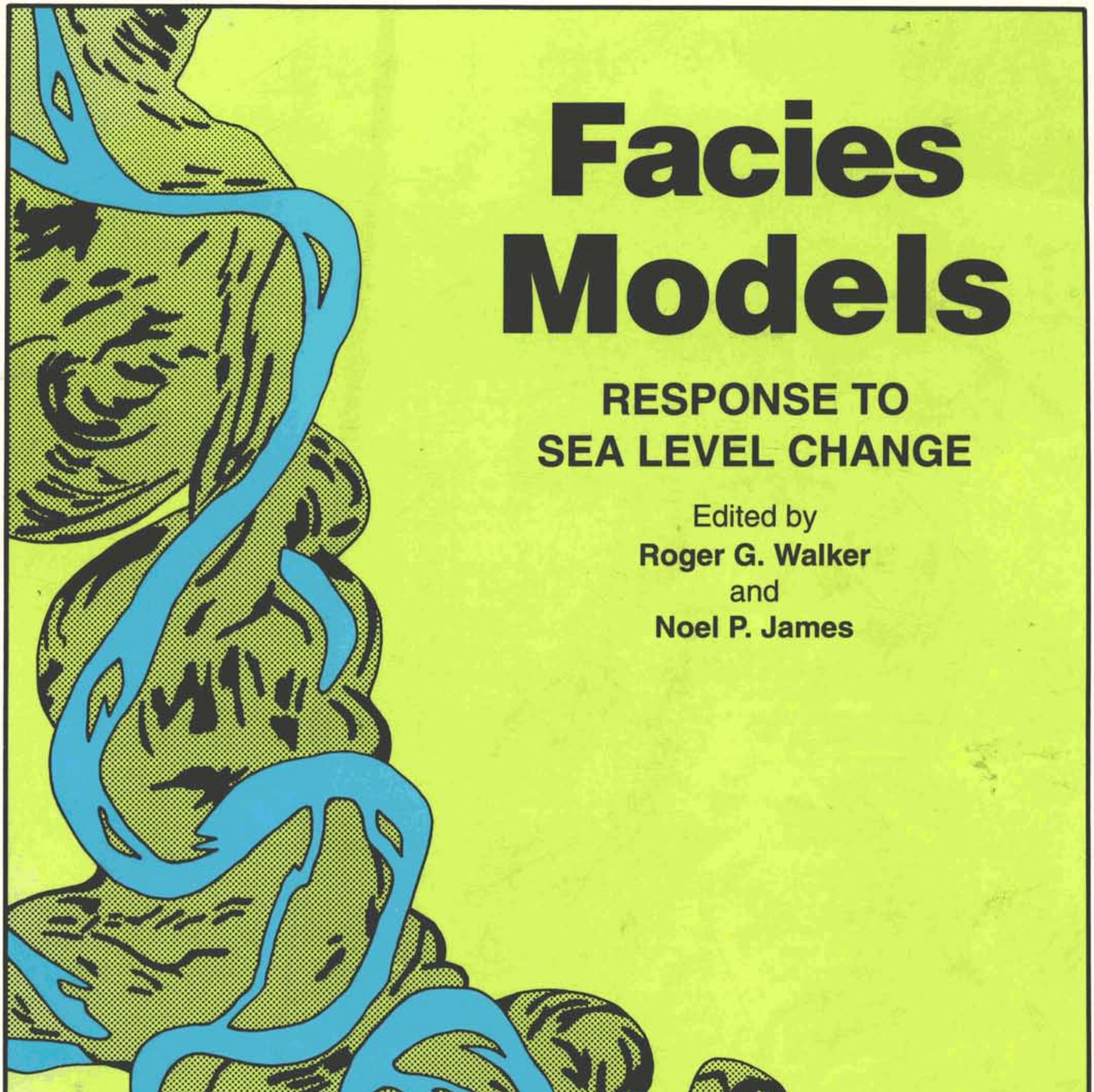

Faces Models

RESPONSE TO SEA LEVEL CHANGE

Edited by
Roger G. Walker
and
Noel P. James

Geological Association of Canada
L'Association géologique du Canada

© Собственность
В. А. Захарова (тел. 35-13-50
35-4994

FACIES MODELS

RESPONSE TO SEA LEVEL CHANGE

Edited by

Roger G. Walker
Department of Geology
McMaster University
Hamilton, Ontario L8S 4M1 Canada

and

Noel P. James
Department of Geological Sciences
Queen's University
Kingston, Ontario K7L 3N6 Canada

Geological Association of Canada
L'Association géologique du Canada

June 1992

Canadian Cataloguing in Publication Data

Main entry under title:

Facies models : response to sea level change

Includes bibliographical references.
ISBN 0-919216-49-8

1. Facies (Geology). I. Walker, Roger G.
II. James, Noel P. III. Geological Association of Canada

QE651.F25 1992 551.7 C92-090412-2

Illustration Concept: Peter Russell, Waterloo

Additional copies may be obtained by writing to:
Geological Association of Canada
Publications
Department of Earth Sciences
Memorial University of Newfoundland
St. John's, Newfoundland A1B 3X5
Canada

 ISBN 0-919216-49-8

Typesetting and Printing
Love Printing Service Ltd.
Stittsville, Ontario

CONTENTS

Preface

In the summer of 1989, the Geological Association of Canada asked us whether it was worthwhile to reprint the second edition of *Facies Models*. Most of the authors felt that the world of sedimentary geology had changed dramatically since the second edition was published in 1984. Rewriting rather than reprinting was necessary. There is now much more information on specific facies. Some fundamental concepts have changed and, most importantly, stratigraphy has re-emerged as a primary analytical tool. Dynamic controls on sedimentation in the form of sea level change, tectonics, climate and biotic evolution, must be incorporated into contemporary facies modelling.

This volume is *not* a third edition, nor is it part of the Geoscience Canada reprint series. Depositional environments have been subdivided in different ways, authors have taken on new responsibilities, new authors are involved, and the volume goes beyond being a mere revision. When preliminary plans for this volume circulated "through the grapevine", Brian Rust was one of the first to volunteer to update his chapter. We discussed plans for this on the day before his trip to Zambia in 1990, where he contracted a fatal case of malaria. We have missed his enthusiasm and knowledge. We will also miss, in the future, the contributions of Bob Frey, who died in January, 1992. His knowledge has enhanced the chapter on Trace Fossils, both in the second edition and in this book.

Of the new concepts incorporated in this book, perhaps the most important concerns the dynamic control of sea level change. Eustatic cycles form the basis of *sequence stratigraphy*, and the bounding discontinuities in the geologic record that formed as a response to sea level change allow *allostratigraphic* subdivision of the stratigraphic column. These fundamental concepts, reviewed in chapter 1, form the underlying theme of the book. All authors have tried to emphasize not only the individual depositional environments, but where appropriate, their response to fluctuations in sea level and other dynamic factors.

Modelling, however, remains an important focus. Models are built on the comparison of modern and ancient examples. In the second edition it seemed possible, when distilling all variables into a static model, to achieve a certain *sedimentological* synthesis which served as a norm, a guide for observations, a predictor, and a basis for interpretation. As more variables are introduced, it is harder to select a group of examples that are homogeneous and can be combined into a model. For example, you might be able to combine the sedimentological features of ten wave-dominated deltas into one model. If sea level change is added as an important descriptive parameter, there may be three deltas that have responded to a relative rise, four to a fall and three in which sea level has not fluctuated. There are now insufficient examples to make powerful integrated models. If tectonic parameters, and the evolving terrestrial biota are included, the problem becomes much worse. In this book we have staked the middle gound. We have tried to explain how the various depositional systems work, and how they respond in general terms to sea level fluctuation and where appropriate, other dynamic factors. At the same time we have still emphasized as much generality as possible (modelling). The models we do present are more complex, and harder to illustrate in block diagrams.

The book is aimed at a general audience, and at students. It is not intended as an advanced research text. All authors have therefore tried to keep the number of citations to a minimum, and we have not necessarily cited the source of every idea presented. The references at the end of each chapter begin with basic sources of information, where more detail on the subject can be found; these references are annotated. The other references are simply in alphabetical order, and are only occasionally annotated.

As editors, we thank the individual authors for building their contributions around the ideas of sedimentation dynamics, in particular the response to sea level change. Although the contributions are largely reviews, there is a lot of original research incorporated in them. Over the years, much of this research has been supported by the Natural Sciences and Engineering Research Council of Canada, and by various universities and government agencies where the authors work. Editors and authors gratefully acknowledge this support.

Bob Baragar (Geological Association of Canada) was extremely helpful in getting this book moving, and Monica Easton took over toward the end and has helped with the technical side of communicating our wishes to the printer. However, there are many other large steps to be taken between writing a manuscript, editing it for technical content, and seeing it appear between the covers of a book. We particularly thank Judith James for editing all nineteen chapters and ensuring that they all follow the same overall style. She has checked on all of those little details that make a contribution as consistent and readable as possible, despite the differing styles of the authors.

Roger G. Walker
Hamilton, Ontario

Noel P. James
Kingston, Ontario

bined (groups) (Fig. 2). Formal methods and rules are given in the North American Stratigraphic Code (NACSN, 1983). Alternative stratigraphic schemes of increasing importance emphasize the *bounding discontinuities* rather than the internal lithological homogeneity. This type of subdivision has been formalized as *allostratigraphy* (Fig. 2; NACSN, 1983). Allostratigraphy is purely descriptive; *sequence stratigraphy* (Van Wagoner *et al.*, 1990) also recognizes units defined by discontinuities and unconformities, but relates them to cycles of sea level fluctuation. *Systems tracts* are linkages of contemporaneous depositional systems. However, different depositional systems occur at different positions of relative sea level, and allow the definition of three main systems tracts; *lowstand, transgressive* and *highstand.*

Certain facies successions and facies geometries in the geological record appear to be characteristic of certain depositional environments. Similar successions and geometries of various ages can be compared with the facies, facies successions and facies geometries observed in modern sediments (Fig. 1). In this way, the general characteristics of various depositional environments can be defined, and used to interpret other parts of the geological record. The

Table 1 *Glossary of terms used in this chapter and throughout the book.*

[redacted] — subdivision of the stratigraphic record into mappable rock bodies "defined and identified on the basis of their bounding discontinuities" (NACSN, 1983, p. 865).

Architectural Element — a morphological subdivision of a particular depositional system characterized by a distinctive assemblage of facies, facies geometries, and depositional processes.

Bounding Discontinuity — a laterally traceable discontinuity; can be an unconformity, ravinement surface, onlap or downlap surface, condensed horizon or hardground. — Non erosional

Depositional Environment — geographic and/or geomorphic area

Depositional System — "three dimensional assemblage of lithofacies, genetically linked by active or inferred processes and environments" (Posamentier *et al.*, 1988, p. 110). It embraces depositional environments and the processes acting therein.

Downlap — the situation where "an initially inclined layer terminates downdip against an initially horizontal or inclined surface" (Mitchum *et al.*, 1977, p. 58).

Eustasy — a world-wide change of sea level relative to a fixed point such as the centre of the earth. Eustatic changes result from variations in the volume of water in the ocean basins (glacial control), or a change in the volume of the basins themselves (related to rates of ocean ridge building and rates of seafloor spreading). The eustatic sea level curve describes cyclic changes in sea level.

Facies — a body of rock characterized by a particular combination of lithology, physical and biological structures that bestow an aspect ("facies") different from the bodies of rock above, below and laterally adjacent.

Facies Association — "groups of facies genetically related to one another and which have some environmental significance" (Collinson, 1969, p. 207).

Facies Succession — a vertical succession of facies characterized by a progressive change in one or more parameters, e.g., abundance of sand, grain size, or sedimentary structures

Facies Model — a general summary of a particular depositional system, involving many individual examples from recent sediments and ancient rocks.

Genetic Stratigraphic Sequence — "the sedimentary product of a depositional episode" (Galloway, 1989, p. 125), where a depositional episode "is bounded by stratal surfaces that reflect major reorganizations in basin paleogeographic framework" (Galloway, 1989, p. 128). These stratal surfaces are maximum flooding surfaces, not the unconformities used to define stratigraphic sequences.

Lithostratigraphy — "a defined body of sedimentary...strata which is distinguished and delimited on the basis of lithic characteristics and stratigraphic position" (NACSN, 1983). It is internally lithologically homogeneous.

Marine Flooding Surface — "a surface separating younger from older strata across which there is evidence of an abrupt increase in water depth" (Van Wagoner *et al.*, 1990, p. 8).

Maximum Flooding Surface — a surface separating a transgressive systems tract (below) from a highstand systems tract (above). It is commonly characterized by a condensed horizon reflecting very slow deposition; markers in the overlying systems tract downlap onto the MFS.

Onlap — the situation where "an initially horizontal stratum laps out against an initially inclined surface" (Mitchum *et al.*, 1977, p. 57-58).

Parasequence — "a relatively conformable succession of genetically related beds or bedsets bounded by marine flooding surfaces and their correlative surfaces" (Posamentier *et al.*, 1988, p. 110).

Ravinement Surface — an erosion surface produced during marine transgression of a formerly subaerial environment.

Seismic Stratigraphy — "a geological approach to the stratigraphic interpretation of seismic data" (Vail and Mitchum, 1977, p. 51).

Sequence — "a relatively conformable succession of genetically related strata bounded at its top and base by unconformities and their correlative conformities...it is composed of a succession of systems tracts and is interpreted to be deposited between eustatic-fall inflection points" (Posamentier *et al.*, 1988, p. 110).

[redacted] — "the study of rock relationships within a chronostratigraphic framework wherein the succession of rocks is cyclic and is composed of genetically related stratal units (sequences and systems tracts)" (Posamentier *et al.*, 1988, p. 110).

[redacted] — "a linkage of contemporaneous depositional systems" (Posamentier *et al.*, 1988, p. 110).

Unconformity — "a surface separating younger from older strata, along which there is evidence of subaerial erosional truncation...or subaerial exposure, with a significant hiatus indicated" (Posamentier *et al.*, 1988, p. 110). This is an extremely restricted definition; Posamentier (personal communication, 1990) now accepts that the "evidence" may be inferred rather than real.

bined (groups) (Fig. 2). Formal methods and rules are given in the North American Stratigraphic Code (NACSN, 1983). Alternative stratigraphic schemes of increasing importance emphasize the *bounding discontinuities* rather than the internal lithological homogeneity. This type of subdivision has been formalized as *allostratigraphy* (Fig. 2; NACSN, 1983). Allostratigraphy is purely descriptive; *sequence stratigraphy* (Van Wagoner *et al.*, 1990) also recognizes units defined by discontinuities and unconformities, but relates them to cycles of sea level fluctuation. *Systems tracts* are linkages of contemporaneous depositional systems. However, different depositional systems occur at different positions of relative sea level, and allow the definition of three main systems tracts; *lowstand, transgressive* and *highstand.*

Certain facies successions and facies geometries in the geological record appear to be characteristic of certain depositional environments. Similar successions and geometries of various ages can be compared with the facies, facies successions and facies geometries observed in modern sediments (Fig. 1). In this way, the general characteristics of various depositional environments can be defined, and used to interpret other parts of the geological record. The

Table 1 *Glossary of terms used in this chapter and throughout the book.*

Allostratigraphy — subdivision of the stratigraphic record into mappable rock bodies "defined and identified on the basis of their bounding discontinuities" (NACSN, 1983, p. 865).

Architectural Element — a morphological subdivision of a particular depositional system characterized by a distinctive assemblage of facies, facies geometries, and depositional processes.

Bounding Discontinuity — a laterally traceable discontinuity; can be an unconformity, ravinement surface, onlap or downlap surface, condensed horizon or hardground. — Non erosional

Depositional Environment — geographic and/or geomorphic area

Depositional System — "three dimensional assemblage of lithofacies, genetically linked by active or inferred processes and environments" (Posamentier *et al.*, 1988, p. 110). It embraces depositional environments and the processes acting therein.

Downlap — the situation where "an initially inclined layer terminates downdip against an initially horizontal or inclined surface" (Mitchum *et al.*, 1977, p. 58).

Eustasy — a world-wide change of sea level relative to a fixed point such as the centre of the earth. Eustatic changes result from variations in the volume of water in the ocean basins (glacial control), or a change in the volume of the basins themselves (related to rates of ocean ridge building and rates of seafloor spreading). The eustatic sea level curve describes cyclic changes in sea level.

Facies — a body of rock characterized by a particular combination of lithology, physical and biological structures that bestow an aspect ("facies") different from the bodies of rock above, below and laterally adjacent.

Facies Association — "groups of facies genetically related to one another and which have some environmental significance" (Collinson, 1969, p. 207).

Facies Succession — a vertical succession of facies characterized by a progressive change in one or more parameters, e.g., abundance of sand, grain size, or sedimentary structures

Facies Model — a general summary of a particular depositional system, involving many individual examples from recent sediments and ancient rocks.

Genetic Stratigraphic Sequence — "the sedimentary product of a depositional episode" (Galloway, 1989, p. 125), where a depositional episode "is bounded by stratal surfaces that reflect major reorganizations in basin paleogeographic framework" (Galloway, 1989, p. 128). These stratal surfaces are maximum flooding surfaces, not the unconformities used to define stratigraphic sequences.

Lithostratigraphy — "a defined body of sedimentary...strata which is distinguished and delimited on the basis of lithic characteristics and stratigraphic position" (NACSN, 1983). It is internally lithologically homogeneous.

Marine Flooding Surface — "a surface separating younger from older strata across which there is evidence of an abrupt increase in water depth" (Van Wagoner *et al.*, 1990, p. 8).

Maximum Flooding Surface — a surface separating a transgressive systems tract (below) from a highstand systems tract (above). It is commonly characterized by a condensed horizon reflecting very slow deposition; markers in the overlying systems tract downlap onto the MFS.

Onlap — the situation where "an initially horizontal stratum laps out against an initially inclined surface" (Mitchum *et al.*, 1977, p. 57-58).

Parasequence — "a relatively conformable succession of genetically related beds or bedsets bounded by marine flooding surfaces and their correlative surfaces" (Posamentier *et al.*, 1988, p. 110).

Ravinement Surface — an erosion surface produced during marine transgression of a formerly subaerial environment.

Seismic Stratigraphy — "a geological approach to the stratigraphic interpretation of seismic data" (Vail and Mitchum, 1977, p. 51).

Sequence — "a relatively conformable succession of genetically related strata bounded at its top and base by unconformities and their correlative conformities...it is composed of a succession of systems tracts and is interpreted to be deposited between eustatic-fall inflection points" (Posamentier *et al.*, 1988, p. 110).

Sequence Stratigraphy — "the study of rock relationships within a chronostratigraphic framework wherein the succession of rocks is cyclic and is composed of genetically related stratal units (sequences and systems tracts)" (Posamentier *et al.*, 1988, p. 110).

Systems Tract — "a linkage of contemporaneous depositional systems" (Posamentier *et al.*, 1988, p. 110).

Unconformity — "a surface separating younger from older strata, along which there is evidence of subaerial erosional truncation...or subaerial exposure, with a significant hiatus indicated" (Posamentier *et al.*, 1988, p. 110). This is an extremely restricted definition; Posamentier (personal communication, 1990) now accepts that the "evidence" may be inferred rather than real.

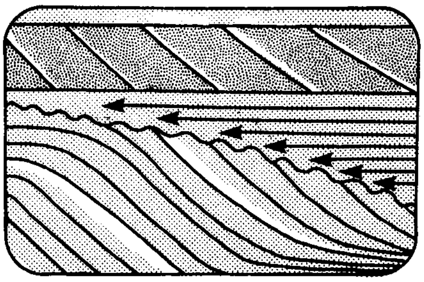

1. Facies, Facies Models and Modern Stratigraphic Concepts

Roger G. Walker, Department of Geology, McMaster University, Hamilton, Ontario L8S 4M1

OBJECTIVES OF FACIES MODELLING

Features of recent sediments and ancient sedimentary rocks can be combined and condensed into idealizations or models that characterize particular sedimentary environments. This combination of features from modern and ancient situations has been emphasized from the earliest days; in 1893 Johannes Walther (quoted by Middleton, 1973, p. 981) "explained that the most satisfying genetic explanations of ancient phenomena were by analogy with modern geological processes". A good model embodies a large amount of information from different examples of the same depositional system, for instance, meandering river channels. It is therefore an excellent point of reference for the interpretation of new examples of the same system, and allows predictions to be made from limited amounts of data. The predictive capabilities of models have largely been used in the exploration for oil and gas (e.g., Chapters 3, 12, 13, 16, 17), and to a lesser extent in exploration for minerals hosted by sedimentary rocks. However, the broad understanding of depositional systems is becoming increasingly important in modelling the movement of ground water and pollutants through surficial unconsolidated sediments, where the movement is partly a function of the geometry of permeable and impermeable layers (Chapter 5). This geometry largely depends on the depositional processes operating in the original sedimentary environment. Facies models also embody ideas about how natural sedimentary systems work, and to what extent they can be "managed". For example, a general understanding of beaches and barriers (Chapter 10) contributes to the solution of coastal erosion problems. In the Mississippi Delta, there is a large annual land loss due to regional subsidence and delta inundation; these aspects of delta behaviour are part of the general deltaic facies model (Chapter 9).

In the first two editions of *Facies Models*, we tried to synthesize and idealize the features of some modern depositional environments and systems (terminology defined in Table 1), and show how their deposits could be identified in the geological record. The models we built tended to be snapshots of specific systems at one time (static block diagrams). They emphasized the sedimentary processes operating within the systems rather than processes external to the environments, such as fluctuations of relative sea level, and tectonics.

The major conceptual change since the second edition (1984) has been the recognition of the importance of relative sea level fluctuation (Chapter 2). This concept now permeates stratigraphy and sedimentology, and brings a dynamic quality to models of depositional environments. Specific environments must be modelled as videos rather than snapshots. The syntheses presented in this book will attempt to convey how the environments respond to sea level fluctuation.

A SEDIMENTOLOGICAL *MODUS OPERANDI*

Over the years, many different methods and concepts have been used in the study of sedimentary rocks. The *modus operandi*, or way of working on sedimentary rocks, depends on the objectives. Studies of ancient depositional environments commonly begin with stratigraphic measurements and correlations, in order to define the rock types present, their three-dimensional geometry, and their internal sedimentary structures.

Overview of terminology

A glossary of terminology used in this chapter, and throughout the book, is given in Table 1. The measurement of a vertical stratigraphic section implies that it will be subdivided into a series of different units, each with different thicknesses and characteristics. The different aspect of each measurement unit is summarized by the term *facies* (from the Latin word for aspect, or "appearance of" something). Primary descriptive characteristics include lithology, sedimentary structures and biological features.

During an individual study, facies can commonly be grouped into *facies associations* (Fig. 1). On a broader scale, certain associations occur sufficiently commonly throughout time and space that they can be regarded as basic *architectural elements* of a particular depositional environment. For example, lateral-accretion deposits form an architectural element within meandering river environments, as discussed in Chapter 7. Facies also tend to occur in specific *facies successions* (Fig. 1), in which one or more of their characteristics changes progressively upsection. Thus a succession might be termed *coarsening-upward* if there is a progressive change of grain size, or *thickening-upward* if there is a change in thickness of individual beds. Progressive changes in rock properties are also shown up in downhole surveys of oil and gas wells (Chapter 3). Progressive facies successions are commonly terminated by abrupt changes in lithology across *discontinuities* of some type (Fig. 2); these might be erosion surfaces, or surfaces of nondeposition. Such surfaces commonly have a distinct trace fossil signature (Chapter 4).

The traditional descriptive stratigraphic scheme for subdividing ancient sedimentary rocks involves the definition of lithologically homogeneous units (formations) that can be further subdivided (members) or com-

comparison of modern and ancient depositional environments, and the search for the processes that control their facies successions and geometries, is now termed *facies modelling*. These terms and concepts are discussed in the following text, beginning at the small scale (facies) and working up to the large scale (systems tracts).

FACIES

The modern geological usage of the term facies was introduced by Gressly in 1838, who used it to imply the sum total of the lithological and paleontological aspects of a stratigraphic unit. Translations of Gressly's extended definition are given by Middleton (1973). The term has been used in many different ways since 1838, with arguments centering on 1) whether the term implies an abstract set of characteristics, as opposed to the rock body itself, 2) whether the term should refer only to "areally restricted parts of a designated stratigraphic unit" (Moore, 1949) or also to stratigraphically unconfined rock bodies (as originally implied by Gressly), and 3) whether the term should be purely descriptive ("mudstone facies") or also interpretive ("fluvial facies"). Succinct discussions of these problems have been given by Middleton (1978), Anderton (1985) and Reading (1986).

Working definition of facies

The most useful modern working definition of facies was given by Middleton (1978), who noted that

> "the more common (modern) usage is exemplified by de Raaf *et al.* (1965) who subdivided a group of three formations into a cyclical repetition of a number of facies distinguished by "lithological, structural and organic aspects detectable in the field". The facies may be given informal designations ("Facies A" etc.) or brief descriptive designations ("laminated siltstone facies") and it is understood that they are units that will ultimately be given an environmental interpretation; but the facies definition is itself quite objective and based on the total field aspect of the rocks themselves... The key to the interpretation of facies is to combine observations made on their spatial relations and internal characteristics (lithology and sedimentary structures) with comparative information from other well-studied stratigraphic units, and particularly from studies of modern sedimentary environments".

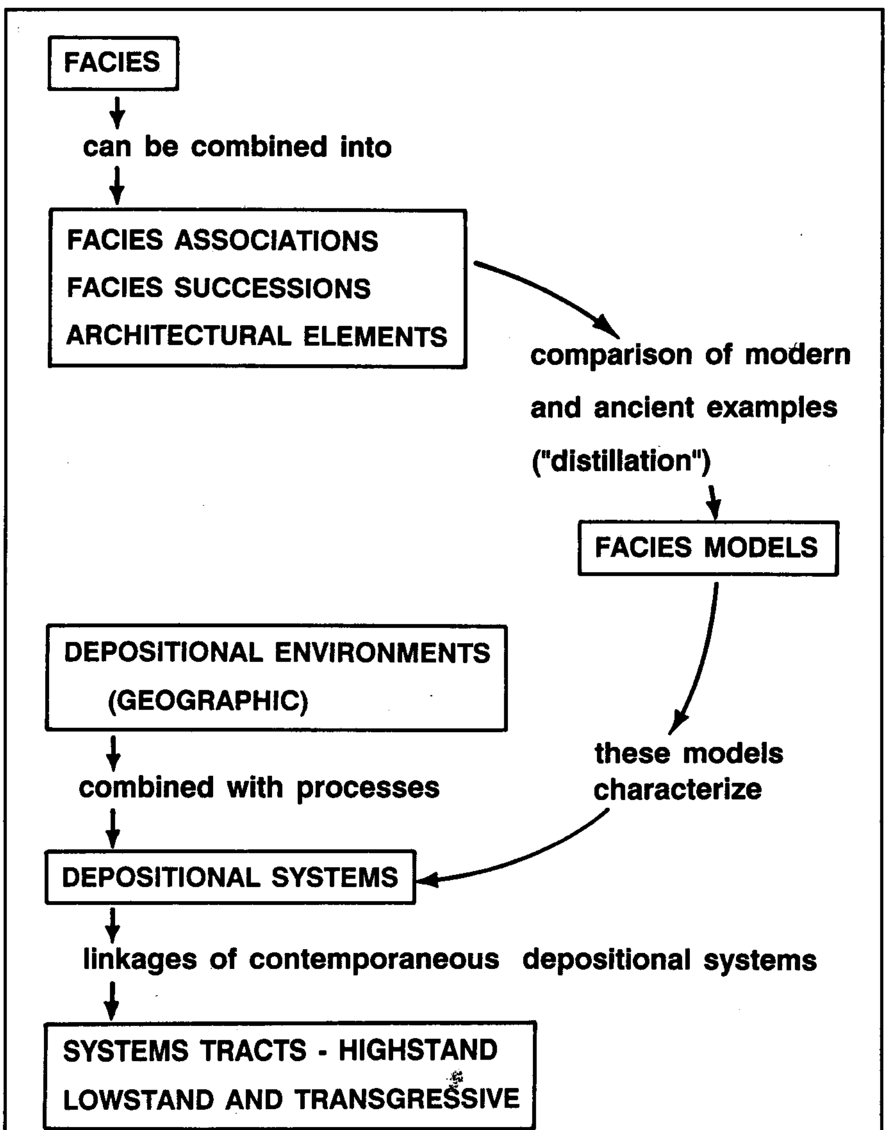

Figure 1 Relationship between facies, depositional environments and systems, and systems tracts, as used throughout this book.

DEFINING FACIES

Facies can be defined on many different scales. In a study specifically devoted to the interpretation of depositional environments, there is usually a deliberate attempt to subdivide a rock body into constituent facies (units of similar aspect). This is a classification procedure, and the degree of subdivision is governed by the objectives of the study. If the objective is routine description and interpretation on a large scale, a fairly broad facies subdivision may suffice. If the objective is more detailed, perhaps involving the refinement of an existing model or the definition of a new one, the facies subdivision must be more detailed.

The *scale* of *subdivision* is dependant not only on the objectives, but on the time available in the field, the degree of preservation, and the abundance of physical and biological structures in the rocks. A thick sequence of massive mudstones or thin-bedded turbidites (Fig. 3) will be difficult to subdivide, but a similar thickness of interbedded sandstones and shales (with abundant and varied examples of ripples, cross bedding [Fig. 4] and trace fossils) might be subdivisible into

Figure 2 Upper diagram shows lithostratigraphic units X (conglomerate), Y (shales) and Z (sandstones). Allostratigraphic units A through E, and systems tracts HST and TST are also indicated. MarFS = Marine Flooding Surface and MaxFS = Maximum Flooding Surface. Solid arrowheads indicate onlap, and open arrowheads indicate downlap. Bounding discontinuities are shown by the small zig-zag serrated symbol (unconformities); the MarFS and MaxFS surfaces are also bounding discontinuities. The large serrated symbol separating the shoreface from the offshore is not a bounding discontinuity — it represents a gradual facies change. Lower diagram shows an interpretation in terms of sea level (SL) fluctuations. During SL1, the shoreface built out to profile 1. With a drop in sea level to SL2, a new shoreface was cut off the right hand edge of the diagram. During a standstill in transgression, and incised shoreface formed at profile 2, and conglomerate was deposited in the shoreface. When the transgression resumed (SL2 to SL3), the top of the conglomerate was eroded, and profile 2 was cut landward to profile 3, making a ravinement surface (profile 3). Note that evidence of subaerial erosion (vegetation on profile 2) is removed during subsequent transgression. Sea level stabilized at SL3-4, and the shoreface sand built out to profile 4. Subsequent fall and rise of sea level resulted in the ravinement surface 5.

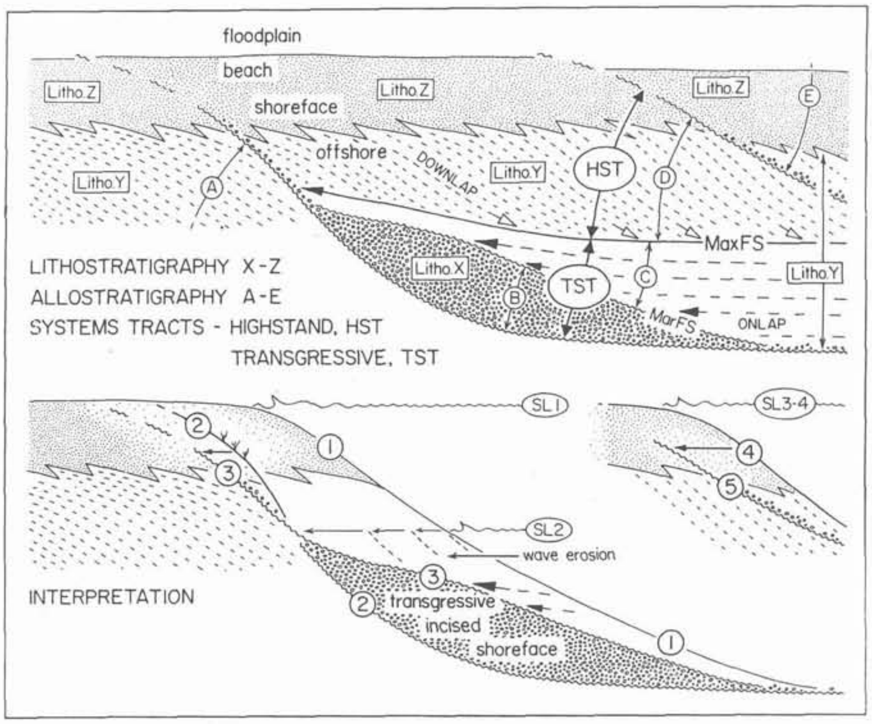

Figure 3 Devonian turbidites near Melbourne, Australia. Stratigraphic top to right.

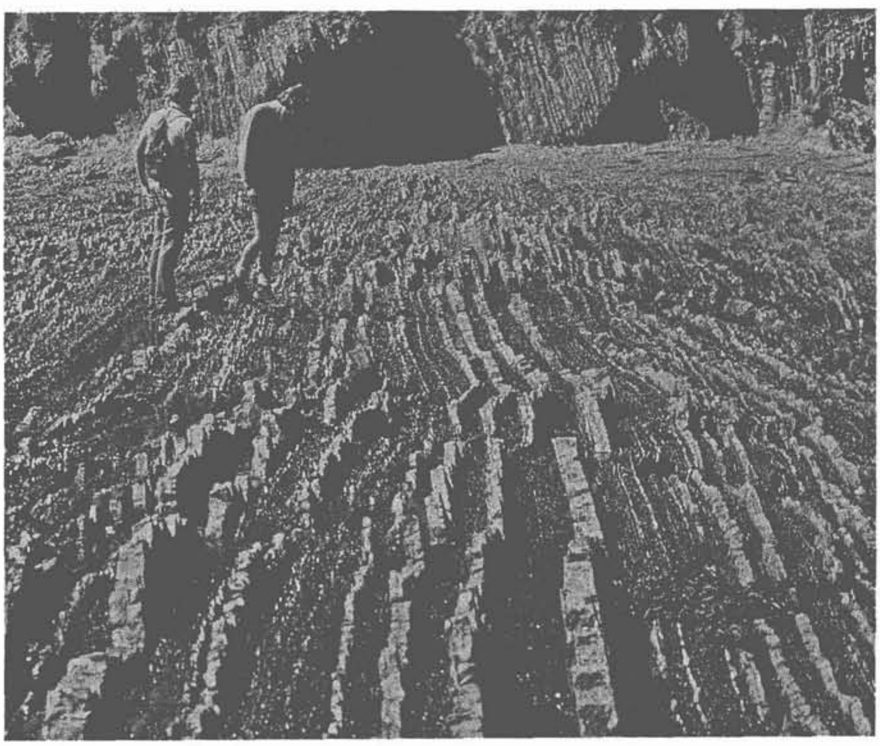

a large number of distinct facies. I would advocate erring on the side of detailed subdivision in the field — facies can always be recombined in the laboratory, but a crude field subdivision cannot be refined in the lab.

Subdivision of a body of rock into facies ideally should not be attempted until one is thoroughly familiar with the rock body. Only then will it be apparent how much variability there is, and how many different facies must be defined to describe the unit adequately. In the field, most facies studies have relied on qualitatively assessed combinations of distinctive sedimentary and organic structures (e.g., de Raaf *et al.*, 1965; Williams and Rust, 1969; Wilson, 1975; Cant and Walker, 1976; Scholle *et al.*, 1983; Walker, 1983). Statistical methods can also be used to define facies, especially where there is considerable agreement among workers as to the important quantifiable, descriptive parameters (e.g., the proportions of different types of clasts in carbonate rocks; Imbrie and Purdy, 1962; Klovan, 1964; Harbaugh and Demirmen, 1964; see also Chapter 7 of the book by Harbaugh and Merriam, 1968). Unfortunately, statistical methods are unsuited to terrigenous clastic rocks, where the most important information (sedimentary and biological structures) cannot easily be quantified.

In the subsurface, rock bodies can be defined seismically, and different parts of the seismic record may have different aspects; this gives rise to the concept of seismic facies (see Chapters 3 and 13). If borehole data are available, the electrical and geophysical well logs also have different aspects, and may allow the definition of facies and facies successions based upon the log characteristics (Chapter 3).

FACIES ASSOCIATIONS AND ARCHITECTURAL ELEMENTS

In many studies, facies have been defined on a small scale — the units are only a few metres in thickness, and differences between facies are subtle, involving (for example) minor changes in proportion of silt and mud, the relative abundance and diversity of fossils, and minor differences in the style of lamination (Walker, 1983). This detailed subdivision commonly results in a facies scheme where the descriptive differences outstrip our ability to interpret the differences. It is therefore useful to combine closely related facies into facies associations (Fig. 1), or "groups of facies genetically related to one another and which have some environmental significance" (Collinson, 1969). These larger scale facies associations have also been termed architectural elements (Allen, 1983), implying that they are the building blocks of the various depositional systems. The concept of *architectural elements* also emphasizes the three dimensional geometry of the facies associations. Good examples are given in Chapter 7.

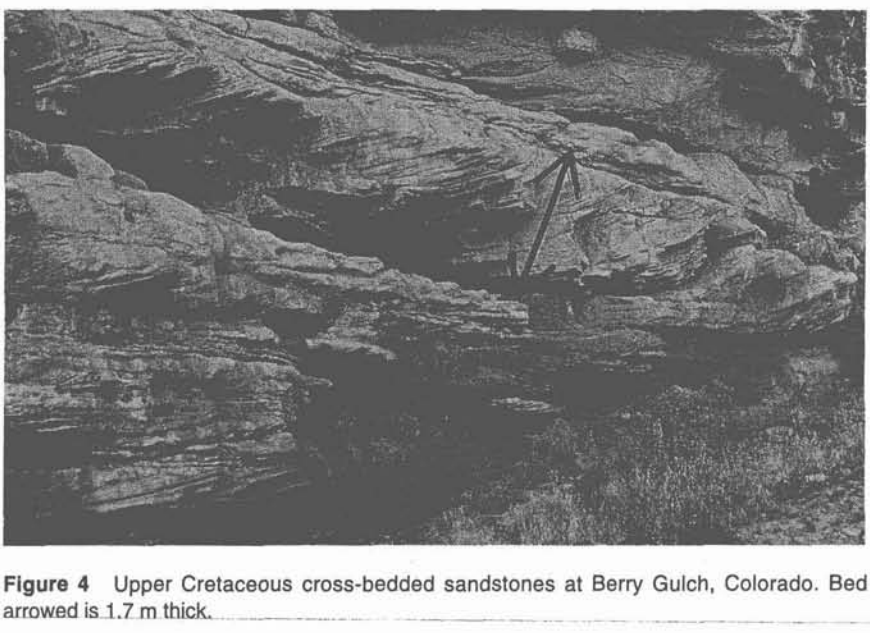

Figure 4 Upper Cretaceous cross-bedded sandstones at Berry Gulch, Colorado. Bed arrowed is 1.7 m thick.

At the scale of architectural elements (but not on the local, small scale facies level), it is becoming clear that in some depositional systems, certain elements occur *universally*, in recent and ancient sediments, and in many different geological settings around the world. The first *universal* facies scheme was proposed for turbidites (Mutti and Ricci Lucchi, 1972; see Chapter 13), and Miall (1977, 1985) has suggested a scheme for fluvial deposits (see Chapter 7). For example, Miall's (1985) *channel* architectural element (CH) consists of any combination of a series of defined lithofacies which communally have a distinctive elongate channel geometry; it is part of the architecture of almost all modern rivers, and can be recognized in most ancient fluvial deposits.

Individual facies are likely to be influenced by many small-scale local factors. In a river, for example, the exact aspect of a local deposit may be controlled by the sinuosity of a meander loop and the erodibility of the bank. Architectural elements are larger scale components of a depositional system (e.g., a river channel). They will be more general in nature, less influenced by local factors, and hence more universal in their application.

FACIES SUCCESSIONS

In stratigraphic studies, the term *sequence* has recently been given a very specific definition (Table 1). The term *facies succession* is now preferable to the older *facies sequence*. The concept of a succession implies that certain facies properties change progressively in a specific direction (vertically or laterally); these properties might include the proportion of sand (*sandier-upward* succession, Fig. 5), the amount of bioturbation, or the grain size of the sand (hence a *coarsening-upward succession*).

Many, if not most individual facies defined in the field have ambiguous environmental interpretations. For example, although the *processes* forming medium-scale cross bedding (Fig. 4) are essentially the same in all settings, a cross-bedded sandstone facies could be formed in a meandering or braided river, a tidal inlet, a shoreface dominated by alongshore currents, or a shelf dominated by tidal currents. Diamict facies (Chapter 5) are particularly difficult to give unambiguous environmental interpretations. Indeed, many facies defined descriptively in the field may at first suggest no particular interpretation at all. The key to interpretation is to analyze all of the facies communally, in context. Thus the *succession* in which they occur contributes important information that the facies, considered individually, cannot contribute.

The relationship between depositional systems in space, and the resulting stratigraphic successions developed through time was first emphasized by Johannes Walther (1894, in Middleton, 1973) in his *Law of the Correlation of Facies.* Walther stated that "it is a basic statement of far-reaching significance that only those facies and facies areas can be superimposed primarily which can be observed beside each other at the present time". Careful application of the law suggests that in a vertical succession, a *gradational* transition from one facies to another implies that the two facies represent environments that were once adjacent laterally. If the contacts between facies or facies associations are sharp and/or erosional, there is no way of knowing whether two vertically adjacent facies represent environments that were once laterally adjacent. Indeed, sharp breaks between facies (marked for example by channel scours, or by thin bioturbated horizons implying nondeposition) may signify fundamental changes in depositional environment and the beginnings of new cycles of sedimentation (de Raaf *et al.*, 1965). These sharp breaks, or *bounding discontinuities*, are now used to separate stratigraphic sequences and allostratigraphic units (as discussed below).

The relationships between facies within facies successions can be expressed quantitatively in facies relationship diagrams (de Raaf *et al.*, 1965), or tabulated in facies transition probabilities. These methods of facies analysis are not as popular as they were a few years ago, but the techniques remain useful. Interested readers are referred to the second edition of *Facies Models* (Walker, 1984; Harper, 1984).

Over the years, it has become ap-

record, in rocks of all ages, in many different geological settings. When these successions are combined with successions observed in certain modern depositional systems, a summary or synthesis of that system emerges. As vertical successions are correlated laterally, developing a three-dimensional picture of a depositional system, we are in effect formulating general statements about that system — a facies model.

FACIES MODELS

A facies model can be defined as a general summary of a given depositional system, written in terms that make the summary useable in at least four different ways. The philosophical assumption made here is that there is system and order in Nature, and that geologists can identify and agree on a limited number of depositional systems. In a well-argued alternative view, Anderton (1985, p. 33) suggests that "if, like me, you have a more nihilistic view of life, the universe and everything, then you have to admit an infinite number of environments, facies and models".

For those who seek order in Nature, the principles, methods and motives of facies modelling are shown in Figure 6, using turbidites and submarine fans as an example. We begin by assuming that if enough modern turbidites can be studied in cores, enough modern fans studied on a larger scale with seismic profiles, and enough ancient turbidites studied in the field, we should be able to make some *general* statements about fans and turbidites rather than statements about one particular example (Chapter 13).

The process of extracting the general information is shown in Figure 6, where the local examples refer to studies of modern fans and ancient rocks. This entire wealth of information is then *distilled*, boiling away the local details but concentrating the important features that they all have in common into a general summary of fans. But what constitutes local detail, and what is general? Which aspects do we dismiss, and which do we extract and consider important?

Answering these questions involves experience, judgement, knowledge and argument among sedimentologists. Models are constantly being refined as more information becomes available, and as the significance of the various constituent parts of the model becomes better understood. For example, extensive debris flow and slump horizons on modern submarine fans were scarcely mentioned in the second edition of *Facies Models*, but these deposits feature prominently in this edition (Chapters 13, 18). Some of the difficulties of modelling, imposed

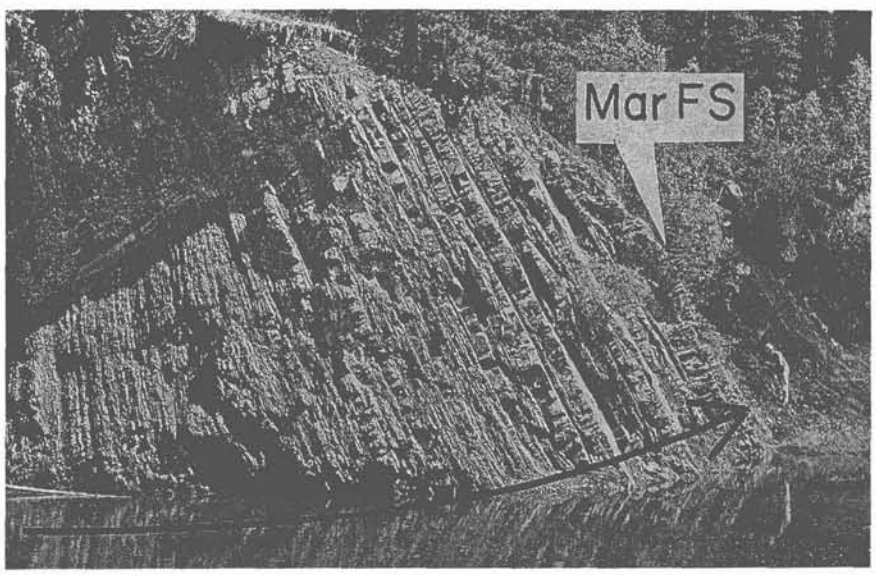

Figure 5 *Sandier-upward facies succession (arrowed) from the Upper Cretaceous* Cardium Formation, Blackstone River, Alberta. Note the overall increase in proportion of sandstone upward, and the tendency for individual sandstone beds to become thicker

by the variability of nature, are discussed by Anderton (1985).

Four main uses of facies models

The generality embodied in a facies model, as opposed to a summary of one particular example, enables the facies model to assume four main functions (Fig. 6):

1) it must act as a *norm*, for purposes of comparison;
2) it must act as a *framework* and *guide* for future observations;
3) it must act as a *predictor* in new geological situations; AUTO EXAMPLE
4) it must act as an integrated basis for *interpretation* for the system that it represents.

Figure 6 also emphasizes the constant comparison and feedback between local examples. If a feature or idea is perceived in one example, does it occur in the others? By these comparisons, the sedimentologist exercises his or her judgement in defining features in common, and identifying "local irregularities". This is the distillation process that allows the initial construction of a facies model.

The model may now act as a *norm*, with which new examples can be compared (Fig. 6). Without a norm we are unable to say whether a hypothetical new example contains any unusual features. If the new example conforms exactly to the facies model, its interpretation is simplified, and the model is strengthened. If the new example differs, we can specify exactly how it differs, and then ask questions about the new example that could not have been asked without the norm. For example, compared with the norm, why is the hypothetical new example thicker, or dominated by debris flow deposits rather than classical turbidites? These questions can open up new avenues of productive thought; without the norm, such questions cannot be asked. This gives rise to yet more feedback between the model and the new examples; some new examples may result in significant modification of the facies model itself.

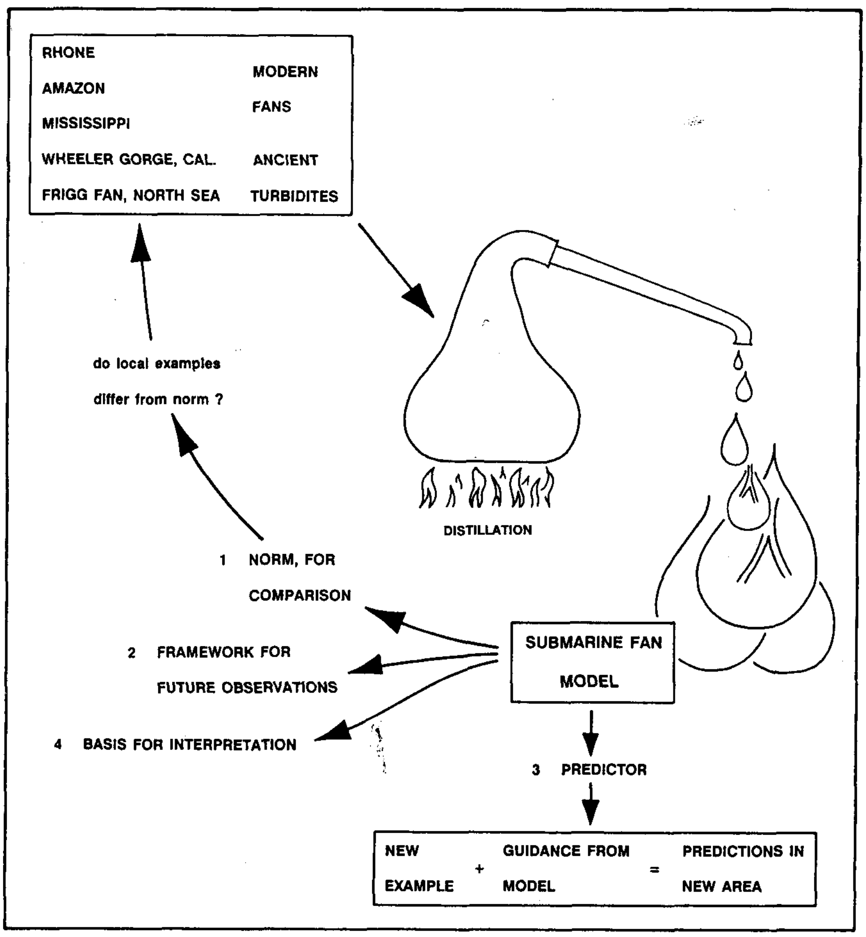

Figure 6 Distillation of a general facies model for submarine fans. See text for details.

The second function of the model is to act as a *guide* for future observations. Inasmuch as the model summarizes all of the important descriptive features of the system, geologists know that similar information must be recorded when working with a new example. This does not exclude the careful search for new information that is not specifically indicated by the model in its present state of evolution.

The third function of the model, as a *predictor*, is probably the most important. I will use an imaginary facies model for automobiles to make my point. A generalized automobile model expresses the relationships between wheels, hood, trunk, doors, etc. What, then, can we say if a radiator is one day discovered in an outcrop? Without a model, one might say little more than "nice radiator". But if the radiator can be identified as part of an automobile system (i.e., an automobile radiator rather than a truck radiator), we can use the automobile model to predict the rest of the car from the discovery of a radiator. Clearly, we will go wrong if we (incorrectly) identify the radiator as part of a truck, and attempt to use a truck facies model to make predictions about an automobile system. In the geological world, we might be able to make predictions within a submarine fan system from one seismic line across a fan channel, or from one outcrop of a fan channel, granted that we could confidently assign the seismic line or outcrop to a submarine fan system rather than to a deltaic distributary channel (for example). Prediction is a vitally important application of facies modelling; good surface or subsurface predictions based on 1) limited data and 2) guidance from a facies model can save unnecessary exploration guesswork, and potentially large amounts of time and money.

AUTOMOBILE EX

The fourth function of the model is to act as an integrated *basis for interpretation*. Before the Bouma (1962) sequence for turbidites was defined, each turbidite bed acted as a basis for its own hydrodynamic interpretation. Bouma generalized the internal sequence of structures for hundreds of individual turbidites, recognizing a massive base, overlain by parallel lamination and ripple cross lamination. This facies model for the internal structures of turbidites then served as the basis for a powerful interpretation of waning flow and deposition from turbidity currents. The interpretation was powerful because it was based on the combined features of hundreds of beds, not one or two local examples. The same principle applies to fluvial point-bar deposits in meander bends, to tidal current ridges on the continental shelf, and in all other situations where there are enough local examples (ancient and modern) to achieve a synthesis in terms of a facies model.

Anderton (1985) is one of very few people who has commented on the four uses of models that I proposed in the first edition of *Facies Models*. He agrees that a model "can and should be used as a framework for future observations and as a predictive tool" (Anderton, 1985, p. 33), but he is not so certain about their use as a norm, and as a basis for interpretation. I would reply that one cannot logically make predictions from a set of unconnected different examples, and that accepting a model as a predictor implies a common body of knowledge, that is, a norm. Philosophically inclined readers are referred to Anderton's thoughtful paper.

WHICH ENVIRONMENTS SHOULD BE MODELLED — THE PROBLEMS OF SCALE

In this chapter, I have referred to models for entire submarine fans, and to models for individual turbidite beds (the Bouma sequence). It is clear that depositional systems and environments can be recognized today on many different scales. Should we build facies models for 1) entire barrier island and lagoonal systems, 2) tidal inlets and channels, or 3) tidal mud flats? An environment is considered to be any distinct geographical entity — thus a washover fan on the back of a barrier island could be the basis for a facies model. The smaller and more distinct the environment, the easier it is to characterize it in a model. Barrier washovers, or Bouma sequences, are relatively simple systems characterized by few descriptive parameters and affected by a small range of physical and biological processes. In contrast, deltas represent large depositional systems characterized by the complex interplay of sediment supply, basin subsidence, and fluvial, wave and tidal redistribution of sediment. It is much more difficult to build a homogeneous model for deltas (i.e., one based on many examples of essentially the same type of delta) because the few that have been well studied have many points of difference and only a few (very general) points of similarity. A model based on homogeneous data (sandy point-bar deposits, for example) is precise and powerful, but a model that contains inhomogeneous data is less precise, and is only a weak predictor. An example of an inhomogeneous model might be one for all sandy rivers, based on examples of both meandering and braided streams. Some models are inhomogeneous because they have been formulated for large depositional systems where only a few examples have been studied. Others are inhomogeneous because they have been constructed poorly, using dissimilar individual examples in an attempt to formulate generality.

WHICH ENVIRONMENTS SHOULD BE MODELLED — THE PROBLEM OF EXTERNAL CONTROLS

Facies models are commonly formulated for depositional systems that today form obvious geographic entities — deltas, reef tracts and barrier islands, for example. However, some modern geographic environments are extremely difficult to preserve in the geological record, and when they are preserved, the deposits look very different from the environment seen in today's snapshot. For example, barrier islands are long, narrow sandbodies which separate the open sea from a lagoon on the landward side (Chapter 10). Few such sandbodies exist in the geological record. Barriers that suffer transgression leave behind a thin smear of lagoonal deposits and almost no record of the sandy barrier superstructure. Barriers that prograde may form a wide sand sheet, with no associated lagoonal deposits (the lagoon was quickly filled in during progradation). It is therefore imperative that in formulating facies models in the 1990's, external controls such as relative sea level changes and tectonics be incorporated into the model.

We have attempted throughout the book to emphasize the concept that geographic environments and depositional systems change as relative sea level changes. This has led to some reorganization of the book, one example being the de-emphasis of the "triangular delta model" (Fig. 7; Galloway, 1975), and the splitting of the shallow-marine system. The delta triangle has served as a useful basis for showing the relative importance of river-, wave- and tide-dominated deltas (Fig. 7). However, most "tide-dominated deltas" in the literature have little morphological relationship to other deltas, and many of them might better be considered as tidal estuaries (Chapter 11). With a few metres of relative sea level rise, tidal deltas have more in common with tidal shelf ridges than with other deltas. Recognizing the importance of relative sea level fluctuation, we have therefore created a chapter on tidal sandstones (Chapter 11), and have torn off the offending corner of the delta triangle (Fig. 7). The new delta chapter (Chapter 9) therefore emphasizes the spectrum of river- and wave-dominated systems, but only briefly touches on tide-influenced systems. Similarly, we recognize that although "the shelf" is a distinct geographical environment, there is little point in creating a "shelf" chapter and immediately splitting the chapter into two distinct parts — storm shelves and tidal shelves. The new siliciclastic shelf chapter (Chapter 12) therefore emphasizes waves and storms; tidal shelf deposits are in the new chapter (11) on tidal sandstones. Likewise, the new chapter on subtidal carbonates (Chapter 15) reflects the recent realization of the importance of the "carbonate factory" in carbonate platform dynamics.

DEPOSITIONAL SYSTEMS AND SYSTEMS TRACTS

Systems tracts are defined as linkages of contemporaneous depositional systems (Table 1). Contemporaneity might be established biostratigraphically, but commonly the systems tracts are identified and correlated on the basis of their bounding discontinuities. Most of the discontinuities are essentially geological time planes, and form as a result of fluctuations in relative sea level. This in turn allows the recognition of three main systems tracts — *highstand, lowstand,* and *transgressive*.

Systems tracts are normally too large to model in the same way as depositional systems. Nevertheless, the concept of systems tracts is extremely important, because it allows predictions from one depositional system to another. For example, in terrigenous clastics, the recognition of a lowstand shelf edge delta predicts the possibility of a contemporaneous deep sea submarine fan. Similarly, a highstand prograding storm-dominated shoreface suggests the possibility of aggrading storm-dominated shelf sediments. Thus facies models are concerned with prediction within specified depositional systems, and systems tracts allow prediction *from one contemporaneous depositional system to another.* Systems tracts now form an integral part of sequence stratigraphy, and are discussed in more detail below.

These comments on highstand, lowstand and transgressive systems tracts necessarily lead into a discussion of stratigraphic schemes based implicitly or explicitly on sea level fluctuation (Haq *et al.*, 1988). Such fluctuations influence 1) the boundaries of the depositional systems to be modelled, and 2) the ways in which depositional systems are preserved in the geological record. There are now two schemes that emphasize bounding discontinuities and unconformities. *Allostratigraphy* is essentially descriptive, and is a formal part of the North American Stratigraphic Code (NACSN, 1983). Although parts of the code need clarification, the scheme is "up and running". *Sequence stratigraphy* is the "study of genetically related facies within a framework of chronostratigraphically significant surfaces" (Van Wagoner *et al.*, 1990). It is theoretical and interpretive rather than descriptive, and the interpretations are couched in terms of global eustatic sea level fluctuations (but see the critique by Miall, 1986). Note that the phrase cited above contains words of debatable meaning, such as *genetically* and *significant*.

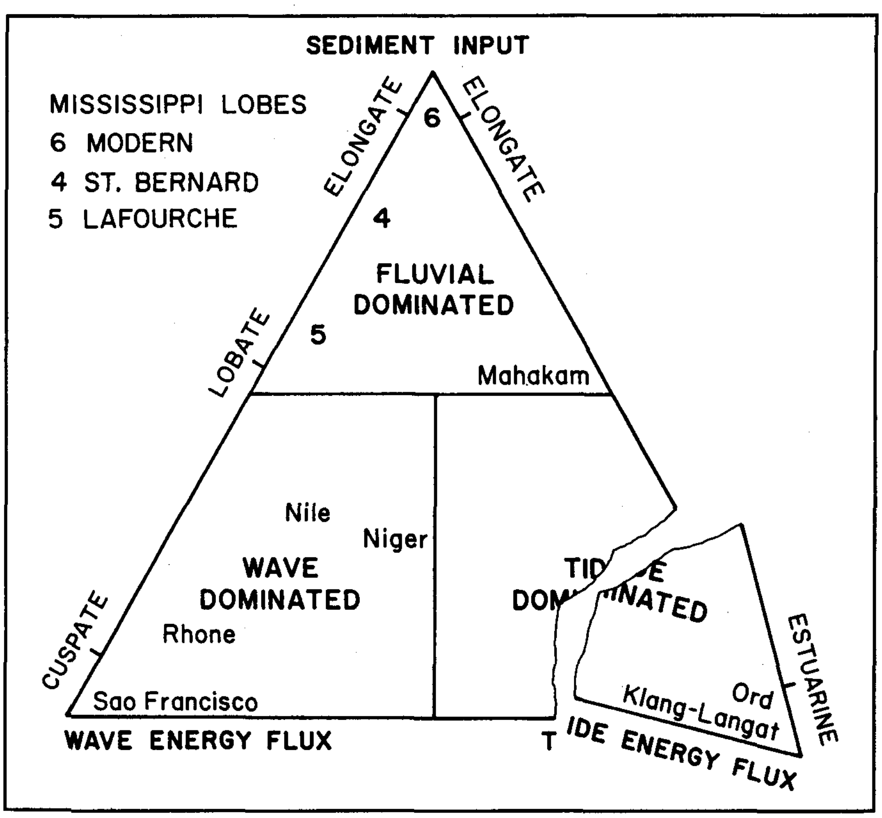

Figure 7 Classification of deltas in terms of river, wave and tide influence, simplified from Galloway (1975). The morphological descriptors (cuspate, lobate, etc.) of Galloway have not been included in subsequent versions of the triangle, and the emphasis that Galloway gave to "estuarine" appears to have been subsequently overlooked or downplayed. Galloway (1975, p. 93) noted that Tide Dominated Deltas tended to be "estuarine to irregular in geometry, and their framework facies were "estuary fill and tidal sand ridges". We also recognize major differences between tide dominated "deltas" and the other types, and suggest that this triangular classification be modified or abandoned.

ALLOSTRATIGRAPHY

Allostratigraphy is formally recognized by the North American Commission on Stratigraphic Nomenclature (NACSN, 1983, p. 865). The stratigraphic code states that "an allostratigraphic unit is a mappable stratiform body of sedimentary rock that is defined and identified on the basis of its *bounding discontinuities* [my emphasis]". I believe that this definition should be extended to read "...bounding discontinuities and *their correlative conformities*". Many different types of bounding discontinuities are discussed in the various chapters of this book. Between these bounding discontinuities, the allostratigraphic unit can be (and usually is) internally heterogeneous (Figs. 2, 5). The units vary in scale, in a manner similar to lithostratigraphic units, and the code recognizes allomembers, alloformations and allogroups.

Allostratigraphy is not intended to replace lithostratigraphy; it is a parallel scheme that emphasizes bounding discontinuities. This *in turn* emphasizes the processes external to the depositional system that initiate and terminate the depositional of a *sedimentologically related* succession of facies. There is no implication in allostratigraphy as to what those external processes might be. Examples of allostratigraphic subdivision and facies modelling within the discontinuity-bounded units are given in Chapters 9, 10, 11, 12, 15, 16 and 17. Although the ideas embodied in allostratigraphy have been widely used, it is surprising that the formal terminology has seldom been adopted.

Bounding discontinuities

Bounding discontinuities can be erosional or nonerosional (conformable). Erosional discontinuities include both angular unconformities (which could be used to define very large scale allostratigraphic units), and subtle erosion surfaces. The latter may have a total erosive relief of a few tens of metres, but extend over 25,000 km^2 or more. On the outcrop scale, the erosive relief may be undetectable, although the erosion surface may be marked by a coarse-grained lag or karst. Relief can be detected by careful correlation of well logs in the subsurface, and superb examples occur in the Cardium Formation of

Alberta, as discussed in detail in Chapter 12.

Nonerosional discontinuities commonly occur at the tops of most carbonate and sandier-upward terrigenous clastic facies successions (Fig. 5 shows a marine flooding surface). The implied discontinuity is in depositional conditions, and may be related to rates of subsidence, sediment production and supply, and eustatic rise of sea level, or some combination of these features. Even more subtle discontinuities may occur within fine-grained successions, and may be expressed as condensed horizons. Here, the rate of terrigenous clastic or carbonate sedimentation is at a minimum, and there tends to be a relative concentration of organic material (e.g., fish scales, forams and other fossils) and chemical deposits (e.g., phosphatic material and glauconite). In other cases, the depositional discontinuity may show up as a firmground or hardground, where there has been induration and some wave scouring, a change in the organisms that colonise the substrate (Chapter 4), but no concentration of organic or chemical deposits. It must be emphasized that subtle erosion surfaces, perhaps marked by gravel lags, can pass basinward into correlative conformities such as condensed horizons or firmgrounds.

Bounding discontinuities highlight important changes in depositional conditions. Thus they define allostratigraphic units in which depositional conditions were either fairly constant, or were progressively changing but without breaks (as in the sandier-upward succession of Figure 5). For this reason, allostratigraphic units are more natural subdivisions of the geological record for interpretive purposes than conventional lithostratigraphic units.

SEISMIC AND SEQUENCE STRATIGRAPHY

The concepts of seismic stratigraphy were introduced and promoted in the literature by geologists and geophysicists from the Exxon Production Research Company in Houston (Payton, 1977). Specifically, Vail and Mitchum (1977, p. 51) described seismic stratigraphy as "a geological approach to the stratigraphic interpretation of seismic data" (as discussed briefly in Chapter 3). Discontinuities in the stratigraphic record can be seen seismically as convergences or truncations of seismic reflectors (Chapter 3; similar convergences [downlap and onlap] are shown with arrowheads in Figure 2).

By incorporating lithological data and facies successions, seismic stratigraphy has given rise to the more geologically oriented concept of *sequence stratigraphy* (Table 1; Van Wagoner *et al.*, 1988, 1990). The basic unit in sequence stratigraphy is the *sequence*, which is "a stratigraphic unit composed of a relatively conformable succession of genetically related strata bounded at its top and base by unconformities and their correlative conformities" (Mitchum *et al.*, 1977). No scale was given in this definition, nor were the terms "relatively conformable" and "genetically related" explained or defined. By defining packages of strata bounded by unconformities, sequence stratigraphy emphasizes the external controls on sedimentation.

Unconformities

In the Exxon scheme, sequences are bounded by *unconformities* (Fig. 8), which are surfaces "separating younger from older strata, along which there is evidence of subaerial erosional truncation (and, in some areas, correlative submarine erosion), or subaerial exposure, with a significant hiatus indicated" (Posamentier *et al.*, 1988, p. 110). Readers will quickly notice that this is a very restrictive definition (as stated in the phrase "evidence of subaerial erosional truncation"), which gives far less flexibility than the bounding discontinuities of allostratigraphy. Moreover, during marine transgression of a subaerial surface, *evidence* of subaerial exposure in terrigenous clastic sediments is normally removed by wave erosion at the shoreline. The diagonal ruling indicates erosion between points A and B in Figure 8, forming a *ravinement surface* or *transgressive surface of erosion*. Posamentier (personal communication, 1990) now recognizes this fact, and agrees that in the field, "evidence" for subaerial exposure may be inferred rather than real.

During a relative fall of sea level, erosion surfaces are cut subaerially behind the shoreline. They also form subaqueously in front of the shoreline, where formerly deep areas of the shelf

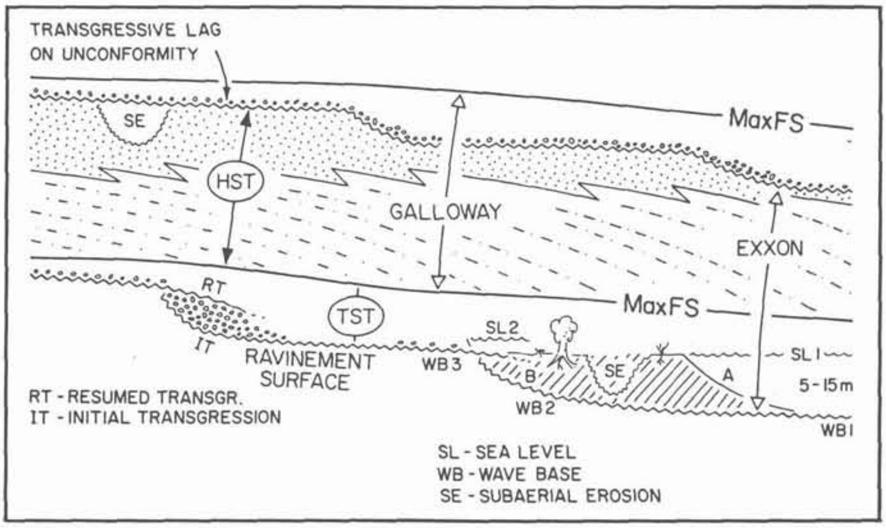

Figure 8 Definition of Exxon sequence boundaries (unconformities) compared with the Galloway genetic stratigraphic sequence boundaries (maximum flooding surfaces, MaxFS). The transgressive erosion surfaces are shown stepped, implying alternations of stillstand or very slow transgression, and more rapid transgression. During very slow transgression (SL1 to SL2), the shoreface erodes landward (A to B lower right), removing the diagonally ruled section between A and B. Note that all evidence of subaerial exposure (trees, roots, shallow incised channels) is removed. During rapid transgression, wave base rises from WB2 to WB3, and the top of the former beach is subsequently eroded (below letters SL2). This gives rise to the concept of separate erosion surfaces associated with Initial Transgression and Resumed Transgression. Only those channels incised more than 5-15 m (SE, top left) can be preserved beneath the ravinement surfaces; this depth approximates the depth from sea level to fairweather erosive wave base. No other vertical or horizontal scale is implied by the diagram.

come within the reach of wave scouring. The subaqueous surface is termed a regressive surface of erosion. In many cases, it will be destroyed by subaerial erosion as the relative lowering of sea level continues. However, when the lowering stops, the surface seaward of the lowstand shoreface can be preserved as a firm or hard ground. Alternatively, the lowstand shoreface may prograde onto the regressive surface of erosion (as described in Chapter 12).

Regressive and transgressive surfaces of erosion can be identified by their morphology, and by the facies that overlie and underlie them. They are important bounding discontinuities, and several examples are given in this book. They form because of relative movements of the land and sea, not exclusively by eustatic changes of sea level, as implied by Van Wagoner *et al.* (1990).

Because of the problems of defining and recognizing unconformities, and the implication that they are eustatically controlled, we suggest that the "generic" *bounding discontinuities* of allostratigraphy offer more flexibility in defining sedimentologically interpretable parts of the stratigraphic record.

Parasequences and marine flooding surfaces

A parasequence is "a relatively conformable succession of genetically related beds or bedsets bounded by marine flooding surfaces or their correlative surfaces...[a marine flooding surface is a surface] separating younger from older strata across which there is evidence of an abrupt increase in water depth" (Fig. 5; Van Wagoner *et al.*, 1990, p. 8). Parasequences and facies successions (as defined earlier in this chapter) are essentially the same thing, except that the concept of facies successions is broader. For example, a fluvial point-bar deposit (Chapter 7) commonly consists of a fining-upward facies succession, but this is not a parasequence because it is not defined by a *marine flooding* surface; it is defined by erosion surfaces with channel lag deposits. In sequence stratigraphic theory, parasequences can be arranged in sets, and have distinctive stacking patterns. However, Posamentier and Vail (1988) and Posamentier *et al.* (1988) give no real examples, and Van Wagoner *et al.* (1990) give a few examples of some stacking patterns, and no examples of others. In this book, we will use the term facies succession rather than parasequence, and will examine vertical and lateral "stacking patterns" only where the data permit (particularly Chapters 9, 12 and 16).

Maximum flooding surfaces

In Exxon theory, unconformities are of regional or inter-regional extent, and develop subaerially during falling relative sea level, and at lowstand. During the opposite part of the sea level cycle, during rising stage (up to the point of maximum transgression), there is marine flooding of the older subaerial surface. Terrigenous clastic deposition is commonly very slow during rising stage because most of the coarser sediment is confined to the alluvial floodplain and to various environments at or very close to the shoreline. After sea level stabilization, sediment may again begin to build out into the sea, generating marker horizons that downlap onto the older surface of very slow deposition (Figs. 2, 8). This older surface, of regional or inter-regional extent, is a *maximum flooding surface* (MaxFS; Fig. 8), and it separates rocks below deposited during transgressive conditions from those above deposited during the next overall regression. There is no doubt that the MaxFS is a key stratigraphic surface. Both marine and maximum flooding surfaces represent deepening but MaxFSs normally have a much greater lateral extent. In many cases, the two could not be distinguished in a single outcrop, and it is the regional mappability that distinguishes the MaxFS. The surface is commonly a condensed horizon, with an unusually thin sedimentary record representing a relatively long period of time. Fossils may be concentrated at the surface, along with other evidence of very slow sedimentation, such as phosphatic or glauconitic material.

Sequence boundaries

There is some controversy regarding the placing of boundaries between genetically related successions of facies. The Exxon group has chosen *unconformities* to define *sequences* (Fig. 8), using the justification (Posamentier, personal communication, 1990) that between unconformities, there is essentially continuous deposition, and that the major break is represented by the unconformity. However, Galloway (1989) prefers to define a *genetic stratigraphic sequence* (GSS) based on the maximum flooding surfaces (Fig. 8). The logic is that, in terrigenous clastic successions "because shelf deposits are derived from reworked transgressed or contemporary retrogradational deposits, their distribution commonly reflects the paleogeography of the precursor depositional episode. *These deposits are best included in and mapped as a facies element of the underlying genetic stratigraphic sequence* (my emphasis)" (Galloway, 1989, p. 132). I cannot agree with Galloway that the transgressive systems tract (Figs. 2, 8) is necessarily derived *from the* systems tract underlying the unconformity (Walker, 1990; *see* Chapter 12), and therefore emphasize the following point. Exxon *sequences* and Galloway *genetic stratigraphic sequences* are only genetic in the sense that they develop during one complete cycle of relative sea level fluctuation. They are *not sedimentologically genetic*, because most if not all of the sedimentological parameters change when an unconformity or a MaxFS is crossed. These parameters include depth of water, waves, tides, basin geometry, salinity, rates of sediment supply, and grain size. The only *sedimentologically related* packages lie 1) between unconformity and MaxFS, 2) between the MaxFS and the next unconformity, or 3) between a subaerial erosion surface (SE in Fig. 8; base of an incised valley) and the overlying unconformity (transgressive *surface of erosion*). These sedimentologically related packages are the systems tracts (Figs. 2, 8).

Systems tracts

Earlier in the paper, systems tracts were defined as linkages of contemporaneous depositional systems. We can now recognize that systems tracts are also defined by unconformities and MaxFSs (Figs. 2, 8), giving three different types; *transgressive, highstand and lowstand*. Transgressive systems tracts are floored by unconformities or bounding discontinuities, and are terminated by MaxFSs (Figs. 2, 8). Highstand systems tracts are floored by MaxFSs and terminated by unconformities or bounding discontinuities (Figs. 2, 8). Lowstand systems tracts commonly form in deep water beyond the shelf edge, commonly as submarine fans (Chapter 13). The base of the lowstand systems tract may be erosional (canyons and channels cut by turbidity currents), and the top is correlative with a MaxFS. Lowstand systems tracts may also include shelf edge deposits, formed at times when lowstand moves the shoreline almost, but not quite to the shelf break (Fig. 25 in Chapter 12). At this time, river valleys become incised, and may fill with lowstand systems tract deposits (fluvial). Alternatively, the valleys remain essentially empty until the next transgression, when they backfill with estuarine deposits of the transgressive systems tract (Chapters 10, 11). The systems tracts in carbonate and evaporite systems are generally quite different (Chapter 14) but the same basic principles apply.

Systems tracts and the eustatic sea level curve

One example will suffice to show that systems tracts are related to the global eustatic sea level curve *only* in a theoretical sense. Real information is either lacking, or has been overlooked in the construction of systems tracts models. In the most recent work, Haq (1991, p. 7) notes that "it is instructive to follow the evolution of a complete cycle of sea level change, starting with a sea level fall from a relative highstand position, followed by a rise and a subsequent fall". The proposed stratigraphic results are shown in Figure 9. Note that sequence boundary 1 (SB1) formed during falling stage, and stimulated deposition of the basin floor fan which is overlain by the leveed channel complex (LCC). The lowstand wedge (LSW) also formed at this time. Subsequent sea level rise cut off sediment supply to the lowstand wedge, [redacted]ve rise to the transgressive [redacted]tract (TST) of shallow-marine [redacted] (Chapter 12). At highstand, [redacted] in Figure 9, there is for- [redacted] "initially aggradational and [redacted]ingly progradational [redacted] (Haq, 1991, p. 12), [redacted] clearly shown to build out over the entire leveed channel complex and lowstand wedge. However, this certainly does not happen during one cycle of sea level fluctuation in most or all modern fans. The Plio-Pleistocene Mississippi Fan has been subjected to over 50 cycles of glacio-eustatic sea level fluctuation (Chapters 2, 13), but the highstand parasequences have not prograded over the fan. Instead, the fan has been buried by a thin layer of hemipelagic deposits that separate the seventeen seismic sequences (Chapter 13). Hemipelagic layers, slumps and debris flows also separate distinct channel-levee complexes in the Rhone and Amazon Fans (Chapter 13), with no indication of complete fan burial by prograding highstand systems tract deposits, as shown in the model reproduced in Figure 9.

Although there are many useful concepts in sequence stratigraphy, models such as that in Figure 9 must be regarded as preliminary, and in need of an infusion of real data from modern examples. Until some of the problems have been worked out, and until the emphasis on control by global eustatic sea level change has been modified, it is safer to subdivide the geological record by bounding discontinuities of all types (allostratigraphy).

The philosophy in this book is that it safer to try to *construct* models from observed facies relationships, and from observed relationships between the larger scale stratigraphic units (depositional systems and systems tracts), than to *propose* hypothetical models that lack a published data base (Fig. 9), and that do not appear to conform to observed situations in recent sediments.

Sequence stratigraphy and sea level change

Seismic and sequence stratigraphy are techniques for subdividing the geological record into related packages of rocks based on their bounding discontinuities and unconformities. This aspect has been emphasized in this chapter. However, both techniques offer powerful ways of interpreting the geological record in terms of sea level changes (Haq *et al.*, 1988). This aspect of seismic and sequence stratigraphy is discussed in Chapter 2.

CONCLUSIONS AND RECOMMENDATIONS

Geographic environments shift rapidly and change their form during relative sea level fluctuations, regardless of how the fluctuations are controlled. Modelling the environments and their depositional systems must take into account, and emphasize, these fluctuations. Contemporaneous linkages of depositional systems can be treated as

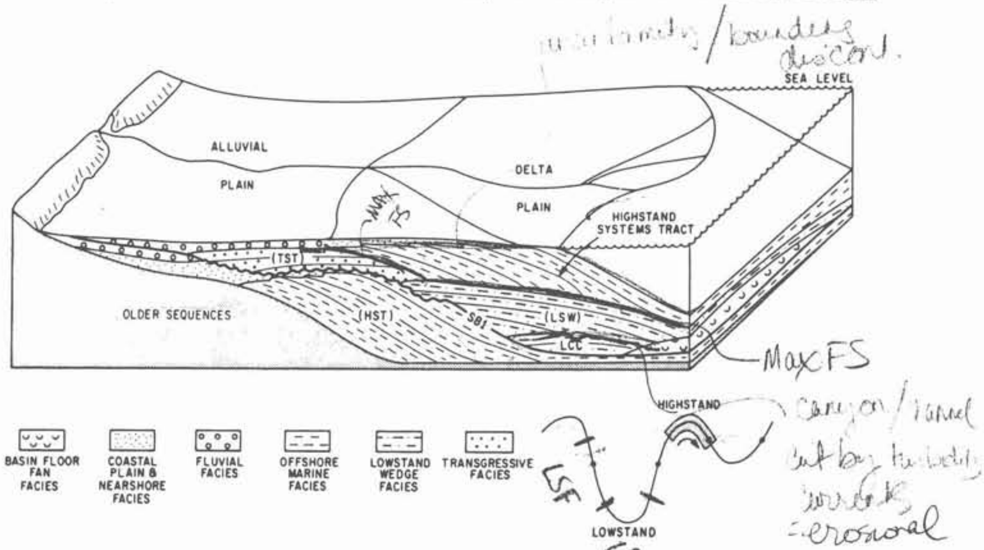

Figure 9 Hypothetical systems tract development during a highstand, and beginning falling stage of sea level. Note that the offshore marine facies of the highstand systems tract are shown to have to have buried the basin floor fan facies, lowstand wedge (LSW) and leveed channel complex (LCC). This is incompatible with information given in Chapter 13 on submarine fan response to sea level change. From Haq (1991). HST, highstand systems tract; TST, transgressive systems tract; SB1, sequence boundary 1.

systems tracts, and systems tracts are defined by unconformities and maximum flooding surfaces (or, in broader terms, bounding discontinuities). Sedimentologically related rocks are packaged between these bounding discontinuities, which are therefore crucial in the establishment of facies models and the understanding of related depositional systems.

The facies models that characterize depositional systems must now take into account the external controls on the systems — particularly relative sea level changes and tectonics. This is best done in the flexible context of allostratigraphy, instead of the rather theoretical and more interpretive framework of sequence stratigraphy.

ACKNOWLEDGEMENTS

The overall format of this chapter, and many of the ideas and emphases, took shape during a meeting in October, 1990, and I particularly thank Mario Coniglio, Bob Dalrymple, Noel James and Andrew Miall for their help. My ideas have also been sharpened by the comments of Janok Bhattacharya, Doug Cant, Nick Eyles, Bill Galloway, Dale Leckie, Gerry Middleton, Guy Plint and Henry Posamentier. I have tried to combine these ideas into a general introduction to this edition and a philosophy that all of the authors can live with, but I am responsible for the final form of the chapter, and hope that I have not misrepresented anyone. The concepts have evolved during research supported by the Natural Sciences and Engineering Research Council of Canada.

REFERENCES

Basic sources of information

Galloway, W.E., 1989, Genetic stratigraphic sequences in basin analysis I: architecture and genesis of flooding-surface bounded depositional units: American Association of Petroleum Geologists, Bulletin, v. 73, p. 125-142.
Gives reasons for preferring stratigraphic units defined by flooding surfaces rather than by unconformities.

Middleton, G.V., 1973, Johannes Walther's Law of the Correlation of Facies: Geological Society of America, Bulletin, v. 84, p. 979-988.
An excellent discussion of the use, misuse and application of Walther's Law.

Middleton, G.V., 1978, Facies, *in* Fairbridge, R.W. and Bourgeois, J., eds., Encyclopedia of sedimentology: Stroudsburg, Pennsylvania, Dowden, Hutchinson and Ross, p. 323-325.
One of the best and most concise statements of the facies concept, discussing various ways in which the term has been used.

Reading, H.G., ed., 1986, Sedimentary environments and facies (2nd. edition): Oxford, Blackwell Scientific Publications, 615 p.
The second edition of this book remains an indispensable reference on depositional environments and facies models.

Van Wagoner, J.C., Posamentier, H.W., Mitchum, R.M., Jr., Vail, P.R., Sarg, J.F., Loutit, T.S. and Hardenbol, J., 1988, An overview of the fundamentals of sequence stratigraphy and key definitions, *in* Wilgus, C.K. *et al.*, eds., Sea-level changes: an integrated approach: Society of Economic Paleontologists and Mineralogists, Special Publication 42, p. 39-45.
A paper which lives up to its title.

Van Wagoner, J.C., Mitchum, R.M., Campion, K.M. and Rahmanian, V.D., 1990, Siliciclastic sequence stratigraphy in well logs, cores, and outcrops: American Association of Petroleum Geologists, Methods in Exploration Series, No. 7, 55 p.
Complete summary, with limited examples, of the "Exxon school of sequence stratigraphy".

Walker, R.G., 1990, Perspectives: facies modelling and sequence stratigraphy: Journal of Sedimentary Petrology, v. 60, p. 777-786.
Some critiques of sequence stratigraphy, along the lines of this chapter.

Wilgus, C.K., Hastings, B.S., Posamentier, H.W., Ross, C.A. and Kendall, C.G.St.C., eds., 1988, Sea level changes: an integrated approach: Society of Economic Paleontologists and Mineralogists, Special publication 42, 407 p.
Collection of papers emphasizing conceptual basis of sequence statigraphy plus numerous case studies of sea level change from the geological record.

Other references

Allen, J.R.L., 1983, Studies in fluviatile sedimentation: bar complexes and sandstone sheets (low sinuosity braided streams) in the Brownstones (L. Devonian), Welsh Borders: Sedimentary Geology, v. 33, p. 237-293.

Anderton, R., 1985, Clastic facies models and facies analysis, *in* Brenchley, P.J. and Williams, B.J.P., eds., Sedimentology: recent developments and applied aspects: Oxford, Blackwell Scientific Publications, p. 31-47.

Bergman, K.M. and Walker, R.G., 1988, Formation of Cardium erosion surface E5, and associated deposition of conglomerate: Carrot Creek field, Cretaceous Western Interior Seaway, Alberta, *in* James, D.P. and Leckie, D.A., eds., Sequences, stratigraphy, sedimentology; surface and subsurface: Canadian Society of Petroleum Geologists, Memoir 15, p. 15-24.

Bouma, A.H., 1962, Sedimentology of some flysch deposits: Amsterdam, Elsevier, 168 p.

Cant, D.J. and Walker, R.G., 1976, Development of a braided fluvial facies model for the Devonian Battery Point Sandstone, Quebec: Canadian Journal of Earth Sciences, v. 13, p. 102-119.

Collinson, J.D., 1969, The sedimentology of the Grindslow Shales and the Kinderscout Grit: a deltaic complex in the Namurian of northern England: Journal of Sedimentary Petrology, v. 39, p. 194-221.

de Raaf, J.F.M., Reading, H.G. and Walker, R.G., 1965, Cyclic sedimentation in the Lower Westphalian of North Devon, England: Sedimentology, v. 4, p. 1-52.
This paper gives the first example of a facies relationship diagram and uses the diagram to establish cyclicity in a series of prograding deltaic deposits. It also shows how facies can be subdivided on a small scale.

Galloway, W.E., 1975, Process framework for describing the morphologic and stratigraphic evolution of deltaic depositional systems, *in* Broussard, M.L., ed., Deltas; models for exploration: Houston Geological Society, p. 87-98.

Haq, B.U., 1991, Sequence stratigraphy, sea level change, and significance for the deep sea, *in* Macdonald, D.I.M., ed., Sedimentation, tectonics and eustasy; sea-level changes at active margins: International Association of Sedimentologists, Special Publication 12, p. 3-39.

Haq, B.U., Hardenbol, J. and Vail, P.R., 1988, Mesozoic and Cenozoic chronostratigraphy and cycles of sea level change, *in* Wilgus, C.K., *et al.*, eds., Sea-level changes: an integrated approach: Society of Economic Paleontologists and Mineralogists, Special Publication 42, p. 71-108.
The most recent discussion of coastal onlap cycles, with big charts of their relative and absolute ages.

Harbaugh, J.W. and Demirmen, F., 1964, Application of factor analysis to petrologic variations of Americus Limestone (Lower Permian), Kansas and Oklahoma. Kansas Geological Survey, Special Distribution Publication 15, 40 p.

Harbaugh, J.W. and Merriam, D.F., 1968, Computer applications in stratigraphic analysis: New York, Wiley, 282 p.

Harper, C.W., Jr., 1984, Improved methods of facies sequence analysis, *in* Walker, R.G., ed., Facies models, 2nd. edition: Geological Association of Canada, Geoscience Canada Reprint Series 1, p. 11-13.

Imbrie, J. and Purdy, E.G., 1962, Classification of modern Bahamian carbonate sediments, *in* Ham, W.E., ed., Classification of carbonate rocks: American Association of Petroleum Geologists, Memoir 1, p. 253-279.

Klovan, J.E., 1964, Facies analysis of the Redwater Reef complex, Alberta, Canada: Bulletin of Canadian Petroleum Geology, v. 12, p. 1-100.

Miall, A.D., 1977, A review of the braided river depositional environment: Earth-Science Reviews, v. 13, p. 1-62.

Miall, A.D., 1985, Architectural element analysis: a new method of facies analysis applied to fluvial deposits: Earth-Science Reviews, v. 22, p. 261-308.

Miall, A.D., 1986, Eustatic sea level changes interpreted from seismic stratigraphy: a critique of the methodology with particular reference to the North Sea Jurassic record: American Association of Petroleum Geologists, Bulletin, v. 70, p. 131-137.

Mitchum, R.M., Jr., Vail, P.R. and Thompson, S., III, 1977, Seismic stratigraphy and global changes of sea level, Part 2: The depositional sequence as a basic unit for stratigraphic analysis, *in* Payton, C.E., ed., Seismic stratigraphy — applications to hydrocarbon exploration: American Association of Petroleum Geologists, Memoir 26, p. 53-62.
Clear and concise discussion of the meaning of depositional sequences, with methods for constructing coastal onlap charts.

Moore, R.C., 1949, Meaning of facies, *in* Longwell, C.R., ed., Sedimentary facies in geological history: Geological Society of America, Memoir 39, p. 1-34.

Mutti, E. and Ricci Lucchi, F., 1972, Le torbiditi dell'Appennino settentrionale: introduzione all'analisi di facies: Memorie della Societa Geologica Italiana, v. 11, p. 161-199. English translation by T.H. Nilsen, 1978, International Geology Review, v. 20, p. 125-166.

North American Commission on Stratigraphic Nomenclature [NACSN], 1983, North American Stratigraphic Code: American Association of Petroleum Geologists, Bulletin, v. 67, p. 841-875.
This is the latest version of the stratigraphic code, where allostratigraphy is spelled out for the first time.

Payton, C.E., ed., 1977, Seismic stratigraphy — applications to hydrocarbon exploration: American Association of Petroleum Geologists, Memoir 26, 516 p.

Posamentier, H.W. and Vail, P.R., 1988, Eustatic controls on clastic deposition II — sequence and systems tract models, *in* Wilgus, C.K., *et al.*, eds., Sea-level changes: an integrated approach: Society of Economic Paleontologists and Mineralogists, Special Publication 42, p. 125-154.
A complex paper that discusses the origin and development of type 1 and type 2 unconformities, and the various systems tracts. All theory, no examples. Do not read this paper unless you are thoroughly familiar with the concepts of sequence stratigraphy (read Van Wagoner et al., 1988, and Posamentier et al., *1988, first).*

Posamentier, H.W., Jervey, M.T. and Vail, P.R., 1988, Eustatic controls on clastic deposition I — conceptual framework, *in* Wilgus, C.K., *et al.*, eds., Sea-level changes: an integrated approach: Society of Economic Paleontologists and Mineralogists, Special Publication 42, p. 109-124.
A complex discussion of eustatic fluctuations, basinal accommodation, and resulting stratal patterns. All theory, no examples.

Sarg, J.F., 1988, Carbonate sequence stratigraphy, *in* Wilgus, C.K., *et al.*, eds., Sea-level changes: an integrated approach: Society of Economic Paleontologists and Mineralogists, Special Publication 42, p. 155-182.

Scholle, P.A., Bebout, D.G. and Moore, C.H., 1983, Carbonate depositional environments. American Association of Petroleum Geologists, Memoir 33, 708 p.

Vail, P.R. and Mitchum, R.M., Jr., 1977, Seismic stratigraphy and global changes of sea level, Part 1: Overview, *in* Payton, C.E., ed., Seismic stratigraphy — applications to hydrocarbon exploration: American Association of Petroleum Geologists, Memoir 26, p. 51-52.

Walker, R.G., 1983, Cardium Formation 3. Sedimentology and Stratigraphy in the Garrington-Caroline area: Bulletin of Canadian Petroleum Geology, v. 31, p. 213-230.
A good illustration of the detailed subdivision of facies using amount and type of bioturbation, presence or absence of silty laminations, grain size, sedimentary structures, nature of bedding contacts and textures of conglomerates.

Walker, R.G., 1984, General introduction: facies, facies sequences and facies models, *in* Walker, R.G., ed., Facies models, 2nd. edition: Geological Association of Canada, Geoscience Canada Reprint Series 1, p. 1-9.

Walker, R.G., 1990, Perspective — facies modelling and sequence stratigraphy: Journal of Sedimentary Petrology, v. 60, p. 777-786.
A critique of some of the concepts of sequence stratigraphy and genetic stratigraphic sequences.

Williams, P.F. and Rust, B.R., 1969, The sedimentology of a braided river: Journal of Sedimentary Petrology, v. 39, p. 646-679.

Wilson, J.E., 1975, Carbonate facies in geologic history: New York, Springer-Verlag, 471 p.

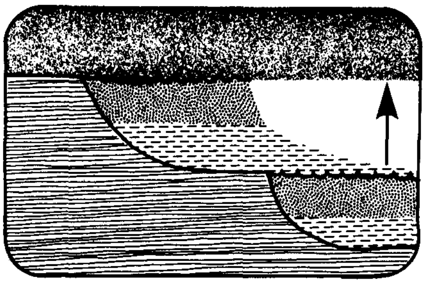

2. Control of Sea Level Change

A. Guy Plint, Department of Geology, University of Western Ontario, London, Ontario N6A 5B7

Nicholas Eyles, Department of Geology, University of Toronto, Scarborough Campus, 1265 Military Trail, Scarborough, Ontario M1C 1A4

Carolyn H. Eyles, Department of Geography, McMaster University, Hamilton, Ontario L8S 4K1

Roger G. Walker, Department of Geology, McMaster University, Hamilton, Ontario L8S 4M1

INTRODUCTION

One theme that runs throughout this book is the recognition of unconformities and bounding discontinuities caused by changes in sea level. At least some of the unconformities and inferred sea level changes *might* be useful for global correlation; this possibility is presently the focus of much research.

Stratigraphic discontinuities allow subdivision of the geological record into purely descriptive allostratigraphic units, and also into the more interpretive *sequences* and *parasequences* of sequence stratigraphy (Chapter 1). It is widely accepted that the most significant stratigraphic discontinuities are 1) *regressive surfaces of erosion*, 2) *transgressive surfaces of erosion*, and 3) *maximum flooding surfaces*. Relative sea level changes affect many marine and coastal depositional environments, their influence being most obvious in shoreline and shallow-marine areas.

EUSTASY, RELATIVE SEA LEVEL AND WATER DEPTH

Changes in water depth in a particular area depend on both global and local controls (Fig. 1, Table 1). The *global* (or *eustatic*) aspect depends on the *motion of the sea surface relative to the centre of the Earth*, which in turn is controlled by two factors. The first concerns changes in the *volume of water* in the ocean; these are largely controlled by the volume of terrestrial ice (*glacio-eustatic* change), and to a lesser extent by the volume of water trapped in terrestrial aquifers. The second concerns changes in the *volume of the ocean basins*; these are largely due to increases or decreases in the volume of oceanic spreading ridges (*tectono-eustatic* change).

Local controls of water depth involve tectonics and sedimentation. *Tectonic movements* of the basin floor (up or down) can amplify, nullify or reverse the effects of eustatic changes. *Sedimentation* results in aggradation of the sea-floor and a reduction in water depth.

vertical upward

Relative changes of sea level in a given area therefore depend on the interplay of eustasy, local tectonics and rates of sedimentation. As an example, we may postulate a basin that is actively subsiding for tectonic reasons. Simultaneously, eustatic sea level is

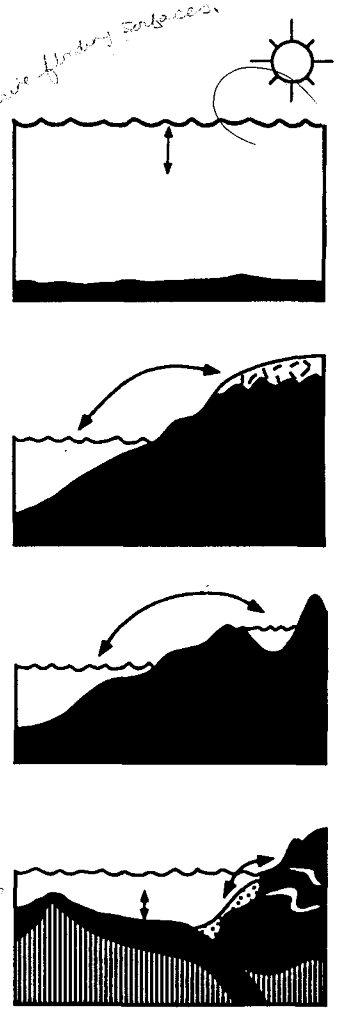

MECHANISM	Time Scale (years)	Order of Magnitude (m)
1) Ocean Steric (thermohaline) Volume Changes		
Shallow (0-500 m)	0.1-100	0.01-1
Deep (500-4000 m)	10-10,000	0.01-10
2) Glacial Accretion and Wastage		
Mountain Glaciers	10-100	0.1-1
Greenland Ice Sheet	100-100,000	0.1-10
East Antarctic Ice Sheet	1,000-100,000	10-100
West Antarctic Ice Sheet	100-10,000	1-10
3) Liquid Water on Land		
Groundwater Aquifers	100-100,000	0.1-10
Lakes and Reservoirs	100-100,000	0.01-0.1
4) Crustal Deformation		
Lithosphere Formation and Subduction	$100,000\text{-}10^8$	1-100
Glacial Isostatic Rebound	100-10,000	0.1-10
Continental Collision	$100,000\text{-}10^8$	10-100
Sea Floor and Continental Epirogeny	$100,000\text{-}10^8$	10-100
Sedimentation	$10,000\text{-}10^8$	1-100

Figure 1 Four mechanisms that can cause sea level changes, showing the time scales over which they operate, and the order of magnitude of the changes. Based on Revelle (1990).

rising. In some areas of the basin, subsidence and eustasy will combine to produce a relative sea level *rise*. However, locally (perhaps in the vicinity of an active delta) the rate of sedimentation may exceed the combined rates of subsidence and eustatic rise, resulting in a relative sea level *fall*.

It is unfortunate that a change in water depth is the only parameter that we can infer from facies analysis, because in order to isolate the effects of one of the independant variables (eustasy, tectonics, sedimentation), we are forced to make *assumptions* about the magnitude and rate of the other two variables (Burton *et al.*, 1987).

The mechanisms, time scales and rates of sea level change (Fig. 1) are currently the subject of vigorous research and debate, particularly with respect to possible anthropogenic climatic changes (e.g., global warming). Current knowledge of the subject is summarized in a number of good reviews, including Devoy (1987a), Nummedal *et al.* (1987), Wilgus *et al.* (1988), Lambeck (1990) and Revelle (1990).

REVOLUTION IN STRATIGRAPHIC ANALYSIS

The current high level of interest in the mechanisms and effects of sea level change has been stimulated, to a large extent, by the publication of various versions of the Exxon sea level curve (Fig. 2; Haq *et al.*, 1988). There is presently considerable debate about the extent to which the curve portrays truly global (eustatic), or more local (relative) changes of sea level (Miall, 1986, 1991). Because this diagram has been the focus of so much attention, it is pertinent here to consider briefly its background, derivation and limitations.

Unconformities generated by major sea level changes have long been recognized and used to subdivide the stratigraphic record. For example, Sloss (1963) defined six continent-wide, unconformity-bounded stratigraphic sequences in the Phanerozoic rocks of North America (Fig. 3). These sequences were subsequently correlated with those of the Russian Platform (Sloss, 1972). The ideas of Sloss provided a basis for the work of Vail and his coworkers at Exxon Production Research who developed the technique termed *seismic stratigraphy* (Vail *et al.*, 1977b). They recognized unconformity-bounded units in seismic cross sections (Chapter 3), and developed inter-regional correlation techniques. On the basis of 1) the recognition, correlation and dating of unconformities, 2) the patterns of onlap, downlap and toplap (Fig. 13 in Chapter 3), and 3) biostratigraphic data from outcrop and boreholes, the Exxon group was able to generate a curve of coastal onlap for the Phanerozoic (Fig. 4). Eustatic changes were inferred from this curve. Good reviews of the methodology underlying seismic stratigraphy are provided by Cross and Lessenger (1988) and Christie-Blick *et al.* (1990).

Sequence stratigraphy, which is an outgrowth of seismic stratigraphy, is a more multidisciplinary approach to stratigraphic analysis. It is based on well-log, core and outcrop data in addition to seismic profiles. The conceptual background to sequence stratigraphy, plus a new and more detailed sea level chart was presented in a series of key papers in SEPM Memoir 42 (Wilgus *et al.*, 1988), and by Van Wagoner *et al.* (1990) and Haq (1991). This work has stimulated an extraordinary amount of research and debate. The application of seismic- and sequence-stratigraphic ideas has revitalized stratigraphic analysis; sedimentary environments and facies are now being discussed as components of *depositional systems* and *systems tracts* which in turn form the building blocks of parasequences and sequences (Chapter 1).

Derivation of the Exxon sea level curve

A portion of the *Exxon sea level curve* (Haq *et al.*, 1988) is reproduced in Figure 2. This chart shows both relative changes in coastal onlap and an

Table 1 *Mechanisms of sea level change. From Revelle (1990).*

MECHANISMS	Time Scale (years)	Order of Magnitude
1) ***Ocean Steric (thermohaline) Volume Changes***		
Shallow (0-500 m)	0.1 – 100	0 – 1 m
Deep (500-4000 m)	10 – 10,000	0.01 – 10 m
2) ***Glacial Accretion and Wastage***		
Mountain Glaciers	10 – 100	0.1 – 1 m
Greenland Ice Sheet	100 – 100,000	0.1 – 10 m
East Antarctic Ice Sheet	1,000 – 100,000	10 – 100 m
West Antarctic Ice Sheet	100 – 10,000	1 – 10 m
3) ***Liquid Water on Land***		
Groundwater Aquifers	100 – 100,000	0.1 – 10 m
Lakes and Reservoirs	100 – 100,000	0.01 – 0.1 m
4) ***Crustal Deformation***		
Lithosphere Formation and Subduction	100,000 – 10^8	1 – 100 m
Glacial Isostatic Rebound	100 – 10,000	0.1 – 10 m
Continental Collision	100,000 – 10^8	10 – 100 m
Seafloor and Continental Epirogeny	100,000 – 10^8	10 – 100 m
Sedimentation	10,000 – 10^8	1 – 100 m

inferred eustatic curve. The relative changes in coastal onlap are derived from analysis of seismic sections (Vail *et al.*, 1977a). In Figure 4, a number of imaginary, paleontologically dated reflectors (80 to 72 Ma) onlap and downlap against an unconformity. Arrows A, B and C show how the vertical component of coastal onlap is measured (interplay of eustatic rise and subsidence). A second unconformity indicates a relative sea level fall, and the position of coastal onlap is shifted seaward and downward (broken arrow D). A second episode of coastal onlap begins at this point (arrow E). The cycle chart (Fig. 2) is compiled from measurement of successive onlap-offlap events, plotted in absolute time. Figure 4 shows how the onlap/offlap cycles are compiled. For example, arrow B on the cross section implies a certain amount of coastal onlap (measured by the two-way travel time of seismic signals, converted to metres and measured vertically) during a certain amount of geologic time (80 to 78 Ma). In the lower part of Figure 4, arrow D is represented by a vertical component (time) and a horizontal component (relative coastal onlap). It is emphasized that the chart shows shifts in coastal onlap, which are due to a *combination* of eustatic sea level change, tectonics, and sediment supply.

Limitations of the seismic stratigraphic approach

Because the concepts and methods underlying the Exxon sea level curve

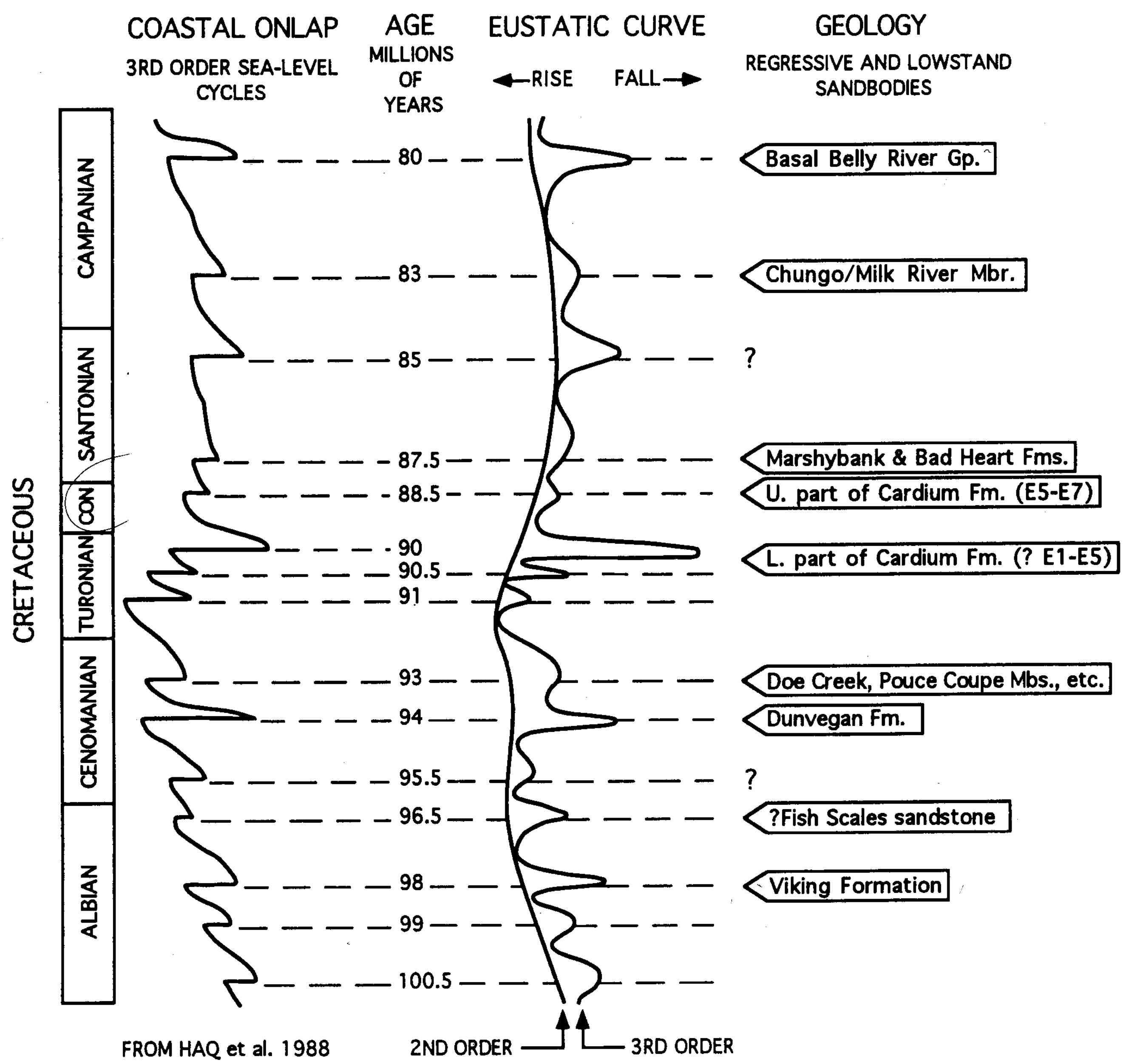

Figure 2 Third-order cycles of coastal onlap for part of the Cretaceous. The long-term (second-order) and short term (third-order) eustatic curves have been derived from the coastal onlap curve (see text). Some of the stratigraphic units in Alberta, discussed elsewhere in this book, are located on the right. Note that there are at least two eustatic falls which do not appear to have given rise to sand bodies in the Alberta Basin.

seem to offer hope for global correlation (Chapter 1), the methods and ideas have been scrutinized and criticized by researchers in both industry and academia (e.g., Parkinson and Summerhayes, 1985; Miall, 1986, 1991; Burton *et al.*, 1987; Walker, 1990). A recent and comprehensive critique of seismic stratigraphy and its role in deciphering the geological record of sea level change has recently been given by Christie-Blick *et al.* (1990). They emphasize three main limitations to the methods of Vail *et al.* (1977b): 1) the uncritical interpretation of all second- and third-order sequence boundaries (Fig. 2) as being of eustatic origin, 2) the uncertainties about absolute ages and correlations, and 3) the extreme difficulty of inferring the amplitude of sea level change. Christie-Blick *et al.* (1990) acknowledge that many second-order sequence boundaries appear to be globally synchronous and therefore probably represent eustatic events. The boundaries of third-order cycles, however, are commonly spaced too closely to permit unequivocal biostratigraphic dating. It is therefore very difficult to demonstrate that the relative sea level changes inferred in different areas were synchronous (and therefore eustatic).

Despite these limitations, the new emphasis on the subdivision of the stratigraphic record by unconformities and bounding discontinuities, and the relationship of these surfaces to relative sea level fluctuations, remains extremely important.

FIVE ORDERS OF CYCLES

Five orders of cyclic sea level change have been defined, with periodicities ranging from hundreds of millions to tens of thousands of years. The definition of the cycles is somewhat subjective (Vail *et al.*, 1977b; Miall, 1990). First-, second- and third-order cycles (Figs. 2, 3) lack a regular periodicity. However, fourth- and fifth-order cycles, with durations of much less than one million years, do appear to reflect a regular cyclic control.

First-order cycles

Two *first-order* cycles lasting 200-400 m.y. are recognized in the Phanerozoic (Fig. 3), and are widely interpreted to be related to the accretion and subsequent splitting apart of supercontinents (Vail *et al.*, 1977b; Worsley *et al.*, 1984). When continents are joined together (as in the Permian Pangea), the volume of spreading ocean ridges is minimized and ocean basin volume is maximized (due to thermal subsidence). This results in a global lowering of eustatic sea level. These conditions are reversed at times of supercontinent breakup, when new

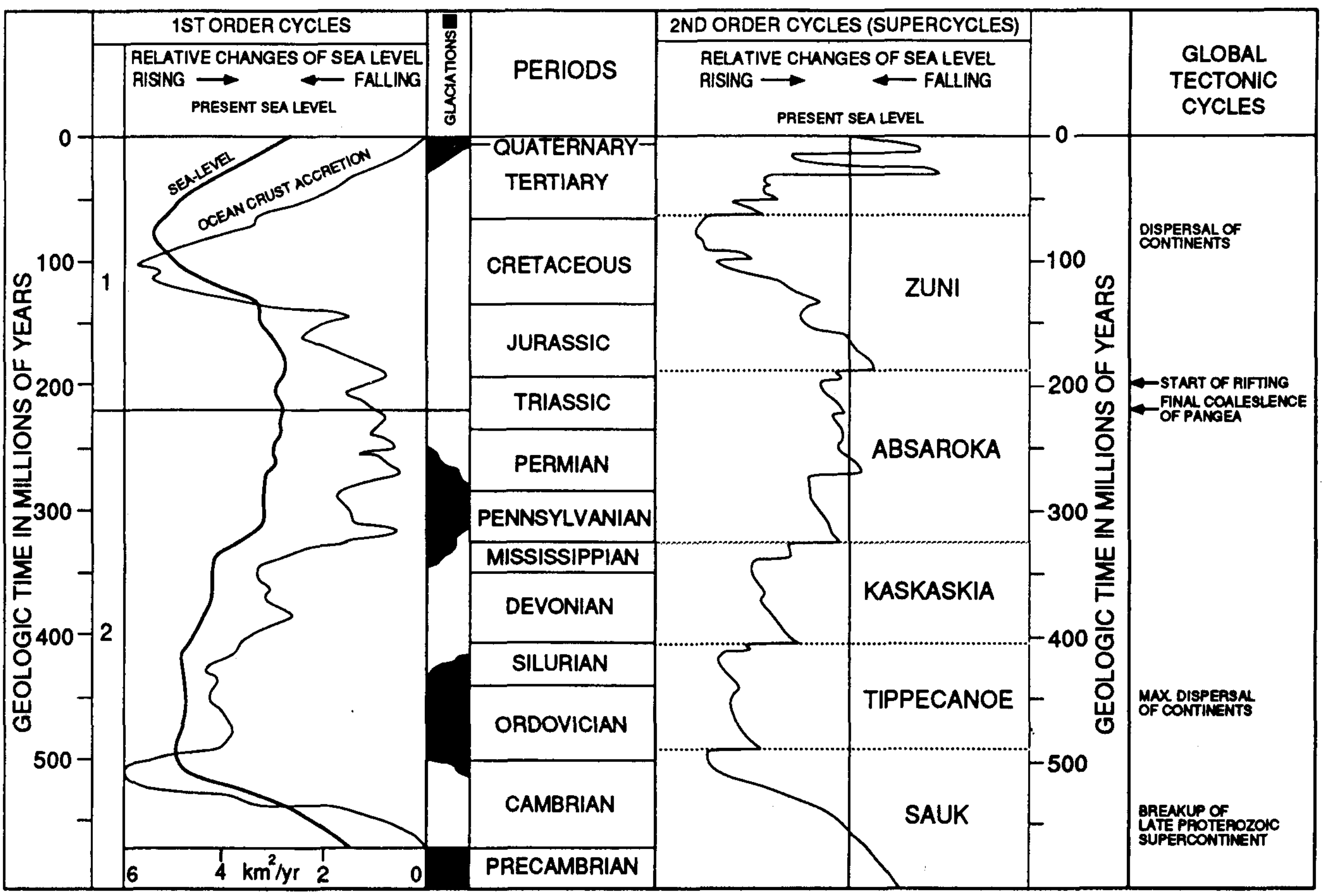

Figure 3 Eustatic sea level variation during the Phanerozoic. First-order sea level cycles reflect long term variations in the production of new oceanic crust (km²/year). This is an index of global tectonic cycles of alternating breakup, dispersal, and amalgamation of supercontinents, as explained in the text. Second-order cycles reflect smaller changes in oceanic crust production, on a 100 million year scale. Associated depositional sequences (Sauk to Zuni) were first defined on the North American craton by Sloss (1963). Periods of widespread glaciation (black) were characterized by short-lived glacio-eustatic changes in sea level (Fig. 6).

spreading ridges form and displace water onto continental margins.

Second- and third-order cycles

Second-order cycles consist of a grouping of third-order cycles (Fig. 2). The third-order cycles represent the highest frequency sea level events portrayed on the Exxon curve.

Second-order cycles span 10 to 100 m.y. and are exemplified by the cratonic sequences documented by Sloss (1963). These sequences have been convincingly correlated between four different continents (Soares *et al.*, 1978), suggesting a *global* sea level control. The explanation of Hallam (1963), now widely accepted, is that second-order cycles reflect changes in the volume of oceanic ridges, related to changes in spreading rate. These ideas were more quantitatively elaborated by Pitman (1978).

Third-order cycles have durations of 1-10 m.y. but are typically shorter than 3 m.y. (Fig. 2). They are ubiquitous in the Phanerozoic record (Haq *et al.*, 1988; Miall, 1990), but their control is problematic and controversial. Vail *et al.* (1977a, b) and Haq *et al.* (1988) suggest that these cycles can be correlated globally. However, because many third-order cycle boundaries are spaced close to or below the limit of biostratigraphic resolution, it may never be possible to resolve their ages with sufficient precision to *prove* precise global synchroneity. Nevertheless, some studies (e.g. Ross and Ross, 1988) provide persuasive evidence that third-order cycle boundaries can be accurately correlated within and between continents. Detailed stratigraphic work in the Cretaceous of the Alberta Basin (examples in Chapters 9, 10 and 12) shows that the chronostratigraphic position of many sequence boundaries and lowstand deposits (Fig. 2) corresponds with those predicted by the third-order cycle chart of Haq *et al.* (1988).

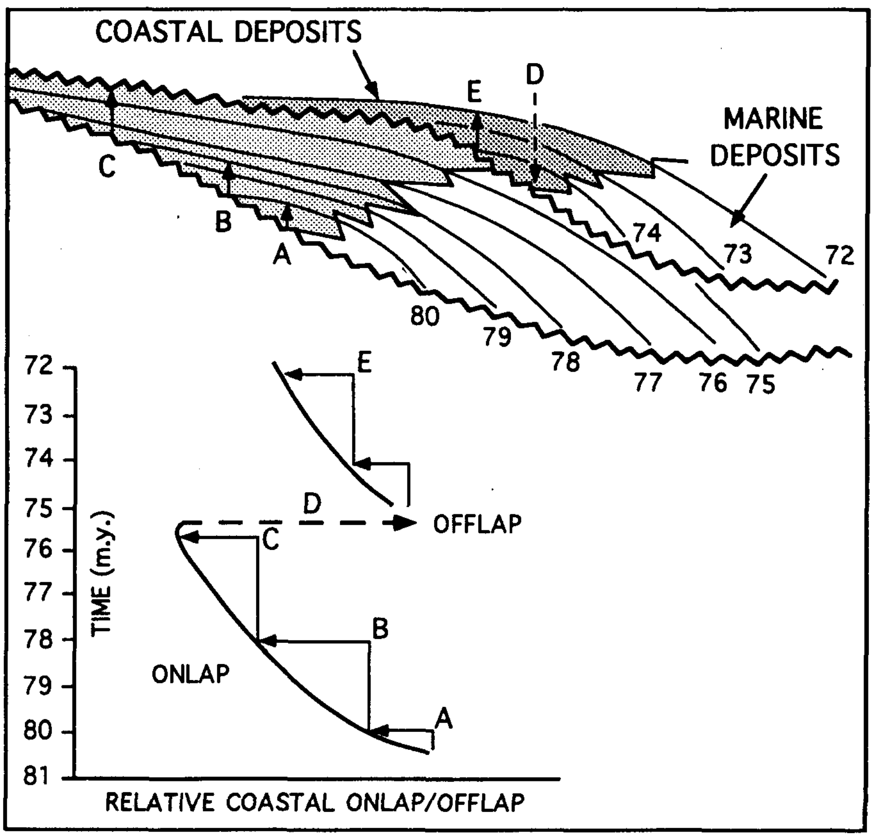

Figure 4 Upper diagram shows two unconformities and a series of numbered seismic reflectors; the numbers indicate geological ages. Note how the left ends of the reflectors *onlap* the unconformities. Arrow A indicates the vertical amount of coastal onlap between times 80+ and 80 Ma, and arrow B indicates the vertical onlap between 80 and 78 Ma, etc. Arrow D indicates the vertical *offlap* between 76- and 74+ Ma. In the lower diagram, the graph shows the measured amounts of onlap/offlap plotted against geological time. For example, arrow B from the cross section is displayed as a vertical sediment (time) and a horizontal segment (which shows the vertical component of coastal onlap). Thus arrows A, B and C (lengths from upper diagram) sum the onlap between 80+ and 76- Ma. Between 76- and 74+ Ma there was a rapid period of coastal offlap, followed by renewed onlap. These are third-order curves; examples from the Cretaceous are shown in Figure 2. After Vail *et al.* (1977).

Possible controls on third-order cyclicity

Although Haq *et al.* (1988) and Vail *et al.* (1977a) imply control of third-order cycles by the waxing and waning of continental ice masses, there is good evidence (e.g., Hayes *et al.*, 1976) that the growth and decay of ice sheets takes place over *much shorter* periods of time (10^4 to 10^5 years; glacio-eustatic sea level changes are discussed in more detail below). Kauffman (1984) noted that third-order marine transgressions in Cretaceous strata in the western United States corresponded to periods of active Cordilleran tectonism and volcanism, whereas lowstands were marked by relative tectonic and volcanic quiescence. These relationships suggested a causative link in which accelerated ocean ridge spreading (causing a eustatic rise), was coupled with accelerated subduction (promoting thrusting and volcanism along convergent margins). Harrison (1990) agreed that variations in spreading rates on ocean ridges (or *segments* of ridges) could account for the *timing* of third-order cycles, but that the amount of eustatic change would be an order of magnitude *less* than that suggested by the rock record. Amplification by tectonic subsidence would result in the greater water depths suggested by the rock record.

In contrast to explanations related to spreading and subduction, Cloetingh (1988) hypothesized that episodic changes in the horizontal stress field within plates might influence third-order cyclicity. The stress changes were postulated to result from the jostling of plates, and were calculated to induce tens of metres of subsidence or uplift over a time scale of about 10^6 years. This in turn would result in simultaneous transgressions and regressions within individual basins. These conclusions have, however, been disputed by Christie-Blick *et al.* (1990), who show that there need be no direct relationship between horizontal stress, basin deformation and the formation of sequence boundaries.

In an attempt to explain inferred regional sea level oscillations of up to 50 m in less than one million years, Cathles and Hallam (1991) suggested that horizontal stress changes within plates could cause rapid, plate-scale changes in lithospheric *density*. These would result in isostatic changes in freeboard of a few metres. Despite the novelty of this hypothesis, it does not explain the cause of *frequent* changes in the stress field.

The idea of geoidal eustasy, as advanced by Mörner (1981, 1987a,b), is based on the discovery (using satellite geodesy) that the ocean surface has "sags" and "bulges" with an amplitude of up to 180 m. This relief reflects irregularities in the gravitational field of the earth. Mörner argued that the migration of these oceanic sags and bulges would result in diachronous sea level changes. However, it has been pointed out (Devoy, 1987b) that changes in the gravitational field probably reflect mantle convection, which is extremely slow. Concomitant drift of the ocean surface topography must be correspondingly slow, on a time scale of millions of years, not thousands of years as inferred by Mörner (1987b). More importantly perhaps, Christie-Blick *et al.* (1990) emphasize the fact that geoidal changes affect not only the oceans but, over geological time, the solid earth as well. The land bulges up under an oceanic bulge, and no net sea level change results. Geoidal eustasy is therefore not likely to produce significant changes in relative sea level.

Sabadini *et al.* (1990) argue that variations in centrifugal force caused by long-term wander of the Earth's axis of rotation produces third-order eustatic sea level fluctuations that are nonsynchronous from hemisphere to hemisphere. Polar wandering results from poorly understood variations in the structure and viscosity of the mantle.

It is clear that an improved understanding of the mechanisms responsible for third-order cycles awaits better geophysical models of the Earth's interior, together with an order of magnitude improvement in the temporal resolution of sea level events from different parts of the world.

Fourth- and fifth-order cyclicity

Fourth- (500,000-200,000 yr) and *fifth-order* (200,000-10,000 yr) cycles are widely documented in many parts of the Phanerozoic, both in shallow-marine and pelagic rocks (see Fischer, 1986 and Kauffman, 1988 for reviews). These cycles are most easily explained by changes in climate driven by various cyclic perturbations of the Earth's tilt and orbit (Fig. 5). These astronomical perturbations are known as *Milankovitch* cycles, after the Serbian mathematician who first calculated their periodicities and effects. The Milankovitch theory holds that fluctuation in the seasonal distribution of incoming solar radiation is the principal control on the growth and decay of Quaternary ice sheets (Imbrie and Imbrie, 1979; Ruddiman *et al.*, 1986; Martinson *et al.*, 1987; Raymo *et al.*, 1989). The simplest way of producing sea level changes at the fourth- and fifth-order scale is by the alternate accumulation and melting of continental ice caps, in response to Milankovitch cycles. This can be convincingly demonstrated for the Quaternary, as elaborated below.

Milankovitch cycles

There are three principal orbital rhythms (periods given in brackets) related to 1) changes in the eccentricity of the Earth's orbit around the sun (400,000 and 100,000 years), 2) changes in the tilt of the Earth's axis with respect to the plane in which it orbits the sun (41,000 years), and 3) a wobble (precession) due to the tilt axis sweeping out a cone (21,000 years). These orbital rhythms (Fig. 5) produce cyclical variations in the intensity and seasonal distribution of incoming solar radiation. In combination, these factors affect the length of the summer melt period, such that at times, the winter snowpack does not melt completely. As the snowpack builds up, ice sheets of continental dimensions can develop, and large amounts of water are removed from the ocean.

SEA LEVEL CHANGES RELATED TO ORBITALLY DRIVEN CLIMATE CYCLES

The existence of Milankovitch rhythms for the last 2 m.y. (Quaternary) can be demonstrated by oxygen isotope studies of deep sea cores. These rhythms have strongly influenced the growth and decay of large continental ice sheets, resulting in changes of sea level. The best available data on the timing and

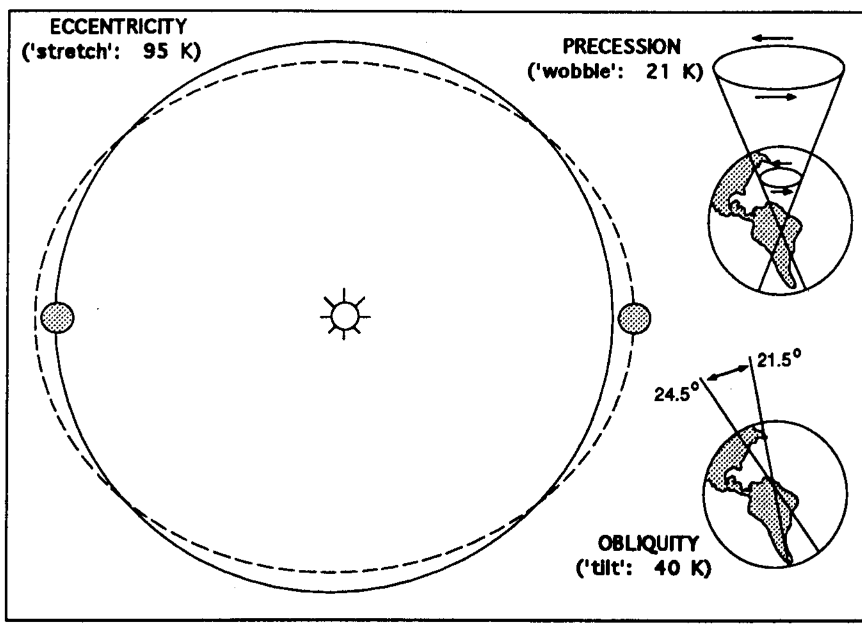

Figure 5 Three causes of "Milankovitch" cyclicity; obliquity, precession and eccentricity. Obliquity refers to changes in the tilt of the earth's axis of rotation. Precession refers to the fact that the earth wobbles like a spinning top; the axis of rotation sweeps out a cone with a period of about 21,000 years. Eccentricity refers to changes in the shape of the earth's orbit around the sun, from more circular to more elliptical. These variables, acting in combination, control incoming solar radiation and affect global climate. This has been termed the "pacemaker" of Quaternary glaciations. Adapted from Imbrie and Imbrie (1979).

magnitude of sea level changes is provided by studies of oxygen isotope ratios in Quaternary deep sea sediments.

Oxygen isotopes, Quaternary ice sheets and sea level change

Glacial control on eustatic sea level variation (termed *glacio-eustasy*) can be clearly demonstrated for Quaternary glaciations by reference to changes in $^{18}O/^{16}O$ ratios from benthic and planktic foraminifera preserved in deep ocean sediments (Matthews, 1986; Chappell and Shackleton, 1986). During the growth of continental ice sheets, seawater becomes progressively enriched in the heavier ^{18}O and the ice sheet in the lighter ^{16}O. This is because the heavier isotope is less mobile. When water evaporates, ^{16}O is concentrated in water vapour. When water vapour condenses into rain, the vapour is still further depleted in ^{18}O. Thus water which eventually falls as snow on the surface of an ice sheet has been relatively enriched in ^{16}O, leaving seawater (and organisms therein) relatively enriched in ^{18}O. In contrast, deglaciation of continental surfaces is recorded in deep sea cores by abrupt ^{16}O *spikes*, produced when isotopically light glacial meltwater returns to the oceans. Relative depletion in ^{18}O is expressed as deviation (δ) in parts per thousand (‰) from a standard interglacial mean (SMOW= Standard Mean Ocean Water). The most depleted (i.e., isotopically lightest) ice in the Antarctic Ice Sheet is about −60‰ (Chappell and Shackleton, 1986). In the North American Laurentide Ice Sheet during the last glaciation, the depletion was about −30‰ (Schwartz and Eyles, 1991). Numerous studies confirm that the average amplitude of the $\delta^{18}O$ signal is about 1.6‰ for the last 700,000 years (Fig. 6).

Over the last 700,000 years, glacial cycles recorded by changes in oxygen isotope ratios have lasted about 100,000 years (Fig. 6). Before this time, higher-frequency cycles (about 40,000 years) are observed (Fig. 6). The timing of the cycles fits very well with the Milankovitch periodicities (Raymo *et al.*, 1989).

Correlation of the isotopic record with sea level changes

The oxygen isotope record derived from deep ocean sediments can be directly correlated with glacio-eustatic sea level changes. The growth of Quaternary ice sheets, which had a maximum volume of about 65 x

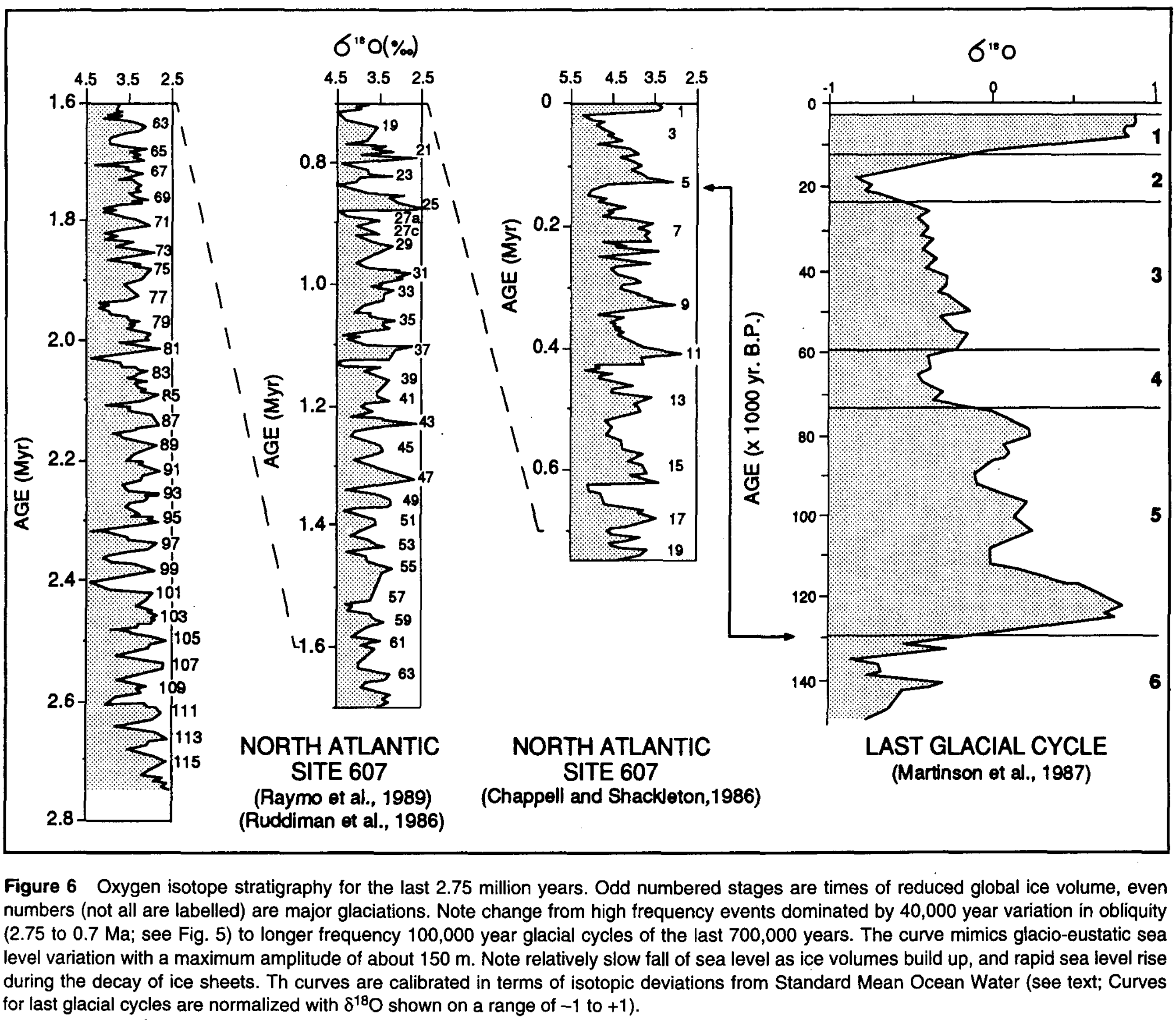

Figure 6 Oxygen isotope stratigraphy for the last 2.75 million years. Odd numbered stages are times of reduced global ice volume, even numbers (not all are labelled) are major glaciations. Note change from high frequency events dominated by 40,000 year variation in obliquity (2.75 to 0.7 Ma; see Fig. 5) to longer frequency 100,000 year glacial cycles of the last 700,000 years. The curve mimics glacio-eustatic sea level variation with a maximum amplitude of about 150 m. Note relatively slow fall of sea level as ice volumes build up, and rapid sea level rise during the decay of ice sheets. Th curves are calibrated in terms of isotopic deviations from Standard Mean Ocean Water (see text; Curves for last glacial cycles are normalized with $\delta^{18}O$ shown on a range of −1 to +1).

10^6 km^3, was accompanied by a glacio-eustatic lowering of sea level of as much as 150 m. If present-day glaciers were to melt, sea level would rise about 70 m, giving a maximum possible sea level fluctuation of over 200 m from full Quaternary glacial conditions to an ice-free Earth. In an ice-free Earth, the oceans would become isotopically lighter by about 1‰, giving a maximum isotopic amplitude from full glacial to ice-free conditions of about 2.6‰. Matthews (1986) suggests a calibration of ^{18}O variation of about 0.011‰ per m of sea level change. Precise calibrations are difficult to make because of uncertainties regarding the amount of ^{18}O-depleted water in floating pack ice rather than continental ice sheets, changing ocean water temperature and possible diagenesis of the foraminiferal tests. Nevertheless, glacio-eustatic variation mimics the ^{18}O record (Fig. 6). It shows a progressive but erratic sea level fall over the 100,000 year glacial cycle as ice sheets grew on the continents. The maximum rate of sea level fall was about 5 m/1000 years. In contrast, sea level rise at the end of a glacial cycle is very rapid (Fig. 6).

During the peak of the last deglaciation (about 12,000 years ago), about 14,000 km^3 of meltwater discharged annually from the North American (Laurentide) and European ice sheets to the North Atlantic Ocean. This is approximately 25 times the present annual discharge of the Mississippi River! At this time, global sea level rose 20 m in less than 1000 years and, for short time periods, as much as 4 m in 100 years (Fairbanks, 1989). Complete sea level recovery from glacial lowstands to interglacial highstands takes about 15,000 years (average rise of 10 m per thousand years). Estimates of rates and magnitudes of glacio-eustatic sea level change over the last glacial cycle (Fig. 6) are provided by study of raised marine terraces, and drowned coral terraces (Chappell and Shackleton, 1986; Fairbanks, 1989; Bard *et al.*, 1990). The growth of coral reefs is particularly responsive to changes in sea level (see Chapter 17).

Stability of the Milankovitch rhythms

The stability of the Milankovitch rhythms is open to question. Mathematical analysis of the motions of the inner planets of the Solar System (Laskar, 1989) suggests that the Milankovitch rhythms can be accurately calculated only for the last 10 m.y. Over longer periods of time, it is postulated that nonlinear amplification of even very small perturbations in planetary orbits, as well as changes in the diameter of the core, and of the earth as a whole, will lead to chaotic, unpredictable planetary motions. This chaotic view of the Solar System is countered by calculations by Berger *et al.* (1989), who suggest that the Milankovitch rhythms are relatively stable. For example, in the Late Cretaceous the tilt cycle would have been shortened by only about 4 per cent and the precession cycle shortened by about 2 per cent. The eccentricity cycle would be unlikely to change. However, Berger *et al.* (1989) suggest that by the Precambrian, it may be impossible to distinguish the precession and tilt cycles.

It must be emphasized that models of glacio-eustatic sea level variation based on well-studied Quaternary deep sea records cannot be applied indiscriminantly to the rock record. Pre-Quaternary glaciations were characterized by radically different distributions of land and sea, ice sheet configurations, tectonic settings and shortened or less effective Milankovitch variables.

PRE-QUATERNARY GLACIO-EUSTATIC CHANGES IN SEA LEVEL

The Earth has a long glacial record, and the distribution of glaciogenic rocks deposited in the past 2700 m.y. is shown in Figure 1 of Chapter 5. However, the ages of most pre-Quaternary glacial deposits are not well established in detail. It is therefore difficult to determine whether sea level changes inferred from the rock record may be attributed to a specific episode of glaciation. The common occurrence of glaciation in Earth history suggests that glacio-eustatic changes in sea level should be represented in the rock record; some examples are given below.

Late Proterozoic deep to shallow water facies successions, up to 1 km thick, have been attributed to glacio-eustatic changes of sea level, and have been correlated from continent to continent (Eisbacher, 1985). Sea level changes have been inferred in late Ordovician and early Silurian strata, and have been attributed to glacio-eustasy related to continental glaciation of the West African Craton (e.g., Johnson and Campbell, 1980).

Boardman and Heckel (1989) identified regionally extensive successions of transgressive limestones and regressive shales in the Pennsylvanian of Texas. These were correlated with fluctuations in the extent of ice sheets on Gondwanaland, implying a glacio-eustatic control. Similar transgressive-regressive successsions have also been recognized in coal-bearing strata in midcontinent North America and in Europe (Crowell, 1978; Veevers and Powell, 1987). However, their glacio-eustatic control has been questioned, and a possible tectonic mechanism has been suggested (Klein and Willard, 1989).

A particularly interesting gap in the glacial record of the Earth occurs from the Triassic to the early Tertiary. During this interval, there is no direct evidence for continental glaciation, although there is good evidence of seasonal pack ice formation at sea level (Spicer, 1987; Frakes and Francis, 1988). Antarctic ice accumulation in the Mesozoic is suggested by modelling experiments (Oglesby, 1989). Despite the lack of direct evidence for continental glaciation, widely distributed shallow-marine strata of Mesozoic age nevertheless contain abundant evidence for sea level oscillations, with frequencies of tens of thousands to a few hundred thousand years (Brandt, 1986; Goldhammer *et al.* 1987; Masetti *et al.* 1991). These sea level oscillations are manifest as regional erosion surfaces within Late Cretaceous shallow-marine units such as the Cardium, Marshybank and Viking formations of Alberta (Fig. 2; Chapter 12; Plint *et al.*, 1986; Plint, 1991; Boreen and Walker, 1991). Neither tectono-eustasy, nor tectonic movement of the basin floor operate on a sufficiently rapid scale to account for the high-frequency Cretaceous sea level changes implied by these erosion surfaces. By default, a glacio-eustatic control with Milankovitch periodicities becomes appealing. Such a control is not precluded by the oxygen isotope record (Prentice and Matthews, 1988), but it is arguable whether any Mesozoic ice masses were large enough to exert a significant glacio-eustatic control on sea level.

Although Milankovitch periodicity cannot be proven to control these Cretaceous sea level cycles, there *is* persuasive evidence for climatically driven *productivity cycles* with Milankovitch periods preserved in Mesozoic pelagic sediments (Fischer, 1986; Kemper, 1987; Herbert and D'Hondt, 1990).

We are therefore presented with a dilemma. Does the *geological evidence* of rapid sea level oscillations in the Mesozoic force us to accept the presence of continental ice, or are other mechanisms available? One possibility involves Milankovitch-scale, climatically controlled changes in the volume of groundwater stored on continents. This mechanism appears to be capable of producing about 10 to 20 m of eustatic change over periods of only 10^4 to 10^5 years (Hay and Leslie, 1990).

In this regard, it is pertinent to note the eustatic effects of human activities. Although present-day sea level has been rising at the rate of 1.6-2 mm/yr for the last several decades (Douglas, 1991), it is far from clear whether this is the result of natural processes or anthropogenic global warming (which results in both steric expansion of the ocean and melting of polar ice caps). A largely overlooked factor involves the construction of reservoirs. At present there are over 10,000 reservoirs on Earth, containing about 10,000 km^3 of water. This corresponds to a *drop* in global sea level of about 30 mm, at a rate of about 0.7 mm/yr over the last 40 years (Chao, 1991). Despite the negative eustatic effect of human water storage systems, global sea level is *still* rising. This raises the alarming possibility that the *true* rate of sea level rise is in fact even higher than that measured today (Chao, 1991).

DISCUSSION

The Exxon sea level curve is here to stay, although it is likely to undergo progressive evolution and refinement as more data are gathered and better chronostratigraphic control becomes available. For example, Mitchum and Van Wagoner (1991) and Plint (1991) have suggested that third-order sequences are in fact built up of fourth-order sequences, each of which yields evidence for deposition during a cycle of relative sea level rise and fall. It is likely that these high-frequency (fourth-order) sea level cycles will be increasingly widely recognized, and this recognition will spur efforts to explain their driving mechanism. Nevertheless, it will remain a major challenge to correlate these cycles on a more than regional scale, although this will be necessary if a eustatic control is to be demonstrated.

Despite the recent emphasis on global cycles of sea level change, the interpretation of cyclic sedimentary successions, particularly those representing relatively short periods of time, must take into account the possible influence of *autocyclic* mechanisms, such as delta-switching. Allocyclic controls such as tectonic uplift or subsidence of the basin and/or hinterland, and fluctuations in sediment supply, such as might result from climatic changes, may also result in pronounced depositional rhythms. Demonstration of a *eustatic* control on deposition must be based on the recognition of *simultaneous* sea level changes (but not necessarily involving changes of similar *magnitude*) in several basins, preferably on different continents. In order to do this, excellent regional biostratigraphic and allostratigraphic control (probably involving both subsurface and outcrop data), is needed. Where sections are widely scattered and correlation uncertain, attention should focus on detailed facies analysis and interpretation of *local* depositional environments, processes and *relative* sea level changes.

ACKNOWLEDGEMENTS

We thank the Natural Sciences and Engineering Research Council of Canada for continuing support of our research.

REFERENCES

Basic sources of information

Devoy, R.J.N., ed., 1987a, Sea surface studies, a global view: New York, Croom Helm, 649 p.
Emphasizes studies of Pleistocene to Recent sea level changes.

Miall, A.D., 1990, Principles of sedimentary basin analysis: New York, Springer-Verlag, 668 p.
Chapter 8 presents a concise review of the main mechanisms thought to be responsible for stratigraphic cycles related to sea level change.

Revelle, R., ed., 1990, Sea level change: National Research Council, Studies in Geophysics, Washington, D.C., National Academy Press, 234 p.
One of the most up to date summaries of processes of sea level change, and the record of past changes.

Wilgus, C.K., Hastings, B.S., Posamentier, H.W., Ross, C.A. and Kendall, C.G. St.C., eds., 1988, Sea level changes: an integrated approach: Society of Economic Paleontologists and Mineralogists, Special Publication 42, 407 p.
Collection of papers emphasizing conceptual basis of sequence stratigraphy (read with a critical eye!) plus numerous case studies of sea level change from the geological record.

Other references

Bard, E., Hamelin, B. and Fairbanks, R.G., 1990, U-Th ages obtained by mass spectrometry in corals from Barbados; sea level during the past 130,000 years: Nature, v. 346, p. 456-458.

Berger, A.L., Loutre, M.F. and Dehant, V., 1989, Influence of the changing lunar orbit on the astronomical frequencies of pre-Quaternary insolation patterns: Paleoceanography, v. 4, p. 555-564.

Boardman, D.R., II and Heckel, P.H., 1989, Glacial-eustatic sea-level curve for early Late Pennsylvanian sequence in north-central Texas and biostratigraphic correlation with curve for midcontinent North America: Geology, v. 17, p. 802-805.

Boreen, T. and Walker, R.G., 1991, Definition of allomembers and their facies assemblages in the Viking Formation, Willesden Green area, Alberta: Bulletin of Canadian Petroleum Geology, v. 39, p. 123-144.

Brandt, K., 1986, Glacioeustatic cycles in the Early Jurassic?: Neues Jahrbuch fur Geologie und Paläontologie, Monatshefte, v. 5, p. 257-274.

Burton, R., Kendall, G.St.C. and Lerche, I., 1987, Out of our depth: on the impossibility of fathoming eustasy from the stratigraphic record: Earth Science Reviews, v. 24, p. 237-277.

Cathles, L.M. and Hallam, A., 1991, Stress-induced changes in plate density, Vail sequences, epirogeny, and short-lived global sea level fluctuations: Tectonics, v. 10, p. 659-671.

Chao, B.F., 1991, Man, water and global sea level: Eos, v. 72, p. 492.

Chappell, J. and Shackleton, N.J., 1986, Oxygen isotopes and sea level: Nature, v. 324, p. 137-140.

Christie-Blick, N., Mountain, G.S. and Miller, K.G., 1990, Seismic stratigraphic record of sea level change, *in* Revelle, R., ed., Sea level change: National Research Council, Studies in Geophysics, Washington, D.C., National Academy Press, p. 116-140.

Cloetingh, S., 1988, Intraplate stresses: a tectonic cause for third-order cycles in apparent sea level? *in* Wilgus, C.K., *et al.*, eds., Sea level changes: an integrated approach: Society of Economic Paleontologists and Mineralogists, Special Publication 42, p. 19-29.

Cross, T.A. and Lessenger, M.A., 1988, Seismic stratigraphy: Annual Review of Earth and Planetary Science, v. 16, p. 319-354.

Crowell, J.C., 1978, Gondwanan glaciation, cyclothems, continental positioning, and climate change: American Journal of Science, v. 278, p. 1345-1372.

Devoy, R.J.N., 1987b, Introduction: first principles and the scope of sea-surface studies, *in* Devoy, R.J.N., ed., Sea surface studies, a global view: New York, Croom Helm, p. 1-30.

Douglas, B.C., 1991, Global sea level rise: Journal of Geophysical Research, v. 96, p. 6981-6992.

Eisbacher, G.H., 1985, Late Proterozoic rifting, glacial sedimentation and sedimentary cycles in the light of Windermere deposition, western Canada: Palaeogeography, Palaeoclimatology, Palaeoecology, v. 51, p. 231-254.

Fairbanks, R.G., 1989, A 17,000-year glacio-eustatic sea level record: influence of glacial melting rates on the Younger Dryas event and deep ocean circulation: Nature, v. 342, p. 637-642.

Fischer, A.G., 1986, Climatic rhythms recorded in strata: Annual Review of Earth and Planetary Sciences, v. 14, p. 351-376.

Frakes, L.A. and Francis, J.E., 1988, A guide to Phanerozoic cold polar climates from high-latitude ice-rafting in the Cretaceous: Nature, v. 333, p. 547-549.

Goldhammer, R.K., Dunn, P.A. and Hardie, L.A., 1987, High-frequency glacio-eustatic sea level oscillations with Milankovitch characteristics recorded in Middle Triassic platform carbonates in northern Italy: American Journal of Science, v. 287, p. 853-892.

Hallam, A., 1963, Major epirogenic and eustatic changes since the Cretaceous and their possible relationship to crustal structure: American Journal of Science, v. 261, p. 164-177.

Haq, B.U., 1991, Sequence stratigraphy, sea level change, and significance for the deep sea, *in* MacDonald, D.I.M., ed., Sedimentation, tectonics and eustasy: International Association of Sedimentologists, Special Publication 12, p. 3-39.

Haq, B.U., Hardenbol, J. and Vail, P.R., 1988, Mesozoic and Cenozoic chronostratigraphy and cycles of sea level change, *in* Wilgus, C.K., *et al.*, eds., Sea level changes: an integrated approach: Society of Economic Paleontologists and Mineralogists, Special Publication 42, p. 71-108.

Harrison, C.G.A., 1990, Long-term eustasy and epirogeny in continents, *in* Revelle, R., ed., Sea level change: National Research Council, Studies in Geophysics, Washington, D.C., National Academy Press, p. 141-158.

Hay, W.W. and Leslie, M.A., 1990, Could possible changes in global groundwater reservoir cause eustatic sea level fluctuations?, *in* Revelle, R., ed., Sea level change: National Research Council, Studies in Geophysics, Washington, D.C., National Academy Press, p. 161-170.

Hayes, J.D., Imbrie, J. and Shackleton, N.J., 1976, Variations in the earth's orbit: pacemaker of the ice ages: Science, v. 194, p. 1121-1132.

Herbert, T.D. and D'Hondt, S.L., 1990, Precessional climate cyclicity in Late Cretaceous-Early Tertiary marine sediments: a high resolution chronometer of Cretaceous-Tertiary boundary events: Earth and Planetary Science Letters, v. 99, p. 263-275.

Imbrie, J. and Imbrie, K.P., 1979, Ice ages: solving the mystery: New York, McMillan Press, 224 p.

Johnson, M.E. and Campbell, G.T., 1980, Recurrent carbonate environments in the lower Silurian of northern Michigan and their inter-regional correlation: Journal of Paleontology, v. 54, p. 1041-1057.

Kauffman, E.G., 1984, Paleobiogeography and evolutionary response dynamic in the Cretaceous Western Interior Seaway of North America, *in* Westermann, G.E.G., ed., Jurassic-Cretaceous biochronology and paleogeography of North America: Geological Association of Canada, Special Paper 27, p. 273-306.

Kauffman, E.G., 1988, Concepts and methods of high-resolution event stratigraphy: Annual Review of Earth and Planetary Sciences, v. 16, p. 605-654.

Kemper, E., 1987, Das klima der Kreide-Zeit (The climate of the Cretaceous Period): Geologisches Jahrbuch, Reihe A, v. 96, p. 5-185.

Klein, G. de V. and Willard, D.A., 1989, Origin of Pennsylvanian coal-bearing cyclothems of North America: Geology, v. 17, p. 152-155.

Lambeck, K., 1990, Late Pleistocene, Holocene and present sea-levels: constraints on future change: Palaeogeography, Palaeoclimatology, Palaeoecology, v. 89, p. 205-217.

Laskar, J., 1989, A numerical experiment on the chaotic behaviour of the Solar System: Nature, v. 338, p. 237-238.

Martinson, D.G., Pisias, N.G., Hays, J.D., Imbrie, J., Moore, T.C. and Shackleton, N.J., 1987, Age dating and the orbital theory of the Ice Ages: development of a high-resolution 0 to 300,000 year chronostratigraphy: Quaternary Research, v. 27, p. 1-29.

Masetti, D., Neri, C. and Bosellini, A., 1991, Deep water asymmetric cycles and progradation of carbonate platforms governed by high-frequency eustatic oscillations (Triassic of the Dolomites, Italy): Geology, v. 19, p. 336-339.

Matthews, R.K., 1986, Oxygen isotope record of ice-volume history: 100 million years of glacio-eustatic sea level fluctuation, *in* Schlee, J.S., ed., Interregional unconformities and hydrocarbon accumulation: American Association of Petroleum Geologists, Memoir 36, p. 97-107.

Miall, A.D., 1986, Eustatic sea level changes interpreted from seismic stratigraphy: a critique of the methodology with particular reference to the North Sea Jurassic record: American Association of Petroleum Geologists, Bulletin, v. 70, p. 131-137.

Miall, A.D., 1991, Stratigraphic sequences and their chronostratigraphic correlation: Journal of Sedimentary Petrology, v. 61, p. 497-505.

Mitchum, R.M. and Van Wagoner, J.C., 1991, High-frequency sequences and their stacking patterns: sequence-stratigraphic evicence of high-frequency eustatic cycles: Sedimentary Geology, v. 70, p. 131-160.

Mörner, N.A., 1981, Revolution in Cretaceous sea level analysis: Geology, v. 9, p. 344-346.

Mörner, N.A., 1987a, Pre-Quaternary long-term changes in sea level, in Devoy, R.J.N., ed., Sea surface studies, a global view: New York, Croom Helm, p. 233-241.

Mörner, N.A., 1987b, Quaternary sea-level changes: northern hemisphere data, *in* Devoy, R.J.N., ed., Sea surface studies, a global view: New York, Croom Helm, p. 242-263.

Nummedal, D., Pilkey, O.H. and Howard, J.D., eds., 1987, Sea level fluctuation and coastal evolution: Society of Economic Paleontologists and Mineralogists, Special Publication 41, 267 p.

Oglesby, R.J., 1989, A GCM study of Antarctic glaciation: Climate Dynamics, v. 3, p. 135-156.

Parkinson, N. and Summerhayes, C., 1985, Synchronous global sequence boundaries: American Association of Petroleum Geologists, Bulletin, v. 69, p. 685-687.

Pitman, W.C., 1978, Relationship between eustasy and stratigraphic sequences of passive margins: Geological Society of America, Bulletin, v. 89, p. 1387-1403.

Plint, A.G., 1991, High-frequency relative sea level fluctuations in Upper Cretaceous shelf clastics of the Alberta Foreland Basin: possible evidence for a glacio-eustatic control?, *in* MacDonald, D.I.M., ed., Sedimentation, tectonics and eustasy: International Association of Sedimentologists, Special Publication 12, p. 409-428.

Plint, A.G., Walker, R.G. and Bergman, K.M., 1986, Cardium Formation 6. Stratigraphic framework of the Cardium in subsurface: Bulletin of Canadian Petroleum Geology, v. 34, p. 213-225.

Posamentier, H.W., Jervey, M.T. and Vail, P.R., 1988, Eustatic controls on clastic deposition 1 — conceptual framework, *in* Wilgus, C.K., *et al.*, eds., Sea level changes: an integrated approach: Society of Economic Paleontologists and Mineralogists, Special Publication 42, p. 109-124.

Prentice, M.L. and Matthews, R.K., 1988, Cenozoic ice-volume history: Development of a composite oxygen isotope record: Geology, v. 16, p. 963-966.

Raymo, M.E., Ruddiman, W.F., Backman, J., Clement, B.M. and Martinson, D.G., 1989, Late Pliocene variation in northern hemisphere ice sheets and north Atlantic deep water circulation: Paleoceanography, v. 4, p. 413-446.

Ross, C.A. and Ross, J.R.P., 1988, Late Paleozoic transgressive-regressive deposition, *in* Wilgus, C.K., *et al.*, eds., Sea level changes: an integrated approach: Society of Economic Paleontologists and Mineralogists, Special Publication 42, p. 227-247.

Ruddiman, W.F., Raymo, M. and McIntyre, A., 1986, Matuyama 41,000-year cycles; North Atlantic Ocean and northern hemisphere ice sheets: Earth and Planetary Science Letters, v. 80, p. 117-129.

Sabadini, R., Doglioni, C. and Yuen, D.A., 1990, Eustatic sea level fluctuations induced by polar wander: Nature, v. 345, p. 708-710.

Schwarcz, H. and Eyles, N., 1991, Laurentide Ice Sheet extent inferred from stable isotopic composition (O, C) of lacustrine ostracodes at Toronto, Canada: Quaternary Research, v. 35, p. 305-320.

Sloss, L.L., 1963, Sequences in the cratonic interior of North America: Geological Society of America, Bulletin, v. 74, p. 93-114.

Sloss, L.L., 1972, Synchrony of Phanerozoic sedimentary-tectonic events of the North American craton and the Russian platform: 24th International Geological Congress, Montreal, Section 6, p. 24-32.

Soares, P.C., Landim, P.M.B. and Sulfaro, V.J., 1978, Tectonic cycles and sedimentary sequences in the Brazilian intracratonic basins: Geological Society of America, Bulletin, v. 89, p. 181-191.

Spicer, R.A., 1987, The significance of the Cretaceous flora of northern Alaska for the reconstruction of the climate of the Cretaceous: Geologisches Jahrbuch, Reihe A, v. 96, p. 265-291.

Vail, P.R., Mitchum, R.M., Jr. and Thompson, S., III, 1977a, Seismic stratigraphy and global changes of sea level, part 3: relative changes of sea level from coastal onlap, *in* Payton, C.E., ed., Seismic stratigraphy — applications to hydrocarbon exploration: American Association of Petroleum Geologists, Memoir 26, p. 63-81.
This paper is one of 11 separate parts of the much longer paper, referenced immediately below.

Vail, P.R., Mitchum, R.M., Todd, R.G., Widmier, J.M., Thompson, S., Sangree, J.B., Bubb, J.N. and Hatlelid, W.G., 1977b, Seismic stratigraphy and global changes of sea level, *in* Payton, C.E., ed., Seismic stratigraphy — applications to hydrocarbon exploration: American Association of Petroleum Geologists, Memoir 26, p. 49-212.
This paper consists of 11 separately authored parts on many different aspects of seismic stratigraphy and sea level change. Titles of individual parts act as a guide to the overall paper.

Van Wagoner, J.C., Mitchum, R.M., Campion, K.M. and Rahmanian, V.D., 1990, Siliciclastic sequence stratigraphy in well logs, cores and outcrops: concepts for high-resolution correlation of time and facies: American Association of Petroleum Geologists, Methods in Exploration Series, No. 7, 55 p.

Veevers, J.J. and Powell, C.M., 1987, Late Paleozoic glacial episodes in Gondwanaland reflected in transgressive-regressive depositional sequences in Euramerica: Geological Society of America, Bulletin, v. 98, p. 475-487.

Walker, R.G., 1990, Facies modelling and sequence stratigraphy: Journal of Sedimentary Petrology, v. 60, p. 777-786.

Worsley, T.W., Nance, D. and Moody, J.B., 1984, Global tectonics and eustasy for the past 2 billion years: Marine Geology, v. 58, p. 373-400

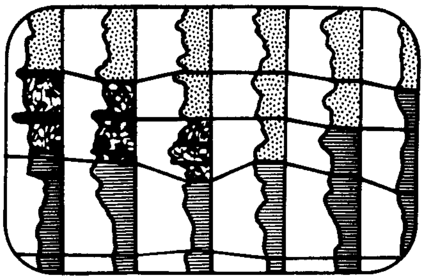

3. Subsurface Facies Analysis

Douglas J. Cant, Geological Survey of Canada, 3303 – 33rd St. N.W., Calgary, Alberta T2L 2A7

INTRODUCTION

This chapter will attempt to bridge the methodological and scale gap between sedimentology based largely on outcrops and modern environments, and techniques and results of large-scale, subsurface investigations. It is an introduction to 1) geophysical logs and correlation, 2) subsurface facies analysis, 3) seismic methods, and 4) larger-scale analysis of sedimentary facies successions and allostratigraphy.

Subsurface work lends itself to the study of facies relationships on a scale larger than can be accomplished on most outcrops. Consequently, many relatively new ideas concerning allostratigraphy, sequence stratigraphy, base-level changes, and global stratigraphic correlations have emerged from subsurface geology, and are based on both geological and geophysical data.

DIFFERENCES FROM SURFACE WORK

Subsurface data provide a differently biased sample of a rock unit than outcrop data. Drill holes and cores are concentrated in localities and zones of economic interest whereas outcrops preferentially expose rocks which are harder and more resistant to weathering. Because drill holes and geophysical logs normally sample a continuous, uninterrupted section (whereas outcrops rarely do), subsurface correlation is based on more complete data. Seismic-reflection data may provide a coherent three-dimensional picture of a basin, along with information on the relationships between the sediments and structural features of a basin.

Subsurface data cannot provide as much local facies information. No matter how closely spaced wells may be, data from geophysical logs, 3 to 20 cm-diameter cores, and cross sections constructed from them, cannot match the level of local detail available from an outcrop. Seismic data give a view of a basin on a very much larger scale than outcrop studies. The differences in the appropriate scales of investigation for outcrop compared with subsurface studies are extremely significant, both scientifically and economically.

Subsurface methods

The following sections will briefly review the principles behind subsurface methods of investigation, including both geological methods (well logs and cores), and geophysical methods (seismic-reflection data). Other publications discuss these techniques in more detail, notably Krumbein and Sloss (1963), Allen

Table 1 *Log types, properties measured, and geological uses.*

Log	Property Measured	Units	Geological Uses
Spontaneous potential	Natural electric potential (compared to drilling mud)	Millivolts	Lithology (in some cases), correlation, curve shape analysis, identification of porous zones.
Resistivity	Resistance to electric current flow	Ohm-metres	Identification of coals, bentonites, fluid evaluation.
Gamma-ray	Natural radioactivity — related to K, Th, U	API units	Lithology (shaliness), correlation, curve shape analysis.
Sonic	Velocity of compressional sound wave	Microseconds/metre	Identification of porous zones, coal, tightly cemented zones.
Caliper	Size of hole	Centimetres	Evaluate hole conditions and reliability of other logs.
Neutron	Concentrations of hydrogen (water and hydrocarbons) in pores	Per cent porosity	Identification of porous zones, cross plots with sonic, density logs for empirical separation of lithologies.
Density	Bulk density (electron density) includes pore fluid in measurement	Kilograms per cubic metre (gm/cm^3)	Identification of some lithologies such as anhydrite, halite, nonporous carbonates.
Dipmeter	Orientation of dipping surfaces by resistivity changes	Degrees (and direction)	Structural analysis, stratigraphic analysis

(1975), Payton (1977), Selley (1978), Anstey (1982), and Miall (1984). Some newly developed methods in subsurface sedimentology, such as the use of resistivity microscanners to detect sedimentary structures, and the analysis of high-resolution dipmeter data, are as yet not widely applied, but are discussed by Hurst *et al.* (1990). The two major types of data, subsurface geological and geophysical, will be treated separately, but where available, both can be integrated.

GEOLOGICAL USES OF WELL LOGS

Well logs are made by pulling an instrumented tool up the hole, and recording the data as a function of depth. They are used extensively in the petroleum industry for evaluation of the fluids in rocks, but this aspect will not be covered here. The interested reader is referred to the various logging company manuals, or to Asquith (1982). Geophysical logs are the fundamental source of data in many subsurface studies because virtually every oil and gas well is logged from near the top to the bottom. Almost all well logging is done by pulling the measurement tool up the hole on the end of a wire. Different types of logs and the properties they measure are shown in Table 1 and are discussed briefly below. On any well log, the absolute elevation of any bed or bed contact is obtained by subtracting its depth in the well from the surveyed elevation of the Kelly Bushing (KB) on the drilling platform; this elevation is given on the top (header) of the well log.

Spontaneous potential (SP) log

This log records the electric potential between an electrode pulled up the hole and a reference electrode at the surface. This potential exists because of electrochemical differences between the waters within the formation and the drilling mud, and because of ionic selection effects in shales (the surfaces of clay minerals selectively allow passage of cations compared to anions). The potential is measured in millivolts on a relative scale only (Fig. 1) because the absolute value depends on the properties of the drilling mud. In shaly sections, the maximum SP response to the right can be used to define a "shale line" (Fig. 1). Deflections of the log from the shale line indicate zones of permeable rock containing interstitial fluid with salinities different from the drilling mud.

Experience in many basins has shown that the SP log may be a good indicator of lithology in areas where sandstones are permeable and water saturated. However, where low-permeability rocks occur, such as the tightly cemented sandstones of the western Alberta Basin or the bitumen-saturated Athabasca Oil Sands, the SP log cannot reliably distinguish lithologies. If subsurface formations contain fresh rather than saline water (such as some Upper Cretaceous rocks of Alberta), SP deflection is suppressed or even reversed

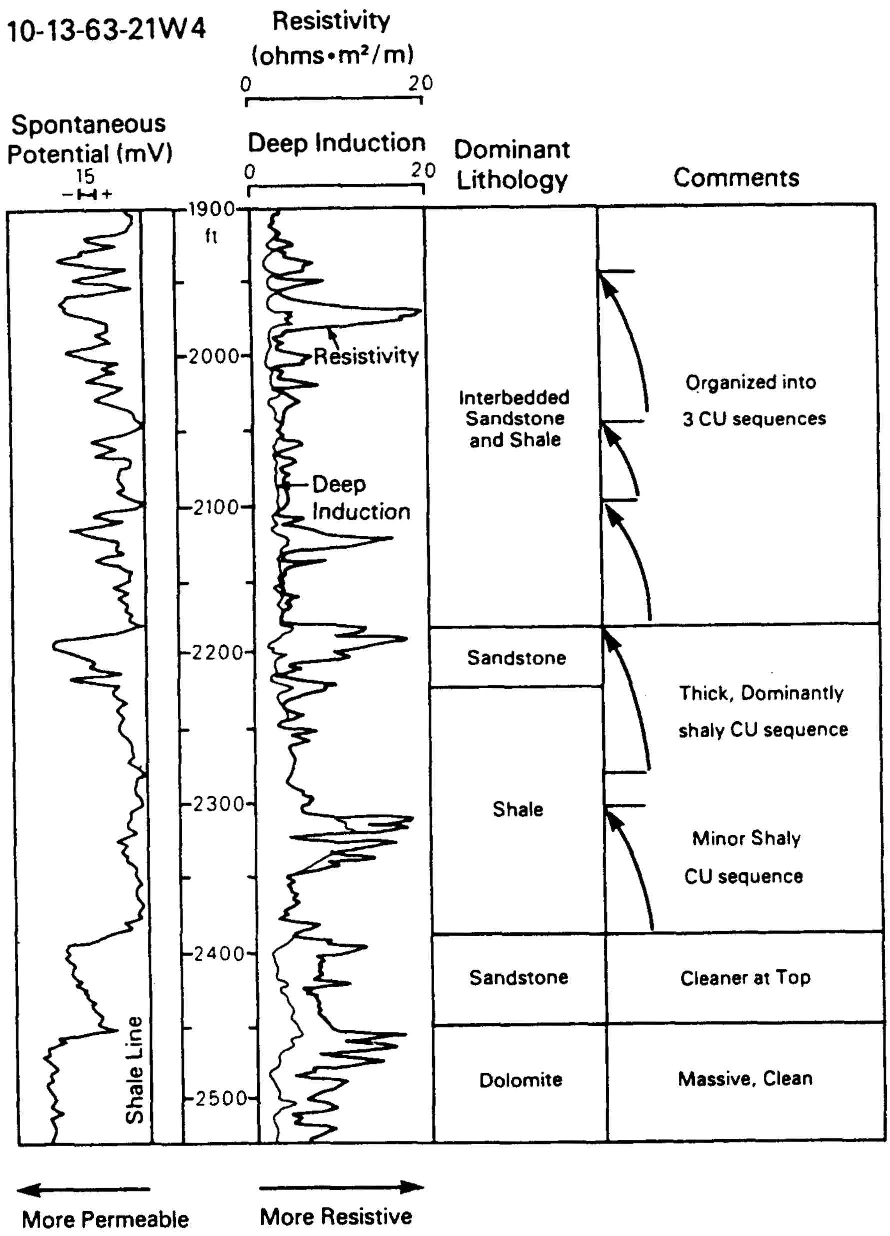

Figure 1 Example of SP and resistivity logs from the Alberta Basin. A shale line is shown on the SP — any deviation from this reflects porous rock. Two resistivity logs are shown — one of medium depth (resistivity) and another (deep induction) which reads farther into the rock beyond the influence of the drilling mud. The deep induction log shows lower resistivity in porous zones, probably indicating salt-water saturation. The carbonates are Devonian Winterburn dolomites overlain by Cretaceous Mannville Group sandstones and shales. The curved arrows indicate individual facies successions; these can be seen as progressive upward deflections in both the SP and resistivity logs.

from normal, depending on the salinity of the drilling mud. The best test of the reliability of the SP log in determining lithology is to calibrate the log against cores and cuttings (cuttings are 1 to 3 mm fragments of rock brought to the surface during normal drilling by the circulating mud) and hence gain experience in a particular area.

Resistivity log

This log records the resistance of interstitial fluids to the flow of an electric current, either transmitted directly to the rock through an electrode, or magnetically induced deeper into the formation from the hole (induction logs; Fig. 1). The term "deep" here refers to horizontal distance from the well bore. Resistivities at different depths into the rock are measured by varying the length of the tool and focusing the induced current. Several resistivity and induction curves are commonly shown on the same track (Fig. 1).

Resistivity logs are used for evaluation of fluids within formations. They can also be used for identification of coals (high resistance), thin limestones in shales (high resistance), and bentonites (low resistance), as shown in Table 1. In older wells where few types of logs were run, the resistivity log may be useful for picking tops and bottoms of formations, and for correlating between wells. Freshwater-saturated porous rocks have high resistivities, so the log can be used in these cases to separate shales from porous sandstones and carbonates.

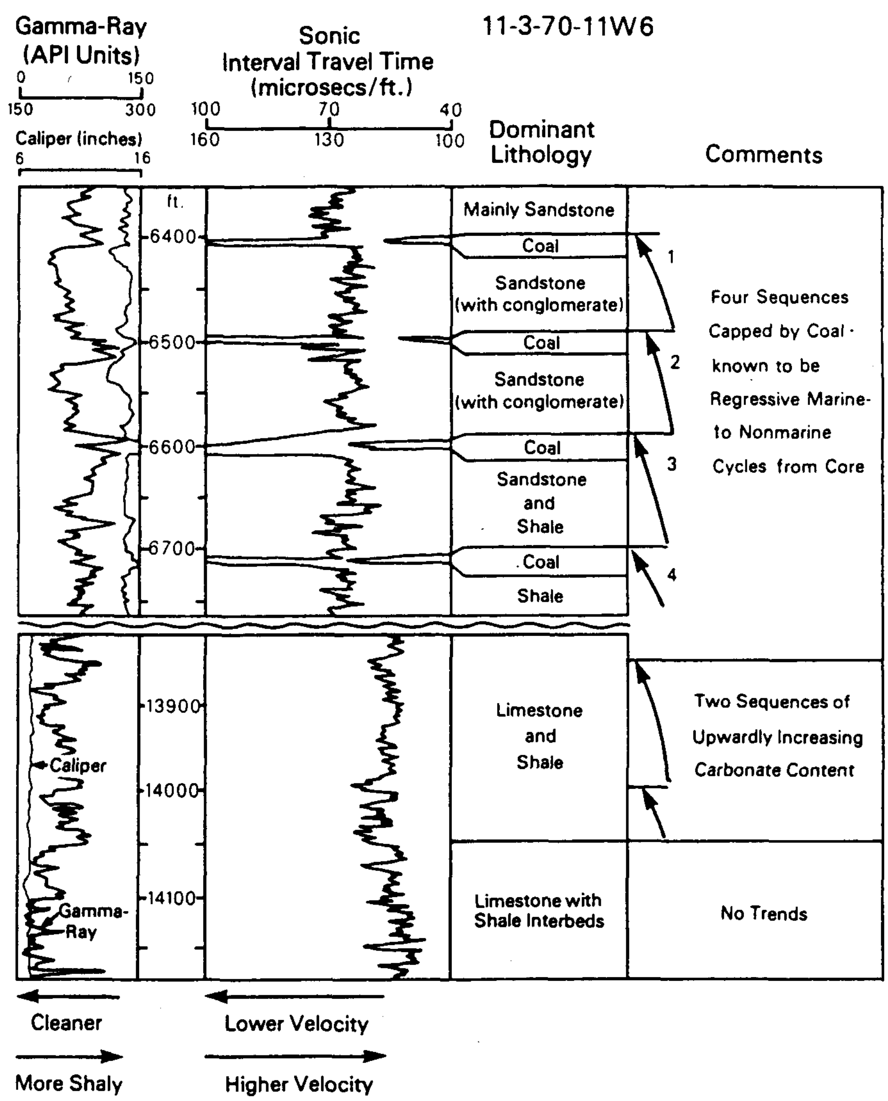

Figure 2 Gamma-ray, caliper, and sonic logs from the Alberta Basin. Because of space limitations, coaly shales (higher gamma-ray readings) are labelled coals. The lower section consists of the Ireton and Leduc Formations and the upper section shows regressive shoreline successions of the Upper Mannville Spirit River Formation.

Gamma-ray log

This log (Fig. 2) measures the natural gamma-ray emission of the various layers penetrated in the well, a property related to their content of radiogenic isotopes of potassium, uranium and thorium. These elements (particularly potassium) are common in clay minerals and some evaporites. In terrigenous clastic successions the log reflects the "cleanness" (lack of clays) or "shaliness" (high radioactivities on the API scale, Fig. 2) of the rock, averaged over an interval of about 2 m. Because of this property, gamma-ray log patterns mimic vertical sand-content or carbonate-content trends of facies successions. It must be emphasized that the gamma-ray reading is *not* a function of grain size or carbonate content, only of the proportion of radioactive elements, which *may* be related to the proportion of shale. For example, clay-free sandstones or conglomerates with any mix of sand and pebble clast sizes generally give similar responses, and lime mudstone gives the same response as grainstone. Distinguishing between clean (clay-free) lithologies such as sandstones, conglomerates, dolomites, and limestones is best done by calibration of one or more logs to cores or cuttings.

Once the main lithologies are known,

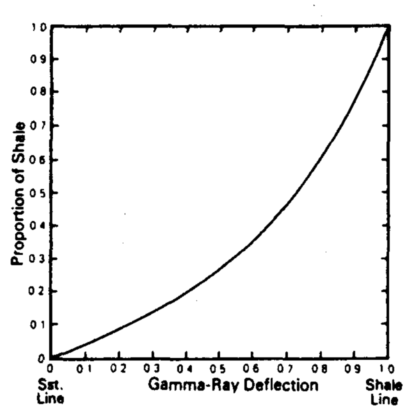

Figure 3 Relationship between gamma-ray deflection and proportion of shale. A cutoff half-way between maximum and minimum values corresponds to about 28 per cent shale, and is commonly used as a criterion for lithologic mapping.

the gamma-ray log can be calibrated to lithology by establishing minimum and maximum readings corresponding to pure carbonate or sandstone versus pure shale end members. The concentration of radioactive elements in shale increases with compaction, so the shale line should be readjusted if a thick section is being studied. The tool response is nonlinear (Fig. 3), so a cutoff halfway between the shale line and sandstone (or other clean lithology) line has a value of roughly 30 per cent shale for purposes such as lithologic mapping.

There are three main interpretation problems with the gamma-ray log, 1) the log response may be affected by diagenetic, radioactive clays in pores, 2) shales rich in illite (high K) are more radioactive than those rich in montmorillonites or chlorites, and 3) arkosic sandstones (high K-feldspars) are more radioactive than those lacking feldspar. Calibration of the log against cores or cuttings may be necessary to distinguish lithologies in some cases.

Sonic log

This log (Fig. 2) measures the velocity of sound waves in rock. This velocity depends on 1) lithology, 2) amount of interconnected pore space, and 3) type of fluid in the pores. The log is useful for delineating beds of low-velocity material such as coal (Fig. 2) or poorly cemented sandstones, as well as high-velocity material such as tightly cemented sandstones and carbonates or igneous basement. Sonic logs are also important in understanding and calibrating seismic lines, as explained below.

Porosity logs

Density and neutron logs can be displayed as estimates of porosities. The density tool emits gamma radiation which is scattered back to the detector in amounts proportional to the electron density of the rock. The electron density, in most cases, is related to the density of the solid material, and the amount and density of pore fluids. Density porosity is calculated by assuming a density of the solid material (2650 kg/m^3 for sandstone and shale, 2710 kg/m^3 for limestone) and fluid (1146 kg/m^3 for salt water).

The neutron log measures the hydrogen concentration (in water or petroleum) in the rock. The tool emits neutrons of a known energy level, then measures the energy of neutrons reflected from the rock. Because energy is transferred most easily to particles of similar mass, the hydrogen concentration can be estimated. Neutron porosities are calculated by assuming that oil or water fills the pore spaces. Gas, or water bound into clay minerals, give anomalously low values.

Caliper log

This log records the diameter of the hole (Fig. 2), and gives an indication of its condition and hence the reliability of other logs. A very large hole indicates that dissolution, caving or falling in of the rock wall has occurred, which can lead to errors in log responses. This log is particularly useful in mixed evaporite successions where dissolution has preferentially leached out soluble evaporites. A hole smaller than the drill bit size may be present because the fluid fraction of the drilling mud invades permeable zones, leaving the solid fraction (mud or filter cake) on the inside of the hole. In one gas field in the Mannville Group of Alberta, very permeable, matrix-free conglomerate can be recognized on the caliper log where the hole size is smaller than the bit size.

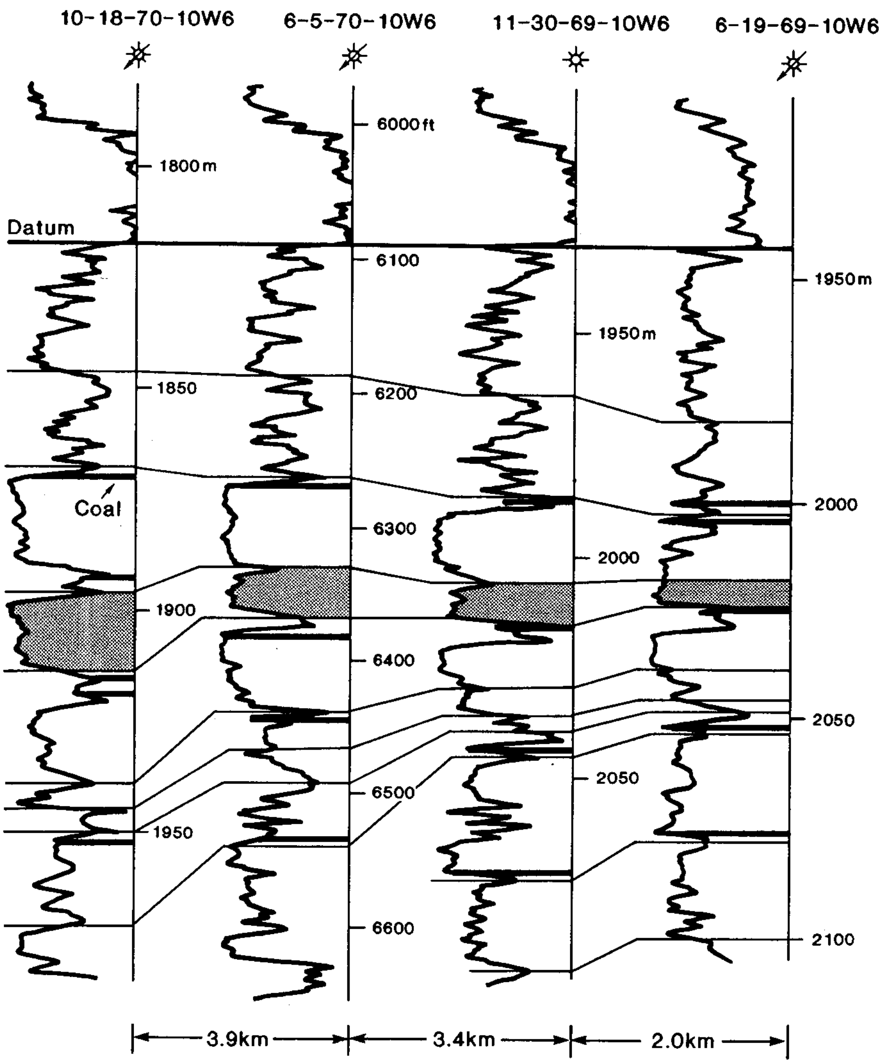

Figure 4 A gamma-ray cross section in the Upper Mannville Group of Alberta illustrating correlation by pattern matching. The correlations have been made using the following criteria, 1) facies successions do not show abrupt lateral changes in character, 2) facies successions do not show abrupt changes in thickness, 3) facies successions do not show seaward (right to left) coarsening, 4) correlated surfaces slope seaward (to the left). Coals (black) were identified on sonic logs. These logs are not spaced proportionally to the distances between wells.

Dipmeter log

This log is made by a resistivity tool with three or four electrodes mounted on separate arms with a common centre point. The orientation of the tool is also continuously recorded. Where a dipping bed is encountered, the response to the lithologic change takes place at different elevations on each arm. The direction and magnitude of dip can be calculated from this information.

The dipmeter measures structural dip, but can also detect various types of sedimentary dips such as a compaction drape over a reef, a sloping mud drape, or even some cross-stratification. In many cases, it is difficult to determine the nature of a dipping surface unless a core has been cut.

CORRELATION OF LOGS

Correct correlation of stratigraphic units is absolutely necessary to make reliable cross sections and maps, and to conduct regional facies analysis. Complex numerical procedures for matching and correlation of logs (such as a method adapted from gene-typing techniques; Griffiths and Bakke, 1990) may be the primary tools in the future. At present, most geologists match log patterns by eye (or by tracing and overlaying logs), allowing for variations in lithologies, thicknesses, and completeness of section. Three major correlation methods will be discussed, 1) marker beds, 2) pattern matching, and 3) slice techniques.

Marker beds

The log response ("kick") of a distinctive bed or series of beds can be used as a marker (e.g., Fig. 19 in Chapter 12) even if the lithology or origin of the bed is not known. Distinctive, laterally extensive groups of beds commonly result from transgressions or regressions or erosional episodes which redistribute proximal sediment far across the basin. Markers that can be mapped regionally may therefore be related to, or include, important allostratigraphic surfaces. For example, condensed sections (possibly expressing maximum flooding surfaces; Chapter 1) are perhaps the most extensive marker beds, and are extremely useful because they are essentially time lines. In the Alberta Basin, the Fish Scale Horizon is a shale rich in organic debris. It can be identified over most of the basin by its characteristic high-gamma ray, slightly high-resistivity, and high-porosity values. It is used in many studies of the units above and below it (particularly the Viking Formation), as a horizontal datum for cross sections. The top of the Middle Mannville Bluesky Sandstone is also a prominent marker in the Mannville Group. The Bluesky is a shoreline deposit abruptly overlain by marine shales; this contact is a bounding discontinuity used to define allostratigraphic units.

In other situations, markers are not related to allostratigraphic units. For example, volcanogenic bentonites are easily recognized on logs (Table 1), providing reliable markers as well as time lines.

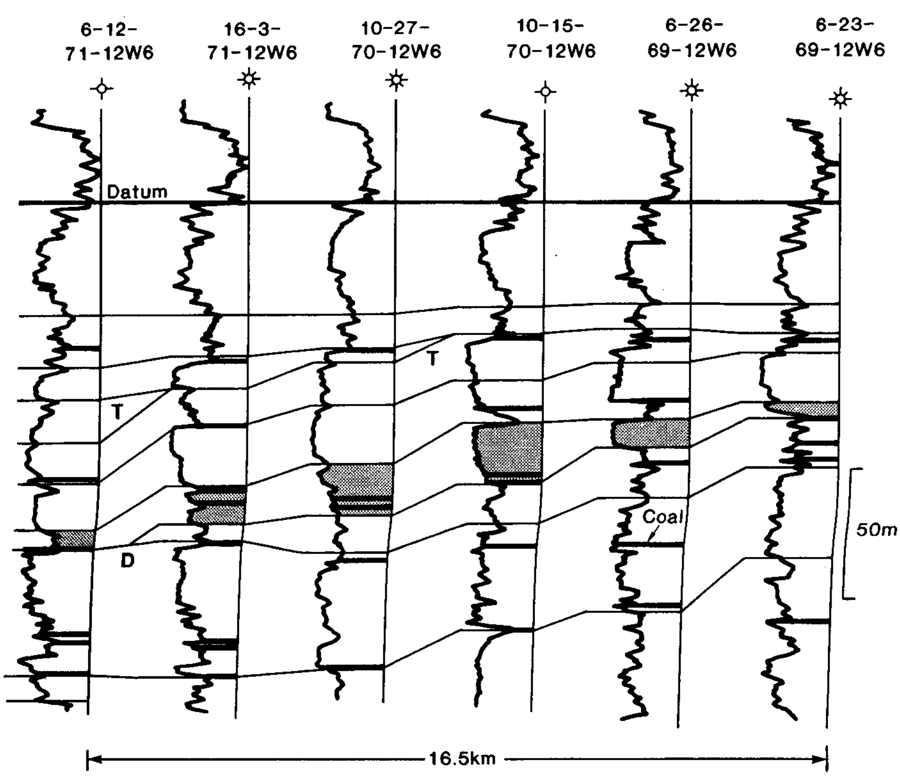

Figure 5 Gamma-ray cross section correlated by pattern matching which shows facies successions sloping seaward and downlapping against a lower surface. Correct pattern matching allows identification of allostratigraphic surfaces such as this. D indicates downlap and T indicates toplap. The logs are not spaced proportionally to distances between wells.

Pattern matching

This technique involves recognition and matching of distinctive log patterns of any origin. The correlated patterns may represent vertical facies successions (Fig. 4), superimposed facies successions, or unconformity-bounded units (Fig. 19 in Chapter 12). The surfaces of the units chosen may be transgressive and separate individual facies successions (Fig. 4). Alternatively, surfaces of maximum transgression separate composite-transgressive from composite-regressive units (to be discussed in more detail below). The bounding surfaces of the chosen units may also be unconformities, such as Cardium Formation surface E5 (Fig. 19 in Chapter 12).

By matching patterns, correlations are made on the basis of log shapes over intervals of metres or tens of metres, rather than on individual peaks, troughs, or markers within the succession. Pattern matching may allow correlation even where lateral variations in lithologies, facies, and thicknesses of units have occurred (Fig. 4). In difficult cases, matching is facilitated by tracing one log and overlaying it on an adjacent log. The logs can be moved up and down until the best overall fit is obtained. Constantly changing positions of fit may indicate lateral facies or thickness changes, and may indicate synsedimentary tectonism.

Pattern matching is extremely useful because it can be used to correlate facies successions or allostratigraphic units as defined from cores or outcrop. It therefore facilitates investigation of regional facies relationships. Examples of this are shown in Figure 15 of Chapter 12, and Figure 16 of Chapter 9. Detailed pattern matching of individual facies successions may delineate surfaces of toplap, downlap or onlap (Fig. 5), and can therefore be used to define large-scale or composite allostratigraphic units. Pattern matching has worked extremely well in many studies of shallow-marine sediments in the Cretaceous Western Interior Seaway of North America, largely because of the lateral uniformity of these rocks (at least compared to other facies).

Certain assumptions about the styles of lateral variation of facies must be made in pattern matching in order to decide between alternative possibilities. For example, the cross sections of Figures 4 and 5 show that in these shoreline-to-shallow-marine clastics, the correlated units satisfy a number of conditions: 1) individual facies successions do not show abrupt changes in thicknesses, log patterns, or inferred grain size patterns; 2) individual successions do not show seaward increases in the thicknesses of sandstones; 3) successions slope gradually seaward (unless synsedimentary or postsedimentary tectonism has occurred); and 4) abrupt lateral changes in facies successions imply that an unconformity exists. Readers may be able to make different correlations through the same wells, depending in part on the initial assumptions made.

Slice techniques

As a method of last resort, when no other method yields results, an interval can be subdivided by arbitrarily slicing it either into units of constant thickness, or into units with thicknesses proportional to the entire interval (Fig. 6). Slicing an interval does not give true correlations; it is only a way of splitting a section which cannot be subdivided any other way. The implicit assumption is made that time lines through the interval are essentially horizontal. Where this assumption is invalid, slice techniques may yield results which are grossly in error. It is a means of last resort, but is necessary in some situations which do not yield to the other methods discussed above.

The thicknesses of slices should be chosen to minimize complications. For example, if sandstones in an area average 30 m in thickness, the choice of slices less than 30 m may not yield interpretable results. In some cases, trial and error is necessary to find the optimum solution.

Slice techniques are most commonly applied in nonmarine deposits. Here, other techniques do not work well because of the lack of continuous beds and absence of laterally extensive facies successions. By noting the stratigraphic position and thickness of each lithologic unit with respect to a marker (commonly the top of the unit), the data is in a form of maximum utility when computerized. Thicknesses of slices can be changed easily until patterns emerge. Note that slice techniques may produce correlations which cut across depositional units or unconformities if they are applied to units with sloping depositional surfaces. Flach (1984) has used this technique to map sandstone-filled channels in the nonmarine to estuarine McMurray Formation of Alberta. He was able to show the locations of the major oil sands reservoirs at different stratigraphic levels even though precise correlation could not be achieved.

SUBSURFACE MAPS

Mapping in the subsurface differs little from surface work except for the huge volume of data which can be collected from a large number of wells. Computerization of data bases and land survey systems has progressed to the point where automatic map production of some attributes is done routinely and quickly.

Subsurface geological maps are either compilations of data, or interpretive summaries. Data compilation maps of many different quantities have been made, but for stratigraphic and sedimentological purposes, there are three main types, 1) structure maps that show the elevation of a surface (the example in Fig. 20 of Chapter 12 is similar to a structure map), 2) isopach maps that show the thickness of a unit (Fig. 21 in Chapter 9), and 3) lithological maps that show the composition of a unit in one of several ways (Fig. 23 in Chapter 9). Examples include maps of the thickness of carbonate rocks as a percentage of the total thickness, maps of net sandstone thickness, or maps of the ratio of clastic to carbonate thicknesses. Full descriptions of the different map types are given by Krumbein and Sloss (1963) and Miall (1984). Interpretive summary maps and block diagrams of such aspects as facies distributions, paleogeographies, and sediment supply directions are also commonly made (Figs. 18, 21, 22 in Chapter 12; Figs. 11, 18 in Chapter 9). Note that all maps depend absolutely on correct correlation of units. If correlations are wrong, the resulting maps will be worthless.

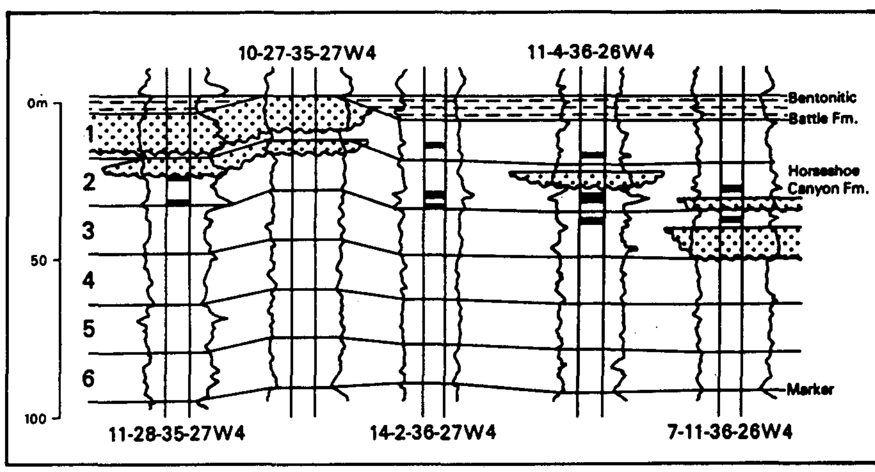

Figure 6 Cross section (gamma-ray logs on left, resistivity logs on right) from the Upper Cretaceous Horseshoe Canyon Formation, Alberta. The section between the Battle Formation and the basal marker was subdivided into six equal slices, chosen to include but not split the major channel sandstones. Simplified from Nurkowski and Rahmani (1984).

SUBSURFACE FACIES ANALYSIS

Without cores, the definition and interpretation of facies in the subsurface are generalized and imprecise. Making lithological logs of cores is similar to the measurement of outcrop sections, the most obvious differences being the scale of features which can be observed in a limited-diameter (commonly 9 cm) core, and the lack of oriented sedimentary structures for paleocurrent analysis. Shales and mudstones, however, are commonly more easily studied in cores than in outcrops (the trace fauna is particularly well displayed in cores, Chapter 4). Cores should always be examined with the logs present to check for completeness of recovery, core-log correlation, and log responses. Well-log cross sections (Fig. 15 in Chapter 12; Fig. 19 in Chapter 9) and appropriate kinds of maps can extend the interpretations made from cores, and set them into a larger-scale stratigraphic and paleogeographic context.

Log curve shapes

The shapes of well-log curves have long been interpreted in terms of depositional facies because of their resemblance to grain size successions (e.g., Selley, 1978). Where SP-Resistivity or Gamma-Sonic pairs of logs are used, the patterns are mirrored, resulting in (among others) bell-shaped and funnel-shaped profiles (note the funnel in the lower half of well 7-10-62-7W5 in Figure 15 of Chapter 12). Much published work uses a simplistic "pigeon-hole" approach to interpretation. An example is the classification of bell-shaped gamma-ray profiles as fining-upward meandering-stream facies successions. Problems with this approach will be discussed below.

The most typical vertical patterns seen on gamma-ray, SP and resistivity logs are shown in Figure 7. *It is emphasized in this diagram that no pattern is unique to, or diagnostic of, any particular depositional environment. It follows that interpretation based on log curve shape alone is extremely imprecise.* In those specific studies where log patterns have been calibrated to well-understood depositional facies successions in cores and/or outcrops, the log-pattern method can be applied successfully to the interpretation of correlative uncored facies successions.

The scale of facies successions is also a very important criterion constraining the interpretation of curve shapes. For example, funnel-shaped patterns (Fig. 7) may range from a few metres to several hundred metres in thickness. These are appropriate scales (respectively) for a crevasse splay building into an interdistributary bay (Fig. 5 in Chapter 9), and a prograding deltaic succession (Figs. 7, 16 in Chapter 9).

Difficulties in interpretation of log patterns may result from deviations of individual facies successions from the general model in Figure 7, possibly in

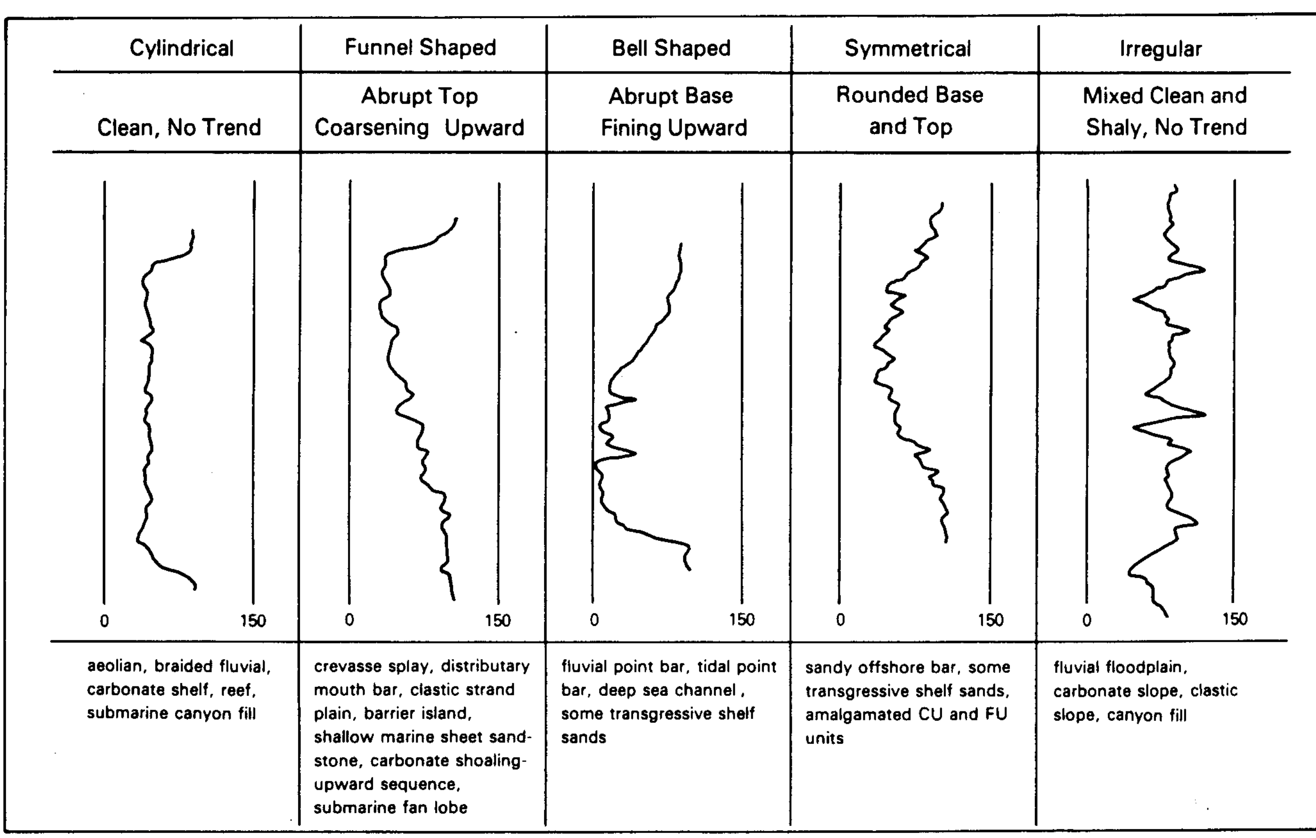

Figure 7 The most common idealized log curve shapes which may be interpreted by correlation with many different core examples (see other chapters). Where resistivity or sonic logs are shown opposite gamma-ray logs, the patterns are mirrored, resulting in the *bell* and *funnel* labels. The limitations of this approach to facies analysis, in the absence of other data, is emphasized in the text, and by the multiple possible environmental interpretations indicated below each curve. Log curve shapes, in the absence of other data, are not diagnostic of particular environments.

some cases because of base-level changes. Other difficulties result from the amalgamation of units. For example, the standard clastic prograding shoreline succession (left side of Fig. 14 in Chapter 12) generates a continuously upward-broadening funnel-shaped gamma-ray pattern (Fig. 7). *Sharp-based* sandy shoreline facies successions (right half of Fig. 14 in Chapter 12, also Fig. 15 in Chapter 12) may result from small drops in relative sea level followed by progradation (forced regression, Chapter 12), or erosional transgression followed by shallow water regressive deposition (Chapter 12). In both of these cases, the typical funnel-shaped log pattern is replaced by a cylindrical or blocky profile (Fig. 15 in Chapter 12), probably not correctly interpretable from log pattern alone.

Amalgamation of facies successions can also alter the standard log profiles of Figure 7. Superimposed channel deposits of meandering rivers can generate a stacked sandstone body characterized by a cylindrical log profile. Similarly, a transgressive sandstone capped by a regressive shoreline sandstone may be characterized by a cylindrical profile and conceal a transgressive unconformity or ravinement (Chapter 12). In the Middle Mannville Bluesky Formation, shoreline sandstones are in some places superimposed directly on nonmarine sandstones in the overall transgressive succession. These form sharp-based, cylindrical log patterns. These examples illustrate that simplistic labelling of log curve shapes in terms of depositional environments, without core or outcrop information, should be avoided.

RECOGNITION OF BOUNDING DISCONTINUITIES

Allostratigraphic units are defined by their bounding discontinuities (Chapter 1). Because subsurface data can be used to document lateral relationships on a large scale, recognition of these discontinuities (maximum flooding surfaces, surfaces of marine transgression and regressive surfaces of erosion) has become extremely important in subsurface investigations. Delineation of these discontinuities allows stratigraphic subdivision of rocks into large-scale genetic packages, with possible implications for large-scale facies relationships.

Condensed sections

These stratigraphic intervals represent periods of very low sedimentation rates in marine depositional environments as a result of major transgressions (Fig. 27 in Chapter 13). They commonly characterize maximum flooding surfaces, and can also be present at marine flooding surfaces (Chapter 1). Condensed sections in clastic rocks are commonly formed as a result of cut-off of clastic supply. In carbonate successions, the sediment-producing environments are drowned. Condensed sections may show up lithologically in carbonate (and some clastic) successions as hardgrounds with early diagenetic carbonate and phosphatic cementation (see Chapter 4). In other clastic successions, they occur as intervals of oolite and lime mud sedimentation. In basinal shales

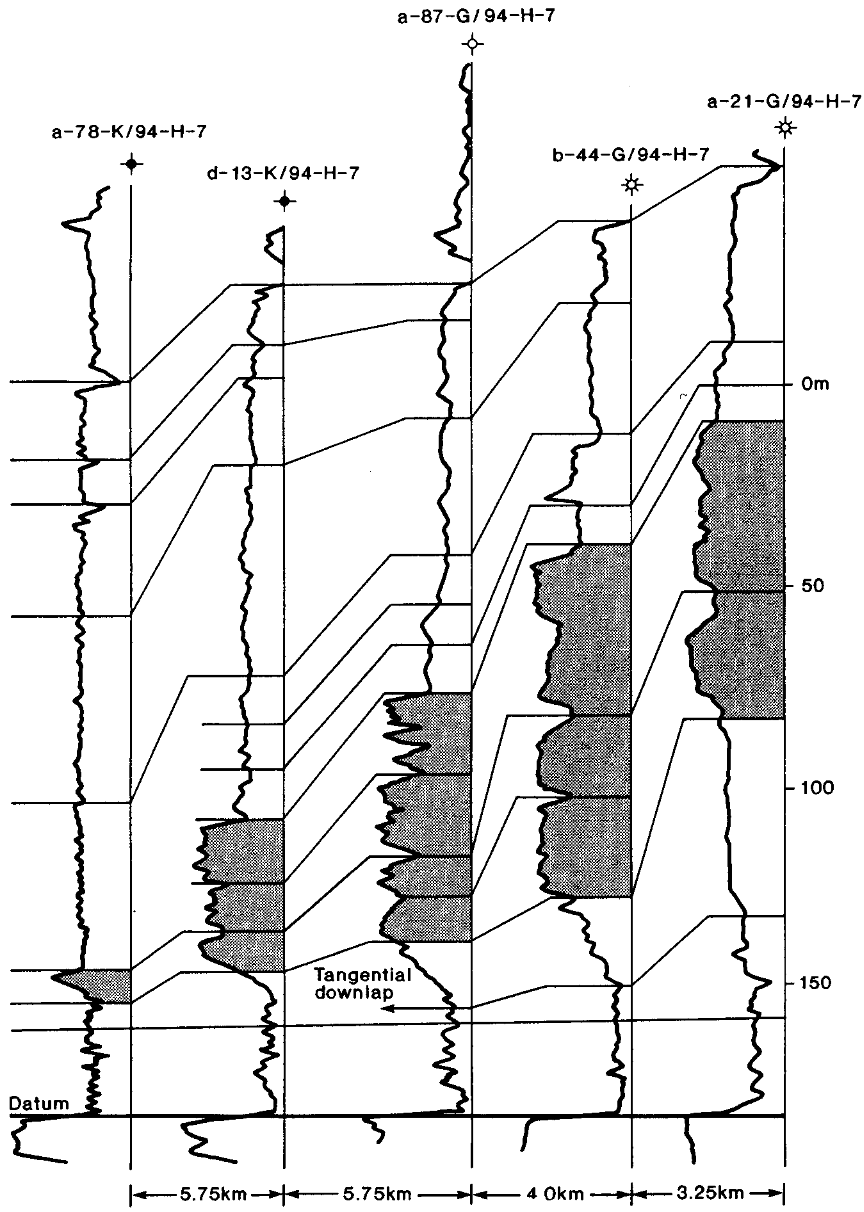

Figure 8 Gamma-ray cross section from the Upper Mannville Group in British Columbia, correlated by pattern matching. The correlation lines slope seaward (to the left), outlining clinoform surfaces which tangentially downlap onto transgressive shallow-marine shales. The section is hung on the top of the Middle Mannville Bluesky Formation (Datum). The maximum flooding surface is the top of the transgressive shale (about 25 m above Datum). The sandstones (shaded) were deposited on the original clinoform slope. The logs are not spaced proportionally to distances between wells.

the condensed horizons may be organic-rich radioactive shales, or pelagic deposits such as chalks or chalky shales. Because of these lithologic contrasts with adjacent rocks, as well as their wide lateral extent in many basins, condensed sections may be recognized on logs as marker beds with characteristically different well-log responses. A good example is the Fish Scale Horizon, which is commonly used as a horizontal datum for regional cross sections in the Cretaceous of the Alberta Basin.

Many condensed sections are overlain by downlapping depositional surfaces or clinoforms which may be recognized on seismic lines (see Seismic Stratigraphy section below), well-log cross sections (Fig. 8), and a few large outcrops. Clinoforms are developed in response to transgressive deepening followed by the re-establishment of laterally prograding sedimentary layers. In Figure 8, regressive shelf-to-shoreline clastic facies successions slope seaward creating a clinoform, and terminate against, or downlap onto the transgressive shales and sandstones below. The condensed section (and in this case, the maximum flooding surface) lies directly below the surface of downlap. In some nonmarine units, surfaces similar to condensed sections may be characterized by thin brackish to marine shales and limestones deposited in lagoons and estuaries as a result of transgression.

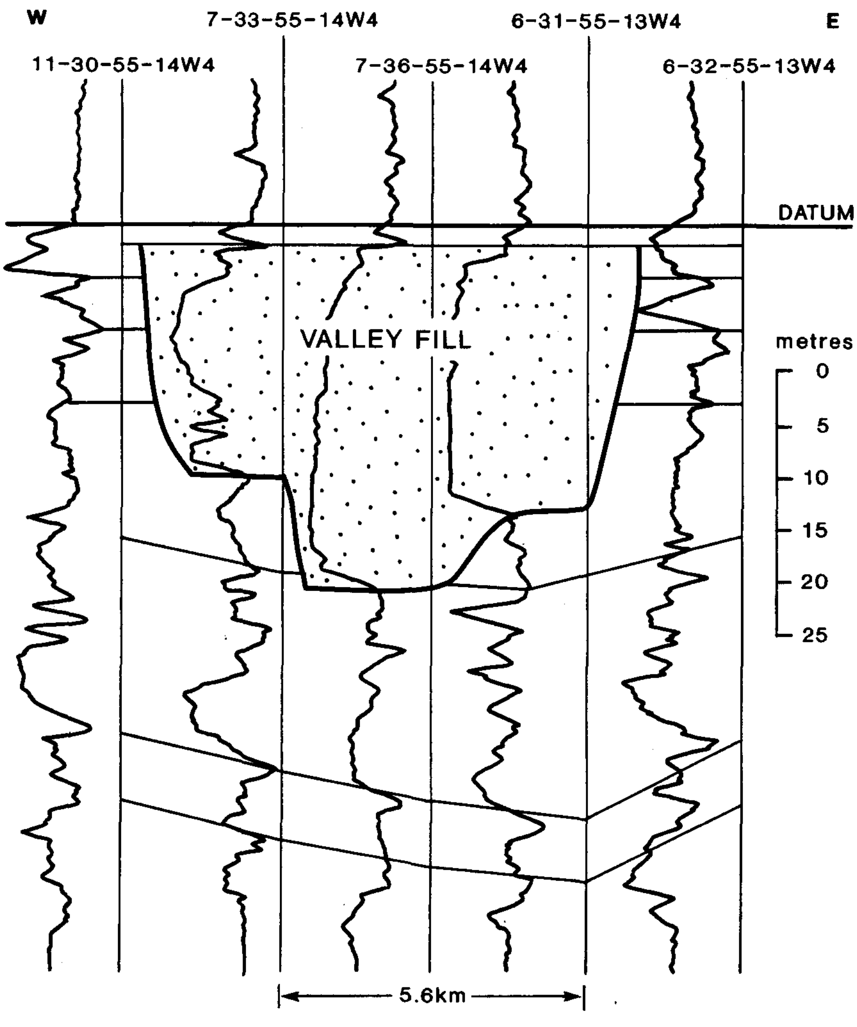

Figure 9 Gamma-ray cross section from the Upper Mannville of eastern Alberta. The regionally correlative log patterns in these fluvio-deltaic deposits (shown at each end) are replaced locally by the valley-fill sandstone. Mapping has shown these anomalous gamma-ray log patterns occur in a linear trend. Detailed pattern matching across the sandstones implies later incision of valleys into the top of the unit, rather than a contemporaneous channel.

Unconformities

Surfaces of erosion or bypass are generally identified where underlying markers or facies successions are truncated (Fig. 19 in Chapter 12), or overlying ones show onlapping relationships. Well-log cross sections of marine rocks commonly allow definition of very low-angle, regional unconformities which may be undetectable on the scale of most outcrops. The Cardium erosion surface designated E5 is a good example (Chapter 12). In shoreline to nonmarine deposits, regional truncations are much more difficult to detect because of the absence of extensive marker beds or easily correlated facies successions. As shown in Figure 5, detailed correlations of shoreline facies successions may show surfaces of onlap and downlap, hence defining minor bounding discontinuities.

In other examples, unconformities may be inferred in shoreline and nonmarine sections where locally distinctive stratigraphic units or successions recognizable locally are cut out and replaced by anomalous units. An example is shown in the cross section (Fig. 9) from the Lower Cretaceous Mannville group of eastern Alberta. Here, the gamma-ray logs in wells 11-30-55-14W4 and 6-32-55-13W4 can be correlated in detail by matching coarsening-upward and fining-upward patterns in these shoreline and nonmarine sediments (interpretations from numerous cores). Sonic and resistivity logs (not shown) were also used to make the best possible pattern matches. The thick sandstones just below the datum in wells 7-33, 7-36 and 6-31 are anomalous deposits which locally replace the interbedded sandstones and shales. Numerous cores and some outcrops show that these thick sandstones are fluvial to estuarine in origin. Mapping has shown that they are linear bodies extending for tens of kilometres along the basin, but generally less than 5 to 8 km wide. Reasonable correlations can be made between the sediments on either side of the channel (Fig. 9, wells 11-30 and 6-32), probably indicating that layers were once continuous, but have subse-

Figure 10 The seismic image of an unconformity (or any other surface) depends on the acoustic impedance across it. The upper diagram shows rock units with their sonic velocities (km/sec). The lower diagram shows reflections, with amplitudes indicated by the thicknesses. The polarity of the reflection (i.e., whether a peak or a trough is generated first) depends on the impedance change, whether positive or negative. Where the polarity is reversed, the unconformity is indicated by a wavy line. The shaded peak of the reflection actually occurs one-half wavelength below the unconformity here.

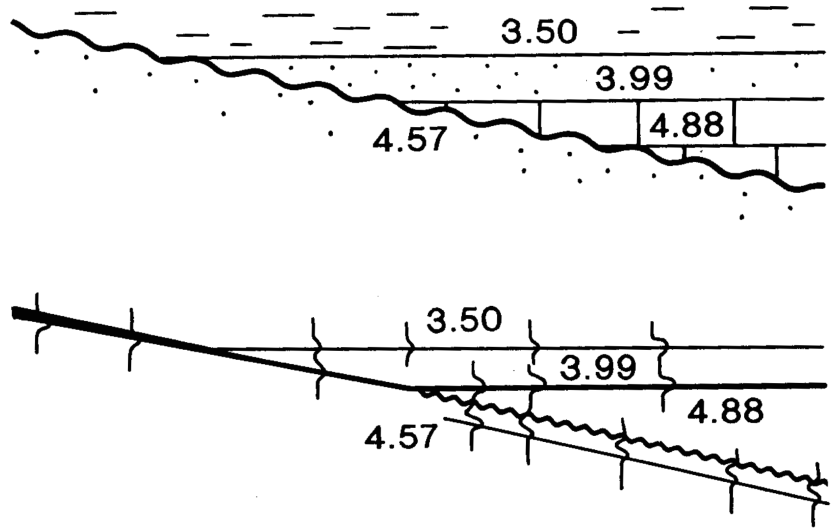

Figure 11 Well 6-33-14-13W4, in southern Alberta, showing (right) a gamma ray log, (top left) a display of sonic log data from the well, seismic data from shot points 194 and 196, with the synthetic seismogram between them, and (bottom left) a seismic line through the well. The tops of the Mannville Group (MNVL), Middle Mannville Ostracod Zone (OCDZ), and Mississippian (MSSP) are marked on each. The shot points (SP) are indicated above the seismic line. The peak (to the right) of each reflection is infilled. Note the lack of vertical resolution of the seismic data compared to the well log. However, the seismic line shows the context of the lower Mannville sandstone in a valley cut on the sub-Cretaceous unconformity. Note the truncations of reflections at the sub-Cretaceous unconformity. Modified from a well-integrated subsurface geology and seismic study by Hopkins *et al.* (1987).

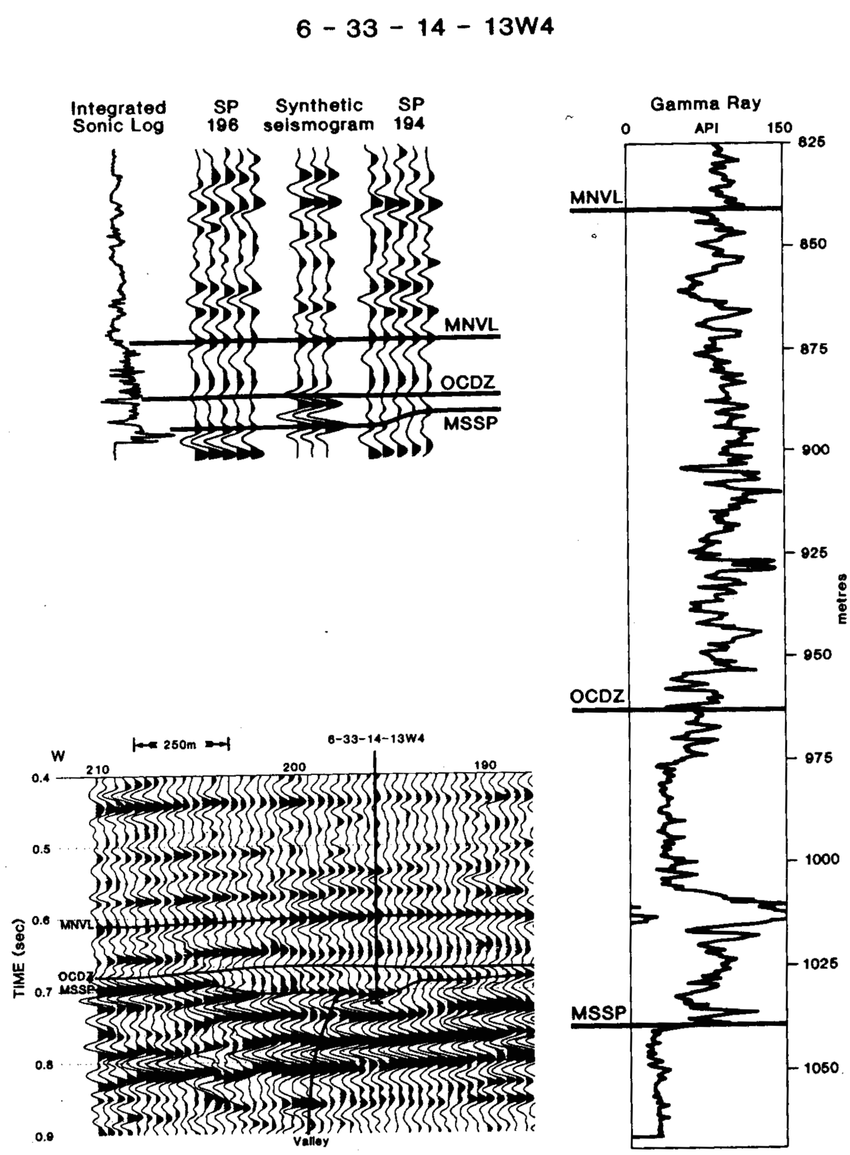

quently been incised by valleys. A series of correlative incision events at the same stratigraphic level marks an unconformity which is undetectable where the channels are absent. These anomalous sandstone units were therefore deposited within valleys cut as part of an unconformity that developed on fluvial and thin deltaic sequences. The most generally accepted interpretation of the series of events in this part of the Mannville Group (Fig. 9) is: 1) deposition of the interbedded fluvial and deltaic sands and shales, 2) drop of relative sea level, allowing the incision of 30 m-deep fluvial valleys through the coastal plain, 3) rise of relative sea level (transgression) and salt water invasion of the valleys, forming linear estuaries, and 4) complete filling of the valley by transgressive sediments grading from fluvial to estuarine deposits.

This interpretation illustrates the integration of facies analysis performed on cores with allostratigraphic analysis essentially done on well-log cross sections. By itself, core logging could not have shown the relationships between the estuarine deposits and the older deltaic sediments. Equally, allostratigraphic analysis of cross sections would not have yielded much information about the nature of the sediments and their relationships to sea level.

SEISMIC REFLECTIONS

Seismic surveys are conducted to investigate subsurface geology by sending compressional sound waves into the earth and detecting the reflected or refracted energy returning to the surface. Shallow (up to several hundreds of metres penetration) single-channel systems (one receiver) or medium depth (up to 10 km penetration) multi-channel systems (many receivers, with digital data added mathematically) record entirely reflected energy. By moving the point of origin of the sound waves (the shot point) and the detectors, a continuous section of any desired length may be obtained. Seismic sections are normally shot in straight lines.

A seismic reflection is generated where a descending sound wave encounters an interface which reflects part of the energy back to the detectors. The reflectivity of a surface has been found to depend on the contrast in the density and sound transmission velocity of the materials above and below it. The product of these quantities is the *acoustic impedance* of the medium, and the strength or amplitude of a reflection from a surface depends on the acoustic impedance contrast or ratio, across it. Reflections are generated from stratigraphic surfaces such as bed contacts or unconformities only where a contrast in acoustic imped-

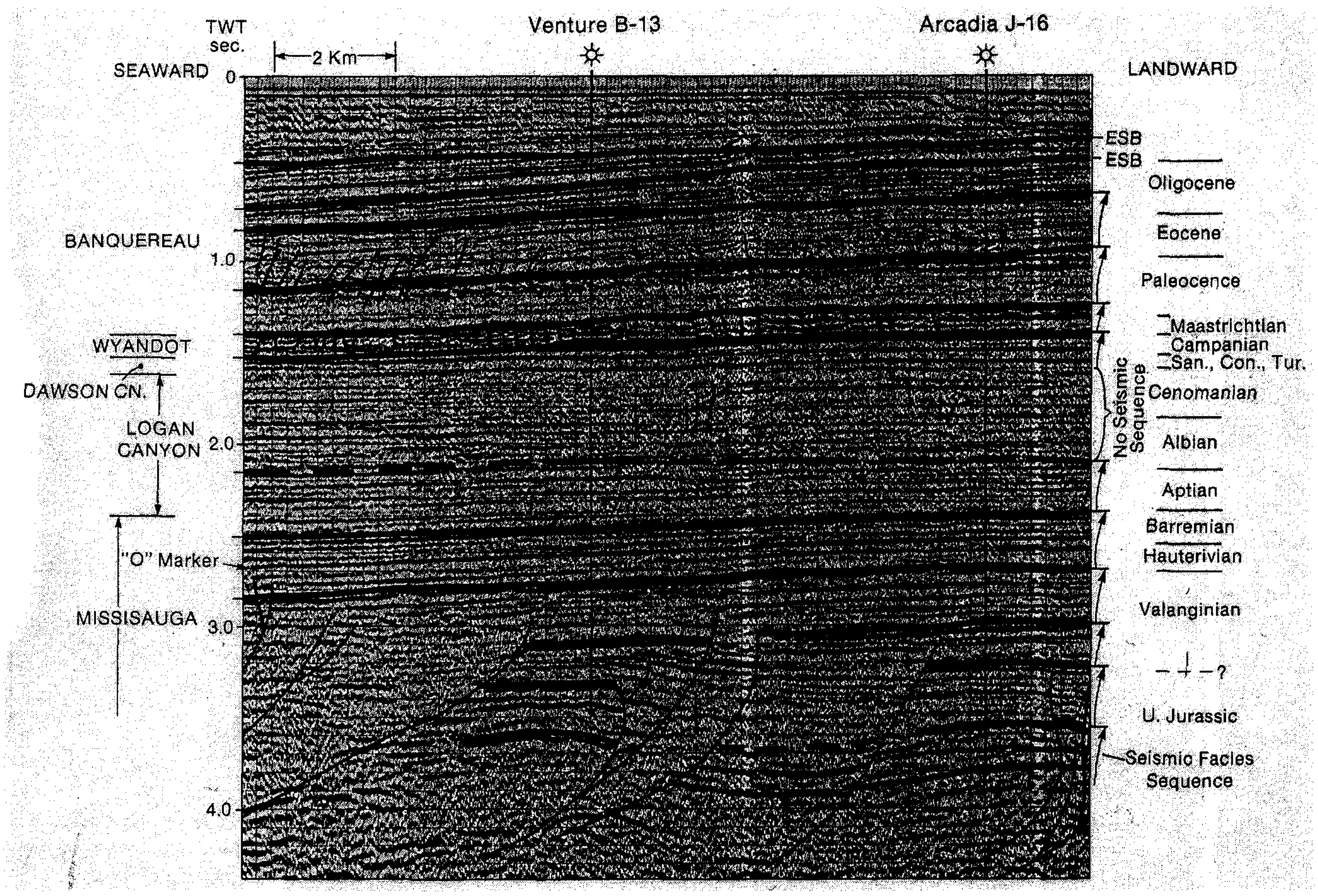

Figure 12 Seismic section from the Venture area, Scotian Shelf of eastern Canada. The horizontal scale is distance, but the vertical scale is two-way travel time (up to 4 seconds), and is nonlinear with respect to depth in metres (the Venture B-13 well is 5219 m deep). The age data and formation picks are from the two wells shown, tied in by synthetic seismograms. In this area, growth faults affect the Upper Jurassic to Lower Cretaceous section, but younger rocks are almost undisturbed. Curved arrows indicate units of upward-increasing reflection frequencies, amplitudes, and continuities. ESB indicates an erosional sequence boundary.

ance occurs across them. For example, an unconformity is not directly imaged if sandstones of similar velocity and density are superimposed above and below it. However, laterally, where the sandstone lies below a shale with lower velocity, a reflection is generated (Fig. 10).

A seismic section comprises a series of shot points displayed horizontally, and a series of reflections shown at different vertical distances. In Figure 11 (lower left), the shot points are 25 m apart, and each shot point has a seismic trace displayed beneath it. By convention, the right half of each trace is filled in (blackened), for illustrative purposes. Where the trace deflects markedly left or right, a reflection from an interface is indicated. Reflections are characterized by their amplitude and frequency, and by the degree of continuity of peaks and troughs from shot point to shot point. A seismic section appears very much like a geological cross section (Fig. 12), with a series of surfaces of contrasting acoustic impedance displayed horizontally, appearing like sedimentary bedding. However, a seismic section is not a geological cross section. Individual sedimentary units are not imaged, regardless of their lithology, if there is no impedance contrast at their surfaces. Also, the vertical dimension of a seismic section is not depth, but the two-way travel time (down and back) of the sonic wave (Figs. 11, 12). Because velocities generally increase with greater depths, the display is nonlinear with respect to depth. Depth conversion can be done roughly by using interval velocities, calculated during data processing, and commonly given at the tops of many sections. In Figure 11, the 200 m-thick Mannville Group is represented by about three peaks and troughs. Therefore the stratigraphic thickness represented by the average reflection (peak to peak) is about 67 m. It is therefore emphasized that one reflection does not represent a single bed, but a stratigraphic interval several tens to hundreds of metres in thickness.

In many cases, depths are obtained by using *synthetic seismograms.* Synthetics are created by assuming or

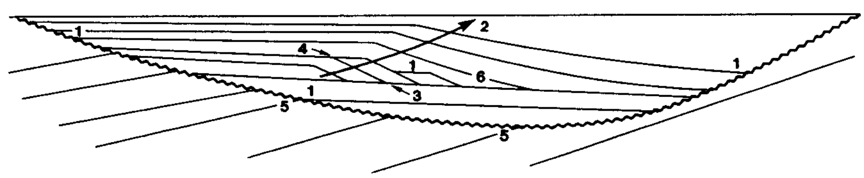

1 - Onlap
2 - Offlap
3 - Downlap
4 - Toplap
5 - Truncation (unconformity)
6 - Clinoforms

Figure 13 Stratigraphic patterns commonly seen on seismic lines, at many different scales. When combined with biostratigraphic dating, these patterns are the basis for interpretation of the stratigraphic history of a basin. Similar patterns but generally of a smaller scale, may be identified on correctly correlated well-log cross sections.

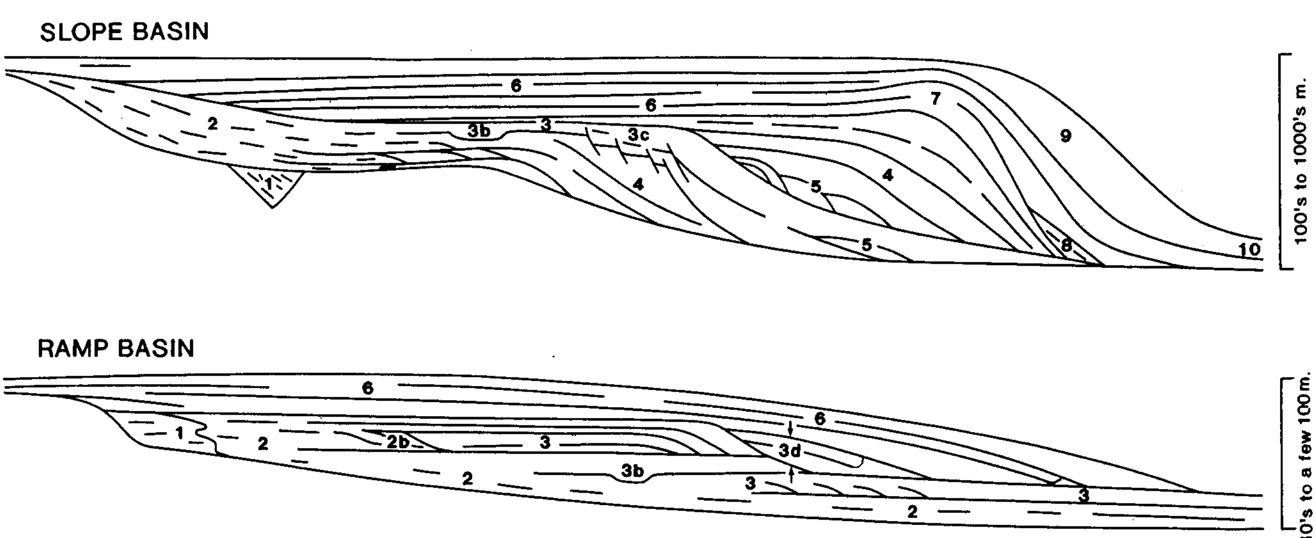

1 - Alluvial conglomerate and sandstones,lacustrine shales
2 - Non-marine clastic and coal
2b - Deltaic facies
3 - Shoreline to regressive shallow marine facies successions
3b - As above,but with incised non-marine fill
3c - As above,but growth faulted
3d - Shoreline deposits-isolated by base-level drop
4 - Slope shales and interbedded sandstones
5 - Deep marine clastic fans
6 - Lagoonal-Shelf carbonates;shale interbeds
7 - Reef
8 - Deep marine carbonate apron
9 - Carbonate slope,micrites and megabreccias
10 - Deep marine pelagic sediments

Figure 14 Composite diagrams of lateral facies relationships shown on seismic data in a slope basin (one with deep water such as a passive continental margin), and a ramp basin (one on the craton lacking very deep water). The depositional facies can be generally identified by the overall lateral relationships, and by the large-scale features such as the slope, the mounds, and the reefs that can be imaged.

measuring a characteristic seismic wavelet for an area, then mathematically combining it with depth, velocity, and density data from sonic logs used to calculate acoustic impedance contrasts. This procedure models or calculates from the sonic log data what the seismic response of the rock units should be. Visual comparison of amplitude and frequency patterns on the synthetic seismogram can be made with the real seismic record to estimate depths (from log depths) to reflections (Figs. 11, 13). Details of synthetic seismogram construction are given in a very understandable and readable form by Anstey (1982). A synthetic seismogram is a very powerful tool for calibrating the seismic response to the stratigraphy of an area, because it shows which lithologic interval is responsible for an individual reflection.

Single-channel seismic data (typical of marine geological investigations of the upper few hundred metres) are recorded directly onto paper by analog processes. Multi-channel seismic data (collected by the petroleum industry for exploration and development) are recorded digitally to allow subsequent numerical processing by large computers. Seismic processing consists of a complex series of numerical operations performed on the raw data. It is designed to enhance the reliability (reduce multiple internal reflections and spurious reflections), sensitivity (increase signal to noise ratio) and positioning (correct locations of reflections from dipping beds) of the data. It also allows the data to be displayed in an interpretable fashion.

Reflection amplitude, as mentioned above, is a function of acoustic impedance contrast. It is well enough preserved during modern processing that the relative strengths of reflections can be observed. Reflection frequency (time interval between peaks) depends on the spacing of reflectors as well as processing. Reflection continuity depends on the lateral extent of the reflector. Within a data set of relatively uniform conditions of acquisition, processing, and display, variations in these characteristics may be interpretable in terms of rock properties and sedimentary facies (see Seismic Facies section below).

A typical seismic line through the Venture gas field, Scotian Shelf, is shown in Figure 12. Individual shot points and traces cannot be seen on this scale, but the more or less horizontal dark lines in Figure 12 are reflections like those in the lower left of Figure 11. The seismic line has been annotated with formation names on the left end, and ages on the right.

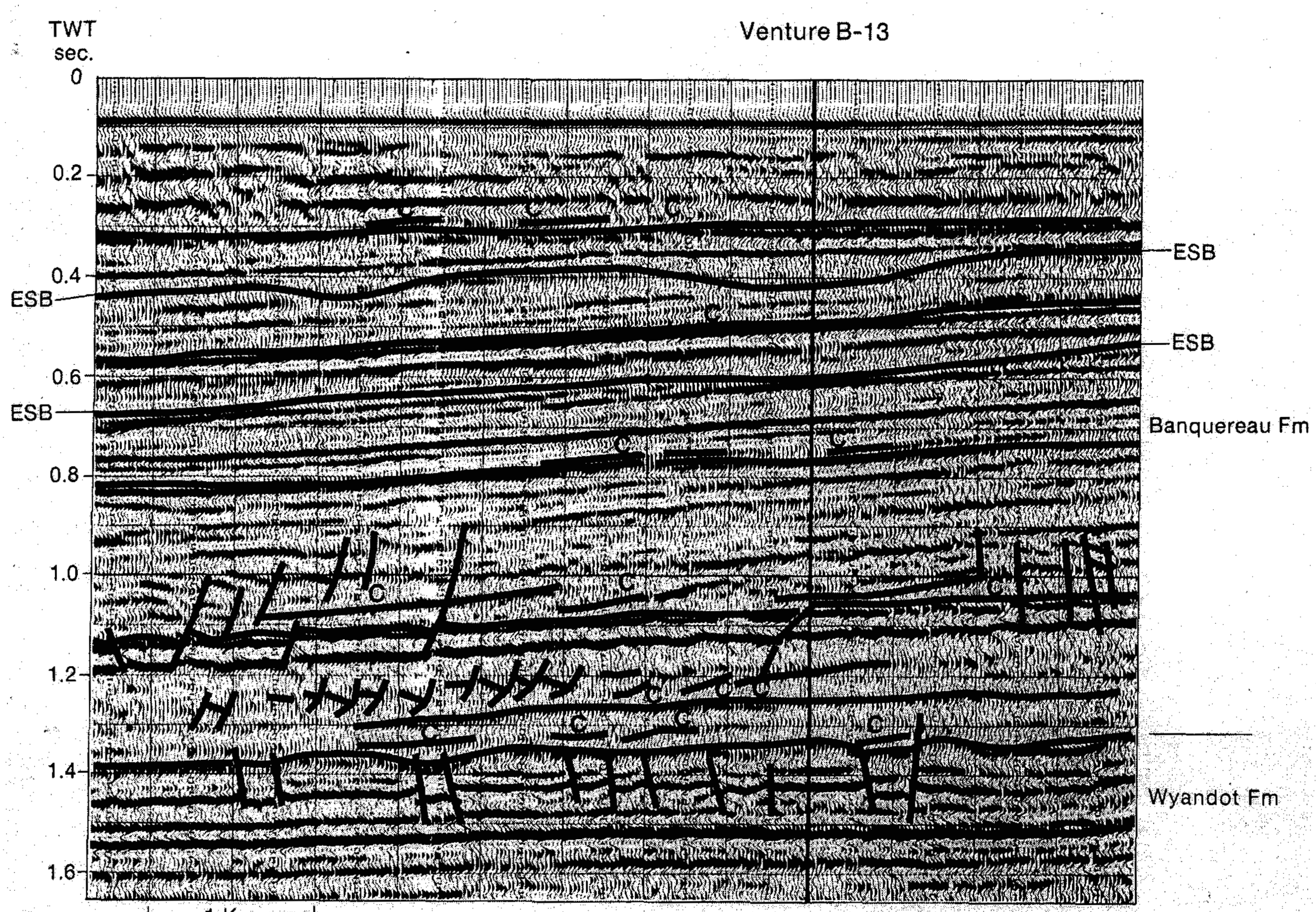

Figure 15 Upper Cretaceous and Tertiary section from the Venture area, Scotian Shelf. Erosional sequence boundaries (ESB) on seismic lines are indicated by truncation or onlap of reflectors. Clinoforms are indicated by "C". Many rotational normal faults disrupt the clinoform sets at the base of the Banquereau Formation. The high-amplitude reflections in the Wyandot Formation originate from chalk beds which are essentially analogous to a condensed section, deposited at the peak of the transgression when clastic input was low.

These data are derived from the two wells, as tied in with synthetic seismograms. In this case, seismic facies sequences were defined on variations in amplitudes, frequencies, and continuities of reflections. The growth faults in the Jurassic section and the minor fractures in the Lower Tertiary were delineated by correlating breaks in reflections. Detailed parts of this line will be discussed later in the chapter.

SEISMIC STRATIGRAPHY

Seismic stratigraphy involves the application of seismic data to the study of regional and global sedimentary sequences and their bounding unconformities. It grew out of investigations performed by the Exxon Production Research Company, summarized initially in Payton (1977). This publication explains many of the fundamentals of large-scale stratigraphic analysis (both seismic and otherwise) and must be understood by anyone attempting this kind of work. The interpretations of relative sea level changes *purely* in terms of eustacy (Vail *et al.*, 1977) have recently been modified by some workers, but the basic principles of seismic stratigraphy are demonstrated in this publication (Payton, 1977).

Figures 11 and 12 emphasize a fundamental condition of seismic stratigraphy, namely that the scale and resolution of multichannel seismic data are very different from outcrop or well-log cross sections. Particularly at great depths where velocities are high, seismic data are generally incapable of resolving stratigraphic features less than 50 to 100 m in thickness. These differences in scale of resolution are emphasized in the example from the Mannville Group of Alberta (Fig. 11), where a gamma-ray log, a synthetic of the well, and a seismic line, show the differences in degree of vertical resolution. Recent detailed work using well-log cross sections (Figures 5 and 9) has revealed several unconformities within the Upper Mannville alone, but these all occur within one *seismic* sequence (definition in Chapter 1). Many recurring stratal patterns are seen on seismic lines that are useful for stratigraphic subdivision and analysis of base-level changes. Figure 13 shows many of the more important configurations and the terminology applied to them. These configurations have been interpreted to result from eustatic variation of sea level, although other mechanisms are now considered possible (Chapter 1). However their origins are interpreted, these configurations are fundamentally important, large-scale features seen on seismic lines and some well-log cross sections.

Seismic reflections are in most cases generated where sharp lithologic contrasts occur between successive stratigraphic units. Lateral gradations of lithology or facies cannot be imaged. Sharp stratigraphic contrasts

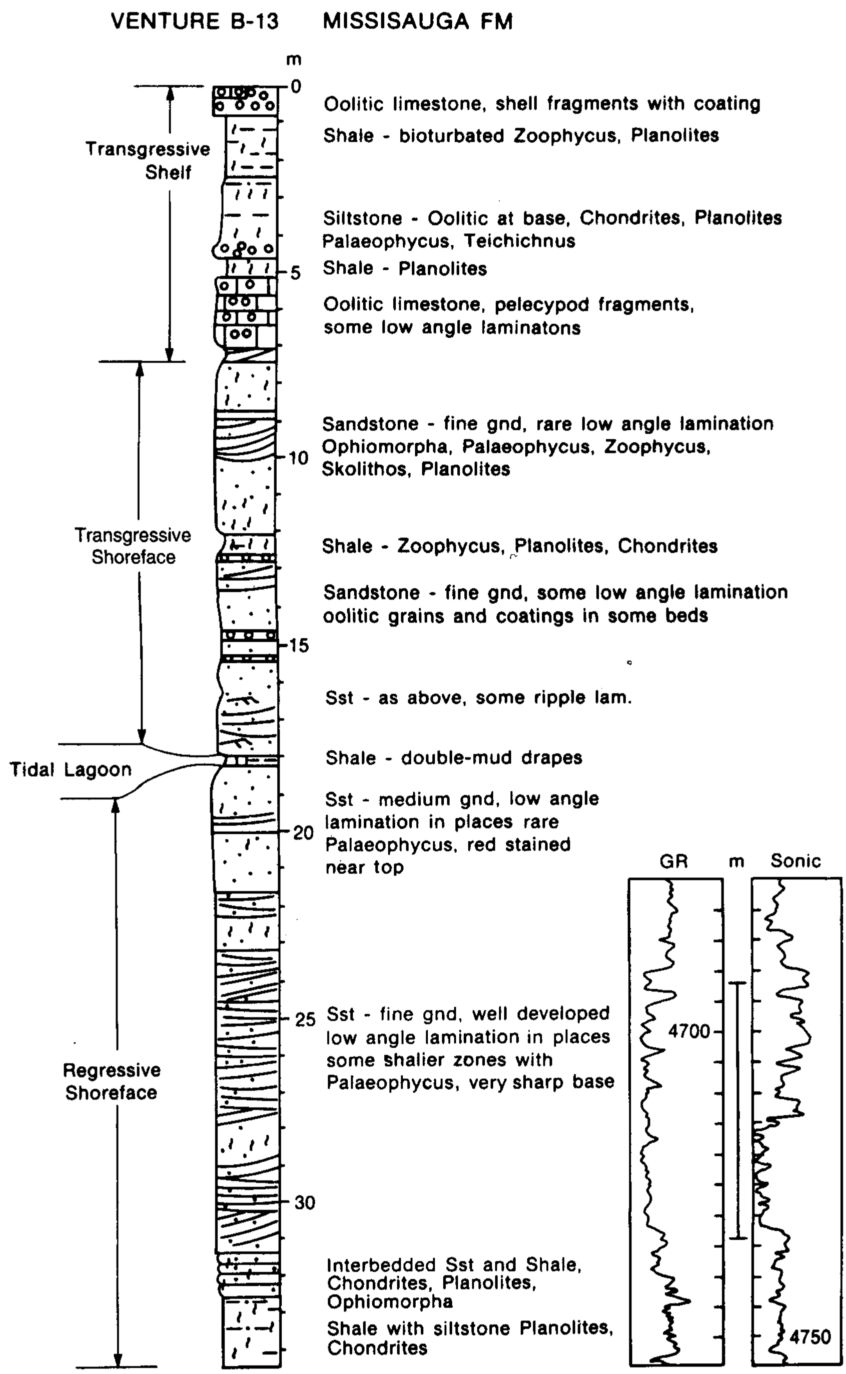

Figure 16 A core log from the Upper Jurassic-Lower Cretaceous Missisauga Formation, Scotian Shelf, showing a regressive shoreface sandstone, followed by a transgressive sandstone. The flooding surface occurs at the top of the oolitic carbonates (just above top of core). These transgressive carbonates generate high-amplitude, laterally continuous reflections on seismic lines. The patterns of upwardly increasing reflection amplitude, frequency, and continuity are shown in Figures 12 (curved arrows) and 17.

commonly develop where marine mudstones overlie sandstones as a result of marine flooding; seismic reflections therefore roughly follow these time surfaces. On many seismic lines (Fig. 14), individual reflections or packages of reflections are composite interference effects generated from stratal boundaries such as interbeds within facies successions, contacts between facies successions, and well-cemented transgressive condensed sections. These reflections follow stratal boundaries but cut laterally through lithologic and facies boundaries. They can commonly be traced from shoreline deposits through shallow and into deep marine deposits. For example, a reflection may follow the top of a shoreline sandstone. Farther offshore, this surface represents the top of a marine coarsening-upward succession, capped only by interbedded siltstones and shales. The interface between the top of the coarsening-upward succession and the succeeding shale is sharp, so that an impedance contrast results which follows the depositional surface. This surface is essentially a time line. No reflection is generated at the laterally gradational contact between the shoreface sandstone and offshore siltstone. This property is a fundamental characteristic of seismic reflections (Vail *et al.*, 1977), which may therefore extend along time surfaces from continental to deep marine facies, commonly following flooding surfaces. Because of the lack of resolution of seismic data at depths, individual facies successions are not generally imaged. Instead, reflections are composite interference effects from several successions. Seismic data can therefore delineate packages of sediment deposited in a wide range of environments, in a given time interval.

Bounding discontinuities and condensed horizons can commonly be identified on seismic sections, allowing for allostratigraphic subdivision (albeit on a relatively large scale). Because of lithologic contrast with the surrounding rocks, many condensed sections show prominently on seismic records (Fig. 15). They can be also be recognized by the presence of overlying clinoform sets (Fig. 15). Unconformities may or may not be directly imaged, depending on the acoustic impedance contrast across them. Angular unconformities can be traced by joining truncation points (Figs. 10, 15) of underlying (erosion) or overlying (onlap) reflections.

SEISMIC FACIES ANALYSIS

Facies concepts can be applied to seismic lines by analyzing portions with differing aspects. *Seismic aspects* include the major external morphologies of seismic features (e.g., the lens-shaped valley fill, lower left in Figure 11), or the internal reflection attributes (amplitudes, frequencies and continuity of reflections). Good examples are illustrated and discussed in Chapter 13.

Major external morphologies

Seismic data have a relatively low resolution, and reflections generally do not follow facies boundaries. Consequently, only those larger-scale depositional features with lithologies that contrast with the surrounding sediments can be imaged directly. These features include reefs, carbonate bank edges, delta complexes (Chapter 9), larger incised valleys, deep water slopes, and submarine fan complexes (Figs. 27-30 in Chapter 13). On some sections, the entire depositional spectrum from nonmarine to deep marine can be recognized (Fig. 14).

This kind of large-scale seismic facies analysis may be as simple as visual examination of reflection morphologies (as in the examples cited above), or may involve mathematical modelling of reflection patterns generated from idealized morphologies and lithologies of different depositional features.

Internal seismic attributes

On a more detailed scale, seismic facies can be based on internal reflection characteristics — the amplitude, frequency, and continuity of reflections. For example, high-amplitude discontinuous reflections indicate the

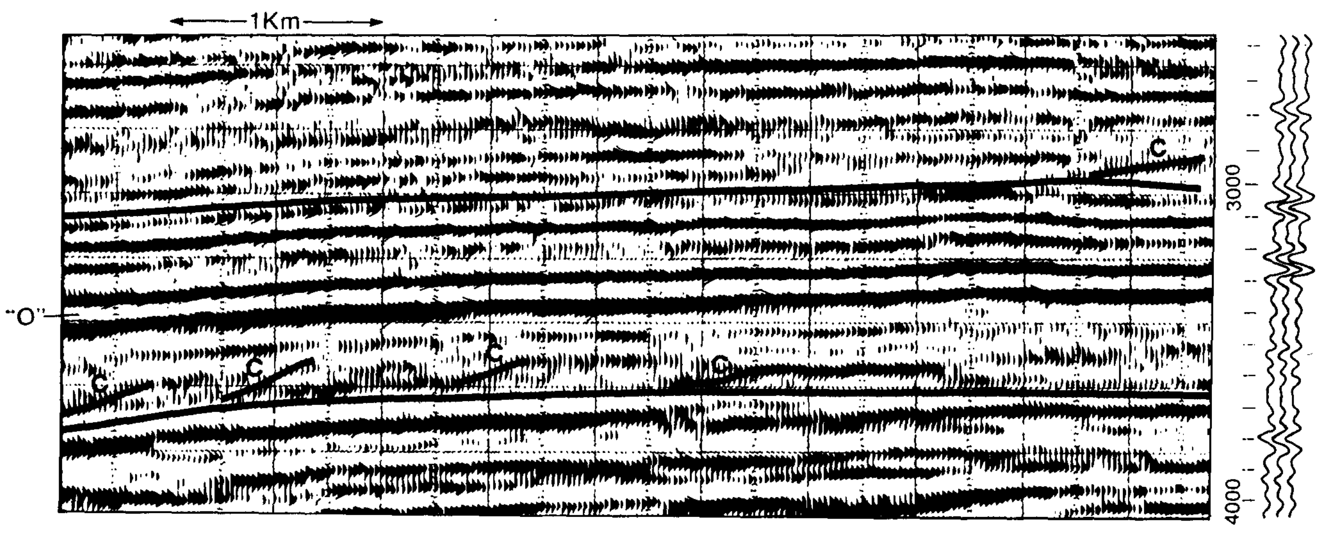

Figure 17 A small section of seismic line with a synthetic made from a well at its end, from the Scotian Shelf. Note the amplitude patterns on the synthetic which correspond to those on the line. The high-amplitude reflections are generated by beds of oolitic limestones deposited during transgressions over the shallow-marine sandstones and shales. "O" indicates one very laterally extensive limestone called the O Marker. "C" indicates small clinoform sets which are laterally discontinuous, but which mark the bases of the units.

complex stacking of thalweg sandstones and overbank mudstones in large submarine fan valleys (Fig. 29 in Chapter 13). Similar seismic facies occur in nonmarine fluvial deposits, with numerous variable-amplitude, discontinuous reflections related to the presence of high-reflectivity coals and discontinuous shales in overbank areas, cut out by sandstone-filled channels. This seismic character differs from the much more continuous, more constant amplitude reflections generated from shoreline and shallow-marine clastics (Fig. 12), and from continuous basin floor turbidites (Fig. 31E in Chapter 13). Highly continuous, high-amplitude reflections from interbedded shelf shales and limestones are easily separable in many examples from chaotic, almost reflection-free reef seismic facies. Some generalizations about clastic seismic facies have been discussed by Sangree and Widmier (1977) and Roksandic (1978), and carbonate seismic facies by Bubb and Hatlelid (1977) and Sarg (1988).

Where uniform seismic data collection, processing, and display have occurred, simple qualitative calibration of reflection characteristics to core and well-log data from a specific area can also be made. This calibration procedure is analogous to the calibration and interpretation of SP or gamma-ray log patterns but is probably even more risky because of the lack of resolution of individual successions on the seismic scale.

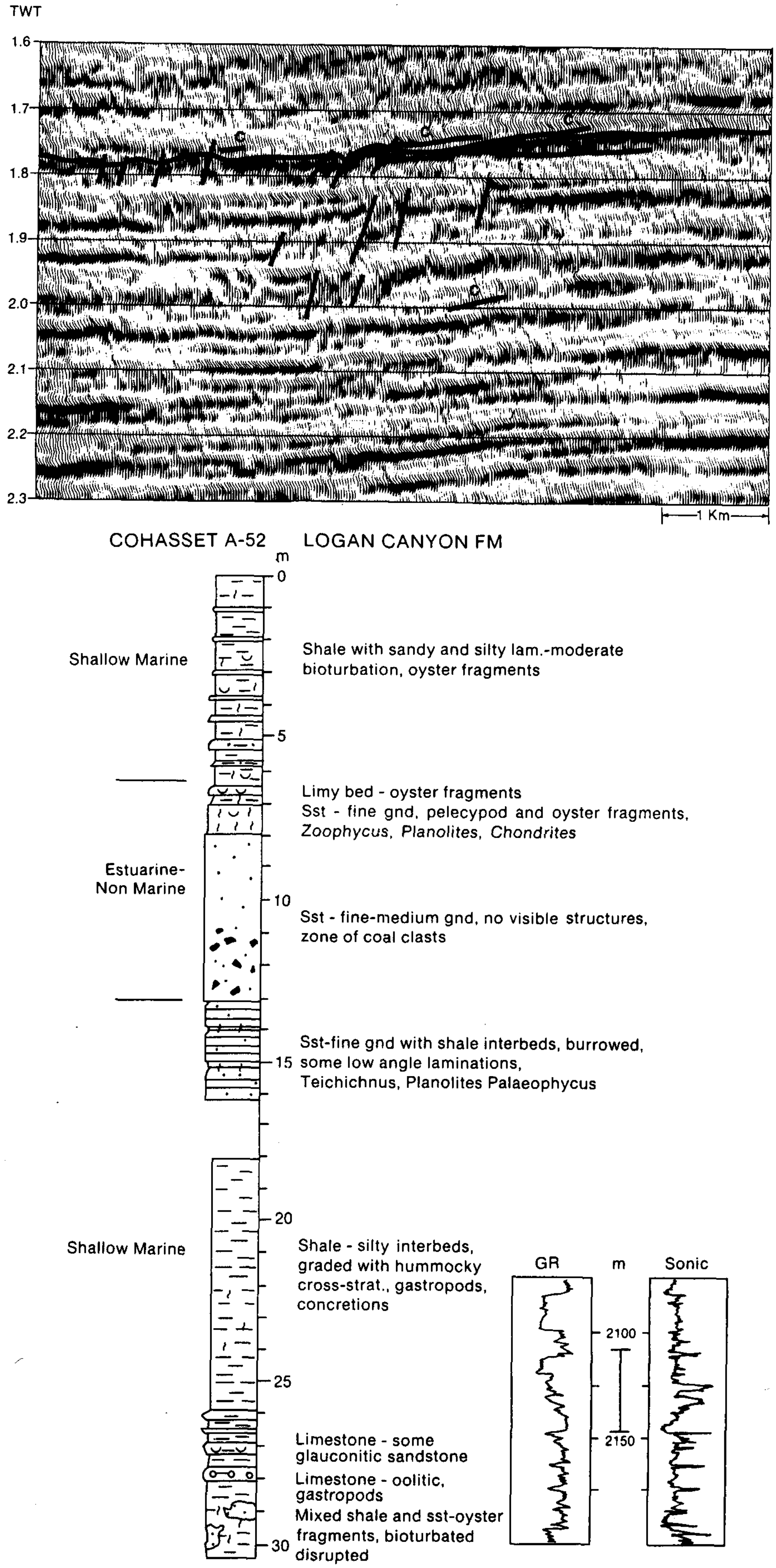

Figure 18 A seismic line with core and well-log control from the Upper Cretaceous Logan Canyon Formation, Scotian Shelf. The core suggests interbedded open marine (from micropaleontology) and estuarine deposits, with erosion and generation of intraclasts and coal clasts. The alternation of open marine and estuarine deposits is interpreted to result from short-period base-level drops which cut erosion surfaces on the shelf (see Chapter 11). The seismic line shows a complete lack of seismic-reflection patterns (compare to Figures 12 and 17). The core is equivalent to the section imaged between 1.9 and 2.0 seconds.

Calibration of well logs, cores and seismic responses: Scotian Shelf
This calibration has been carried out on two intervals of shallow-marine sediments on the Scotian Shelf of eastern Canada. The Upper Jurassic to Lower Cretaceous Missisauga Formation (Fig. 16) consists mainly of stacked coarsening-upward shallow marine to shoreline clastic facies successions, with apparent transgressive shelf deposits as shown by many cores and logs (Fig. 17) from Venture gas field. The transgressive units commonly are capped by oolitic carbonate beds on the flooding surfaces that generate strong seismic reflections. These surfaces are in many examples overlain by small clinoform sets (C in Fig. 17) of the basal, slightly deeper-water shelf deposits above. The patterns of upward-increasing reflection amplitudes, continuities, and frequencies can be used to interpret the same style of sedimentation in uncored areas.

The shaly Albian to Cenomanian Logan Canyon Formation shows completely different shallow-marine facies in cores (Figs. 12, 18). The sharp-based sandstones do not appear to be parts of regressive coarsening-upward successions; they are more randomly interbedded. On the basis of their sedimentary and biogenic structures in cores, they can be interpreted as estuarine or even nonmarine deposits intercalated within the marine shales. Although well control is not adequate to map incised valleys, it is believed that the basal surfaces of the sandstones represent erosional events resulting from short-term base-level drops.

The seismic response of this shallow-marine facies (Fig. 18) is completely different from that of the Missisauga interval (Fig. 12) discussed above. Amplitudes and times of arrival (depths) of individual reflections vary laterally in an irregular fashion across the interval. No vertical patterns of reflection amplitudes or frequencies can be documented. Some sloping reflections with apparent onlaps exist (Fig. 18) which could be interpreted as delineating erosion surfaces, but resolution of these is poor. Small (less than 50 m high), laterally restricted clinoforms and minor growth faults also occur in places (Fig. 18). The overall aspect of the seismic response of this interval is an absence of patterns of any seismic attributes, either vertically or horizontally. The discontinuous reflections have variable amplitudes which are not organized into any larger-scale patterns; this is due to lateral variation in the amount of sandstone, minor growth faults, and absence of major transgressive or condensed horizons. This seismic facies should be contrasted with the packages of upwardly increasing reflection amplitudes, frequencies and continuities shown in Figure 17.

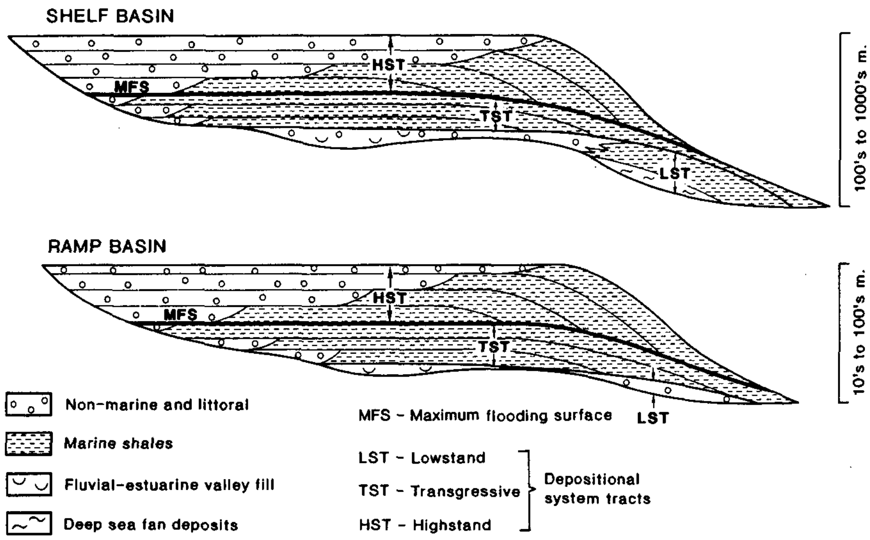

Figure 19 Generalized diagram of systems tracts in unconformity-bounded sequences in shelf and ramp basins. MFS is the maximum flooding surface.

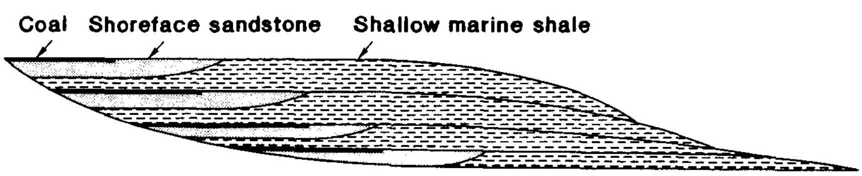

Figure 20 Diagram illustrating four progradational facies successions stacked in an overall retrogradational or transgressive pattern. The stacking pattern is important in determining the systems tract.

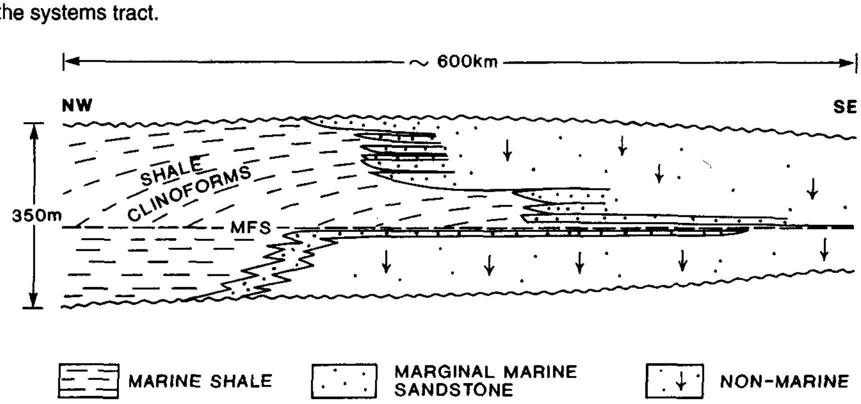

Figure 21 Stratigraphy of the Mannville Group of the Alberta Basin from a proximal area (SE) to a distal one (NW). The lower part of the succession (up to the MFS, maximum flooding surface) consists of a transgressive systems tract, and the upper part is a highstand systems tract. The shale clinoforms are shown in Figure 8. Depositional environments from outcrop and subsurface work are shown.

LARGE-SCALE FACIES RELATIONSHIPS

Subsurface work has contributed a great deal in recent years to knowledge of large-scale facies relationships. It has particularly helped in understanding the way in which facies successions relate to one another and to the different types of bounding surfaces. This section presents, in the most abbreviated form possible, a few of the most general conclusions achieved by subsurface study of these large-scale relationships.

Large-scale facies associations can be grouped into depositional systems tracts, depending on relationships to allostratigraphic bounding discontinuities, positions in the basin with respect to other systems tracts, and whether they have overall progradational or retrogradational patterns (Fig. 19). Depositional systems tracts are associated with specific bounding discontinuities. For example, a transgressive systems tract is capped by a maximum flooding surface or condensed section (Fig. 19), whereas a highstand systems tract is capped by an unconformity (Fig. 19). The facies associations or systems tracts are normally composed of several vertical facies successions (Fig. 20). Individual successions do not necessarily show the same trend. The associations of bounding discontinuities systems tracts have been reviewed by Posamentier and Vail (1988). These authors interpret the organization of depositional systems and erosional discontinuities almost entirely in terms of eustatic sea level variation. However, other interpretations can be made in terms of tectonic subsidence and variations in the rate of sedimentation. An example of this is shown in Figure 21, from the Lower Cretaceous Mannville Group of Alberta. The Lower to Middle Mannville (below MFS in Fig. 21) comprises a lowstand to transgressive systems tract made up of individual progradational facies successions. The thin shale directly above the Bluesky Sandstone contains the maximum flooding surface, as shown by regional cross sections. The Upper Mannville is a strongly progradational highstand depositional systems tract. The stratigraphy of this clastic wedge has been interpreted as the result of variations in tectonic subsidence and sediment supply rates from the Cordillera to the foreland basin, rather than eustatic variations in sea level. The Mannville systems tracts occur in the same arrangement as shown in Figure 19, but the interpretation may differ from that of Posamentier and Vail (1988).

Large-scale subsurface analysis in terms of systems tracts has also led to a greater understanding of relationships between siliciclastic and carbonate sediments in many areas. Figure 22 shows a cross section of one side of a basin rimmed by carbonate banks and reefs. The basin centre facies was deposited beyond the bank edge, and consists dominantly of sandstones and shales. The relationships between these systems tracts imply that clastics were supplied from the land and transported across the carbonate shelf, probably in incised valleys during periods of relative sea level fall. At the slope break, they were deposited as deltas, shorelines, or deep sea fans, depending on the local basin depth compared to sea level. During subsequent transgressions, some shelves were covered by thin siliciclastics but others completely lack this facies. Rapid production of carbonate sediments during the relative rising sea level phase allowed aggradation and progradation of the carbonate complex (Chapter 18). This kind of alternating highstand-lowstand deposition of carbonates and clastics has been termed reciprocal sedimentation. Most well-established examples have been imaged on seismic lines, but well-log cross sections and rare outcrops also show these relationships.

CONCLUSIONS

Large-scale subsurface facies analysis, combined with allostratigraphy and/or sequence stratigraphy, is now one of the most dynamic fields of research in sedimentary geology. Comparison of this volume with previous editions of *Facies Models* shows the increase in understanding of sedimentary systems and the extent of the contribution of subsurface work. While many ideas about individual facies have not changed markedly in the last ten years, ideas of facies relationships and the nature and significance of the bounding surfaces between them have been revolutionized.

REFERENCES

Basic sources of information

Anstey, N.A., 1982, Simple seismics: Boston, International Human Resources Development Corporation, 168 p.
An exceptionally entertaining book explaining the basics of the seismic method. Nonmathematical, for nonspecialists.

Asquith, G.B., 1982, Basic well-log analysis for geologists: American Association of Petroleum Geologists, Methods in Exploration, 216 p.
An excellent introduction to well-log analysis, directed at the interpretation of fluids in rocks by use of mathematical equations and calibrations. Very clearly presented.

Payton, C.E., 1977, Seismic stratigraphy — applications to hydrocarbon exploration: American Association of Petroleum Geologists, Memoir 26, 516 p.
A basic, necessary reference, now somewhat dated by advances in the field.

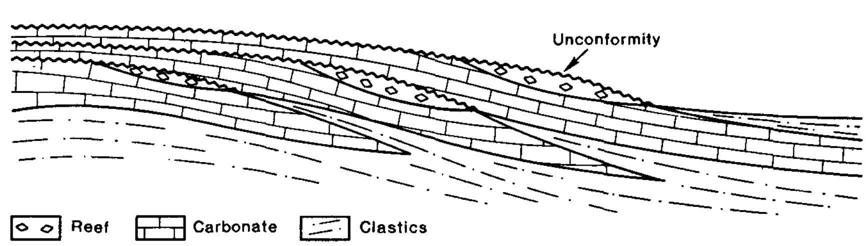

Figure 22 Cross section illustrating a succession that results from "reciprocal" sedimentation. Note that carbonate platforms and bank edges intertongue basinward with clastics, commonly sandstones proximally and shales distally. This configuration of lithofacies is interpreted to result from a carbonate shelf prograding and aggrading under conditions of rising relative sea level. During a base-level drop, the clastics are transported through breaks and channels in the carbonate margin, and deposited either as turbidites and other deep sea deposits, or in other situations as coarse-grained deltas. Because of the low relative sea level, carbonate deposition is minimal at that time. Thus relative sea level fluctuation results in deposition of highstand carbonates alternating with lowstand clastics in this setting. The cross section is a composite from the Permian Guadeloupe Reef Complex of west Texas, and seismic lines across the northwest Australian shelf.

Van Wagoner, J.C., Mitchum, R.M. Jr., Posamentier, H.W. and Vail, P.R., 1987, Key definitions of sequence stratigraphy, *in* Bally, A.W., ed., Atlas of seismic stratigraphy: American Association of Petroleum Geologists, Studies in Geology 27, p. 11-14.
Many basic definitions presented graphically in a large format. All the genetic associations of sequence stratigraphy are shown, with the assumption that eustatic sea level variation is the controlling parameter of stratigraphic units.

Van Wagoner, J.C., Mitchum, R.M., Campion, K.M. and Rahmanian, V.D., 1990, Siliciclastic sequence stratigraphy in well logs, cores and outcrops: concepts for high-resolution correlation of time and facies: American Association of Petroleum Geologists, Methods in Exploration Series no. 7, 55 p.
This is the latest comprehensive discussion of sequence stratigraphy, with many subsurface examples.

Wilgus, C.K., Hastings, B.S., Posamentier, H.W., Ross, C.A. and Kendall, C.G.St.C., eds., 1988, *Sea level changes: an intergrated approach*: Society of Economic Paleontologists and Mineralogists, Special Publication 42, 407 p.
Collection of papers emphasizing conceptual basis of sequence stratigraphy plus numerous case studies of sea level change from the geological record.

Other references

Allen, D.R., 1975, Identification of sediments — their depositional environment and degree of compaction — from well logs, *in* Chilingarian, G.V. and Wolf, K.H., eds., Compaction of coarse-grained sediments I: New York, Elsevier, p. 349-402.

Bubb, J.N. and Hatlelid, W.G., 1977, Seismic stratigraphy and global changes of sea level, Part 10: Seismic recognition of carbonate buildups, *in* Payton, C.E., ed., Seismic stratigraphy — applications to hydrocarbon exploration: American Association of Petroleum Geologists, Memoir 26, p. 185-204.

Flach, P.D., 1984. Oil sands geology — Athabasca deposit north: Alberta Research Council, Bulletin 46, 31 p.

Griffiths, C.M. and Bakke, S., 1990, Interwell matching using a combination of petrophysically derived numerical lithologies and gene-typing techniques, *in* Hurst, A., Lovell, M.A., and Morton, A.C., eds., Geological applications of wireline logs: Geological Society of London, Special Publication 48, p. 133-151.
An example of one numerical technique for log correlation, not as yet widely used by geologists.

Hopkins, J.C., Lawton, D.C. and Gunn, J.D., 1987, Geologic and seismic evaluation of a Lower Mannville valley system; Aldesson prospect, Rolling Hills, southwestern Alberta: Bulletin of Canadian Petroleum Geology, v. 35, p. 296-315.

Hurst, A., Lovell, M.A. and Morton, A.C., 1990, Geological applications of wireline logs: Geological Society of London, Special Publication 48, 357 p.

Krumbein, W.C. and Sloss, L.L., 1963, Stratigraphy and sedimentation: San Francisco, W.H.Freeman and Co., 660 p.

Miall, A.D., 1984, *Principles of Basin Analysis*: New York, Springer Verlag, 490 p.

Nurkowski, J.R. and Rahmani, R.A., 1984, An Upper Cretaceous fluvio-lacustrine coal-bearing sequence, Red Deer area, Alberta, Canada, *in* Rahmani, R.A. and Flores, R.M., eds., Sedimentology of coal and coal-bearing sequences: International Association of Sedimentologists, Special Publication 7, p. 163-176.
Example of the use of bentonitic marker beds and slices in subdividing an uncorrelatable unit.

Posamentier, H.W. and Vail, P.R., 1988, Eustatic controls on clastic deposition II — Sequence and systems tract models, *in* Wilgus, C.K., *et al.*, eds., Sea-level changes — an integrated approach: Society of Economic Paleontologists and Mineralogists, Special Publication 42, p. 125-154.
A complete exposition of the relationships between facies, facies successions, depositional systems tracts, transgressive surfaces, and erosional surfaces. The interpretation of eustasy as the only controlling parameter may be overstated, but the basic relationships discussed in this paper are of prime importance in large-scale stratigraphic and sedimentological analysis.

Roksandic, M.M., 1978, Seismic facies analysis concepts: Geophysical Prospecting, v. 26, p. 383-398.

Sangree, J.B. and Widmier, J.M., 1977, *Seismic stratigraphy and global* changes of sea level, Part 9: Seismic interpretation of clastic depositional facies, *in* Payton, C.E., ed., Seismic stratigraphy — applications to hydrocarbon exploration: American Association of Petroleum Geologists, Memoir 26, p. 165-184.

Sarg, J.F., 1988, Carbonate sequence stratigraphy, *in* Wilgus, C.K., *et al.*, eds., Sea-level changes — an integrated approach: Society of Economic Paleontologists and Mineralogists, Special Publication 42, p. 155-181.

Selley, R.C., 1978, Concepts and methods of subsurface facies analysis: American Association of Petroleum Geologists, Continuing Education Course Notes Series 9, 82 p.

Vail, P.R., Todd, R.G. and Sangree, J.B., 1977, Seismic stratigraphy and global changes of sea level, Part 5: chronostratigraphic significance of seismic reflections, *in* Payton, C.E., ed., Seismic stratigraphy, — applications to hydrocarbon exploration: American Association of Petroleum Geologists, Memoir 26, p. 99-133.

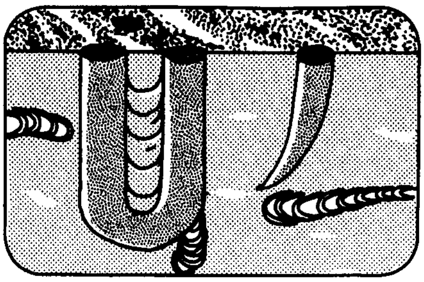

4. Trace Fossil Facies Models: Environmental and Allostratigraphic Significance

S. George Pemberton and James A. MacEachern, Department of Geology, University of Alberta, Edmonton, Alberta T6G 2E3

Robert W. Frey, Department of Geology, University of Georgia, Athens, Georgia 30602, U.S.A.

INTRODUCTION

Trace fossils contribute a unique blend of sedimentological and paleontological information about depositional environments. They record the behaviour of active, in situ organisms to a much greater extent than body fossils. *Ichnology*, the study of trace fossils, is therefore concerned with the behavioral record of benthic organisms, as dictated or modified by environmental constraints.

Biogenic structures appear in many forms (Frey and Pemberton, 1985), but this chapter is concerned mainly with tracks, trails, burrows, and borings. In order to define the facies implications of these biogenic structures, it is first necessary to discuss their behavioral *(ethological)* significance. The two main objectives of the chapter are 1) to describe and interpret nine associations of trace fossils *(ichnofacies)*, and 2) to show how these ichnofacies can be used in stratigraphic reconstructions, and in defining allostratigraphic bounding discontinuities.

FACTORS INFLUENCING THE CLASSIFICATION OF TRACE FOSSILS

Special classification schemes have been developed for trace fossils, because they represent *behaviour* rather than actual body remains. Historically, trace fossils have been classified in descriptive, preservational, taxonomic, and ethological terms. Of these, the ethological scheme is by far the most important, because the behavioral record of benthic organisms is dictated and modified not only by genetic preadaptations, but also by prevailing environmental parameters.

Ekdale *et al.* (1984) recognized seven basic categories of behaviour; resting traces *(cubichnia)*, locomotion traces *(repichnia)*, dwelling structures *(domichnia)*, grazing traces *(paschnia)*, feeding burrows *(fodinichnia)*, farming systems *(agrichnia)*, and escape traces *(fugichnia)*. Ekdale (1985) added predation traces *(praedichnia)*, and Frey *et al.* (1987) emphasized the importance of equilibria *(fugichnia)* to all other behavioral patterns (Fig. 1).

These fundamental behavioral patterns are genetically controlled, but are not phylogenetically restricted. The basic ethological categories have mostly persisted throughout the Phanerozoic. Individual tracemakers have evolved, but basic benthic behaviour essentially has not. For example, deposit feeders are preadapted to low-energy environments where deposited foodstuffs are most abundant; they do not fare well in turbulent water settings. The opposite is true for suspension feeders. Similarly, locomotion traces can be preserved only in fine-grained, low-energy quiescent environments such as lagoons. This ability to discern behavioral trends of benthic organisms represented in the rock record greatly facilitates environmental interpretations.

THE ICHNOFACIES CONCEPT

Just as various physical sedimentary structures can be grouped together to define facies (Chapter 1), so individual ichnofossils can be grouped into *ichnofacies*. Experience has shown that there is a limited number of groups or associations of ichnofossils. This grouping, developed by Adolf Seilacher (1967) in the 1950s and 1960s, was originally based on the concept that many of the parameters controlling the distribution of tracemakers tend to change progressively with increased water depth (Fig. 2).

Because of the geological value of this bathymetric relationship (Fig. 2), the ichnofacies sequence devised by Seilacher soon came to be regarded almost exclusively (albeit erroneously) as a relative paleobathometer. Today the ichnofacies remain valuable in environmental reconstructions, but paleobathymetry is only one aspect of the modern ichnofacies concept (Frey *et al.*, 1990).

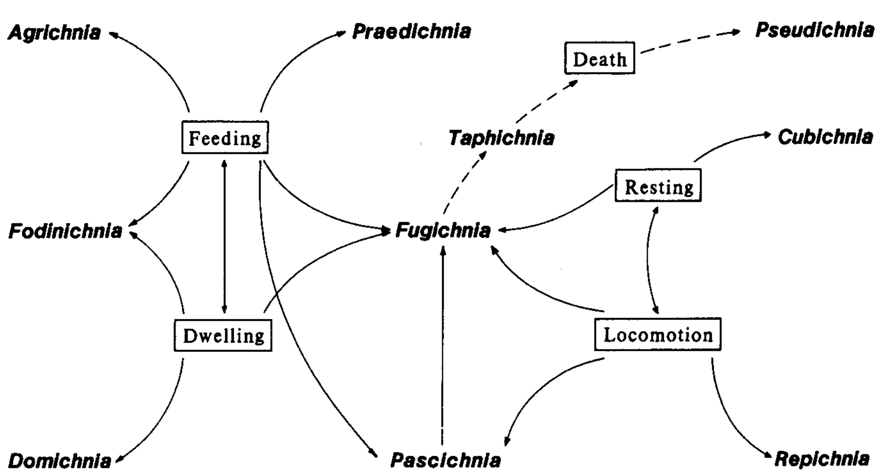

Figure 1 Behavioral classification of trace fossils. With environmental fluctuation, virtually all traces are intergradational with the *fugichnia* — escape or equilibrium structures. Extended stress may lead to death throes and the *taphichnia*, some of which might be confused with inorganic structures resembling trace fossils, the *pseudichnia*. Adapted from Frey *et al.* (1987).

The ichnofacies concept is closely related to the concept of *ichnocoenoses*. An ichnocoenose (sometimes spelled ichnocoenosis) is an association of contemporaneous, environmentally related traces, somewhat analogous to a community of organisms. An *ichnofacies* is the preserved record of that ichnocoenose (Frey and Pemberton, 1985, p. 90-94, their table 2). Seilacher's ichnofacies, therefore, are merely distinctive, recurrent, archetypal associations of traces.

In practice the term ichnocoenose has been applied in different ways by different workers (Bromley, 1990, p. 181-182). The concept clearly applies not only to traces in modern settings but also to their ancient counterparts in the rock record (Radwanski and Roniewicz, 1970; Frey and Pemberton, 1987). Modern ichnocoenoses (Dörjes and Hertweck, 1975) are studied as a basis for the interpretation of fossil equivalents.

Ichnofacies and reconstructed ichnocoenoses are part of the total aspect of the rock. Isolated bored shells or clasts, for example, do not in themselves constitute the *Trypanites* ichnofacies. Rather, they must conform to Walther's Law where there should be some semblance of stratification, lateral continuity, and vertical succession. It follows that interpretations of ichnofaunas are improved substantially when the traces are studied in the context of the host rocks, the physical sedimentary structures, and the stratigraphic position within an overall facies succession.

RECURRING ARCHETYPAL ICHNOFACIES

Nine recurring ichnofacies have been recognized, each named for a representative ichnogenus, namely *Scoyenia, Glossifungites, Trypanites, Teredolites, Psilonichnus, Skolithos, Cruziana, Zoophycos,* and *Nereites*. These ichnofacies (Fig. 2) reflect adaptations of tracemaking organisms to environmental factors such as substrate consistency, food supply, hydrodynamic energy, and salinity and oxygen levels (Frey and Pemberton, 1984; Frey *et al.*, 1990).

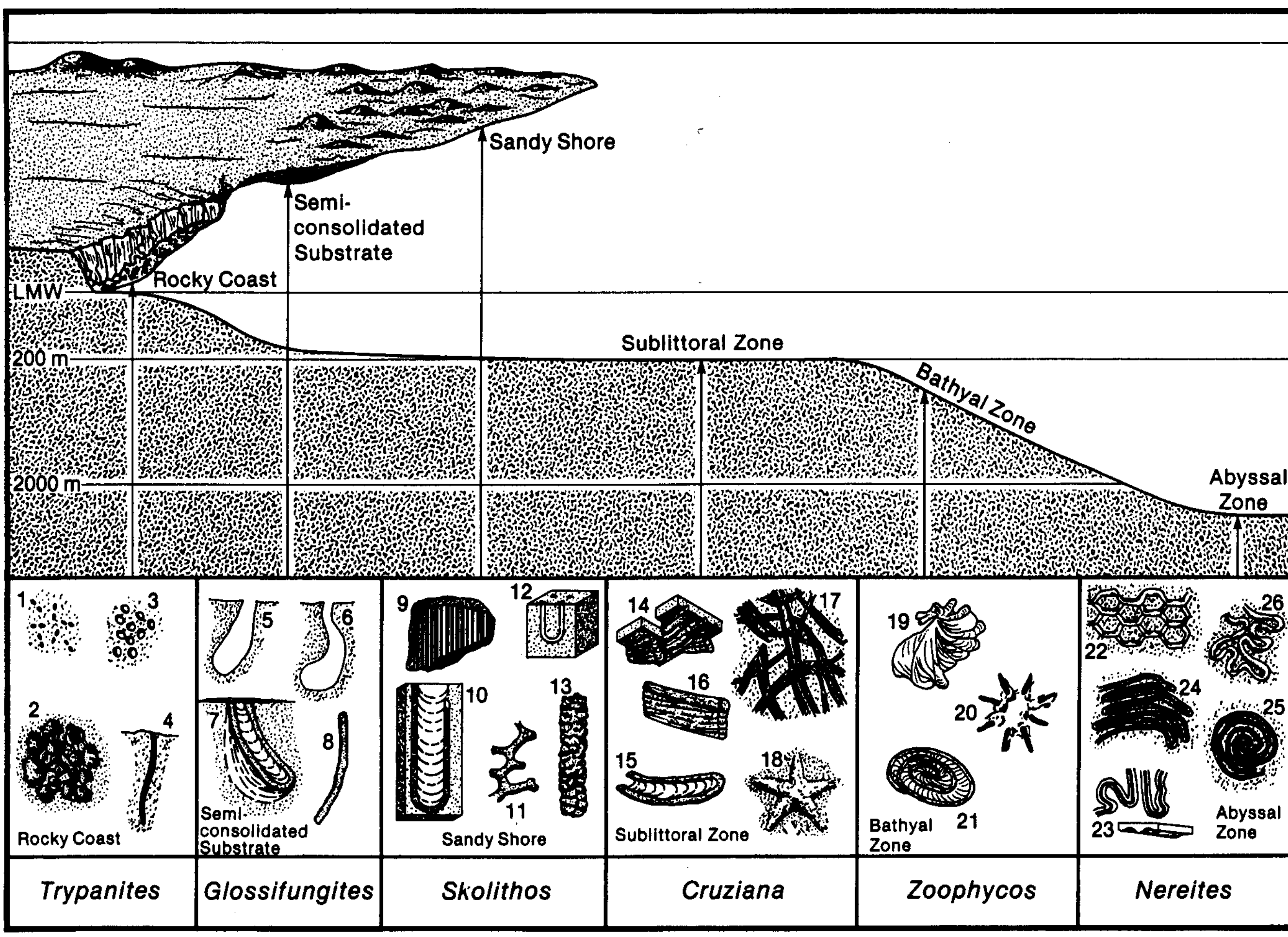

Figure 2 Recurring marine ichnofacies, placed in a representative, but not exclusive, suite of environmental gradients. Local physical, chemical, and biological factors ultimately determine which traces occur at which sites. Typical trace fossils include 1) *Caulostrepsis*, 2) *Entobia*, 3) echinoid borings, unnamed, 4) *Trypanites*, 5,6) *Gastrochaenolites* or related ichnogenera, 7) *Diplocraterion*, 8) *Psilonichnus*, 9) *Skolithos*, 10) *Diplocraterion*, 11) *Thalassinoides*, 12) *Arenicolites*, 13) *Ophiomorpha*, 14) *Phycodes*, 15) *Rhizocorallium*, 16) *Teichichnus*, 17) *Crossopodia*, 18) *Asteriacites*, 19) *Zoophycos*, 20) *Lorenzinia*, 21) *Zoophycos*, 22) *Paleodictyon*, 23) *Taphrhelminthopsis*, 24) *Helminthoida*, 25) *Spirorhaphe*, 26) *Cosmorhaphe*. Modified from Crimes (1975); Frey and Seilacher (1980). Bathymetric terms are from Ager (1963), mainly from the Treatise on Marine Ecology and Paleoecology. Not to scale.

ORGANIZATION OF THE DESCRIPTIVE PART OF THIS CHAPTER

Nonmarine ichnofacies are described first, but most (other than the *Scoyenia* assemblage) are in need of further study. *Marine softground ichnofacies* are described under two subheadings, *nearshore marine and coastal (Psilonichnus, Skolithos, Cruziana)*, and *open marine and deep marine (Zoophycos and Nereites)*. *Substrate-controlled* ichnofacies, associated with firmgrounds *(Glossifungites)*, woodgrounds *(Teredolites)*, and hardgrounds *(Trypanites)*, are described on the basis of substrate type and consistency.

Most of these ichnofacies form in soft to fairly soft substrates. Representative occurrences are described below. However, members of particular ichnofacies can appear in other settings, depending on the correct set of characteristic environmental parameters. For example, from the standpoint of the ethological requirements of the trace-making organisms, certain intertidal back-barrier environments are not all that different from certain subtidal fore-barrier environments. They may contain virtually identical suites of trace fossils.

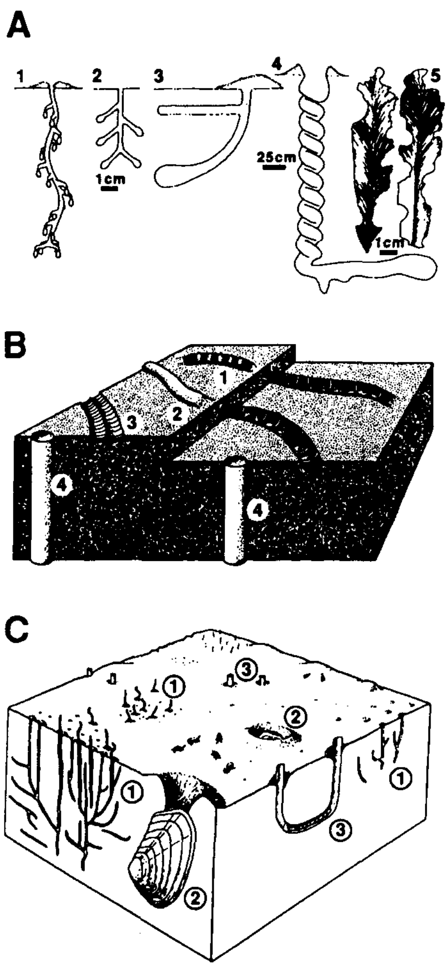

Figure 3 Characteristic types of biogenic structures in nonmarine environments. A) Structures typical of modern and ancient soil zones; 1) bee burrows, 2) wasp burrows, 3) beetle burrows, 4) vertebrats burrows, and 5) insect bite traces in leaves. B) Structures representative of the *Scoyenia* ichnofacies, which typifies the shore zone of ephemeral lakes and the overbank of rivers; 1) *Scoyenia*, 2) *Ancorichnus*, 3) *Cruziana*, and 4) *Skolithos*. C) Structures typical of shallow lacustrine settings; 1) oligochaete burrows (e.g., *Tubifex*), 2) sphaerid and unionid bivalve burrows, and 3) chironomid larvae burrows. Modified after Ekdale *et al.* (1984).

NONMARINE ICHNOFACIES

***Scoyenia* ichnofacies, and the ichnology of nonmarine environments**

At present, the only recognized named ichnofacies for nonmarine environments is the *Scoyenia* ichnofacies (Fig. 3B). Frey *et al.* (1984) concluded that the *Scoyenia* ichnofacies remains a valid concept within appropriate limits and is suggestive of deposition in the shore zone of ephemeral lakes and along the overbank of sluggish rivers. Other distinctive assemblages characterizing nonmarine aquatic environments remain unnamed, because of a paucity of ancient examples. For instance, modern lacustrine environments are characterized by traces generated by oligochaete annelids, amphipod crustaceans, sphaerid and unionid bivalves, and insect larvae (most notably midge larvae or chironomids; Fig. 3C). Unfortunately, ancient examples have not been widely documented.

The nonmarine realm includes both terrestrial and aquatic environments. Contrary to popular misconception, the *Scoyenia* ichnofacies is only one of many nonmarine ichnofacies (Frey *et al.*, 1984; Bromley and Asgaard, 1991; Gierlowski-Kordesch, 1991). Although the ichnological record of most nonmarine environments is indeed meagre, in some cases distinct suites of trace fossils are present that may prove useful as diagnostic tools in paleoenvironmental interpretation. Useful summaries of nonmarine ichnology, from both practical and philosophical points of view, were given by Ekdale *et al.* (1984), Miller (1984), Maples and Archer (1989), Bromley (1990), and Bromley and Asgaard (1991).

Prospects for the recognition of additional archetypal nonmarine ichnofacies remain encouraging. For example, Ekdale *et al.* (1984) and Frey and Pemberton (1987) noted that distinct suites of trace fossils characterize aeolian dunes and fluvial, paleosol, and lake environments, among others. The environments and deposits essentially devoid of water include eolian settings (Chapter 8) and paleosols. Most eolian deposits have a meagre trace fossil record, but reptile and mammal trackways, scorpionid, millepede, and isopod trails, and a variety of other nondescript surface trails and burrows made by dune-dwelling invertebrates can be present, as described by Ahlbrandt *et al.* (1978). They concluded that modern eolian deposits are dominated by only three distinctive types of biogenic structures (Fig. 4), 1) vertical unlined shafts constructed by numerous insects (e.g., sand wasps, crickets, beetle larvae) and arachnids, 2) horizontal meniscate burrows produced by crane fly larvae, and 3) footprints attributed to various reptiles, mammals, and invertebrates that commonly crawl or walk across the dunes.

Paleosols also have a meagre trace fossil record (Fig. 3A) which includes 1) invertebrate burrows that tend to be dominated by the larval cells of dung beetles (Retallack, 1984), 2) vertical unlined shafts possibly created by small insects and arachnids, 3) indentations on fossil plant leaves interpreted as insect bite traces or leaf mines, 4) vertebrate structures, including tracks, burrows, and coprolites from a variety of mammals and reptiles, and 5) rhizoliths representing the traces of roots.

Other nonmarine deposits are formed in running water (rivers, streams, wave-swept beaches) and standing water (ponds, pools and deep lakes) environments. The ichnofossils of these environments were summarized recently by Ekdale *et al.* (1984), Frey *et al.* (1984), Miller (1984), Gray (1988), Pollard (1988), Maples and Archer (1989), Bromley (1990), and Bromley and Asgaard (1991).

Even though sediments of modern nonmarine environments are subjected to intense bioturbation, most ancient examples are characterized by a sparse ichnofossil assemblage. This difference is probably due to numerous evolutionary and taphonomic factors, including 1) the fact that most organism groups originated in marine environments, 2) subsequently, representatives of some groups adapted to brackish and freshwater conditions, 3) diverse Tertiary nonmarine ichnofossil suites are related to the evolution of angiosperms (seed-bearing plants) in the Late Cretaceous, 4) angiosperm development led to an evolutionary explosion in the insects, 5) with the increase in insects came a corresponding increase in terrestrial and nonmarine crustaceans, and 6) most biogenic structures generated by nonmarine organisms are surficial and therefore ephemeral. These trends are reflected in examples documented from the Cretaceous-Tertiary of the Western Interior of North America (Table 1). Such trends must be considered when evaluating the use of trace fossils in delineating marine to nonmarine transitions. Pre-Cretaceous occurrences, for instance, may not bear close resemblance to later ones and must be evaluated with care.

The trace fossils are characterized by 1) small horizontal, lined, backfilled feeding burrows, 2) curved to tortuous unlined feeding burrows, 3) sinuous crawling traces, 4) vertical cylindrical to irregular shafts, and 5) tracks and trails. The invertebrates are mostly deposit feeders or predators, whereas the vertebrates are predators, herbivores or grovellers. Invertebrate diversity is very low, yet some traces may be abundant.

GENERAL CHARACTERISTICS OF MARINE CLASTIC SOFTGROUND ICHNOFACIES

Softground ichnofacies tend to be differentiated one from another by variables that typically are depth related. The *Zoophycos* and *Nereites* assemblages are more characteristic of deep water environments, whereas the *Psilonichnus, Skolithos*, and *Cruziana ichnofacies* are represented in nearshore marine or coastal environments. For example, in the Cretaceous of the Western Interior of North America, the interdeltaic marine shoreface can be zoned ichnologically (Fig. 5). This zonation is based on the way in which relative energy levels influence the distribution of food resources.

Recent summaries of the ichnology of marine shoreface environments have been presented by Saunders and Pemberton (1986), Frey and Pemberton (1987), Frey and Howard (1990), and Bromley (1990). Details of the effect of storms on the distrbution of trace fossils in shoreface settings were given by Pemberton and Frey (1984), Vossler and Pemberton (1988a), and Frey (1990). The ichnological distinction between river-dominated delta-front environments and the interdeltaic shoreface was summarized recently by Moslow and Pemberton (1988).

The *Zoophycos* and especially the *Nereites* ichnofacies tend to characterize deep water environments, including outer shelf, slope, and bathyal to abyssal settings (Fig. 2), as discussed by Crimes *et al.* (1981), Ekdale *et al.* (1984), McCann and Pickerill (1988), Pickerill and Harland (1988), and Crimes and Crossley (1991).

NEARSHORE MARINE AND COASTAL ICHNOFACIES

Marginal marine environments, including the intertidal zone, shallow lagoons, estuaries, and delta platforms, characteristically display steep salinity gradients resulting from variations in 1) amounts of freshwater input from rivers and runoff from land, 2) rainfall, 3) evaporation, 4) tidal range and salinity content in adjacent open-ocean coastal waters, 5) morphology of the coastal area, and 6) differences in wind direction and velocity (Dörjes and Howard, 1975). Such salinity fluctuations (combined with corresponding

Table 1 *Evolution of nonmarine trace fossil suites from the Early Cretaceous to Tertiary; examples are from Western Interior Basin.*

AGE	Early Cretaceous	Late Cretaceous	Tertiary
TYPES OF TRACE FOSSILS	*Skolithos, Planolites*	*Planolites, Conichnus, Lockeia, Imbrichnus Thalassinoides, ?Palaeophycus, Skolithos, Psammichnites*	*Celliforma, Edapichnium, Scaphichnium, Macanopsis, Ichnogyrus, Planolites, Taenidium, ?Ophiomorpha, Skolithos, Pallichnus*
PROBABLE PRODUCERS	worms, insects	worms, insects, bivalves, crustaceans	worms, oligochaetes, bivalves, spiders, insects, beetles, bees, wasps, crustaceans, crabs, mammals

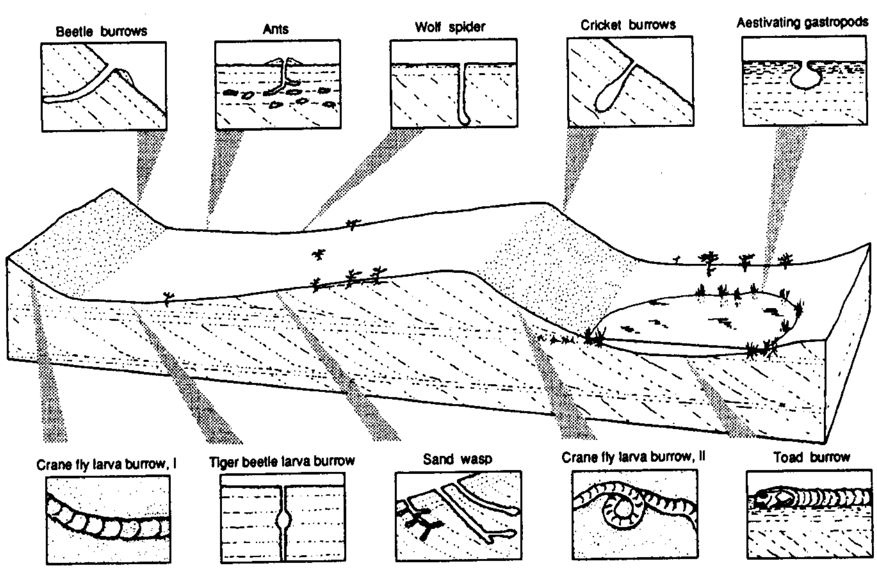

Figure 4 Schematic representation of characteristic organism traces in modern eolianites. Modified after Ahlbrandt *et al.* (1978) and Ekdale *et al.* (1984).

changes in temperature, turbulence, oxygen content, etc.) result in a physiologically stressful environment for numerous organism groups.

It is commonly held that most invertebrates originated in marine environments (Whitfield, 1976) and representatives of some groups subsequently adapted to brackish and freshwater conditions. The physiological mechanisms involved in the adaptive process centre on the capability of the organisms to control osmotic flooding (osmoregulation) and the ionic concentration of body fluids (ionic regulation) due to lower salt concentrations (Croghan, 1983). The extent to which these adaptations occur in different organism groups is highly variable and thus their

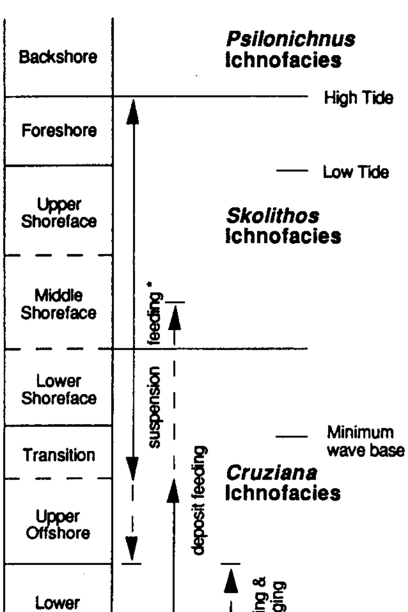

Figure 5 Idealised shoreface model for ichnofacies, based mainly on facies observations in the Cretaceous Interior Seaway. For organism behaviour or feeding strategy, dashed intervals reflect a presence, whereas solid lines indicate a dominance. Deposit-feeding strategies are characteristic of lower offshore to lower shoreface settings; associated grazing and foraging tracemakers typical of lower offshore settings mostly supplant the suspension feeders and passive carnivores of shallower settings, reflecting increased water depths and decreased energy levels, among other parameters (Frey *et al.*, 1990).

distribution in relation to salinity gradients shows marked differences. Therefore, based on physiological criteria, freshwater and fully saline faunas constitute somewhat stable end members. The freshwater fauna is impoverished and is dominated by relatively few groups, most notably branchiopods (freshwater crustaceans) and insects (Croghan, 1983). By sharp contrast, the brackish water fauna is characterized by opportunistic euryhaline (tolerant to wide ranges of salinities) species and consists of numerous elements, including 1) a freshwater component consisting of euryhaline species restricted to low salinity, 2) a marine component comprising euryhaline species, 3) a brackish component consisting of species that penetrate neither fresh nor fully saline waters, and 4) a migratory component comprising species that spend only a portion of their life cycles in brackish water (Perkins, 1974).

Investigations on modern brackish water environments indicate that although their biotic component is highly variable, the following generalizations may have significant ecological and paleoecological ramifications. 1) Brackish waters are generally reduced in species numbers with respect to both freshwater and fully saline water (Dörjes and Howard, 1975). 2) Whereas the number of freshwater species decreases rapidly even with slight increases in salinity, the reduction of marine species is more gradual. Therefore, the brackish water fauna can be considered more as an impoverished marine assemblage than a true mixture of freshwater and marine elements. 3) With reduced salinities, the marine macrofauna decreases more rapidly than the microfauna (Remane and Schieper, 1971). 4) Infaunal organisms are more abundant in low-salinity waters than are epifaunal organisms (Sanders *et al.*, 1965). 5) With decreasing salinity, the reduction of species in groups forming a calcareous skeleton is greater than in their counterparts lacking such a skeleton (Remane and Schlieper, 1971). 6) Many marine organisms undergo a size reduction when subjected to less saline water (Milne, 1940). 7) There is a distinct shift in the bathymetric range of marine organisms when subjected to salinity reductions (Remane and Schieper, 1971). Thus the influence of salinity gradients can hardly be divorced from the ichnocoenose concept as suggested by Bromley and Asgaard (1991).

Such trends reflect a stressful environment, and successful colonization depends (aside from physiological constraints) on the ability of the organisms to develop an effective adaptive strategy. Sediments of estuaries and other brackish water environments are effective at dampening the influence of salinity fluctuations within the substrate (Sanders *et al.*, 1965). Therefore, the deep infaunal habitat serves as a refuge to buffer the organism against rapid and extreme salinity variations. As a result, burrowing organisms are able to penetrate a greater distance up an estuary than epifaunal (animals living on the substrate surface) organisms, which are subjected to fluctuating salinities of the overlying water column (Alexander *et al.*, 1935).

Although an unfortunate paucity of studies deals specifically with biogenic structures in modern brackish water environments, work by Howard and Frey (1973) on estuaries of the Georgia coast indicates that 1) the diversity and abundance of biogenic structures increases seaward, 2) distinct biogenic structures and bioturbate textures are also more diverse and abundant along the margins of the estuaries than in the deeper channels, 3) distinct burrows and dwelling tubes characterize most muds whereas sandy muds or muddy sands may exhibit both distinct burrows and various types of bioturbate textures, and 4) coarser sediments tend to lack biogenic sedimentary structures. In addition, they also recognized that the entire suite of estuarine biogenic structures generally consists of both vertical and horizontal burrows or burrow systems and thus does not fall conveniently into any of Seilacher's (1967) universal ichnofacies. Instead, the assemblage tends to be composed of a mixture of structures typical of both the *Skolithos* and *Cruziana* ichnofacies. This assemblage is characterized by burrows that, if preserved, would consist of *Skolithos, Monocraterion, Thalassinoides, Ophiomorpha, Planolites*, and *Palaeophycus* (Howard and Frey, 1973). Burrows typical of freshwater deposits (i.e., *Scoyenia* and insect perturbations) were not observed. Similarly, although sediments and physical sedimentary structures in tidal stream bars are very similar to those in terrestrial bars, biogenic structures in the two are very different (Frey and Pemberton, 1984).

Although brackish marginal-marine environments are widespread in the modern realm, relatively few have been documented from the rock record. Notable exceptions, in which the authors mention ichnofossils, include parts of the following units; the Devonian-Mississippian Price Formation of the central Appalachians (Bjerstedt, 1987), the Middle Jurassic Great Estuarine Group (Hudson, 1980), the Upper Jurassic of Portugal (Fürsich, 1981), the Lower Cretaceous Wealden Group of Great Britain (Stewart, 1981), the Lower Cretaceous Fall River Formation of Wyoming (Campbell and Oaks, 1973), the Grand Rapids Formation of Alberta (Beynon *et al.*, 1988), the McMurray Formation of Alberta (Pemberton *et al.*, 1982), various members in the Mannville Group of Alberta (Wightman *et al.*, 1987), the Upper Cretaceous Fox Hills Formation of Wyoming (Land, 1972), and the Eocene Bagshot Beds of southern England (Goldring *et al.*, 1978). All these units contain well-developed suites of biogenic structures which, in most instances, have been used as evidence of at least some saline influence. The general assemblage reflects inherently fluctuating environmental parameters and is characterized by 1) low diversity, 2) forms typically found in marine environments, 3) structures constructed by trophic generalists, 4) suites that are commonly dominated by a single ichnogenus (Fig. 6), and 5) vertical and horizontal ichnofossils that are common to both the *Skolithos* and *Cruziana* ichnofacies (Fig. 7).

Psilonichnus ichnofacies

The *Psilonichnus* ichnofacies (Fig. 8) represents a mixture of marine, quasi-marine, and nonmarine conditions. Typical environments include the backshore of the beach, dunes, washover fans, and supratidal flats. Frey and Pemberton (1987) noted that such environments are subject to extreme variations in energy levels, sediment types, and physical and biogenic sedimentary structures. The environments may also be strongly affected by torrential rains and storm surges. Marine processes generally dominate during spring tides and storms, whereas eolian processes predominate during neap tides and nonstorm periods.

Because of their topographic position few such substrates are available to benthic marine animals. The only persistent, notable exceptions are amphibious crabs of the family Ocypodidae (ghost crabs), which include both scavengers and surficial deposit feeders. These animals typically excavate J-, Y-, or U-shaped dwelling burrows, some with bulbous basal cells, referable to the trace fossil *Psilonichnus* (Fig. 8). Other biogenic structures are generated by essentially terrestrial organisms and include 1) the vertical shafts of insects and spiders, 2) the horizontal tunnels formed by the crawling and foraging of

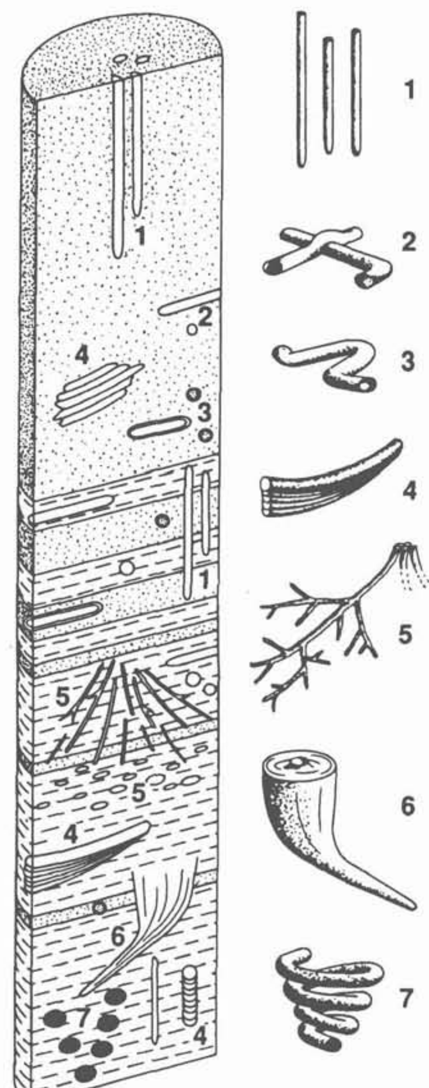

Figure 7 Association of trace fossils that are typically found in both marine and brackish water environments. 1) *Skolithos*, 2) *Planolites*, 3) *Palaeophycus*, 4) *Teichichnus*, 5) *Chondrites*, 6) *Rosselia*, 7) *Gyrolithes*. Modified after Wightman *et al.* (1987).

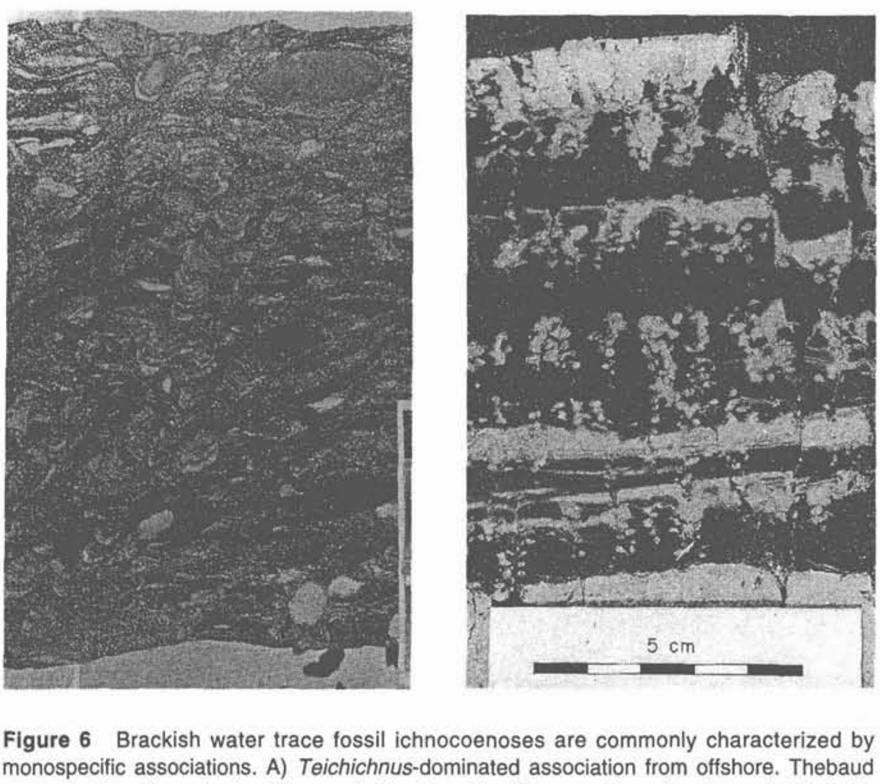

Figure 6 Brackish water trace fossil ichnocoenoses are commonly characterized by monospecific associations. A) *Teichichnus*-dominated association from offshore. Thebaud core. B) *Gyrolithes*-dominated association from the Waseca Formation (core A10-34-47-23W3, 489.5 m) of the Golden Lake Field, Saskatchewan.

insects and tetrapods, and 3) the ephemeral tracks, trails, and fecal pellets of insects, reptiles, birds, and mammals; these are mostly predators or herbivores. The *Psilonichnus* ichnofacies includes plant-root penetrations. The types of plants able to exploit these substrates range from intertidal halophytes (plants tolerant of saltwater) on the distal margins of some washover fans, to maritime or terrestrial grasses, weeds, vines, shrubs, bushes, and trees on dunes.

To the extent that ocypodid crab burrows may appear in the uppermost foreshore or the upper part of estuarine point bars, the *Psilonichnus* ichnofacies may slightly overlap the *Skolithos* ichnofacies; nevertheless, the boundary between these two ichnofacies is normally distinct. Because of its potentially large numbers of terrestrial traces, however, the *Psilonichnus* ichnofacies may be broadly intergradational not only with the *Scoyenia* ichnofacies but also with several other, as yet unnamed nonmarine ichnocoenoses.

The naming of the *Psilonichnus* ichnofacies has caused some problems. It was founded on fossil examples (Frey and Pemberton, 1987, p. 336) but the modern ichnocoenoses were emphasized to show the richness that one might reasonably expect to have existed for various ancient ichnofaunas. This follows one of the major tenets of ichnofacies reconstruction, namely that the namebearer need not be present in every occurrence of the ichnofacies. Thus just as *Cruziana* is rare in post-Paleozoic occurrences of the *Cruziana* ichnofacies, *Psilonichnus* may well be absent in pre-Mesozoic occurrences of the Psilonichnus ichnofacies.

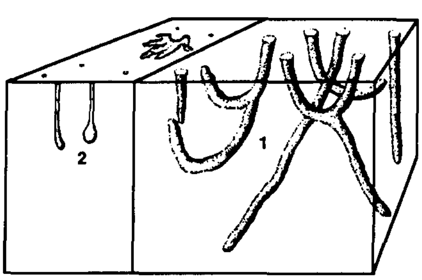

Figure 8 Trace fossil association characteristic of the *Psilonichnus* ichnofacies. 1) *Psilonichnus*, 2) *Macanopsis*.

Skolithos ichnofacies

The *Skolithos* ichnofacies (Fig. 9) is indicative of relatively high levels of wave or current energy, and typically is developed in slightly muddy to clean, well-sorted, loose or shifting particulate substrates. Increasing energy levels enhance physical reworking, thus obliterating the biogenic structures and preserving physical sedimentary structures. Abrupt changes in rates of deposition, erosion, and physical reworking of sediments are frequent. Such conditions commonly occur on the foreshore and shoreface of beaches, bars, and spits, but the same conditions sometimes occur on estuarine point bars, tidal deltas and submarine fans. As dictated by fundamental relationships between water agitation, sediment transport and animal distribution, most tracemakers found here are suspension feeders. Substrates serve mainly as an anchoring medium. The organisms typically construct deeply penetrating, more or less permanent domiciles (Fig. 9). Depth of burrowing in the intertidal zone is controlled in part by tidal range and height of the low water table. During low tide, moist sediments at depth help buffer the organisms against desiccation and salinity or temperature shock, and also help provide respiratory water. In both intertidal and high-energy subtidal settings, deep burrowing is one means of escaping the instability of the ever-shifting substrate surface.

The trace fossils are characterized by 1) predominantly vertical, cylindrical or U-shaped burrows, 2) protrusive and retrusive spreiten in some U-burrows, which develop in response to substrate aggradation or degradation, 3) few horizontal structures, 4) few structures produced by mobile organisms, 5) low diversity, although individual forms may be abundant, 6) mostly dwelling burrows constructed by suspension feeders or passive carnivores, and 7) vertebrate traces, particularly in low-energy intertidal settings.

The *Skolithos* ichnofacies ordinarily grades landward into supratidal or terrestrial zones and seaward into the *Cruziana* ichnofacies. The landward boundary tends to be more abrupt than the seaward boundary. With reduced energy, it may also grade into intertidal or shallow subtidal extensions of the *Cruziana* ichnofacies. Mixed *Skolithos-Cruziana* associations are common in both recent (Howard and Frey, 1973) and ancient settings.

Finally, the *Skolithos* ichnofacies may appear in slightly to substantially deeper water deposits wherever energy levels, food supplies, and hydrographic and substrate characteristics are suitable (Crimes *et al.*, 1981). Potential examples include submarine canyons, deep sea fans, and bathyal slopes swept by strong contour currents. Therefore, as emphasized previously, paleobathymetric interpretations cannot be based solely on checklists of trace fossil names. Evaluation of associated physical sedimentary structures, stratigraphic position, and other evidence is essential, even in normal beach-to-offshore sequences.

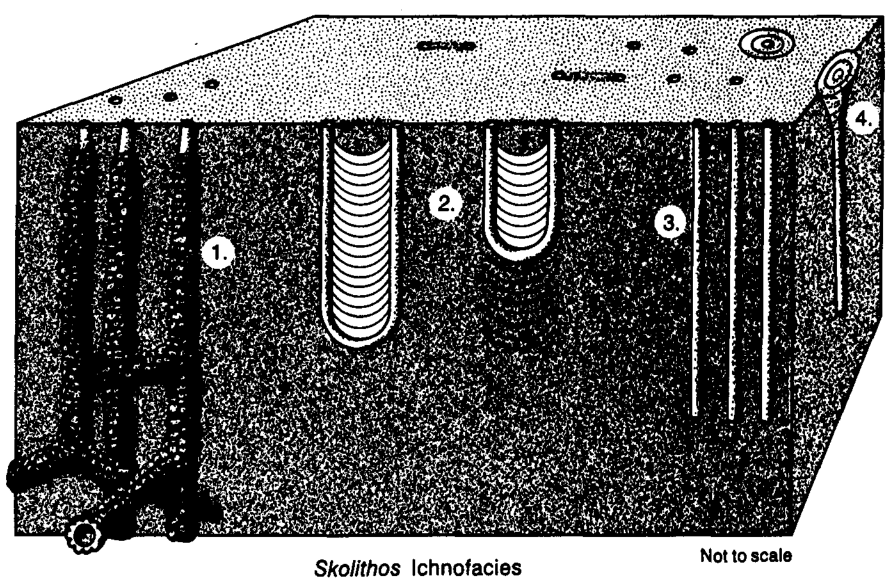

Figure 9 Trace fossil association characteristic of the *Skolithos* ichnofacies. After Frey and Pemberton (1984). 1) *Ophiomorpha*, 2) *Diplocraterion*, 3) *Skolithos*, 4) *Moncraterion*.

Cruziana ichnofacies

The *Cruziana* ichnofacies (Fig. 10) is most characteristic of subtidal, poorly sorted and unconsolidated substrates. Conditions typically range from moderate energy levels in shallow waters below fairweather wave base but above storm wave base, to low energy levels in deeper, quieter waters. The ichnofacies is also found in the littoral to sublittoral parts of some estuaries, bays, lagoons and tidal flats. Sediment deposition is negligible to appreciable, but is not necessarily rapid. Sediment textures and bedding styles exhibit considerable diversity. They include 1) thinly bedded, well-sorted silts and sands, 2) discrete mud and shell layers, 3) interbedded muddy and clean silts and sands, and 4) extremely poorly sorted beds derived from any of the above through intense bioturbation.

With reduced but not negligible energy levels, food supplies consist of both suspended and deposited components. Either fraction may predominate locally, or the two may be intermixed. Characteristic organisms therefore include both suspension and deposit feeders, as well as mobile carnivores and scavengers. Because of lowered energy and abrupt shifts in temperature and salinity levels, burrows tend to be constructed horizontally rather than vertically, although scattered vertical or steeply inclined burrows occur. Profusions of burrows may be present at stable, low-energy sites. Trails of epibenthic (living on the seafloor) and endobenthic (living within the substrate) foragers also may be common and reflect the abundance, diversity, and accessibility of food.

In shallow waters, periodic scour by storm waves, and renewed deposition after the storm may incorporate storm layers within a sequence of otherwise low-energy deposits (Pemberton and Frey, 1984). Development of hummocky cross stratification may involve the introduction of new sediment as well as the reworking of previously deposited sediment. Any of these conditions may yield burrow truncations and escape structures. Increased energy and allied parameters thus represent a temporary excursion of *Skolithos*-type conditions into a *Cruziana*-type setting. However, this overall bedding style differs from that of the main *Skolithos* ichnofacies, in which stratification features, substrate scour, burrow truncations, and escape structures are contained entirely within sequences of high-energy deposits. Furthermore, the storm layers eventually are overprinted with *Cruziana*-type traces.

The trace fossils are characterized by 1) a mixed association of vertical, inclined, and horizontal structures, 2) presence of traces constructed by mobile organisms, 3) generally high diversity and abundance, and 4) mostly feeding and grazing structures constructed by deposit feeders, except where crawling traces are predominant (as in some Paleozoic nearshore settings). Inclined U-burrows mostly have protrusive spreiten indicating feeding swaths (soft-sediment *Rhizocorallium*), and forms of *Ophiomorpha* and *Thalassinoides* have irregularly inclined to horizontal components.

OPEN MARINE AND DEEP MARINE ICHNOFACIES

Zoophycos ichnofacies

Of all recurrent marine ichnofacies, this assemblage is most debated and least understood. The ichnogenus *Zoophycos* has an extremely broad paleobathymetric range, hence its designation as namebearer for a supposedly depth-related ichnofacies has long been controversial. In popular bathymetric schemes, the *Zoophycos* ichnofacies (Fig. 11) typically is portrayed as an intermediary between the *Cruziana* and *Nereites* ichnofacies, at a position corresponding more or less to the continental slope. More specifically, the original designation placed it in areas below storm wave base but free of turbidity currents, within the broad depositional gradient that defines the outer shelf-to-slope transition (Seilacher, 1967).

As re-evaluated recently (Frey and Seilacher, 1980), one of the major environmental controls represented by the ichnofacies is *lowered oxygen levels* associated with *abundant organic material* in *quiet water settings.* To some extent, these conditions do occur in the broad area across the shelf-slope break, and hence the popularized bathymetric placement of the ichnofacies (Fig. 2) is suitable. However, such reducing conditions replete with a dominance of *Zoophycos,* are perhaps even better known in shallower water, epeiric deposits (Marintsch and Finks, 1982).

Considering the above characteristics of the ichnofacies, together with the widespread distribution of indivi-

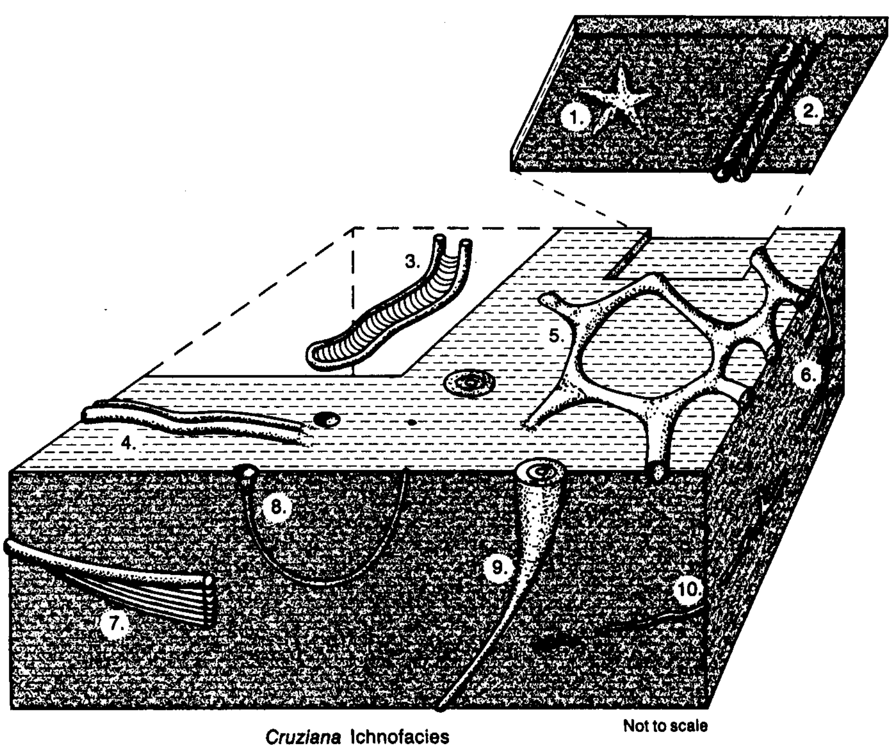

Figure 10 Trace fossil association characteristic of the *Cruziana* ichnofacies. After Frey and Pemberton (1984). 1) *Asteriacites,* 2) *Cruziana,* 3) *Rhizocorallium,* 4) *Aulichnites,* 5) *Thalassinoides,* 6) *Chondrites,* 7) *Teichichnus,* 8) *Arenicolites,* 9) *Rossella,* 10) *Planolites.*

dual specimens of *Zoophycos* in both shallow- and deep-water deposits (Frey *et al*., 1990), we speculate that the *Zoophycos* animal was broadly adapted in most ecologic respects. It tolerated not only a considerable range of water depths but also numerous substrate types, variable food resources, and different energy and oxygen levels. Its traces therefore appear in the *Cruziana* through *Nereites* ichnofacies (Crimes *et al*., 1981). Indeed, its tolerance may be its most distinguishing environmental characteristic. The animal was able to compete successfully with diverse tracemakers under the conditions associated with the *Cruziana* and *Nereites* ichnofacies, but few other animals were able to compete with it under the restricted conditions outlined above.

Because of its singular prominence in many restricted settings, the association seems to warrant its own ichnofacies designation. Conversely, the less restrictive the environment at a given site, the less distinctive the ichnofacies as a separate entity. In numerous places, the ichnofacies is hard to recognize in the transition from the *Cruziana* to the *Nereites* ichnofacies, especially on unstable ancient slopes originally subjected to turbidity flows or contour currents.

The exact environmental implications of the *Zoophycos* ichnofacies and its variants have not yet been determined. The most important factors in the distribution of the animal, in addition to its own opportunism, evidently include water depth, depth of burrowing, sediment cohesiveness, and interstitial or bottom-water oxygen levels. Stressed quiet water environments, particularly those exhibiting anoxia, seem to be the primary common denominator, even though the animal itself was cosmopolitan.

The ichnofacies may also occur in restricted intracoastal settings, particularly in Paleozoic sequences. The ichnogenus *Zoophycos* possibly represents greater paleobathymetry in Mesozoic and Cenozoic deposits than in Paleozoic deposits (Frey and Pemberton, 1984, p. 201-202). The character of the *Zoophycos* ichnofacies may therefore vary from one part of the stratigraphic column to the next.

The trace fossils are characterized by 1) low diversity, though individual traces may be abundant, 2) simple to moderately complex, efficiently executed grazing and feeding structures produced by deposit feeders, and 3) horizontal to gently inclined spreiten structures distributed in delicate sheets, ribbons, lobes or spirals (flattened forms of *Zoophycos* or, in pelitic sediments, *Phycosiphon*).

***Nereites* ichnofacies**

The Nereites ichnofacies occurs in bathyal to abyssal quiet but oxygenated waters, commonly influenced by turbidity currents. Thus the bathymetric implications of the *Nereites* ichnofacies (Fig. 12) are less equivocal than those of any other recurrent ichnofacies. Although numerous trace fossils otherwise typical of shallow water deposits occasionally range into deep sea deposits, the reverse is not ordinarily true. The depth- and energy-related variables seem to be more important influences than turbidity current deposition (Crimes *et al*., 1981). For example, the trace assemblage persists today on distal abyssal plains essentially beyond reach of turbidity currents but is absent among well-developed, shallow water turbidite sequences.

Nevertheless, most *Nereites* associations studied to date occur in turbidites, probably because the stratigraphic record of deep water deposits is mainly from subsiding basins rather than the broad abyssal plain.

Animals exploiting lower bathyal to abyssal environments have two major concerns, 1) scarcity of food, relative to more abundant supplies in shallower settings, and 2) periodic disruption by strong downcanyon bottom currents or actual sediment-gravity flows. Over long spans of geologic time, the overall community ultimately developed two component parts; preturbidite and post-turbidite. The preturbidite resident association is characteristic of quiet, normal conditions and is dominant wherever the substrate is free of the influence of turbidity currents. It tends to be overwhelmed or eliminated by severe erosion or turbulence, however, and is replaced by the post-turbidite association immediately after a turbidity current. Later, as conditions revert to a normal, low-energy setting, the preturbidite association gradually re-establishes itself. Preturbidite animals thus comprise a stable, persistent community well adapted to quiet conditions, derived mainly from original early-Paleozoic colonizers of the deep-sea floor. In contrast, post-turbidite animals represent a more opportunistic, less stable community better adapted to turbidite colonization, derived mainly from subsequent evolutionary immigrants from shallower waters (Frey and Seilacher, 1980).

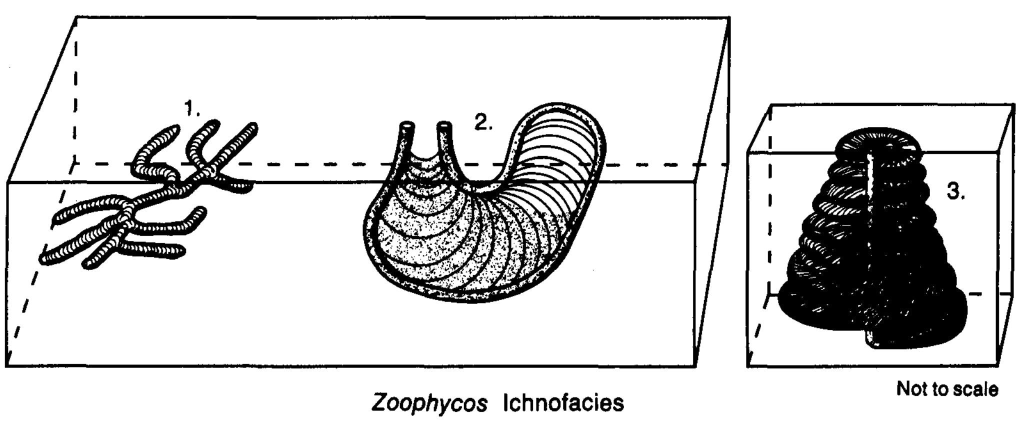

Figure 11 Trace fossil association characteristic of the *Zoophycos* ichnofacies. After Frey and Pemberton (1984). 1) *Phycosiphon*, 2) *Zoophycos*, 3) *Spirophyton*.

In addition to pre- and post-turbidite associations, numerous turbidites display ichnologic gradients down depositional dips (Crimes *et al.*, 1981). Where strong bottom currents issue from submarine canyons or flow along fan channels, components of the *Skolithos* ichnofacies may be present. Otherwise, proximal parts of turbidites may be characterized by rosetted or radiating traces, and the gently meandering forms of *Scolicia*. Medial parts may be indicated by spiralled or tightly meandering traces (Figs. 12-1, 12-6 and 12-7). Distal parts are typified by patterned networks (Figs. 12-2, 12-4, and 12-5) although other traces are generally present. *Zoophycos* is common locally in various settings, but it tends to be multilobed and in places is more complex than in the *Zoophycos* ichnofacies.

Finally, the *Nereites* ichnofacies has been recognized in cores of ancient, unconsolidated, well-bedded fine sediments, including distal turbidites and pelagic rhythmites of the present ocean basins. However, the association, if present, tends not to be preserved on great expanses of abyssal plain, where sedimentation and bioturbation are more or less constant rather than episodic.

The trace fossils are characterized by 1) high diversity but low abundance, 2) complex horizontal grazing traces and patterned feeding/dwelling structures reflecting highly organized efficient behaviour, 3) spreite are typically nearly planar, although *Zoophycos* forms are spiralled, multilobed and complex, 4) numerous crawling and/or grazing traces and sinuous fecal castings *(Helminthoida, Cosmorhaphe)* that are mostly intrastratal, 5) structures produced by deposit feeders and scavengers, and 6) possible structures associated with trapping or farming microbes within essentially permanent open domiciles *(Paleodictyon, Megagrapton*; Ekdale *et al.*, 1984).

As presently understood, the *Nereites* ichnofacies is restricted primarily to turbidite successions. Sediments on the basin plains beyond the influence of turbidity currents are mostly characterized by bioturbate textures rather than discrete traces (Frey and Wheatcroft, 1989).

SUBSTRATE-CONTROLLED ICHNOFACIES

The ichnofacies described above are characteristic of soft substrates, in nonmarine, marginal marine and open marine, and deep marine settings. However, there are three ichnofacies related to firm, hard and woody substrates.

Glossifungites ichnofacies

The *Glossifungites* ichnofacies is environmentally wide ranging, but only develops in firm unlithified substrates such as dewatered muds. Dewatering results from burial and the substrates are made available to tracemakers if exhumed by later erosion (Pemberton and Frey, 1985). Exhumation can occur in shallow water environments as a result of coastal erosion, or as a result of submarine channels cutting through previously deposited sediments. Such horizons commonly form important bounding discontinuities (Chapter 1).

The traces are characterized by 1) vertical, cylindrical, U- or tear-shaped pseudo-borings, or sparsely to densely branching dwelling burrows, or mixtures of borings and burrows, 2) protrusive spreiten in some burrows that develop mostly through animal growth (fan-shaped *Rhizocorallium* and *Diplocraterion* [formerly *Glossifungites*]), 3) animals that leave the burrow to feed (e.g., crabs), as well as suspension feeders, 4) low diversity, yet individual structures may be abundant. *Glossifungites* excavations tend to avoid obstructions within the substrate, demonstrating a preference for firm, rather than hard, substrates.

Trypanites Ichnofacies

This is also a specialized ichnofacies that characterizes fully lithified marine substrates such as hardgrounds, reefs, rocky coasts, beachrock, and omission surfaces. The ichnofacies may develop even on igneous substrates (Fischer, 1981), and the collective volume of bioeroded sediments may be substantial. (Torunski, 1979).

The traces are characterized by 1) cylindrical to vase-, tear- or U-shaped to irregular domiciles of organisms living within the borings, 2) borings oriented perpendicular to the substrate, or consisting of shallow anastomosing systems of borings (sponges, bryozoans), 3) borings excavated by suspension feeders or passive carnivores, 4) raspings and gnawings of algal grazers and similar organisms (mainly chitons, limpets and echinoids), 5) moderately low diversity, although borings and scrapings of individual ichnogenera may be abundant. In contrast to the *Glossifungites* ichnofacies, the walls of the borings cut through hard parts of the substrate (larger grains, shells) rather than skirting around them.

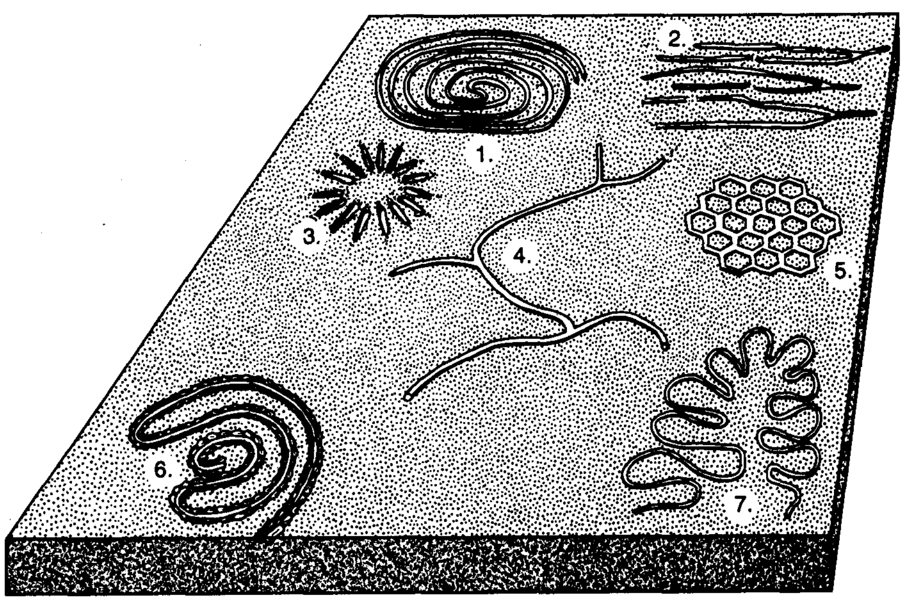

Figure 12 Trace fossil association characteristic of the *Nereites* ichnofacies. After Frey and Pemberton (1984). 1) *Spirorhaphe,* 2) *Uroheiminthoida,* 3) *Lorenzinia,* 4) *Megagrapton,* 5) *Paleodictyon,* 6) *Nereites,* 7) *Cosmorhaphe.*

Teredolites Ichnofacies

The *Teredolites* ichnofacies consists of a characteristic assemblage of borings in woody (xylic) substrates. These differ from lithic substrates in three main ways (Bromley *et al.*, 1984); 1) they may be flexible instead of rigid, 2) they are composed of combustible material instead of mineral matter, and 3) they are readily biodegradable. Woodgrounds may appear in freshwater settings such as logjams in fluvial cutoffs, and freshwater ichnocoenoses consist principally of isopod and allied borings. Because wood substrates can be moved by currents, it is important to determine whether the borings are autochthonous (Arua, 1989) or allochthonous (Dewey and Keady, 1987). Only the autochthonous forms are true members of the *Teredolites ichnofacies*. These assemblages may also be important in defining sequence and parasequence boundaries.

The traces are characterized by 1) sparse to profuse clavate (club-shaped) borings, 2) dense excavations, but without interpenetrating borings, 3) walls ornamented with the texture of the host substrate (e.g., tree ring impressions), 4) stumpy to elongate subcylindrical, subparallel excavations in marine or marginal marine settings, 5) shallower, sparse to profuse nonclavate etchings (isopod borings) in freshwater settings.

EVALUATION OF THE NINE RECURRING ICHNOFACIES MODELS

These archetypal models, particularly the marine ones, have proven to be valuable in characterizing general environmental conditions. In many cases, physical sedimentary structures cannot be used to distinguish environments — for example, the structures of fluvial point bars may be very similar to those of estuarine point bars. However, the two settings can easily be distinguished because the biogenic sedimentary structures are very different.

Perhaps the most misunderstood aspect of these recurrent ichnofacies is their use in paleobathymetry. Although some workers have been complacent regarding this aspect of environmental reconstruction (as discussed by Frey *et al.*, 1990), other ichnologists have long and persistently emphasized that *local sets of environmental factors* are most important in controlling the distribution of tracemakers, whether or not these parameters occur at specific water depths. For instance, many estuarine point bars exhibit a high-energy, channelward side typified by a *Skolithos* association and a low-energy bankward side typified by a *Cruziana* association (Howard and Frey, 1985). The respective associations occur in close proximity, at the same stratigraphic or bathymetric level.

However, many environmental parameters do tend to change progressively with water depth and distance from shore (e.g., grain size, energy levels, suspended food, water turbidity), and these gradients effect corresponding changes in the distribution of physical and biogenic sedimentary structures (Fig. 2). To that extent, trace fossil associations are indeed useful in paleobathymetry.

The long temporal duration of most kinds of trace fossils is very important. These basic benthic behavioral patterns are more nearly like stable ecologic niches than individualistic records of particular animal species (Frey and Seilacher, 1980, p. 202-203). As long as the functional niche remains advantageous under given environmental conditions, many different animal species, over long intervals of geological time, may be expected to exploit it. Their preserved traces are strikingly similar and have equivalent significance. Hence, although we conveniently and informally speak of the "*Skolithos* animal" as the architect for a particular kind of dwelling structure, numerous different animal species actually were involved (i.e., many biological species construct the same type of burrow). The longevity of recurrent ichnofacies thereby exceeds the longevity of recurrent biofacies by a considerable margin. Such ichnofacies are more useful as archetypal models not only for environmental interpretation but also for comparisons of depositional environments of widely differing ages.

These recurrent ichnofacies have been designated as archetypal facies models, with which particular local ichnofacies can be compared. The archetypes are intended to supplement, not supplant, local ichnofacies designations, some of which are quite distinctive; corresponding ichnofaunas may be restricted (Serna, 1986), intergradational (Marintsch and Finks, 1982), or diverse (Dam, 1990).

The idealized ichnofacies succession (Fig. 2) works well in most "normal" situations (Frey and Pemberton, 1984, their fig. 5), including salinity gradients (Bromley and Asgaard, 1991). However, nearshore assemblages can be found in offshore sediments, and vice versa, if the particular sediments accumulated under conditions preferred by the tracemaking organisms. The basic controls are not physical constraints such as water depth, distance from shore, or some particular tectonic or physiographic setting. Rather, they involve substrate consistency, hydraulic energy, rates of deposition, turbidity, oxygen and salinity levels, toxic substances, the quality and quantity of available food, and the ecologic or ichnologic prowess of tracemakers themselves (Vossler and Pemberton, 1988a).

Finally, the models should not be divorced from associated patterns of bioturbation. Numerous local ichnofacies, particularly those representing low-energy conditions and slow rates of deposition, are set in a totally bioturbated texture (Fig. 13). Several generations of burrows may be discernible via their cross-cutting relationships, showing that the same volume of sediment passed repeatedly through various styles of reworking. In environmental reconstruction, such ichnologic fabrics may be equally as important as the individual, named trace fossils (Pemberton and Frey, 1984; Howard and Frey, 1984).

PALEOENVIRONMENTAL SIGNIFICANCE OF ICHNOFOSSILS

The application of ichnology to paleoenvironmental analysis goes far beyond the mere establishment of general recurring ichnofacies. For instance, shallow water coastal marine environments (Chapters 9, 10, 11, 12) consist of many smaller sedimentological regimes characterized by large fluctuations in many physical and chemical parameters. In order to comprehend fully the depositional history of such regimes, it is necessary to have reliable means of differentiating subtle changes in these physical and chemical parameters. Physical sedimentary structures definitely help, but biogenic sedimentary structures can better delineate ecological parameters such as oxygenation, salinity, and energy levels. An example is given by Dörjes and Hertweck (1975), who subdivided the coastal zone into three major environments, based primarily on the position of mean high water, mean low water, and wave base. Their faunistic investigations also confirmed the importance of minimum and maximum wave base as distinct boundaries separating animal communities (Fig. 5).

ICHNOLOGIC APPLICATIONS TO ALLOSTRATIGRAPHY

Allostratigraphy (Chapter 1) is based on the recognition of units that can be defined by their *bounding discontinuities*. Many discontinuities are marked by major lithological changes (Figs. 2 and 8 in Chapter 1), but other equally important discontinuities may have a very subtle expression. It is here that trace fossils and trace fossil suites (along with all other available sedimentological, stratigraphic and paleontological information) can be employed effectively, both to aid in the recognition of various types of discontinuities and to assist in their genetic interpretation.

Figure 13 Complex bioturbate textures in chalk. Textures progress from obscure background mottling to increasingly sharp, well-preserved burrows. Cross cutting relations within these chalks reveal as many as 7 tiers of traces. Demopolis Chalk, Upper Cretaceous, Alabama. Scale bar 1 cm. Adapted from Frey and Bromley 1(985.)

RECOGNITION AND INTERPRETATION OF DISCONTINUITIES USING ICHNOLOGY

It is a commonly held belief that sharp breaks in the vertical stratigraphic record may signify fundamental changes in the depositional environment and initiation of new cycles of sedimentation. However, many facies contacts are sharp, despite the superposed facies being at least somewhat genetically related. The emplacement of sandy storm beds in the offshore transition zone, for example, yields abrupt basal contacts with the fairweather silty shales, but clearly reflects a penecontemporaneous relationship. Despite an erosional relationship, the absence of a significant temporal break indicates that such contacts probably do not have allostratigraphic significance.

In contrast, gradational facies contacts are generally regarded to imply a more gradual shift in depositional conditions. Nonetheless, intense burrowing, for example, can destroy erosion surfaces through biogenic homogenization, making the contact between two superposed facies appear to be gradational. The presence of dispersed pebbles or rip-up clasts may be the only preserved evidence of such a surface, and such evidence must be sought carefully when logging core or measuring outcrop sections. The action of organisms within the substrate may serve to either *enhance* or *obscure* breaks in the stratigraphic succession. In this chapter, we are primarily concerned with the ichnological characteristics which serve to enhance the recognition and interpretation of discontinuities.

Ichnology may be employed to resolve breaks in the section in two main ways. The first is by recognition of substrate-controlled ichnofacies, which mark time gaps between the *original* deposition of a unit (with or without softground burrowing) and later superimposition of a *postdepositional* trace assemblage. The second is through careful analysis of vertical ichnologic successions analogous to facies successions (Chapter 1). Vertical changes in ichnological character which *may* reflect fundamental changes in depositional setting include changes in 1) interpreted organism behaviour (e.g., feeding strategy, dwelling style), 2) trace fossil diversity, reflecting environmental stresses such as decreased salinity, increased water turbidity, and reduced

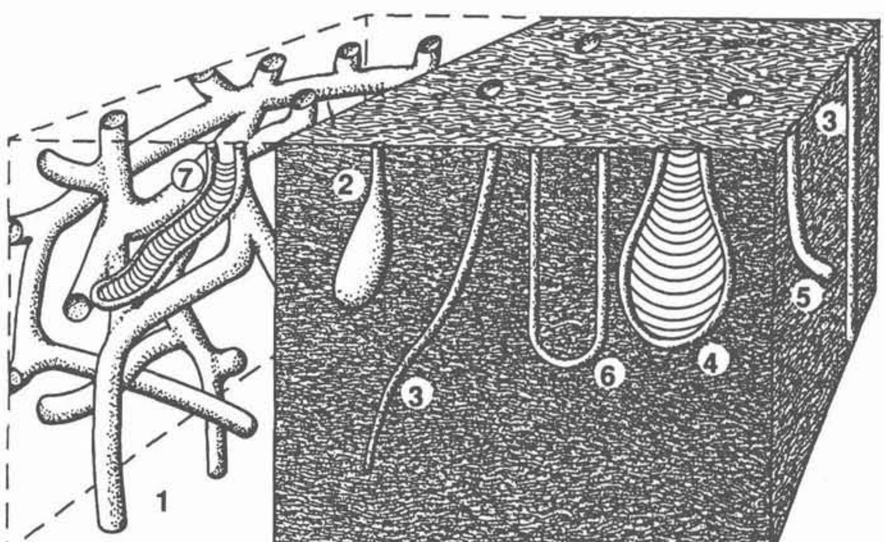

Figure 14 Trace fossil association characteristic of the *Glossifungites* ichnofacies. 1) *Thalassinoides* or *Spongeliomorpha*, 2) *Gastrochaenolites* or related ichnogenera, 3) *Skolithos* or *Trypanites*-like structures, 4) *Diplocraterion*, 5) *Psilonichnus*, 6) *Arenicolites*, 7) *Rhizocorallium*. Modified from Frey and Pemberton (1984).

oxygenation, and 3) ichnofossil abundance. Integrating the data derived from substrate-controlled ichnofacies with data from vertical ichnologic successions provides a powerful tool for the recognition and interpretation of discontinuities.

Discontinuities

All breaks in the stratigraphic record are important but may not have allostratigraphic importance. Allostratigraphic boundaries typically correspond to fundamental shifts in the depositional systems, related to allocyclic controls. Such bounding discontinuities are regional in extent and correspond to significant temporal breaks, aspects that require careful stratigraphic, sedimentological, biostratigraphic, paleomagnetic, and/or radiometric analysis.

Three major types of discontinuity commonly regarded to have allostratigraphic significance will be considered, 1) *erosional discontinuities*, 2) *nondepositional hiatuses*, and 3) *depositional discontinuities*. The *erosional discontinuities* include lowstand incised valleys, incised submarine canyons, regressive surfaces of erosion (forced regressions, Chapter 12), transgressive surfaces of erosion (ravinement surfaces), and coplanar surfaces of lowstand erosion and transgressive ravinement (E/T surfaces in the Cardium Formation, Plint *et al.*, 1986). *Nondepositional hiatuses* correspond to diastems or nonsequences. They reflect cessation of deposition, with minimal or no erosion; they may be manifest by submarine firmgrounds or hardgrounds. *Depositional discontinuities* are unusually thin intervals of slow but continuous accumulation. They include condensed sections, which are thin deposits reflecting long spans of time, such that underlying facies successions are fundamentally unrelated to overlying successions. Marine flooding surfaces can also be depositional discontinuities, in as much as they represent abrupt deepening with minimal or no development of intermediate facies due to insufficient time for "normal" environmental response to the changing conditions. It is emphasized that both condensed sections and marine flooding surfaces form important stratigraphic discontinuities, despite the fact that there has been no actual removal of strata nor cessation of deposition.

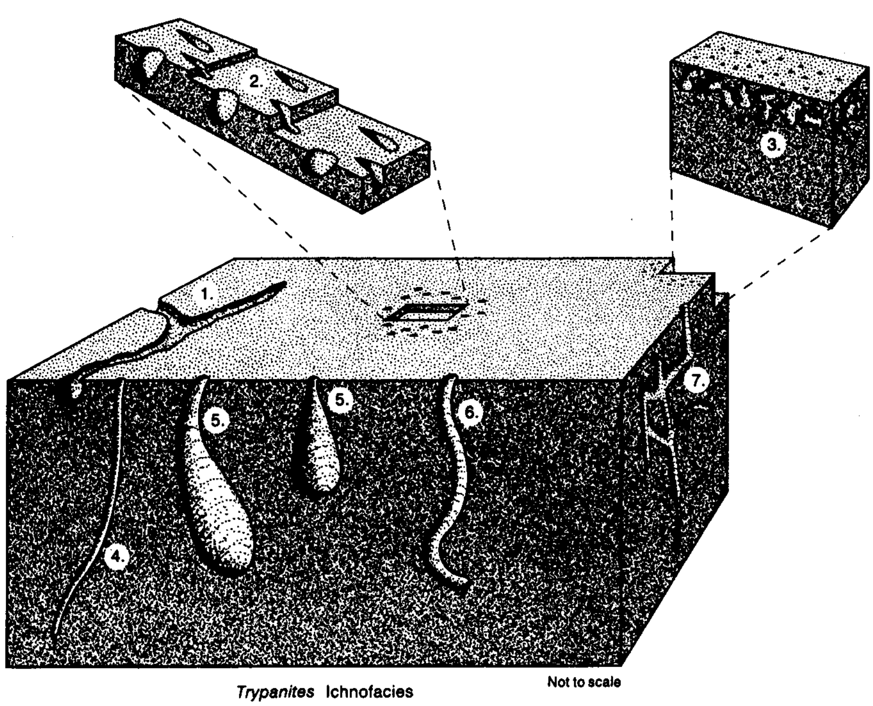

Figure 15 Trace fossil association characteristic of the *Trypanites* ichnofacies. 1) echinoid grooves, unnamed, 2) *Rogeralla*, 3) *Entobia*, 4) *Trypanites*, 5) *Gastrochaenolites*, 6) *Trypanites*, 7) polychaete boring, unnamed. Adapted from Frey and Pemberton (1984).

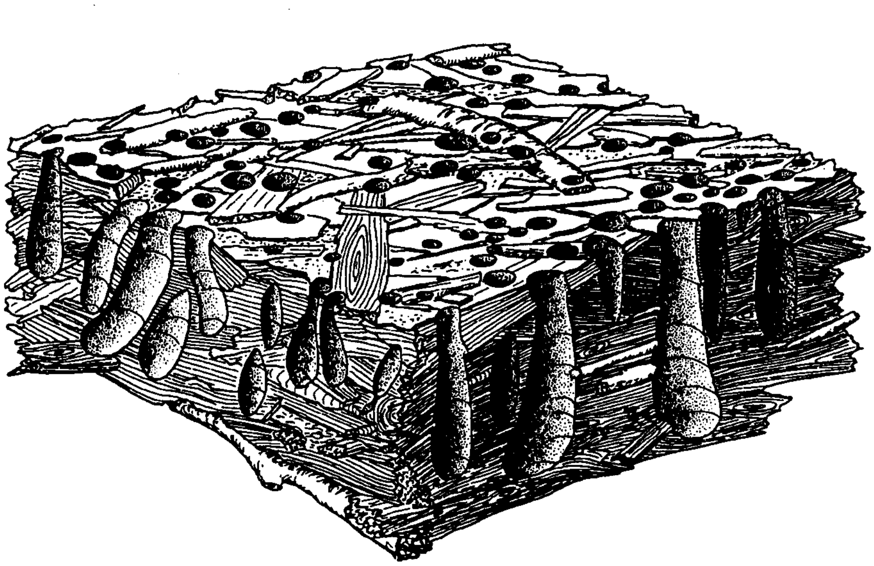

Figure 16 Trace fossil association characteristic of the *Teredolites* ichnofacies. Adapted from Bromley *et al.* (1984).

Substrate-controlled ichnofacies

Three substrate-controlled ichnofacies have been established (Ekdale *et al.*, 1984), *Glossifungites* (firmground, Figs. 14, 17A, B), *Trypanites* (hardground, Figs. 15, 17C), and *Teredolites* (woodground, Figs. 16, 17D; Table 2). In clastic settings, most of these trace assemblages are associated with erosionally exhumed (dewatered and compacted or cemented) substrates and therefore correspond to erosional discontinuities. Woodgrounds consist of xylic clasts or interwoven mats of vegetation, forming resilient substrates that are not necessarily erosionally exhumed. In carbonate settings, firmground or hardground surfaces may occur at the sediment-water interface, due either to erosional exhumation or nondepositional breaks with associated submarine cementation (Bromley, 1975). Depositional breaks, in particular condensed sections, may also be semilithified or lithified (Loutit *et al.*, 1988), presumably at the upper contact. A condensed section may be colonized without erosion, and the upper surface may subsequently form a downlap surface (Chapter 1). In general, however, the recognition of substrate-controlled ichnofacies may be regarded as equivalent to the recognition of discontinuities in the stratigraphic record.

Although certain insect and animal burrows in the terrestrial realm may be properly regarded as firmground suites (Fürsich and Mayr, 1981) or more rarely, hardground suites, they have a low preservation potential and constitute a relatively minor component in the geological record of such associations. The overwhelming majority of these firmground assemblage faunas form in marine or marginal-marine settings. A discontinuity may be generated in either subaerial or submarine settings, but colonization of the surface may be regarded as marine influenced, particularly in pre-Tertiary rocks. This has important implications regarding the genetic interpretation of the discontinuity.

The substrate-controlled ichnocoenose typically cross cuts a pre-existing softground suite. It therefore reflects conditions *postdating* both initial deposition of the unit and its subsequent erosion (Fig. 17). The suite also corresponds to a hiatus between the erosion event (which exhumes the substrate) and deposition of the overlying unit. During this time gap, the substrate is colonized by organisms. By studying 1) the softground ichnofacies (contemporaneous with deposition of the unit), 2) the ichnofacies associated with the exhumed substrate, and 3) the ichnofacies of the overlying unit, it is possible to make some interpretation regarding the origin of the surface and the allocyclic or autocyclic mechanisms responsible.

EROSIONAL DISCONTINUITIES

There are numerous examples in the ancient record of ichnologically demarcated erosional discontinuities (Table 2), many of which have allostratigraphic significance. These discontinuities include *lowstand unconformities, transgressive surfaces of erosion,* and *amalgamated lowstand erosion* and *transgressive surfaces.*

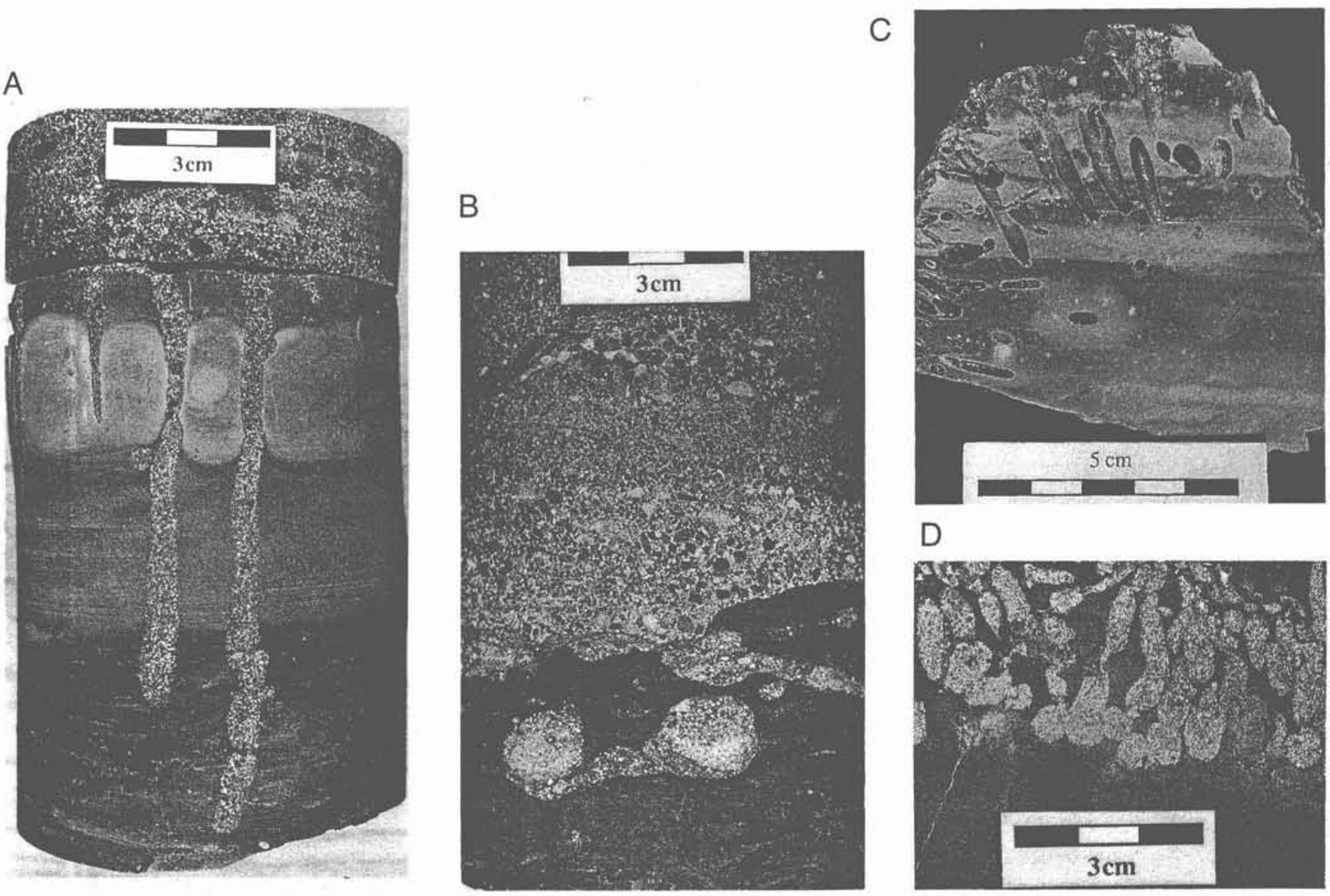

Figure 17 Substrate-controlled ichnofacies. A) *Glossifungites* ichnofacies consisting of *Skolithos* and ?*Arenicolites/Diplocraterion* penetrating a sideritized shale. The firmground suite cross-cuts offshore shales containing *Helminthopsis, Terebellina, Planolites*, and *Chondrites.* Pebbly fill has been piped down from the overlying conglomerate. Albian Viking Formation, Gilby A Field, Alberta. B) *Glossifungites* ichnofacies consisting of *Rhizocorallium* excavated into offshore shales and cross cutting a resident softground suite of *Helminthopsis, Planolites, Terebellina, Chondrites*, and *Zoophycos.* The firmground suite marks the base of an incised valley fill. Albian Viking Formation, Willesden Green Field, Alberta. C) *Trypanites* ichnofacies consisting of *Trypanites weisei* from the Silurian/Devonian disconformity (Bois Blanc/Bertie Formations), southern Ontario. D) *Teredolites* ichnofacies consisting of borings into slightly coalified wood. The medium to coarse sand fill is [illegible] Grand Rapids Formation, Wabasca area, Alberta.

Lowstand unconformities

Subaerial exposure and/or erosion produced during a lowstand of relative sea level permits the widespread development of dewatered and firm or cemented substrates. Such surfaces may initially be mantled by a thin veneer of nonmarine deposits, although their preservational potential is low. In any case, unless the exhumed surface is exposed to marine or marginal marine conditions prior to final burial, it will not become colonized by tracemakers of the *Glossifungites*, *Trypanites* or *Teredolites* ichnofacies.

In the exceptional case of submarine canyons, the erosional discontinuity lies within a marine setting at the time of its development, and colonization of the walls and floor has a much higher probability than those in terrestrial valleys. Outcrops of the Lower Miocene Nihotupu and Tirikohua formations in Northland, New Zealand, contain a noteworthy substrate-controlled trace fossil association (Hayward, 1976; Fig. 18; Table 2). The underlying Nihotupu Formation consists of largely unburrowed mudstones, sandstones and subaqueous mass flow conglomerates (all of volcanic origin), together with submarine piles of pillow lavas. Ichnofossils are rare, but solitary burrows and burrowed horizons, including *Thalassinoides*, *Planolites*, and *Scalarituba*, occur locally. Sediments of the Nihotupu Formation are interpreted to have been deposited as turbidites at bathyal water depths (based on faunal content) within an interarc basin on the lower eastern flanks of the west Northland volcanic arc.

The contact with the overlying Tirikohua Formation is sharp and erosional, and exhibits visible relief. The exhumed substrate contains a Glossifungites assemblage of burrows, consisting of *Skolithos* (called *Tigillites* by the original author), *Rhizocorallium*, and ?*Thalassinoides*. Mechanical borings are absent, indicating that the surface was not lithified at the time of colonization. Steep trench walls with small overhangs demonstrate that underlying sediments were stiff and semiconsolidated at the time of colonization by tracemakers of the *Glossifungites* suite (Fig. 18). The overlying Tirikohua Formation consists of fairly coarse-grained volcaniclastics (sandstones and conglomerates), deposited as canyon floor and neritic sediment gravity flows, similar to proximal turbidites. The sediments contain a sparse trace suite consisting of *Planolites*, *Scalarituba*, *Skolithos*, *Thalassinoides*, and escape traces. Hayward (1976) interpreted the erosional discontinuity as a submarine canyon, excavated into bathyal to neritic interarc sediment gravity flow deposits due to tectonic uplift of the basin margin (e.g., relative lowering of sea level). Colonization of the canyon walls by the firmground tracemakers preceded eventual burial by canyon floor and neritic turbidite deposits of the Tirikohua Formation, probably corresponding to late stage relative sea level lowstand or early transgressive fill of the submarine canyon.

Within terrestrial incised valleys, colonization of the discontinuity may occur during lowstand conditions at the seaward (estuarine) end of the valley. In this case, the distribution of substrate-controlled ichnofacies can be used to map the maximum marine limit within the valley. Alternatively, colonization of the valley walls and floor may not occur until an ensuing transgressive event. Under these conditions, initial lowstand deposits are removed during the transgression, exposing the unconformity to marginal marine conditions. Transgressively related estuarine deposits are ultimately laid down on the substrate-controlled trace suite as the valley fills. Whether a substrate-controlled trace fossil suite at the base of a valley fill represents the marginal-marine portion of the valley during lowstand or later transgressively related fill is a problem to be resolved through stratigraphic, sedimentological, and paleontologic analysis.

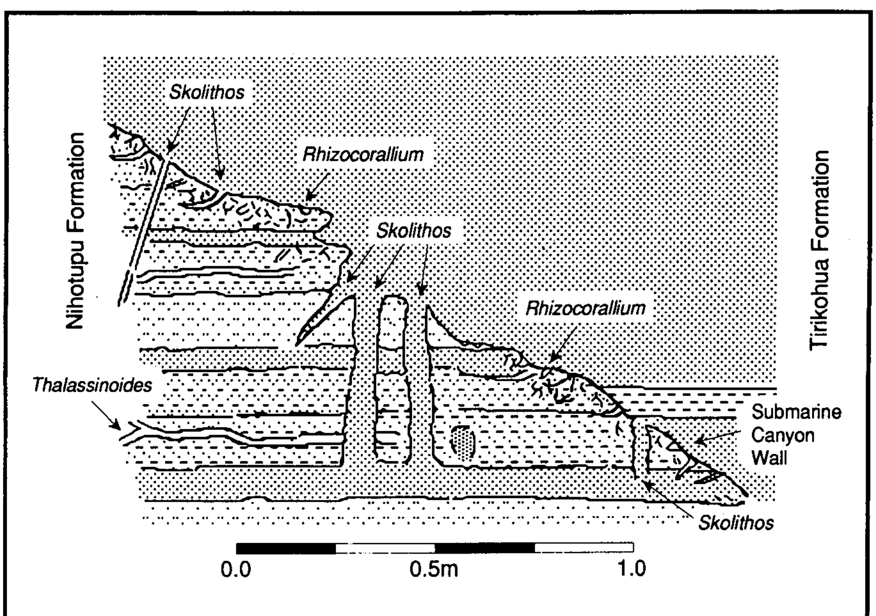

Figure 18 Submarine canyon wall ichnocoenose at Tirikohua Point, New Zealand. The Miocene Nihotupu Formation consists of volcanogenic clastics deposited as turbidites in bathyal water depths in an inner-arc basin. A submarine canyon is incised into these sediments as a result of a relative fall in sea level and is marked by a substrate-controlled ichnocoenose. The presence of the *Glossifungites* ichnofacies, as well as the steep trench walls having small overhangs, attest to semiconsolidated underlying sediments at the time of colonization. The Tirikohua Formation corresponds to canyon floor deposits and neritic sediment gravity flows, which filled the submarine canyon during an ensuing transgression. Modified after Hayward (1976).

Lowstand unconformities — examples from the Viking Formation

The Lower Cretaceous (Albian) Viking Formation of Alberta contains an excellent example of subaerial erosion (valley incision) and subsequent estuarine colonization. The subsurface Crystal field (Figs. 19, 20) consists of a linear sandstone body up to 30 m thick, generally interpreted to be some form

Table 2 *Ichnologically Demarcated Erosional Discontinuity Surfaces. The table outlines outcrop and subsurface examples of substrate-controlled ichnofacies and the interpreted allostratigraphic significance of the demarcated discontinuity. Most omission suite traces are referable to the* Glossifungites *ichnofacies, but some are referable to the* Trypanites *or* Teredolites *ichnofacies. WCSB refers to the Western Canada Sedimentary Basin.*

AGE	LOCATION	FORMATION	PRE-EROSION TRACE SUITE	EROSION SURFACE TRACE SUITE
Ordovician	Michigan Basin U.S.A.	Glenwood Fm (subsurface)	Dark, phosphatic silt-bearing shale; no visible trace fossils.	*Glossifungites* assemblage consisting of robust *Thalassinoides.*
Sil-Dev unconformity	S. Ontario Canada	Bertie/Bois Blanc Fm contact (outcrop)	Bertie Fm dolomites with *Thalassinoides.*	Karsted surface bored by tracemakers of the *Trypanites* assemblage, consisting of *Trypanites weisei* & *Gastrochaenolites.*
Jurassic (Pliensbachian)	East Greenland	Kap Stewart/ Neill Klinter Fm contact (outcrop)	Unburrowed and rooted deltaplain sandstones and coals.	*Glossifungites* assemblage consisting of abundant *Diplocraterion parallelum.* Pebble lag is present.
Cretaceous (L. Albian)	WCSB NE B.C.	Gething/ Bluesky Fm contact (subsurface)	Unburrowed, finely laminated and rooted mudstones and coals (Gething Fm).	*Glossifungites* assemblage consisting of *Skolithos* and *Thalassinoides* with associated pebble lag.
Cretaceous (U. Albian)	WCSB Joffre Field Alberta	Viking Fm (subsurface)	Silty shales & distal storm sands with *Planolites, Helminthopsis, Chondrites, Terebellina,* rare *Zoophycos, Asterosoma* & *Rhizocorallium.*	*Glossifungites* assemblage consisting of *Skolithos, ?Arenicolites/Diplocraterion* and *Thalassinoides* with associated pebble lag.
Cretaceous (U. Albian)	WCSB Kaybob Field Alberta	Viking Fm (subsurface)	Intensely burrowed sandy shale with *Teichichnus, Helminthopsis, Planolites, Zoophycos, Chondrites, Asterosoma,Terebellina* & rare *Rosselia* & *Rhizocorallium.*	*Glossifungites* assemblage consisting of *Thalassinoides* and *Skolithos* with associated rip-up clasts and pebbles.
Cretaceous (U. Albian)	WCSB Crystal Field Alberta	Viking Fm (subsurface)	Intensely burrowed muddy sandstone with *Helminthopsis, Terebellina, Chondrites, Planolites Asterosoma* & rare *Zoophycos.*	*Glossifungites* assemblage consisting of *Diplocraterion* shafts.
Cretaceous (U. Albian)	WCSB Sinclair Field Alberta	Peace River Fm Paddy Mbr (subsurface)	Intensely burrowed pebbly shale with *Chondrites, Helminthopsis, Terebellina, Asterosoma* & *Planolites.*	*Glossifungites* assemblage consisting of *Diplocraterion,* associated with dispersed pebbles.
Cretaceous (Cenomanian)	WCSB Jayar Field Alberta	Dunvegan Fm (subsurface)	Largely unburrowed and locally rooted mudstones in shallow water (lacustrine?) and deltaplain settings	*Glossifungites* assemblage consisting of *Thalassinoides* systems.
Cretaceous (Turonian)	WCSB Pembina Field Alberta	Cardium Fm (subsurface)	Silty shales with *Helminthopsis, Planolites, Chondrites, Terebellina* and rare *Zoophycos,* reflecting a distal *Cruziana* ichnofacies.	*Glossifungites* ichnofacies consisting of *Thalassinoides.*
Cretaceous (Maastrichtian)	WCSB Drumheller Alberta	Horseshoe Canyon Fm (outcrop)	Unburrowed and rooted shales and coals formed within a backbarrier setting.	*Teredolites* assemblage consisting of abundant *Diplocraterion parallelum* subtending into a backbarrier coal.
Cretaceous-Tertiary contact	Alabama U.S.A.	Prarie Bluff/ Clayton Fm	Burrowed (ichnogenera not disclosed) fossiliferous chalk (*cf.* Frey and Bromley, 1985).	Vertical *Thalassinoides paradoxicus* & *Spongeliomorpha* system of the *Glossifungites* assemblage.
Tertiary	Tirikohua Pt	Nihotupu /	Largely unburrowed thin bedded	*Glossifungites* ichnofacies, represented

Table 2 *cont'd.*

POST-EROSION TRACE SUITE	INTERPRETATION OF SURFACE
Intensely burrowed coarsening-upward cycle of sandstone & shale with a shallow water suite of *Teichichnus, Asterosoma, Planolites,* small *Terebellina* & rare *Chondrites.*	Lower facies reflects a condensed section (R. Dott Jr., G. Nadon and D. Rodrigues de Miranda, pers. comm., 1991), possibly with submarine cementation. A shallowing event, probably accompanied by erosion (rip-up clasts within burrow fill) may indicate lowered relative sea level.
Oriskany sandstone of the Bois Blanc Fm is unburrowed.	Bertie Fm reflects final stages of marine regression. Disconformity at top represents shallowing and subaerial exposure. Transgression permitted colonisation and boring of E/T surface, followed by Oriskany sandstone deposition (Pemberton *et al.*, 1980).
Poorly-sorted, medium to very coarse, massive to cross-bedded sandstone with *Diplocraterion, Ophiomorpha, Gyrochorte, Monocraterion* & *Rhizocorallium.*	The contact is interpreted as a transgressive omission surface (?ravinement), separating Sinemurian deltaplain deposits from overlying barred shoreline sediments (Dam, 1990).
Bar margin: intensely burrowed shaly sands with *Rosselia, Helminthopsis, Asterosoma, Palaeophycus, Teichichnus, Planolites* & *Terebellina.* Brackish pro-delta: interbedded sands & shales with *Teichichnus, Planolites* & *Palaeophycus.*	Subaerial exposure and progradation of coal-bearing deltaplain sediments, followed by transgressive ravinement (amalgamated E/T surface). Colonisation of the erosion surface preceded main transgressive lag deposition. Overlying facies reflect prograding bar margin or brackish water pro-delta deposits of the next progradational cycle (Oppelt, 1988).
Sparsely burrowed, cross-bedded pebbly and coarse sandstone with rip-up clasts. Mud drapes contain *Planolites.*	Erosion surface cut into offshore deposits during lowstand of relative sea level, sharply overlain by middle or lower shoreface sandstones. Reflects basinward shift of lowstand shoreface or final shoreface position due to transgressive shoreface retreat (Downing and Walker, 1988).
Trough and low angle parallel laminated sandstone containing *Arenicolites, Skolithos, Ophiomorpha, Teichichnus, Palaeophycus, Helminthopsis, Chondrites, Rosselia, Planolites, Terebellina* and *Asterosoma,* reflecting a middle shoreface setting.	Surface is an erosional unconformity (generated by lowstand of relative sea level) incised into underlying offshore/inner shelf deposits. Proximally, an abrupt basinward shift of the shoreline ("forced regression") resulted in deposition of directly overlying middle shoreface deposits. Distally, shoreface progradation produced a coarsening-upward lower to middle shoreface cycle.
Sandstones, interbedded sands and shales, and shales with *Teichichnus, Ophiomorpha, Palaeophycus, Diplocraterion, Terebellina, Planolites, Skolithos, Asterosoma* & *Rosselia.*	The surface is interpreted to reflect an incised valley, generated during a lowstand of relative sea level. The surface is incised into underlying shelf to lower shoreface deposits. Overlying valley fill is part of an estuarine tidal-channel complex (Reinson *et al.*, 1988).
Pebbly shale, intensely burrowed, with *Helminthopsis, Zoophycos* and *Chondrites,* grading into less burrowed sandstone & shale with *Asterosoma, Planolites* and *Chondrites.*	The surface is interpreted to reflect transgressive ravinement associated with continued (stepwise?) Colorado Sea advance. Underlying transgressively reworked deposits reflect slightly more proximal conditions than the immediately overlying sediments.
Medium grained sandstones, intensely burrowed, with *Ophiomorpha* (transgressive sheet sand), passing into marine shales with *Zoophycos, Planolites* and *Chondrites.*	Deltaplain facies capped by subaerial exposure surface, reflecting a lowstand of relative sea level. Transgressive surface of erosion was cut, and reworking of underlying facies produced an overlying transgressive sheet sand, passing into marine shale (Bhattacharya and Walker, 1991).
Largely unburrowed conglomerate, overlain by marine shale with dispersed pebbles; shales contain *Helminthopsis, Planolites, Chondrites, Terebellina* and *Zoophycos.*	The surface may reflect erosion due to a lowstand of relative sea level followed by shoreface progradation (Plint *et al.*, 1988) or ravinement (initial transgression) followed by stillstand shoreface progradation, capped by shales of a resumed transgression (*cf.* Walker, 1990).
Low angle parallel laminated (HCS and SCS) sandstone with *Ophiomorpha, Rhizocorallium, Teichichnus, Conichnus, Skolithos* & *Rosselia* in a storm-dominated lower shoreface setting.	The erosion surface is interpreted to reflect transgressive ravinement, separating backbarrier deposits from overlying prograding storm-dominated shoreface deposits (Saunders and Pemberton, 1986).
Sandy glauconitic marls with reworked Cretaceous fossils, thoroughly burrowed; replete with *Thalassinoides suevicus.*	Prarie Bluff Chalk was subaerially exposed and locally incised by valleys during a lowstand of relative sea level. Subsequent transgression with ravinement permitted colonisation of the E/T surface (Savrda, 1991).
Coarse-grained volcanogenic sandstone (Tirikohua Fm) similar to proximal turbidites; sparse suite of *Skolithos, Planolites, Scalarituba, Thalassinoides* and escape traces.	The surface reflects submarine canyon incision into deep water clastics in response to tectonic uplift of an inter-arc basin margin. Canyon walls are intensely burrowed by the *Glossifungites* suite. The surface is overlain by canyon floor sediment gravity flow deposits (Hayward, 1976).

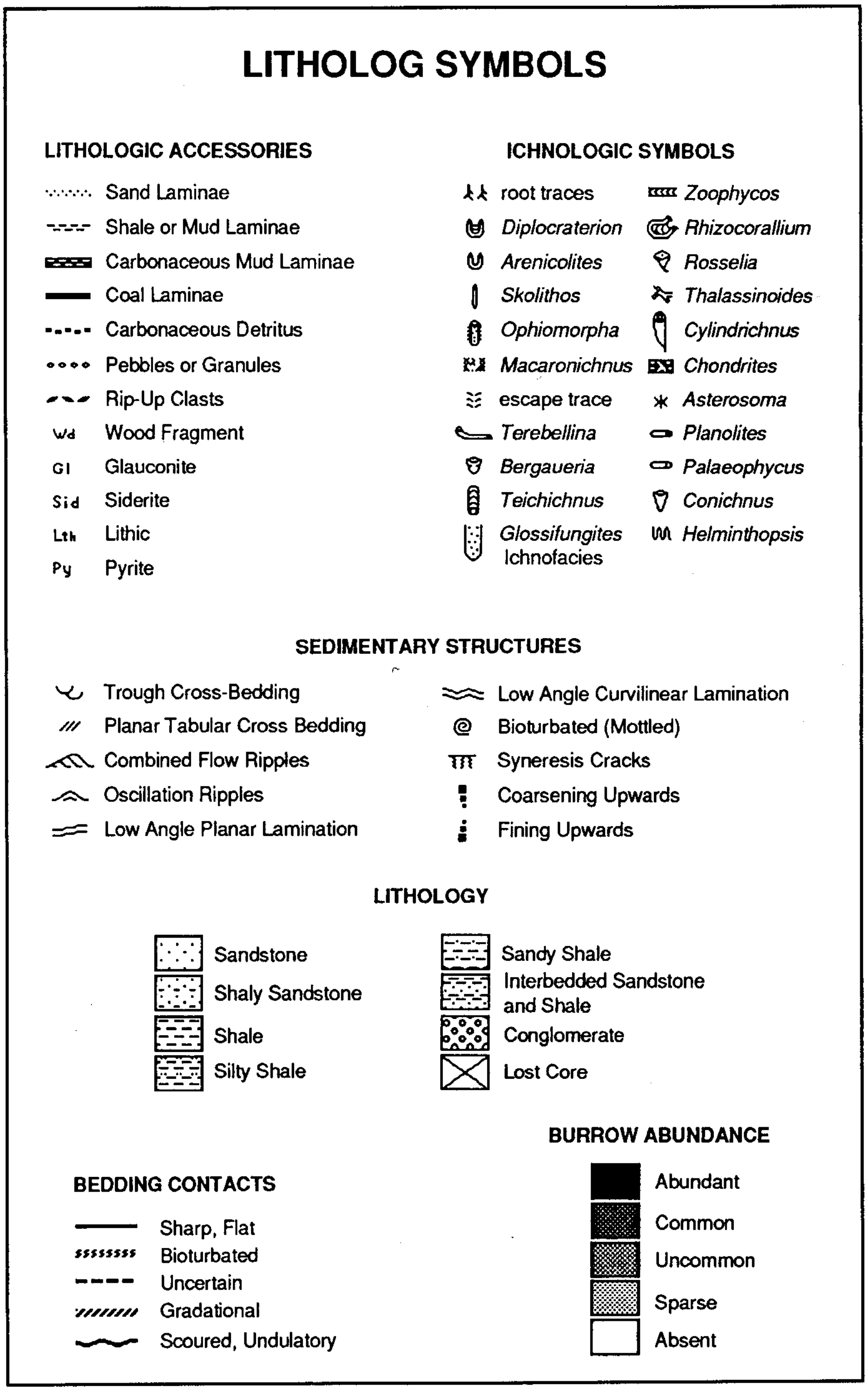

Figure 19 Symbols used in strip logs of Figures 20, 22 and 25.

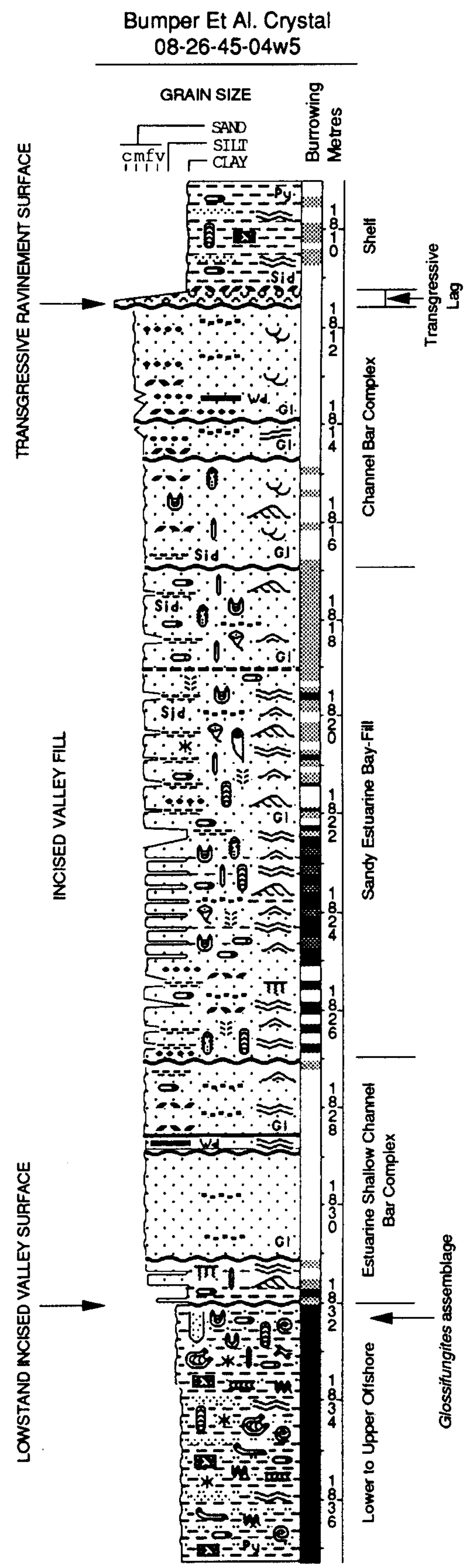

Figure 20 Strip log of a cored interval of the Viking Formation (Albian) in the Crystal Field, south-central Alberta (symbols explained in Fig. 19). Facies interpretations are listed on the right-hand side of the log; key surfaces are marked on the left. The section shows an incised valley, excavated into offshore deposits during a relative lowstand of sea level. The incision surface is marked by a *Glossifungites* assemblage consisting of *Diplocraterion.* The valley fill is a heterolithic succession of sandstones, interbedded sandstones and shales, and shales deposited in estuarine to marine settings during a relative rise in sea level. The valley fill is capped by a transgressive lag, suggesting ravinement, followed by shelfal deposition of shales.

of estuary filling (Reinson *et al.*, 1988). Beneath the basal incision of the valley, the older silty shales contain a diverse softground *Cruziana* suite of abundant *Terebellina*, *Chondrites*, *Planolites*, *Helminthopsis*, *Asterosoma*, and rare *Zoophycos* (Fig. 21A). At the erosional truncation, a large number of sharp-walled, unlined *Diplocraterion* shafts, constituting the *Glossifungites* assemblage (Fig. 21B), extend downward into the underlying facies and cross cut the original softground suite. Elsewhere, the *Glossifungites* suite consists of firmground *Gastrochaenolites.* The overlying estuary-fill facies consists of a heterolithic association of sandstones and shales. A low-diversity suite of *Skolithos* and *Planolites* (Fig. 21C) with associated syneresis cracks occurs near the base, and reflects brackish water conditions. This association passes into more fully marine suites, consisting of *Ophiomorpha*, *Teichichnus*, small *Rosselia*, *Asterosoma*, *Diplocraterion*, *Skolithos*, *Planolites*, *Palaeophycus*, and escape traces. The erosion surface is interpreted as an incised valley, excavated into underlying lower to upper offshore deposits during a relative lowering of sea level. The overlying heterolithic facies succession was interpreted by Reinson *et al.* (1988) as multistage tidal channel-fill within a larger estuarine channel-bay complex, which accumulated in response to an ensuing period of transgression.

The base of a similar incised valley in the Viking Formation at Willesden Green field is also marked by a *Glossifungites* assemblage locally consisting of *Rhizocorallium* (Fig. 17B), *Diplocraterion* and *Thalassinoides.*

The Viking Kaybob field in central Alberta (Fig. 22) produces hydrocarbons from a coarsening-upward, NW-SE-trending sandstone body. The sandstone overlies an extensive erosion surface incised into thoroughly burrowed silty to sandy shales containing a diverse Cruziana assemblage of *Teichichnus*, *Helminthopsis*, *Asterosoma*, *Terebellina*, *Planolites*, *Zoophycos*, *Chondrites*, rare *Rosselia*, and *Rhizocorallium*. The mixture of grazing and deposit-feeding traces suggests offshore shallow-marine deposition. Cores in proximal positions (Fig. 22) show the underlying sandier-upward offshore facies succession abruptly truncated by the erosional discontinuity. The discontinuity is marked by a *Glossifungites* assemblage consisting of robust *Skolithos* and *Thalassinoides*, passively filled with medium to coarse sand which infiltrated the burrows from the overlying facies. The overlying sandstone is medium grained and contains low-angle parallel lamination and rarer oscillation ripples. The trace fossil suite mainly consists of structures made by deposit feeders, suspension feeders, and passive carnivores with less abundant grazing traces, and is manifest by *Skolithos*, *Ophiomorpha*, *Bergaueria*, *Palaeophycus*, *Teichichnus*, *Asterosoma*, *Rosselia*, *Planolites*, *Terebellina*, *Helminthopsis*, and *Chon-*

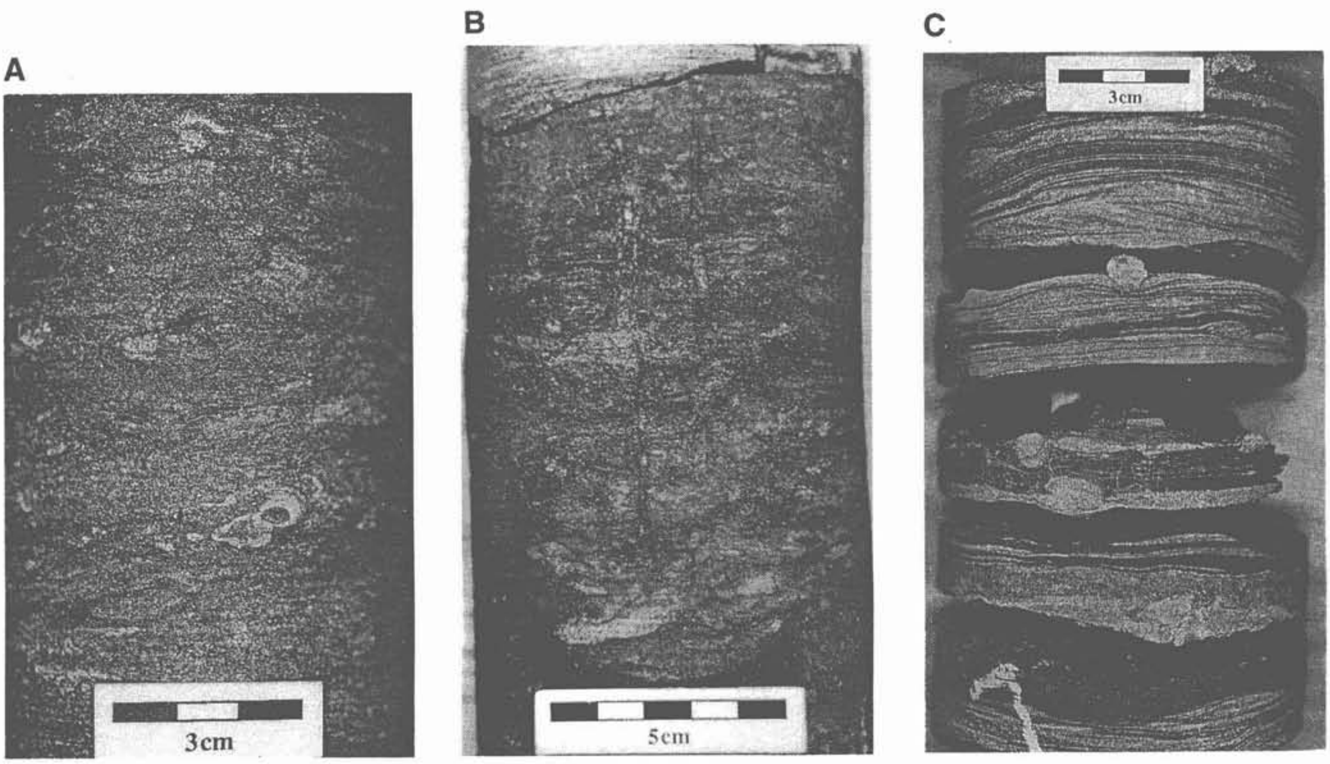

Figure 21 Pre-erosion (A), erosion (B), and posterosion (C) trace fossil suites, Albian Viking Formation, Crystal Field, Alberta. A) Pre-erosion softground suite representing a distal *Cruziana* assemblage in intensely burrowed offshore, to lower shoreface silty to sandy shales. Traces include *Helminthopsis, Planolites, Thalassinoides, Terebellina, Teichichnus, Rhizocorallium,* and rare *Arenicolites, Skolithos,* and *Palaeophycus.* B) Erosion suite, consisting of a *Glossifungites* assemblage of sharp walled, unlined, mud filled *Diplocraterion* shafts, cross cutting a distal *Cruziana* suite. Contact between the sandstone at the top of the photograph and the sandy shale corresponds to the base of the incised valley fill. C) posterosion suite consists of a low-diversity assemblage of sparse *Planolites* and rare *Skolithos.* Traces are developed in wavy bedded oscillation and combined flow ripple laminated fine sandstones and dark shale drapes. Suite reflects a stressed (brackish?) environment.

drites. This sharp-based sandstone is interpreted to reflect a storm-dominated lower- to middle-shoreface setting.

Farther seaward to the northeast, the same erosion surface lacks a *Glossifungites* suite, but is marked by dispersed pebbles and medium- to coarse-sand grains. The erosion surface is overlain by a gradually coarsening upward succession of intensely burrowed silty and sandy shales containing a diverse *Cruziana* suite of abundant *Asterosoma, Terebellina, Planolites, Zoophycos, Chondrites*, and *Helminthopsis*; upward, *Teichichnus, Rosselia, Rhizocorallium, Skolithos*, and *Arenicolites* are more common, reflecting offshore to lower shoreface progradation. Finally, the sandy shales grade upward into intensely burrowed shaly sandstones containing *Skolithos, Arenicolites, Cylindrichnus, Palaeophycus, Asterosoma, Terebellina, Chondrites, Planolites*, and *Helminthopsis*, reflecting lower- to middle-shoreface conditions.

The discontinuity is interpreted to be a regressive surface of erosion, formed as a result of a lowering of relative sea level and incision into the underlying offshore shales. In proximal areas, the erosion surface is abruptly overlain by incised lower- to middle-shoreface deposits. In more basinal settings, the discontinuity is overlain by distal equivalents of the incised shoreface, which prograded basinward and generated a more gradual coarsening-upward succession. This relationship defines a *forced regression* (Chapter 12; Plint, 1988; Posamentier and Vail, 1988).

Transgressive surfaces of erosion

Transgressive surfaces of erosion (ravinement surfaces) afford the most elegant mode of developing widespread substrate-controlled ichnofacies. This is principally because the exhumed surfaces are generated within a marine or marginal marine environment, favouring colonization by organisms as the surface is cut, and prior to significant deposition of overlying sediment.

Transgressive surfaces of erosion — example from the Viking Formation

The Viking Formation can be used again, this time providing excellent examples of transgressive surfaces of erosion. Several such surfaces occur near the top of the formation. In the Kaybob field, the lowstand incised shoreface setting discussed previously (Fig. 22) is overlain by pebbly shales with thin gritty sands, containing a trace suite of *Terebellina, Helminthopsis, Planolites, Teichichnus, Chondrites*, and *Zoophycos*. This style of sedimentation is interrupted by Glossifungites assemblages *(Skolithos, Arenicolites, Diplocraterion*, and *Thalassinoides)* that occur at "hidden" bed junctions, associated with periods of erosion (ravinement) and stillstand. These deposits are overlain by indistinctly burrowed marine shales having thin silty sand stringers and rare *Planolites*.

The incised shoreface succession (Fig. 22) is interpreted to reflect basinward progradation, following the forced regression. This was terminated by a relative rise in sea level, when associated ravinement stripped off the upper shoreface and coastal plain facies. Periodic stillstands during the overall transgression permitted deposition of the pebbly shale facies, while resumed transgression generated erosional discontinuities marked by *Glossifungites* suites (Fig. 23). Continued transgression of the Colorado sea resulted in deposition of distal offshore to shelfal shales. Similar facies successions occur in other parts of the Viking Formation (e.g. Joarcam field, Power, 1988; Joffre field, Downing and Walker, 1988).

Amalgamated lowstand erosion and transgressive surfaces

Amalgamated (or coplanar) lowstand erosion and transgressive surfaces are commonly colonized by substrate-controlled tracemakers. Erosion during lowstand typically produces widespread firmground, hardground, and woodground surfaces. The following transgressive event tends to remove much of the lowstand deposits and exposes the discontinuity to marine or marginal marine conditions (Chapter 12). Organisms then colonize the re-exhumed flooded surface. Savrda (1991) noted that the lowstand unconformity at the Cretaceous-Tertiary contact in Alabama contained a substrate-controlled ichnofacies only where an overlying transgressive surface of erosion was amalgamated with it. Localities where valley fill deposits separate the unconformity from the

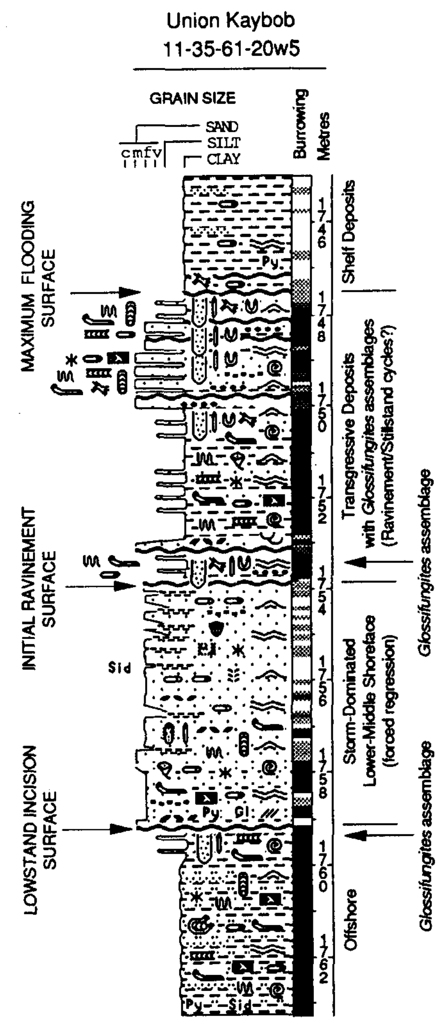

Figure 22 Strip log of a cored interval of the Viking Formation (Albian) in the Kaybob Field in central Alberta (symbols explained in Fig. 19). Facies interpretations are shown on the right -hand side of the log; key surfaces are marked on the left. The lower half of the section shows lower- to middle-shoreface deposits abruptly attenuating offshore sandy shale deposits. The erosional discontinuity is marked by a *Glossifungites* assemblage consisting of *Skolithos*. The shoreface is interpreted to be a result of "forced regression", due to a relative lowering of sea level. The lowstand shoreface is truncated by sandy and pebbly shales containing numerous *Glossifungites* assemblages developed at hidden bed junctions. The overlying assemblage reflects transgressive deposition resulting from ravinement/stillstand cycles, ultimately being capped by shelf deposits produced during maximum marine flooding.

ravinement surface lack *Glossifungites* suites (see Table 2) and suggest the fill may have been fluvial.

The Turonian Cardium Formation of the Pembina field, central Alberta (Fig. 16 in Chapter 12), contains a series of shorefaces associated with transgressive surfaces of erosion (Walker and Eyles, 1991). Below erosion surface E5 (Chapter 12), silty shales contain a diverse trace assemblage, including *Planolites, Chondrites, Helminthopsis, Terebellina, Asterosoma*, and rare *Zoophycos*. This suite reflects a distal Cruziana ichnofacies, suggesting offshore to shelfal accumulation. The erosion surface (E5) cut into this facies is marked by a *Glossifungites* assemblage consisting of robust *Thalassinoides* that penetrate into the underlying silty shales. The burrows are passively filled with pebbles and sand from overlying structureless conglomerates (Vossler and Pemberton, 1988b). The conglomerates grade upward into overlying marine shelfal shales that contain *Helminthopsis, Planolites, Chondrites, Terebellina*, and *Zoophycos*. The erosional discontinuity is interpreted to have initially formed during lowstand of relative sea level, but was extensively modified during transgression. In places, the conglomerates rest on a surface of initial transgression (E5) and are erosively truncated during a resumption of transgression (T5; see Figs. 15 and 17 in Chapter 12). In other places, the T5 surface cuts down to become coplanar with E5 (Fig. 17 in Chapter 12). Colonization of the surface by the omission suite tracemakers corresponds to a hiatus in deposition between initial transgression (forming E5) and shoreface progradation associated with a period of stillstand. The stillstand shoreface was ultimately drowned during resumed transgression (T5), marked by the capping marine shelfal shales. The transgression/stillstand shoreface model has also been applied to the Viking Formation of the Joffre field (Table 2; Downing and Walker, 1988).

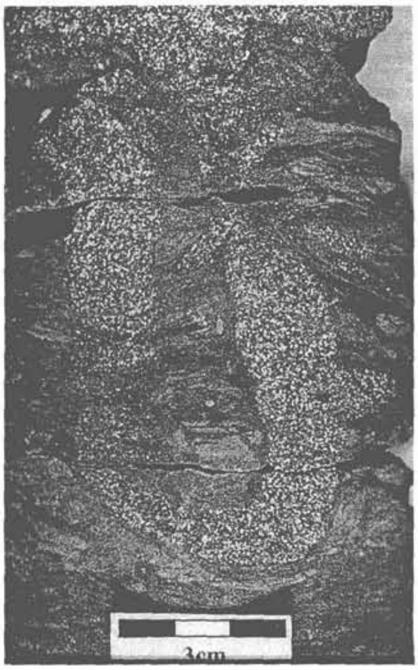

Figure 23 Robust, unlined, coarse sand-filled *Arenicolites* shaft excavated into a silty to sandy shale. The firmground suite cross cuts a *Planolites, Helminthopsis, Asterosoma, Chondrites*, and *Terebellina* softground assemblage. The *Glossifungites* suite corresponds to a transgressive ravinement surface followed by stillstand progradation of coarser clastics. Albian Viking Formation, Kaybob S. Field, Alberta.

Another example of bioturbation at an amalgamated lowstand/transgressive surface is in the Bertie and Bois Blanc formations of southern Ontario. The contact between them corresponds to the Silurian/Devonian unconformity (Pemberton *et al.*, 1980). Dolomites of the Bertie Formation contain softground *Thalassinoides* systems and reflect the final stages of transgression in the Silurian. The Silurian/Devonian unconformity was initiated during a period of extreme shallowing and subaerial exposure, which produced a karsted surface. Subsequent transgression is indicated by colonization of the karsted hardground by boring organisms and development of a *Trypanites* ichnofacies (Fig. 17C), manifest by abundant *Trypanites weisei* and *Gastrochaenolites*. Sediment of the overlying unburrowed Oriskany sandstone of the Bois Blanc Formation was deposited as a widespread sheet which subsequently suffered localised removal. The surface corresponds to an amalgamated lowstand erosion and transgressive ravinement (E/T) surface.

Nondepositional hiatuses (diastems or nonsequences)

Nondepositional hiatuses are commonly formed in carbonate settings where cessation of deposition results in synsedimentary lithification of the seafloor and development of hardgrounds. These hardground surfaces are colonized rapidly by marine organisms. The absence of significant deposition of sediment related to hardground formation strongly favours the colonization of such surfaces, and unbored hardgrounds are more the exception than the rule.

In Upper Cretaceous chalks of northwestern Europe, nonerosional (nondepositional) omission surfaces are abundant through much of the succession (Bromley, 1975), particularly in some of the Cenomanian grey chalks of southern England (Kennedy, 1967). In the Upper Cretaceous (Campanian-Maastrichtian boundary) white chalks of Kronsmoor, Schlesswig-Holstein, Germany, many of the more obvious omission surfaces have been termed "pseudo-hardgrounds" (Bromley, 1975). Three main trace fossil associations typically occur in such settings; pre-omission, omission, and post-omission suites. The pre-omission suite consists of *Thalassinoides, Chondrites*, and *Zoophycos*; the traces have a pale blue fill because of disseminated pyrite. The omission suite corresponds to the *Glossifungites* ichnofacies, and consists of a monospecific assemblage of *Thalassinoides*. These are distinguished by a grey, clayey chalk fill from the overlying unit and a faintly ferruginous coating on the burrow walls because of exposure to seawater during the period of nondeposition. The post-omission suite occupies the overlying unit and consists of *Thalassinoides, Chondrites*, and *Zoophycos*, which are virtually identical to the pre-omission suite. This last suite penetrates the discontinuity surface through re-excavation of the omission suite burrow fill. Bromley (1975) interpreted this reburrowing to be a function of low nutrient content of the underlying chalk rather than of substrate hardness. The lack of new ichnofossil forms introduced in the omission suite and post-omission suite strongly suggests that negligible change occurred in the depositional setting before or after development of the omission surface (Bromley, 1975).

Where synsedimentary lithification occurs at the seafloor, omission suites are separated into prelithification *burrows* and postlithification *borings*

(Bromley, 1975). Prelithification suites may include both softground suites and firmground suites. Recognition of a bored (rather than burrowed) sedimentary surface is unequivocal evidence of sediment omission (erosional or non-depositional) and the presence of a hardground (Bromley, 1975).

Depositional Discontinuities

Condensed Sections

Condensed sections were deposited over a long span of time, but are thin because of slow rates of hemipelagic or pelagic sedimentation. They are typically most extensive during periods of maximum transgression (Loutit *et al.*, 1988), when the basin is starved of terrigenous material (Van Wagoner *et al.*, 1990), and form *maximum flooding surfaces*. Recognition of condensed sections is important, both from a stratigraphic and facies analysis point of view. Such thin deposits may easily be missed during biostratigraphic analysis, if sampling is not conducted carefully. Missing the condensed section would result in the interpretation of an *apparent* time gap in the biostratigraphic record. This in turn would imply a major unconformity even though sedimentation was actually continuous (Van Wagoner *et al.*, 1990).

Condensed sections tend to contain abundant and diverse deep water faunas, whereas over- and underlying deposits, particularly those accumulated in fluvial, estuarine, and shallow-marine settings, tend to be nonfossiliferous or only slightly fossiliferous. If faunas are collected from successive condensed sections, in several discrete sequences (in the sequence stratigraphy sense), the sedimentologist might erroneously conclude that continuous deep water conditions prevailed across that interval, and could misinterpret the intervening nonfossiliferous sandstones as being deep water in origin (Van Wagoner *et al.*, 1990).

Several condensed sections have been described from the rock record (Legget, 1980; Jenkyns, 1980; Leckie *et al.*, 1990), and Loutit *et al.* (1988) summarized most of their common characteristics (Fig. 24).

The ichnological signatures of condensed sections have yet to be documented adequately. In general, the units tend to be unburrowed, which is commonly attributed to low oxygen content and overall stressful conditions for benthic organisms. Six selected condensed sections from epeiric settings show a general adherence to conditions of higher total organic carbon, reduced oxygen values, low concentrations of benthic foraminifera, and minimal or no burrowing (Fig. 24). The relationships of low oxygen, preservation of organic carbon, and biologically lethal seafloor conditions have been discussed by numerous authors (Byers and Larson, 1979; Jenkyns, 1980; Legget, 1980; Savrda and Bottjer, 1987). Savrda and Bottjer (1987) noted that ichnofaunas are generally more indicative of both magnitudes of, and rates of change in, oxygen levels than are macrobenthic body fossil suites. Bromley and Ekdale (1984) found that with decreasing oxygenation at the seafloor, *Planolites*, *Thalassinoides*, and *Zoophycos* progressively disappear before *Chondrites* does, suggesting that the *Chondrites* tracemaker may have been capable of surviving conditions of anoxia. Savrda and Bottjer (1987) also found that burrow sizes decrease with increasing depth and decreasing oxygen levels.

In a study of the Monterey Formation (Miocene) of California and the Niobrara Formation (Cretaceous) of Colorado, Savrda and Bottjer (1987) indicated that *oxygen-related ichnocoenoses* could be defined, and used to distinguish units of more uniform or less uniform bottom-water oxygenation. One possible means of recognising condensed sections characterised by dysaerobic or anaerobic conditions may be by the presence of a suspiciously unburrowed or only slightly burrowed dark carbonaceous shale lying between more intensely burrowed marine deposits.

Condensed sections overlying transgressive lags, and coinciding with maximum flooding, are shown in Figure 25. This core is from the Lower Cretaceous (Albian) Bluesky Formation of the Knopcik Field, west-central Alberta. Near the base of the core, foreshore and upper shoreface sandstones containing *Macaronichnus*, are erosionally truncated and overlain by a conglomerate and pebbly shale, interpreted to reflect transgressive ravinement. The overlying shale is black, slightly fissile, pyritic, and glauconitic, and is conspicuously unburrowed. It is interpreted as a condensed section, deposited during maximum flooding. The condensed section grades upward into offshore silty shales and sandy shales burrowed with a diverse *Cruziana* ichnofacies, consisting of

COMMON CHARACTERISTICS OF CONDENSED SECTIONS

Legend: X = present; ? = not addressed; Blank = not present

	Cambro-Ordovician, Baltic Shield	Jet Rock Shales	Shaftesbury Fm	Mowry Shale	Awgu Shale	Eocene-Oligocene Boundary, Alabama
1. Slow sedimentation rates	X	X	X	X	X	X
2. Reduced oxygen values	X	X	X	X	X	X
3. High organic matter content (TOC)	X	X	X	X	X	X
4. High concentration of Platinum elements (iridium)	?	?		?	?	?
5. Presence of authigenic minerals (e.g. glauconite, phosphate, siderite)	X	X		?	X	X
6. High Gamma-ray counts	?	?	X	X	?	X
7. Abundant and diverse plankton	X			X	X	X
8. Abundant and diverse microfauna	X			X	X	X
9. Abundant open-ocean planktonic foraminifera	?			?	X	X
10. Low concentrations of benthic foraminifera	X	X	X	X	X	X
11. Abruptly overlies nonmarine or shallow marine sediments	X		X	X		X
12. Section overlain by downlap surface	?	?		X		X
13. Associated with burrowed, bored or slightly lithified tops	X	?		X	?	?
14. *Generally unburrowed* or sparsely burrowed interval	X	X	X	X	X	?

Figure 24 Six condensed sections selected from epeiric settings are summarized. Data were collected as follows: Cambro-Ordovician (Baltic Shield) – Lindstrom (1963) and Jenkyns (1986); Jet Rock Shales (Toarcian; U.K.) – Morris (1979); Shaftsbury Formation (Albian; Alberta, Canada) – Leckie *et al.* (1990); Mowry Shale (Late Albian; Wyoming, U.S.A.) – Byers and Larson (1979) and Jenkyns (1980); Awgu Shale (Turonian; Benue Trough, Nigeria) – Petters (1978) and Jenkyns (1980); Eocene-Oligocene Boundary (Alabama, U.S.A.) – Loutit *et al.* (1988).

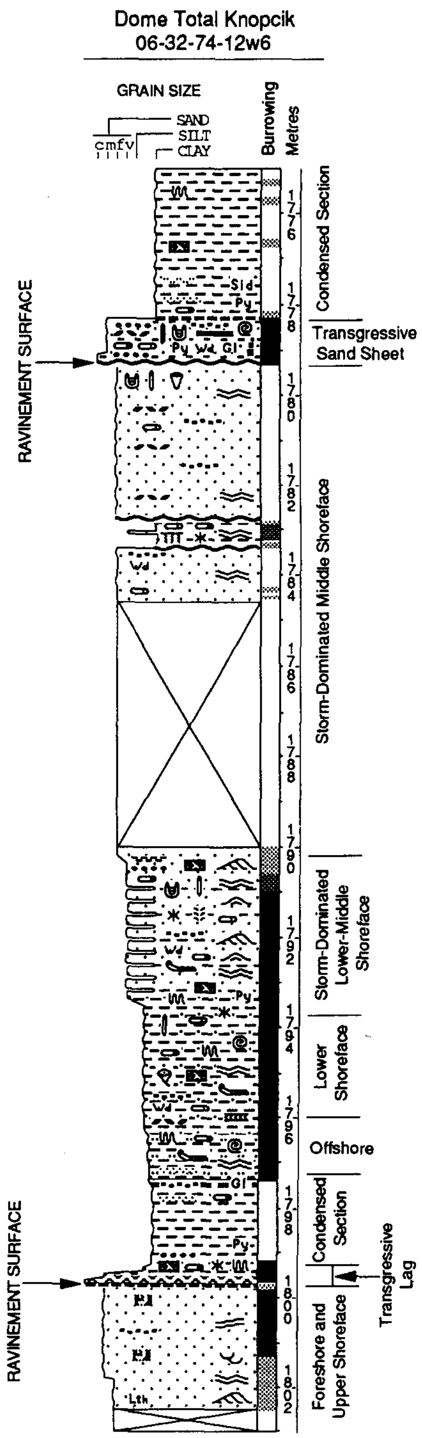

Figure 25 Strip log of a cored interval of the Bluesky Formation (Lower Albian) in the Knopcik Field in west-central Alberta (symbols explained in Fig. 19). Facies interpretations are given on the right-hand side of the log; key surfaces are marked on the left. The basal section shows an upper shoreface sandstone transgressed with ravinement, overlain by a condensed section. A second offshore to shoreface progradational cycle is developed (near top of section) and is also erosively transgressed, capped by a transgressive sand sheet and followed by a second condensed section.

Terebellina, Planolites, Chondrites, Helminthopsis, Zoophycos, small Rosselia, *Palaeophycus, Teichichnus, Asterosoma,* and rare *Skolithos.* This passes into storm-dominated lower- to middle-shoreface sandstones, reflecting shoreface progradation. Towards the top of the core (Fig. 25), a ravinement surface is overlain by intensely but indistinctly burrowed, pebbly medium to coarse sandstone interpreted as a transgressive sand sheet. It is abruptly overlain by dark, slightly fissile, pyritic silty shale containing sparse *Planolites* and *Chondrites,* interpreted as another condensed section.

SUMMARY

In the second edition of *Facies Models* (Frey and Pemberton, 1984), we showed that recurrent ichnofacies are not only valuable environmental indicators but also archetypal facies models. The same holds true today (Frey *et al.*, 1990). However, in 1984, trace fossils had little or no place in refined genetic stratigraphic applications. This is certainly not true today; trace fossils are very important both in defining bounding discontinuities of various types, and in contributing to their interpretation. The particular tracemakers colonizing the discontinuities, and the intensity of burrowing or boring, are independent of the genesis and regional extent of the surface itself, except in situations where there is an environmental gradient (e.g., freshwater/brackish-water/marine). The allostratigraphic significance of any given discontinuity is a problem that can be resolved only through the integration of sedimentological, stratigraphic, ichnological, and paleontological techniques.

ACKNOWLEDGEMENTS

Mike Ranger kindly permitted use of his computer program to draft the strip logs presented in the paper. Don McPhee and Howard Brekke spent numerous hours scanning and constructing the figures, and Ms. Cathy Gendron typed numerous drafts of the text. Roger Walker made many editorial suggestions that helped to improve the manuscript. Funding was provided by the Natural Sciences and Engineering Research Council of Canada and is gratefully acknowledged.

After helping to complete this paper,

Bob Frey passed away on January 1, 1992. He will be long remembered for his classic work that helped lay the foundation for modern ichnology. We dedicate this paper in his honour.

REFERENCES

Basic sources of information

Bromley, R.G., 1990, Trace fossils, biology and taphonomy: Special Topics in Palaeontology 3: London, Unwin Hyman, 280 p.
New book on ichnology outlining basic principles and concepts, aimed at graduate students and professionals. Excellent illustrations and good treatment on the burrowing behaviour of modern organisms.

Ekdale, A.A., 1985, Paleoecology of the marine endobenthos: Palaeogeography, Palaeoclimatology, Palaeoecology, v. 50, p. 63-81.
Good review paper on basic principles, especially on feeding strategies employed by benthic organisms.

Ekdale, A.A., Bromley, R.G. and Pemberton, S.G., eds., 1984, Ichnology: the use of trace fossils in sedimentology and stratigraphy: Society of Economic Paleontologists and Mineralogists, Short Course Notes 15, 317 p.
Comprehensive review of the significance of ichnology in stratigraphy and sedimentology. Good starting point for information on paleoenvironmental interpretation using trace fossils.

Frey, R.W. and Seilacher, A., 1980, Uniformity in marine invertebrate ichnology: Lethaia, v. 13, p. 183-207.
Comprehensive evaluation of the uniformitarian approach in ichnology, emphasizing the interaction of benthic behavioral patterns and prevailing environmental conditions.

Frey, R.W. and Pemberton, S.G., 1985, Biogenic structures in outcrops and cores. I. Approaches to ichnology: Bulletin of Canadian Petroleum Geology, v. 33, p. 72-115.
Extensive review of the disciplinary framework of ichnology, including definitions of major concepts.

Frey, R.W., and Wheatcroft, R.A., 1989, Organism-substrate relations and their impact on sedimentary petrology: Journal of Geological Education, v. 37, p. 261-279.
Excellent review of basic principles in ichnology, especially with regard to sediment reworking, aimed at beginning graduate or senior undergraduate students.

Wilgus, C.K., Hastings, B.S., Posamentier, H.W., Ross, C.A. and Kendall, C.G.St.C., eds., 1988, Sea level changes: an integrated approach: Society of Economic Paleontologists and Mineralogists, Special Publication 42, 407 p.
Collection of papers emphasizing conceptual basis of sequence stratigraphy plus nimerous case studies of sea level change from the geological record.

Other references

Ager, D.V., 1963, Principles of paleoecology: New York, McGraw-Hill, 371 p.

Ahlbrandt, T.S., Andrews, S. and Gwynne, D.T., 1978, Bioturbation of eolian deposits: Journal of Sedimentary Petrology, v. 48, p. 839-848.

Alexander, W.B., Southgate, A. and Bassindale, R., 1935, Survey of the River Tes, Part II. The estuary – chemical and biological: Department of Science Industrial Research, Water Pollution Research Technical Paper 5, 171 p.

Arua, I., 1989, Clavate borings in a Maastrichtian woodground in southeastern Nigeria: Palaeogeography, Palaeoclimatology, Palaeoecology, v. 69, p. 321-326.

Beynon, B.M., Pemberton, S.G., Bell, D.A. and Logan, C.A., 1988, Environmental implications of ichnofossils from the Lower Cretaceous Grand Rapids Formation, Cold Lake Oil Sands Deposit. *in* James, D.P. and Leckie, D.A., eds., Sequences, stratigraphy, sedimentology: surface and subsurface: Canadian Society of Petroleum Geologists, Memoir 15, p. 275-290.

Bhattacharya, J. and Walker, R.G., 1991, Allostratigraphic subdivision of the Upper Cretaceous Dunvegan, Shaftesbury, and Kaskapau formations, northwestern Alberta subsurface: Bulletin of Canadian Petroleum Geology v. 39, p. 145-164.

Bjerstedt, T.W., 1987, Trace fossils indicating estuarine deposystems for the Devonian-Mississippian Cloyd Conglomerate Member, Price Formation, Central Appalachians: Palaios, v. 2, p. 339-349.

Bradshaw, M.A., 1981, Paleoenvironmental interpretations and systematics of Devonian trace fossils from the Taylor Group (lower Beacon Supergroup), Antarctica: New Zealand Journal of Geology and Geophysics, v. 24, p. 615-652.

Bromley, R.G., 1975, Trace fossils at omission surfaces, *in* Frey, R.W., ed., The study of trace fossils: New York, Springer-Verlag, p. 399-428.

Bromley, R.G. and Ekdale, A.A., 1984, Composite ichnofabrics and tiering of burrows: Geological Magazine, v. 123, p. 59-65.

Bromley, R.G., and Asgaard, U., 1991, Ichnofacies: a mixture of taphofacies and biofacies: Lethaia, v. 24, p. 153-163.

Bromley, R.G., Pemberton, S.G. and Rahmani, R.A., 1984, A Cretaceous woodground: the *Teredolites* ichnofacies: Journal of Paleontology, v. 58, p. 488-498.

Byers, C.W. and Larson, D.W., 1979, Paleoenvironments of Mowry Shale (Lower Cretaceous), western and central Wyoming: American Association of Petroleum Geologists, Bulletin, v. 63, p. 354-361.

Campbell, C.V. and Oaks, R.W., 1973, Estuarine sandstone filling tidal scours, Lower Cretaceous Fall River Formation, Wyoming: Journal of Sedimentary Petrology, v. 43, p. 765-778.

Crimes, T.P. and Crossley, J.D., 1991, A diverse ichnofauna from Silurian flysch of the Aberystwyth Grits formation, Wales: Geological Journal, v. 26, p. 27-64.

Crimes, T.P., Goldring, R., Homewood, P., van Stuijvenberg, J. and Winkler, W., 1981, Trace fossil assemblages of deep-sea fan deposits, Gurnigel and Schlieren flysch (Cretaceous-Eocene, Switzerland): Eclogae Geologicae Helvetiae, v. 74, p. 953-995.

Croghan, P.C., 1983, Osmotic regulation and the evolution of brackish- and freshwater faunas: Journal of the Geological Society of London, v. 140, p. 39-46.

Dam, G., 1990, Palaeoenvironmental significance of trace fossils from the shallow marine Lower Jurassic Neill Klinter Formation, East Greenland: Palaeogeography, Palaeoclimatology, Palaeoecology, v. 79, p. 221-248.

Dewey, C.P. and Keady, D.M., 1987, An allochthonous preserved woodground in the Upper Cretaceous Eutaw Formation in Mississippi: Southeastern Geology, v. 27, p. 165-170.

Dörjes, J. and Hertweck, G., 1975, Recent biocoenoses and ichnocoenoses in shallow-water marine environments, *in* Frey, R.W., ed., The study of trace fossils: New York, Springer-Verlag, p. 459-491.

Dörjes, J. and Howard, J.D., 1975, Fluvial-marine transition indicators in an esturine environment, Ogeechee River, Ossabaw Sound: Senckenbergiana Maritima, v. 7, p. 137-179.

Downing, K.P. and Walker, R.G., 1988, Viking Formation, Joffre Field, Alberta: Shoreface origin of long, narrow sand body encased in marine mudstones: American Association of Petroleum Geologists, Bulletin, v. 72, p. 1212-1228.

Fischer, R., 1981, Bioerosion of basalt of the Pacific coast of Costa Rica: Senckenbergiana maritima, v. 13, p. 1-41.

Frey, R.W., 1990, Trace fossils and hummocky cross-stratification, Upper Cretaceous of Utah: Palaios, v. 5, p. 203-218.

Frey, R.W. and Pemberton, S.G., 1984, Trace fossil facies models, *in* Walker, R.G., ed., Facies models: Geological Association of Canada, Geoscience Canada Reprint Series 1, p. 189-207.

Frey, R.W. and Bromley, R.G., 1985, Ichnology of American chalks: The Selma Group (Upper Cretaceous), western Alabama: Canadian Journal of Earth Sciences, v. 22, p. 801-828.

Frey, R.W. and Pemberton, S.G., 1987, The *Psilonichnus* ichnocoenose and its relationship to adjacent marine and nonmarine ichnocoenoses along the Georgia coast: Bulletin of Canadian Petroleum Geology, v. 35, p. 333-357.

Frey, R.W. and Howard, J.D., 1990, Trace fossils and depositional sequences in a clastic shelf setting, Upper Cretaceous of Utah: Journal of Paleontology, v. 64, p. 803-820.

Frey, R.W., Pemberton, S.G. and Fagerstrom, J.A., 1984, Morphological, ethological, and environmental significance of the ichnogenera *Scoyenia* and *Ancorichnus*: Journal of Paleontology, v. 58, p. 511-528.

Frey, R.W., Howard, J.D. and Hong, J.-S., 1987, Prevalent lebensspuren on a modern macrotidal flat, Inchon, Korea: ethological and environmental significance: Palaios, v. 2, p. 571-593.

Frey, R.W., Pemberton, S.G. and Saunders, T.D.A., 1990, Ichnofacies and bathymetry: a passive relationship: Journal of Paleontology, v. 64, p. 155-158.

Fürsich, F.T., 1981, Salinity-controlled benthic associations from the Upper Jurassic of Portugal: Lethaia, v. 14, p. 203-220.

Fürsich, F.T. and Mayr, H., 1981, Nonmarine *Rhizocorallium* (trace fossils) from the Upper Freshwater Molasse (Upper Miocene) of southern Germany: Neues Jahrbuch für Geologie und Paleontologie, Monatshefte, v. 6, p. 321-333.

Gierlowski-Kordesch, E., 1991, Ichnology of an ephemeral lacustrine/alluvial plain system: Jurassic East Berlin Formation, Hartford Basin, USA: Ichnos, v. 1, p. 221-232.

Goldring, R., Bosence, D.W.J., and Blake, T., 1978, Estuarine sedimentation in the Eocene of southern England: Sedimentology, v. 25, p. 861-876.

Gray, J. 1988, Evolution of the freshwater ecosystem: the fossil record: Palaeogeography, Palaeoclimatology, Palaeoecology, v. 62, p. 1-214.

Hayward, B.W., 1976, Lower Miocene bathyal and submarine canyon ichnocoenoses from Northland, New Zealand: Lethaia, v. 9, p. 149-162.

Howard, J.D. and Frey, R.W., 1973, Characteristic physical and biogenic sedimentary structures in Georgia estuaries: American Association of Petroleum Geologists, Bulletin, v. 57, p. 1159-1184.

Howard J.D. and Frey, R.W., 1984, Characteristic trace fossils in nearshore to offshore sequences, Upper Cretaceous of east-central Utah: Canadian Journal of Earth Sciences, v. 21, p. 200-219.

Howard, J D. and Frey, R.W., 1985, Physical and biogenic aspects of backbarrier sedimentary sequences, Georgia coast, U.S.A.: Marine Geology, v. 63, p. 77-127.

Hudson, J.D., 1980, Aspects of brackish-water facies and faunas from the Jurassic of north-west Scotland: Proceedings of the Geologists Association, v. 91, p. 99-105.

Jenkyns, H.C., 1980, Cretaceous anoxic events: from continents to oceans: Journal of the Geological Society of London, v. 137, p. 171-188.

Jenkyns, H.C., 1986, Pelagic environments, *in* Reading, H.G., ed., Sedimentary environments and facies: Oxford, Blackwell Scientific Publications, p. 343-397.

Kennedy, W.J., 1967, Burrows and surface traces from the Lower Chalk of Southern England: British Museum (Natural History), Geological Bulletin, v. 15, p. 127-167.

Land, C.B., 1972, Stratigraphy of Fox Hills Sandstone and associated formations, Rock Springs Uplift and Wamsutter Arch Area, Sweetwater County, Wyoming: a shoreline-estuary sandstone model for the Late Cretaceous: Colorado School of Mines, Quarterly, v. 67, p. 1-69.

Leckie, D.A., Singh, C., Goodarzi, F. and Wall, J.H., 1990, Organic-rich, radioactive marine shale: a case study of a shallow-water condensed section, Cretaceous Shaftesbury Formation, Alberta, Canada: Journal of Sedimentary Petrology, v. 60, p. 101-117.

Legget, J.K., 1980, British lower Paleozoic black shales and their palaeo-oceanographic significance: Journal of the Geological Society of London, v. 137, p. 139-156.

Lindstrom, M., 1963, Sedimentary folds and the development of limestone in an early Ordovician sea: Sedimentology, v. 2, p. 243-292.

Loutit, T.S., Hardenbol, J., Vail, P.R. and Baum, G.R., 1988, Condensed sections: the key to age dating and correlation of continental margin sequences, *in* Wilgus, C.R. *et al.*, eds., Sea-level changes; an integrated approach: Society of Economic Paleontologists and Mineralogists, Special Publication 42, p. 183-213.

Maples, C.G. and Archer, A.W., 1989, The potential of Paleozoic nonmarine trace fossils for paleoecological interpretations: Palaeogeography, Palaeoclimatology, Palaeoecology, v. 73, p. 185-195.

Marintsch, E.J. and Finks, R.M., 1982, Lower Devonian ichnofacies at Highland Mills, New York and their gradual replacement across environmental gradients: Journal of Paleontology, v. 56, p. 1050-1078.

McCann, T. and Pickerill, R.K., 1988, Flysch trace fossils from the Cretaceous Kodiak Formation of Alaska: Journal of Paleontology, v. 62, p. 330-348.

Miller, M.F., 1984, Distribution of biogenic structures in Paleozoic non-marine and marine margin sequences: an actualistic model: Journal of Paleontology, v. 58, p. 550-570.

Milne, A., 1940, The ecology of the Tamar Estuary, iv. The distribution of the fauna and flora on buoys: Journal of the Marine Biological Association of the United Kingdom, v. 24, p. 69-87.

Morris, K., 1979, A classification of Jurassic marine shale sequences; an example from the Toarcian (Lower Jurassic) of Great Britain: Palaeogeography, Pa laeoclimatology, Palaeoecology, v. 26, p. 117-126.

Moslow, T.F. and Pemberton, S.G., 1988, An integrated approach to the sedimentological analysis of some Lower Cretaceous shoreface and delta front sandstone sequences, *in* James, D.P. and Leckie, D.A., eds., Sequences, stratigraphy, sedimentology: surface and subsurface: Canadian Society of Petroleum Geologists, Memoir 15, p. 337-386.

North American Commission on Stratigraphic Nomenclature (NACSN), 1983, North American stratigraphic code: American Association of Petroleum Geologists, Bulletin, v. 67, p. 841-875.

Oppelt, H., 1988, Sedimentology and ichnology of the Bluesky Formation in northeastern British Columbia, *in* James, D.P. and Leckie, D.A., eds., Sequences, stratigraphy, sedimentology: surface and subsurface: Canadian Society of Petroleum Geologists, Memoir 15, p. 401-416.

Pemberton, S.G. and Frey, R.W, 1984, Ichnology of storm-influenced shallow marine sequence: Cardium Formation (Upper Cretaceous) at Seebe, Alberta, *in* Stott, D.F. and Glass, D.J., eds., The Mesozoic of middle North America: Canadian Society of Petroleum Geologists, Memoir 9, p. 281-304.

Pemberton, S.G. and Frey, R.W., 1985, The *Glossifungites* ichnofacies: modern examples from the Georgia coast, U.S.A., *in* Curran, H.A., ed., Biogenic structures; their use in interpreting depositional environments: Society of Economic Paleontologists and Mineralogists, Special Publication 35, p. 237-259.

Pemberton, S.G., Kobluk, D.R., Yeo, R.K. and Risk, M.J., 1980, The boring *Trypanites* at the Silurian-Devonian disconformity in southern Ontario: Journal of Paleontology, v. 54, p. 1258-1266.

Pemberton, S.G., Flach, P.D. and Mossop, G.D., 1982, Trace fossils of the Athabasca Oil Sands, Alberta, Canada: Science, v. 217, p. 825-827.

Perkins, E.J., 1974, The biology of estuaries and coastal waters: London, Academic Press, 678 p.

Petters, S.W., 1978, Mid-Cretaceous paleoenvironments and biostratigraphy of the Benue Trough, Nigeria: Geological Society of America, Bulletin, v. 89, p. 151-154.

Pickerill, R.K. and Harland, T.L., 1988, Trace fossils from Silurian slope deposits, North Greenland: Grønlands Geologiske Undersøgelse, v. 137, p. 199-133.

Plint, A.G., 1988, Sharp-based shoreface sequences and "offshore bars" in the Cardium Formation of Alberta: their relationship to relative changes in sea level, *in* Wilgus, C.R., *et al.*, eds., Sea-level changes: an integrated approach: Society of Economic Paleontologists and Mineralogists, Special Publication 42, p. 357-370.

Plint, A.G. and Walker, R.G., 1987, Cardium Formation 8. Facies and environments of the Cardium shoreline and coastal plain in the Kakwa field and adjacent areas, northwestern Alberta: Bulletin of Canadian Petroleum Geology, v. 35, p. 48-64.

Plint, A.G., Walker, R.G. and Bergman, K.M., 1986, Cardium Formation 6. Stratigraphic framework of the Cardium: Bulletin of Canadian Petroleum Geology, v. 34, p. 213-225.

Plint, A.G., Walker, R.G. and Duke, W.L., 1988, An outcrop to subsurface correlation of the Cardium Formation in Alberta, *in* James, D.P. and Leckie, D.A., eds., Sequences, stratigraphy, sedimentology: surface and subsurface: Canadian Society of Petroleum Geologists, Memoir 15, p. 167-184.

Pollard, J.E., 1988, Trace fossils in coal-bearing sequences: Journal of the Geological Society of London, v. 145, p. 339-350.

Posamentier, H.W. and Vail, P.R., 1988, Eustatic controls on clastic deposition II — sequence and systems tract models, *in* Wilgus, C.K., *et al.*, eds., Sea-level changes: an integrated approach: Society of Economic Paleontologists and Mineralogists, Special Publication 42, p. 125-154.

Posamentier, H.W. and Chamberlain, C.J., in press, Sequence stratigraphic analysis of Viking Formation lowstand beach deposits at Joarcam Field, Alberta, Canada, *in* Posamentier, H.W., Summerhayes, C.P., Haq, B.U. and Allen, G.P., eds., Stratigraphy and facies associations in a sequence stratigraphic framework: International Associatyion of Sedimentologists, Special Publication

Power, B.A., 1988, Coarsening-upwards shoreface and shelf sequences: examples from the Lower Cretaceous Viking Formation at Joarcam, Alberta Canada, *in* James, D.P. and Leckie, D.A., eds., Sequences, stratigraphy, sedimentology: surface and subsurface: Canadian Society of Petroleum Geologists, Memoir 15, p. 185-194.

Radwanski, A. and Roniewicz, P., 1970, General remarks on the Ichnocoenose concept: Bulletin de l'Academie Polonaise des Sciences, Serie des sciences géologie et géographie, v. 18, p. 51-56.

Reinson, G.E., Clark, J.E. and Foscolos, A.E., 1988, Reservoir geology of Crystal Viking Field, Lower Cretaceous estuarine tidal channel-bay complex, south-central Alberta: American Association of Petroleum Geologists, Bulletin, v. 72, p. 1270-1294.

Remane, A. and Schlieper, C., 1971, Biology of brackish water: New York, Wiley, 372 p.

Retallack, G.J., 1984, Trace fossils of burrowing beetles and bees in an Oligocene paleosol, Badlands National Park, South Dakota: Journal of Paleontology, v. 58, p. 571-592.

Sanders, H.L., Mangelsdorf, P.C., Jr. and Hampson, G.R., 1985, Salinity and faunal distribution in the Pocasset River, Massachusetts: Limnology and Oceanography, v. 10, p. R216-R229.

Saunders, T. and Pemberton, S.G., 1986, Trace fossils and sedimentology of the Appaloosa Sandstone: Bearpaw-Horseshoe Canyon Formation transition, Dorothy, Alberta: Canadian Society of Petroleum Geologists, Field Trip Guide Book, 117 p.

Savrda, C.E., 1991, Ichnology in sequence stratigraphic studies: An example from the Lower Paleocene of Alabama: Palaios, v. 6, p. 39-53.

Savrda, C.E. and Bottjer, D.J., 1987, The exaerobic zone, a new oxygen-deficient marine biofacies: Nature, v. 327, p. 54-56.

Seilacher, A., 1967, Bathymetry of trace

Serna, F.E., 1986, La ichnofacies *Zoophycos-Chondrites* del Cretacico de la cordillera Occidental de Colombia y su posible signification paleoambiental: Caldasia, v. 15 (Nos. 71-75), p. 405-422.

Stewart, D.J., 1981, A field guide to Wealden Group of Hastings area and the Isle of Wight, *in* Elliott, T., ed., Field guides to modern and ancient fluvial systems in Britain and Spain: International Fluvial Conference, Keele University, U.K., p. 3.1-3.32.

Torunski, H., 1979, Biological erosion and its significance for the morphogenesis of limestone coasts and for nearshore sedimentation (northern Adriatic): Senckenbergiana maritima, v. 11, p. 193-265.

Van Wagoner, J.C., Mitchum, R.M., Campion, K.M. and Rahamnian, V.D., 1990, Siliciclastic sequence stratigraphy in well logs, cores, and outcrops: American Association of Petroleum Geologists, Methods in Exploration Series 7, 55 p.

Vossler, S.M. and Pemberton, S.G., 1988a, *Skolithos* in the Upper Cretaceous Cardium Formation: an ichnofossil example of opportunistic ecology: Lethaia, v. 21, p. 351-362.

Vossler, S.M. and Pemberton, S.G., 1988b, Ichnology of the Cardium Formation (Pembina oilfield): implications for depositional and sequence stratigraphic interpretations, *in* James, D.P. and Leckie, D.A., eds., Sequences, stratigraphy, sedimentology; surface and subsurface: Canadian Society of Petroleum Geo logists, Memoir 15, p. 237-253.

Walker, R.G., 1990, Facies modelling and sequence stratigraphy: Journal of Seimentary Petrology, v. 60, p. 777-786.

Walker, R.G. and Eyles, C.H., 1991, Topography and significance of a basin-wide sequence-bounding erosion surface in the Cretaceous Cardium Formation, Alberta, Canada: Journal of Sedimentary Petrology, v. 61, p. 473-496.

Wetzel, A, 1991, Ecologic interpretation of deep-sea trace fossil communities: Palaeogeography, Palaeoclimatology, Palaeoecology, v. 85, p. 47-69.

Whitfield, M., 1976, The evolution of the oceans and the atmosphere, *in* Bligh, J., Cloudsley-Thompson, J.L. and MacDonald, A.G., eds., Environmental physiology of animals: New York, Wiley, p. 30-45.

Wightman, D.M., Pemberton, S.G. and Singh, C., 1987, Depositional modelling of the Upper Mannville (Lower Cretaceous) central Alberta. Implications for the recognition of brackish water deposits, *in* Tillman, R.W. and Weber, K.J., eds., Reservoir sedimentology: Society of Economic Paleontologists and Mineralogists, Special Publication 40, p. 189-220.

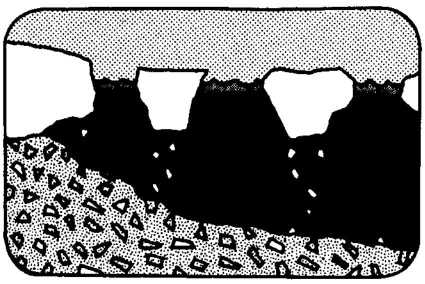

5. Glacial Depositional Systems

Nicholas Eyles, Department of Geology, University of Toronto, Scarborough Campus, Scarborough, Ontario M1C 1A4

Carolyn H. Eyles, Department of Geography, McMaster University, Hamilton, Ontario L8S 4K1

INTRODUCTION

An understanding of glacial depositional systems and models has many important applications. First, glacial deposits contain data that can be used to unravel the long, but intermittent, record of global change and glaciation during geological time (Fig. 1, and see Chapter 2). Second, glacial deposits are fundamental to studies of environmental geology in heavily urbanized mid-latitude areas of North America and Europe. The investigation of geo-engineering characteristics, hydrogeological regimes and contaminant migration in glacial sediments is currently a major stimulus of glacial sedimentological research. It is akin to the stimulus of hydrocarbon reservoir studies on aspects of clastic and carbonate sedimentology in the 1950s. A third and closely related aspect of glacial studies is their application to economic geology. This involves exploration for mineral deposits hosted in glacial sediments and rocks (placers; Eyles, 1990), and the use of glacial sediments in the search for mineral deposits on glaciated shields (drift prospecting; DiLabio and Coker, 1989). Glacial strata have traditionally been ignored by petroleum geologists, but Late Paleozoic glaciated basins contain significant reserves of oil and gas in Australia, Argentina, Brazil, Bolivia, northern Saudi Arabia, Jordan and Oman (Levell *et al.*, 1988; Franca and Potter, 1991).

In many people's minds, glacial sedimentary facies are still uniquely characterized by *tills* (or if lithified, *tillites*). These are unsorted mixtures of all available sizes, from boulders to clay, deposited directly by glaciers and ice sheets. However, sediments having the same outcrop appearance (hence the same aspect, or facies) can be deposited in a wide range of glacial and nonglacial environments (Fig. 2). The term *diamict* (if lithified, *diamictite*) should therefore be used as a descriptive, nongenetic term for such poorly sorted facies regardless of origin. Only those diamict(ite)s known to be deposited directly by glacier ice can be identified as true till(ite)s. A central problem in stratigraphic studies is therefore to determine whether specific diamict(ite) facies are glacial or nonglacial in origin. There are many examples in the literature where sediments originally described as tills and tillites have been shown to have a nonglacial origin. Diamict(ite)s are

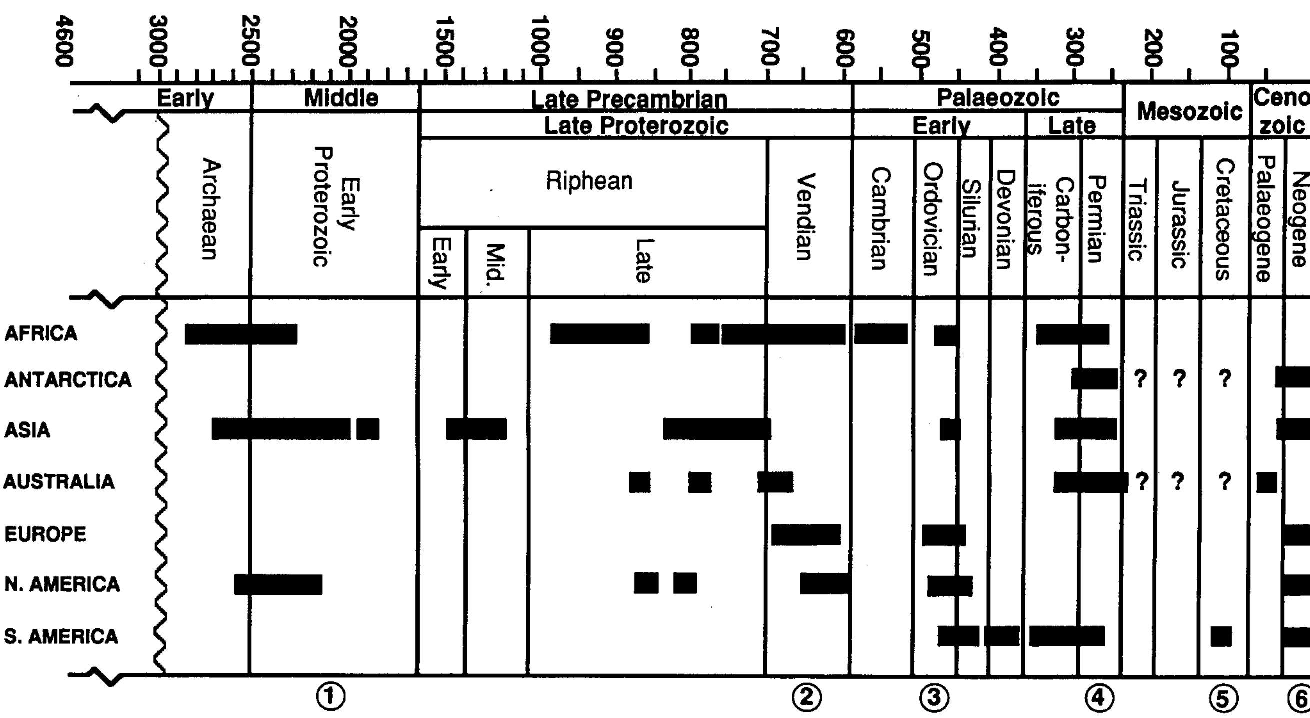

Figure 1 Earth's glacial record. Black bars depict glacial strata where ages are constrained by radiometric dating. Cretaceous ice caps may have existed in the interior of Antarctica and northern Siberia. Data compiled principally from Hambrey and Harland (1981). Representative references: (1) Miall (1985), (2) Eisbacher (1985), Eyles, C.H. (1988), Nystuen (1985), (3) Vaslet (1990), (4) Crowell and Frakes (1975), Visser (1983, 1989), Levell *et al.* (1988), Franca and Potter (1991), (5) Frakes and Francis (1988), (6) Martinson *et al.* (1987), Andrews (1987).

merely a common facies type and are produced in a range of sedimentary environments and climates. It is commonly impossible to deduce the origin of a diamict(ite) from a single small outcrop. It is always important to examine the related facies in conformable stratigraphic context above and below the diamict (Chapter 1), in order to assess the evidence for its depositional environment by reference to associated facies. This approach is based on the premise that diamict facies produced, for example, by sediment gravity flows, will tend to be intimately associated with other gravity-emplaced diagnostic facies such as turbidites (see later in

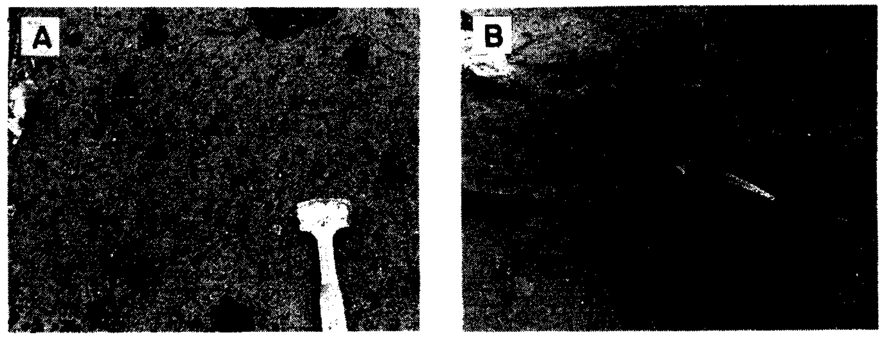

Figure 2 Diamict(ite) facies. A) Clast-rich massive diamict produced by ice-rafting and settling of suspended fines in a glaciomarine environment. Late Cenozoic Yakataga Fm., Alaska. B) clast-poor massive diamict produced by ice-rafting and settling of suspended fines in an ice-contact glaciolacustrine setting. Note thin silt wisps above ice-axe. Late Wisconsin Sunnybrook diamict, Scarborough Bluffs, Ontario.

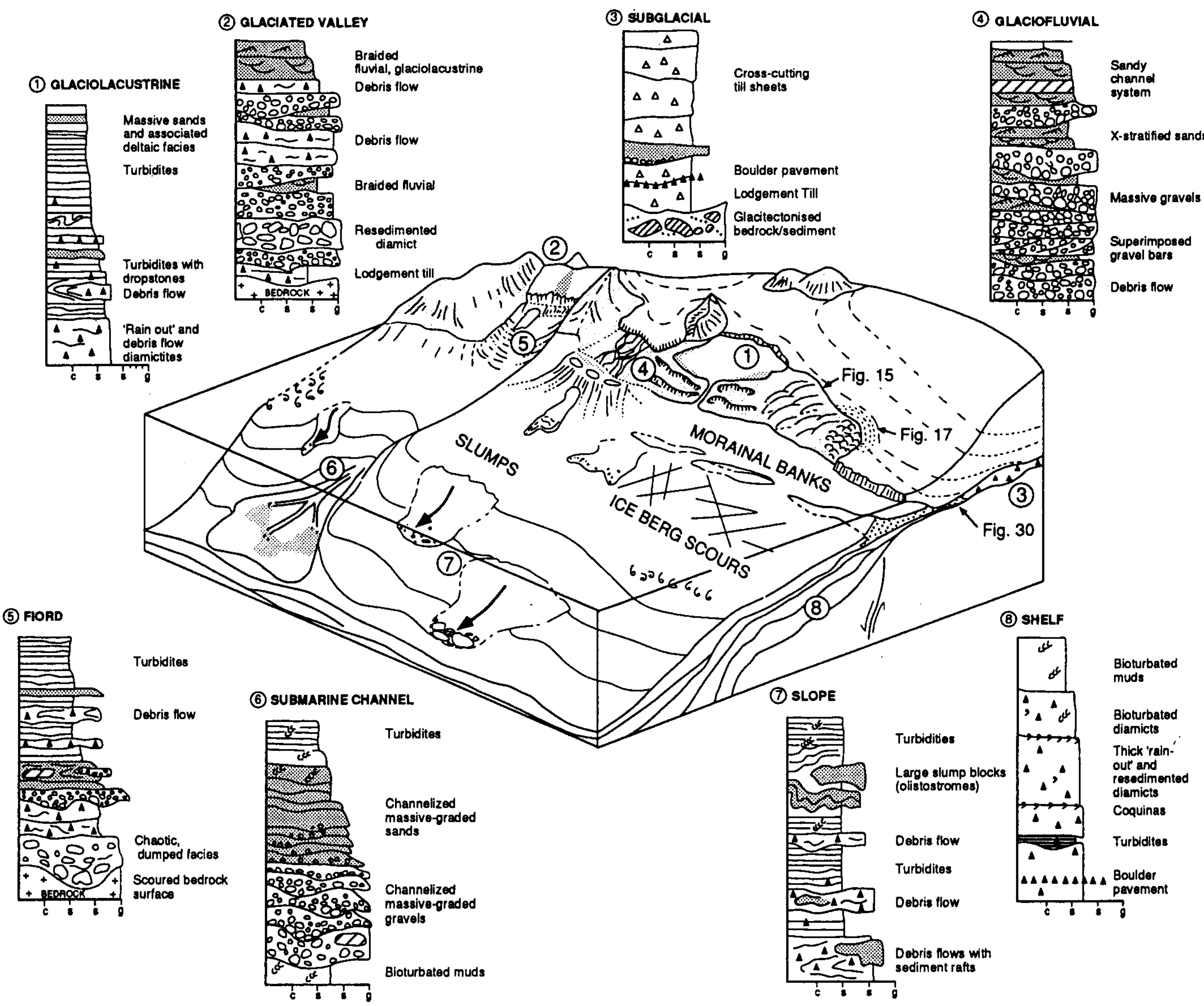

Figure 3 Depositional environments and typical vertical profiles of facies deposited during a single phase of glacier advance and retreat in various glacioterrestrial and glaciomarine environments.

this chapter, and in Chapter 13). Facies associations vary in different depositional environments, as does the geometry or three-dimensional shape of the deposit. The best interpretations therefore require detailed vertical profiles of the deposits, along with information on lateral variability and depositional geometry (architecture) beyond the local outcrop.

Commonly, glacial facies are intimately associated with the deposits of many other environments, particularly rivers, lakes, continental shelves, and slopes. In most cases, the role of the glacier has been to deliver large volumes of sediment to a marine or lacustrine basin, where primary glacial sediments are then reworked by nonglacial sedimentary processes. However, sedimentary products (facies) found within different glacial and glacially influenced environments can be identified, and occur in distinct facies associations (families of related facies). Glacial *depositional systems* can be recognized as distinct three-dimensional assemblages of process-related facies that record major paleogeomorphic basin elements. The spatial and chronological linkage of these depositional systems identifies two distinctive systems tracts, *glacioterrestrial and glaciomarine* (Fig. 3).

THE GLACIOTERRESTRIAL SYSTEMS TRACT

Glaciation of continental interiors creates a variety of glacioterrestrial depositional environments which can be grouped into four depositional systems; *subglacial, supraglacial, glaciolacustrine* and *glaciofluvial* (Fig. 3). Substrate relief and tectonic setting play a fundamental role in the deposition and preservation of terrestrial glacial sediments in these environments. Extensive Quaternary glacial deposits of cratonic continental interiors (Figs. 4 and 5) record the growth of large ice sheets but are relatively poorly preserved in the Earth's glacial record. On the other hand, reworked continental glacial deposits are a very common stratigraphic component of orogenic belts. They record the growth of cordilleran ice masses and preservation of glacial sediments in tectonically active basins. The bulk of glacially derived sediment is preserved in the ocean basins (Fig. 4; Bell and Laine, 1985). Cold climate (periglacial) processes also affect terrestrial glacial deposits beyond the ice margin, causing extensive deformation of sediments, and influencing the deposition of fluvial and eolian facies.

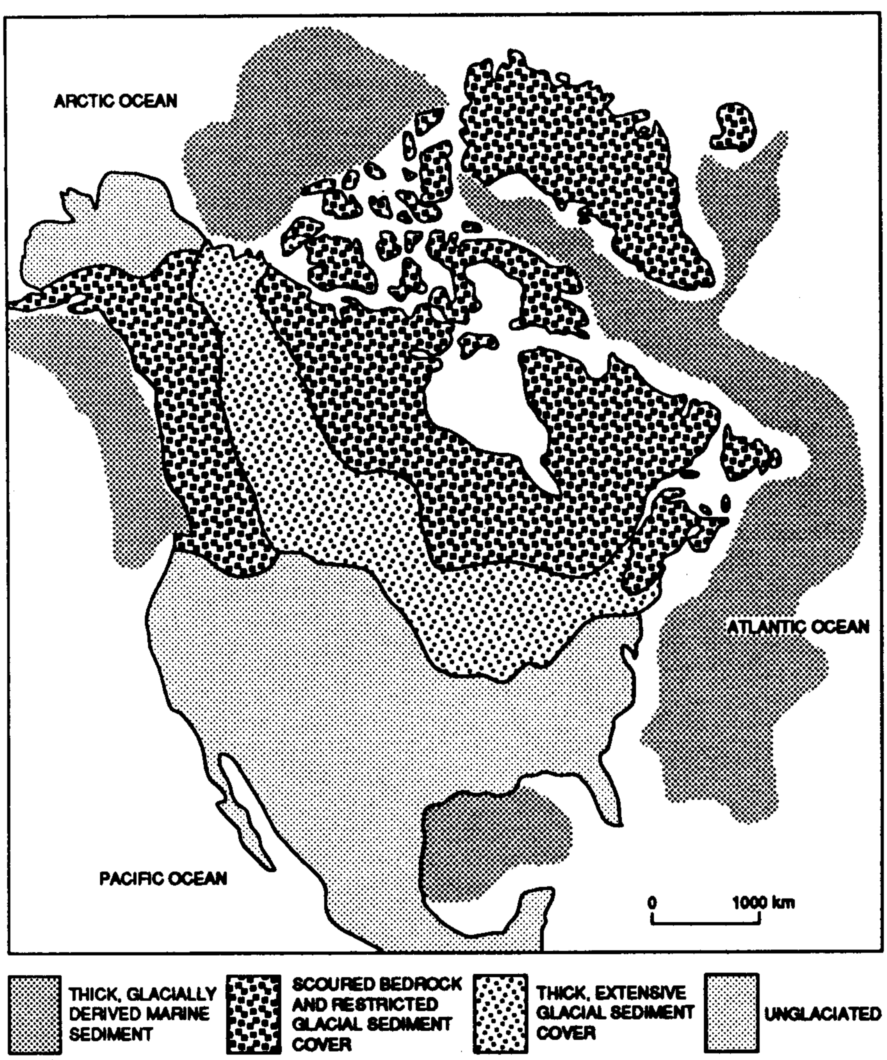

Figure 4 Schematic distribution of sediments resulting from Quaternary glaciation of northern North America. Note widespread distribution of thick, glacially derived marine sediment in ocean basins; these sediments are preferentially preserved in the Earth's glacial record.

LOW-RELIEF GLACIOTERRESTRIAL SETTINGS

Glaciation of low-relief, continental interiors results in crudely concentric belts of different glaciated terrains that reflect the growth and shrinkage of large ice sheets. This is well shown by the distribution of Pleistocene glacial deposits in North America (Figs. 4, 5). Several depositional systems can be recognized (Fig. 3).

Subglacial depositional systems

Conditions at the base of large ice sheets vary widely in response to different ice temperatures and velocities. Wet-based ice (Figs. 6A, B) occurs where conditions are close to the pressure melting point, and the ice slides over the substrate. In dry-based conditions (Fig. 6A) the ice remains frozen to the bed and moves mostly by internal deformation. Subglacially deposited diamict facies occur principally below wet-based ice (Figs. 6C, D). Englacial debris is transported within a thin (1 m) basal layer that consists of irregular layers of ice and debris. Intense abrasion occurs both between particles in the base of the layer, and between these particles and the substrate. Clasts or masses of debris that collide with the bed may become lodged against the substrate as a result of pressure-melting and release from the ice base. The process is akin to smearing peanut butter across a piece of toast. A characteristic glacially faceted clast shape (*bullets*, Fig. 7) evolves as a result of overlying dirty ice moving over the lodged clast. Continued lodgement produces lenticular beds of dense, overconsolidated diamict termed *lodgement till* (Figs. 8, 9, 10). Long axes of the clasts have a strongly preferred alignment parallel to ice flow. Measurement of long axis orientation for a few bullet clasts gives a rapid indication of ice flow direction.

Lodgement tills lie on marked local and regional unconformities, and tend to have regional sheet-like geometries (Figs. 8, 9). Total thicknesses rarely exceed 50 m. Strongly lenticular till units occur locally within the sheet-like forms. They have cross cutting and overlapping relationships as a result of intermittent erosion of the substrate in response to change in ice velocities. Changes in ice flow direction and the introduction of differing debris lithologies can result in a stack of several lodgement tills, superimposed during a single glaciation (Fig. 8). Each till unit contains clasts and matrix from contrasting bedrock sources. This emphasizes the need for care in interpreting ice advance/retreat cycles from multiple-till stratigraphies.

Gravel-filled channels resulting from subglacial stream drainage are also integral components of the subglacial stratigraphy (Fig. 8; Eyles *et al.*, 1982). Channels have a planar upper surface truncated by overlying diamict. They are oriented subparallel to ice flow direction and are genetically related to esker ridges (Fig. 8). Therefore, the presence of glaciofluvial facies within lodgement-till complexes does not necessarily indicate glacier retreat.

Sediments and poorly lithified rocks below lodgement-till successions are commonly observed to be extensively deformed as a result of subglacial tectonism (Fig. 11; Croot, 1988). This is akin to spreading peanut butter on very soft bread. These *glaciotectonized* substrates are particularly common over large areas of the Prairie Provinces in western Canada, and consist of weak mud rocks and poorly lithified sandstones (Sauer *et al.*, 1990).

Eskers record transient water flow below the ice sheet. They infill tunnel networks that may be cut either into the bed or up into the overlying ice

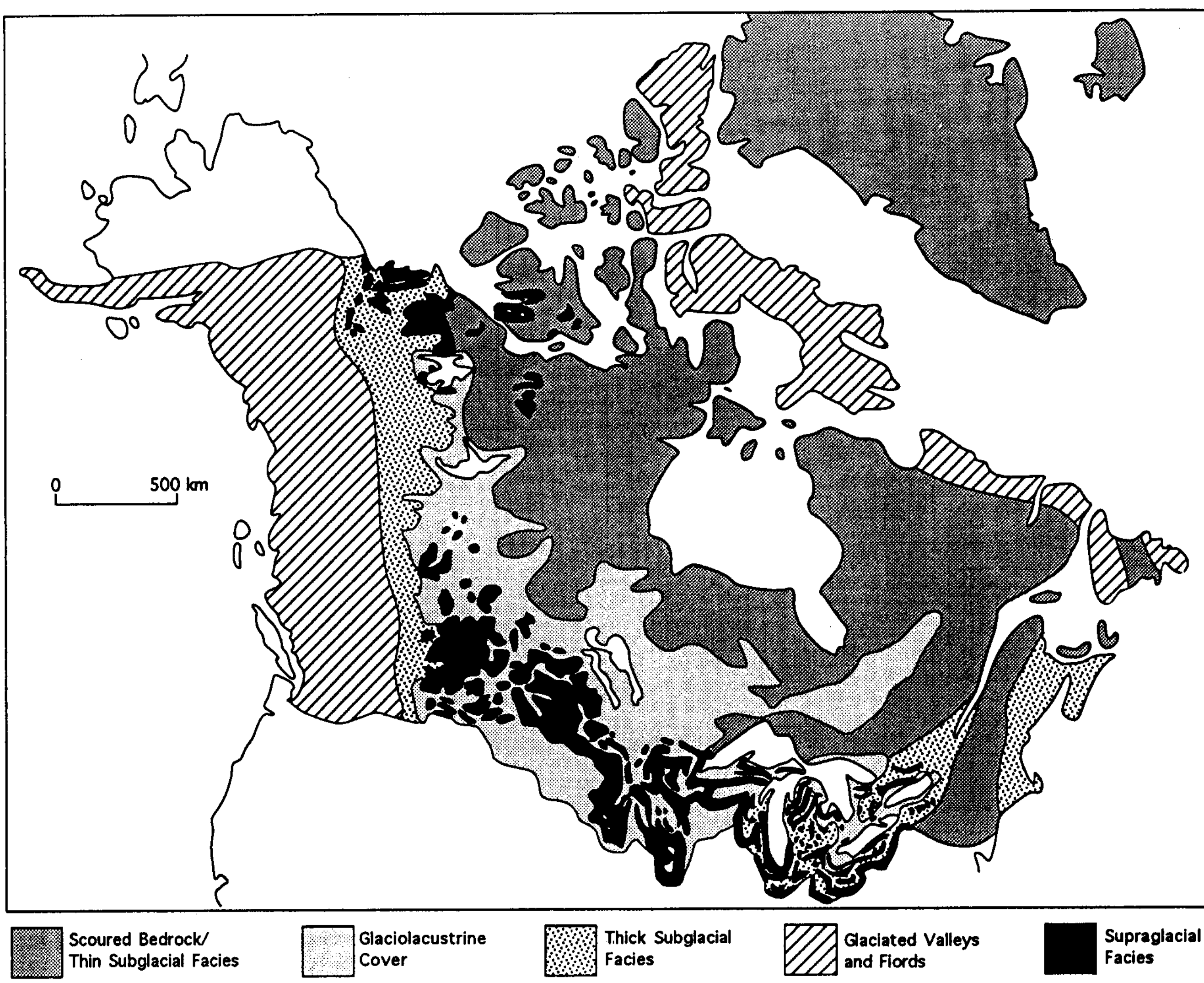

Figure 5 Schematic distribution of Quaternary glacioterrestrial sediments in northern North America. Glaciolacustrine sediments obscure large areas.

base. Such tunnel fill eskers are exposed by ice retreat as steep-sided ridges that record the internal plumbing system of the ice sheet (Fig. 12). Internally, the eskers contain cross-bedded sand and gravel facies with restricted variance in paleocurrent directions. A beaded form is typical of eskers deposited as overlapping subaqueous fans in water ponded against the retreating ice front. Beaded eskers show rapid downstream transitions into fine-grained glaciolacustrine facies.

Other bedforms exposed by the retreat of wet-based, sliding glaciers are streamlined *drumlins*, which form part of extensive swarms (Fig. 13). Their formation is not well understood, but most inferred mechanisms invoke either incremental lodgement around subglacial obstacles such as rock highs, or erosion of sediment over-run by the ice sheet. Studies of drumlins at modern ice margins, and geophysical investigations in Antarctica (Alley *et al.*, 1987), show that subglacial sediments can be pervasively deformed below rapidly flowing ice (Fig. 6D). In this case, sliding along the ice/substrate interface is less important than movement resulting from internal deformation of the substrate. These beds are composed of diamicts (deformation till; Fig. 14) and formed by the mechanical mixing and homogenization of eroded sediments, as in a concrete mixer. Indeed, the glacier base can be regarded as a giant shear zone, with *deformation till being equivalent to fault* gouge and drumlins as large-scale slickensides. The thickness of the deforming layer below large Quaternary ice sheets is not yet established, but could have reached several tens of metres. The deformability of sediments overridden by the ice sheet is dictated by their geotechnical and hydrogeological properties. Spatial variation in the shear-strength of subglacial substrate sediments gives rise to streams of deforming diamict separated by areas of the bed that are resistant to deformation (Fig. 15). Erosion around these more resistant portions of the bed results in streamlined *residual* drumlins. Detailed subsurface investigations show that many drumlins originate by erosion of pre-existing sediment, with deformation till resting unconformably on a resistant core of overridden proglacial sediments (Fig. 15; Boyce and Eyles, 1991). Other models of drumlin genesis involve the release of catastrophic subglacial sheet floods (Shaw and Sharpe, 1987) but this hypothesis has yet to be adequately tested by studies of the internal

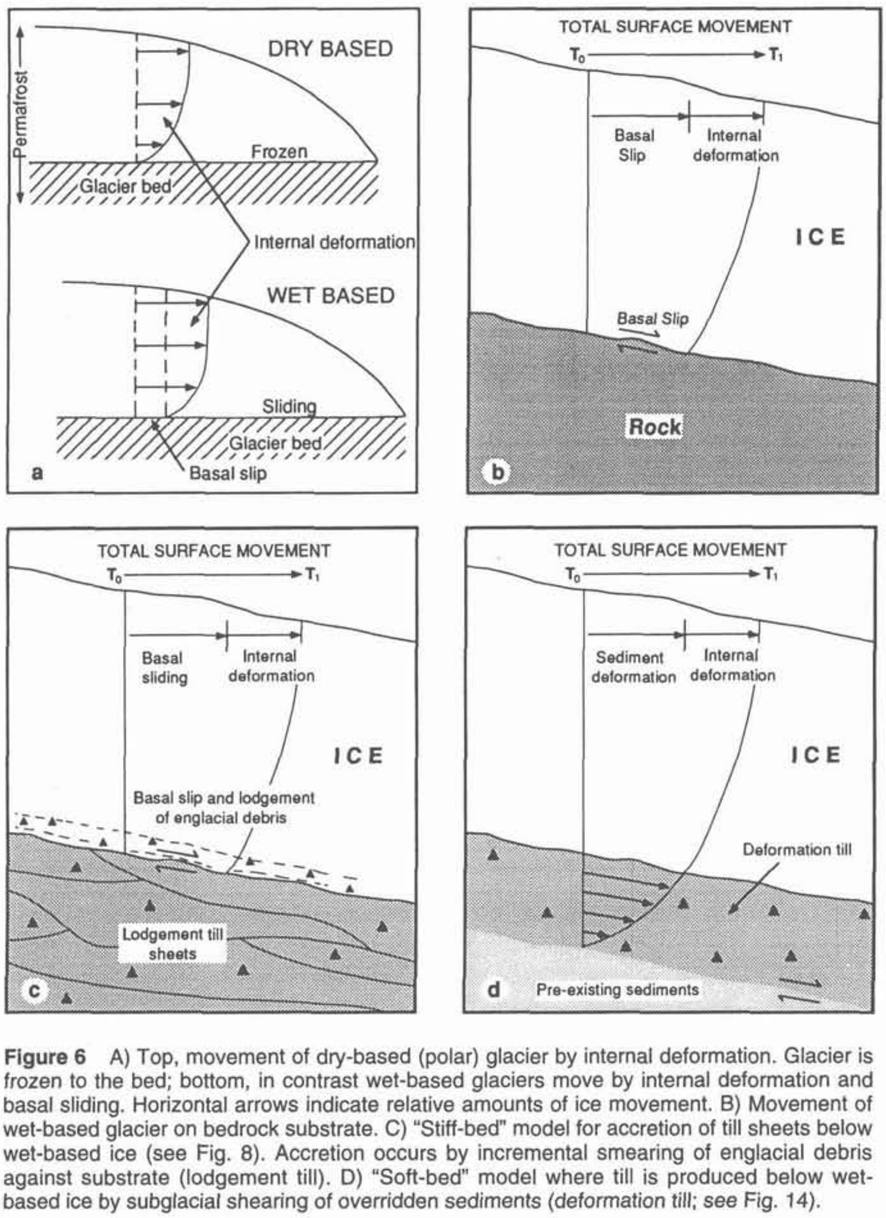

Figure 6 A) Top, movement of dry-based (polar) glacier by internal deformation. Glacier is frozen to the bed; bottom, in contrast wet-based glaciers move by internal deformation and basal sliding. Horizontal arrows indicate relative amounts of ice movement. B) Movement of wet-based glacier on bedrock substrate. C) "Stiff-bed" model for accretion of till sheets below wet-based ice (see Fig. 8). Accretion occurs by incremental smearing of englacial debris against substrate (lodgement till). D) "Soft-bed" model where till is produced below wet-based ice by subglacial shearing of overridden sediments (*deformation till; see* Fig. 14).

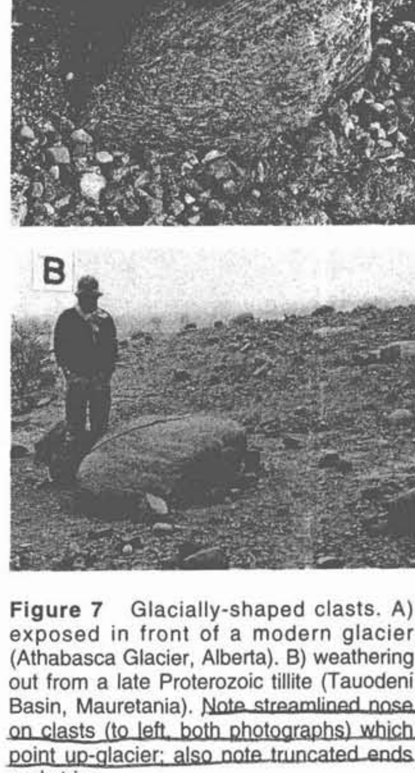

Figure 7 Glacially-shaped clasts. A) exposed in front of a modern glacier (Athabasca Glacier, Alberta). B) weathering out from a late Proterozoic tillite (Tauodeni Basin, Mauretania). Note streamlined nose on clasts (to left, both photographs) which point up-glacier; also note truncated ends and *striae*.

structure and facies of the drumlins.

The important criteria for identifying *continental glacial facies* are 1) the presence of underlying regionally extensive unconformities and 2) the restricted regional thickness of individual subglacially deposited diamict(ite) units. This thickness is generally less than 50 m, and is commonly much less. By contrast with the subglacial environment, diamict(ite) thicknesses in glaciolacustrine and glaciomarine environments are much greater (see below). The second criterion of restricted regional thickness applies regardless of the relative importance of lodgement (stiff-bed) and deformation (deforming bed) below the ice sheets (Fig. 6) and regardless of the precise origin of subglacial bedforms. The presence or absence of subglacial bedforms (drumlins, eskers and glaciotectonic structures), subaerial outwash and other cold climate facies, provides further contextual criteria for the identification of subglacially deposited till(ite)s.

Supraglacial depositional system

The thin, outer margin of an ice sheet commonly stagnates, leaving broad zones of hummocky topography underlain by highly variable sediments with complex geometries. During the last glaciation, stagnant ice extended over many thousands of square kilometres in North America (Figs. 4, 5). Strong compression between active ice upglacier and the dam of stagnant marginal ice results in complex folding and thickening of the basal debris layer (Fig. 16). This debris may be slowly melted out in situ to form *basal melt-out till*. The melt-out till, together with other diamict facies released on the ice surface, is associated with a distinct hummocky topography that records complex disintegration of the ice margin (Fig. 17D, E; Shaw, 1979; Lawson, 1982; Kasizcki, 1987; Paul and Eyles, 1990). If the thin outer margin of the ice sheet becomes frozen to the substrate, large bedrock slabs may be detached and glaciotectonized. This is because ice movement is accomplished not by basal sliding, but by deformation of underlying substrate sediments.

An inactive or retreating margin of this type becomes buried under a drape of diamict formed by the melt-out of englacial debris on the ice surface (Figs. 16, 17A, B, C). This drape is very unstable and is moved by sediment gravity flows into kettle basins generated by the local melt of buried ice (Boulton, 1972; Fig. 17b, c). Kettle fills are subsequently preserved as hummocks when adjacent ice cores, under a thinner sediment cover, meltdown more rapidly to produce topographic lows (*relief-inversion*). Typical vertical profiles through hummocks

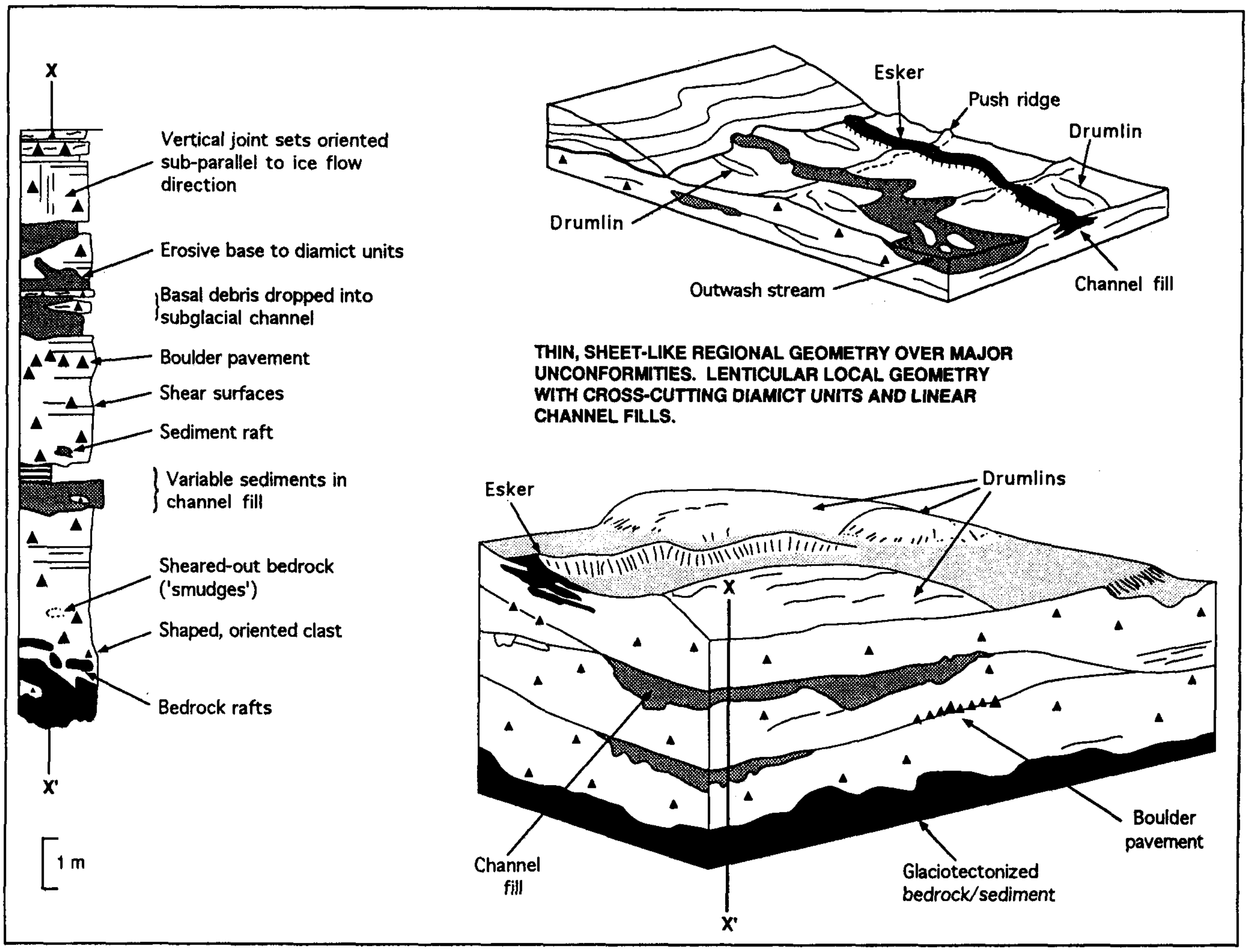

Figure 8 Depositional environment, stratigraphy and generalized vertical profile for lodgement till

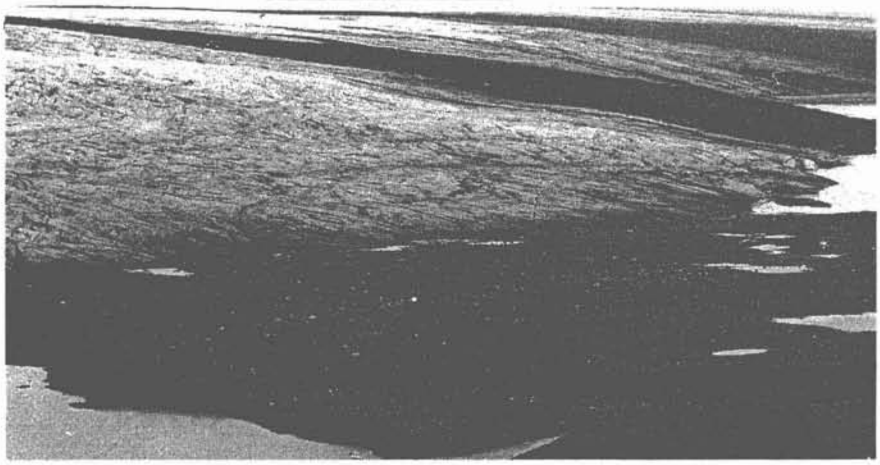

Figure 9 Low relief till plain being exposed by retreat of an Icelandic glacier; lines parallel to ice margin are annual push ridges. Section in centre of photograph is 8 m high.

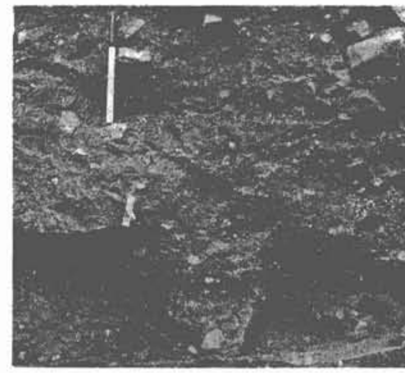

Figure 10 Massive, overconsolidated lodgement till showing subhorizontal shear planes. Late Wisconsin deposits at Sandy Bay, Northumberland, England.

Figure 11 (left) Folded rafts of Cretaceous Chalk in glaciotectonized glaciomarine deposits of N.E. Norfolk, England. Ice movement was from right to left. Sea wall in front of section is 2 m high.

Figure 12 (lower left) Sinuous esker ridge (8m high) exposed by retreat of Icelandic ice margin 1 km distant.

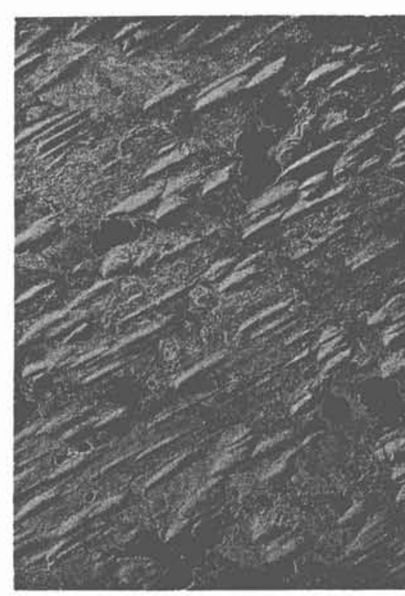

Figure 13 Drumlin swarm and flutes in Saskatchewan produced by ice sheet flowing toward top right. Note *en echelon* arrangement of drumlins suggesting erosional streamlining of pre-existing sediment (see Fig. 15). Scale bar (centre-right) is 2 km.

show uppermost successions of resedimented massive, graded and stratified diamicts (Fig. 16). Supraglacial diamicts resedimented as debris flows are generally conformable, have clast imbrication parallel to flow, clasts that project from the tops of beds, rafts and fragments of pre-existing sediments, channelized cross sectional form, lenticular downslope-thickening geometry, an absence of relief on upper bed surfaces and a tendency to fill topographic lows. Massive and crudely bedded diamict facies predominate; the crudely bedded facies result from successive superimposition of thin massive flows. These diamict facies are interbedded with glaciofluvial and lacustrine facies. They overlie basal melt-out till (Fig. 16), which may drape over bedrock rafts that were present in the former ice base. Glaciotectonized (ice thrust) bedrock and incorporated substrate sediments can be an important component of the sedimentary succession (Fig. 16). Under certain conditions, englacial structures such as folded basal debris successions survive basal melt-out in the form of ridge-like bedforms oriented transverse to former ice flow direction (Shaw, 1979).

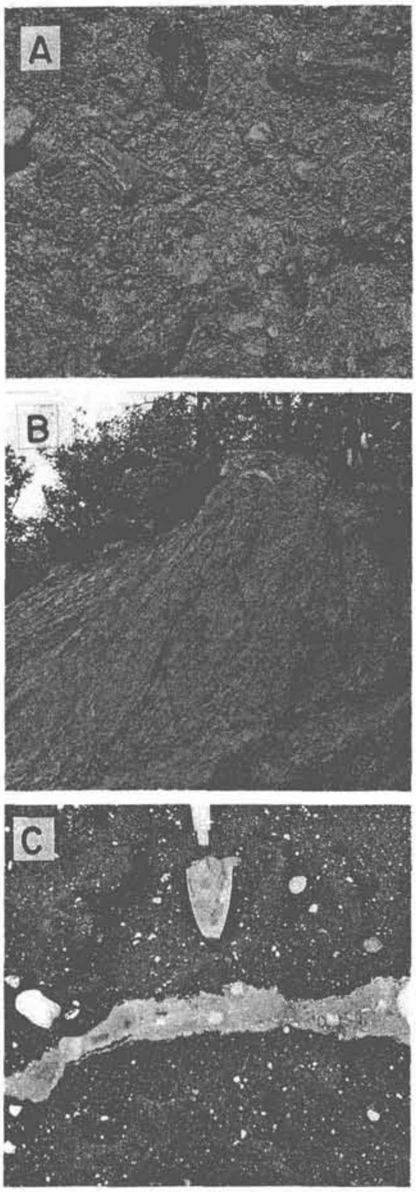

Figure 14 Deformation till. A) Deformation till recently exposed at the margin of Saskatchewan Glacier, Alberta. Note "chaotic" appearance and lack of any clast fabric. Largest clast shown is approximately 15 cm diameter. B) 10 m thick exposure of Halton Till at Toronto, Ontario, deposited during the Late Wisconsin glaciation (about 25-15,000 years ago). Till rests erosively on sands. C) Sheared-out lens of chalk in clay-rich deformation till; Late Wisconsin deposits of the east Yorkshire coast, England.

Glaciolacustrine depositional system

Glaciolacustrine ponding results from overdeepening by glacial erosion, glacial disruption of former drainage systems, and the release of large volumes of meltwater. Basins vary from narrow alpine types in areas of high relief (see below), to large continental-scale lakes akin to interior seaways. These large lakes are ponded in isostatically depressed continental interiors evacuated by ice sheets (Fig. 5). Lake Agassiz is the most famous example, extending over an area of about 1,000,000 km^2 of North America (Teller and Clayton, 1983). A simple distinction between ice-contact and non ice-contact lake bodies can be made (Fig. 18). One of the most characteristic glaciolacustrine facies consists of *varves*, which are annually produced couplets of contrasting grain sizes resulting from different conditions of sedimentation in winter and summer. A varve typically comprises a couplet of a coarser summer layer (sand and/or silt) and a finer winter layer (clay). Proximal equivalents may include varved gravels, but these are difficult to recognize. The classic model of varve formation in non ice-contact glacial lakes emphasizes a strongly seasonal regime driven by summer supraglacial melting across the ice margin. Significant supraglacial melt is

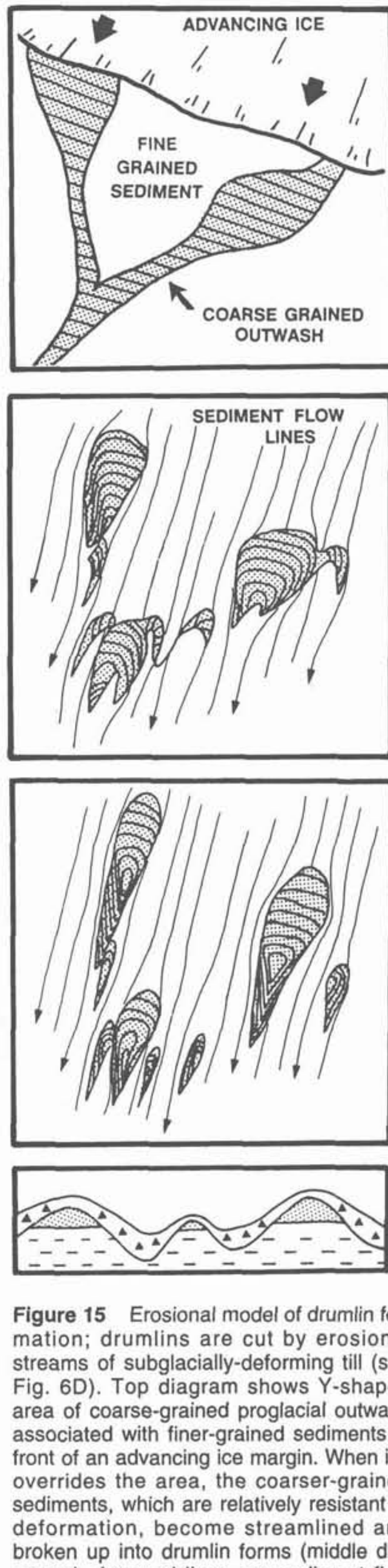

Figure 15 Erosional model of drumlin formation; drumlins are cut by erosional streams of subglacially-deforming till (see Fig. 6D). Top diagram shows Y-shaped area of coarse-grained proglacial outwash associated with finer-grained sediments in front of an advancing ice margin. When ice overrides the area, the coarser-grained sediments, which are relatively resistant to deformation, become streamlined and broken up into drumlin forms (middle diagrams). Arrowed lines are sediment flow lines. Bottom diagram shows cross section through resultant drumlins which have a sandy core (stippled), overlie fine-grained sediments (dashes) and are draped with a thin veneer of deformation till (triangles). After Boulton (1987), and Boyce and Eyles (1991).

suppressed in winter. Under this regime sedimentation is dominated by the growth of fan-delta lobes. In summer, sediment laden, higher density meltwaters move down these lobes as density underflows. A distinct succession of sandy lithofacies is deposited in each summer melt season (Fig. 19) and records the start, increase and ultimate decline of density underflow activity (Ashley, 1975). The succession is bounded top and bottom by a winter clay layer deposited from suspension (Figs. 19, 20A, B). The summer sandy layers thin distally into silts with isolated starved ripples and rare ripple-drift cross lamination. The base of the coarser layer is commonly sharp, and the layer may be graded (Figs. 19, 20D). It may contain multiple laminations representing deposition by a single pulsating or intermittent density underflow. There may also be a minor contribution of pelagic material from interflows or overflow plumes of suspended sediment. The dark clay unit (winter layer) may show normal grading indicating deposition of suspended sediment under the ice cover of a closed lake. Clay layer thicknesses are generally uniform across the basin but may contain massive or cross-stratified sands and laminated silts which record the winter drawdown of lake levels and delta foreslope slumping (Fig. 19; Shaw, 1977). Burrowing and trace fossils are commonly present in the summer layer but not the winter clay.

Unfortunately, the term *varve* (or varvite) continues to be used as a routine descriptive term for sediments that are better termed rhythmically laminated (rhythmites), or laminated sediments (laminites). The real significance of many varved successions as indicators of seasonally controlled sedimentation remains to be assessed rigorously. Many of the layers described as varves comprise single or multiple-graded units of silt and clay with divisions C, D and E of the Bouma sequence for turbidites (Fig. 3 in Chapter 13). These may have been deposited by discrete-event turbidity currents with no evident seasonal control. In pre-Quaternary successions varvites are used to infer glaciolacustrine (i.e., continental) environments and seasonality of climate. These inferences may be incorrect if the layers are discrete-event turbidites of marine origin (or even tidally formed laminites, see Chapter 11). However, thin-bedded turbidites may also be interbedded with seasonally controlled layers so the identification of varved successions and varvites requires detailed field study (e.g., Ashley, 1975).

A seasonal, varved, depositional regime is characteristic of non ice-contact lakes in low-relief basins where sedimentation is driven solely by seasonal surface melting of the ice sheet. In high-relief lake basins in mountain

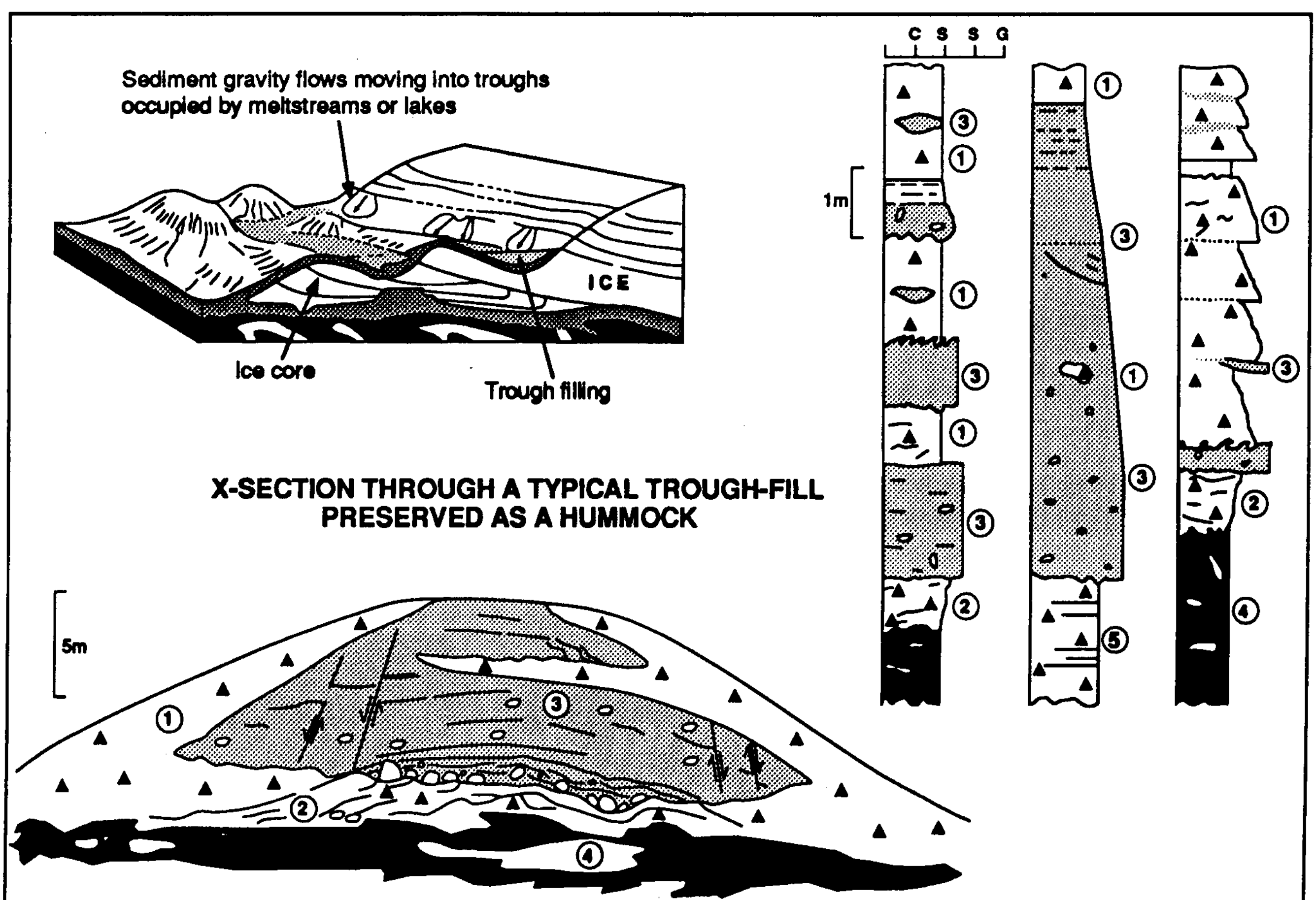

Figure 16 Depositional environment, stratigraphy and generalized vertical profile for supraglacial deposits at margin of stagnant, debris-rich, ice margin (see Fig. 17). (1) debris flows, (2) melt-out till, (3) outwash, (4) deformed substrate, (5) lodgement till (see Fig. 8) or deformation till (see Fig. 14).

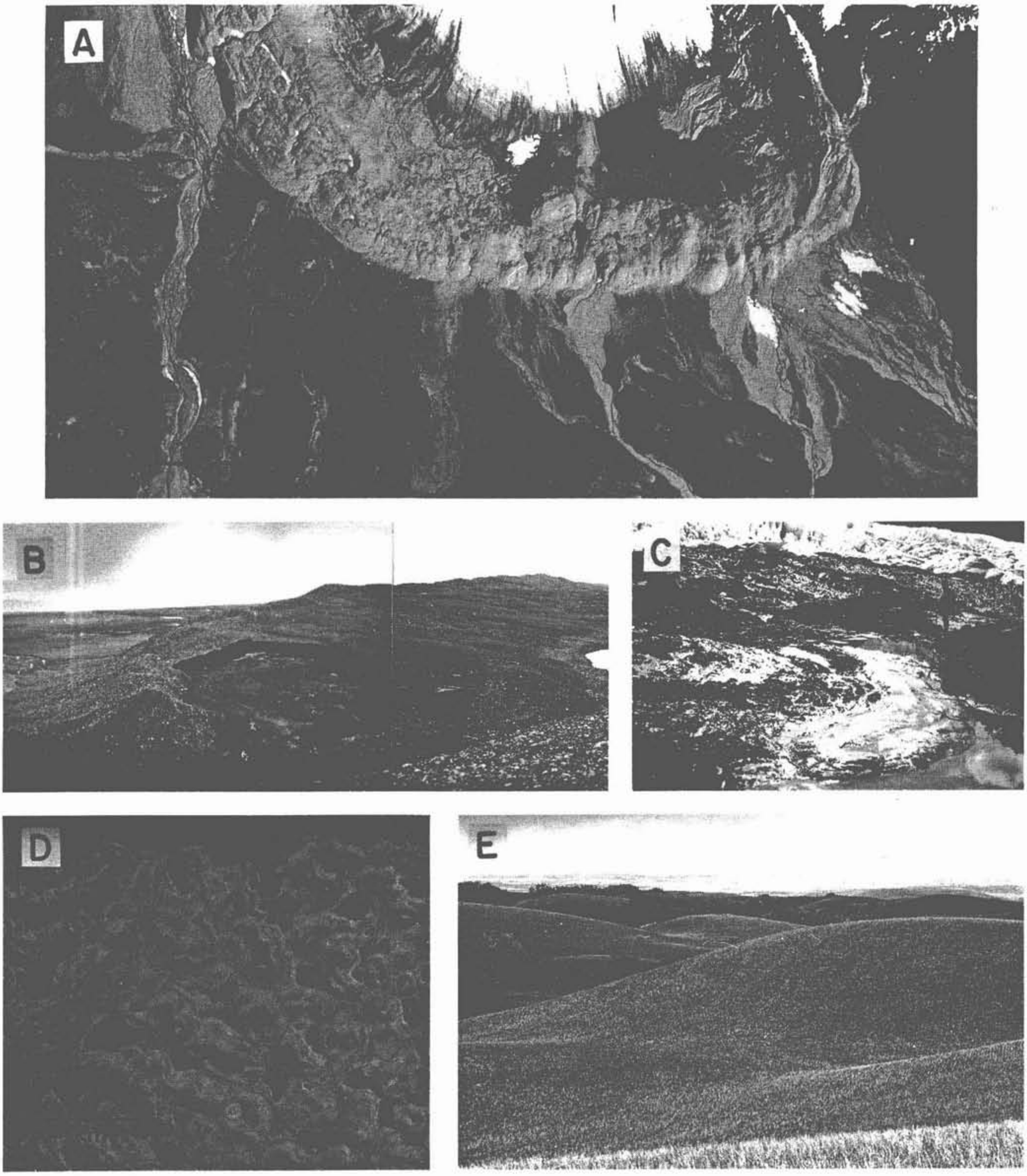

Figure 17 Supraglacial environments and facies. A) Vertical air photograph of stagnant downwasting ice margin in Spitzbergen showing hummocky, disintegration topography. B) Large ice-cored hummock (15 m high) in Spitzbergen with surface cover of debris being stripped by debris flow. Ice margin (not shown) lies to right. C) Supraglacial debris flow lobe on Matanuska Glacier, Alaska. Ice in central part of photograph contains much supraglacial debris; ice in background is relatively clean. D) Air photograph showing hummocky, supraglacially-deposited, disintegration topography in western plains of Canada (see Fig. 5). E) Rolling landscape of hummocky disintegration topography in western Canada.

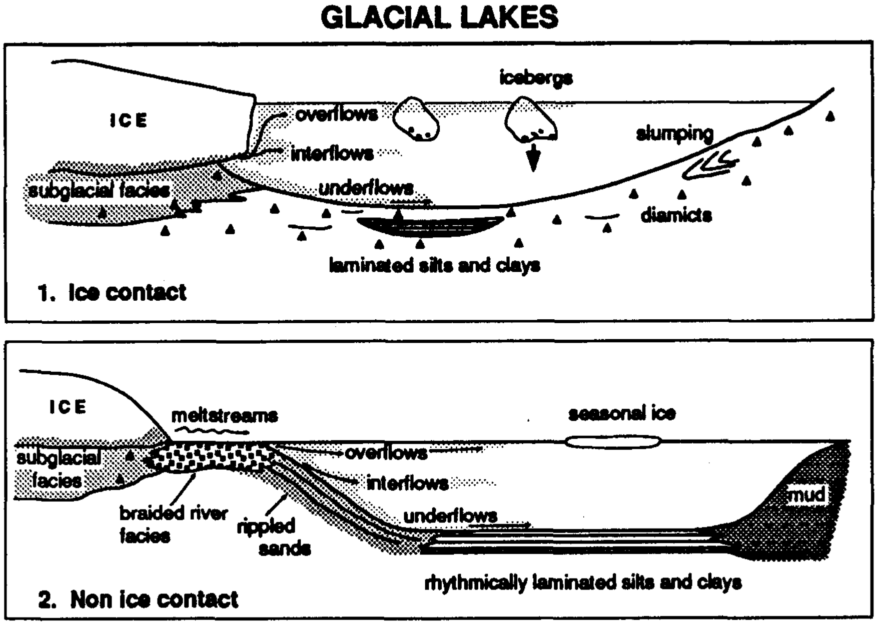

Figure 18 Contrasting depositional conditions in ice-contact and non ice-contact lakes.

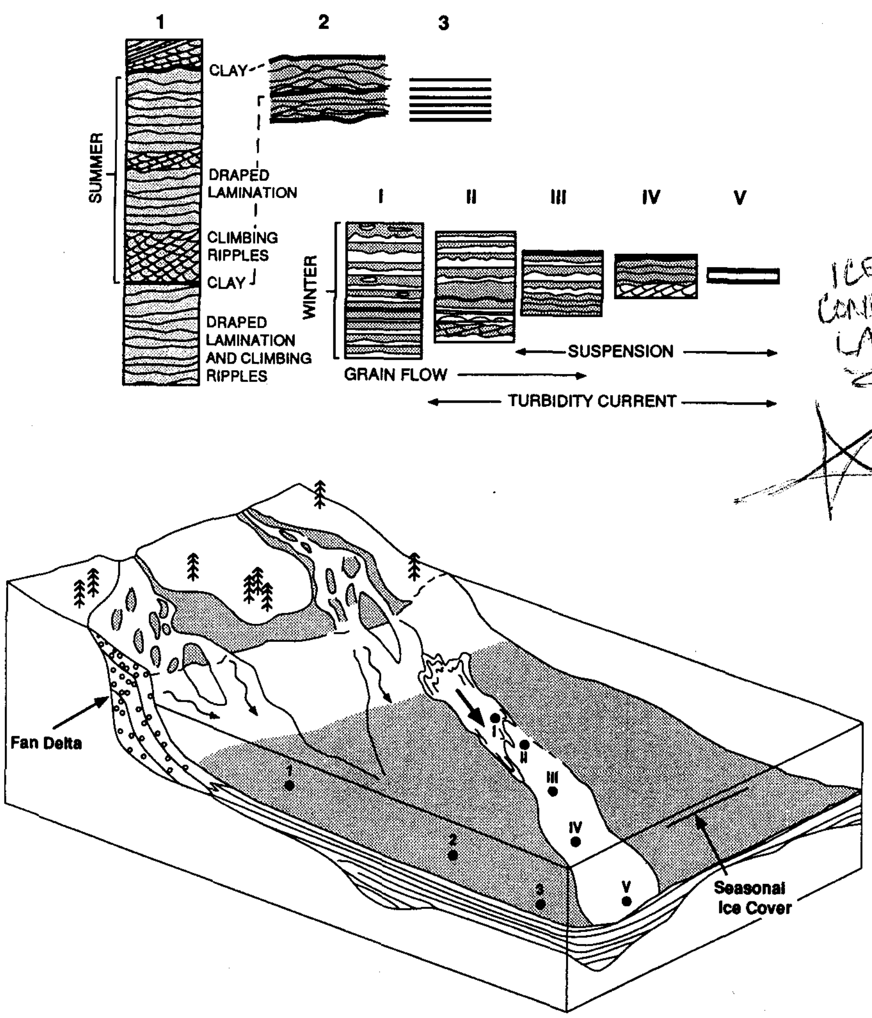

Figure 19 Deposition of seasonally-controlled (varved) sediments in non ice-contact lake. Note proximal to distal (1, 2, 3) trend from thick (cm to m) variably-rippled sands to thin (cm) silts bounded top and bottom, by a winter clay layer. Slope failure of the delta front in winter may result in more complex successions (I-V; see Shaw, 1977).

zones, seasonality is easily suppressed because resedimentation processes operate year round (see below). Sedimentological modelling of ice-contact glacial lakes is frustrated by the logistic difficulty of working on modern proglacial lakes, and the small size of modern lake basins compared to Pleistocene and older examples.

Extensive Pleistocene glaciolacustrine deposits exposed around the modern Great Lakes in North America are of considerable significance to the study of sedimentation in large, ice-contact lakes in low-relief settings (Figs. 21, 22). The deposits consist predominantly of stacked successions of diamicts and variably bedded sands (Eyles and Eyles, 1983). Diamicts are fine grained and have a blanket-like geometry, thickening in topographic lows and thinning over highs. Internally, they are complex assemblages of massive and stratified facies (Figs. 20E, 21, 22). The massive diamict facies result from the rapid rain out of suspended sediment and ice-rafted debris onto the basin floor. Stratification may subsequently be developed by reworking of this sediment by traction currents or downslope resedimentation. ICE CONTACT LAKES Diamicts are commonly overlain by channelled units of laminated silty clays, probably of turbidite origin, containing *dropstones* (Fig. 20C). These are in turn overlain by a coarsening-upwards succession of ripple-laminated, planar and trough cross-bedded sands which record delta progradation over sites of diamict accumulation. The most common deltaic facies is a crudely bedded silty sand with abundant liquefaction structures indicating rapid subaqueous deposition. Sands are commonly loaded into the upper surfaces of diamict as a result of rapid deposition of sand onto a water-saturated diamict substrate. Littoral and shallow water sediments of such large lakes are commonly storm influenced (Eyles and Clark, 1988) and subject to scouring by floating ice masses (Teller and Clayton, 1983; Woodworth-Lynas and Guigné, 1990). Extremely rapid changes in lake levels, caused by the creation or removal of ice or sediment dams, allows the close juxtaposition of shallow and deep water facies (sands and diamicts respectively; Figs. 21, 22) and may trigger large-scale slumping events.

Glaciofluvial deposits
The depositional systems described above contain significant volumes of sediment deposited by glacial meltwater rivers (Fig. 23). At the ice margin, aggradation at the head of outwash fans is commonly rapid enough to bury portions of the ice margin. This leads to deformation structures in coarse-grained, crudely bedded or massive proximal outwash gravels when the buried ice subsequently melts. Outwash surfaces pitted (with *kettles* or *craters*) by the melt of buried ice, may extend over many square kilometres. They are flanked by eskers or complex ice-contact diamict successions (Fig. 16).

The outwash plain or *sandur* (plural: *sandar* in Icelandic) lies beyond the immediate ice terminus. Glacial outwash rivers are typically of multiple-channel (braided) type (Chapter 7). Deposition is commonly dominated by large floods (jokulhlaups), to the extent that a single flood event may accomplish most of the sediment transport each year. Wind action, in the absence of vegetation, results in deposition of wind-blown silts (loess) and sand (see below). During early postglacial conditions, swamps may become established in the proximity of water bodies and anastomosed river systems may develop in areas experiencing glacio-isostatic rebound and rising base level (Chapter 7). Thick peat accumulations may ultimately generate coals, such as those of the Permo-Carboniferous

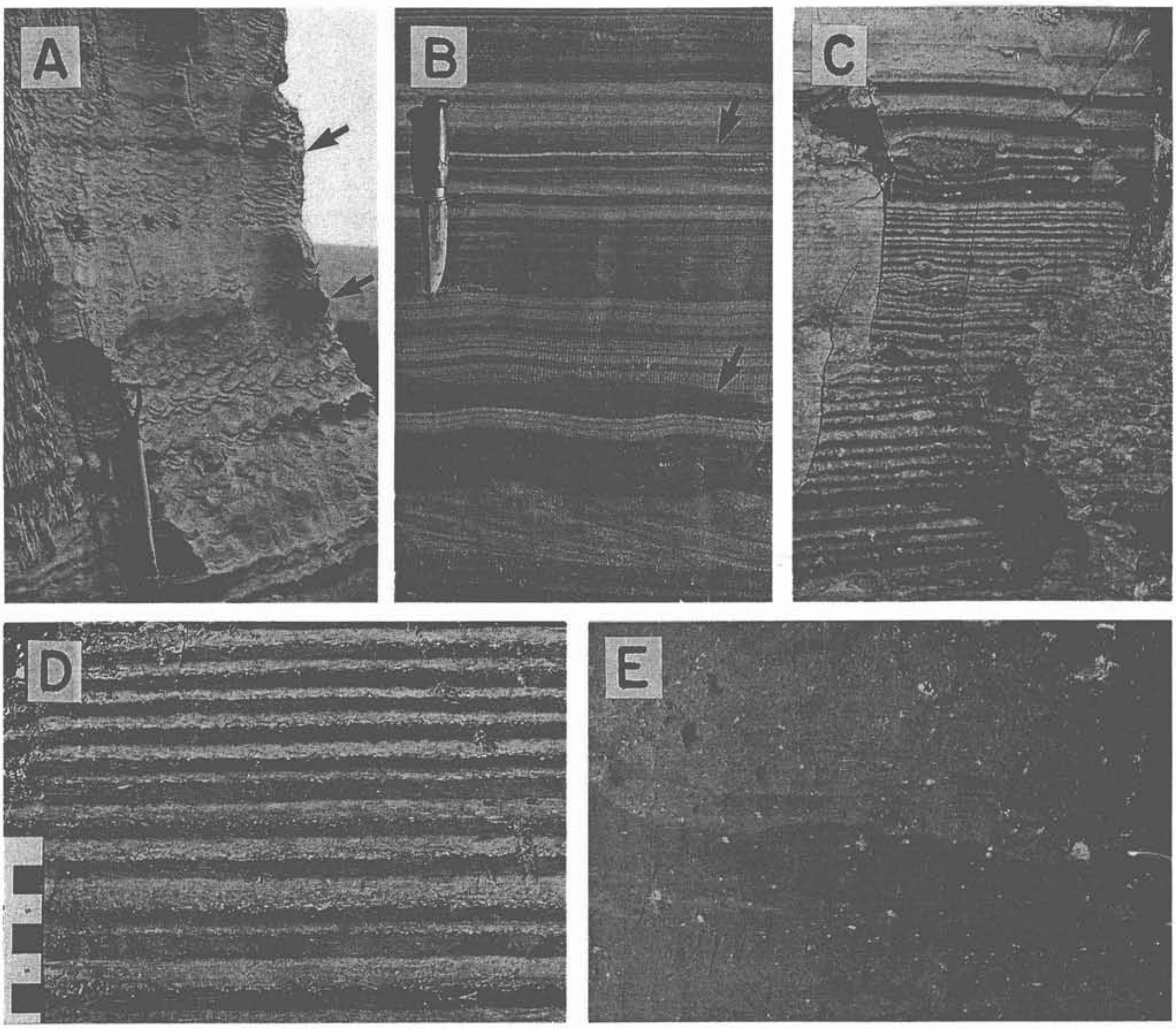

Figure 20 Glaciolacustrine facies. A) Proximal varved sands (e.g., 1 in Fig. 19) with winter clay layers arrowed. These facies were deposited in a non ice-contact lake (Fraser River valley, British Columbia). B) Lowermost rippled sands with overlying draped lamination (silt) with winter clay layers arrowed (e.g., 2 in Fig. 19). Deposited in a non ice-contact lake (Glacial Lake Hitchcock, Massachussetts). C) Laminated silts and clays containing abundant ice-rafted material. Some laminae show normal grading from silt to clay. Note variable thickness of laminae. Deposited in an ice-contact lake; Don Valley Brickyard, Toronto, Ontario. D) Varved silts and clays deposited in Lake Agassiz, northern Ontario. Note relatively constant thickness of laminations. Scale in cm; photograph courtesy T. Warman. E) crudely stratified muddy diamict formed by ice-rafting and settling of suspended fines in an ice-contact glaciolacustrine environment; photo shows about 1 m of outcrop. Late Wisconsin deposits, Scarborough Bluffs, Ontario.

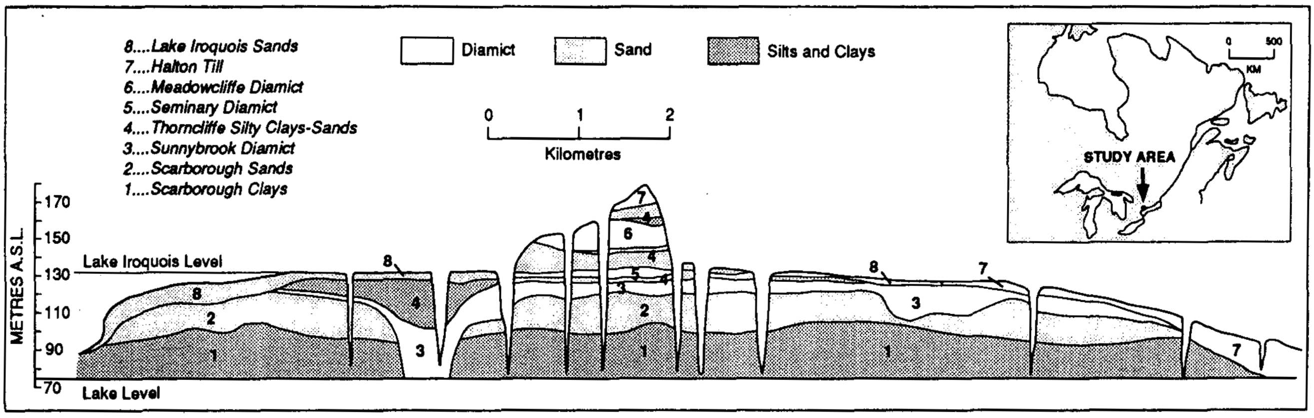

Figure 21 Outcrop geometry of last glaciation (Wisconsin) glaciolacustrine complex (diamicts, sands, silts, clays) exposed at Scarborough Bluffs, Ontario.

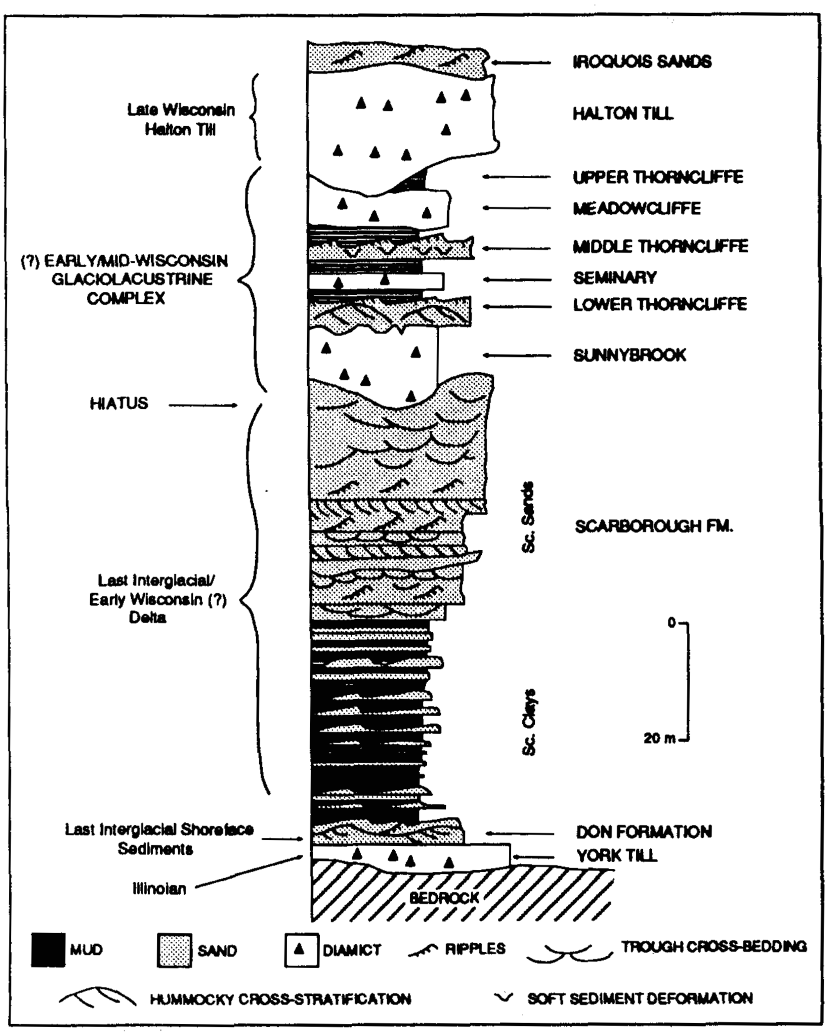

Figure 22 Idealized vertical profile through Late Wisconsin glaciolacustrine complex exposed at Scarborough Bluffs, Ontario. See Fig. 21 for outcrop geometries.

coal-bearing glaciated basins of the southern continents (Martini and Glooschenko, 1985).

Glaciofluvial processes are important because they may completely rework sediment deposited by the glacier (Fig. 23). The sedimentary record indicating the presence of ice may therefore be destroyed. This is a problem in the interpretation of ancient deposits, because braided river deposits occur in many depositional settings (Chapter 7). A glacial connection may be very difficult, if not impossible to identify. Evidence must be sought from the presence or absence of cold climate (see below) periglacial structures, or from the occurrence of glacial clast shapes (Fig. 7) and striations. This is a particular problem in high-relief settings.

HIGH-RELIEF GLACIOTERRESTRIAL SETTINGS

In mountainous areas typical of active tectonic settings, steep substrate slopes and valley floor rivers are the dominant influence on sedimentation. Late glacial resedimentation processes rework primary glacial sediment downslope into braided river systems or fan-deltas on the margins of lakes. Deposits are dominated by interbedded debris flow diamicts, braided river gravels and glaciolacustrine facies (Fig. 24) and comprise a relatively distinct *glaciated valley* depositional system. The term *paraglacial* has been used to identify a short-lived transitional period from glacial to fluvial environments (Ryder, 1971). Downslope transport of large volumes of poorly sorted debris is common, particularly in glaciated volcanic areas where large volumes of coarse-grained poorly sorted volcanic sediments are remobilized downslope as *lahars* (Eyles and Eyles, 1989; see Chapter 6). The presence of glacially streamlined bullet boulders within a diamict(ite) may be the only indication of a glacial contribution to the sediment

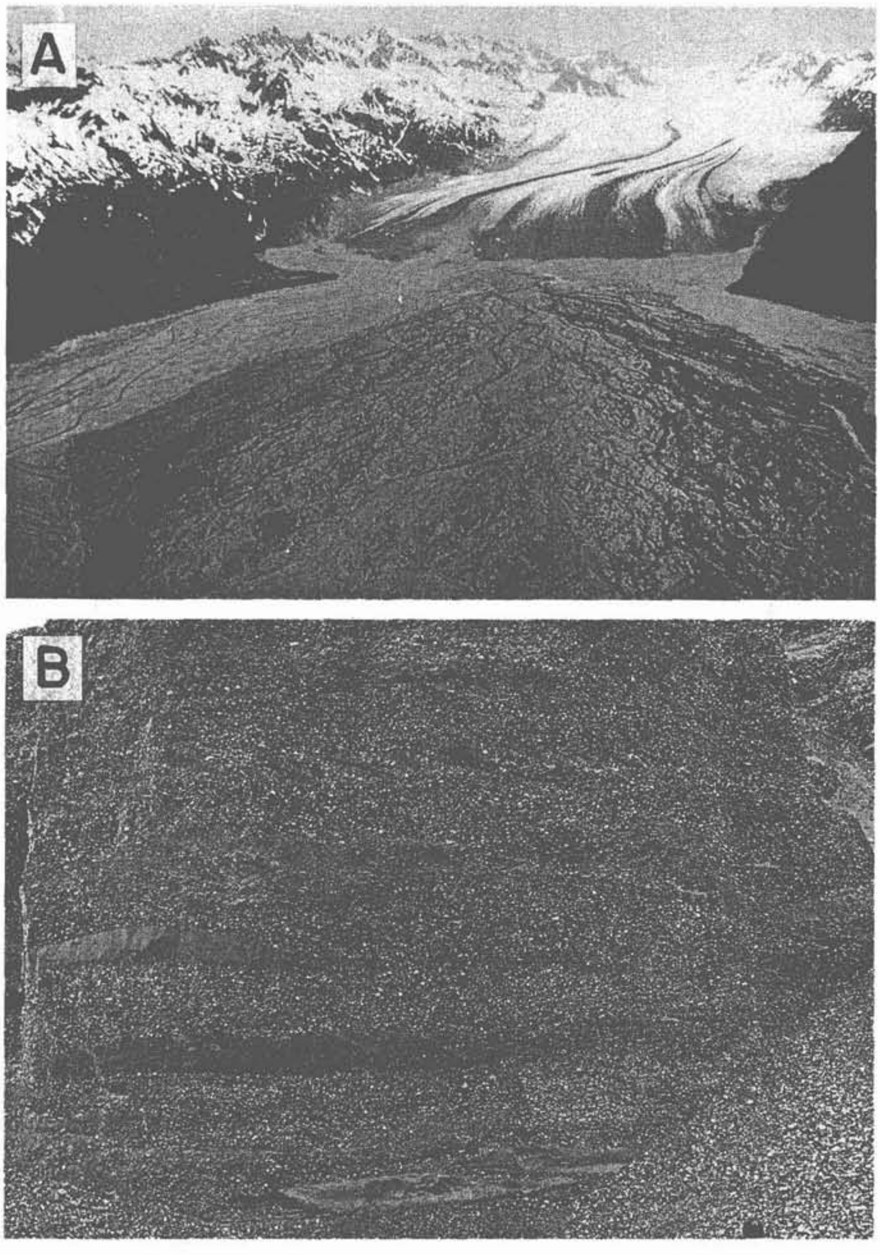

Figure 23 Glaciofluvial environments and facies. A) Scott outwash fan, Alaska. B) Typical braided river gravel facies showing planar tabular sheets of massive to poorly-stratified gravels deposited on longitudinal bars. Note thin (30 cm) wedges of sand deposited along trailing edge of gravel bars (see Chapter 7). Section is approximately 8 m high.

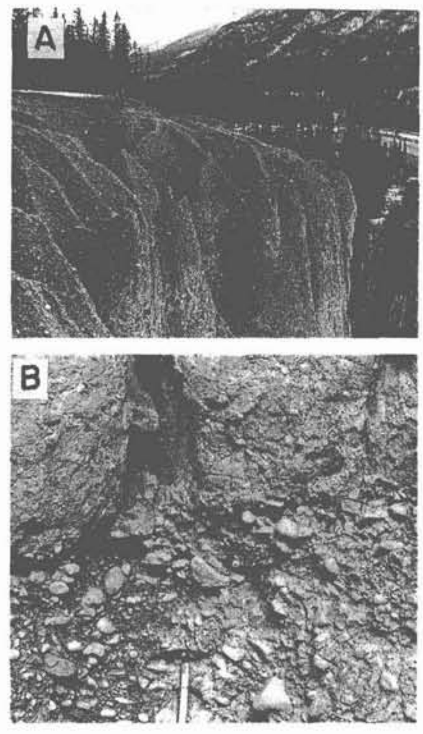

Figure 24 High relief valley infill facies. A) Late Wisconsin crudely bedded debris flow diamictites cropping out along the Bow Valley, Alberta. These deposits are preferentially cemented and eroded into steep-sided pillars (hoodoos). Cliff approximately 14 m high. B) Valley infill stratigraphy near Banff, Alberta, comprising crudely bedded debris flow diamictites overlying glaciofluvial outwash deposits.

(Eyles and Eyles, 1989).

Ice contact glaciolacustrine sedimentation in high-relief settings is comparable to glaciomarine sedimentation in fiords (see below). The presence of structural lineaments in the bedrock allows glaciers to erode their valleys well below sea level. Alpine areas in western Canada and Europe contain elongate overdeepened lakes, commonly termed *fiord-lakes* because of similarity to their marine counterparts. The predominant lacustrine deposits are massive and deformed silts deposited during deglaciation (Hsu and Kelts, 1984). For example, seismic-reflection investigations of the Quaternary fill of Okanagan Lake in British Columbia suggest that up to 800 m of silt accumulated during a single phase of late Wisconsin glaciolacustrine sedimentation (Eyles *et al.*, 1991; Figs. 25, 26). Under such conditions, a varved depositional regime is suppressed by the focusing of large volumes of sediment into the basin. This regime is also suppressed by downslope resedimentation processes that operate year-round in response to depositional oversteepening. The burial of stagnant ice under supraglacial water bodies is also important in promoting mass movement (Postma *et al.*, 1983). Varved silts and clays are deposited only during the very latest *starved* stage of lake infilling, when the glacier has retreated from the basin and meltwater inputs are driven by summer supraglacial melting.

Cold climate modification

Cold climate weathering processes greatly affect continental glacial sediment and ground surfaces beyond the ice margin. The term *periglacial* is used as a broad umbrella term to identify glacial and nonglacial cold climates. However, definitions and environments encompassed by this term vary greatly (Washburn, 1980; Dionne, 1985).

Cold climate environments are characterized by 1) eolian deflation and deposition, 2) downslope mass-wasting processes, 3) mechanical disturbance of nearsurface strata by the growth of ice lenses, and 4) aggradation by braided rivers. Cold climate structures and facies are most commonly associated with major unconformities separating stratigraphic successions. Where mean annual temperatures are less than –4°C the ground is perennially frozen *(permafrost)*. Permafrost reaches a maximum reported depth of 1450 m in Siberia (Williams and Smith, 1989); much of this formed during Quaternary ice ages and is now actively degrading. However, during the summer the surface melts to a depth of only 2 m (the *active layer*).

Permafrozen substrates are characterized by the growth of subsurface ice layers. Near the surface (less than 50 m), ice occurs as *segregated* masses in the form of layers, lenses, dikes, or massive tabular masses many metres thick. Considerable mechanical disturbance of the frozen strata occurs. At depth, ice occurs as a pore filling. Large areas of submarine permafrost occur in the arctic as a result of deep freezing of strata first exposed and then flooded by glacio-eustatic sea level change (see below).

Despite the widespread extent and depth of present-day permafrost, sedimentary structures produced by permafrost have not been widely described from the geological record. This is due to lack of preservation or recognition. Structures most diagnostic of former frozen ground are ice wedge casts formed by severe ground contraction, cracking, and the freezing of melt-waters in contraction cracks (Black, 1976). Host sediments experience mechanical disturbance caused by wedge growth. The resultant ice wedge (Fig. 27A) comprises part of extensive poly-gonal networks. With climatic amelioration, ice wedges melt to leave ice wedge casts filled with debris derived from surface slumping (Fig. 27B; Williams, 1986). The recognition of Quaternary ice wedge casts is not straightforward (see Black, 1976); many Late Proterozoic examples may be sand dikes produced by seismic

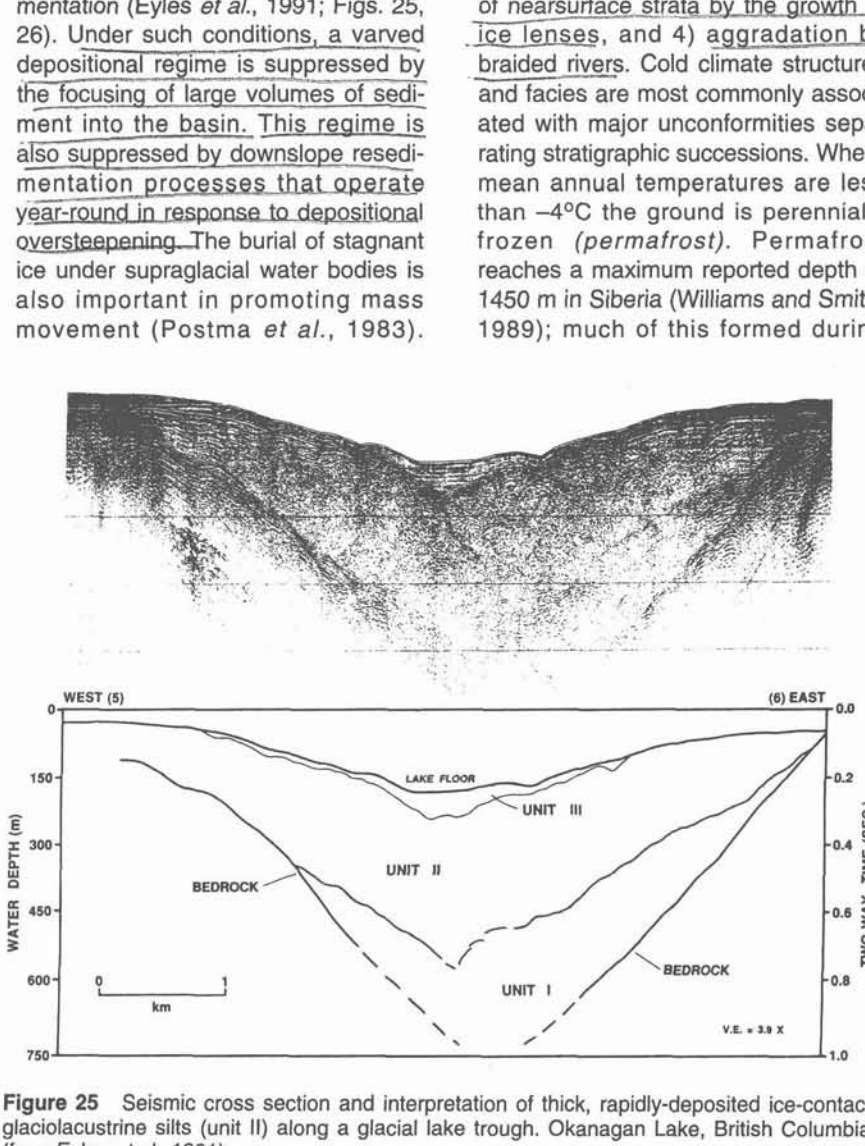

Figure 25 Seismic cross section and interpretation of thick, rapidly-deposited ice-contact glaciolacustrine silts (unit II) along a glacial lake trough. Okanagan Lake, British Columbia (from Eyles *et al.*, 1991).

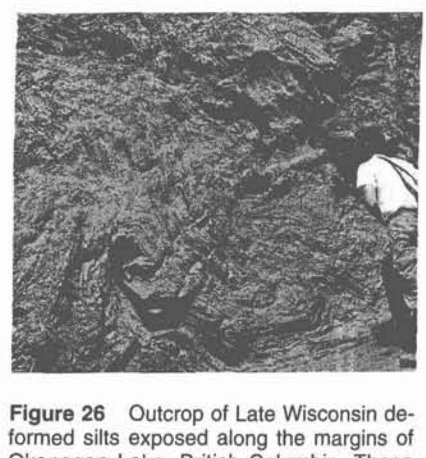

Figure 26 Outcrop of Late Wisconsin deformed silts exposed along the margins of Okanagan Lake, British Columbia. These silts are probably the same as those represented by seismic unit II on Fig. 25.

shock (Fig. 28a; Eyles and Clark, 1985).

Complexly involuted *cryoturbation* structures are alleged to form when late summer refreezing generates high pore water pressures in the surface active layer. Pore water movement in the active layer sets up a series of slow-moving convection cells which texturally sort sediment. This process of soil *churning* produces sorted stone polygons on the ground surface (Fig. 28B). Collapse structures and faulting may accompany the melt of larger ice lenses in the permafrost (thermokarst). Cryoturbation structures used to infer periglacial climates are not unique to cold climates. Similar structures occur as a result of subaqueous loading, liquefaction, and seismic shock. Their common presence in glaciated areas may simply record the widespread occurrence of thawed, saturated sediments.

Windblown silt (*loess*) and sand derived from deflation of large braided stream networks are distinctive periglacial features (Deynoux *et al.*, 1989). Extensive loess blankets and dune fields occur in Quaternary continental interiors, such as the Nebraska Sand Hills where a periglacial sand sea covers over 50,000 km^2 (see Wright *et al.*, 1984). Loess has a thickness of more than 300 m in parts of China. However, there is only one report of a pre-Quaternary loessite (Edwards, 1979).

The predominant periglacial facies in areas of Pleistocene glaciation are coarse-grained fluvial sediments. These record seasonal braided

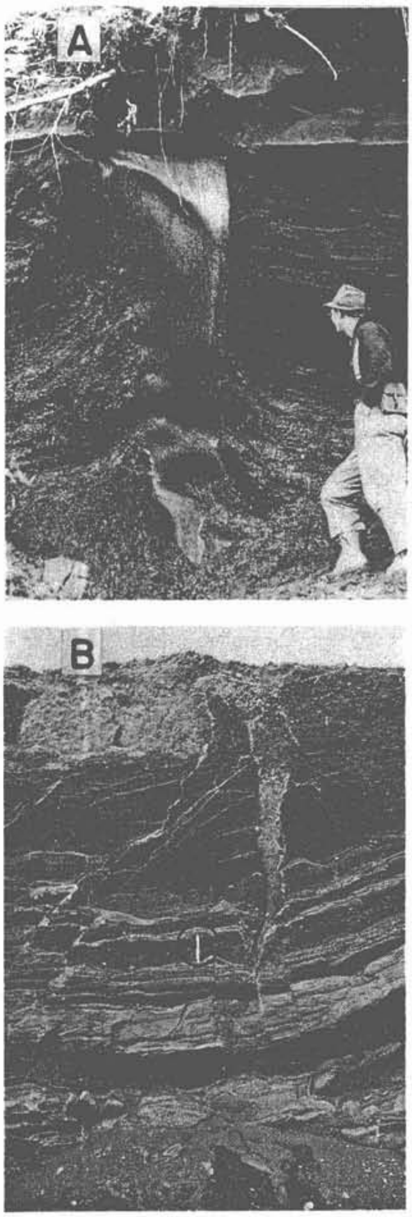

Figure 27 Periglacial ice wedges. A) Modern ice wedge in silts, Alaska. B) Ice wedge cast filled with sand and gravel penetrating Late Wisconsin glaciolacustrine sands and silts; Newfoundland, Canada. Hammer (circled) for scale.

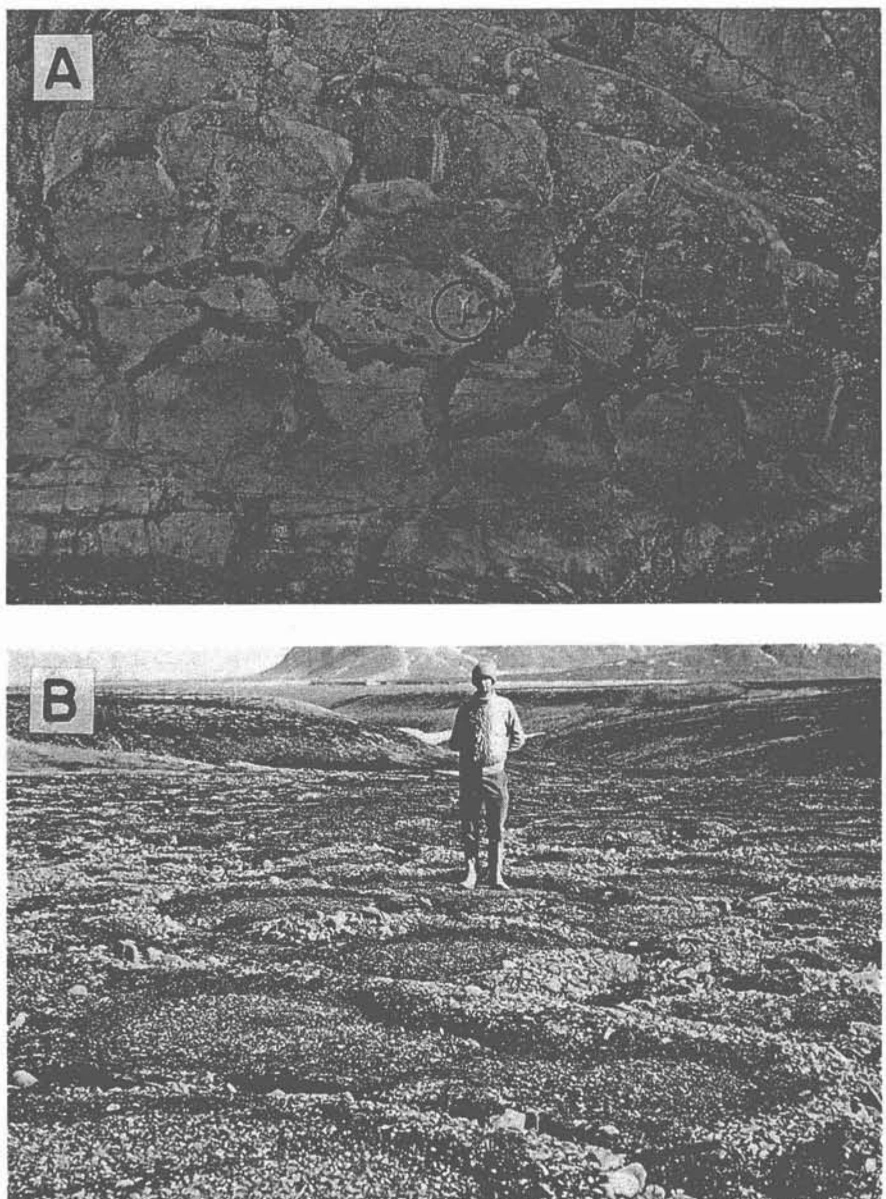

Figure 28 Periglacial structures. A) Bedding plain view of polygonal sandstone dykes interpreted as periglacial in origin; Late Proterozoic Port Askaig Formation, Scotland. These features have also been interpreted as soft sediment deformation structures (Eyles and Clarke, 1985). Hammer (circled) for scale. B) Modern polygonal structures (sorted stone circles) in Spitzbergen, produced by periglacial churning of saturated sediments.

stream activity and indicate stream access to large volumes of coarse, mechanically weathered debris. Stratified diamicts are also important periglacial facies. They result from a wide variety of downslope mass movement processes (*solifluction* or *gelifluction*; French, 1976) when seasonally thawed surface layers become water saturated. These facies commonly infill the lower points of the topography and interfinger with braided river facies.

GLACIOMARINE SYSTEMS TRACT

A simple division of marine glacial depositional systems distinguishes continental shelf settings from continental slopes and fiords. Proximity to an ice margin determines whether the environment is dominated by glacial processes *(ice proximal)* or marine processes (*ice distal*; Fig. 29). Regional climate is another important control because it dictates the volume of meltwater reaching the marine environment. Temperate oceanic environments, for example, receive large volumes of meltwater and mud which are supplied directly to the shelf (Fig. 3). These sediment-nourished environments can be contrasted with sediment-starved settings that are typical of deeply frozen polar areas. Meltwater inputs are severely restricted and chemical and biogenic deposition become relatively important, as in Antarctica (Fig. 30; Domack, 1988). Clearly, the thicker glaciomarine deposits of temperate oceanic areas are more likely to be preserved in the rock record (Anderson and Ashley, 1991).

LOW-RELIEF GLACIOMARINE SETTINGS

Continental shelf: ice proximal

Given sufficient ice volume, ice margins extend onto continental shelves where they construct large submarine moraine complexes *(morainal banks)*. Figure 31 summarizes the morainal bank environment as identified from modern and Quaternary tidewater settings (Powell and Elverhoi, 1989; Dowdeswell and Scourse, 1990; Anderson and Ashley, 1991). There is little information from pre-Quaternary settings. Morainal banks are characterized by the presence of strong meltwater flows from the ice margin, structural complexity caused by bulldozing (due to ice margin advances) and iceberg scouring, and the release of large volumes of mud from meltwaters. Meltwaters are released as *efflux jets* (Fig. 31) that deposit proximal gravels and sands by strong underflows moving across subaqueous fan systems. As the jet moves seaward, lower density meltwaters containing fine-grained suspended sediment rise to the surface, or to intermediate depths in the water column. These *suspended sediment plumes* can extend many tens of kilometres from the ice front, and result in distal mud belts (Syvitski *et al.*, 1987). Tidal current interaction with the rain-out of fine-grained suspended sediment results in laminated muds that may be difficult to distinguish from varves in glaciolacustrine settings.

Massive and/or variably graded diamict facies are deposited by sediment gravity flows originating from the collapse of structurally or depositionally oversteepened slopes. Sediment is reworked and mixed during downslope movement. Poorly sorted basal debris issuing from the ice front may be spilled downslope as debris flows. This occurs where grounded ice begins to float (at the *grounding line*) and subglacial slurries are dumped to form grounding-line fans (the till deltas of Alley *et al.*, 1987).

The combination of ice-rafting, deposition of fines from efflux jets and associated plumes, and size sorting by currents either on the seafloor or in the water column, gives rise to a wide range of *rain-out* diamict facies produced in situ on the seafloor (Fig. 31). The finer-grained facies include laminated and massive muds with variable clast contents. Coarser, commonly stratified diamict facies accumulate in areas of episodic traction currents (Fig. 32B). They contain ice-rafted dropstones, abundant traction-current structures, and rounded clasts rolled along as bed load. The sandy facies occur as part of a lithofacies continuum with pebbly sands and poorly sorted gravels. Where present, microfauna and macrofauna provide evi-

PROXIMAL: (ice margin to several km) **VS.** **DISTAL: (several km to '000 km)**

"DIRECT GLACIAL SEDIMENTATION INTO THE MARINE ENVIRONMENT"

- **glacial processes dominate**
- **rapid deposition and resedimentation of meltwater deposits and ice 'dumped' material on morainal banks and ice-contact subaqueous fans; ice-push features**
- **complex facies associations and geometries**

"GLACIALLY INFLUENCED CONTINENTAL MARGIN SEDIMENTATION"

- **marine processes dominate**
- **glacial influences limited to ice-rafting, 'berg scouring', release of suspended sediment, sea-level change and sediment starvation**

CONTINENTAL SHELF **CONTINENTAL SLOPE** **ABYSSAL PLAIN**

Figure 29 Differentiation in glaciomarine environments.

dence of marine influence in ancient successions. However, brackish water may inhibit biological activity in ice-proximal glaciomarine settings.

Morainal banks consist of subaqueously deposited ice-contact facies which are characterized by heterogeneous facies types, rapid lateral and vertical facies variability and irregular bed geometries (Fig. 31). These landforms commonly record the outer limit of grounded ice on continental shelves, and are the marine equivalents of the moraine systems deposited onshore (Fig. 3). Eyles and McCabe (1989) showed that morainal banks on a Late Pleistocene glaciated shelf (Irish Sea Basin) are systematically related to drumlin swarms onshore. Drumlins record deforming bed conditions (Fig. 15) and the offshore morainal banks were constructed when large volumes of basal debris were flushed to the ice sheet margin to be deposited subaqueously.

Glacier retreat from morainal banks results in fining-upward facies successions, with the upper parts of the successions dominated by laminated and massive muds and fine-grained 'rainout' diamicts. Later, isostatic emergence and rapid sediment accumulation may bring these retreat successions up above wave base, resulting in erosion and deposition of a cap of gravelly nearshore facies.

Continental shelf: ice distal

Ice distal environments are influenced

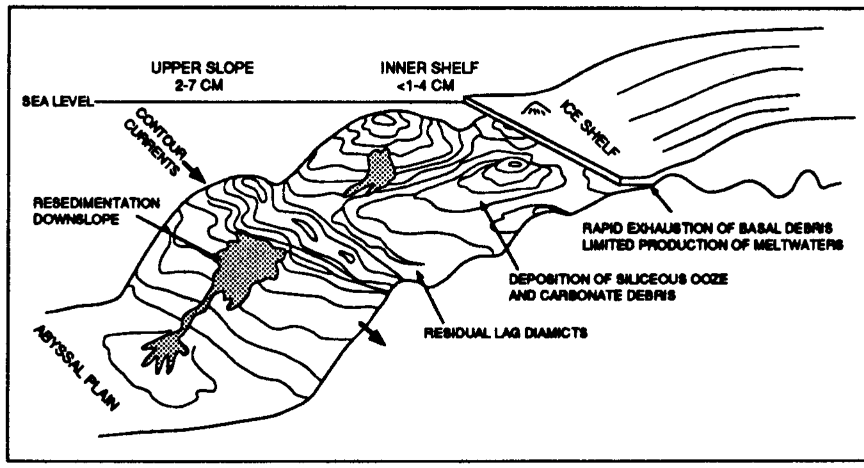

Figure 30 Glaciomarine deposition along high relief Antarctic continental margin. Subglacial deposits accumulate when ice extends across shelf. Postglacial reworking and resedimentation of these deposits is coeval with deposition of siliceous and organic oozes under conditions of clastic starvation (see Domack, 1988). Numbers refer to sedimentation rates (cm/1000 yr).

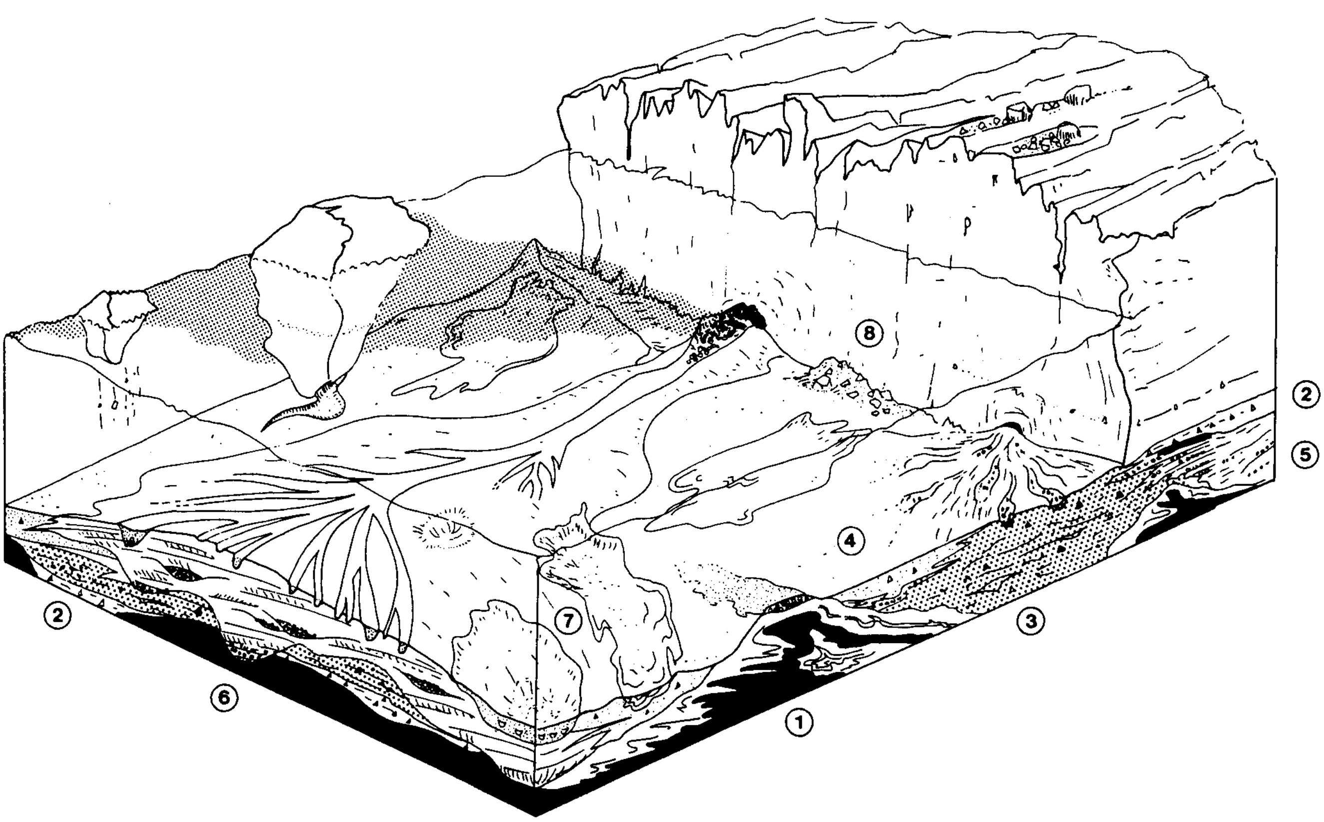

Figure 31 Proximal subaqueous sedimentation. 1) glaciotectonized marine sediments; 2) lenticular lodgment or deformation till units (see Figs. 10 and 14); 3) coarse-grained stratified diamictc (Fig. 32 B); 4) pelagic muds, sandy diamicts; 5) coarse-grained proximal outwash; 6) interchannel cross stratified sands with channel gravels; 7) resedimented facies (debris flow, slides and turbidites); and 8) supraglacial debris. Deformation results from ice advances, melt of buried ice and iceberg turbation. Suspended sediment plumes shown by shading. Same model may apply, with modifications, to sedimentation adjacent to grounding lines below large ice shelves.

by 1) deposition of fine-grained suspended sediment from plumes; 2) downslope resedimentation of sediments; 3) water depth changes resulting from both variation in the volume of continental ice (glacio-eustatic sea level changes) and crustal response to ice-sheet loading (glacio-isostatic sea level change); 4) scour by icebergs, storms and currents; and 5) bioturbation. The dominant sedimentary process on many temperate glacially influenced continental shelves is the production of extensive, blanket-like *rain-out diamict* facies by the settling of mud from suspended sediment plumes and coarser debris from icebergs (Figs. 32a, C). Rain-out diamicts can reach thicknesses of many tens of metres and may be massive or crudely stratified, depending on the textural characteristics of the incoming sediment plumes. The diamicts commonly contain abundant microfauna (foraminifera) and macrofauna. Rates of deposition can be as high as 1 m per thousand years. Most ice-rafted debris is carried into the marine environment by icebergs released from tidewater ice margins. Sediment laden bergs can travel many hundred kilometres from their source areas. Modern rain-out diamict facies are largely absent from the Antarctic continental shelf, because insignificant volumes of meltwater and fine-grained sediment are released to the marine environment by the cold-based Antarctic ice sheet. The ice sheet is grounded below sea level, and is fringed by extensive floating ice margins *(ice shelves)*, which make up about 80 per cent of the Antarctic coastline. Icebergs released from the front of ice shelves contain no debris. Any englacial debris is melted out close to the point where the ice shelf begins to float, and is not transported to the ice shelf edge. Consequently, sedimentation rates are less than 1 cm per thousand years (Domack, 1988; Fig. 30).

Resedimentation processes operate readily on glacially influenced continental shelves as a result of high porewater pressures generated in rapidly deposited fine-grained sediment. Seismic shock and grounding icebergs can also cause resedimentation. Resedimented diamicts may be either massive or crudely stratified, and contain folded interbeds of sand and/or mud. They are commonly associated with turbidites. In many cases it may be difficult to differentiate massive rain-out diamicts from those formed by resedimentation processes unless a displaced fauna can be identified.

Sea level changes on glacially influenced continental shelves may be recorded by disconformities and/or

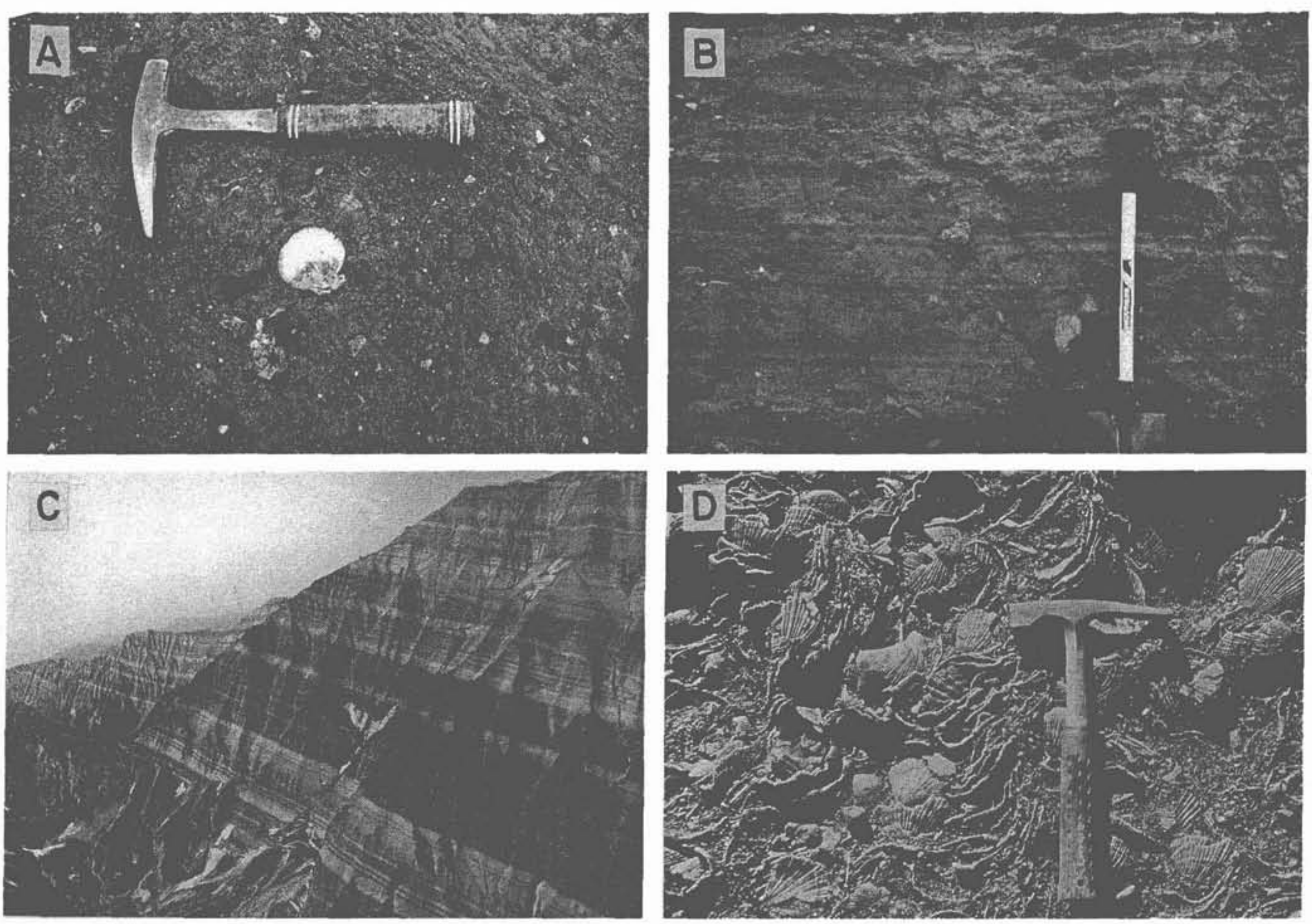

Figure 32 Glaciomarine facies in low relief settings. A) Massive rain-out diamictite containing abundant micro and macrofauna; Late Cenozoic Yakataga Fm., Alaska (see Lagoe *et al.*, 1989). B) Stratified, sandy diamictite recording interplay of rain-out and traction-currents in ice-proximal environment. Late Wisconsin deposits of the Isle of Man, U.K. C) Interbedded diamictites (dark coloured) and shelf-sandstones (light coloured) in 1000 m thick outcrop of the Yakataga Fm., Alaska. Note planar tabular geometry of units. D) Coquina bed consisting of pecten shells in a coarse sand matrix. Yakataga Fm., Middleton Island, Alaska.

erosion surfaces, and by the deposition of extensive mud blankets (Fig. 33). Boulder lag horizons result from winnowing of diamicts on the seafloor under high-energy regimes (lowered sea levels). These lags may be subsequently striated by grounding glacier ice to form marine *boulder pavements* (Fig. 33; Eyles, 1987). Starvation of clastic sediment under high-energy conditions may also allow the formation of biogenic deposits such as *coquinas* (Figs. 32D, 33). Flooding of the shelf is recorded by extensive horizons of bioturbated muds. These horizons may represent relatively deep water interglacial conditions (Fig. 33). However, paleoclimatic interpretation of disconformities, erosion surfaces and mud blankets in shelf successions is extremely difficult, because of the complex interactions between glacioeustatic and glacio-isostatic sea level changes, discussed below.

Linear or curved furrows, produced by the scouring of iceberg and seasonal ice keels, are abundant on modern high-latitude shelves (and some lakes) but uncertainty still surrounds their identification in the ancient record (Woodworth-Lynas and Guigné, 1990). Berg scours can be as wide as 50 m and as deep as 2 m, and may extend for several tens of kilometres. Scours are easily destroyed by wave processes in shallow water or by downslope resedimentation, and are not likely to be preserved in the geological re-cord. Seafloor sediments subject to repeated ice scouring (*iceberg turbates*) are not well understood and may resemble diamicts produced subglacially. It is likely that iceberg turbates have been described in the literature as tills or tillites.

Burrowing is common in glacially influenced distal marine environments but the tracemakers themselves are seldom preserved. Ichnofacies distributions differ in several ways from the classic shoreline-nearshore-shelf-slope model for nonglacial continental margins (Chapter 4). Rapid deposition rates and poorly consolidated muddy sediments exclude suspension feeders. This limits the development of the *Skolithos* ichnofacies characteristic of clean, shifting sand substrates in nonglacial settings. The *Cruziana* ichnofacies assemblage predominates on muddy glaciated shelves (Eyles *et al.*, in press,b). Evidence for rapid sedimentation is provided by common escape structures (fugichnia) and the mass mortality of bivalves. Firm ground burrows typical of the *Glossifungites* ichnofacies are restricted to sediment surfaces undergoing erosion in shallow water. These surfaces may be veneered by coquinas or boulder lags, described above. Changes in salinity and the development of brackish water conditions resulting from meltwater inputs, may be recorded by dwarf feeding traces. Elsewhere, the role of turbidity currents and debris flows is to promote downslope transport of food. This explains the development of a diverse *Cruziana* ichnofacies in slope areas where, under nonglacial conditions, the *Nereites* ichnofacies characterized by grazing traces is found.

The 5 km-thick Late Cenozoic Yakataga Formation of Alaska provides an excellent example of an ancient glacially influenced shelf deposit. It contains stratiform successions of fossiliferous rainout and resedimented diamicts interbedded with marine muds, coquinas, boulder pavements, and storm-deposited sandstones (Figs. 32, 33). Another example of a preserved shelf succession is the Late Precambrian Port Askaig Formation. Its shelf origin is suggested by the presence of tidally influenced sandstones interbedded with diamictites (Eyles, 1988).

HIGH-RELIEF GLACIOMARINE SETTINGS

Fiords

Fiords are high-latitude, glacially overdeepened coastal valleys with floors cut several hundred meters below sea level. Many are still occupied by active tidewater ice margins and associated ice-contact depositional systems (Fig. 3). Others receive meltwaters from inland ice margins, and the transported sediment is deposited as fiord-head fan deltas. Comprehensive reviews of fiord oceanography and sedimentation (both in the presence and absence of ice margins) have been presented by Syvitski *et al.* (1987). When ice advances downfiord, any pre-existing glacial or nonglacial sediments are largely removed. Glacial sedimentation is restricted to the end of the glacial cycle when ice retreats upfiord. Slow retreat occurs in relatively shallow water and is marked by deposition of morainal banks. By contrast, in deep water, fiord glaciers undergo rapid calving and retreat.

Muds and pebbly muds are an important facies type in fiords. Variation in meltwater discharge, tidal flows and

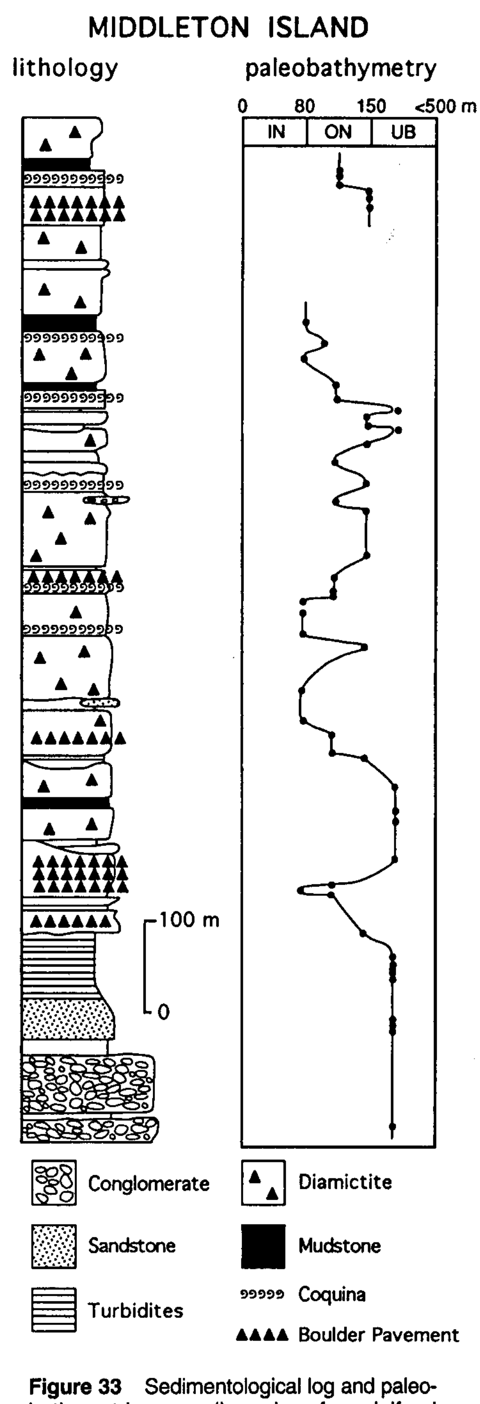

Figure 33 Sedimentological log and paleobathymetric curve (based on foraminiferal data), for the Yakataga Fm. exposed on Middleton Island, Alaska. Note relatively deep water conditions during deposition of the bioturbated mudstones near the top of the log and relatively shallow conditions during formation of coquinas and boulder pavements.

waves produce finely laminated couplets of coarser and finer sediment derived from suspended sediment plumes. Fiord-head sediment accumulations are very prone to downslope resedimentation. Slumping and sediment gravity flows down active channels are ubiquitous and generate turbidity currents. Similar sedimentation patterns occur on glacially influenced continental slopes (see above).

Continental slope and abyssal plain

Glacially influenced slopes are major repositories of glacial sediment and are preferentially preserved in the ancient record. Most Late Proterozoic "tillite" successions probably consist of deep marine debris flows intimately associated with turbidites, recording the downslope reworking of glacial sediment by mass flow into a deep water base-of-slope setting. Late Cenozoic slope deposits in the Gulf of Alaska and eastern Canada (Laurentian Fan, Piper *et al.*, 1985; Chapter 13) formed under very different tectonic regimes but reveal similar slope morphologies and depositional processes. The Surveyor Fan lies adjacent to the heavily glaciated coast of southern Alaska and records marine glacial sedimentation since the Late Miocene; the fan contains about 175,000 km^3 of glacially derived sediment. Slopes show channel systems separated by smooth interchannel slope

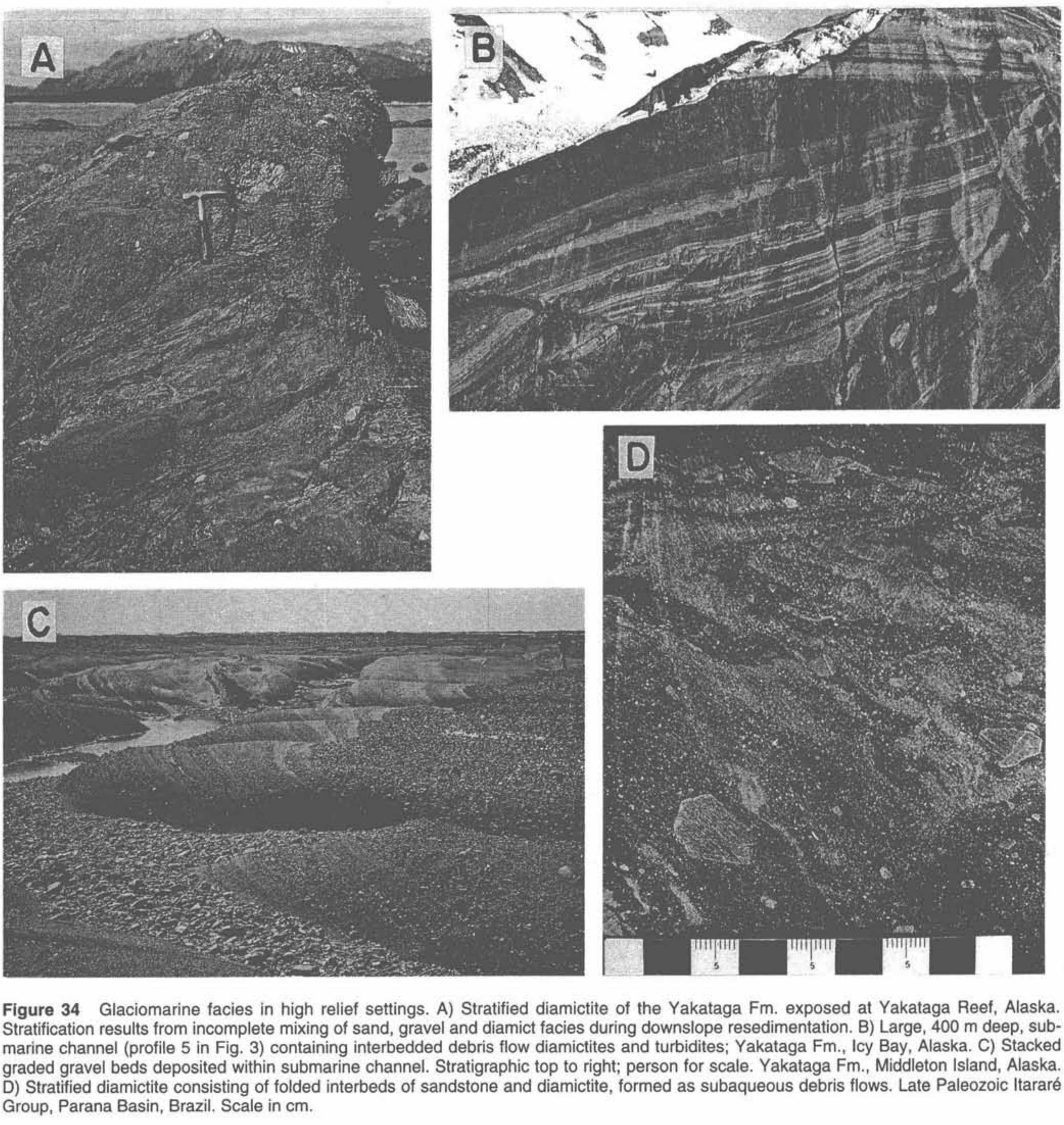

Figure 34 Glaciomarine facies in high relief settings. A) Stratified diamictite of the Yakataga Fm. exposed at Yakataga Reef, Alaska. Stratification results from incomplete mixing of sand, gravel and diamict facies during downslope resedimentation. B) Large, 400 m deep, submarine channel (profile 5 in Fig. 3) containing interbedded debris flow diamictites and turbidites; Yakataga Fm., Icy Bay, Alaska. C) Stacked graded gravel beds deposited within submarine channel. Stratigraphic top to right; person for scale. Yakataga Fm., Middleton Island, Alaska. D) Stratified diamictite consisting of folded interbeds of sandstone and diamictite, formed as subaqueous debris flows. Late Paleozoic Itararé Group, Parana Basin, Brazil. Scale in cm.

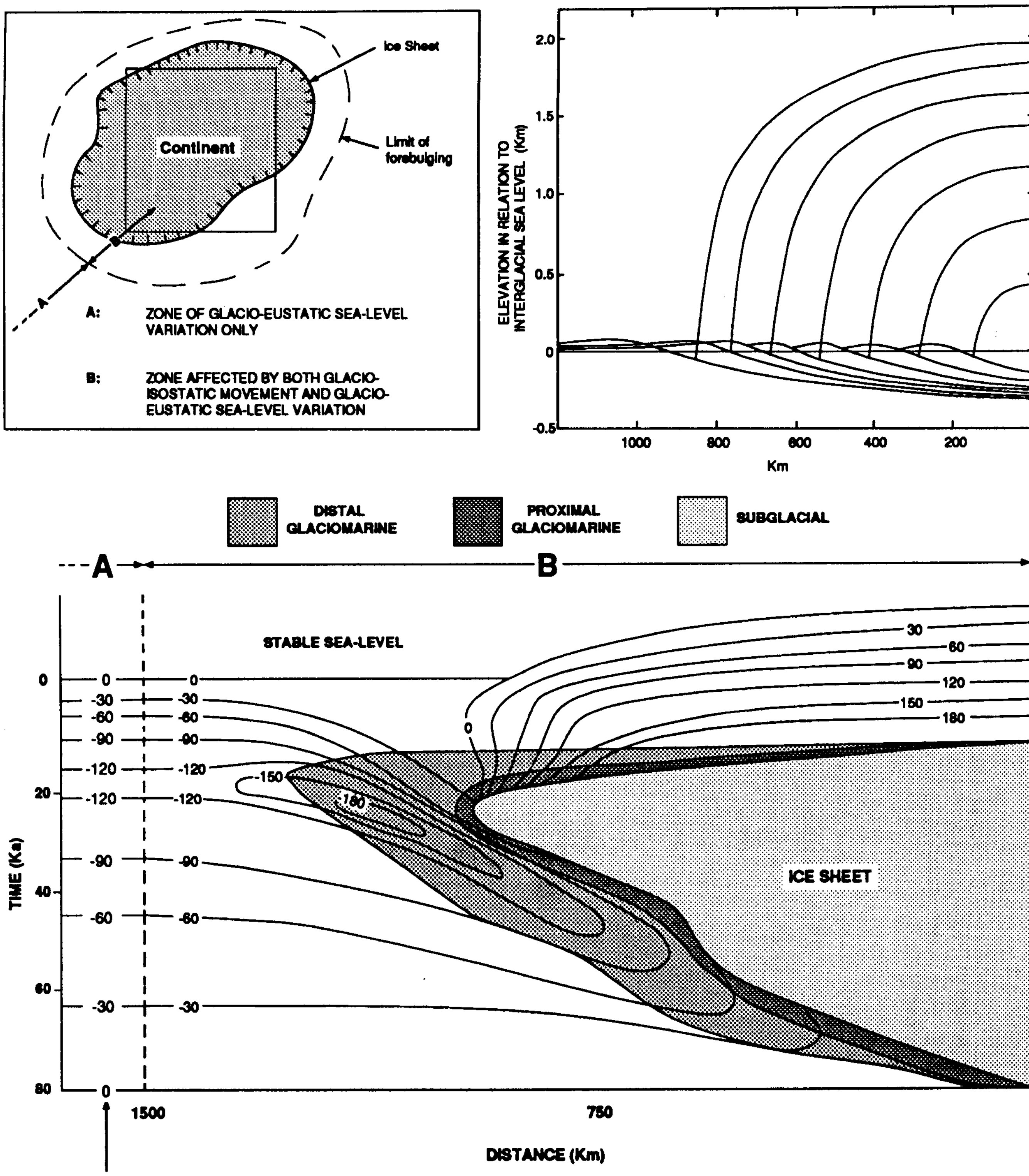

Figure 35 Schematic model to show relationship between glacio-eustatic and glacio-isostatic sea level change around a glaciated continental margin. Top left; hypothetical glaciated continent showing spatial extent of glacio-isostatic crustal depression (Zone B) and limit of forebulging (dashed lines). Zone outside of forebulge (A) experiences glacio-eustatic sea-level change only. Pattern of sea level variation in Zone B results from interaction of glacio-eustasy and glacio-isostasy. Top right; progressive crustal deformation accompanying growth of ice sheet. Ice sheet grows from right to left on diagram. Note development of peripheral zone of relatively deep water between ice margin and forebulged crust. Bottom; spatial and temporal (0-80 ka) variation in relative sea level and associated sedimentary environments at the margin of a continental ice sheet. Zones A and B are defined in diagram top right. Adapted from Boulton (1990). Note that ice retreat is in direction of increasing glacio-isostatic downwarping; ice margin may float and calve back to coastal margin catastrophically. Also note relative slow fall of glacio-eustatic sea level in Zone A compared to rise (see Chapter 2).

areas. Sediment gravity flows and other mass movements are the dominant processes in both Alaska and eastern Canada. Active channels typically tend to fill with graded gravels (Fig. 34C). Abandoned channels are plugged by muds and rain-out diamict facies (see base of log shown in Fig. 33; Eyles, 1987), recording the release of coarse glacial outwash from glaciers that have advanced to the shelf break (Fig. 3). Interchannel areas receive large volumes of suspended sediment, together with debris bulldozed over the shelf break by the ice sheet. Interpretation of seismic profiles suggests the presence of massive debris flow facies (reworked muds with scattered clasts; Figs. 34A, B, D) that are broadly channelled in cross section and which thin downslope and interfinger with laminated muddy turbidites. The term till tongue is unfortunately still used to describe such debris flow units. Large-scale slumping of the upper and mid slope areas generates large rafts of slumped sediment, and creates an irregular slope relief subsequently infilled and smoothed by sediment ponding.

The formation of ice sheets results in global lowstands of sea level, with shorelines close to the shelf-slope break. The sediment delivered directly to the shelf-slope break is largely resedimented downslope as turbidity currents. Consequently, base of slope and basin plain settings during periods of global lowstand are dominated by thick, sandy turbidites, as discussed in Chapter 13.

FACIES SUCCESSIONS AND BOUNDING DISCONTINUITIES IN GLACIATED BASINS

The concepts of *sequence stratigraphy* allow the subdivision of the sedimentary record into depositional sequences bounded by unconformities (Chapters 1, 2). The unconformities are thought to have formed as a result of globally synchronous *(eustatic)* sea level changes and have been used to construct worldwide stratigraphic correlations. However, the recognition of eustatic sea level changes in glaciated basins is very difficult, given the number of other processes which create relative changes in sea level. The development of large continental ice sheets produces global changes in sea level (glacio-eustacy) because large volumes of water are locked up as ice (Chapter 2). In addition to glacio-eustatic changes, *glacio-isostatic* sea level changes are caused by ice loading and unloading of the Earth's crust. This results in elevation or depression of the seafloor and thus creates *relative* changes in sea level and water depths *local* to the glaciated basin. Variation in the magnitude of crustal loading across a glaciated basin can cause one part of the basin to experience a *fall* in relative sea level at the same time as water depths are *increasing* elsewhere in the basin. The combination of these effects in glaciated basins makes assessment of the stratigraphic significance of individual unconformity surfaces extremely difficult.

A simple model for the deposition of sequences on glaciated shelves is based on the movement of ice out onto the shelf at times of glacio-eustatically lowered sea level. This erosional event creates a sequence boundary. Ice-contact depositional systems (Fig. 3) deposited against the advancing ice margin will not survive glacial advance but will be reworked subglacially as deformation till and/or be recycled to the ice front as a morainal bank. The shelf break and deep water will ultimately stop the advance of the ice margin. Much of the sediment pushed across the continental shelf by advancing ice will be discharged down the slope.

The position of ice margins that have moved onto continental shelves is controlled not so much by climate but by crustal downwarping below and around the ice sheet (Fig. 35). Downward flexing of the crust, and displacement of mantle material beneath and immediately adjacent to the ice sheet, is reflected in the formation of a peripheral forebulge (Fig. 35, top right and left). The crust can be depressed by as much as 600 m below the ice sheet and for some distance beyond the ice margin. Such crustal depression far exceeds the magnitude of glacio-eustatic sea level drop (approximately 150 m; see Chapter 2) and so creates the situation where *high* relative sea levels occur around the ice margin at times of global glacio-eustatic sea level *low* stand. The forebulge migrates away from a growing ice sheet to a distance of several hundred kilometres from the ice margin, and collapses as the ice sheet retreats. This gives rise to a very complex succession of sea level changes (resulting from both glacio-eustatic and glacio-isostatic adjustments) throughout the glacial cycle and across glaciated continental shelves.

In the simple model of an ice sheet margin that has moved out to the continental shelf edge, the increase in water depths caused by glacio-isostatic downwarping (i.e. a deepening of *relative* sea level) may be sufficient to initiate deglaciation by extensive calving along the ice margin. This situation produces high ice flow rates (Hughes, 1987) which cause large volumes of subglacial debris and meltwater to be flushed to the ice margin (Eyles *et al.*, 1991). Poorly integrated networks of tunnel valleys composed of steep-sided, flat-floored channels, and cut by meltwater or fluidized sediment, may result from this process. These valleys are a common feature of unconformity surfaces on glaciated shelves (Boulton and Hindmarsh, 1987).

Most glaciomarine sedimentation occurs during glacier retreat when large volumes of meltwater are available. Thick *fining-upward* successions, consisting of relatively coarse-grained ice-contact deposits overlain by finely laminated proglacial silts, result from glacier retreat. At the end of the glacial cycle when ice has retreated from the marine environment, crustal rebound results in rapid shallowing of the coastal margin (Fig. 35, bottom). Deeper water muds will be uplifted and eroded, thereby creating sequence bounding unconformities in shallower parts of the basin. Initial rates of rebound are extremely rapid and may approach several metres per year. Thereafter, rates decrease exponentially and about 10,000 years after the end of the glacial cycle, isostatic rebound is essentially complete (Fig. 35, bottom). The coastal margin may subsequently be flooded by continuing postglacial eustatic sea level rise (Fig. 35, bottom). In offshore areas that escaped rebound into shallow water, postglacial flooding of the shelf results in mud deposition. Thus, erosion in one part of the basin can be coeval with flooding and deposition elsewhere. Boulton (1990) presents a very useful summary of complex sea level variations across glaciated basins and describes the resulting architecture of glaciomarine sedimentary sequences and their bounding unconformities. Even where detailed biofacies and paleobathymetric data are available in relatively young Late Cenozoic successions, the effects of glacio-eustacy and glacio-isostasy cannot be readily discriminated (e.g., Fig. 33).

Recognition of glacio-eustatic cycles in the rock record

Analysis of Quaternary deep ocean sediments shows that glaciations are strongly cyclic in nature, alternating with interglacial conditions in a steady rhythm driven by Milankovitch astronomical variables (Chapter 2). At first sight, repeated glacio-eustatic sea level cycles provide an obvious mechanism for the formation of stratigraphic sequences in pre-Quaternary glacial deposits. However, complex changes in water depths and relative sea level *within* glaciated basins are generated by crustal loading by the ice sheet and other processes. These tend to mask any change in water depth caused by glacio-eustacy, as has been clearly demonstrated for many Quaternary basins (see above).

Tectonics have been the overriding control on the deposition of stratigraphic successions in most pre-Quaternary glaciated basins, negating any simple identification of glacio-eustatic sea level changes. For example, many Late Proterozoic glacial successions comprise lowermost deep water mass-flow diamictites overlain by a thick, shoaling-upward turbidite succession. These successions, up to 1 km thick, are defined by bounding unconformities and have been attributed to glacio-eustacy (Eisbacher, 1985). A more likely explanation is that they record deposition in rapidly subsiding rift basins. Other Late Proterozoic shelf successions also show repeated diamictite and sandstone strata (e.g., Eyles, 1988) that could be interpreted as a record of glacially controlled cycles of sea level change.

However, short-term glacio-eustatic oscillation of one hundred metres or less cannot, by itself, account for the preservation of unconformity-bounded stratigraphic sequences. Without tectonic subsidence or a sufficient supply of sediment, repeated glacio-eustatically driven oscillations of sea level produce erosion surfaces. This is clearly demonstrated on tectonically stable continental shelves that were subject to repeated glaciation during the Quaternary. These shelves commonly show

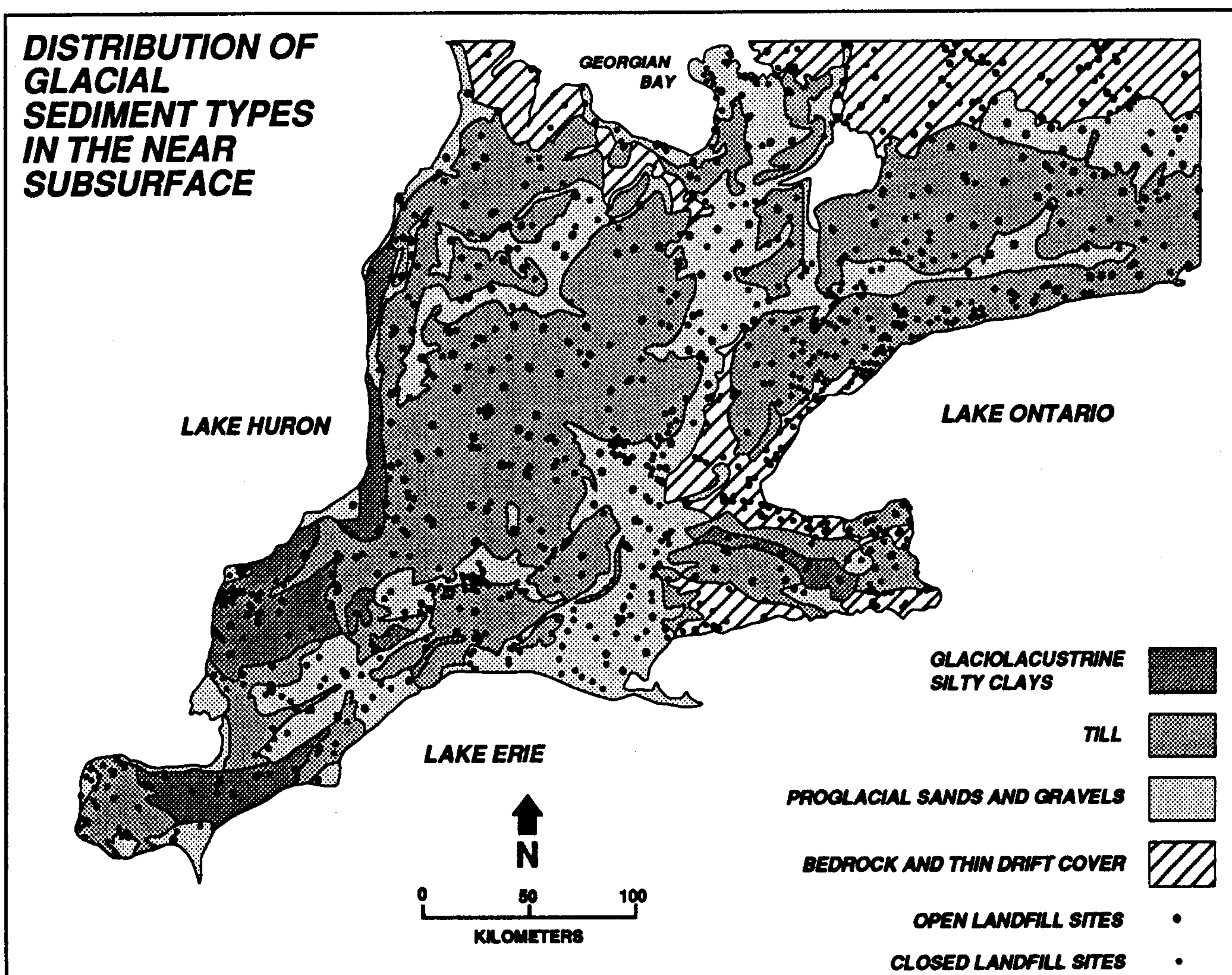

Distribution of landfill sites and glacial geology of southern Ontario thin (less than 100 m) glacial deposits of the last glacial cycle (younger than 125,000 years) resting on a regional erosion surface cut across Mesozoic and older strata. Without subsidence, no older glacial record has been preserved. In contrast, along the central graben of the North Sea Basin, where subsidence is active, over 1 km of Quaternary sediments are preserved.

Glacio-eustatic sea level changes are most likely to be recorded in slowly subsiding, nonglaciated basins far removed from glaciated areas. In North America, glacio-eustatic changes during the Late Paleozoic glaciation of Gondwanaland (about 250-350 m.y. ago) are recorded by well-developed coal-bearing depositional successions (cyclothems; Veevers and Powell, 1987). The recognition of possible glacio-eustatic sea level change in the Mesozoic (Chapter 12) is one argument for the existence of ice sheets at this time, even though no direct evidence of glacial sedimentation has been found (Chapter 2).

APPLIED GEOLOGY OF GLACIAL DEPOSITS

Two recent developments in the fields of petroleum geology and environmental geology are having a major effect on the future direction of studies in glacial sedimentology.

Oil, gas, and coal

Until recently, glacial strata have been overlooked by petroleum geologists. However, in the southern Gondwana continents there is now active exploration for hydrocarbon resources in Permo-Carboniferous glacial strata. The largest field discovered so far is in Oman, where the Al Khlata Formation contains about 5.6 x 10^8 m^3 (3.5 billion barrels) of oil (Levell *et al.*, 1988). Reservoirs occur in ice-contact deltaic deposits around the basin edge, and glaciolacustrine silts and clays form stratigraphic seals on top of the reservoirs (Figs. 21, 22). In Bolivia, the Bermejo, Palmer and Santa Cruz fields are important producers. Correlative strata in Argentina host the Duran, Icua and Madrejones fields, and in Brazil the Itararé Group has sig-

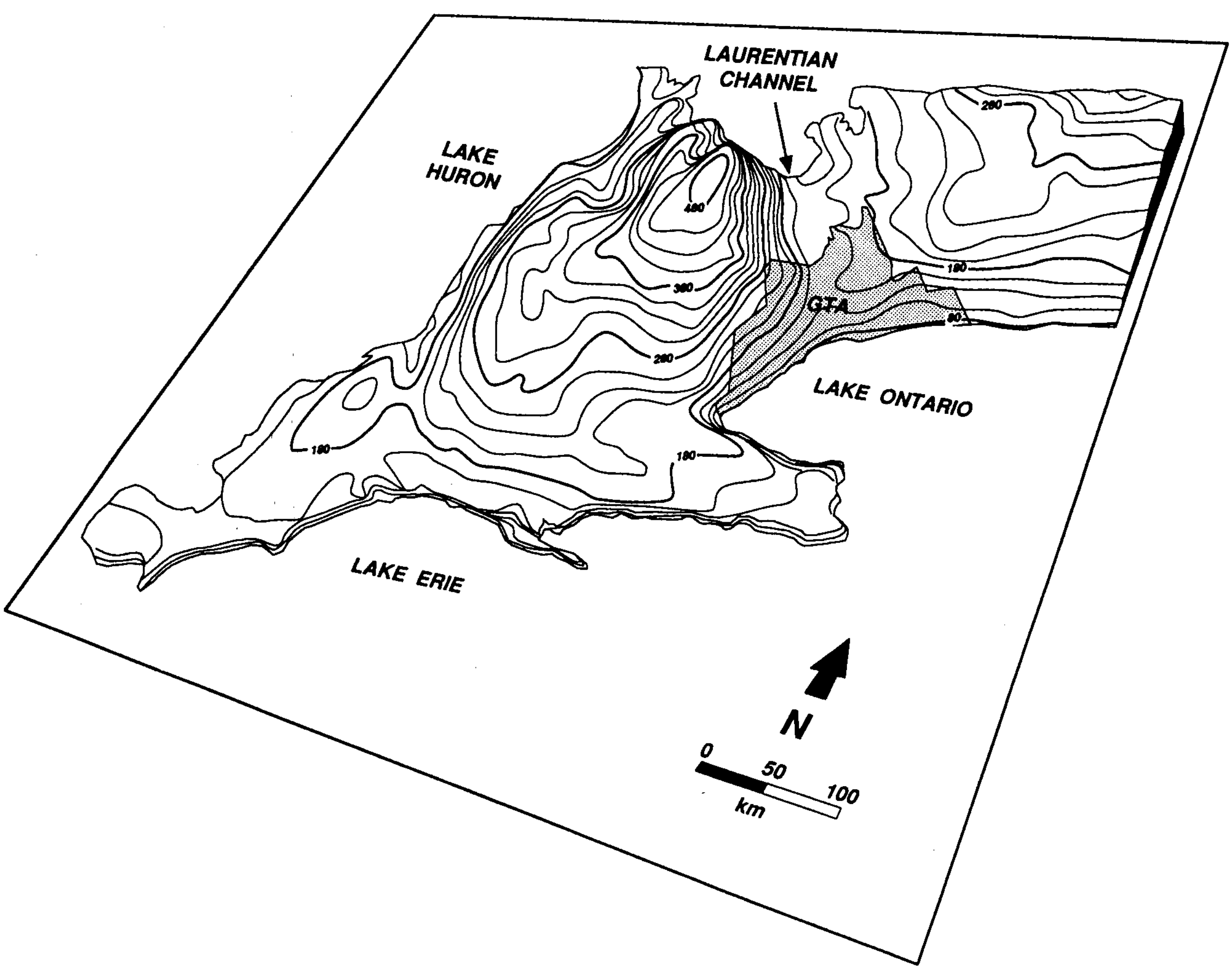

Figure 37 Computer drawn three-dimensional block diagram showing bedrock topography of southern Ontario. Contour intervals are 25 m and represent bedrock elevations above sea level. Note prominent bedrock channel (Laurentian Channel) linking Lake Huron with Lake Ontario. This channel focusses regional groundwater flow towards the south. GTA = Greater Toronto Area. Data compiled from water well records.

nificant but as yet subcommercial gas shows within the Parana Basin (Franca and Potter, 1991). Within these fields, the principal reservoirs occur in thick, sandy turbidites deposited around the basin margin. Rain-out and debris flow diamictites are the stratigraphic seals. In northern Saudi Arabia and Jordan, hydrocarbons occur in Lower Silurian glacial outwash channels. In Australia, cold climate, wind-blown sands are exploration targets in Permo-Carboniferous glacial deposits of the Cooper Basin. As well as oil and gas, coal deposits are a major resource in many Permo-Carboniferous cold climate basins of the Gondwana continents (e.g., Martini and Glooschenko, 1985).

Environmental geology

Recent concerns with environmental geology have led to much new research on Quaternary glacial depositional systems. Urbanization and increasing demand on groundwater resources is a stimulus to detailed subsurface investigations. Southern Ontario, which supports 35 per cent of the Canadian population, provides a good example of an area where industry, agriculture and urban development are having a major impact on groundwater supply and quality. Particular problems include waste management, the proper design of landfills, and the tracing of subsurface contaminant plumes (Rowe and Booker, 1990). Solving these problems requires a detailed understanding of the three-dimensional geometry of glacial facies and their hydrogeology. For example, more than 1200 active and inactive landfill sites occur in southern Ontario (Fig. 36). Most of these are located in abandoned glaciofluvial sand and gravel quarries and are associated with subsurface plumes of chemically contaminated water (leachate). Fine-grained, relatively impermeable glaciolacustrine sediments afford some protection from leachate migration into underlying groundwaters. However, many clay deposits are fractured and afford little protection. Silt- and sand-rich tills dominate the surficial geology of southern Ontario, but despite their massive, dense character, they have significant bulk permeabilities and contain intraformational coarser-grained sediments.

In southern Ontario, the regional ground water flow in Quaternary glacial sediments is controlled by the slope of the underlying bedrock surface. The bedrock surface is characterized by a major south-draining paleochannel (Laurentian Channel; Fig. 37), in which glacial sediments reach thickness of over 100 m. Drilling and downhole geophysical logging (Chapter 3) allow regional correlation of the major glacial stratigraphic units (Figs. 21, 22). The more permeable units *(aquifers)* include the Scarborough Sands, and the impermeable units *(aquitards)* include the glaciolacustrine sediments that overlie these sands. Groundwater flow is generally within the permeable stratigraphic units, but fracturing and changes in the local facies geometry allows flow between separate aquifers (e.g., Howard and Beck, 1986; Eyles and Howard, 1988). Thus an understanding of the original glacial depositional system is fundamental to prediction of local facies geometries, the delineation of aquifers and aquitards, and hence the movement of natural and contaminated groundwater.

Close spacing of boreholes allows local facies geometries and groundwater flow paths to be established at various scales, some as fine as individual landfill sites (about the size of several football fields). Techniques such as drilling, digging test pits, shallow seismic reflection, and the use of ground-penetrating radar are used to establish the detailed site stratigraphy. However, an understanding of glacial depositional models is the key to the prediction of lateral variability in facies characteristics and hydrogeological properties. Water origin and flow in different aquifers can be traced by study of major and minor ions, isotopes, and by radiocarbon dating. These techniques establish the overall *hydrostratigraphy* of the site, and provide a means of modelling groundwater flow through the various glacial facies. Examples of such studies are provided by Desaulniers *et al.* (1981), Rowe and Booker (1990) and Eyles *et al.* (in press, a). Determining fluid flow paths in Quaternary and pre-Quaternary glaciated basins not only provides fundamental information about the geometry of permeable and impermeable facies, but also the detailed disposition of facies in the glacial depositional system. In this way, data from individual case studies are fed back into, and help refine, general models.

GLACIAL FACIES MODELLING

The development of comprehensive glacial facies models is still at an early stage as a result of relatively recent sedimentological interest in glacial deposits. A high priority for future work must be integration of different data sets from Proterozoic and Phanerozoic glaciated basins. Most ancient glacial strata are still poorly known. The models presented in this chapter have considerable value in applied projects, particularly in the prediction of facies geometries and associations in the subsurface. In particular, these models can be used to predict the extent and form of permeable and impermeable facies in the subsurface or the three-dimensional variability of geotechnical properties. This is extremely important in the search for hydrocarbons in glaciated basins and in hydrogeological assessments of Quaternary glacial deposits, where the relationship of reservoirs (aquifers) and seals (aquitards) must be evaluated.

REFERENCES

Basic sources of information

Anderson, J.W. and Ashley, G.M., eds., 1991, Glacial marine sedimentation; paleoclimatic significance: Geological Society of America, Special Paper 261, 232 p.
Contains good descriptions of Quaternary and pre-Quaternary glaciomarine strata deposited in polar and temperate glacial settings. See also Powell and Elverhoi (1989), and Dowdeswell and Scourse (1990).

Boulton, G.S., 1972, Modern arctic glaciers as depositional models for former ice sheets: Journal of the Geological Society of London, v. 127, p. 361-393.
A classic paper on the importance of understanding modern ice marginal sedimentation as a basis for work in ancient basins.

Dowdeswell, J.D. and Scourse, J.D., eds., 1990, Glaciomarine environments: process and sediments: Geological Society of London, Special Publication 53, 423 p.

Drewry, D., 1986, Glacial geologic processes: Baltimore, Edward Arnold, 276 p.
Excellent overall summary of physical sedimentation processes in glacial environments.

Eyles, N., Eyles, C.H. and Miall, A.D., 1983, Lithofacies types and vertical profile analysis; an alternative approach to the description and environmental interpretation of glacial diamict and diamictite sequences: Sedimentology, v. 30, p. 393-410.
Describes widely-used sedimentological approach to field description of glacial facies.

Eyles, C.H., Eyles, N. and Miall, A.D., 1985, Models of glaciomarine sedimentation and their application to the ancient glacial record: Palaeogeography, Palaeoclimatology and Palaeoecology, v. 51, p. 15-84.
A thorough review of glaciomarine environments, facies types and associations in Quaternary and pre-Quaternary settings.

Powell, R.D. and Elverhoi, A., eds., 1989, Modern glaciomarine environments: glacial and marine controls of modern lithofacies and biofacies: Marine Geology, v. 85, p. 101-418.

Ruddiman, W.F. and Wright, H.E., Jr., eds., 1987, North America and adjacent oceans during the last glaciation: Geological Society of America, The Geology of North America, v. K-3, p. 13-37.
Contains excellent papers on glaciology and dynamics of the last North American ice sheet.

Wilgus, C.K., Hastings, B.S., Posamentier, H.W., Ross, C.A. and Kendall, C.G.St.C., eds., 1988, Sea level changes: an integrated approach: Society of Economic Paleontologists and Mineralogists, Special Publication 42, 407 p.
Collection of papers emphasizing conceptual basis of sequence stratigraphy plus numerous case studies of sea level change from the geological record.

Other references

Alley, R.B., Blankenship, D.D., Bentley, C.R., and Rooney, S.T, 1987, Till beneath ice stream B, 3. Till deformation: Evidence and implications: Journal of Geophysical Research, v. 92, p. 8921-8929.

Andrews, J.T., 1987, The Late Wisconsin glaciation and deglaciation of the Laurentide Ice Sheet, *in* Ruddiman, W.F. and Wright, H.E., Jr., eds., North America and adjacent oceans during the last deglaciation: Geological Society of America, The Geology of North America, v. K-3, p. 13-38.

Ashley, G.M., 1975, Rhythmic sedimentation in glacial Lake Hitchcock, Massachusetts-Connecticut, *in* Jopling, A.V. and McDonald, B.C, eds., Glaciofluvial and glaciolacustrine sedimentation: Society of Economic Paleontologists and Mineralogists, Special Publication 23, p. 304-320.

Bell, M. and Laine, E.P., 1985, Erosion of the Laurentide Ice Sheet by glacial and glaciofluvial processes: Quaternary Research, v. 23, p. 154-174.

Black, R.F., 1976, Periglacial features indicative of permafrost; ice and soil wedges: Quaternary Research, v. 6, p. 3-26.

Boulton, G.S., 1987, A theory of drumlin formation by subglacial sediment deformation, *in* Menzies, J. and Rose, J., eds., Drumlin symposium: Rotterdam, Balkema, p. 25-80.

Boulton, G.S., 1990, Sedimentary and sea-level changes during glacial cycles and their control on glaciomarine facies architecture, *in* Dowdeswell, J.A. and Scourse, J.D., eds., Glaciomarine environments: processes and sediments: Geological Society of London, Special Publication 53, p. 15-52.

Boulton, G.S. and Hindmarsh, R.C.A., 1987, Sediment deformation beneath glaciers: rheology and geological consequences: Journal of Geophysical Research, v. 42, p. 9059-9082.

Boyce, J.I. and Eyles, N., 1991, Drumlins carved by deforming till streams below the Laurentide Ice Sheet: Geology, v. 19, p. 787-790.

Crowell, J.C. and Frakes, L.A., 1975, The late Palaeozoic Glaciation, *in* Campbell, K.W.W., ed., Gondwana Geology 3: Australian National University Press, p. 313-331.

Croot, D., ed., 1988, Glaciotectonics: forms and processes: Rotterdam, Balkema, 212 p.

Desaulniers, D.E., Cherry, J.A. and Fritz, P., 1981, Origin, age and movement of porewater in argillaceous Quaternary deposits at four sites in southwestern Ontario: Journal of Hydrogeology, v. 50, p. 231-257.

Deynoux, M., Kocurek, G. and Proust, J.N., 1989, Late Proterozoic periglacial aeolian deposits on the West African Platform, Taoudeni Basin, Western Mali: Sedimentology, v. 36, p. 531-549.

DiLabio, R.N.W. and Coker, W.B., 1989, Drift prospecting: Geological Survey of Canada, Paper 89-20, 30 p.

Dionne, J.C., 1985, Formes, figures et faciés; sedimentaires glaciels des estrans vaseux des regions froides: Palaeogeography, Palaeoclimatology, Palaeoecology, v. 51, p. 415-451.

Domack, E.W., 1988, Biogenic facies in the Antarctic glaciomarine environment: basis for a Polar glaciomarine summary: Palaeogeography, Palaeoclimatology, Palaeoecology, v. 63, p. 357-372.

Edwards, M.B., 1979, Late Precambrian glacial loessites from North Norway and Svalbard: Journal of Sedimentary Petrology, v. 49, p. 85-92.

Eisbacher, G.H., 1985, Late Proterozoic rifting, glacial sedimentation, and sedimentary cycles in the light of Windermere deposition, Western Canada: Palaeogeography, Palaeoclimatology, Palaeoecology, v. 51, p. 231-254.

Eyles, C.H., 1987, Glacially-influenced submarine channel sedimentation in the Yakataga Formation, Middleton Island, Alaska: Journal of Sedimentary Petrology, v. 57, p. 1004-1017.

Eyles, C.H., 1988, Glacially- and tidally-influenced shallow marine sedimentation of the late Precambrian Port Askaig Formation, Scotland: Palaeogeography, Palaeoclimatology, Palaeoecology, v. 68, p. 1-25.

Eyles, C.H. and Eyles, N., 1983, Sedimentation in a large lake; a reinterpretation of the Late Pleistocene stratigraphy at Scarborough Bluffs, Ontario, Canada: Geology, v. 11, p. 146-152.

Eyles, C.H. and Eyles, N., 1989, The Late Cenozoic White River "Tillites" of southern Alaska; subaerial slope and fan delta deposits in a strike-slip setting: Geological Society of America, Bulletin, v. 101, p. 1091-1102.

Eyles, N., 1990, Glacially-derived, shallow marine gold placers of the Cape Yakataga district, Gulf of Alaska: Sedimentary Geology, v. 66, p. 171-185.

Eyles, N. and Clark, B.M., 1985, Gravity induced soft-sediment deformation structures in glaciomarine sequences of the Late Proterozoic Port Askaig Formation, Scotland: Sedimentology, v. 32, p. 784-814.

Eyles, N. and Clark, B.M., 1988, Storm-influenced deltas and ice-scouring in a Late Pleistocene glacial lake: Geological Society of America, Bulletin, v. 100, p. 793-809.

Eyles, N. and Howard, K.W.F., 1988, A hydrochemical study of urban landslides caused by heavy rain; Scarborough Bluffs, Ontario, Canada: Canadian Geotechnical Journal, v. 25, p. 455-466.

Eyles, N. and McCabe, A., 1989, The Late Devensian (<22,000 YBP) Irish Sea Basin: the sedimentary record of a collapsed ice sheet margin: Quaternary Science Reviews, v. 8, p. 307-351.

Eyles, N., Sladen, J. and Gilroy, S., 1982, A depositional model for stratigraphic complexes and facies superimposition in lodgement tills: Boreas, v. 11, p. 317-333.

Eyles, N., Mullins, H. and Hine, A.C., 1991, The seismic stratigraphy of Okanagan Lake, British Columbia; a record of rapid deglaciation in a deep "fiord-lake" basin: Sedimentary Geology, v. 73, p. 13-41.

Eyles, N., Boyce, J. and Hibbert, J., in press, a, Geology of garbage in southern Ontario: Geoscience Canada.

Eyles, N., Vossler, S. and Lagoe, M.B., in press, b, Ichnology of a glacially-influenced continental shelf and slope: the Late Cenozoic Gulf of Alaska (Yakataga Formation): Palaeogeography, Palaeoecology, Palaeoclimatology.

Frakes, L.A. and Francis, J.E., 1988, A guide to Phanerozoic cold polar climates from high latitude ice-rafting in the Cretaceous: Nature, v. 333, p. 547-549.

Franca, A.B. and Potter, P.E., 1991, Stratigraphy and reservoir potential of glacial deposits of the Itarare Group (Carboniferous to Permian), Parana Basin, Brazil: American Association of Petroleum Geologists, Bulletin, v. 75, p. 62-85.

French, H.M., 1976, The periglacial environment: London, Longmans, 309 p.

Hambrey, M.J. and Harland, W.B., eds., 1981, Earth's pre-Pleistocene glacial record: Cambridge, Cambridge University Press, 1004 p.

Howard, K.W.F. and Beck, P., 1986, Hydrochemical interpretation of groundwater flow systems in Quaternary sediments of southern Ontario: Canadian Journal of Earth Sciences, v. 23, p. 938-947.

Hsü, K.J. and Kelts, K.R., eds., 1984, Quaternary geology of Lake Zurich: an interdisciplinary investigation by deep lake drilling: Amsterdam, Elsevier, Contributions to Sedimentology, v. 13, 210 p.

Hughes, T., 1987, Ice dynamics and deglaciation models when ice sheets collapsed, *in* Ruddiman, W.F. and Wright, H.E., eds., North American and adjacent oceans during the last deglaciation: Geological Society of America, The Geology of North America, v. K-3, p. 183-220.

Kasizcki, C.A., 1987, A model for glacial and proglacial sedimentation in the shield terrane of southern Ontario: Canadian Journal of Earth Sciences, v. 24, p. 2373-2391.

Lagoe, M.B., Eyles, C.H. and Eyles, N., 1989, Paleoenvironmental and paleoclimatic significance of foraminiferal biofacies in the glaciomarine Yakataga Formation, Middleton Island, Gulf of Alaska: Journal of Foraminiferal Research, v. 19, p. 194-204.

Lawson, D.E., 1982, Mobilization, movement and deposition of active subaerial sediment flows, Matanuska Glacier, Alaska: Journal of Geology, v. 90, p. 279-300.

Levell, B.K., Braakman, J.H. and Ruttenk, V., 1988, Oil-bearing sediments of Gondwana glaciation in Oman: American Association of Petroleum Geologists, Bulletin, v. 72, p. 775-796.

Martini, I.P. and Glooschenko, W.A., 1985, Cold climate peat formation in Canada, and its relevance to lower Permian coal measures of Australia: Earth Science Reviews, v. 22, p. 107-140.

Martinson, D.G., Pisias, N.G., Hays, J.D., Imbrie, J., Moore, T.C. and Shackleton, N.J., 1987, Age dating and the orbital theory of the ice ages: development of a high-resolution 0 to 3,000,000 year chronostratigraphy: Quaternary Research, v. 27, p. 1-29.

Miall, A.D., 1985, Sedimentation on an early Proterozoic continental margin under glacial influence: the Gowganda For-mation (Huronian) Elliot Lake area, northern Ontario, Canada: Sedimentology, v. 32, p. 763-788.

Nystuen, J.P., 1985, Facies and presentation of glaciogenic sequences from the Varanger ice age in Scandinavia and other parts of the North Atlantic region: Palaeogeography, Palaeoclimatology, Palaeoecology, v. 51, p. 209-229.

Paul, M.A. and Eyles, N., 1990, Constraints on the preservation of diamict facies (melt-out tills) at the margins of stagnant glaciers: Quaternary Science Reviews, v. 9, p. 51-69.

Piper, D.J.W., Stow, D.A.V. and W.R. Normark, 1985, Laurentian Fan, Atlantic Ocean, *in* Bouma, A.H., Normark, W.R. and Barnes, N.E., eds., Submarine fans and related turbidite systems: New York, Springer-Verlag, p. 137-142.

Postma, G., Roep, T.R. and Ruegg, G.H.J., 1983, Sandy gravelly mass flow deposits in an ice marginal lake (Saalian, Leuvenumsche Beek Valley, Veluwe, the Netherlands) with emphasis on plug-flow deposits: Sedimentary Geology, v. 34, p. 59-82.

Rowe, K.R. and Booker, J.R, 1990, Contaminant migration through fractured till into an underlying aquifer: Canadian Geotechnical Journal, v. 27, p. 484-495.

Ryder, J.M., 1971, The stratigraphy and morphology of paraglacial alluvial fans in south-central British Columbia: Canadian Journal of Earth Sciences, v. 8, p. 279-298.

Sauer, E.K., Gareau, L.F. and Christiansen, E.A., 1990, Softening of overconsolidated Cretaceous clays by glacial erosion: Quarterly Journal of Engineering Geology, v. 23, p. 307-324.

Shaw, J., 1977, Sedimentation in an alpine lake during deglaciation: Okanagan Valley, British Columbia, Canada: Geografiska Annaler, v. 59A, p. 221-240.

Shaw, J., 1979, Genesis of the Sveg tills and Rogen moraines of central Sweden; a model of basal melt-out: Boreas, v. 8, p. 409-426.

Shaw, J. and Sharpe, D.R., 1987, Drumlin formation by subglacial meltwater erosion: Canadian Journal of Earth Sciences, v. 24, p. 2316-2322.

Syvitski, J.P.M., Burell, D.C. and Skei, J.M., 1987, Fjords: processes and products: New York, Springer-Verlag, 379 p.

Teller, J.T. and Clayton, L., eds., 1983, Glacier Lake Agassiz: Geological Association of Canada, Special Paper 26, 451 p.

Vaslet, D., 1990, Upper Ordovician glacial deposits in Saudi Arabia: Episodes, v. 13, p. 147-161.

Veevers, J.J. and Powell, C. M., 1987, Late Paleozoic glacial episodes in Gondwanaland reflected in transgressive-regressive depositional sequences in Euramerica: Geological Society of America, Bulletin, v. 98, p. 475-487.

Visser, J.N.J., 1983, Submarine debris flow deposits from the Upper Carboniferous Dwyka Tillite Formation in the Kalahari Basin, South Africa: Sedimentology, v. 30, p. 511-523.

Visser, J.N.J., 1989, The Permo-Carboniferous Dwyka Formation of southern Africa: deposition by a predominantly subpolar marine ice sheet: Palaeogeography, Palaeoclimatology, Palaeoecology, v. 70, p. 377-391.

Washburn, A.L., 1980, Permafrost features as evidence of climatic change: Earth Science Reviews, v. 15, p. 327-402.

Williams, G.E., 1986, Precambrian permafrost horizons as indicators of paleoclimate: Precambrian Research, v. 32, p. 233-242.

Williams, P.J. and Smith, M.W., 1989, The frozen earth: fundamentals of geocryology: Cambridge, Cambridge University Press, 305 p.

Woodworth-Lynas, C.M.T. and Guigné, J.Y., 1990, Iceberg scours in the geological record; examples from glacial Lake Agassiz, *in* Dowdeswell, J.A. and Scourse, J.D., eds., Glaciomarine environments: processes and sediments: Geological Society of London, Special Publication 53, p. 217-234.

Wright, H.E., Jr., Almendinger, J.C. and Grüger, J., 1984, Pollen diagram from the Nebraska Sandhills and the age of the dunes: Quaternary Research, v. 24, p. 115-120.

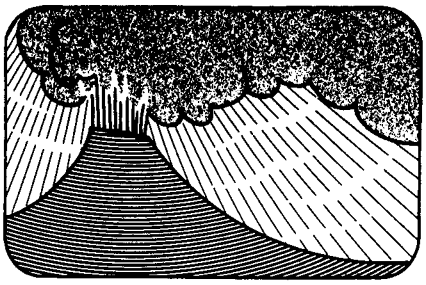

6. Volcaniclastic Rocks

Jean Lajoie and John Stix, Département de géologie,
Université de Montréal, Montréal, Québec H3C 3J7

INTRODUCTION

As in all other facies models, ancient volcaniclastic rocks must be interpreted by comparison with recent accumulations. In this chapter we will present the major characteristics of volcaniclastic deposits.

In a general plate tectonic framework (Fig. 1), oceanic volcanism at midocean ridges, seamounts, and oceanic islands is dominantly basaltic. Due to the lower volatile content of basaltic magmas, volcaniclastic rocks in these regions tend to be formed by fragmentation of lava flows rather than by explosive eruptions. Pillow breccias and hyaloclastites are commonly formed. By contrast, island arc environments are dominantly basaltic to andesitic in composition. Explosive volcanoes commonly produce subaerial and subaqueous pyroclastic fallout and flows. Remobilized volcaniclastic mass flows and turbidites may be deposited in the submarine environment. Continental magmatic arc environments are dominantly andesitic to rhyolitic in composition. Here, subaerial pyroclastic flows and fallout deposits are common, as are their remobilized equivalents. The forearc environment, however, may be partly submarine. Continental rift environments are commonly associated with caldera structures where acid subaerial pyroclastic deposits are found. Basaltic cinder cones and tuff rings also occur here, and are commonly associated with lava flows. In summary, oceanic extension produces effusive volcanoes where the magma is mostly basic, whereas subduction produces explosive volcanoes (e.g., Indonesia, Japan, the Cascades, and the Lesser Antilles), where the magma is intermediate to acid in composition. Thus, different tectonic environments have distinctive volcaniclastic facies.

The models discussed in this chapter are best used as general frameworks for future observations. A few models, particularly for pyroclastic rocks, have been tested on different volcanoes and may thus be used to initiate interpretations, but more work needs to be done before they can be considered norms and predictors. One should keep in mind that most pyroclastic models discussed in the present chapter were developed in subaerial deposits. We shall see that subaqueous accumulations may have different characteristics.

TERMINOLOGY

Volcaniclastic rocks include all fragmental volcanic rocks that result from any mechanism of fragmentation. *Epiclastic* fragments result from the weathering of volcanic rocks. *Autoclastic* fragments are formed by mechanical breakage or gaseous explosion of lava during movement. *Hyaloclastic* fragments, a variety of autoclastic, are produced by quenching lava that enters

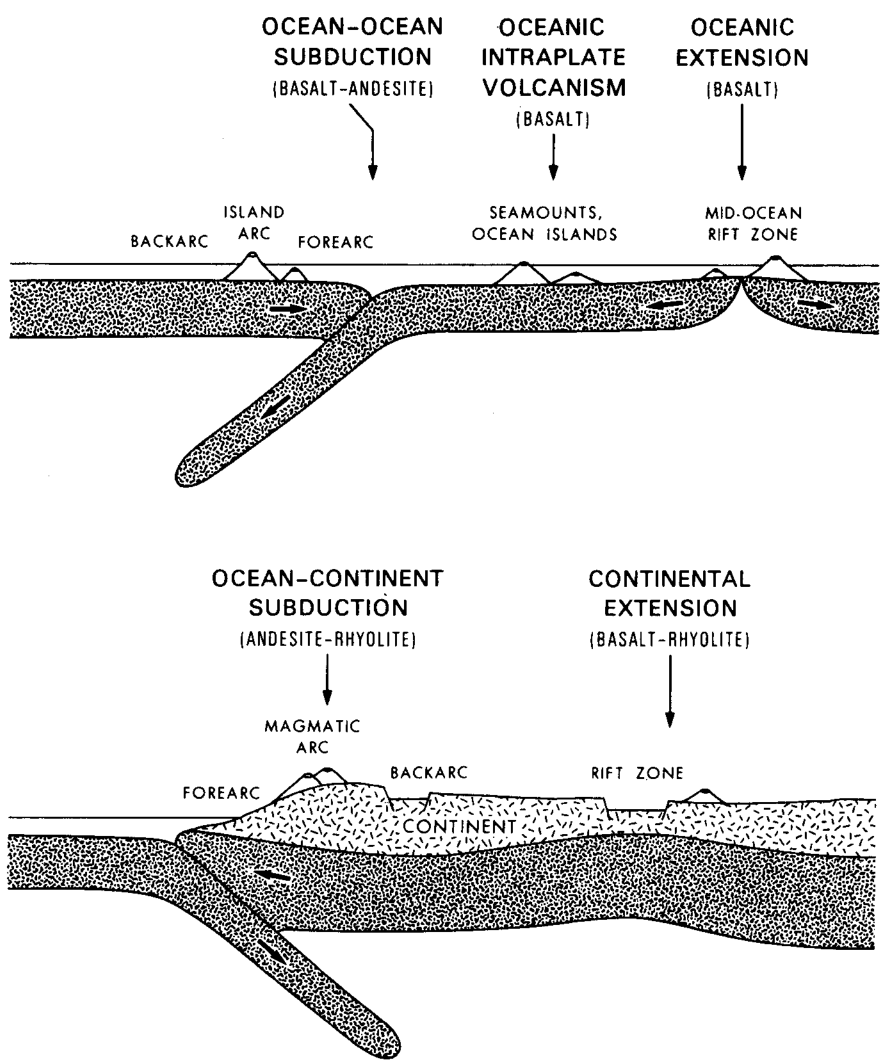

Figure 1 Tectonic setting of volcaniclastic deposits.

water, water-saturated fragmental deposits, or ice. *Pyroclastic* fragments originate from explosive eruptions and are projected from volcanic vents. Showers of pyroclastic debris produce *fall deposits*. Clasts ejected from vents may be transported *en masse* on land or in water by *nuées ardentes*. This descriptive term was proposed by Lacroix (1904) from his studies of the 1902 eruption of Mount Pelée, to refer to hot pyroclastic density currents. These deposits may thus result from more than one transporting mechanism.

In the volcanic literature, pyroclastic deposits originating from laminar transport of hot, high-concentration mixtures of fragments in gas are commonly referred to as *flow* deposits. Those that accumulate from hot, relatively low-concentration turbulent suspensions are termed *surge* deposits (Fisher and Schmincke, 1984; Cas and Wright, 1987). Surges are further subdivided into *base, ground,* and *ash-cloud* surges depending on the position of the turbulent cloud relative to the entire density current. This highly genetic terminology is certainly very useful to volcanologists working on recent volcanoes and is well entrenched in the volcanic literature. However, it is ambiguous because both pyroclastic *flows* and *surges* are flows *sensu stricto*. Furthermore, there is no consensus among workers as to what are *flow* and *surge deposits* (Lipman and Mullineaux, 1981), raising a few questions as to the applicability of this nomenclature to ancient deposits. Cas and Wright (1987, p. 355) note that "it is a brave person who walks to an outcrop (of pyroclastic deposits) and applies a genetic classification or terminology". In the present chapter we shall therefore favour the more descriptive terminology whenever possible.

Pyroclastic fragments are called *primary* if ejected from a vent, and *secondary* if they are recycled from *unconsolidated* primary deposits. Lahar, a term first used at Kelud volcano on Java, refers to coarse remobilized primary pyroclasts where the interstitial fluid is water. In ancient deposits it may not always be possible to distinguish between primary and secondary pyroclastic debris.

Pyroclastic fragments coarser than 64 mm (-6ϕ) are called *bombs* or

Table 1 *Differences between pyroclastic flow and epiclastic deposits.*

	Epiclastic	Pyroclastic
Texture	Rounded grains of volcanic rocks and crystals. Depending on environment of deposition, sorting may be excellent to poor.	Angular to subrounded pumice, scoria, shards, accretionary and armoured lapilli that may be deformed or welded. Sorting is poor to very poor.
Composition	Volcanic rock fragments which tend to be polygenetic, with common incompatible phases such as quartz and basalt.	Mostly acid to intemdiate fragments which tend to be monogenetic.
Structure	Normal sedimentary structures.	Common presence of normal or reverse grading, of thick diffuse strata, low angle cross laminae, and bomb sags.

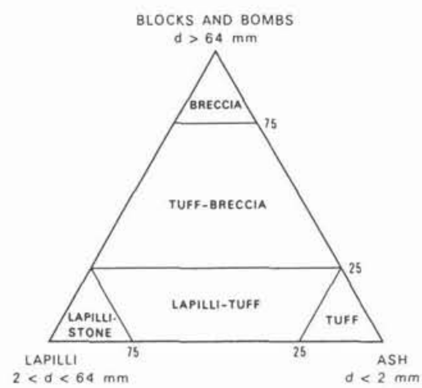

Figure 2 Pyroclastic grain-size classification with rock nomenclature. Modified from Fisher and Schmincke (1984, p. 92).

Figure 4 Hyaloclastite transitional with pillow lava, Rouyn-Noranda region, Québec.

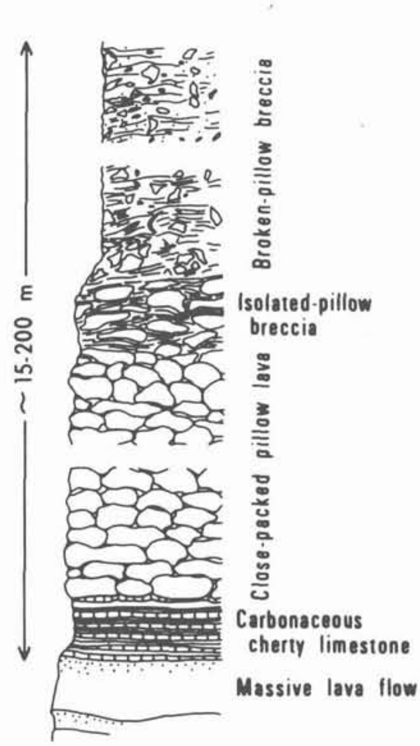

Figure 3 Typical pillow breccia-hyaloclastite sequence in the Triassic of Quadra Island, British Columbia. From Carlisle (1963).

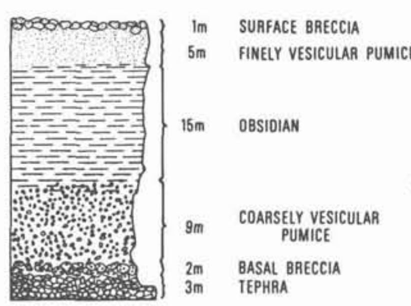

Figure 5 Schematic cross section of rhyolitic obsidian flow. After Fink (1980).

blocks, lapilli if grain size ranges from 64 to 2 mm (–6 to 1ϕ), and *ash* if finer than 2 mm (–1ϕ). Ashes are further subdivided into coarse and *fine* at 1/16 mm (4ϕ). Pyroclastic *rocks* with mixtures of these fundamental size subpopulations are classified in Figure 2.

Volcaniclastic sedimentation is a vast subject and has so many variables that it will not be possible to treat all of its aspects. Except for composition, epiclastic rocks do not differ from other siliciclastic rocks. They thus will not be treated here except to summarize the petrographic differences with pyroclastic fragments (Table 1). These differences are in part due to the different fragmentation processes, and in part to the temperature of accumulation. We will describe briefly the characteristics of autoclastic and pyroclastic rocks, and discuss their observed and possible variations in time and space (facies). The reader will find good descriptions of the morphology and petrography of volcaniclastic fragments in Fisher and Schmincke (1984), and Heiken and Wohletz (1985).

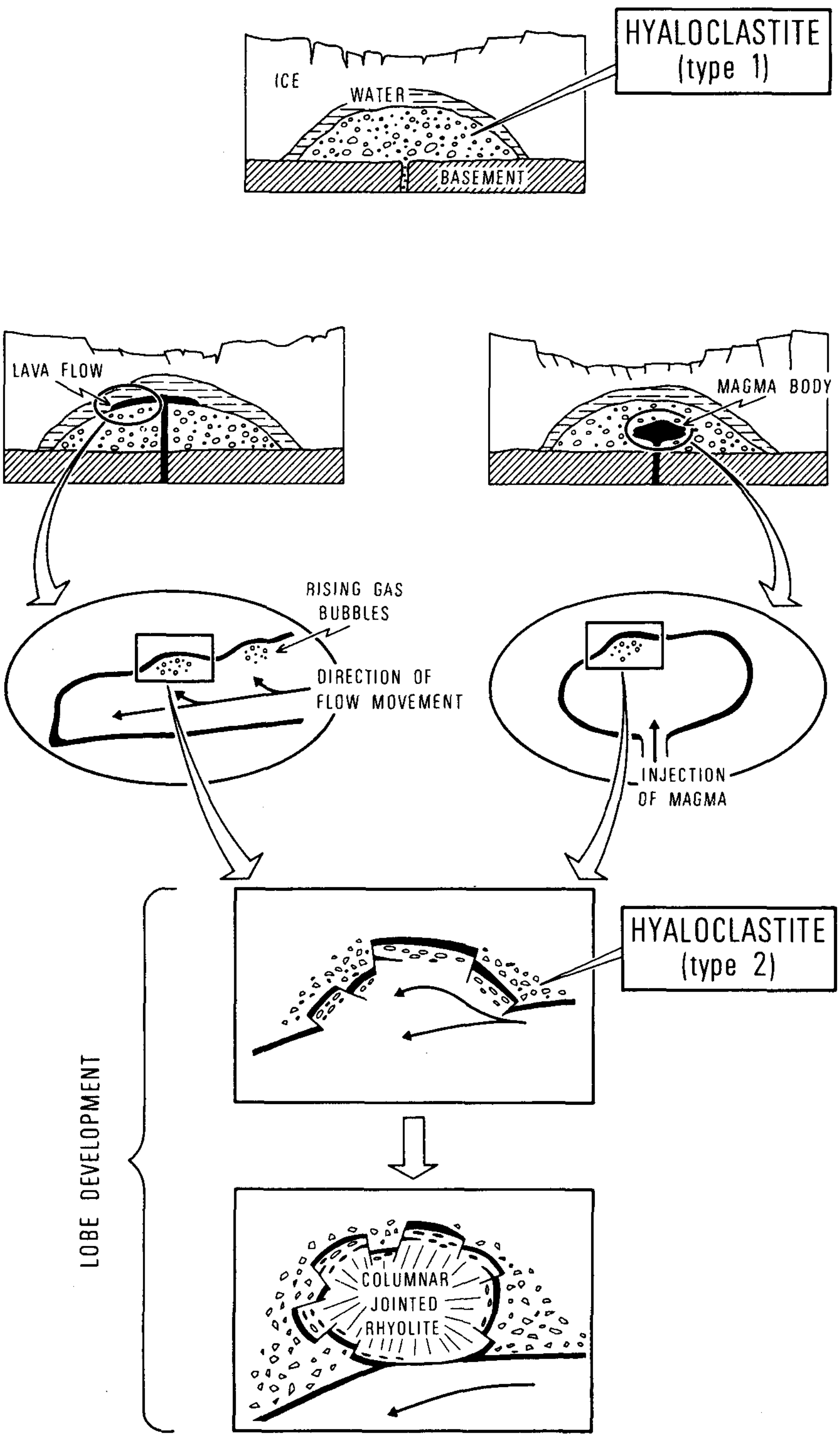

Figure 6 Evolutionary model of the two types of acid hyaloclastites and lobes. From Furnes *et al.* (1980).

AUTOCLASTIC ROCKS

Flow breccias and hyaloclastites are common in basaltic sequences and uncommon in acid sequences. This is because basic lavas flow more readily than acid ones, due to their lower viscosity. In these two types of autoclastic rocks, the clasts are generally monogenetic, with most fragments being derived from the same parent liquid. Lava may erode vent walls or rip up fragments as it flows, but such exotic fragments are rarely reported in descriptions of flow breccias. In basaltic sequences, the breccias commonly consist of complete pillows and/or pillow fragments set in a matrix of devitrified glass shards and lumps. Acid flow breccias are made up of abundant angular blocks with coarse and fine sand size fragments set in a glassy matrix.

Facies in flow breccias and hyaloclastites

Due to their mode of origin, in situ flow breccias and hyaloclastites should show little or no systematic lateral variations in clast content, size, and composition. Autoclastic associations, however, are much more complex.

The vertical variations in a typical flow breccia of basaltic composition are summarized in Figures 3 and 4. The pillowed lava grades upward into an isolated-pillow breccia that is overlain and transitional with a broken-pillow breccia. In the Archean of the Noranda region, similar sequences are occasionally overlain by fine-grained hyaloclastites (Fig. 4). In this succession, clast size decreases from base to top. This grain size variation cannot properly be called graded bedding because there is no bedding to begin with. The clasts are formed in situ rather than being transported and deposited. The distinctive characteristics of this type of breccia are the monogenetic composition of the clasts and the transitional contact with the underlying lava. Since the fragmentation is formed by quenching, the shards are not welded.

Subaerial lava flows of acid composition commonly have flow breccias which underlie and/or overlie the lavas. Fink (1980) presented a schematic cross section of subaerial rhyolitic obsidian flows based on studies from California, New Mexico, and Lipari in the Eolian Islands (Fig. 5). The approximately 30 m-thick lava flow has a two m-thick breccia at the base and a one m-thick flow-top breccia. The texture and composition of the fragments are similar to those of the associated parent lava flow. Compared to flow breccias of basaltic composition, however, the breccias of acid flows are thinner; the transition with the parent lava is more abrupt, and may even be sharp; and the fragments are large and chaotically organized.

There are few modern examples of submarine acid lava flows, and they are rare in the rock record. Subglacial acid hyaloclastites from Iceland show a greater lithological diversity than basaltic hyaloclastites (Furnes *et al.*, 1980). They are made of structureless to strongly flow-banded fragments of pumice and obsidian, commonly associated with large (long axes average 7 m) irregular to subspherical bodies (lobes) of vesicular to nonvesicular rhyolite. Two genetically different types of hyaloclastites are described (Fig. 6). Type 1 hyaloclastites, said to be by far the most common, consist entirely of pumiceous fragments that vary considerably in size and shape, and result from phreatic explosive events. Type 2 hyaloclastites consist of fragments of obsidian, flow-banded or flow-folded pumices, and lithic rhyolite invariably associated with ellipsoidal to irregularly shaped bodies (lobes) that may commonly reach 70 m in length. These lobes, which are mineralogically and chemically similar to the pumice, consist of an outer shell of obsidian adjacent to a zone of flow-banded and flow-folded vesiculated and glassy rhyolite. Type 2 hyaloclastites are derived from the lobes during the fragmentation of lava flows or magma bodies (Fig. 6) that have intruded water-saturated Type 1 hyaloclastites. These Type 2 hyaloclastites are closely related, are in sharp contact with the parental lava, and have no internal structures indicative of transport.

Autoclastic fragments may be reworked by bottom currents or resedimented from density currents. In certain cases the deposit may show some of the characteristics of pyroclastic rocks. These secondary hyaloclastites may be difficult to distinguish from pyroclastic rocks, because both types of fragmentation may form similar textures. Pumice and scoria should, however, be more common in pyroclastic deposits. Honnorez and Kirst (1975) have shown that the percentages of concave, convex, and planar grain boundaries can be used to distinguish a hyaloclastic from a pyroclastic fragment.

The model proposed for basaltic flow breccias and hyaloclastites is sufficiently well established to be used as a norm.

PYROCLASTIC ROCKS

Pyroclastic debris consists of pumice, scoria, glass shards, crystals, and accessory lithic fragments. All of this material is explosively ejected from vents and then falls or flows in air or water under the influence of gravity. There is a consensus among workers that gravity plays a major role in the en masse transport of pyroclasts. Settling velocities of pyroclasts are proportional to fragment size, shape, and density. Therefore, the principles that govern the sedimentation of pyroclasts are similar to those controlling the deposition of other clastic debris.

The lateral extent and geometry of pyroclastic deposits are influenced in part by magma composition and in part by the environment in which the eruption takes place. Basaltic subaerial eruptions generally produce cones of scoria and ash of limited areal extent around or downwind of the cones. Basaltic eruptions that take place in shallow water, or where water has access to the vent, are more strongly explosive and produce ash rings and ash layers that may have considerable lateral extent. Eruptions of acid and intermediate compositions are generally explosive due to the volatile content of the magma. These eruptions may project very large volumes of pyroclastic debris to heights well in excess of 25 km and may produce thick fall and flow deposits.

The influence of the environment is illustrated by the asymmetric distribution of pyroclastic deposits east and west of the Lesser Antilles arc (Fig. 7). On the west side of the arc, nuées ardentes entering the Caribbean Sea descend on steep slopes and are transported into deep water where their characteristics

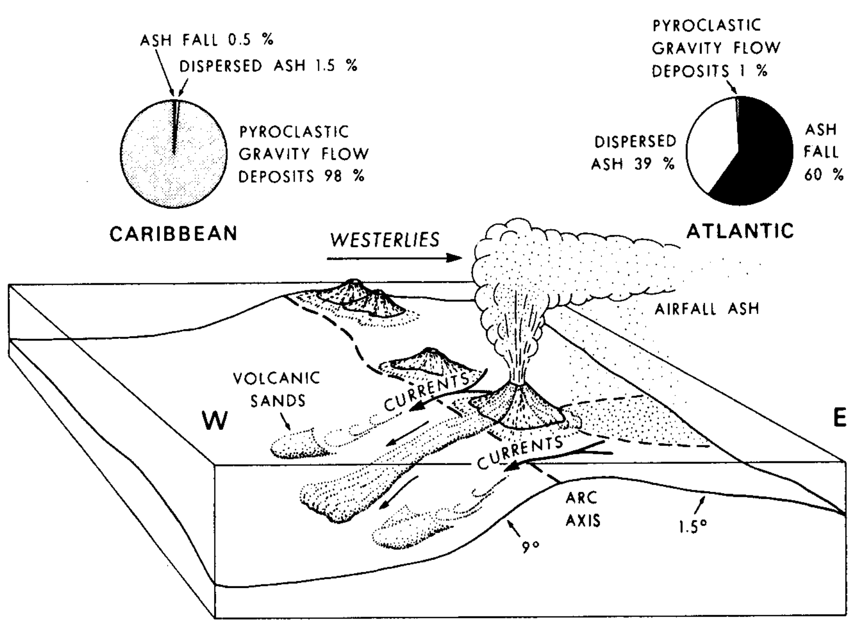

Figure 7 Asymmetric distribution of pyroclastic deposits east and west of the Lesser Antilles arc. Volcanic islands are roughly 10 km apart. From Sigurdsson *et al.* (1980).

are preserved, and they form various types of density-current deposits. Those entering the east side of the arc, in relatively shallow water, are reworked and lose their original characteristics, thus becoming epiclastic deposits. Also, due to the prevailing winds, most of the fallout deposits are found on the Atlantic side of the arc.

Facies in pyroclastic fall deposits
Pyroclastic fallout deposits range from small volume, localized scoria and cinder cone accumulations to large volume sequences that mantle topography over large distances. The deposits are the products of ballistic fallout and turbulent convection in the eruption column. Large volume fallout deposits commonly are associated with flow deposits from the same eruption. The change from fallout to flow is caused by an increase in the magma discharge rate and/or a decrease in the magmatic volatile content. Two classifications of fallout deposits are presented (Fig. 8). The deposits are grouped according to their dispersal and degree of particle fragmentation. Small magnitude eruptions form *hawaiian, microplinian (strombolian)*, and surtseyan fallout units. Larger magnitude eruptions deposit *subplinian, plinian, ultraplinian*, and *phreatoplinian* fallout sheets. Surtseyan and phreatoplinian deposits are characteristically fine grained (−1 to 5 ϕ), even close to the source vent, indicating efficient fragmentation by interaction of magma and external water. Another type of fall deposit, termed *co-ignimbrite fallout ash*, may be formed during the emplacement of a pumiceous pyroclastic flow *(ignimbrite)* by the preferential loss of vitric material from the flow to the atmosphere. Co-ignimbrite ashes also are fine grained and cover large areas.

Basaltic pyroclastic eruptions frequently build scoria and cinder cones. The resulting fallout deposits are termed hawaiian, strombolian, or microplinian (Fig. 8A). The deposits dip both away from and into the cone, generally have small volumes (< 1 km^3), and are localized in areal extent (Fig. 9A). The juvenile material has a range of vesicularities and grain sizes, the fragments being crudely bedded and framework supported. The deposits are variably sorted because of 1) fragments with different vesicularities and densities, 2) particle agglomeration in fine-grained layers, 3) mixing of turbulently suspended material and ballistic blocks and bombs, and 4) welded spatter that results from high eruption rates. Fallout material that accumulates on the steep slopes of the cone may be mobilized downslope by grain flows, resulting in beds that are inversely graded. Scoria and cinder cone sequences may have rapid vertical and lateral transitions among scoria and cinder layers, welded agglutinated units, and fine-grained beds, reflecting changes in eruptive conditions, distance from the vent, and phreatomagmatic influences.

Widespread fallout tephra sheets of large volume (10-10^3 km^3) are usually silicic in composition, although basaltic examples do exist. Large explosive eruptions frequently show a progression from fallout to pyroclastic flows during the course of the eruption. The fallout deposits consist primarily of framework-supported pumice or scoria clasts with subordinate crystal and lithic

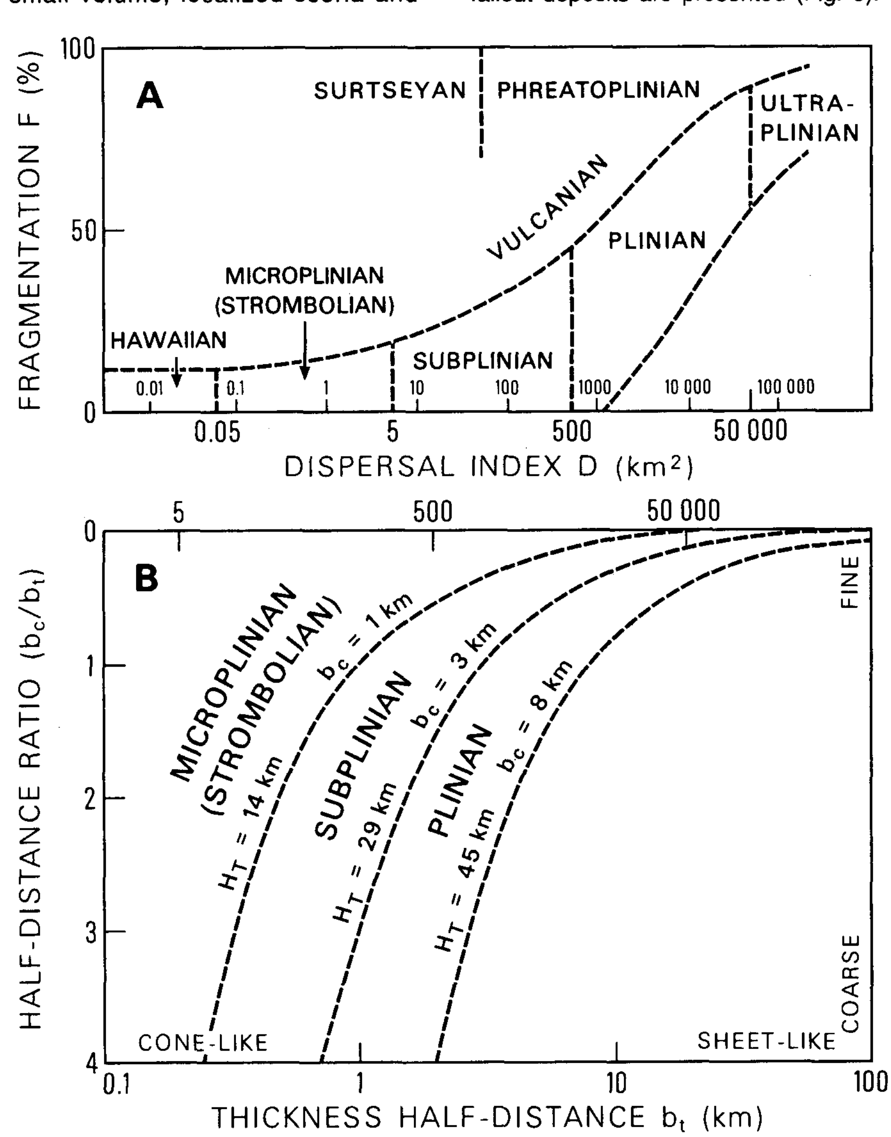

Figure 8 Two classifications of pyroclastic fall deposits. A) Classification in terms of dispersal D (area enclosed by the $0.01T_{max}$ isopach, where T_{max} is the maximum thickness of the deposit) and degree of magma fragmentation F (percentage of a deposit finer than 1 mm at the intersection of the dispersal axis and the $0.1T_{max}$ isopach). Modified from Walker (1973), Self and Sparks (1978), Walker (1980), and Francis *et al.* (1990). B) Classification in terms of thickness half-distance b_t (distance over which the thickness of a deposit halves) and half-distance ratio b_c/b_t, where b_c is the maximum clast half-distance (distance across which maximum clast size halves). Curves show eruption column heights (H_T) for different values of b_c. As with (A) above, fragmentation increases toward the top, and dispersal increases from left to right. Modified from Pyle (1989).

fragments. Pumices are commonly angular and fractured from impact. Pumices near the vent can have pink oxidized interiors, indicating hot emplacement. As a rough guide, in these deposits lithic fragments are half as large as pumices, depending on the differences in density.

Fallout deposits can be massive and/or stratified. Massive sequences suggest sustained eruptions, while stratified parts may indicate fluctuations in eruption intensity or wind direction (Fig. 10). In fallout deposits it may not be easy to distinguish between primary stratification due to factors stated above and stratification due to reworking after deposition where sorting improves, and pumices commonly are subrounded. Mantle bedding, in which thickness over a limited area is uniform, is common except in topographic depressions where thicker deposits can accumulate due to secondary movement of material. In this case, however, the deposits are no longer primary. Fallout deposits are commonly better sorted than flow deposits, but fine-grained ash that has agglomerated in clusters can result in poorly sorted fall deposits. Ash clusters have been documented in the deposits from the May 18th, 1980 eruption of Mt. St. Helens and the 1982 El Chichon eruptions. On the other hand, low-density ash clusters can transport higher-density crystals (e.g., magnetite, pyroxene) to greater distances from the volcano than would normally be the case if the grains fell individually (see Kittleman, 1973; Fisher and Schmincke, 1984, p. 159-160). Fallout deposits may be ungraded, normally graded, inversely graded, or a combination of the above (Figs. 11, 12). Normally graded sequences indicate that the eruption was most intense during its initial phases. By contrast, inversely graded fallout deposits can be overlain directly by flow deposits from the same eruption, suggesting that eruption intensity increased during the eruption. Beds that exhibit both normal and inverse grading imply that the intensity varied during the course of the eruption. Some fallout deposits have a fine-grained base with accretionary lapilli, suggesting that the magma interacted with meteoric water during eruption, possibly through a crater or caldera lake. Such deposits

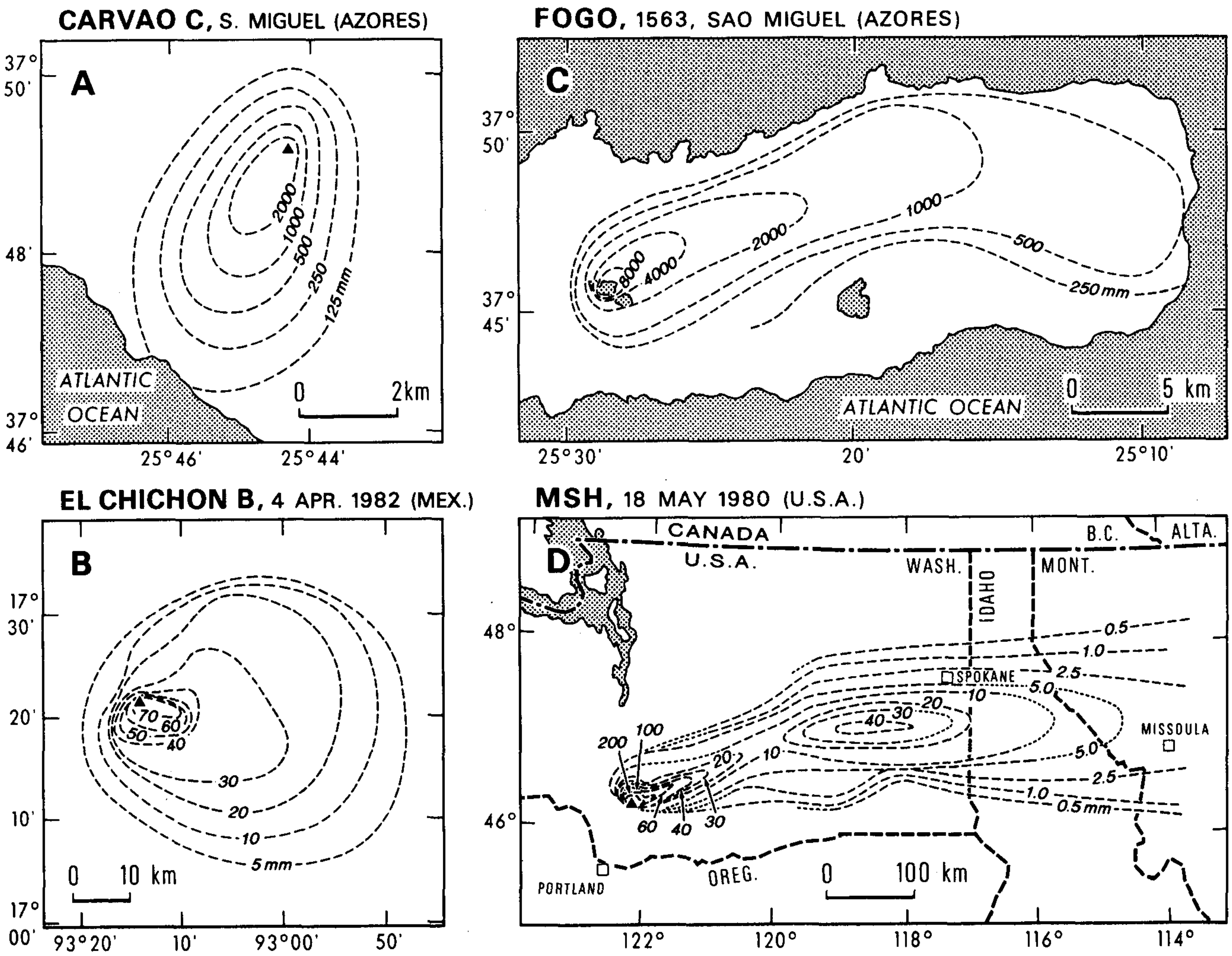

Figure 9 Isopach maps for four fallout deposits. All thicknesses in mm. A) Map of the Carvao C deposit, Azores. Note the limited areal extent of the pyroclasts. From Booth *et al.* (1978). B) Isopach map of the El Chichon B deposit, Mexico. Note the relatively concentric isopachs. From Carey and Sigurdsson (1986). C) Isopach map of the Fogo 1563 deposit, Azores. The deposit is strongly asymmetric. From Walker and Croasdale (1971). D) Isopach map of the 18 May 1980 Mt. St. Helens deposit. Secondary thickening occurs 300 km downwind of the volcano. From Sarna-Wojcicki *et al.* (1981).

are termed phreatomagmatic.

Fallout distributions may be uniformly dispersed around the source, indicating little influence from wind (Fig. 9B), or may be asymmetrically distributed due to prevailing winds (Fig. 9C). In general, fallout deposits from large magnitude eruptions tend to be more uniformly distributed than deposits from smaller magnitude eruptions (Carey and Sparks, 1986). However, fallout patterns can be very complex if there are different winds at different altitudes or if wind directions change during the course of an eruption.

Fallout sheets exhibit systematic changes in thickness, maximum clast size, and proportions of pumice, crystals, and lithic fragments from near-vent to distal environments. Thicknesses generally decrease exponentially away from the vent (Pyle, 1989). Fine-grained fallout deposits are not necessarily distal, however, as they may result from low-intensity eruptions, phreatomagmatic explosions, or co-ignimbrite ash deposition. In asymmetrically distributed deposits (Fig. 9C), thicknesses decrease more gradually along the dispersal axis than on its margins or upwind of the source volcano. Maximum thicknesses may not necessarily occur in proximity to the vent, due to erosion of fallout material by pyroclastic flows. Secondary thickening of the May 18th, 1980 Mt. St. Helens fallout ash occurred 300 km downwind of the volcano (Fig. 9D). This may have been a result of premature fallout of fine-grained agglomerates and/or additions from co-ignimbrite ash generated by the pyroclastic flows on the flanks of the volcano. This indicates that the thicknesses of distal plinian ashes may have been overestimated by not recognizing the co-ignimbrite ash component. The distinction between plinian fallout ashes and co-ignimbrite ashes (ash derived from a pumiceous pyroclastic flow) is indeed difficult in distal regions. Both are fine grained and rich in vitric material. Co-ignimbrite ash layers do not thin exponentially and

Figure 10 Rhyolite fallout bed showing the transition from massive pumice below the hammer to stratified pumice above. A pyroclastic flow deposit directly overlies the stratified fallout sequence. Guaje Pumice Bed, Jemez Mountains, New Mexico, USA.

Figure 11 Normal grading in a rhyolite pumice fallout unit. Pre-Bandelier plinian deposit, Jemez Mountains, New Mexico, USA.

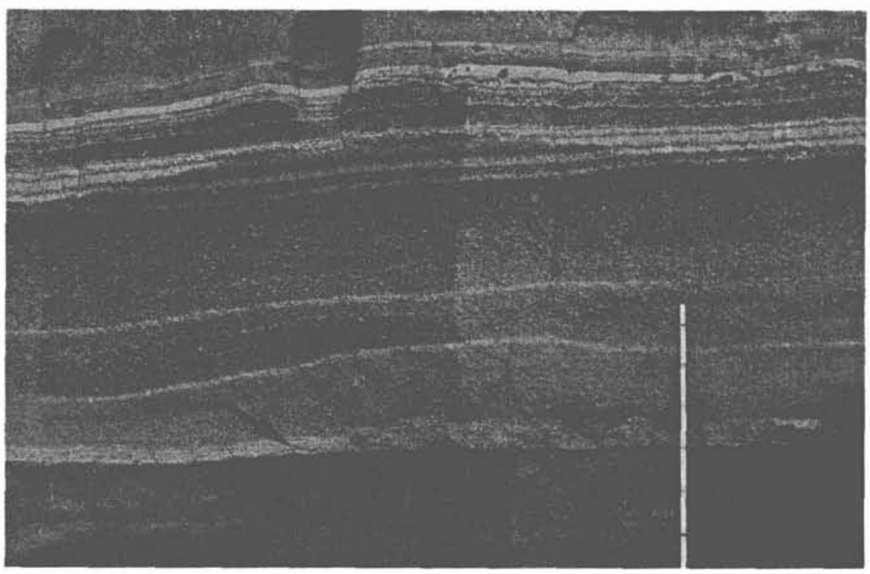

Figure 12 Inverse grading in a rhyolite pumice fallout deposit. The thin white beds are fine-grained units which may represent episodic phreatomagmatic activity. Note the relatively thick fine-grained unit, marked by the arrow at the base of the inversely graded bed, which may indicate an initial phreatomagmatic phase of the eruption. Scale is graduated in 10-cm increments. Cerro Toledo Rhyolite, Jemez Mountains, New Mexico, USA.

thus have a much more uniform thickness over a wide area than do plinian units. Trace element geochemistry of the glass shards may be able to distinguish between distal plinian and co-ignimbrite ashes from one eruption. If the plinian phase of the eruption is erupted before the pyroclastic flow phase, the plinian eruption will tap the upper regions of the magma chamber, which are most enriched in incompatible trace elements (e.g., uranium and niobium). Therefore, the plinian ash will have higher concentrations of incompatible trace elements than the co-ignimbrite ash.

The maximum size of pumices and lithic fragments in outcrops of a fallout deposit decreases exponentially from the source (Pyle, 1989), although clasts in proximity to the vent may be anomalously large due to ballistic emplacement. These maximum size variations can be mapped as isopleths of equivalent clast diameter (Fig. 13). It is preferable to examine lithic fragments because of the problems of breakage and variable densities associated with pumices. Systematic lateral changes in the isopleths can be related to the height of the eruption column. The width of a particular isopleth is a function of the height of the column, while the maximum downwind range of the isopleth depends upon both the column height and the wind speed (Carey and Sparks, 1986). The distribution of maximum lithic isopleths is generally less asymmetric than thickness isopachs (compare Figs. 9A and 13B), implying that the isopleths are less affected by wind.

The grain size and proportions of the three major components in a fallout deposit (pumice, crystals, and lithic fragments) also change from proximal to distal regions (Fig. 14). The deposit as a whole becomes finer grained away from the source. This is reflected in the distal fining of the pumice and lithic populations. The size of the crystals does not change laterally, however, because crystal size is controlled by pre-eruptive conditions in the magma chamber. The proportion of lithic fragments remains approximately constant, while the percentage of pumice decreases and percentage of crystals increases distally. This reflects the progressive liberation of crystals from pumice fragments as the grain size of the pumices approaches that of the crystals.

Facies in nuée-ardente deposits

Three different types of nuées ardentes are recognized by volcanologists, 1) the *Pelée* type where the nuées are produced by directed explosions generating high-velocity, low-concentration, turbulent suspensions, 2) the *St. Vincent* type which results from column collapse, with the flow descending the slopes of the volcano in radial directions, and 3) the *Merapi* type caused by avalanche of solidified, but hot, blocks of the lava dome which break up into smaller pieces during their descent in high-concentration suspensions (Escher, 1933; Macdonald, 1972; Williams and McBirney, 1979; Fig. 15).

There is general agreement among workers that although the Pelée nuées ardentes are initiated by a lateral explosive thrust, and St. Vincent nuées ardentes by vertical explosion, once in motion they behave as gravity-controlled density currents. It follows that the mechanisms responsible for transporting the debris are similar to those of other density currents. It is therefore not surprising that *debris* and *grain flows* have been invoked to explain the features found in a number of coarse pyroclastic deposits, and *turbidity current* for a limited number of turbulent nuée-ardente deposits.

The *Pelée nuées ardentes* are produced by strong lateral thrusts leading to high velocities, roughly 130 m/sec over St-Pierre at the base of Mount Pelée, for the May 8th and 20th nuées ardentes of 1902 (Lacroix, 1904; Brissette and Lajoie, 1991). Such high velocities resulted in turbulent low-concentration density currents which left characteristic deposits which have been well documented at Mount Pelée.

At their type locality, the Pelée nuée-ardente deposits are characterized by the common presence of three well-defined strata (beds I, II, and III; Fig. 16; Boudon and Lajoie, 1989; Charland and Lajoie, 1989). The basal bed (I) is thinner than the middle bed and contains the coarsest grain size of the deposit. It is massive, reversely and more rarely normally graded, and poor in fines with less than 2 per cent of grains finer than 4ϕ (1/16 mm). The middle bed (II), which may rest either in sharp or transitional contact with the underlying bed, represents most of the deposit. It shows well-developed normal-population grading (Fig. 16) with the fines (4ϕ) increasing to 30 per cent at the top of the bed. Stratification is superimposed on the grading in the upper portion of the bed (Fig. 16). In more proximal sections these strata are relatively crude and thick, dipping upflow at less than 10° (Fig. 16), and are interpreted as antidunes. In more distal sections, bedding is better defined, with thinner laminae dipping downflow, and interpreted as dune bedforms (Boudon and Lajoie, 1989). The upper bed is relatively thin and contains the finest grain size of the deposit (50 per cent finer than 4ϕ). The coarse fraction increases at the top of the deposit (Fig. 16) due to the presence of accretionary lapilli (small spheres made up of agglutinated fine ashes). Generally the upper bed is normally graded, with rare parallel laminae and ripple cross bedding at its very top. The entire deposit of a typical

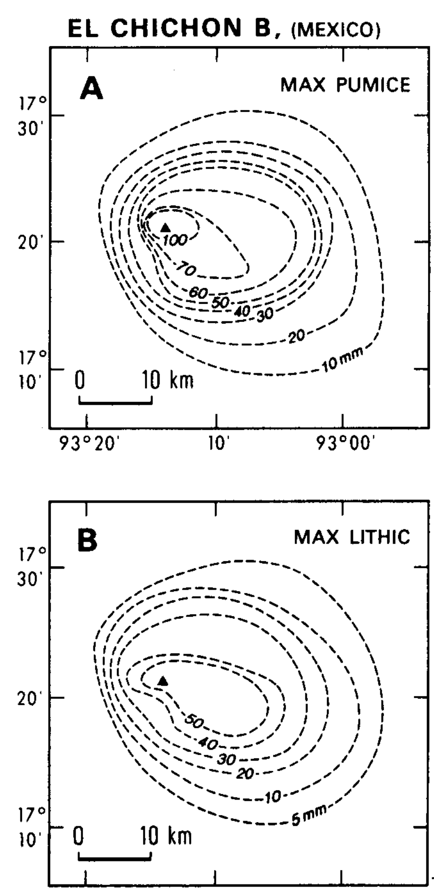

Figure 13 Isopleths of the largest pumice clasts (A) and lithic fragments (B) in the El Chichon B fallout deposit, Mexico. From Carey and Sigurdsson (1986).

Pelée nuée ardente is therefore normally graded. Sorting (σ_i) ranges from more than 2.5ϕ at the base, improving to 1.2-1.5ϕ in the finer-grained part of the deposit, which by standard sedimentary nomenclature would be termed poorly to very poorly sorted. The typical Pelée nuée-ardente deposit is interpreted as having accumulated from a low-concentration turbulent suspension where bed I represents a thick traction carpet formed by gravity segregation of the coarser fraction within the nuée. Here, dispersive pressure played an important role as the clast supporting

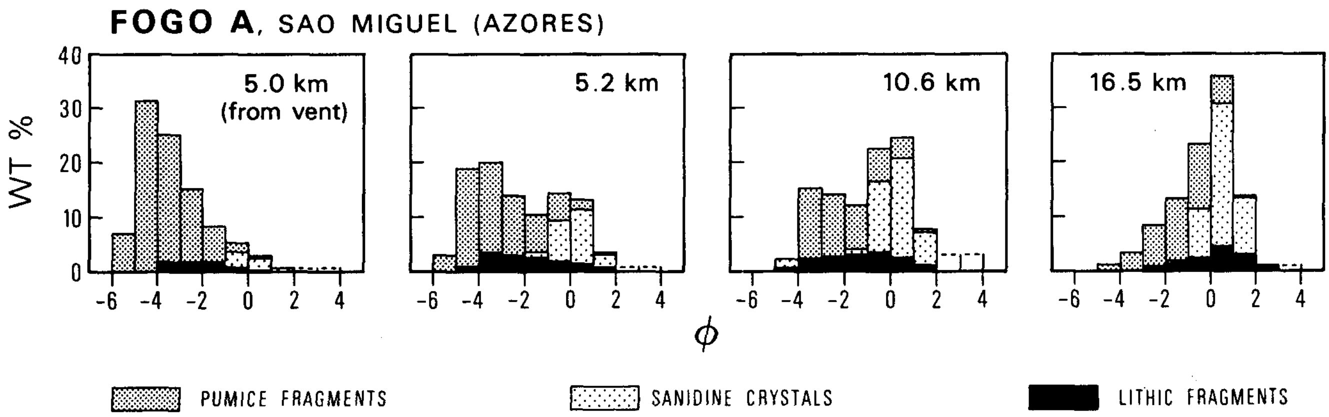

Figure 14 Proximal to distal variations in proportions of pumice, crystals, and lithic fragments for different size fractions in a fallout deposit. Fogo A sequence, Azores. Modified from Walker (1971).

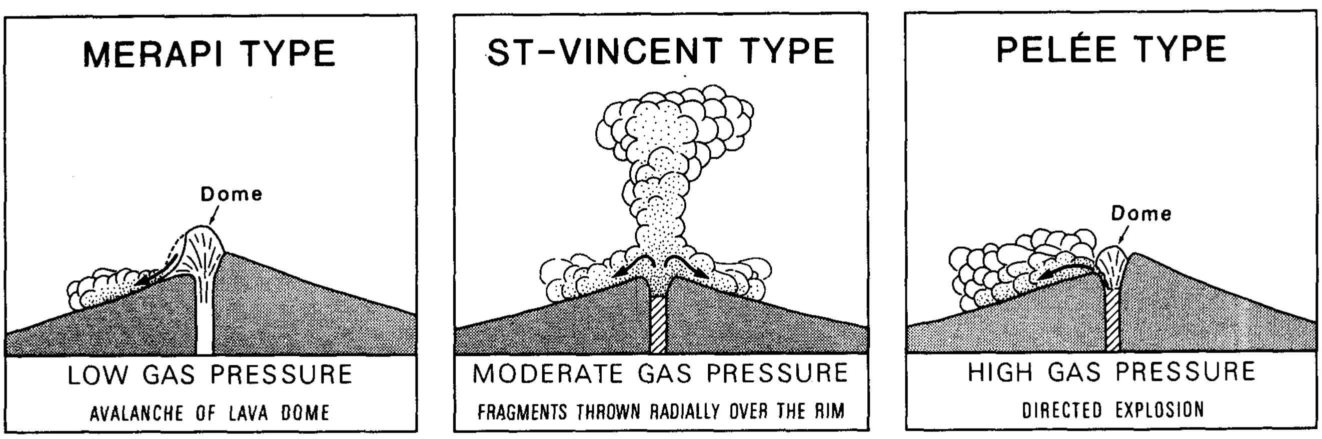

Figure 15 The three different types of nuées ardentes, modified from Escher (1933).

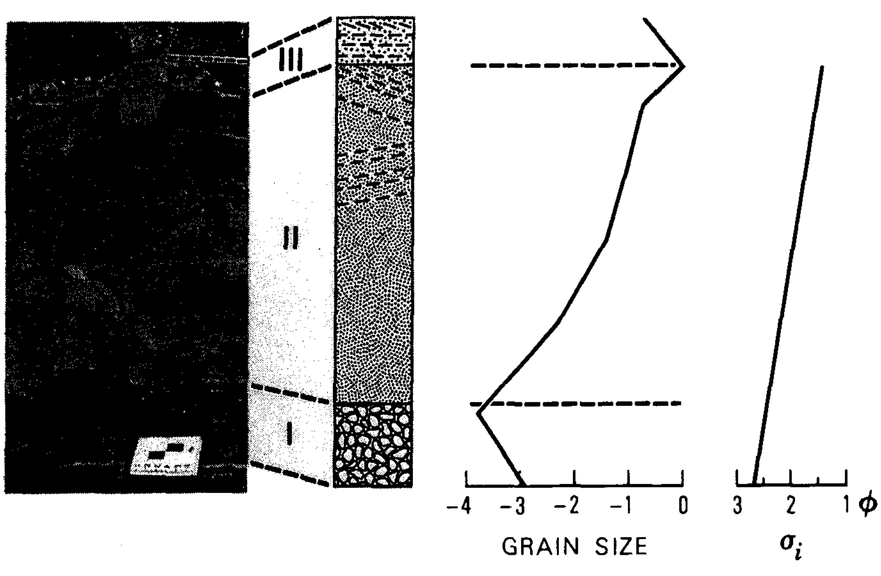

Figure 16 Depositional sequence in a typical Pelée nuée-ardente, at the type section with upbed variations of mean grain size (M_z) and sorting (σ_i).

mechanism. The primary structure sequence in the deposit was interpreted as resulting from a decelerating subaerial particulate suspension where the fluid was hot gas.

The causes responsible for the May 18th, 1980 Mount St. Helens "blast surge" are different from those of the 1902 nuées ardentes at Mount Pelée (Boudon *et al.*, 1990). However, both eruptions left similar deposits (Fig. 17), with a massive or normally graded coarse basal "layer", overlain by a finer "layer" whose base is massive or normally graded, passing upward into laminated and cross-bedded ash. In the Mt. St. Helens deposit, the coarser basal bed is channelled in its central portion, and the thickness of the overlying bed decreases laterally away from the axis, where parallel- and cross-laminae become increasingly better developed.

The *Merapi nuée ardentes* are primarily controlled by gravity and lack the initial lateral thrust of the Pelée and Mount St. Helens nuées ardentes. Their velocities are therefore much slower (Lacroix, 1904, witnessed velocities ranging from 15 to 50 m/sec for this type of nuée). These nuées are sometimes referred to as block-and-ash flows. At the type section the deposits consist of coarse blocks, lapilli, and ashes, in which the general bedding and primary structure characteristics do not change downflow over the entire 7 km length. Typically, the deposit of the 1984 Merapi eruption consists of a single bed of reversely graded lapilli-tuff which lacks stratification. The lower contact with the underlying deposit is sharp and nonerosive. The entire population is graded (Fig. 18A), and the deposit is fines-poor, with less than 5 per cent fines (4 ϕ). Generally, the deposit is very poorly sorted, but grain size characteristics are not easy to describe due to the polymodality of the distributions. Some of these subpopulations fit a Rosin law better than the more standard log-normal distribution, which suggests that fragmentation rather than transport played an important role in the grain size distributions. The long axes of the lithic fragments are preferentially oriented parallel to flow. In such coarse-grained deposits, it is generally assumed that bed thickness and maximum grain size decrease downflow with distance from the source vent. However, the 1984 Merapi deposit shows a regular and significant increase in both maximum grain size and bed thickness, downflow for 7 km.

The characteristics of the studied Merapi deposit have been interpreted as the result of a concentrated suspension of cohesionless solids exhibiting non-Newtonian behaviour. Here, dispersive pressure played an important role in the suspension of the clasts, such as for an inertial, density-modified grain flow. The flow travelled on a 35° slope for the first km, and on a 20° slope for the next 2 km. It began depositing on a 6° slope, dissipating all its energy in the next 4 km.

The deposits of the *St. Vincent nuées ardentes* have not been described in detail. In their pioneer work, Anderson and Flett (1903) depict the original phenomena as a highly concentrated mass which descended radially from the crater for a distance of 4 km at a relatively low velocity of about 15 m/sec. These authors report that the most striking feature of the 1902 deposit is its fine grain size, 90 per cent of the deposit being ash, with fragments coarser than 7 cm making up less than 3 per cent of the mass. The deposit also contains many scoriaceous lapilli, and less frequently, large rounded bombs up to 1 m in diameter. The deposit is massive, with no grading or stratification of any sort, and has a sharp lower contact. These characteristics are indicative of a highly concentrated suspension of cohesionless solids exhibiting non-Newtonian behaviour.

Facies in hydrovolcanic deposits

Hydrovolcanism is the effect of the interaction of magma with water. It affects all shallow subaquatic volcanoes and many subaerial vents, forming tuff cones and tuff rings which are second in pyroclastic-deposit abundance only to scoria cones. Explosions which result from the conversion of groundwater to steam by ascending magma are called phreatomagmatic eruptions. The products are water, steam, and brecciated country rocks, and must include juvenile clasts. Hydroexplosions may generate ejecta plumes with an additional horizontal component known as a *base surge* or a *pyroclastic*

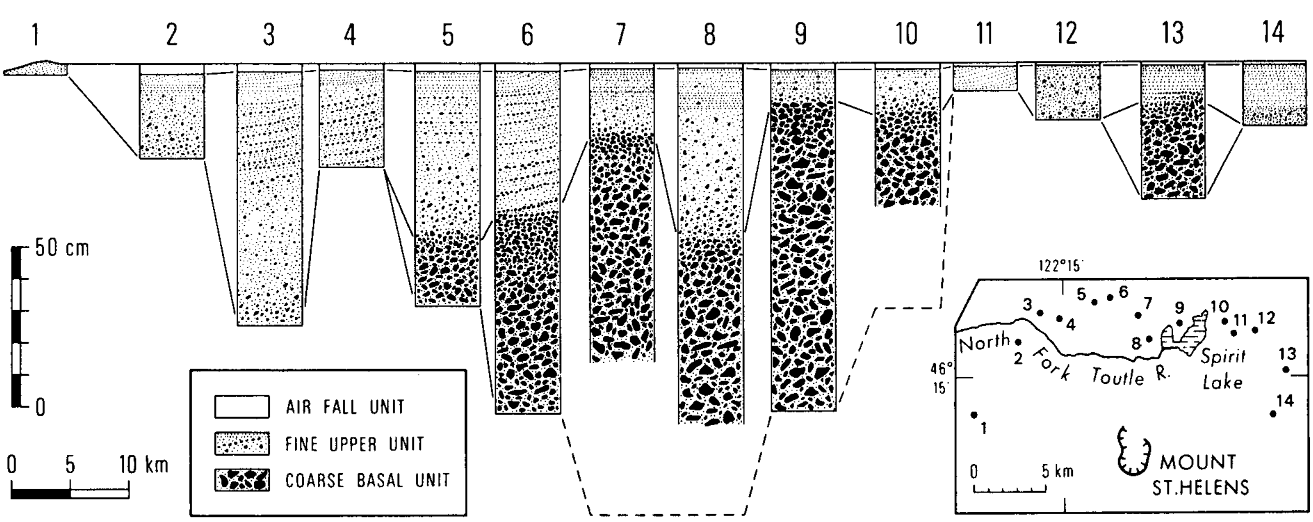

Figure 17 Lateral and vertical variations of bed thickness and primary structures in the May 18, 1980, "surge" deposit of Mount St. Helens. From Moore and Sisson (1981).

surge that may be dry (superheated steam media) or wet (condensing steam media). The general consensus is that, although initiated by an explosive thrust, once in motion surges behave largely as gravity-controlled density currents in which turbulence is a major grain-supporting mechanism. Cas and Wright (1987, p. 205-214) argue that surges can be compared to turbidity currents in a general way. However, they also suggest that in the case of wet surges there is no direct analogy with "normal" sedimentary processes, because of the three-phase media (solid-liquid-gas). The differences between sedimentary and volcanic processes certainly do exist but they could have minor effects on flow rheology as shown by the proposed models of lateral facies variations in dry- and wet-surge deposits.

Wohletz and Sheridan (1979) offer a model for dry-surge deposits in which a proximal, *cross-bedded facies* passes downflow within some 500 m (the scale is important) to a massive and reversely graded bed facies, to be replaced further away by what they call a "planar" facies in the more distal sections (Fig. 19). These "planar" beds are not planar or plane beds in the sedimentological sense. They may be 10 cm thick, are reversely graded, and are believed to have formed from a laminar grainflow mechanism. In this model, bed thickness decreases very rapidly in the direction of transport in the cross-bedded facies, but not in the massive facies where the variation is not systematic. Sorting is poor throughout the deposit (ϕ ranging from 1.6 to 1.88), but grain size increases downflow from a mean of 2.6ϕ (0.177 mm) in the cross-bedded facies to −0.48ϕ (30 mm) in the more distal massive beds, a very significant increase. Wohletz and Sheridan (1979) suggest that on eruption, the surge is inflated (fluidized) by volatiles to such an extent that velocities are extremely high and *viscosities very low*. Therefore, turbulence occurs close to the vent, resulting in traction that produces the observed primary structures. The cloud travels downslope, away from the vent, aided by gravity. Gases escape rapidly and the cloud deflates, resulting in a higher grain concentration. This leads to laminar flow, which is responsible for the massive and reversely graded distal facies. Cloud deflation, however, cannot explain the large lateral increase in grain size from fine sand to coarse pebbles in the direction of transport. Fisher and Schmincke (1984, p. 254) argue that this model may provide statistical summations of many flows through time at a particular locality. They also suggest that these facies variations cannot apply to processes which occur laterally within a single event.

An alternative model for the lateral

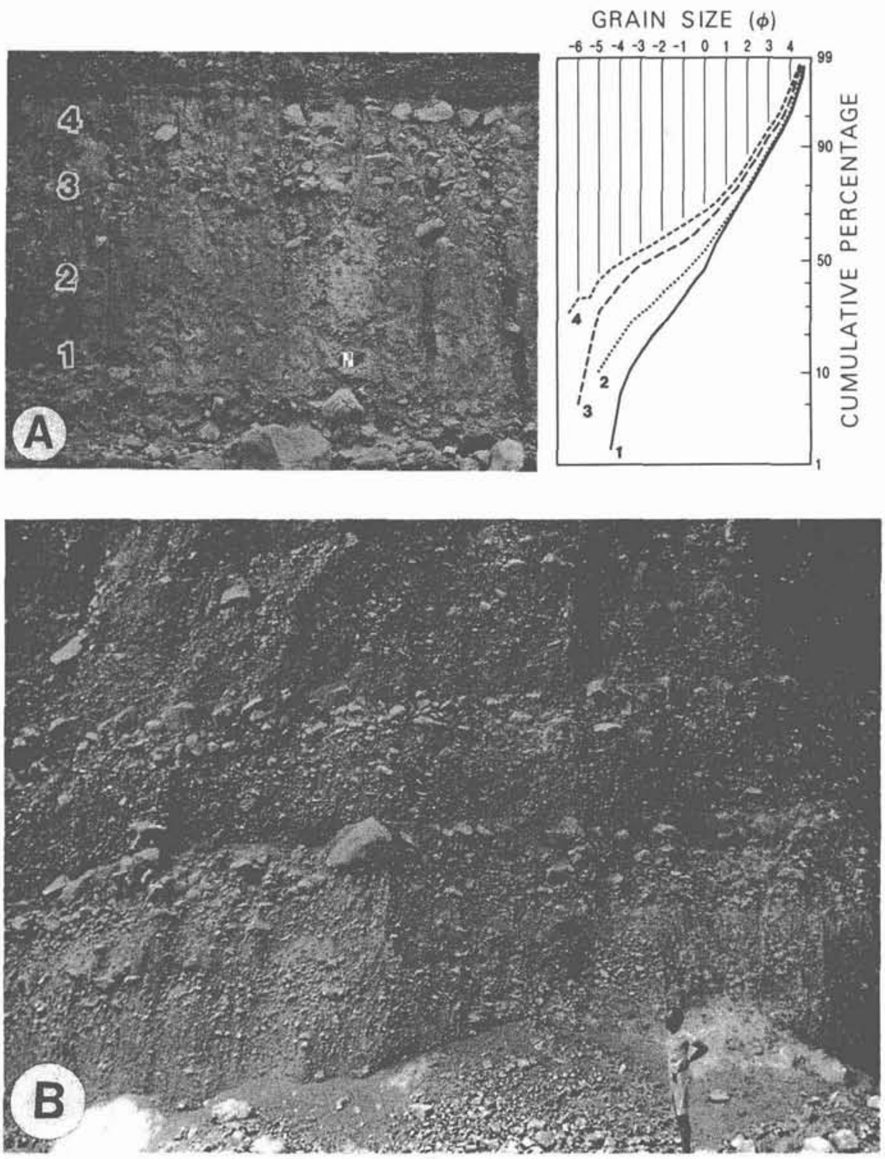

Figure 18 Typical Merapi nuée-ardente deposits, at Merapi (A) with cumulative distributions from base to top showing reverse population grading (notebook for scale is 19 cm high), and at Mount Pelée (B).

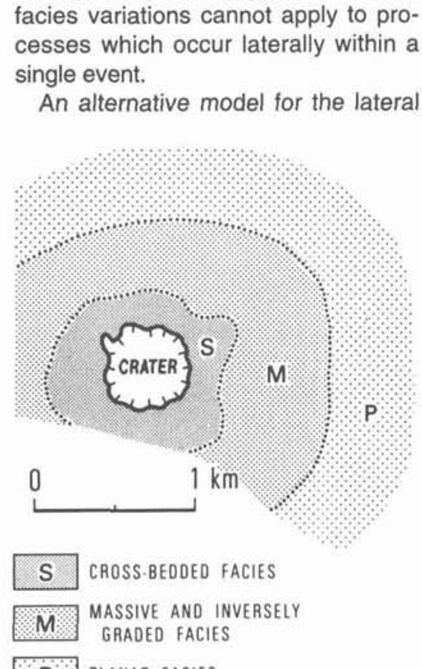

Figure 19 Lateral facies variations in dry *pyroclastic surges according to* Wohletz and Sheridan (1979).

facies variations in dry-surge deposits was proposed by Sohn and Chough (1989) from the Suwolbong tuff ring on the island of Chaju in Korea and has been verified at one other tuff ring (Chough and Sohn, 1990). In this model (Fig. 20), the general thickness of the deposit, as well as the individual bed thickness and grain size, decrease in the direction of transport for almost three kilometres. The most proximal facies consists of a majority of massive beds passing laterally into a crudely stratified parallel-laminated bed facies, which is in turn replaced downflow by a dune cross-bedded facies in the most distal sections. The model is interpreted in terms of decelerating turbulent suspensions with increasing distance travelled and is therefore very similar in its variations and process to that observed in many turbidity-current deposits.

The lateral facies variations in wet-surge deposits described here were observed on the island of Linosa, located in the Sicilian channel south of Agrigento where the deposits are the result of phreatomagmatic activity (Lanti *et al.*, 1988). The presence of vesiculated tuffs, abundant mud-coated clasts and accretionary lapilli in these deposits is considered good evidence that the surges which transported the clasts were wet. The lateral variations of facies in these wet-surge deposits show a general decrease of bed thickness and grain size downcurrent from the vent (Fossa Cappellano, Fig. 21) to the more distal section (Punta Calcarella), for a distance of 2.5 km. The general primary-structure sequences vary as in turbidites. In the most proximal section (Section 1, Fig. 21) more than 80 per cent of the beds are massive. This massive facies passes downflow into a sequence where nearly 50 per cent of the beds show a parallel-laminated division overlying a normally graded or massive division (Section 2, Fig. 21). This second lateral facies is replaced at about 1 km from the vent by a sequence of thinner beds with a primary-structure sequence of normal grading overlain by parallel laminae. Here, however, dune cross beds make up an important proportion of the section (Section 3, Fig. 21). In the most distal section (Section 4, Fig. 21), most beds exhibit dune-type cross bedding. This lateral variation of facies

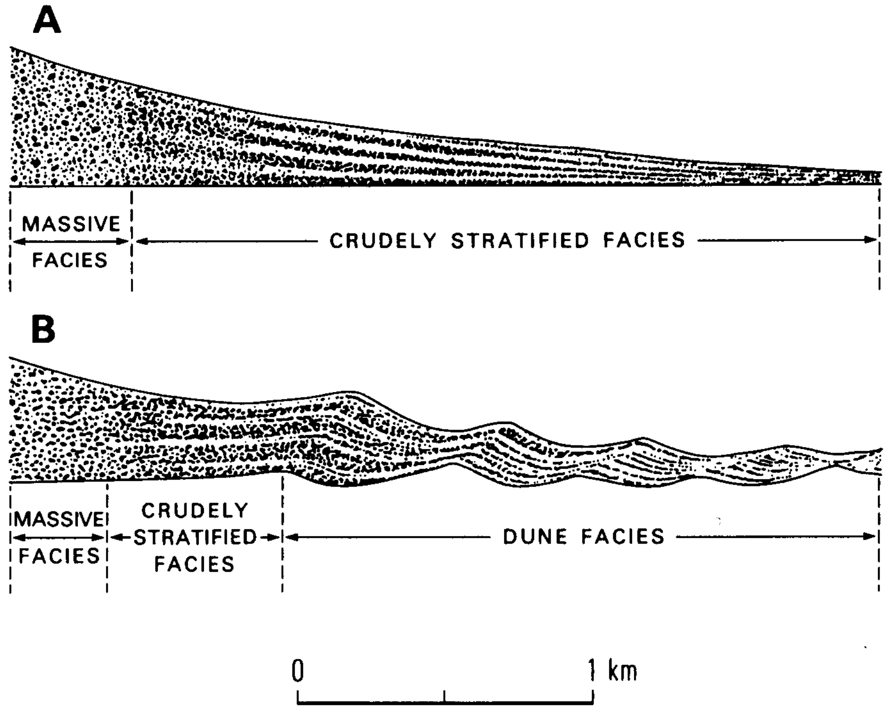

Figure 20 Lateral facies variations in dry-surge deposits from Cheju Island, Korea. Modified from Sohn and Chough (1989).

Table 2 *Differences that may be observed between beds of pyroclastic fall and flow deposits.*

	Fall	Flow
Sorting	Well sorted.	Poorly sorted.
Bed thickness	Regular and drapes the underlying surface (mantle bedding).	Irregular; thins over highs, thickens in depressions; thins laterally towards channel margins.
Grading and laminae	Massive beds are rare; normal grading is rare, but present. Absence of well-defined traction structures such as parallel and oblique laminae, but crude strata are common.	Massive beds, reverse grading are common in deposits having accumulated from laminar suspensions (debris and grain flows). Normal grading is common in deposits from turbulent suspensions and is commonly found underlying or overlying a laminae division.
Other primary structures	Bomb-sags and accretionary lapilli are common in subaerial or shallow water deposits. Gas-escape pipes are absent.	Accretionary lapilli occur in upper beds of some subaerial nuées ardentes. Rare or absent in subaqueous deposits. Gas-escape pipes are common.
Primary structure sequences	Absent.	Common, and are generally similar to those observed in other mass-transported sediments.

in a wet-surge deposit is identical to the above model proposed by the Koreans for dry-surge deposits, and in all probability both sequential variations originate from similar processes.

The above proposed models of lateral facies variations in the Korean and Italian surge deposits are new and insufficiently tested to be considered predictors. However, they are in our opinion excellent working hypotheses.

Subaqueous pyroclastic deposits

Pyroclastic fragmentation is explosive by definition. Explosions caused by magmatic volatiles can only occur when pressure within the magma exceeds the water pressure of the subaqueous environment. This is the pressure compensation level (PCL; Fisher, 1984), which should normally be at relatively shallow depths. The evidence suggests that the PCL for most explosive basaltic eruptions is less than 200 m, and it seems

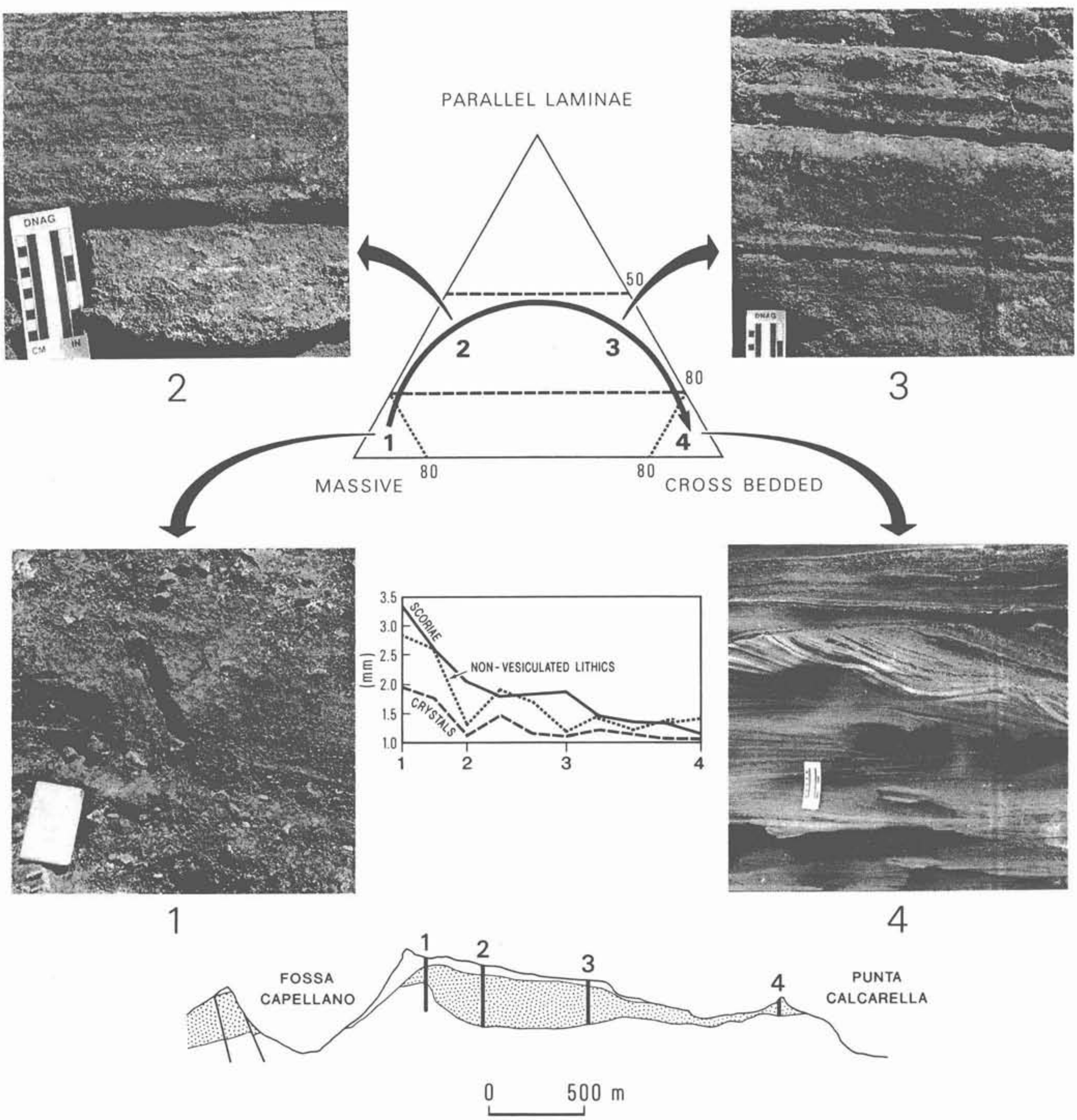

Figure 21 Lateral facies variations in wet-surge deposits from Linosa Island, Italy. The upper triangle gives the relative proportion of the primary structures in the stratigraphic sections which are localized in the lower cross section. Grain-size variations are given for the different grain textures. The small bars on the scale in photos 2, 3, and 4 are cm. The notebook in photo 1 is 19 cm in height.

that acid magma cannot vesiculate significantly at depths greater than a few tens of metres. Consequently most authors favour a shallow water or a subaerial origin for the pyroclasts found in subaqueous pyroclastic deposits.

Subaqueous pyroclastic flows can develop from subaerial nuées ardentes that moved into water. Because of their high density, the Merapi and St. Vincent nuées ardentes should continue to flow along the bottom, as they reach water level. Where the slope is sufficiently steep, these flows may become turbulent, mix with water, and produce cool, unwelded deposits. They may, however, enter water without mixing and retain enough heat to produce welded deposits. Many workers do not believe that hot pyroclastic flows can be deposited under water, although a few authors report welded tuffs from marine sequences. The water interaction should be different for the low-density, high-velocity Pelée-type nuées ardentes. As these turbulent nuées reach water, the ash cloud overlying the denser lower portion of the flow floats on the denser water (Anderson and Flett, 1903; Lacroix, 1904). The denser lower portion is assumed to continue its route under water. Here, mixing with ambient fluid is almost certain because the flow is turbulent as it enters water. There are no examples of Pelée-type deposits reported from the literature on subaqueous pyroclastic deposits. It may be that the three-bed division which is observed in subaerial deposits is lost due to flow separation of the upper part and mixing with water of the lower portion of the flow.

Descriptions of subaqueous pyroclastic deposits are rare. The evidence for subaqueous deposition is generally determined indirectly on stratigraphic arguments using sequence associations, interbedded pillow lavas, or fossils, and is not always convincing. The presence of normal grading, cross laminae, and slump structures, for example, is not very solid evidence for subaqueous transport and accumulation, as is shown by the above descriptions of the St. Helens and Mount Pelée subaerial deposits.

The two examples that will be used to describe the lateral facies variations in subaqueous pyroclastic deposits are taken from the Neogene of Japan, and from the Archean of Rouyn-Noranda, Canada.

The subaqueous deposits of Japan were erupted just above water level and deposited in a lake 200 to 500 m deep (Yamada, 1984). Flows travelled for a maximum of 8 km. The proximal facies, observed over the first 2 km (Fig. 22) consists of massive or chaotic breccia with cobble- and pebble-sized lithic fragments, some of the larger blocks showing radial jointing due to quenching, which suggests that they were hot at the time of deposition.

The intermediate facies, 2 to 4 km downcurrent, is characterized by a sequence of beds which have erosive lower contacts and are normally graded, and in which parallel laminae gradually develop upwards. Shattered crystals, the result of rapid cooling, are common in this facies. In the uppermost units, cross laminae may be present. Locally, accretionary lapilli are scattered in the upper tuffs.

The distal facies, 4 km downflow, is distinguished by finer grain sizes and the absence of the massive lower portion of the vertical sequence (Fig. 22).

Yamada (1984) compared the vertical primary structure sequence in these subaqueous deposits to that observed in high-density turbidity current deposits (the R-S-T sequence of Lowe, 1982).

The deposits of the Archean example extend laterally for 17 km, and range in thickness from some 260 m in the proximal sections to 120 m in the distal sections (Tassé *et al.*, 1978). Pillow lavas are found both underlying and overlying the pyroclastic sequence. The pyroclasts are andesitic in composition, consisting of lithic fragments, crystals, and scoriae. The presence of abundant and large scoriae suggests very shallow water or subaerial eruptions. The scoriae are more deformed than the whole rock, indicating that they were still hot at the time of deposition. These Archean pyroclastic deposits are therefore believed to be primary. In these deposits the ratio between lithic fragments and scoriae decreases with distance from the vent, that is, the amount of scoriae increases downflow. This relationship has also been observed in recent deposits, and is opposite to the scoria-lithic ratio commonly found in pyroclastic fall deposits. This is due to the lower density of the scoria which settles at lower velocity, and is thus found further downflow.

In the studied sections of the Archean deposits, there are two distinct bed types with different mean thickness, grain size, and primary structures. The two bed types were treated in two different statistical assemblages (A and B beds, Fig. 23). Type A beds (Fig. 24) are thicker than type B (Fig. 25). Mean bed thickness increases downflow in type A, whereas it decreases in type B. Grain size varies upsection, but generally it decreases in the direction of transport in both bed types. Primary structure sequences vary systematically away from the vent, but the sequences are different in both bed types. In type A beds, the most abundant structure is grading, and parallel laminae are rare. The proximal section has a high proportion of massive or reversely graded beds, whereas the distal section is characterized by normal grading with a greater number of beds where parallel laminae are present. The two intermediate sections show a gradation from the proximal to the distal facies. Normal grading is the rule in type B beds. Traction structures, such as parallel and oblique laminae (dunes and ripples) are more abundant than in type A, and their proportion increases

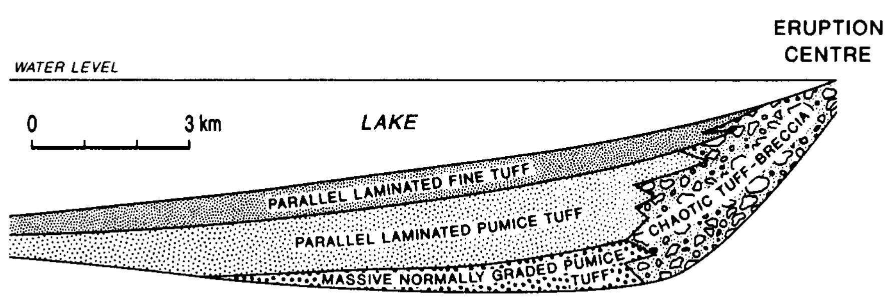

Figure 22 Lateral variations of size and primary structures in a subaqueous pyroclastic deposit of Japan. No vertical scale. Modified from Yamada (1984).

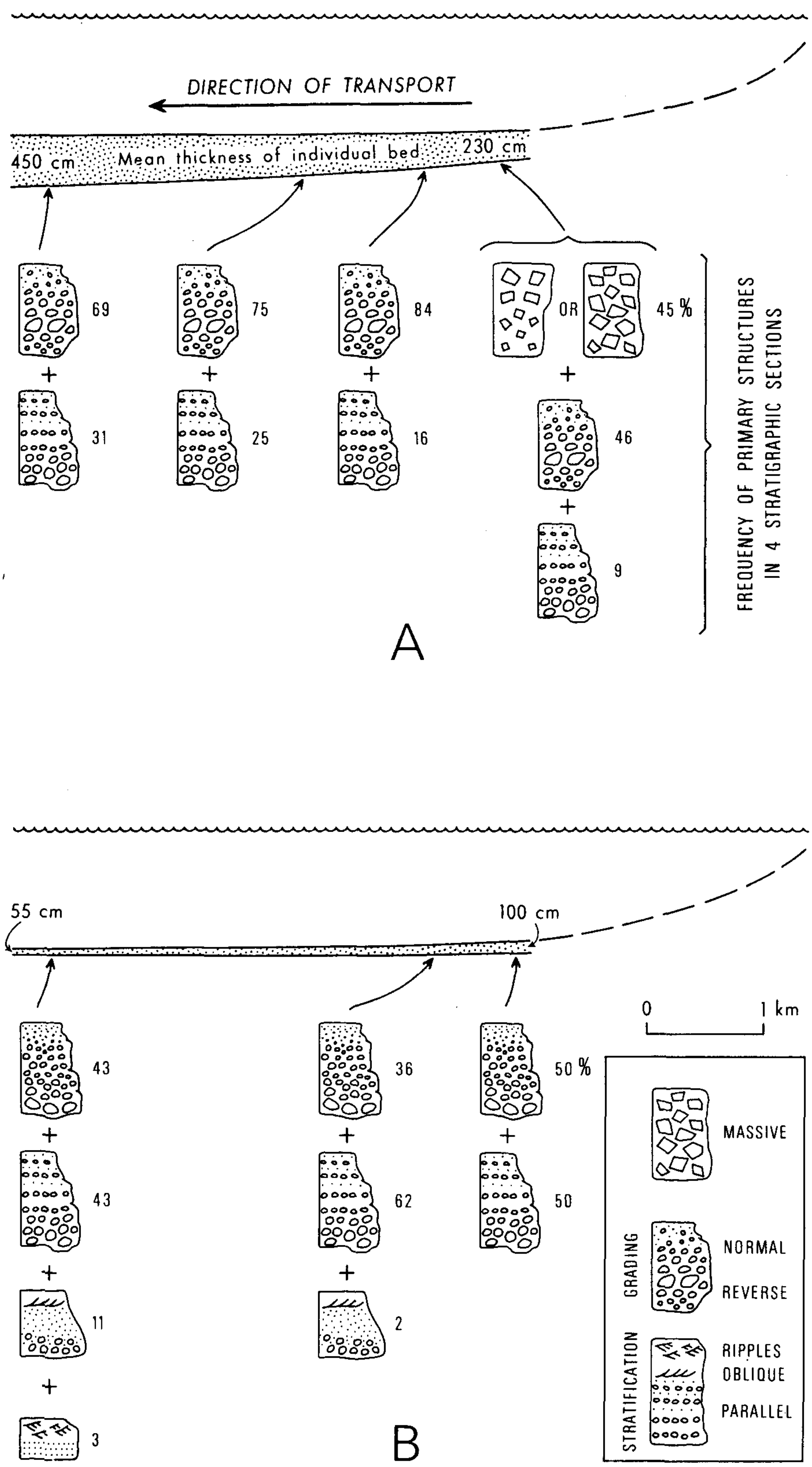

Figure 23 Lateral variations of mean bed thickness and primary structure sequences in the direction of transport in an Archean subaqueous pyroclastic deposit. The variations are shown for high concentration (A) and low-concentration (B) suspensions (see text). The frequency distributions of structure sequences, in percentages, total 100 at each locality or section. Modified from Tassé *et al.* (1978).

with distance of transport.

Tassé *et al.* (1978) interpreted the above lateral facies variations in subaqueous pyroclastic flow deposits by analogy with sedimentary density flows. Type B beds probably result from the accumulation of decelerating turbulent suspensions of low density (turbidity currents). Most of the flows responsible for type A beds appear to have been turbulent in distal regions. Almost half (45 per cent) of the beds in the more proximal section have characteristics that are best interpreted as the result of a concentrated suspension of cohesionless solids exhibiting non-Newtonian behaviour. Here, dispersive pressure played an important role in the suspension of the clasts, (inertial, density-modified, grain flow).

An integrated working hypothesis

Although there has been much work done on pyroclastic deposits since the publication of the second edition of *Facies Models*, the data are still spotty. Most models of vertical and lateral variations in volcaniclastic rocks are recent, and have not been tested adequately. However, the data presently available may be used to propose an integrated, idealized working hypothesis for facies variations from a subaerial vent to a subaqueous environment. Facies in pyroclastic rocks reflect variations in flow density, viscosity and velocity, as well as transport distance from the vent. For example, there are Pelée nuée-ardente deposits on Merapi volcano, and Merapi deposits on Mount Pelée (Fig. 18). Most models of lateral and vertical facies variations that have been proposed can be explained by analogy with other sedimentary mass-flow deposits. This approach is used to suggest an idealized scenario of lateral facies variations in pyroclastic rocks (Fig. 26). In this model, deposits of Pelée-type nuées ardentes are restricted to subaerial aprons and lobes. The Merapi and St. Vincent nuée-ardente deposits are channelled and are not restricted to the subaerial environment. Entering water, there is a high probability that the flow mixes with water and that it transforms into lower concentration turbulent suspensions, resulting in subaqueous type B beds described above. From the vent to the most distal sections, bed thickness and grain size decrease, and as in other sedimentary mass-flow deposits, primary structure sequences evolve from high flow power sequences to low flow power ones.

Distinctions between pyroclastic flow and fall deposits

It is commonly not an easy exercise to distinguish between pyroclastic fall and flow, and some of the differences (Table 2) may be very subtle. Mantle bedding is characteristic of fall deposits. The deposit drapes underlying irregularities with little or no thickness variations except on relatively steep slopes. Since the pioneer work of Murai (1961), much work has been done with statistical parameters of grain size distributions to help distinguish the various types of unconsolidated and consolidated pyroclastic deposits, but with limited success. Most of the problems with the techniques originate from the almost universal use of 1ϕ intervals in these analyses, leading to useless data. Commonly, the distributions are not log-normal and better fit a Rosin law. Thus the median, generally used as a defining parameter of the distributions, is inappropriate. On the other hand, primary structures, and particularly primary structure sequences, can be used successfully to distinguish among the various types of pyroclastic deposits.

SUMMARY

In this chapter we have presented what is known of facies relationships in autoclastic and pyroclastic deposits. Autoclastic fragments that are formed in situ are monogenetic and not welded. They may be transitional with the parent lava flow, and have the same composition. The internal structures in these deposits suggest the absence or near absence of transport.

Pyroclastic fall deposits are crudely stratified and commonly show a systematic lateral decrease in grain size and bed thickness downwind. In these deposits, sorting is poorest close to source due to ballistic emplacement and settling of fragments of different densities. In fall deposits, the vertical variations are controlled by eruption intensity and are therefore unpredictable.

In nuée ardente deposits, bed thickness and grain size generally decrease downflow, but close to vent the variations are not systematic and may even be reversed. Beds are commonly graded in these deposits. In subaqueous deposits the grading of all fragments is generally normal, but in many subaerial deposits pumices and scoriae are reversely graded. The primary structure sequences vary systematically downflow in most of the deposits and depict changing flow conditions and grain sizes that are being transported.

ACKNOWLEDGEMENTS

Léopold Gélinas, John Ludden, and Roger Walker read the earlier editions of this chapter and offered many helpful suggestions. We thank Michel Demidoff for careful work on the illustrations. The research leading to many of the proposed models in this chapter was supported by the Natural Sciences and Engineering Research Council of Canada.

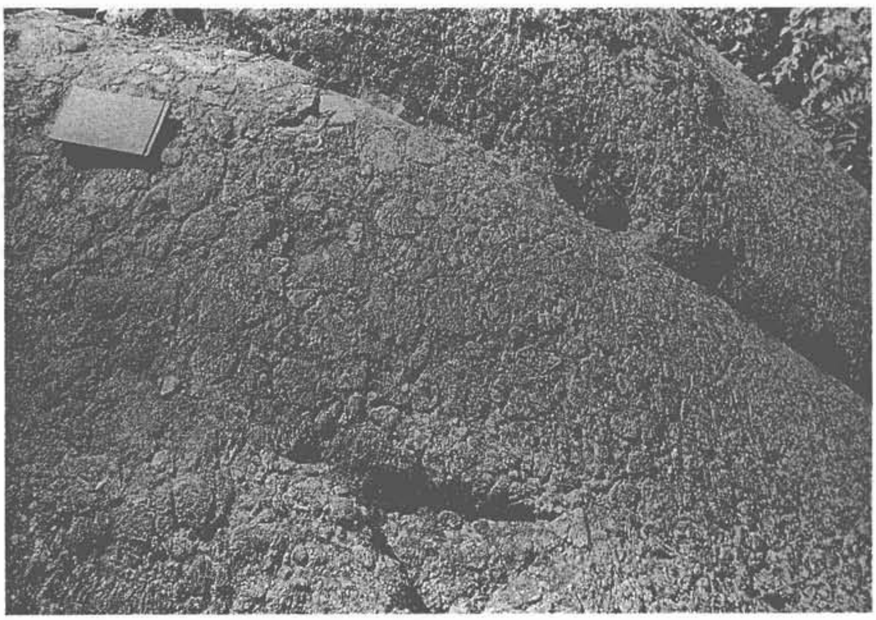

Figure 24 Reversely graded subaqueous pyroclastic flow deposit of Archean age, Rouyn-Noranda, Québec. Top is left. Notebook is 30 cm long.

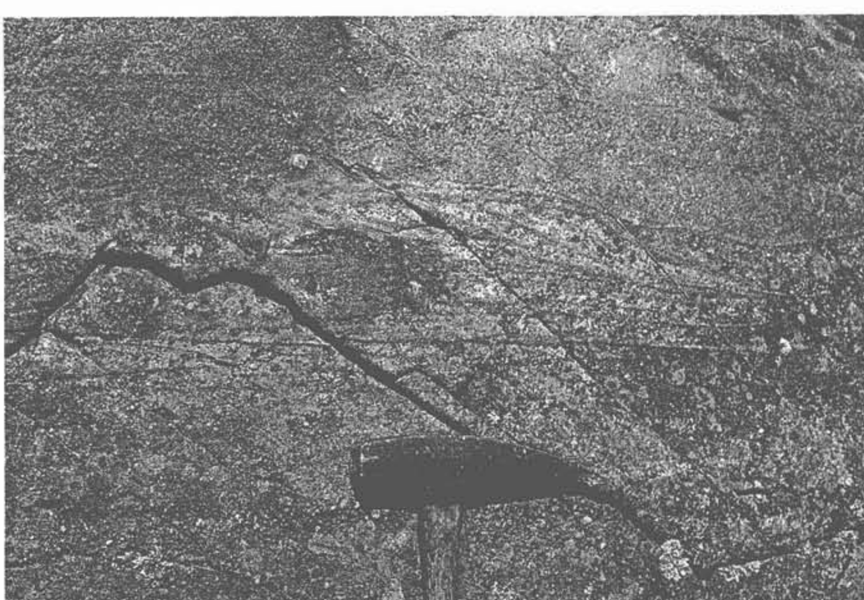

Figure 25 Primary-structure sequence in a type B bed. From base to top: normal grading, parallel laminae, ripples. Archean of Rouyn-Noranda.

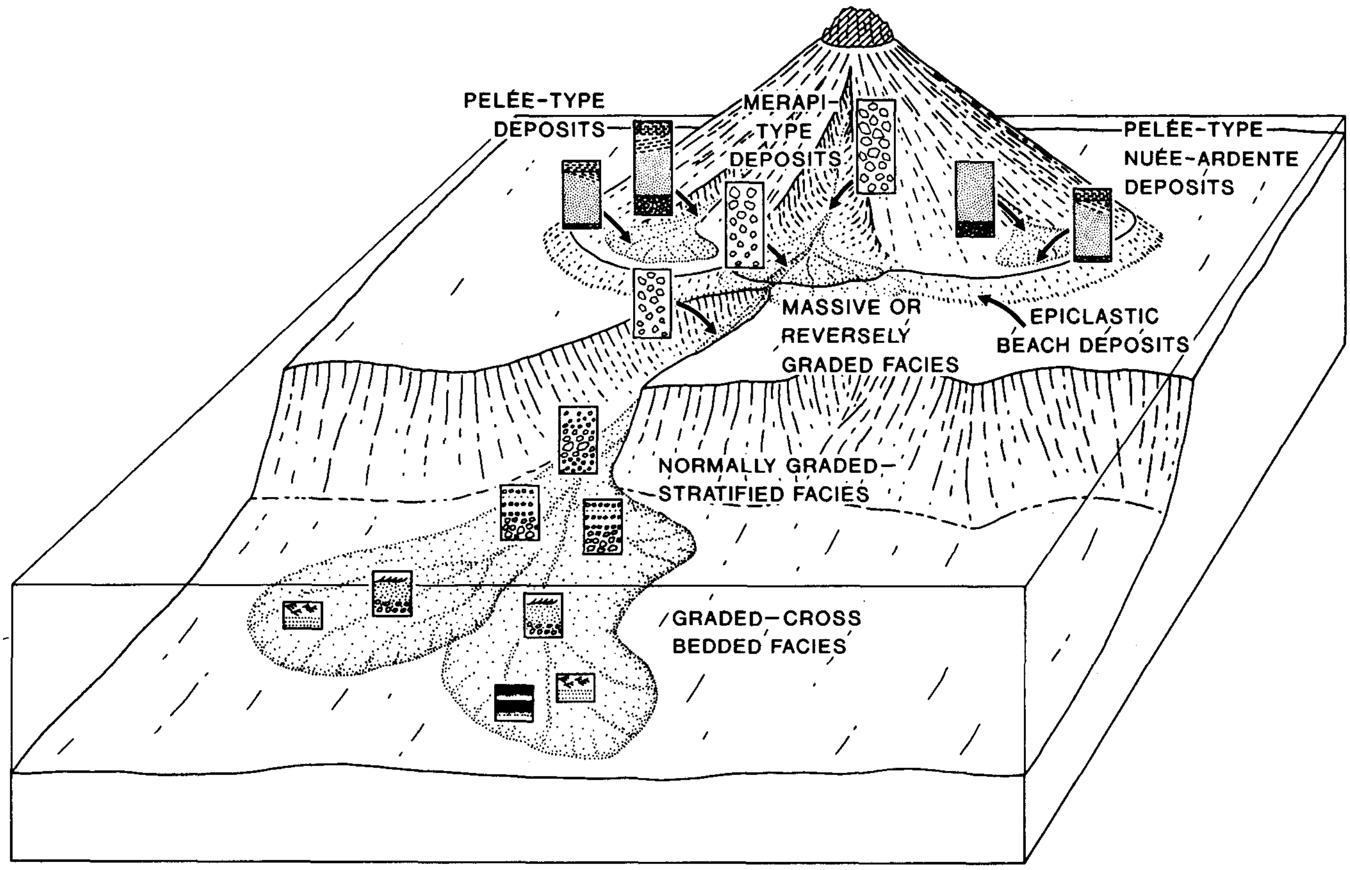

Figure 26 Idealized vertical and lateral facies variations in subaerial and subaqueous environments for an explosive island volcano.

REFERENCES

Basic sources of information

Anderson, T. and Flett, J.S., 1903, Report on the eruptions of the Soufrière in St. Vincent, in 1902, and on a visit to Montagne Pelée, in Martinique — Part I: Royal Society of London, Philosophical Transactions, v. A200, p. 353-553.
A classic study of the St. Vincent-type nuées ardentes, at the type locality. Good descriptions of the phenomena and of the deposits. Recommended reading for those working on pyroclastic flow deposits.

Carey, S. and Sparks, R.S.J., 1986, Quantitative models of the fallout and dispersal of tephra from volcanic eruption columns: Bulletin of Volcanology, v. 48, p. 109-125.
The application of lithic clast size isopleths in determining eruption column heights.

Cas, R.A.F. and Wright, J.V., 1987, Volcanic successions: modern and ancient: Boston, Allen & Unwin, 528 p.

Escher, B.G., 1933, On a classification of central eruptions according to gas pressure of the magma and viscosity of the lava and on the character of the Merapi eruption in central Java: Leidsche Geologische Mededelingen, v. 6, p. 45-58.
An old, but classic classification of volcanic eruptions.

Fisher, R.V. and Schmincke, H.-U., 1984, Pyroclastic rocks: New York, Springer-Verlag, 528 p.
An excellent text with good descriptions and illustrations, with many personal comments and suggestions. Makes interesting reading.

Heiken, G.H. and Wohletz, K.H., 1985, Volcanic ash: Berkeley, University of California Press, 246 p.
Petrography, chemical analyses, electron microscopy with grain size analyses and standard accumulation sequences of most types of ash deposits. Excellent descriptions and photographs.

Kokelaar, B.P. and Howells, M.F., eds., 1984, Marginal Basin Geology. Volcanic and associated sedimentary and tectonic processes in modern and ancient marginel basins: Geological Society of London, Special Publication, 322 p.

Lacroix, A., 1904, La montagne pelée et ses éruptions: Paris, Masson et cie, 662 p.
The classic study that defined the three different types of nuée ardente. A must for anyone working on these rocks.

Lipman, P.W. and Mullineaux, D.R., 1981, The 1980 eruptions of Mount St. Helens, Washington. United States Geological Survey, Professional Paper 1250, 844 p.
Perhaps the most comprehensive study of a single eruption with excellent text, illustrations and photographs. Considering its price, it is a gift from the U.S. Government. A must for students of pyroclastic deposits.

Macdonald, G.A., 1972, Volcanoes: Englewood Cliffs, NJ, Prentice-Hall Inc., 510 p.

Pyle, D.M., 1989, The thickness, volume and grain size of tephra fall deposits: Bulletin of Volcanology, v. 51, p. 1-15.
An interesting article that examines exponential behaviour of fallout thicknesses and granulometry. The author presents new ways to calculate volumes and classify deposits.

Williams, H. and McBirney, A.H., 1979, Volcanology: San Francisco, Freeman, Cooper and Company, 387 p.

Walker, G.P.L., 1973, Explosive volcanic eruptions — a new classification scheme: Geologische Rundschau, v. 62, p. 431-446.
An important article that looks at the characteristics of different fallout deposits and proposes a dispersal-fragmentation classification scheme.

Wilgus, C.K., Hastings, B.S., Posamentier, H.W., Ross, C.A. and Kendall, C.G.St.C., eds., 1988, Sea level changes: an integrated approach: Society of Economic Paleontologists and Mineralogists, Special Publication 42, 402 p.
Collection of papers emphasizing conceptual basis of sequence stratigraphy plus numerous case studies of sea level change from the geological record.

Other references

Booth, B., Croasdale, R. and Walker, G.P.L., 1978, A quantitative study of five thousand years of volcanism on Sao Miguel, Azores: Royal Society of London, Philosophical Transactions, v. A288, p. 271-319.

Boudon, G. and Lajoie, J., 1989, The 1902 Pelean deposits in the Fort Cemetery of St. Pierre, Martinique: a model for the accumulation of turbulent nuées ardentes: Journal of Volcanology and Geothermal Research, v. 38, p. 113-130.
A new model of Pelée-type nuée-ardente deposit from the type locality.

Boudon, G., Bourdier, J.L., Gourgaud, A. and Lajoie, J., 1990, The May 1902 eruptions of Mount Pelée: high-velocity directed blasts or column-collapse nuées ardentes? Journal of Volcanology and Geothermal Research, v. 43, p. 359-364.

Brissette, F.P. and Lajoie, J., 1991, Depositional mechanics of turbulent nuées ardentes (surges) from their grain sizes: Bulletin of Volcanology, v. 53, p. 60-66.
Discussion of settling velocities of pyroclasts of different grain size parameters (mean, coarse, fine) in suspensions of varying densities. A method to evaluate mean-flow velocity in low concentration, turbulent nuées ardentes, independently of flow density.

Carey, S. and Sigurdsson, H., 1986, The 1982 eruptions of El Chichon volcano, Mexico (2): Observations and numerical modelling of tephra-fall distribution: Bulletin of Volcanology, v. 48, p. 127-141.

Carlisle, D., 1963, Pillow breccias and their aquagene tuffs. Quadra Island, British Columbia: Journal of Geology, v. 71, p. 48-71.

Charland A. and Lajoie J., 1989. Characteristics of pyroclastic deposits at the margin of Fond Canonville, Martinique, and the implications for the transport of the 1902 nuées ardentes of Mount Pelée: Journal of Volcanology and Geothermal Research, v. 38, p. 97-112.

Chough, S.K. and Sohn, Y.K., 1990, Depositional mechanics and sequences of base surges, Songaksan tuff ring, Cheju Island, Korea: Sedimentology, v. 37, p. 1115-1135.

Fink, J., 1980, Surface folding and viscosity of rhyolite flows: Geology, v. 8, p. 250-254.

Fisher, R.V., 1984, Submarine volcaniclastic rocks, *in* Kokelaar, B.P. and Howells, M.F.,eds., Marginal Basin Geology. Volcanic and associated sedimentary and tectonic processes in modern and ancient marginal basins: Geological Society of London, Special Publication, p. 5-27.

Francis, P.W., Glaze, L.S., Pieri, D., Oppenheimer, C.M.M. and Rothery, D.A., 1990, Eruption terms: Nature, v. 346, p. 519.

Furnes, H., Fridleifsson, I.B. and Atkins, F.B., 1980, Subglacial volcanics-on the formation of acid hyaloclastite: Journal of Volcanology and Geothermal Research, v. 8, p. 95-110.

Honnorez, J. and Kirst, P., 1975, Submarine basaltic volcanism: morphometric parameters for discriminating hyaloclastites from hyalotuffs: Bulletin Volcanologique, v. 39, p. 441-465.

Kittleman, L.R., 1973, Mineralogy, correlation, and grain-size distributions of Mazama tephra and other post-glacial pyroclastic layers; Pacific Northwest: Geological Society of America Bulletin, v. 84, p. 2957-2980.

Lanti, E., Lanzafame, G., Rossi, P.L., Tranne, C.A. and Calanchi, N., 1988, Vulcanisimo e tettonica nel Canale di Sicilia: l'isola di Linosa: Mineralogia e Petrographia Acta, v. 31, p. 69-94.

Lowe, D.R., 1982, Sediment gravity flows: II. Depositional models with special reference to the deposits of high-density turbidity currents: Journal of Sedimentary Petrology, v, 52, p. 279-297.

Moore, J.M. and Sisson, T.W., 1981, Deposits and effects of the May 18 pyroclastic surge, *in* Lipman, P.W. and Mullineaux, D.R., eds., The 1980 eruptions of Mount St. Helens, Washington: United States Geological Survey, Professional Paper 1250, p. 421-438.

Murai, I., 1961, A study of the textural characteristics of the pyroclastic flows of Japan: Bulletin of the Earthquake Research Institute, v. 39, p. 133-248.

Sarna-Wojcicki, A.M., Shipley, S., Waitt, R.B., Dzurisin, D. and Wood, S.H., 1981, Areal distribution, thickness, mass, volume, and grain size of air-fall ash from six major eruptions of 1980, *in* Lipman, P.W. and Mullineaux, D.R., eds., The 1980 eruptions of Mount St. Helens, Washington: United States Geological Survey, Professional Paper 1250, p. 577-600.

Self, S. and Sparks, R.S.J., 1978, Characteristics of widespread pyroclastic deposits formed by the interaction of silicic magma and water: Bulletin Volcanologique, v. 41, p. 196-212.

Sigurdsson, H., Sparks, R.S.J., Carey, S.N. and Huang, T.C., 1980, Volcanogenic sedimentation in the Lesser Antilles Arc: Journal of Geology, v. 88, p. 523-540.

Sohn, Y.K. and Chough, S.K., 1989, Depositional processes of the Suwolbong tuff ring, Cheju Island (Korea): Sedimentology, v. 36, p. 837-855.

Tassé, N., Lajoie, J. and Dimroth, E., 1978, The anatomy and interpretation of an Archean volcaniclastic sequence, Noranda region, Québec: Canadian Journal of Earth Sciences, v. 15, p. 874-888.

Walker, G.P.L., 1971, Grain-size characteristics of pyroclastic deposits: Journal of Geology, v, 79, p. 696-714.

Walker, G.P.L., 1980, The Taupo Pumice: product of the most powerful known (ultraplinian) eruption?: Journal of Volcanology and Geothermal Research, v. 8, p. 69-94.

Walker, G.P.L. and Croasdale, R., 1971, Two plinian-type eruptions in the Azores: Journal of the Geological Society of London, v. 127, p. 17-55.

Walker, G.P.L., Self, S. and Wilson, L., 1980, Tarawera 1886, New Zealand — a basaltic plinian fissure eruption: Journal of Volcanology and Geothermal Research, v. 21, p. 61-78.

Wohletz, K.H. and Sheridan, M.F., 1979, A model of pyroclastic surge, *in* Chapin, C.E. and Elston, W.E., eds., Ash-flow tuffs: Geological Society of America, Special Paper 180, p. 177-194.

Yamada, E., 1984, Subaqueous pyroclastic flows: their development and their deposits, *in* Kokelaar, B.P. and Howells, M.F., eds., Marginal Basin Geology. Volcanic and associated sedimentary and tectonic processes in modern and ancient marginal basins: Geological Society of London, Special Publication, p. 29-35.

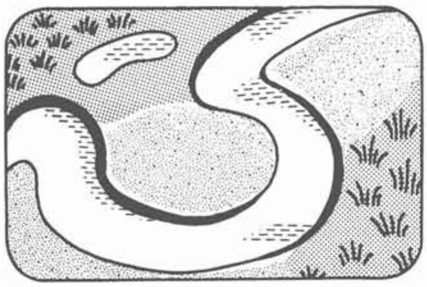

7. Alluvial Deposits

Andrew D. Miall, Department of Geology, University of Toronto,
Toronto, Ontario M5S 3B1

INTRODUCTION

Alluvial deposits are an important component of the stratigraphic record. They occur in a wide range of tectonic settings, and are sensitive indicators of *allogenic* (extrabasinal) controls such as tectonism and sea level change. They host major nonrenewable resources such as petroleum, placer gold and uranium. Much of the oil in the giant fields at Prudhoe Bay (Alaska), Brent (North Sea), and Daqing (China) occurs in fluvial reservoirs. Mineral deposits include gold, uranium and diamonds in the Witwatersrand Supergroup (South Africa). Uranium is found in the Huronian Supergroup (Ontario), and in the Morrison Formation (Colorado Plateau). Many important coal deposits are of fluvial origin, including some of the Pennsylvanian coals of West Virginia and Kentucky, and some Tertiary coals of the Western Interior Basin in Alberta, Wyoming and Colorado.

Alluvial sediments are predominantly clastic, ranging in grain size from the finest mud to the coarsest boulder conglomerates. Minor chemical sediments are formed in floodplain environments. They include nodular carbonate deposits formed in fossil soils *(paleosols)*, some coals, and minor evaporites deposited in nonmarine sabkhas.

SUBDIVISION OF ALLUVIAL DEPOSITS IN THIS CHAPTER

On a small scale, various types of stratification and bedforms can be recognized in alluvial deposits. Larger depositional units are termed *bars* (Fig. 1). Channels are filled by a wide variety of bars and bedforms. There are some common patterns of geometry and composition in these deposits, whatever the channel style. This has enabled sedimentologists to erect standardized classifications of the deposits at two distinct scales. The smaller scale includes the individual building-blocks, or *facies*, of the deposit. At a somewhat larger scale, these facies assemblages can be grouped into *architectural elements* characterized by distinctive shapes and internal geometries that represent some of the major types of bar and channel formation within fluvial systems.

On a still larger scale, four styles of fluvial channels have traditionally been recognized, *meandering, braided, anastomosed* and *straight*. Most of the coarse, porous beds that host petroleum and mineral deposits are formed within the channels and their associated bar deposits, and so an understanding of the architecture of the various types of channel fill is critical. In nature, there are many variations between the four basic end member channel styles.

On a much broader scale, important aspects of alluvial sediments concern their location on the earth's surface, and the control of their large-scale architecture. The study of alluvial deposits plays a key role in the reconstruction of the plate-tectonic evolution of sedimentary basins, and in deducing the history of relative changes in sea level within sed-

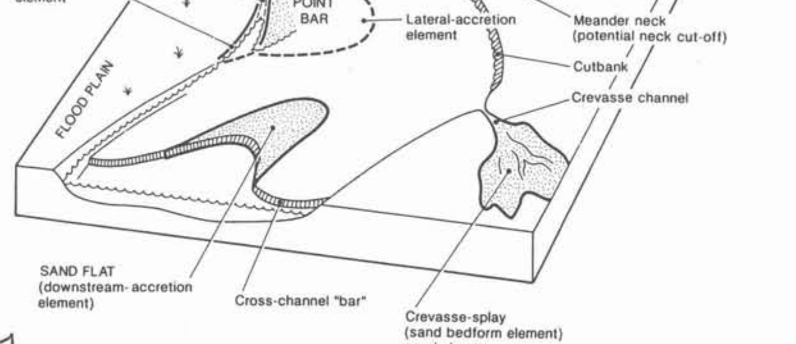

Figure 1 Block diagram of a hypothetical river, to illustrate some of the terms used in this chapter.

Figure 2 An exposed bar surface at the edge of a river channel (Congaree River, South Carolina). A field of dunes (10-20 cm high) was deposited on this surface when the water level was higher, and has now been abandoned. The crests are oriented perpendicular to flow (which is toward the viewer) and extend under water to the right, where the dunes may still be actively advancing. Photo courtesy of M.O. Hayes.

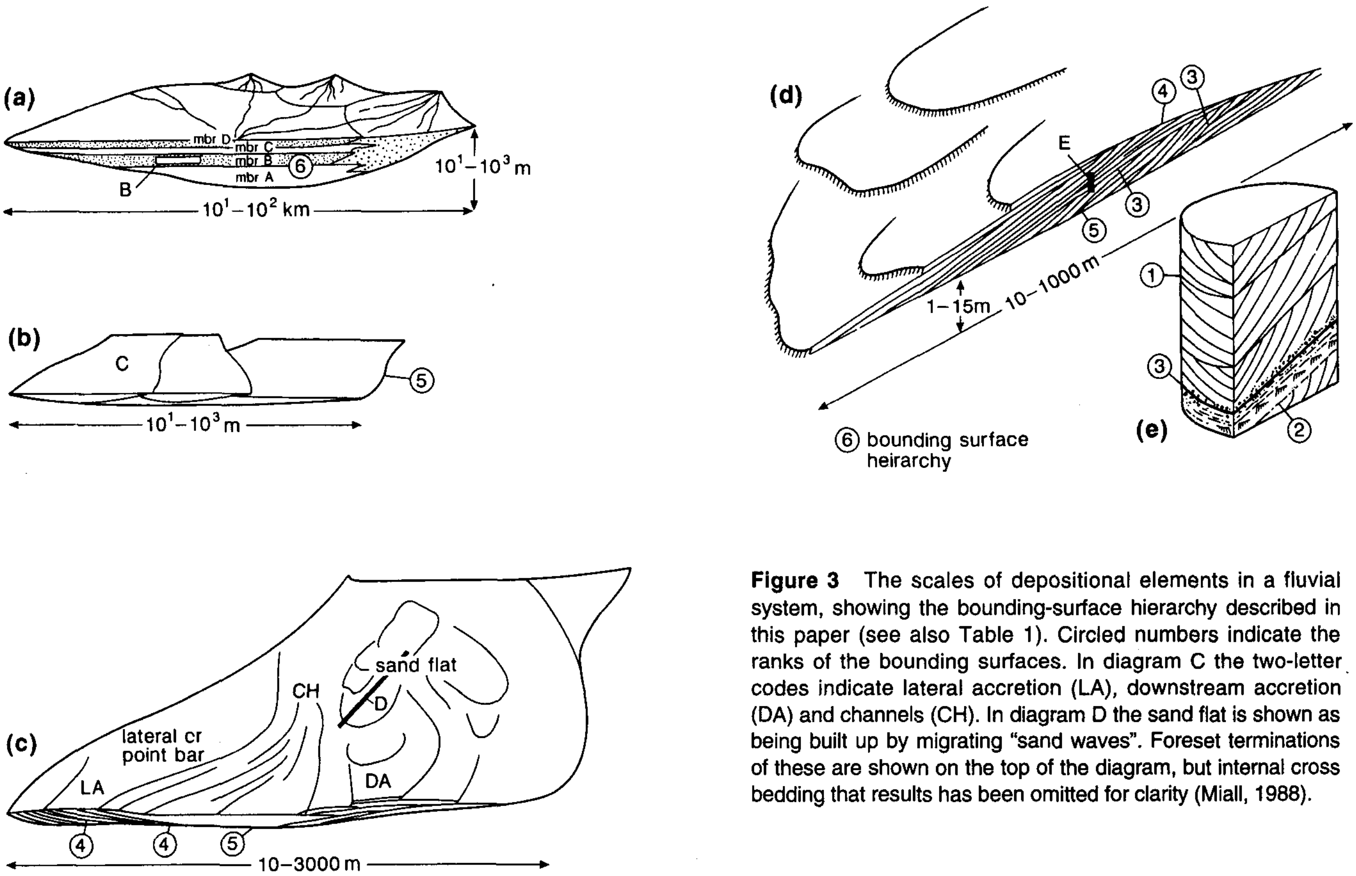

Figure 3 The scales of depositional elements in a fluvial system, showing the bounding-surface hierarchy described in this paper (see also Table 1). Circled numbers indicate the ranks of the bounding surfaces. In diagram C the two-letter codes indicate lateral accretion (LA), downstream accretion (DA) and channels (CH). In diagram D the sand flat is shown as being built up by migrating "sand waves". Foreset terminations of these are shown on the top of the diagram, but internal cross bedding that results has been omitted for clarity (Miall, 1988).

Table 1 *Hierarchy of depositional units in alluvial deposits. Modified from Miall (1991b).*

Group	Time scale of processes (a)	Examples or processes	Instantaneous sedimentation rate (m/ka)	Fluvial, deltaic depositional units	Rank and characteristics of bounding surfaces
1	10^{-6}	burst-sweep cycle		lamina	0th-order, lamination surface
2	10^{-5} - 10^{-4}	bedform migration	10^5	ripple (microform)	1st-order, set bounding surface
3	10^{-3}	bedform migration	10^5	diurnal dune increment, reactivation surface	1st-order, set bounding surface
4	10^{-2} - 10^{-1}	bedform migration	10^4	dune (mesoform)	2nd-order, coset bounding surface
5	10^0 - 10^1	seasonal events, 10-year flood	10^2 - 10^3	macroform growth increment	3rd-order, slipping 5-20° in direction of accretion
6	10^2 - 10^3	100-year flood, bar migration	10^2 - 10^3	macroform, e.g., point bar, levee, splay	4th-order, convex-up macroform top
7	10^3 - 10^4	long term geomorphic processes	10^0 - 10^1	channel, delta lobe	5th-order, flat to concave-up channel base
8	10^4 - 10^5	5th-order (Milankovitch) cycles	10^{-1}	channel belt sequence	6th-order, flat, regionally extensive
9	10^5 - 10^6	4th-order (Milankovitch) cycles	10^{-1} - 10^{-2}	depositional system alluvial fan, sequence	7th-order, sequence boundary; flat, regionally extensive
10	10^6 - 10^7	3rd-order cycles, Tectonic and eustatic processes	10^{-1} - 10^{-2}	*basin-fill complex*	*8th-order, regional disconformity*

imentary basins. Generally, alluvial sediments occur in two main settings, thick clastic wedges resulting from tectonic uplift of a major source area, and thinner, pod- or sheet-like bodies deposited on regional unconformity surfaces.

SEDIMENT TRANSPORT

Sediment is transported in rivers by two mechanisms, *traction currents* and *sediment gravity flows.* Traction currents are those which transport cohesionless sediment as dispersed grains, each moving individually. Large grains are moved by sliding or rolling along the bed *(bedload)*, smaller grains bounce along the bed or are swept along for short distances in suspension *(bed contact load).* Grains moved as bedload and by intermittent suspension typically accumulate in a variety of bedforms (Fig. 2). Migration of the bedforms produces the sedimentary structures seen in ancient deposits. The structures are characterized by their surface form or their internal stratification in cross section. The smallest grains, including the clay fraction, remain in suspension unless the water body comes to a complete rest, as in a floodplain pond or abandoned channel. At this time the grains will slowly settle out. The style in which the grains accumulate to form stratification and sedimentary structures is the basis for the definition of facies in traction-current deposits, as noted in the next section.

Most alluvial sediments are deposited from traction currents, but in certain settings sediment gravity flows may be important. These occur when large masses of loose sediment are mobilised by liquefaction on a sloping surface. Such occurrences are particularly common under water, but also occur subaerially, typically at times of heavy rainfall. The flow may start as a landslide, and develop into a moving body of wet, unsorted sediment termed a *debris flow.* Movement ceases when the flow loses momentum on a flat basin floor, and when the lubricating effect of the pore waters has been lost by the water draining out into the substrate. The result is an apparently chaotic deposit of poorly sorted debris, with large pebbles, cobbles, even giant boulders, mixed in together and usually separated from each other by a finer grained matrix of sand, silt and mud. Close examination may reveal a subtle sorting (grading) of the grains or the matrix, and a regular orientation of the larger clasts.

Two terms, *competence* and *capacity*, are used to describe the ability of a river to transport sediment. Competence indicates the grain size of sediment that can be transported, and relates to the strength of the flow (velocity, shear stress). Capacity indicates the total volume of sediment that can be moved, and is a reflection of the magnitude of the discharge.

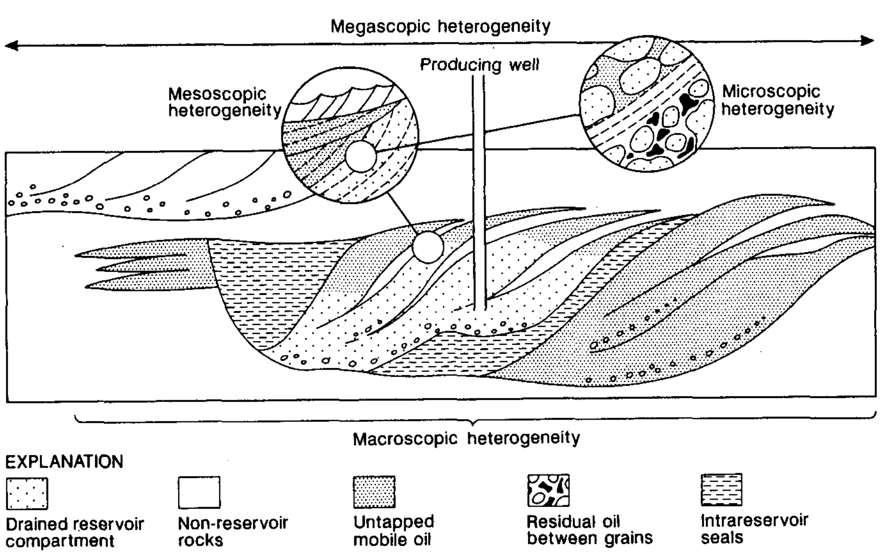

Figure 4 Schematic cross section through a meander belt sandstone, showing the various scales of heterogeneity, and the relation of these heterogeneities to the distribution of reservoir fluids. Note that much of the potential production will remain unproduced unless the geologist can reconstruct the architectural complexities of the reservoir, and position wells accordingly (Tyler, 1988).

A HIERARCHY OF SCALES OF DEPOSITIONAL UNITS

Geologists describe clastic deposits in terms of their natural depositional units, such as (in order of increasing scale) the bedform, bed, stratigraphic unit (member, formation, group), and basin fill complex. Fluvial depositional units can be subdivided into ten natural groups, based on their physical dimensions, their sedimentation rate, and the time scale represented by each type of unit (Table 1, Fig. 3). At each of these scales rock bodies are enclosed by *bounding discontinuities.* These include the contacts between beds and sedimentary structures, channel scours, the base and top of stratigraphic units, and the surfaces which define the major allogenic subdivisions of alluvial successions, such as regional unconformities. A sedimentological classification of these surfaces (Table 1, Fig. 3) is a useful tool for field studies, facilitating field description and leading to more comprehensive interpretations. Petroleum reservoir geologists recognize at least five scales of heterogeneity for purposes of calculating volumes and rates of production. Four of these are shown in Figure 4. Microscopic heterogeneity is concerned with porosity variations at the scale of individual sand grains (within group 1 of Table 1). Mesoscopic heterogeneity is that of bedding units and sedimentary structures (groups 1-4). Macroscopic heterogeneity includes the variability associated with the deposition of channels and bars (groups 5-7). Megascopic heterogeneity deals with the variations across major sedimentary units and entire basins (groups 8-10).

A wide variety of sedimentation rates are shown in Table 1. At each level of the hierarchy, instantaneous rates of sedimentation can be estimated from measurements in the laboratory, or determined from study of modern river sediments and ancient deposits (Miall, 1991b). However, rates measured from modern sediments usually bear little relation to geologically meaningful accumulation rates calculated from ancient rock units. Depositional rates in modern sediments can be estimated using ^{14}C techniques, or by studying the evolution of meanders and bars on maps and aerial photographs. These rates are typically far higher than those estimated from ancient geological units. This is because individual depositional units have a limited preservation potential, and any given sedimentary structure, bar or channel may be removed by erosion rather than become buried and preserved. The preservation potential becomes successively lower for smaller-scale units (smaller group numbers in Table 1). Long-term geological sedimentation rates necessarily include numerous episodes of nondeposition and erosion. The contrast between the average sediment accumulation rates in the upper and lower parts of Table 1 emphasizes how many depositional units and how much sediment may be deposited, only to be removed before it can be permanently preserved by burial.

FACIES

The study of sedimentary structures in modern river deposits played an important part in the development of our understanding of their hydrodynamic formation. Experimental work has recently been summarized by Ashley (1990) in a series of *phase diagrams*. These set out the flow depths, flow velocities and grain sizes that control the formation and stability of the various bedforms.

The recognition of sedimentary structures, and the ways in which they group together, is one of the main means by which geologists define facies (Chapter 1). Many years of study by fluvial sedimentologists have shown that a limited number of facies occur in alluvial environments. A classification erected by Miall (1977, 1978b; Table 2) is now in widespread use for surface outcrop studies and subsurface core analysis. Examples of facies types are given in Figures 5 and 6.

In gravels, an important distinction is that between matrix-supported (facies Gms; Fig. 5A) and clast-supported types (Figs. 5B, C). Matrix support indicates that clasts and matrix were deposited together, a characteristic of debris flows. The other facies are those deposited by traction currents.

Sand facies are characterized by a range of sedimentary structures indicating various conditions of deposition (Fig. 5D-G). The vertical succession of such facies is commonly repetitive, or cyclic, and indicates progressive change in depositional conditions. For example, a vertical decrease in grain size and in scale of cross bedding is a feature of the classic fining-upward point-bar succession (Allen, 1963), which is discussed in a later section of this chapter.

ARCHITECTURAL ELEMENTS

Definitions

A river consist of various straight and curved channel reaches, with large areas of exposed gravel, sand, or mud, termed *bars* (Fig. 7). The development and distribution of these features follows certain relatively predictable patterns that leave their record in the resulting deposits. The channels and bars are the basic depositional elements of the river, and can be subdivided into *architectural*

Table 2 *Facies classification. From Miall (1978b).*

Facies code	Facies	Sedimentary Structures	Interpretation
Gms	massive, matrix supported gravel	grading	debris flow deposits
Gm	massive or crudely bedded gravel	horizontal bedding, imbrication	longitudinal bars, lag deposits, sieve deposits
Gt	gravel, stratisfied	trough cross beds	minor channel fills
Gp	gravel, stratisfied	planer cross beds	longitudinal bars, deltaic growths from older bar remnants
St	sand, medium to very coarse, may be pebbly	solitary or grouped trough cross beds	dunes (lower flow regime)
Sp	sand, medium to very coarse, may be pebbly	solitary or grouped planer cross beds	linguoid, transverse bars, sand waves (lower flow regime)
Sr	sand, very fine to coarse	ripple cross lamination	ripples (lower flow regime)
Sh	sand, very fine to very coarse may be pebbly	horizontal lamination parting or streaming lineation	planer bed flow (upper flow regime)
Sl	sand, very fine to very coarse may be pebbly	low angle (<10°) cross beds	scour fills, washed-out dunes, antidunes
Se	erosional scours with intraclasts	crude cross bedding	scour fills
Ss	sand, fine to very coarse, may be pebbly	broad, shallow scours	scour fills
Fl	sand, silt, mud deposits	fine lamination, vey small ripples	overbank or waning flood
Fsc	silt, mud	laminated to massive	backswamp deposit
Fcf	mud	massive, with freshwater molluscs	backswamp pond deposits
Fm	mud, silt	massive, desiccation cracks	overbank or drape deposits
C	coal, carbonaceous mud	plant, mud films	swamp deposits
P	carbonate	pedogenic features	paleosol

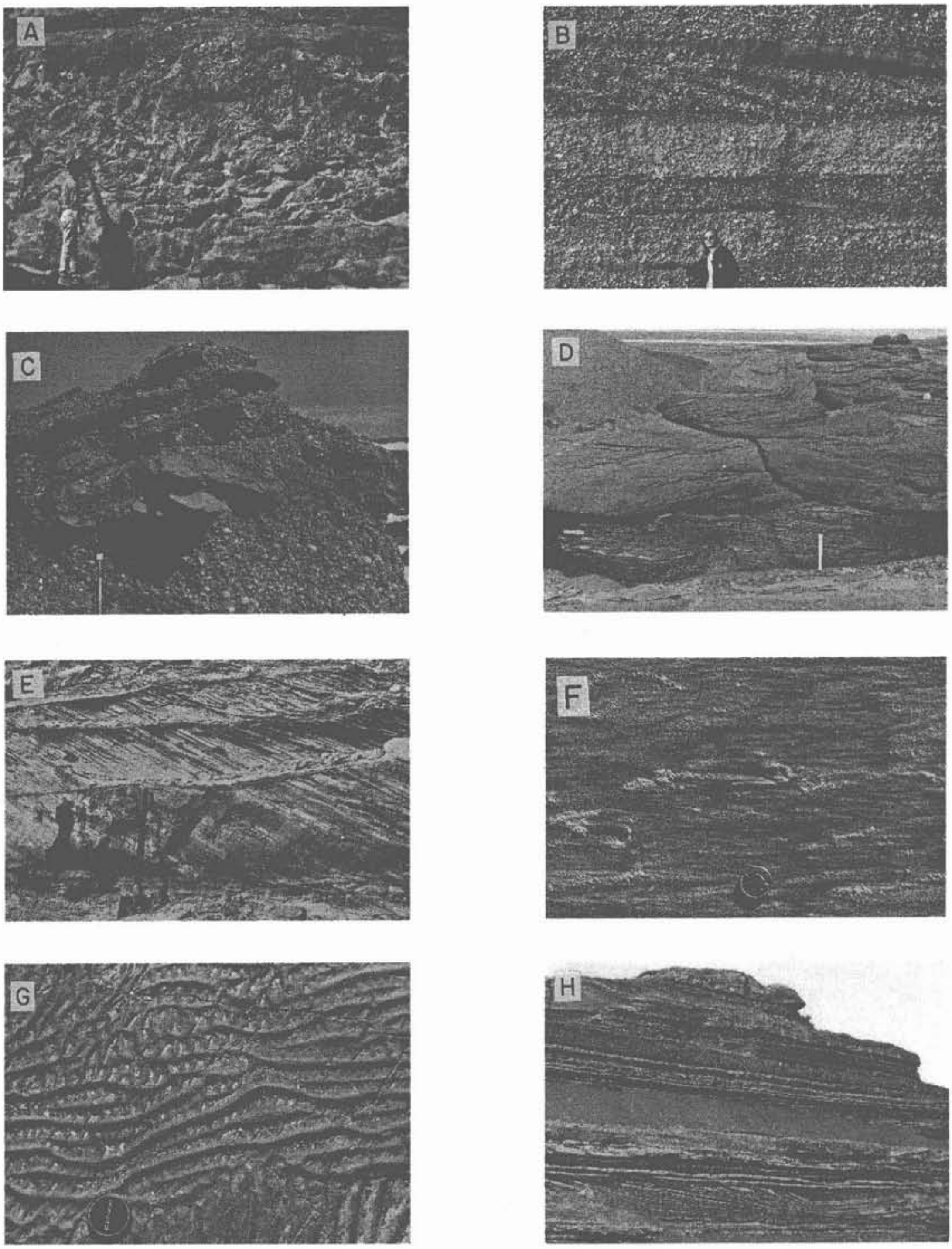

Figure 5 Examples of typical facies in alluvial deposits. The two-letter facies code is explained in Table 2. A) Debris-flow deposit (facies Gms), consisting of large tree trunks in a sand matrix; Tertiary, Japan. B) Several beds of facies Gm with varying grain size and texture, enclosing a unit of planar cross-bedded gravel, facies Gp. Glacial outwash, Quaternary, Banff, Canada. C) Typical ancient alluvial fan deposit, consisting of units of crudely bedded conglomerate (facies Gm), with interbedded lenses of sandstone (facies St, Sr) deposited in minor channels during low water; Devonian, Arctic Canada. Scale is 1.5 m long. D) Trough cross-bedded sandstone. Outcrop is viewed down trough axes; Devonian, Arctic Canada. E) Superimposed planar-tabular cross bed sets (facies Sp) typical of shallow, sand-bed braided rivers, such as the Platte River of Nebraska. Cretaceous of Banks Island, Arctic Canada. F) View of underside of bedding plane in unit of horizontally laminated sandstone showing parting lineation (facies Sh). Note scour shadows formed around pebbles, as flow crossed the bed from right to left; Ordovician, Ontario, Canada. Diameter of coin is 2 cm. G) Ladderback ripples (facies Sr) formed in a pool of standing water adjacent to a bar; Jurassic, Karoo basin, South Africa. H) Various floodplain units, including floodplain muds and silts (homogeneous units, facies Fl), a shallow channel filled with thin-bedded sands and silts (facies Fl, Sr), and thin crevasse-splay sandstones (facies Sr, St). Height of outcrop approximately 20 m; Triassic, Arizona.

elements (Allen, 1983; Ramos and Sopeña, 1983). These are components of a depositional system equivalent in size to, or smaller than a channel fill, and larger than an individual facies unit. They are characterized by a distinctive facies assemblage, internal geometry, external form and (in some instances) vertical profile (Fig. 1). Work on fluvial architectural elements has been expanded and synthesized by Miall (1985, 1988), who proposed eight basic types (Table 3; Fig. 8). Many elements are *macroforms*, or large-scale components of the fluvial landscape. They represent the cumulative effects of depositional and erosional processes over periods of tens to thousands of years (e.g., the sand flats in Fig. 7B), and are group 6 deposits in the classification of Table 1. In fluvial systems, macroforms include major channels and bars, such as point bars, side bars, sand flats and islands (Fig. 7). In the rock record, bars are typically bounded at the top by convex-up fourth-order surfaces (although many bars are truncated by a succeeding sand sheet). The bars are cut internally by third-order surfaces, indicating the presence of separate growth increments. Each depositional unit bounded by a third-order surface represents a period of active bar growth, for example, during seasonal runoff peaks or during flash floods in a desert. Intervening periods of low water are represented by mud drapes. Periods of erosion are represented by low-angle disconformity surfaces that commonly truncate underlying bedding at a low angle. Comparable cross-cutting erosion surfaces occur within individual cross bed units, where they are termed *reactivation surfaces*. They represent surfaces where the bedform became reactivated following a pause in deposition (Collinson, 1970). The same term can be used for the third-order surfaces that separate macroform growth increments.

Following Ashley (1990), the term *bar* is now restricted to these large forms. The simple cross-bedded bars that have been termed linguoid, lobate or transverse bars in earlier literature, are now recognized to be simple dunes. They are two-dimensional or three-dimensional depending on whether they are simple, straight-crested forms (2-D), or sinuous crested (Fig. 7B).

Lateral-accretion deposits

Point bars (Fig. 7A) are examples of the *lateral-accretion* architectural element (LA in Table 3; Figs. 1, 7A, 8), so termed because the direction of accretion is at a high angle to the main channel trend. The term is now preferred to "point bar" for descriptive purposes, because lateral-accretion deposits occur in many fluvial settings that are not point bars, such as in mid-channel settings. In meandering streams they develop on the insides of meander bends as the bend widens or migrates downstream. Surface flow impinges against the outer bank, where it maintains a cutbank by active erosion (Figs. 7A, 9). The flow turns downward, developing a helical overturn pattern. The return flow, at depth, passes obliquely over the point-bar surface (Fig. 9). The helical flow pattern decays as the flow emerges from the bend, and is replaced by a helical overturn in the opposite direction, as the flow impinges on the cutbank of the next bend downstream.

Sediment removed from the cutbank is incorporated in the overall sediment load of the river. Large slump blocks may accumulate in the deepest part of the channel as a lag deposit. Material broken down into individual grains is incorporated into the bedload and suspension load, and is swept downstream. Much of it becomes deposited in bedforms and bars. Sediment is added to the point-bar surface at a rate comparable to that at which it is removed by erosion along the outer

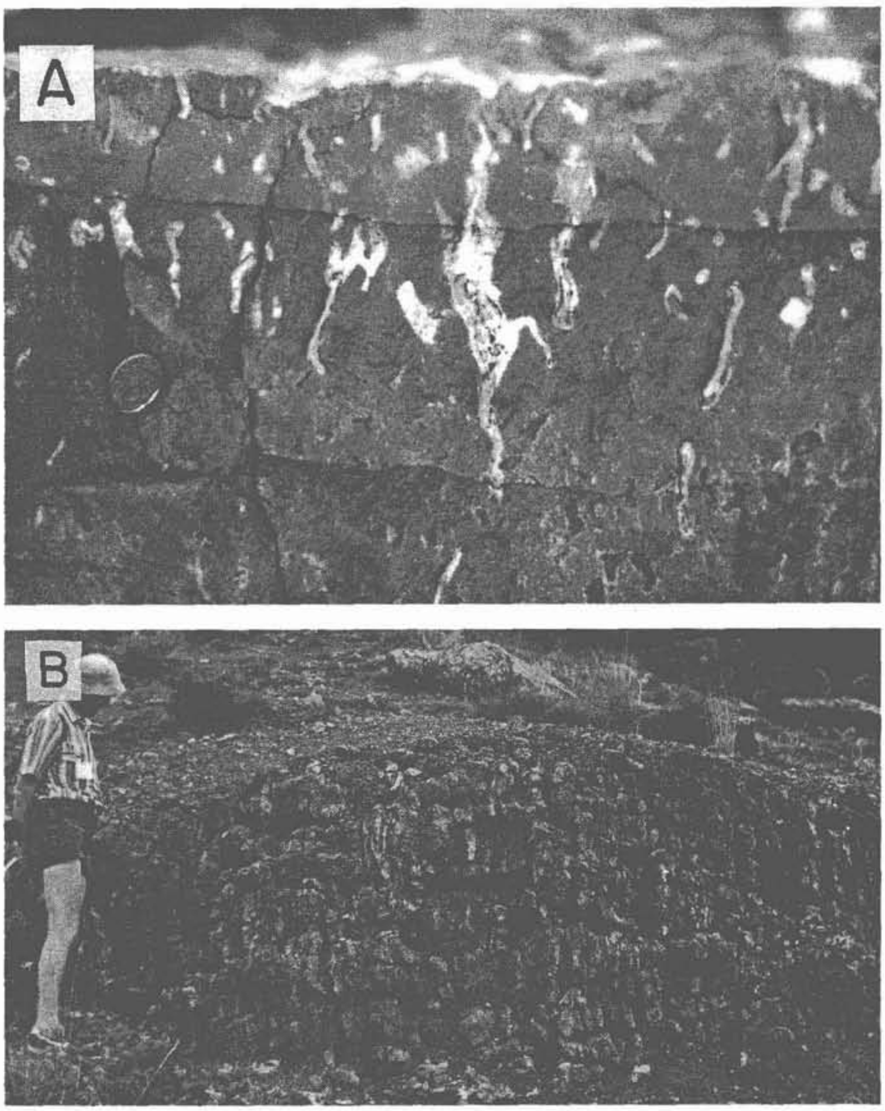

Figure 6 Floodplain deposits. A) Close-up view of floodplain siltstones (facies Fm) containing rootlets; Triassic, Spain. B) A well-developed calcrete (facies P); Buntsandstein (Triassic), Spain.

bank of the meander. The resulting lateral growth can easily be detected in many modern bars by the curved ridges and depressions (swales) on the bar surface. In Figure 7A from the Milk River, the centre of each point bar is covered by old trees, with the size and density of vegetation decreasing outward to the vegetation-free bar surface at the edge of the channel. This spectrum of vegetation illustrates the bar evolution and indicates the time available for growth on each part of the bar. Variations in depth and velocity over the point-bar surface result in sediment sorting and variations in the assemblage of sedimentary structures, with a tendency for finer grain sizes and structures of lower flow regime to occur in the upper part of the bar. Figure 2 shows the edge of a modern point bar, with the active depositional surface covered with two-dimensional dunes.

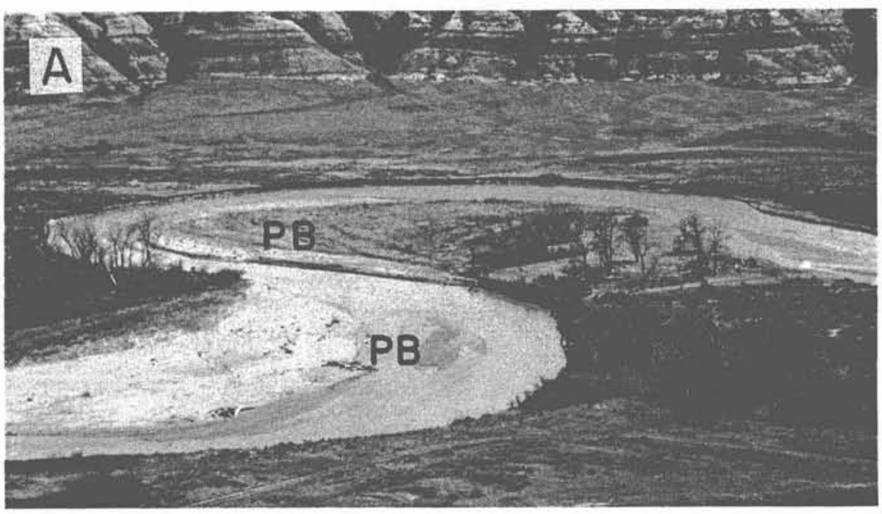

Figure 7 Examples of different styles of river channels and bars. A) The Milk River, southern Alberta, an example of a highly sinuous, *meandering* river. The bare sand surfaces at the edge of the channel on the inside of each meander bend are good examples of point bars (PB). Channel is about 20 m wide. B) The William River, northern Saskatchewan, an example of a multiple-channel, *braided* river. The large pale-coloured exposed areas in the distance are examples of what are commonly termed sand flats. They are compound bars built by depositional and erosional processes over many years. In the foreground is a series of large, lobate, three-dimensional dunes (formerly termed linguoid bars) advancing toward the viewer. Channel is about 60 m wide. Both photos courtesy of D. G. Smith.

Continued enlargement of a meander loop results in increased sinuosity. Eventually a cutbank may incise into an adjacent reach of the channel. This typically occurs at the neck of a meander (Fig. 1; see also the area of large trees in the centre of Fig. 7A), and results in a *neck cut-off.* Flow is diverted through the break, and the channel reach between the points of cut-off is abandoned. Fine-grained floodplain sediments or new point-bar deposits then seal off the ends of the abandoned channel and it becomes a curved pond, colloquially termed an *oxbow lake. Chute channels* (Figs. 1, 8) and chute cutoffs occur where an erosional channel develops across the top of the active point bar during flood events.

Figure 10 illustrates cross sections through a range of examples of LA deposits, and Figure 11 is a photograph of a typical outcrop. LA elements range in thickness from a minimum of about 2 m (Fig. 10D), up to the giant bars of the Athabasca Oil Sands, Alberta, which are at least 25 m thick (Fig. 10F). The most distinctive features of LA deposits are the *lateral-accretion surfaces.* These may be the boundaries of facies sets or cosets (1st- or 2nd-order bounding surfaces of Fig. 3), or they may be surfaces of minor erosion (3rd-order surfaces), indicating pauses in the development of the deposit. They dip at about 3-25°, with typical dips in the 5-15° range. The direction of dip of these surfaces indicates the direction of bar growth, and is approximately perpendicular to the direction of bedform migration (Fig. 2). The crests of the dunes in this illustration are oriented parallel to the dip of the accretion surface, which can be seen dipping underwater to the right. This relative orientation of dips and migration directions is a useful clue for the identification of lateral-accretion deposits in the ancient record.

Bars composed of cobble gravel occur in some basin-margin conglomerates, but most lateral-accretion deposits are sand-dominated. Many, but by no means all accretion surfaces in LA deposits show fining updip, parallel to bedding, reflecting the range of water depths and flow velocities that occurs across each accretion surface

(Figs. 9, 11). As the bar accretes laterally, beds deposited in successively shallower water are superimposed on each other. Thus the resulting deposit tends to show a vertical upward fining, that can readily be recognized in vertical sections, such as drill cores (Fig. 9; see also Chapter 3). Fluvial models of meandering and braided systems that contain lateral-accretion deposits are illustrated later.

Downstream-accretion deposits
Many gravel- and sand-bed rivers contain active bars and islands in mid-channel positions (Fig. 7B). These develop by accretionary processes, in particular by the capture of trains of bedforms at the upstream edges or on the flanks of the bar. In this way the bar may accrete upstream, lateral to the channel trend, or downstream. Lateral accretion (LA) and *downstream accretion* (DA) are the most common styles. Some large sand flats may show both styles in different parts of the bar (Allen, 1983). DA deposits are particularly characteristic of braided streams. They range in height from 1-15 m, and in length from 10-1000 m.

The essential characteristic of a downstream-accretion element is that it consists of several (possibly many) cosets deposited by bedform migration that are dynamically related to each other by a hierarchy of internal

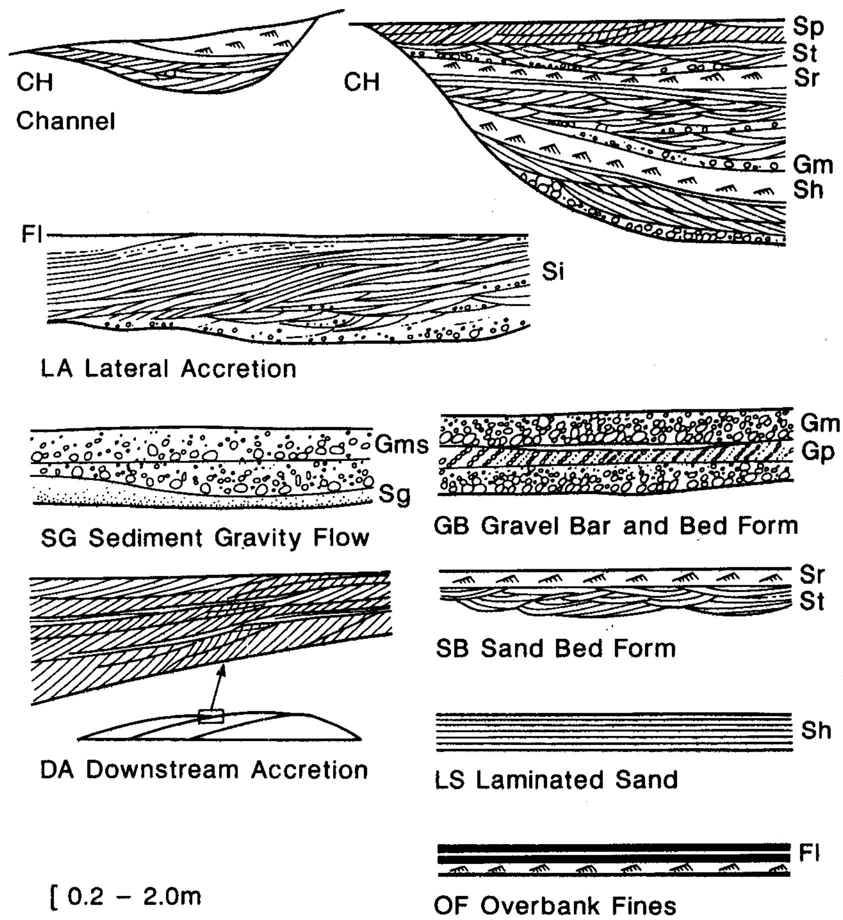

Figure 8 The eight basic architectural elements in fluvial deposits. No vertical exaggeration. Note the variable scale. Modified from Miall (1985).

Table 3 *Architectural elements in fluvial deposits. Modified from Miall (1985). Facies classification from Miall (1978b).*

Element	Symbol	Principal facies assemblage	Geometry and relationships
Channels	CH	any combination	finger, lens or sheet; concave-up erosional base; scale and shape highly variable; internal concave-up 3rd-order erosion surfaces common
Gravel bars and bedforms	GB	Gm, Gp, Gt	lens, blanket; usually tabular bodies; commonly interbedded with SB
Sandy bedform	SB	St, Sp, Sh, Sl, Sr, Se, Ss	lens, sheet, blanket, wedge, occurs as channel-fills, crevasse splays, minor bars
Downstream-accretion macroforms	DA	St, Sp, Sh, Sl, Sr, Se, Ss	lens resting on flat or channelled base, with convex-up 3rd-order internal erosion surfaces and upper 4th-order bounding surface
Lateral- accretion macroform	LA	St, Sp, Sh, Sl, Se, Ss, less commonly Gm, Gt, Gp	wedge, sheet, lobe; characterized by internal lateral-accretion 3rd-order surfaces
Sediment gravity flow	SG	Gm, Gms	lobe, sheet, typically interbedded with GB
Laminated sand sheet	LS	Sh, Sl; minor Sp, Sr	sheet, blanket
Overbank fines	OF	Fm, Fl	thin to thick blankets; commonly interbedded with SB; may fill abandoned channels

bounding surfaces (Figs. 12, 13). This assemblage of cross-bedded deposits and their enclosing surfaces reveals the former existence of an active, non-periodic, possibly irregular-shaped bar form comparable in height and width to the channel in which it formed. The bounding surfaces are of first-, second-, and third-order type; they dip gently (<10°) downstream, oblique to flow, or gently upstream around and over a low-relief bar core. Between these surfaces are sets or cosets of St, Sp, Sh, Sl, or Sr (see Figs. 5D-G, for examples of these facies). The Sh and Sl laminae are organized parallel or subparallel to the internal bounding surfaces. Detailed paleocurrent studies show that the bedforms advance generally down the slopes defined by the first- to third-order surfaces, or oblique to the surfaces draping the bar cores. These data reveal a picture of fields of bedforms driving across, around and down the bar forms.

Cant and Walker (1978) referred to the large, mid-channel bars in the South Saskatchewan River as *sand flats.* These evolve from large, simple,

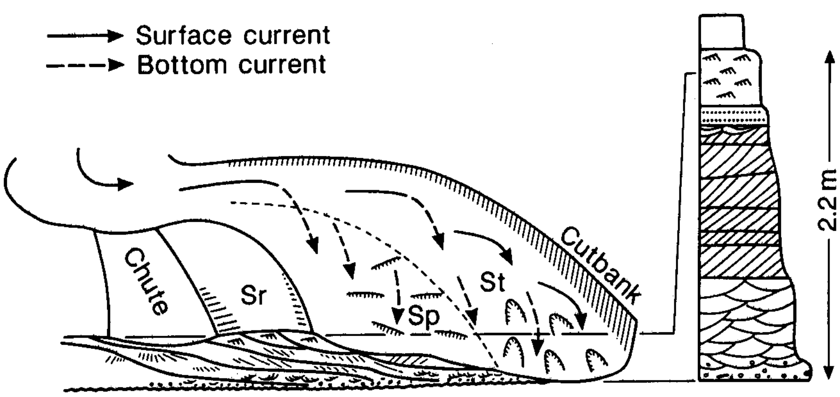

Figure 9 Three-dimensional diagram that illustrates the formation of lateral-accretion deposits on the inside of a meander bend. Surface flow around the bend impinges against the outer bank, where it maintains an active cutbank. The flow turns down and passes obliquely across the point-bar surface, setting up a helical overturn pattern. Sediment is carried up onto the point bar, and sorted under conditions of decreasing depth and velocity. This accounts for the decrease in grain size and in scale of hydrodynamic structures up the point-bar surface. A vertical section through the bar is bracketed at the right. It is capped by fine-grained floodplain deposits accumulated by vertical accretion following continued channel migration. This model is the basis for the classic fluvial fining-upward cycle of Bernard *et al.* (1962), Allen (1963), Visher (1965), and others.

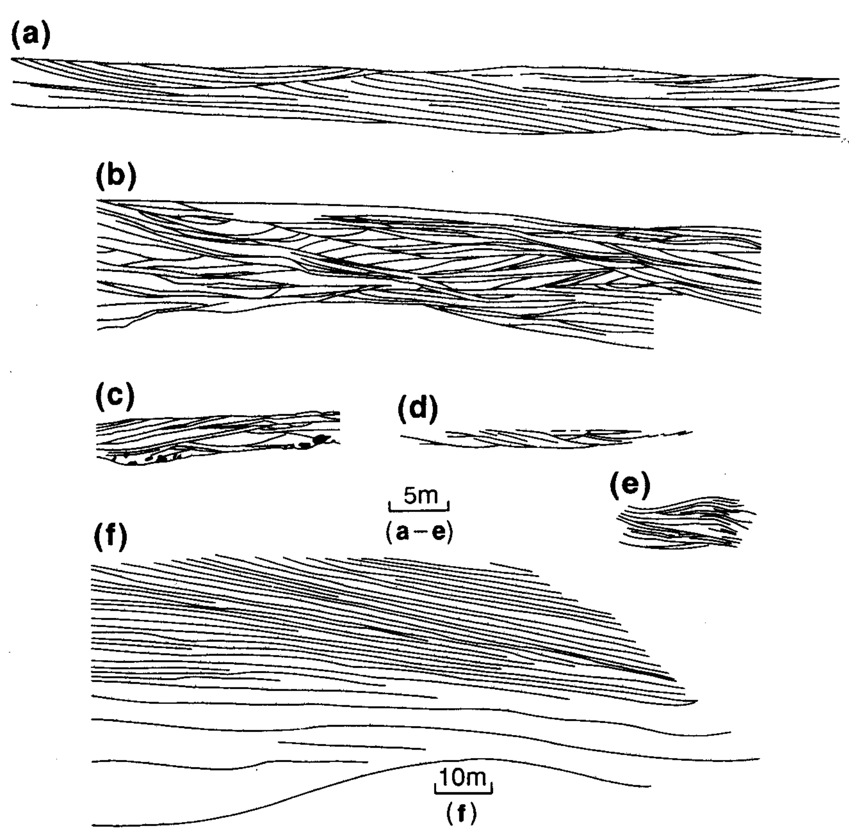

Figure 10 Examples of lateral-accretion elements, illustrating the wide range of scales and facies (from Miall, 1985). No vertical exaggeration. All sections are oriented approximately perpendicular to the channel (comparable to the cross-section shown in Fig. 9). Facies codes are given in Table 2. A) Conglomerate point bar (facies Gm), with chute channels (facies Gt; Quaternary alluvial fan gravels, Italy); B) Element composed of medium-grained sandstone, with abundant internal planar-tabular cross bedding (facies Sp; Pennsylvanian, Appalachian coal basin); C) Fine- to very-coarse sandstone and pebbly sandstone with cobble to boulder conglomerate lag. Abundant internal cross bedding (facies Sp, St, Sh, and Sl; Devonian, Wales); D) Small sandy point bar with abundant dune and ripple cross bedding (facies St, Sr; Miocene, Spain); E) Point bar composed mainly of fine sandstone and siltstone (facies Sl) with minor medium- to coarse-grained, cross-bedded sandstone (facies St) at base (modern river, British Columbia); F) Giant point bar with thick, fine-grained trough cross-bedded sandstone at base (facies St) passing up into accretionary sets of alternating fine sandstone and argillaceous siltstone showing evidence of tidal bundling (facies Se; Athabasca Oil Sands, Alberta).

cross-bedded flow-transverse bedforms, termed cross-channel bars by Cant and Walker (1978). Elevated parts of these bedforms become emergent at low water and then form the nuclei of new sand flats, which anchor part of the bar in the middle of the channel. Sediment is added to the cross-channel bedforms by the migration of fields of dunes and ripples. Those parts of the crestline in deeper water continue to advance more rapidly than the sand flat nucleus, so that the entire bedform swings around oblique to the channel direction (Cant and Walker, 1978; Allen, 1983, his Fig. 20). The macroforms accrete sediment partly by the process of bedform capture on the upstream or flanks, and partly by rapid burial and preservation of superimposed bedforms on the advancing downstream face (Fig. 12).

Many of the variations in composition and geometry between described macroforms probably reflect fluctuations in *stage* (the depth of water in the river). The bar surfaces may be cut by numerous erosional channels during falling stage, and may be abandoned altogether at low stage, or as a result of a shift in channel position, leading to overall nondeposition or erosion (Fig. 11). The minor channels, and the cross-cutting erosion surfaces that separate growth increments, are defined as third-order surfaces.

Other architectural elements

Characteristics of the other main element types are listed in Table 3. The *channel element* (CH) may be defined for small channels within a channel complex (the main channel-fill deposits typically may be broken down into component elements). *Sediment gravity flow deposits* (element SG; Fig. 5A) are common in some proximal alluvial fans. Here, abundant loose sediment may be available in the source area, and can be transported by occasional sudden run-off events related to severe weather systems. *Sandy bedforms* (SB) are typical of crevasse splays (mini-deltas which accrete into the floodplain from breaks in the channel bank; see Fig. 1), bar tops, and some sand sheets in shallow rivers where major sand flats are not able to develop. Commonly they show upward fining. *Laminated sand sheets* (LS) are tabular units characterized by parting

Figure 11 Typical point bar deposit; an example of a lateral-accretion (LA) deposit. Each accretionary unit consists of a resistant sandstone unit at the base, which becomes more thinly bedded and more recessive laterally upward, along the bedding surface. Carboniferous, Black Warrior Basin, Alabama. Thickness of point bar, between the two coal beds, approximately 8 m.

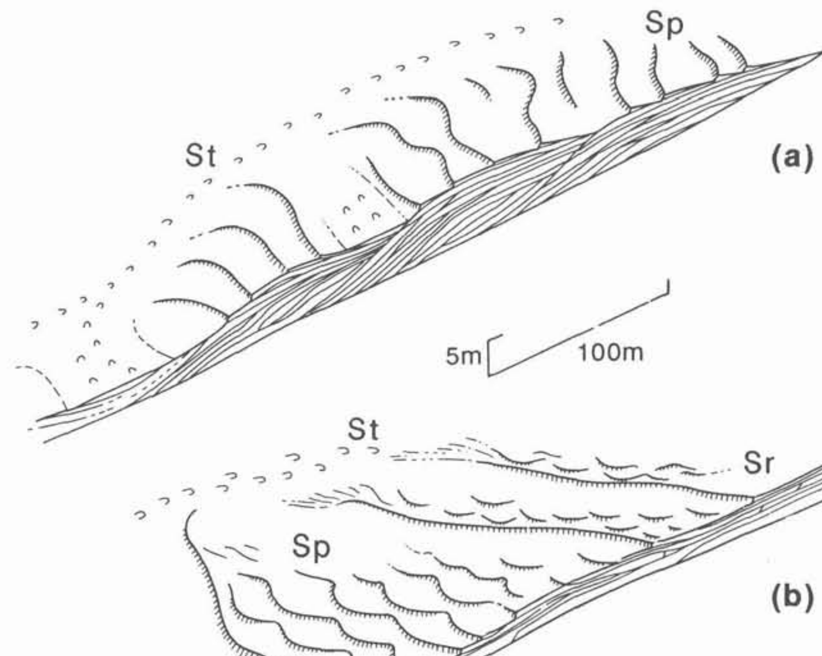

Figure 12 Generalized models of downstream-accretion (DA) architectural elements. Scales are approximate. Internal geometry varies considerably, depending on channel depth, grain size, discharge amount and variability. The upper diagram shows a deposit accumulated as three separate increments, separated by internal, dipping, third-order erosion surfaces. Two minor channels formed by surface runoff at times of falling discharge, are also shown (Miall, 1985).

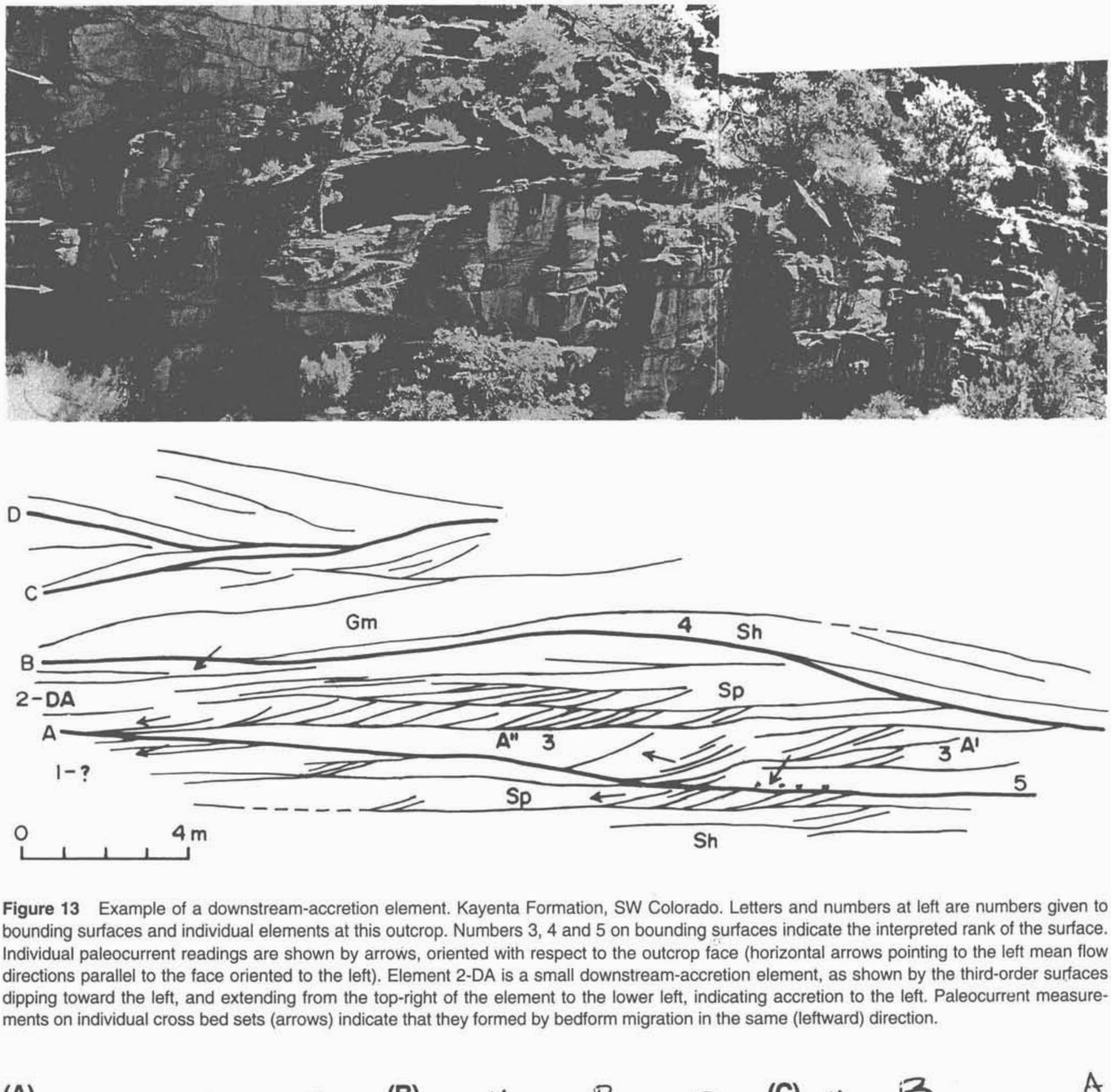

Figure 13 Example of a downstream-accretion element. Kayenta Formation, SW Colorado. Letters and numbers at left are numbers given to bounding surfaces and individual elements at this outcrop. Numbers 3, 4 and 5 on bounding surfaces indicate the interpreted rank of the surface. Individual paleocurrent readings are shown by arrows, oriented with respect to the outcrop face (horizontal arrows pointing to the left mean flow directions parallel to the face oriented to the left). Element 2-DA is a small downstream-accretion element, as shown by the third-order surfaces dipping toward the left, and extending from the top-right of the element to the lower left, indicating accretion to the left. Paleocurrent measurements on individual cross bed sets (arrows) indicate that they formed by bedform migration in the same (leftward) direction.

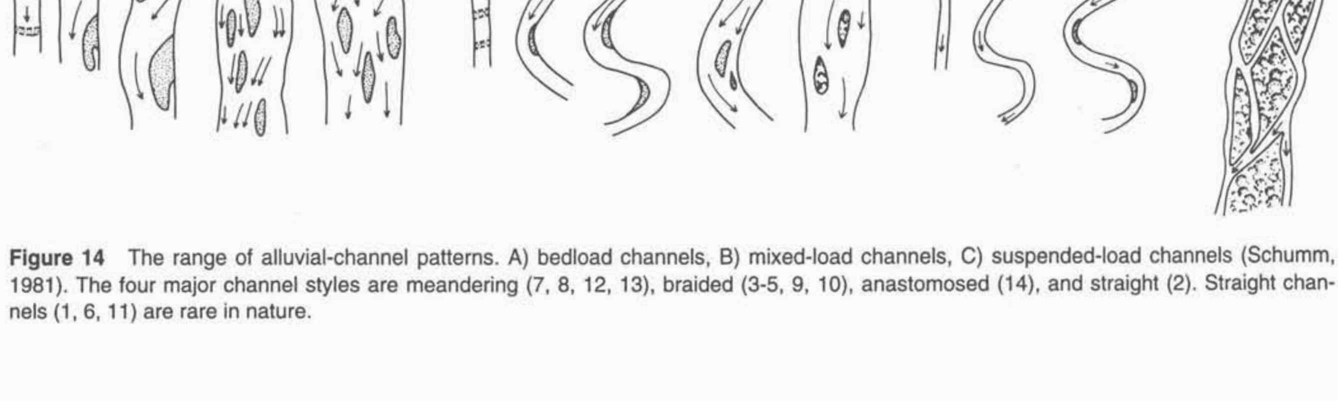

Figure 14 The range of alluvial-channel patterns. A) bedload channels, B) mixed-load channels, C) suspended-load channels (Schumm, 1981). The four major channel styles are meandering (7, 8, 12, 13), braided (3-5, 9, 10), anastomosed (14), and straight (2). Straight channels (1, 6, 11) are rare in nature.

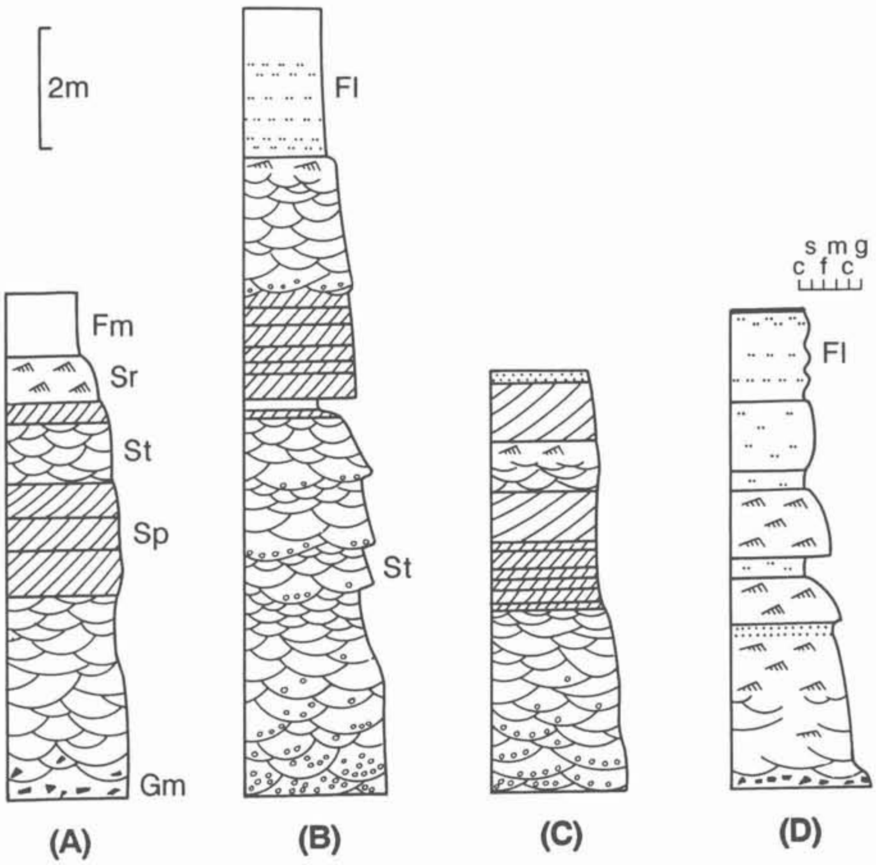

Figure 15 Comparison of four vertical profiles, showing how similar fining-upward cycles may be produced in several different ways. A) Model cyclic sequence, Battery Point Formation (Devonian), Quebec, probably formed by vertical bar aggradation in a low-sinuosity (braided) river. B) Sequence formed by lateral accretion of a point bar, Castisent Sandstone (Eocene), Spain. C) Sequence formed by lateral accretion of a point bar, modern Amite River, Louisiana. D) Sequence formed by vertical aggradation and progressive channel abandonment on an alluvial fan, under conditions of tectonic quiescence (allogenic control), Upper Carboniferous coal measures, northern Spain. Columns A, B and D include fine-grained overbank deposits at the top formed by vertical accretion on the floodplain following the abandonment of the bar. Diagram from Miall (1980).

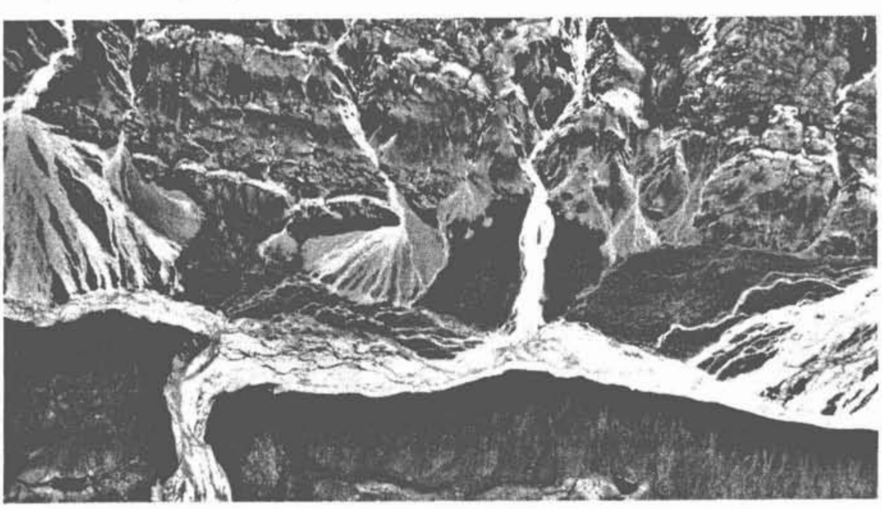

Figure 16 Aerial view of alluvial fans along the flank of the Mackenzie Mountains, Canada. Note the varying size of these fans, their tendency to merge laterally, and the fact that in most instances only a small area of each fan is occupied by active distributaries. Field of view approximately 4 km wide.

lineation (facies Sh; Fig. 5F), and develop by upper flow regime conditions during flash floods in arid environments.

The *overbank fines element* (OF; Fig. 5H) is highly variable. Its characteristics depend primarily on climate. In humid-tropical regions coal may be important, although it may be necessary for the overbank region to develop as a raised swamp, in order to prevent clastic influxes infiltrating the accumulating peat and downgrading the resulting deposit to carbonaceous shale (McCabe, 1984). In more arid regions alternation of evaporation and rain infiltration concentrates dissolved carbonates and silicates near the sediment surface, leading to nodular *calcretes* (Fig. 6B) and *silcretes*. Commonly these develop in association with soil formation. Several authors have shown how the structure and colour of calcretes can be used to estimate the time of maturation of these deposits (Leeder, 1975; Bown and Kraus, 1987; Kraus, 1987). Small, isolated nodules and grey and orange colours indicate immature soils, whereas layers of large, possibly laterally coalesced nodules, and red and purple colours indicate greater maturation times.

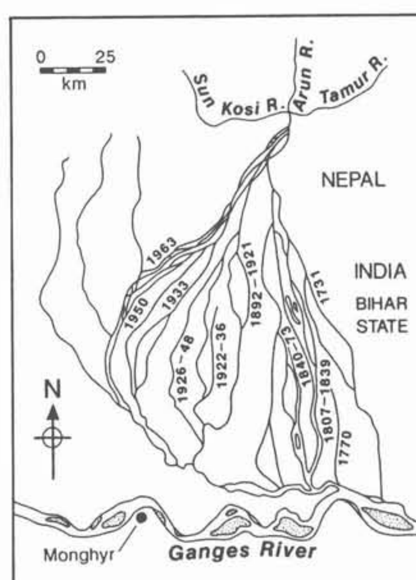

Figure 17 The Kosi fan, India. This is probably the world's largest fan. The dates occupied by each distributary channel are shown — note the gradual westward migration of the main distributary. Sediments range from boulder conglomerate near the apex, to fine sand and silt at the foot.

Thick, well-developed calcrete beds indicate that the floodplain has been abandoned in a state of nondeposition for tens of thousands of years. Such surfaces may extend for many kilometres, and may have significance as regional sixth- or seventh-order bounding surfaces indicating times of tectonic quiescence and stable base level.

Apart from these chemical sediments the overbank area may accumulate thick muds in swamps or temporary ponds, and may also contain sandstone sheets (element SB) deposited as crevasse splays.

CHANNEL STYLES

Four traditional channel patterns form the basis of most textbook discussions of alluvial depositional systems. There are both scientific and historical reasons for this; the straight, meandering, braided and anastomosed patterns are certainly common in nature, but these patterns have been overemphasized in the search for simple models by sedimentologists and petroleum geologists in the 1950s and 1960s. A full review of the historical development of fluvial studies has been given by Miall (1978a). It is now accepted that, although these patterns are common, there are many gradations between them.

Areal variations in channel styles, and their causes

Why are there so many different fluvial channels styles (Fig. 14)? This is an extremely complex question, to which there is no simple answer. *Braided* channels (patterns 3-5, 9, 10 in Fig. 14) have numerous bars and islands that represent temporary sediment storage during downstream transport. This indicates that the capacity of the river has been exceeded for some or most of the time. Thus abundant sediment supply, for example from easily eroded banks, is one cause of braiding. A second factor favouring a braided channel pattern is a highly variable discharge. Large volumes of sediment can be carried during periods of high discharge, but the river does not have the competence or capacity to move the load at other times, hence the storage of sediment in braid bars and islands. Rivers characterized by large discharge fluctuations related to seasonal variations in temperate, arctic, and alpine climates, or the more random discharge variations in arid regions, therefore tend to be braided, given adequate sediment supply.

Meandering (Fig. 14, patterns 7, 8, 12, 13) and *anastomosed* (Fig. 14, pattern 14) rivers characteristically occur on lower slopes and carry finer grained sediment loads. Anastomosed rivers have numerous channels of variable sinuosity. They are rather stable in position, and do not migrate laterally, as do the meander bends of meandering rivers. There is growing evidence that the anastomosed pattern develops where the river is affected by a downstream damming or backtilting process. This may occur where a river crosses a tectonically positive area, or flows toward an area of postglacial rebound. Vegetation is also an important control on channel style. Dense vegetation along river

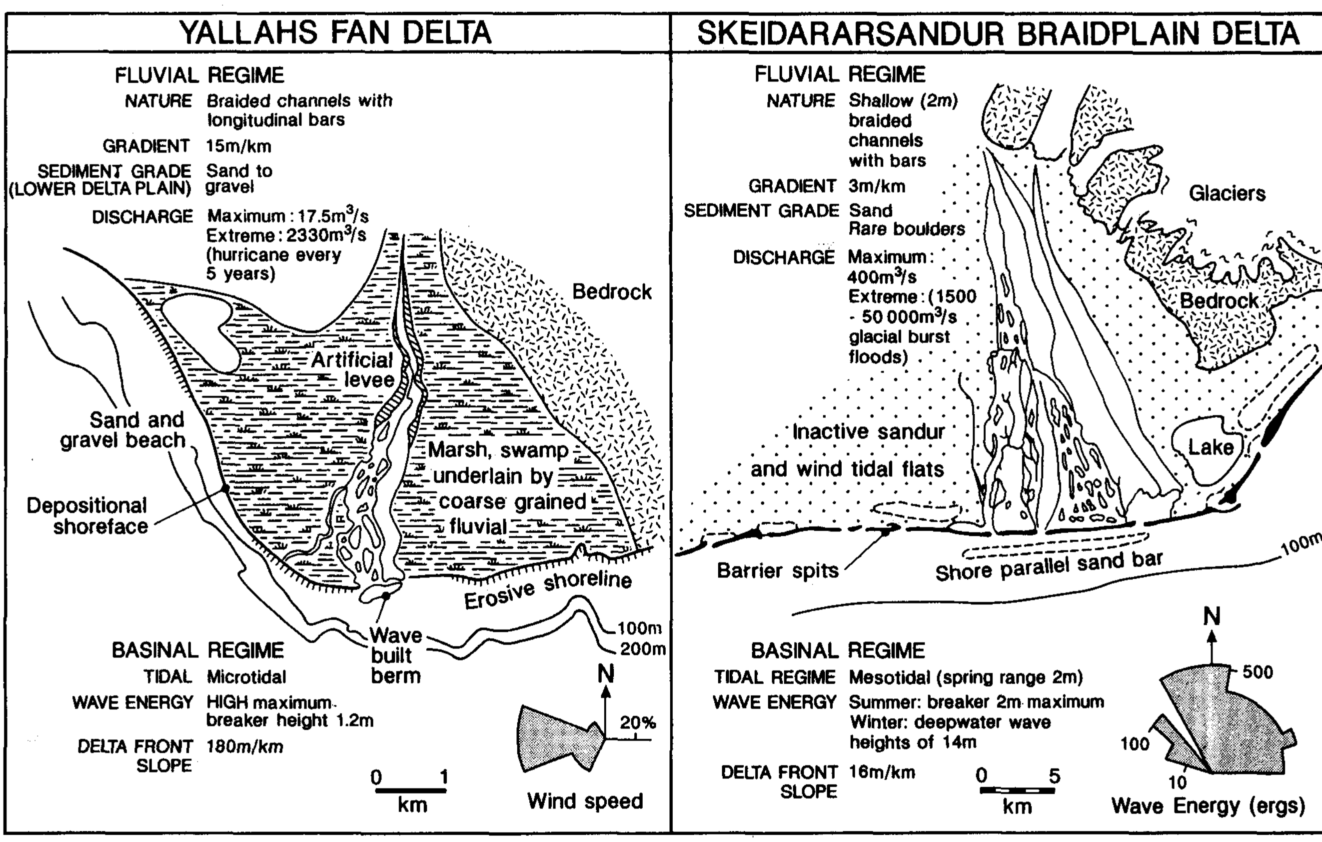

Figure 18 *Examples of modern coastal alluvial depositional systems. The Yallahs fan delta is in Jamaica, a tropical setting. The Skeidararsandur braidplain delta is on the south coast of Iceland, a cool-temperate setting. Diagram compiled by Orton (1988).*

banks, such as grasses or tropical-tree roots, tends to inhibit bank widening and prevent the development of braiding. Vegetation is climatically dependent, and has only been an important control on channel style since the Silurian or Devonian, when land plants first became a significant component of the subaerial landscape. Until that time poorly consolidated banks were probably the norm, with a consequent tendency for braided-channel styles to predominate (Schumm, 1968).

Given these controls, there is a tendency within most alluvial basins for proximal rivers (including alluvial fans if present) to be braided, whereas more distal rivers, at least in perennial, humid environments, are more likely to be meandering. Anastomosed rivers are also more likely to occur in distal settings, but may also occur in proximal settings where the river crosses an area undergoing gentle tectonic uplift, such as a fault.

Whatever the actual channel style, channels are always characterized by some sinuosity; meandering is a characteristic of large-scale turbulence of moving water bodies. Even in straight channels there may be a meandering *thalweg* (line of deepest channel), with bank-attached *side bars* deposited on alternate sides of the channel inside each bend in the thalweg (Fig. 14, pattern 2). Completely straight channels, such as patterns 1, 6 and 11 in Figure 14, are rare.

Standardized facies models were built during the 1960s and 1970s, based on the basic depositional characteristics of the four main channel styles, plus such variables as sediment-load grain size and climatic criteria. A considerable increase in the volume of descriptive data during the last decade or so has demonstrated that these models are inadequate to convey the full variability of fluvial depositional styles, and it has also been shown that they contain some contradictory features. For example, it is now known that the process of lateral accretion, which gives rise to the distinctive architecture of the point bar (Fig. 9-11), is not confined to meandering rivers, as was once thought, but is common in braided streams, and also occurs in minor or modified form in anastomosed and straight channels.

In the past, considerable reliance

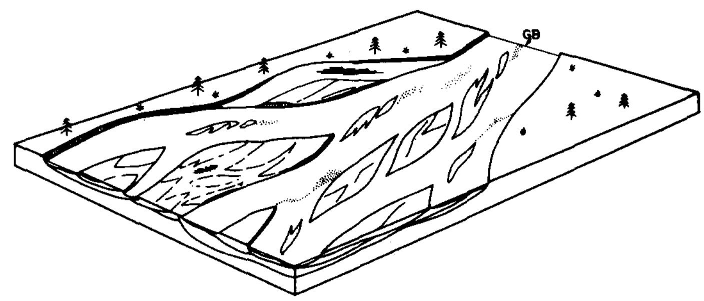

Figure 19 Block diagram of typical gravel-bed braided river. Element and facies codes for this and subsequent diagrams are given in Tables 2 and 3.

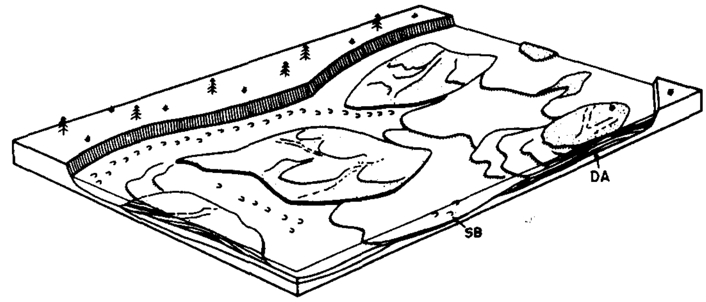

Figure 20 Block diagram of a large, perennial, sand-bed braided river, in which large sand flats are developing. Note the internal complexity of the sand flats, which typically include LA and DA elements (Figs. 9-13).

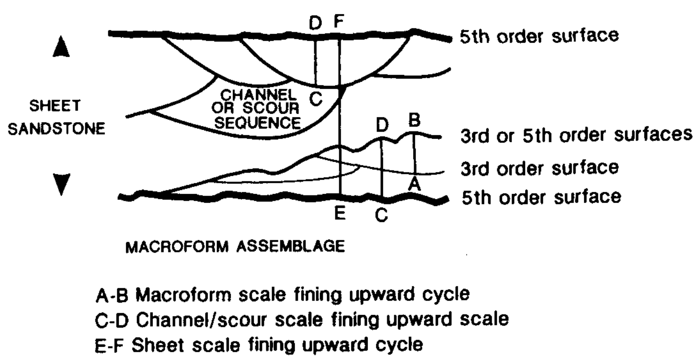

Figure 21 The three scales of fining-upward cycle in a typical sandy-braided deposit, the Westwater Canyon Member of the Morrison Formation (Godin, 1991). The depositional environment of this river was similar to that shown in Figure 20.

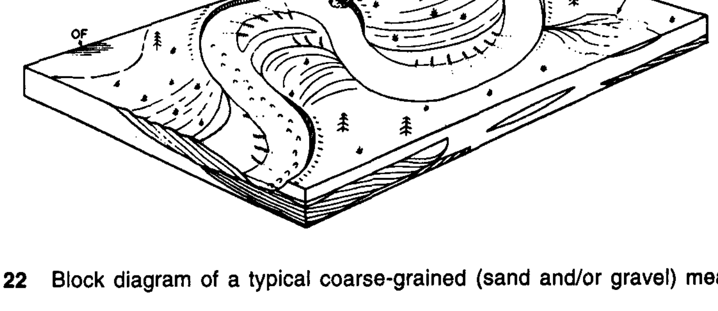

Figure 22 Block diagram of a typical coarse-grained (sand and/or gravel) meandering river.

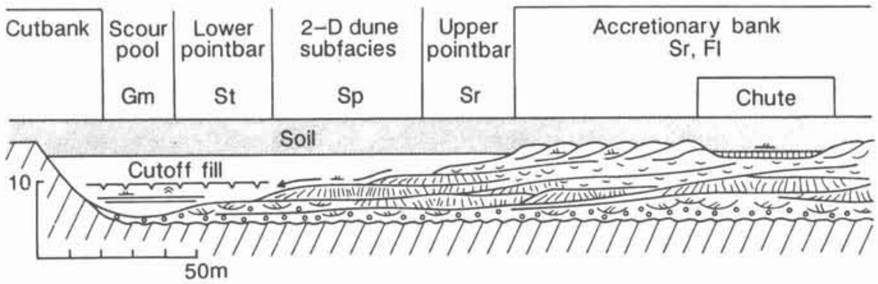

Figure 23 Diagrammatic cross section across a point bar in the Castisent Sandstone, Spain, showing the architecture of the deposit, and the range of sedimentary structures. (Modified from Nijman and Puigdefabregas, 1978).

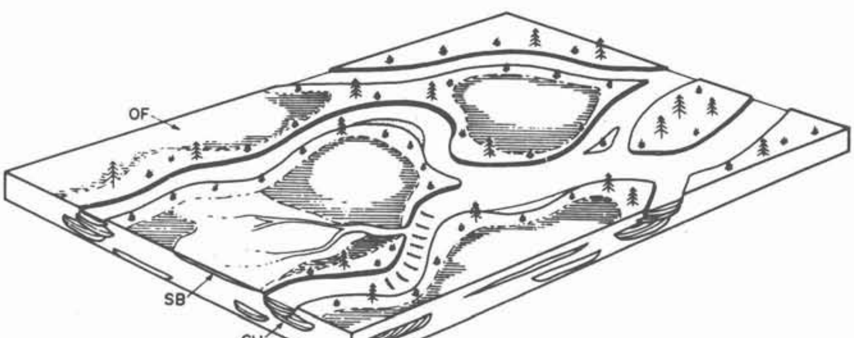

Figure 24 Block diagram of anastomosed river. Horizontal ruling on the top surface of the diagram indicates swamp vegetation, and encloses areas of open water comprising small, shallow, floodplain ponds.

Figure 25 An interpreted example of an anastomosed river deposit. The sandstone lens is 8 m thick, and represents a channel deposit. It is encased in thick floodplain siltstones and sandstones which, in this case, also include nodular calcrete deposits. Cutler Group, northern New Mexico (Eberth and Miall, 1991).

has also been placed on the characteristics of vertical profiles as indicators of channel style. For example, the presence of fining-upward successions with their characteristic assemblage of sedimentary structures (Allen, 1963; Visher, 1965) was regarded with near certainty as proof of a meandering-fluvial environment. We now know that vertical profiles are unreliable diagnostic tools. For example, Figure 15 shows four fining-upward cycles, three produced by different *autogenic* (within basin) processes and the fourth developed by a tectonic *(allogenic)* control.

Modern architectural studies of fluvial deposits demonstrate an enormous variety of fluvial styles. Twelve different styles were illustrated by Miall (1985), who emphasized that this was not intended to provide a complete coverage of the subject. Indeed, continued field research has provided the basis for defining several additional fluvial styles, none of them exactly similar to the published twelve. However, each style is characterized by a particular assemblage of the architectural elements described in this chapter. This suggests the basis for a modified approach to facies analysis for use in complex systems such as alluvial deposits, where a deposit may be encapsulated by a unique *summary of the environment.* It is the architectural elements that provide the recognizable, common thread running through the analysis. In a subsequent section a few common fluvial styles are selected, and it is shown how the corresponding deposits can be analyzed in terms of the standard elements described in this chapter.

ALLUVIAL FANS AND FAN DELTAS

These environments have become widely recognized by sedimentologists, but the use of the terms may be confusing. An *alluvial fan* is a distributary fluvial system, formed where rivers emerge from a confined, mountain valley onto the basin floor, where the channels are no longer confined (Fig. 16). The fluvial system fans out from a point source (the feeder channel) into a series of distributaries, although only one or two may be active at any one time. Typically deposition within a narrow channel belt builds up the fan surface in one area and reduces the slope. Eventually a channel-switching *(avulsion)* event occurs, normally during a high-discharge event, when flooding overtops the channel banks, and discharge switches to a region of the fan having a steeper slope. In this way the water and sediment gradually shift across the entire fan, building the typical fan-shaped depositional lobe (Fig. 17). In arid environments the fluvial discharge may be in the form of sheet floods or lobate sediment-gravity flows that are not confined to channels. Nevertheless, the flow radiates from a point source, and may therefore be said to be formed within a fan-like distributary system. A *fan delta* (Fig. 18) is an alluvial fan that progrades directly into a standing body of water (sea, lake; Nemec and Steel, 1988).

For most geologists the terms alluvial fan and fan delta imply coarse-grained sediments deposited in braided channels. There is a tendency for geologists to use the terms in a descriptive sense for any ancient basin-margin conglomeratic unit, hence the evolution of the term *fanglomerate*. Such sediments are assigned to element GB (Fig. 5C), and may or may not contain interbedded sediment-gravity-flow deposits (element SG; Fig. 5A). The gravel facies illustrated in Figure 5 are typical of those formed within fan environments. The fluvial styles of gravel-dominated braided channels are illustrated in the next section. However, the terms alluvial fan and fan delta do not, in fact, have a unique facies sense. There are giant modern fans, such as the Kosi, of India (Fig. 17), which grade from boulder conglomerate near the mountains to fine sand-silt-mud 140 km downslope at its distal end. Hirst and Nichols (1986) described an ancient example of a basin-margin distributary-alluvial-fan system (documented by paleocurrent data) which consisted predominantly of sandstone organised into ribbons (element CH) and sheets (elements SB, LS). Parkash *et al.* (1983) described a modern *terminal fan*, which is an ephemeral fluvial distributary system 12 km long that deposits fine sand, silt and mud at the edges of playas or tidal flats in arid regions (element SB).

There is some ambiguity in the terms alluvial fan and fan delta. Not all basin-margin talus prisms are built by distributary systems emanating from point sources. Many, particularly in arid environments, are deposited by an array of individual, parallel streams. Coastal glacial-outwash systems, such as those on the south coast of Iceland and Alaska consist of parallel braided systems fed from several or many meltwater sources (Fig. 18; see Chapter 5). They have been termed fan deltas by some writers, but the dispersal may differ from the classical radial pattern. If the geomorphic implication of the two terms is considered important, they cannot be used for all basin-margin alluvial environments. The alternative term *braidplain* may be used for fluvial systems consisting of an array of parallel streams with multiple sources. The corresponding coastal system may be called a *braidplain delta*. In practice the difficulty of distinguishing single from multiple sources and parallel versus radiating dispersion in the ancient record may make these distinctions difficult to apply. Orton (1988) suggested that most fans and fan deltas have a transverse relationship to regional structural grain, contrasting with the axial or lon-

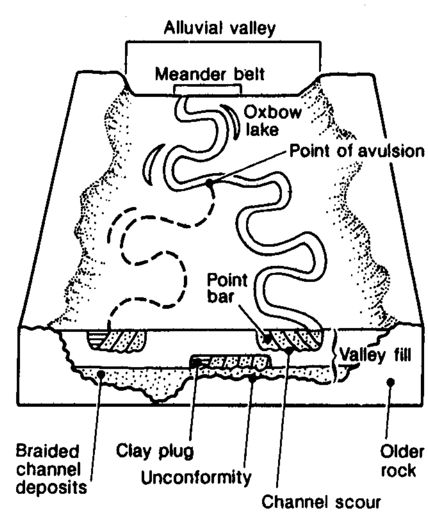

Figure 27 Schematic block diagram of the valley-fill deposits of the Mississippi River. The basal bounding discontinuity of the valley formed during the Pleistocene lowstand of sea level, when the river incised bedrock to adjust itself to a lower base level. As sea level rose following glaciation the valley filled first with coarse sands deposited in a braided-stream environment, and then with lower energy meandering-stream deposits. Many ancient valley-fill alluvial successions formed in this way. In some, the uppermost deposits are estuarine to marine in depositional environment, and may be followed by widespread transgressive-marine blanket deposits (Weimer, 1986; based on the work of H. Fisk)

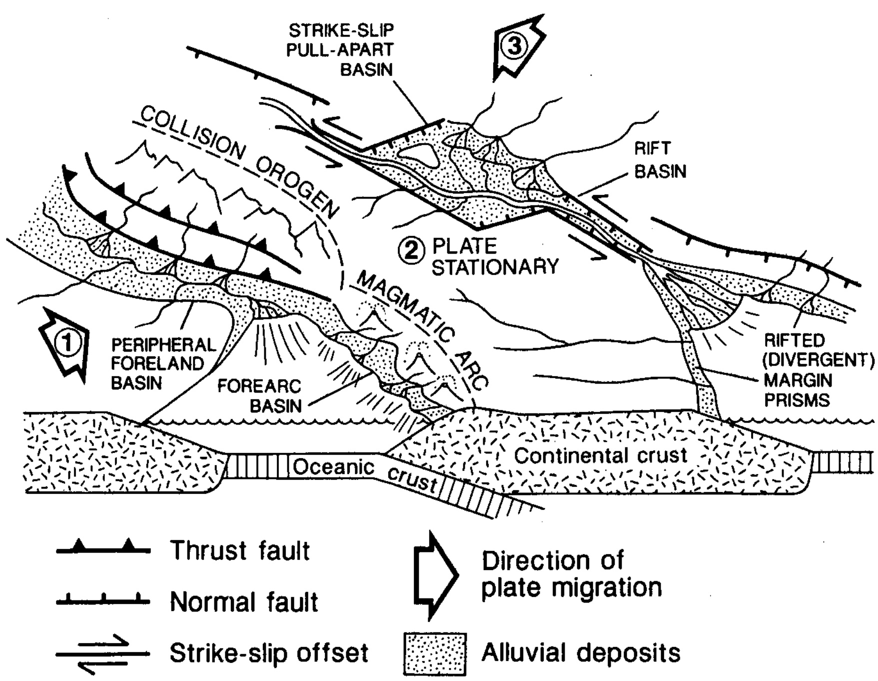

Figure 26 Tectonic setting of fluvial deposits. Note the distinction between *transverse* drainage, which is oriented perpendicular to structural grain, and *axial*, or *longitudinal* drainage, which typically consists of trunk streams flowing along the basin axis.

gitudinal orientation of typical braidplains. He also suggested that debris flow deposits and sheetflood deposits were more likely to occur on fans, as opposed to braidplains.

In light of the problems discussed above, the terms alluvial fan and fan delta should clearly be used with extreme caution when applied to the rock record. Because the primary criterion in modern environments is diverging distributary patterns, these should be demonstrated in ancient rocks if this terminology is to be used meaningfully. Excellent descriptions of alluvial fans and fan deltas are given by Nilsen (1985) and Nemec and Steel (1988), respectively.

EXAMPLES OF FLUVIAL STYLES

Given the variability in nature of the many controls that govern fluvial style (climate, discharge amount and variability, sediment size and amount, regional slope, subsidence rate, bank stability) it is not surprising that fluvial systems show a very wide range of depositional styles. The basic sedimentary processes are comparable in all rivers, which is why it is possible to use a single facies classification for all alluvial deposits. The major architectural elements are also comparable in all rivers. Thus lateral-accretion deposits occur in gravel- and sand-bed braided rivers and all types of meandering rivers and, to a minor extent, also in anastomosing and straight rivers. But the geometry of the channels and the way by which the elements are stacked on each other show a wide degree of variability. A few of the better known examples of fluvial style are described briefly in this section.

Gravel bed rivers

Gravel bed rivers occur as the distributaries of many alluvial fans, and also form the proximal reaches of many fluvioglacial outwash plains. Many channels may be active within a single broad valley. Element GB predominates (Fig. 19). This is built up by the development of low gravel sheets during high-discharge events (facies Gm; Fig. 5B), and by the migration of gravel bedforms (Gp, Gt; Fig. 5B). Typically gravel comprises up to 95 per cent of the total thickness, the remainder being sand deposited in minor channels, during low-water stage.

A variation of this style includes sheets or lobes of element SG (Fig. 5A), representing catastrophic run-off events. This fluvial style is most typical of alluvial fans in unvegetated areas, where there is little to inhibit rapid runoff from sudden rain storms.

Sand bed braided rivers

There is a wide variety of styles of sand bed braided rivers. Shallow pe-

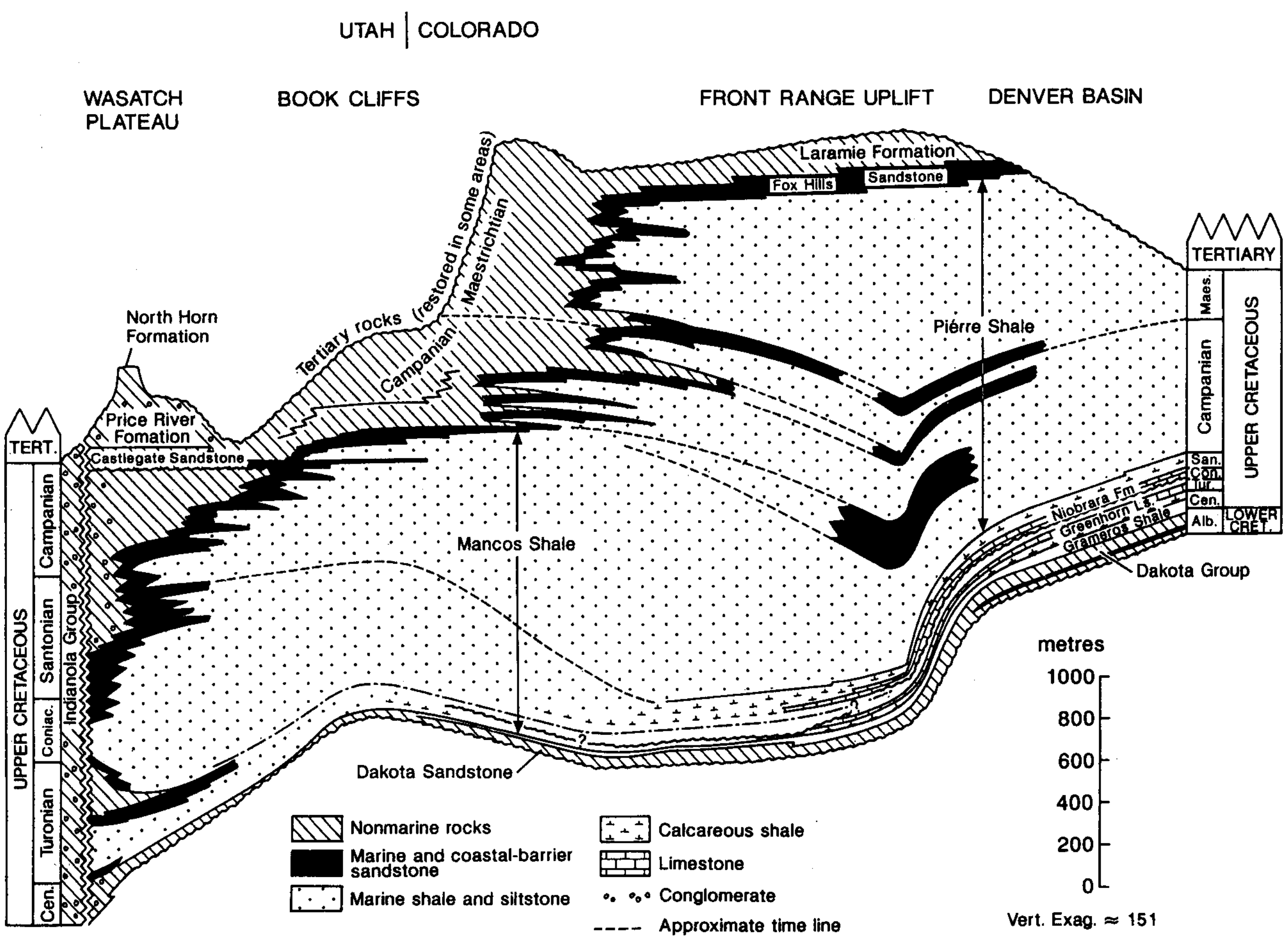

Figure 28 Stratigraphic cross section of Cretaceous-Tertiary rocks from central Utah to northeastern Colorado. Clastic wedges of this type are very common in retroarc and peripheral foreland basins. This example is from the foreland basin of the North American Western Interior. Note interfingering of marine and nonmarine strata (Molenaar and Rice, 1988).

rennial rivers, such as much of the Platte River of Nebraska, are characterized by the migration of large, lobate 3-D dunes, which deposit suites of planar-tabular cross bedding and associated minor structures (element SB; Fig. 5E). Braidplains in arid environments may be ephemeral, and are then characterized by tabular sandbodies up to several metres thick consisting of plane-laminated sand (element LS; Fig. 5F), or by flood sheets comprising thinning- and fining-upward assemblages of cross bedding and ripples (SB). The most complex sandy-braided deposits are those developed in large, perennial rivers, in which a wide variety of large bar forms (macroforms) develops. Side bars, which evolve in a similar style to point bars and deposit element LA are common. Mid-channel bars are also common, and may accrete in any direction within the channel, but most typically grow laterally and downstream (Figs. 12, 13). The deposits then may consist of elements LA and DA, and these may grade into each other within the same sand sheet. Figure 20 is a block diagram of such a river.

Fining-upward cycles are common in sandy-braided rivers (Miall, 1977; Fig. 15A of this paper). However, they are generated by several different processes. Godin (1991), in a detailed study of one ancient deposit defined three types of cycle (Fig. 21): 1) cycles 1-6 m thick developed by the generation of a macroform (e.g., sand flat) or the fill of a large scour hollow; 2) stacked macroform cycles constituting the fill of a channel, 1-10 m thick, and 3) cycles representing the thickness of major sandstone sheets 4-16 m thick and up to several or many kilometres in lateral extent. Unlike the first two types of cycle, sheet cycles may have allogenic causes, reflecting gentle basin tilting or base-level change. Definition and outcrop mapping of the various ranks of bounding surface are essential for the correct identification of these various types of cycle.

Coarse-grained meandering streams

The coarse-grained (sand and/or gravel) meandering stream (Figs. 22, 23) is characterized by point-bar deposits (element LA; Fig. 10) that typically have a lag deposit of caved bank material, waterlogged plant material, or calcrete pebbles and cobbles at their base. The accretionary face of the bar is crossed by numerous sandy bedforms, such as sand waves and dunes (2-D and 3-D). The point bar may show upward fining (Fig. 15B, C), as illustrated in the early models of Allen (1963) and Visher (1965), depending on such factors as meander sinuosity and flow patterns around the bend. In the ideal case, the sediment transported across the bar is sorted in an environment in which flow depth and velocity decrease up the bar surface, as a result of the helical flow patterns that develop around the meander bend (Fig. 9). Meander scars and abandoned channels (oxbow lakes) are common in the floodplain.

There are several other classes of meandering river, which differ from each other primarily in the grain size of the sediment load and the corresponding sedimentary structures. They range from vigorous, gravel bed rivers with gravel point bars that develop in some basin-margin environments, to sluggish, suspended-load streams in which the dominant deposits are mud, silt and very fine-grained sand.

Anastomosed rivers

Anastomosed rivers consist of several or many active channels of low to high sinuosity (Fig. 24). They are relatively

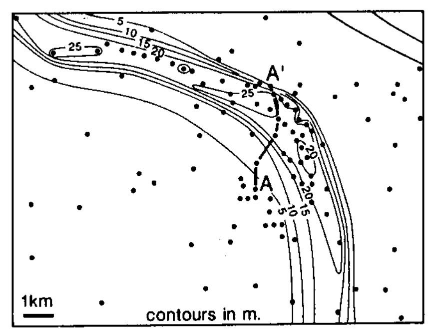

Figure 29 Isopach map (contours in metres) of valley-fill sandstone, Little Bow Field, Mannville Group, Alberta. The cross section is shown in Figure 30 (Wood and Hopkins, 1989)

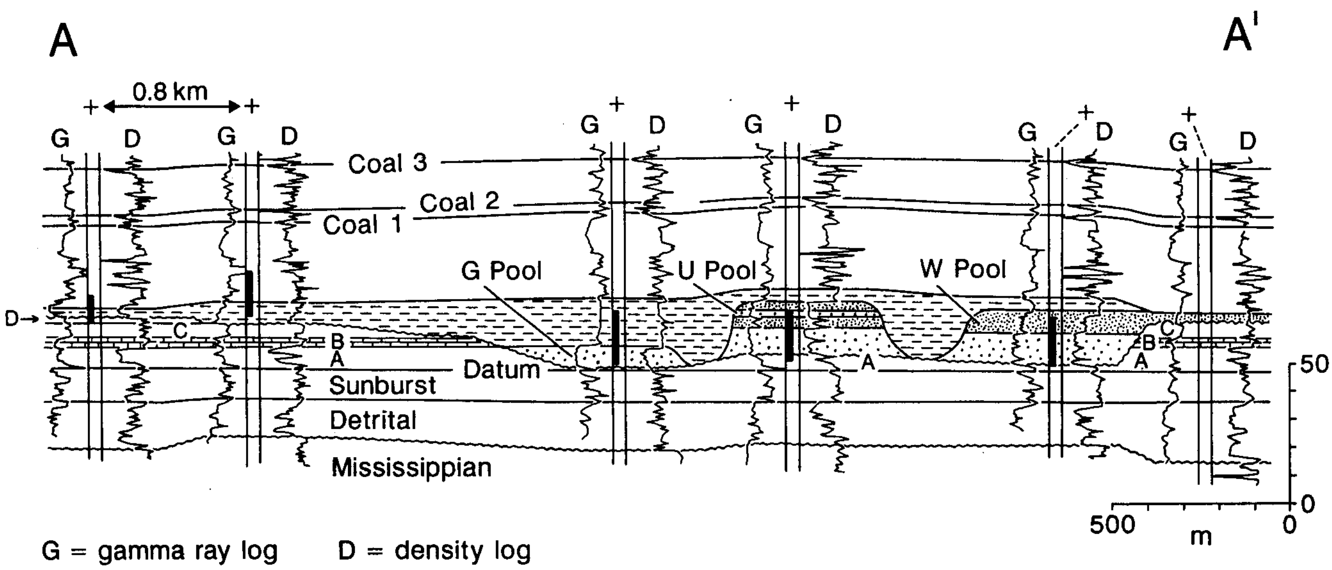

Figure 30 Stratigraphic cross sections across the valley-fill at Little Bow field. Note the presence of three separate pools in the valley-fill, separated by shale-filled channels. The location of the cross section is given in Figure 29 (Wood and Hopkins, 1989).

stable in position, unlike braided and meandering rivers. The channels develop ribbon sand bodies that are typically isolated within thick floodplain fines and crevasse splays (Fig. 25). The system evolves by the plugging of channels with bedload deposits, which encourages crevassing to occur. Crevasse splays become large enough that the discharge which deposits them eventually escapes into an adjacent channel, causing the diversion of channel flow (Smith and Smith, 1980; Smith, 1983).

TECTONIC SETTING

Alluvial deposits are sensitive indicators of allogenic processes, such as tectonism and base-level change. An examination of these controls is therefore an essential element of a basin analysis of a fluvial system. One of the most important allogenic controls is tectonic setting (Fig. 26). The thickest successions of alluvial deposits occur in rift basins (including failed rifts and aulacogens), forearc basins, retroarc and peripheral foreland basins, and those associated with plate-collision hinterland deformation, particularly foreland and strike-slip basins. Note that some of these basin types are one-sided, in that the alluvial apron forms a prismatic-shaped body flanking the sea or a major lake (Fig. 26). Drainage (paleocurrent directions) and the orientation of proximal-distal facies changes are essentially perpendicular to the basin margin. Ocean-margin basins on passive or divergent plate margins are of this type, as are some foreland basins. In other cases the basin is two-sided, with alluvial aprons on both sides. The basin centre may be occupied by a water body, or by a major trunk river that collects runoff and sediment, and disperses it along the axis of the basin. The facies characteristics and orientation of this trunk river system are typically very different from those of the feeder systems draining from the sides. Most rift basins, strike-slip fault-bounded basins, and many foreland basins are of this second type. These various types of basin-fill patterns have been reviewed by Miall (1981, 1990). Fluvial deposits do not occur in some types of basin, such as oceanic trenches, subduction complexes, and remnant ocean basins, because these basins are floored by oceanic crust, and therefore are unlikely to include any areas of nonmarine deposition.

Proximal (near-source) deposits may reach enormous thicknesses (17 km of Tertiary fluvial and associated marine strata in the Western Trough of Burma; 7 km of fluvial deposits in the Indus-Ganges Trough of northern Pakistan). Commonly they are structurally deformed and uplifted, indicating that the tectonism that uplifted the source area continued during deposition. Early basin-fill sediment may be cannibalized by uplift and erosion and fed back into the basin, where it is incorporated into the younger basin fill. It is common for proximal deposits to make up large-scale coarsening-upward cycles tens to hundreds of metres thick, recording the increasing source-area relief and depositional slope during active tectonism (Heward, 1978; Steel *et al.*, 1977). The *distal* deposits occupying the basin centre may interfinger with shallow-marine or lacustrine deposits, the style of the interfingering providing a sensitive record of the local fluctuations in base level, as discussed in the next section.

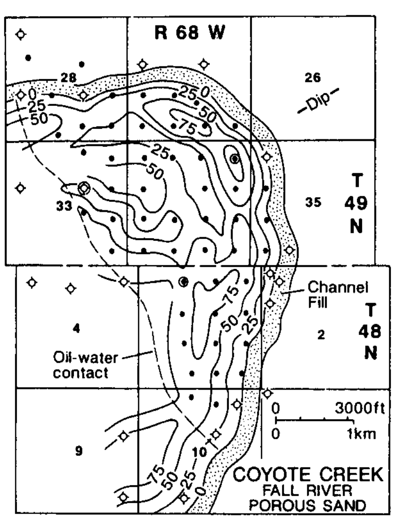

Figure 31 Isopach map (contours in feet) of the Coyote Creek field, Wyoming. Regional dip is toward the west. Oil is trapped against the updip flank of the point bar, which is bordered by the impermeable shale of the abandoned channel. Detailed wireline-log cross sections show that the point-bar lens is probably a composite of more than one bar, with the mapped channel representing the final channel position at the time of abandonment (Berg, 1968).

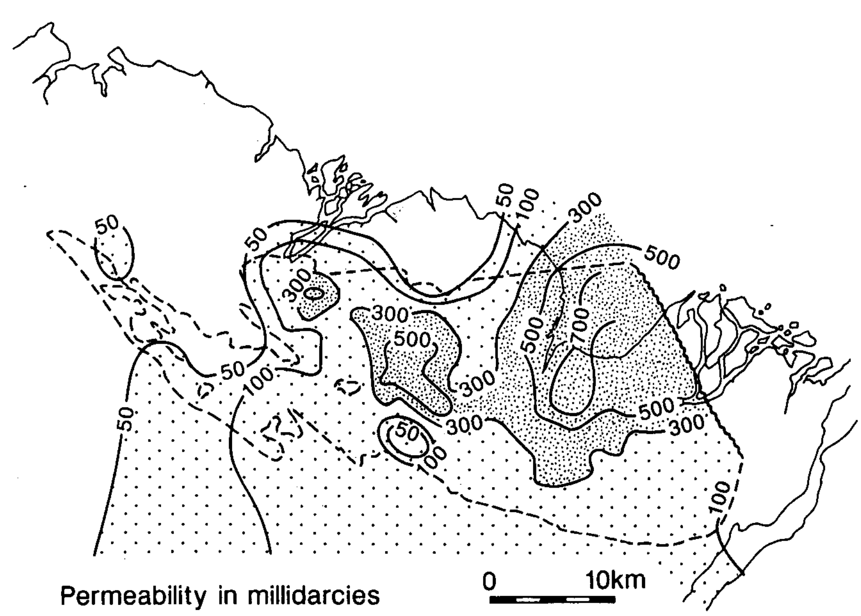

Figure 32 Isopermeability map of the braided channel complex in the Sadlerochit Formation, Alaska North Slope. The Prudhoe Bay field is outlined by the dashed line. The wavy line indicates the faulted margin of the field. High permeability values (the larger millidarcy numbers) are yielded by the coarse, texturally more mature deposits formed in proximal reaches of the complex. Note the crudely lobate shape of the area of high permeability, corresponding to the distribution of the sand sheet, in the form of a large, fan-shaped braided delta complex (Wadman *et al.*, 1979).

BASE-LEVEL CHANGE AND ITS CONTROL OF ALLUVIAL ARCHITECTURE

There is no doubting the primary control of tectonism in creating most alluvial successions. The geometry and timing of alluvial clastic wedges and associated coastal plain deposits can typically be related to tectonic episodes in the source area(s). For example, Cenozoic clastic wedges of the Gulf Coast can be correlated with tectonism in the headwaters region of the Gulf Coast rivers - the Cordilleran mountains of the western United States (Galloway, 1989). At the distal fringes of an alluvial succession, however, where it interfingers with marine deposits, the question of tectonic versus sedimentary controls is a more difficult one. Many basins contain regional unconformity surfaces crossed by incised-channel systems. The fluvial and estuarine deposits filling these channels may be important petroleum reservoirs, as in the Mannville Group of Alberta (Farshori and Hopkins, 1989; Wood and Hopkins, 1989) and the "J" Sandstone of the Denver Basin (Weimer, 1986). Is the unconformity the result of falling sea level or basin uplift? Many modern river systems show a similar incised architecture (Fig. 27), reflecting their response to the lower sea levels during the Pliocene-Quaternary ice age. Suter *et al.* (1987) described examples from the Quaternary deposits of the Louisiana continental shelf.

In other basins wedges of fluvial sediment up to hundreds of metres thick are interbedded in complex stratigraphic relationships with marine shoreface and shelf deposits. Examples include many of the mid-Cretaceous deposits of the Alberta foreland basin (Plint and Norris, 1991) and Upper Cretaceous-Tertiary rocks of the Book Cliffs, Utah (Molenaar and Rice, 1988; Fig. 28). Is the alternation of regression and transgression driven by variations in sediment supply and depositional slope (tectonic controls), or by changes in base level? In the case of the Book Cliffs succession (Fig. 28) there is no question about the overriding tectonic control. The development of the clastic wedge as a whole can be correlated with orogenic episodes to the west (Sevier Orogeny). Different fluvial tongues have different paleocurrent patterns, indicating shifts in paleoslope, and they also have different detrital sandstone compositions indicating changes in sediment source areas. These effects can only be explained by tilting of the basin and uplift of the basin margin as a result of contemporary tectonism (Lawton, 1986). A similar conclusion was reached by Embry (1990) regarding Mesozoic depositional successions in Sverdrup basin, Arctic Canada. However, in detail, changes in base level, such as those related to eustasy, may control the architecture of the coastal plain deposits. This is the view of Van Wagoner

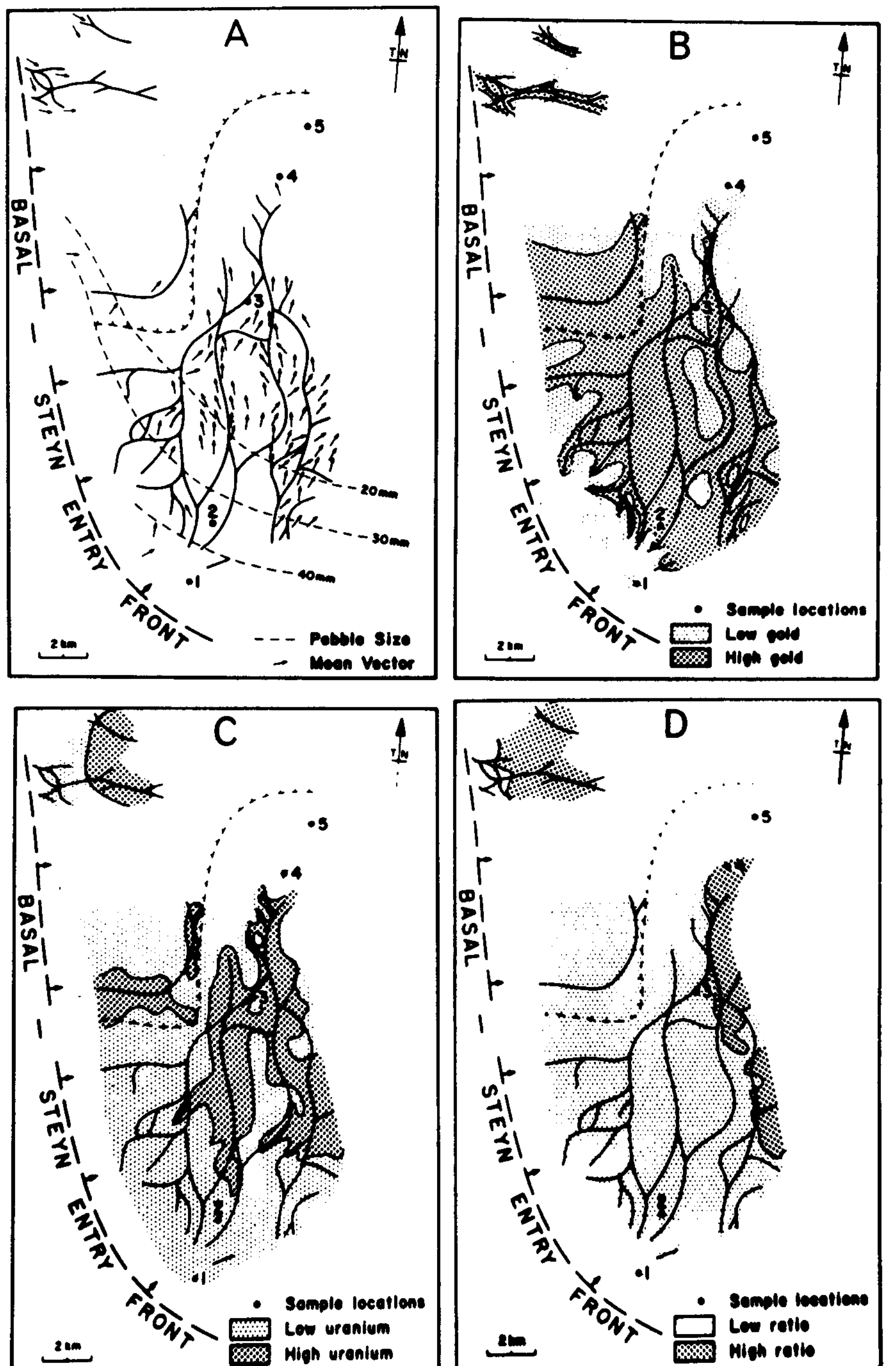

Figure 33 Distribution of gold and uranium placer particles in a Witwatersrand braidplain deposit: A) contours showing maximum pebble size, and vector-mean paleocurrent directions; B, C) distribution of gold and uranium particles (relative values); D) uranium/gold ratio (Minter, 1978).

et al. (1990), who interpreted the Castlegate and other sandstone tongues of Book Cliffs in terms of changes in base level (Posamentier and Vail, 1988; Posamentier *et al.*, 1988). Tongues of fluvial sandstone were interpreted as resting on regional scour surfaces (of 6th-order rank or higher; Table 1). They extend far into the basin over marginal-marine deposits. They were designated by Van Wagoner *et al.* (1990) as "lowstand" deposits, formed by backfilling above an erosion surface that truncates underlying shoreface deposits. Separating the effects of tectonism from eustasy in such cases is extremely difficult.

A quite different configuration occurs where fluvial deposits represent the coarse upper member of coarsening-upward successions that develop by progradation into a basin. Such fluvial deposits may, in this case, represent "highstand" deposits, formed at a time of high, stable base level, when the continental shelf is filled by progradation of the coastal plain (Posamentier *et al.*, 1988). This depositional pattern is typically terminated by incision accompanying a fall in base level (Miall, 1991a).

ECONOMIC DEPOSITS IN ALLUVIAL SEDIMENTS

A knowledge of alluvial architecture is of importance in the exploitation of the fuels and minerals stored in the rocks, and for understanding the flow of groundwaters (including toxic wastes) through aquifers. A knowledge of facies assemblages and successions and of depositional architecture can lead to useful predictions regarding the extent and orientation of porous bodies in the subsurface. Petroleum geologists were among the first to recognize the importance of such information. The first well-documented example of a fluvial stratigraphic trap was the point-bar study published by Berg (1968).

Oil and gas occur in several types of reservoir body. Paleovalley-fills form linear reservoirs, in which the petroleum is trapped updip against any impermeable rocks that are incised by the valley. Fields in the Mannville Group of Alberta and the "J" sandstone of the Denver Basin are good examples (Figs. 29, 30). Note the narrowness of the sandstone body, and the consequent need for excellent well control to locate and map the reservoir. The reservoir may consist of several separate valley-fill tongues, and may be incised by mud-filled channels separating it into isolated sandbodies. As a result, a field may contain several separate hydrocarbon pools, with oil-water and gas-oil contacts at different levels (Fig. 30). A different type of stratigraphic trap is formed where the depositional style of the fluvial system produces sand lenses isolated within floodplain fines. The point-bar fields of the Fall River Sandstone, Wyoming, are classic examples (Fig. 31). Such fields tend to be small, but the point bars may occur in connected meander belts at more than one stratigraphic level, leading to large cumulative production from dozens or even hundreds of separate pools. The giant Daqing field of China is an excellent example of this type (Yinan *et al.*, 1987). Production from such fields requires an ability to understand the origins of the sand lens geometry and predict its distribution in the subsurface from knowledge of regional paleogeography.

Finally, there are the reservoirs formed by braided sheet sands. These may be volumetrically large, and provide reasonably continuous reservoir bodies, reflecting a simple architecture of amalgamated sheet-sandstone bodies. However, production problems in some mature fields show that there may be important internal heterogeneities formed by poorly sorted sands, or mud drapes situated on third- to fifth-order bounding surfaces. The Prudhoe Bay field, Alaska, is an excellent example of this type of field (Fig. 32). Another is Messla field, Libya (Clifford *et al.*, 1980).

Among the best known mineral deposits in alluvial sediments are the placer gold and uranium in the Witwatersrand Supergroup, South Africa. The distribution of the placer particles is controlled by downstream sorting processes, and maps of their concentration outline bars and channels in a braidplain system (Fig. 33).

CONCLUSIONS

This chapter has considered facies analysis and facies models at four main levels of scale and complexity.

1. Individual clastic facies may be recognised and classified primarily according to their grain size and sedimentary structures. A limited number of facies states occur in fluvial deposits (Table 2). Successions of facies in the rock record may indicate progressively changing conditions, for example, the gradual shallowing of the water and reduction in flow strength up a point-bar surface. Primary mesoscopic heterogeneities in petroleum reservoirs and aquifers relate to depositional controls at this scale.

2. Architectural elements are assemblages of facies organized into deposits of a particular overall shape and internal geometry. They represent the major depositional features of fluvial systems, as shown in Table 3, and are the source of macroscopic heterogeneities in reservoirs and aquifers. Analysis of architectural elements requires a study of the bounding surfaces in fluvial deposits, including their extent, shape and facies relations.

3. River systems as a whole vary in terms of the amount and distribution of the discharge (large rivers versus small streams; ephemeral, perennial, seasonal, and other patterns of discharge variability), the number of active channels and their sinuosity, and the grain-size range of the sediment load. These factors determine the assemblage of facies and architectural elements that are preserved. These factors also control the scale and geometry of the architectural elements. Outcrop studies should incorporate detailed bounding-surface and paleocurrent information into the analysis — data that are hard to assemble from subsurface sources. Variations at this scale affect reservoir and aquifer heterogeneity at the macroscopic scale.

Facies models can be built for different fluvial styles, to illustrate the major depositional processes and products. The sandy meandering river system (Fig. 22) and the sandy braided system with sand flats (Fig. 20) are among the best known, and were emphasized in previous editions of this book.

4. At the basin scale, the stratigraphic architecture of fluvial deposits yields information on the major allogenic controls of deposition. For example, clastic wedges develop in response to basin-margin tectonism. Sheets and tongues bounded at the base by regional disconformities are typically valley-fill deposits formed at times of low base level.

REFERENCES

Basic sources of information

Collinson, J. D., 1986, Alluvial sediments, *in* Reading, H. G., ed., Sedimentary environments and facies: Oxford, Blackwell Scientific Publications Ltd., p. 20-62.
The best general summary of fluvial processes and facies, but does not deal with architectural elements.

Collinson, J.D. and Lewin, J., eds., 1983, Modern and ancient fluvial systems: International Association of Sedimentologists, Special Publication 6, 575 p.
A useful collection of papers emphasizing present-day channel processes and facies models.

Ethridge, F.G., Flores, R.M. and Harvey, M.D., eds., 1987, Recent developments in fluvial sedimentology: Society of Economic Paleontologists and Mineralogists, Special Publication 39, 389 p.
A collection of useful, up to date papers on many aspects of fluvial deposition.

Flores, R.M., Ethridge, F.G., Miall, A.D., Galloway, W.E. and Fouch, T.D., 1985, Recognition of fluvial depositional systems and their resource potential: Society of Economic Paleontologists and Mineralogists, Short Course 19, 290 p.
Facies descriptions and modern and ancient examples from five different perspectives.

Miall, A.D., ed., 1978, Fluvial sedimentology: Canadian Society of Petroleum Geologists, Memoir 5, 859 p.
Although a little dated, this volume contains several classic papers and remains an excellent source of information.

Nemec, W. and Steel, R.J., eds., 1988, Fan deltas: sedimentology and tectonic setting: Glasgow, Blackie, 444 p.
An excellent compilation of research papers on fan deltas. Several papers discuss definitions of fan deltas and related depositional systems, presenting several different (and in places confusing) ideas.

Nilsen, T.H., ed., 1984, Fluvial sedimentation and related tectonic framework, western North America: Sedimentary Geology, v. 36, 523 p.
A special issue of Sedimentary Geology with a collection of regional basin-analysis papers, including discussions of basin architecture and tectonic control.

Wilgus, C.K., Hastings, B.S., Posamentier, H.W., Ross, C.A. and Kendall, C.G.St.C., eds., 1988, Sea level changes: an integrated approach: Society of Economic Paleontologists and Mineralogists, Special Publication 42, 407 p.
Collection of papers emphasizing conceptual basis of sequence stratigraphy plus numerous case studies of sea level change from the geological record.

Other references

Allen, J.R.L., 1963, Henry Clifton Sorby and the sedimentary structures of sands and sandstones in relation to flow conditions: Geologie en Mijnbouw, v. 42, p. 223-228.

Allen, J.R.L., 1965, A review of the origin and characteristics of recent alluvial sediments: Sedimentology, v. 5, p. 89-191.
A classic early review, focusing on meandering streams, with many examples and diagrams.

Allen, J.R.L., 1983: Studies in fluviatile sedimentation: bars, bar complexes and sandstone sheets (low-sinuosity braided streams) in the Brownstones (L. Devonian), Welsh Borders: Sedimentary Geology, v. 33, p. 237-293.
A very well illustrated architectural study of an ancient braided stream deposit, with the author's own classification of elements and bounding surfaces.

Allen, J.R.L., 1985, Principles of physical sedimentology: London, George Allen and Unwin, 272 p.

Ashley, G.M., 1990, Classification of large-scale subaqueous bedforms: a new look at an old problem: Journal of Sedimentary Petrology, v. 60, p. 160-172.
A major synthesis of new ideas regarding the generation of bedforms, with some suggestions regarding documentation, and an elegant classification.

Berg, R.R., 1968, Point-bar origin of Fall River Sandstone reservoirs: American Association of Petroleum Geologists Bulletin, v. 52, p. 2116-2122.

Bernard, H.A., Leblanc, R.J. and Major, C.J., 1962, Recent and Pleistocene geology of southeast Texas, *in* Rainwater, E.H. and Zingula, R.P., eds., Geology of the Gulf Coast and central Texas; Geological Society of America, Guidebook for 1962 Annual Meeting, p. 175-224.

Blatt, H., Middleton, G.V. and Murray, R., 1980. Origin of sedimentary rocks, 2nd edition: Englewood Cliffs, NJ, Prentice-Hall Inc., 782 p.

Bown, T.M. and Kraus, M.J. 1987, Integration of channel and floodplain suites, I. Development of sequence and lateral relations of alluvial paleosols: Journal of Sedimentary Petrology, v. 57, p. 587-601.

Cant, D.J. and Walker, R.G., 1978, Fluvial processes and facies sequences in the sandy braided South Saskatchewan River, Canada: Sedimentology, v. 25, p. 625-648.
One of the best descriptions of the surface processes of sand-flat formation in a sandy-braided river. Illustrated with many photographs.

Clifford, H.J., Grund, R. and Musrati, H., 1980, Geology of a stratigraphic giant: Messla Oil Field, Libya, *in* Halbouty, M.T., ed., Giant oil and gas fields of the decade 1968-1978: American Association of Petroleum Geologists, Memoir 30, p. 507-524.

Collinson, J.D., 1970, Bedforms of the Tana River, Norway: Geografiska Annaler, v. 52A, p. 31-55.

Doeglas, D.J., 1962, The structure of sedimentary deposits of braided rivers: Sedimentology, v. 1, p. 167-190.

Eberth, D.A. and Miall, A.D., 1991, Stratigraphy, sedimentology and evolution of a vertebrate-bearing, braided to anastomosed fluvial system, Cutler Formation (Permian-Pennsylvanian), north-central New Mexico: Sedimentary Geology, v. 72, p. 225-252.

Embry, A.F., 1990, A tectonic origin for third-order depositional sequences in extensional basins — implications for basin modelling, *in* Cross, T.A., ed., Quantitative dynamic stratigraphy: Englewood Cliffs, N.J., Prentice-Hall, p. 491-501.

Farshori, M.Z. and Hopkins, J.C., 1989, Sedimentology and petroleum geology of fluvial and shoreline deposits of the Lower Cretaceous Sunburst Sandstone Member, Mannville Group, southern Alberta: Bulletin of Canadian Petroleum Geology, v. 37, p. 371-388.

Galloway, W.E., 1989, Genetic stratigraphic sequences in basin analysis II: application to northwest Gulf of Mexico Cenozoic basin: American Association of Petroleum Geologists, Bulletin, v. 73, p. 143-154.

Godin, P.D., 1991, Fining-upward cycles in the sandy braided-river deposits of the Westwater Canyon Member (Upper Jurassic), Morrison Formation, New Mexico: Sedimentary Geology, v. 70, p. 61-82.

Harms, J.C. and Fahnestock, R.K., 1965, Stratification, bed forms, and flow phenomena (with an example from the Rio Grande), *in* Middleton, G.V., ed., Primary sedimentary structures and their hydrodynamic interpretation: Society of Economic Paleontologists and Mineralogists, Special Publication 12, p. 84-115.

Heward, A.P., 1978, Alluvial fan sequence and megasequence models: with examples from Westphalian D - Stephanian B coalfields, northern Spain, *in* Miall, A.D., ed., Fluvial Sedimentology: Canadian Society of Petroleum Geologists, Memoir 5, p. 669-702.

Hirst, J.P.P. and Nichols, G.J., 1986, Thrust tectonic controls on Miocene alluvial distribution patterns, southern Pyrenees, *in* Allen, P.A. and Homewood, P., eds., Foreland basins: International Association of Sedimentologists, Special Publication 8, p. 247-258.

Holmes, A., 1965, Principles of physical geology: London, Thomas Nelson, 1288 p.

Jackson, R.G., II, 1975: Hierarchical attributes and a unifying model of bedforms composed of cohesionless material and produced by shearing flow; Geological Society of America, Bulletin, v. 86, p. 1523-1533.

Kraus, M.J., 1987, Integration of channel and floodplain suites, II. Vertical relations of alluvial paleosols: Journal of Sedimentary Petrology, v. 57, p. 602-612.

Lawton, T.F., 1986, Fluvial systems of the Upper Cretaceous Mesaverde Group and Paleocene North Horn Formation, central Utah: a record of transition from thin-skinned to thick-skinned in the foreland region, *in* Peterson, J.A., ed., Paleotectonics and sedimentation in the Rocky Mountain region, United States: American Association of Petroleum Geologists, Memoir 41, p. 423-442.

Leeder, M.R., 1975, Pedogenic carbonate and flood sediment accretion rates: a quantitative model for alluvial, arid-zone facies: Geological Magazine, v. 112, p. 257-270.

McCabe, P.J., 1984, Depositional environments of coal and coal-bearing strata, *in* Rahmani, R.A. and Flores, R.M., eds., Sedimentology of coal and coal-bearing sequences: International Association of Sedimentologists, Special Publication 7, p. 13-42.

A thought-provoking review of our ideas regarding the depositional environment of coal. Concludes that the exclusion of clastic detritus from peat deposits by the development of raised swamps is an important component of the process of coal development.

Miall, A.D., 1977, A review of the braided river depositional environment: Earth Science Reviews, v. 13, p. 1-62.

A comprehensive review of the sedimentary processes of braided rivers. The facies classification used in this chapter is first proposed here.

Miall, A.D., 1978a, Fluvial sedimentology: an historical review, *in* Miall, A.D., ed., Fluvial sedimentology, Canadian Society of Petroleum Geologists, Memoir 5, p. 1-47.

Miall, A.D., 1978b, Facies types and vertical profile models in braided river deposits: a summary, *in* Miall, A.D., ed., Fluvial sedimentology: Canadian Society of Petroleum Geologists, Memoir 5, p. 597-604.

An updating of the facies classification and the description of braided-river vertical profile models from the 1977 paper.

Miall, A.D., 1980, Cyclicity and the facies model concept in geology: Bulletin of Canadian Petroleum Geology, v. 28, p. 59-80.

Miall, A.D., 1981, Alluvial sedimentary basins: tectonic setting and basin architecture, *in* Miall, A.D., ed., Sedimentation and tectonics in alluvial basins: Geological Association of Canada, Special Paper 23, p. 1-33.

Miall, A.D., 1985, Architectural-element analysis: a new method of facies analysis applied to fluvial deposits: Earth Science Reviews, v. 22, p. 261-308.

An attempt to develop a standardized approach to the description and classification of architectural elements.

Miall, A.D., 1988, Reservoir heterogeneities in fluvial sandstones: lessons from outcrop studies: American Association of Petroleum Geologists, Bulletin, v. 72, p. 682-697.

Miall, A.D., 1990, Principles of sedimentary basin analysis: New York, Springer-Verlag, 668 p.

Miall, A.D., 1991a, Stratigraphic sequences and their chronostratigraphic correlation: Journal of Sedimentary Petrology, v. 61, p. 497-505.

A critique of the Exxon sequence models, focusing on problems with their ideas regarding fluvial accommodation space, and problems of biostratigraphic precision.

Miall, A.D. 1991b, Hierarchies of architectural units in clastic rocks, and their relationship to sedimentation rate, *in* Miall, A.D., and Tyler, N., eds., The three-dimensional facies architecture of terrigenous clastic sediments, and its implications for hydrocarbon discovery and recovery: Society of Economic Paleontologists and Mineralogists, Concepts in Sedimentology and Paleontology, v. 3, p. 6-12.

Miall, A.D., and Smith, N.D., 1989: Rivers and their deposits; Society of Economic Paleontologists and Mineralogists, Slide Set 4.

Carefully selected set of photographs of modern and ancient alluvial deposits, with a concise descriptive text.

Minter, W.E.L., 1978, A sedimentological synthesis of placer gold, uranium and pyrite concentrations in Proterozoic Witwatersrand sediments, *in* Miall, A.D., ed., Fluvial sedimentology: Canadian Society of Petroleum Geologists, Memoir 5, p. 801-829.

Molenaar, C.M. and Rice, D.D., 1988, Cretaceous rocks of the Western Interior Basin, in Sloss, L.L., ed., Sedimentary cover — North American Craton: U.S.: Geological Society of America, The geology of North America, v. D-2, p. 77-82.

Moody-Stuart, M., 1966, High and low sinuosity stream deposits, with examples from the Devonian of Spitzbergen: Journal of Sedimentary Petrology, v. 36, p. 1102-1117.

Nanz, R.H., Jr., 1954, Genesis of Oligocene sandstone reservoir, Seeligson field, Jim Wells and Kleberg Counties, Texas: American Association of Petroleum Geologists, Bulletin, v. 38, p. 96-117.

Nijman, W. and Puigdefabregas, C., 1978, Coarse-grained point bar structure in a molasse-type fluvial system, Eocene Castisent sandstone Formation, south Pyrenean Basin, *in* Miall, A.D., ed., Fluvial sedimentology: Canadian Society of Petroleum Geologists, Memoir 5, p. 487-510.

Nilsen, T.H., 1985, Modern and ancient alluvial fan deposits: New York, Van Nostrand Reinhold, 372 p.

Ore, H.T., 1964, Some criteria for recognition of braided stream deposits: Wyoming Contributions to Geology, v. 3, p. 1-14.

Orton, G.J., 1988, A spectrum of Middle Ordovician fan deltas and braidplain deltas, North Wales: a consequence of varying fluvial clastic input, *in* Nemec, W. and Steel, R.J., eds., Fan deltas: sedimentology and tectonic setting: Glasgow, Blackie, p. 23-49.

Parkash, B., Awasthi, A.K. and Gohain, K., 1983, Facies of the Markanda terminal fan, Kurukshetra district, Haryana, India, *in* Collinson, J.D. and Lewin, J., eds., Modern and ancient fluvial systems: International Association of Sedimentologists, Special Publication 6, p. 337-344.

Plint, A.G. and Norris, B., 1991, Anatomy of a ramp margin sequence: facies successions, paleogeography and sediment dispersal patterns in the Muskiki and Marshybank formations, Alberta Foreland Basin: Bulletin of Canadian Petroleum Geology, v. 39, p. 18-42.

Posamentier, H.W. and Vail, P.R., 1988, Eustatic controls on clastic deposition II — sequence and systems tracts models, *in* Wilgus, C.K., *et al.*, eds., Sea-level changes: an integrated approach: Society of Economic Paleontologists and Mineralogists, Special Publication 42, p. 125-154.

Posamentier, H.W., Jervey, M.T. and Vail, P.R., 1988, Eustatic controls on clastic deposition I — conceptual framework, *in* Wilgus, C.K., *et al.*, eds., Sea-level changes: an integrated approach: Society of Economic Paleontologists and Mineralogists, Special Publication 42, p. 109-124.

These two papers set out the Exxon view of sequence stratigraphy. Very persuasive, with lots of coloured diagrams, but difficult papers to read (and see Miall, 1991a for a different opinion).

Ramos, A. and Sopeña, A., 1983, Gravel bars in low-sinuosity streams (Permian and Triassic, central Spain), *in* Collinson, J.D. and Lewin, J., eds., Modern and ancient fluvial systems: International Association of Sedimentologists, Special Publication 6, p. 301-312.

Ramos, A., Sopeña, A. and Perez-Arlucea, M., 1986, Evolution of Buntsandstein fluvial sedimentation in the northwest Iberian Ranges (Central Spain); Journal of Sedimentary Petrology, v. 56, p. 862-875.

These two papers present the results of detailed architectural studies of some beautifully exposed Triassic fluvial deposits. The authors erect their own classification of architectural elements.

Schumm, S.A., 1968, Speculations concerning paleohydrologic controls of terrestrial sedimentation: Geological Society of America, Bulletin, v. 79, p. 1573-1588.

Schumm, S.A., 1981, Evolution and response of the fluvial system, sedimentological implications, *in* Ethridge, F.G., and Flores, R.M., eds., Recent and ancient nonmarine depositional environments: models for exploration: Society of Economic Paleontologists and Mineralogists, Special Publication 31, p. 19-29.

Smith, D.G., 1983, Anastomosed fluvial deposits: modern examples from western Canada, *in* Collinson, J.D., and Lewin, J., eds., Modern and ancient fluvial systems: International Association of Sedimentologists, Special Publication 6, p. 155-168.

Smith, D.G. and Smith, N.D., 1980, Sedimentation in anastomosed river systems: examples from alluvial valleys near Banff, Alberta: Journal of Sedimentary Petrology, v. 50, p. 157-164.

Smith, N.D., 1970, The braided stream depositional environment: comparison of the Platte River with some Silurian clastic rocks, north central Appalachians: Geological Society of America, Bulletin, v. 81, p. 2993-3014.

Steel, R.J., Machi, S., Nilsen, H., Roe S.L. and Spinnangr, A., 1977, Coarsening-upward cycles in the alluvium of Hornelen Basin (Devonian), Norway; sedimentary response to tectonic events: Geological Society of America, Bulletin, v. 88, p. 1124-1134.

Suter, J.R., Berryhill, H.L. and Penland, S., 1987, Late Quaternary sea-level fluctuations and depositional sequences, southwest Louisiana continental shelf, *in* Nummedal, D., Pilkey, O.H. and Howard, J.D., eds., Sea-level fluctuation and coastal evolution: Society of Economic Paleontologists and Mineralogists, Special Publication 41, p. 199-219.

Tyler, N., 1988, New oil from old fields: Geotimes, v. 33, #7, p. 8-10.

Van Wagoner, J.C., Mitchum, R.M., Campion, K.M. and Rahmanian, V.D., 1990, Siliciclastic sequence stratigraphy in well logs, cores, and outcrops: American Association of Petroleum Geologists, Methods in Exploration Series 7, 55 p.

Visher, G.S., 1965, Use of vertical profile in environmental reconstruction: American Association of Petroleum Geologists, Bulletin, v. 49, p. 41-61.

Wadman, D.H., Lamprecht, D.E. and Mrosovsky, I., 1979, Joint geologic/engineering analysis of the Sadlerochit reservoir, Prudhoe Bay field: Journal of Petroleum Technology, v. 31, p. 933-940.

Weimer, R.J., 1986, Relationship of unconformities, tectonics, and sea level change in the Cretaceous of the Western Interior, United States, *in* Peterson, J.A., ed., Paleotectonics and sedimentation in the Rocky Mountain region, United States: American Association of Petroleum Geologists, Memoir 41, p. 397-422.

Williams, P.F. and Rust, B.R., 1969, The sedimentology of a braided river: Journal of Sedimentary Petrology, v. 39, p. 649-679.

Wood, J.M. and Hopkins, J.C., 1989, Reservoir sandstone bodies in estuarine valley fill: Lower Cretaceous Glauconitic Member, Little Bow Field, Alberta, Canada: American Association of Petroleum Geologists, Bulletin, v. 73, p. 1361-1382.

Yinan Q., Peihua X. and Jingsiu X., 1987, Fluvial sandstone bodies as hydrocarbon reservoirs in lake basins, *in* Ethridge, F.G., Flores, R.M., and Harvey, M.D., eds., Recent developments in fluvial sedimentology: Society of Economic Paleontologists and Mineralogists, Special Publication 39, p. 329-342.

8. Eolian Systems

Michael E. Brookfield, Department of Land Resource Science,
University of Guelph, Guelph, Ontario N1G 2W1

INTRODUCTION

Eolian facies commonly form cliffs of pink or white sandstones characterized by very large sets of cross bedding (Fig. 1). Although this cross bedding has fascinated sedimentologists for many years, little detailed sedimentology has been attempted until recently. Eolian deposits were among the last to have coherent facies models developed. With the integration of studies on both modern and ancient eolian sediments, fairly detailed models can now been presented. The models involve the recognition of the different parts, as well as different types, of dune/interdune systems. The integration of patterns seen among the various systems may then give a coherent view of the development of an entire desert. The fluctuating sea levels emphasized in other chapters of this book have little influence on the development of inland sand seas, but may be important in areas of coastal dunes.

This chapter examines some of the features of modern eolian sands as the basis of eolian facies models. It will then show how the models can be applied to eolian sandstones. Finally, some of the possible external controls on sand sea development will be considered.

MODERN EOLIAN SANDS

Modern eolian sands occur mostly in sandy deserts and coastal dunes. Deposits in deserts are the most extensive. Arid and semi-arid conditions affect about one-third of the present land surface and include three main sedimentary environments, 1) alluvial fans and ephemeral streams, 2) inland sabkhas or playas, and 3) sandy deserts — also called "sand seas" or *ergs* (Fig. 2). Areas of sand accumulation form only about twenty per cent of the area of modern deserts. The rest comprises eroding mountains (40 per cent), stony areas or *serirs* (10-20 per cent) and desert flats (10-20 per cent). There are also smaller areas of dry washes, volcanic cones and badlands, where erosion rather than deposition takes place (Cooke and Warren, 1973). Within these desert environments, the amount of eolian sand varies greatly, depending on climate, wind regime, basin area and source rocks. Thus the wide enclosed basins of western China contain abundant eolian sand, whereas the small desert basins of western North America contain very little. In North America, alluvial fans are much more important (30 per cent), and sandy deserts much less (less than 1 per cent), than elsewhere. The one exception is the Gran Desierto, Sonora, Mexico (Fig. 2B), which is a sand sea.

The Sahara is the largest desert in the world (7 million km^2), and has several major ergs arranged in three belts. Individual ergs cover areas as large as 500,000 km^2 (twice the area of Nevada). They are located in physiographic or structural basins with long histories of sediment accumulation, including extensive Tertiary and Pleistocene fluvial sediments. However, the modern eolian deposits are rarely more than 100 m thick (Mainguet, 1976;

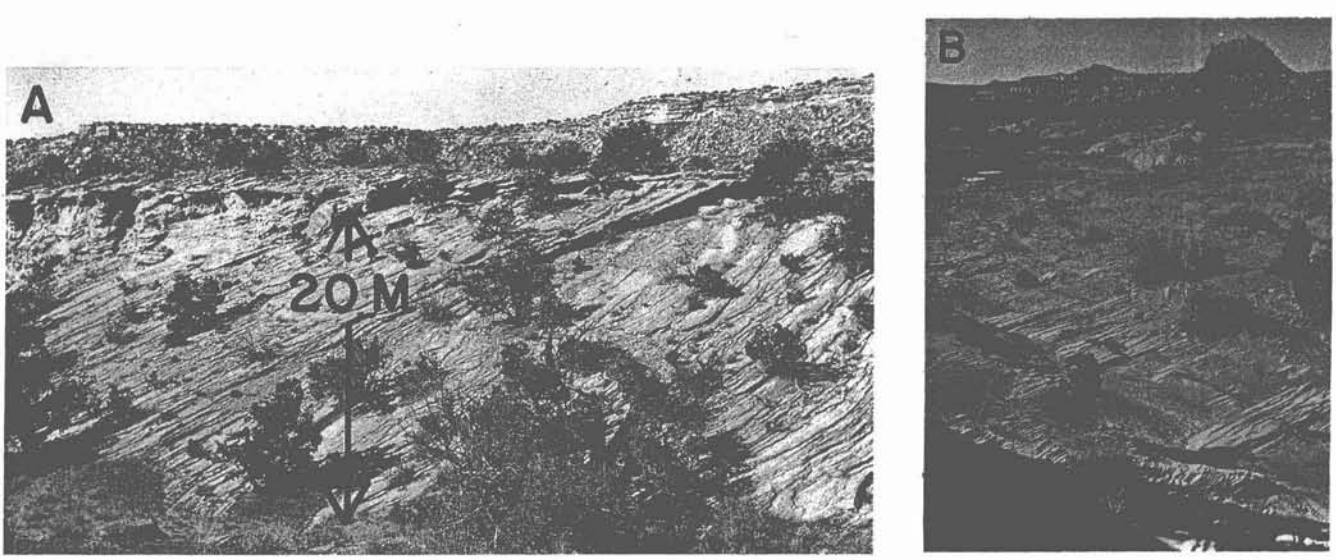

Figure 1 A) Twenty-metre-thick set of cross bedding in the eolian White Rim sandstone (Permian, Canyonlands, Utah). These cross sets have straight lines of intersection with the floor of the dry wash B) and indicate extensive migration of the dune to the left. Note truck for scale. Photos courtesy Roger Walker.

Mainguet and Callot, 1974; Wilson, 1971, 1972, 1973). Sand accumulates in an erg mainly because of an original topographic depression. As in aqueous accumulations, deposition is frequently the result of increasing depth of flow and consequent drop in fluid velocity. In the case of ergs the flow depth is the height of the atmospheric boundary layer, commonly between 1 and 2 km. The importance of wind patterns has been recognized in the Fachi Bilma erg, which is situated in the southern Sahara. It has been studied using satellite and aerial photography, and some features have been checked in the field (Mainguet and Callot, 1974; Fig. 2A). This erg is partly developed in the wind shadow of the Tibesti massif that deflects the winds around it. Within the erg there is a definite spatial zonation of dune types. Barchans occur on all sides, and mark zones of intermittent deposition. Toward the centre of the erg, wind velocities decrease. The barchans coalesce into larger sinuous longitudinal *(seif)* dunes, and then into larger compound longitudinal features *(silks)* composed of *draa* (large sand bedforms 20-450 m high). In the upwind part of the erg, a zone of large star-shaped draa over 100 m high occurs in the zone of turbulence and fluctuating winds immediately downwind of the Tibesti massif. This erg is dominated by longitudinal bedforms generally parallel to the mean wind direction. Other Saharan ergs are dominated by transverse bedforms or mixtures of bedforms. The Gran Desierto of Mexico shows both mixed and transverse-dominated areas (Fig. 2B). These ergs can be used to develop facies models for deserts with dominantly longitudinal and dominantly transverse bedforms. Similar regular patterns can be seen in bedform maps based on satellite photography of many of the major ergs in the world (Breed *et al.*, 1979). Although this review concentrates on warm, lowland deserts, sandy deserts can also occur in cold polar areas and at high altitudes (Koster, 1988).

Bedforms

Wilson's (1971, 1972) studies of Saharan bedforms led him to propose three main scales of eolian bedforms: ripples, dunes and draa. Ripples are flatter than those in water and usually have more regular crest lines (Sharp, 1963). Dunes are larger than ripples, and vary from 0.1 to 100 m in height. Draa are large sand bedforms between 20 and 450 m high, and are characterized by the superimposition of smaller dunes on them. Nevertheless, the dune-draa distinction is not universally accepted. A descriptive classification based on form and complexity should probably be used (Table 1). Dune form has been related by Fryberger (1979) to the variability of the wind and its ability to transport sand (Fig. 3).

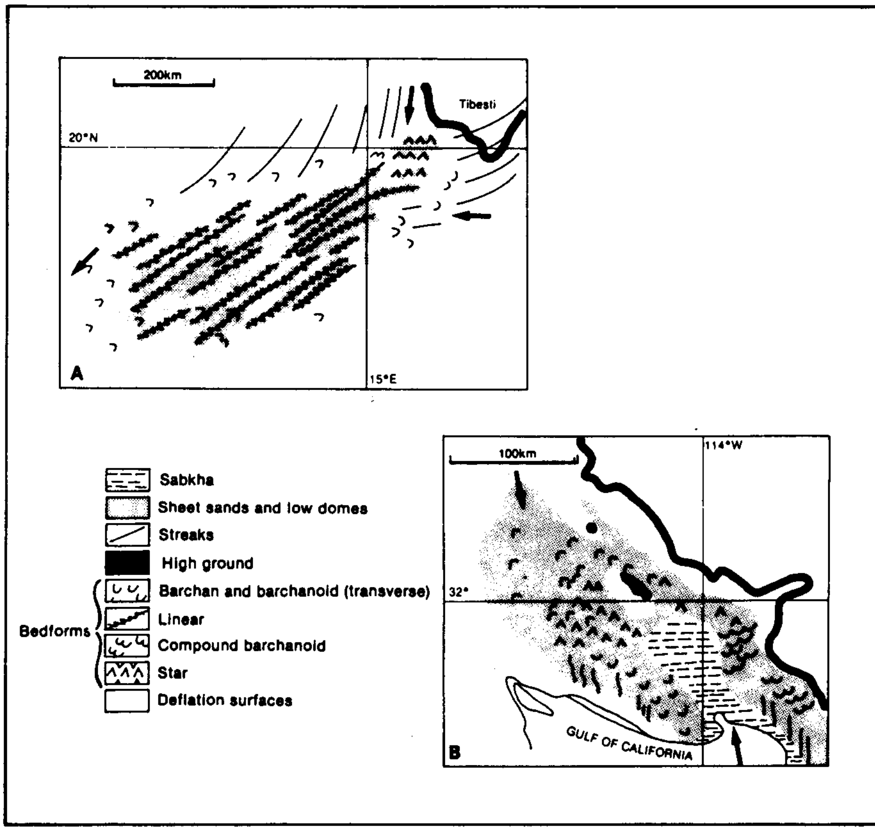

Figure 2 Bedform map of: A) the Fachi Bilma erg, southeastern Sahara (after Mainguet and Callot, 1974), and B) El Gran Desierto, Sonora, Mexico (M. Brookfield). Note difference in scale — the Mexican desert is one quarter the size of the Fachi Bilma erg. Arrows show dominant wind directions.

Table 1 *Morphology and classification of eolian bedforms. After McKee (1979).*

Morphology	Name	Associations
Sheet-like	Sheet sands	
Thin elongate strips	Streaks	COMPOUND — two or more of the same type combined by overlap or superimposition (Wilson's draa)
Circular to elliptical mound, dome-shaped	Dome	
Crescent in plan	Barchan	
Connected crescents	Barchanoid (akle)	
Asymmetrical ridge	Transverse (reversing)	COMPLEX — two different basic types occurring together, either superimposed (Wilson's draa), or adjacent.
Symmetrical ridge	Linear (seif)	
Central peak with arms	Star (pryamidal)	
U-shaped	Parabolic	

Sand transport

The gross amount of sand that can potentially be moved by the wind during a given period of time, weighted for the wind velocity, is the *drift potential* (DP). The amount moved depends also on sand availability. The *resultant drift direction* (RDD) is the vector resultant of all drift directions (Fig. 3). The *resultant drift potential* (RDP) is the vector sum of all drift potentials; it gives a value for the net movement of sand. These three measures give a very useful way of quantifying the direction (RDD) and rate of net sand movement (RDP) as well as the gross amount of sand movement (DP). These measures can then be related to wind regime. Barchanoid and transverse dunes occur in areas of fairly unidirectional winds (high RDP/DP ratios). Longitudinal dunes result from more variable winds (moderate RDP/DP ratios), and star bedforms

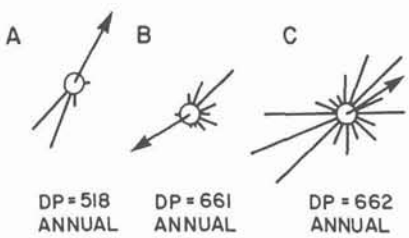

Figure 3 Characteristic high-energy wind regimes: A) narrow unimodal, barchanoid dunes, Peru; B) bimodal, linear dunes, Mauritania; C) complex, star dunes, Libya. DP = drift potential (see text), and arrows indicate resultant drift direction (RDD). After Fryberger (1979)

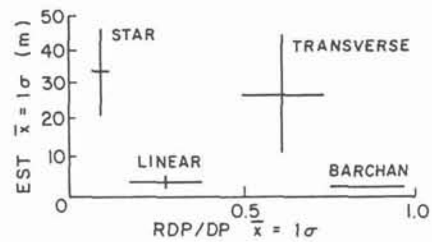

Figure 4 Statistically significant (P=0.001) separation of the four elemental dune types by means of two variables — equivalent sand thickness (EST) and a measure of wind directional variability (RDP/DP). The $\bar{x} \pm 1$ for EST in barchans is 0.02 ± 0.005 m (n=8). From Wasson and Hyde (1983a).

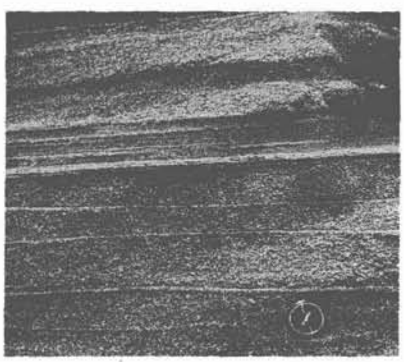

Figure 5 Plane bed lamination in coarse and fine sand (Permian, Arran, Scotland). Camera cover is 5 cm across.

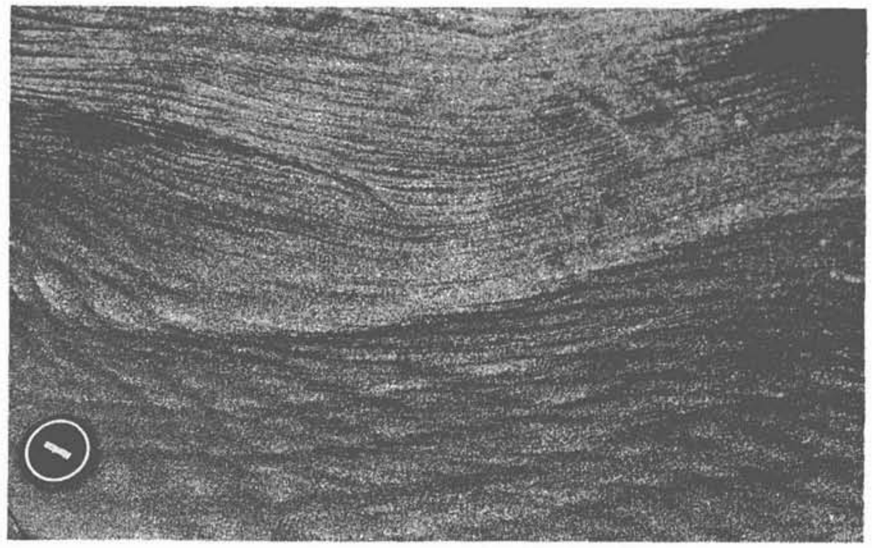

Figure 6 Highly oblique section through supercritical to subcritical climbing translatent strata (Permian, Arran, Scotland). Camera cover is 5 cm across.

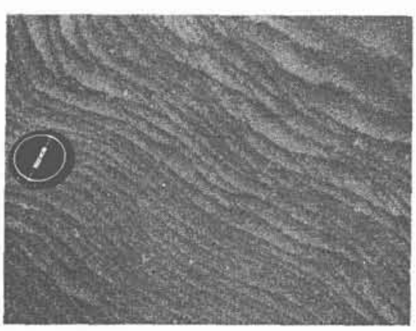

Figure 7 Oblique section through grainfall lamination with interbedded sandflows in upper part (Permian, Arran, Scotland). Camera cover is 5 cm across.

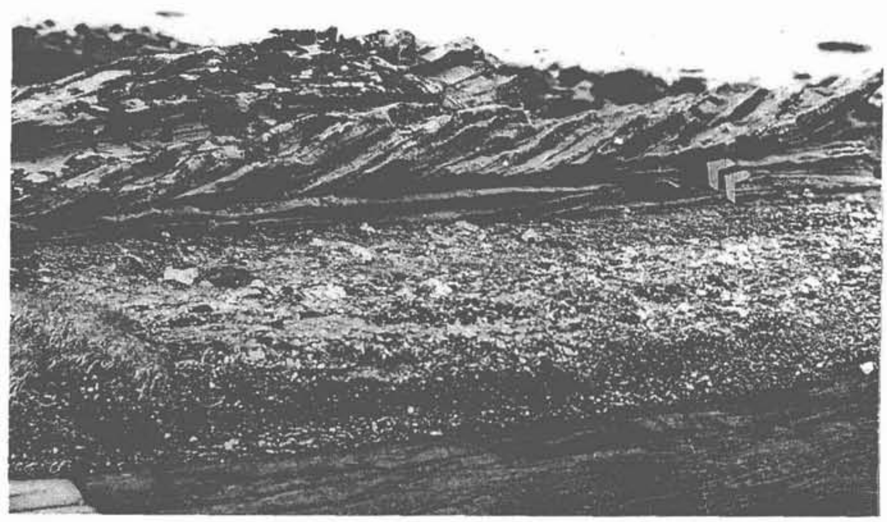

Figure 8 Sandflow cross strata, 20 cm thick, (arrowed top right) on plane bed lamination over alluvial fan breccia and sandstone (Permian, Arran, Scotland).

occur in regions of very variable winds (low RDP/DP ratios). Wasson and Hyde (1983a) found that various bedforms plotted in separate fields if wind variability was plotted against "spread-out" sand thickness (Fig. 4). This indicates that the form of the dunes may be controlled both by wind regime and availability of sand. What is missing here is any consideration of the ratio of flow saturation/deposition to flow undersaturation/erosion, which is basically what "spread-out" sand thickness measures.

Textures

Ahlbrandt (1979) summarized the textural parameters of eolian sands in terms of three depositional sub-environments, 1) well- to very well-sorted fine coastal dune sands, 2) moderately to well-sorted, fine- to medium-grained inland dune sands, and 3) poorly sorted interdune and serir sands. The dune samples vary in mean grain size from about 1.6 to 0.1 mm. Most interdune and serir sands are bimodal in the sand fraction. They also have higher silt and clay contents when compared with adjacent dune samples. In inland dune fields with predominantly unidirectional winds, there is progressively improved sorting and finer mean grain size downwind from the sand sources, through a sequence of dome, transverse, barchanoid and parabolic dunes. In reversing and multidirectional wind regimes, sand accumulates in dunes that have very slow net rates of migration. The clastic material in these dunes is a combination of available source materials. Because of the fluctuating conditions, the crests and bases of the dunes tend to have more divergent means than in unidirectional wind regimes. Attempts to relate grain size properties to bedform hierarchies have so far been unsuccessful (Wilson, 1973; Wasson and Hyde, 1983b).

Sedimentary structures

The scale of internal cross bedding in eolian dunes is determined by the size and rate of climb of the bedforms. In general, eolian and subaqueous bedforms make similar structures (Rubin and Hunter, 1982), but the detailed structure of eolian lamination differs from that of subaqueous lamination. Hunter (1977) proposed four main types of eolian lamination based on his study of small coastal dunes. Examples of the above types of stratification have now been found in ancient eolian sandstones (Clemmensen and Abrahamson, 1983; Fryberger and Schenk, 1981; Hunter, 1981). 1) *Plane-bed lamination*, produced by wind velocities too high for ripple formation, is analogous to the upper flat bed in

Figure 9 Sandflows on star draa overlying climbing translatent strata at the base of the slipface and overlain by grainfall strata on the upper slipface (Recent, El Gran Desierto, Mexico). Slipface height seen is 20 m.

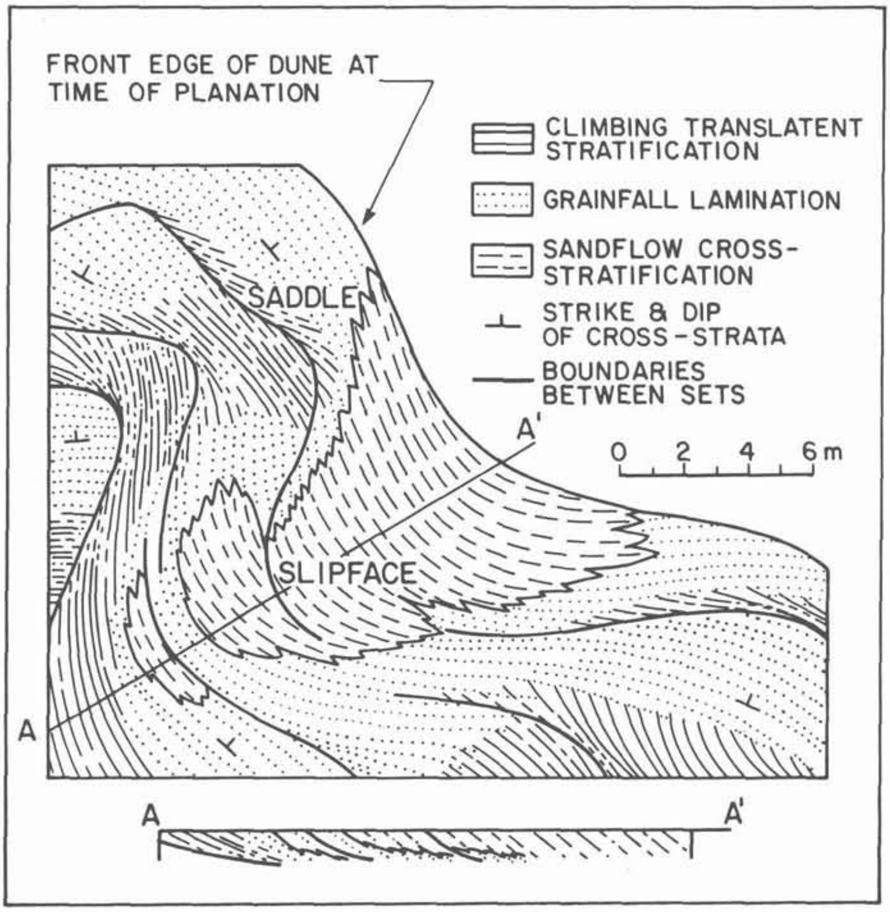

Figure 10 Horizontal cross section of dune foreset cross stratification exposed on a planed-off sinuous transverse or barchanoid dune, showing distribution of stratification types. A – A' shows a vertical cross section through these laminations. Simplified from Hunter (1977) using an example from Padre Island, Texas.

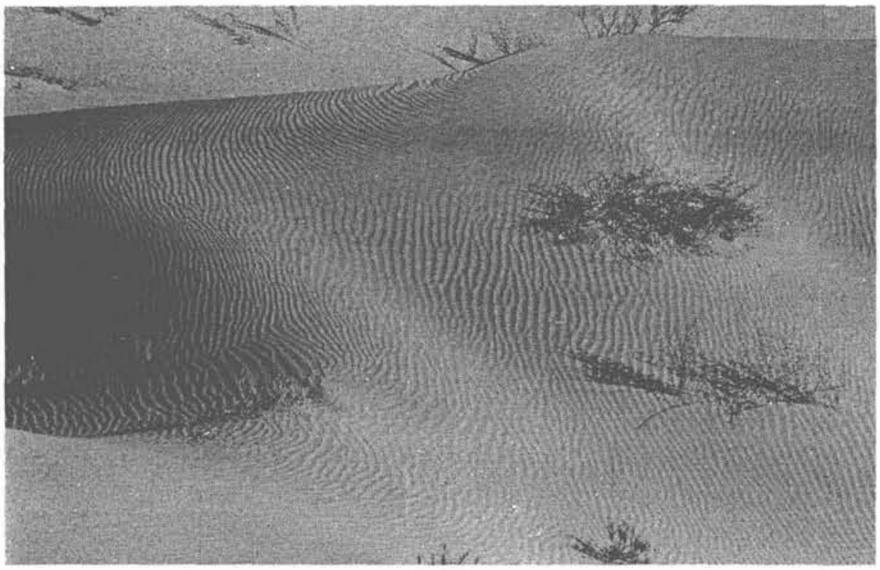

Figure 11 Wind ripples (maximum wave length seen is 5 cm) in fine sand (El Gran Desierto, Mexico)

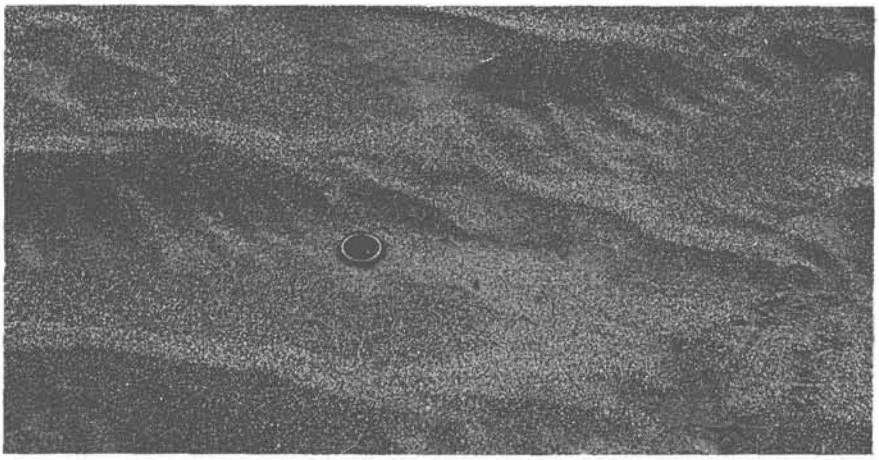

Figure 12 Wind ripples (maximum wave length seen is 25 cm) in coarse sand (El Gran Desierto, Mexico).

Figure 13 Adhesion structures at margin of permanent salt lake (El Gran Desierto, Mexico).

aqueous deposits (Fig. 5). 2) *Climbing ripple lamination* closely resembles subaqueous varieties, but the ripple foresets are difficult to recognize because of their low relief except in oblique sections (Fig. 6). Hunter (1977) distinguishes translatent strata (where only the bounding surfaces between migrating ripples are visible) from rippleform strata (where the ripple foresets can be identified). Both are inversely graded and relatively closely packed. 3) *Grainfall lamination* is produced in zones of flow separation (commonly in the lee of dune crests) by deposition from suspension (Fig. 7). Segregation of different grain sizes is relatively poor and laminae and grading are difficult to see. The average porosity is about 40 per cent, due to a packing that is intermediate between the closely packed traction laminae of planebed and climbing ripple laminae, and the loosely packed sandflow strata described below. 4) *Sandflow lamination* (avalanche cross bedding) is caused by slumping and consequent grainflow down slopes (Figs. 7 top, 8). Sandflow cross strata are loosely packed (average porosity 45 per cent), interfinger with grainfall laminae near their base, and form lenses parallel to the slipfaces (Fig. 9).

Internal structures are difficult to study in modern dunes, hence the emphasis on stratification models. Large-scale cross bedding was formerly considered typical of eolian sands, but large bedforms also occur in shallow shelf seas (Chapter 12) and in large deep rivers (Chapter 7), where the cross beds may resemble eolian cross bedding (Allen, 1982). Nevertheless, many superimposed sets, each thicker than about 10 m, occur *far* more commonly in eolian than in other depositional environments. Eolian cross bedding can be deformed into huge convolutions, caused by slumping of water-saturated dune sands. Convolute stratification is found in ergs being inundated by the sea, but may also form by seasonal melting of ice in cold-climate dunes (Koster, 1988).

Each type is found on different parts of a dune and can be recognised even where the dune is deflated. For example, the slipfaces (sandflow cross strata), saddles (climbing translatent strata) and the passage between the slipfaces and saddles (grainfall lamination) can be recognized in barchanoid dunes, even after deflation (Fig. 10). Further information on stratification types and their relationship to dune morphology is given by Hunter (1981), Hunter and Rubin (1983), Rubin and Hunter (1983).

Our knowledge of the larger internal structures of modern dunes is due almost entirely to the work of McKee (McKee, 1966; McKee and Tibbitts, 1964; McKee and Douglass, 1971; McKee and Moiola, 1975) and Bigarella (Bigarella, 1972; Bigarella *et al.*, 1969). These studies are summarized in McKee (1979).

The most detailed studies were done in the White Sands dune field of New Mexico. This area is not analogous to most ancient eolian deposits because the dunes are composed of gypsum and are easily stabilized after occasional wetting by rain. Also, we cannot be sure that the deeper structures relate to the modern wind regime. Therefore, an alternative approach to the understanding of internal structures is the computer modelling of a diversity of migrating bedforms (Rubin, 1987).

Interdunes are an integral part of the eolian bedform system (Ahlbrandt and Fryberger, 1981; Kocurek, 1981b). In deserts with a limited sand supply, interdunes consist of lag deposits, coarse sand sheets and small isolated dunes and sabkhas. Here, the water table may reach the surface and control the amount and type of sediment deposition (Stokes, 1968; Fryberger *et al.*, 1988). Because of the way in which sand is transported through the system, longitudinal bedforms tend to have coarse lag and coarse sand sheets and dunes in the interdune areas. Transverse bedforms tend to have sabkhas and fine sand dunes between them (Glennie, 1970; Sharp, 1979). The size of interdunes is also dependent on sand supply and on the stage of development of the surrounding erg. Most modern deserts have extensive interdunes because of their relatively recent development (Mainguet and Chemin, 1983).

Surface structures are common on eolian bedforms and include ripple marks (Figs. 2, 11, 12), adhesion structures (Fig. 13), animal tracks (Fig. 14) and trails, and marks made by vegetation (Fig. 15), rain, hail and lightning (Fig. 16). All may be preserved by rip-

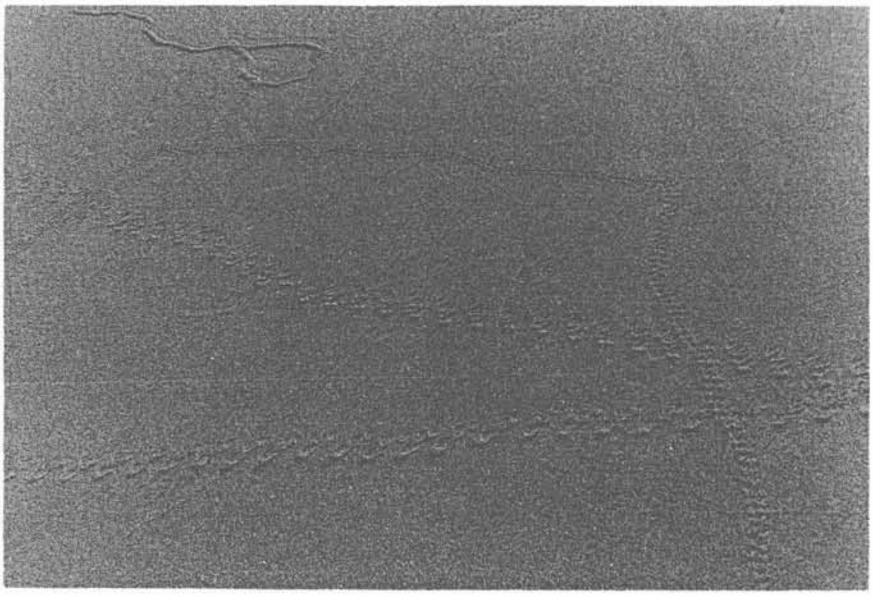

Figure 14 Various lizard and beetle tracks on dune surface (El Gran Desierto, Mexico). Width of biggest track set is 5 cm.

Figure 15 Concentric grooves (0.5 to 1.0 m in diameter) created by plants moving in the wind. Photo courtesy Rodney Stevens.

Figure 16 Fulgurite-sand fused by lightening strike (Permian, Arran, Scotland). Pen is 7 cm long.

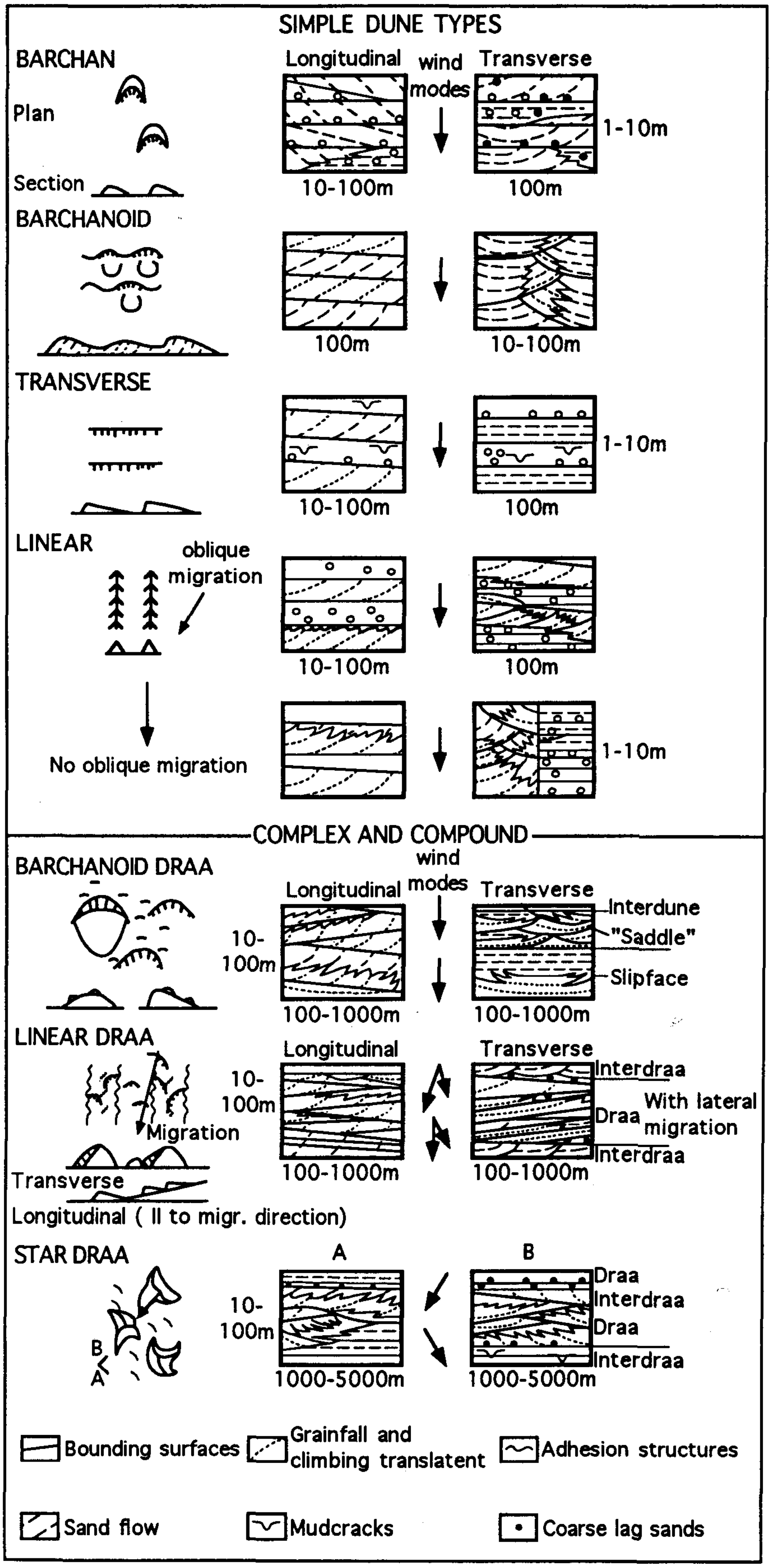

ple climbing and grainfall deposition (Ahlbrandt and Fryberger, 1981; Kocurek and Fielder, 1982; McKee, 1982; Steidtmann, 1973). Between sand layers there may be soil horizons and plant and animal traces (Loope, 1988).

The features described above suggest that the input for a facies model should consist of 1) the different types of bedforms and interdunes in modern deserts, and 2) the types of stratification formed by the migration of different parts of the various bedforms. However, a good model must also consider how the characteristic strata of various combinations of migrating bedforms can form thick, extensive ancient eolian sandstones.

STRATIFICATION AND BOUNDING SURFACE MODELS

Stratification results from the migration of bedforms as they climb at various angles and directions over one another (Fig. 17). Simple stratification models involve simple migrating bedform systems and form simple architectural assemblages. For example, simple transverse dunes migrating across a desert form tabular cross beds separated by planar bounding surfaces. Simple transverse dunes migrating over larger transverse draa form slightly more complicated patterns, including downwind-dipping second-order surfaces (discussed below). However, bedforms generated by moving sand are rarely simple and are also affected by existing structures. Changing winds cause modification of existing bedforms and these changing bedforms also interact with the wind to produce a variety of disequilibrium forms (Mader and Yardley, 1985).

The models of Figure 17 assume unidirectional climbing of ideal bedforms in a fully developed dune, draa and interdune system, but only indicate some of the possible stratification styles. Rubin (1987) has used computer models to show the enormous variety and complexity possible if the bedforms are neither climbing unidirectionally nor fully developed.

Figure 17 Stratification models for simple and complex/compound dune types. Longitudinal and transverse sections are parallel and perpendicular to resultant wind directions respectively.

Bounding surfaces

Where bedforms climb at angles lower than their windward slopes, the underlying and preceding bedforms are eroded. This leads to the formation of *bounding surfaces* that define sets of cross strata (Brookfield, 1977; Figs. 18, 19). These bounding surfaces occur at all scales, and even translatent strata are really only ripple bounding surfaces. Bounding surfaces can only form from a migrating train of bedforms.

First-order surfaces (Fig. 18) are flat-lying bedding planes cutting across all underlying eolian structures and are attributed to the migration of draa.

Second-order surfaces (Fig. 18) commonly lie between first-order surfaces and usually dip downwind with variable inclinations. These surfaces are attributed to transverse dunes climbing down the lee slopes of draa, or to lateral migration of linear dunes across the draa lee slope.

Third-order surfaces form the boundaries of bundles of laminae within cosets of cross laminae, and are attributed to erosion followed by renewed deposition due to local fluctuations in wind direction and velocity. They are reactivation surfaces.

Simple dune and draa systems should lack the second-order surfaces. However, they occur only because few systems are in the dynamic equilibrium assumed in climbing bedform theories. Second-order surfaces can be formed by dunes periodically overtaking one another and coalescing (Mader and Yardley, 1985), and occur especially in seasonally reversing dune systems (Fig. 20). All dune-draa systems must show a resultant sand drift except at the sand-flow nodes (Wilson, 1971). Net unidirectional climbing is thus a near certainty (Hesp *et al.*, 1989), although some star draa systems may only climb very slowly. Theoretical models suggest very low rates of dune and draa climbing, since most eolian sandstones seem to preserve only a small basal part of the original bedforms. Nevertheless, the models can be modified for steep rates of climb where necessary (Rubin and Hunter, 1982; Rubin, 1987). These stratification models are for uniform assemblages of one type of dune-interdune or draa-dune-interdune system.

As well as the bounding surfaces discussed above, there may be other extensive surfaces that cut across ancient eolian sandstones, truncating all underlying surfaces. These *supersurfaces* form in response to external controls on the desert and are discussed in a later section.

In deserts, many different systems are present, and it is necessary to consider the possible stacking of different systems during the evolution of a desert. This requires knowledge of the typical areal distribution of bedform types in a desert, and the vertical and lateral varisations in stratification formed as they migrate and the desert evolves.

FACIES MODELS

The facies models developed here are based on the two fundamental concepts discussed above. First, strata are generated by hierarchies of migrating bedforms of differing sizes and shapes. These climb over one another at different angles and in differing directions. The resulting bounding surfaces can be used to recognize the nature of the bedform systems in ancient eolian sandstones (Brookfield, 1977; Rubin and Hunter, 1982; Rubin, 1987). Second, the stratification types vary in proportion and location in different types of bedforms in modern deserts. The stratification types, together with bounding surfaces, can be used to identify bedforms in ancient eolian sandstones (Hunter, 1977).

Application of studies of modern sediments

There are many problems in using studies of modern eolian sediments to

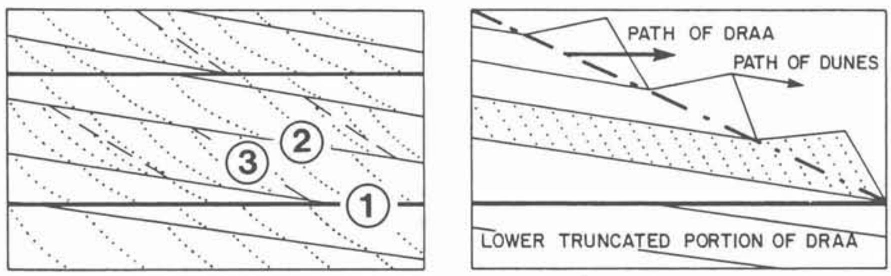

Figure 18 First-order bounding surfaces are generated by the migration of draa. Second-order surfaces are generated by the movement of individual dunes climbing down the draa lee slope. Third-order surfaces represent eolian lamination. From Brookfield (1977).

Figure 19 Bounding surfaces, mostly first order, in the Jurassic Navajo Sandstone at Page, Utah. Note decrease in thickness upwards toward contact with overlying fluvial sediment, suggesting decrease in bedform size with time.

Figure 20 Reversing barchanoid dunes between rows of large star draa; one is being traversed by the truck, others can be seen in the distance. Note deflation surfaces on lee slopes of both draas and dunes (El Gran Desierto, Mexico).

formulate general facies models. General models must incorporate modern and ancient examples, as well as theoretical results. Modern large eolian bedforms commonly rest on alluvium and are usually Quaternary in age (Wilson, 1973). No thick eolian deposits comparable to ancient examples seem to be forming today. Deposits observed today are unlikely to be even approximately in equilibrium with present wind conditions. This is because large dunes and draa take thousands of years to re-equilibrate with changing wind conditions. Those observed today could not possibly have adjusted to the rapid alternations of climate and wind regimes during and since the Pleistocene (Wilson, 1973). Ancient ergs may have formed under more uniform conditions, which might explain why ancient eolian sandstone systems appear simpler than modern ones.

Stratification in Recent large dunes and draa of uncemented quartz sand is almost impossible to examine by trenching, because the trench walls rapidly collapse. Because of the Recent climate and wind changes, any stratification observed in trenches would be difficult to relate to processes of formation. Direct comparison between cross sections of modern dunes and ancient eolian sandstones is also difficult because normally, only the lowest parts of eolian bedforms are preserved. Rates of bedform migration tend to be at least one order of magnitude greater than vertical buildup. It follows that only the lowest parts of the dunes are preserved, and reconstruction of large bedforms depends almost entirely upon structures formed at their basal lee slopes.

The two different models presented in Figures 21 and 22 are based on the migration of predominantly transverse and predominantly longitudinal bedforms, respectively. These models are based largely on simplifications of the western part of the Gran Desierto (Fig. 2B) and of the Fachi-Bilma erg (Fig. 2A).

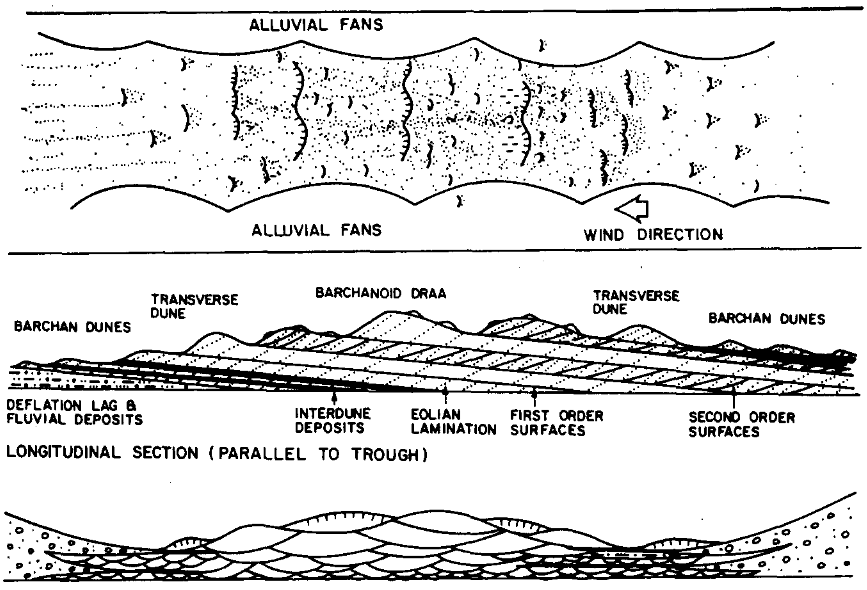

Figure 21 Synthetic model for desert with transverse bedforms. Vertical scale is exaggerated, such that bedforms appear to be climbing too steeply, and the troughs shown in the transverse section are too concave. Only first-order surfaces are shown on the transverse section; some second-order surfaces are shown on the longitudinal section. For scale, the basin is at least 5 km across.

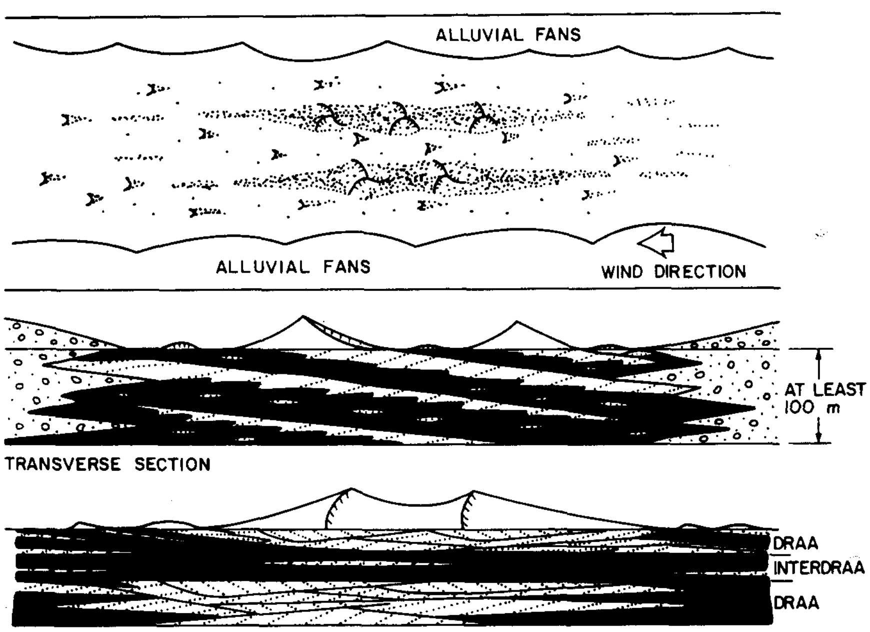

Figure 22 Synthetic model for desert with longitudinal bedforms in an enclosed basin. Note that some lateral migration of longitudinal star draas is permitted — without migration, vertical stacks of longitudinal-star draa deposits would be separated by thick interdraa lags, barchan dunes, and fluvial deposits (lags, dunes and fluvial deposits shown in black). For scale, the basin is at least 5 km across.

Transverse bedform model

The transverse bedform model (Fig. 21) is based on unidirectional winds, with upward and lateral buildup of sand within an enclosed basin with marginal fans. The constriction of the fans keeps the first-order bounding surfaces horizontal; by contrast, on an unconfined extensive plain, these bounding surfaces would tend to be convex-upward on a large scale. The model involves the initial development of sand patches and barchan dunes with the onset of aridity, followed by the successive development of transverse dunes and compound transverse draa at the climax of aridity. Finally, with decreasing aridity and/or reduction in sand supply, there would be a gradual contraction of the erg and eventual covering over by fluvial or lacustrine sediments. Fluctuations during erg development lead to complex interfingering of fluvial and eolian deposits (Langford, 1989; Langford and Chan, 1989).

Longitudinal bedform model

In this model (Fig. 22), the bedforms rest on alluvium and lag deposits, as in the Fachi Bilma erg. The early sand patches and barchans are followed by linear dunes and linear complex draa, and eventually (in complex wind regimes) by star draa. These longitudinal patterns have rarely been reconstructed in ancient eolian sandstones. This is possibly because such bedforms are characteristic of deserts with a net through-flow of sand and little deposition, or because such bedforms migrate laterally, laying down deposits that mimic those of transverse bedforms (Hesp *et al.*, 1989; Rubin and Hunter, 1983). Changes in climate over a long period of time would probably lead either to partial preservation of the bedforms below a soil and alluvial cover, or almost complete deflation. Isolated sand lenses may be the only remnants of the large star draa.

In both the transverse and longitudinal models, the thickest units are in the centre of the erg, where the largest bedforms occur. Erg migration may lead to systematic changes in the nature and thickness of eolian strata in specific areas (Porter, 1986). In an ideal desert, the thick compound superimposed cross strata would characterize the interior. Toward the margins, there would be an increasing amount of thicker interdune deposits with smaller, simpler cross strata and possibly interbeds of fluvial deposits. The areal relationships and paleo-winds of such sequences are shown on Figure 23.

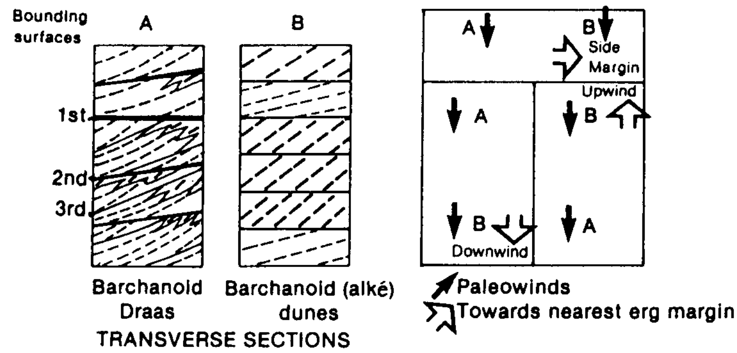

Figure 23 (top) Synthetic transverse sections A and B, related to the nearest inferred erg margins and resultant wind direction.

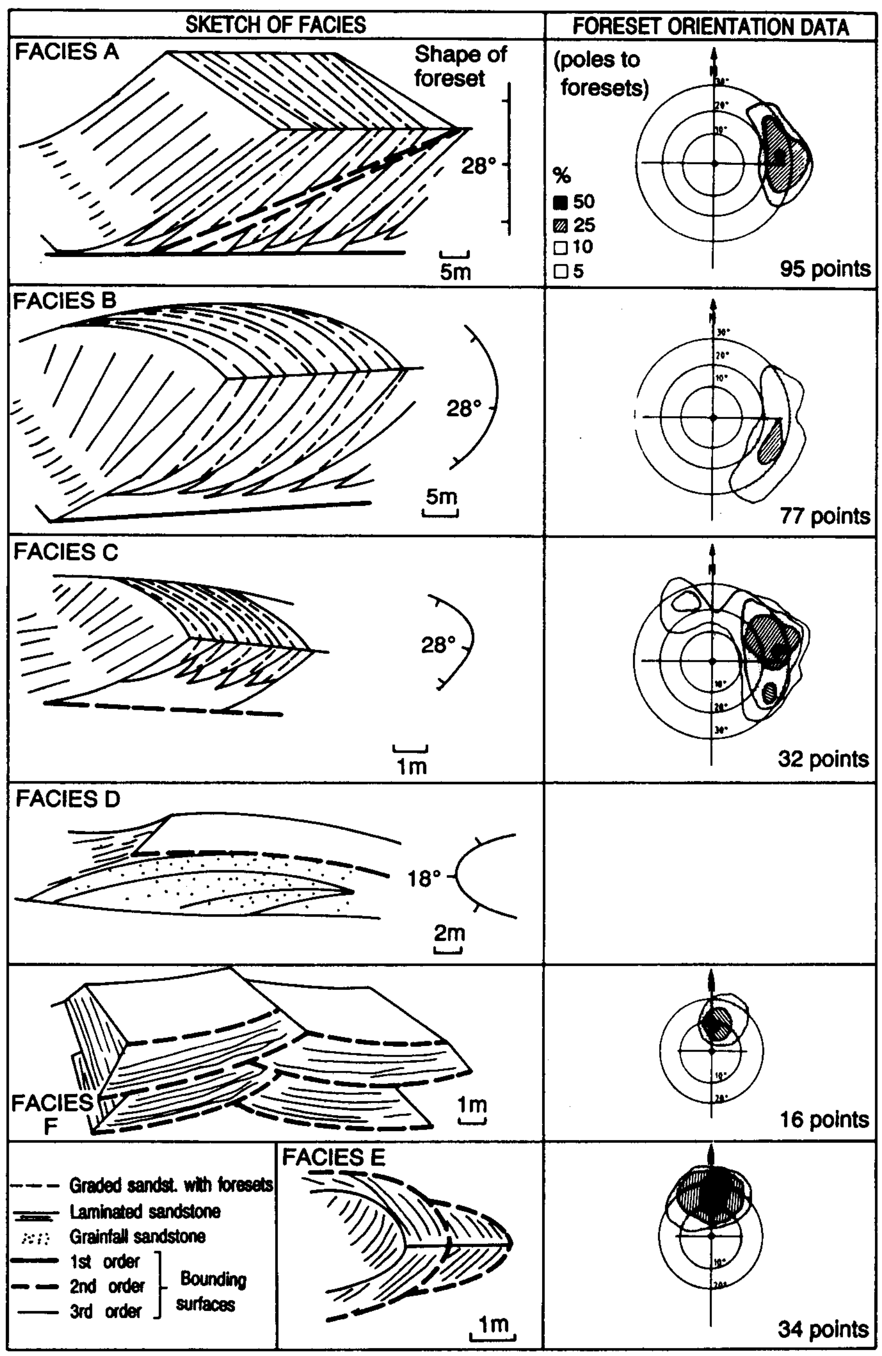

Figure 24 (right) Three dimensional sketches of facies based on foreset orientations and shapes, Bridgnorth Sandstone, Permian, Britain. Modified from Karpeta (1990).

Application of models to ancient rocks

Similar interpretations have been developed for ancient ergs (Karpeta, 1990; Kocurek, 1981a; Ross, 1983). Karpeta (1990) distinguished six facies in the Permian Bridgnorth Sandstone in Britain, based on the nature of the stratification and orientation of the foresets (Fig. 24), as in the stratification and bounding surface models discussed above. He then grouped different facies into three facies associations, which were interpreted as various dune-interdune systems (Fig. 25). Kocurek (1981a) made a particularly detailed reconstruction of the large Jurassic Entrada erg in the western U.S.A. Using stratification types, bounding surfaces, foreset dip dispersion, and interdune characteristics, he estimated the actual wavelength and sizes of the bedforms and their distribution in the desert (Figs. 26, 27). This study remains the best published analysis of an ancient erg. Kocurek (1981a) also estimated the wavelengths of the individual draa from the intersection of first-order surfaces with supposed synchronous horizons (supersurfaces, see below). These horizons represent major changes in the environment within an erg.

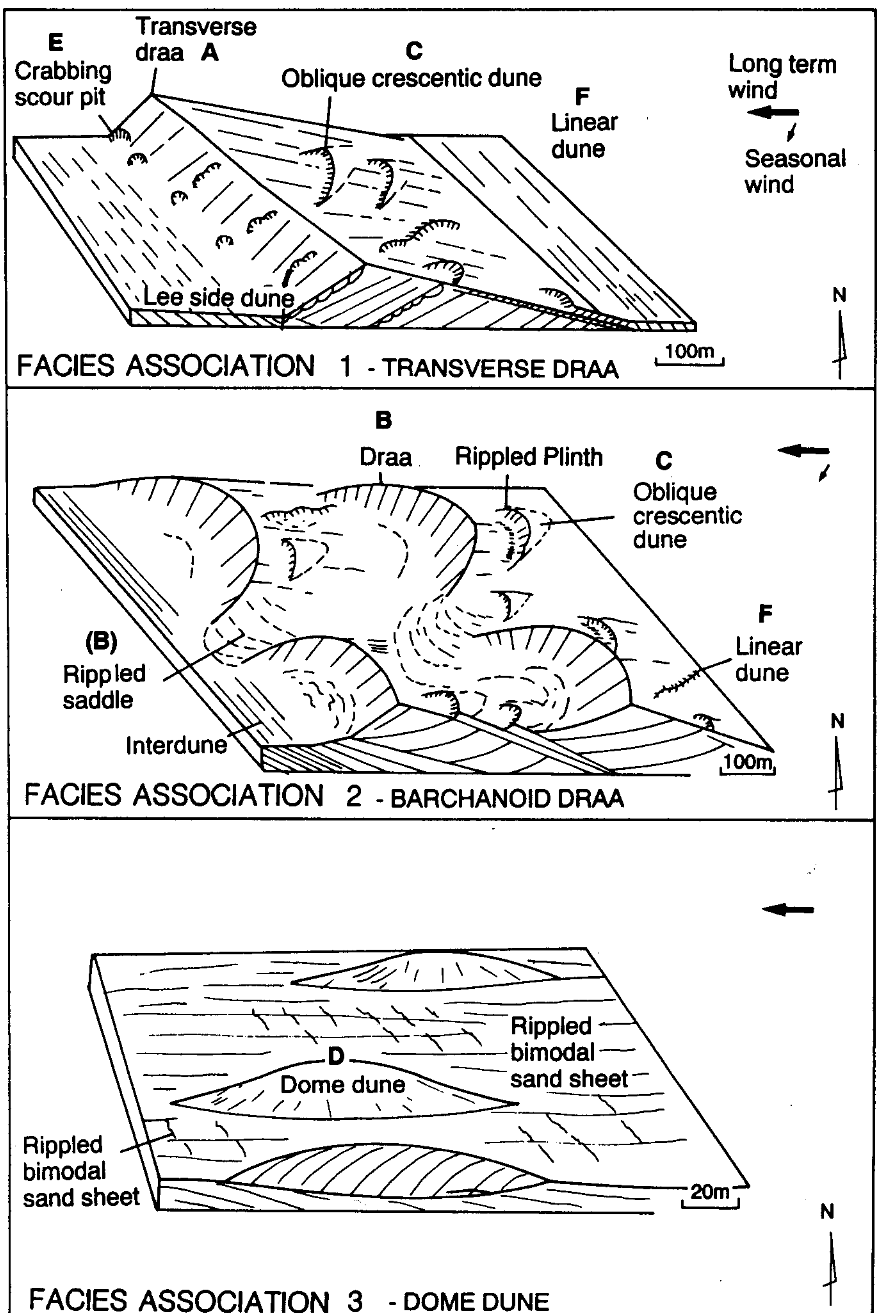

Figure 25 Facies associations in the Bridgnorth Sandstone, Permian, Britain. Modified from Karpeta (1990). Crabbing scour pit is a scour moving sideways across the slipface. Rippled plinth is a flat upwind surface with ripples.

SUPERSURFACES

Kocurek's (1981a) supposed synchronous horizons that cut all earlier surfaces are now known as *supersurfaces*. They may consist only of a thin coarse lag between identical eolian sands, and can therefore be very difficult to detect. These horizons separate stratigraphic packages and record major interruptions in basin history (Galloway, 1989). They are *bounding discontinuities* (Chapter 1), and can be used to place eolian deposits within the context of allostratigraphy and sequence stratigraphy. Although often considered isochronous on a geological time scale, the supersurfaces need not be.

Origin of supersurfaces

The origin of eolian supersurfaces has been considered most thoughtfully by Kocurek (1988), who placed the surfaces into three broad categories. The categories are not mutually exclusive; for example, sea level changes may cause changes in climate.

Climatic change

Supersurfaces can form during the regional termination of an erg because of climatic change. Quaternary examples are common. In the Sahel, southern Sahara, vegetation-covered dunes are now being reactivated due to overgrazing (Talbot, 1985). A similar stratigraphic break occurs in the rolling vegetation-covered Nebraska sand hills, which were once a large early Quaternary erg (Warren, 1976). In these examples, the form of the inactive erg is preserved beneath covering vegetation. The supersurface is essentially the complex rolling land surface that is forming as erosion smoothes the hills and causes deposition in the depressions. An unusual surface of this type surmounts the Permian Yellow Sands of northeastern England. Here, linear draa were rapidly buried by the flooding of the Zechstein Sea (Glennie and Buller, 1983; Steele, 1983). This flooding was so rapid that rounded profiles of individual draa up to 50 m high are preserved below the overlying transgressive mudstones (the Marl Slate). However, most ancient ergs have undergone much greater erosion before being preserved (Langford and Chan, 1989).

Changes of relative sea level, or tectonic setting

The Gran Desierto (Fig. 2B; 9, in background) shows deflating bedforms around its western and southern margins due to a combination of climatic, sea level and tectonic causes (Blount and Lancaster, 1990). This deflation results in supersurfaces of local or desert-wide extent. Many examples were noted by Blakey and Middleton (1983) in the Mesozoic of the western U.S.A. (Fig. 28). Supersurfaces of this type are especially common in coastal deserts where sea level changes directly affect the desert (Chan and Kocurek, 1988). However, sea level changes can also affect groundwater levels farther inland, which in turn can cause chemical cementation and "fixing" of interdune and upwind sources (see Fig. 13). The dunes can then be entirely deflated, leaving a planar scoured or Stokes surface (Fryberger *et al.*, 1988; Loope, 1985). Sand sheets may subsequently form on these surfaces (Kocurek and Nielson, 1986).

Migration of sand seas

The lower and upper bounding surfaces of an eolian deposit may be formed by the migration of an entire sand sea through time (Porter, 1986). Within an extensive inland basin, changes in climate, sea level, tectonics or source could trigger the migration of Wilson's (1971) sand nodes. Migration of an erg within a basin could therefore lead to multiple, closely spaced, intersecting supersurfaces. However, there are no published examples of this.

DYNAMIC INTERPRETATION

Dynamic interpretations of both modern and ancient sand seas are controversial, because there is no consensus about what causes the form, shape and distribution of bedforms in modern deserts. Experimentation is difficult for bedforms larger than ripples. The larger the bedforms, the greater the lag effects, and the harder it is to determine whether they are adjusted to the current wind regime. The development of theoretical models relating bedform development to atmospheric structure, sand transport patterns and bedform/airflow interactions, may therefore be an important direction for future research.

ACKNOWLEDGEMENTS

I thank the Natural Sciences and Engineering Research Council of Canada for their generous and continuing support of my research. Roger Walker criticized and improved the manuscript.

REFERENCES

Basic sources of information

Allen, J.R.L., 1982, Sedimentary structures; their character and physical basis: Amsterdam, Elsevier, v. 1, 594 p. and v. 2, 644 p.
The most comprehensive text ever written on sedimentary structures. Essential reading for all sedimentologists.

Bagnold, R.A., 1941, The physics of blown sand and desert dunes: London, Methuen, 265 p.
Still an essential, marvellous, thought-provoking study of recent eolian bedforms.

Brookfield, M.E. and Ahlbrandt, T.S., eds., 1983, Eolian sediments and processes: Amsterdam, Elsevier, 660 p.

Cooke, R.V. and Warren, A., 1973, Geomorphology in deserts: London, Batsford, 394 p.

Kocurek, G., ed., 1988, Late Paleozoic and Mesozoic eolian deposits of the western interior of the United States: Sedimentary Geology, v. 56, p. 1-413.
Many good papers on the best studied, large extensive ancient sand seas.

Kocurek, G., 1991, Interpretation of ancient eolian sand dunes: Annual Review of Earth and Planetary Sciences, v. 19, p. 43-75.

Koster, E.A., 1988, Ancient and modern cold-climate aeolian sand deposition; a review: Journal of Quaternary Science, v. 3, p. 69-83.
Do not forget that large sand dunes occur next to glaciers and in Antarctica.

McKee, E.D., ed., 1979, A study of global sand seas: United States Geological Survey, Professional Paper 1052, 429 p.
A lot of good stuff.

Rubin, D.M., 1987, Cross-bedding, bedforms and paleocurrents: Society of Economic Paleontologists and Mineralogists, Concepts in Sedimentology and Paleontology, v. 1, 187 p.
An essential guide to the relationships of bedforms, bedding and bounding surfaces.

Wilson, I.G., 1973, Ergs: Sedimentary Geology, v. 10, p. 77-106.
The impetus for modern studies on sand seas.

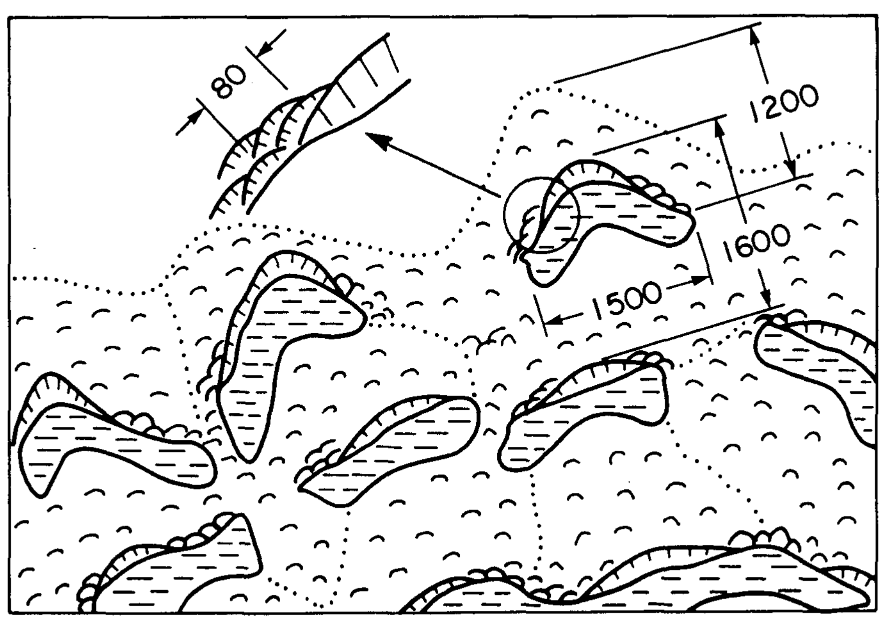

Figure 26 Interpretation of the overall structure, and dimensions of bedforms and interdune areas, in the central erg facies of the Entrada Sandstone. Draa slipfaces are up to 110 m high, and individual barchanoid dunes have slipfaces up to 8 m high. Scales in m. Redrawn from Kocurek (1981a).

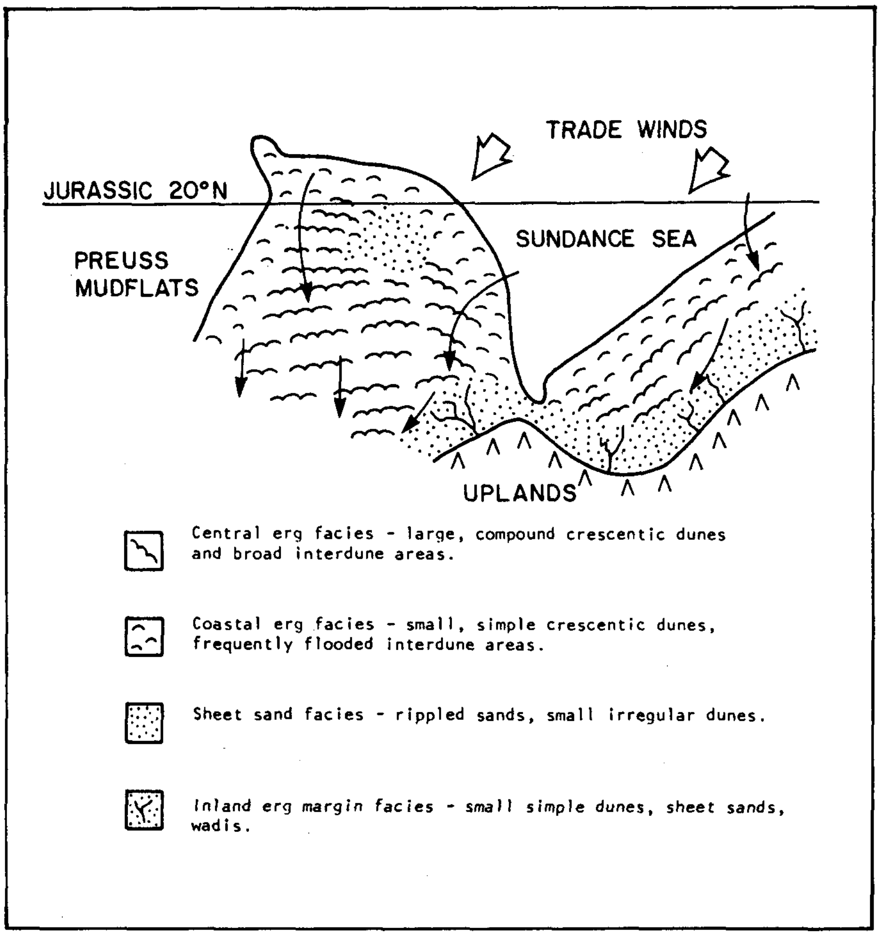

Figure 27 Reconstruction of the Entrada erg over the study area in N.E. Utah and N.W. Colorado. The region has been rotated such that Jurassic lines of latitude are shown horizontally. Arrows indicate inferred erg circulation pattern. Redrawn from Kocurek (1981a).

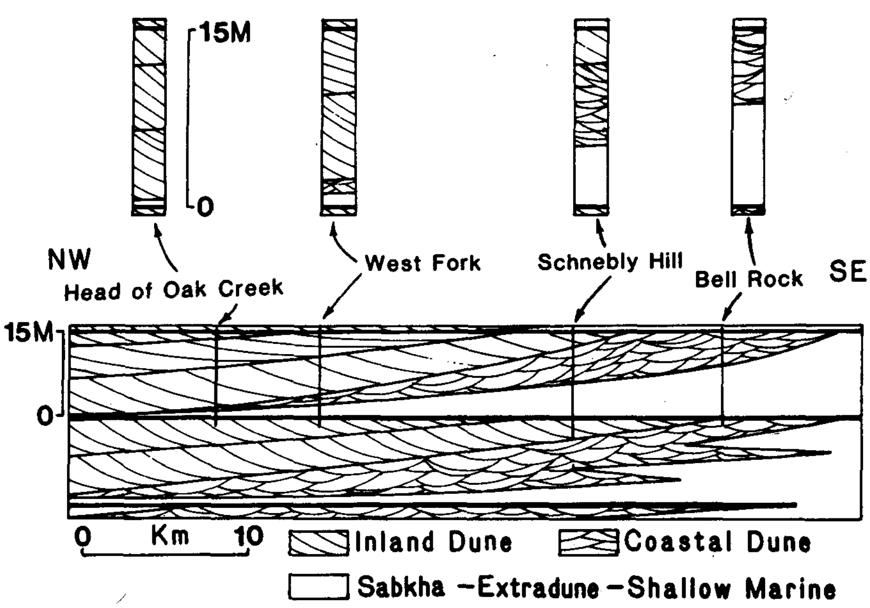

Figure 28 Correlation of supersurfaces (heavy lines) in part of the Coconino Sandstone, western U.S.A. From Blakey and Middleton (1983).

Other references

Ahlbrandt, T.S., 1979, Textural parameters of eolian deposits: United States Geological Survey, Professional Paper 1052, p. 21-51.

Ahlbrandt, T.S. and Fryberger, S.G., 1981, Sedimentary features and significance of interdune deposits, *in* Ethridge, F.G. and Flores, R.M., eds., Modern and ancient non-marine depositional environments: models for exploration: Society of Economic Paleontologists and Mineralogists, Special Publication 31, p. 293-314.

Bigarella, J.J., 1972, Eolian environments: their characteristics, recognition and importance, *in* Rigby, J.K. and Hamblin, W.K., eds., Recognition of ancient sedimentary environments: Society of Economic Paleontologists and Mineralogists, Special Publication 16, p. 12-62.

Bigarella, J.J., Becker, R.D. and Duarte, G.M., 1969, Coastal dune structures from Parana (Brazil): Marine Geology, v. 7, p. 5-55.

Blakey, R.C. and Middleton, L.T., 1983, Permian shoreline aeolian complexes in central Arizona; dune changes in response to cyclic sea level changes, *in* Brookfield, M.E. and Ahlbrandt, T.S., eds., Eolian sediments and processes: Amsterdam, Elsevier, p. 551-581.

Blount, G.D. and Lancaster, N., 1990, Development of the Gran Desierto sand sea, northwestern Mexico: Geology, v. 18, p. 724-728.

Breed, C.S., Fryberger, S.G., Andrews, S., McCauley, C., Lennartz, F., Gebel, D. and Horstman, K., 1979, Regional studies of sand seas using Landsat (ERTS) imagery: United States Geological Survey, Professional Paper 1052, p. 305-397.

Brookfield, M.E., 1977, The origin of bounding surfaces in ancient eolian sandstones: Sedimentology, v. 24, p. 303-332.

Chan, M.A. and Kocurek, G., 1988, Complexities in eolian and marine interactions; processes and eustatic controls on erg development: Sedimentary Geology, v. 56, p. 283-300.

Clemmensen, L.B. and Abrahamson, K., 1983, Aeolian stratification and facies association in desert sediments, Arran Basin (Permian) Scotland: Sedimentology, v. 30, p. 311-339.

Fryberger, S.G., 1979, Dune form and wind regime: United States Geological Survey, Professional Paper 1052, p. 137-169.

Fryberger, S.G. and Schenk, C.J., 1981, Wind sedimentation tunnel experiments on the origin of eolian strata: Sedimentology, v. 28, p. 805-821.

Fryberger, S.G., Schenk, V.J. and Krystinik, L.F., 1988, Stokes surfaces and the effects of near-surface groundwater-table on aeolian deposition: Sedimentology, v. 35, p. 21-41.

Galloway, W.E., 1989, Genetic stratigraphic sequences in basin analysis I: architecture and genesis of flooding-surface bounded depositional units: American Association of Petroleum Geologists, Bulletin, v. 73, p. 125-142.
Glennie, K.W., 1970, Desert sedimentary environments: Amsterdam, Elsevier, 222 p.
Glennie, K.W. and Buller, A.T., 1983, The Permian Weissliegend of N.W. Europe; the partial deformation of aeolian dune sands caused by the Zechstein transgression: Sedimentary Geology, v. 35, p. 43-81.
Hesp, P., Hyde, R., Hesp., V. and Qian Zhengyu, 1989, Longitudinal dunes can move sideways: Earth Surface Processes and Landforms, v. 14, p. 447-451.
Hunter, R.E., 1977, Basic types of stratification in small eolian dunes: Sedimentology, v. 24, p. 361-387.
Hunter, R.E., 1981, Stratification styles in eolian sandstones; some Pennsylvanian to Jurassic examples from the Western Interior, U.S.A, *in* Ethridge, F.G. and Flores, R.M., eds., Modern and ancient non-marine depositional environments: models for exploration: Society of Economic Paleontologists and Mineralogists, Special Publication 31, p. 315-329.
Hunter, R.E. and Rubin, D.M., 1983, Interpreting cyclic cross-bedding with an example from the Navajo sandstone, *in* Brookfield, M.E. and Ahlbrandt, T.S., eds., Eolian sediments and processes: Amsterdam, Elsevier, p. 429-454.
Karpeta, W.P., 1990, The morphology of Permian paleodunes — a reinterpretation of the Bridgnorth Sandstone around Bridgnorth, England in the light of modern dune studies: Sedimentary Geology, v. 69, p. 59-75.
Kocurek, G., 1981a, Erg reconstruction; the Entrada sandstone (Jurassic) of northern Utah and Colorado: Palaeogeography, Palaeoclimatology, Palaeoecology, v. 36, p. 125-153.
Kocurek, G., 1981b, Significance of interdune deposits and bounding surfaces in aeolian dune sands: Sedimentology, v. 28, p. 753-780.
Kocurek, G., 1988, First-order and super bounding surfaces in eolian sequences —bounding surfaces revisited: Sedimentary Geology, v. 56, p. 193-206.
Kocurek, G. and Fielder, G., 1982, Adhesion structures: Journal of Sedimentary Petrology, v. 52, p. 1229-1241.
Kocurek, G. and Nielson, J., 1986, Conditions for the formation of warm-climate aeolian sand sheets: Sedimentology, v. 33, p. 795-816.
Koster, E.A., 1988, Ancient and modern cold-climate aeolian sand deposition: a review: Journal of Quaternary Science, v. 3, p. 69-83.
Langford, R.P., 1989, Fluvial-aeolian interactions: Part 1, modern systems: Sedimentology, v. 36, p. 1023-1035.
Langford, R.P. and Chan, M.A., 1989, Fluvial-aeolian interactions: Part II, ancient systems: Sedimentology, v. 36, p. 1037-1051.
Loope, D.B., 1985, Episodic deposition and preservation of eolian sands; a late Paleozoic example from southern Utah: Geology, v. 13, p. 73-76.
Loope, D.B., 1988, Rhizoliths in ancient eolianites: Sedimentary Geology, v. 56, p. 301-314.
Mader, D. and Yardley, M.J., 1985, Migration, modification and merging in aeolian systems and the significance of the depositional mechanisms in Permian and Triassic dune sands of Europe and North America: Sedimentary Geology, v. 43, p. 85-218.
Mainguet, M., 1976, Propositions pour une nouvelle classification des edifices sableux eoliens d'apres les images des satellites Landsat 1, Gemini, NOAA 3: Zeitschrift fur Geomorphologie, Supplement Band 20, p. 275-296.
Mainguet, M. and Callot, Y., 1974, Air photo study of typology and interrelations between the texture and structure of dune patterns in the Fachi-Bilma Erg, Sahara: Zeitschrift fur Geomorphologie, Band 20, p. 62-69.
Mainguet, M. and Chemin, M.C., 1983, Sand seas of the Sahara and Sahel — an explanation of their thickness and sand dune type by the sand budget principle, *in* Brookfield, M.E. and Ahlbrandt, T.S., eds., Eolian sediments and processes: Amsterdam, Elsevier, p. 353-364.
McKee, E.D., 1966, Structure of dunes at White Sands National Monument, New Mexico (and a comparison with structures of dunes from other selected areas): Sedimentology, v. 7, p. 1-70.
McKee, E.D., 1982, Sedimentary structures in dunes of the Namib desert, Southwest Africa: Geological Society of America, Special Paper 108, 64 p.
McKee, E.D. and Douglass, J.R., 1971, Growth and movement of dunes at White Sands National Monument, New Mexico: United States Geological Survey, Professional Paper 750-D, p. 109-114.
McKee, E.D. and Moiola, R.J., 1975, Geometry and growth of the White Sands dune field, New Mexico: Journal of Research, United States Geological Survey, v. 3, p. 59-66.
McKee, E.D. and Tibbits, G.C.,Jr., 1964, Primary structures of a seif dune and associated deposits in Libya: Journal of Sedimentary Petrology, v. 34, p. 5-17.
Porter, M.L., 1986, Sedimentary record of erg migration: Geology, v. 14, p. 497-500.
Ross, G.M., 1983, Bigbear erg: a Proterozoic intermontane eolian sand sea in the Hornby Bay Group, Northwest Territories, Canada, *in* Brookfield, M.E. and Ahlbrandt, T.S., eds., Eolian sediments and processes: Amsterdam, Elsevier, p. 483-519.
Rubin, D.M. and Hunter, R.E., 1982, Bedform climbing in theory and nature: Sedimentology, v. 29, p. 121-138.
Rubin, D.M. and Hunter, R.E., 1983, Reconstructing bedform assemblages from compound cross-bedding, *in* Brookfield, M.E. and Ahlbrandt, T.S., eds., Eolian sediments and processes: Amsterdam, Elsevier, p. 407-427.
Sharp, R.P., 1963, Wind ripples: Journal of Geology, v. 71, p. 617-636.
Sharp, R.P., 1979, Intradune flats of the Algodones Chain, Imperial Valley, California: Geological Society of America, Bulletin, v. 90, p. 908-916.
Steele, R.P., 1983, Longitudinal draa in the Permian Yellow Sands of north-east England, *in* Brookfield, M.E. and Ahlbrandt, T.S., eds., Eolian sediments and processes: Amsterdam, Elsevier, p. 543-550.
Steidtmann, J.R., 1973, Ice and snow in eolian sand dunes of southwestern Wyoming: Science, v. 179, p. 796-798.
Stokes, W.L., 1968, Multiple parallel truncation bedding planes — a feature of wind-deposited sandstone formations: Journal of Sedimentary Petrology, v. 38, p. 510-515.
Talbot, M.R., 1985, Major bounding surfaces in aeolian sandstones — a climatic model: Sedimentology, v. 32, p. 257-265.
Warren, A., 1976, Morphology and sediments of the Nebraska Sand Hills in relation to Pleistocene winds and the development of aeolian bedforms: Journal of Geology, v. 84, p. 685-700.
Wasson, R.J. and Hyde, R., 1983a, Factors determining desert dune type: Nature, v. 304, p. 337-339.
Wasson, R.J. and Hyde, R., 1983b, A test of granulometric control on desert dune geometry: Earth Surface Processes and Landforms, v. 8, p. 301-312.
Wilson, I.G., 1971, Desert sandflow basins and a model for the origin of ergs: Geographical Journal, v. 137, p. 180-199.
Wilson, I.G., 1972, Aeolian bedforms — their development and origin: Sedimentology, v. 19, p. 173-210.

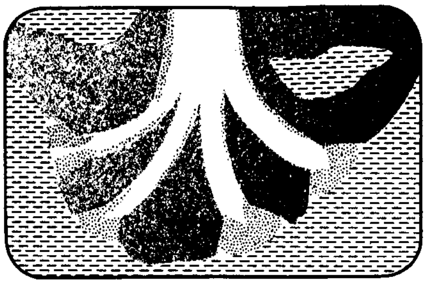

9. Deltas

Janok P. Bhattacharya, Alberta Geological Survey, P.O. Box 8330, Edmonton, Alberta T6H 5X2
Present Address: Arco Exploration and Production Technology, 2300 West Plano Parkway, Plano, Texas 75075

Roger G. Walker, Department of Geology, McMaster University, Hamilton, Ontario L8S 4M1

INTRODUCTION

A delta is a discrete shoreline protuberance formed at a point where a river enters an ocean or other large body of water. Many deltas cover a large area, and have been influenced by a variety of fluvial and marine processes. Several distinct sub-environments of deposition can therefore be identified within a delta. This makes it difficult or impossible to characterize an ancient deposit as "deltaic" simply on the basis of a single core or outcrop section; a restored plan view of the system is necessary. Ancient deltas are economically important because they are commonly associated with major coal, oil and gas reserves. As a result, deltas have been intensively studied, and deltaic facies models have become relatively well established. Readers are referred to several recent summaries for general information (Colella and Prior, 1990; Whateley and Pickering, 1989; Elliott, 1986; Miall, 1984; Coleman and Prior, 1982; Broussard, 1975).

HISTORICAL BACKGROUND

The concept of a delta dates back to the time of Herodotus (ca. 400 B.C.) who recognized that the alluvial plain at the mouth of the Nile had the form of the Greek letter DELTA (Fig. 1). The first study of ancient deltas was that of Gilbert (1885), who described Pleistocene freshwater gravelly deltas in Lake Bonneville, Utah. Barrell (1912) extended Gilbert's ideas to the much larger scale of the Devonian Catskill delta in the Appalachians, and also provided the first explicit definition of the essential features of a delta, as

> "a deposit partly subaerial built by a river into or against a body of permanent water. The outer and lower parts are necessarily constructed below water level, but its upper and inner surface must be land maintained or reclaimed by river building from the sea. A delta, therefore, consists of a combination of terrestrial and marine, or at least lacustrine strata, and differs from other modes of sedimentation in this respect" (Barrell, 1912, p. 381).

Barrell therefore considered the recognition of associated nonmarine facies crucial in distinguishing ancient deltas.

Our understanding of modern deltas has developed during the last 40 years, beginning with work on the Mississippi Delta published in the 1950s and early 1960s (Shepard *et al.*, 1960). Scruton (1960) recognized that deltas are essentially cyclic in nature and consist of a progradational, *constructive* phase usually followed by a retrogradational *destructive* phase coinciding with delta abandonment. He also illustrated a vertical "deltaic sequence" (Scruton, 1960, p. 89) of coarsening- and sandier-upward bottomset, foreset and topset beds related to the seaward migration of depositional environments. Although the Gulf Coast (Florida to Texas) continues to be an important focus for research on modern and ancient deltas (primarily because of the economic importance of deltas in this region as oil and gas reservoirs), studies have spread worldwide. Coleman and Wright (1975) compiled data on 34 modern deltas and developed a six-fold classification based on sand distribution patterns (Fig. 2). However, the most widely used classification scheme today is that of Galloway (1975), who subdivided deltas according to the dominant processes controlling their morphology; rivers, waves and tides (see Chapter 1, Fig. 7). Improvements in technology in the late seventies and early eighties, particularly side-scan sonar imaging, led to the recognition of the abundance and importance of synsedimentary deformation in the subaqueous parts of modern deltas (Coleman *et al.*, 1983; Winker and Edwards, 1983). Similar features have now been recognized in ancient deltas (Martinsen, 1989; Pulham, 1989; Nemec *et al.*, 1988). The present research emphasis concerns the evolution of modern deltas in the context of eustatic sea level changes (Dominguez *et al.*, 1987; Boyd *et al.*, 1989; Williams and Roberts, 1989; Carbonel and Moyes, 1987), and the application of the concepts of sequence stratigraphy to ancient deltas (Galloway, 1989; Bhattacharya and Walker, 1991).

DEFINITIONS

Deltas are "discrete shoreline protuberances formed where rivers enter oceans, semi-enclosed seas, lakes or lagoons and supply sediment more rapidly than it can be redistributed by basinal processes" (Elliott, 1986, p. 113). By this definition, all deltas are to some degree river dominated.

The sediment in a delta is normally derived directly from the river that feeds it. This contrasts with estuaries and many so-called tide-dominated "deltas", in which sediment is derived from the marine realm. These *tide-dominated* systems are dealt with in Chapter 11, although *tide-influenced* deltas are considered in this chapter. Where basinal processes redistribute sediment to the point that the fluvial source and delta morphology can no longer be recognized, more general environmental terms such as paralic, strandplain or coastal plain are preferable. The term delta has also been loosely applied to ancient facies successions that show a transition from marine to nonmarine, or which contain a marine-fluvial or lacustrine-fluvial interface (Alexander, 1989). Although a shoreline must be crossed in such a transition or interface, the identification of the shoreline as specifically deltaic usually requires good three-dimensional control of facies patterns. This may consist of maps of lithofacies distributions showing a thickening and narrowing of the clastic succession toward the point of fluvial input, and the required seaward protuberance of the shoreline (Fig. 2).

Deltas occur at a wide variety of scales ranging from large-scale depositional systems such as the modern Mississippi delta, with an area of about 28,500 km^2, to components of other depositional systems such as flood-tidal deltas within barrier-lagoon depositional systems (Chapter 10) or bayhead deltas within estuarine systems (Chapter 11). The larger-scale systems will be reviewed in this chapter.

DELTA-FORMING PROCESSES

A delta forms when a river of sediment-laden freshwater enters a standing body of water, loses its competence to carry sediment, and deposits it. The general form of the deltaic deposit depends upon 1) whether the river outflow is more dense (hyperpycnal flow), equally dense (homopycnal) or less dense (hypopycnal) than the standing body of water, and 2) the extent to which the deposits are reworked by marine (wave and tide) processes.

Where the flows are hyperpycnal and the sediment load is relatively coarse grained, small, steeply dipping elongate deltas tend to form. Finer grained material may be deposited further offshore as density underflows. This kind of deposition is common where sediment-laden streams enter freshwater lakes, as occurs in many alpine or periglacial environments (Chapter 5). Such mouth bars have been referred to as inertia dominated (Bates, 1953).

In homopycnal settings there may be a greater degree of mixing between the river and standing body of water. These situations are also common in fresh water deltas, especially where the suspended sediment load is high. In shallow water, friction at the bed causes rapid deceleration and development of a middle-ground bar that tends to cause the associated distributary to bifurcate (Wright, 1977). So-called friction-dominated mouth bars also tend to be more fan shaped and may be dominated by traction current features such as ripples and cross bedding. These types of deltas are commonly characterized by steeply dipping foreset beds, separating less steeply dipping topset and bottomset beds. They are characteristic of the small gravelly freshwater deltas described by Gilbert (1885) and now commonly termed "Gilbert-type deltas".

In most cases where a river enters salt water, the density of the river plus sediment load is less than that of the sea water (hypopycnal flow). The suspended sediment is relatively fine grained, and tends to be carried farther out into the receiving basin as a buoyant plume, resulting in lower depositional slopes and more extensive deltaic deposits. These are sometimes referred to as buoyancy-dominated

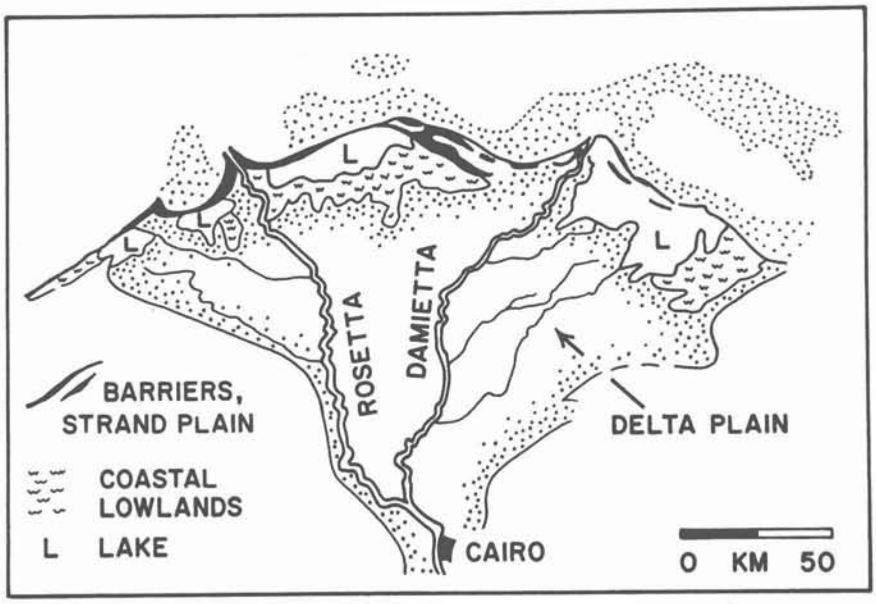

Figure 1 Environments and facies in the modern Nile delta. Only the Rosetta and Damietta Branches are presently active. Stipple north of delta margin indicates older reworked delta sands (Scheihing and Gaynor, 1991) rather than active "sand plumes" (Coleman *et al.*, 1981). Since construction of the Aswan Dam, water and sediment discharge to the delta have decreased, and the entire delta is undergoing transgression. After Fisher *et al.* (1969) and Sestini (1989).

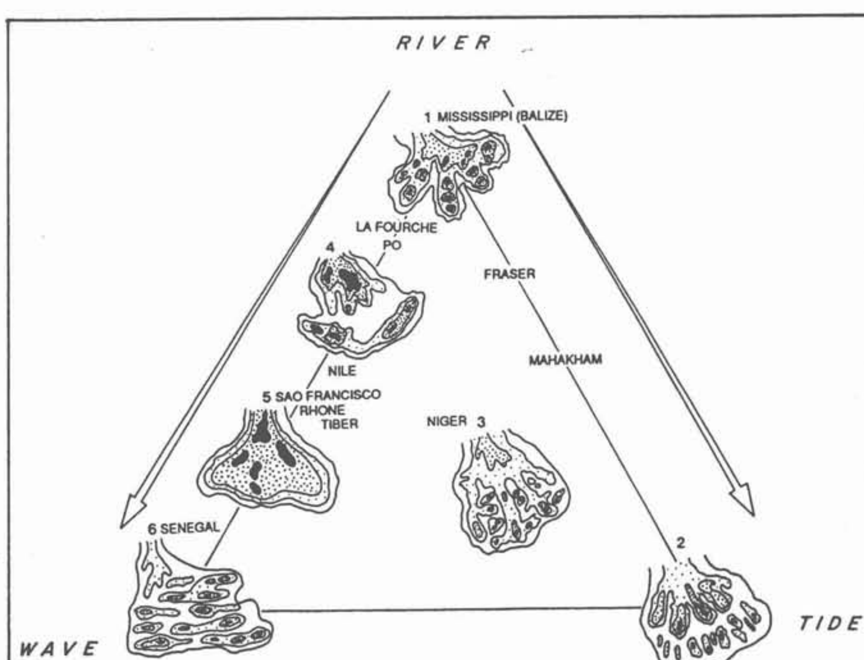

Figure 2 Sandbody geometries of the six delta types of Coleman and Wright (1975) plotted on the river-, wave- and tide-dominated tripartite classification of Galloway (1975).

mouth bars. In any given river mouth or delta, inertial, frictional, and buoyant forces may be operative in varying proportions. Recent work has attempted to distinguish the relative importance of these processes in classifying ancient river mouth sediments (Martinsen, 1990; Pulham, 1989; Harris, 1989).

Deltas comprise three main subenvironments; the *delta plain* (where river processes dominate), the *delta front* (where river and basinal processes are both important) and the *prodelta* (where basinal processes dominate). Several examples are shown in Figure 3.

Delta plains usually contain distributary channels and a wide variety of nonmarine to brackish environments including swamps, marshes, tidal flats, and interdistributary bays.

The delta front is the site of much of the active deposition in deltaic environments, particularly at the mouths of distributaries where the coarsest sediment is deposited in distinct bars. *Distributary mouth bars* (also referred to as stream mouth or middle-ground bars) are relatively small features in modern deltas; their development is influenced by marine processes and grain size. In deeper water mud-dominated deltas that build into relatively quiet marine basins (low tidal range, low wave action), the positions of distributary channels may be fixed for long periods. The sandier distributary mouth bars then prograde to form elongate bar fingers, as in the modern Mississippi "birdfoot" delta (Fig. 3). By contrast, in siltier or sandier systems deposited in shallower water, distributaries switch more rapidly and coalesce to form more lobate deltas, as in the Lafourche (Fig. 3) and Atchafalaya (Fig. 4) deltas.

The prodelta is the area where fine material settles quietly out of suspension. It is commonly extensively bioturbated, and merges seaward with fine-grained sediment of the basin floor. The preservation of some silty lamination is commonly taken to mark the influence of the delta, as opposed to total bioturbation of the basin floor sediments. Where the sediments are rhythmically laminated, there may be a tidal influence (Smith *et al.*, 1990).

Apart from the nature of the fluvial input and the reworking of the deposits by waves and tides, other factors may also influence the delta form. Coleman and Wright (1975) emphasize the geometry and nature of the receiving basin, the nature of the drainage basin, the tectonic setting, the gradient of the shelf, and the climate. In addition, relative sea level changes (due to the interaction of eustasy and rates of subsidence) will influence the extent of delta growth and destruction. Reading and Orton (1991) also emphasize that sediment size and compositions affect the nature and distribution of deltaic facies.

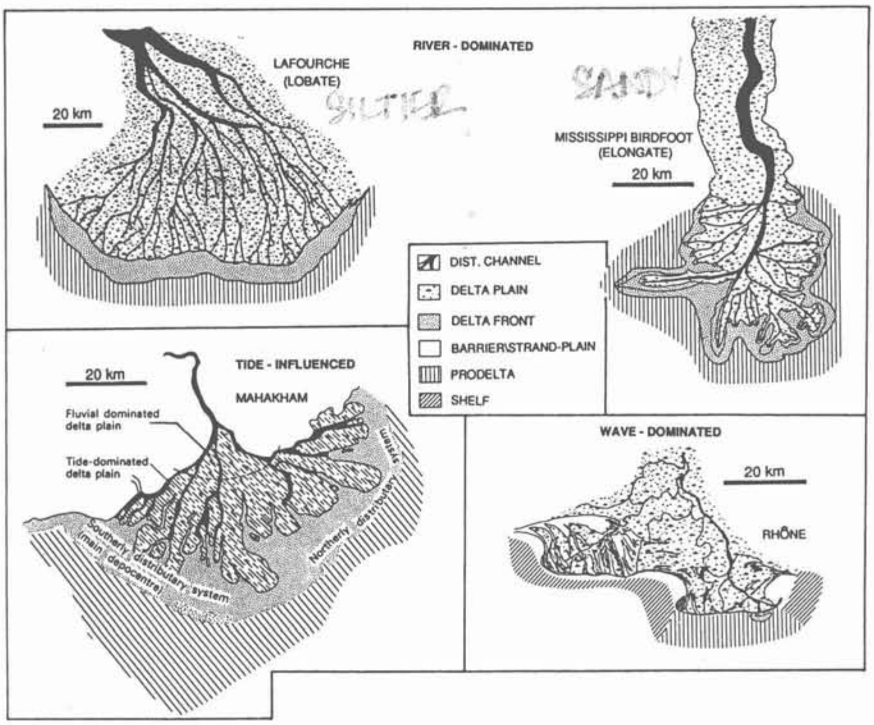

Figure 3 Representative modern examples of river-dominated, wave-dominated and tide-influenced deltas. Modified from Fisher *et al.* (1969). River-dominated deltas are classified into lobate (shoal-water), and elongate (deep-water or birdfoot deltas). In the Mahakham example (after Allen *et al.*, 1979), delta front deposits comprise sandy siltstones and mudstones.

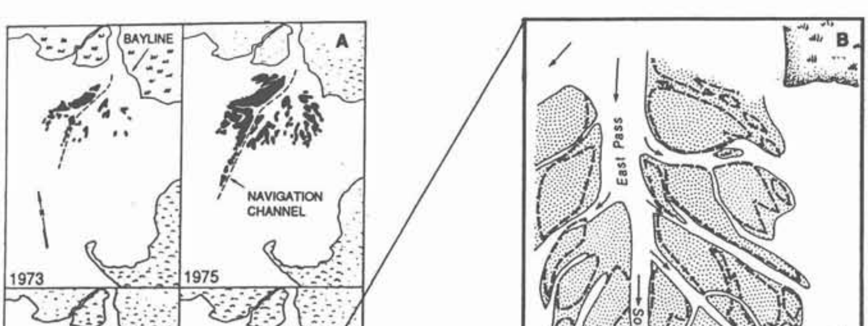

Figure 4 Development of a shallow water delta in Atchafalaya Bay, Mississippi Delta. A) River-dominated lobe forms by the coalescing of distributary mouth bars (black), suggesting friction dominance. B) As the delta grows, the mouth bars accrete upstream and downstream (compare 1976 and 1982 shorelines). After Van Heerden and Roberts (1988).

These factors are not all independent. Sediment type and rate of supply, for example, will be a function of the size, relief, and climate in the drainage basin. Relief may be dependent on the tectonics of the drainage basin. Wave or tide energy may be a function of eustasy, shelf slope, size and shape of the receiving basin, and climate. Sediment type and rate of supply were also influenced by the absence of land plants in pre-Devonian rocks, resulting in higher sedimentation rates and a greater proportion of fan-deltas (Miall,1984; Stow, 1986). Fan deltas occur where alluvial fan systems, consisting of many rivers, build directly into a standing body of water with no intervening coastal or delta plain and are usually coarse grained. The topic is dealt with most recently by Colella and Prior (1990).

BASIC DELTAIC MORPHOLOGY

The term *delta* includes all the *delta plain*, *delta front* and *prodelta* deposits of a particular river. A delta may be composed of several distinct *lobes*, which stack irregularly or shingle side by side as the river changes position from time to time. Thus one lobe may be forming while earlier lobes are subsiding and being transgressed.

Deltas basically consist of a sandy framework fleshed out with finer grained deposits. In river-dominated systems such as the Mississippi, the sandbodies reflect positions of distributary channels, and generally trend perpendicular to shoreline. Finer grained sediment is deposited as overbank material during flood stages of the river, on the floodplain, in bays, swamps, marshes, and in other standing bodies of water, commonly as crevasse splays (Fig. 5).

With increasing wave influence, the sand fraction tends to be reworked alongshore and the finer fraction swept out to sea, as in the Rhone delta in southern France (Fig. 3). Sandbodies trend parallel to the shoreline, and within the delta proper, fines only accumulate in lagoons behind the shore-parallel beaches and beach ridges. This spectrum of delta morphologies is shown in Figs. 1, 2 and 3. These differing processes and morphologies form the basis for delta classifications.

CLASSIFICATION OF DELTAS

The commonly used tripartite classification (Figure 6 in Chapter 1, from Galloway, 1975) is based on the relative importance of fluvial processes versus basinal processes (waves and tides, Fig. 2). Fluvially dominated deltas tend to display an overall digitate morphology. These types of deltas have also been termed "high-constructive" by Fisher *et al.* (1969). In contrast, wave-dominated deltas tend to be more lobate and to have smooth, arcuate to cuspate margins (Figs. 1, 2 and 3). These were termed "high-destructive" (Fisher *et al.*, 1969), but because all deltas are to some degree "constructive", the term "high-destructive" is misleading. Tidal processes form sandbodies oriented parallel to the directions of the tidal currents; these are roughly perpendicular to regional shorelines, but may be parallel to the banks of estuaries and large embayments of the coastline.

Coleman and Wright (1975) recognized that the sandbody geometry of a delta should uniquely reflect the relative importance of fluvial and marine processes. All of their delta geometries (Fig. 2) emphasize narrowing and thickening of sands toward a point (i.e., fluvial) source, but the seaward margins differ as explained above.

More recent work on deltas at continental margins has resulted in recognition of a new type of delta, termed a shelf margin or shelf edge delta (Edwards, 1981; Fig. 6). Sandbodies in these settings are often aligned along strike, but are controlled by large-scale and rapid subsidence along growth faults, rather than wave processes.

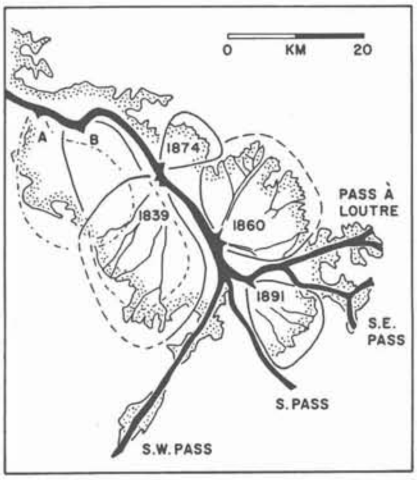

Figure 5 Infilling of interdistributary bays by historically dated crevasse "subdeltas" in the modern Mississippi birdfoot delta. Simplified from Coleman and Gagliano (1964, Fig. 5).

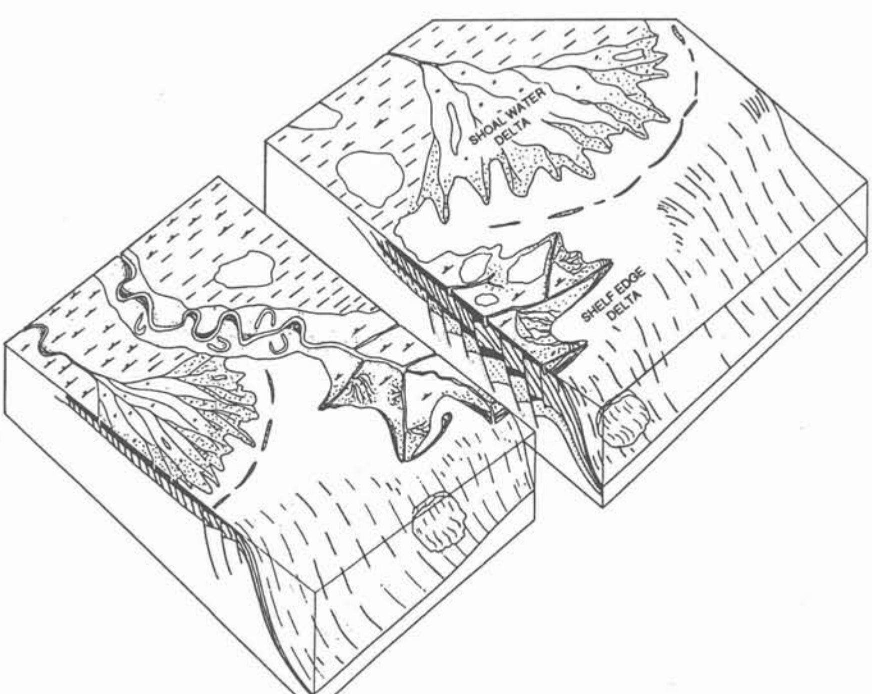

Figure 6 Block diagram contrasting lobate shoal-water (or shelf phase) deltas and shelf edge deltas. Note thickening of facies across growth faults in the shelf edge delta. After Edwards (1981).

FACIES SUCCESSIONS WITHIN DELTAIC DEPOSITIONAL SYSTEMS

In addition to sandbody geometries, Coleman and Wright (1975) presented a series of composite vertical facies successions through the prodelta, delta front and delta plain environments of each of their delta types. Idealized facies successions represent "norms", and may be very useful points of reference for outcrop studies where three-dimensional control may be limited, but, as with all norms, they should not be used unthinkingly. Typical facies successions through the dominantly marine (prodelta and delta front) and dominantly nonmarine (delta plain) parts of deltas, mostly in river- and wave-dominated settings, are outlined below.

Prodelta and delta front successions

Progradation of a delta lobe will tend to produce a single, relatively thick coarsening-upward facies succession (Fig. 7) showing a transition from muddier facies of the prodelta into the sandier facies of the delta front and mouth bar environments (Elliott, 1986; Coleman and Wright, 1975). Thicknesses may range from a few metres to a hundred metres depending on the scale of the delta and the water depth. Continued progradation may result in delta plain facies overlying the delta front sands in a continuous succession. However, delta front sands may be partially eroded by progradation of the distributary channel over its own mouth bar (Fig. 7). Commonly, progradational delta lobe successions are truncated by thin transgressive abandonment facies (Fig. 8).

In shelf edge deltas (Fig. 6), thick coarsening-upward delta front successions are commonly completely preserved in thicker deposits across the seaward downthrown portion of growth faults. In the shallower landward portions, greater reworking by shallow-marine processes can result in more complex facies successions (Winker and Edwards, 1983).

The specific nature of the facies in prograding prodelta and delta front successions will depend on the processes influencing sediment transport, deposition, and reworking. In addition, coarsening-upward facies successions can be produced by the progradation of other types of depositional systems, as discussed in the definitions above.

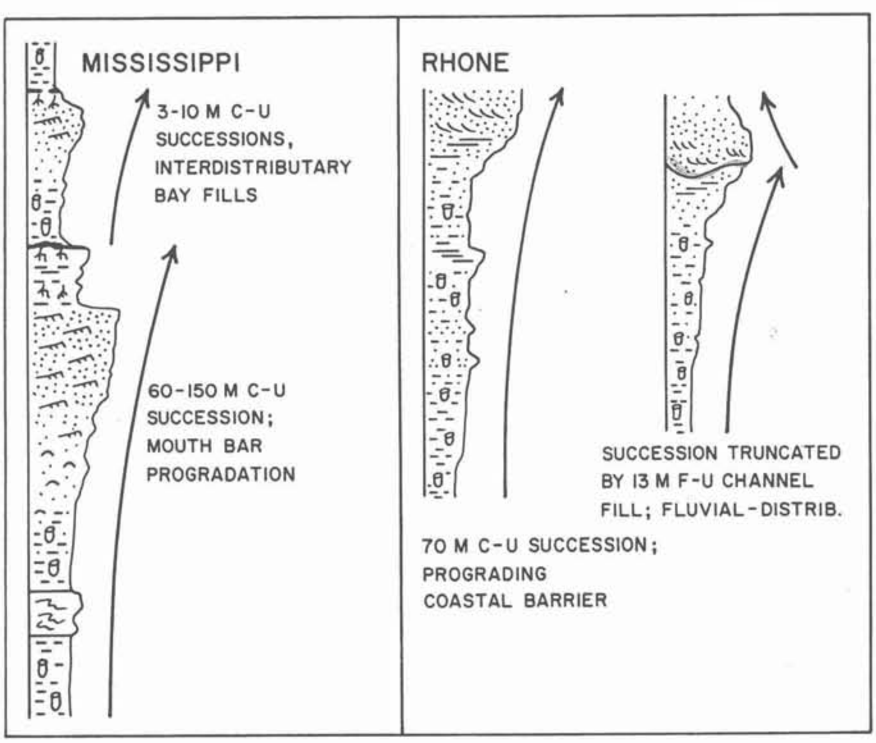

Figure 7 Typical coarsening-upward facies succession formed as a result of prograding deltaic lobes and mouth bars. Mississippi example shows a composite of a thicker mouth bar succession below and the more irregular bay fill successions above. From Elliott (1986); modified after Coleman and Wright (1975). Rhone example (left) shows progradation of a mouth bar forming an asymmetrical coarsening-upward succession, whereas Rhone example (right) shows truncation by a distributary channel, and has a more symmetrical profile. Rhone examples from Elliott (1986; modified after Oomkens, 1970).

River-dominated deltas

In river-dominated deltas, prodelta mudstones and siltstones are typically massive to well stratified and may show graded bedding (Figs. 7 and 8A). The graded beds may result from 1) the settling of material carried out in suspension as a buoyant plume, or 2) from density underflows generated at the river mouth during times of high discharge (Wright *et al.*, 1988). The amount of bioturbation is variable, depending on rates of sedimentation and grain size of sediment supplied. Wave-formed structures are uncommon. Soft-sediment deformation features, resulting from high sedimentation rates, are common in river-dominated deltas, and may be on a very large scale and involve large proportions of the delta front sediments, as in the Mississippi (Coleman *et al.*, 1983).

Sandy delta front facies show the predominance of deposition by fluvial processes in distributary mouth bar environments. This may include unidirectional current ripples and cross bedding or massive graded beds, depending on the importance of frictional versus inertial processes (Martinsen, 1990). High rates of deposition may result in rapid burial, and preservation of the fluvially formed structures. Variations in discharge in the fluvial system may produce a somewhat irregular coarsening-upward, with interbedded burrowed mudstones throughout the succession (Fig. 8A). Preserved organic matter is commonly high in river-dominated delta fronts. Fresh or brackish water influence may be reflected in brackish faunal and trace faunal assemblages (Moslow and Pemberton, 1988; Bhattacharya and Walker, 1991), syneresis cracks (Plummer and Gostin, 1981), and early diagenetic siderite (Coleman and Prior, 1982; Bhattacharya and Walker, 1991).

Wave-dominated deltas

Storm- and wave-dominated deltas commonly consist of a series of prograding beach and beach-ridge complexes, with sand fed from a nearby

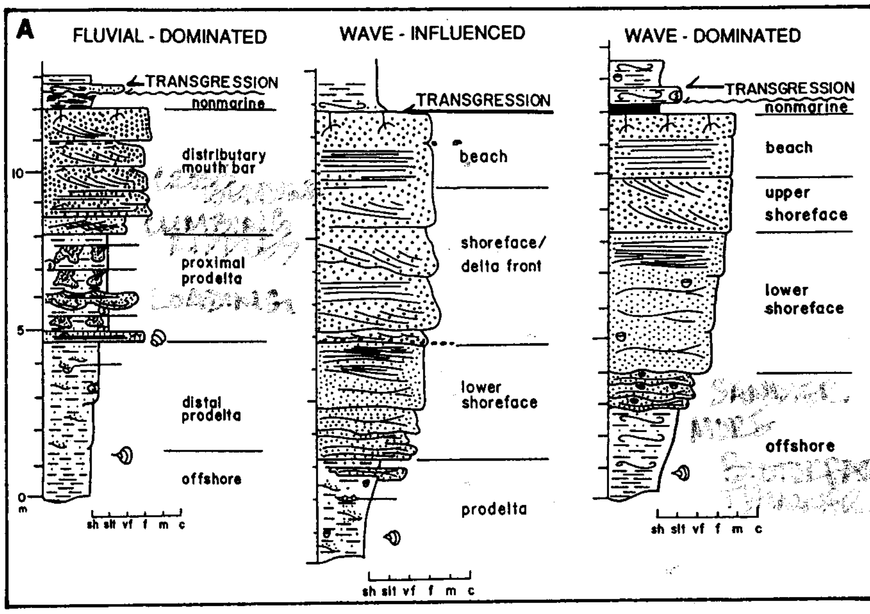

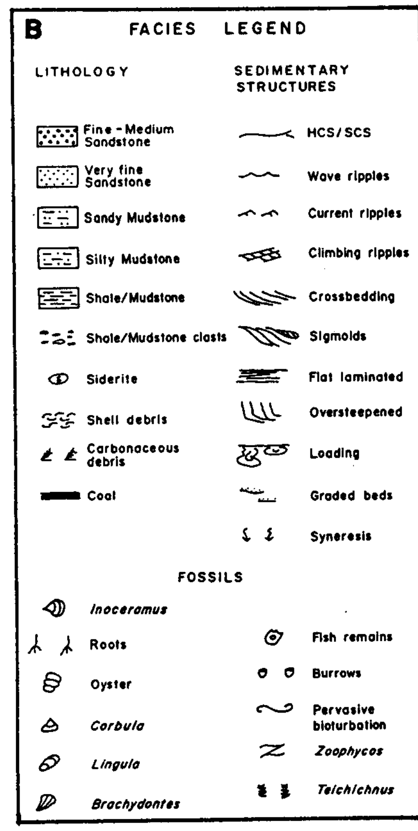

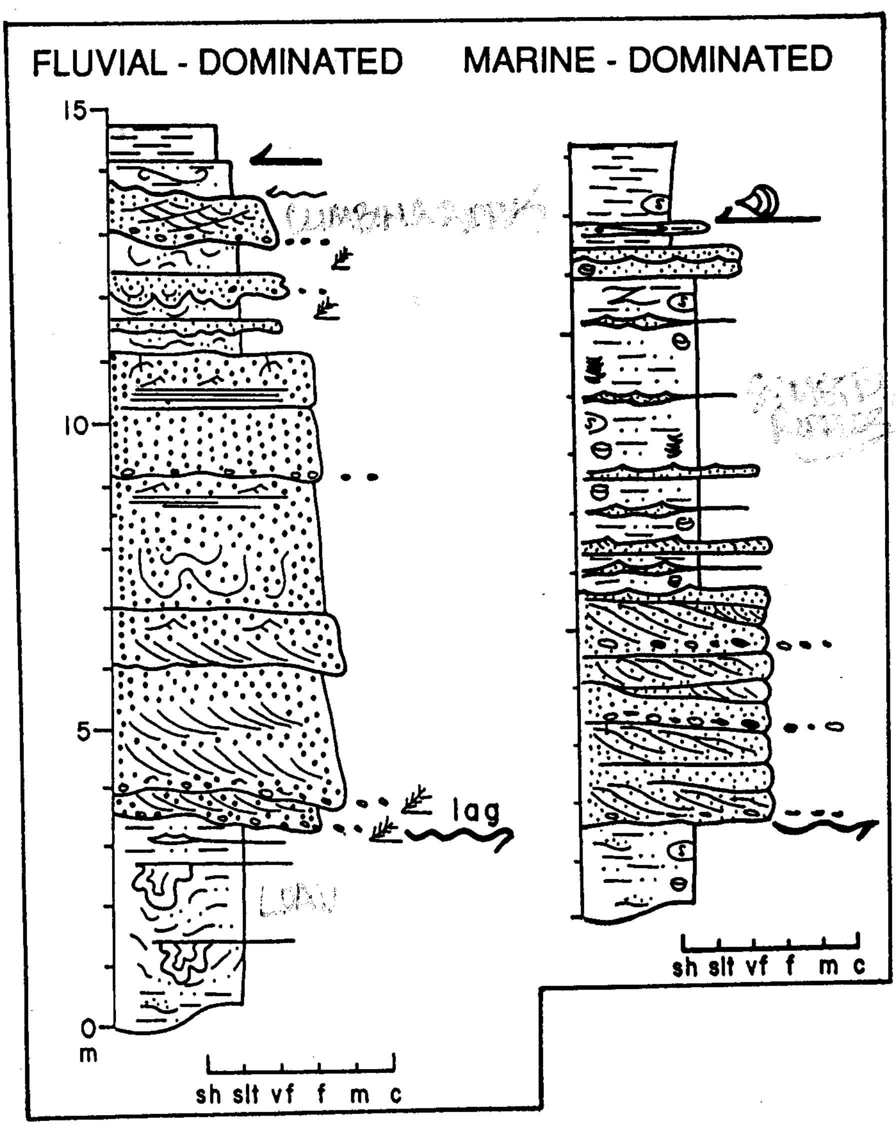

Figure 8 A) (above left) Comparison of delta front successions in river-dominated, wave-influenced, and wave-dominated deltas in the Upper Cretaceous Dunvegan Formation, Alberta. After Bhattacharya and Walker (1991). The river-dominated succession is the most irregular. Basal mudstones are increasingly bioturbated with decreasing fluvial influence. B) (above) facies legend for Dunvegan figures 8, 9 and 10.

Figure 9 **(left)** Comparison of distributary channel fill successions in fluvial- and marine-dominated deltas of the Dunvegan Formation (Cretaceous, Alberta). In the marine-dominated system, the distributary fill reflects transformation of the distributary into an estuary. After Bhattacharya and Walker (1991). Arrow indicates transgression.

river (e.g., Rhone). The delta front (Figs. 7 and 8 [wave-dominated column]) is usually characterized by a relatively continuous coarsening-upward facies succession characteristic of a wave-dominated shoreface (Chapter 12). The proportion of wave-produced structures (such as wave ripples and hummocky cross stratification) tends to be greater, whereas indicators of high sedimentation rates and fresh water influence (e.g., soft sediment deformation, climbing current ripples, brackish fauna, syneresis cracks) tend to be fewer. Prodelta mudstones may be more bioturbated, thinner, and sandier than in river-dominated settings. In the geological record, one vertical facies succession of this type indicates only a prograding wave- or storm-dominated shoreface. Good three-dimensional control is necessary before such a shoreface can be positively associated with a *delta*.

really important

river dom structures

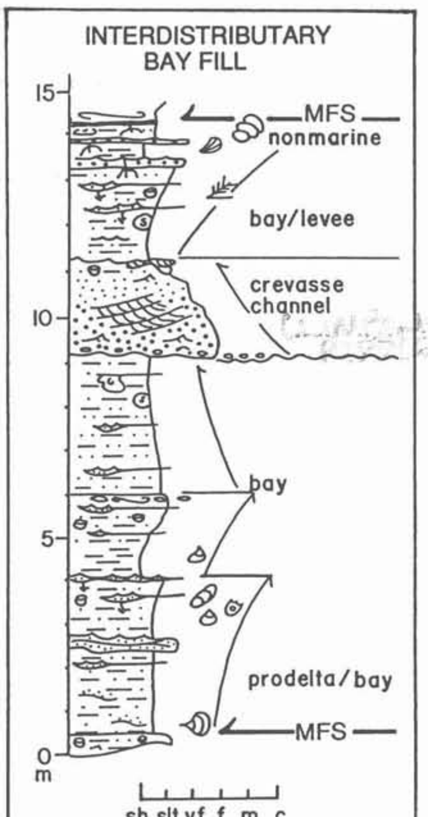

Figure 10 Interdistributary bay fill in a river-dominated delta lobe in the Dunvegan Formation (Cretaceous, Alberta), showing thin irregular cycles and overall increase in proportion of nonmarine facies upward. After Bhattacharya and Walker (1991). MFS, maximum flooding surface.

Tide-influenced deltas

Tidally influenced prograding delta fronts, such as the Fraser in Canada, the Mahakham in Indonesia, and the Niger in Africa, also show an overall coarsening upward but the facies reflect tidal influence. Smith *et al.* (1990) describe tidal rhythmites (see Chapter 11) in glacio-marine prodelta sediments in Alaska and suggest that similar pro-

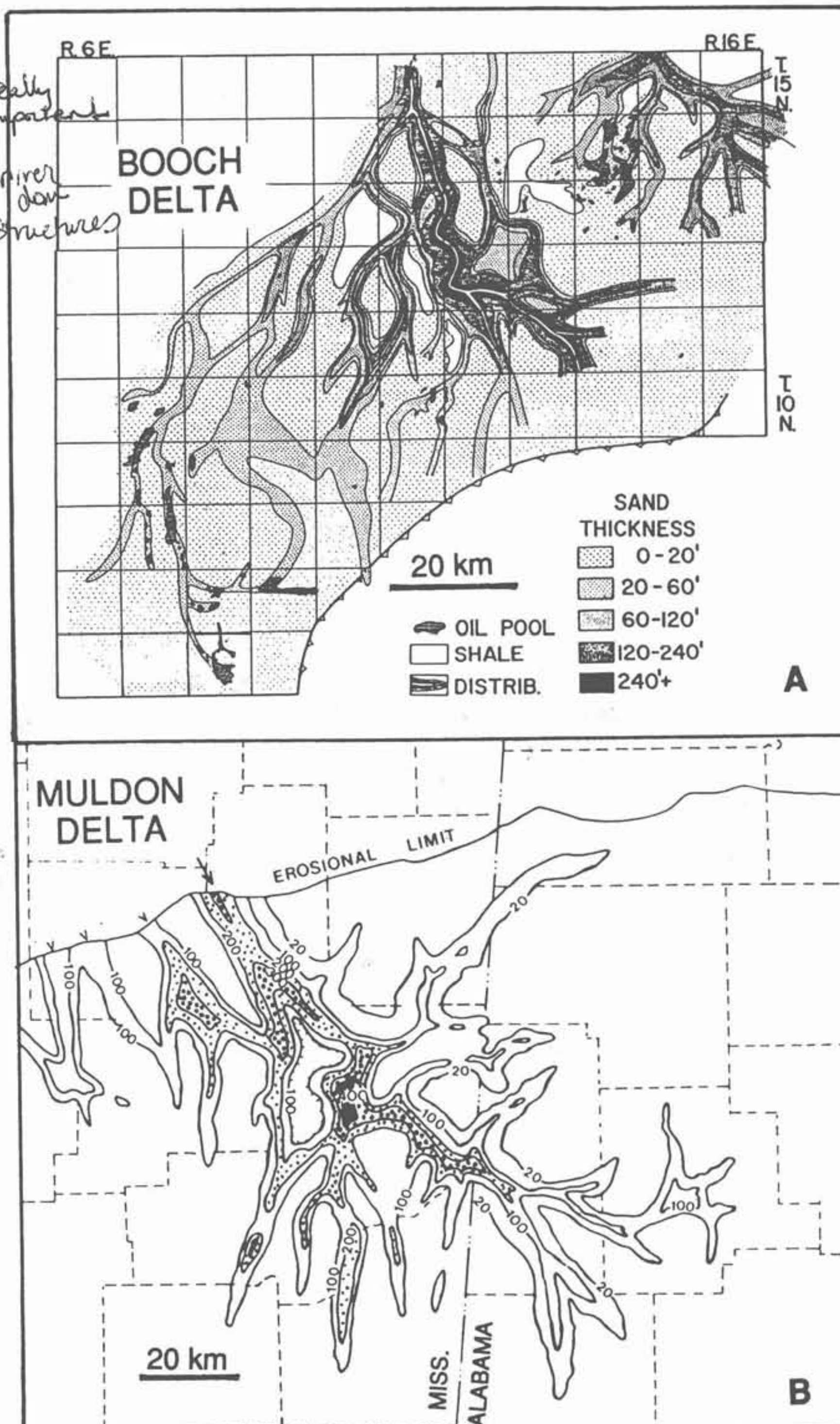

Figure 11 Ancient examples of dendritic "shoestring" sandstones interpreted as river-dominated, elongate deltas. A) Pennsylvanian Booch sandstone (Oklahoma), after Busch (1971). B) Muldon delta (Pennsylvanian, Mississippi/Louisiana) after Cleaves and Broussard (1980).

cesses may be applicable to nonglacial meso- and macro-tidal deltaic settings. Leithold *et al.* (1989) and Kreisa *et al.* (1989) document tidal cyclicity in ancient prodelta sediments.

Tidal indicators in delta front sands include herringbone cross bedding, tidal bundles, and reactivation surfaces (Chapter 11), although these features are also found in many nondeltaic tidal settings. Some of the "tide-*dominated* deltas" that have been identified in the literature fall equally well into other descriptive settings, for example, offshore tidal sand ridges (Klang-Langat in Malaysia) or estuaries (Ord River in Australia). We therefore emphasize that the deltaic terminology can only be applied where three-dimensional control exists and where the systems clearly show evidence of seaward progradation.

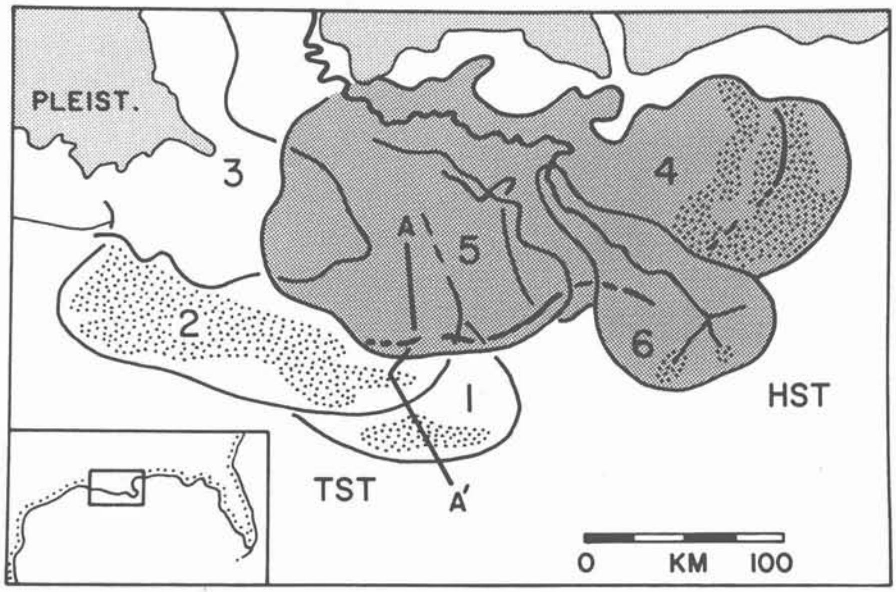

Figure 12 Major deltaic lobes of the Mississippi Delta; 1 – Outer Shoal, 2 – Maringouin, 3 – Teche, 4 – St. Bernard, 5 – Lafourche, 6 – Modern. Lobes 1-3 (plain) belong to transgressive systems tracts (TST), and lobes 4-6 (stippled) belong to a highstand systems tract (HST) (see Fig. 13). Heavy dots indicate subaqueous sand bodies; in lobe 1, Outer Shoal and in lobe 2, Ship Shoal. The heavy line, particularly around the margins of lobes 4 and 5, indicates barrier islands. The line A-A' shows the location of Figure 13. Simplified from Boyd *et al.* (1989).

Delta plain successions

Distributary channels

Facies successions through distributaries (Fig. 9) are erosionally based. Filling commonly takes place after channel switching and lobe abandonment. At this time, the distributary channel may develop into an estuary, and the fill is commonly transgressive (see also Chapter 11). The facies succession will tend to fine upward, with some preserved fluvially derived facies at the base, and a greater proportion of marine facies in the upper part of the channel fill. The extent of marine facies development will depend on the degree of fluvial dominance. Examples of these different types were presented by Bhattacharya and Walker (1991) from distributaries in Cretaceous deltaic systems in Alberta (Fig. 9).

The overall proportion of distributary channel facies is a function of the type of delta. In general, the more wave-dominated the delta, the greater will be

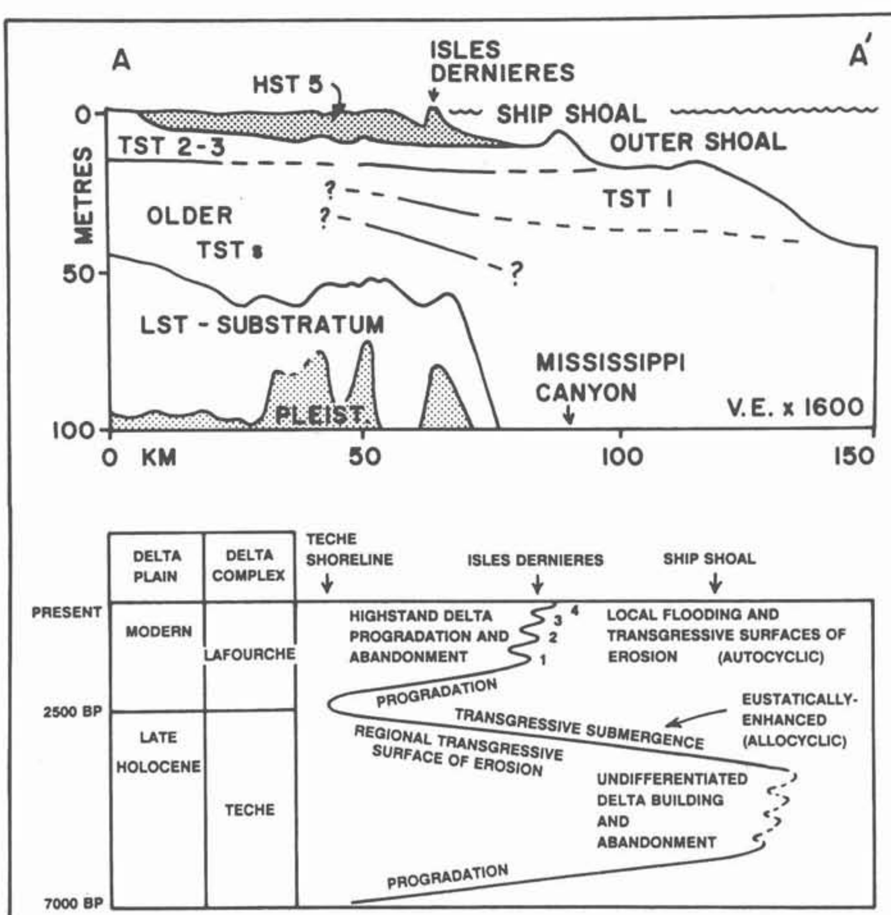

Figure 13 Sequence stratigraphic interpretation of the Mississippi delta plain based on identification of a major eustatically enhanced transgression between the Teche/Maringouin delta complex (TST, lobes 2-3), and the younger Lafourche/Modern complex (HST, lobes 4-6). The cross section shows the major systems tracts, located in Figure 12. The sea level history chart shows autocyclic and allocyclic units; the major lobes are interpreted as autocyclic in origin, while the lobe complexes are allocyclic. After Boyd *et al.* (1989).

the proportion of lobe sediment with more limited amounts of interlobe and distributary channel facies.

Interdistributary areas

Interdistributary and interlobe areas tend to be less sandy, and commonly contain a series of relatively thin, stacked coarsening- and fining-upward facies successions (Fig. 10). These are usually less than ten metres thick, and much more irregular than the successions found in prograding deltaic lobes (compare Figs. 8 and 10; also see Elliott, 1974). The proportion of lobe versus interlobe successions will depend on the nature and type of delta system and will tend to be greater in more river- or tide-influenced systems and less in wave-dominated deltas.

Interdistributary areas in river-dominated deltas

An interdistributary bay is filled by overbank spilling of fine-grained material from the river during flood stages. There is an overall shallowing-upward facies succession, associated with a trend from more marine to more nonmarine facies, but commonly without the deposition of thick sands (Fig. 10). This represents the transition from offshore prodelta mudstones into delta top facies without the development of a sandy shoreline (Walker and Harms, 1971; Bhattacharya and Walker, 1991). The muddy nature of interdistributary bay successions may be punctuated by sandy crevasse splay or channel deposits that may produce thin coarsening or fining cycles (Coleman and Prior, 1982; Elliott, 1974). The succession may grade into rooted coaly mudstones or coals representing a variety of swamp, marsh and lacustrine environments. In addition, beach sands associated with the development of barrier strandplains, spits, or cheniers may be present at the tops of these successions, although they will probably be relatively thin. Interlobe areas may also act as the locus for progradation of the next lobe and may be erosively truncated by younger distributary channels.

Interdistributary areas in wave-influenced deltas

Interdistributary bays may often be completely closed off by barrier/beach complexes in wave-dominated deltas (e.g., the Nile, and the Sao Francisco in Brazil), resulting in extensive backbarrier lagoons. These may be filled from the landward side by progradation of bayhead deltas or from the barrier side by storm washovers (as discussed in Chapter 10). Deposits are commonly organic-rich, with marsh vegetation or mangroves.

Interdistributary areas in tide-influenced deltas

Tidal processes may be important in interdistributary bays (even in river-dominated deltas) resulting in tidally

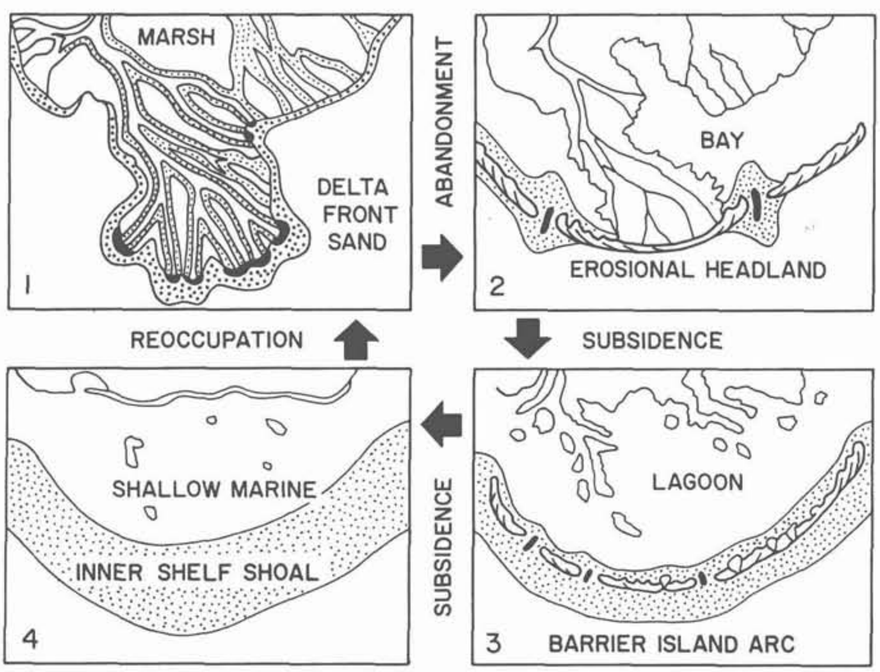

Figure 14 *Stages in the evolution of a delta, based on Mississippi examples. Note the contrast between the constructional (active) phase (panel 1) and the transgressive destructional (or nondeltaic) stages (panels 2-4).* In panel 1, levees and delta front sands are stippled, and mouth bars are black. In panels 2-4, stipple indicates sand that is reworked during transgression. This reworking forms barrier island arcs (panels 2-3), which can be submerged to form inner shelf shoals (panel 4). Simplified from Boyd and Penland (1988).

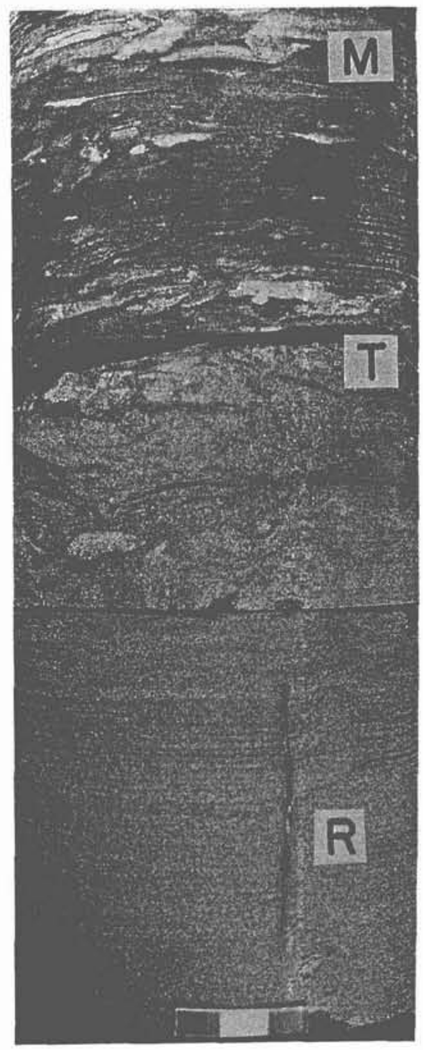

Figure 15 Transgressive surface (T) *capping interdistributary sediments of the* Dunvegan Formation. The surface separates nonmarine heterolithic sandstones and mudstones containing root traces (R) below, from the deeper marine mudstones (M) above. Note the absence of an intervening shoreline sandstone or distinctive transgressive lag. From well 12-31-62-2W6, 7556 feet. Scale in cm.

influenced facies such as tidal flats or tidal channels (Allen *et al.*, 1979; Ramos and Galloway, 1990). These are especially common in modern tidally influenced deltas such as the Niger, Fraser, and Mahakham deltas. Ancient examples of tidally influenced facies in delta plain settings include those published by Ramos and Galloway (1990), Eriksson (1979) and Rahmani (1988).

CASE STUDIES OF MODERN DELTAS AND THEIR ANCIENT COUNTERPARTS

The delta models described above are based on the morphologies and facies patterns of several modern deltas. A few case studies will be discussed, to place the facies successions into a larger context.

River-dominated deltas

The modern Mississippi birdfoot lobe (Balize delta) is the type example of an elongate, river-dominated delta (Fig. 3). It is characterized by a skeleton of radiating, shore-normal bar finger sands that formed by the progradation of distributary mouth bars (Fisk, 1961). The very straight nature of the bar fingers is largely due to lack of reworking of sands in the marine environment and the muddy nature of the sediments; wave action is slight and the tidal range is very low. The birdfoot is also situated in relatively deep water, close to the edge of the continental shelf, where the subaerial levees of the distributaries can only build straight forward on top of the mouth bar deposits. Overall, the facies are dominated by muds with well-developed coarsening-upward mouth bar successions (Fig. 7) within the bar fingers. Associated sands in the immediate subsurface (Coleman, 1981) show a greater degree of strike alignment related to growth faults. The rate of fluvial sediment input is so great, and the marine processes relatively so weak, that the skeleton of bar finger sands, radiating from the Head of Passes, has developed during the last 600-800 years. The skeleton has been fleshed-out by deposition in interdistributary bays from historically dated crevasses in the channel levees (Fig. 5). Each bay fill is in effect a small delta, building from the crevasse in the levee.

The modern Mississippi birdfoot delta owes its morphology to an unusual set of circumstances (very high

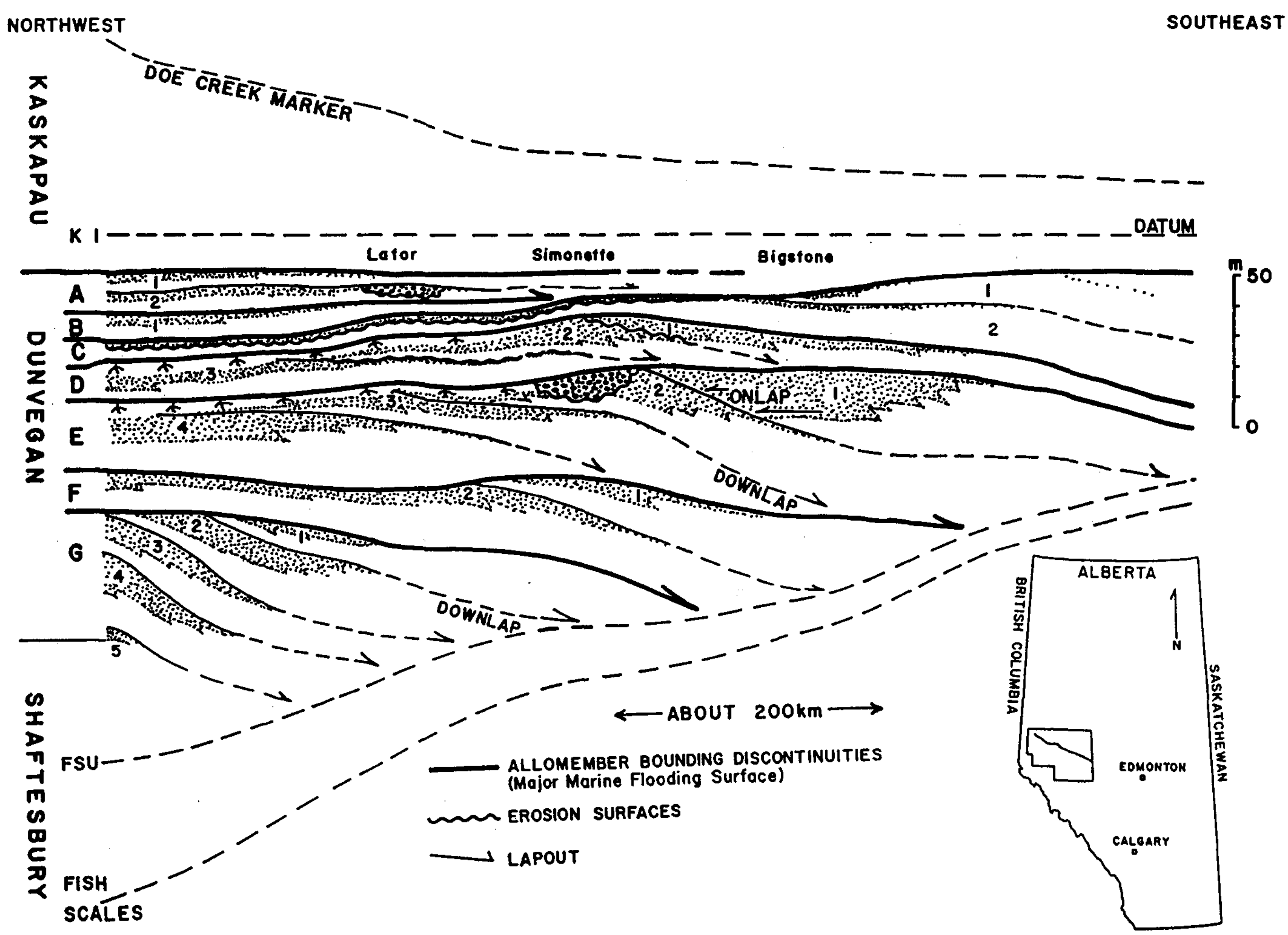

Figure 16 Subdivision of the Dunvegan clastic wedge into seven allomembers (A to G) bounded by major marine flooding surfaces. The allomembers contain offlapping shingled units (numbered) which provided the basis for mapping discrete deltaic depositional systems. The cross section is based on hundreds of well logs and cores, and is condensed from Bhattacharya and Walker (1991).

river input into a relatively deep marine basin with low wave action and tidal range). The birdfoot is artificially maintained in its present position by the U.S. Army Corps of Engineers, who restrict or prevent the diversion of the Mississippi River into other channels hundreds of kilometres upstream, and who protect the banks and dredge the channels within the birdfoot to keep the shipping channel to the port of New Orleans open.

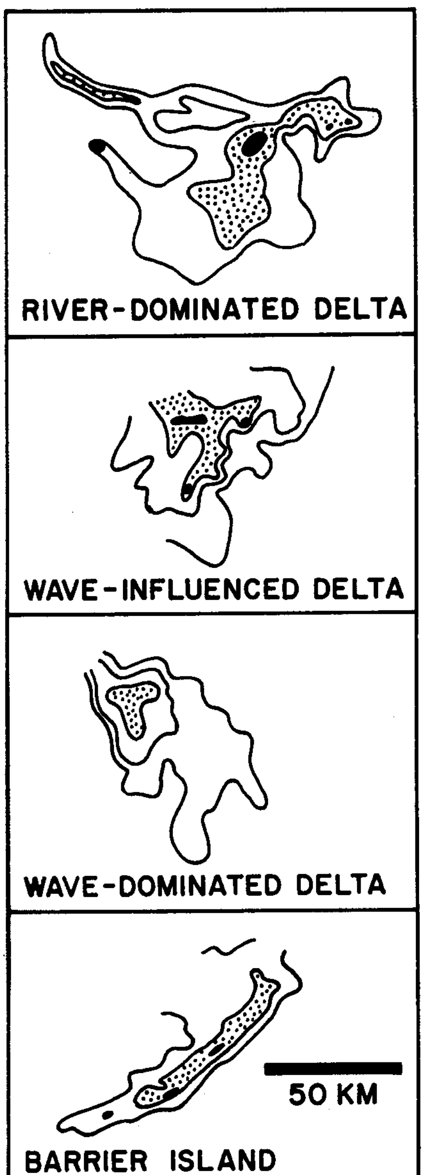

Figure 17 Spectrum of sandbody geometries shown by sandstone isolith maps of shingles within various allomembers in the Upper Cretaceous Dunvegan Formation (Alberta). Based on data presented by Bhattacharya and Walker (1991).

Despite the artificial setting of the Mississippi birdfoot delta, there do appear to be some Paleozoic analogs (Fig. 11; Busch, 1971; Cleaves and Broussard, 1980). Similar analogs have been described from the subsurface of the Texas Gulf Coast (e.g., Fisher *et al.*, 1969), and Ayers (1986) documented elongate and lobate deltas in Cretaceous lacustrine strata in the Western Interior Seaway of North America.

By contrast, river-dominated deltas in shallower water are characterized by a greater degree of lobe and river-mouth switching, which tends to form thinner and more lobate deltas. Most of the other lobes in the Mississippi delta plain were deposited in shallower water than the modern birdfoot delta. They are lobate in shape and the best example is the Lafourche delta lobe (Fig. 3).

There are many well-documented examples of ancient river-dominated deltas of this type (e.g., Elliott, 1975; Bhattacharya and Walker, 1991; Bhattacharya, 1991; Miall, 1976; Horne *et al.*, 1978; Pulham, 1989). Cretaceous and Tertiary examples in the Gulf Coast are summarized by Fisher and McGowen (1967) and Galloway (1975).

Lobe abandonment in the Mississippi Delta

As well as the present birdfoot, there are several distinct older lobes (Figs. 12, 13). These have been abandoned due to river avulsions, and regional subsidence is now causing them to sink beneath the waves. In the earliest stages of transgression, sand is winnowed at the lobe margin to form beaches and beach ridges (Fig. 14). During storms, sand is washed over the beach ridges onto the abandoned delta top, and the beach – beach-ridge complex moves landward, keeping pace with the transgressing sea. The preserved deposits of this transgression consist essentially of washovers and beaches, although as older beaches are in turn transgressed, the beach stratification is extensively bioturbated. Thus a transgression of this type might be identified by a thin (tens of centimetres) bioturbated sandstone (with other coarse winnowed fragments, pebbles and shells) resting abruptly on vegetated delta top facies with in situ root traces.

In some of the Mississippi lobes, the rate of subsidence has been so great that the delta top has become submerged as a shallow sea, before the passage of the beach-ridge complex; this has been stranded out to sea as a barrier island. An example is the St. Bernard Lobe (Figs. 12, 14), which is now separated from the Chandeleur Islands (barrier) by Chandeleur Sound. The sound is protected by the barrier from most wave action, and the continuing transgression of the St. Bernard lobe is extremely quiet, with no wave action and no winnowing of the edge of the lobe. It follows that no distinct win-

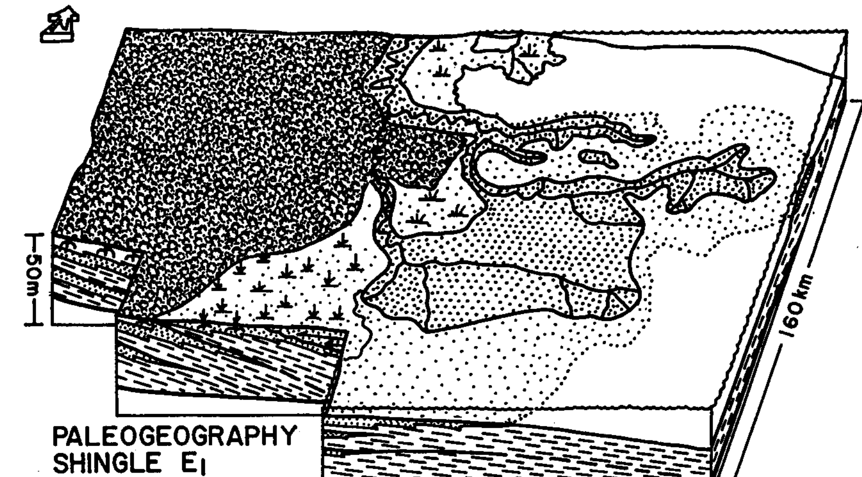

Figure 18 Reconstruction of a river-dominated delta in shingle E1 of the Dunvegan, based on sand isolith maps (Fig. 17) and facies successions in cores (Figs. 8, 9 and 10). Modified after Bhattacharya (in press) and Bhattacharya and Walker (1991).

nowed deposit or transgressive lag will be formed. Instead, brackish-water and marine mudstones will overlie delta top mudstones and siltstones (with in situ root traces) with the most subtle and imperceptible transition (i.e., the transgression of the mainland in Stage 2 of Figure 14). A possible ancient analog for subtle transgression is shown in Figure 15, from the Cretaceous Dunvegan Formation in Alberta. In allostratigraphic terminology, these subtle surfaces are important bounding discontinuities; they could easily be overlooked in the stratigraphic record.

The Dunvegan Delta

The Dunvegan Formation of Alberta represents a heterolithic wedge of mudstones and sandstones, up to 300 m thick, deposited from the actively rising Western Cordillera into the adjacent Cretaceous Interior Seaway. The term "Dunvegan Delta" has been applied to this entire undifferentiated sedimentary package.

In a study area of about 30,000 km^2 in the subsurface of Alberta, Bhattacharya and Walker (1991) recognized seven through-going transgressive surfaces. These were used to subdivide the Dunvegan wedge into seven allomembers (Fig. 16). Each of the allomembers could be further subdivided into several shingled offlapping units separated by less extensive surfaces of transgression and regression. The discontinuity-bounded shingles and allomembers provided the stratigraphic basis for facies mapping and paleogeographic reconstruction.

Sandbody geometries within individual shingles (Fig. 17) revealed a wide range of deltaic to shoreline related depositional systems, including some superb examples of ancient river-dominated deltas (Fig. 18; Bhattacharya, 1991). The abundance of core data allowed reconstruction of the lateral facies relationships both down dip (Fig. 19) and along depositional strike. The cores also facilitated the development of summary vertical facies successions for the various components in the different deltaic systems (Figs. 8, 9, and 10).

Wave-dominated deltas

Well-studied modern wave-dominated deltas include the Rhone (France; Oomkens, 1970), Nile (Egypt; Sestini, 1989), and Tiber (Italy; Bellotti *et al.*, 1989). These deltas are built of broad sandy lobes with an arcuate to cuspate geometry (Figs. 1, 2 and 3). The Rhone (Fig. 3) has at least two major lobes, whereas the Nile (Fig. 1) represents a single broad lobe with two presently active distributaries. These deltas prograde as sand, supplied by one or more distributaries, is reworked along the shoreface by wave-induced currents, and deposited in the shoreface, and in beach and beach-ridge complexes. Beach-ridge complexes can detach from the delta to form spits, cutting off lagoons behind the spits (Fig. 20). Distributary feeder channels make up only a small part of the areal facies distribution. Other associated channelized facies include tidal inlets within the spit and barrier sands.

The Sao Francisco delta of Brazil has long been quoted as the classic example of a wave-dominated delta (Coleman and Wright, 1975). However, recent work by Dominguez *et al.* (1987) has emphasized the importance of sea level fluctuations on delta development, particularly a relative *fall* of about 5 m during the last 5000 years. This fall has made a new source of sand available to the shoreline, namely the inner shelf. These sands are incorporated into the longshore drift, and are deposited at places where the lon shore drift system is interrupted, such as at river mouths. These processes are illustrated in Figure 12 of Chapter 12. Dominguez *et al.* (1987, p. 125) note that "along the Brazilian coast, sediments provided in this way were more important than the fluvial input". Nevertheless, the Sao Francisco can still be regarded as a delta, because it is a "protuberance in the shoreline at a point where a river enters the ocean".

Wave-dominated deltas have been identified in the geological record. One of the best examples occurs in the Upper Cretaceous San Miguel Formation in the subsurface of Texas

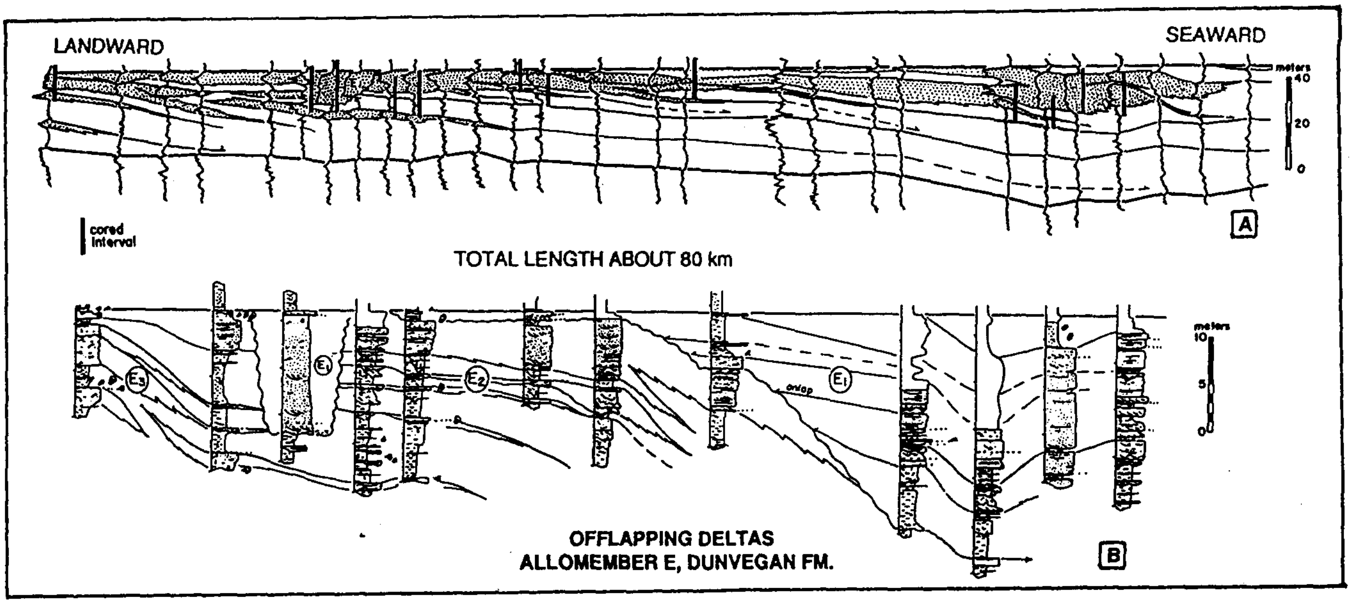

Figure 19 Dip-oriented well log (A) and core (B) cross sections of the Upper Cretaceous Dunvegan Formation, showing offlapping clinoforms.

(Weise, 1980). Isopach maps of ten sandy stacked lobes in the San Miguel showed a wide variety of different sandbody morphologies (Fig. 21), including some text-book examples of wave-dominated cuspate deltas. Weise (1980) related the differences in sandbody geometry to differences in wave and fluvial energy. Limited core information suggested that many of the sandbodies were extensively reworked, giving the facies the signature of storm- and wave-dominated shelf sandbodies (Chapter 12). The sandbody geometries, however, are more suggestive of a deltaic origin.

Wave-influenced deltas

Wave-*influenced* deltaic systems show facies successions that are intermediate between the river- and wave-dominated end members. Examples from the Upper Cretaceous Dunvegan Formation in Alberta (Fig. 8, middle column; Bhattacharya and Walker, 1991) and from the Carboniferous (Namurian) of Western Ireland (Pulham, 1989) show well-developed coarsening-upward facies successions. In the Dunvegan, plan view geometries shown in isopach maps (Fig. 17) clearly establish the deltaic origin. Soft sediment deformation features, relatively little burrowing, and abundant graded bedding are common in the prodelta mudstones (as in the prodelta mudstones in many river-dominated deltas), and indicate relatively high sedimentation rates (Fig. 8, middle column). The delta front sandstones, however, are wave rippled to hummocky cross stratified, suggesting that storm and wave processes were significant.

Figure 20 Gascoyne River delta, Western Australia. R = river flow; A = alongshore drift; W = wave reworking of deltaic sediments onshore; L = lagoon cut off by alongshore drift of sand. Photo courtesy of Dave Feary.

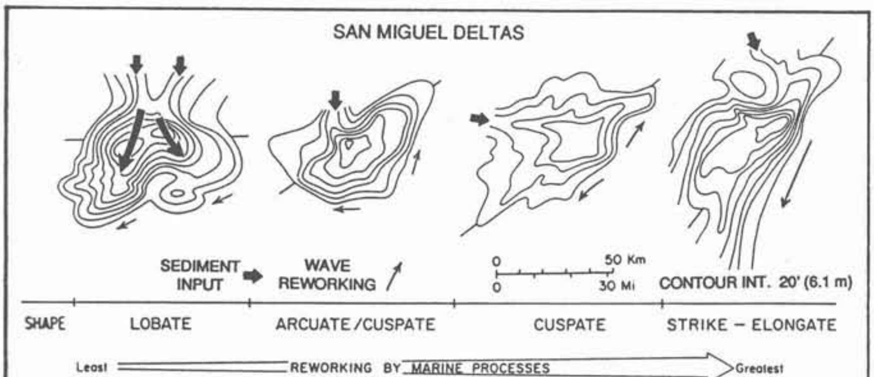

Figure 21 Spectrum of river-dominated (left) to wave-dominated (right) deltas in the Upper Cretaceous San Miguel Formation (Texas) after Weise (1980). The isopach maps are contoured in 20 foot (6.1 m) intervals, with maximum thicknesses of about 120-140 feet (36-43 m).

Tide-influenced deltas

Mixed-influence deltas show a combination of the effects of river, wave, and tidal processes. The Niger (Africa; Fig. 22) and Mahakam (Indonesia; Fig. 3) are classic examples (Allen, 1965; 1970; Allen *et al.*, 1979). The Niger (Fig. 22) comprises a well-developed, sandy wave-dominated beach ridge system cut by numerous tidal channels, with an extensive tidally influenced delta plain behind. Sandy distributary mouth bars are also present.

Tides also affect sediment transport patterns in the Niger. During flood tides, sediment is trapped on the delta plain but is flushed seaward during ebb tides, in similar manner to that described by Smith *et al.* (1990). Prodelta sediments in the Niger comprise heterolithic mudstones, silts and sandstones.

Tidal ranges in the Mahakam delta area are in the 2-4 m (mesotidal) range (Allen *et al.*, 1979), although wave energy is far less than in the Niger. Sand is relatively minor in the system and is largely confined to the distributaries and tidally modified mouth bars (Fig. 3). Interdistributary tidal channels may actually incise deeper than the distributary channels, but are usually mud filled. Beach ridges are developed, but are composed of retransported lignite rather than quartz sand. Mapping on the basis of sandbody geometry indicates a dendritic, shoestring pattern, similar to those shown in Fig. 11; in the absence of core information, the tidal influence might easily be overlooked.

Ancient tide-influenced deltas have been described from the subsurface underneath the modern Mahakham (Verdier *et al.*, 1981), from the Precambrian in South Africa (Eriksson, 1979), and the Eocene of Oregon (Kreisa *et al.*, 1989; Leithold *et al.*, 1989).

Shelf edge deltas

Shelf edge deltas (Fig. 6) are better known from Quaternary and older units beneath the Rhone shelf (France, Tesson *et al.*, 1990) and the Gulf Coast (Suter and Berryhill, 1985; and Edwards, 1981). The modern Mississippi is probably the closest modern analogy. In many shallow shelf settings and shallow epeiric seaways, where fault-induced subsidence is not a significant control, sand thickness and facies maps are good indicators of delta type (e.g., Horne *et al.*, 1978;

Cleaves and Broussard, 1980; Weise, 1980; Bhattacharya and Walker, 1991). In shelf margin deltas, percentage sand maps, rather than sand thickness, may show geometries more comparable with those of Coleman and Wright (1975). Thus they may give a better indication of the degree of wave versus fluvial influence (Fig. 23; Winker and Edwards, 1983; Duncan, 1983).

In outcrop, shelf edge deltas may show spectacular soft sedimentary deformation features (Fig. 24) related to growth faults and shelf/slope instability, analogous to those seen on seismic sections (Coleman *et al.*, 1983).

STRATIGRAPHIC ARCHITECTURE AND LATERAL FACIES VARIABILITY

Deltaic deposits are characterized by a prograding clinoform geometry (Fig. 19, 25, 26; Berg, 1982), as was first recognized by Barrell (1912) and Scruton (1960). This geometry can be seen in downdip seismic profiles of modern and ancient deltas, and can be reconstructed in core and well-log cross sections (Fig. 19; Bhattacharya, 1991). It can also be seen in rare outcrops (Fig. 26), where there is enough lateral continuity of exposure to show the facies relationships and facies geometry. Berg (1982) discussed typical seismic facies in deltaic depositional systems and suggested that sandy wave-dominated systems tend to be characterized by a more shingled pattern. The muddier river-dominated delta types tend to show more of an oblique-sigmoidal pattern (Fig. 25A). The steeply dipping, sigmoid-shaped portions are probably characteristic of the mud-dominated prodelta facies whereas the more flat-lying upper reflectors represent the sandier delta front and delta plain facies (Fig. 25A). Frazier (1974) showed a similar geometry based on geological studies of the Mississippi delta plain (Fig. 25B). Offlapping clinoformal geometries have also been recognized in the Late Quaternary wave-dominated sediments of the Rhone shelf (Tesson *et al.*, 1990) and in many other studies (Suter and Berryhill, 1985; Brown and Fisher, 1977; see Figure 26).

Depositional clinoform gradients have a wide range of values in different settings. Clinoform gradients of shelf edge deltas in the Gulf of Mexico average between 4 and 8 degrees

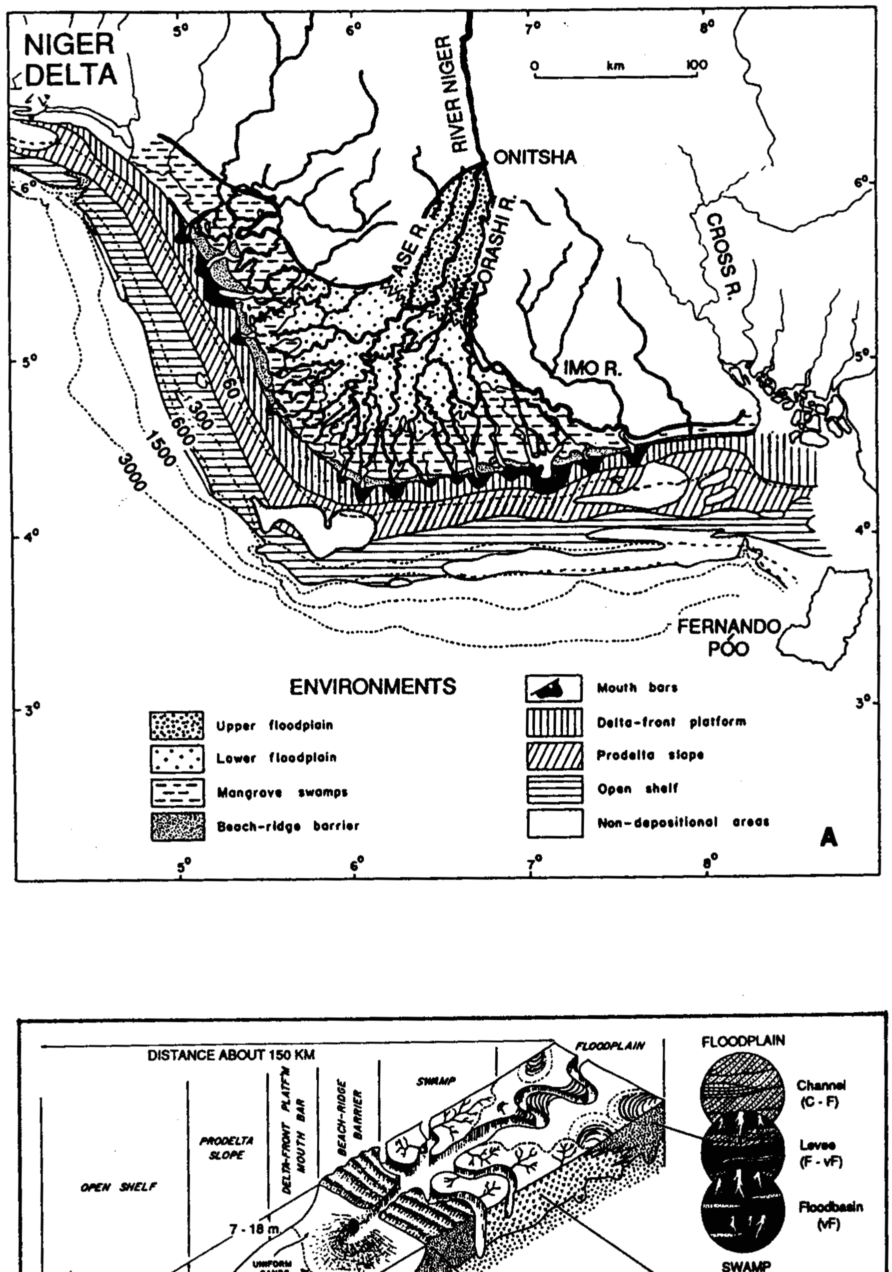

Figure 22 Environments and facies in the modern Niger delta, a mixed wave- and tide-influenced delta. A) Plan view, showing overall cuspate shape (wave influence) and meandering channels within mangrove swamps (tide influence). B) Schematic facies distribution from landward to seaward. Modified after Allen (1970).

the same !
in Priobskoe !

(Suter and Berryhill, 1985). Gradients of the Rhone shelf edge deltas average about 1 degree, whereas gradients in late Cretaceous deltas in the Alberta basin average 0.1 degrees. The much higher slopes in the Gulf Coast and Rhone shelves result in greater instability of the shelf edge sediments where large-scale synsedimentary deformation features are common. Soft-sediment deformation features in the Alberta examples are apparently limited to loading rather than large-scale slumps, slides, or growth faults.

The clinoform model provides a norm that predicts that surfaces should dip seaward as facies become finer-grained. Along strike, facies relationships may be less predictable and depositional surfaces may dip in different directions. This is particularly so in more river-dominated deltas where along-strike reworking is not significant and abrupt facies transitions may occur between distributaries and interdistributary areas (Bhattacharya, 1991). Overlapping delta lobes result in lens-shaped stratigraphic units that exhibit a mounded appearance on seismic lines (Fig. 25A).

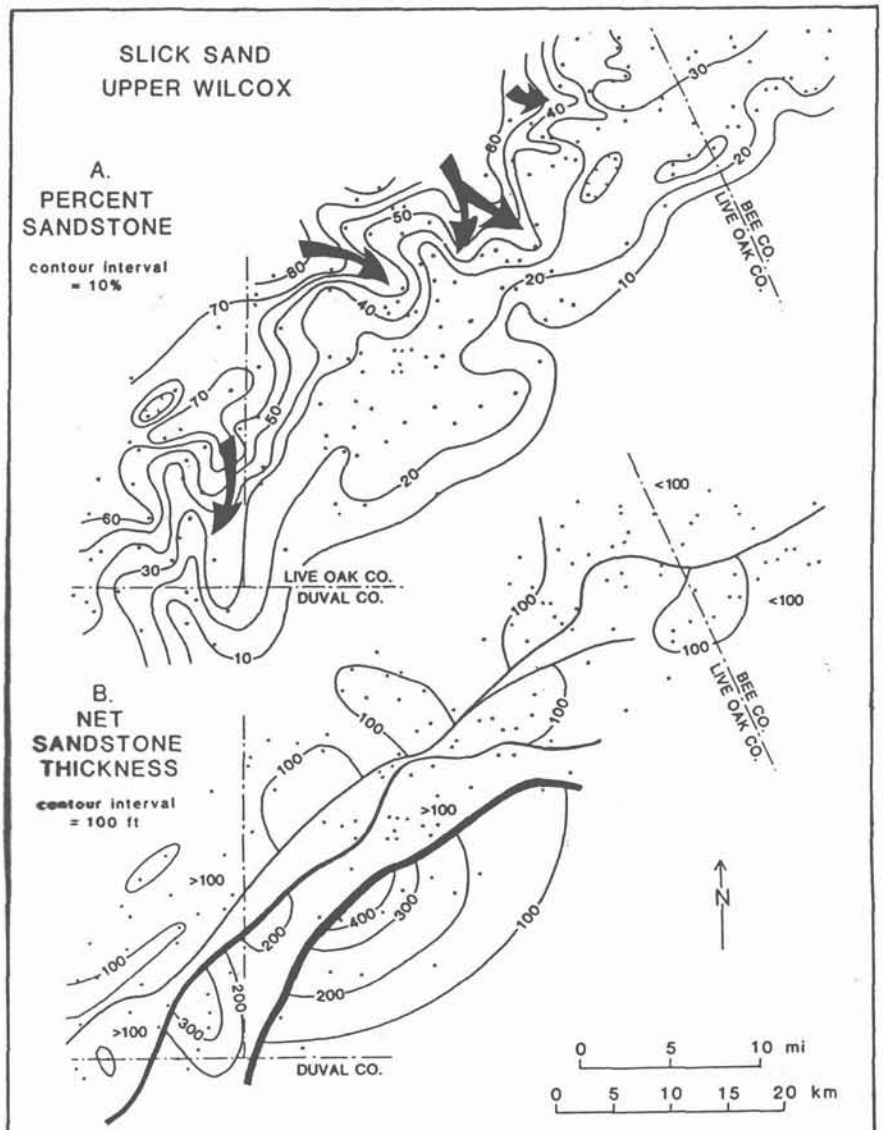

Figure 23 Per cent sandstone, and net sandstone thickness maps of the Eocene Slick Sand (interpreted as a shelf edge delta), Texas Gulf Coast. Per cent sandstone map gives best indication of lobate nature. Growth faults (heavy lines on net sandstone thickness map) have a fundamental control of facies distribution, with thickening on the downdip (southeastern) side. After Winker and Edwards (1983).

DELTAIC SYSTEMS TRACTS

Systems tracts (linkages of related contemporaneous depositional systems) form an important conceptual framework for understanding the larger scale relationships between depositional systems. They also help in the interpretation of relative sea level changes and allow sedimentary rocks to be studied in the context of sequence stratigraphy (Brown and Fisher, 1977; Van Wagoner *et al.*, 1990). Deltas deposited during times of relatively high sea level (highstand systems tracts) are usually confined to the shelf and deposited in shallow water. These shallow water deltas are characterized by rapid lobe switching. In fluvially dominated systems, Lafourche-type shoal-water lobate deltas are formed (Figs. 3, 6). During times of sea level fall, elongate deltas may result from progradation into deeper water on the mid to lower shelf, especially when sediments are relatively fine grained. If sedimentation rate just keeps up with relative sea level fall, lobe and channel switching will be suppressed, enhancing the elongate geometry. These types of elongate deltas have been discussed by Suter and Berryhill (1985) and Galloway (1975).

Deltas deposited after a relative fall of sea level (lowstand or shelf margin systems tracts) commonly overlie an

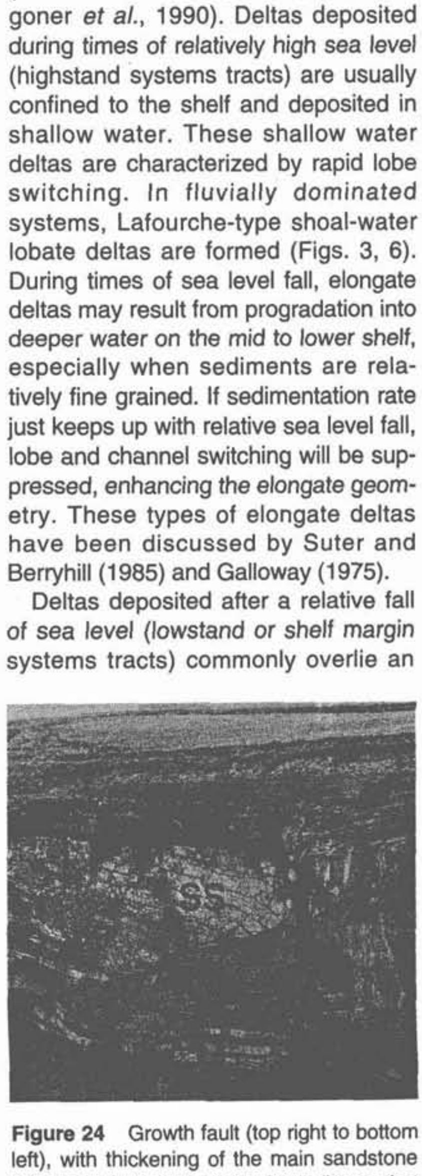

Figure 24 Growth fault (top right to bottom left), with thickening of the main sandstone (SS) beds toward the fault; this indicates that the fault was active during sand deposition. Fault activity is also indicated by the curvature (rolling over) of the sandstones toward the fault. The fault stopped mobing after deposotion of these sandstones, and a triangular (T) wedge of sediment was deposited before the uppermost layers were deposited flat across the area. Foohagh Point, County Clare, western Ireland; Pennsylvanian Central Clare Group.

incised topographic surface caused by the preceding fall. Lowstand deltas commonly prograde into deeper water than deltas confined farther landward on the shelf and their morphology may be partly controlled by the underlying topography. This topography may also be controlled by seaward-directed growth faults, especially in passive margin settings, resulting in sandbodies oriented parallel to depositional strike (Fig. 6). Wave power is commonly more concentrated at the shelf edge resulting in wave- and storm-influenced deltas. Examples include the Quaternary lowstand deltas on the Northwest Gulf Coast (Suter and Berryhill, 1985), and interpreted wave-dominated shelf edge deltas associated with the Rhone (Tesson *et al.*, 1990).

During times of active sea level rise, (transgressive systems tracts) deltaic deposition will commonly be suppressed because river-borne sediment accumulates on the aggrading floodplain. Where active deltaic deposition does occur, the fluvial influence is minimal and tide- and wave-dominated deltas will tend to dominate. Perhaps more importantly, flooding of river valleys during transgression forms estuaries. In many estuaries, the constriction amplifies the tidal range, forming a series of tidally influenced sandbodies parallel to the trend of the estuary. Some of these sandbodies have been termed "tide-dominated deltas" (e.g., the Ord in Australia, Coleman and Wright, 1975). Similarly, continued transgression may result in a series of tidally influenced sandbodies on the shelf. Some of these have also been termed deltas (e.g., the Klang-Langat in Malaysia, Coleman and Wright, 1975). In this edition of *Facies Models*, these so-called "tidal deltas" are discussed along with other tidally influenced sandbodies in Chapter 11. The transgressive to relatively highstand position of sea level today may result in the present preponderance of estuarine shorelines and tidally dominated shelf sandbodies. In the past, during times when sea level was

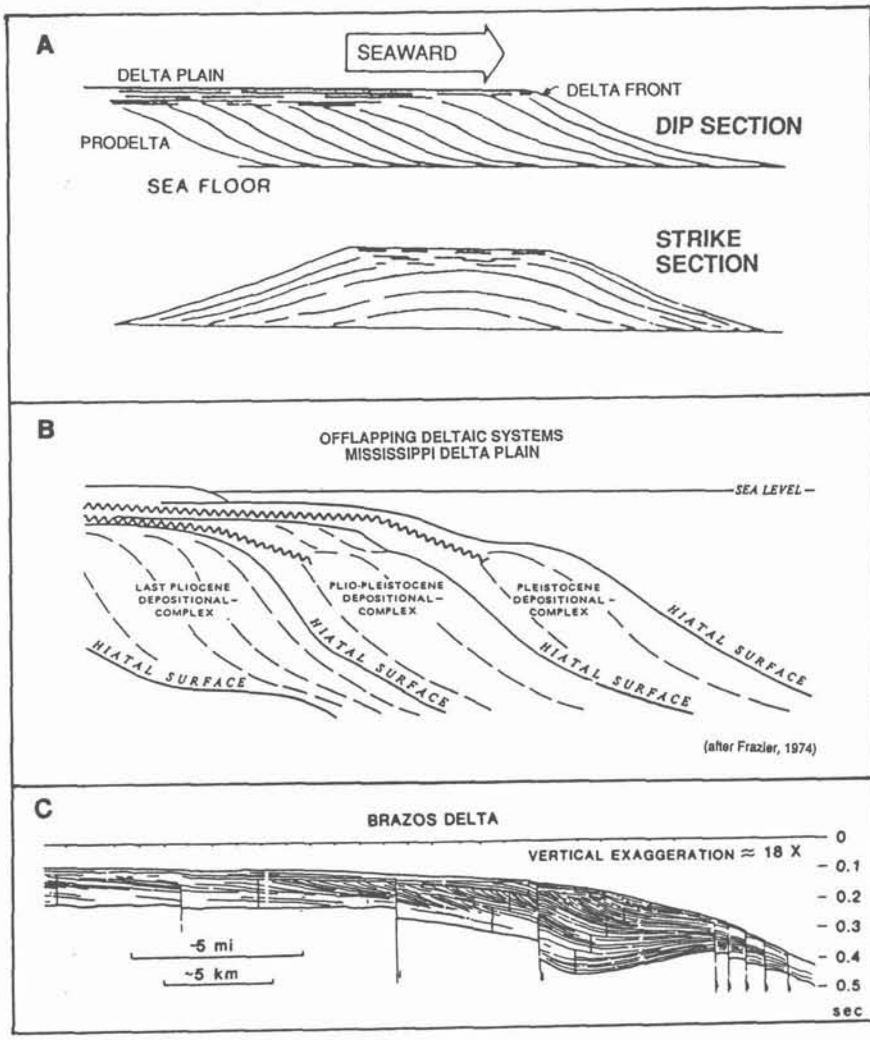

Figure 25 Typical stratigraphic geometries of deltaic depositional systems showing offlapping clinoforms. A) schematic from Berg (1982). B) offlapping clinoforms in the Mississippi delta plain (after Frazier, 1974). C) Seismic (sparker) profile through the modern Brazos delta showing offlapping clinoforms, and thickening of section across growth faults. A similar thickening is seen in sediments of the modern Mississippi Delta lobe (Fig. 12). Compare with Fig. 19.

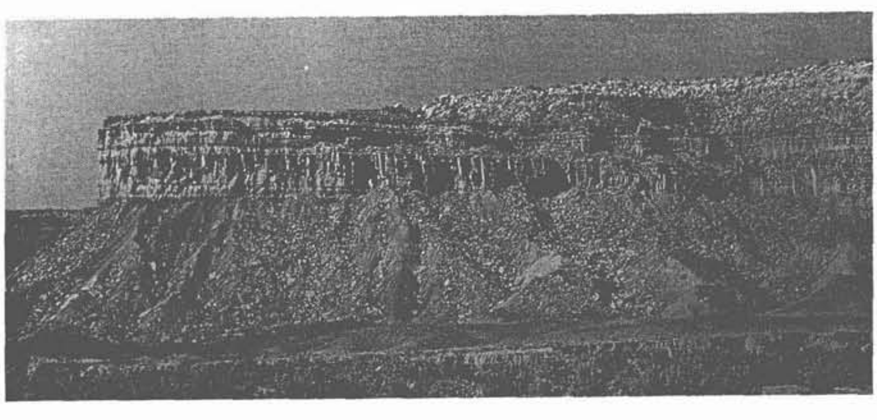

Figure 26 Seaward-dipping clinoform beds in river-dominated delta front sandstones of the Upper Cretaceous Ferron Member of the Mancos Shale, Utah. Photo has been reversed so that beds are shown dipping to the right (compare with Figure 25). Deltaic beds pass laterally into prodelta shales of the underlying Tununk Member. Width of outcrop about 340 m.

either stable or falling, there may have been fewer tidally dominated sandbodies.

The concept of systems tracts also provides a way of linking the different types of depositional systems reviewed in this book. Active development of deep water submarine fans is commonly related to the development of shelf edge deltas in lowstand systems tracts. Development of fans may also correlate with the incision of alluvial systems in a landward direction. Active submarine fan development commonly ends with a rise of relative sea level, and may coincide with development of shoal water deltas in a transgressive or highstand systems tract. Thus the generalizations embodied in the definitions of systems tracts allow the tracts to be used predictively in the sense of large-scale facies models. Thus one part of a given systems tract may be important in predicting the appearance and nature of a related part.

AUTOCYCLIC AND ALLOCYCLIC CONTROLS OF DELTA DEVELOPMENT

The paralic setting of deltaic depositional systems means that they tend to be very sensitive indicators of relative sea level change. The repeated development of similar facies successions ("cyclicity") due to switching delta lobes is a very common feature in many deltaic depositional settings, such as coal-bearing successions in the Pennsylvanian of the U.S. (Horne *et al.*, 1978), the Carboniferous cyclothems of the U.K. (Elliott, 1975; Pulham, 1989), and the Devonian Catskill deltaic wedge of the Appalachians (Woodrow and Sevon, 1985). The cause of this cyclicity has long been a matter of debate, comparing and contrasting autocyclic and allocyclic processes. Autocyclic processes are intrabasinal in origin, and are related to the sedimentological behaviour of the depositional system. In deltaic systems they include lobe switching and river avulsion. Allocyclic processes are extrabasinal in origin and can include eustasy, tectonics in the source area and receiving basin, climate and other factors. Allocyclic processes tend to produce more widespread effects.

In many deltas, the switch from one lobe to another is due to river avulsion (an autocyclic change). As the older lobe subsides, its coarsening-upward facies succession is capped by a bounding discontinuity or marine flooding surface (Chapter 1) due to local transgression. A group of delta lobes, represented by a group of shingled and/or stacked coarsening-upward facies successions (perhaps formed in a highstand systems tract), might be separated from another group of lobes by a more extensive bounding discontinuity (formed during a eustatic rise of sea level (an allocyclic change). The regional transgression would lead to the development of a transgressive systems tract, topped in turn by a maximum flooding surface, before re-establishment of the next deltaic system of the highstand systems tract.

AUTOCYCLIC AND ALLOCYCLIC EVOLUTION OF THE MODERN MISSISSIPPI DELTA PLAIN

Until very recently, the seven successively younger overlapping delta lobes that make up the Mississippi delta plain were interpreted to have formed as a result of autocyclic processes, with major river avulsions leading to lobe switching (Scruton, 1960; Kolb and van Lopik, 1966; Frazier, 1967). Shifts in the shoreline position were local, and applied to individual lobes rather than the delta complex as a whole. In this interpretation, the transgressive abandonment facies capping one lobe are time-equivalent to an entire, actively prograding lobe elsewhere.

This model of Mississippi delta development has recently been modified due to the discovery of a eustatically enhanced transgressive surface of erosion (Boyd *et al.*, 1989). The surface is dated about 3340 years ago, and separates the older Maringouin–Teche delta complex from the younger Lafourche–St. Bernard–Modern complexes (Fig. 13), strongly suggesting an allocyclic control. The older Maringouin–Teche system is interpreted to represent deposition of progressively backstepping lobes, formed during an overall transgression, which culminated in the laterally extensive Teche shoreline. The younger lobes prograded during the ensuing highstand, to form a highstand systems tract. All lobes except the modern birdfoot are presently being transgressed as the delta complex subsides (due to underlying tectonic control in the Gulf of Mexico).

The less extensive transgressive surfaces (marine flooding surfaces) between successive lobes within the transgressive and highstand systems tracts are interpreted as autocyclic in origin (Fig. 13). They are different from the more extensive eustatically enhanced allocyclic transgressive surface of erosion that separates the two major delta systems. As discussed earlier, the expression of some of the marine flooding surfaces may be extremely subtle.

The youngest (Balize) Mississippi delta lobe shows some similarities to the Quaternary lowstand shelf edge deltas described by Suter and Berryhill (1985), deposited during the late Wisconsinian drop of sea level. This is clearly the result of an artificially controlled increase in sedimentation rate resulting from the efforts of the U.S. Army Corps of Engineers to keep the existing distributaries open. Human interference is clearly at odds with the autocyclic tendencies of the Mississippi River, which is presently attempting to switch into the course of the Atchafalaya River and flow into Atchafalaya Bay.

OTHER EXAMPLES OF ALLOCYCLIC CONTROL IN DELTA DEVELOPMENT

In many delta studies, it is difficult to separate autocyclic and allocyclic controls, although as a rule, bounding discontinuities developed during autocyclic changes tend to be more widespread. The problem may be compounded if other factors (e.g., sedimentation rates) are important. For example, Winker (1982) has shown that progradation of pre-Pleistocene shelf margin deltas was not synchronous across the Gulf Coast and therefore argues against a purely eustatic control. Rather he invokes an allocyclic control caused by increases in sedimentation rates induced by periods of tectonically induced uplift in the associated Cordilleran drainage basins. This resulted in localized deposition of shelf margin systems tracts. Human interference can also be regarded as extrabasinal (allocyclic), and has affected other rivers than the Mississippi. In Italy, the progradation of the Po delta (Nelson, 1970) has largely been caused by man-made efforts to maintain the course of the Po River, resulting in an increase in long-term sedimentation rate. In contrast, the Nile delta (Sestini, 1989) is currently undergoing an overall transgression as a result of decreasing sedimentation rates caused by construction of the Aswan Dam farther upstream.

Allocyclic processes (such as a lowering of relative sea level) may result in valley incision and juxtaposition of unlike facies. In the Upper Cretaceous Horseshoe Canyon Formation in Alberta, estuarine valley fills are incised into the older deposits of wave-dominated prograding shorefaces and deltas (Rahmani, 1989). These deltas had been previously interpreted as tide dominated. However, it is now realized that the tidally dominated estuarine valley fills are not genetically related to the older prograding shorefaces characterized by hummocky and swaly cross stratification, and interpreted as wave- and storm-dominated. As has been shown above (Fig. 14), during transgression, a deltaic depositional system may evolve into an estuary or barrier island system, thereby losing its deltaic character. The transgressive deposits are commonly underlain by a transgressive surface of erosion, resulting in facies that are genetically unrelated to the underlying progradational deltaic phase (Fig. 8).

In the Dunvegan example discussed above (Fig. 16), the basin-wide allomember-bounding transgressive surfaces were interpreted as allocyclic in origin, resulting from times of tectonically induced increases in subsidence. In contrast, most of the less extensive shingle boundaries were interpreted as autocyclic (Bhattacharya, 1988). Progradation of the Dunvegan wedge as a whole has been inferred to be partly forced by a eustatic drop of sea level (Bhattacharya, 1988).

CONCLUSIONS

This chapter has attempted to look at the traditional river-, wave- and tide-dominated deltaic facies models, incorporating the latest ideas of fluctuations of relative sea level. Deltas are complex three-dimensional progradational depositional systems. However, in response to changes in controlling parameters, the deltas may be transformed into other depositional systems and vice-versa. An increase in sedimentation rate, or a channel avulsion, could transform a prograding strandplain into a delta. Alternatively, given a steady rise of relative sea level, a river channel or distributary might widen into an estuary with tidally influenced sand bars (i.e., a tidal "delta" such as the Ord River in Australia). The estuary might in turn be drowned, and the system would evolve into a series of shallow-marine, tidal sand ridges (Yang and Sun, 1988).

In other settings, waves are important in modifying deltaic sediments during transgressions. Around the margins of the Mississippi delta, such modification has produced winnowed sandbodies that began as beach ridge complexes, were detached as barriers, and have now been drowned as shoals (e.g., Ship Shoal in Fig. 13; Penland *et al.*, 1987). Depending on the larger stratigraphic context, these may be regarded as components of deltaic systems or as distinct depositional systems.

The definition and understanding of a depositional system depend partly upon the scale of observation and objectives of the study. The distribution of sand at the surface in many modern deltas may not characterize the sandbody geometry in the immediately underlying deposits. In many so-called tide-dominated deltas, transgressive reworking of the uppermost veneer of sediments (i.e., destructional phase) may not reflect the sedimentary processes in the major proportion of the underlying regressive deltaic package (i.e., constructional phase). The same may be true for modern wave-dominated deltas such as the Nile. This delta is currently being transgressed, but it contained better developed lobes in the past and may have been more river dominated (Sestini, 1989). Nevertheless, the important point is the understanding of how environments change as the controlling parameters (particularly relative sea level) change, rather than assigning names to depositional systems. These changes are now becoming fairly well understood in many deltaic settings, and deltaic systems are therefore ideal for testing other stratigraphic concepts, and for making predictions about other parts of a basin. This perhaps explains the present emphasis on deltas and shorelines in sequence stratigraphic models (Van Wagoner *et al.*, 1990; Boyd *et al.*, 1989; Bhattacharya and Walker, 1991).

ACKNOWLEDGMENTS

Most of this chapter was written by Bhattacharya during his tenure of a Postdoctoral Fellowship from the Natural Sciences and Engineering Research Council of Canada. The Alberta Geological Survey is thanked for technical support. Ideas have been sharpened by conversations with many friends, particularly R.W. Dalrymple, R.D. Kreisa, T. Elliott, B. Zaitlin, and W.E. Galloway. The authors, however, shoulder all responsibility for any shortfalls in the synthesis presented herein.

REFERENCES

Basic sources of information

Berg, O.R., 1982, Seismic detection and evaluation of delta and turbidite sequences: their application to exploration for the subtle trap: American Association of Petroleum Geologists, Bulletin, v. 66, p. 1271-1288.
General models for the seismic expression of deltaic depositional systems emphasizing the clinoform geometry and their relationship to associated deep water turbidite systems.

Broussard, M.L., ed., 1975, Deltas, Models for Exploration: Houston, Houston Geological Society, 555 p.
A compendium of important papers, including classic reviews of the state-of-the-art in the mid seventies by Galloway, and Coleman and Wright (see other references).

Colella, A. and Prior, D.B., 1990, Coarse-grained deltas: International Association of Sedimentologists, Special Publication 10, 357 p.
Compendium of 19 papers on fan deltas, alluvial deltas, and other coarse-grained delta systems including summary papers by Nemec and by Postma on classification and general models.

Coleman, J.M., 1981, Deltas: processes of deposition and models for exploration. Minneapolis, Burgess Publishing Co., 2nd. Ed., 124 p.
Summary of results of worldwide research by Coastal Studies Institute with an emphasis on modern deltas.

Coleman, J.M. and Prior, D.B., 1982, Deltaic environments, *in* Scholle, P.A. and Spearing, D.R., eds., Sandstone Depositional Environments: American Association of Petroleum Geologists, Memoir 31, p. 139-178.
Well-illustrated review of deltaic environments with lots of colour photographs, including cores through the Mississippi.

Elliott, T., 1986, Deltas, in Reading, H.G., ed., Sedimentary environments and facies: Oxford, Blackwell Scientific Publications, p. 113-154.
The most comprehensive and up-to-date summary of deltaic facies models.

Elliott, T., 1989, Deltaic systems and their contribution to an understanding of basin-fill successions, *in* Whateley, M.K.G. and Pickering, K.T., eds., Deltas: sites and traps for fossil fuels: Oxford, Blackwell Scientific Publications, Geological Society, Special Publication 41, p. 3-10.
State of the art discussion of most of the major problems and future directions of deltaic research, including the integration of deltaic studies in basin analysis.

Fisher, W.L., Brown, L.F., Scott, A.J. and McGowen, J.H., 1969, Delta systems in the exploration for oil and gas, a research colloquium, Austin, TX, Texas Bureau of Economic Geology, 204 p.
Thorough presentation of modern and ancient examples emphasizing the depositional systems approach, with an emphasis on the Gulf Coast. Old, but still very useful.

LeBlanc, R.J., 1976a, Modern deltas: American Association of Petroleum Geologists, Reprint Series 18, 205 p.

LeBlanc, R.J., 1976b, Ancient deltas: American Association of Petroleum Geologists, Reprint Series 19, 226 p.
Two collections of important papers, mostly from the AAPG Bulletin.

Morgan, J.P., ed., 1970, Deltaic sedimentation, modern and ancient: Society of Economic Paleontologists and Mineralogists, Special Publication 15, 312 p.
Compendium of papers including important reviews of the Niger (Allen) and Rhone (Oomkens) deltas.

Whateley, M.K.G. and Pickering, K.T., eds., 1989, Deltas: sites and traps for fossil fuels: Oxford, Blackwell Scientific Publications, Geological Society, Special Publication 41, 360 p.
Many useful and up to date papers, with both modern and ancient examples, including general summaries by Elliott and Alexander.

Wright, L.D., 1977, Sediment transport and deposition at river mouths: a synthesis: Geological Society of America, Bulletin, v. 88, p. 857-868.
Important paper that integrates processes of deposition and morphology of resulting deposit. Effects of tides and waves are also discussed but no ancient examples.

Other references

Alexander, J., 1989, Deltas or coastal plain? With an example of the controversy from the Middle Jurassic of Yorkshire, *in* Whateley, M.K.G. and Pickering, K.T., eds., Deltas: sites and traps for fossil fuels: Oxford, Blackwell Scientific Publications, Geological Society, Special Publication 41, p.11-19.

Allen, G.P., Laurier, D. and Thouvenenin, J., 1979, Etude sedimentologique du delta de la Mahakam: Paris, TOTAL, Compagnie Francaise des Petroles, Notes et Memoires 15, 156 p.
Thorough study of a tide-influenced delta incorporating core, surface samples, hydrodynamic, and geomorphic data. Includes a ten page English summary.

Allen, J.R.L., 1965, Late Quaternary Niger Delta, and adjacent areas: sedimentary environments and lithofacies: American Association of Petroleum Geologists, Bulletin, v. 49, p. 547-600.

Allen, J.R.L., 1970, Sediments of the modern Niger delta, a summary and review, *in* Morgan, J.P., ed., Deltaic sedimentation modern and ancient: Society of Economic Paleontologists and Mineralogists, Special Publication 15, p. 138-151.

Ayers, W.B., Jr., 1986, Lacustrine and fluvial-deltaic depositional systems, Fort Union Formation (Paleocene), Powder River Basin, Wyoming and Montana: American Association of Petroleum Geologists, Bulletin, v. 70, p. 1651-1673.

Barrell, J., 1912, Criteria for the recognition of ancient delta deposits: Geological Society of America, Bulletin, v. 23, p. 377-446.

Bates, C.D., 1953, Rational theory of delta formation: American Association of Petroleum Geologists, Bulletin, v. 37, p. 2119-2162.

Bellotti, P., Tortora, P. and Valeri, P., 1989, Sedimentological and morphological features of the Tiber delta: Sedimentology, v. 36 (supplementary chart).
Well-illustrated chart integrating core, seismic, and geomorphologic studies of a wave-dominated delta.

Bhattacharya, J., 1988, Autocyclic and allocyclic sequences in river- and wave-dominated deltaic sediments of the Upper Cretaceous Dunvegan Formation, Alberta: core examples, *in* James, D.P. and Leckie, D.A., eds., Sequences, stratigraphy, sedimentology; surface and subsurface: Canadian Society of Petroleum Geologists, Memoir 15, p. 25-32.

Bhattacharya, J., 1991, Regional to sub-regional facies architecture of river-dominated deltas, Upper Cretaceous Dunvegan Formation, Alberta sub-surface, *in* Miall, A.D. and Tyler, N., eds., The three-dimensional facies architecture of terrigenous clastic sediments, and its implications for hydrocarbon discovery and recovery: Society of Economic Paleontologists and Mineralogists, Concepts in Sedimentology and Paleontology, v. 3, p. 189-206.

Bhattacharya, J. and Walker, R.G., 1991, River- and wave-dominated depositional systems of the Upper Cretaceous Dunvegan Formation, northwestern Alberta: Bulletin of Canadian Petroleum Geology, v. 39, p. 165-191.
The two Bhattacharya papers summarize a regional subsurface study of shallow water deltas in a foreland basin setting combining well logs, cores and allostratigraphy.

Boyd, R. and Penland. S., 1988, A geomorphic model for Mississippi delta evolution: Gulf Coast Association of Geological Societies, Transactions, v. 38, p. 443-452.

Boyd, R., Suter, J. and Penland, S., 1989, Sequence stratigraphy of the Mississippi delta: Gulf Coast Association of Geological Societies, Transactions, v. 39, p. 331-340.
Important paper reinterpreting formation of successive Mississippi lobe complexes by allocyclic processes (eustasy).

Brown, L.F. and Fisher, W.L., 1977, Seismic-stratigraphic interpretation of depositional systems: examples from Brazilian rift and pull-apart basins, *in* Payton, C.E., ed., Seismic stratigraphy – applications to hydrocarbon exploration: American Association of Petroleum Geologists, Memoir 26, p. 213-248.
First paper to tie seismic stratigraphy and systems tracts together.

Busch, D.A., 1971, Genetic units in delta prospecting: American Association of Petroleum Geologists, Bulletin, v. 55, p. 1137-1154.

Carbonel, P. and Moyes, J., 1987, Late Quaternary paleoenvironments of the Mahakham delta (Kalimantan, Indonesia): Palaeogeography, Palaeoclimatology, Palaeoecology, v. 61, p. 265-284.

Cleaves, A.W. and Broussard, M.C., 1980, Chester and Pottsville depositional systems, outcrop and subsurface, in the Black Warrior Basin of Mississippi and Alabama: Gulf Coast Association of Geological Societies, Transactions, v. 30, p. 49-60.

Coleman, J.M. and Gagliano, S.W., 1964, Cyclic sedimentation in the Mississippi River deltaic plain: Transactions of the Gulf Coast Association of Geological Societies, v. 14, p. 67-80.

Coleman, J.M., Prior, D.B. and Lindsay, J.F., 1983, Deltaic influences on shelf edge instability processes, *in* Stanley, D.J. and Moore, G.T., eds., The shelfbreak: critical interface on continental margins: Society of Economic Paleontologists and Mineralogists, Special Publication 33, p. 121-137.
An important paper on sediment instability in the modern Mississippi shelf, slope, and canyon.

Coleman, J.M. and Wright, L.D., 1975, Modern river deltas: variability of processes and sand bodies, *in* Broussard, M.L., ed., Deltas, models for exploration: Houston, TX, Houston Geological Society, p. 99-149.
Comprehensive study of a large number of modern deltas, presented as a review of general principles followed by development of six delta types.

Dominguez, J.M.L., Martin, L. and Bittencourt, A.C.S.P., 1987, Sea-level history and Quaternary evolution of river mouth-associated beach-ridge plains along the east-southeast Brazilian Coast: a summary, *in* Nummedal, D., Pilkey, O.H. and Howard, J.D., eds., Sea-level fluctuations and coastal evolution: Society of Economic Paleontologists and Mineralogists, Special Publication 41, p. 115-127.
Important re-interpretation of the development of the Sao Francisco and other Brazilian wave-dominated "deltas" as nondeltaic strandplains.

Duncan, E.A., 1983, Delineation of delta types: Norias delta system, Frio Formation, South Texas: Gulf Coast Association of Geological Societies, Transactions, v. 33, p. 269-273.

Edwards, M.B., 1981, Upper Wilcox Rosita delta system of South Texas: growth-faulted shelf-edge deltas: American Association of Petroleum Geologists, Bulletin, v. 65, p. 54-73.

Elliott, T., 1974, Interdistributary bay sequences and their genesis: Sedimentology, v. 21, p. 611-622.

Elliott, T., 1975, The sedimentary history of a delta lobe from a Yoredale (Carboniferous) cyclothem: Yorkshire Geological Society, Proceedings, v. 40, p. 505-536.

Eriksson, K.A., 1979, Marginal marine processes from the Archaen Moodies Group, Barberton Mountain Land, South Africa: evidence and significance: Precambrian Research, v. 8, p. 153-182.

Fisher, W.L. and McGowen, J.H., 1967, Depositional systems in the Wilcox Group of Texas and their relationship to the occurrence of oil and gas: Gulf Coast Association of Geological Societies, Transactions, v. 17, p. 105-125.
First major paper to introduce the idea of depositional systems. Reprinted in the American Association of Petroleum Geologists, Bulletin, 1969, v. 53, p. 30-54, as well as in the volume edited by LeBlanc (1976b).

Fisk, H.N., 1961, Bar finger sands of the Mississippi delta, *in* Peterson, J.A. and Osmond, J.C., eds., Geometry of sandstone bodies – a symposium: Tulsa, American Association of Petroleum Geologists, p. 29-52.
One of the best known of Fisk's many papers on the Mississippi. It presents the model for bar finger sands.

Frazier, D.E., 1967, Recent deltaic deposits of the Mississippi delta: their development and chronology: Gulf Coast Associations of Geological Societies, Transactions, v. 17, p. 287-315.

Frazier, D.E., 1974, Depositional episodes: their relationship to the Quaternary stratigraphic framework in the northwestern portion of the Gulf basin: Austin, TX, Bureau of Economic Geology, Geological Circular 74-1, 28 p.

Galloway, W.E., 1975, Process framework for describing the morphologic and stratigraphic evolution of deltaic depositional systems, *in* Broussard, M.L., ed., Deltas, models for exploration: Houston, TX, Houston Geological Society, p. 87-98.

Galloway, W.E., 1989, Genetic stratigraphic sequences in basin analysis II: application to northwest Gulf of Mexico Cenozoic basin: American Association of Petroleum Geologists, Bulletin, v. 73, p. 143-154.

Gilbert, G.K., 1885, The topographic features of lake shores: United States Geological Survey, Annual Report, 5th (1883 - 1884), p. 69-123.

Harris, J.P., 1989, The sedimentology of a Middle Jurassic lagoonal delta system: Elgol Formation (Great Estuarine Group), N.W. Scotland, *in* Whateley, M.K.G. and Pickering, K.T., eds., Deltas: sites and traps for fossil fuels: Oxford, Blackwell Scientific Publications, Geological Society, Special Publication 41, p.147-165.

Horne J.C., Ferm, J.C., Caruccio, F.T. and Baganz, B.P., 1978, Depositional models in coal exploration and mine planning in Appalachian region: American Association of Petroleum Geologists, Bulletin, v. 62, p. 2379-2411.
Detailed outcrop based study of intracratonic river-dominated deltas ranging from local to subregional scale. Lots of figures showing lateral facies relationships and block diagrams.

Kolb, C.R. and van Lopik, J.R., 1966, Depositional environments of the Mississippi River deltaic plain – southeastern Louisiana, *in* Shirley, M.L. and Ragsdale, J.A., eds., Deltas in their geologic framework: Houston, TX, Houston Geological Society, p. 17-61.

Kreisa, R.D., Leithold, E.L. and Bourgeois, J., 1989, Tidal signature in mixed-energy deltaic facies: Second International Research Symposium on Clastic Tidal Deposits, Calgary, 1989, p. 49 (abs.).

Leithold, E.L, Bourgeois, J. and Kreisa, R.D., 1989, Genesis of tidal rhythmites of an Eocene delta slope, S.W. Oregon, U.S.A.: Second International Research Symposium on Clastic Tidal Deposits, Calgary, 1989, p. 55 (abs.).

Martinsen, O.J., 1989, Styles of soft-sediment deformation on a Namurian (Carboniferous) delta slope, Western Irish Namurian basin, Ireland, *in* Whateley, M.K.G. and Pickering, K.T., eds., Deltas: sites and traps for fossil fuels: Oxford, Blackwell Scientific Publications, Geological Society, Special Publication 41, p.167-177.
Sub-regional outcrop-based study, a possible ancient analogue to delta slopes associated with shelf margin deltas.

Martinsen, O.J., 1990, Fluvial, inertia-dominated deltaic deposition in the Namurian (Carboniferous) of northern England: Sedimentology, v. 37, p. 1099-1113.

Miall, A.D., 1976, Sedimentary structures and paleocurrents in a Tertiary deltaic succession, northern Banks Basin, Arctic Canada: Canadian Journal of Earth Sciences, v. 13, p. 1422-1432.

Miall, A.D., 1984, Deltas, *in* Walker, R.G., ed., Facies Models, 2nd Edition: Geological Association of Canada, Geoscience Canada Reprint Series 1, p. 105-118.

Moslow, T.F. and Pemberton, S.G., 1988, An integrated approach to the sedimentological analysis of some lower Cretaceous shoreface and delta front sandstone sequences, *in* James, D.P. and Leckie, D.A., eds., Sequences, stratigraphy, sedimentology; surface and subsurface: Canadian Society of Petroleum Geologists, Memoir 15, p. 373 - 386.

Nelson, B.W., 1970, Hydrography, sediment dispersal, and recent historical development of the Po River delta, Italy, *in* Morgan, J.P., ed., Deltaic sedimentation modern and ancient: Society of Economic Paleontologists and Mineralogists, Special Publication 15 , p. 152-184.

Nemec, W., Steel, R.J., Gjelberg, J., Collinson, J.D., Prestholm, E. and Oxnevad, I.E., 1988, Anatomy of a collapsed and re-established delta front in Lower Cretaceous of Eastern Spitsbergen: gravitational sliding and sedimentation processes: American Association of Petroleum Geologists, Bulletin, v. 72, p. 454-476.

Oomkens, E., 1970, Depositional sequences and sand distribution in the postglacial Rhone delta complex, *in* Morgan, J.P., ed., Deltaic sedimentation modern and ancient: Society of Economic Paleontologists and Mineralogists, Special Publication 15, p. 198-212.

Penland, S., Suter, J.R. and McBride, R.A., 1987, Delta plain development and sea level history in the Terrebonne coastal region, Louisiana, *in* Coastal Sediments '87, Water Ways Division: American Society of Coastal Engineers, New Orleans, LA, p. 1689-1705.

Plummer, P.S. and Gostin, V.A., 1981, Shrinkage cracks: desiccation or synaeresis?: Journal of Sedimentary Petrology, v. 51, p. 1147-1156.

Pulham, A.J., 1989, Controls on internal structure and architecture of sandstone bodies within Upper Carboniferous fluvial-dominated deltas, County Clare, western Ireland, *in* Whateley, M.K.G. and Pickering, K.T., eds., Deltas: sites and traps for fossil fuels: Oxford, Blackwell Scientific Publications, Geological Society, Special Publication 41, p. 179-203.
Outcrop-based study incorporating a comprehensive biostratigraphic framework. Superb cross sectional exposure along basin strike allows correlation of lateral geometries and incorporation of paleocurrent data.

Rahmani, R.A., 1988, Estuarine tidal channel and nearshore sedimentation of a Late Cretaceous epicontinental sea, Drumheller, Alberta, Canada, *in* de Boer, P.L., van Gelder, A. and Nio, S.D., eds., Tide-influenced sedimentary environments and facies: Dordrecht, D. Riedel Publishing Company, p. 433-471.

Ramos, A. and Galloway, W.E., 1990, Facies and sand-body geometry of the Queen City (Eocene) tide-dominated delta-margin embayment, NW Gulf of Mexico basin: Sedimentology, v. 37, p. 1079-1098.

Reading, H.G. and Orton, G.J., 1991, Sediment calibre: a control on facies models with special reference to deep-sea depositional systems, *in* Muller, D.W., McKenzie, J.A. and Weissert, H., eds., Controversies in modern geology: New York, Academic Press, p. 85-111.

Scheihing, M.H. and Gaynor, G.C., 1991, The shelf sand-plume model: a critique: Sedimentology, v. 38, p. 433-444.

Scruton, P.C., 1960, Delta building and the deltaic sequence, *in* Shepard, F.P., Phleger, F.B. and van Andel, T.H., eds., Recent sediments northwest Gulf of Mexico: Tulsa, OK, American Association of Petroleum Geologists, p. 82-102.

Sestini, G., 1989, Nile delta: a review of depositional environments and geological history, *in* Whateley, M.K.G. and Pickering, K.T., eds., Deltas: sites and traps for fossil fuels: Oxford, Blackwell Scientific Publications, Geological Society Special Publication 41, p. 99-127.

Shepard, F.P., Phleger, F.B. and Van Andel, T.H., eds., 1960, Recent sediments, Northwest Gulf of Mexico: Tulsa, OK, American Association of Petroleum Geologists, 394 p.

Smith, N.D., Phillips, A.C. and Powell, R.D., 1990, Tidal drawdown: a mechanism for producing cyclic laminations in glaciomarine deltas: Geology, v. 18, p. 10-13.

Stow, D.A.V., 1986, Deep clastic seas, *in* Reading, H.G., ed., Sedimentary environments and facies, 2nd. edition: Oxford, Blackwell Scientific Publications, p. 399-444.

Suter, J.H. and Berryhill, H.L., Jr., 1985, Late Quaternary shelf-margin deltas, Northwest Gulf of Mexico: American Association of Petroleum Geologists, Bulletin, v. 69, p. 77-91.

Tesson, M., Gensous, B., Allen, G.P. and Ravenne, C., 1990, Late Quaternary deltaic lowstand wedges on the Rhone continental shelf, France: Marine Geology, v. 91, p. 325-332.

Van Heerden, I.L. and Roberts, H.H., 1988, Facies development of Atchafalaya delta, Louisiana: a modern bayhead delta: American Association of Petroleum Geologists, Bulletin, v. 72, p. 439-453.

Van Wagoner, J.C., Mitchum, R.M., Campion, K.M. and Rhamanian, V.D., 1990, Siliciclastic sequence stratigraphy in well logs, cores, and outcrops: Tulsa, OK, American Association of Petroleum Geologists, Methods in exploration series 7, 55 p.

Verdier, A.C., Oki, T. and Suardy, A., 1981, Geology of the Handil field (east Kalimantan-Indonesia), *in* Halbouty, M., ed., Giant oil and gas fields of the decade 1968-1978: American Association of Petroleum Geologists, Memoir 30, p. 399- 421.

Walker, R.G. and Harms, J.C., 1971, The "Catskill Delta": a prograding muddy shoreline in central Pennsylvania: Journal of Geology, v. 79, p. 381-399.

Wanless, H.R., Baroffio, J.R., Gamble, J.C., Horne, J.C., Orlopp, D.R., Rocha-Campos, A., Souter, J.E., Trescott, P.C., Vail, R.S. and Wright, C.R., 1970, Late Paleozoic deltas in the central and eastern United States, *in* Morgan, J.P., ed., Deltaic sedimentation modern and ancient: Society of Economic Paleontologists and Mineralogists, Special Publication 15, p. 215-245.

Weise, B.R., 1980, Wave-dominated deltaic systems of the Upper Cretaceous San Miguel Formation, Maverick Basin, South Texas: Austin, TX, Texas Bureau of Economic Geology, Report of Investigations 107, 39 p.
Regional subsurface study of deltaic cycles in a transgressive systems tract combining well logs, some cores, and some outcrop data — a superb example of shallow water wave-dominated deltas.

Williams, H.F.L. and Roberts, M.C., 1989, Holocene sea-level change and delta growth: Fraser River delta, British Columbia: Canadian Journal of Earth Sciences, v. 26, p. 1657-1666.

Winker, C.D., 1982, Cenozoic shelf margins: Gulf Coast Association of Geological Societies, Transactions, v. 32, p. 427-448.

Winker, C.D. and Edwards, M.B., 1983, Unstable progradational clastic shelf margins, *in* Stanley, D.J. and Moore, G.T., eds., The shelfbreak: critical interface on continental margins: Society of Economic Paleontologists and Mineralogists, Special Publication 33, p. 139-157.
Important summary paper based largely on examples from Atlantic passive margin.

Woodrow, D.L. and Sevon, W.D., eds., 1985, The Catskill Delta: Geological Society of America, Special Paper 201, 246p.

Wright, L.D., Wiseman, W.J., Bornhold, B.D., Prior, D.B., Suhayda, J.N., Keller, G.H., Yang, Z.S. and Fan, Y.B., 1988, Marine dispersal and deposition of Yellow River silts by gravity-driven underflows: Nature, v. 332, p. 629-632.

Yang, C.S. and Sun, J.S., 1988, Tidal sand ridges on the East China Sea shelf, *in* de Boer, P.L., van Gelder, A. and Nio, S.D., eds., Tide-influenced sedimentary environments and facies: Dordrecht, D. Riedel Publishing Company, p. 23-38.

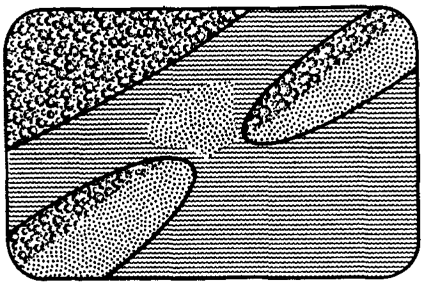

10. Transgressive Barrier Island and Estuarine Systems

Gerald E. Reinson, Institute of Sedimentary and Petroleum Geology,
Geological Survey of Canada, 3303 – 33rd St. N.W.,
Calgary, Alberta T2L 2A7

INTRODUCTION

In the simplest sense, modern barrier islands consist of long, narrow sand bodies that separate offshore muddy sediments from lagoonal muddy sediments. However, barrier island systems seldom retain their initial geometry and facies relationships when preserved in the geological record. Relative fluctuations of sea level result in their preservation either as *transgressive lagoonal and back-barrier deposits, or as regressive (prograding) shoreface successions.* In the latter situation, the lagoon commonly fills in, and the barrier system becomes a prograding strandplain.

This chapter focuses on *transgressive* barrier island and related estuary and lagoon environments in wave-dominated settings, where tidal ranges are usually micro (0-2 m) or mesotidal (2-4 m). It has been estimated that only about ten per cent of the world's barriers occur on coastlines where the tidal range exceeds 3 m (Glaeser, 1978), and barrier islands are extremely rare in macrotidal (greater than 4 m) coastal areas.

The objectives of this chapter are 1) to describe the facies and environments of transgressive barrier island and estuary systems, 2) to document the various facies successions formed during barrier evolution, and compile these successions into depositional models for use in interpreting ancient rocks, and 3) to relate the models to concepts of allostratigraphy and sequence stratigraphy.

DEPOSITIONAL SETTING OF BARRIER ISLAND AND ESTUARINE SYSTEMS

Wave-dominated shorelines in interdeltaic and nondeltaic coastal regions are characterized by elongate, shore-parallel sand deposits. These can occur as 1) a single mainland-attached beach (Fig. 1A), 2) a broader strandplain consisting of multiple parallel beach ridges (Fig. 1B), 3) a broad regressive barrier island also composed of multiple parallel beach ridges (Fig. 1C), or 4) a narrow transgressive barrier island (Fig. 1D). The barrier islands are wholly or partially separated from the mainland by a lagoon, estuary or marsh. A regressive barrier (Fig. 1C) is similar to a strandplain (Fig. 1B), but the latter is much wider and connected to the mainland. Strandplains also lack extensive enclosed lagoonal environments and tidal channels. As regressive barriers build seaward, the associated lagoon and tidal channels commonly fill in, and the barrier develops into a strandplain. These *regressive* barrier deposits and genetically related strandplains are discussed in Chapter 12.

Barrier island chains contain three main geomorphological elements (Fig. 2), 1) the sandy *barrier islands* themselves, 2) the enclosed *lagoons or estuaries* behind the barriers, and 3) the *tidal channels* that cut through the barriers and connect the lagoons to the open sea. Thus the barrier island systems contain three major clastic depositional environments (Fig. 3), 1) the subtidal to subaerial barrier-beach-dune complex, 2) the subtidal-intertidal lagoon, tidal flats and marsh, and 3) the subtidal-intertidal channels and tidal delta complexes. In strandplain settings (Fig. 1B) the subaerial beach-dune complex would be the dominant depositional environment, whereas in bay-mouth-barrier systems (Figs. 1C, D), subtidal lagoonal, estuarine, tidal channel and tidal delta environments would be most prevalent. Thus barrier islands are composite depositional systems, each displaying a combination of the three environments, within the broad spectrum of depositional settings ranging from barrier island to strandplain.

In *transgressive* settings, there is also a spectrum of depositional settings ranging from 1) barrier islands that protect lagoons with few rivers flowing into the lagoons (Fig. 4A), through 2) more extensive lagoons with several drowned river mouths (Fig. 4B), into 3) funnel-shaped drowned river valleys *(estuaries)* with few or no barriers at the estuary mouth (Fig. 4C). This gradational relationship between lagoons, lagoonal estuaries and estuaries (Fig. 4) was related to tidal range by Hayes (1975, 1979). Hayes observed not only that barrier *islands* were rare on macrotidal coastlines, but that there were morphological differences between barrier islands on microtidal and mesotidal coastlines. *Microtidal barrier islands* tend to be long and narrow, with abundant storm washover features (Fig. 5) but few well-developed *tidal channels and associated tidal* deltas. Because there are few channels, storm surges tend to overtop the barrier forming extensive overwash

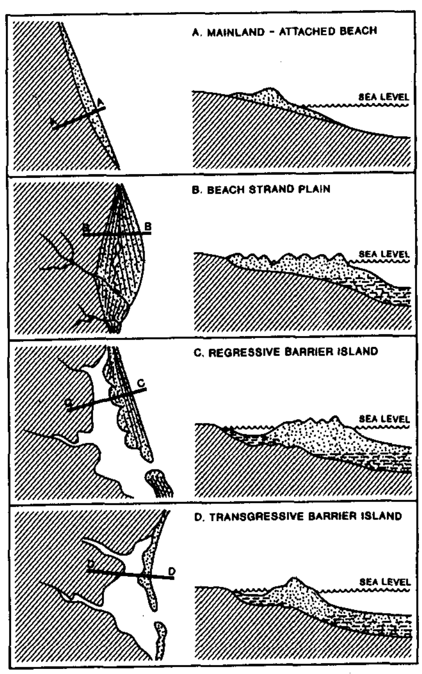

Figure 1 Generalized diagram illustrating the morphological relationship between beaches, strandplains and barrier islands, in regressive and transgressive settings.

conduits. *Mesotidal barrier islands* tend to be shorter and stunted, and characterized by large well-developed tidal channels and tidal deltas. According to Hayes (1975, 1979), microtidal barrier islands can be considered to be wave-dominated as opposed to mesotidal barriers which are affected by both wave and tidal current processes.

In general, wave-dominated coasts will be subjected to low tidal ranges and tide-dominated coasts to high tidal ranges. However, as pointed out by Reinson (1981) and Davis and Hayes (1984), exceptions to this generalization are common due to other controlling factors such as wave energy and tidal prism. In particular, the overprinting by the tidal prism can also produce tide-dominated morphologies on coasts with microtidal ranges.

ORIGIN AND OCCURRENCE OF BARRIER ISLANDS AND ESTUARIES

Barrier islands

The three main hypotheses for the origin of barrier islands have been reviewed at length by Schwartz (1973), Swift (1975), Field and Duane (1976), and Kraft and Chrzastowski (1985). They include 1) the aggradation and *emergence of submarine bars*, 2) *spit progradation* parallel to the coast and segmentation of the spit by channels, and 3) *isolation of beach and beach-dune complexes* due to coastal submergence. The controversy remains largely unresolved because most of the evidence pertaining to origin has usually been destroyed by subsequent modification.

Swift (1975) and Field and Duane (1976) consider that barrier formation by the emergence of submarine bars is insignificant compared to the other two mechanisms. This is because a submarine bar would have to aggrade through the surf zone; it is more likely that wave action would wash away the bar crest and prevent emergence. Swift (1975) favours submergence of coastal plain beach-dune complexes as the most important mode of formation. This mechanism is pictured elsewhere in this book (Figure 14 of Chapter 9), with reference to barriers around parts of the Mississippi Delta. With an overall sea level rise during the Holocene, it is certainly the most feasible mechanism for explaining the evolution, if not the initial origin, of most of the extensive barrier island regions existing today.

Spit progradation parallel to the coast initiates and modifies modern barriers. Many extensive barrier island chains probably have had a composite mode of origin, both by spit progradation and coastal submergence. Variations in sediment supply and wave climate could easily induce periodic spit elongation in specific localities while submergence of coastal ridges was occurring on a more regional scale.

Barrier islands and strandplains are more prevalent in coastal settings which have a low-gradient continental shelf adjacent to a low-relief coastal plain, an abundant sediment supply, and moderate to low tidal ranges (Glaeser, 1978). Both the shelf and coastal plain are composed of unconsolidated sediments which provide a source for the littoral drift necessary to accrete barrier islands.

Estuaries

Estuaries are found worldwide in all types of climates and tidal conditions

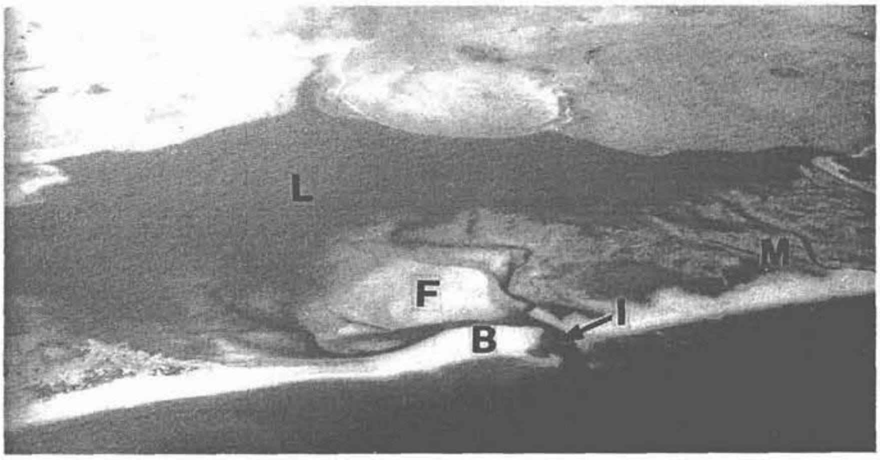

Figure 2 Oblique aerial view in September, 1980, of a small barrier-island system on the northeast coast of New Brunswick, showing the linear barrier-beach (B), the tidal inlet (I) through the barrier, and the lagoon (L) behind the barrier. Note the flood-tidal delta (F) and the back-barrier marsh (M) developed on abandoned delta deposits.

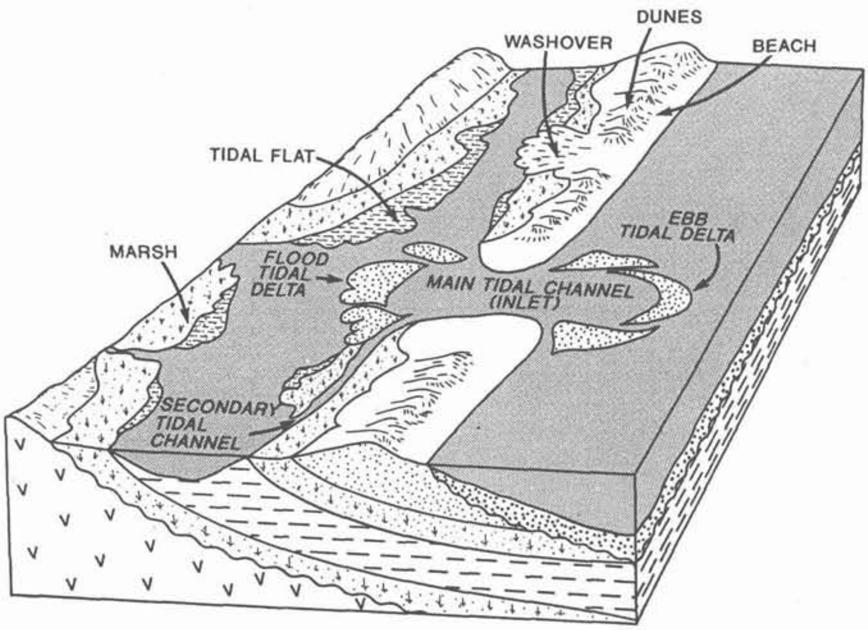

Figure 3 Block diagram illustrating the various subenvironments in a transgressing barrier-island system. Note the development of bounding discontinuities (undulating lines) below the transgressing marsh, and in the shoreface.

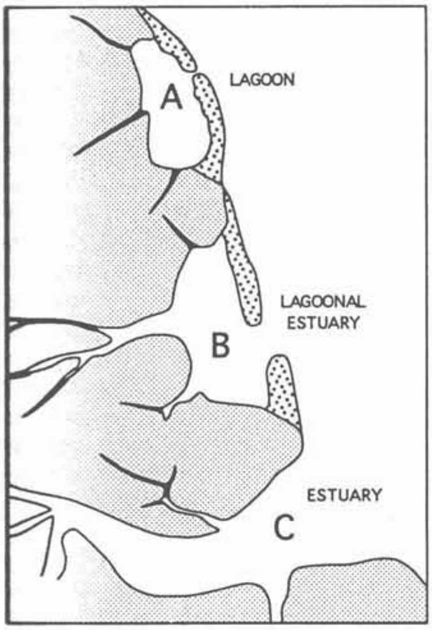

Figure 4 Diagram illustrating the gradational morphological relationships between lagoons (A), lagoonal estuaries (B), drowned river-valley estuaries (C), and barrier-islands.

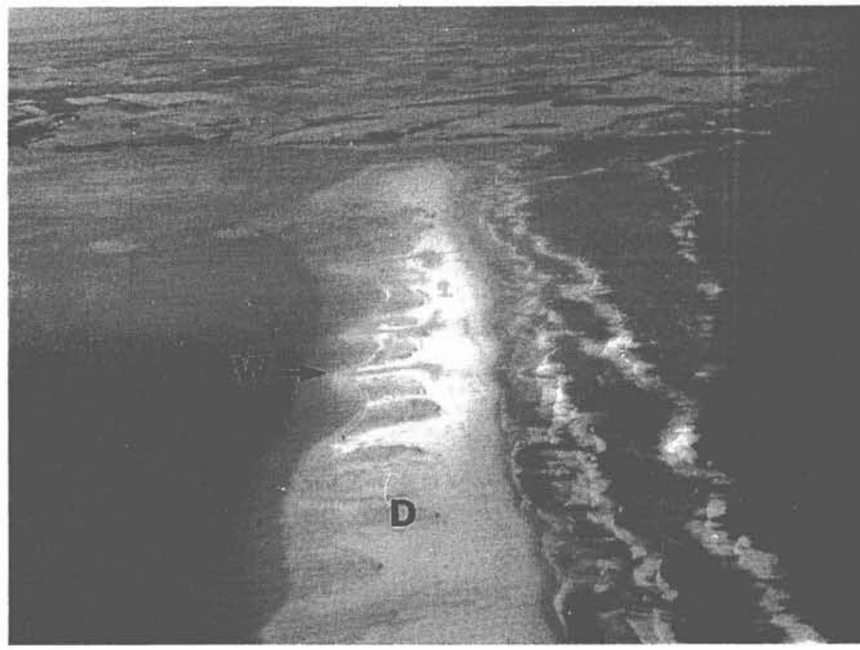

Figure 5 Oblique aerial photo of the barrier beach at Cavendish, Prince Edward Island, Canada, illustrating lobate washover fan deposits (W) extending into the lagoon (left). The dune ridge (D) is dissected by many washover channels. Note the occurrence of a dual bar system (delineated by the zones of breaking waves) in the nearshore zone (right). This is a microtidal area, with a tidal range of about 0.7 m. Photo taken in September, 1980.

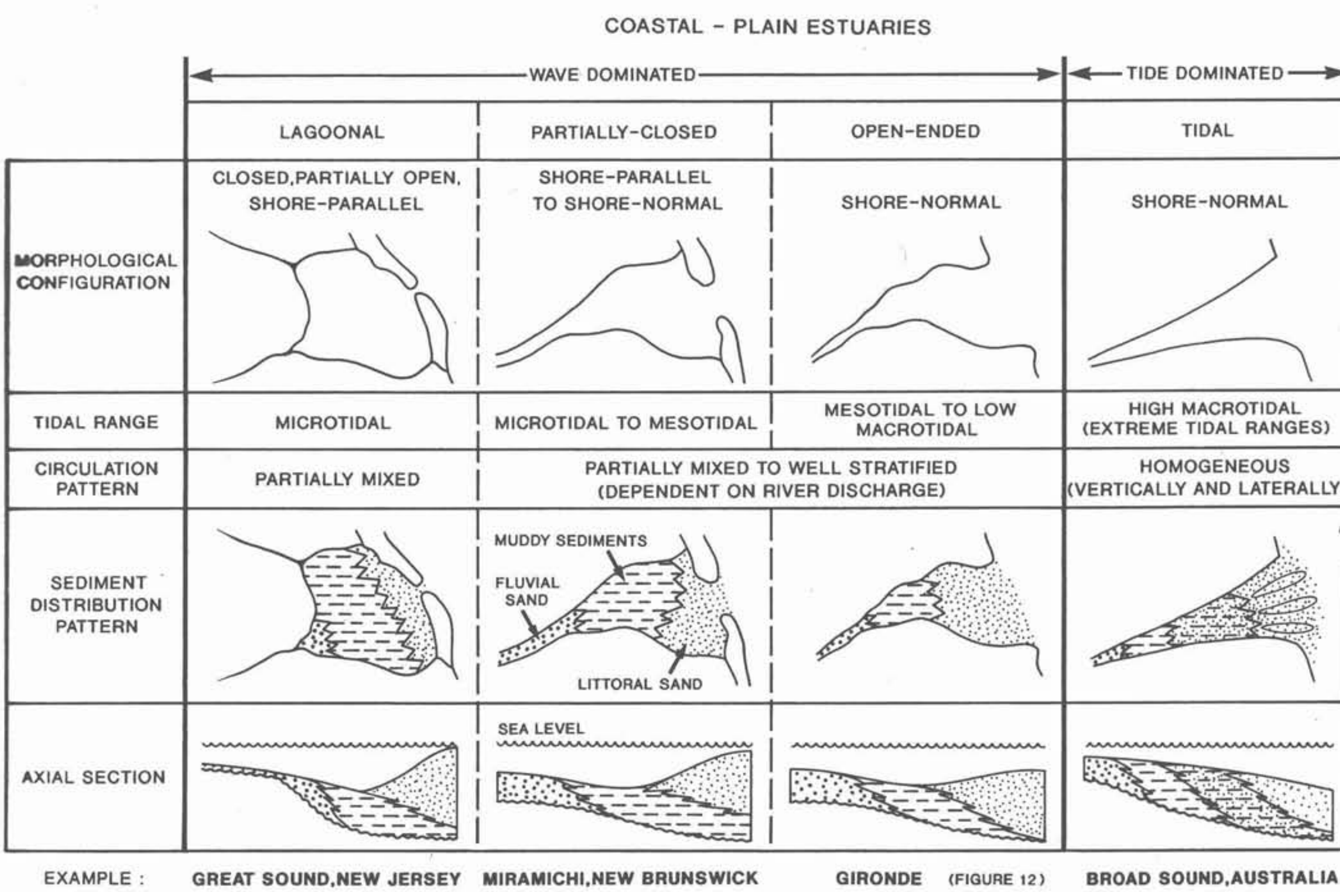

Figure 6 Classification of estuaries (based on volume of the tidal prism) illustrating morphological, oceanographic, and sedimentological characteristics of each estuary type. See Ashley (1988) and Cook and Mayo (1977) for Great Sound and Broad Sound examples, respectively.

(Olausson and Cato, 1980). They are best developed on mid-latitude coastal plains, with wide continental shelves that are undergoing marine submergence. Estuaries also occur on coasts with overdeepened valleys resulting from glaciation or tectonic activity. However, the underlying reason for the existence of estuaries is the Holocene rise of sea level. This began about 15,000 years before present (B.P.), when sea level was about 120 m below its present level (Emery, 1967; Milliman and Emery, 1968). The rapidity of sea level rise during early Holocene was instrumental in the formation of estuaries, because river valleys were inundated so quickly that infilling could not keep pace with the rise of sea level. From about 3,000 years B.P. to the present, sea level has been rising relatively slowly, and the rate of infilling of estuaries over that time period has been rapid (Meade, 1969). Thus the formation and lifespan of an estuary depends on the balance between relative sea level rise and volume of sediment input (Nichols and Biggs, 1985). Clearly, with respect to the ancient record, estuarine deposits provide evidence of transgressive events, and form part of the transgressive systems tract.

ESTUARINE SYSTEMS — DEFINITION AND CLASSIFICATION

There is presently much debate as to what constitutes an estuary. Most geologists think of an estuary as a drowned river valley, whereas hydrologists consider bodies of water to be estuarine if the salinity is less than that of seawater. Oceanographers regard estuaries as bodies of water in which river water mixes with and dilutes seawater. The most widely used, and best general definition states that "an estuary is a semi-enclosed coastal body of water which has free access to the ocean and within which seawater is measurably diluted by freshwater from land drainage" (Pritchard, 1967).

The oceanographic and geomorphological classifications of estuaries (Pritchard, 1967; Fairbridge, 1980; Kennedy, 1982; Nichols and Biggs, 1985) are not very useful for delineating estuarine facies or characteristic facies successions that can be used to interpret rock sequences. The sedimentological and morphological classification proposed here for coastal plain estuaries (Fig. 6) is probably applicable on a worldwide basis, and can be applied to the interpretation of ancient estuarine sequences, as will be shown later.

The classification (Fig. 6) is based on the premise that the interaction of the tidal prism and freshwater discharge are responsible for generating characteristic circulation types and sedimentary response patterns. In coastal plain settings, the volume of the tidal prism in microtidal and mesotidal estuaries increases with estuary surface area. At any given time during a transgression, the estuary surface area is a function of drainage basin area and therefore freshwater discharge. In macrotidal estuaries, tidal prism is largely a function of tidal range, which completely overwhelms the effects of freshwater discharge. As mentioned previously, obvious wave-dominated coasts generally experience relatively low tidal ranges, and the effects of ever increasing tidal range (from microtidal to high mesotidal) are clearly evident in a spectrum of depositional morphologies (Hayes 1975, 1979). The classification recognizes such a spectrum of estuarine types (lagoonal to open-ended) based on variation in tidal prism and freshwater discharge, and a singular estuarine type (tidal) that is dominated by tides (discussed in Chapter 11).

The terms used in Figure 6 have a descriptive physiographic connotation, but also imply a level of interaction

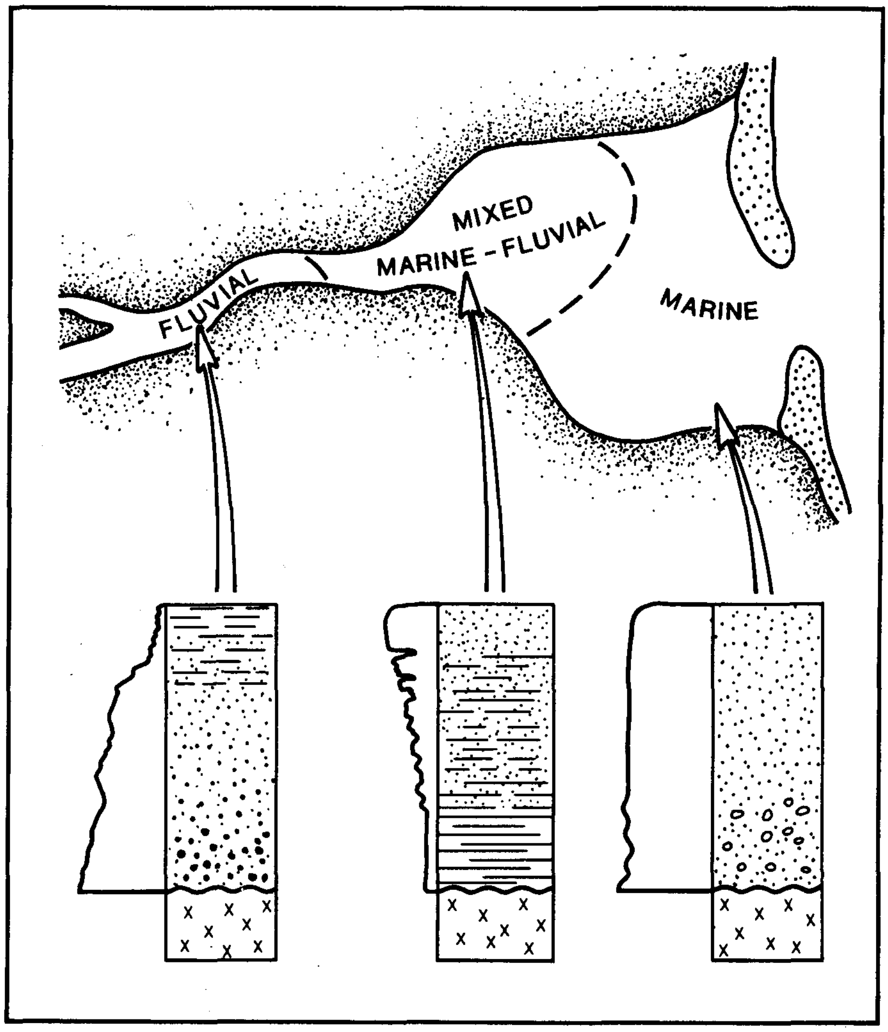

Figure 7 Schematic diagram illustrating the tripartite depositional realm characteristic of most partially closed to open-ended estuaries. The stratigraphic columns illustrate grain size trends associated with 1) fluvial fining-upward successions, 2) coarsening-upward trends in the turbidity maximum zone (mixed marine-fluvial), and 3) fining-upward trends associated with marine sands filling the estuary mouth; here, the fining upward reflects continuing transgression.

between the opposing river and tidal forces. *Lagoonal* implies a relatively quiescent system, *open-ended* an active but balanced system, and *tidal* a system dominated by one process.

The *lagoonal estuary* is small, generally shallow, and almost completely enclosed by a barrier bar. It has a small tidal prism, low freshwater input (relative to other estuarine types) and is characteristic of microtidal coastal areas. Such estuaries are usually partially stratified to well mixed, depending on the magnitude of seasonal variations in freshwater input. Winds play a dominant role in the mixing process.

The *open-ended* estuary is generally wide-mouthed with no entrance restrictions. It has an intermediate tidal prism, with intermediate to high freshwater input. It occurs in mesotidal and low macrotidal areas and in microtidal areas where freshwater inputs are high enough to affect the size of the tidal prism. The circulation in such estuaries generally varies between partially stratified and highly stratified, and winds play a minor role in the mixing process.

The *partially-closed estuary* is transitional between the lagoonal and open-ended types (Fig. 6). Freshwater input is sufficient to form partially- to highly-stratified circulation patterns. Seasonal variations in freshwater input, and winds, appear to affect the circulation in the transitional estuarine type more than in the open-ended type.

Tidal estuaries have large tidal prisms and occur only in areas subjected to extreme tidal ranges. Estuaries that are transitional between the open-ended and tidal types may occur. However, it appears that there is a critical tidal range at which the continuous depositional spectrum (Fig. 6) is broken, and tides dominate all other processes.

In estuaries that lie in the lagoonal to open-ended spectrum (Fig. 6), there is commonly a tripartite subdivision of depositional realms (Fig. 7), 1) *marine*, 2) *mixed marine-fluvial* and 3) *fluvial*. These correspond to the *estuary mouth* (where littoral sand is swept into the estuary from the ocean), the *central basin area* (characterized by silts and muds) and the *bayhead delta*, or upper reaches of the estuary (characterized by alluvial sands and gravels), respectively. The three-fold depositional concept was introduced by Bird (1967) and Kulm and Byrne (1967), and further refined in subsequent studies by Reinson (1977a), Roy (1984), Boyd *et al.* (1987), and Zaitlin and Shultz (1990). Tidal estuaries do not have a tripartite sand-mud-sand zonation, but tend to change from coarse-grained tidal bars to high-energy sand flats to extensive intertidal fluvial mudflats in the landward direction (Zaitlin and Shultz, 1990; Dalrymple *et al.*, 1992).

It is noteworthy that the well-studied macrotidal Gironde estuary (France) has a pronounced tripartite depositional framework (Figure 8). This is not inconsistent with the classification in Figure 6, since spring tides in the Gironde are only in the 5 m range. This low macrotidal range thus allows wave processes and fluvial discharge to affect the estuarine realm sufficiently to render it open ended rather than tidal.

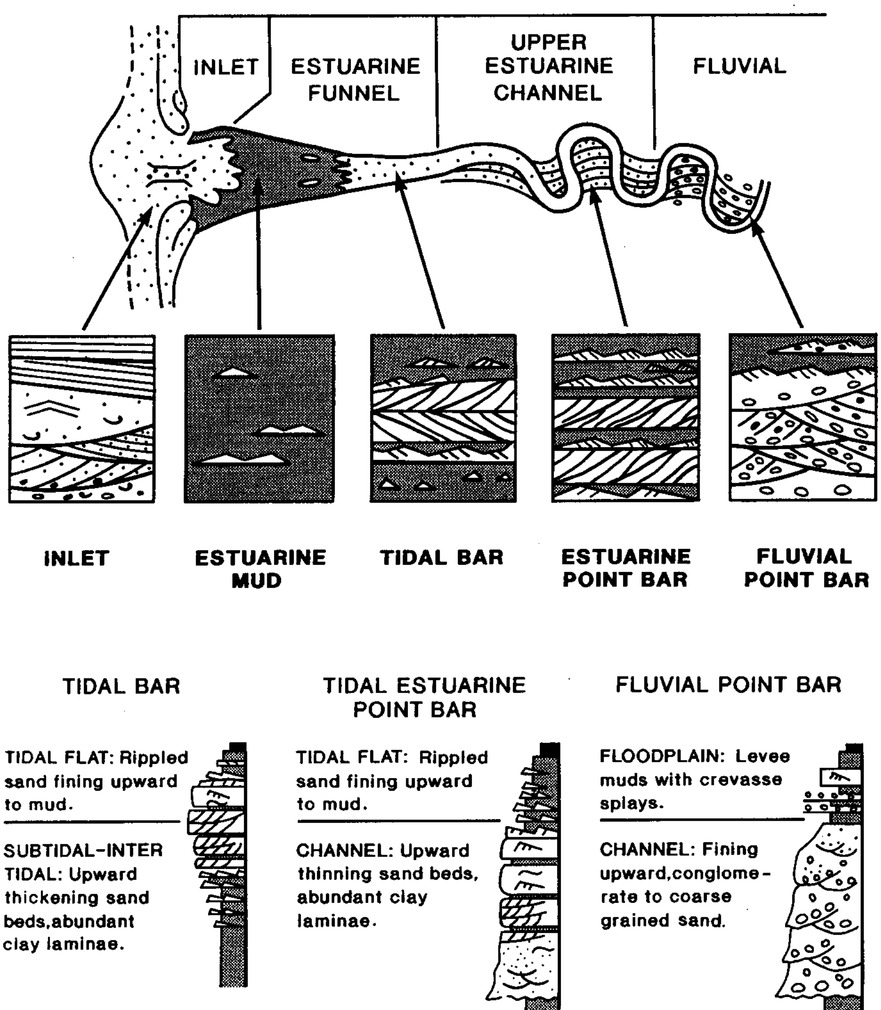

Figure 8 Schematic illustration of the variable facies successions occurring along a longitudinal profile within a Gironde-type macrotidal, or open-ended, estuary. Modified from Allen (1991).

FACIES AND FACIES SUCCESSIONS OF BARRIER ISLAND SYSTEMS AND ESTUARIES

The three main environments of a barrier island system (barrier beach, lagoon, tidal channel-and-delta complex) are made up of a number of subenvironments (Fig. 3), each of which is characterized by distinct lithofacies. Facies of the barrier beach, channel and delta environments are mainly sand and gravel, whereas the lagoonal (back barrier) deposits can consist of both mud and sand. Barrier beach deposits are elongate bodies which parallel the strandline and enclose finer grained deposits of the lagoon. Tidal channel and associated tidal delta sands are generally oriented perpendicular or oblique to the barrier complex, and can extend into the lagoon and seaward into the nearshore zone (Fig. 3). The transition between lagoon deposits and barrier, channel and delta deposits occurs in the overlapping subenvironments of the back-barrier tidal flats, marsh, washover fans and flood tidal deltas.

Estuaries contain several subenvironments, including tidal channels, tidal deltas, tidal flats, marshes and subtidal bays. The close morphological association of estuaries with lagoons, and in turn, lagoons with barrier islands, makes discussion of specific facies somewhat repetitive. Estuarine deposits will in general be aligned oblique to perpendicular to the shoreline particularly if they tend to the *tidal* as opposed to *lagoonal* type (Fig. 6).

The extent and occurrence of transitional deposits in the estuarine system (e.g., tidal flats, marshes, washovers), and of specific facies within the barrier island system, will depend on the degree of tide or wave dominance. For example, tidal flat deposits will not be an important facies in microtidal environments because of the limited tidal range, whereas they may be extensive in mesotidal environments. Similarly, tidal channel and delta deposits are likely to be more prevalent in mesotidal than in microtidal environments because of the stronger tidal currents generated by the larger tidal range. The following discussion covers all the depositional environments and corresponding deposits of barrier island systems, beach-ridge strandplains, and estuaries.

Barrier beach and related facies

The depositional subenvironments of a barrier beach complex include 1) the subtidal zone or *shoreface*, 2) the intertidal zone or *beach*, 3) the subaerial zone or *backshore-dune* landward of the beachface and, 4) the supratidal to subaerial wave- and wind-formed *washover* flats which extend across the barrier into the lagoon (Figs. 3, 5). All of these subenvironments and corresponding facies and facies successions have been described in detail by Reinson (1984), Elliott (1986), and Thom (1984).

Shoreface and *beach* subenvironments in progradational settings are discussed in Chapter 12. In transgressive settings, shoreface, beach and backshore-dune environments are subjected to extensive wave erosion. In contrast, the deposits of washover and lagoonal environments tend to be preserved during transgression, and will be described in some detail below.

Washover deposits are formed when wind-generated storm surges cut through and spill over barriers, creating lobate or sheet-like deposits of sand which extend into the lagoon (Figs. 3, 5). These washover flats then

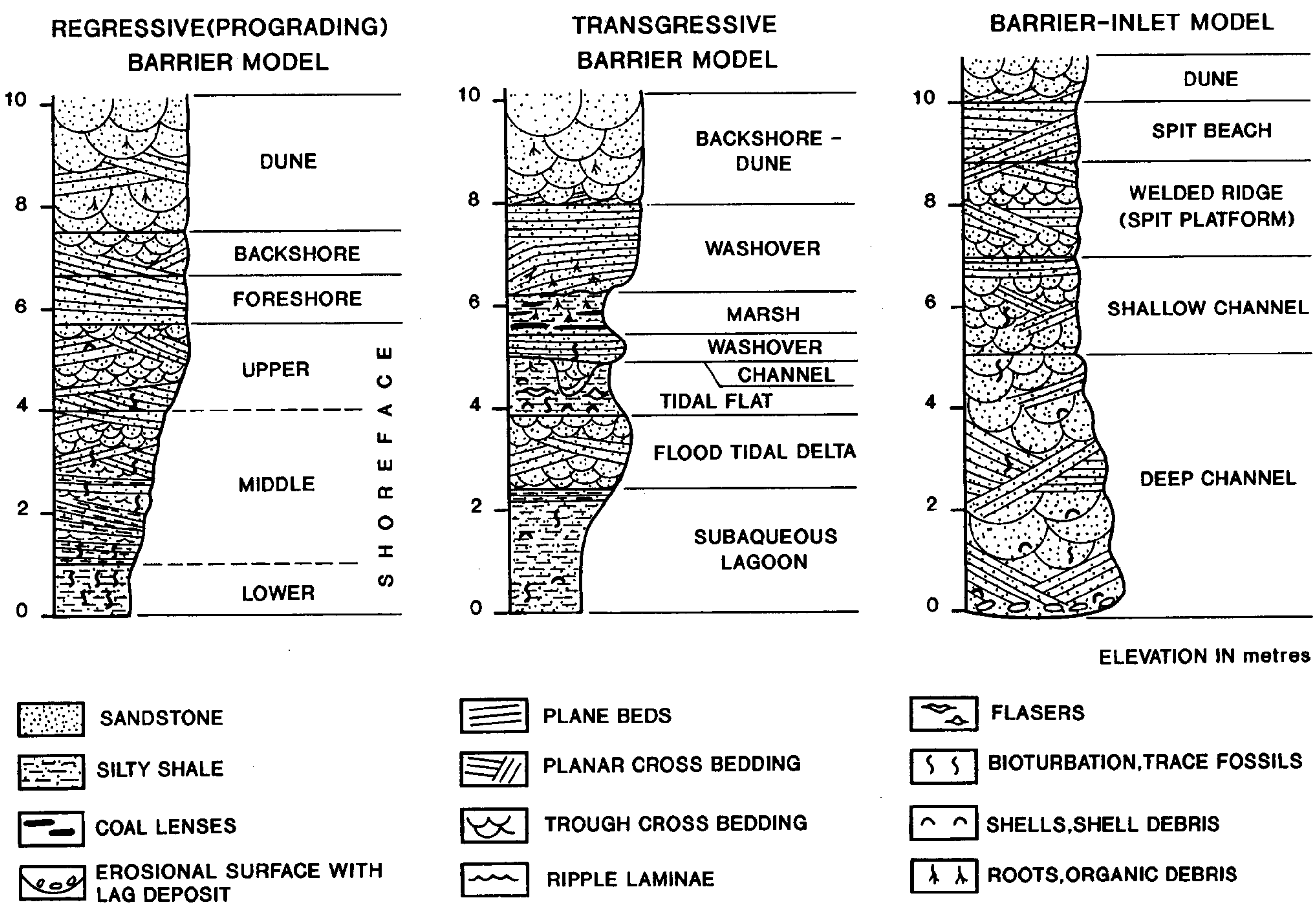

Figure 9 Three "end-member" facies successions associated with regressive and transgressive barrier islands, and inlet migration. After Reinson (1984).

provide corridors for transferring wind-transported sand across the foredune belt to form back-barrier sand flats. This mechanism increases the width of the barrier, and creates environments favourable for stabilization by marsh growth. Modern studies of washover deposits indicate that there are two dominant sedimentary structures, sub-horizontal (planar) stratification, and small- to medium-scale foreset strata where the washover detritus builds into the lagoon (Schwartz, 1982). The deposits range from fine-grained sands to gravel, with fine- to medium-grained sand being most common. The deposits are generally thin, ranging from a few centimetres to two metres for each overwash event. In plan, they form elongate, semicircular, sheet-like or tabular bodies a few hundred metres in width and oriented normal to the shoreline. Coalescing washover fans can be kilometres in width, creating extensive washover flats which cover large tracts of the inner barrier.

Recent studies on modern barrier island systems have shown that washover deposits form a significant portion of transgressive barrier sand bodies (Fig. 5), especially in microtidal regions (Boothroyd *et al.*, 1985; Nichols, 1989). During transgression, washover is one of the main processes by which the barrier island migrates landward. Further scouring associated with washover is probably one of the main mechanisms responsible for the initiation of new tidal channels.

Washover deposits have a high potential for preservation in a transgressive succession (Fig. 9). Washover facies in the stratigraphic record have been described by Bridges (1976), Horne and Ferm (1978), and Hobday and Jackson (1979), and they are probably much more common than has been recognized to date.

Tidal channel and tidal delta facies

Tidal channel and tidal delta deposits are closely related facies, both geographically, and with regard to their internal sedimentary structures and textures (Boothroyd, 1985). The occurrence of tidal delta deposits is governed by tidal current processes directed normal or oblique to the strandline. The *ebb tidal delta* forms seaward of the barrier (Fig. 3), and is affected by longshore and wave-generated currents. The *flood tidal delta* forms landward of the barrier, and is only slightly influenced by wave- and wind-generated processes (Fig. 3).

There are two types of *tidal channel* environments, the main channels (inlets) that connect the lagoon to the ocean, and the secondary channels located adjacent to the tidal deltas and back-barrier estuary/lagoon margins. Tidal channel facies can occur independently of tidal deltas, as in open-ended estuaries, whereas the occurrence of tidal delta facies is dependent on the presence of tidal channels.

Tidal channel deposits

Tidal channel deposits (Fig. 10) are formed by lateral migration (Fig. 11), as in a meander bend in a river. The direction and rate of inlet channel migration is controlled by the magnitude of net longshore sediment supply. Barriers lengthen by spit accretion on the updrift side, with a corresponding erosion of the downdrift channel margin (Fig. 11). The shifting of the main channel through a barrier causes the subordinate tidal channels both land-

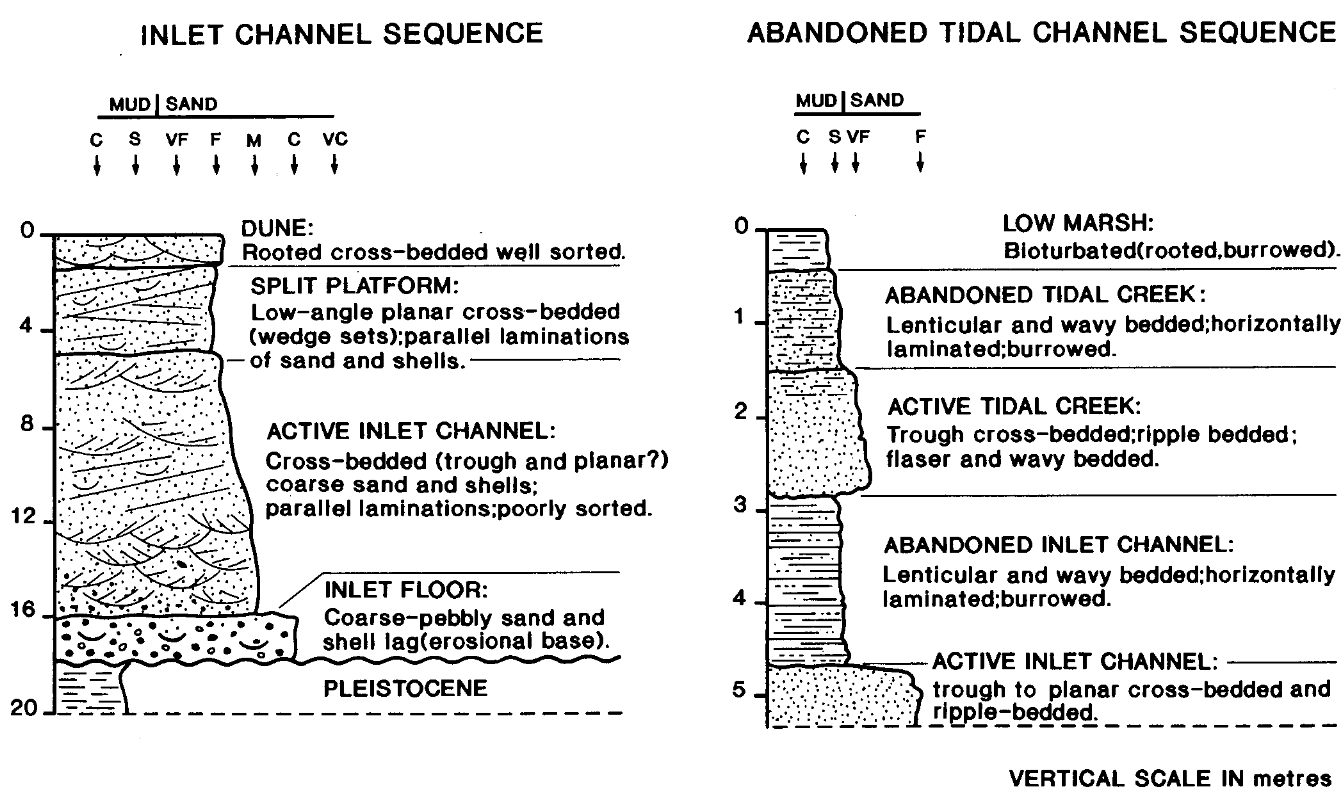

Figure 10 Tidal channel-fill sequences for an inlet channel located along an active barrier-island, and an abandoned channel situated in a back barrier position. After Moslow and Tye (1985).

ward and seaward of the barrier, and the tidal deltas, to shift position also. The sand body that is deposited by channel migration will be elongated parallel to the barrier island, having a length equal to the distance the channel has migrated. The thickness of the *channel facies succession* (Fig. 10) will be equal to the depth of the channel, if no subsequent erosion of the upper boundary occurs during transgression.

Channel fill successions resulting from barrier inlet migration are characterized by 1) an erosional base often marked by a coarse lag deposit, 2) a deep active channel facies consisting of bidirectional large-scale planar and/or medium-scale trough cross beds, 3) a shallow channel (spit platform) facies consisting of bidirectional medium-scale planar cross-beds and "washed-out" ripple laminae, and 4) a fining-upward textural trend and a reduction in cross bed set thickness upward (Kumar and Sanders, 1974; Hayes, 1980; Heron *et al.*, 1984; Moslow and Tye, 1985).

Ancient tidal channel successions have been described by Cheel and Leckie (1990), Ricketts (1991), Barwis and Makurath (1978) and Land (1972). The Silurian inlet sequence of Barwis and Makurath (1978) consists of a channel lag deposit overlain by 4.1 m of bidirectional trough and planar cross bedded, medium-grained sandstone, with set thickness averaging 15 cm. The cross bed orientations reflect deposition from reversing tidal currents, along an axis oblique to the paleostrand. This deep channel facies is overlain gradationally by a fine-grained sandstone unit (1.8 m thick) dominated by bidirectional trough cross bed sets averaging 2.5 cm in thickness, and "washed-out" ripples. The tidal channel sequence described by Land (1972) averages 8 m in thickness and consists of bimodal to polymodal trough cross bed sets (from 10 cm to 90 cm in thickness) in the lower 5 to 6 m, and subparallel beds in the upper 2 to 3 m.

A vertical succession resulting from tidal channel abandonment (Fig. 10) should consist largely of mud which caps thin active inlet channel sands. This contrasts with the thick active channel sands that form as the result of lateral barrier inlet migration. Channel fills resulting from abandonment should be present in flood tidal delta regions of mesotidal estuaries where tidal channel switching is common. Examples of ancient back-barrier sand-filled tidal channels (Carter, 1978; Devine, 1991) could also be interpreted as part of a flood tidal delta complex, as will become evident in the following discussion.

Tidal delta deposits

Hayes (1975) recognized that tidal deltas display a common morphological pattern governed by segregated zones of ebb and flood flow, and was the first to propose generalized models for both ebb- and flood-tidal delta deposition. Generalized vertical facies successions (Fig. 12) were proposed by Boothroyd (1985). Ebb tidal deltas are almost impossible to preserve in the geological record. As the tidal channel migrates downdrift, ebb tidal deposits become reincorporated into the longshore drift system, thereby losing their distinctive deltaic morphology and sedimentary structures. Flood tidal deltas can be preserved, as part of the lagoon filling (Fig. 9), and examples have been described by Murakoshi and Masuda (1991), Boersma (1991), Barwis (1990), Cheel and Leckie (1990), and Van Wagoner *et al.* (1990).

Estuary and Lagoon Facies

Despite many studies of the geomorphology and sedimentation processes of modern estuaries, few geological models for estuarine environments have been proposed that can be applied to the stratigraphic record. Estuarine deposits are usually associated with submergence and transgression, and have a good preservation potential in the stratigraphic record. However, estuarine successions are complex because they straddle several coastal and shallow marine environments. Consequently, ancient

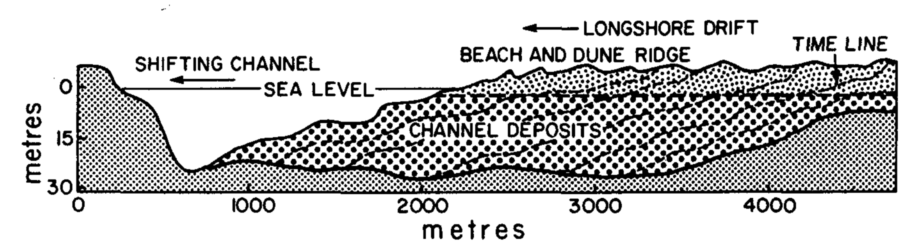

Figure 11 Generalized cross section parallel to shoreline illustrating the development of a barrier-inlet sand body by lateral inlet migration. Modified from Hoyt and Henry (1965).

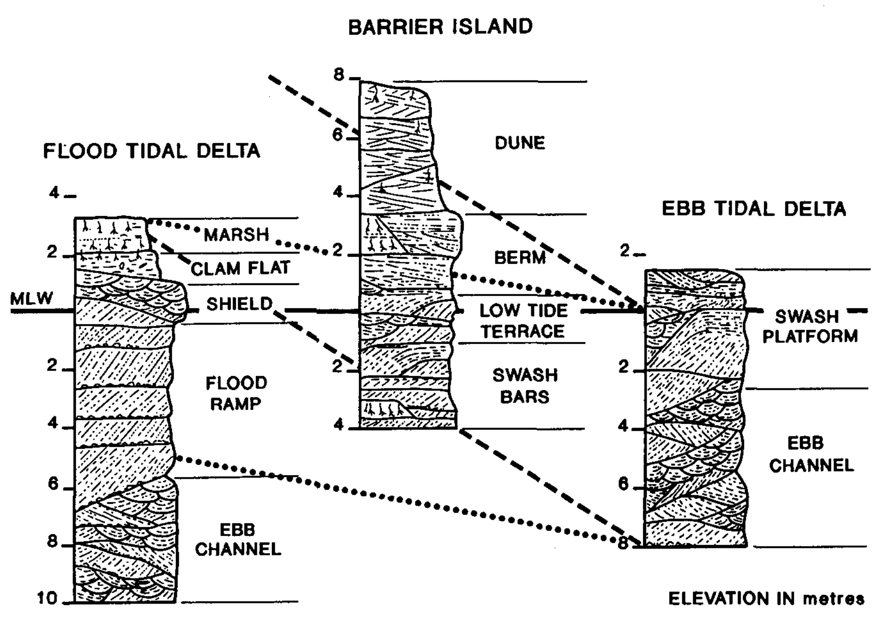

Figure 12 Ebb- and flood-tidal delta successions, as postulated by Boothroyd (1985).

estuarine deposits are difficult to compare with facies distributions in modern estuaries, making model building difficult. In the 1980s, the development of sequence stratigraphic concepts has led to a revival of estuarine sedimentary environments as appropriate analogues for interpreting many ancient coastal and incised valley fill successions (Rahmani, 1988; Reinson *et al.*, 1988; Wood and Hopkins, 1989; Leckie and Singh, 1991).

Frey and Howard (1986) define an *estuarine sequence* as "a complex of intertidal and shallow subtidal, mostly channel-form intracoastal facies dominated to some extent by tidal processes, exhibiting conspicuous variations in sediment texture, composition, and provenance, and in physical and biogenic sedimentary structures". The depositional environments comprising this complex of facies may encompass any number (or all) of the following: tidal deltas, inlets, shoals, back-barrier beaches and spits, washover fans, swash and point bars, tidal flats, marshes, stream banks and channels. Thus deposits of estuaries and lagoons can be recognized as distinct entities but consisting of numerous component facies. Depending on location within an estuary, vertical facies successions could consist entirely of cross-bedded sands or of laminated muds, or some combination of the two. Good examples of vertical facies variability within a single system are shown in Figures 7 and 8, and are illustrated by Fletcher *et al.* (1990).

Lagoonal sequences generally consist of interbedded and interfingering sandstone, shale, siltstone and coal facies characteristic of a number of overlapping subenvironments (Fig. 13). This variability is clearly illustrated in studies of modern lagoons (Boothroyd *et al.*, 1985; Hennessy and Zarillo, 1987; Ashley, 1988; Oertel *et al.* 1989; Nichols, 1989). Sand facies include *washover* sheet deposits and sheet and channel fill deposits of *flood-tidal* delta origin. Fine-grained facies include those of the *subaqueous lagoon* and the *tidal flats*, which are situated adjacent to the barrier or on the landward side of the lagoon abutting the hinterland *marsh* and *swamp* flatland (Fig. 3). Organic deposits of coal and peat record marsh and swamp environments, and usually are very thin, having formed on sand and mud flats of the lagoonal margin, and on emergent washover flats. Abandoned or mature flood tidal

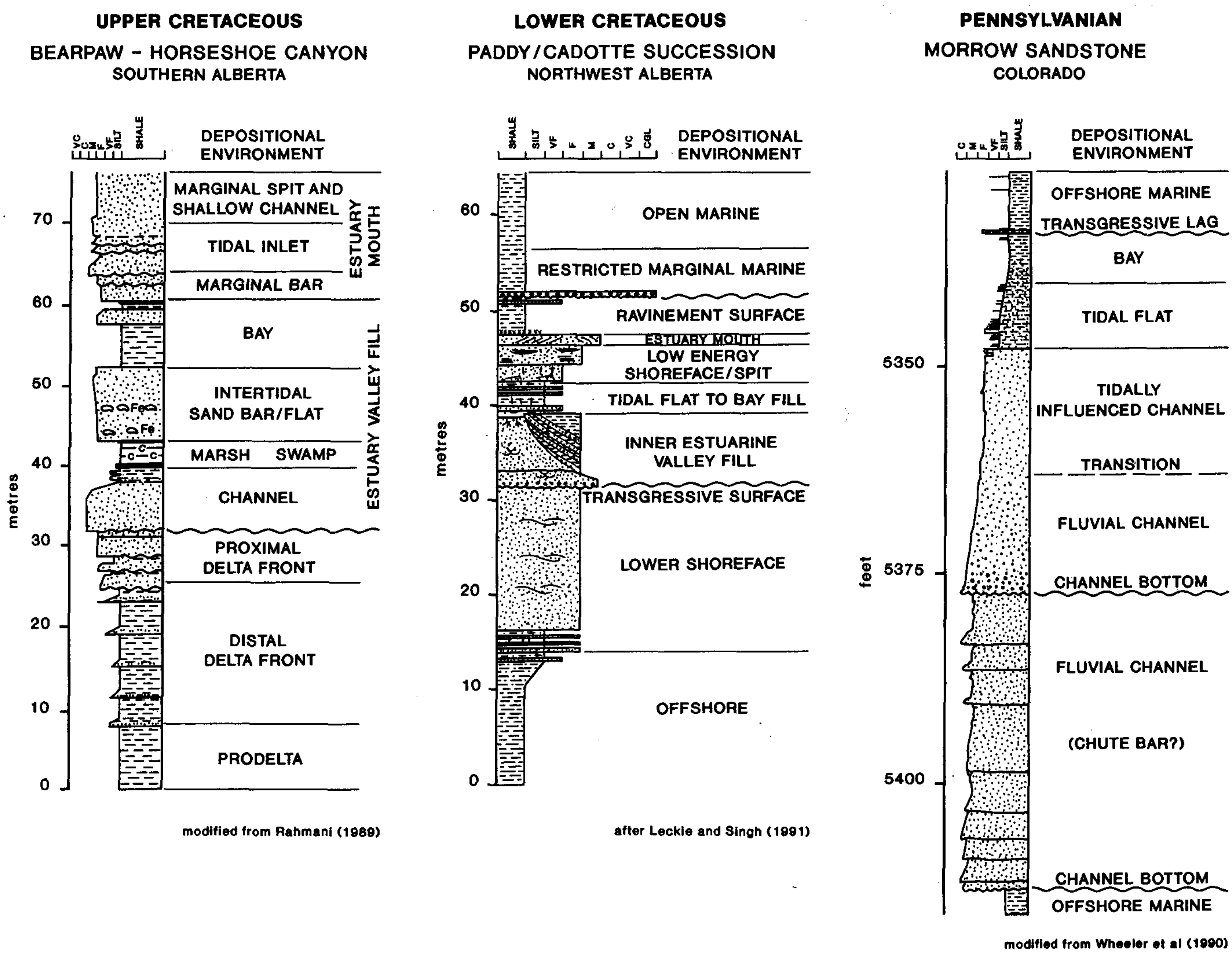

Figure 13 Vertical facies successions of three rock sequences interpreted as containing estuary valley-fill deposits. Note that each valley fill succession begins above a bounding discontinuity (undulating lines), and reflects a transgressive situation.

deltas can also become stabilized by marsh vegetation. This situation and that of the vegetated washover flat can lead to the presence of very thin coal lenses overlying organic-rich sheet sandstones in the rock record (Fig. 14). Subaqueous shale and siltstone facies in Cretaceous lagoon deposits are often characterized by brackish water bivalve shells, (Kirschbaum, 1989) and coquinid oyster beds (Land, 1972). Disseminated carbonaceous material, imprints of plant remains, and root and reed fragments are common in some shale beds, indicating the interfingering of proximal marsh and subaqueous lagoonal environments.

Estuarine sequences from partially closed and open-ended estuaries will also be characterized by stacked facies representative of several depositional subenvironments, although vertical successions will tend to be less variable than those generated in shallow lagoons. Examples of such modern estuaries include the Miramichi, New Brunswick (Reinson, 1977b); Georgia and South Carolina estuaries (Frey and Howard, 1986), and those situated on the New South Wales coast, Australia (Roy, 1984). Typical generalized successions are described by Clifton (1982), and Frey and Howard (1986).

Ancient estuarine facies are characterized by a set of sedimentary structures which indicate tidal influence and biotic stress. Physical sedimentary structures diagnostic of diurnal and lunar tidal-flow responses include tidal bundles, mud-layer couplets, sigmoidal bedding and inclined heterolithic stratification (Chapter 11; Nio and Yang, 1991; Thomas *et al.*, 1987; Kreisa and Moiola, 1986). Examples of these structures in ancient successions are documented also by Rahmani (1989), Reinson *et al.* (1988), Reinson (1989) and Kuecher *et al.* (1990). Characteristic trace fossil assemblages reflect brackish to stressed conditions (Chapter 4), and have been illustrated in several rock studies (Reinson *et al.*, 1988; Wightman *et al.*, 1987).

Because the occurrence of estuarine deposits is usually related to submergence or transgression, complete axial facies successions should reflect the tripartite depositional realms, from fluvial at the base through mixed fluvial-marine, to marine at the top (Nichols and Biggs, 1985). The Gironde estuary model (Fig. 8) depicts marine estuary-mouth deposits overlying estuary muds, and the rock sequences illustrated in Figure 13 depict similar superposition of progressively more seaward deposits over landward inner estuarine and fluvial deposits, within the continuous valley fill succession. Wave-dominated coastal plain estuaries (whether partially closed or open-ended) will be characterized by a set of vertical successions that reflect position within the estuarine depositional system. In ancient sequences, for example, the recognition of fluvial deposits grading upwards to estuarine facies should reflect location in the upper reaches or fluvial realm. Accretionary channel fill and tidal delta facies should indicate littoral deposits situated at the estuary mouth. The tidal range and geomorphological configuration of ancient estuaries could be determined if laterally accreting estuarine point-bar or coarsening-upward bay fill facies successions were encountered.

Estuary bounding discontinuities

Vertical facies successions containing stressed trace fossil assemblages and tidal bedform structures do not unequivocally identify ancient estuarine deposits. Recognition of the overall geometry and bounding discontinuities is important for identifying allostratigraphic units, and for defining the internally complex but genetically related estuarine rock bodies. The bounding unconformities must also be identified in order that sequence stratigraphic ideas can be applied; they include ravinement surfaces (transgressive surfaces of erosion, Chapter 1), marine flooding surfaces, surfaces of onlap and downlap, channel bases, and regressive surfaces of erosion (Chapter 1). Most important of all is the recognition of *incised valleys* (SE, subaerial erosion in Figure 8 of Chapter 1), in which the estuaries form. A vertical facies progression from fluvial to estuarine in some valley fill successions can be expected (Howard and Whittaker, 1990; Wheeler *et al.*, 1990). In other successions, reworking of the fluvial sediments and modification of the original river valley topography early in the transgressive phase have obscured or erased the evidence of initial fluvial incision. A fluvial origin can commonly be inferred from the valley orientation with respect to regional dip and strike directions, and the stratigraphic context of the valley fill deposits.

The placement of estuary fill facies in the *lowstand* systems tract by the Exxon sequence stratigraphic school (Van Wagoner *et al.*, 1990) should probably be revised. The river valley is *incised* during falling stage and lowstand, but is only transformed into an estuary during rising stage of sea level. The deposits are therefore better placed in the *transgressive* systems tract. The base of the incised valley, as seen in the geological record, may

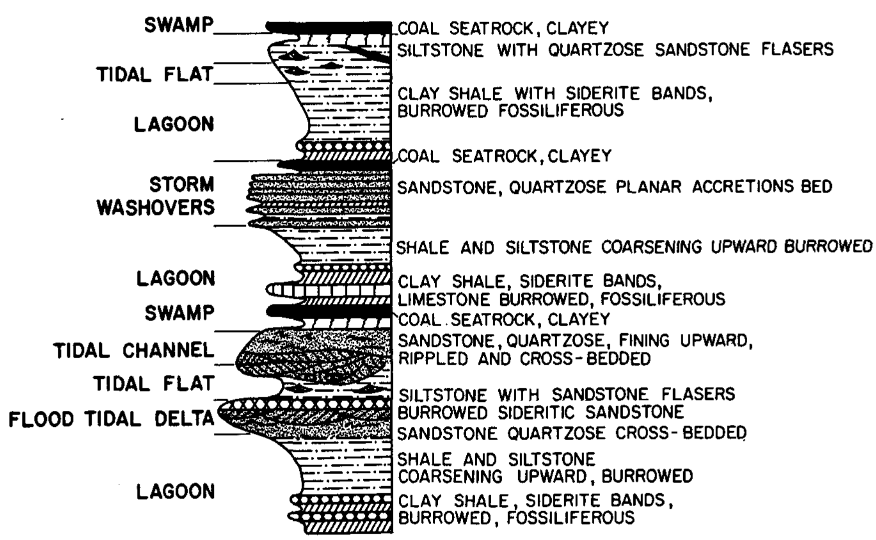

Figure 14 Generalized lagoonal sequence through back barrier deposits in the Carboniferous of eastern Kentucky and southern West Virginia. Such sequences range from 7.5 to 24 m thick. From Horne and Ferm (1978).

be 1) the original fluvial incision surface, or 2) an original fluvial incision totally modified by the initial stages of marine transgression. In the first case, fluvial facies may immediately overlie the incision and pass upward into estuarine facies. In the second case, no fluvial facies will be preserved, and the valley fill will begin with brackish to estuarine facies, as in the estuary fills in the Viking Formation, Alberta (Reinson *et al.*, 1988; Boreen and Walker, 1991).

The correct identification of sequence-bounding unconformities and ravinement surfaces on transgressed barrier island and estuary coasts may be difficult and controversial. The problem has been discussed, with several useful examples (Fig. 15), by Demarest and Kraft (1987).

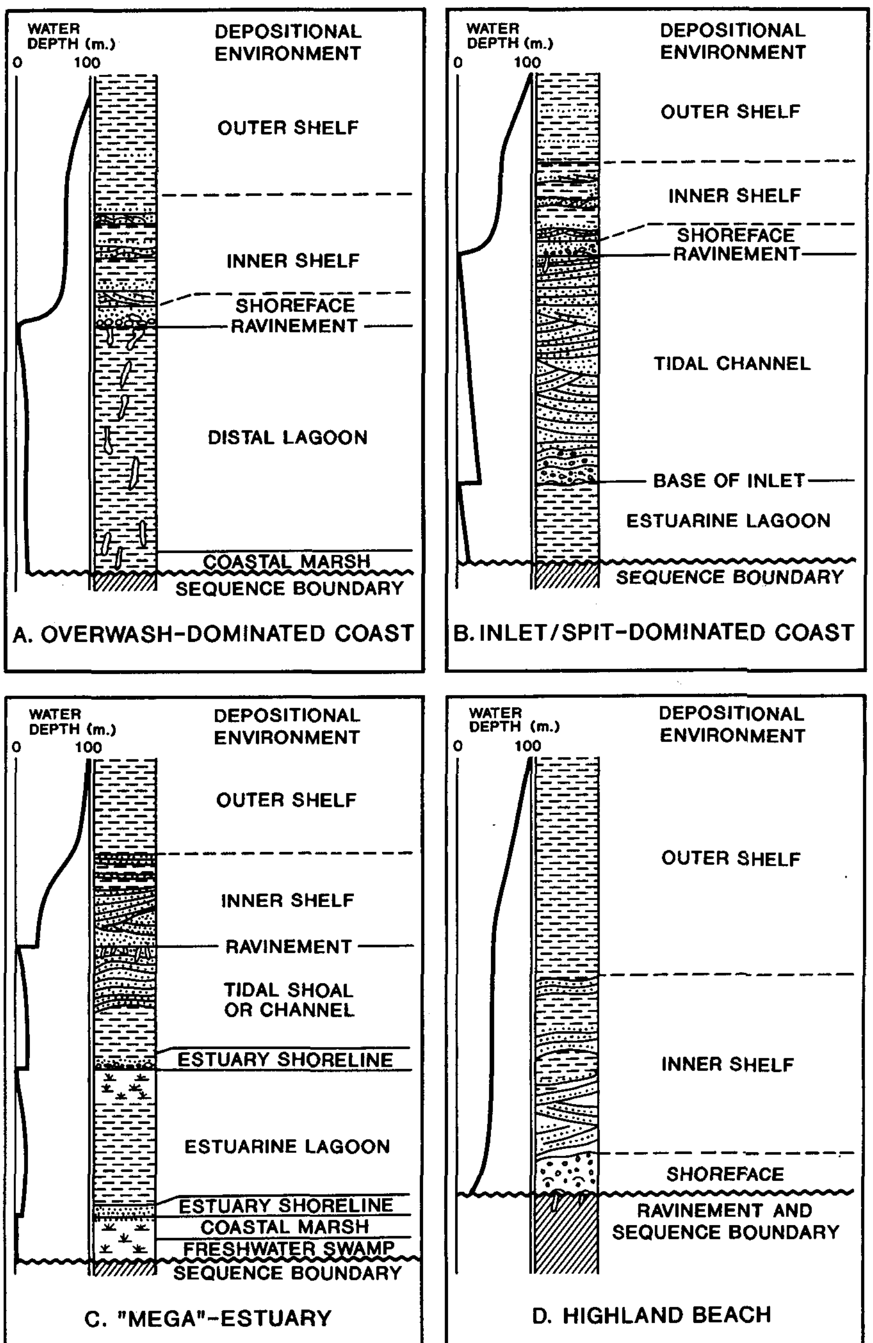

Figure 15 Vertical sequences produced through transgression of different types of coastal environments. Modified from Demarest and Kraft (1987).

TRANSGRESSIVE STRATIGRAPHIC MODELS

Estuarine valley fill deposits rarely consist of a single fill cycle formed during one rising stage of sea level (Clifton, 1982). Rather, several successions may be represented in the valley fill deposits because the estuary would probably occupy the same valley during several minor sea level fluctuations. The recognition of estuarine deposits within incised valleys is important in understanding transgressive systems tracts, bounding discontinuities (ravinements, flooding surfaces), and overall transgressive stratigraphic models.

Transgressive depositional systems

Barrier island and estuarine depositional systems commonly form part of the transgressive systems tract. Barrier islands can also prograde (normally in the highstand systems tract), but commonly are transformed into strandplains (Chapter 12). Estuaries have a uniquely transgressive origin, and rarely occur as significant components of the highstand systems tract. Transgressive and regressive barrier shoreline migrations produce very different facies successions, related to transgression, regression and inlet migration (Fig. 9; Reinson, 1984).

Beaches, barrier islands and estuarine shorelines retreat landward in response to sea level rise or subsidence or a reduction in sediment supply. Most modern barrier island systems have migrated landward in response to the Holocene transgression, and the trend is continuing today (Kraft and Chrzastowski, 1985). Modern coastal plain estuaries also formed during the Holocene transgression, and major estuary tracts usually are juxtaposed or associated with barrier shoreline coasts (Meade, 1969; Hayes, 1975, 1979; Frey and Howard, 1986).

Transgressive systems; continuous shoreface retreat versus in situ drowning

The idealized transgressive barrier island facies succession (Fig. 9) will be extremely modified and attenuated as the depositional system migrates landward in response to sea level rise. This is evident from the two proposed mechanisms of barrier island shoreline behaviour during marine transgression (Fig. 16). The mechanism of *erosional shoreface retreat* is widely accepted because of strong evidence from detailed studies of the U.S. Atlantic shoreface and inner continental shelf (Niedoroda *et al.*, 1985). This involves sediment being eroded from the upper shoreface and transported 1) to the lower shoreface or offshore as storm beds, or 2) to the lagoonal estuary as washover deposits. As the upper shoreface zone moves landward and upward during continued transgression, it erodes the barrier, washover and lagoonal facies to form a planar erosional surface (ravinement surface), upon which the redistributed lower shoreface-inner shelf sands are deposited (Fig. 16A; Nummedal and Swift, 1987). This model predicts that the thickness of transgressive facies successions will depend on the rate of relative rise of sea level. If sea level rise is slow compared with the rate of landward erosion, almost all of the barrier system may be destroyed. The only stratigraphic record will be a thin layer of lagoonal, tidal channel and washover facies resting unconformably on older sediments (Pleistocene in Fig. 16A). This thin layer is truncated by the ravinement surface, which in turn is overlain by offshore storm deposits in an overall transgressive, fining-upward succession.

Under conditions of continuous but slow erosional shoreface retreat, certain architectural elements of transgressive depositional systems may be preserved. Transgression of a coastal plain previously dissected by an episode of significant sea level fall will produce shore-normal estuaries and shore-parallel lagoons (both with associated tidal channels). The resultant stratigraphic succession would be characterized by an inner-shelf sand sheet that overlies fluvial and estuarine sediments which fill former subaerial valleys (Nummedal and Swift, 1987; Reinson *et al.*, 1988; Boreen and Walker, 1991). Indeed, relict tidal inlets and channels have been interpreted for the numerous incised channels found to be cutting the middle-inner continental shelf off North Carolina (Hine and Snyder, 1985).

The *in place drowning* model (Fig. 16B) has been proposed as an alternative to erosional shoreface retreat. It is suggested that the barrier remains in place as sea level rises, until the wave zone reaches the top of the barrier. The wave zone then oversteps landward and a new sand barrier forms on the inner side of the lagoonal estuary. The old barrier system is essentially drowned in place (Rampino and Sanders, 1980). This in place drowning model predicts successions with a high preservation potential, such that with rapid relative rise of sea level, almost complete transgressive sequences could be preserved (Fischer, 1961; Swift, 1975).

Transgressive vertical successions

Specific vertical successions can indicate the type of shoreline being transgressed, whether it is tide or storm

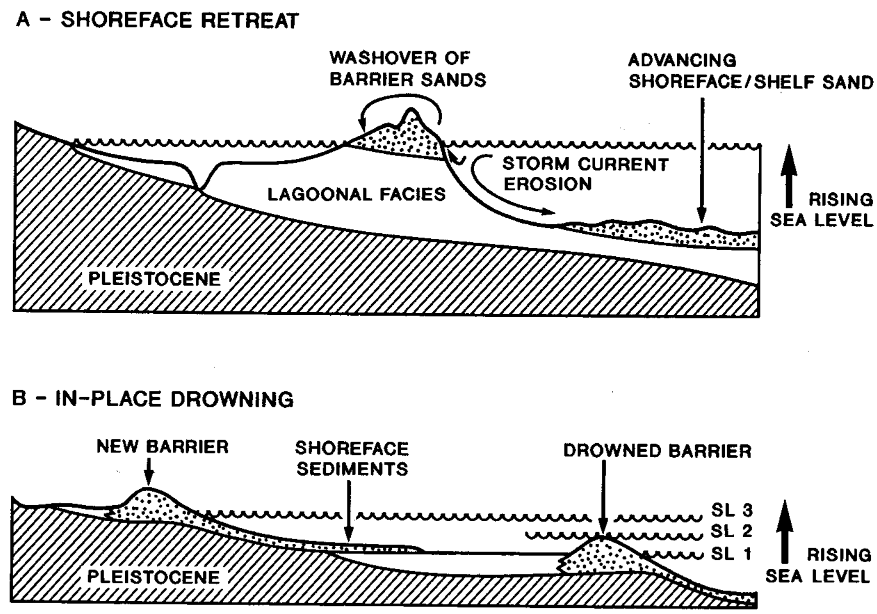

Figure 16 Mechanisms of landward barrier migration during a transgression by shoreface retreat (A) and by in place drowning (B). Modified after Rampino and Sanders (1980) and Elliott (1986).

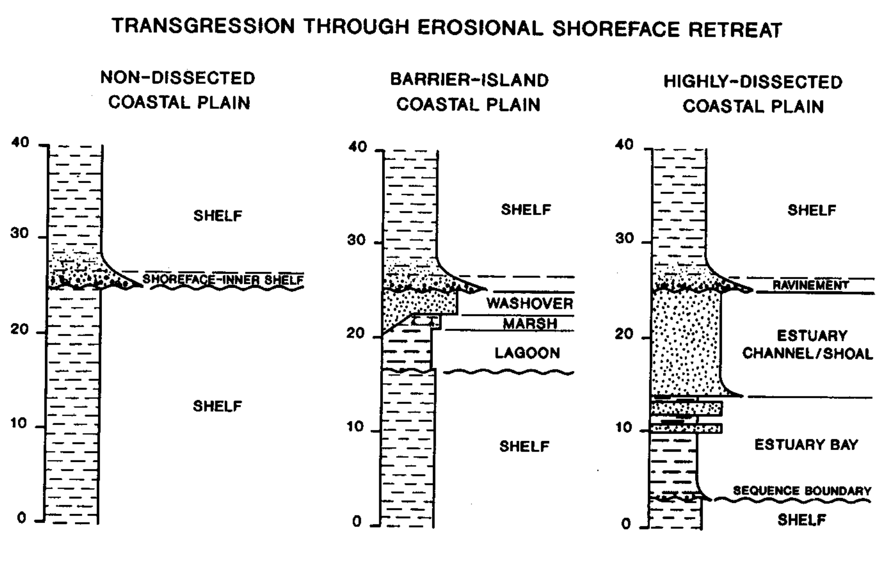

Figure 17 Generalized "end-member" transgressive facies successions for nondissected, barrier-island, and highly dissected coastal plain settings.

wave dominated, whether there may be thick shore-parallel or shore-normal sand bodies along depositional strike, or whether extensive estuarine channel or valley-fill deposits are likely to be present. For example, the transgressive vertical succession expected on an overwash-dominated coast (Fig. 15A) will indicate a high wave energy, microtidal coast with abundant shore-parallel lagoons and a paucity of large active tidal inlets. This is in contrast to the facies succession indicative of a mesotidal coast dominated by tidal channels and spits. Here, thick channel sands occur below the ravinement surface (Fig. 15B). The vertical facies succession generated in a large estuary (Fig. 15C) should exhibit an overall coarsening-upward succession that represents the superposition of distal over proximal deposits as the estuary mouth transgresses landward. Note the similarity of this succession to the estuary bay sequences illustrated in Figure 13. The thinnest transgressive vertical succession (Fig. 15D) is produced when shoreface retreat erodes below the sequence boundary; for practical purposes, the sequence boundary and ravinement surface are coincident. The thin transgressive shoreface deposits of Figure 15D are similar to many of the transgressive coarse-grained deposits in the Cardium Formation (Chapter 12, and Figure 8 in Chapter 1). Careful study of Figure 15 shows that many bounding discontinuities are difficult to identify, and may be even more difficult to interpret. They raise many problems in the use of sequence stratigraphic concepts (Chapter 1).

Transgression due to erosional shoreface retreat will tend to create thin facies successions, with only partial preservation or nonpreservation of many of the diagnostic depositional facies. In place drowning would result in preservation of more complete barrier successions, as in the idealized end member models of Figure 9. However, recognition of the partially preserved successions may be difficult. Erosional shoreface retreat may occur in different coastal plain settings (Fig. 17), and different transgressive vertical facies successions would be generated. Figure 17 is generalized, but encompasses several variations which have been discussed and illustrated in Figures 13 and 15.

TRANSGRESSIVE BARRIER AND ESTUARY MODELS

Vertical facies successions formed during transgression of barrier island and estuarine systems can be highly variable in terms of thickness and facies complexity. Their degree of preservation in the rock record will also be varied and dependent upon the factors that govern the mechanism and rate of transgression (erosional shoreface retreat versus rapid inundation). Intense shoreface erosion during transgression will tend to favour preservation of only partial sequences whereas rapid inundation should result in the preservation of almost complete successions. If complete successions are present in the geological record, they should be similar to the "end member" barrier model described by Reinson (1984).

Transgressions commonly affect coastal plains that have recently been dissected during a significant base level drop. This may lead to the preservation of characteristic incised valley fill and estuary sequences overlain by inner shelf deposits (Fig. 17). Estuaries are by definition transgressive depositional systems; therefore estuarine successions should be associated with other transgressive deposits as part of the transgressive systems tract. On wave-dominated and microtidal barrier island coasts which have not been highly dissected by a preceding base level drop, intense transgressive erosion of the shoreface will lead to preservation of a thin back-barrier lagoon deposit capped by an extremely thin coarse lag which records the ravinement surface. This, in turn, will be overlain by offshore deposits (partly bioturbated mudstones, partly storm-emplaced sandstones). In the extreme case of a nondissected mainland coast the only evidence of transgression by erosional shoreface retreat will be the thin ravinement lag deposit encased in shelf sediments (Fig. 17).

Barrier island and estuarine systems clearly respond rapidly and sensitively to relative fluctuations of sea level. It is therefore very important to identify correctly the various bounding discontinuities, in order that the discrete units (allostratigraphic units) can be recognized, and interpreted in vertical succession. A fall in sea level may result in valley downcutting (incision) with corresponding erosion in the marine realm (regressive surface of erosion; Chapters 1 and 12). During rising sea level, the surface of initial transgression is very important in estuarine deposits. It may lie above a preserved lag of fluvial deposits in the estuary, or it may coincide with the basal (initially fluvial) erosion surface if all of the fluvial deposits have been reworked during initial transgression. The estuary fill may be truncated by a second transgressive erosion surface (ravinement surface) or, in open-ended estuaries, the estuary fill may grade vertically into nearshore marine deposits. Elucidation of estuary type and the history of sea level fluctuation is therefore dependent largely on the identification and correct interpretation of the bounding discontinuities.

ACKNOWLEDGEMENTS

I thank Roger Walker and Douglas Cant for critical review of the preliminary manuscript. I am grateful to Eleanor Gordon for typing the various manuscripts and Peter Gubitz who drafted the figures.

REFERENCES

Basic sources of information

Davis, R.A., Jr., ed., 1985, Coastal sedimentary environments: New York, Springer-Verlag, 716 p.
Contains excellent review chapters on estuaries (M.M. Nichols and R.B. Biggs), tidal inlets and deltas (J.C. Boothroyd), and shoreface environments (A.W. Niedoroda, D.J.P. Swift and T.S. Hopkins).

Elliott, T., 1986, Clastic shorelines, *in* Reading, H.G., ed., Sedimentary environments and facies: Oxford, Blackwell Scientific Publications, p. 143-177.
Excellent general synthesis of nondeltaic shoreline deposits including barrier-islands, strandplains, estuaries and tidal flats.

Lauff, G.H., ed., 1967, Estuaries: Washington, D.C., American Association for the Advancement of Science, Publication 83, 747 p.
Although 25 years old, this book remains one of the best integrated compilations of sedimentological, hydrological and biological studies on modern estuarine environments.

Nummedal, D., Pilkey, O.H. and Howard, J.D., eds., 1987, Sea-level fluctuation and coastal evolution: Society of Economic Paleontologists and Mineralogists, Special Publication 41, 267 p.
This volume includes several excellent papers (Davis and Clifton, Demarest and Kraft, Nummedal and Swift), dealing with the stratigraphic implications of transgressions on marginal marine and coastal plain successions.

Oertel, G.F. and Leatherman, S.P., eds., 1985, Barrier islands: Marine Geology, v. 63, p. 1-396.
Comprehensive special issue of the journal Marine Geology, including 13 papers on barrier islands, inlets, deltas, lagoons and associated shoreline and barrier platform elements.

Smith, D.G., Reinson, G.E., Zaitlin, B.A. and Rahmani, R.A., eds., 1991, Clastic tidal sedimentology: Canadian Society of Petroleum Geologists, Memoir 16, 307 p.
This volume contains several excellent papers on estuaries and related tidal-inshore deposits and facies.

Wilgus, C.K., Hastings, B.S., Posamentier, H.W., Ross, C.A. and Kendall, C.G.St.C., eds., 1988, Sea level changes: an integrated approach: Society of Economic Paleontologists and Mineralogists, Special Publication 42, 407 p.
Collection of papers emphasizing conceptual basis of sequence stratigraphy plus numerous case studies of sea level change from the geological record.

Other references

Allen, G.P., 1991, Sedimentary processes and facies in the Gironde estuary: a model for macrotidal estuarine systems, *in* Smith, D.G., Reinson, G.E., Zaitlin, B.A. and Rahmani, R.A., eds., Clastic tidal sedimentology: Canadian Society of Petroleum Geologists, Memoir 16, p. 219-226.

Ashley, G.M., ed., 1988, The hydrodynamics and sedimentology of a back-barrier lagoon-salt marsh system, Great Sound, New Jersey: Marine Geology, v. 82, p. 1-132.

Barwis, J.H., 1990, Flood-tidal delta reservoirs, Medota-Dickinson Trend, North Dakota, *in* Barwis, J.H., McPherson, J.G. and Studlick, R.J., eds., Sandstone petroleum reservoirs: New York, Springer-Verlag, p. 389-412.

Barwis, J.H. and Makurath, J.H., 1978, Recognition of ancient tidal inlet sequences: an example from the Upper Silurian Keyser Limestone in Virginia: Sedimentology, v. 25, p. 61-82.

Bird, E.C.F., 1967, Depositional features in estuaries and lagoons on the south Coast of New South Wales: Australian Geographical Studies, v. 5, p. 113-124.

Boersma, J.R., 1991, A large flood-tidal delta and its successive spillover apron: detailed proximal-distal facies relationships (Miogene lignite Suite, Lower Rhine Embayment, Germany), *in* Smith, D.G., Reinson, G.E., Zaitlin, B.A. and Rahmani, R.A., eds., Clastic tidal sedimentology: Canadian Society of Petroleum Geologists, Memoir 16, p. 227-254.

Boothroyd, J.C., 1985, Tidal inlets and tidal deltas, *in* Davis, R.A., Jr., ed., Coastal sedimentary environments: New York, Springer-Verlag, p. 445-533.

Boothroyd, J.C., Friedrich, N.E. and McGinn, S.R., 1985, Geology of microtidal coastal lagoons: Rhode Island: Marine Geology, v. 63, p. 35-76.

Boreen, T. and Walker, R.G., 1991, Definition of allomembers and their facies assemblages in the Viking Formation, Willesden Green area, Alberta: Bulletin of Canadian Petroleum Geology, v. 39, p. 123-144.

Boyd, R., Bowen, A.J. and Hall, R.K., 1987, An evolutionary model for transgressive sedimentation on the eastern shore of Nova Scotia, *in* FitzGerald, D.M. and Rosen, P.S., eds., Glaciated coasts: New York, Academic Press, p. 87-114.

Bridges, P.H., 1976, Lower Silurian transgressive barrier islands, southwest Wales: Sedimentology, v. 23, p. 374-362.

Carter, C.H., 1978, A regressive barrier and barrier-protected deposit: depositional environment and geographic setting of the Late Tertiary Cohansey Sand: Journal of Sedimentary Petrology, v. 48, p. 933-950.

Cheel, R.J. and Leckie, D.A., 1990, A tidal-inlet complex in the Cretaceous epeiric sea of North America: Virgelle Member, Milk River Formation, southern Alberta, Canada: Sedimentology, v. 37, p. 67-81.

Clark, J.E. and Reinson, G.E., 1990, Continuity and performance of an estuarine reservoir, Crystal Field, Alberta, Canada, *in* Barwis, J.H., McPherson, J.G. and Studlick, J.R.J., eds., Sandstone petroleum reservoirs: New York, Springer-Verlag, p. 342-362.

Clifton, H.E., 1982, Estuarine deposits, *in* Scholle, P.A. and Spearing, D., eds., Sandstone depositional environments American Association of Petroleum Geologists, Memoir 31, p. 179-189.

Cook, P.J. and Mayo, W., 1977, Sedimentology and Holocene history of a tropical estuary (Broad Sound, Queensland): Australian Bureau of Mineral Resources, Geology and Geophysics, Bulletin 170, 206 p.

Dalrymple, R.W., Zaitlin, B.A. and Boyd, R., 1992, A conceptual model of estuarine sedimentation: Journal of Sedimentary Petrology (in press).

Davis, R.A., Jr. and Hayes, M.O., 1984, What is a wave-dominated coast: Marine Geology, v. 60, p. 313-329.

Demarest, J.M., II and Kraft, J.C., 1987, Stratigraphic record of Quaternay sea levels: implication for more ancient strata, *in* Nummedal, D., Pilkey, O.H. and Howard, J.D., eds., Sea-level fluctuation and coastal evolution: Society of Economic Paleontologists and Mineralogists, Special Publication 41, 267 p.

Devine, P.E., 1991, Transgressive origin of channelled estuarine deposits in the Point Lookout Sandstone, northwestern New Mexico: a model for Upper Cretaceous, cyclic regressive parasequences of the U.S. Western Interior: American Association of Petroleum Geologists, Bulletin, v. 75, p. 1039-1063.

Emery, K.O., 1967, Estuaries and lagoons in relation to continental shelves, *in* Lauff, G.H., ed., Estuaries: American Association for the Advancement of Science, Special Publication 83, p. 9-11.

Fairbridge, R.W., 1980, The estuary: its definition and geodynamic cycle, *in* Olausson, E. and Cato, I., eds., Chemistry and biogeochemistry of estuaries: New York, John Wiley and Sons, p. 1-36.

Field, M.E. and Duane, D.B., 1976, Post-Pleistocene history of the United States inner continental shelf. Significance to origin of barrier islands: Geological Society of America, Bulletin, v. 87, p. 691-702.

Fischer, A.G., 1961, Stratigraphic record of transgressing seas in light of sedimentation on Atlantic Coast of New Jersey: American Association of Petroleum Geologists, Bulletin, v. 45, p. 1656-1666.

Fletcher, C.H., III, Knebel, H.J. and Kraft, J.C., 1990, Holocene evolution of an estuarine coast and tidal wetlands: Geological Society of America, Bulletin, v. 102, p. 283-297.

Frey, R.W. and Howard, J.D., 1986, Mesotidal estuarine sequences: a perspective from the Georgia Bight: Journal of Sedimentary Petrology, v. 56, p. 911-924.

Glaeser, J.E., 1978, Global distribution of barrier islands in terms of tectonic setting: Journal of Geology, v. 86, p. 283-297.

Hayes, M.O., 1975, Morphology of sand accumulations in estuaries, *in* Cronin, L.E., ed., Estuarine research, v. 2, Geology and engineering: New York, Academic Press, p. 3-22.

Hayes, M.O., 1979, Barrier-island morphology as a function of tidal and wave regime, *in* Leatherman, S.P., ed., Barrier islands — from the Gulf of St. Lawrence to the Gulf of Mexico: New York, Academic Press, p. 1-28.

Hayes, M.O., 1980, General morphology and sediment patterns in tidal inlets: Sedimentary Geology, v. 26, p. 139-156.

Hennessy, J.T. and Zarillo, G.A., 1987, The interrelation and distinction between flood-tidal delta and washover deposits in a transgressive barrier island: Marine Geology, v. 78, p. 35-56.

Heron, S.D., Jr., Moslow, T.F., Berelson, W.M., Herbert, J.R., Steele, G.A., III and Susman, K.R., 1984, Holocene sedimentation of a wave-dominated barrier-island shoreline: Cape Lookout, North Carolina, *in* Greenwood, B. and Davis, R.A., Jr., eds., Hydrodynamics and sedimentation in wave-dominated coastal environments: Marine Geology, v. 60, p. 413-434.

Hine, A.C. and Snyder, S.W., 1985, Coastal lithosome preservation: evidence from the shoreface and inner continental shelf off Bogue Banks, North Carolina: Marine Geology v. 63, p. 307-330.

Hobday, D.K. and Jackson, M.P.A., 1979, Transgressive shore zone sedimentation and syndepositional deformation in the Pleistocene of Zululand, South Africa: Journal of Sedimentary Petrology, v. 49, p. 145-158.

Horne, J.C. and Ferm, J.C., 1978, Carboniferous depositional environments: eastern Kentucky and southern West Virginia: Department of Geology, University of South Carolina, 151 p.

Howard, R.H. and Whitaker, S.T., 1990, Fluvial-estuarine valley fill at the Mississippian-Pennsylvanian unconformity, Main Consolidated field, Illinois, *in* Barwis, J.H., McPherson, J.G. and Studlick, R.J., eds., Sandstone petroleum reservoirs: New York, Springer-Verlag, p. 319-341.

Hoyt, J.H. and Henry, V.J., Jr., 1965, Significance of inlet sedimentation in the recognition of ancient barrier islands: Wyoming Geological Association, 19th Field Conference Guidebook, p. 190-194.

Kennedy, V.S., ed., 1982, Estuarine comparisons: New York, Academic Press, 609 p.

Kirschbaum, M.A., 1989, Lagoonal deposits in the Upper Cretaceous Rock Springs Formation (Mesaverde Group) southwest Wyoming: Marine Geology, v. 88, p. 349-364.

Kraft, J.C. and Chrzastowski, M.J., 1985, Coastal stratigraphic sequences, *in* Davis, R.A., Jr., ed., Coastal sedimentary environments: New York, Springer-Verlag, p. 625-663.

Kreisa, R.D. and Moiola, R.J., 1986, Sigmoidal tidal bundles and other tide-generated sedimentary structures of the Curtis Formation, Utah: Geological Society of America, Bulletin, v. 97, p. 381-387.

Kuecher, G.J., Woodland, B.G. and Broadhurst, F.M., 1990, Evidence of deposition from individual tides and of tidal cycles from the Francis Creek Shale (host rock to the Mazon Creek biota), Westphalian D (Pennsylvanian), northeastern Illinois: Sedimentary Geology, v. 68, p. 211-221.

Kulm, L.D. and Byrne, J.V., 1967, Sediments of Yaquina Bay, Oregon, *in* Lauff, G.H., ed., Estuaries: Washington, D.C., American Association for the Advancement of Science, Special Publication 83, p. 226-238.

Kumar, N. and Sanders, J.E., 1974, Inlet sequence: a vertical succession of sedimentary structures and textures created by the lateral migration of tidal inlets: Sedimentology, v. 21, p. 491-532.

Land, C.B., Jr., 1972, Stratigraphy of Fox Hills Sandstone and associated formations, Rock Springs uplift and Wamsutter arch area, Sweetwater County, Wyoming: a shoreline-estuary sandstone model for the Late Cretaceous: Colorado School of Mines, Quarterly Journal, v. 67, 69 p.

Leckie, D.A. and Singh, C., 1991, Estuarine deposits of the Albian Paddy Member (Peace River Formation) and lowermost Shaftesbury Formation, Alberta, Canada: Journal of Sedimentary Petrology, v. 61, p. 825-850.

Meade, R.H., 1969, Landward transport of bottom sediments in estuaries of the Atlantic coastal plain: Journal of Sedimentary Petrology, v. 39, p. 222-234.

Milliman, J.D. and Emery, K.D., 1968, Sea levels during the past 35,000 years: Science, v. 162, p. 1121-1123.

Moslow, T.F. and Tye, R.S., 1985, Recognition and characterization of Holocene tidal inlet sequences: Marine Geology, v. 63, p. 129-151.

Murakoshi, N. and Masuda, F., 1991, A depositional model for a flood-tidal delta and washover sands in the late Pleistocene Paleo-Tokyo Bay, Japan, *in* Smith, D.G., Reinson, G.E., Zaitlin, B.A. and Rahmani, R.A., eds., Clastic tidal sedimentology: Canadian Society of Petroleum Geologists, Memoir 16, p. 219-226.

Nichol, S.L., 1991, Zonation and sedimentology of estuarine facies in an incised-valley, wave-dominated, microtidal setting, New South Wales, Australia, *in* Smith, D.G., Reinson, G.E., Zaitlin, B.A. and Rahmani, R.A., eds., Clastic tidal sedimentology: Canadian Society of Petroleum Geologists, Memoir 16, p. 41-58.

Nichols, M.J., 1989, Sediment accumulation rates and relative sea level rise in lagoons: Marine Geology, v. 88, p. 201-220.

Nichols, M.M. and Biggs, R.B., 1985, Estuaries, *in* Davis, R.A., Jr., ed., Coastal sedimentary environments: New York, Springer-Verlag, p. 77-173.

Nichols, M.M., Johnson, G.H. and Peebles, P.C., 1991, Modern sediments and facies model for a microtidal coastal plain estuary, the James Estuary, Virginia: Journal of Sedimentary Petrology, v. 61, p. 883-899.

Niedoroda, A.W., Swift, D.J.P. and Hopkins, T.S., 1985, The shoreface, *in* Davis, R.A., Jr., ed., Coastal sedimentary environments: New York, Springer-Verlag, p. 533-624.

Nio, S.D. and Yang, C.S., 1991, Diagnostic attributes of clastic tidal deposits: a review, *in* Smith, D.G., Reinson, G.E., Zaitlin, B.A. and Rahmani, R.A., eds., Clastic tidal sedimentology: Canadian Society of Petroleum Geologists, Memoir 16, p. 3-28.

Nummedal, D. and Swift, D.J.P., 1987, Transgressive stratigraphy at sequence-bounding unconformities: some principles derived from Holocene and Cretaceous examples, *in* Nummedal, D., Pilkey, O.H. and Howard, J.D., eds., Sea-level fluctuation and coastal evolution: Society of Economic Paleontologists and Mineralogists, Special Publication 41, p. 241-260.

Oertel, G.F., Kearney, M.S., Leatherman, S.P. and Woo, J., 1989, Anatomy of a barrier platform: outer barrier lagoon, southern Delmarva Peninsula, Virginia: Marine Geology, v. 88, p. 303-318.

Olausson, E. and Cato, I., eds., 1980, Chemistry and biogeochemistry of estuaries: New York, John Wiley and Sons, 452 p.

Pritchard, D.W., 1967, What is an estuary: physical standpoint?, *in* Lauff, G.H., ed., Estuaries: Washington, D.C., American Association for Advancement of Science, Publication 83, p. 3-5.

Rahmani, R.A., 1988, Estuarine tidal channel and nearshore sedimentation of a late Cretaceous epicontinental sea, Drumheller, Alberta, Canada, *in* de Boer, P.L., Van Gelder, A. and Nio, S.D., eds., Tide-influenced sedimentary environments and facies: Dordrecht, D. Riedel Publishing Company, p. 433-471.

Rahmani, R., 1989, Cretaceous tidal estuarine and deltaic deposits, Drumheller, Alberta: Canadian Society of Petroleum Geologists, Second International Research Symposium on Clastic Tidal Deposits, Field trip guidebook, 55 p.

Rampino, M.R. and Sanders, J.E., 1980, Holocene transgression in south-central Long Island, New York: Journal of Sedimentary Petrology, v. 50, p. 1063-1080.

Reinson, G.E., 1977a, Hydrology and sediments of a temperate estuary — Mallacoota Inlet, Victoria: Australian Bureau of Mineral Resources, Geology and Geophysics, Bulletin 178, 91 p.

Reinson, G.E., 1977b, Tidal current control of submarine morphology at the mouth of the Miramichi estuary, New Brunswick: Canadian Journal of Earth Sciences, v. 14, p. 2524-2532.

Reinson, G.E., 1981, Variations in tidal-inlet morphology and stability, northeast New Brunswick, *in* McCann, S.B., ed., The coastline of Canada: Geological Survey of Canada, Paper 80-10, p. 23-39

Reinson, G.E., 1984, Barrier-island and associated strand-plain systems, *in* Walker, R.G., ed., Facies models: Geological Association of Canada, Geoscience Canada Reprint Series 1, p. 119-140.

Reinson, G.E., ed., 1989, Modern and ancient examples of clastic tidal deposits — a core and peel workshop: Canadian Society of Petroleum Geologists, Second International Research Symposium on Clastic Tidal Deposits, 126 p.

Reinson, G.E., Clark, J.E. and Foscolos, A.E., 1988, Reservoir geology of Crystal Viking field, Lower Cretaceous estuarine tidal channel-bay complex, south-central Alberta: American Association of Petroleum Geologists, Bulletin, v. 72, p. 1270-1294.

Ricketts, B.D., 1991, Lower Paleocene drowned valley and barred estuaries, Canadian Arctic Islands: aspects of their geomorphological and sedimentological evolution, *in* Smith, D.G., Reinson, G.E., Zaitlin, B.A. and Rahmani, R.A., eds., Clastic tidal sedimentology: Canadian Society of Petroleum Geologists, Memoir 16, p. 81-106.

Roy, P.S., 1984, New South Wales estuaries: their origin and evolution, *in* Thom, B.G., ed., Coastal geomorphology in Australia: Sydney, Academic Press, p. 99-121.

Schwartz, M.L., ed., 1973, Barrier islands: Stroudsburg, PA, Dowden, Hutchinson and Ross, 451 p.

Schwartz, R.K., 1982, Bedforms and stratification characteristics of some modern small-scale washover sand bodies: Sedimentology, v. 29, p. 835-850.

Swift, D.J.P., 1975, Barrier island genesis: evidence from the Middle Atlantic shelf of North America: Sedimentary Geology, v. 14, p. 1-43.

Thom, B.G., 1984, Sand barriers of eastern Australia: Gippsland — a case study, *in* Thom, B.G., ed., Coastal geomorphology in Australia: Sydney, Academic Press, p. 233-261.

Thomas, R.G., Smith, D.G., Wood, J.M., Visser, J., Calverley-Range, E.A. and Koster, E.H., 1987, Inclined heterolithic stratification — terminology, description, interpretation and significance: Sedimentary Geology, v. 53, p. 123-179.

Van Wagoner, J.C., Mitchum, R.M., Campion, K.M. and Rahmanian, V.D., 1990, Siliciclastic sequence stratigraphy in well logs, cores, and outcrops: American Association of Petroleum Geologists, Methods in Exploration Series 7, 55 p.

Ward, L.G. and Ashley, G.M., eds., 1989, Physical processes and sedimentology of siliciclastic-dominated lagoonal systems: Marine Geology, v. 88, p. 181-364.

Wheeler, D.M., Scott, A.J., Coringrato, V.J. and Devine, P.E., 1990, Stratigraphy and depositional history of the Morrow Formation, southeast Colorado and southwest Kansas, *in* Sonnenberg, S.A., Shannon, L.T., Rader, K., Von Drehle, W.F. and Martin, G.W., eds., Morrow Sandstones of Southeast Colorado and adjacent areas: Denver, Rocky Mountain Association of Geologists, p. 9-37.

Wightman, D.M., Pemberton, S.G. and Singh, C., 1987, Depositional modelling of the upper Mannville (Lower Cretaceous), east central Alberta: implications for the recognition of brackish water deposits, *in* Tillman, R.W. and Weber, K.J., eds., Reservoir sedimentology: Society of Economic Paleontologists and Mineralogists, Special Publication 40, p. 190-220.

Wood, J.M. and Hopkins, J.C., 1989, Reservoir sandstone bodies in estuarine valley-fill: Lower Cretaceous Glauconitic Member, Little Bow field, Alberta, Canada: American Association of Petroleum Geologists, Bulletin, v. 73, p. 1361-1382.

Zaitlin, B.A. and Shultz, B.C., 1990, Wave-influenced estuarine sand body, Senlac heavy oil pool, Saskatchewan, Canada, *in* Barwis, J.H., McPherson, J.G. and Studlick R.J., eds., Sandstone petroleum reservoirs: New York, Springer-Verlag, p. 363-387.

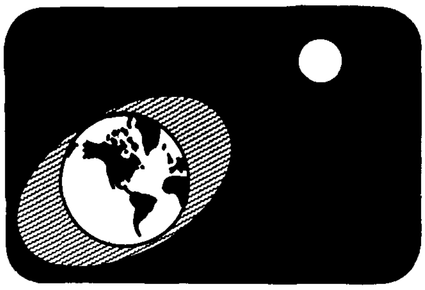

11. Tidal Depositional Systems

Robert W. Dalrymple, Department of Geological Sciences, Queen's University, Kingston, Ontario K7L 3N6

INTRODUCTION

Most books, including former editions of *Facies Models*, subdivide coastal and shallow marine environments on the basis of geomorphology (e.g., deltas, barrier islands, shelves). As a result, tide-dominated environments are discussed in several different chapters. However, the tidal sand ridges that characterize tide-dominated deltas have more in common with tidal shelf and estuarine sand ridges than with the distributary mouth bars of fluvially dominated deltas, or with the shoreface of wave-dominated deltas and barrier coastlines.

This chapter takes a new approach, examining all tide-dominated depositional systems together (tidal flats, estuaries, deltas and shelves), and discussing their response to changes of relative sea level. Thus it is recognized that the relative intensity of the *processes* (tidal currents, waves, storm-generated currents, and fluvial currents) determines the character of the deposits as much, if not more, than the geomorphological setting (Galloway, 1975; Hayes, 1979; Johnson and Baldwin, 1986).

Tidal dominance over other processes is most common in areas where the tidal range is large, because this results in strong tidal currents. Consequently, most *microtidal* (0-2 m tidal range) and *mesotidal* (2-4 m range) areas are wave (or storm) dominated, whereas some *mesotidal* and most *macrotidal* (>4 m range) areas are tide dominated. However, if wave action is limited due to topographic sheltering, or the tidal current speeds are increased by a topographic constriction, tidal dominance can even occur in microtidal areas.

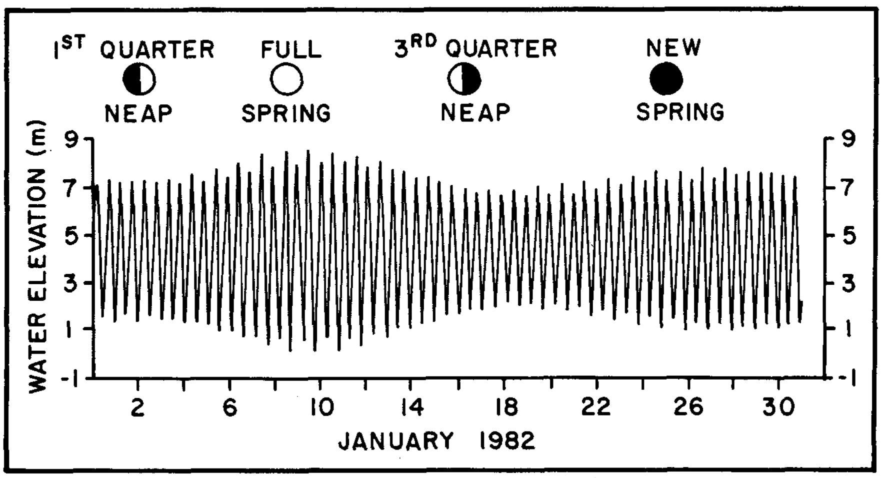

Figure 1 Predicted tidal variations in water level at Saint John, New Brunswick. Following standard practice, the datum is approximately the spring low-tide elevation. The tides are semidiurnal with a pronounced variation in range between neap and spring tides. Tidal-current speeds mimic the variations in tidal range because the range determines the tidal discharge which passes a point each half tidal cycle. After Forrester (1983).

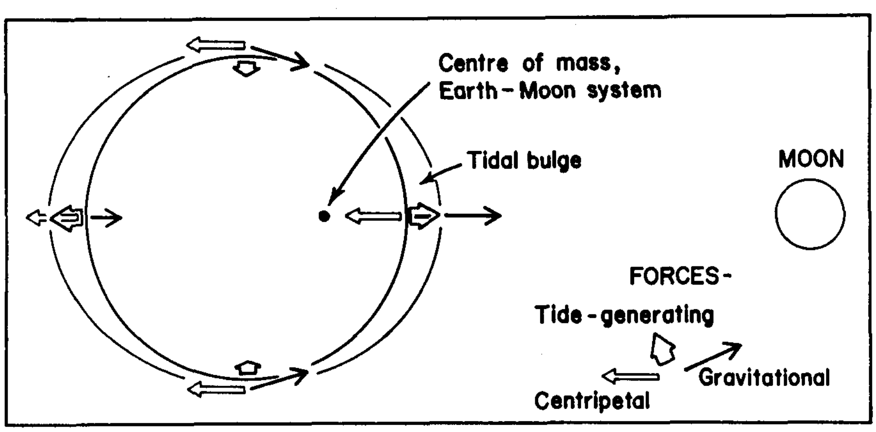

Figure 2 Origin of the tides. On the side of the Earth facing the moon, the tide-generating force is gravitational-minus-centripetal. On the opposite side of the Earth, the gravitational force from the moon is weaker, and the tide-generating force is centripetal-minus-gravitational. At the top and bottom of the Earth, as drawn, the tide-generating force is directed inward, as the resultant of a gravitational force directed toward the moon, and the centripetal force. The centripetal forces affecting the ocean all operate in the same direction, and result from movement of the Earth around the centre of mass of the Earth-moon system. This point is about one-quarter of the distance from the surface to the centre of the Earth. The effects of the gravitational field of the sun have been omitted. Diagram courtesy Roger Walker.

TIDES AND TIDAL CURRENTS

Origin of tides

A *tide* is any *periodic* (regularly repeating) fluctuation in water level (Fig. 1) that is generated by the gravitational attraction of the moon and sun. The moon, because it is closer to the Earth, exerts a tide-generating force which is twice as large as that of the sun. One of the best nonmathematical discussions of the origin of tides is given by the Open University Course Team (1989). More mathematical descriptions are given by Howarth (1982) and Forrester (1983).

Tides represent the vector sum of two forces: 1) the gravitational attraction of the moon, which is strongest on the side of the Earth facing the moon, and 2) the centripetal force caused by the revolution of the Earth-moon system about its common centre of mass. This centripetal force is of uniform intensity all over the Earth (Fig. 2). On the side of the Earth facing the moon, the gravitational attraction of the moon is greater than the oppositely directed centripetal force, while the reverse is true on the other side of the Earth. The water in the oceans therefore piles up in two bulges, one underneath the moon, and the other on the opposite side of the Earth. Because the Earth rotates, the bulges appear to travel around the Earth as two "tidal waves", causing water levels to rise and fall regularly. Rising water levels are known as the *flood* tide, whereas the fall is the *ebb* tide. The most commonly observed period for one complete *tidal cycle* is the *semidiurnal* (twice a day) period of 12.42 hours (Fig. 1). This is longer than 12 hours because the moon orbits in the same

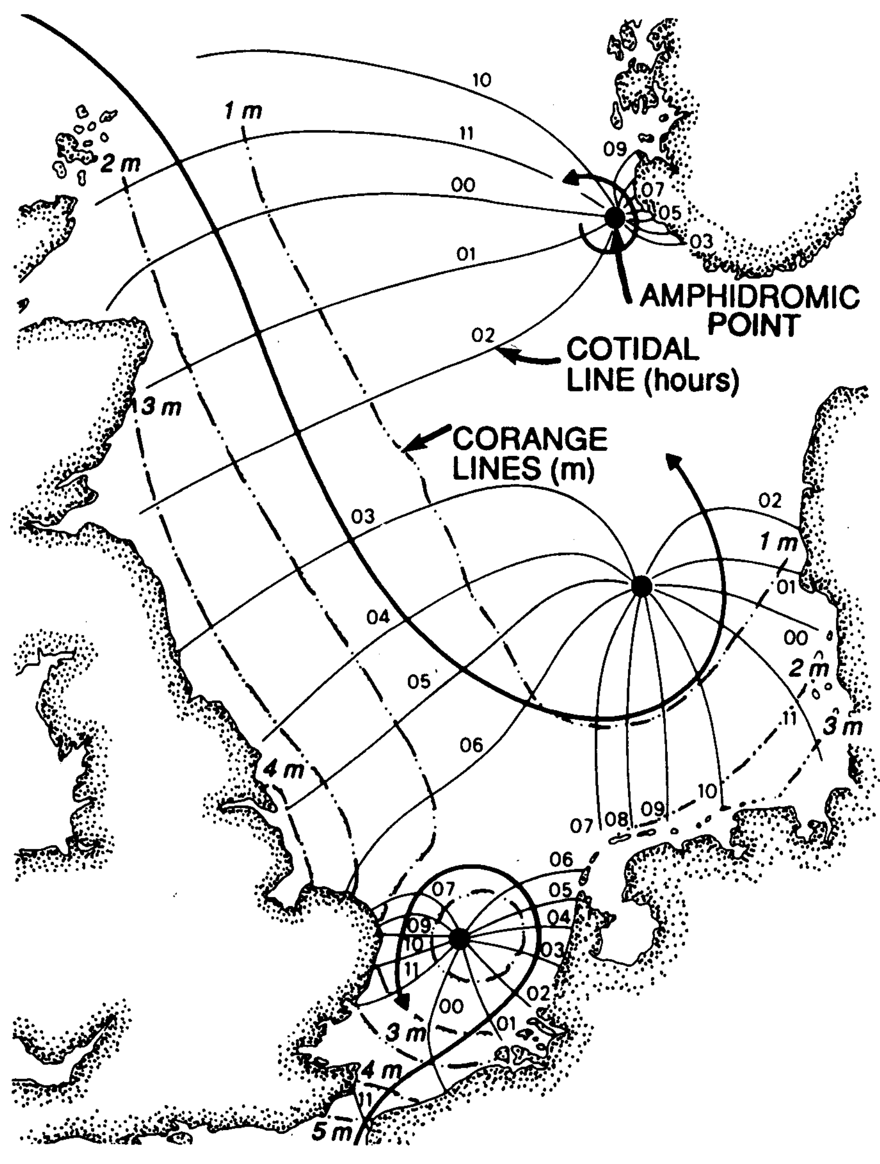

Figure 3 Amphidromic tidal system in the North Sea. The tidal range (dotted corange lines) increases outward from each of the three amphidromic points, with the highest ranges occurring in coastal embayments such as the German Bight (3 m) and those on the east coast of England (4 m). The solid cotidal lines show the times of high water in lunar hours, and indicate the direction of propagation of the tidal wave (anticlockwise). After Houbolt (1968).

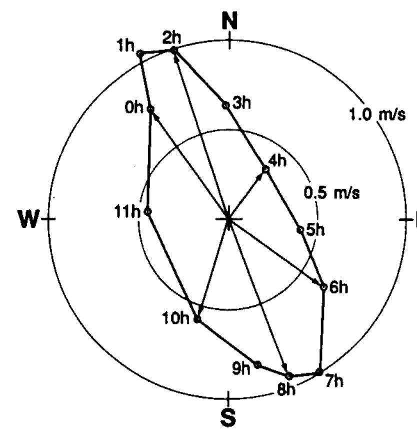

Figure 4 Rotary tidal currents and the tidal ellipse for a site on Georges Bank. The tidal ellipse is constructed by joining the tips of the successive current-velocity vectors which have a length scaled to the current speed. Note that current speeds never fall below 0.3 m/s. After Stewart and Jordan (1964).

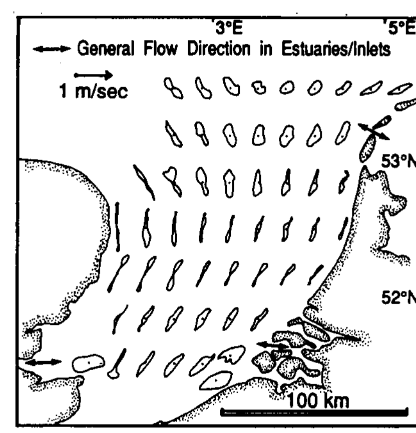

Figure 5 Tidal current ellipses for computed velocities 1 m above the bed in the southern North Sea. Note the extreme elongation of ellipses in the south due to the coastal constriction, and the more circular shapes in the north. Current directions in the mouth of the Thames River and Dutch estuaries are approximately perpendicular to those on the shelf. After McCave (1971).

direction as the Earth rotates, and any point on the surface of the Earth requires a little more than one revolution to return to the peak of the tidal bulge. Because the rotational axis of the Earth is inclined with respect to the orbital plane of the moon most of the time, any given point on the Earth's surface passes closer to the crest of one tidal bulge than the other, thereby adding a *diurnal* (once a day) component to the tidal spectrum. The diurnal component is generally small relative to the semidiurnal tide, but it is the main tidal period in areas where the semidiurnal tide is damped out by destructive interference.

The interaction of the moon and sun produces a still longer periodic variation in *tidal range* (the difference in water level between successive high-tide and low-tide levels). When the sun and moon lie in a straight line relative to the Earth, their effects add to produce greater than average tidal ranges (*spring tides*; Fig. 1). When the sun and moon are at right angles, their forces counteract each other and the tidal range is smaller than average *(neap tides)*. For semidiurnal tides, the spring-neap cycle has a period of 14.77 days, and contains 28 tidal cycles. Diurnal tides have a neap-spring period of 13.66 days that contains 14 tidal cycles.

Tidal range

Because the tide-generating forces are small, only the open oceans develop significant tides, and even these typically have a range of less than 1 m. Smaller bodies of water (including enclosed seas such as the Mediterranean and the water overlying the present-day continental shelves) cannot develop an appreciable tide of their own. The tides which are observed on continental shelves are due to the *forcing* action of the oceanic tide. As the tidal wave moves from the open ocean onto a continental shelf, shoaling, and convergence associated with coastal embayments concentrate the energy within the tidal wave into a smaller cross sectional area, and the tidal range increases. Particularly large ranges occur if the *natural period* of the water body (i.e., the period for the water to "slosh" back and forth in the absence of any forcing action) is close to one of the astronomically determined tidal periods, in which case *resonant amplification* takes place. This is shown dramatically by the Bay of Fundy-Gulf of Maine system where tidal ranges reach 16.3 m.

Tidal currents

Tidal current speeds and flow directions vary systematically over a single tidal cycle. In open shelf settings, far from the confining influence of a coastline, the *Coriolis* force causes the tidal wave to rotate about a fixed *(amphidromic)* point (Fig. 3). Consequently, the tidal current speed and direction are constantly changing, and the tip of the current velocity vector traces out a path termed a *tidal ellipse* over a single tidal cycle (Fig. 4). In the northern hemisphere, the tidal wave typically moves in an anticlockwise direction about an amphidromic point, while the current vectors rotate in a clockwise sense. These *rotary* tides have no *slack-water* period when current speeds decrease to zero. In the ideal case, the tidal ellipse is a circle, but in nearshore areas, the presence of the shoreline causes current speeds to be higher parallel to the coast, and weaker in an onshore-offshore direction (Fig. 5). At the shore, these *rectilinear* currents simply reverse by 180° at each slack water period. In estuaries and coastal embayments, the currents tend to flow into and out of the basin, with flow directions that are at a high angle to the general trend of the shoreline (Fig. 5).

The maximum current speed at any location is controlled by the volume of water that must pass that point in each half tidal cycle. The volume of water is a function of the tidal range *and* the size of the area being drained or flooded. Strong tidal currents are commonly associated with large tidal ranges. However, they can also occur in areas with small tidal ranges if the estuary or embayment is large relative to the cross sectional area of the mouth

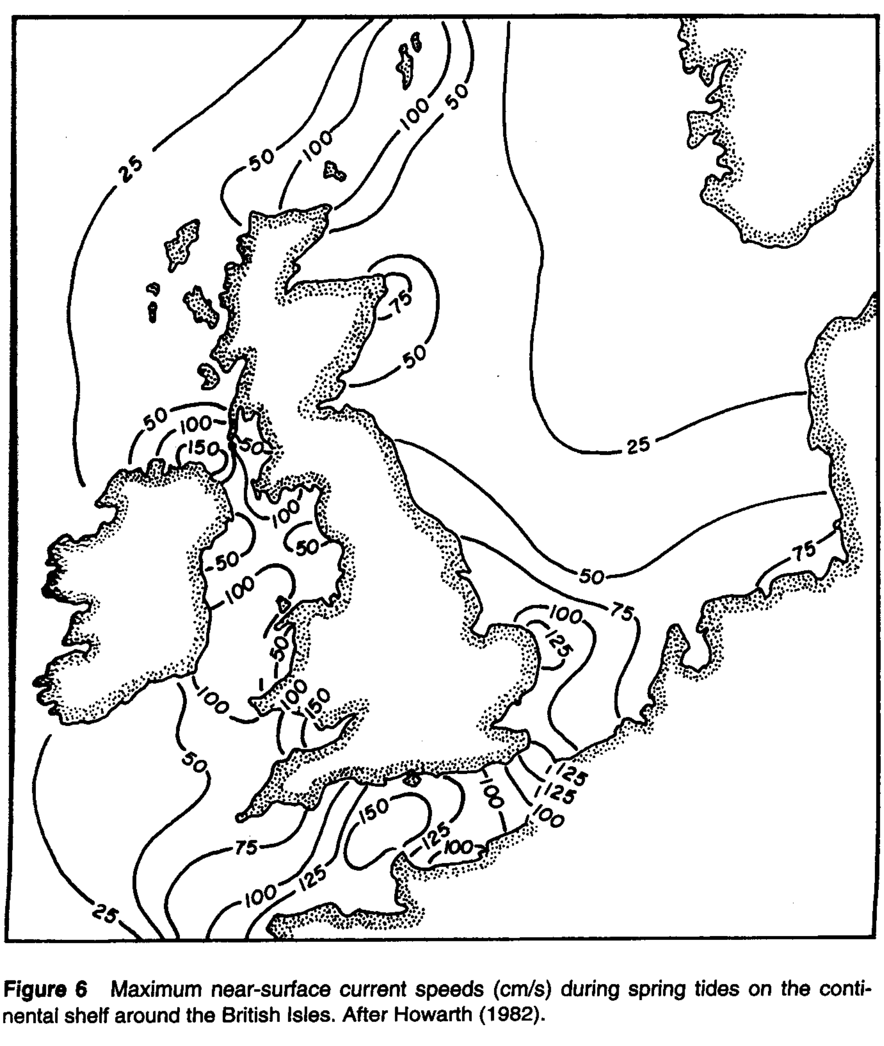

Figure 6 Maximum near-surface current speeds (cm/s) during spring tides on the continental shelf around the British Isles. After Howarth (1982).

through which the flow passes. For example, Chesapeake Bay on the east coast of the United States is microtidal (tidal range 1 m) but has a very small mouth relative to its size. Therefore, maximum, near surface speeds at the entrance are typically greater than 0.5 m/s, and locally exceed 1 m/s. Within the broader inner estuary, current speeds are much less. Similar tidal current speeds typify most tide-dominated environments, including such areas as the macrotidal Bay of Fundy and the southern North Sea and English Channel (Fig. 6). Only very locally in these areas do speeds exceed 1.5 m/s. Thus, the major influence of a large tidal range is not to cause appreciably faster currents, but to increase the area that experiences strong tidal influence.

In general, the fastest tidal currents occur in coastal areas because onshore shallowing increases the tidal range and decreases the cross-sectional area. Topographic constrictions associated with tidal inlets and estuaries also accentuate the currents. Strong tidal currents may also occur on the outer part of the continental shelf if the offshore increase in the volume of water flowing through any shore-parallel section is not compensated by a sufficient increase in water depth. A particularly well-developed example is given by Georges Bank, at the outer edge of the shelf between Nova Scotia and Cape Cod. Tidal current speeds exceed 0.5 m/s in all areas shallower than 60 m, with peak values up to 1.2 m/s (Twichell, 1983). In the deeper water to the north, current speeds are typically less than 0.2 m/s.

Ideally, the speed and duration of the ebb and flood currents are equal, and no net transport of water or sediment occurs. In many coastal areas, however, deformation of the tidal wave and the interaction of the currents with the bottom topography produce inequalities between the flood and ebb currents. As a result, many areas experience a *net* or *residual* transport of sediment in the direction of the stronger *(dominant)* current. The weaker current which flows in the opposite direction is termed the *subordinate* current. Typically, areas of ebb and flood dominance alternate spatially in a system of mutually-evasive, flood-dominated and ebb-dominated channels, producing complicated patterns of sediment transport, as in Bay of Fundy estuaries (Dalrymple *et al.*, 1990).

TIDAL SEDIMENTARY STRUCTURES

The *periodic* changes in current speed and direction which characterize tidal systems produce several sedimentary structures which are diagnostic of tidal deposition. A full discussion is given by Nio and Yang (1991).

Cross bedding containing some type of regularly spaced, internal discontinuities will be formed in areas where the maximum speed of the dominant current is capable of producing dunes. If the subordinate current is capable of eroding the lee face of the dunes formed by the preceding dominant current, *reactivation surfaces* will be produced (Fig. 7). Mud drapes may also be deposited on the lee face during one or both slack-water periods if suspended sediment concentrations are high enough (Figs. 7, 8). Much of this mud may be in the form of fecal pellets rather than individual clay

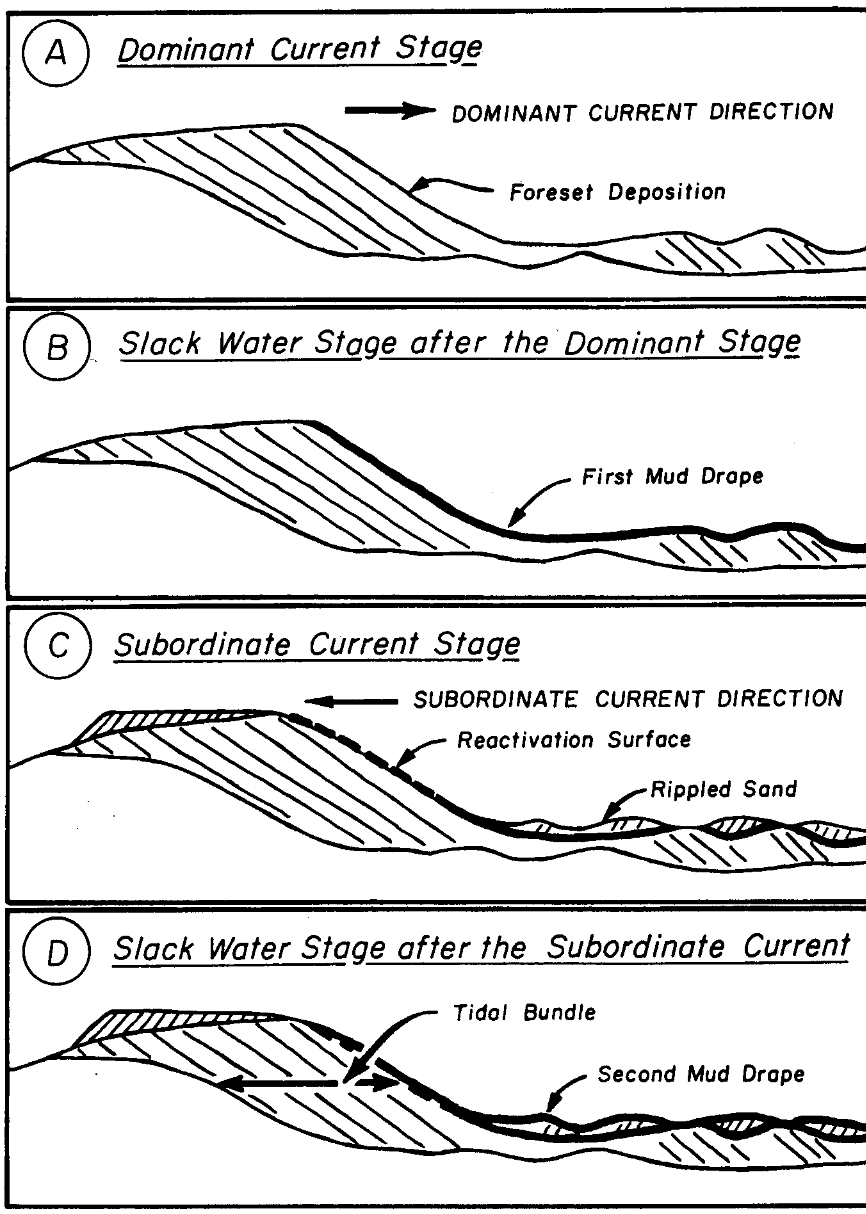

Figure 7 Structures produced in a dune during a tidal cycle. In this example, the currents exhibit a pronounced asymmetry and suspended sediment concentrations are moderately high. A tidal bundle is the deposit of the dominant portion of the tidal cycle. After Visser (1980).

flakes. Typically the amount of sand deposited by the subordinate current is small, and hence the mud drapes deposited after the dominant and subordinate tides are closely spaced (first to second drapes in Figure 7). Mud drapes may not be deposited if there is wave action, or if there are rotary tides that have no slack-water period. The deposit of a single, dominant tide is called a *tidal bundle*, whether bounded by reactivation surfaces or mud drapes (Fig. 7).

Because of the variations in tidal current speed associated with the neap-spring cycle, sequences of tidal bundles commonly show cyclic variations in thickness, with thicker bundles forming during spring tides when currents are stronger and the dune migrates further. Thinner bundles form during neap tides (Fig. 9). If the tides are semidiurnal, there should be 28 tidal bundles within a complete neap-spring cycle of 14.77 days (Fig. 1). There will be fewer than 28 if the maximum current speeds drop below the threshold for sand movement during neap tides (Visser, 1980). There will be 14 or fewer bundles if the tides are diurnal. Excellent ancient examples of tidal bundles have been described by Allen (1982) and Allen and Homewood (1984).

The above structures form only within dunes which do not bear smaller, superimposed dunes. The internal structure of large compound dunes (which are commonly called *sand waves*) is much more complicated, as discussed below.

Herringbone cross stratification, which is marked by opposed *(bipolar)* dip directions in adjacent sets of cross bedding, is widely used as an indication of tidal deposition. However, bipolar cross bedding is not universally developed in tidal sands because the development of either flood or ebb dominance commonly produces a unidirectional paleocurrent pattern. Herringbone cross bedding is most easily recognized in planar tabular cross bedding. In limited outcrops of trough cross bedding, care must be taken to avoid misinterpreting a partial end-on view of troughs.

In many areas, current ripples are the stable bedform instead of dunes. The structures formed in these situations generally belong to the continuum from *flaser bedding* to *lenticular bedding* (Fig. 10; Reineck and Wunderlich, 1968). In the ideal case, a unit of ripples will be formed by the maximum currents of the dominant tide, followed by deposition of a mud layer during the ensuing slack-water period (Fig. 11). If the subordinate current is strong enough, a second rippled unit with an opposite paleocurrent direction will be deposited on top of the first mud drape, followed by another mud drape during the second slack-water interval. More commonly, however, the subordinate current is too weak to deposit sand, and the two mud drapes are amalgamated. Tidal currents which are too slow to produce ripples may still deposit thin sand layers from suspension that alternate with mud laminae. Beds which show cyclic changes in layer thickness due to neap-spring variations in tidal current speed are termed *tidal rhythmites* (Kvale and Archer, 1990; Dalrymple et al., 1991; Williams, 1991).

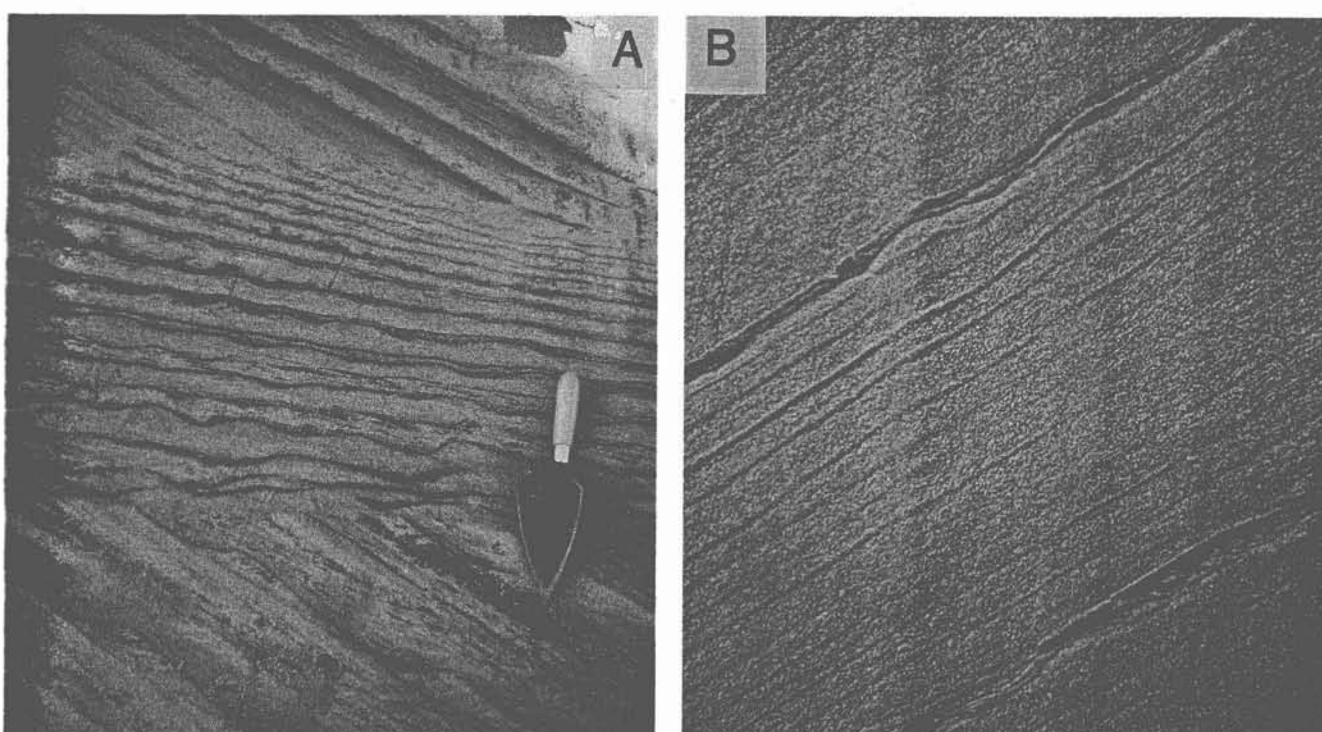

Figure 8 Bundled cross bedding in subtidal sands of the Oosterschelde estuary, the Netherlands. A) Outcrop photo showing repetitive mud drapes in the foresets and bottomsets of two large-scale cross beds. The dark flecks are either organic debris or mud pebbles. Trowel 24 cm long. B) Close-up of foresets showing a complete tidal bundle bounded by mud couplets that enclose subordinate-current ripples. The tidal bundle is approximately 20 cm thick.

TIDE-DOMINATED ENVIRONMENTS

Two environments are common to many tide-dominated depositional systems, 1) sandy to muddy tidal flats which fringe the shoreline, and 2) elongate *tidal sand ridges* or bars, with their superimposed sand waves, that occur offshore from the flats, in estuarine, deltaic and open shallow marine settings.

Tidal flats

In areas with a large tidal range, tidal flats typically rim the margins of back-barrier lagoons, estuaries and the open coast. They may be up to several km wide, and form flat to gently sloping areas (typically <1°) that extend from the *supratidal zone*, through the *intertidal zone*, and into the shallow portion of the *subtidal zone* (Fig. 12; see also Fig. 22). The outer edge of the flats in back-barrier and estuarine settings is commonly bordered by a major tidal channel in which flow is subparallel to the local shoreline. The speeds of both the flood and ebb tidal currents are greatest in these channels, and decrease landward. Consequently, the sediments adjacent to the channel are typically sandy, and pass gradually into muds near the high-tide line. In some lagoons, the tidal flats pass outward into subtidal muds.

The *sand flats* which occupy the lower portion of most tidal flats commonly contain dune cross bedding in areas with high current speeds, and ripple cross lamination in places where the current speed is lower (Fig. 12). The thickness of the cross bed sets generally decreases toward the shore. Parallel lamination may also occur in

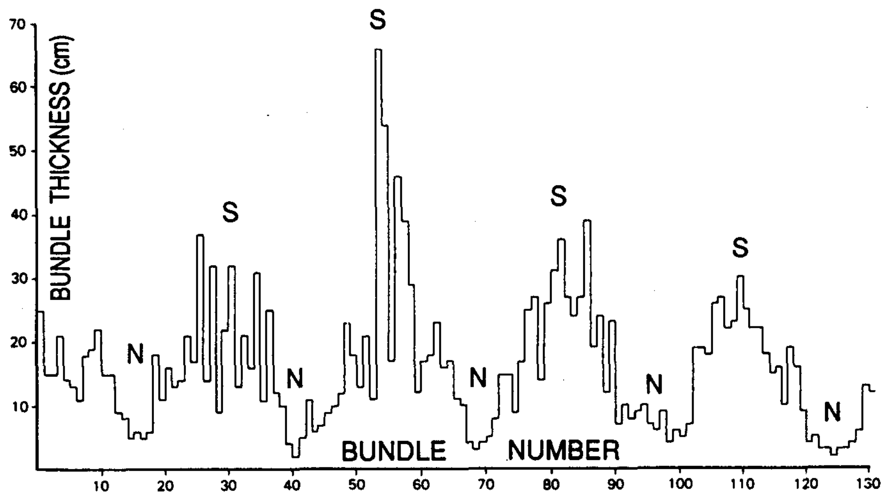

Figure 9 Variation of bundle thickness within a cross bed from the Oosterschelde estuary, the Netherlands. N = neap tides; S = spring tides. The average number of bundles between successive neap tides is 27. The tendency for the thickness of successive bundles to be alternately larger and smaller is due to the diurnal inequality. After Visser (1980).

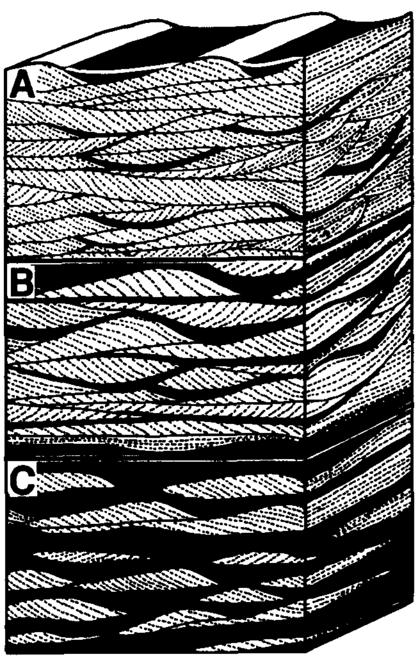

Figure 10 Flaser bedding (A), wavy ("tidal") bedding (B), and lenticular bedding (C). The progression from A to C results from a net decrease in current speed and increased deposition and preservation of mud drapes. After Reineck and Singh (1980).

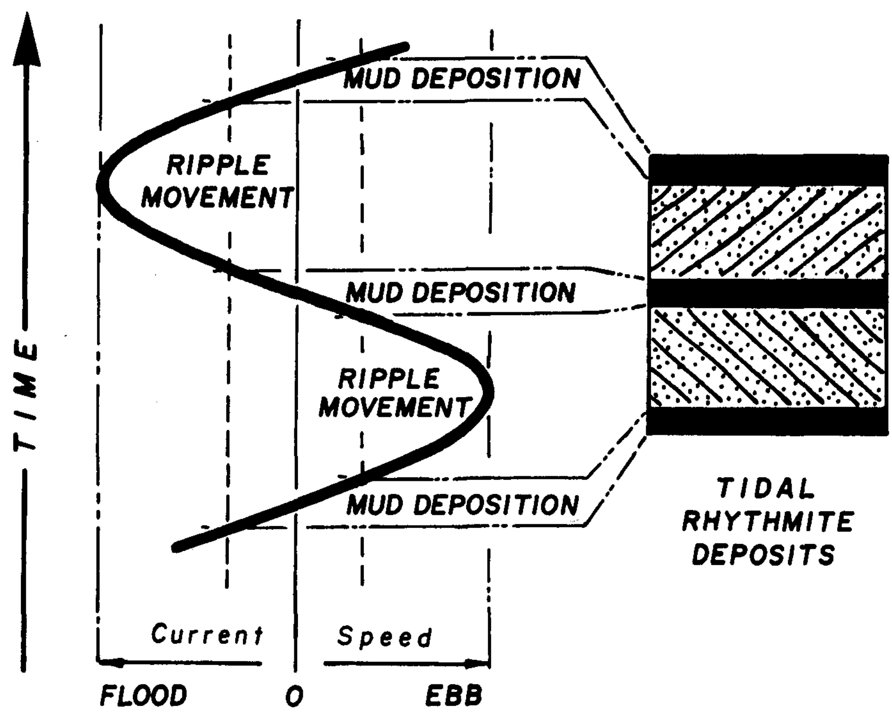

Figure 11 Variation in tidal current speed over a single tidal cycle and the origin of tidal rhythmites. The tidal currents in this example are of equal speed in both directions. As the difference in speed between the dominant and subordinate currents increases, the thickness of the two sand layers will become more unequal. After Dalrymple *et al.* (1991).

the sand flats located in the headward portions of macrotidal estuaries (Dalrymple et al., 1990). *Mixed flats,* in which mud layers become more abundant as the distance from the channel increases, lie shoreward of the sand flats. *Mud flats* consisting of laminated muds with relatively little sand lie still further landward (Fig. 12). Flaser bedding passing landward into lenticular bedding is typical of the transition from mixed flats to mud flats. Burrows belonging to the *Skolithos* ichnofacies (Chapter 4) may partially to completely obliterate the physical structures on any part of the tidal flat where sediment movement is not too intense. The highest parts of the tidal flats may become vegetated to produce *salt marshes* where the stratification is largely destroyed by rootlets. Saltwater and freshwater peats can accumulate here. Desiccation cracks are most abundant in the upper intertidal and supratidal zones.

Tidal flats along exposed, open coasts exhibit the landward-fining trend described above, but because of greater wave action they may be coarser grained, and contain more wave-generated structures, than tidal flats in protected areas (Thompson, 1968; Larsonneur, 1975). During periods of reduced sediment supply, wave erosion concentrates the sand and shells into beach ridges or swash bars that pass seaward into a thin erosional lag.

In tropical climates, sea grasses and mangroves commonly colonize large parts of the tidal flats (Gostin *et al.*, 1984). The carbonate content is generally higher than in temperate tidal flats, and evaporites may form in the upper intertidal and supratidal zones if the climate is arid. By contrast, tidal flats in mid to high latitudes commonly contain ice-rafted debris and soft-sediment deformation produced by the grounding of ice blocks.

The muddy parts of the intertidal flats

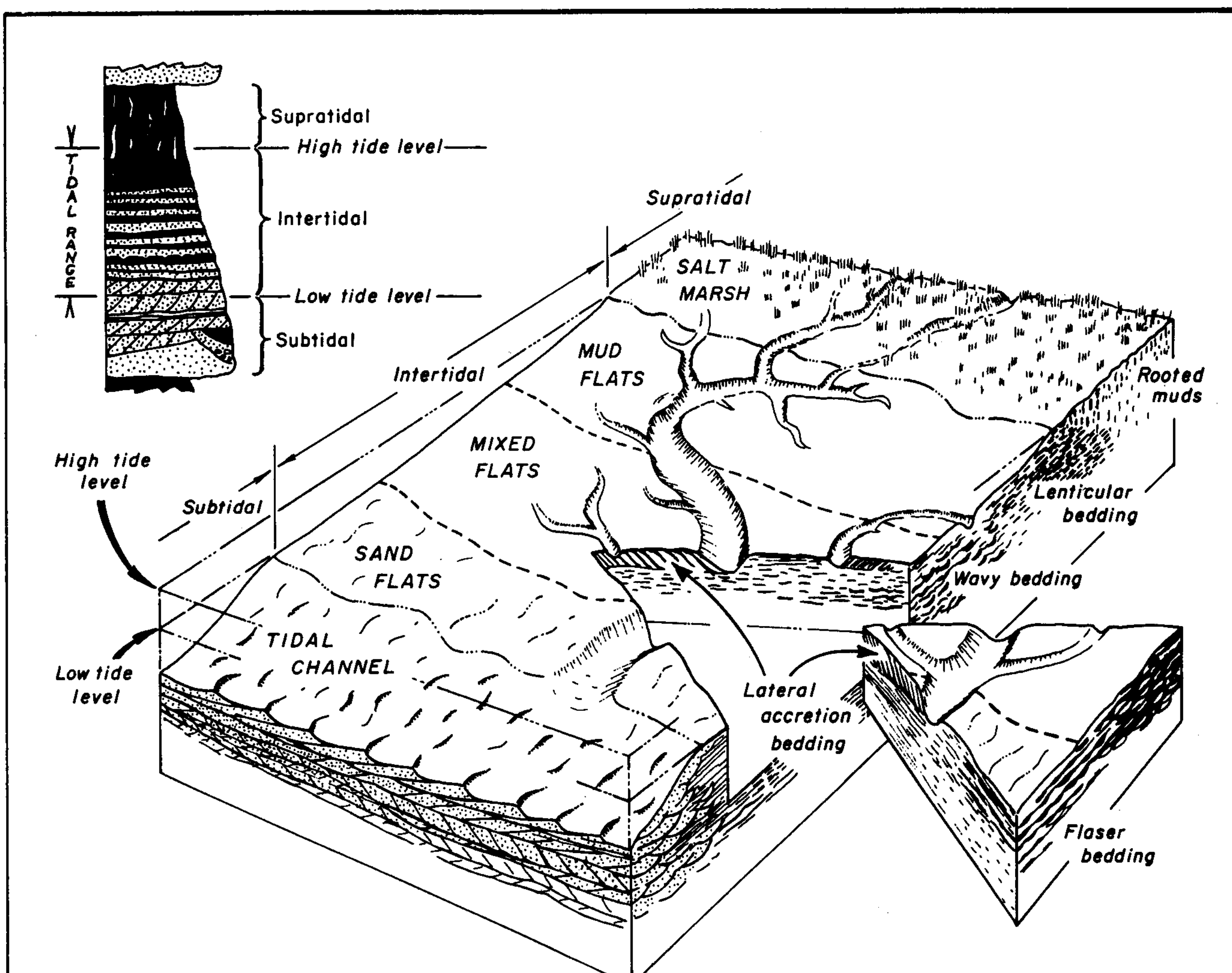

Figure 12 Block diagram of a typical siliciclastic tidal flat. The tidal flats fine toward the high-tide level, passing gradationally from sand flats, through mixed flats, to mud flats and salt marshes. An example of the upward-fining succession produced by tidal flat progradation is shown in the upper left corner. The sedimentary structures reflect a landward decrease in tidal-current speeds. The cross bedding deposited on the lower portion of the sand flats, and in the adjacent tidal channel, is commonly oriented parallel to the local coastline (which parallels the back edge of the diagram).

are dissected by a network of small- to medium-sized meandering *tidal gullies* that increase in width and depth as they coalesce seaward (Fig. 12). The floors of the gullies commonly contain a lag of shells and mud clasts. Sand is only abundant in the more seaward parts. The main site of deposition is on the point bars where lateral-accretion bedding (also called *inclined heterolithic stratification*) is developed (Fig. 13; Bridges and Leeder, 1976; Thomas *et al.*, 1987). These deposits consist of interbedded sand and mud which may contain tidal rhythmites. Burrowing is generally less intense than on the adjacent flats because deposition is more rapid. The vertical thickness of the lateral-accretion sets approximates the depth of the channel, and ranges from a few tens of centimetres to many metres in the main tidal channels. The dips are typically 5-15°, but may exceed 25°. The proportion of a tidal flat which is underlain by point-bar deposits varies widely. In some North Sea tidal flats, lateral-accretion bedding comprises a high proportion of the tidal flat deposits, whereas in other areas (e.g., the Bay of Fundy and Korean west coast) gulleys, if present, have stable positions, and most of the deposits are horizontally bedded (Alexander *et al.*, 1991; Dalrymple *et al.*, 1991).

Progradation of a tidal flat generates an upward-fining succession (Weimer *et al.*, 1982; Terwindt, 1988). The successions typically begin with an erosional base that is scoured by tidal

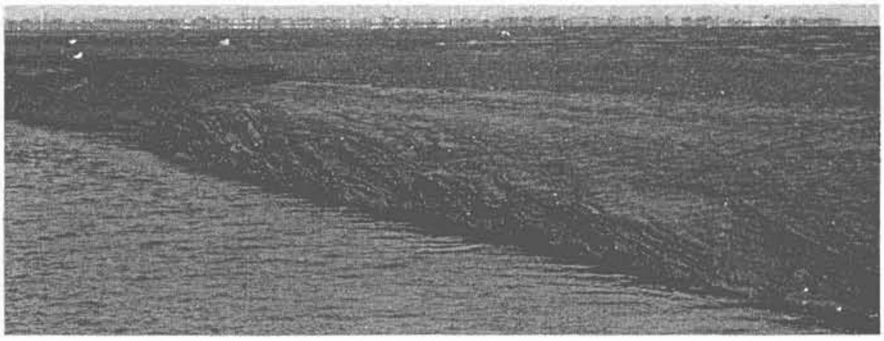

Figure 13 Cut bank of tidal creek in Jade Bay, Germany, showing lateral-accretion bedding of an earlier tidal channel. The exposure is approximately 1 m high.

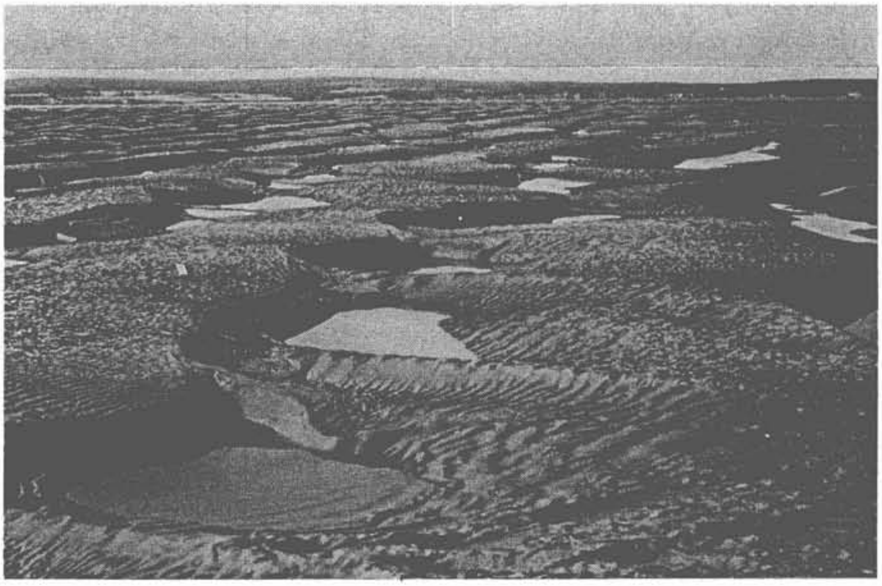

Figure 14 Extensive field of three-dimensional megaripples with well-developed scour pits, on a tidal sand bar in the outer part of the Cobequid Bay-Salmon River estuary. These dunes have a wavelength of approximately 7 m. Note the late-ebb stage current ripples that cover the dunes. Similar dunes occur on tidal sand ridges in deltaic and shelf environments.

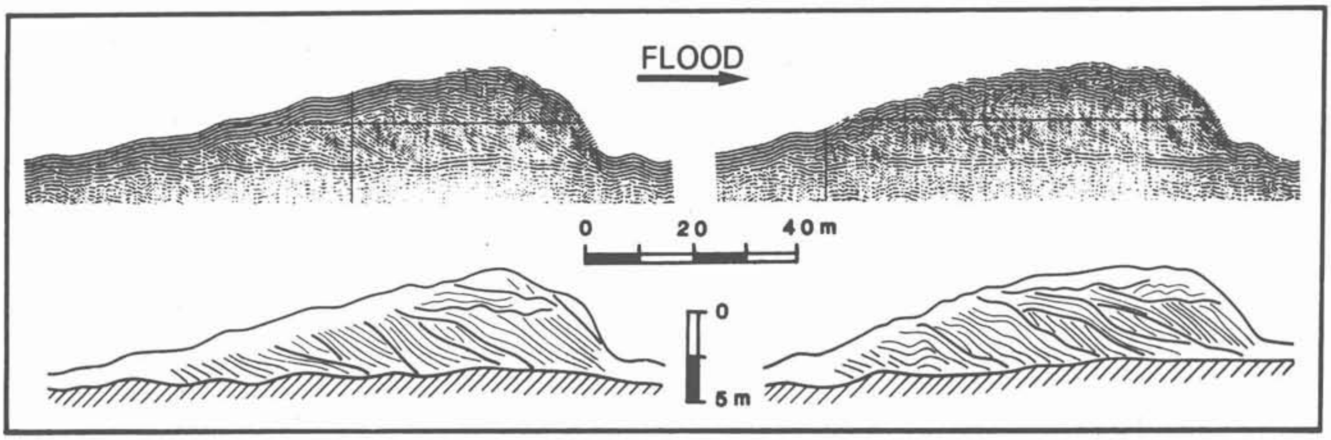

Figure 15 High-resolution seismic-reflection profiles and interpreted sections through flood-asymmetric sand waves from the northern French coast. The vertical exaggeration is x4, and maximum lee-face slopes are approximately 20°. All of the stratification surfaces shown are master bedding planes, and the structures belong to classes IV or V of Allen (1980; Fig. 16). From Berné *et al.* (1988).

channels during a local transgression. Above this there is a gradual upward decrease in the grain size and thickness of sand beds, and an increase in the proportion of mud (Fig. 12). Commonly encountered structures in the sands of the subtidal and lower intertidal zone include mud-draped foresets, reactivation surfaces and local herringbone cross bedding. Variable amounts of wave-generated structures, perhaps including hummocky cross stratification, are present in open coast settings. The intertidal mud flats contain abundant flaser and lenticular bedding, and erosionally based tidal gulley sediments with lateral-accretion bedding. Rooted horizons, coals and/or paleosols occur in the capping salt marsh. Bioturbation may range from minimal to intense in any facies. The thickness of such successions ranges from about 1 m to more than 10 m. Some workers have attempted to estimate the tidal range by determining the sediment thickness between the interpreted levels of high and low tide (Fig. 12; Terwindt, 1988), but such attempts have met with limited success.

Tidal sand waves and sand ridges

Sand waves and sand ridges are common in shallow subtidal areas such as 1) the axial portions of tide-dominated estuaries, 2) distributary mouth and subaqueous delta plain regions of tide-dominated deltas, and 3) large parts of tide-dominated shelves. These environments commonly experience tidal currents with speeds of 0.5-1.5 m/s, and the sediments consist predominantly of sand. As a result, dunes of various types (megaripples and sand waves of previous authors) are widely developed (Fig. 14). These bedforms are commonly superimposed on still larger features called tidal sand ridges or bars that are oriented nearly parallel to the main tidal flow..

Tidal sand waves

Large-scale, compound dunes (i.e., sand waves) are particularly abundant in sandy subtidal settings. These bedforms range in height from about 1 m to more than 20 m, and have wavelengths of 10 m to several hundred metres (McCave, 1971; Belderson *et al.*, 1982). In general, the larger bedforms occur in deeper water. Because of the widespread dominance of flow in one direction, sand waves are typically asymmetrical (Fig. 15), with their steeper (lee) face inclined in the direction of net sediment transport and bedform migration. Lee face inclinations vary from the angle of repose (32-35°) to nearly zero, but are typically about 5° (Belderson *et al.*, 1982). Allen (1980) has produced a set of theoretical models of the internal structure of large sand waves (Fig. 16). Two examples are shown in Figures 17 and 18. At one extreme, the deposits consist of high-angle cross stratification (dips >25-30°; Fig. 16 I and II) in which there are few erosional breaks (Fig. 17). This structure most likely forms where the subordinate current is below the threshold of sediment movement (Allen, 1980), and where any superimposed dunes are small (Dalrymple, 1984). As the power of the subordinate and dominant currents becomes more equal, or as the superimposed dunes become larger, the number of erosional surfaces (the *master bedding planes* of Allen, 1980) increases and their angle of dip decreases, until the deposit consists entirely of *compound cross bedding* (smaller-scale cross beds separated by inclined set boundaries; Figs. 16 V and VI, 18) that is produced as smaller dunes migrate down (or up) the lee face of the sand wave. Note that bipolar cross stratification becomes more pre-

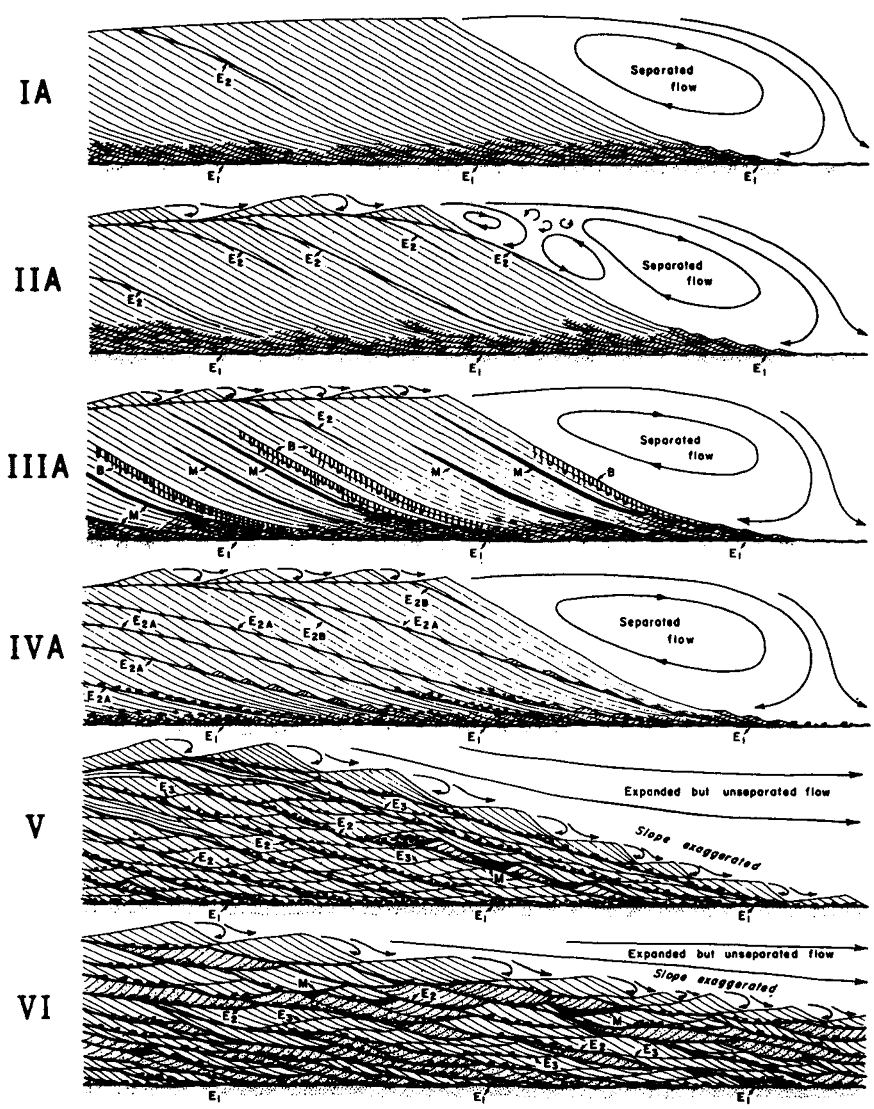

Figure 16 Theoretical models of the structures within tidal sand waves as proposed by Allen (1980). M = mud drape; B = bioturbation. The letters E refer to the hierarchy of erosion surfaces; E2 surfaces are the master bedding planes. The hydrodynamic interpretation of the various structures provided by Allen (1980) has been questioned (Dalrymple, 1984), but the structures depicted are matched qualitatively by many ancient examples.

valent as the inclination of the master bedding planes decreases. The abundance of mud drapes, mud clasts and bioturbation varies markedly between examples. At one extreme, mud and bioturbation may be entirely absent, but in other cases, the bottomsets and lower part of the lee face contain significant amounts of mud. Such deposits commonly show a concave-upward geometry and have been termed *sigmoidal cross stratification* (Mutti *et al.*, 1985).

High-resolution, seismic-reflection profiles through modern sand waves confirm the general features of Allen's models (Fig. 15; Berné *et al.*, 1988). The reflectors in these profiles have dips of less than 15° (do not be fooled by the vertical exaggeration!) and represent master bedding planes. Cores show that the structures between these planes consist of smaller cross beds.

Tidal sand ridges

Sand ridges cover thousands of square kilometres in tide-dominated shallow-marine settings (Fig. 19) and in the delta front region of tide-dominated deltas. Morphologically similar features also occur in estuaries where they are called tidal sand bars. These features have spacings of 1-30 km, lengths of 10-120 km, and heights of 7.5-40 m (Houbolt, 1968; Swift, 1975; Stride *et al.*, 1982; Twichell, 1983). They are nearly flow parallel, but are always oriented at a small angle (<20°) to the maximum tidal currents. The local, net sediment movement is in opposite directions on either side of the crest (Fig. 20). The ridges are generally asymmetrical, with a steeper (lee) side facing in the direction of regional sediment transport. Shelf ridges which have been examined seismically contain gently-inclined reflectors which lie parallel to this "steep" face (Figs. 20, 21; Houbolt, 1968; Johnson *et al.*, 1982; Yang and Sun, 1988). Dips of these lateral-accretion surfaces range from 5-10° in ridges which are presently active, to less than 2° in moribund (inactive) ridges. No published information exists on the internal architecture of modern estuarine and delta mouth ridges.

Active ridges in all settings are covered by sand waves and megaripples, and the limited core information indicates that these ridges contain cross bedding of various types (Houbolt, 1968; Dalrymple *et al.*, 1990). Shelf ridges which have become moribund due to the postglacial sea level rise lack large-scale bedforms. They may be draped by strata containing ripple cross lamination and/or storm deposits with greater degrees of burrowing. These sediments may also contain larger amounts of mud than the deposits of active ridges. The vertical succession of grain sizes in ridges may either coarsen or fine upward, depending on the depositional setting and sea level history.

TIDE-DOMINATED DEPOSITIONAL SYSTEMS

It is generally not appreciated that the new concepts of allostratigraphy and sequence stratigraphy discussed in Chapter 1 were primarily developed in *wave-dominated* settings. Few studies have examined how *tidal* systems respond to sea level change. As a result, the material in the following sections on the stratigraphy of tide-dominated systems contains a certain amount of "educated speculation" that is based to varying degrees on documented examples.

Figure 17 Large-scale cross bedding in the Lower Greensand (L. Cretaceous) near Leighton Buzzard, England. The large set at the base is about 5 m thick. It is overlain by smaller sets which interfinger with the major foresets, indicating that the smaller sets were produced by superimposed bedforms. Many of the foreset beds are bioturbated. This example would correspond to structure class II or III of Figure 16.

Figure 18 Low-angle (5°), compound cross bedding in the Lower Greensand (L. Cretaceous) near Leighton Buzzard, England. Regional bedding is horizontal. This example corresponds with class IV or V of Figure 16. A wet and cold Roger Walker (1.6 m) for scale.

Tidal systems are potentially more sensitive to sea level change than wave-dominated systems, because tidal resonance, which favours tidal sedimentation, is a sensitive function of basin geometry. Basin geometry, in turn, may be dramatically altered by small changes in sea level. Thus, tide-dominated conditions may be turned on and off in a "geological instant" because of sea level rise or fall.

Transgressive systems tracts

During a lowstand of sea level, river valleys commonly become incised. With the succeeding transgression, the lower reaches of these valleys are flooded by saltwater and experience tidal action. These areas are termed *estuaries.* They trap the sediment supplied by the rivers, and consequently little sediment reaches the shelf. As a result, pre-existing material, including estuarine facies which are abandoned on the shelf as transgression continues, may be eroded from the seafloor by strong tidal currents. The mud component commonly moves offshore into deeper water, while the sands are either transported onshore or left in place on the shelf as the water deepens.

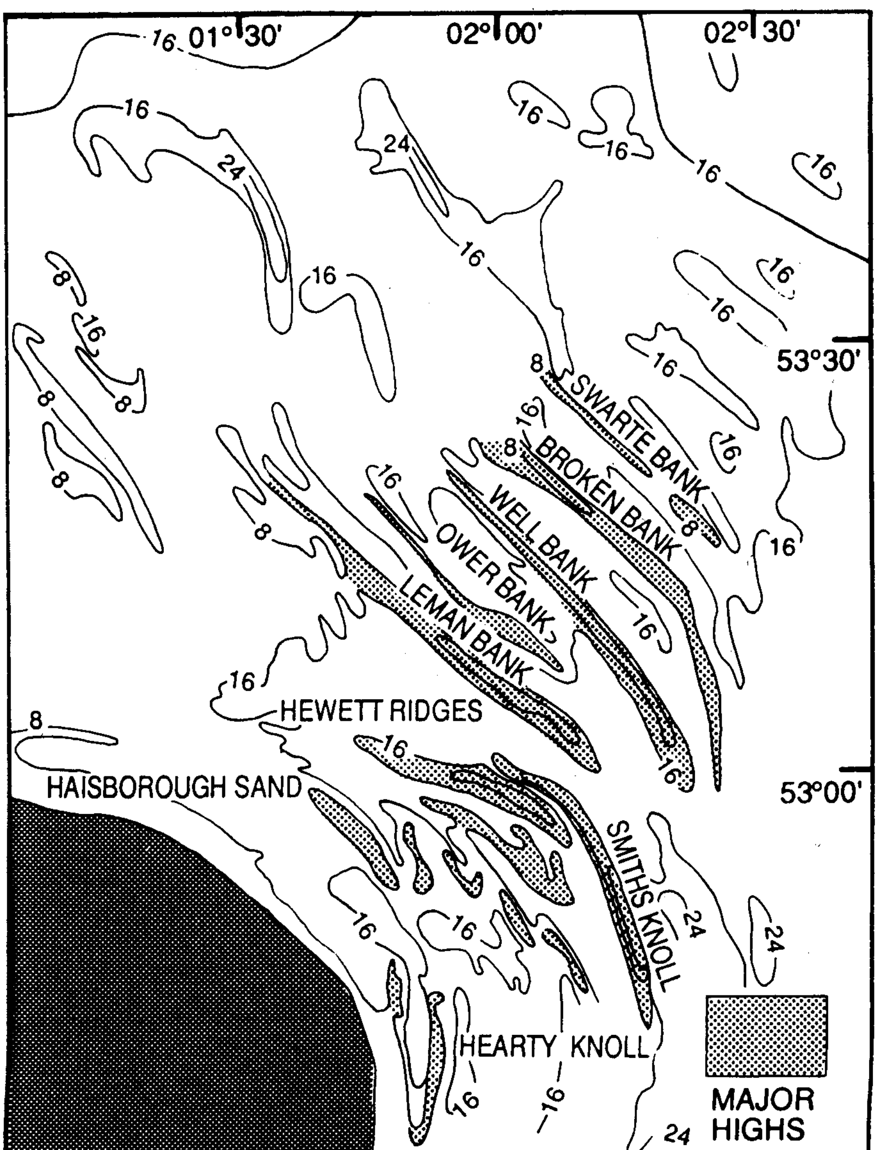

Figure 19 Distribution of tidal sand ridges off Norfolk, England, in the southern North Sea. *Depths in fathoms (1 fathom = 6 feet, or roughly 2 m). The ridges are 35-40 m high, with their crests in 10-15 m of water. The steepest ridge flank (5°) is on the northeastern side of each ridge because the strongest tidal currents flow to the north. From Swift (1975) after Houbolt (1968).*

Tide-dominated estuaries

The Cobequid Bay-Salmon River system in the Bay of Fundy (Dalrymple *et al.*, 1990, 1991) shows the typical facies of a tide-dominated estuary (Figs. 22, 23). A similar situation is presented by the Ord River in Australia (Wright *et al.*, 1975) and the Severn River, England (Allen, 1990). The patterns of sedimentation in these estuaries, and differences between tide-dominated and wave-dominated estuaries are discussed by Dalrymple *et al.* (1992). Wave-dominated estuaries are described in Chapter 10. It is worth noting that the morphological distinction between tide-dominated estuaries and deltas is not well documented, and that many so-called tide-dominated deltas (e.g., the Ord River) may be better classified as estuaries (see discussions in Chapters 1 and 9).

Tide-dominated estuaries receive sediment both from the river at the head of the estuary, and from the adjacent shelf by tidal currents. As a result, grain sizes are coarsest at the mouth and head of the estuary. Unlike wave-dominated estuaries, however, no fine-grained lagoonal facies are present, because tidal currents penetrate into the estuary much more easily than waves do (Dalrymple *et al.*, 1992). Consequently, the distinct *tripartite* facies distribution (sandy barrier – muddy lagoon – sandy bay-head delta; see Chapter 10) of wave-dominated estuaries does not occur in tide-dominated systems. Instead, tide-dominated estuaries are bordered by muddy tidal flats and marshes because tidal currents are strongest in the sandy channels that run along the entire length of the estuary axis (Fig. 22). The axial sands are finest grained and contain the greatest number of mud drapes in the vicinity of the tidal-fluvial transition, where the suspended sediment *turbidity maximum* is situated.

The most seaward, estuarine facies consists of elongate sand bars (Fig. 22) which are separated by ebb-dominant and flood-dominant channels (Dalrymple *et al.*, 1990). The bars are covered by dunes of various types and sizes, and the bar sediments are composed primarily of cross bedded, medium to coarse sand. Lateral shifting of the bars produces an upward-fining trend (Fig. 23) because current speeds are greatest in the channels and decrease toward the bar crests. On average, the tidal current speeds increase into the estuary, so that the area headward of the bars is characterized by extensive sand flats with parallel lamination. Still farther headward, these flats grade into the tidally influenced portion of the river channel (Fig. 22). Parallel lamination is present here, but cross bedding containing mud drapes may become abundant headward. Tidal rhythmites occur in the bordering mud flats (Dalrymple *et al.*, 1991), and inclined heterolithic stratification may be present in the meanders that occur in this region. At the tidal limit, which can be situated several hundred kilometres inland, the muddy channel sands of the inner estuary pass gradationally into coarser fluvial sediments.

The Gironde estuary (France) is commonly cited as a typical tide-dominated estuary, but it has many of the attributes of a wave-dominated estuary, including a tripartite facies distribution (Allen, 1991). This estuary contains tidal sand ridges, but these represent a tide-dominated bay-head delta within the inner estuary. As a result, these ridges coarsen upward because they prograde seaward over central estuary muds (Allen, 1991).

During active transgression, the facies within a tide-dominated estuary shift headward. This appears to be the case in the Severn estuary today (Allen, 1990). In the process, migrating tidal channels coupled with wave action erode all or part of the more headward facies, leaving an incomplete record of the estuary in shallow marine areas that lie seaward of the final shoreline. In the ideal case of essentially complete preservation, the *transgressive* valley-fill sediments will fine upwards from fluvial sands and/or gravels to interbedded sands and muds deposited in the tidal-fluvial transition of the inner estuary (Fig. 24). This is followed by an overall upward coarsening into fine-grained, parallel-

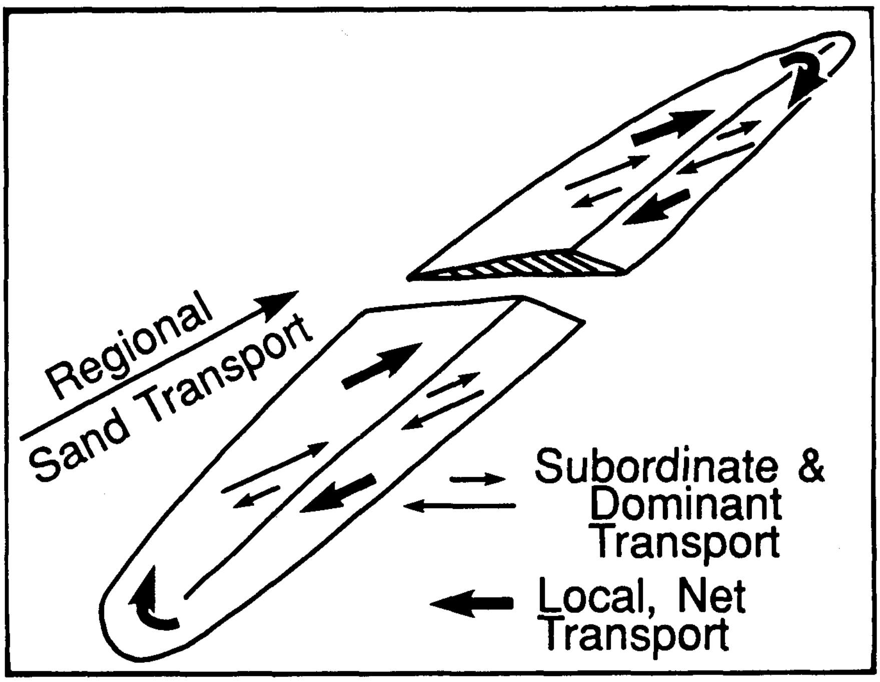

Figure 20 Model of sediment transport around, and internal structure within, a tidal sand ridge. The peak tidal currents flow at a slightly oblique angle to the ridge crest so that local, net transport is in opposite directions on either side of the crest. In most cases, net accretion occurs on the steeper (regionally downstream) side of the ridge. Thus most of the small-scale cross bedding in the ridge should be oriented in the opposite direction to the regional transport. After Stride *et al.* (1982).

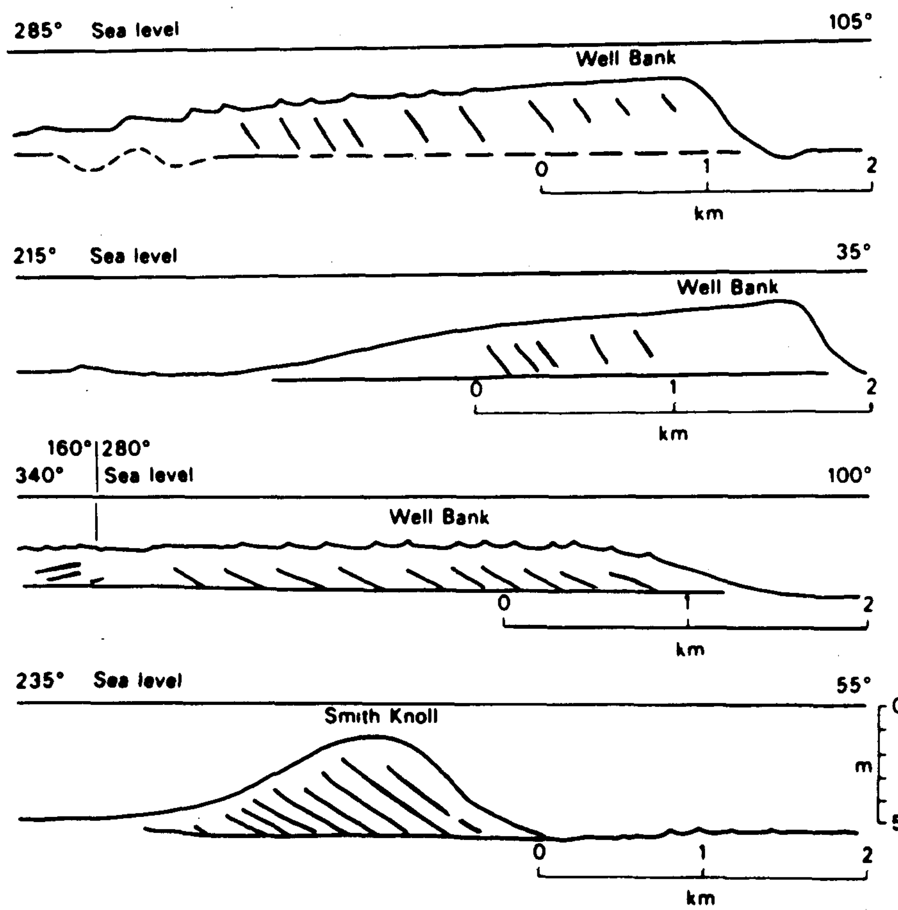

Figure 21 Seismic-reflection profiles through tidal sand ridges from the North Sea; see Figure 19 for ridge locations. The vertical exaggeration is approximately 13 times; none of the inclined reflectors is steeper than 5°. From Houbolt (1968).

laminated sand flat sediments and ultimately into cross-bedded, medium sand of the elongate sand bars. These sands may be enclosed laterally by, and interfinger with, mud flat and salt marsh sediment. There will be numerous local discontinuities produced by tidal channel erosion. The units bounded by these erosion surfaces are deposited by tidal flat progradation or sand bar migration, and fine upward. The lower portion of this succession has the highest preservation potential, but it is possible for the deeper channels between the sand bars to scour completely to the base of the valley, remove any fluvial deposits, and modify the geometry of the bounding discontinuity.

At the limit of the transgression, when the estuary reaches its most landward position, the estuary will infill and a *progradational* succession will be developed. This process has begun in the Cobequid Bay-Salmon River estuary (Dalrymple *et al.*, 1990). Such regressive estuary filling will generate an upward-fining facies succession in which cross-bedded sands of the sand bars are overlain by parallel-laminated sand of the sand flats, and by mixed flat, mud flat and marsh deposits (Fig. 23).

Continental shelves

The shallow marine area surrounding the British Isles is the classic example of a transgressive, tide-dominated continental shelf (Stride, 1982). Georges Bank in the outer part of the Gulf of Maine (Twichell, 1983) is another example. In such settings, inequalities between the flood and ebb currents produce large areas in which the residual sediment transport is in one direction. In each of these regionally extensive *transport paths*, sediment is eroded from the seafloor in the *bed load parting* (Fig. 25) at the upstream end, leaving a shelly gravel lag in which large wave ripples may be present (Fig. 26). The reworked sediment is transported downcurrent, and deposited where tidal current speeds decrease. Flow-parallel sand ribbons and isolated dunes occur in the zone of bypassing where neither erosion nor deposition occurs. In depositional areas, sand sheets may cover thousands of square kilometres. Sand waves are extensively developed on these sheets, and sand ridges occur if there is sufficient sediment and the maximum current speeds exceed 1 m/s (Stride *et al.*, 1982). Even farther down the transport path, where tidal current speeds are less than about 50 cm/s (Fig. 26), rippled sand sheets and isolated sand patches are developed. Mud accumulates at the distal end of the transport path, if it is available. In general, however, transgressive sand sheets are composed of clean sand that contains little mud.

Transgressive tidal sand sheets are typically only a few metres thick (the one in the southern North Sea averages less than 5 m), except in the sand ridges where thicknesses reach 30 m. The structures in the proximal portion consist of cross bedding produced within the sand waves. Due to the dominance of one current, cross bedding orientations are primarily unidirectional. Within sand ridge fields, however, deposition occurs preferentially on the side that is dominated by the regionally-weaker current (Fig. 20). These sand ridge deposits may therefore have a paleocurrent direction which is the opposite of that in other parts of the sand sheet. Cross bed set thicknesses decrease in the down-transport direction, due to the decreasing current speeds (Fig. 26), and pass distally into rippled and burrowed fine sand and mud. The relative influence of storms increases as the tidal

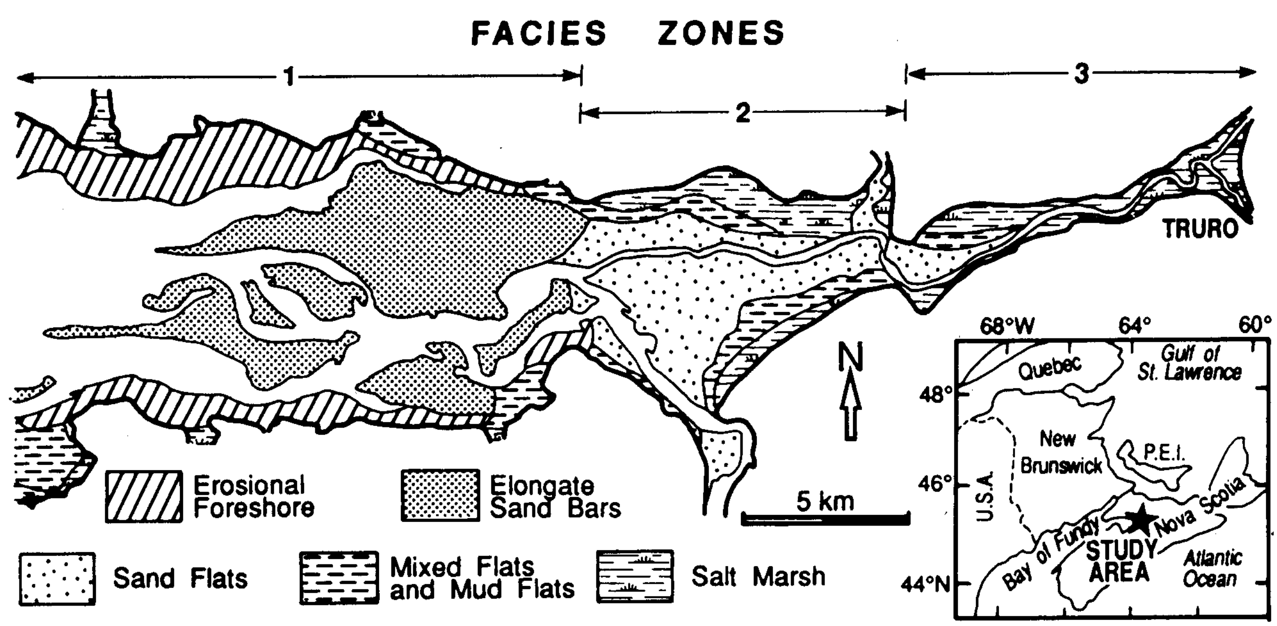

Figure 22 Facies distribution in the Cobequid Bay – Salmon River macrotidal estuary, Bay of Fundy. Facies zone 1, elongate sand bars (medium to coarse sand); zone 2, upper-flow-regime sand flats (fine sand); and zone 3, tidal-fluvial transition. The erosional foreshores bordering zone 1 are unique to Cobequid Bay. Sand bars in estuaries such as the Severn River are bordered by mud flats and salt marshes. After Dalrymple *et al.* (1990).

current speeds decrease, and the distal parts of the sand sheet may contain storm-generated structures.

Within active sand ridges, it is believed that the sediments coarsen upward because wave action is most intense on the ridge crests. During a transgression, however, the progressive increase in water depth causes current speeds at any location to decrease through time. This causes the bedform zones (Fig. 26) to shift in an upcurrent direction. In the process, the sand ridges become moribund. Sediment is eroded from the ridge crests by storm waves, and deposited as a drape on the ridge flanks (Fig. 24). Shell accumulations may also form on the ridge crest at this time. It is possible, based on modern examples, that some ridge topography will remain, but the lack of published ancient examples with a preserved topography suggests that complete flattening occurs in many cases. As the transgression proceeds, there is an upward change from cross bedding to finer-grained, rippled and burrowed sediment as current speeds decrease. The subdued or flattened ridge is eventually mantled by mud (Fig. 24).

In some circumstances transgression leads to the abandonment of estuary-mouth ridges on the shelf. For example, Yang and Sun (1988) and Yang (1989) have proposed that the sand ridges seaward of the Changjiang River in the East China Sea originated in an estuarine setting, and were stranded on the shelf as the coast moved westward during the Holocene transgression (Fig. 27). Seismic data show that the internal structure of these ridges is similar to that in North Sea shelf ridges (Fig. 21), but the East China Sea ridges are inactive now, and are draped by a layer of shelf mud. Their relief is subdued but not obliterated. The extent to which these estuarine ridges have been remoulded on the shelf is unknown.

Transgressive stratigraphy

The transgressive systems tract rests on a bounding disconformity (Fig. 24) which was formed subaerially during the preceding lowstand. The base of any incised valleys may contain fluvial sediments that represent part of the lowstand systems tract, unless they have been scoured out by tidal cur-

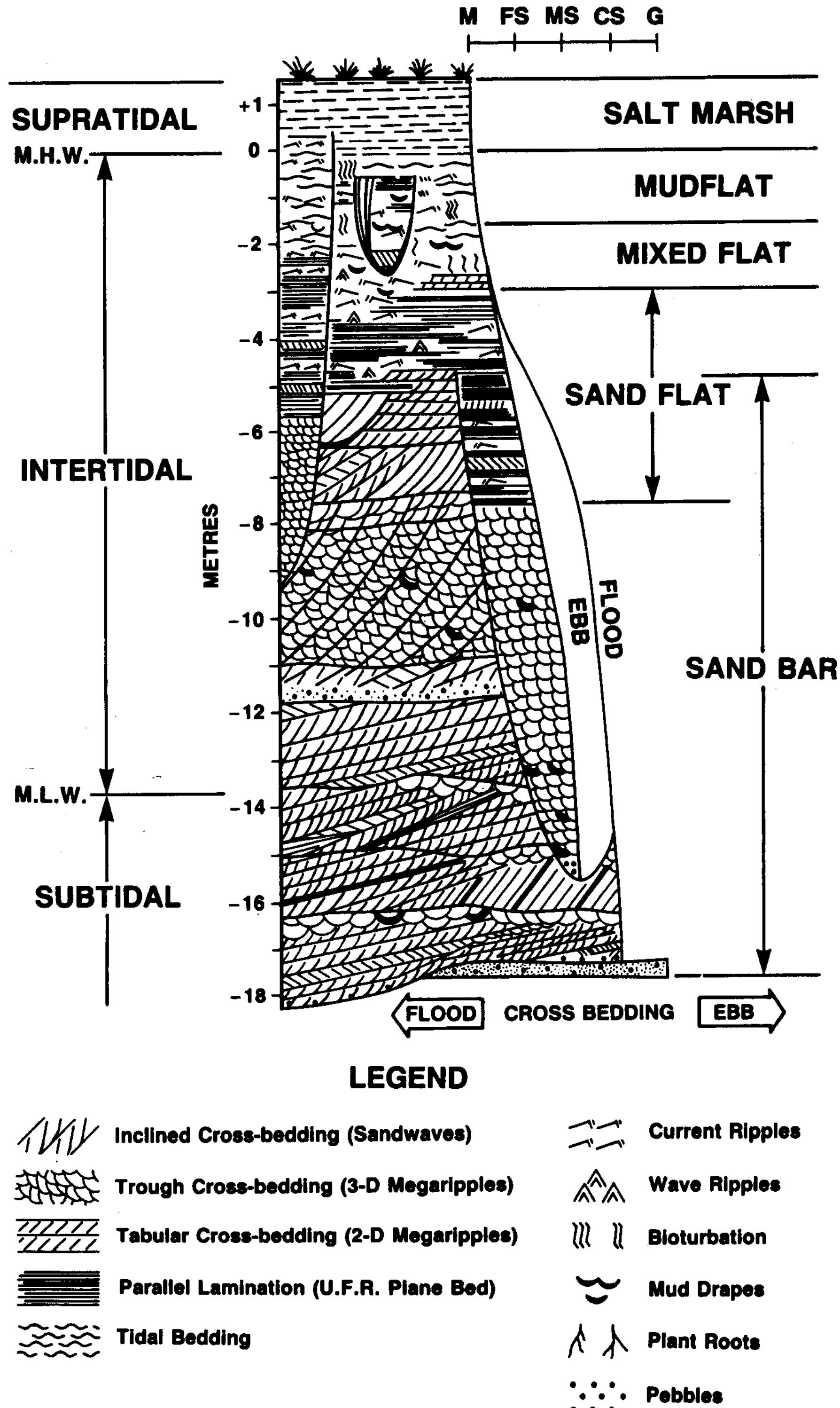

Figure 23 Vertical facies succession which would be developed if a tide-dominated estuary such as the Cobequid Bay-Salmon River estuary filled by progradation. M – mud; FS – fine sand; MS – medium sand; CS – coarse sand; G – gravel; M.H.W. – mean high water; M.L.W. – mean low water; U.F.R. – upper flow regime. The sediments underlying this succession may consist of preserved remnants of transgressive estuarine or fluvial deposits, or of older material, depending on the amount of tidal-current erosion during the transgression. From Dalrymple *et al.* (1990).

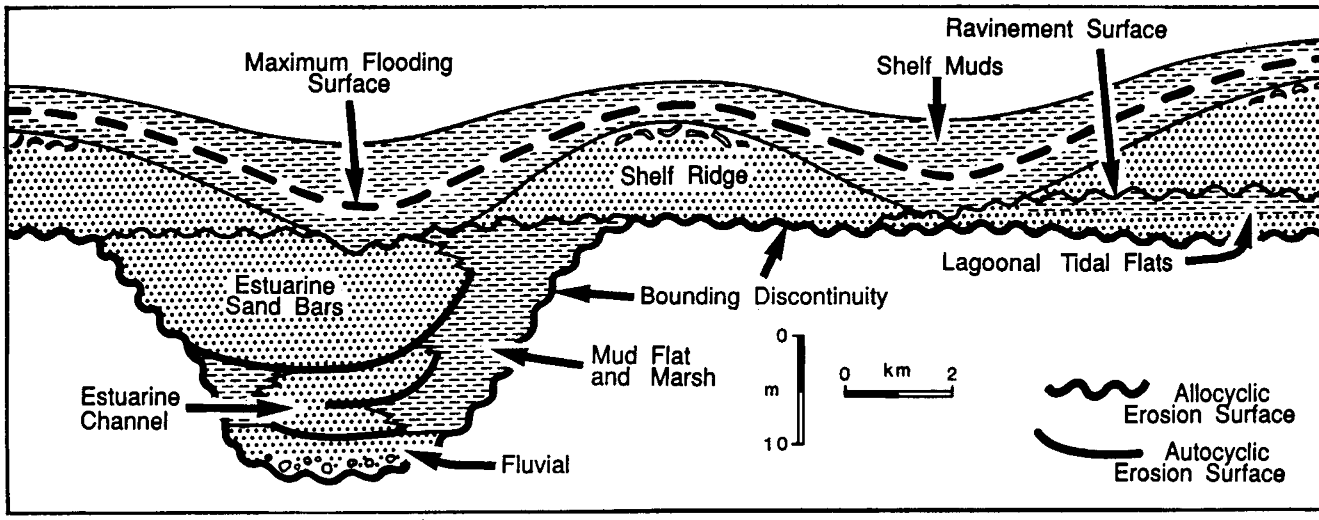

Figure 24 Hypothetical, coast parallel section showing the stratigraphy of a transgressive systems tract, assuming complete preservation of the estuarine deposits for the purposes of illustration. Less than complete preservation is more likely. The estuarine portion of this figure is based on the Cobequid Bay – Salmon River and Severn River estuaries, while the marine part is based on the southern North Sea. Autocyclic erosion surfaces are generated by tidal channel migration, whereas allocyclic erosion surfaces are related to relative changes in sea level.

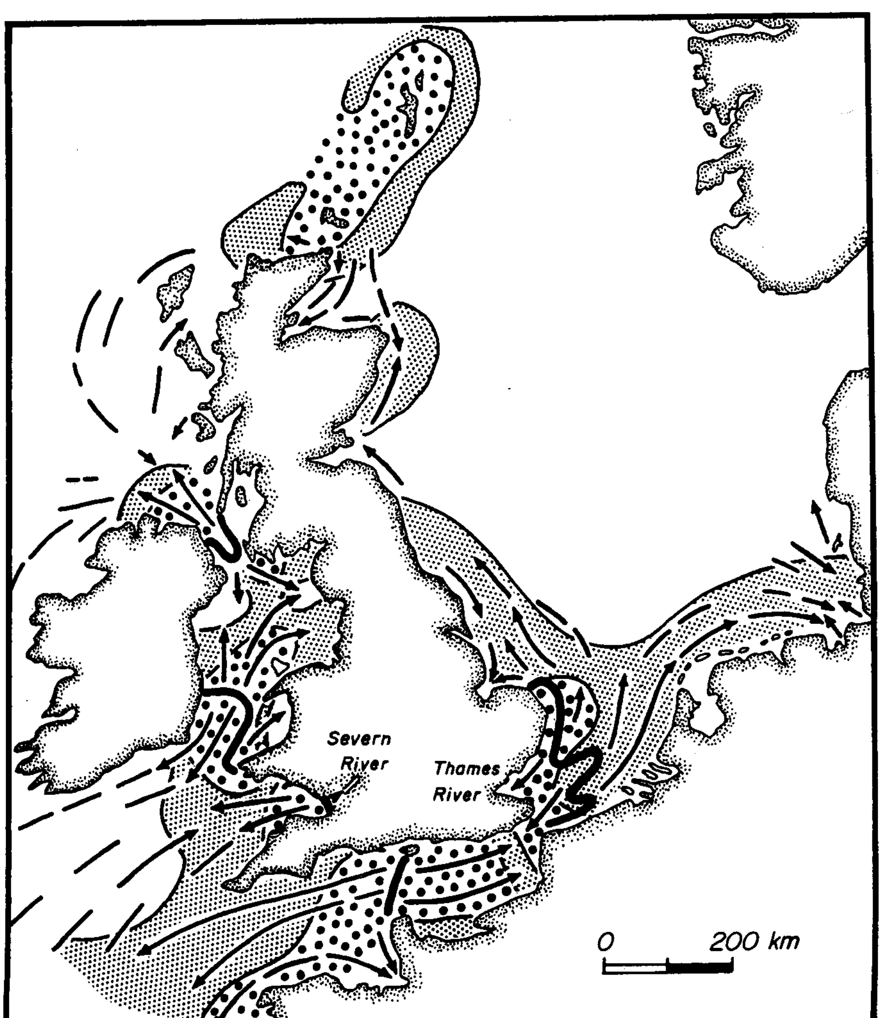

Figure 25 Map showing the net tidal-transport paths and distribution of grain sizes on the continental shelf around the British Isles (coarse stipple = gravel; fine stipple = sand; blank areas = mud). Each sediment transport path, which extends from a bed load parting (heavy lines) to a bed load convergence is tens to hundreds of kilometres long. Deposition occurs in areas where sediment moves into an area with lower speeds, and not necessarily at sites of bed load convergence. Note the transport into the Severn and Thames estuaries. After Johnson *et al.* (1982) and Stride *et al.* (1982).

rents. They will be overlain by tide-dominated estuarine deposits which comprise the lower portion of the transgressive systems tract. Exxon's assignment of estuarine deposits primarily to the lowstand systems tract (Van Wagoner *et al.*, 1990) seems illogical because the estuary only exists because of transgression. The contact between the fluvial and estuarine sediments is a flooding surface (Chapter 1), although it need not be abrupt everywhere.

The top of the estuarine sediments may or may not be marked by an erosion surface. In the East China Sea example discussed above (Fig. 27), the estuarine ridges are stranded on the shelf without major erosion, and are draped by shelf muds. There should be no transgressive surface of erosion in such cases. By contrast, sand ridges are not present seaward of the mouth of the Severn River, England. Instead, this area is the site of a bed load parting (Fig. 25), and the seafloor is eroded by strong tidal currents. The marine erosion surface that is formed as the bed load parting migrates landward during the transgression is the tidal equivalent of the *ravinement surface* formed by shoreface erosion in wave-dominated settings (see Chapters 10, 12). In such situations, the shallow marine sand sheet that forms from reworked older sediment will rest disconformably on any preserved remnants of estuarine deposits (Fig. 24).

The coastline between major estuaries is typically characterized by a mixed energy (wave plus tide) regime which creates short barrier islands with numerous tidal inlets. The Dutch and German coasts provide an example of this (Fig. 6). Landward movement of the barrier island shoreface will generate a true ravinement surface, in the manner described in Chapter 10. As a result, the shelf ridges seaward of the Dutch coast erosionally overlie and locally contain remnants of lagoonal, tidal flat deposits (Cameron *et al.*, 1989). The discontinuity which separates the lagoonal and shelf ridge sediments was originally formed by shoreface erosion, but subsequent scour in the ridge troughs has modified its form (Fig. 24).

Continued transgression leads to abandonment of the shelf ridges and their ultimate burial beneath shelf muds. At some level within the transgressive muds, and probably close to their base, there is a *maximum flooding surface* (Fig. 24) which is the upper bounding discontinuity of the transgressive systems tract.

If estuarine ridge sediments survive the transgression, distinction between estuarine and shelf sands is crucial for a correct interpretation of the stratigraphic succession. In addition to potentially having differing grain-size trends (estuarine ridges fine upwards, whereas active shelf ridges coarsen upwards beneath an upward-fining transgressive drape), estuarine sands are likely to contain more mud in the form of mud drapes and/or mud pebbles than their shelf counterparts because of the higher suspended sediment concentrations in estuaries. Neap-spring bundle sequences will be more clearly developed in estuaries because of less disruption of the cyclicity by storms. The shelly fossils and ichnofauna (Chapter 4) of estuarine deposits should show evidence of

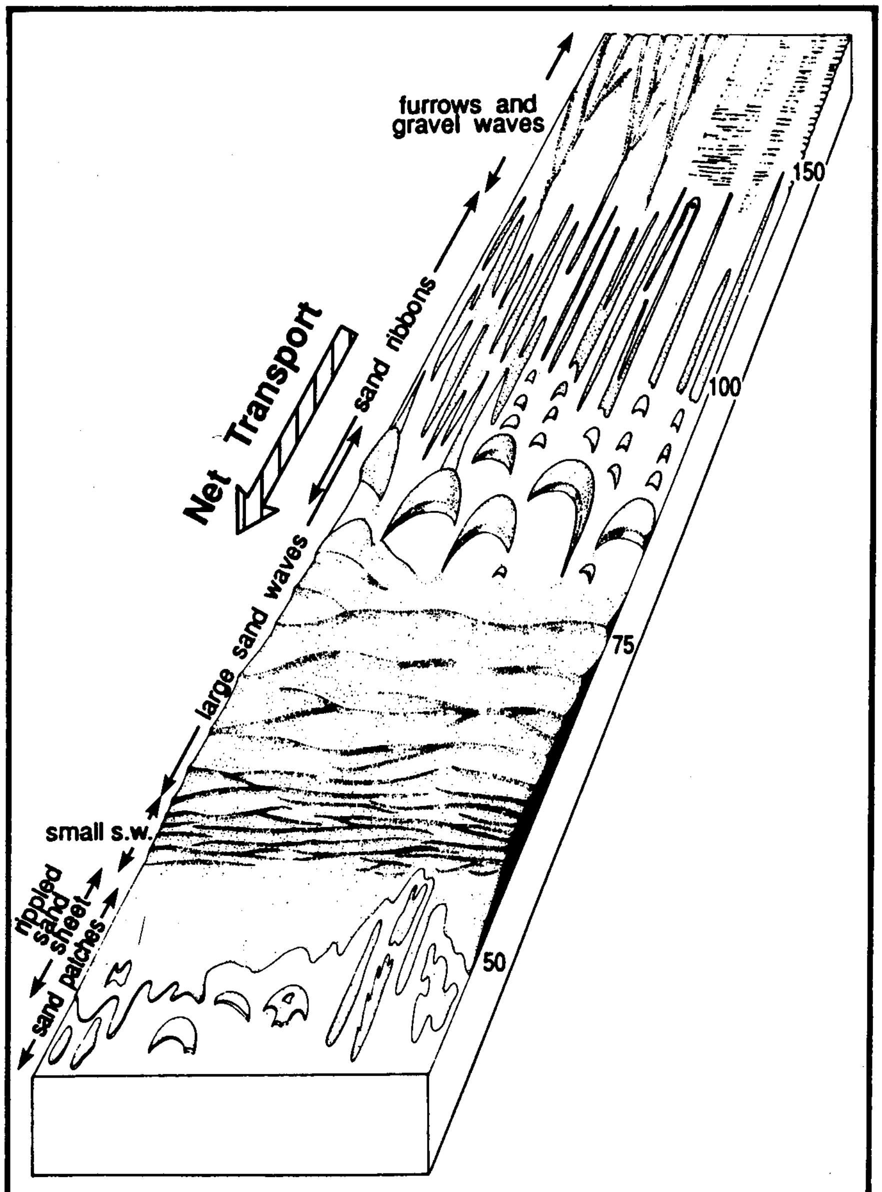

Figure 26 Idealized distribution of bedforms along a sediment transport path, with the typical maximum (spring-tide), near-surface current speeds (cm/s) associated with each bedform type. Sand ridges will be developed in the sand-wave zone if there is sufficient sand. From Belderson *et al.* (1982).

brackish water conditions. Estuarine sands are also intimately associated with tidal flat sediments, and should be contained within an incised valley. Shelf sands will occur as an areally extensive sheet that is probably less than 15 m thick on average.

Highstand systems tracts

As the rate of sea level rise slows at the end of a transgression, estuaries become filled. Consequently, there are no highstand estuaries, and fluvial sediment is delivered directly to the shoreline and shelf. Therefore, tide-dominated, highstand systems tracts are characterized by progradation, either of tide-dominated deltas and/or open-coast tidal flats. Both of these should extend seaward into a regressive shelf.

Tide-dominated deltas

Deltas which experience strong tidal action represent one of three end members within the continuum of delta types (Chapters 1, 9; Coleman and Wright, 1975; Galloway, 1975). Several examples have been described, including the Klang-Langat (Malaysia; Coleman *et al.*, 1970), the Colorado River delta (Gulf of California; Meckel, 1975), and the Ord River (northern Australia; Wright *et al.*, 1975), although this latter system may be an estuary. The Mahakam delta (Indonesia; Allen *et al.*, 1979) also displays a strong tidal influence. These deltas tend to occur at the heads of embayments where the tidal range is amplified, or adjacent to narrow straits where tidal current speeds are high.

The subaqueous delta plain of tide-dominated deltas is characterized by tidal sand ridges which are oriented at a high angle to the general trend of the coastline (Fig. 28), unless the delta borders a strait. Near the shoreline these ridges may have a relief of up to 15-20 m, but the relief gradually decreases away from the distributaries and they pass outward into the smooth, muddy delta front and prodelta in depths of 10-30 m. These ridges are best developed where the ratio of tidal to fluvial discharge is high. Thus, the abandoned portion of the delta plain which receives little fluvial discharge is the part most likely to contain tidal sand bars (Allen *et al.*, 1979), especially if the tidal range is mesotidal. In macrotidal areas, even the active distributaries contain sand ridges.

The subaerial portion of the delta plain is characterized by broad tidal flats that grade seaward into the sand bars, and landward into either vegetated marshes if the climate is humid (the Klang-Langat delta), or evaporative flats if the climate is arid (Colorado and Ord Rivers). The tidal flats and marshes are dissected by tidal gulleys that have highly meandering channel patterns. Such gulleys are especially abundant in inactive portions of the delta plain (Fig. 28).

Progradation of the active distributaries generates a gradational, upward-coarsening succession which passes from prodelta muds into interbedded sands, silts and muds of the delta front. These are in turn gradationally overlain by the fine to medium sands of the tidal ridges (Fig. 29B; Coleman and Wright, 1975; Meckel, 1975; Allen *et al.*, 1979). Tidal modulation of the sediment discharge (sediment output is impeded during the flooding tide and enhanced on the ebb tide) may produce tidal rhythmites in the portions of the delta front where wave action does not disrupt the regularity of the stratification (Williams, 1991). The medium sands of the ridges contain abundant cross bedding, with ebb-oriented paleocurrents predominating near the active distributaries. Continued progradation causes the distributary channel(s) themselves to extend into the sand ridge field, erosionally truncating the ridge deposits locally (Fig. 29A). The distributary channel sediments fine upward and contain more slack-water mud drapes than do either the nontidal fluvial channels up river (Allen *et al.*, 1979), or the sands of the ridges further seaward where wave action inhibits mud deposition.

In the abandoned parts of the delta plain which are undergoing local transgression due to compactional subsidence, tidal current scour in the channels between the ridges erosionally truncates the underlying delta front sediments (Fig. 29C). As a result, the sand ridges in these areas are commonly erosionally based (Allen *et al.*, 1979), and fine upward like estuarine ridges. Flood-oriented cross bedding and shell accumulations will be more common here than in areas adjacent to the active distributaries.

In all parts of the delta plain, the ridge sands are gradationally overlain by an upward-fining succession of tidal

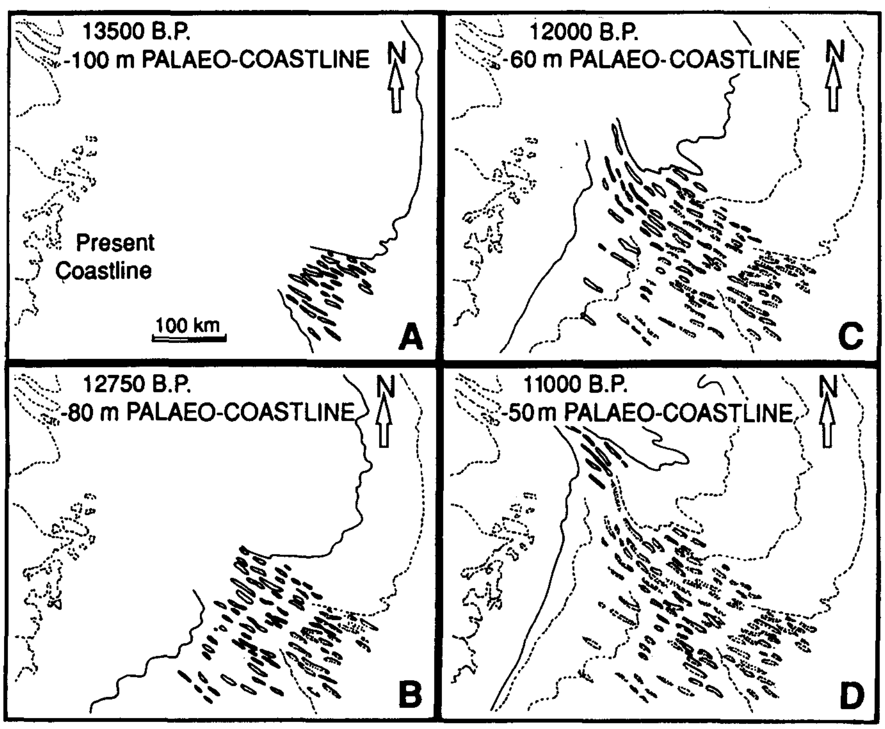

Figure 27 Evolution of the tidal sand-ridge field in the East China Sea during the Late Wisconsinan-Holocene transgression. These ridges overlie incised channels which are interpreted to be filled with fluvial and estuarine deposits. From Yang and Sun (1988).

flat and marsh sediments (Fig. 29). Erosionally based tidal creek deposits that contain lateral-accretion bedding are common. In humid tropical areas, saltwater and freshwater peat swamps are widespread on the delta plain, and organic detritus is a major constituent of the "mud" drapes. In arid areas, the tidal flats are barren, mud cracks are abundant, and evaporites may be developed.

Open-coast tidal flats

In coastal areas adjacent to a major delta, alongshore transport of sediment by tidal and shelf currents leads to the development of open-coast tidal flats like those downdrift from the Colorado River delta (Thompson, 1968). These tidal flats are generally muddy near the delta, but become progressively more sandy as the distance from the delta increases (Fig. 28) and eventually grade alongshore into beaches because of the increasing influence of waves. Variations in the supply of sediment due to delta switching cause periods of tidal flat progradation to alternate with episodes of wave erosion when beach ridges composed of sand and/or shells are formed. Tidal flat *chenier plains* formed in this manner are present in areas adjacent to the Colorado River delta (Thompson, 1968), and at various places along the Chinese coast (Wang, 1983).

Regressive shelves

Sediment supply to the shelf during a highstand should lead to gradual shallowing and the development of regressive conditions. Unfortunately, no modern examples of regressive, prograding tidal systems are sufficiently well documented to serve as a model. There are also surprisingly few ancient examples (Mutti *et al.*, 1985), in contrast to the abundance of regressive storm/wave-dominated shelves (Chapter 12). Because of this, the following description cannot be considered as a facies model in the sense discussed in Chapter 1.

Because the processes which produce unidirectional, net sediment transport paths are not dependent on the history of relative sea level, regressive shelves are expected to show regional changes in facies which are similar to those on transgressive shelves (Fig. 26), although there will be notable differences. As sediment is most likely input at the upstream end of a transport path, the erosional zone with furrows and sand ribbons will not be present. Instead, there may be direct passage from deltaic sand ridges into shelf ridges with little clear separation. Sand waves should be abundant. From here, the sediment will fine down the transport path, passing outward into shelf muds. The overall grain size is likely to be finer than in transgressive settings, and mud will be relatively abundant.

Progradation of an individual shelf ridge produces an upward-coarsening succession (Fig. 30) that may reach 10 m in thickness. It begins with bioturbated muds and sands that contain a *Cruziana* ichnofacies (Chapter 4). The sand beds become thicker and the proportion of muddy interbeds decreases upward. The succession is capped by cross-bedded medium to fine sand of the ridge crest, which is in turn abruptly overlain by shelf mud of the next succession. Evidence of tidal

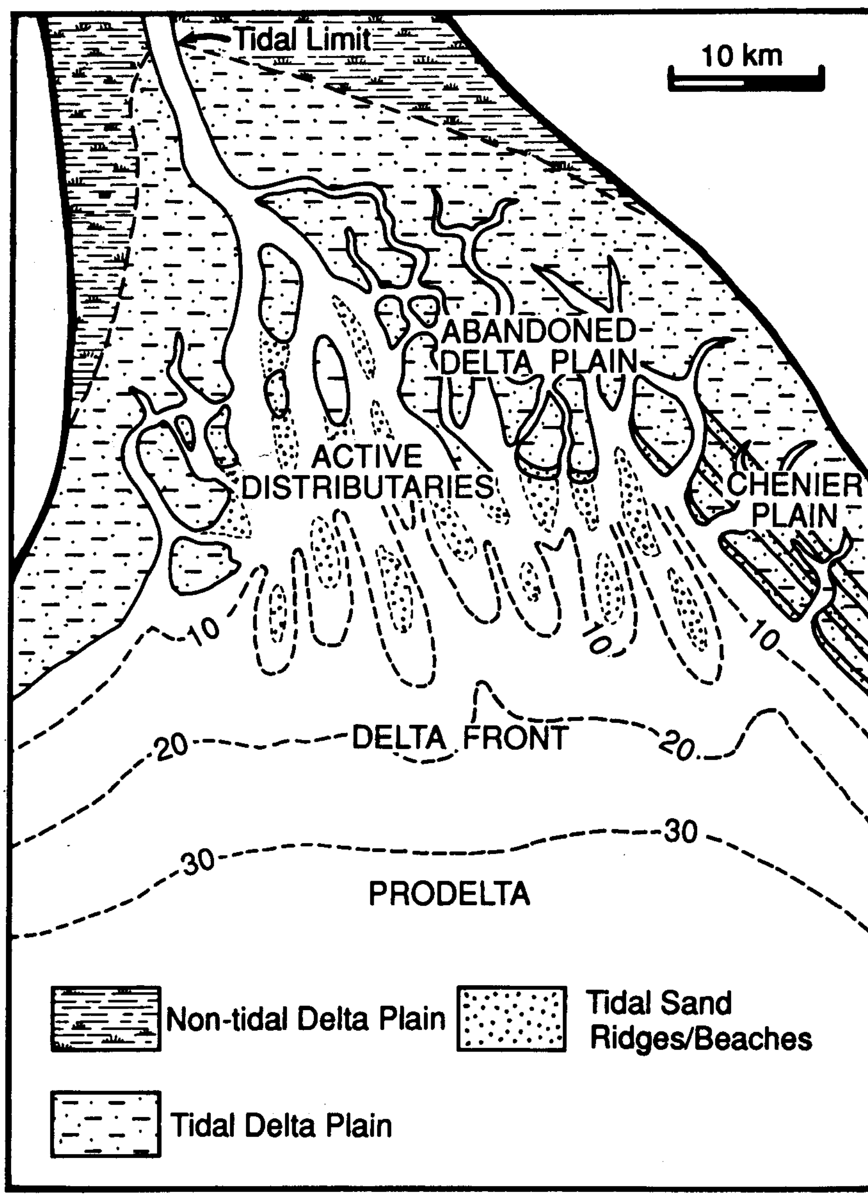

Figure 28 Schematic map of a tide-dominated delta, based on the Ganges-Brahmaputra, Ord, Colorado and Klang-Langat deltas. Note the morphological distinction between the active and inactive (abandoned) portions of the delta plain, and the outward transition from salt marsh, through mud flats and sand ridges, to the muddy prodelta. In areas adjacent to the embayment, open-coast tidal flats and chenier plains are developed.

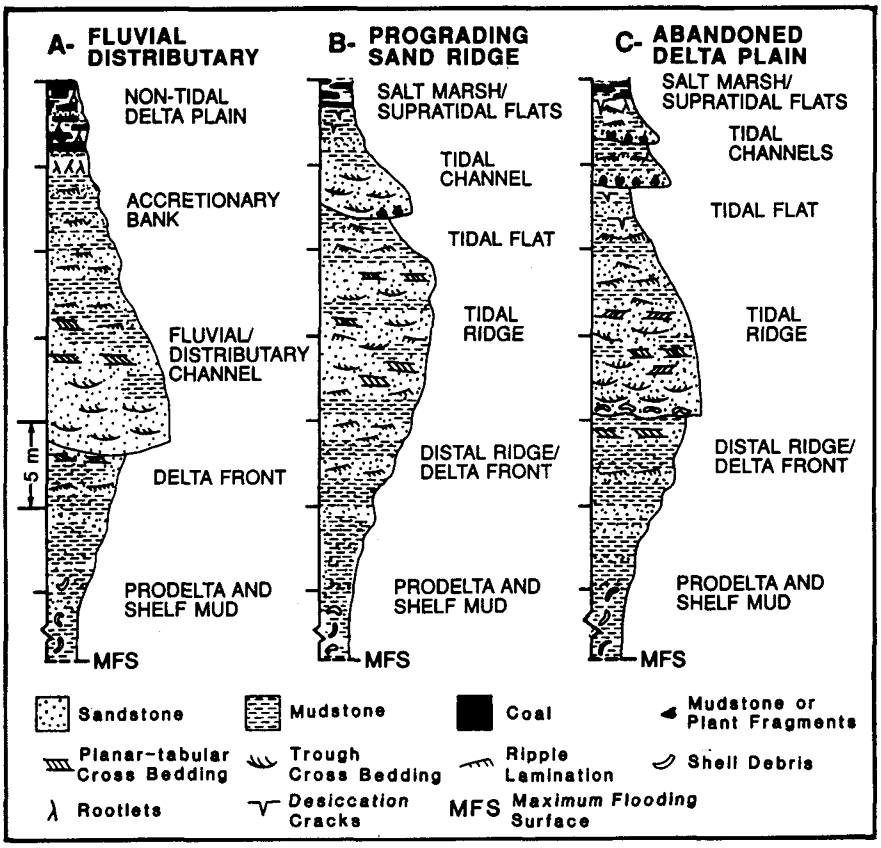

Figure 29 Three hypothetical, vertical facies successions within tide-dominated deltas, based on Coleman and Wright (1975), Meckel (1975) and Allen *et al.* (1979). In this example, the climate is humid, leading to the development of coal (black) in the subaerial portions of the delta plain. MFS – maximum flooding surface.

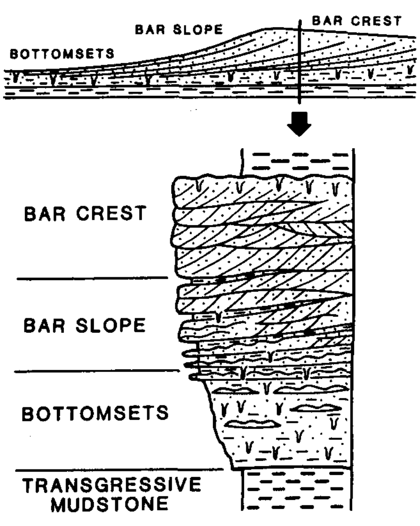

Figure 30 Schematic vertical succession through a prograding sand ridge in a regressive shelf setting, based on the Eocene of the Ager Basin, northern Spain. The vertical succession is typically about 5 m thick. After Mutti *et al.* (1985).

Figure 31 (right) Stratigraphic section through Ordovician tidal flat deposits, Capetown, South Africa, showing repeated upward-fining tidal flat successions (A.J. Tankard, pers. comm., 1991). The sandier middle portion of the section contains a greater proportion of subtidal sands, and accumulated in deeper water, on average, than the base and top of the formation. After Tankard and Hobday (1977).

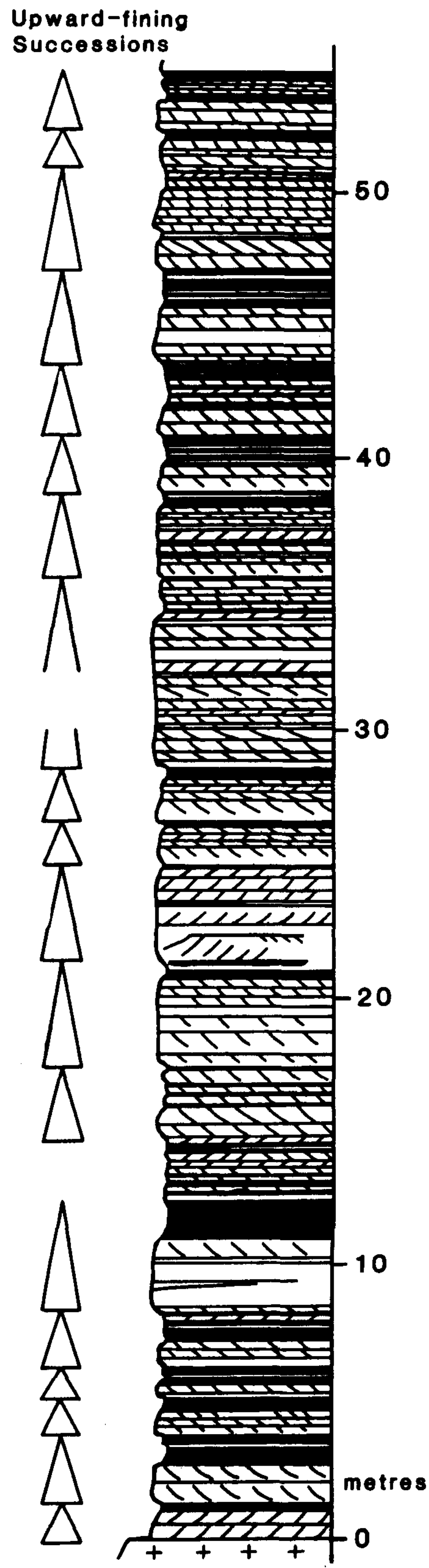

activity is provided by reactivation surfaces, mud drapes and local bipolar paleocurrents. Bioturbation of the sands may range from negligible to intense, but is probably greater on average than in estuarine sediments.

Unlike the relatively thin nature of transgressive shelf units, regressive shelf deposits are typically several tens to hundreds of metres thick.

Regressive stratigraphy

The stratigraphy of tide-dominated, highstand systems tracts remains largely speculative because of the scarcity of documented examples. The shelf, deltaic and coastal tidal flat deposits should downlap onto the maximum flooding surface at the top of the underlying transgressive systems tract, in the same manner as is seen in storm-dominated shelves (Chapter 12). The overall facies succession will be upward coarsening and upward shallowing, from offshore and/or prodelta muds, into the burrowed to cross-bedded sands of the shelf or deltaic sand ridge zone (Fig. 29B). Numerous small, upward-coarsening sand ridge successions (Fig. 30) may be present. In deltaic settings, these ridge deposits will be erosionally overlain by distributary channels (Fig. 29A). Tidal current scour in the abandoned portion of the delta plain may also truncate the sand ridges (Fig. 29C). Along nondeltaic shorelines, open-coast tidal flats will overlie the shelf sediments. The contact may be marked by an erosional discontinuity produced by wave erosion during the formation of chenier ridges. Above these various discontinuities, the sediments will generally fine upward, due to deposition on tidal flats or in distributary channels. The upper bounding discontinuity of the systems tract will be a terrestrial erosion surface produced during the subsequent sea level fall.

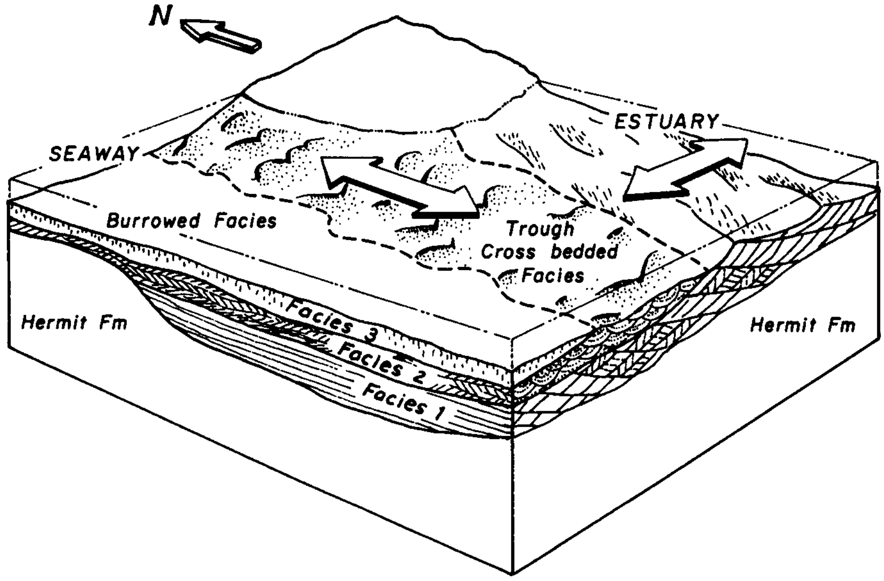

Figure 32 Reconstructed paleogeography of the Rancho Rojo Sandstone, Arizona. The upward decrease in set thickness and grain size from facies 1 to facies 3 is interpreted to represent progressive deepening, erosional transgression of an estuary, and establishment of shallow marine conditions. After Kreisa *et al.* (1986).

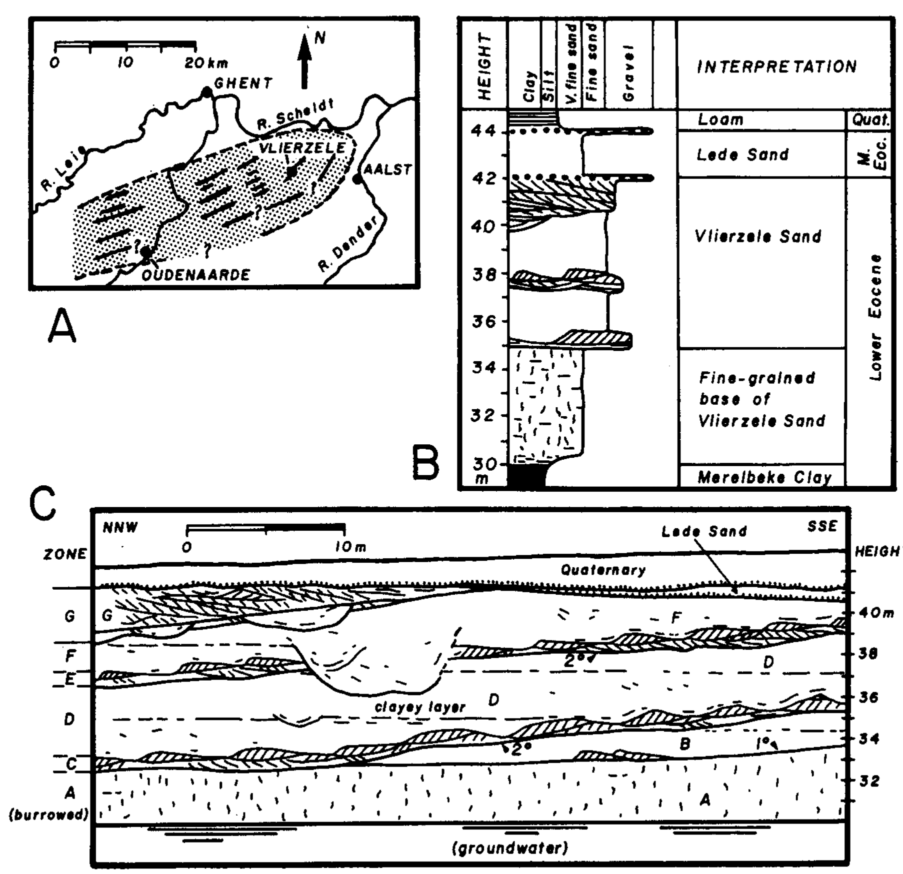

Figure 33 A) Distribution of Eocene tidal sand ridges (heavy lines) in the Vlierzele Sands (Eocene, Belgium). B) and C) Vertical profile and section through a sand ridge. Note the inclination of the stratigraphic units (C), and the overall upward-coarsening succession (B). The enigmatic massive sands of units D and F are interpreted as rapidly formed storm deposits, even though they do not have the typical features of storm beds (see Chapter 12). From Houthuys and Gullentops (1988).

ANCIENT EXAMPLES OF TIDE-DOMINATED DEPOSITS

Coastal successions

There are numerous descriptions of ancient tidal flat deposits (e.g., Sellwood, 1975; Tankard and Hobday, 1977; Kvale and Archer, 1990). Most of these display many or all of the features typical of tidal flat progradation (Fig. 12), even if the overall stratigraphic setting is transgressive. The paleogeographic and sequence-stratigraphic context of many of the documented tidal flat successions is not well known, but most are interpreted as lagoonal and estuarine deposits, and thus occur within transgressive systems tracts. Sellwood (1975) describes one such tidal flat deposit in the Jurassic of Bornholm, Denmark. Here, a single 13 m-thick, upward-fining, tidal flat succession overlies fluvial deposits and is in turn erosionally overlain by shallow-marine sandstones. Open-coast and delta-associated tidal flats and their accompanying chenier ridges in a highstand systems tract have been identified much less commonly. However, Kvale and Archer (1990) have described an 8 m-thick unit of tidal flat sediments that is interbedded between coals in a deltaic succession. Tidal rhythmites are well developed. This interval of tidal sediments, which shows an unusual symmetric, upward-coarsening upward-fining succession, represents a transgressive-regressive episode in the overall progradation of the delta plain.

Thicker sections containing a large number of stacked, tidal flat successions have been described from many localities, including the Ordovician of South Africa (Tankard and Hobday, 1977). In this example, the 55 m-thick Graafwater Formation consists of repeated, erosionally based, upward-fining (progradational) tidal flat successions that are typically 1-5 m thick (Fig. 31). This remarkable vertical stacking of tidal flat sediments implies that a close balance existed between accumulation and subsidence. Similar successions in carbonate rocks have received considerable attention in recent years (Chapter 16) because it is believed that they contain a detailed record of sea level fluctuations.

Shelf successions

The deposits of ancient tide-dominated shelves are characterized by cross-bedded sandstone. In most examples, the paleocurrents are essentially unimodal, although bipolar cross stratification is present locally. This paleocurrent pattern is usually attributed to the presence of regional, net sediment transport paths, and/or to the superposition of a unidirectional oceanic current. Reactivation surfaces are abundant, but regularly spaced mud drapes and neap-spring cyclicity are not particularly common.

Tidal shelf deposits are known from both transgressive and regressive (highstand) systems tracts, even though several authors (Banerjee, 1991) have suggested that tidal deposition is favoured by transgressions.

The Permian Rancho Rojo Sandstone of Arizona (Kreisa *et al.*, 1986) illustrates the main features of a transgressive, tidal systems tract (Fig. 32). Like most transgressive deposits, this unit is thin (maximum 18 m), and disconformably overlies and onlaps terrestrial sediments. The lowest part (facies 1) is interpreted to lie within an incised valley, and contains very large, simple and compound cross bedding (3-12 m-thick sets) with a bipolar (east-west) paleocurrent pattern. Reactivation surfaces, mud drapes and mud intraclasts are abundant. This is erosionally overlain by a unit of smaller-scale cross bedding (sets <1 m thick) that has a bipolar (north-south) paleocurrent (facies 2). Re-activation surfaces occur, but mud drapes are not reported. This is followed by rippled and bioturbated marine sands (facies 3) which become finer grained upwards. The entire succession reflects a decrease in tidal energy, due to increasing water depth as the transgression proceeded. The 90° change in paleocurrent direction, the decrease in the abundance of mud drapes, and the erosional contact between facies 1 and 2 are interpreted as resulting from transgression of an estuary, followed by shelf sedimentation.

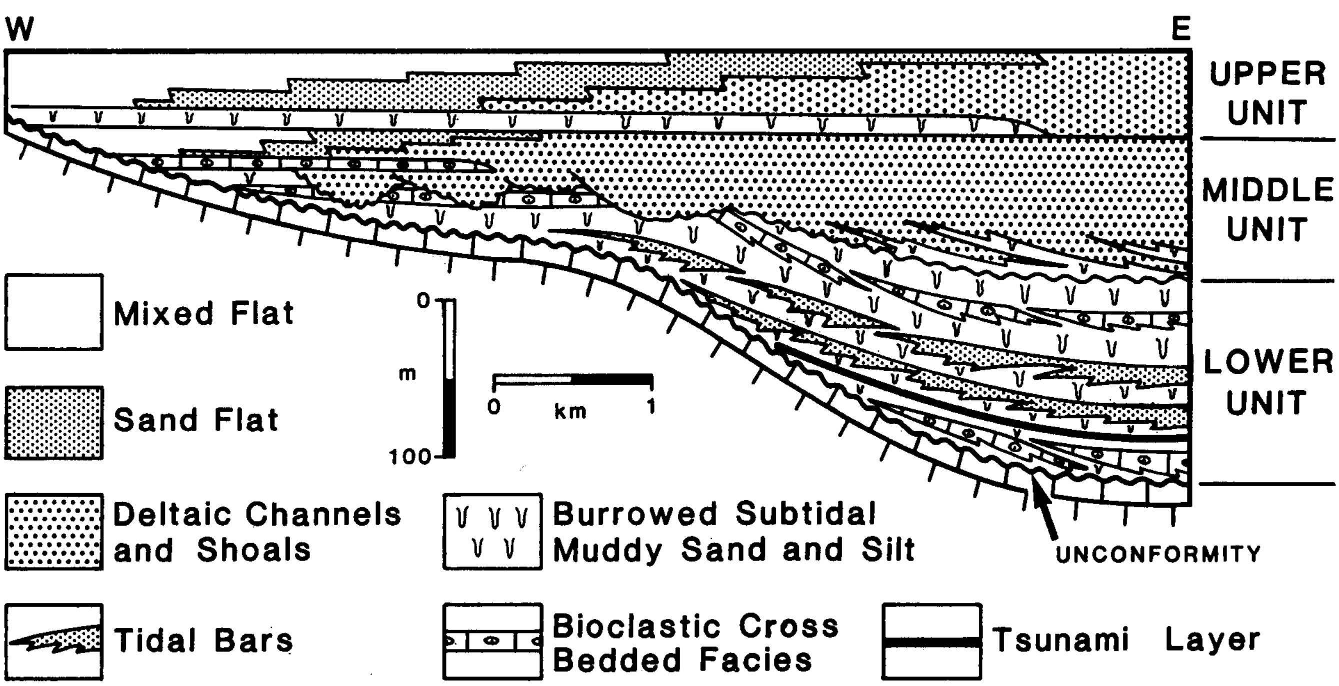

Figure 34 Diagrammatic cross section of the Baronia tide-dominated deltaic and regressive shelf depositional system, Ager Syncline, northern Spain. After Mutti *et al.* (1985).

Although abundant in modern shallow seas, tidal sand ridges are rarely described from the stratigraphic record. One of the most convincing examples occurs in Eocene sands in Belgium (Fig. 33; Houthuys and Gullentops, 1988), which are 10-20 m thick in the axes of the ridges. Cross bedding is the dominant structure, and there is abundant evidence of regularly varying current speeds and directions in the form of thin mud layers, reactivation surfaces and bipolar paleocurrents. The cross bedding is oriented parallel or slightly oblique to the ridge axis, as is expected from modern ridges, and the boundaries between cosets dip at low angles (2-3°; Fig. 33C) perpendicular to the ridge length. These surfaces are presumably equivalent to the inclined seismic reflectors seen in modern ridges (Fig. 21). Both vertical and horizontal burrowing are locally abundant. The ridge sediments erosionally overlie an upward-coarsening, regressive succession of marine clays and bioturbated fine sands (Fig. 33B). The limited thickness of the succession suggests that deposition occurred during a sea level fall, and represents a *forced regression* (Chapter 12).

A particularly good example of a tide-dominated regressive shelf and delta is provided by the Eocene Baronia deltaic system of northern Spain (Fig. 34; Mutti *et al.*, 1985), which consists of up to 275 m of interbedded sandstones and mudstones. The basal part is transgressive, and onlaps onto bedrock highs (Fig. 34). This lower unit accumulated in an eastward-closing embayment, and consists primarily of upward-coarsening, shelf sand ridge deposits (Fig. 30), each 5-6 m thick, that are encased in bioturbated shelf muds. Regressive periods are characterized by seaward-prograding ridges composed of siliciclastic sands, whereas transgressive episodes are marked by landward-migrating ridges composed of cross-bedded bioclastic material. The lower unit is capped by a deeper water, bioturbated sandy mudstone that represents the culmination of the transgression.

Following a hiatus that may be related to tectonic activity, progradation began from a deltaic sediment source along the southern margin of a through-going seaway (Fig. 34, middle unit). Deltaic sand ridges (the "estuary mouth shoals" of Mutti *et al.*, 1985) and regressive shelf ridges prograded to the east, in the direction of the dominant tidal currents, producing an upward-coarsening succession that downlaps onto the underlying discontinuity (Fig. 34). This regressive succession is then erosionally overlain by upward-fining, delta distributary channels ("estuary channels" of Mutti *et al.*, 1985). Individual channels are 5-20 m thick, but occur in amalgamated complexes up to 40 m thick. Almost all of the cross bedding dips seaward, and mud drapes are abundant. These channels are overlain by upward-fining tidal flat deposits. Delta progradation is terminated by another transgression, which is followed by a final phase of deltaic and tidal flat progradation from the west (Fig. 34, upper unit).

Many Late Precambrian and Cambrian tidal shelf deposits are not easily divisible into transgressive and regressive intervals. Such units are hundreds to thousands of metres thick, and consist largely of cross-bedded sandstone with little or no mud. For example, the Lower Sandfjord Formation (Late Precambrian) of northern Norway (Levell, 1980) is 1.5 km thick, and contains a variety of sizes and styles of simple and compound cross bedding. The paleocurrents are predominantly unimodal, although reversals occur. Numerous reactivation surfaces are present. Storm-generated event beds are rare. A clearly defined sequential ordering of grain sizes or facies is lacking in this and similar units, but from their thickness it is evident that deposition must have occurred over numerous sea level cycles.

Portions of the Gog quartzites (Cambrian) of the southern Canadian Rockies have similar characteristics, but with somewhat greater amounts of shale. Hein (1987) interprets the relatively disordered succession as resulting from the lateral migration of offshore sand ridges, without a strong overprint related to fluctuations of sea level.

PRESENT STATUS AND FUTURE DIRECTIONS

The recent recognition of neap-spring tidal-bundle sequences and tidal rhythmites has provided major new criteria for the identification of tidal sediments. Care must be exercized in the application of these criteria because not every thinly interbedded unit of sand and mud is a tidal rhythmite, nor do mud-draped foresets necessarily indicate the presence of tidal bundles. However, if tidal periodicities can be determined with confidence (De Boer *et al.*, 1989), then unequivocal evidence of tidal deposition is present. In the absence of these diagnostic structures, the presence of abundant reactivation surfaces and mud drapes, bipolar paleocurrents, the various types of so-called "tidal" bedding (Fig. 10), and emergence indicators may be used to infer a tidal origin. As with any environmental reconstruction, tidal interpretations should be based on the entire association of structures within the deposit.

Despite the large body of literature on tidal sedimentation, not all environments are known in equal detail. Tidal flats, which are the most accessible of tidal environments, are best known, and tide-dominated estuaries are becoming better understood through work in such areas as the Bay of Fundy and the Severn River. The morphological and textural attributes of transgressive shelves are well documented, but our understanding of the internal structure of subtidal sand waves and sand ridges remains largely theoretical. Our greatest knowledge gap lies with regressive tidal settings, for which there are few modern or ancient examples. Is this due to a real scarcity of such deposits, or to the absence of appropriate models?

Tidal facies models which include the influence of relative sea level changes are only beginning to emerge. Research on this aspect of tidal sedimentation has lagged behind that in wave-dominated systems. Models for transgressive systems tracts are the most firmly established (Fig. 24) because of the abundance of modern transgressive environments, but remain partially theoretical. The models for highstand systems tracts are even less well constrained, being based mainly on a few ancient examples (Fig. 34). None of these models, with the exception of that for an individual tidal flat succession (Fig 12), has the generality that the models for wave/storm-dominated coasts and shelves have.

ACKNOWLEDGEMENTS

I thank Roger Walker for his helpful editorial comments on earlier versions of the manuscript. Ela Rusak Mazur and John Glew drafted the figures. My research on tidal sedimentation has been funded by the Natural Sciences and Engineering Research Council of Canada.

REFERENCES

Basic sources of information

Allen, J.R.L., 1980, Sand waves; a model of origin and internal structure: Sedimentary Geology, v. 26, p. 281-328.
A good summary of the internal structure of large sand waves, even if the hydrodynamic model is flawed.

Dalrymple, R.W., Knight, R.J., Zaitlin, B.A. and Middleton, G.V., 1990, Dynamics and facies model of a macrotidal sandbar complex, Cobequid Bay–Salmon River estuary (Bay of Fundy): Sedimentology, v. 37, p. 577-612.
Comprehensive description of a tide-dominated estuary, with emphasis on the tidal sand ridges at the mouth.

Meckel, L.D., 1975, Holocene sand bodies in the Colorado delta area, northern Gulf of California, in Broussard, M.L., ed., Deltas: models for exploration: Houston, Houston Geological Society, p. 239-265.
The best description of a modern tide-dominated delta.

Nio, S.-D. and Yang, C.-S., 1991, Diagnostic attributes of clastic tidal deposits: a review, *in* Smith, D.G., Reinson, G.E., Zaitlin, B.A. and Rahmani, R.A., eds., Clastic tidal sedimentology: Canadian Society of Petroleum Geologists, Memoir 16, p. 3-28.
This is the place to start reading about the origin of tidal bundles, rhythmites and neap-spring cycles.

Smith, D.G., Reinson, G.E., Zaitlin, B.A. and Rahmani, R.A., eds., 1991, Clastic tidal sedimentology: Canadian Society of Petroleum Geologists, Memoir 16, 387 p.
Contains many examples of modern and ancient tidal deposits, including several descriptions of tidal rhythmites.

Stride, A.H., ed., 1982, Offshore tidal sands: processes and deposits: New York, Chapman and Hall, 222 p.
The definitive summary of sedimentation on transgressive shelves; do not expect to find anything on regressive settings. Excellent chapters on tidal processes, bedforms and facies distribution.

Weimer, R.J., Howard, J.D. and Lindsay, D.R., 1982, Tidal flats and associated tidal channels, *in* Scholle, P.A. and Spearing, D., eds., Sandstone depositional environments: American Association of Petroleum Geologists, Memoir 31, p. 191-245.
A review of tidal flat sedimentation, with modern and ancient examples.

Other references

Alexander, C.R., Nittrouer, C.A., Demaster, D.J., Park, Y.-A. and Park, S.-C., 1991, Macrotidal mud flats of the southwestern Korean coast: A model for interpretation of intertidal deposits: Journal of Sedimentary Petrology, v. 61, p. 805-824.

Allen, G.P., 1991, Sedimentary processes and facies in the Gironde estuary; A Recent model for macrotidal estuarine systems, *in* Smith, D.G., Reinson, G.E., Zaitlin, B.A. and Rahmani, R.A., eds., Clastic tidal sedimentology: Canadian Society of Petroleum Geologists, Memoir 16, p. 29-39.

Allen, G.P., Laurier, D. and Thouvenin, J., 1979, Étude sédimentologique du delta de la Mahakam: Compagnie Française des Petroles, Notes et Memoires 15, 156 p.

Allen, J.R.L., 1982, Mud drapes in sandwave deposits: physical model with application to the Folkestone Beds (Early Cretaceous, southeast England): Philosophical Transactions of the Royal Society, v. A306, p. 291-345.

Allen, J.R.L., 1990, The Severn Estuary in southwest Britain: its retreat under marine transgression, and fine sediment regime: Sedimentary Geology, v. 66, p. 13-28.

Allen, P.A. and Homewood, P., 1984, Evolution and mechanics of a Miocene tidal sandwave: Sedimentology, v. 31, p. 63-81.

Banerjee, I., 1991, Tidal sand sheets of the Late Albian Joli Fou–Kiowa–Skull Creek marine transgression, Western Interior Seaway of North America, *in* Smith, D.G., Reinson, G.E., Zaitlin, B.A. and Rahmani, R.A., eds., Clastic tidal sedimentology: Canadian Society of Petroleum Geologists, Memoir 16, p. 335-348.

Belderson, R.H., Johnson, M.A. and Kenyon, N.H., 1982, Bedforms, *in* Stride, A.H., ed., Offshore tidal sands: processes and deposits: New York, Chapman and Hall, p. 27-57.

Berné, S., Auffret, J.-P. and Walker, P., 1988, Internal structure of subtidal sandwaves revealed by high-resolution seismic reflection: Sedimentology, v. 35, p. 5-20.

Bridges, P.H. and Leeder, M.R., 1976, Sedimentary model for intertidal mudflat channels, with examples from the Solway Firth, Scotland: Sedimentology, v. 23, p. 533-552.

Cameron, T.D.J., Laban, C. and Schuttenhelm, R.T.E., 1989, Middle and Upper Pleistocene and Holocene stratigraphy in the southern North Sea between 52° and 54°N, 2° to 4°E, *in* Henriet, J.P. and deMoor, G., eds., The Quaternary and Tertiary geology of the southern bight, North Sea: Ghent, Belgian Geological Survey, p. 119-135.

Coleman, J.M., Gagliano, S.M. and Smith, W.G., 1970, Sedimentation in a Malaysian high tide tropical delta, in Morgan, J.P., ed., Deltaic sedimentation: modern and ancient: Society of Economic Paleontologists and Mineralogists, Special Publication 15, p. 185-197.

Coleman, J.M. and Wright, L.D., 1975, Modern river deltas: variability of processes and sand bodies, *in* Broussard, M.L., ed., Deltas: models for exploration: Houston, Houston Geological Society, p. 99-149.

Dalrymple, R.W., 1984, Morphology and internal structure of sand waves in the Bay of Fundy: Sedimentology, v. 31, p. 365-382.

Dalrymple, R.W., Makino, Y. and Zaitlin, B.A., 1991, Temporal and spatial patterns of rhythmite deposition on mudflats in the macrotidal, Cobequid Bay-Salmon River estuary, Bay of Fundy, Canada, *in* Smith, D.G., Reinson, G.E., Zaitlin, B.A. and Rahmani, R.A., eds., Clastic tidal sedimentology: Canadian Society of Petroleum Geologists, Memoir 16, p. 137-160.

Dalrymple, R.W., Zaitlin, B.A. and Boyd, R., 1992, A conceptual model of estuarine sedimentation: Journal of Sedimentary Petrology, v. 62, in press.

De Boer, R.L., Oost, A.P. and Visser, M.J., 1989, The diurnal inequality of the tide as a parameter for recognizing tidal influences: Journal of Sedimentary Petrology, v. 59, p. 912-921.

Forrester, W.D., 1983, Canadian tidal manual: Ottawa, Department of Fisheries and Oceans, 138 p.

Galloway, W.E., 1975, Process framework for describing the morphologic and stratigraphic evolution of deltaic depositional systems, *in* Broussard, M.L., ed., Deltas: models for exploration: Houston, Houston Geological Society, p. 87-98.

Gostin, V.A., Hails, J.R. and Belperio, A.P., 1984, The sedimentary framework of northern Spencer Gulf, South Australia: Marine Geology, v. 61, p. 111-138.

Hayes, M.O., 1979, Barrier island morphology as a function of tidal and wave regime, *in* Leatherman, S.P., ed., Barrier islands — from the Gulf of St. Lawrence to the Gulf of Mexico: New York, Academic Press, p. 1-27.

Hein, F.J., 1987, Tidal/littoral offshore shelf deposits — Lower Cambrian Gog Group, southern Rocky Mountains, Canada: Sedimentary Geology, v. 52, p. 155-182.

Houbolt, J.J.H.C., 1968, Recent sediments in the southern bight of the North Sea: Geologie en Mijnbouw, v. 47, p. 245-273.

Houthuys, R. and Gullentops, F., 1988, The Vlierzele Sands (Eocene, Belgium): a tidal ridge system, *in* de Boer, P.L., van Gelder, A. and Nio, S.D., eds., Tide-influenced sedimentary environments and facies: Boston, D. Reidel Publishing Company, p. 139-152.

Howarth, M.J., 1982, Tidal currents of the continental shelf, *in* Stride, A.H., ed., Offshore tidal sands: processes and deposits: New York, Chapman and Hall, p. 10-26.

Johnson, H.D. and Baldwin, C.T., 1986, Shallow siliciclastic seas, *in* Reading, H.G., ed., Sedimentary environments and facies: Oxford, Blackwell Scientific Publications, p. 229-282.

Johnson, M.A., Kenyon, N.H., Belderson, R.H. and Stride, A.H., 1982, Sand transport, *in* Stride, A.H., ed., Offshore tidal sands: processes and deposits: New York, Chapman and Hall, p. 58-94.

Kreisa, R.D., Moiola, R.J. and Nottvedt, A., 1986, Tidal sand wave facies, Rancho Rojo Sandstone (Permian), Arizona, *in* Knight, R.J. and McLean, J.R., eds., Shelf sands and sandstones: Canadian Society of Petroleum Geologists, Memoir 11, p. 277-291.

Kvale, E.P. and Archer, A.W., 1990, Tidal deposits associated with low-sulphur coals, Brazil Fm. (Lower Pennsylvanian), Indiana: Journal of Sedimentary Petrology, v. 60, p. 563-574.

Larsonneur, C., 1975, Tidal deposits, Mont Saint-Michel Bay, France, *in* Ginsburg, R.N., ed., Tidal deposits: a casebook of recent examples and fossil counterparts: New York, Springer-Verlag, p. 21-30.

Levell, B.K., 1980, A late Precambrian tidal shelf deposit, the Lower Sandfjord Formation, Finnmark, North Norway: Sedimentology, v. 27, p. 539-557.

McCave, I.N., 1971, Sand waves in the North sea off the coast of Holland: Marine Geology, v. 10, p. 199-225.

Mutti, E., Rosell, J., Allen, G.P., Fonnesu, F. and Sgavetti, M., 1985, The Eocene Baronia tide dominated delta-shelf system in the Ager Basin, *in* Mila, M.D. and Rosell, J., eds., Excursion guidebook: 6th European Regional Meeting, International Association of Sedimentologists, Lleida, Spain, p. 579-600.

Open University Course Team, 1989, Waves, tides and shallow-water processes: Oxford, Pergamon Press, 187 p.

Reineck, H.E. and Singh, I.B., 1980, Depositional sedimentary environments: New York, Springer-Verlag, 549 p.

Reineck, H.E. and Wunderlich, F., 1968, Classification and origin of flaser and lenticular bedding: Sedimentology, v. 11, p. 99-104.

Sellwood, B. W., 1975, Lower Jurassic tidal-flat deposits, Bornholm, Denmark, *in* Ginsburg, R.N., ed., Tidal deposits: a casebook of recent examples and fossil counterparts: New York, Springer-Verlag, p. 93-101.

Stewart, H.B. and Jordan, G.F., 1964, Underwater sand ridges on Georges Shoal, *in* Miller, R.L., ed., Papers in marine geology: Shepard commemorative volume: New York, McMillan, p. 102-116.

Stride, A.H., Belderson, R.H., Kenyon, N.H. and Johnson, M.A., 1982, Offshore tidal deposits: sand sheet and sand bank facies, *in* Stride, A.H., ed., Offshore tidal sands: processes and deposits; New York, Chapman and Hall, p. 95-125.

Swift, D.J.P., 1975, Tidal sand ridges and shoal retreat massifs: Marine Geology, v. 18, p. 105-134.

Tankard, A.J. and Hobday, D.K., 1977, Tide-dominated back-barrier sedimentation, early Ordovician Cape Basin, Cape Peninsula, South Africa: Sedimentary Geology, v. 18, p. 135-159.

Terwindt, J.H.J., 1988, Palaeo-tidal reconstructions of inshore tidal depositional environments, *in* De Boer, P.L., van Gelder, A. and Nio, S.D., eds., Tide-influenced sedimentary environments and facies: Boston, D. Reidel Publishing Company, p. 233-263.

Thomas, R.G., Smith, D.G., Wood, J.M., Visser, J., Calverley-Range, E.A. and Koster, E.H., 1987, Inclined heterolithic stratification — terminology, description, interpretation and significance: Sedimentary Geology, v. 53, p. 123-179.

Thompson, R.W., 1968, Tidal flat sedimentation on the Colorado River delta, northwestern Gulf of California: Geological Society of America, Memoir 107, 413 p.

Twichell, D.C., 1983, Bedform distribution and inferred sand transport on Georges Bank, United States Atlantic continental shelf: Sedimentology, v. 30, p. 695-710.

Van Wagoner, J.C., Mitchum, R.M., Campion, K.M. and Rahmanian, V.D., 1990, Siliciclastic sequence stratigraphy in well logs, cores, and outcrops: concepts of high-resolution correlation of time and facies: American Association of Petroleum Geologists, Methods in Exploration Series, No. 7, 55 p.

Visser, M.J., 1980, Neap-spring cycles reflected in Holocene subtidal large-scale bedform deposits: a preliminary note: Geology, v. 8, p. 543-546.

Wang, Y., 1983, The mudflat system of China, *in* Gordon, D.C., Jr. and Hourston, A.S., eds., Proceedings of the symposium on the dynamics of turbid coastal environments: Canadian Journal of Fisheries and Aquatic Science, v. 40, supplement 1, p. 160-171.

Williams, G.E., 1991, Upper Proterozoic tidal rhythmites, South Australia: sedimentary features, deposition, and implications for the Earth's paleorotation, *in* Smith, D.G., Reinson, G.E., Zaitlin, B.A. and Rahmani, R.A., eds., Clastic tidal sedimentology: Canadian Society of Petroleum Geologists, Memoir 16, p. 161-178.

Wright, L.D., Coleman, J.M. and Thom, B.G., 1975, Sediment transport and deposition in a macrotidal river channel, Ord River, Western Australia, *in* Cronin, L.E., ed., Estuarine research, v. II: New York, Academic Press, p. 309-322.

Yang, C.-S., 1989, Active, moribund and buried tidal sand ridges in the East China Sea and the southern Yellow Sea: Marine Geology, v. 88, p. 97-116.

Yang, C.-S. and Sun, J., 1988, Tidal sand ridges on the East China Sea shelf, *in* De Boer, P.L., van Gelder, A. and Nio, S.D., eds., Tide-influenced sedimentary environments and facies: Boston, D. Reidel Publishing Company, p. 23-38.

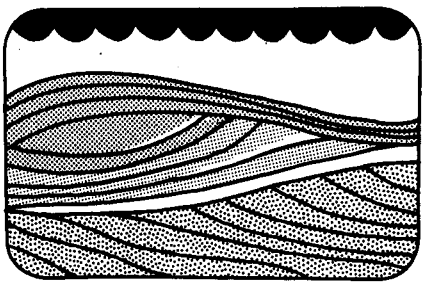

12. Wave- and Storm-Dominated Shallow Marine Systems

Roger G. Walker, Department of Geology,
McMaster University, Hamilton, Ontario L8S 4M1

A. Guy Plint, Department of Geology, University of Western Ontario,
London, Ontario N6A 5B7

INTRODUCTION

Shallow marine systems include a continuum of depositional environments, from beach and shoreface, through inner to outer shelf settings. The environments are laterally gradational, and are linked by a variety of geological processes. Wave- and storm-dominated shallow marine sediments can occur in highstand, lowstand and transgressive systems tracts. Highstand deposits are commonly typified by sandier-upward facies successions that accumulate during coastal progradation and shelf aggradation. Lowstand shelf deposits also shoal upward; they commonly form isolated sandbodies, bounded by erosion surfaces and enclosed in marine mudstone. Transgressive systems tract deposits commonly consist of coarse lags that pass upward into transgressive mudstones. The sedimentary record may be even more complex if tidal and oceanic currents were operating; the distinctive suite of tidally influenced facies is discussed in Chapter 11.

The geological record of shoreline and shallow marine systems is further complicated by their sensitivity to even minor fluctuations of sea level. This sensitivity was not fully appreciated when the second edition of *Facies Models* was written (Walker, 1984), but its effect on the distribution and geometry of sandbodies is now much better understood. For example, erosion can result from both falling and rising sea levels, and can be as important as depositional processes in controlling sandbody geometry.

The abundance of erosion surfaces (bounding discontinuities) makes an allostratigraphic (Chapter 1) approach to shoreline and shallow marine systems very important. Readers interested in the history of studies of shallow marine systems, and in some of the older case histories, are referred to the second edition (Walker, 1984).

Modelling depositional systems involves the comparison of modern and ancient examples. Sandbodies around modern shorelines and on modern shelves have been severely influenced by the Holocene transgression. This began about 18,000 years ago as a result of the onset of deglaciation, and involved a relative sea level rise of more than 100 m. Consequently, modern transgressive systems tract deposits can be examined, but few prograding highstand systems are available for study.

DEFINITIONS AND TERMS USED IN THIS CHAPTER

The term *bar* includes all ancient elongate, narrow accumulations of coarse sediment, and the term *sandbody* includes accumulations of sandstone and/or conglomerate. *Shallow marine* will be used as a general term for environments affected by waves, regardless of their tectonic setting. It includes modern shelves as well as epeiric seas and the shallow parts of foreland basins.

MORPHOLOGICAL ELEMENTS

The main morphological elements of a

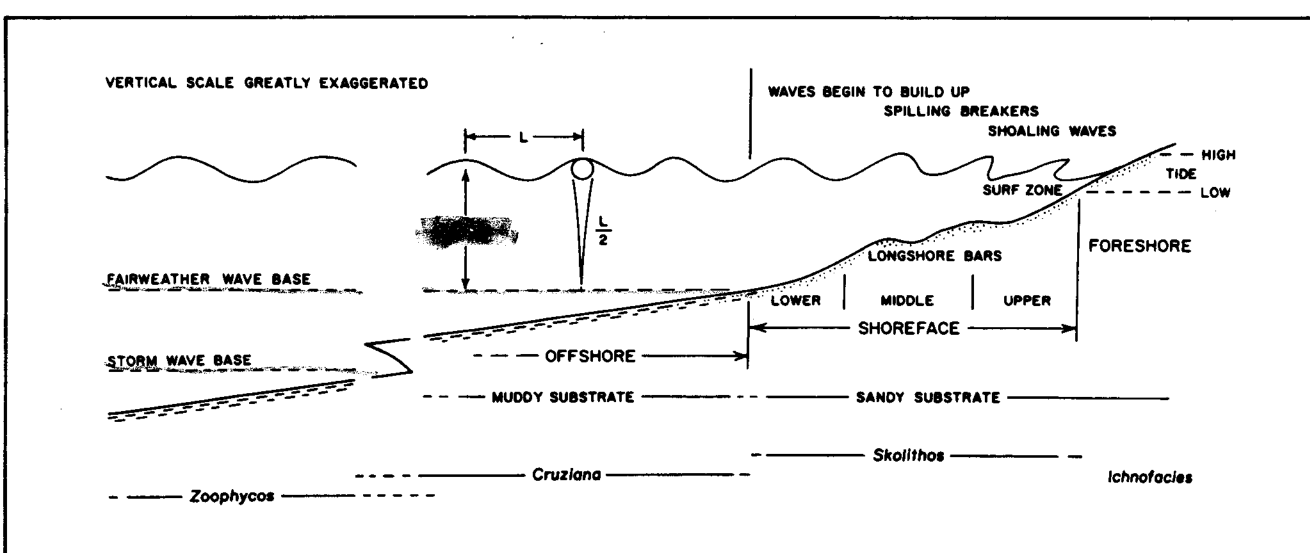

Figure 1 Shoreline to shallow marine profile locating foreshore, shoreface and offshore areas, as well as fairweather wave base and approximate ichnofacies occurrences. Note that fairweather waves of wavelength L cannot agitate the bed at depths greater than approximately L/2. *Fairweather wave base lies at depths of about 5-15 m.*

modern shoreline-to-shallow-marine depositional system are shown in Figure 1. The *foreshore*, which is essentially synonymous with *beach*, consists of the portion above low tide line, and is dominated by the swash and backwash of breaking waves. The *shoreface* lies consistently below low tide level and is characterized by day-to-day sand transport above fair-weather wave base. The depth of fair-weather wave base varies from about 5-15 m, depending on the general wave climate of the basin. The shoreface normally has a concave-upward profile, which is in equilibrium with the waves that shape it. The shoreface gradient of about 1:200 (about 0.3°) decreases seaward, and the sand-dominated shoreface passes into the mud-dominated *offshore zone* where the gradient is closer to 1:2000 (about 0.03°). In a prograding sedimentary succession, it is impossible to identify the topographic change that marks the transition from offshore to shoreface. In practice, the base of the shoreface can be defined at the point where interbedded sandstones and mudstones pass upward into relatively clean sandstones.

A variety of small bedforms, bars and runnels exist in the shoreface. Their migration produces both scoured surfaces and medium-scale angle-of-repose cross stratification, and these features can be preserved in the stratigraphic record.

In many places, large shoreface ridges (Swift and Field, 1981) originate in the middle to lower shoreface, and trend obliquely seaward (Fig. 2). Off the coast of Maryland (U.S. Atlantic shelf), for example, the shoreface ridges pass seaward into shelf ridges with heights of 6-9 m, lengths of 8-14 km and widths of 1-2 km. Both shelf and shoreface ridges rest on an erosion surface cut during the Holocene transgression. The more seaward ridges are now isolated on the shelf where they form fields of *ridges and swales* in nearshore and offshore areas. The morphology and internal structure of these ridges are slowly being modified by storm currents (Fig. 2).

The ridges and bars observed in shallow marine settings today originally formed at or close to the shoreline. They were subsequently drowned during the Holocene transgression and now appear "abandoned" on the shelf. There is no well-documented example of a modern sandy "offshore bar" that has developed on a contemporaneous muddy substrate in a totally offshore setting.

PHYSICAL PROCESSES IN THE BEACH AND UPPER SHOREFACE

Sediment transport in the beach and upper shoreface is driven by waves. Good reviews of the processes are given by Komar (1976, 1983) and Swift *et al.* (1986). As waves enter shallow water, they begin to move sediment on the seafloor at a maximum depth roughly equal to half their wavelength (Fig. 1). The wave-induced orbital water motion close to the bed is asymmetrical, resulting in a net onshore movement of sand.

In the *foreshore* and *upper shoreface*, the onshore, longshore and offshore (rip) currents are shown in Figure 3. Waves transport water *onshore*; when they break on the beach they drive a thin sheet of water rapidly up the beachface. This swash is capable of moving sand and gravel, and typically produces plane lamination parallel to the beachface. There are two dominant current systems — longshore currents produced by oblique wave approach to the shoreline and a cell circulation of rip currents and longshore currents (Komar, 1976; Fig. 3).

Longshore currents are driven by waves breaking at an angle to the shoreline (Fig. 3). Measurements show that the current velocity drops quickly to zero outside the breaker zone, indicating that waves rather than tidal currents or oceanic circulation control the flow. Predicting sand movement by these longshore currents is very important in studies of coastal stability and erosion (Komar, 1983; Everts, 1987; Pilkey and Davis, 1987). The dip

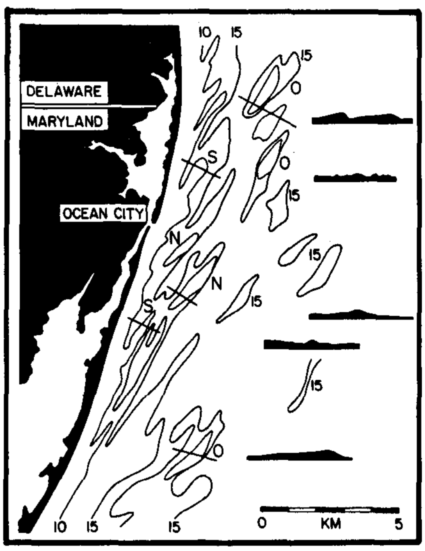

Figure 2 Bathymetry (in metres) of the Assateague ridge field, offshore Maryland, U.S.A. Note typical shoreface (S), nearshore (N) and offshore (O) ridges, with their typical bathymetric cross sections (which are presented at a greater scale than the map itself). Ridges appear to be more symmetrical in the shoreface, and more asymmetrical offshore. Simplified from Swift and Field (1981).

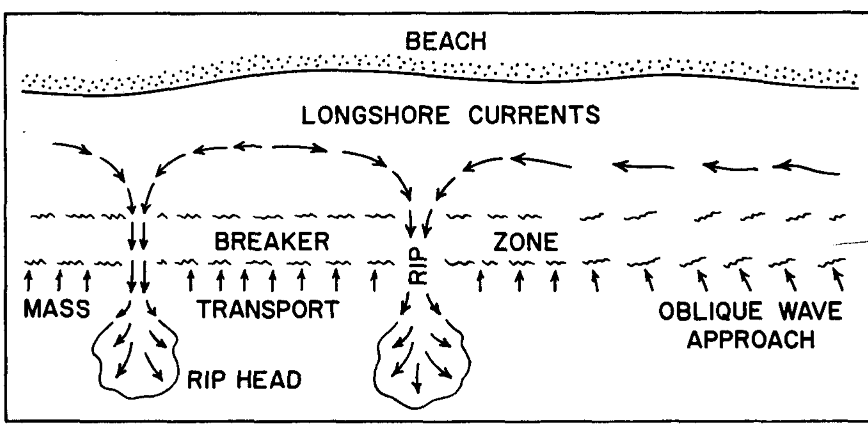

Figure 3 In the shoreface, there is mass onshore transport of water, driven by waves. Landward of the breaker zone, this water moves as longshore currents. If wave crests are roughly parallel to shore, the longshore currents flow in opposite directions to form cells. Water is transported seaward as rip currents where two longshore currents converge (left half of figure). Seaward of the breaker zone, the rip currents spread in the rip heads and die out. If wave crests approach the beach obliquely, the longshore currents tend to move in one direction (right half of figure). Rip cell portion of the figure is based on Komar (1976, fig. 7-1).

of the beachface is influenced by grain size (steeper on coarser grained beachfaces) and by wave conditions. During fair weather sand tends to move onshore, steepening the beach profile, whereas storms remove sand from the beach and flatten the profile.

In the cell circulation, water returns seaward in rip currents that can transport sand and gravel, and cut channels in the upper shoreface. However, the currents die out seaward of the breaker zone, and do not transport sediment more than a few hundred metres offshore.

STORM-INDUCED SHELF CURRENTS

Although storm conditions exist for only a small part of the year at any given point on the shelf, their effects in terms of erosion and sediment transport are disproportionately large. During a storm, frictional coupling between the wind and the water surface causes water to be driven forward. The moving surface waters entrain deeper and deeper layers, all of which are deflected to the right (in the northern hemisphere) by *Coriolis force*. Sediment-moving currents on the seafloor therefore flow at angles of up to 90° to the wind direction. A very clear discussion of these wind-driven currents is given by the Open University Course Team (1989).

Water blown onshore by the wind also results in an ocean surface that is higher at the coast than offshore (a *coastal set up*). The superelevation can also be augmented by very low atmospheric pressures. The different water levels at the coast and offshore result in hydrostatic pressure differences on the ocean floor. These pressure differences drive a bottom flow down the pressure gradient (relaxation flow, Fig. 4). This flow is also deflected by Coriolis force, resulting in a geostrophic flow that moves obliquely offshore, veering through time to flow shore-parallel. The flow persists as long as there is a pressure gradient, typically for a few days in the case of a winter storm on the present Atlantic shelf (Swift *et al.*, 1986). We emphasize that the flow is a continuous response to the pressure gradient; it is *not* a sudden surge of water related to the end of the storm winds.

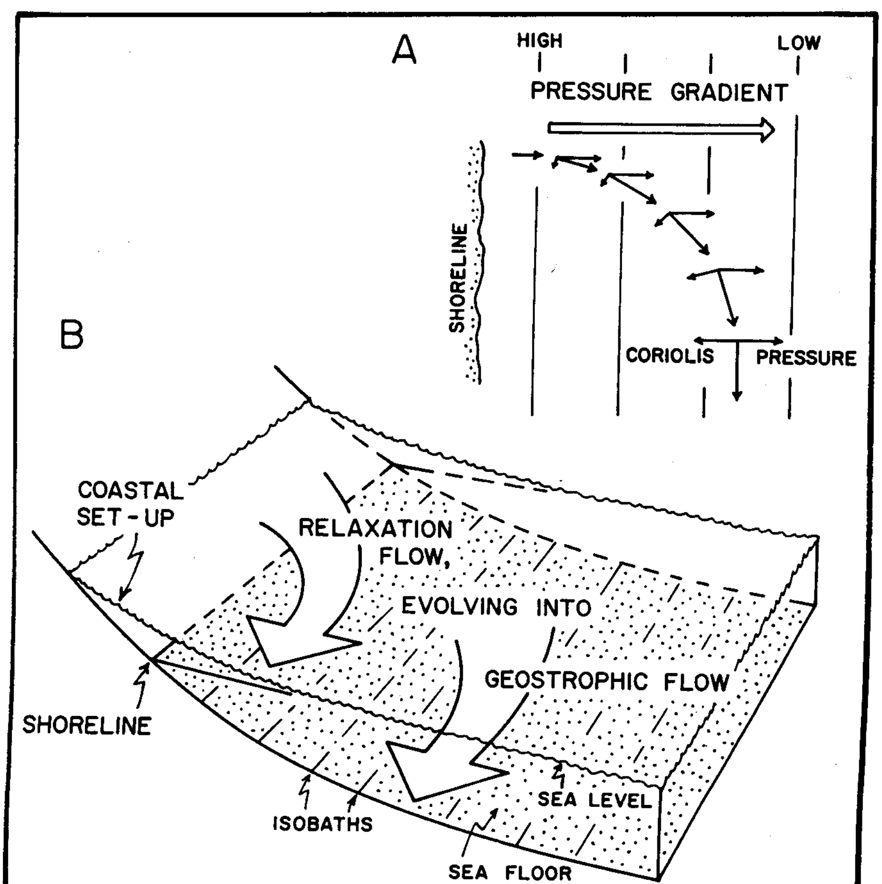

Figure 4 Coastal set-up ("storm surge") creates a seaward pressure gradient (A). Bottom water flows seaward as a result, but is deflected to the right (northern hemisphere) by Coriolis force to form a geostrophic flow (B) parallel to isobaths. The extent of the deflection is controversial (see "The sand transport problem" in text). In theory it depends upon the latitude, mass of water in motion and its velocity, as well as the duration of the flow. No scale is implied in the diagram, which is constructed after Swift and Niedoroda (1985) and Strahler (1963).

Storms and hurricanes on modern shelves

Flow velocities associated with annual northeasterly storms on the Atlantic shelf have been measured by Swift and colleagues (Swift *et al.*, 1981; Swift and Field, 1981). In depths of 10-20 m, near-bottom velocities are up to about 60 cm/sec. These flows, by themselves, are incapable of moving much sand. However, the currents are usually accompanied by a powerful wave-driven oscillatory motion at the bed (Swift *et al.*, 1986). Unidirectional and oscillatory currents, operating together, are termed *combined flows*. The waves provide the high shear stresses needed to lift the sediment off the bed, and the grains are gradually dispersed in the direction of the geostrophic bottom currents.

Tropical storms and hurricanes generate much higher flow velocities close to the bed. Classic examples have been reviewed by Morton (1988), and recent data from the Texas shelf have been discussed by Snedden *et al.* (1988). Hurricane Camille, in 1969, was one of the most intense Gulf of Mexico hurricanes in modern times. Current meters in the shoreface to the east of the path of Camille showed a longshore flow strengthening and veering offshore, with peak velocities of about 160 cm/sec. Farther out on the shelf, just east of the birdfoot delta of the Mississippi, the storm waves appear to have liquefied the bed, causing sediment flowage and slumping. Parts of the bed appear to have been lowered by about 2 m, and other parts raised by 10 m.

Tropical Storm Delia (1973) moved northwestward across the Texas shelf. Near bottom current measurements were made from an offshore drilling platform situated 50 km off Galveston Island in 21 m of water (Fig. 5; Forristall *et al.*, 1977). Shore-parallel flows reached nearly 2 m/sec, and offshore flows were between 50 and 75 cm/sec. The coastal set up of 2 m at Galveston Island did not occur until 30 hours after the storm reached the shoreline (landfall, Fig. 5), whereas the maximum shore-parallel velocity occurred about 38 hours before peak coastal set up (Fig. 5). Thus the shore-parallel (geostrophic) flow was driven by wind stresses, not storm surge ebb. Hurricane Alicia (1983) followed roughly the same path as Delia, causing a coastal set up of about 3 m. Longshore and slightly offshore currents were measured up to 1 m/sec, and flows of about 50 cm/sec were sustained for about two days. Hurricane Alicia appears to have formed a graded bed, probably by in situ reworking and size fractionation of pre-existing shelf sediments (Morton, 1988). However, the graded bed had largely been reworked by organisms only three months later.

These examples show that storms and hurricanes move sediment in shallow marine settings. The direction of sediment movement appears to be obliquely offshore with some sand moving from the shoreface into offshore settings.

SEDIMENTARY STRUCTURES IN SHOREFACE AND SHALLOW MARINE SETTINGS

In these environments, structures form in response to unidirectional and oscillatory (wave) currents; these flows commonly co-exist, to form combined flow sedimentary structures.

Ripples and dunes

In sand-sized sediment, oscillation ripples are ubiquitous, and are characterized by straight crests and symmetrical profiles. Symmetrical gravel ripples, which can form at depths of up to 160 m, have also been reported in modern (Forbes and Boyd, 1987; Hart and Plint, 1989) and ancient (Leckie, 1988) sediments. Combined flow ripples (Fig. 6) tend to have symmetrical profiles, but an internal cross lamination that dips consistently in one direction. In the geological record, where the ripple profile may not be preserved, combined flow and current ripples can be very difficult to distinguish.

Two- and three-dimensional dunes are common in modern shorefaces where they are formed by fairweather longshore and onshore currents (Clifton *et al.*, 1971; Greenwood and Mittler, 1985). Their migration forms medium-scale cross bedding. In wave- and particularly storm-dominated shorefaces, however, the cross bedding tends to be obliterated by storm waves and replaced by parallel lamination and/or swaly cross stratification (Greenwood and Sherman, 1986). Dunes are also observed on modern shelves, with wavelengths of 1-40 m, and dune heights of several metres. The smaller 3-D dunes actively migrate during storm-induced geostrophic flows (Swift *et al.*, 1981), but may be reworked to ripples during waning flows. The larger 2-D dunes, with spacings of 20-400 m, migrate more slowly and are not reformed from storm to storm.

Hummocky cross stratification (HCS)

This structure (Fig. 7), which forms mainly in fine- and very fine-grained sandstones, was not commonly identified in the geological record until the name *hummocky cross stratification* (HCS) was created by John Harms (Harms *et al.*, 1975). He compared the hummocky bedform to large-scale wave ripples, and interpreted HCS as a storm deposit. HCS has now been recognized in many basins of different ages (Duke, 1985), and the storm interpretation is widely accepted. Debate continues on the mechanics of its formation; some authors favour combined flows whereas the experimental results of Southard *et al.* (1990) favour strong, purely oscillatory flows. Because HCS is probably formed during major storms, there is no direct observational evidence from modern shallow seas. Cores of possible HCS have been obtained from the shoreface (Greenwood and Sherman, 1986), and it has been tentatively identified in offshore areas.

In the geological record, HCS sandstones are commonly interbedded with bioturbated mudstones. The sandstone beds are commonly 10-50 cm thick, with a few beds thicker than 1 m. Most beds have sharp bases, and a few also have directional sole marks (which often suggest flow perpendicular to regional shoreline trends). In most examples, there is no associated medium-scale angle-of-repose cross bedding; this is probably a function of grain-size control, with the cross bedding forming mainly in medium- and coarse-grained sands. HCS is generally preserved in areas of weak tidal activity that lie below fairweather wave base. The main problem presented by HCS sandstones interbedded with bioturbated mudstones is not so much the formation of HCS as the mechanism of sand transport to the final depositional site; this is discussed later.

Swaly cross stratification

In the geological record, some HCS sandstone beds amalgamate together,

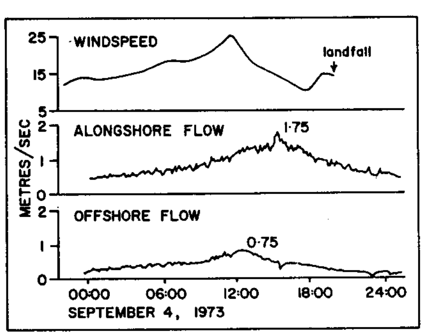

Figure 5 Windspeed, longshore (shore-parallel) and offshore currents measured during Tropical Storm Delia, September 3-5, 1973. Data recorded at a drilling platform 50 km offshore from Galveston Island, Texas, in a depth of 21 m. Redrawn and simplified from Forristall *et al.* (1977).

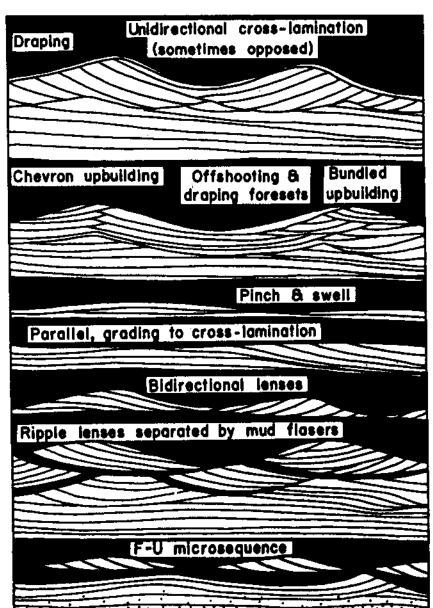

Figure 6 Sketch showing the various types of ripple cross stratification formed by waves. Modified from de Raaf *et al.* (1977).

and the interbedded mudstones are thin or absent. There appears to have been little opportunity for the deposition and preservation of mud, suggesting a generally shallower, more agitated environment. If the HCS sandstones amalgamate so thoroughly that there is no interbedded mudstone,

Figure 7 Hummocky cross stratification, Cardium Formation, Ram River, Alberta. Arrows show curvature of lamination within the HCS. Also note low angle convergence of curved laminae at C.

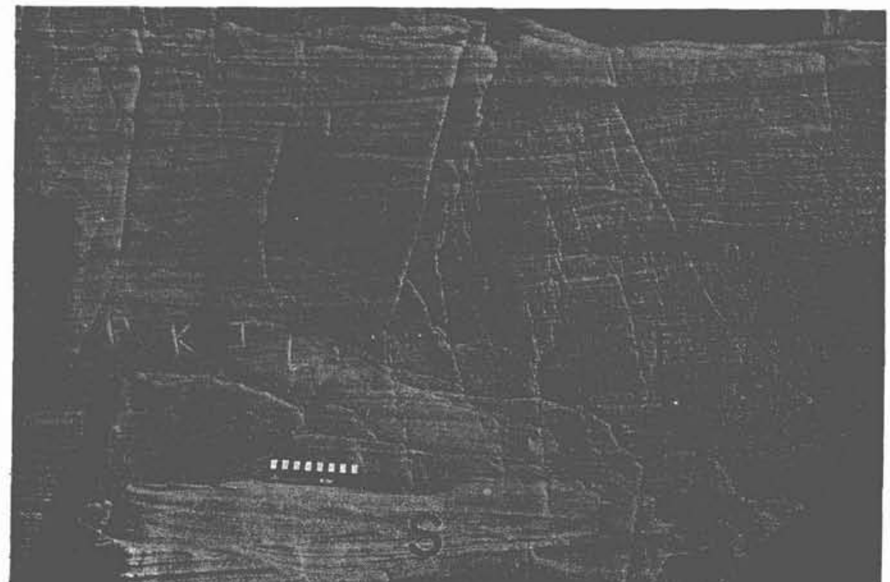

Figure 8 *Swaly cross stratification in Permian rocks at Thirroul, near Woollongong, N.S.W.,* Australia. Much of the stratification is relatively flat (F), with isolated swales (S). Note low angle, curved intersecting laminae in upper one-third of the photograph. Scale is 15 cm long.

and no distinct parting planes or amalgamation surfaces, a thick sandbody several metres thick can form (Fig. 8). The term *swaly cross stratification* (SCS) was created by Leckie and Walker (1982) for sandbodies by definition thicker than 2 m. The internal stratification is dominantly flattish to very gently undulating, and the swales cut into this lamination. The swales are circular to elliptical in plan view, a metre or more in diameter and a few tens of centimetres deep. The infilling laminae conform to the shape of the swale, gradually flattening out upward. The swales rarely pass laterally into hummocks, although there are enough convex-upward laminae in a swaly sandbody to indicate a descriptive (and probably genetic) similarity to classical HCS.

In many examples from the geological record, SCS sandbodies occur stratigraphically above HCS sandstones and interbedded mudstones. Commonly, the sandbodies are 10-15 m thick and contain SCS throughout. Alternatively, the lower part contains SCS, with cross-bedded and horizontally bedded sandstones at the top (upper shoreface and beach). These may be capped by coaly horizons with in situ root traces. This stratigraphic context suggests that many or most SCS sandbodies represent prograding storm-dominated shorefaces, in which storm processes have overprinted all record of fairweather sedimentation, except in the upper shoreface and beach.

SHELF MUDSTONES

The attention paid to sandstones outweighs that devoted to mudstones, although the latter comprise the bulk of shelf sediments. Mud and silt washed into the sea by rivers can be transported for many tens of kilometres in suspension. Final deposition onto the bed is commonly accelerated by filter-feeding organisms that ingest mud from the water column and deposit it as fecal pellets. Where the concentration of suspended mud is very high, ocean waves are damped and the shoreface itself may consist of mud (Rine and Ginsberg, 1985). Physical and biological structures in mudstones are commonly difficult to study in outcrop, but can be well displayed in unweathered polished slabs or in cores. In most shelf mudstones, all physically formed structures have been partly or completely destroyed by the burrowing and grazing activities of organisms, as discussed in Chapter 4.

In situations where the water close to the bed was depleted in oxygen, and benthonic organisms consequently scarce, primary sedimentary structures may be preserved. The most common feature consists of a subtle colour banding that reflects milimetre- to centimetre-scale graded siltstone-mudstone beds (Fig. 9; Davis *et al.*, 1989). The sharp-based graded beds were probably deposited from waning, storm-generated flows; the muddy portion of each bed is probably partly storm emplaced, and partly reflects pelagic deposition between storms.

THE SAND TRANSPORT PROBLEM

For medium to large shallow marine sandbodies, the most important problem can be simply stated: *did the sand move from the shoreline to the sandbody, or did the sandbody form at the shoreline and become subsequently abandoned on the shelf by transgression?*

Where mudstones interbedded with the sandstones suggest an offshore depositional environment, the question arises as to the direction and process of sand transport from the shoreface to its depositional site. Directions of transport can be perpendicular, oblique or parallel to the shoreline. Transport mechanisms might include combined flows driven by waves and/or pressure differences, or density currents similar to turbidity currents.

Parallel-laminated to current-rippled sandstone beds

Some ancient sandstones, deposited in offshore environments, are characterized by sharp bases with sole marks, parallel lamination, and ripple cross lamination (Fig. 10). In the Bouma terminology for turbidites, these beds would be described as BC beds (see Chapter 13). Although the sedimentary structures indicate waning flow, it is not always clear whether the flows were unidirectional or oscillatory.

Duke (1990) has suggested that the parallel lamination may be formed by oscillatory currents, and that the ripples are combined flow ripples. The sharp bases would reflect scouring of the muddy shelf floor during the rising phase of the storm, followed by the emplacement of sand as the storm waned. The sedimentary structures would reflect diminishing wave orbital velocities as the storm waves died down. This interpretation can be applied to situations where sand moves incrementally, storm by storm, to its final depositional site.

In other situations, apparently unidirectional currents also form BC beds with sharp bases. The best-known example is in the Jurassic of Alberta, where the BC beds and interbedded mudstones form a section about 60 m thick. This section is overlain by HCS beds (20 m) and finally by SCS shoreface sandstones and coals (Hamblin and Walker, 1979). It was suggested that the BC beds were emplaced by turbidity currents that deposited sediment below storm wave base. The sharp-based HCS beds have identical sole mark directions to the BC beds below, and hence were also believed to be turbidity current deposits. However, because the sand was deposited above storm wave base, the normal turbidite sedimentary structures were reworked into HCS. The problems raised by this interpretation are 1) that there are no actualistic examples of turbidity currents on modern shelves, and 2) that generating mechanisms for turbidity currents at or close to the shoreface are difficult to envisage.

Arguments concerning the direction of sand emplacement are fuelled by the geological observation that many ancient storm-emplaced sandstone beds have sole marks indicating dominantly shore-perpendicular flow directions (Leckie and Krystinik, 1989; but see Hart *et al.*, 1990 and Plint and Norris, 1991 for contrasting observa-

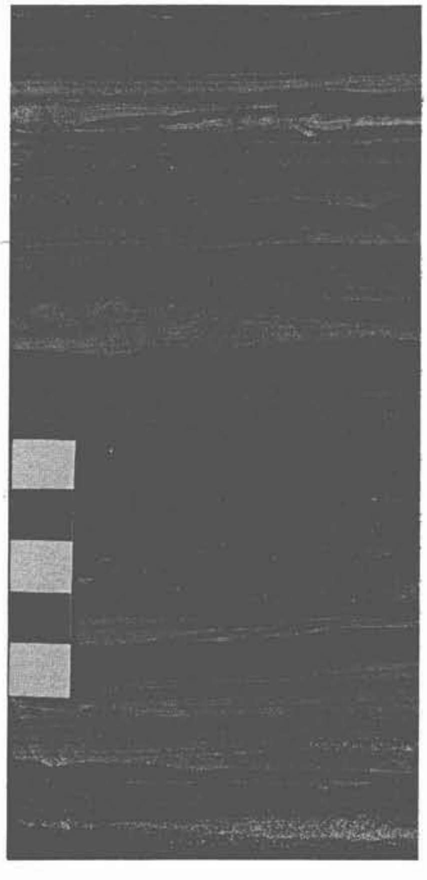

Figure 9 Core photo shows sharp-based siltstone beds, many with subtle colour grading indicating more mud in the upper part of the bed. Note faint flat to very gently inclined lamination within some beds. There is an absence of ripple cross lamination. Viking Formation at Judy Creek, Alberta: well 10-36V-64-13W5, 4745 feet. Scale in centimetres.

Figure 10 Sharp-based bed of fine sandstone showing parallel lamination throughout most of the bed, and a single layer of ripple cross lamination at the top. Cardium Formation at Ricinus field, Alberta; well 3-5-35-8W5, 8845 feet.

tions). The apparent conflict between flow on modern shelves (largely shore-parallel) and paleocurrent evidence in ancient rocks (largely shore-perpendicular) has been discussed by Duke (1990) and Duke *et al.* (1991). They point out that the paleocurrent evidence is largely derived from small-scale sole marks that were made by the instantaneous action of waves; these are typically shore-perpendicular. If angle-of-repose cross stratification is present, the paleoflow directions are commonly shore-parallel. However, the dunes that formed the cross stratification responded to a longer term *time-averaged* flow and better reflect the net, geostrophically driven along-shelf flow.

ANCIENT SHALLOW MARINE SANDBODIES

The processes described earlier in this chapter appear to have combined to form three main types of shoreface and shallow marine sandbodies in the geological record. The first consists of sheet-like sandbodies up to about 20 m thick, representing prograding shorefaces. The second consists of sheet-like or patchy bodies of interbedded HCS sandstones and bioturbated mudstones, representing an aggrading offshore marine environment. The third type consists of long narrow bodies that may be much coarser (medium sandstone to conglomerate) than the surrounding sediments. These long, narrow bodies tend to be more or less parallel to regional shoreline trends, and they also tend to be under- and overlain by regionally extensive erosion surfaces. Features directly analogous to the offshore ridges and swales of modern shelves have not been identified in the geological record.

Prograding shorefaces and aggrading offshore HCS sandstones are characteristic of highstand systems tracts; the long, narrow sandstone and conglomerate bodies more commonly form lowstand and parts of transgressive systems tracts.

PROGRADING STORM-DOMINATED SHOREFACE SYSTEMS

Modern prograding shorefaces

Relatively few modern shorefaces are actively prograding. The best example is the broadly arcuate, 200 km-long microtidal coast of Nayarit on the Pacific coast of Mexico (Fig. 11). It has prograded up to about 15 km during the last 3,600 years, at an average rate of about 3 m/year (Curray *et al.*, 1969). Sand is supplied to the strandplain by the Rio Grande de Santiago and a number of smaller rivers, as well as by marine erosion of older transgressive deposits. The well-sorted fine and medium sand is distributed along the coast by a powerful wave-driven longshore drift system, forming a sandbody about 7 m thick. The shore face sands grade seaward into silts and clays at a depth of about 10 m.

The importance of sand supply to the shoreface by reworking of the inner shelf has been discussed by Dominguez *et al.* (1987) from a study of the southeastern coast of Brazil. Here, strandplains are associated with several river mouths (Fig. 12). On the downdrift side of the river mouths, the strandplain contains some sand supplied directly from the rivers. On the updrift side, the mineralogy of the sand is different, suggesting derivation from the shelf by reworking in response to an approximately 5 m relative fall in sea level during the last 5,100 years. This hypothesis is strengthened by the fact that the Caravelas strandplain (Dominguez *et al.*, 1987, fig. 4) is not associated with a river at all. It has been built in a zone of convergent longshore drift with sand supplied by erosion of the shelf. This work in Brazil suggests that regressive sheet sandbodies are most likely to develop following a relative sea level fall, when dispersed sand on the inner shelf is eroded and concentrated in the shoreface.

Ancient shoreface sandbodies

Many examples of sheet-like sand-

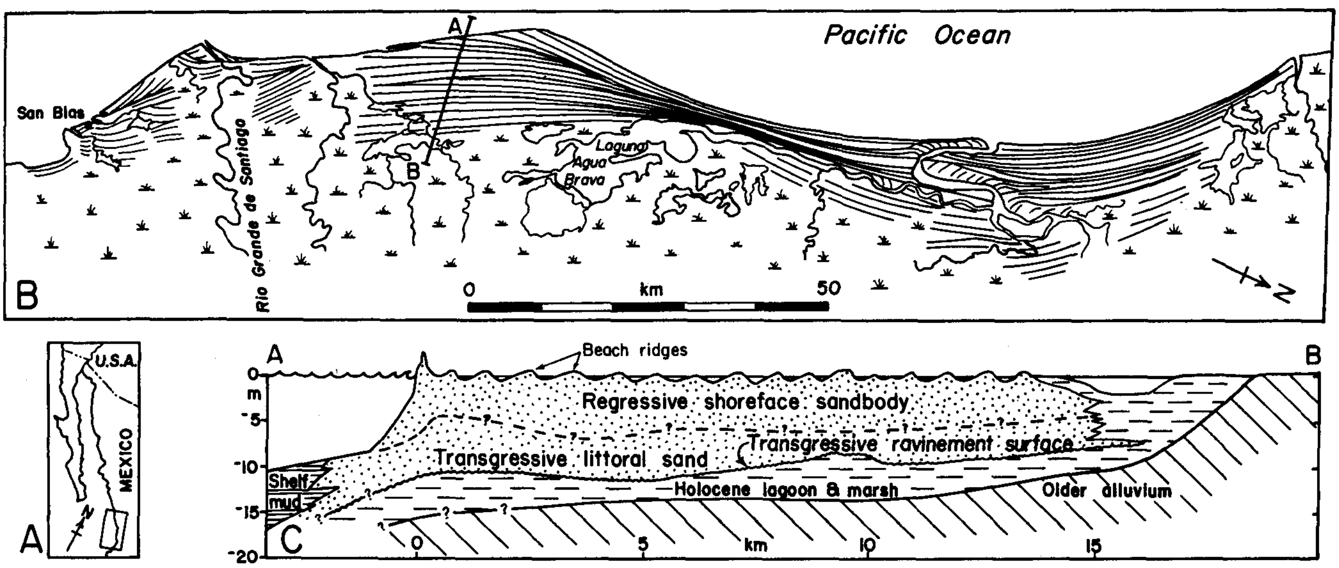

Figure 11 A) Coast of Nayarit, Mexico, showing (B) arcuate wave-dominated strandplain with up to 280 sub-parallel beach ridges which have accreted during about 4500 years of coastal progradation. Changes in wind patterns, and in the positions of river mouths have resulted in localized erosion and reorientation of the shoreline. C) cross section showing a Holocene transgressive ravinement surface overlain by a transgressive littoral sand, in turn overlain by the prograding beach and beach-ridge complex (regressive shoreface sandbody). Modified from Curray *et al.* (1969).

bodies characterized by SCS, and interpreted to have been deposited in prograding wave-dominated shorefaces, have now been recognized (see Heward, 1981; McCubbin, 1982; Johnson and Baldwin, 1986 for recent reviews). This literature is strongly biased toward the Cretaceous of the Western Interior Seaway of North America, where the sandbodies form important hydrocarbon reservoirs (McCrory and Walker, 1986; Nummedal and Swift, 1987; Plint and Walker, 1987; Rosenthal and Walker, 1987; Swift *et al.*, 1987; Plint and Norris, 1991; Hart and Plint, in press; and references therein). Examples in other settings include the Tertiary Cohansey Sand of New Jersey (Carter, 1978) and the Oligocene Frio Formation of Texas (Tyler and Ambrose, 1986). Each sandbody typically extends many hundreds of kilometres along depositional strike, and may prograde over 300 km seaward. Where sandbody geometry can be well defined using isopach maps, localized bulges in the shoreline trend probably indicate the former position of major river mouths.

The SCS shoreface sandbodies characteristically occur in the upper parts of sandier-upward facies successions (Figs. 13, 14). These successions (such as the one at Lundbreck,

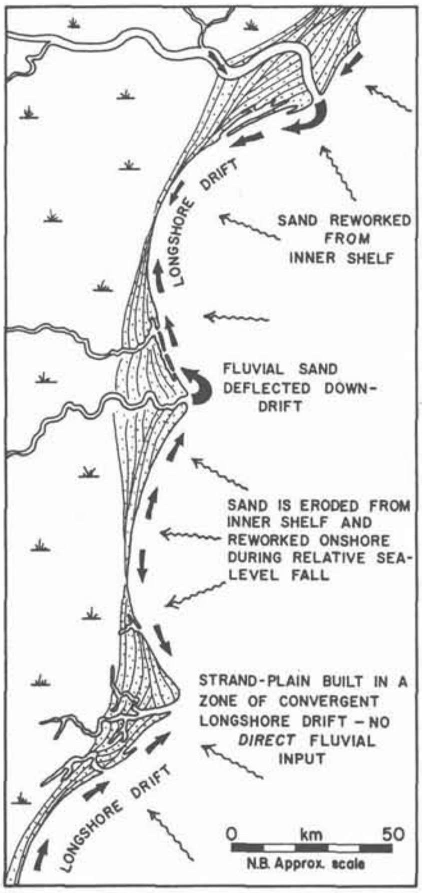

Figure 12 Development of beach-ridge strandplains on a wave-dominated coast undergiong relative sea level fall. Sand supplied by rivers is deflected alongshore and contributes to the downdrift side of the strandplain. The updrift side is built largely of sand reworked in the onshore direction through erosion of the inner shelf, as a result of increased wave scouring during relative sea level fall. Note that a strandplain can accumulate in an area *lacking a direct fluvial input*. Idealized after diagrams of Dominguez *et al.* (1987).

Figure 13 Prograding shoreface succession in the Cretaceous Chungo Member, Wapiabi Formation, at Lundbreck, Alberta. Stratigraphic top to left. M = offshore bioturbated mudstones; H = interbedded HCS sandstones and bioturbated mudstones; S = SCS shoreface sandstones. Thickness of H plus S is about 100 m. Note progressive increase in proportion of sand upward.

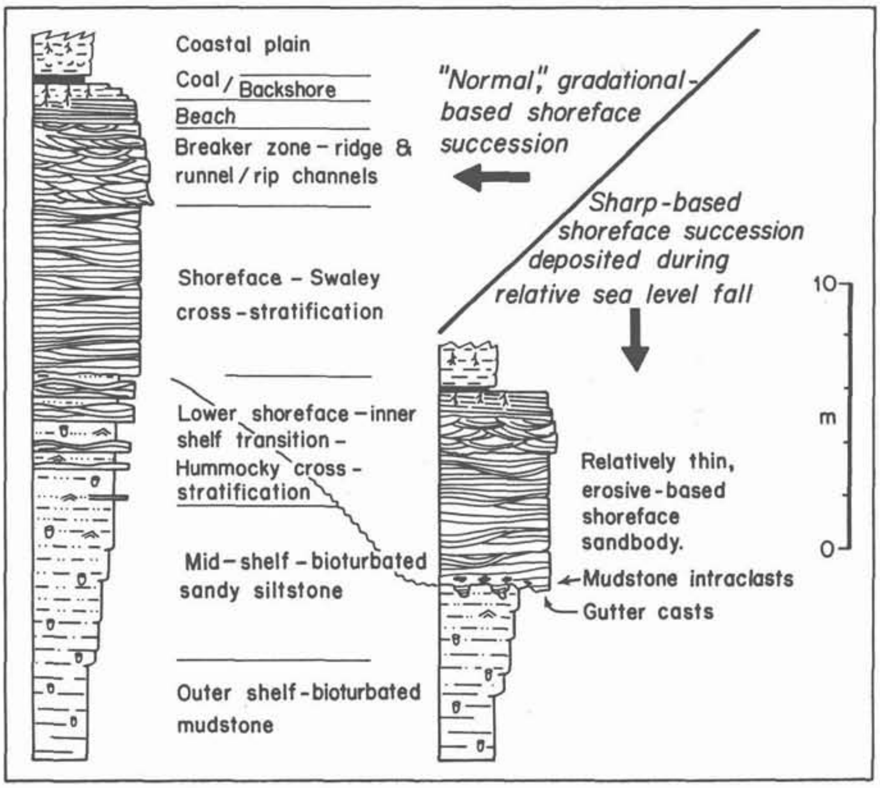

Figure 14 Wave-dominated shoreface successions. Left, a gradationally based succession passing from outer through inner shelf deposits into sand-dominated shoreface and beach sediments. Right, shows a succession characterized by a *sharp-based shoreface* deposited during a period of relative sea level fall (a *forced regression)*. At such times, reduced accommodation space eliminates the shelf-to-shoreface transitional zone, and the shoreface sands rest abruptly on a wave-scoured erosion surface.

Alberta; Fig. 13; Rosenthal and Walker, 1987) typically begin with bioturbated mudstones and interbedded fine to very fine sandstone beds a few centimetres or tens of centimetres thick; these may contain HCS, planar lamination or ripple cross lamination. Upward, the sandstone beds thicken, the proportion of HCS increases and beds become more amalgamated. The mudstone interbeds finally disappear and SCS predominates. Toward the top of the SCS sandbody, there may be a few metres of somewhat coarser (upper fine to medium grained) trough cross-bedded sandstone, representative of longshore bars and troughs. The top 1-2 m of the succession typically consists of fine sandstone with planar lamination, representing the beach. It may be capped by somewhat silty, structureless and rooted sandstone representing a backshore environment.

Although fine sandstone commonly dominates the SCS shoreface successions, coarser sediment may also be present. For example, coarse, cross- and planar-bedded sandstone and/or conglomerate may be important near river mouths (Clifton, 1981; DeCelles, 1987; Leckie and Walker, 1982; Plint and Walker, 1987; Hart and Plint, 1989; Plint and Norris, 1991).

Sharp-based shoreface sandbodies

In some progradational facies successions, the base of the SCS sandbody is sharp rather than gradational (Fig. 14). The contact with underlying thinly interbedded shelf mudstones and siltstones can also be marked by large load casts and/or elongate gutter casts (Rosenthal and Walker, 1987; Davis and Byers, 1989; Plint, 1991). The gutter casts have the geometry of gutters (eavestroughs), and are narrow sand-filled scours oriented perpendicular to regional shoreline trends. They are believed to be formed by wave scour on the bed (Duke, 1990).

Lateral relationships between gradational and sharp-based sandbodies can be demonstrated in subsurface studies. For example, in the Cardium Formation of Alberta (discussed in detail later in this chapter), Plint (1988) showed that gradational-based shoreface successions could be traced laterally into thinner, sharp-based sandbodies (Fig. 15). The slight drop in stratigraphic position of the base of the shoreface, along with its change to a sharp base, was interpreted to be the result of progradation due to a relative sea level fall. This would cause wave scouring of the inner shelf, resulting in shoreface progradation over an erosion surface. The transitional lower shoreface zone would be eliminated. Because the water was shallower, less sediment would be needed for aggradation, and therefore the progradation rate would increase. More information is provided by the Marshybank Formation of Alberta (Plint, 1990, 1991; Plint and Norris, 1991), which contains a succession of very thin (3-5 m), erosive-based SCS shoreface sandstones. These sandbodies prograded for many tens of kilometres over a muddy shelf in response to relative sea level falls. Comparable sandbodies have recently been described from the Paleozoic of Greenland (Bryant and

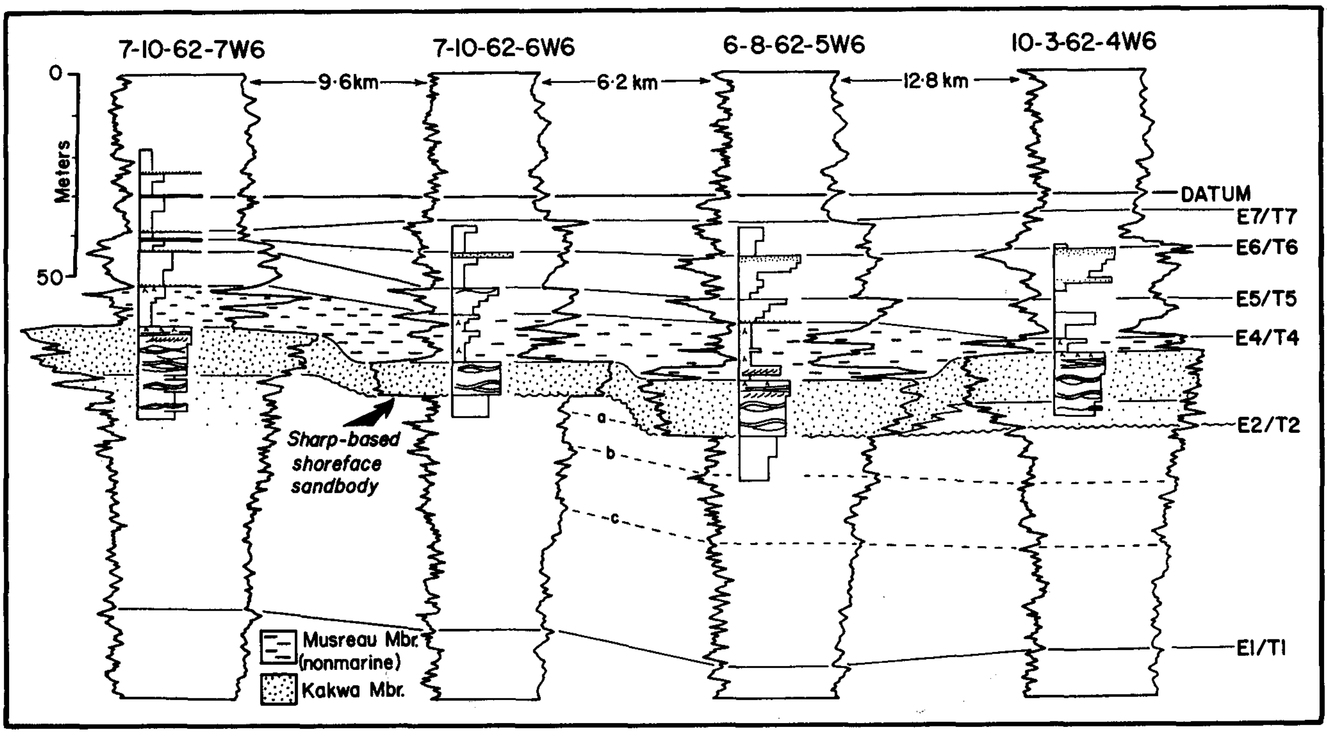

Figure 15 Representative log and core cross section through shoreface sandstones of the Kakwa allomember of the Cardium Formation. Section is located in Figure 16, and progradation was left to right (eastward). The base of the shoreface (stippled) is gradational in 7-10-62-7, *but is stratigraphically a little lower, and sharp-based, in 7-10-62-6 and 6-8-62-5.* Thus the stratigraphic drop in shoreface position is coincident with the change from gradational to sharp base. Note also the erosion of well log marker "a" between 7-10-62-6 and 6-8-62-5. The sharp-based shoreface is interpreted to result from a small lowering of sea level during progradation (a *forced regression).* The shoreface rises stratigraphically between 6-8-62-5 and 10-3-62-4, and becomes gradational again; this is interpreted to be due to a slight relative sea level *rise during progradation. Modified from Plint (1988).*

Smith, 1990). This type of coastal progradation was termed a *forced regression* by Plint (1991), to emphasize its dependence on relative sea level fall, rather than simple progradation of the shoreline in response to sedimentation. A good analogue for these Cretaceous Cardium and Marshybank sandbodies is the Pleistocene Ingleside Sand, which represents a strandplain that prograded many kilometres across the Gulf of Mexico shelf in response to a Wisconsinian glacio-eustatic lowstand (Wilkinson *et al.*, 1975).

SHEET-LIKE AND PATCHY HCS SANDBODIES

This facies consists of HCS sandstones interbedded with bioturbated mudstones. In almost all cases, the physical sedimentology and trace fauna suggest an environment below fairweather wave base but above storm wave base. HCS sandstones interbedded with bioturbated mudstones have not yet been unequivocally documented on modern shelves and all information is derived from the geological record.

Sandstone beds commonly become thinner in the dispersal direction, and form sandier-upward stratigraphic successions, although muddier-upward successions are also known (Bourgeois, 1980). The sandier-upward successions in ancient shallow marine settings are commonly interpreted to reflect coastal progradation.

There is no information on the geometry of individual HCS sandstone beds, but packets of HCS sandstones and interbedded bioturbated mudstones a few to several metres thick can be traced for tens of kilometres in the Book Cliffs of Utah (Swift *et al.*, 1987). In the Raven River allomember of the Cardium Formation (subsurface of Alberta; Figs. 16, 17), there are several discrete sandier-upward successions of HCS sandstones. The successions are each about 7.5 m thick, and they are irregularly stacked and shingled against each other (Walker and Eyles, 1988). Isopach maps of each succession (Fig. 18) show lobe-like geometries. The shifting lobe positions were hypothesized to be the result of changes in the position of river mouths (Walker and Eyles, 1988; Fig. 18). The shingled lobes have coalesced to form a sheet-like sandbody at the top of the Raven River allomember. This sandbody forms major reservoirs at Pembina, Willesden Green and Ferrier (Figs. 16, 17).

The sheet sandstones at Pembina are erosively overlain by conglomerates, mostly forming a veneer but in places up to 10 m thick. This erosion surface (E5; Fig. 17) has greatly influenced ideas about sandstone and conglomerate body geometry, and is now known to separate highstand from lowstand/transgressive systems tract deposits.

SANDBODY GEOMETRY DETERMINED BY EROSIONAL DISSECTION

In the subsurface of the Alberta Basin (Fig. 16), the Cardium Formation is essentially flat lying, unfaulted, and is penetrated by over 10,000 wells. There are more than 1500 preserved cores. In the mudstones below and above the Cardium, there are excellent well log markers that form continuous and planar datums. This superb control is unmatched anywhere else in the world. It is therefore possible to demonstrate erosion at the base of Cardium conglomerates in cross sections (Fig. 19), and to map the geometry of the erosion surface in three dimensions (Fig. 20; Walker and Eyles, 1991). In the Pembina, Willesden Green and Ferrier area (Fig. 16), the sandbodies that form the individual reservoirs have a topographic relief of

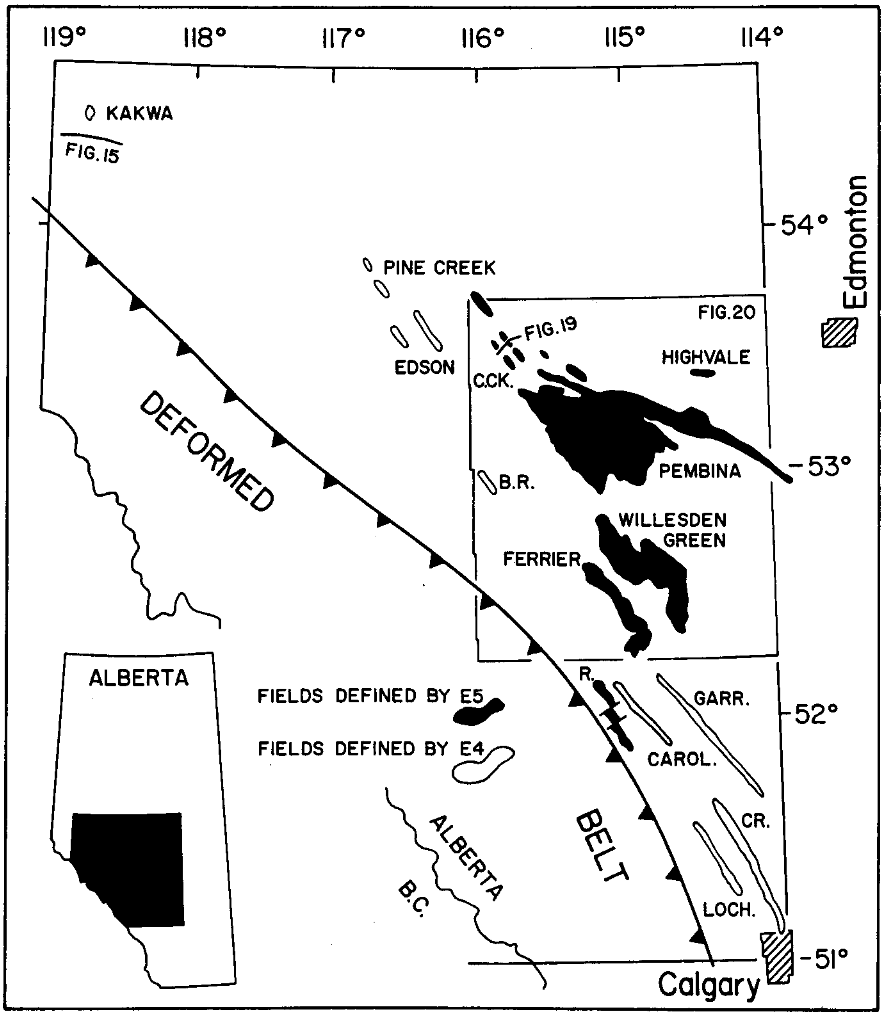

Figure 16 Location map, Cardium Formation oil and gas fields, southern Alberta. Thrust symbol shows edge of deformed belt; southwest of this line the Cardium is exposed in outcrop, commonly steeply dipping in a series of thrusts. Locations of cross sections (Figs. 15, 19) are shown, and area covered by mesh diagram (Fig. 20) is outlined. B.R. = Brazeau River; R = Ricinus; CAROL. = Caroline; GARR. = Garrington; CR. = Crossfield; LOCH. = Lochend. For scale, the rectangle enclosing Pembina and adjacent fields is 140 x 170 km.

up to 20 m with respect to upper and lower datums (as shown in Figure 19 for the sandstones below E5 at Carrot Creek). This relief, along with the map pattern (Fig. 16), has traditionally been interpreted to indicate some form of "shelf bar" that grew in situ in an open marine setting. It has now been established that this is *not* the case. The relief observed is demonstrably *entirely erosional* (Plint *et al.*, 1986; Bergman and Walker, 1988; Walker and Eyles, 1988, 1991), and is interpreted to have formed as a result of 1) a relative sea level fall, followed by 2) emergence of the shelf, and then 3) erosional dissection of the former shelf sandstones during transgression (Fig. 21).

Following the Cardium work, similar erosion surfaces have been identified throughout the Cretaceous section in the Alberta Basin. Interpretations of the Cardium data suggest a re-examination of other "offshore bars" (such as the conglomerate-capped sandier-upward successions of the Carboniferous Kinsale Formation; Cotter, 1985; de Raaf *et al.*, 1977). These might also be examples of sheet sandbodies dissected during relative lowering of sea level, and erosively modified during subsequent transgression. We conclude that patchy HCS shelf sandbodies may owe their shapes to 1) original deposition in particular lobes, and/or 2) subsequent erosional dissection during sea level fluctuations. The importance of sea level fluctuations and accompanying erosion will form the main theme of the rest of this chapter.

LONG NARROW SANDSTONE BODIES ENCASED IN MARINE MUDSTONE

The Cretaceous rocks of the Western Interior Seaway (foreland basin) of North America contain numerous long (tens of km), narrow (few km) sandstone and conglomerate bodies that are totally encased in marine mudstones (Fig. 16). Because subsurface control is normally necessary to define sandbody geometry in three dimensions, it is difficult to know how common such sandbodies are in other areas where well control is not so good. The sandbodies are normally parallel or subparallel to regional shoreline trends, but they have no physical connection with a time-equivalent shoreface sandbody. The isolated position of these sandbodies, along with their tendency to coarsen and become sandier upward, has led to their interpretation as "offshore bars" that "grew" on a muddy seafloor, tens of kilometres from the shoreline. One of the most intensely studied examples is the Shannon Sandstone in Wyoming (Fig. 22; Tillman and Martinsen, 1984, 1987; Gaynor and Swift, 1988), where the geological setting makes an "offshore bar" interpretation appealing. However, several problems with such an interpretation must be emphasized.

Problems posed by "offshore bars"

The problems can be listed very simply, and will be discussed below:

1) Exactly how was the sand (and gra-

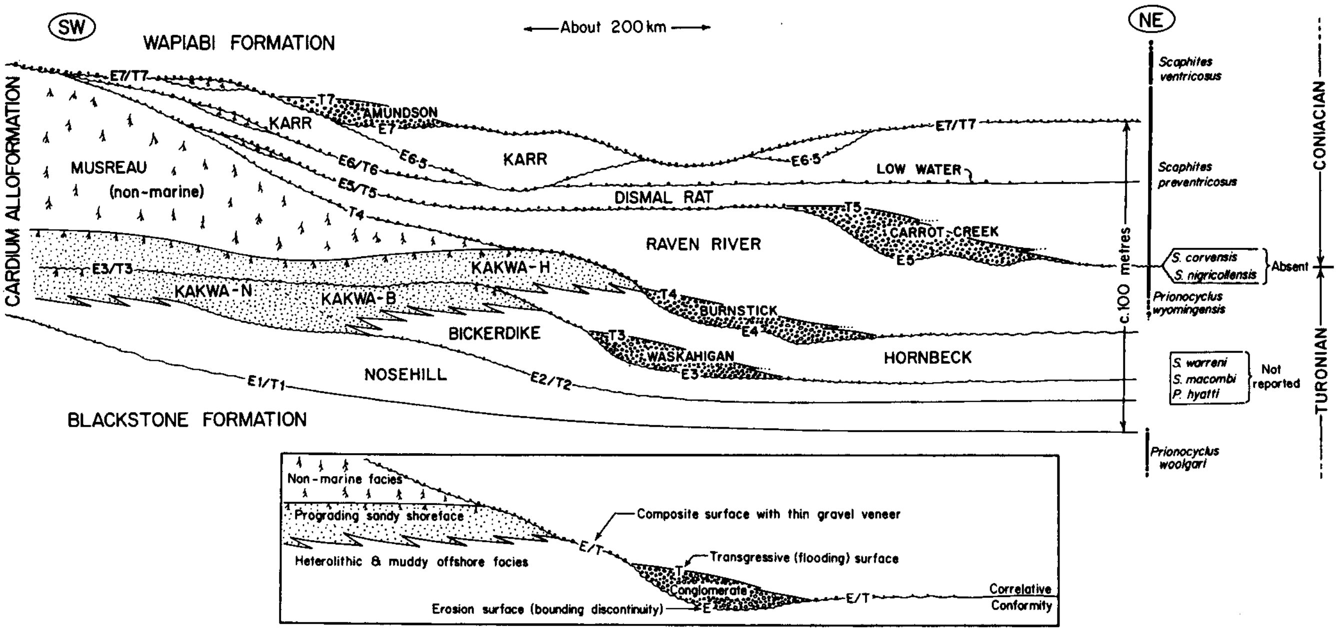

Figure 17 Allostratigraphy of the Cardium Formation, Alberta Basin. The diagram is slightly modified from Plint *et al.* (1986) and Walker and Eyles (1991), using work by Hart and Plint (in press), Hall *et al.* (1991), Wadsworth and Walker (1991), Hart (pers. comm., 1991) and other unpublished information. The erosional surfaces (E) initially formed as a result of relative sea level fall, with wave scour in inshore areas and subaerial erosion in the exposed portions of the former shelf. Long, narrow bodies of conglomerate formed in the maximum lowstand shorefaces, or in shorefaces cut during stillstands in the subsequent transgression. During transgression, erosion in the shoreface removed physical evidence of subaerial exposure in areas landward of the lowstand shoreface. The resulting shorefaces are in part of composite origin, with episodes of erosion having taken place during 1) marine regression; 2) subaerial exposure; and finally 3) marine transgression. The T surfaces represent modification of the subaerial surface, and the reworking of subaqueous lowstand deposits during marine transgression. In many places between incised shorefaces, the E and T surfaces are co-planar. Available ammonite biostratigraphy suggests that the erosional hiatuses at the E5/T5 and E7/T7 surfaces correspond, respectively, with third-order eustatic falls of sea level (Haq *et al.*, 1988) in the late Turonian and mid-Coniacian.

vel) transported from the shoreline to the offshore bar?

2) If the coarse sediment moved as a thin sheet on the seafloor, what marine processes concentrated and focused the sediment into long narrow sandbodies?

3) Why did the sand moving out across the seafloor become progressively concentrated on the bar *top*, forming sandier-upward facies successions?

The reader need only refer to the Shannon "offshore bars" 160 km from shore (Fig. 22) to appreciate how severe these problems are.

1) The problem of sediment transport has been discussed earlier; the literature contains some classically all-embracing (but unhelpful) interpretations such as "shelf currents" (Fig. 22), "storm-driven currents", "normal tidal currents" and "regional circulation currents".

2) There are no known modern situations in which sand supplied from the shoreline is presently being transported across a muddy shelf and concentrated into long narrow bars. Explanations for ancient long narrow ridges include, among others, i) deposition in the lee of a pre-existing break in slope (origin of break not explained; e.g., Swagor *et al.*,

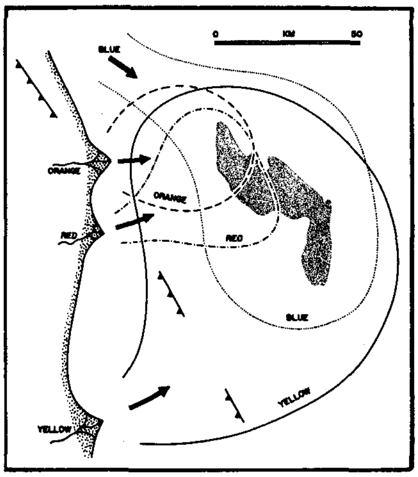

Figure 18 Willesden Green field (stippled) is located in Fig. 16. Four "lobate" sandier-upward successions can be identified immediately beneath erosion surface E5, from bottom upward designated yellow, red orange and blue. Data from the immediate area of Willesden Green shows the direction and rate of thinning of these lobes. Projections in the direction of thickening to where the lobes would be about 20-30 m thick suggest possible shoreline positions. Thrust symbol indicates position of deformed belt (Fig. 16). From Walker and Eyles (1988).

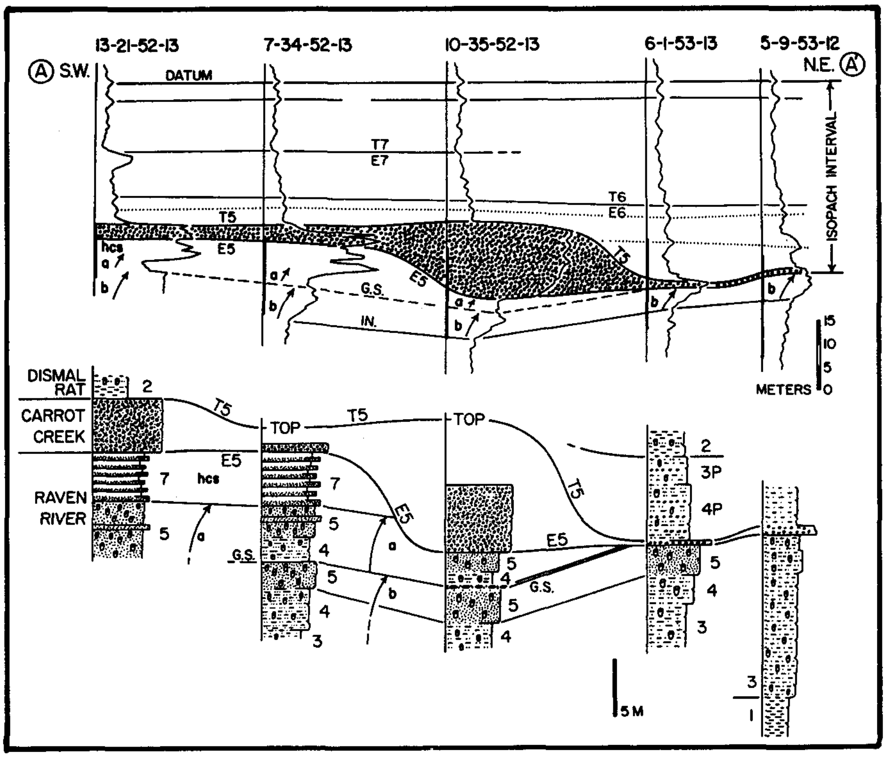

Figure 19 Resistivity well log and core cross sections through part of Carrot Creek (section located in Figure 16). Note the truncation of sandier-upward successions "a" and "b" (arrows) by the base of the conglomerate, and particularly the erosion of the HCS sandstones between wells 7-34-52-13 and 10-35-52-13. Numbers 3, 4 and 5 indicate increasingly sandy bioturbated facies; GS indicates "gritty (coarse sand) siderite", and IN (inflection) indicates the first rightward deflection of the well logs. E5, E6 and E7 indicate Cardium erosion and (T) transgressive surfaces. The interpreted positions of three of these wells are shown in Figure 23. From Bergman and Walker (1988).

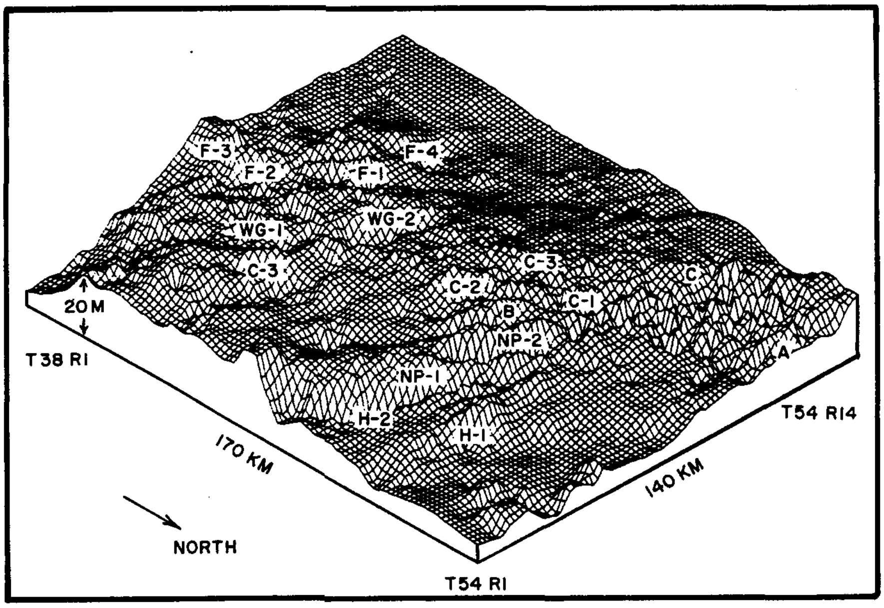

Figure 20 Mesh diagram of the topography of the E5 erosion surface, viewed from NE toward SW (i.e., from the basin toward the sediment source). Note that the topography is characterized by a series of asymmetrical highs and lows, with the steeper sides of the highs facing northeastward (toward the viewer). Vertical relief (up to 20 m) is greatly exaggerated, and the area of the diagram (140 x 170 km) is shown in Figure 16. H = Highvale, NP = North Pembina, WG = Willesden Green, and F = Ferrier. A and C refer to highs in the Carrot Creek and Pembina areas. From Walker and Eyles (1991).

1976; La Fon, 1981), ii) convergence and expansion of along-shelf geostrophic storm flows over an initial topographic irregularity (origin unexplained) which then becomes "self-propagating" (Swift and Rice, 1984; Gaynor and Swift, 1988), and iii) nucleation over a tectonic "paleo-high" (Tillman and Martinsen, 1984).

3) The sandier-upward successions have been related to the topographic expression of the ridge (a few to about 15 m), where the crest is coarser grained because of greater wave and current action than on the flanks (Hobson *et al.*, 1982; Boyles and Scott, 1982). This does not explain how the coarse sediment was moved to the top of the ridge if currents on the flanks are weaker, and prompts one to question whether the 'trough-to-crest' differences in current and wave strength are geologically significant if the "bar" has a topographic height of only a few metres but is situated in water several tens of metres deep.

The three problems posed above are hard to explain, and our brief review of some proposed solutions indicates no consensus. Many interpretations simply push the problem farther out of sight (e.g., proposing the existence of pre-existing topographic elements on which the "bars" allegedly grew). We will examine the possibility that many of the ridges did *not* form tens of kilometres from the shoreline, and that they owe their present 'offshore' position, encased in marine mudstone, to major regressions and transgressions. We will again use the Cardium Formation as a case history, and then examine other situations.

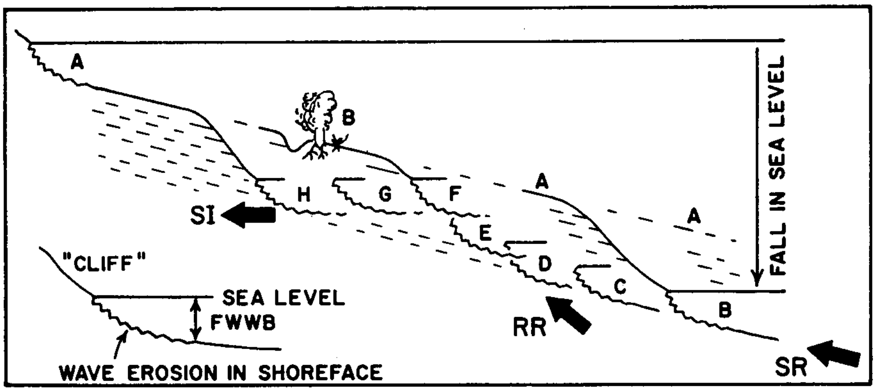

Figure 21 The initial shoreface is at A, with a sediment surface dipping gently basinward (letters A, A). A fall of relative sea level moves the shoreface to B (lower right), where it is incised, with a low "cliff" of former marine strata behind the shoreface. The old sediment surface A – A is now subaerially exposed and has become vegetated, with small incised streams at B. Slow, steady sea level rise (SR) forms shorefaces C and D, and BCD defines an erosive shoreface envelope. If the rise is more rapid (RR), the shoreface envelope rises at a steeper angle with respect to the underlying beds (DEF). If there is a pause in sea level rise, wave erosion will cause the shoreface to cut horizontally landward (erosional envelope FGH, formed during stillstand incision, SI). The overall transgressive erosion surface, from B to H, will be stepped, and any evidence of subaerial exposure (the vegetation at B) will be removed. The erosion surface will be overlain by a transgressive lag, and transgressive marine mudstones.

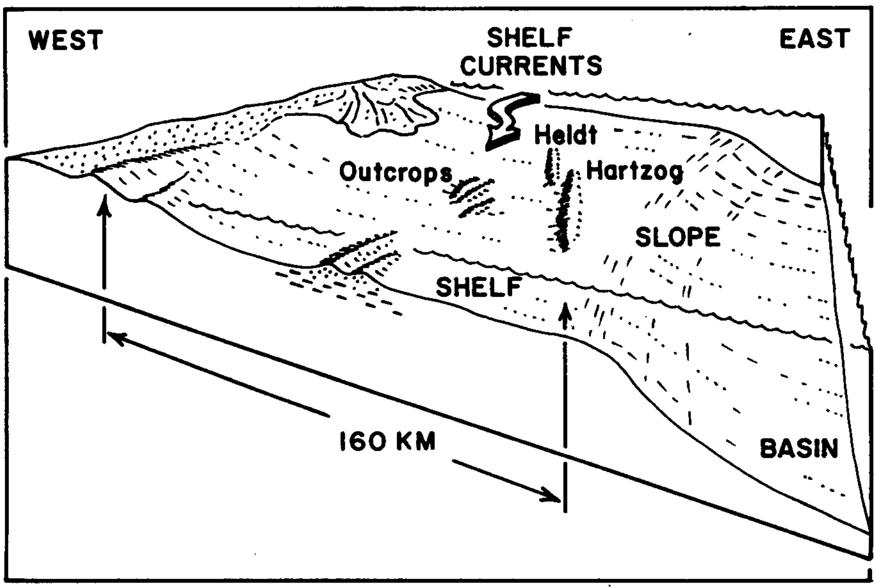

Figure 22 Block diagram (simplified from Tillman and Martinsen, 1987) showing the positions of Shannon outcrops in the Salt Creek anticline, and positions of Shannon oil and gas fields at Heldt Draw and Hartzog Draw. Note that these "offshore bars" are gradationally rooted in shelf mudstones (front face of diagram), and appear to be up to 160 km from the contemporaneous shoreline. In this interpretation, it is obvious that the sand has to be moved to Hartzog Draw by "shelf currents", but the nature of these currents is not stated.

LONG NARROW SANDBODIES: A CASE HISTORY OF THE CARDIUM FORMATION

The Turonian-Coniacian Cardium Formation of Alberta (Fig. 16) has been subdivided into eight sedimentary successions, each bounded by regionally extensive discontinuities (termed E1 through E7 in Fig. 17). The elongate shapes of the sandstone and conglomerate reservoirs (Fig. 16), encased in marine mudstones, have formerly suggested interpretations in terms of "offshore bars". Because the Cardium hosts several large oil fields (with at least 2 billion barrels of recoverable oil), there is a superb subsurface data base of well logs and cores. Numerous outcrops are also available in the adjacent Foothills. This unparalleled stratigraphic and sedimentological control permits detailed interpretations that are both specific to the Cardium, and of more general applicability.

The Cardium is characterized by a series of sandier-upward facies successions that pass from bioturbated mudstones to interbedded HCS sandstones and bioturbated mudstones. These successions are capped by conglomerates, in the form of thin veneers, and as deposits up to almost 20 m thick (Fig. 17). The erosive break between the conglomerates and underlying sandstones can be easily illustrated in cross sections from Carrot Creek (Fig. 19). Eight distinct erosional surfaces, or "bounding discontinuities", have now been mapped (Fig. 17; Plint *et al.*, 1986, 1987, 1988; Wadsworth and Walker, 1991), and they allow the Cardium to be divided into several allomembers (Fig. 17). In the southwest, the section is dominated by a prograding shoreface (Kakwa allomember) overlain by nonmarine sediments (Musreau allomember). Toward the northeast, shallow marine facies are characterized by sandier-upward facies successions, most notably in the Raven River allomember. Shoreface progradation and shelf aggradation were periodically interrupted by relative lowering of sea level, forming erosion surfaces that extended basinward many tens of kilometres from the original shoreface.

The erosion surfaces are generally marked by conglomerate veneers which locally thicken into linear accumulations ("bars") up to 20 m thick, subparallel to the trend of the Kakwa shoreface. These regional erosion surfaces can be studied in two dimensions in cross sections (Fig. 19) and in three dimensions in isopach maps and mesh diagrams (Fig. 20). Maps have now been published for surfaces E4 (Pattison and Walker, 1992), E5 (Fig. 20; Walker and Eyles, 1991), E6, E6.5 and E7 (Wadsworth and Walker, 1991). The E4 and E5 surfaces are characterized by a series of northwest-southeast trending asymmetrical "steps" (Fig. 20; Fig. 21 envelope FGH), with the steeper side of the step facing northeastward. The thick conglomerate deposits occur banked up against these erosional steps (Fig. 23; Bergman and Walker, 1988).

Formation of Cardium erosion surfaces

In general, erosion surfaces might form 1) in an open marine setting, 2) in a subaerial setting, or 3) in a transgressive shoreface setting with partial or total modification of an older subaerial surface. These possibilities have been discussed with respect to the Cardium Formation by Walker and Eyles (1991), and extremely brief arguments are presented here. *Erosion in open marine settings* takes place during storms, forming scours no more than a few metres deep. These eroded areas tend to fill in again during fairweather conditions, and no examples of linear scours, up to 20 m deep, are known to have formed in open marine settings on modern shelves. *Subaerial erosion* by rivers on floodplains can easily produce 20 m of relative topography. However, the Cardium erosional lows are consistently asymmetrical, parallel to each other and parallel to regional strike. Most river patterns are sinuous, and oriented downdip, not parallel to strike. We therefore suggest that erosion took place in a *transgressive shoreface setting*, with complete removal of any evidence of former subaerial exposure.

During transgression, erosion is largely due to wave action in the shoreface, between sea level and fairweather wave base (FWWB, Fig. 21). If the rate of transgression is steady, a more or less planar erosion surface may form as the shoreface moves across the subaerial surface (Fig. 21, erosional envelope BCD formed by steady rise, SR). If the rate of relative rise increases, the erosional envelope will be at a steeper angle with respect to the underlying beds (Fig. 21, rapid rise RR, forming erosional envelope DEF). However, if there is a relative sea level stillstand, the shoreface may become locally incised (Fig. 21, stillstand incision SI, forming erosional envelope FGH), cutting a distinct notch into the underlying sediments. These incised notches may be preserved, as on the continental shelf off Brazil (Kowsmann *et al.*, 1977) and Spain (Diaz and Maldonado, 1990).

In a scenario of this type, the events forming the rocks below and above E5 can be itemized.

1) Deposition began with a sandier-upward succession on the shelf, forming a succession of mudstones that pass upward into HCS sandstones in the Raven River allomember (Fig. 21, surface A).

2) A relative fall of sea level exposed the former shallow marine sediments to subaerial erosion (Fig. 21, vegetation and trees at B). The shoreface moved to an unknown position to the northeast. Subaerial erosion probably took place, with rivers cutting shallow

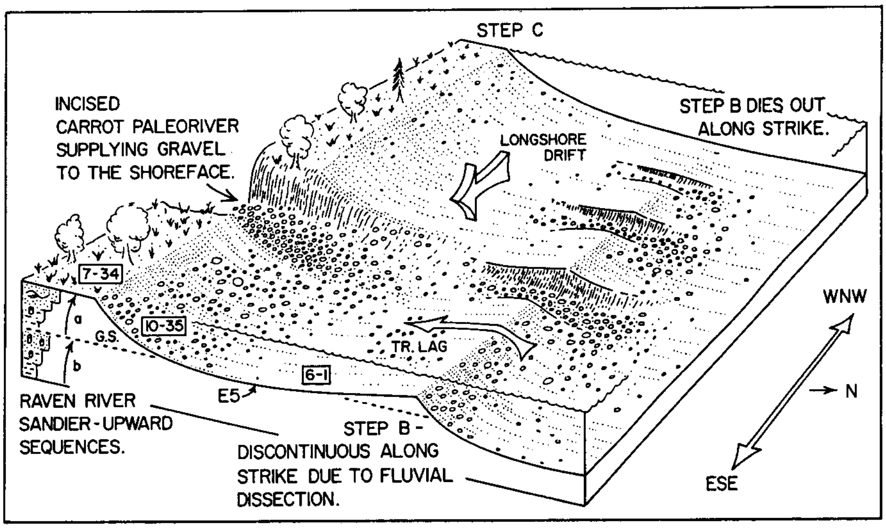

Figure 23 Interpretation of Cardium Formation conglomerate deposition in the Carrot Creek area (see Fig. 16). The origin of the stepped erosion surface E5 is shown in Figure 21. Conglomerates were supplied by rivers and were banked up against steps on the erosion surface, suggesting deposition in the shoreface. The upper shoreface and beach were eroded during subsequent transgression, forming a transgressive lag (TR. LAG). Interpretation is based on the cross section in Figure 19, and shows successions "a" and "b" separated by gritty siderite G.S. Locations of wells 7-34-52-13, 10-35-52-13 and 6-1-53-13, from Figure 19, are shown above. Note that in the interpretation, vegetation is still present at 7-34; it will be eroded, along with the beach, before the transgressive lag is deposited (as seen in the core, Fig. 19). The position of step C can also be seen in Figure 20. Note the incision of gravelly distributaries into the shoreface of step B, which is very discontinuous along strike. Modified slightly from Bergman and Walker (1988).

channels into this surface.

3) The rivers flowing across the subaerially exposed shelf supplied gravelly sediment to the new shoreface, which prograded a short distance. This *maximum lowstand shoreface* is hard to identify at the E5 horizon.

4) Sea level began to rise again, causing the shoreline to retreat southwestward. Wave erosion in the transgressing shoreface removed all evidence of subaerial exposure (e.g., root traces, paleosols, incised river channels). New erosional level is shown by the erosive envelope BCDEFGH in Figure 21.

5) During steady transgression, the erosion (or *ravinement)* surface is cut essentially parallel to the original stratigraphic dip. During relative stillstands in the overall transgression, erosion in the shoreface cut horizontal steps into the gently dipping coastal plain (Fig. 21, step FGH). Sand and gravel supplied to these shorefaces may be sufficient to cause local progradation near river mouths, and in those parts of the shorefaces downdrift from the river mouth.

6) Resumed transgression truncated the former shoreface sand/gravel body, and spread former beach gravel southwestward as a thin transgressive lag (Fig. 23). Some of the beach gravel was moved a short distance seaward during storms to form stringers in mudstones accumulating offshore. Bioturbation may mix the sediment to produce a structureless pebbly mudstone.

Figure 24 Two superimposed sandier-upward successions (arrowed) in the Shannon Sandstone, Castle Rocks, Salt Creek Anticline, Wyoming.

7) Continued transgression and deepening finally ended the reworking of the former shoreface deposits, and mudstones were deposited on top of the conglomerates. It is not possible in the Cardium to locate the maximum flooding surface. For practical purposes, we assume that it is within the mudstones but close to the contact with the conglomerates.

Solutions to the problems posed by "offshore bars"

Earlier in the chapter, three problems were introduced, 1) the transport of sediment across the shelf, 2) its concentration into long narrow bars, and 3) the formation of sandier-upward successions within the bars. The Cardium case history provides plausible solutions to the questions.

1) The topography of erosion surfaces (Figs. 19-21, 23) suggests that the overlying coarse sandstones and conglomerates formed in incised *shorefaces.* If so, the sandstones and conglomerates are not offshore bars, and the problem of sediment transport into offshore areas no longer exists.

2) The problem of focusing or concentrating the sediment into long, narrow bodies is easily solved — the bodies form along linear shorefaces by longshore drift of coarse sediment from river mouths.

3) Because the conglomerates are separated from the underlying successions of HCS sandstones by regional erosion surfaces, they are *not genetically related* to the underlying sandier-upward successions, which form during shelf aggradation.

At the E5 horizon, the conglomerate bodies at Carrot Creek rest within incised steps on the erosion surface. The long narrow fields at Willesden Green and Ferrier are not "offshore bars", but represent *erosional remnants* of the HCS sheet-like sandstones *below* the E5 erosion surface (Fig. 20). Thus the erosion surfaces influence the morphology of sandstone and conglomerate bodies in two different ways: 1) by forming elongate erosional remnants of sheet-like sandbodies below the erosion surfaces, and 2) by localizing the deposition of long, narrow coarse-grained lowstand shoreface deposits above the erosion surfaces.

IS THE SHANNON SANDSTONE A LOWSTAND SHOREFACE ?

The Shannon Sandstone occurs as a series of long, narrow sandbodies in central Wyoming, about 160 km seaward of time-equivalent shorelines (Fig. 22). In outcrops in the Salt Creek area, there are two stacked sandier- and coarsening-upward successions (Fig. 24) that begin with bioturbated mudstones and pass upward into cross-bedded medium- to coarse-grained sandstones (Tillman and Martinsen, 1984). Paleocurrent directions are mostly southward, with some northward flows. There are no convincing explanations of how the sand was moved 160 km from the shoreface to the bars, nor how it was concentrated into long narrow sandbodies. Perhaps the biggest problem is the failure to explain how the coarsest sediment moved to the tops of the bars, where the largest sets of cross bedding occur.

Careful examinations of the outcrop have not revealed erosion surfaces *immediately* below the sandbodies, although a regionally extensive phosphatic pebble bed *does* lie 5-10 m below the lower sandbody at Salt Creek (Gaynor and Swift, 1988). We direct the reader's thoughts to the following speculations.

A major relative sea level fall might have rapidly moved the Shannon shoreline almost to the area of central Wyoming. There would have been simultaneous moderate scouring and winnowing of shelf mudstones seaward of the new shoreline, generating a subtle, lag-strewn erosion surface. The lowstand shoreface then *prograded,* forming a sandier- and coarsening-upward shoreface succession which began with offshore bioturbated mudstones (Fig. 25, column 5). These were succeeded vertically by sandstones, with cross bedding forming in coarse sands in the upper shoreface. A minor transgression was followed by a second progradation, leading to the two stacked successions at Salt Creek. Finally, a major transgression truncated the succession in central Wyoming and cut an erosion surface back to the "time-equivalent shoreline" shown in Figure 22 (and Fig. 25, column 8). Although most reports illustrate the Shannon as an isolated sandbody, it is of interest to note that Gill and Cobban (1973, fig. 10) show, in some areas, a *continuous* sand sheet extending westward to link with shoreline sandstones of the Mesaverde Formation. This sand sheet may be a locally preserved remnant of the shoreface sandbody deposited during rapid regression, as illustrated in Figure 25A, between sea levels D and F.

In our scenario, the Shannon "offshore bars" become prograding lowstand shorefaces, effectively solving the problems of sediment transport from the shoreline, its concentration into bars, and the formation of sandier- and coarsening-upward successions. These shorefaces appear to have prograded farther than those in the Cardium, because they have complete gradationally based successions that begin with offshore mudstones (similar to Fig. 25, succession 5). In the Cardium, shoreface progradation in the Waskahigan, Burnstick and Carrot Creek allomembers was restricted to the area of the wave-scoured surface. No offshore mudstones related to shoreface progradation are present below the sharp-based shoreface sandstones (Figure 25, column 4). The differences reflect sediment supply and time available for progradation before transgression resumes, as well as differences in slopes and subsidence rates. Steeper slopes and faster subsidence would generate greater accomodation space and hence favour mud accumulation below fairweather wave base.

FACIES MODELLING — SYNTHESIS

Two models emerge from this chapter — one well understood and one embryonic. The well-understood *prograding shoreface* (Figs. 13, 14, 15) can be summarized in two vertical succes-

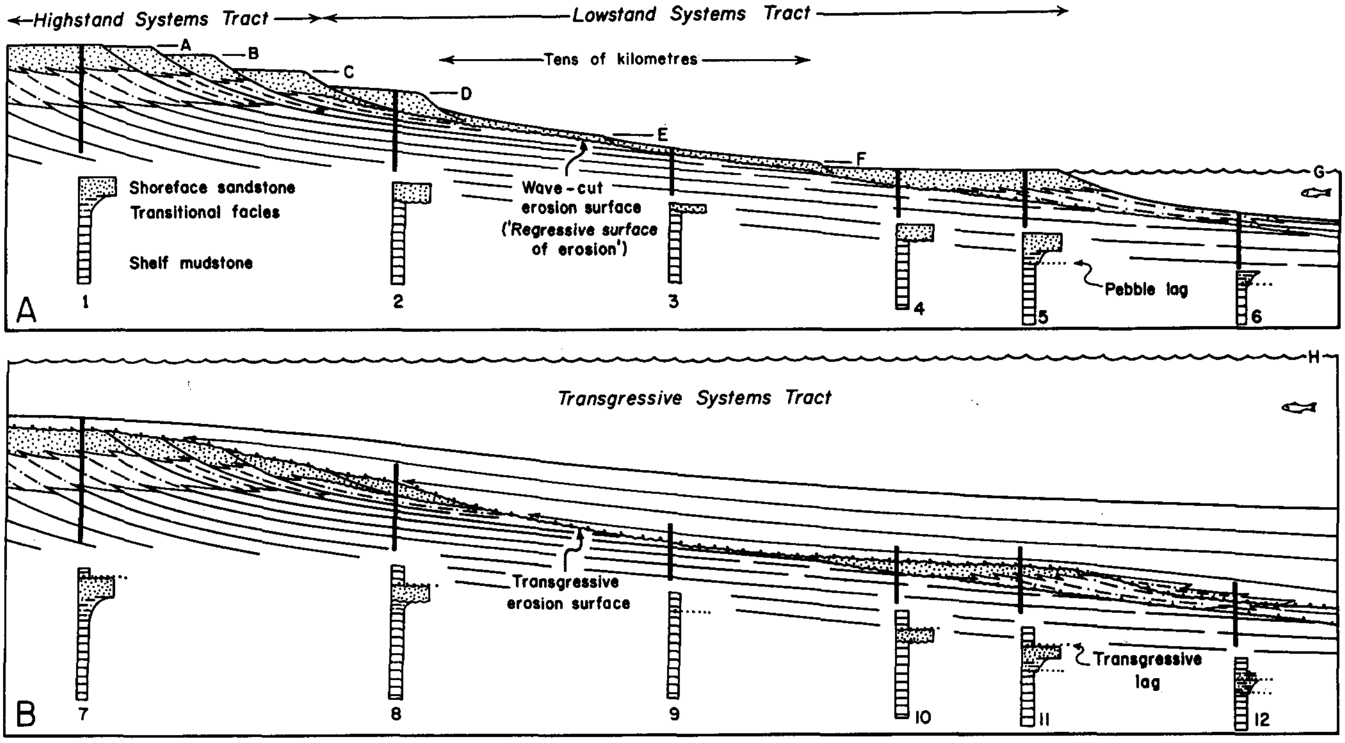

Figure 25 Generalized model for origin of "offshore bars" in a shallow marine setting. In cross section A, a wave-dominated strandplain (highstand systems tract) progrades during sea level A. Shelf muds grade progressively up into shoreface sands (column 1). Subsequently, relative sea level lowers through B, C and D, and with reduced accommodation space, the shoreface-to-shelf transitional facies are progressively eliminated, resulting in shoreface sands resting directly on shelf muds (column 2). Relative sea level lowers rapidly from D through F, forming a very thin, erosively based shoreface sandbody (column 3). It stabilizes at G, permitting development of a new, *lowstand shoreface*. The landward portion of the lowstand shoreface sandbody rests abruptly on an erosion surface (column 4), but as the lowstand shoreface sands prograde into deeper water, transitional and offshore facies can be formed and preserved (column 5). In columns 5 and 6, there will be either an abrupt or rapidly-gradational contact, possibly marked by an intraclast lag, between distal shelf muds and the coarser silts and sands of the shoreface. The deposits associated with sea levels D through G can be assigned to a *lowstand* systems tract. In cross section B, the lowstand deposition is terminated by a relative sea level rise, to position H. The shoreline is driven landward, and wave scour in the transgressing shoreface forms a gently undulating erosion surface (*ravinement* surface). This may be mantled by a transgressive lag, and all evidence of subaerial exposure may be removed (columns 10, 11, 12). The thin regressive sandstone veneer in column 3 is completely removed, and the only evidence of the passage of the shoreline is a veneer of pebbles separating shelf mudstones (below) from shelf mudstones (above) (column 9). Such veneers may be very hard to identify in the geological record. Continued transgression results in the erosional removal of the upper part of the shoreface sandstones of columns 2 and 1, resulting in columns 8 and 7; the older shoreface sands are blanketed by transgressive marine mudstones. This entire cycle of progradation and transgression results in a lenticular, marine, shore-parallel sandbody with an abrupt or sharply gradational base (columns 10, 11, 12), isolated offshore and wholly enclosed in offshore marine mudstones — a lowstand shoreface masquerading as a classic "offshore bar". Diagram based on Plint (1988).

sions (Fig. 14) which begin with bioturbated open marine mudstones and pass upward into interbedded HCS sandstones and interbedded mudstones. The successions are capped by SCS shoreface sandbodies. The two successions in Figure 14 differ with respect to the sharp or gradational base of the SCS sandbody. The model has predictive value inasmuch as the discovery of an SCS sandbody predicts the occurrence of open marine HCS sandstones in a basinward direction, and vice versa. The model acts as a guide for future observations, particularly directing attention to the sedimentary structures within the SCS sandbody, and the relative proportions of SCS and angle-of-repose cross stratification. Prograding shorefaces are common within the highstand systems tract, and may also occur in some lowstand situations (as postulated for the Shannon; Fig. 25).

One emphasis of this chapter has been the difficulty of forming "offshore bars". This model is now hard to justify, and the tabulation in the second edition of *Facies Models* is definitely misleading (Walker, 1984, p. 163-164). Instead, we propose the embryonic *incised shoreface* model exemplified by the Cardium Formation (Figs. 19-21, 23). In this embryonic model, the norm consists of a sandbody aligned parallel to regional strike, resting abruptly on an erosion surface, and surrounded by marine mudstones. It formed within a shoreface during maximum lowstand, or during a pause in an overall transgression. Its along-strike extent depends upon the positions and numbers of rivers supplying sediment to the shoreface, and the rate of wave-driven sediment transport alongshore. Its extent in the seaward direction depends on the rate of sediment supply and the duration of the relative sea level stillstand. The Cardium sandbodies prograded about 1-2 km. Similar sandbodies in the Lower Cretaceous Viking Formation prograded up to about 15 km, and in the Lower Cretaceous Glauconite Formation, several tens of kilometres of progradation have been suggested by Rosenthal (1988). Commonly only the lower, or lower plus middle shoreface is preserved. The upper shoreface is eroded and spread landward as a transgressive lag during resumed transgression (Fig. 23). Structures within the shoreface reflect either storm or fairweather processes. Because the pause in transgression is short and little new sediment is supplied, there is little opportunity for the development of offshore sandy facies, and these are not predicted by this model. Finally, we point out the importance of isolated pebble beds in muddy, apparently continuous offshore successions (similar to column 9 in Fig. 25B). We tentatively suggest that some of them could be lags resulting from shoreface ravinement, and may predict the existence of lowstand shoreface deposits farther seaward (as in columns 10 and 11 in Fig. 25B). However, more modern and ancient examples must be studied before the incised shoreface model can be developed further.

ACKNOWLEDGEMENTS

Our work in western Canada has been supported by the Natural Sciences and Engineering Research Council, and the Department of Energy, Mines and Resources, Canada. Many oil companies have also given logistical help, particularly Amoco, Canadian Hunter, Esso, Home, Husky, Texaco and Unocal. Many friends have contributed ideas over the years, and for this chapter we particularly thank Bruce Hart and Bill Duke. The chapter has also been improved by comments from the 1991 graduate class in Shelf Sedimentation at McMaster.

REFERENCES

Basic sources of information

James, D.P. and Leckie, D.A., eds., 1988, Sequences, stratigraphy, sedimentology: surface and subsurface: Canadian Society of Petroleum Geologists, Memoir 15, 586 p.
A collection of papers emphasizing sequence stratigraphy and sedimentology, with emphasis on subsurface core studies in the Western Canadian sedimentary basin.

Knight, R.J. and McLean, J.R., eds., 1986, Shelf sands and sandstones: Canadian Society of Petroleum Geologists, Memoir 11, 347 p.
Collection of papers reviewing many aspects of storm and tide-dominated shelves, ancient and modern.

Moslow, T.F. and Rhodes, E.G., eds., 1986, Modern and ancient shelf clastics: a core workshop: Society of Economic Paleontologists and Mineralogists, Core workshop No. 9, 459 p.
The papers in this volume are profusely illustrated with core photographs — a very useful source of information.

Open University Course Team, 1989, Ocean circulation: Oxford, Pergamon Press, 238 p.
Contains an excellent discussion of geostrophic currents.

Open University Course Team, 1989, Waves, tides and shallow-water processes: Oxford, Pergamon Press, 187 p.
Very well-written and well-illustrated discussion of waves and tides, and sediment movement. Controlling processes for beaches and the littoral zone, tidal flats and estuaries, deltas, and shelf seas are explained in detail using only very simple mathematics.

Nummedal, D., Pilkey, O.H. and Howard, J.D., eds., 1987, Sea-level fluctuations and coastal evolution: Society of Economic Paleontologists and Mineralogists, Special Publication 41, 267 p.
A useful collection of papers relating sea level fluctuations, Quaternary and Holocene coastal depositional systems, and sequence-bounding unconformities.

Tillman, R.W., Swift, D.J.P. and Walker, R.G., eds., 1985, Shelf sands and sandstone reservoirs: Society of Economic Paleontologists and Mineralogists, Short Course 13, Notes, 708 p.
Good reviews of processes affecting modern shelf sands (242 pages), followed by case histories of selected ancient shelf sandstones. The concepts applied to some of the case histories are now a little out of date.

Wilgus, C.K., Hastings, B.S., Posamentier, H.W., Ross, C.A. and Kendall, C.G.St.C., eds., 1988, Sea level changes: an integrated approach: Society of Economic Paleontologists and Mineralogists, Special Publication 42, 407 p.
Collection of papers emphasizing conceptual basis of sequence stratigraphy plus numerous case studies of sea level change from the geological record.

Other references

Bergman, K.M. and Walker, R.G., 1988, Formation of Cardium erosion surface E5, and associated deposition of conglomerate: Carrot Creek field, Cretaceous Western Interior Seaway, Alberta, *in* James, D.P. and Leckie, D.A., eds., Sequences, stratigraphy, sedimentology; surface and subsurface: Canadian Society of Petroleum Geologists, Memoir 15, p. 15-24.

Bourgeois, J., 1980, A transgressive shelf sequence exhibiting hummocky cross stratification: the Cape Sebastian Sandstone (Upper Cretaceous), southwestern Oregon: Journal of Sedimentary Petrology, v. 50, p. 681-702.

Boyles, J.M. and Scott, A.J., 1982, A model for migrating shelf-bar sandstones in the Upper Mancos Shale (Campanian), northwestern Colorado: American Association of Petroleum Geologists, Bulletin, v. 66, p. 491-508.

Bryant, I.D. and Smith, M.P., 1990, A composite tectonic-eustatic origin for shelf sandstones at the Cambrian-Ordovician boundary in north Greenland: Journal of the Geological Society of London, v. 147, p. 795-809.

Carter, C.H., 1978, A regressive barrier and barrier-protected deposit: depositional environments and geographic setting of the Late Tertiary Cohansey sand: Journal of Sedimentary Petrology, v. 48, p. 933-950.

Clifton, H.E., 1981, Progradational sequences in Miocene shoreline deposits, southeastern Caliente Range, California: Journal of Sedimentary Petrology, v. 51, p. 165-184.

Clifton, H.E., Hunter, R.E. and Phillips, R.L., 1971, Depositional structures and processes in the non-barred, high-energy nearshore: Journal of Sedimentary Petrology, v. 41, p. 651-670.

Cotter, E., 1985, Gravel-topped offshore bar sequences in the Lower Carboniferous of southern Ireland: Sedimentology, v. 32, p. 195-213.

Curray, J.R., Emmel, F.J. and Crampton, P.J.S., 1969, Holocene history of a strand plain, lagoonal coast, Nayarit, Mexico, *in* Castanares, A.A. and Phleger, F.B., eds., Coastal lagoons — a symposium: Mexico City, Universidad Nacional Autonoma, p. 63-100.

Davis, H.R. and Byers, C.W., 1989, Shelf sandstones in the Mowry shale: evidence for deposition during Cretaceous sea level falls: Journal of Sedimentary Petrology, v. 59, p. 548-560.

Davis, H.R., Byers, C.W. and Pratt, L.M., 1989, Depositional mechanisms and organic matter in Mowry Shale (Cretaceous), Wyoming: American Association of Petroleum Geologists, Bulletin, v. 73, p. 1103-1116.

DeCelles, P.G., 1987, Variable preservation of Middle Tertiary, coarse-grained, nearshore to outer-shelf storm deposits in southern California: Journal of Sedimentary Petrology, v. 57, p. 250-264.

de Raaf, J.F.M., Boersma, J.R. and van Gelder, A., 1977, Wave-generated structures and sequences from a shallow marine succession, Lower Carboniferous, County Cork, Ireland: Sedimentology, v. 24, p. 451-483.

Diaz, J.I. and Maldonado, A., 1990, Transgressive sand bodies on the Maresme continental shelf, western Mediterranean Sea: Marine Geology, v. 91, p. 53-72.

Dominguez, J.M.L., Martin, L. and Bittencourt, A.C.S.P., 1987, Sea-level history and Quaternary evolution of river mouth-associated beach-ridge plains along the east-southeast Brazilian coast: a summary, *in* Nummedal, D., Pilkey, O.H. and Howard, J.D., eds., Sea-level fluctuations and coastal evolution: Society of Economic Paleontologists and Mineralogists, Special Publication 41, p. 115-127.

Duke, W.L., 1985, Hummocky cross stratification, tropical hurricanes, and intense winter storms: Sedimentology, v. 32, p. 167-194.

Duke, W.L., 1990, Geostrophic circulation or shallow marine turbidity currents? The dilemma of paleoflow patterns in storm-influenced prograding shoreline systems: Journal of Sedimentary Petrology, v. 60, p. 870-883.

Duke, W.L., Arnott, R.W. and Cheel, R.J., 1991, Shelf sandstones and hummocky cross stratification; new insights on a stormy debate: Geology, v. 19, p. 625-628.

Everts, C.H., 1987, Continental shelf evolution in response to a rise in sea level, *in* Nummedal, D., Pilkey, O.H. and Howard, J.D., eds., Sea-level fluctuations and coastal evolution: Society of Economic Paleontologists and Mineralogists, Special Publication 41, p. 49-57.

Forbes, D.L. and Boyd, R., 1987, Gravel ripples on the inner Scotian Shelf: Journal of Sedimentary Petrology, v. 57, p. 46-54.

Forristall, G.Z., Hamilton, R.C. and Cardone, V.J., 1977, Continental shelf currents in tropical storm Delia: observations and theory: Journal of Physical Oceanography, v. 87, p. 532-546.

Gaynor, G.C. and Swift, D.J.P., 1988, Shannon Sandstone depositional model: sand ridge dynamics on the Campanian Western Interior shelf: Journal of Sedimentary Petrology, v. 58, p. 868-880.

Gill, J.R. and Cobban, W.A., 1973, Stratigraphy and geologic history of the Montana Group and equivalent rocks, Montana, Wyoming, and North and South Dakota: United States Geological Survey, Professional Paper 776, 37 p.

Greenwood, B. and Mittler, P.R., 1985, Vertical sequence and lateral transitions in the facies of a barred nearshore environment: Journal of Sedimentary Petrology, v. 55, p. 366-375.

Greenwood, B. and Sherman, D.J., 1986, Hummocky cross stratification in the surf zone: flow parameters and bedding genesis: Sedimentology, v. 33, p. 33-45.

Hall, R.L., Krause, F.F., Joiner, S.D. and Deutsch, K.B., 1991, Biostratigraphy and allostratigraphy in the Cardium Formation, Upper Cretaceous, Canada: Geological Association of Canada—Mineralogical Association of Canada, Annual Meeting, Abstracts, v. 19, p. A49.

Hamblin, A.P. and Walker, R.G., 1979, Storm dominated shallow marine deposits: the Fernie-Kootenay (Jurassic) transition, southern Rocky Mountains: Canadian Journal of Earth Sciences, v. 16, p. 1673-1690.

Haq, B.U., Hardenbol, J. and Vail, P.R., 1988, Mesozoic and Cenozoic chronostratigraphy and cycles of sea level change, *in* Wilgus, C.K., *et al.*, eds., Sea-level change; an integrated approach: Society of Economic Paleontologists and Mineralogists, Special Publication 42, p. 71-108.

Harms, J.C., Southard, J.B., Spearing, D.R. and Walker, R.G., 1975, Depositional environments as interpreted from primary sedimentary structures and stratification sequences: Society of Economic Paleontologists and Mineralogists, Short Course 2, 161 p.

Hart, B.S. and Plint, A.G., 1989, Gravelly shoreface deposits: a comparison of modern and ancient facies sequences: Sedimentology, v. 36, p. 551-557.

Hart, B.S. and Plint, A.G., in press, Origin of erosion surfaces in shoreface sandstones of the Kakwa Member (Upper Cretaceous Cardium Formation, Alberta): importance for recognition of stratal geometry and depositional history, *in* Posamentier, H.W., Summerhayes, C.P., Haq, B.U. and Allen, G.P., eds., Stratigraphy and facies associations in a sequence-stratigraphic framework: International Association of Sedimentologists, Special Publication.

Hart, B.S., Vantfoort, R.M. and Plint, A.G., 1990, Is there any evidence for geostrophic currents preserved in the sedimentary record of inner to middle-shelf deposits? — Discussion: Journal of Sedimentary Petrology, v. 60, p. 633-635.

Heward, A.P., 1981, A review of wave-dominated clastic shoreline deposits: Earth-Science Reviews, v. 17, p. 223-276.

Hobson, J.P., Jr., Fowler, M.L. and Beaumont, E.A., 1982, Depositional and statistical exploration models, Upper Cretaceous offshore sandstone complex, House Creek field, Wyoming: American Association of Petroleum Geologists, Bulletin, v. 66, p. 689-707.

Johnson, H.D. and Baldwin, C.T., 1986, Shallow siliciclastic seas, *in* Reading, H.G., ed., Sedimentary environments and facies: Oxford, Blackwell Scientific Publications, p. 229-282.

Komar, P.D., 1976, Beach processes and sedimentation: Englewood Cliffs, New Jersey, Prentice Hall, 429 p.

Komar, P.D., ed., 1983, CRC Handbook of coastal processes and erosion: Boca Raton, Florida, CRC Press, Inc., 305 p.

Kowsmann, R.O., Costa, M.P.A., Vicalvi, M.A., Coutinho, M.G.N. and Gamboa, L.A.P., 1977, Modelo da sedimentacao holocenica na platforma continental sul brasileira, *in* Projeto REMAC, Evolucao sedimentar holocenica da platforma continental e do talude do sul do Brasil: Rio de Janeiro, PETROBRAS, Divisao de informacao tecnica e propriedade indistrial (DINTEP), p. 8-26.

La Fon, N.A., 1981, Offshore bar deposits of Semilla Sandstone Member of Mancos Shale (Upper Cretaceous), San Juan Basin, New Mexico: American Association of Petroleum Geologists, Bulletin, v. 65, p. 706-721.

Leckie, D.A., 1988, Wave-formed coarse-grained ripples and their relationship to hummocky cross stratification: Journal of Sedimentary Petrology, v. 58, p. 607-622.

Leckie, D.A. and Krystinik, L.F., 1989, Is there evidence for geostrophic currents preserved in the sedimentary record of inner to middle-shelf deposits?: Journal of Sedimentary Petrology, v. 59, p. 862-870.

Leckie, D.A. and Walker, R.G., 1982, Storm- and tide-dominated shorelines in Late Cretaceous Moosebar-Lower Gates interval — outcrop equivalents of deep basin gas trap in western Canada: American Association of Petroleum Geologists, Bulletin, v. 66, p. 138-157.

McCrory, V.L.C. and Walker, R.G., 1986, A storm- and tidally-influenced prograding shoreline — Upper Cretaceous Milk River Formation of southern Alberta, Canada: Sedimentology, v. 33, p. 47-60.

McCubbin, D.G., 1982, Barrier island and strand plain facies, *in* Scholle, P.A. and Spearing, D., eds., Sandstone depositional environments: American Association of Petroleum Geologists, Memoir 31, p. 247-279.

Morton, R.A., 1988, Nearshore responses to great storms, *in* Clifton, H.E., ed., Sedimentologic consequences of convulsive geologic events: Geological Society of America, Special Paper 229, p. 7-22.

Nummedal, D. and Swift, D.J.P., 1987, Transgressive stratigraphy at sequence-bounding unconformities: Some principles derived from Holocene and Cretaceous examples, *in* Nummedal, D., Pilkey, O.H. and Howard, J.D., eds., Sea-level fluctuations and coastal evolution: Society of Economic Paleontologists and Mineralogists, Special Publication 41, p. 241-260.

Pattison, S.A.J. and Walker, R.G., 1992, Deposition and interpretation of long, narrow sandbodies underlain by a basinwide erosion surface: Cardium alloformation, Cretaceous Western Interior Seaway, Alberta, Canada: Journal of Sedimentary Petrology, v. 62, p. 292-309.

Pilkey, O.H. and Davis, T.W., 1987, An analysis of coastal recession models: North Carolina coast, *in* Nummedal, D., Pilkey, O.H. and Howard, J.D., eds., Sea-level fluctuations and coastal evolution: Society of Economic Paleontologists and Mineralogists, Special Publication 41, p. 59-68.

Plint, A.G., 1988, Sharp-based shoreface sequences and "offshore bars" in the Cardium Formation of Alberta: their relationship to relative changes in sea level, *in* Wilgus, C.K., et al., eds., Sea level changes, an integrated approach: Society of Economic Paleontologists and Mineralogists, Special Publication 42, p. 357-370.

Plint, A.G., 1990, An allostratigraphic correlation of the Muskiki and Marshybank Formations (Coniacian-Santonian) in the foothills and subsurface of the Alberta Basin: Bulletin of Canadian Petroleum Geology, v. 38, p. 288-306.

Plint, A.G., 1991, High-frequency relative sea level oscillations in Upper Cretaceous shelf clastics of the Alberta foreland basin: possible evidence for a glacio-eustatic control?, *in* MacDonald, D.I.M., ed., Sedimentation, tectonics and eustasy: International Association of Sedimentologists, Special Publication 12, p. 409-428.

Plint, A.G. and Norris, B., 1991, Anatomy of a ramp margin sequence: facies successions, paleogeography and sediment dispersal patterns in the Muskiki and Marshybank Formations, Alberta foreland basin: Bulletin of Canadian Petroleum Geology, v. 39, p. 18-42.

Plint, A.G. and Walker, R.G., 1987, Cardium Formation 8. Facies and environments of the Cardium shoreline in the Kakwa field and adjacent areas, northwestern Alberta: Bulletin of Canadian Petroleum Geology, v. 35, p. 48-64.

Plint, A.G., Walker, R.G. and Bergman, K.M., 1986, Cardium Formation 6. Stratigraphic framework of the Cardium in subsurface: Bulletin of Canadian Petroleum Geology, v. 34, p. 213-225.

Plint, A.G., Walker, R.G. and Bergman, K.M., 1987, Cardium Formation 6. Stratigraphic framework of the Cardium in subsurface: reply: Bulletin of Canadian Petroleum Geology, v. 35, p. 365-374.

Plint, A.G., Walker, R.G. and Duke, W.L., 1988, An outcrop to subsurface correlation of the Cardium Formation in Alberta, *in* James, D.P. and Leckie, D.A., eds., Sequences, stratigraphy, sedimentology; surface and subsurface: Canadian Society of Petroleum Geologists, Memoir 15, p. 167-184.

Rosenthal, L.R.P., 1988, Wave-dominated shorelines and incised channel trends: Lower Cretaceous Glauconite Formation, west-central Alberta, *in* James, D.P. and Leckie, D.A., eds., Sequences, stratigraphy, sedimentology; surface and subsurface: Canadian Society of Petroleum Geologists, Memoir 15, p. 207-220.

Rosenthal, L.R.P. and Walker, R.G., 1987, Lateral and vertical facies sequences in the Upper Cretaceous Chungo Member, Wapiabi Formation, southern Alberta: Canadian Journal of Earth Sciences, v. 24, p. 771-783.

Rine, J.M. and Ginsburg, R.N., 1985, Depositional facies of a mud shoreface in Suriname, South America — a mud analogue to sandy shallow-marine deposits: Journal of Sedimentary Petrology, v. 55, p. 633-652.

Snedden, J.W., Nummedal, D. and Amos, A.F., 1988, Storm and fair-weather combined flow on the central Texas continental shelf: Journal of Sedimentary Petrology, v. 58, p. 580-595.

Southard, J.B., Lambie, J.M., Federico, D.C., Pile, H.T. and Weidman, C.R., 1990, Experiments on bed configurations in fine sand under bidirectional purely oscillatory flow, and the origin of hummocky cross stratification: Journal of Sedimentary Petrology, v. 60, p. 1-17.

Strahler, A., 1963, The earth sciences: New York, Harper and Row, 681 p.

Swagor, N.S., Oliver, T.A. and Johnson, B.A., 1976, Carrot Creek field, central Alberta, *in* Lerand, M.M., ed., The sedimentology of selected clastic oil and gas reservoirs in Alberta: Calgary, Canadian Society of Petroleum Geologists, p. 78-95.

Swift, D.J.P. and Field, M.E., 1981, Evolution of a classic sand ridge field; Maryland sector, North American inner shelf: Sedimentology, v. 28, p. 461-481.

Swift, D.J.P., Han, G. and Vincent, C.E., 1986, Fluid processes and sea floor response on a modern storm-dominated shelf; middle Atlantic shelf of North America. Part I: the storm-current regime, *in* Knight, R.J. and McLean, J.R., eds., Shelf sands and sandstones: Canadian Society of Petroleum Geologists, Memoir 11, p. 99-119.

Swift, D.J.P., Hudelson, P.M., Brenner, R.L. and Thompson, P., 1987, Shelf construction in a foreland basin: storm beds, shelf sandbodies, and shelf-slope depositional sequences in the Upper Cretaceous Mesaverde Group, Book Cliffs, Utah: Sedimentology, v. 34, p. 423-457.

Swift, D.J.P. and Niedoroda, A.W., 1985, Fluid and sediment dynamics on Continental Shelves, *in* Tillman, R.W., Swift, D.J.P. and Walker, R.G., eds., Shelf sands and sandstone reservoirs: Society of Economic Paleontologists and Mineralogists, Short Course 13, Notes, p. 47-133.

Swift, D.J.P. and Rice, D.D., 1984, Sand bodies on muddy shelves: a model for sedimentation in the Western Interior Seaway, North America, *in* Tillman, R.W. and Siemers, C.T., eds., Siliciclastic shelf sediments: Society of Economic Paleontologists and Mineralogists, Special Publication 34, p. 43-62.

Swift, D.J.P., Young, R.A., Clarke, T.L., Vincent, C.E., Niedoroda, A. and Lesht, B., 1981, Sediment transport in the Middle Atlantic Bight of North America: synopsis of recent observations, *in* Nio, S.D., Shuttenhelm, R.T.E. and van Weering, T.C.E., eds., Holocene marine sedimentation in the North Sea basin: International Association of Sedimentologists, Special Publication 5, p. 361-383.

Tillman, R.W. and Martinsen, R.S., 1984, The Shannon shelf-ridge sandstone complex, Salt Creek anticline area, Powder River basin, Wyoming, *in* Tillman, R.W. and Siemers, C.T., eds., Siliciclastic shelf sediments: Society of Economic Paleontologists and Mineralogists, Special Publication 34, p. 85-142.

Tillman, R.W. and Martinsen, R.S., 1987, Sedimentologic model and production characteristics of Hartzog Draw field, Wyoming, a Shannon shelf-ridge sandstone, *in* Tillman, R.W. and Weber, K.J., eds., Reservoir sedimentology: Society of Economic Paleontologists and Mineralogists, Special Publication 40, p. 15-112.

Tyler, N. and Ambrose, W.A., 1986, Facies architecture and production characteristics of strand plain reservoirs in North Markham-North Bay City field, Frio Formation, Texas: American Association of Petroleum Geologists, Bulletin, v. 70, p. 809-829.

Wadsworth, J.A. and Walker, R.G., 1991, Morphology and origin of erosion surfaces in the Cardium Formation (Upper Cretaceous, Western Interior Seaway, Alberta), and their implications for rapid sea level fluctuations: Canadian Journal of Earth Sciences, v. 28, p. 1507-1520.

Walker, R.G., 1984, Shelf and shallow marine sands, *in* Walker, R.G., ed., Facies models (2nd. Edition), Geological Association of Canada, Geoscience Canada Reprint Series 1, p. 141-170.

Walker, R.G. and Eyles, C.H., 1988, Geometry and facies of stacked shallow-marine sandier-upward sequences dissected by erosion surface, Cardium Formation, Willesden Green, Alberta: American Association of Petroleum Geologists, Bulletin, v. 72, p. 1469-1494.

Walker, R.G. and Eyles, C.H., 1991, Topography and significance of a basin-wide sequence-bounding erosion surface in the Cretaceous Cardium Formation, Alberta, Canada: Journal of Sedimentary Petrology, v. 61, p. 473-496.

Wilkinson, B.H., McGowen, J.H. and Lewis, C.R., 1975, Ingleside strandplain of sand of central Texas coast: American Association of Petroleum Geologists, Bulletin, v. 59, p. 347-352.

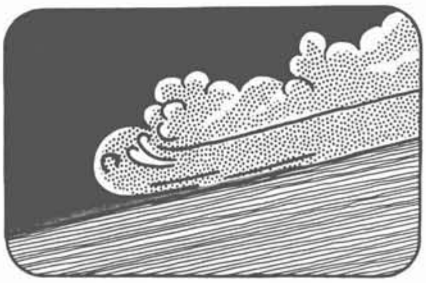

13. Turbidites and Submarine Fans

Roger G. Walker, Department of Geology, McMaster University,
Hamilton, Ontario L8S 4M1

INTRODUCTION

This chapter discusses turbidites and submarine fans on many different scales. Individual turbidites may be a few centimetres or tens of centimetres in thickness. However, vast numbers of such beds can build up submarine fan deposits with volumes up to four million cubic kilometres in the Bengal Fan.

The turbidity current concept is both simple and elegant. Simple, because each turbidite is the result of a single short-lived event, and once deposited, it is unlikely to be reworked by other currents. Elegant, because it suggests that the deposition of thousands of graded sandstone beds, alternating with shales, results from a series of similar events. No large volume of sedimentary rock, other than turbidites, can be interpreted so simply.

In the early days of turbidite studies (1950-1965), the emphasis was on ancient rocks. After 1965, information slowly became available on modern submarine fans. Since about 1980, the emphasis has been on the large-scale seismic characterization of modern fans, the sequence stratigraphy of their deposits, and the influence of relative sea level fluctuations. All of these aspects will be discussed in this chapter.

TURBIDITY CURRENTS AND TURBIDITES

Density currents move downslope on the ocean floor, driven by gravity that acts on the density difference between the current and the surrounding seawater. The excess density of the current could be due to colder temperatures, higher salinities, or suspended sediment in the current. Where the density is due to suspended sediment, the flow is termed a *turbidity current* (Fig. 1). A *turbidite* is defined as the deposit of a turbidity current.

The turbidity current concept was introduced into the geological literature by Kuenen and Migliorini in 1950, at a time when no-one had observed a modern turbidity current in the ocean. In writing their classic paper "Turbidity currents as a cause of graded bedding" (Kuenen and Migliorini, 1950), they pulled together evidence from density currents in lakes, from observations of modern submarine canyons, from geology and paleontology, and from experimental studies. A full review of how and why the concept was established in geology was published by Walker (1973).

Turbidites are generally regarded as deep water deposits. The turbidity current *process* can operate in any depth, but to preserve the deposits as turbidites, they must not be reworked into different-looking deposits by other currents. This effectively places turbidites below storm wave base; depending on the basin, this probably implies *minimum* depths of 250-300 m.

FLOW GENERATION AND MOVEMENT

The initiation of a large turbidity current in the ocean has never been observed. Nevertheless, mechanisms for flow generation can be deduced from three different situations, and other studies give information on flow volumes and distances of flow.

Grand Banks of Newfoundland

Classic information on flow genesis and movement came from a series of submarine cable breaks off the Grand Banks of Newfoundland. Many of the cables broke instantaneously following an earthquake in 1929 (Fig. 2, where epicentre is shown by a triangle, and area of instantaneous cable breaks IB outlined). Others broke in sequence farther and farther from the epicentre, over a period of time from 59 minutes to 797 minutes from the quake (Fig. 2). It is now apparent that the sequential breaks were made by a turbidity current. The 1929 earthquake appears to have caused liquefaction of sands and gravels in the upper valleys of Laurentian Fan, and the turbidity current developed from this liquefied material. The mechanics of the flow have been reconstructed by Piper *et al.* (1988), who suggest velocities up to about 20 m/sec, flow thicknesses of several hundred metres, and a mini-

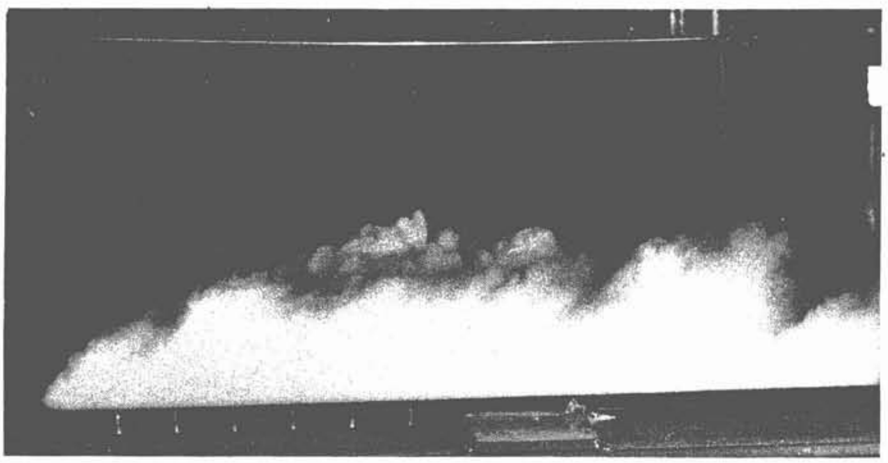

Figure 1 Experimental turbidity current in a flume at Caltech. Water depth is 28 cm. Note characteristic shape of the head, and eddies behind the head. Sediment is thrown out of the main flow by these eddies, and the body of the flow is only about half the height of the head.

mum volume for the Grand Banks turbidite of 175 km^3. The deposit of the Grand Banks turbidity current now covers a large part of the Sohm Abyssal Plain, and a turbidite in places over 1 m thick extends hundreds of kilometres from the upper fan valleys (Fig. 2).

Congo River, Africa
Powerful flows have also broken telegraph cables off the Congo (Zaire) River in Africa. The Congo has no delta; instead, it has a large estuary that feeds directly into the head of a submarine canyon (Heezen *et al.*, 1964). Cables on the shelf and slope were preferentially broken 1) during months when the Congo River was in flood, and 2) during the years when the Congo River was shifting its route through the estuary and sweeping estuarine sandbodies into the canyon head. Cables have been broken in depths as great as 2800 m, in the lower part of the Congo submarine canyon, suggesting that sand moved down the canyon as a powerful, cable-breaking flow (turbidity current). Even during today's relative highstand of sea level, there have been 26 cable breaks in the period 1893-1937, at the average rate of one flow every 1.7 years.

Magdalena River, Colombia
A slump off the mouth of the Magdalena River in Colombia in 1935 had an estimated volume of sand of 3×10^8 m^3. The slump was probably a response to rapid deposition and overloading in the delta front. It generated a turbidity current that broke telegraph cables in depths of 1400 m about 28 km from the delta. Other Magdalena turbidity currents have broken cables up to 100 km from the delta (Heezen, 1956). During the period 1932-1955, there have been 15 cable breaks (averaging one every 1.5 years).

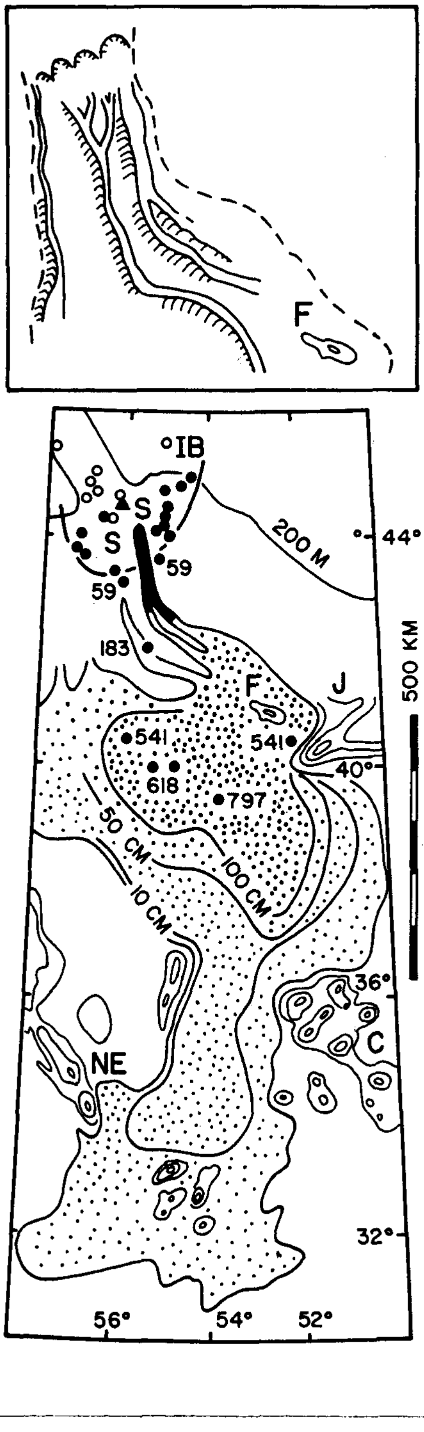

Figure 2 (left) Map of the Laurentian Fan – Sohm Abyssal Plain, off the Grand Banks of Newfoundland. Shelf edge marked by the 200 m isobath, with Laurentian Channel entering map area from the northwest. Black dots show cable breaks that followed the 1929 earthquake (epicentre shown by triangle, with post 1929 quake epicentres shown with open circles). North of the line IB, the breaks were instantaneous (IB = instantaneous breaks, S = zone of slumping). South of the line, cables were broken in sequence, 59 to 797 minutes from the quake. Isopachs show the resulting turbidite (stippled), and the canyon fill (black) indicates debris flow deposits. Seafloor topography locally deflected the turbidity current, particularly the J Anomaly Ridge (J), the Fogo (F) and Corner (C) Seamounts, and part of the New England Seamount Chain (NE). Diagram at top shows detail of the upper fan channels and levees. Redrawn from Piper *et al.* (1984).

Extent of Turbidites on Basin Plains
Individual turbidite sand beds cover large areas of modern basin plains (Fig. 2), as reviewed by Pilkey (1988). The largest single bed is the "Black Shell turbidite" (named for its distinctive corroded and transported mollusc fragments), which covers an area of 44,000 km^2 on the Hatteras Abyssal Plain (western North Atlantic Ocean). It is up to 4 m thick, with a volume estimated at between 100 and 200 km^3. It extends for at least 500 km along the length of the abyssal plain, and was deposited about 16,000 years ago during a lowstand of relative sea level (Elmore *et al.*, 1979).

Several important points emerge from this brief summary. Turbidity currents can be generated at various times with respect to low- and highstands of relative sea level. Initiating mechanisms include earthquakes (Grand Banks), rivers in flood (Congo) and sediment failure in rapidly deposited delta fronts (Magdalena). The initial sediment in the current will reflect the source; in the case of the Congo, the sediment will be the clean, well-sorted sand of the estuarine sand bars. Individual flows can be thick and rapid, up to at least 20 m/sec. At that velocity they could suspend by *fluid turbulence* alone clasts up to about 3-4 cm in diameter (the exact size

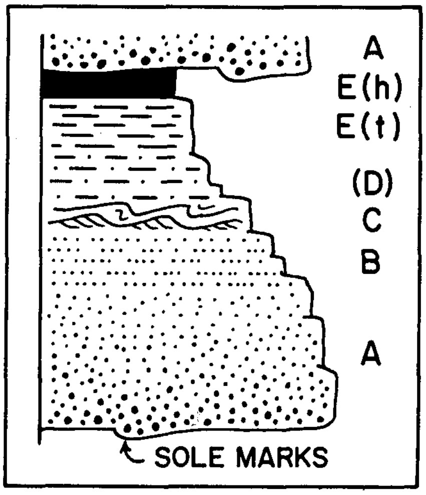

Figure 3 Bouma (1962) sequence; division A is structureless, B is parallel-laminated sand, C is rippled and/or convoluted, (D) is hard to see in weathered or tectonized outcrops, and consists of parallel-laminated silt and mud. The pelitic interval E is partly of turbidite origin (t) and partly hemipelagic (h).

depends on assumptions made in the calculation). On the flat abyssal plains (gradients typically less than 1:1000), large turbidity currents can flow for several hundred kilometres, and deposit beds a metre or more in thickness.

TURBIDITE FEATURES

Immediately after introduction of the turbidity current concept in 1950, studies emphasized a vast array of new sedimentary structures and their use in determining paleoflow directions. In the absence of a turbidite facies model, there was no norm with which to compare new examples, no framework for organizing observations, no logical basis for prediction, and no unified basis for hydrodynamic interpretation. As a result of continued work during the 1950's, a small but consistent set of features began to be associated with beds here termed *classical turbidites*:

1) Sandstones and shales are monotonously interbedded through tens or hundreds of metres of section.

2) Beds tend to have sharp, flat bases, with no indications of erosion of the seafloor on a scale exceeding a few tens of centimetres (i.e., the seafloor was flat and unchannellized).

3) The sharp bases (soles) of the beds have abundant markings, now classified into three types; *tool marks*, which are carved into the underlying mud by rigid objects (sticks, stones, shells); *scour marks*, which are cut into the underlying mud by fluid scour; and *organic marks*, which represent trails and burrows made by organisms and filled in by the turbidity current. Tool and scour marks give accurate indications of local flow directions.

4) Within the sandstone beds (Fig. 3), the grain size commonly decreases upward (graded bedding); the basal division A of the bed is commonly structureless, and grades up into a sandy, parallel-laminated division B — this in turn grades into a current-rippled division C. Both divisions B and C can also contain convolute lamination. The rippled division C is overlain by parallel-laminated silt and mud (division D) — this division is difficult to see in weathered and/or tectonized outcrops. The uppermost division E is pelitic, and mostly deposited by the turbidity current E(t). Only the uppermost part of the pelitic division represents the slow accumulation of mud deposited directly from the ocean after the passage of the turbidity current (hemipelagic deposition, E(h)). This grouping of sedimentary structures and lithologies was first published by Bouma (1962), and is now known as the "Bouma sequence" (Fig. 3).

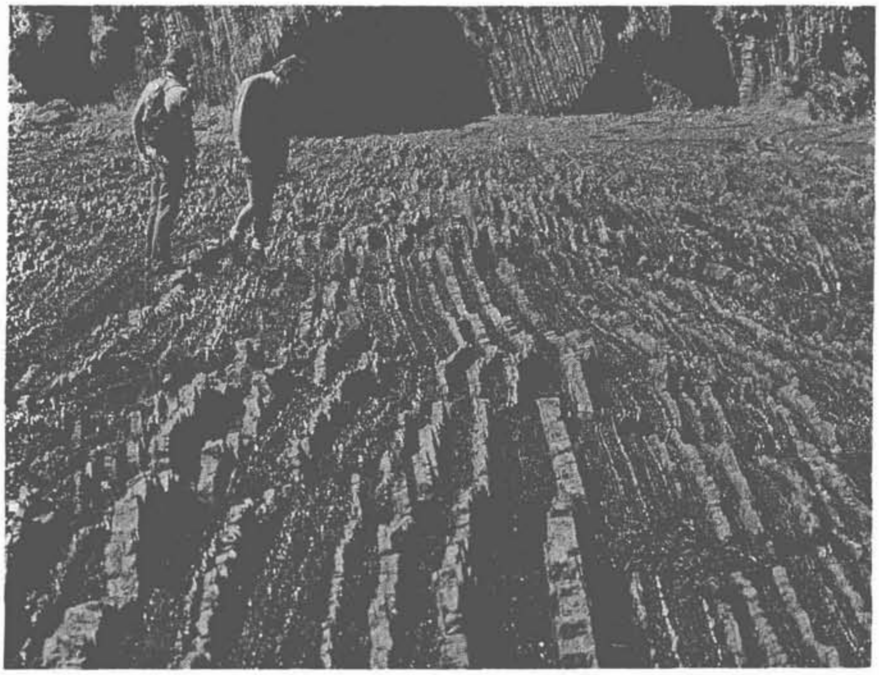

Figure 4 Classical turbidites; monotonous interbeds of sandstone and shale, with no evidence of topography on the seafloor. Stratigraphic top to right; Devonian, Cape Liptrap, near Melbourne, Australia.

The Bouma sequence as a facies model

On a small scale, the Bouma sequence has functioned well as a facies model in its own right. The sequence has been distilled from thousands of individual beds, and therefore forms a homogeneous model of great generality.

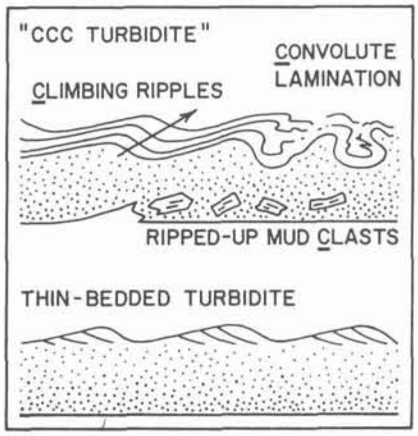

Figure 5 Comparison of distal, or basin plain thin-bedded turbidite, with a CCC turbidite interpreted to be a levee deposit. Arrow indicates climbing ripples.

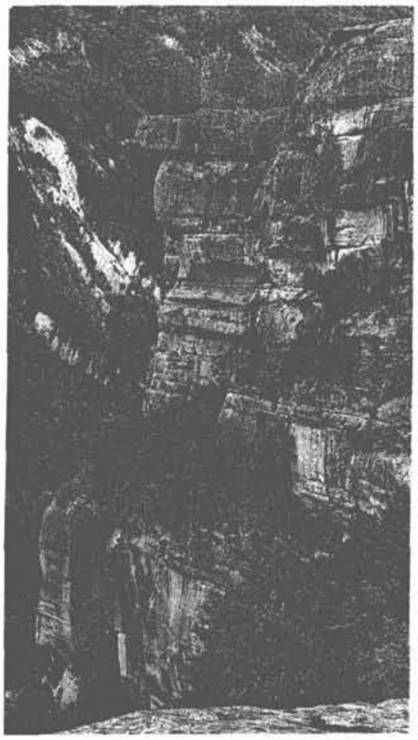

Figure 6 Massive sandstone facies in the Upper Eocene Annot Sandstone, southern France. About 180 m of section can be seen; note thickness of individual sandstone beds and absence of mudstone interbeds.

It functions very well as a *norm*, or point of comparison between different turbidite beds, and also serves well as a *guide* for making observations. As a *predictor*, it indicates (for example) that beds beginning with division A might be expected in more proximal settings. However, as the turbidity current slows down in more distal areas, the model predicts that beds should begin with division B, or division C. Finally the Bouma sequence acts as the *basis for an integrated hydrodynamic interpretation* (Walker, 1965).

Figure 7 Dish structures in Upper Cretaceous sandstones, Wheeler Gorge, California. Note darker less permeable layers, and paler cleaner layers where escaping fluid has broken through the darker layers and curved them upward.

Figure 8 Pebbly sandstone facies, Cambro-Ordovician Cap Enragé Formation, Québec. Note excellent graded bedding but absence of interbedded mudstones. Tape 30 cm long.

THE FAMILY OF TURBIDITE FACIES

Descriptively, the whole family of deep water clastic rocks can be subdivided into five main facies associations, 1) classical turbidites, 2) massive sandstones, 3) pebbly sandstones, 4) conglomerates, and 5) pebbly mudstones, debris flows, slumps and slides. These associations (Walker, 1978) represent a simplification of the scheme suggested by Mutti and Ricci Lucchi (1972); this latter scheme has been widely used but can now be improved in some ways. I use the term *facies associations* because many of them can be divided into individual facies.

Classical turbidites

This facies association is characterized by a monotonous alternation of sharp-based sandstones and interbedded mudstones (Fig. 4). There is no evidence of erosion of the seafloor on a scale greater than a few tens of centimetres, and almost all the sandstones can be described using the Bouma sequence (Fig. 3). The term *classical* implies that these beds would quickly be identified as typical turbidites by most people today. This association contains two main facies; thin-bedded and thick-bedded turbidites. These terms are not precisely defined, but thin bedded is commonly used for beds thinner than a few tens of centimetres, and thick bedded for beds over one metre. There is a complete spectrum of thicknesses, and any subdivision is arbitrary.

The thin-bedded turbidites can be separated into two distinct types. The first is characterized by one row of current ripples, rare convolute lamination and rare ripped-up mudstone clasts (the features described do not necessarily occur in every bed, but characterize the facies as a whole). The second is characterized by climbing ripples, abundant convolution, and many ripped-up mud clasts (Fig. 5). This type has been termed CCC *turbidites*, for Clasts, Convolution and Climbing ripples (Walker, 1985). Both the climbing ripples and the convolution suggest high rates of deposition from suspension, and the clasts suggest erosive turbidity currents. This combination of features in relatively thin beds could be explained by deposition high on channel margins or on levees. By contrast, the single row of ripples indicates a turbidity current that has almost run out of suspended sand. The scarcity of convolution suggests slow deposition from suspension and the absence of ripped-up clasts indicates turbidity currents that are flowing too slowly to achieve much erosion of the bed. In thin-bedded turbidites, this combination of features implies a distal, basin floor environment of deposition.

Massive sandstones

There is a gradation in facies from thick-bedded classical turbidites into

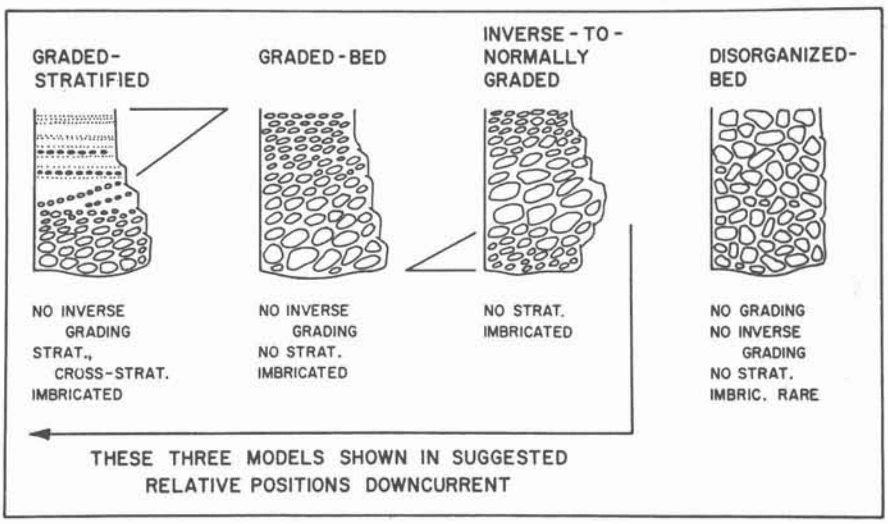

Figure 9 Four models for resedimented conglomerates, shown in their inferred downcurrent relative positions. From Walker (1975a).

massive sandstones. In massive sandstones (Fig. 6), there is much more evidence of erosion of the substrate; beds are commonly associated with channels many metres deep. The deposits of successive flows also join together (amalgamation) to make composite beds. Thus the monotonous aspect of sandstone-shale interbedding, characteristic of classical turbidites, is also lost. Individual massive sandstones range in thickness from about 50 cm to many metres, and normally the only Bouma division present is A. Graded bedding is commonly subtle or absent. The most common sedimentary structures found in massive sandstones are *dish* (Fig. 7) and *pillar structures*, which indicate abundant fluid escape during deposition (Lowe, 1975).

Pebbly sandstones

Beds in this facies association tend to be well graded (Fig. 8). Internal stratification is fairly abundant, and consists of a rather coarse, crude horizontal stratification, or (much less commonly) a well-developed trough or planar-tabular cross bedding. Imbrication of individual pebbles is common. No "Bouma-like" model has been proposed for the pebbly sandstone facies association, although Hein (1982) has distinguished different pebbly sandstone facies in the Cambro-Ordovician Cap Enragé Formation (Quebec) and interpreted their mechanisms of deposition. Pebbly sandstone beds are commonly channelled and laterally discontinuous, and interbedded shales are very uncommon.

Conglomerates

Conglomerates are volumetrically less abundant than other deep water facies, but make up an important part of the deep sea sedimentary record. They have been subdivided into four facies (Walker, 1975a), but because of the small data base, the models lack the authority of the Bouma sequence. In Figure 9, it can be seen that the descriptors include the type of graded bedding (normal or inverse), the type of stratification, and the fabric (Fig. 10). In different combinations, the descriptors allow the definition of the four facies shown in Figure 9. One of the most important features is the imbrication, which is typified by clasts whose long axes lie parallel to flow and dip upstream. The significance of this fabric (that the clasts have *not* rolled on the bed) has been discussed in detail by Walker (1975a).

In the absence of experimental work, interpretations of conglomeratic facies are rather speculative, as are the proposed relationships of the four facies to each other in the downstream direction (Fig. 9).

Figure 10 Inverse to normal grading in conglomerates of the Cretaceous La Jolla Formation, Tourmaline State Surfing Beach, near San Diego, California. Note also the well-developed imbrication, with clasts dipping upstream (to the right).

Pebbly mudstones, debris flows, slumps and slides

Pebbly mudstones (Crowell, 1957) consist of pebbles and distorted clasts of sandstone and mudstone, dispersed in a silty mudstone matrix (Fig. 11). One origin for such a texture is the rapid deposition of sand and gravel on top of very watery, uncompacted mudstones — the gravel load causes dewatering and mixing of gravel and mud. Alternatively, some pebbly mudstones may be the deposits of debris flows. These are mud-rich flows in which the mud-water mixture has matrix strength. This strength supports the coarser clasts during their transport in a semirigid

Figure 11 Pebbly mudstone in the Upper Cretaceous Pigeon Point Formation at Pigeon Point, California. Note pebbles, boulders, and rolled up sandstone clasts irregularly distributed within mudstone matrix.

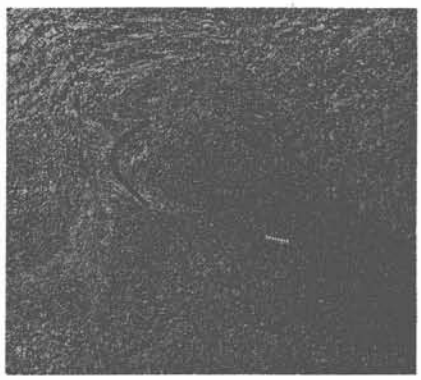

Figure 12 Soft sediment folds within Eocene slope mudstones of the Cozy Dell Formation. Highway 33 north of Wheeler Gorge, California.

plug of material. The resulting deposit commonly has large blocks projecting up above the top of the bed, or even resting almost entirely on top of the bed. The deposits show no internal evidence of slumping.

The terms slump and slide are used to describe deformed groups of beds, with slide implying a little less internal deformation. Slumps can range from coherently deformed beds (where many if not most beds can be traced part way through the slump) to totally disrupted strata. Thicknesses range from a few metres (only a few beds deformed) to over 100 m, and the material deformed can range from almost all shale to thick classical turbidites interbedded with mudstones. The following distinct slump facies may have environmental significance, but more work on slumped facies will probably show that this list is incomplete.

1) *Slumped shales and mudstones.* This facies contains relatively few sandstone beds, and is characterized by many subtle soft-sediment folds on a variety of scales (Fig. 12). The dominance of mudstone, along with abundant slumping, suggests deposition on the slope into the basin. A good example has been given by Clari and Ghibaudo (1979).

2) *Slumped thin-bedded turbidites.* These slumps occur on a variety of scales, and can involve a few beds (Fig. 13) or great thicknesses of beds (Fig. 14; Gregory, 1969). Thin-bedded turbidites originally deposited on the basin floor are less likely to slump than those deposited on channel margins or levees. On modern fans (discussed below), levee failure leads to slump/debris flow deposits tens of metres

Figure 13 Long arrow shows thinning-upward succession of beds in Cretaceous rocks of Wheeler Gorge, California. Smaller arrows show way up of a single bed within a complex, soft-sediment fold (nose at top of photo).

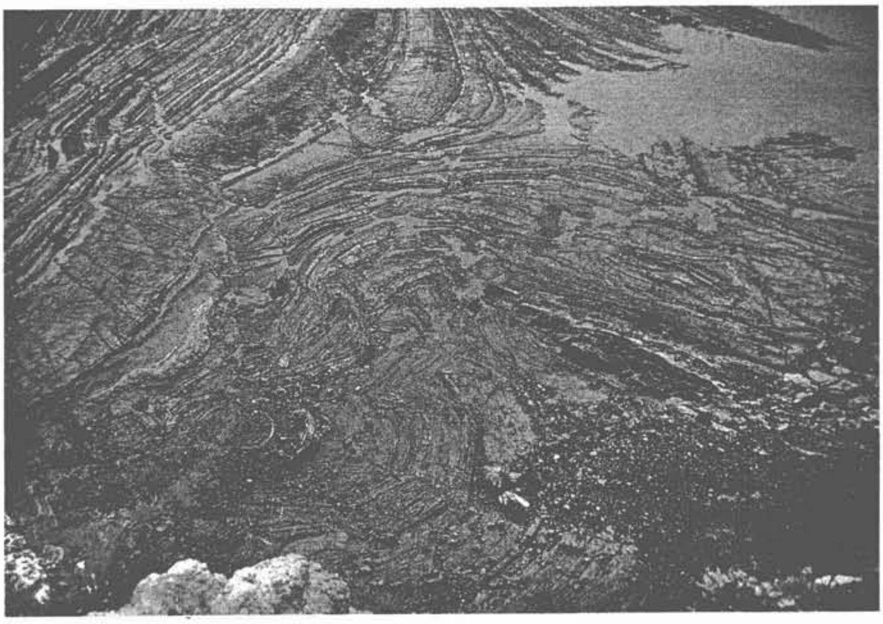

Figure 14 Large slump involving thin-bedded turbidites of the Lower Miocene Waitemata Group. Exposure is on the wave-cut platform east of Army Bay, Whangaparaoa Peninsula, near Auckland, New Zealand. Width of wave cut platform in centre of photo is about 60 m.

Figure 15 Soft sediment slump in the Upper Cretaceous Great Valley Sequence at Lake Berryessa, California. The matrix is a silty mudstone, which contains a large variety of pebbles and cobbles. Note particularly the stratified blocks (SB) of interbedded sandstone and mudstone; they cannot have been transported more than a few metres, or they would have peeled apart. Such blocks probably collapsed into a channel from an immediately adjacent channel wall. Double black lines indicate regional bedding; their convergence is due to perspective because the camera is pointed up a steep cliff. Stratigraphic top is to the left, and the slumped bed is about 7 m thick.

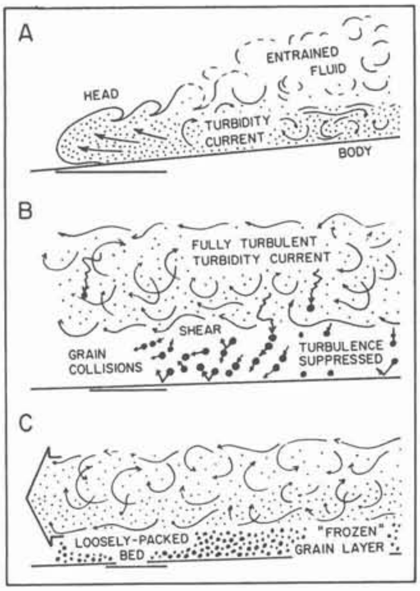

Figure 16 A) a fully turbulent turbidity current maintains all of its sediment load in suspension by fluid turbulence. B) as it slows down, the coarser grains settle toward the base of the flow (large black dots with wiggly arrows). They continue to be transported as a layer of colliding grains, the friction being overcome by the shear stress applied by the main body of the turbidity current. C) when the shear stress can no longer overcome the friction (too many grains, or the flow has slowed down too much, or both), the layer of colliding grains stops moving ("freezes"), and the initial loosely packed bed compacts down to form a sandy or pebbly deposit without sedimentary structures.

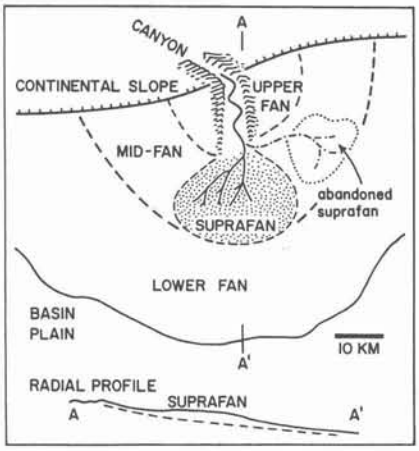

Figure 17 Model of a submarine fan, after Normark (1978). Fan is divided into upper, mid and lower fan; the mid-fan grows by the switching in position of suprafan lobes. These have a distinct depositional topography (see radial profile), and their margins are sedimentologically determined rather than being constrained by topographic elements within the basin. The upper fan is characterized by one leveed channel with a meandering thalweg, and the lower fan is topographically featureless.

thick. It is therefore tempting to interpret thick slumped masses of thin-bedded turbidites (Fig. 14) as originally having been deposited on levees.

3) *Slumps with angular stratified blocks.* Angular stratified blocks (Fig. 15) suggest that the slumped mass has not moved very far, because the cohesionless sandy layers in the blocks have not broken apart. Deposits containing such blocks may represent collapse of a channel wall rather than erosion of a channel floor (Walker, 1985).

TURBIDITY CURRENT DEPOSITION

The facies described above, with the exception of boulder conglomerates and the various debris flows and slumps, can be interpreted in terms of the way in which sediment is deposited from the turbidity current (Lowe, 1982; Middleton and Southard, 1984). In the current, all the sand and most of the granules and pebbles, are supported above the bed by fluid turbulence (Fig. 16A). As the flow decelerates, the upward components of turbulence become too weak to support the coarser grains, which gradually settle toward the base of the flow. Here, they may collide with each other, and with the bed, in a dispersed grain layer (Fig. 16B). The dispersion is maintained by the shear stress applied by the main body of the turbidity current. At some point, the applied shear stress will become insufficient to overcome the friction within the dispersed grain layer. The layer will then rapidly "freeze" (stop moving), forming Bouma's division A or a thick massive sandstone (Fig. 16C). Graded bedding is present in some layers. In thicker beds (commonly more than one metre), escape of fluid during initial compaction of the dispersed grains forms vertical fluid escape pillars and dish structures

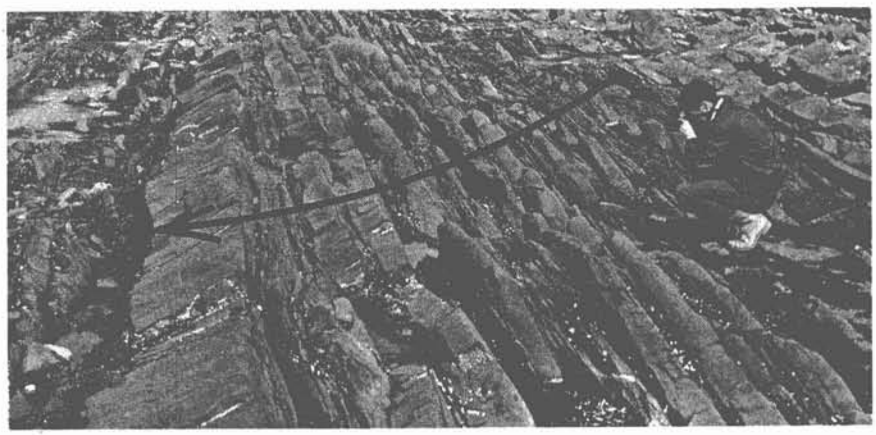

Figure 18 Classical turbidites in the Ordovician Cloridorme Formation at Grande Vallée, Québec. Beds are slightly overturned with stratigraphic top to left. Arrow marks a thickening-upward succession.

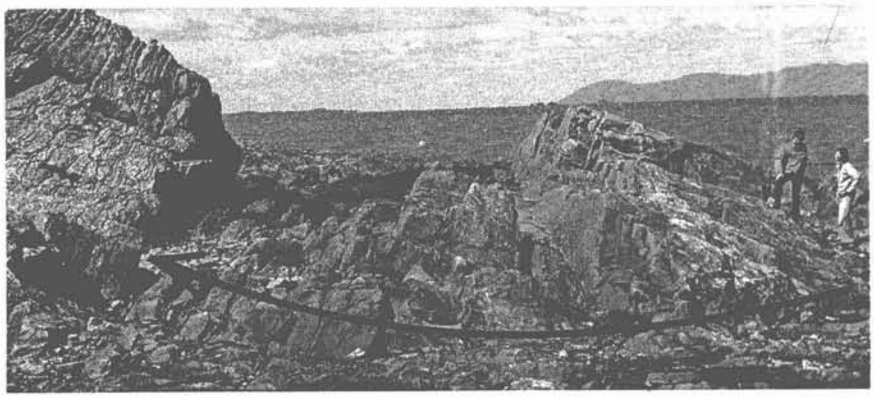

Figure 19 Thinning-upward succession beginning with massive sandstones and passing upward (arrow) into classical turbidites. Cambrian St. Roch Formation at St.-Jean-Port-Joli, Québec.

(Fig. 7).

In classical turbidites, the continued deceleration of the flow forms parallel lamination (Bouma's division B), either by deposition of new sand from the suspension, or by reworking the top of division A. Similarly, ripple cross lamination (division C) forms by the reworking of division B, or by deposition of new sand from suspension; in the latter case, the ripples commonly climb. Rapid deposition from suspension in division C traps fluid between the grains, and climbing ripples can easily be deformed into convolute lamination. This is more common on channel margins and levees (CCC turbidites; Fig. 5), where the turbidity current still has an abundant suspended load, than on the deep basin floor.

FACIES SUCCESSIONS IN TURBIDITES

One of the first steps in linking studies on the scale of facies to studies on the scale of submarine fans is to identify distinctive successions of facies. It has been suggested that some successions can be interpreted in terms of deposition in particular topographic parts of fans.

Fans are largely built up of the deposits of turbidity currents. They commonly occur at the end of a submarine canyon or feeder channel (Fig. 17), and consist of channelized and unchannellized deposits. The channels commonly have levees, and together build up channel-levee complexes. Levees tend to decrease in height downfan, and the channels become shallower. As a result, the turbidity currents spread out to form topographically distinct depositional lobes (suprafan in Fig. 17), or more extensive sheet-like deposits.

Successions of turbidite facies were first compared with these elements of fan topography by Mutti and Ricci Lucchi (1972). They described two types of succession, those in which individual beds became thicker upsection *(thickening-upward)* or thinner

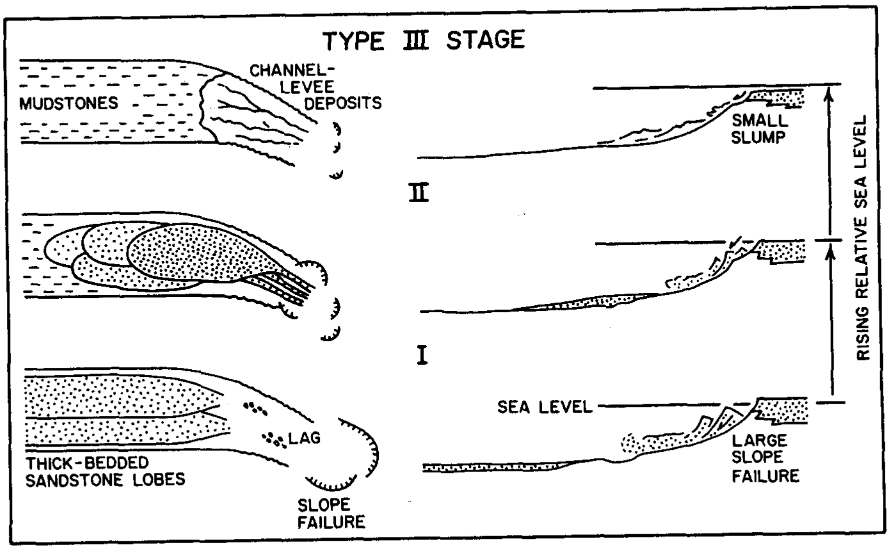

Figure 21 **(Left)** three types of submarine fans related (right) to three proposed stages of fan evolution, after Mutti (1985). The detached lobes without channel deposits (Type I fan) are believed to result from large slope failures and the generation of large, sandy turbidity currents. Type II resembles the channel and lobe model of Normark (1978; Fig. 17), and type III consists of muddy channel-levee deposits believed to form from small, muddy turbidity currents that develop during a rising stage of sea level. The fan models, and their relationship to relative sea level, are controversial (see text).

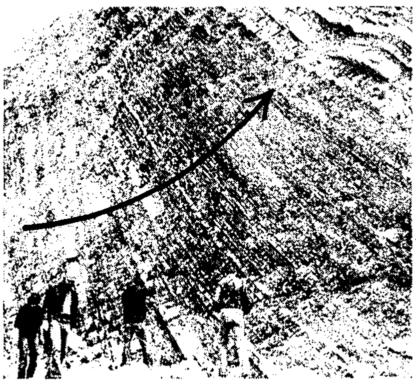

Figure 20 Thinning-upward succession of classical turbidites in Paleocene rocks at Shelter Cove, Point San Pedro, California. Note the absence of massive sandstones, and the monotonous interbedding of classical turbidites with no indication of topography on the seafloor. The sequence may be due to lateral lobe shifting, or to distal overbank deposition in a situation where the channel is progressively migrating away from this area.

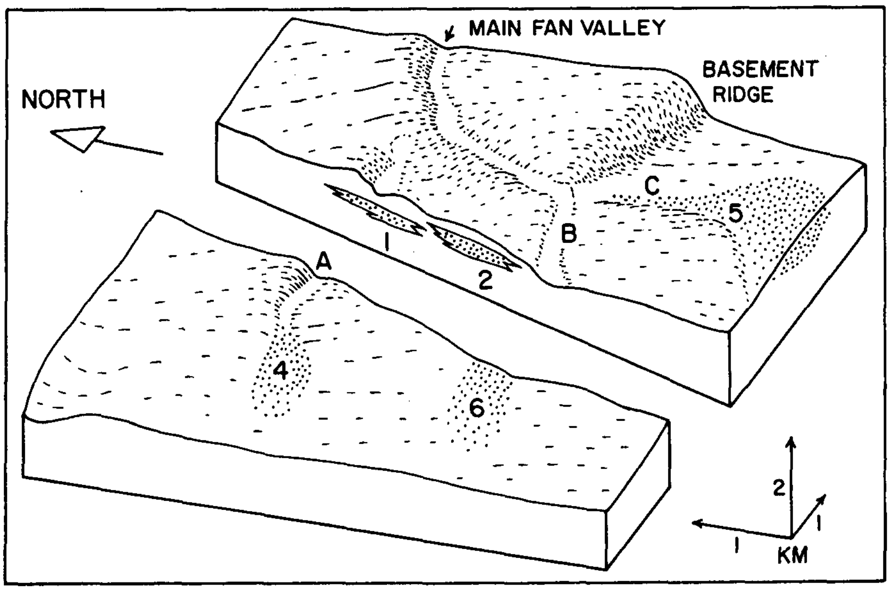

Figure 22 Block diagram of Navy Fan, California, simplified from Normark *et al.* (1979). Fan lobes 1, 2 and 3 (not shown) occur in the subsurface, and lobes 4, 5 and 6 have slight topographic expression on the present fan surface. Channels A and C are no longer connected to the main fan valley (channel B).

upsection *(thinning-upward)*. The thickening-upward successions (Fig. 18) were compared with prograding delta lobes, and were therefore interpreted as having been formed during the progradation of a submarine fan lobe (Fig. 17). The thinning-upward successions (Fig. 19) were compared with channel fills on the delta plain, and were interpreted as the fills of submarine channels (Fig. 17). These two types of succession definitely exist, but their recognition in the field is sometimes subjective — many individual "successions" exist only in the eye of the beholder. Interpretations are difficult in the absence of abundant core information from modern fans. For thinning-upward successions, there are at least three ways in which the succession can be controlled *autocyclically* (i.e., by sedimentary processes operating within the fan, rather than by external [*allocyclic*] processes such as tectonics or sea level fluctuation). First, successions about 10-40 m thick that begin with thick massive sandstones, and pass upward into classical turbidites, can be recognized in many places and probably indicate channel filling (Fig. 19). Second, thick successions that show thinning upward without the presence of massive sandstones (Fig. 20) suggest the possibility of gradual lobe shifting, with lobe margin replacing lobe centre depositional environments. Third, other thinning-upward sequences, with CCC turbidites and small soft-sediment slumps (Fig. 13), represent successive deposition of thinner beds on a levee rather than channel filling.

The interpretation of facies successions has presented many problems. Mutti (1985) has recently rejected his original autocyclic ideas concerning channel filling and lobe progradation in favour of an allocyclic origin for the successions related to the sizes of flows generated by slumping at the shelf edge (Fig. 21). He has sug-

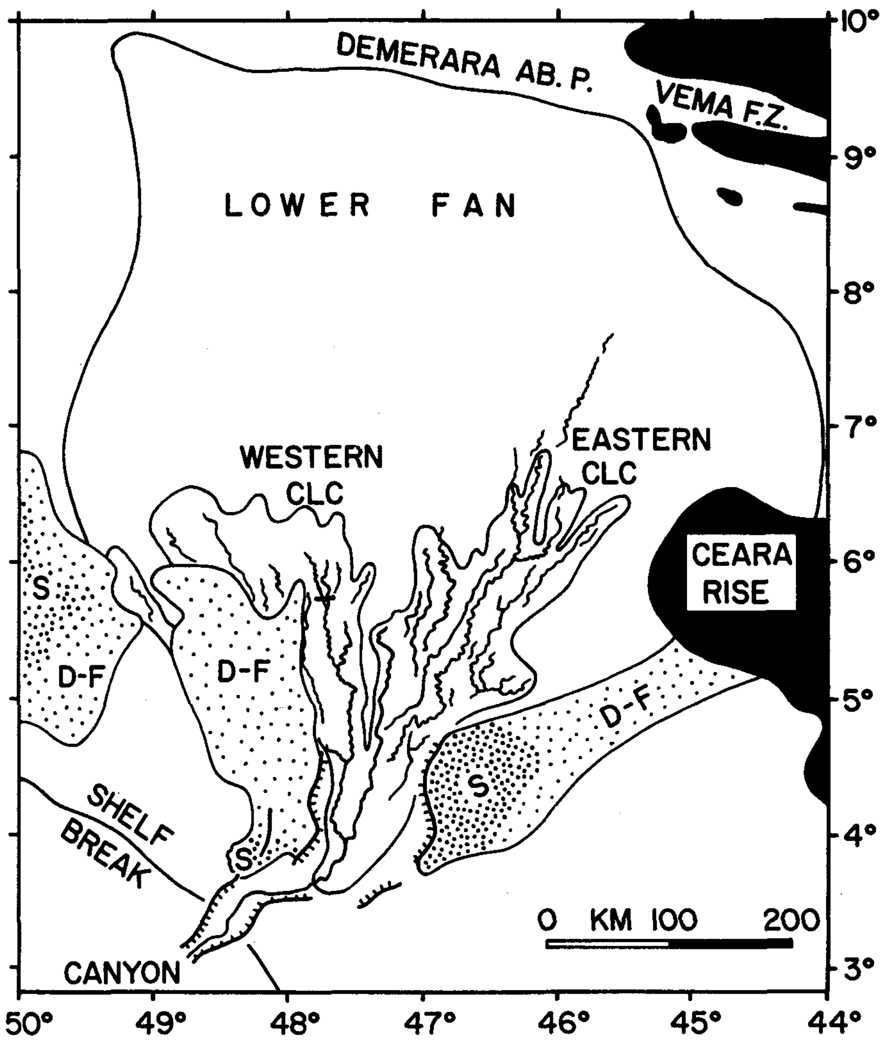

Figure 23 Main components of the Amazon submarine fan in the south Atlantic. S D-F indicates slump/debris flow complexes, and CLC indicates channel-levee complexes. Sinuous lines show positions of the main channels on the fan surface. Fan passes seaward into the Demerara Abyssal Plain, and abuts against the irregular topography of the mid-Atlantic Ridge (black). Short, heavy line toward northern end of the Western channel-levee complex indicates the location of Figure 29.

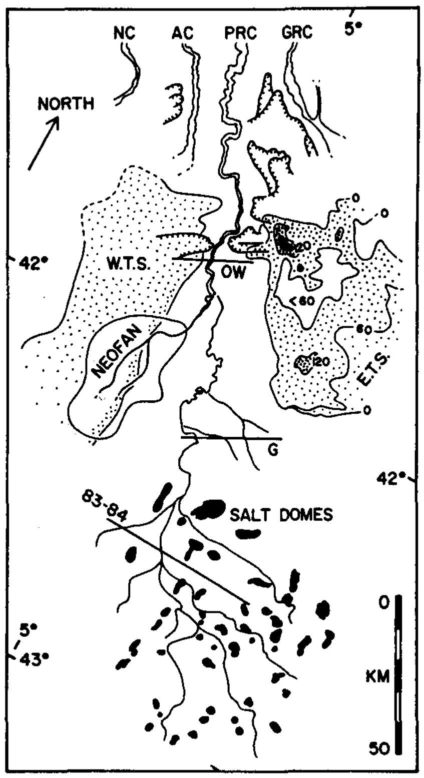

Figure 24 Map of the Rhone Fan in the Mediterranean Sea. Feeder canyons are the Nimes (NC), Arles (AC), Petit Rhone (PRC) and Grande Rhone Canyons (GRC). There are two seismically transparent layers close to the fan surface, the Eastern and Western Transparent Series (ETS, WTS). The ETS is contoured in milliseconds (ms of two way travel time), and the black area is thicker than 160 ms. One ms roughly equals a thickness of one metre if the velocity of sound is taken at 2 km/s. OW, G and 83-84 locate the cross sections shown in Figure 30. The most recent event on the fan surface was the construction of a neofan at the end of the sinuous Petit Rhone Canyon. The black areas on the lower fan are salt domes.

gested (Mutti, 1985, p. 73) that flow size is a function of the position of relative sea level (Fig. 21), with large slumps forming sand-rich turbidity currents at times of relative lowstand, and small slumps forming mud-rich turbidity currents during rising stage or at highstand. He therefore suggests (p. 88) that "small-scale fluctuations of sea level...probably account for a large part of the medium- to small-scale cyclicity observed in ancient turbidite lobe and channel-fill deposits". This hypothesis depends on a single generating mechanism for turbidity currents (shelf edge slumping), and a definite relationship between slump size, grain size of sediment within the slump, and the position of relative sea level; Fig. 21). By completely rejecting earlier autocyclic interpretations, Mutti may have thrown the baby out with the bathwater.

MODERN SUBMARINE FANS AND FAN MODELS: 1970-1983

The facies and facies successions described above form the main interpretive link between the geological record and modern submarine fans. The study of modern fans blossomed in the 1970s, following the first attempt at synthesis — "Growth patterns of deep-sea fans" (Normark, 1970). With added information, Normark (1978) improved the model (Fig. 17), suggesting that fans consisted of three parts, 1) a single leveed valley on the upper fan, 2) a mid fan built up of suprafan depositional lobes at the ends of channels - these lobes switched in position periodically, and 3) a topographically smooth lower fan without channels (Fig. 17). This three part *channel-feeding-lobe* model is largely based upon Navy Fan (Fig. 22), where there is a wealth of high-resolution depth sounding and seismic profiling, and side-scan sonographs. However, the Navy Fan lobes are only 2-3 km in length, and bathymetric maps (Normark *et al.*, 1979, p. 754) indicate that their topographic relief is very small, and always much less than 5 m. Although there are more than 100 cores from Navy Fan, few are longer than 6 m, and sand recovery is not always good. It is not known whether the Navy depositional lobes contain sandier- and thickening-upward successions, nor if the lobes have prograded in the manner of the models of Mutti and Ricci Lucchi (1972). Despite the appealing simplicity of channel-feeding-lobe models of the type pictured by Mutti and Ricci Lucchi (1972), Normark (1978; Fig. 17), Normark *et al.* (1979; Fig. 22), Walker (1978) and Mutti (1985; Fig. 21), the data base for such models is poor.

The fan models that flourished in the 1970-1983 period were purely sedimentological (autocyclic). They did not incorporate the effects of relative sea level fluctuation, changes in the grain size of the sediment supplied, and basinal tectonics. The effect of grain size on fan development was first hypothesized by Mutti (1979), who was also among the first workers to incorporate the effects of sea level fluctuation into fan models (Mutti, 1985). Again based on theory, he introduced three types of submarine fans (I, II and III; Fig. 21), and implied that these types corresponded with stages I, II and III in the evolution of a single turbidite system during rising relative sea level. Mutti's Type II is close to the channel-feeding-lobe model of Normark (1978). His type I implies that large sandy flows can move a long way from the base of slope, resulting in a deposit that is detached from its feeder channel(s). His type III implies that muddy channel-levee complexes can form during rising sea level without time-equivalent depositional lobes. These theoretical models are not well supported by data from modern fans.

SEISMIC STUDIES OF MODERN FANS (1983-PRESENT): INTRODUCTION

The year 1983 represents a major turning point in the study of modern fans, with the publication of sidescan sonographs of the modern Amazon submarine fan (Damuth *et al.*, 1983a, b). They revealed a pattern of continuous channels a few tens of metres deep and up to about 1 km wide. However, the really surprising feature was the extreme sinuosity of the channels, with bifurcations, avulsions, cutoffs and oxbows. The channels marked the

Table1 *Dimensions of modern submarine fans.*

	Amazon	Rhone	Indus	Laurentian	Mississippi
Length km	700+	440	1500	700+	540
Width km	250-700	210	960	450	570
Area km^2	3.3×10^5	7×10^4	1.1×10^6	3×10^5	3×10^5
Thickness km	4.2	1.2	3 +	2	4
Volume km^3	7×10^5	1.2×10^4	1×10^6	1×10^5?	2.9×10^5

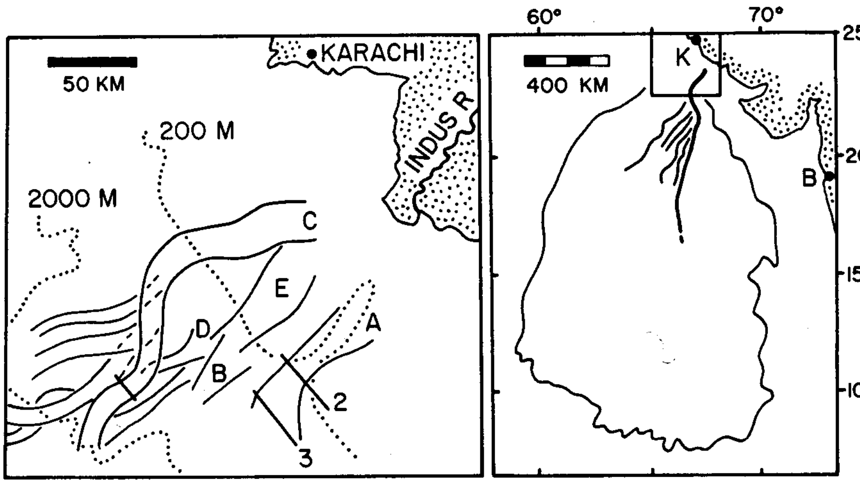

Figure 25 Location (right) of the Indus Fan off the coast of Pakistan and India; K and B indicate Karachi and Bombay, respectively; after Kolla and Coumes (1985). Boxed area (right; top centre) is enlarged to left, showing shelf edge (200 m) and continental rise (2000 m). After McHargue and Webb (1986). Channels are lettered in sequence from the modern channel (A) backward in time. Short heavy lines A2, A3 and the line crossing channel C (C7) refer to the cross sections in Figure 28.

crests of broad (25-40 km) channel-levee complexes up to 1000 m thick that could be traced from the end of the Amazon Canyon for over 300 km to the lower fan (Fig. 23). None of the channels had a depositional lobe at the end. It was difficult in 1983 (and it remains difficult today) to envisage how huge rapid turbidity currents could follow such a tight, sinuous channel. It has recently been suggested that the sinuous channels were occupied by more continuous density underflows (i.e., relatively slow but continuous muddy currents; Damuth *et al.*, 1988, p. 904-909).

There are now excellent studies of many submarine fans (data given in Table 1), particularly the Amazon (Fig. 23), Rhone (Fig. 24), Indus (Fig. 25), Laurentian (Fig. 2) and Mississippi (Fig. 26). These fans have a data base of 1) multichannel seismic lines that show the deep internal structure of the fans, 2) 3.5 kHz surveys that give good detail near the surface but only penetrate a few tens of metres into the fan and 3) sidescan sonar images of fan topography. Distinct seismic facies can be recognized, and can be used to define depositional environments and infer depositional processes on these fans.

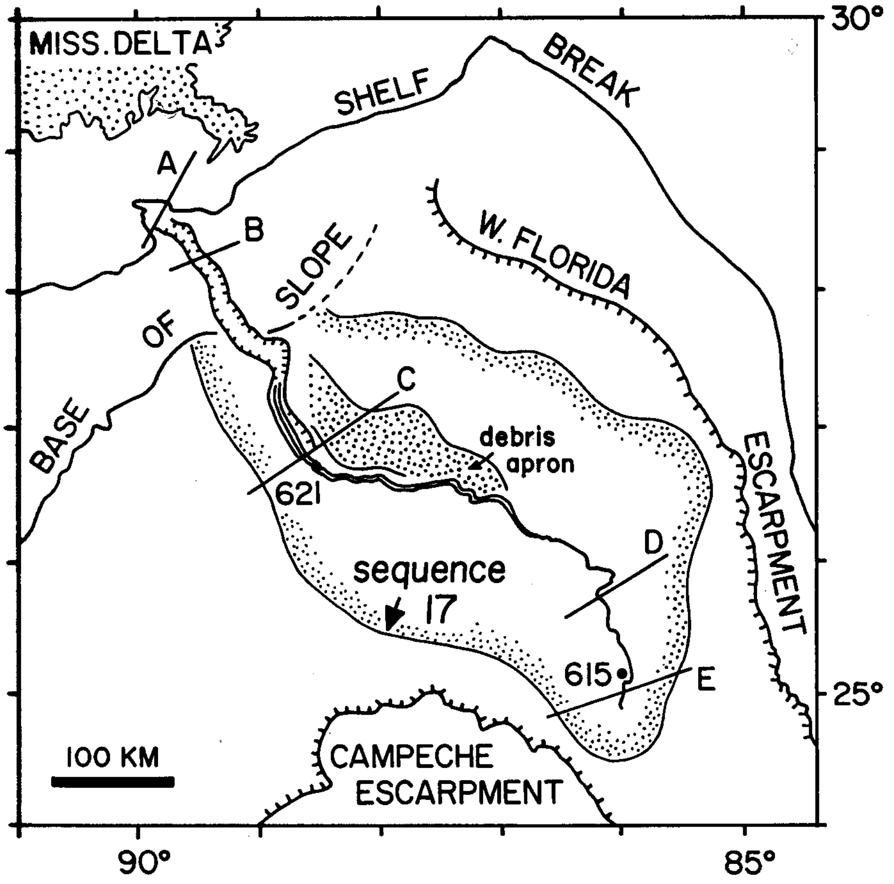

Figure 26 (left) Location of the youngest Mississippi Fan "lobe" (stippled edge), or fan sequence 17. From Weimer (1989). 621 and 615 indicate the locations of cores, and cross sections A through E are shown in Figure 31.

Seismic descriptors

The overall appearance of seismic reflectors can be used to define *seismic*

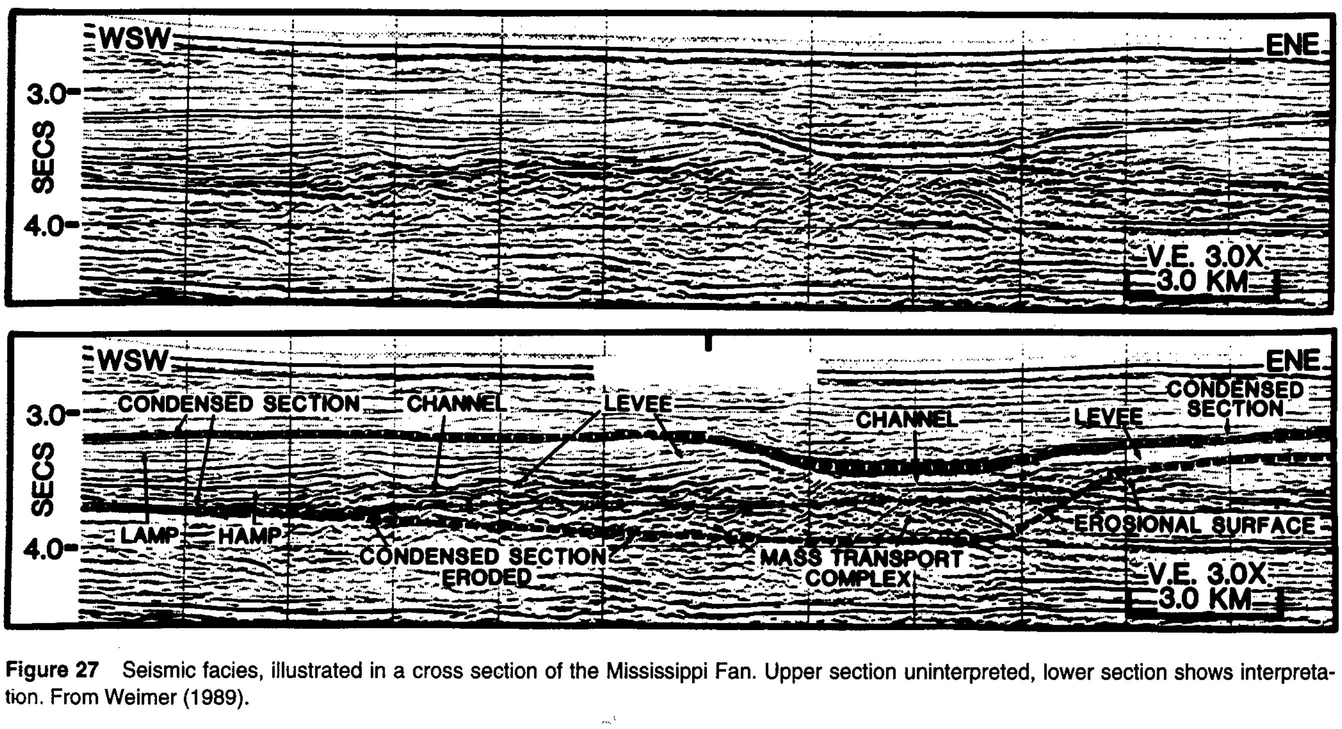

Figure 27 Seismic facies, illustrated in a cross section of the Mississippi Fan. Upper section uninterpreted, lower section shows interpretation. From Weimer (1989).

facies on various scales, in the same way as sedimentary structures and lithologies can be used to define geological facies. The most important descriptive parameters are 1) the amplitude of the seismic signal, 2) the continuity of the seismic reflectors, 3) the external form (or three dimensional geometry) of seismic packages, and 4) the configuration of reflectors within 3-D packages (Table 2). In Figure 27, high-amplitude (HAMP) and low-amplitude (LAMP) signals are illustrated. Continuous reflectors are shown (e.g., where they are paired and interpreted as a condensed section), and can be contrasted with the much more discontinuous reflectors within the mass transport complex. The external forms include sheets (above the upper condensed section), wedges (levees), lenses (channel) and mounds (mass transport complex). Internal configurations include parallel, subparallel and hummocky or mounded shapes.

In the following text, the terms HAD (high amplitude discontinuous), LAD, HAC and LAC (low amplitude continuous) will be used. If the reflectors are very discontinuous and of extremely low amplitude (the end member LAD facies), there is almost no acoustic response at all; such facies will be termed *acoustically transparent.*

LARGE-SCALE SEISMIC FACIES ON MODERN FANS

The characteristics of the seismic signals (Table 2), and their mutual relationships, allow the definition of four large-scale facies associations, 1) channel-levee systems, 2) continuous unchannelized sheet-like deposits (overbank or basin plain), 3) mass transport complexes, and 4) slumps and debris flows associated with levee failure.

Channel-levee systems

Channel deposits are characterized by HAD reflectors that probably indicate the interbedding of coarse sands and gravels with muddier horizons. Channel deposits may also be acoustically transparent, suggesting a single lithology without distinct interbeds. This could be sand (as in Figure 6), or it could be mud filling the channel after abandonment (central portion of channel fill in Figure 28-C7).

The coarser facies may be restricted to thalweg channels, and the acoustically contrasting beds may be finer grained, accumulating at times when the channel is disused. In many channel-levee systems, the HAD reflectors stack vertically, indicating channel aggradation (Figs. 29, 30, 31). In other examples (Indus, Fig. 28) there is abundant evidence of lateral migration of the thalweg during overall fan aggradation; up to 15 km in Figure 28-A3. In six of the seventeen channel-levee systems in the Mississippi Fan (Figs. 32, 33), there is no evidence of lateral channel migration during aggradation. In the other eleven, the channels migrate laterally from 1 to 12 km during aggradation (Weimer, 1989). Clearly, the resulting channel sandbody geometry will be greatly affected by the degree of vertical aggradation and lateral migration.

In the Indus, the HAD reflectors suggest aggraded thalweg deposits between 130 and 580 m thick (Fig. 28). The spectacularly sinuous channels on the surface of the Amazon Fan are 30-80 m deep and 400-3000 m wide in the mid-fan area; their aggraded thickness of 70-350 m is equal to the thickness of the channel-levee system (Fig. 29). In the Mississippi, the stacked and aggraded channel deposits at Deep Sea Drilling Project (DSDP) site 621 (Fig. 34) are about 350 m thick, of which the lower 200 m is dominantly sandy (with some gravel). Stacks of massive sandstones occur in the geological record, and about 180 m of amalgamated classical turbidites and massive sandstones are shown in Figure 6.

The levees are characterized by LAD to LAC divergent reflectors within wedge-shaped external forms (Figs. 28-31). There is a suggestion that levee reflectors have slightly higher amplitudes, and become a little more continuous away from the levee crests. This may indicate slower rates of deposition and more interbedded hemipelagic beds away from the crests (Fig. 29). Near the crests, the levees can be as steep as 3.5°, and are prone to slumping. The thickness of channel-levee systems (and hence thickness of aggraded channel deposits) on various fans varies from about 150-500 m (Table 3), and widths vary from about 30-250 km. Channel depths and thicknesses of channel-levee systems both decrease downfan, and the channel-levee systems grade into more sheet-like deposits.

Table 2 *Nature of seismic facies in various environments.*

	Amplitude	Continuity	External Form	Internal Configuration	Lateral Distribution
Channels	High	Fair/Low	Lens	Sub-parallel	Narrow, Linear
Levees	Low/Fair	Mod.	Wedge	Sub-parallel, diverging toward channel	Parallel to channel
Overbank	Low/Fair	Fair	Sheet	Sub-parallel	Widespread away from channel
Un-chann. Basin Floor	Low/Mod.	Fair	Sheet	Sub-parallel	Widesread
Mass Transport Complex	Low	Poor	Mounds	Mounded, hummocky	Underlies and is subparallel to channel
Levee Failure	Low/Fair	Fair/Poor	Wedge	Mounded, hummocky	Limited

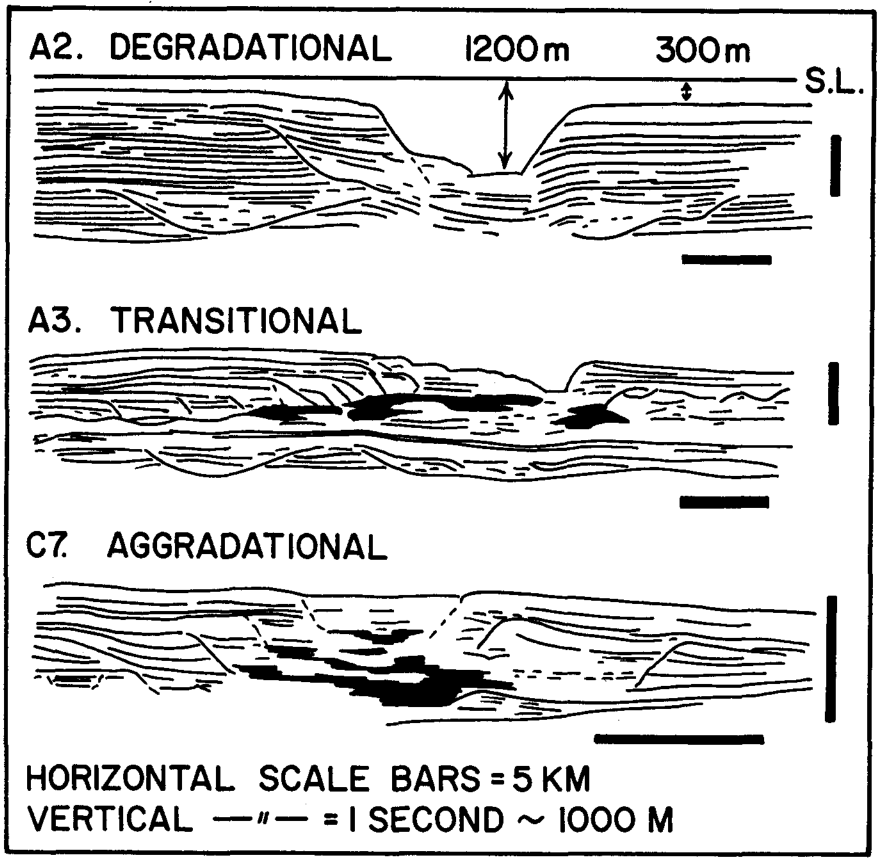

Figure 28 Seismic cross sections A2, A3 and C7, located in Figure 25. After McHargue and Webb (1986). Note that the sections are presented at different vertical and horizontal scales. Degradational channels have erosional bases and no levee deposits. Transitional channels also have erosional bases, but with the development of sandy thalweg deposits (black), the levees appear to grow. In A3, the thalweg shifts progressively to the right (southeast), and the levee builds laterally over the thalweg deposits. Aggradational channels have more conformable bases; as well as thalweg migration, C7 also shows some vertical stacking of channel-levee systems.

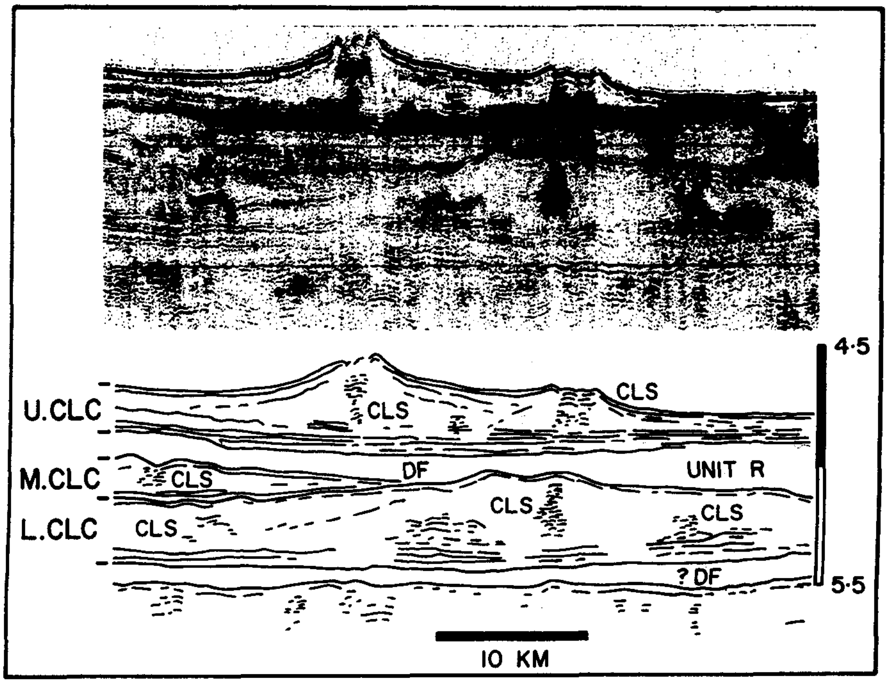

Figure 29 (left) East (left) to west high-resolution seismic-reflection profile across part of the western channel-levee complex of the Amazon Fan (located by short, heavy line in Figure 23). Interpretation (below) shows an upper channel-levee complex made up of individual channel-levee systems that shingle upon each other. DF indicates seismically transparent areas interpreted as debris flow deposits. Note the presence of continuous reflectors above unit R at the base of the upper channel-levee complex. Upper, middle and lower channel-levee complexes are shown, and the vertical scale is two-way travel time, in seconds. If the speed of sound in poorly consolidated sediments is taken as roughly 2 km/s, then 1 second of *two-way* travel time is equivalent to 2000 m of travel, or a sediment *thickness* of about 1000 m. Diagram simplified from Manley and Flood (1988).

Continuous sheet-like deposits

Sheet-like deposits typically occur in the lower fan, as seen in the Rhone (Fig. 30) and Mississippi Fans (Fig. 31). Sheet-like deposits also underlie the channel-levee systems in the Amazon Fan (Fig. 29). Reflectors tend to be LAC and HAC, and probably represent the deposits of widespread unchannelized turbidity currents. In the Mississippi, cores taken during Leg 96 of DSDP (Fig. 34) suggest that sand can bypass the mid-fan channels (Fig. 34 site 621, located in Fig. 26) and become concentrated in the lower fan (site 615). Here, individual sand and coarse silt beds are "from 10 cm to at least 12 m in thickness" (O'Connell *et al.*, 1985).

In the Amazon, the lower fan also contains highly reflective, conformable but discontinuous reflectors that reflect more sheet-like turbidite deposition than in the mid-fan channel-levee systems. Cores show medium- to fine-grained turbidite sands (much coarser than the turbidites in the mid-fan channel axes) in beds up to a few metres thick (Ciro *et al.*, 1988). The turbidites of the mid-fan channel axes and the lower fan "cannot be related in time and event to the thicker and coarser turbidites sampled on the lower fan and abyssal plain, which are certainly older" (Ciro *et al.*, 1988, p. 451). Thus these coarser lower fan sands have also bypassed the mid-fan area, as in the Mississippi.

Sheet-like reflectors also occur in levees (away from levee crests) and overbank areas. There is almost no core control of the nature of the geological facies present. The seafloor slopes are low (0.7° to 1.1° estimated from Figs. 29 and 30 respectively) and the lateral extent is great (tens of km), suggesting that the turbidites would be laterally extensive and unchannellized. Because they have been deposited from the portion of the turbidity current that spilled over the levee crest, the beds are probably relatively fine grained, with a low sand/shale ratio. These overbank classical turbidites might be distinguished from lower fan and basin plain turbidites by their thin bedding and low sand/shale ratios.

Mass transport complexes

This seismic facies has best been described from the Mississippi Fan (Weimer, 1989, 1990), where it is characterized by mounded external forms and hummocky to subparallel internal reflectors of low- to fair-amplitude and poor continuity (Fig. 27). The mass transport complexes erode up to 200 m into underlying sequences (Fig. 33), and average about 180 m (range 90-256 m) in thickness. The sedimentological aspect of the mass transport complex deposits is unknown; they are probably poorly sorted and poorly stratified debris flow deposits.

Slumps and debris flows associated with levee failure

Acoustically transparent deposits occur on the present-day surfaces of several fans, especially the Amazon (Fig. 23), Rhone (Fig. 24) and Mississippi. The slump/debris-flow deposits of the Amazon are 10-50 m thick, and have volumes of 300-1500 km^3. The flows head in scarps 25 to 250 m high, and have travelled for 200-300 km on slopes as low as 0.35 to 0.6°. In the few cores from this facies, the beds show "zones of disturbed, contorted bedding, colour changes and angular contacts" (Damuth and Embley, 1981). Similar transparent seismic facies occur on the Rhone Fan, as Eastern (E.T.S.) and Western (W.T.S.) Transparent Series (Fig. 24). The ETS is up to 160 m thick, and covers an area of about 2250 km^2. Droz and Bellaiche (1985, p. 467) state that it "clearly shows [derivation] from a slump originating in the north in the area of curvilinear escarpments on the continental slope". However, the thickest part of the slump (black area at eastern end of line OW in Fig. 24) is very close to slump scars in the back of the upper fan levee, suggesting some levee failure also.

The beds originally deposited on the backs of the levees were probably thin-bedded classical turbidites with a low sand/shale ratio. Slumping without too much lateral displacement and mixing of lithologies might lead to thick slump deposits of thin-bedded turbidites similar to those in Figure 14. With more displacement and mixing, these slumps might evolve into muddy debris flows which could continue for many tens of km across the fan surface (Figs. 23, 24).

FACIES RELATIONSHIPS AND FAN EVOLUTION

The facies relationships suggested here result from the comparison and contrast of the fans mentioned above.

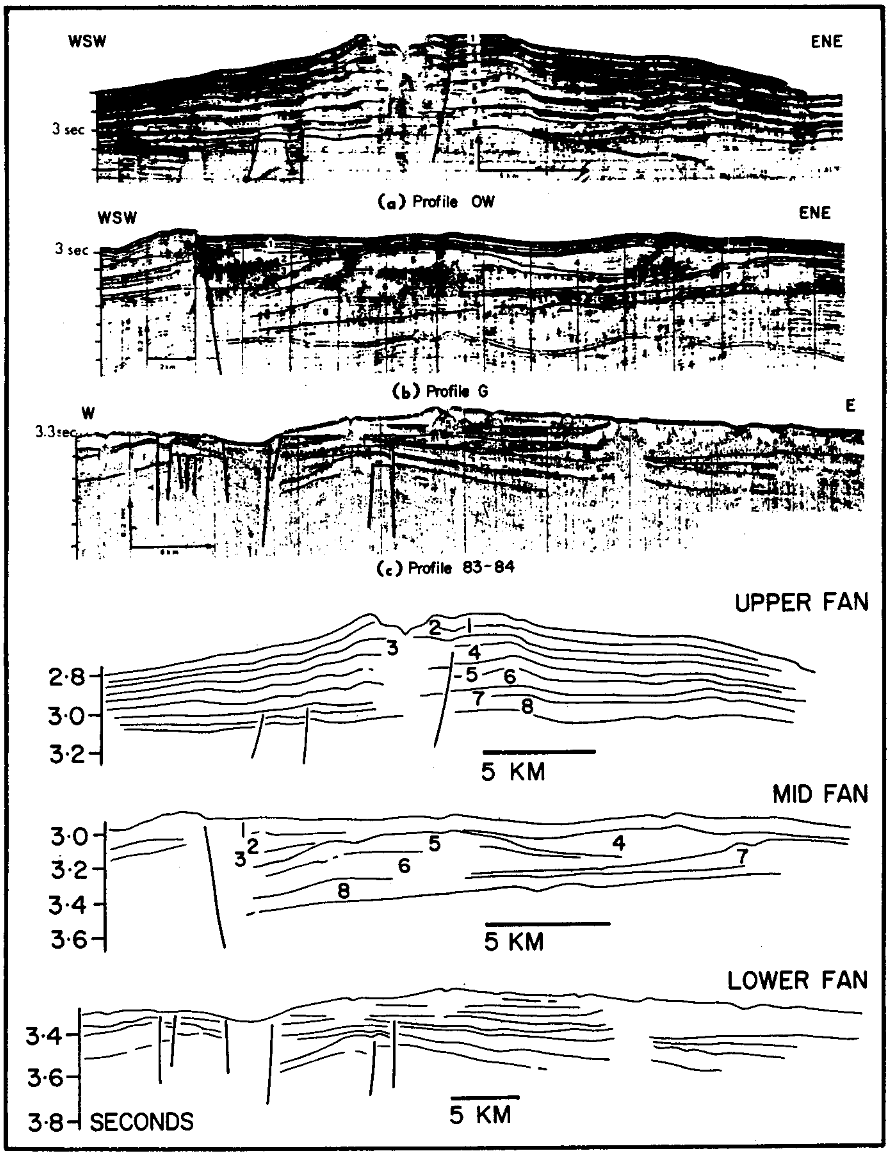

Figure 30 Seismic profiles OW, G and 83-84, located in Figure 24. From Droz and Bellaiche (1985). The numbered units (channel-levee systems) in the upper part of the diagram are sketched below for more clarity. Note the vertical stacking pattern on the upper fan, and the lateral shingling of the channel-levee systems on the mid fan. The channel-levee systems are more laterally extensive on the lower fan, but individual systems cannot be mapped because of interference by the salt domes.

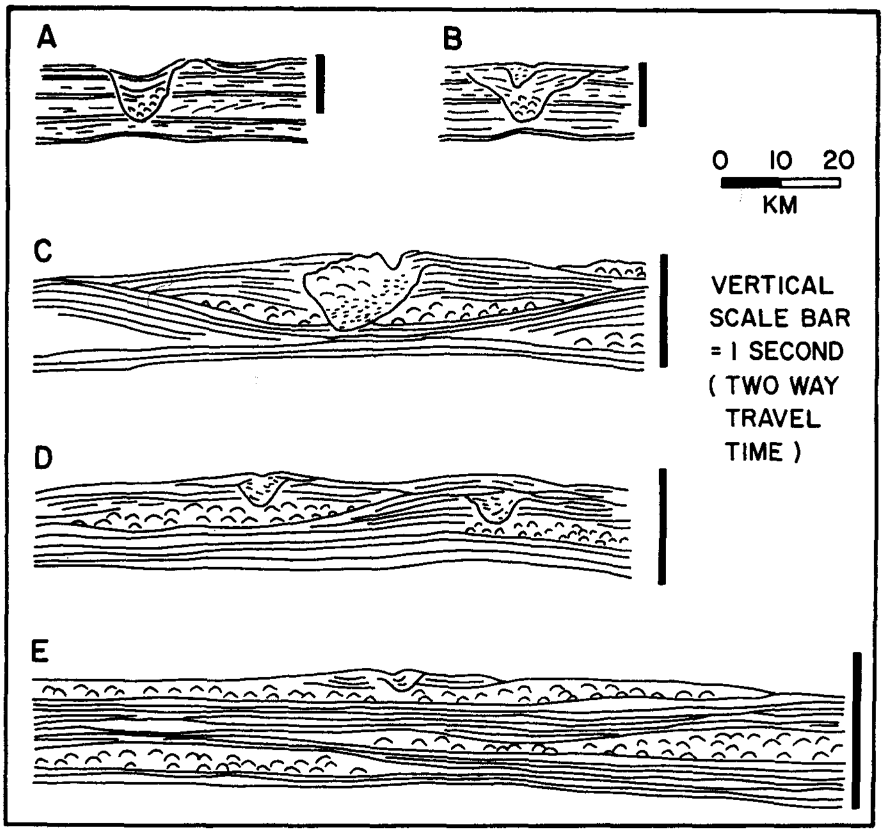

Figure 31 Cross sections A through E (see Fig. 26) of Mississippi Fan channel. Horizontal scale is the same for all sections, but vertical scale varies. Note tendency for lateral shingling of channel-levee systems (especially in C and D), and more sheet-like reflectors, with smaller channels, in the lower fan (E). Short dashes in channels indicate HAD reflectors, and "bumpy" symbol indicates hummocky reflectors and probable mass flow deposits. After Bouma and Coleman (1985).

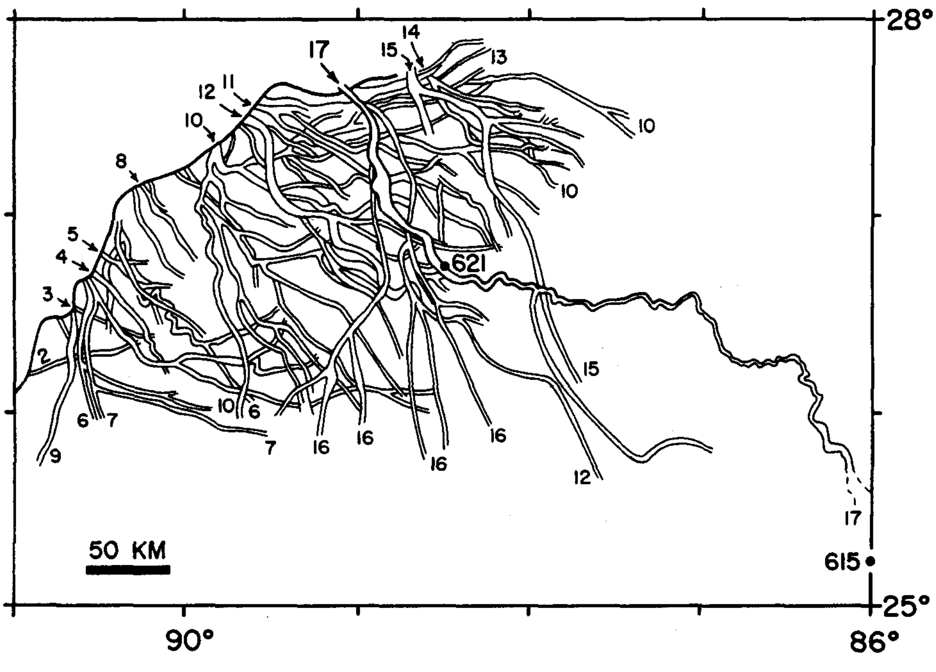

Figure 32 Channel patterns for sequences 1-17 on the Mississippi Fan, from Weimer (1989). 621 and 615 indicate core locations, and other numbers identify the channels of particular sequences.

This distillation does not yet have the power of a good facies model because 1) few examples are included, 2) the facies relationships in each example are not identical, and 3) individual fans may be evolving in different ways.

The first generalization is that the lower fan is much sandier than the mid-fan, and contains deposits that are much more extensive laterally. In some cases, these lower fan deposits are older than those of the mid-fan. The mid-fan is characterized by channel-levee systems that shingle against one another to form channel-levee complexes. The Amazon contains at least three channel-levee complexes (Fig. 35). Here, the upper channel-levee complex contains six shingled channel-levee systems; the lower channel-levee complex is less well defined but appears to contain five channel-levee systems. Individual channel-levee systems build up above the general level of the fan surface by 200-300 m until there is an avulsion. Then a new channel-levee system begins to build on the flanks of an older one.

In the Amazon, there is a distinct stratigraphy consisting of debris flows overlain by sheet-like reflectors, overlain in turn by channel-levee systems (Fig. 29). The debris flows in Figure 29 (? DF – about 100 m thick; and the DF of Unit R – about 150 to 225 m thick) are overlain by parallel sheet-like reflectors, perhaps indicating that the channel-levee systems develop, not immediately on top of a debris flow deposit, but on top of older laterally extensive (? sandy) turbidites. This might be yet another example of mid-fan channel-levee systems prograding over older lower fan sandy sheet-like turbidites.

The importance of the mass transport complexes in the Mississippi Fan has been emphasized by Weimer (1989, 1990). He relates the mass transport complexes to the initiation of a phase of fan growth (a new seismic sequence), when there is erosion at the base of slope "as submarine canyons were forming ... [also] ... as the slope-derived sediments are transported basinward, they have tremendous erosive abilities that scour into the underlying sequence and are deposited farther downfan in the form of mass transport complexes" (Weimer, 1989, p. 270). Further mass transport complex deposition results from retrogressive slumping in the canyon head. When the canyon head has cut back far enough to join up with the incised channels on the shelf, sand is fed directly to the submarine fan (Goodwin and Prior, 1989), probably as turbidity currents.

The Rhone is constructed in a very similar way, with eight shingled channel-levee systems making up a channel-levee complex (Fig. 30). In both the Amazon and Rhone fans, the channel-levee complexes are separated stratigraphically by seismically transparent facies (Figs. 29, 36). Unfortunately, it is not clear whether these are early-formed mass transport complexes, or later-formed slope and levee failure deposits. However, there is clear evidence in the Rhone that episodes of channel-levee system development are terminated by major slides and slumps, at least partly from the slope.

RELATIONSHIP OF FAN DEVELOPMENT TO SEA LEVEL FLUCTUATIONS

There is almost no detailed dating of modern fans that permits the facies and facies successions described above to be related to Plio-Pleistocene fluctuations of relative sea level. However, it is fairly well established that highstands of relative sea level result in fan abandonment, and the draping of the fan surface with hemipelagic mudstones to form *condensed horizons* (Fig. 27). In the Mississippi, the mass transport complexes rest on, or scour into condensed horizons (Weimer, 1989), suggesting that mass transport complexes initiate new phases of fan growth during lowering of relative sea level, slumping on the slope, and canyon formation. By contrast, the debris flows related to levee failures on the Rhone and Amazon fans seem to be almost the youngest features on the fan surfaces, suggesting formation during rising Holocene sea level and fan abandonment. Some acoustically transparent or chaotic facies within the fans (e.g., ?DF and the DF of Unit R, Amazon Fan, Fig. 29) cannot reliably be assigned either to mass transport complexes or to levee failures, making it difficult to know whether these layers initiate or terminate a phase of fan growth. The same problem exists in the Rhone (Fig. 36), where the slumps and slides clearly divert turbidity currents and initiate new locations of fan growth. However, in the absence of dating, it is not possible to relate the Rhone slide and slump facies to relative sea level lowering (mass transport complex) or rising (levee failure).

In the absence of dating, the channel-levee complexes are also difficult to relate to sea level fluctuations. The Plio-Pleistocene record of relative sea level fluctuations has been worked out from studies of oxygen isotopes (Chapter 2). There have been seven major fluctuations in the last 700,000 years, and each of these fluctuations may have resulted in one of the Mississippi seismic sequences. The older 10 sequences may have been influenced by one or many of the sea level fluctuations older than 700,000 years. However, these fluctuations have smaller absolute ranges, and appear to be tuned to a cyclicity of about 41,000 years (Chapter 2). In fans other than the Mississippi, the correlation between Plio-Pleistocene fluctuations and numbers of fan lobes is even more difficult to investigate. In the Amazon, for example, Manley and Flood (1988) argue persuasively that the Upper channel-levee complex (Fig. 35) developed during the Wisconsin lowstand of sea level (85,000-12,000 years ago). In the Mississippi, foraminiferal dating of fan sequences 16 and 17 (Fig. 34) indicate deposition during the Wisconsin lowstand, but the presence of two sequences within one lowstand also suggests that an autocyclic process is operating. Thus it is currently almost impossible to relate fan lobes or seismic sequences to specific fluctuations of relative sea level.

In a theoretical sense, fan facies are tentatively related to relative sea level fluctuations in the following scheme:

1) Lowering of relative sea level initiates a phase of fan growth. Coastal depocentres prograde out to the shelf-slope break, where the added sediment load may cause slope failure, slumping and canyon development. The upslope edge of the first slump scar will tend to be unstable, and will result in retrogressive slumping and canyon enlargement. The slumped sediment will move into the basin and be deposited as mass transport complexes. If canyons already exist, the shift of coastal depocentres to the shelf edge may result in the direct funnelling of sand down the canyons in turbidity currents. These will deposit sheet-like sandy turbidites in pre-existing topographic lows on the basin floor.

2) During continued falling stage, and/or during lowstand, channel-levee complexes build out onto the fan surface. It is not clear what controls the change from unconfined sheet-like flow of sandy turbidity currents to confined flow of muddier currents within channel-levee systems. One possibility is that levees initially form on the walls of the incised canyon. As more and more flows use the canyon, with fines spilling up onto and over the levees, the levees lengthen onto the fan surface, and grow in height and width as more and more fine-grained material spills overbank. The suspended fines will lead to levee growth, and the sand will bypass the leveed

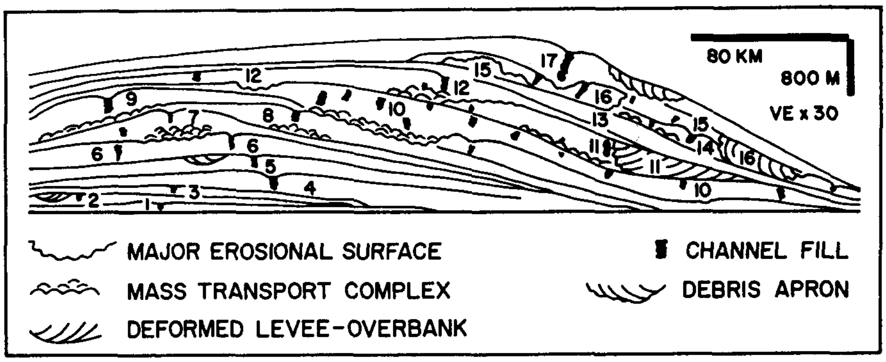

Figure 33 West (left) to east (right) composite cross section of the Mississippi Fan, showing the stacking pattern of the 17 sequences, from Weimer (1989). Note vertical exaggeration of 30 times.

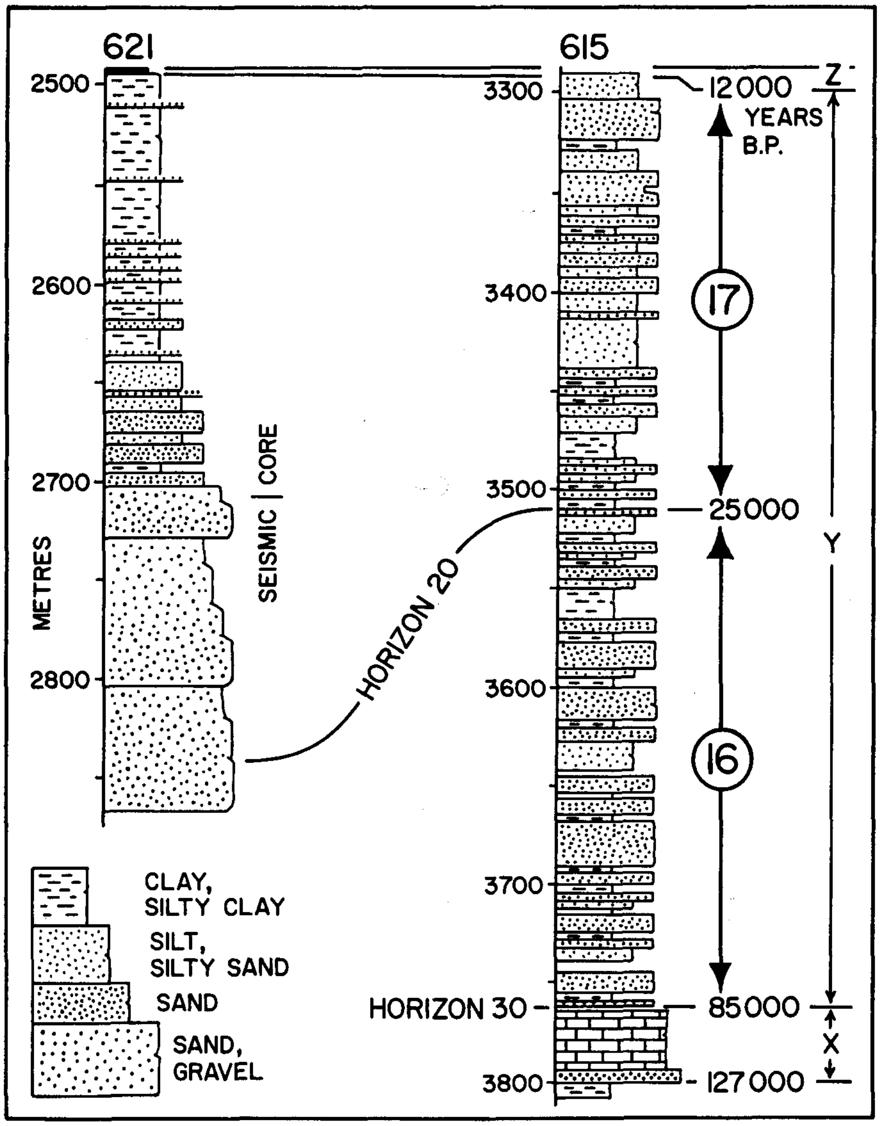

Figure 34 Graphic logs of Deep Sea Drilling Project (Leg 96) cores from sites 621 (mid-fan channel) and 615 (lower fan). Note that 621 has been extended down below the cored interval using interpretations of seismic data. Z, Y and X refer to biostratigraphic zones, with ages given in years before present. Zone Y corresponds to the Wisconsin late glacial stage, and X to the Wisconsin interstadial. Horizons 20 and 30 are distinctive seismic markers; horizon 30 marks the beginning of sequence 16, and 20 marks the beginning of sequence 17. Depths in core are given below sea level, with datum at the present sediment-water interface. Note particularly the sandy nature of the lower fan, and implied sediment bypassing of the mid-fan (where the core shows much more mud in the upper part of sequence 17).

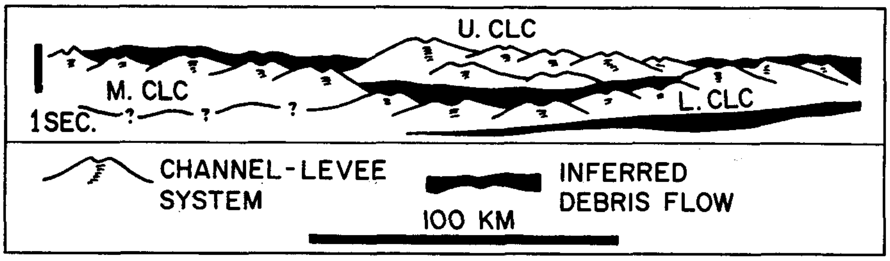

Figure 35 Schematic diagram, after Manley and Flood (1988), showing the proposed sequence of fan growth-debris flows (black) overlain by channel-levee complexes. No debris flow deposits are known beneath the middle channel-levee complex. Note construction of each channel-levee complex from five or six individual channel-levee systems.

part of the fan *en route* to the sandy lower fan. Alternatively, if the sediment introduced into the basin becomes progressively muddier and impoverished in sand, the flows may evolve into continuous low-density underflows. The fan channels will become much more sinuous, and no sand will be funnelled through the channels to the lower fan.

3) The active construction of channel-levee complexes is probably terminated by a relative rise in sea level. At this time, empty channels (and feeder canyons) may fill with mud. Sediment failures on the lower slope and on levees may lead to slumps and debris flows that travel over large parts of the fan surface.

4) During continued rising stage, and during highstand, the fan surface is passively blanketed by hemipelagic fines, resulting in a condensed horizon.

5) Despite the present relative highstand of sea level, turbidity currents are now being generated at the rate of about one every two years in the Congo and Magdalena systems. Even on passive margins, there are also enough earthquakes that sediment can be catastrophically dislodged from canyon heads and resedimented into deep water (as in Laurentian Fan). Fan growth is therefore not entirely restricted to times of relative lowstand.

These ideas are embodied in the two models of Figure 37, where model A incorporates mass transport complexes and channel switching in the upper fan (based largely on the Mississippi). Model B incorporates sheet-like sandy turbidites without mass transport complexes but with some vertical channel stacking in the upper fan (based more upon the Rhone Fan). In the models, phases of fan growth related to sea level cycles (seismic sequences) are separated by hemipelagic layers (Fig. 37).

FANS IN A SEQUENCE-STRATIGRAPHIC CONTEXT

Fan stratigraphy has been related to global eustatic sea level fluctuations in widely published but misleading schemes such as that shown in Figure 38. In sequence stratigraphic theory, one complete cycle of sea level fluctuation takes place between the sequence boundaries (SB, Fig. 38). In one terminology, the sediments have been subdivided into *lowstand fans* and *lowstand wedges* (Posamentier and Vail, 1988), representing falling stage and lowstand, respectively. In an alternative terminology, Vail (1987) recognizes a *basin floor fan*, a *slope fan* (channel-levee complex), and a *lowstand wedge – prograding complex* that progrades and buries both the slope fan and basin floor fan (Fig. 38). Note also that prograding highstand systems tract deposits are shown burying the lowstand wedge. In the examples described in this chapter, there are no lowstand wedge – prograding complexes (and certainly no prograding HST deposits) that bury the basin floor fan and slope fan (channel-levee system) deposits (compare Figure 38 with Figures 29, 30, 33, 35). In fans where the data are available (Mississippi), the condensed section (CS, Fig. 38) overlies the basin floor fan and slope fan (channel-levee system), not a thick lowstand wedge – prograding complex. Figure 38 shows too much theory and not enough real geological relationships! Another problem is the use of the term *slope fan* (Vail, 1987) and placement of the channel-levee complex on the *slope* (Posamentier *et al.*, 1988). On fans such as the Amazon, Rhone and Mississippi, the channel-levee complexes form on the fan surface, seaward of both the slope and the rise.

Widely published diagrams similar to Figure 38 have not been carefully constructed by the distillation of real examples; they do not act as "norms", and cannot be used for prediction.

COMPARISON OF MODERN FANS AND ANCIENT ROCKS

This comparison is very difficult, the first problem being one of *scale.* From outcrops, it is almost impossible to reconstruct features as large as those seen on modern fans (e.g., a channel-levee system 200 m thick and tens of km wide). Scale remains a problem in most subsurface studies, although some examples approach the scale of, and have the same sedimentary features as, modern fans (e.g., Lower Eocene Frigg Fan, North Sea, McGovney and Radovich, 1985; Fig. 39). The second major problem concerns the *features* of modern fans, particularly the abundance of channel-levee systems and scarcity of depositional lobes. Most overall interpretations of ancient turbidite systems rely heavily on the individual interpretations of thinning- and thickening-upward successions. With the scarcity of lobes on modern fans, the interpretations of ancient thickening-upward successions becomes much more difficult. It is not yet known whether thickening-upward successions can be understood in the context of deposition in channel and levees, or on the smooth sand-rich lower fan. Indeed, the facies and facies geometries of lower fan deposits are probably less well known than any other part of the fan, despite their sandiness and hence importance in understanding ancient sandy turbidite oil and gas reservoirs.

The following discussion is mostly concerned with ancient rocks, in four situations; large feeder channels, channel-levee systems, sheet-like turbidites and slump/debris-flow facies.

Large feeder channels

No large (deeper than 500 m) feeders, or canyons have been described from outcrop, but several are known in the subsurface, including Eocene and early Oligocene canyons in Czechoslovakia (1-3 [max. 10] km wide, 800-1060 m deep; Picha, 1979), the Eocene Yoakum canyon of Texas (16 km wide, 1067 m deep; Dingus and Galloway, 1990), the Paleocene Meganos canyon of California (16 km wide, up to 760 m deep; Fischer,

Table 3 *Dimensions of mid-fan channel-levee systems.*

	Amazon	Rhone	Mississippi
CHANNEL-LEVEE SYSTEMS			
Average thickness (m)	330-360	150	140
Average width (km)	20-40	70	250
INDIVIDUAL CHANNELS			
Aggraded HAD thickness			
(range, milliseconds [ms])	(70-350)	(70-140)	(60-530)
average (ms)	180	90	210
Width of HAD reflectors (km)	1.7	0.44	3.0

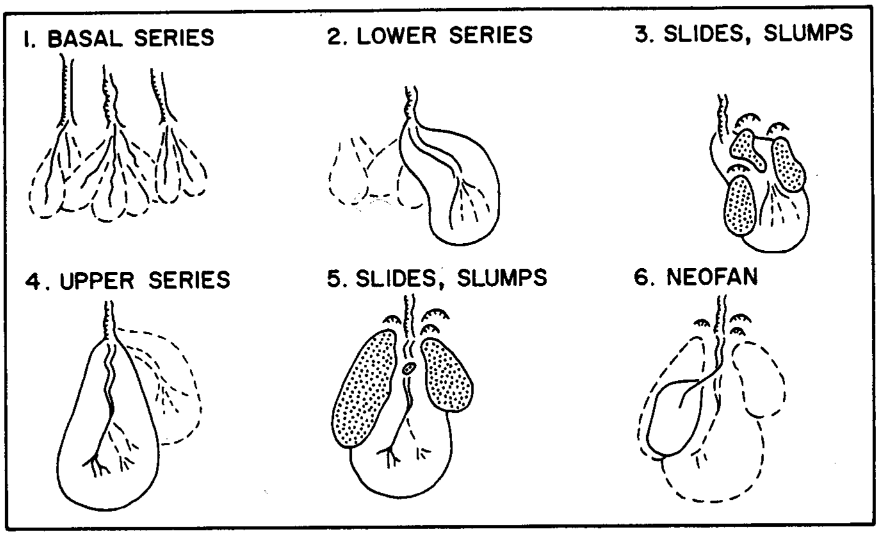

Figure 36 Growth pattern for the Rhone Fan, after Droz and Bellaiche (1985). The basal series (1) is poorly understood. The lower series (2) consists of several individual channel-levee systems, and their deposition was terminated by slumps and slides (3). These caused a westward diversion of the fan (4) and deposition of the upper series of channel-levee systems. Slumping and debris flow (5) covered a large part of the fan surface and blocked fan channels, causing channel diversion and deposition of the neofan (6).

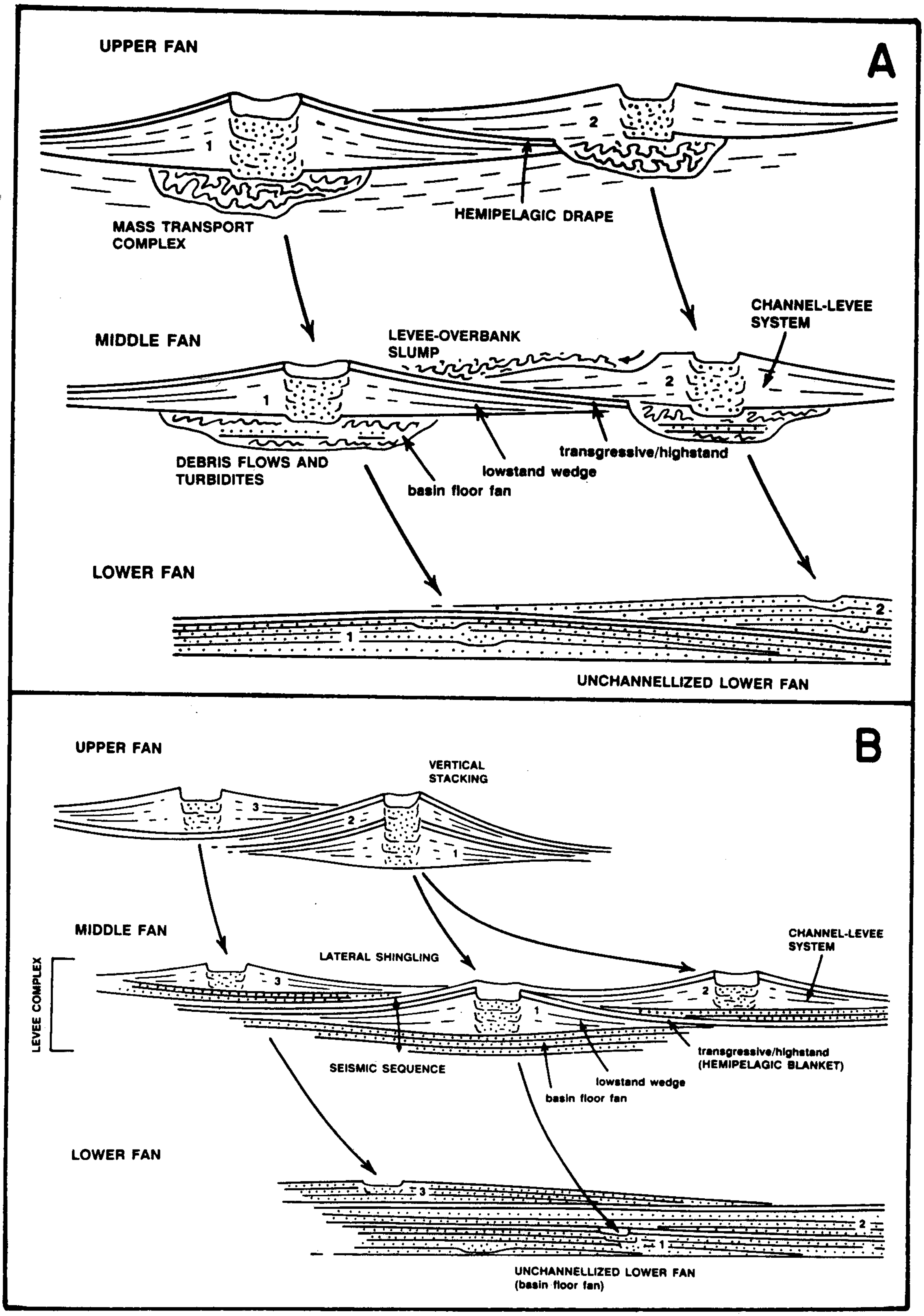

Figure 37 Preliminary fan models. A) model in which fan deposition begins with a Mass Transport Complex (basin floor fan in the terminology of Fig. 38), overlain by channel-levee systems. B) model in which fan deposition begins with sheet-like basin floor turbidites (basin floor fan, Fig. 38), overlain by channel-levee systems. Note stacking on upper fan (as in the Rhone) and lateral shingling on the mid-fan.

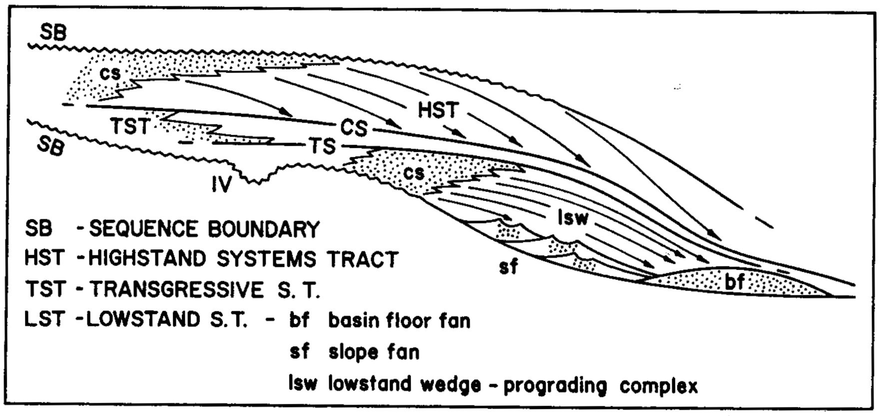

Figure 38 Submarine fans in a sequence-stratigraphic context. This diagram is a combination of similar diagrams published by Vail (1987) and Posamentier and Vail (1988). Diagram shows the conceptual development of a fan within one sequence (i.e., the result of one cycle of sea level fluctuation). SB = sequence boundary, TS = transgressive surface, CS = condensed section (or maximum flooding surface), and cs = coastal sandstones. None of the modern fans discussed in this chapter has a thick lowstand wedge (with downlapping shallow-marine Highstand Systems Tract deposits) on top of the "slope fan" (channel-levee complex, which does *not* occur on the slope). See text for further discussion of this controversial model.

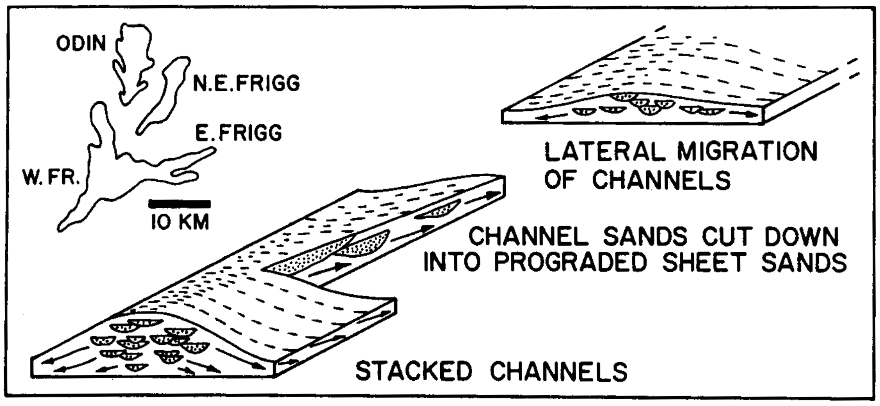

Figure 39 Interpretation of sheet sandstones and overlying channelized sandstones in Frigg Fan, North Sea. From McGovney and Radovich (1985).

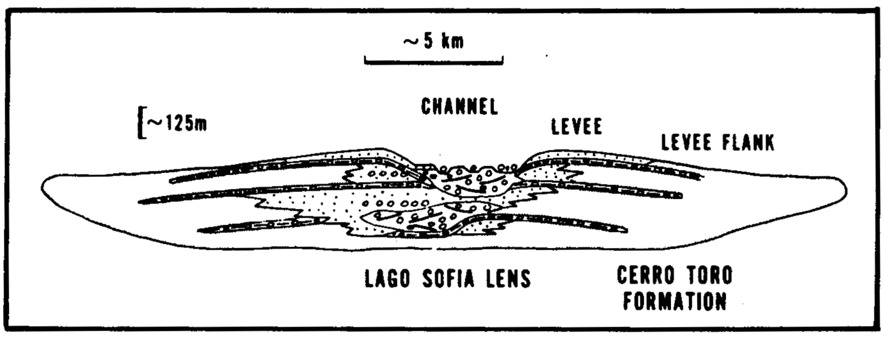

Figure 40 Schematic cross section through a coarse "Lago Sofia" lens in the Cretaceous Cerro Torro Formation, southern Chile. From Winn and Dott (1979).

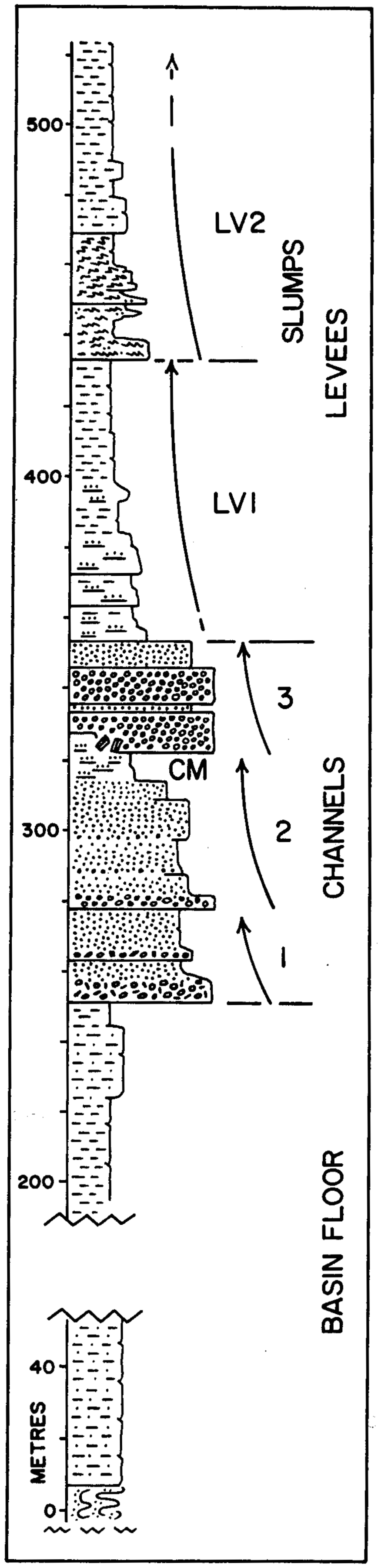

Figure 41 (right) Stratigraphic section through Cretaceous rocks at Wheeler Gorge, California. Base of section is faulted (Santa Ynez Fault), and overlain by a small slump. The lower part of the section consists of 250 m of mudstones. CM = channel margin deposits, LV = levee. Arrows indicate thinning- and fining-upward facies successions.

1979), and the early Cretaceous Gevaram canyon of Israel (7 km wide, 1000 m deep; Cohen, 1976). Of these, only the Czechoslovakian example contains appreciable sandstone and conglomerate (up to 300 m) in the canyon fill; the others are mudstone filled.

The Yoakum canyon appears to have formed by retrogressive slumping at the shelf break (Dingus and Galloway, 1990), as has been suggested for the canyons and feeders of the Plio-Pleistocene Mississippi fan. By contrast, the cutting of the Meganos canyon has been related to Paleocene fault movements (Fischer, 1979, p. 7). Both the Czechoslovakian canyons and the Gevaram canyon appear to be submerged fluvial valleys further developed and enlarged by marine processes. It would now appear that the initiation of all of these canyons except Meganos is directly related to a lowering of relative sea level. The canyons appear to have widened and deepened whilst they acted as conduits for turbidity currents, but because of relatively steep axial gradients, little turbidite sand or gravel remains in the canyon. The canyons are all mudstone filled (except for the lower parts of the Czechoslovakian canyons), presumably during a rise of relative sea level. The size of the canyons suggests some turbidity current scouring (not just retrogressive slumping), and hence the model predicts submarine fan sandstone and conglomerate deposits at the ends of the canyons. For various reasons, these deposits have not yet been discovered.

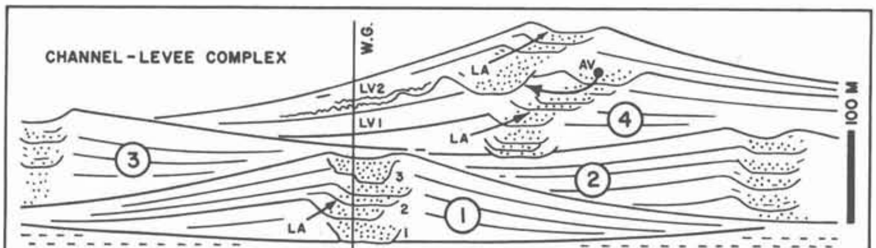

Figure 42 Interpretation of the Wheeler Gorge section in terms of the models of Figure 37. WG indicates the vertical profile of Wheeler Gorge. Circled numbers suggest the order of channel-levee system development, and uncircled numbers 1-3 indicate the stacked channels at Wheeler Gorge. LA = lateral accretion and AV = avulsion. Thus the thinning-and fining-upward levee sequences are interpreted to reflect lateral migration of the channel away from Wheeler Gorge. Channel-levee systems 2 and 3 are necessary in order that the levee sequences of system 4 can build on top of the stacked channel deposits of system 1. No horizontal scale is implied; systems 2 and 3 could equally well be on opposite sides of system 1, and system 4 could be a mirror image of what is shown, on the left of Wheeler Gorge. Stipple indicates sandstone and conglomerate within channels.

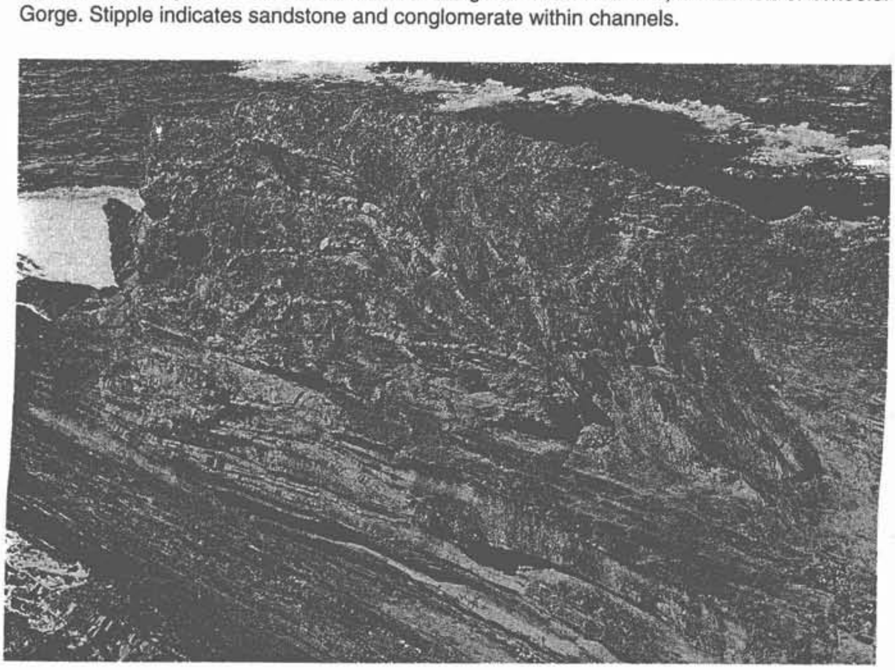

Figure 43 Slumped slope deposits in the Carboniferous Gull Island Formation of County Clare, western Ireland.

Channel-levee systems

Channels seen on the surfaces of modern fans in mid-fan areas average about 40 m deep, but aggraded HAD thicknesses of channel-fill facies range from about 60-530 m (Table 3). Levee and overbank deposits of modern fans have similar thicknesses, and widths of tens of kilometres. In the geological record, they are probably made up of laterally continuous and extensive thin-bedded turbidites.

In the literature, the interpretation that most closely approaches the model of channel-levee systems developed in this chapter is the Eocene Frigg Fan (subsurface, North Sea; McGovney and Radovich, 1985). The interpretation is based on seismic lines, well logs and cores, and shows four radiating finger-like sandbodies (Fig. 39) 4-5 km wide and 10-20 km long. The stacks of channelized sandstones occur along the central parts of the fingers, and vary from 20-200 m in thickness, with thin shale partings 2-5 m thick. The channelized sandstones cut into older sheet-like sandstones that have a much greater lateral extent, and show very gently mounded seismic reflectors. In the interpretation (Fig. 39), it is notable that the channel sands are stacked in the upcurrent position, but are shown as thinner and laterally migrating in the downcurrent position (as in the modern Rhone and Mississippi fans, Figs. 30, 31).

In outcrop, the scale of channel-levee systems makes them difficult to reconstruct. Many of the finer-grained facies may be obscured by cover, and the section may be broken up by folds and faults. The best reconstruction is probably that of Winn and Dott (1979), from Late Cretaceous rocks of southern Chile. They summarise their observations in a cross section that shows two superimposed channel-levee systems, with a total aggraded channel thickness of about 300 m (Fig. 40). The channel deposits consist of sandstones and conglomerates. Thinner-bedded turbidites make up the levee deposits, and the proposed width of the channel-levee system is about 20 km. Some of the thinner-bedded turbidites occur in slumped horizons up to about 15 m thick; reconstructed directions of slumping tend to be mostly eastward, whereas regional paleoflow in the channels is southward. This suggests the possibility that the slumped horizons represent levee failure (cf., Rhone and Amazon fans).

There is also one superb vertical section through a channel-levee system in the Cretaceous Wheeler Gorge section in California (Walker, 1985; Fig. 41). In Figure 41, the section is truncated at the base by the Santa Ynez Fault. A basal slump is overlain by a fine-grained section about 250 m thick, dominated by 1-cm-thick graded siltstones — there are about 6000 such beds present. The depositional environment appears to have been very quiet and monotonous, far from the action of large turbidity currents (the "basin floor" of Figure 41). Stacked channels overlie the basin floor deposits extremely abruptly, suggesting a lowering of relative sea level and rapid progradation of a channel-levee system. Channels 1 and 2 are both conglomeratic at the base and fine upward through pebbly and massive sandstones. The sandstones of channel 2 are overlain by thin-bedded turbidites (CM in Fig. 41), characterized by bedding lenticularity and CCC turbidites (Fig. 5). These features, along with the stratigraphic position, suggest a channel margin (CM, Fig. 41). Channel 3 has an erosive base, and a spectacular example of a collapsed channel wall with stratified blocks similar to those in Figure 15. The bulk of the fill is unstratified conglomerate, but there is a fining upward at the top through massive sandstones into classical turbidites. The two levee successions (LV1 and LV2) both fine upward, from classical turbidites into mudstones. Succession LV2 (Fig. 41) is dominated by multiple horizons of soft-sediment slumping within a thin-bedded turbidite facies (Fig. 13). The levee interpretation is based particularly on the association with coarse channelized deposits, and the abundance of deformation within thin-bedded CCC turbidites.

The scale (100-m channel stack, 80-m-thick levees) invites comparison with channel-levee systems of the Amazon (Fig. 29) or Rhone Fans (Fig. 30). The interpretation of Figure 42 shows how guidance from the channel-levee fan model developed in this chapter (Fig. 37) can suggest predictions from one new piece of information (the Wheeler Gorge section). Note that the use of a Rhone- and Amazon-based model suggests that channel-levee systems must shingle at the same stratigraphic level as the Wheeler Gorge channels before thick levee deposits (LV1 in Fig. 42) can spread across the channels at a higher stratigraphic horizon.

Other channel-levee interpretations in the literature commonly refer to sandy systems of limited lateral extent, and with channel depths of only a few tens of metres (e.g., Cretaceous Chatsworth Formation of California; Advocate and Link, 1981). Alternatively, there are interpretations of shifting and nested channel and channel-margin facies 20-40 m thick, where the interbedding of sandstones and mudstones may respond acoustically as an HAD facies (Upper Miocene Capistrano Formation, California, Walker, 1975b). It is possible that these examples, or systems like them, represent thalweg channels within a much larger canyon (Figure 28), rather than individual channel-levee or channel-margin systems.

Sheet-like turbidites

There are many examples of apparently unchannelized, sheet-like turbidites in the geological record. In some cases, individual beds can be traced for kilometres or tens of kilometres, implying very smooth basin floors (Enos, 1969; Hesse, 1974; Ricci Lucchi and Valmori, 1980). The topography of modern fans shows that smooth, low-gradient depositional areas exist 1) on the lower fan, and 2) on the flatter parts of levees some distance from the levee crest. Limited data from modern fans suggest that the lower fan setting would contain much sandier turbidites than on the distal parts of levees. It is important to develop criteria for distinguishing the two settings, in order to make better predictions of lateral facies changes, and in order to place the deposits correctly within a fan stratigraphy (the lower fan sandy sheet-like facies would commonly be older than the distal levee facies).

In the geological record, classical turbidites in apparently unchannelled settings commonly occur in thickening-upward successions. These have been related to the progradation of depositional lobes (Mutti and Ricci Lucchi, 1972), although this interpretation must now be questioned because 1) depositional lobes are *not* common on modern fans, and 2) some thickening-upward successions might be related to fluctuations of relative sea level (Mutti, 1985). It is not known whether thickening-upward successions occur in the lower sandy parts of modern fans. Conversely, depositional lobes in the geological record can only confidently be identified by their external form, not by the presence of thickening-upward successions. There are few good examples where the external form can be defined. One example is the Cretaceous Forbes Formation, California (Weagant, 1972), where the stack of sandy lobes and interbedded mudstones is about 1000 m thick. Individual lobes are up to 60 m thick and 10 km in diameter in the Grimes gas field. The lobes appear to be irregularly stacked, and are separated by blanketing mudstones that partly trap gas in the reservoirs.

Slump/debris flow facies

Although there are many examples of slumps and debris flows in the geological record, there are very few that approach the scale of the chaotic and acoustically transparent layers on modern fans (many tens up to about 200 m). One of the best examples of a slumped slope facies is in Pennsylvanian rocks on the coast of western Ireland, where there is an almost continuously exposed section up to 550 m thick (Martinsen, 1989; Fig. 43). The styles of deformation include mud slumps 0.5 to 15 m thick (with composite thicknesses to about 50 m) and mud and sand slides involving sediment thicknesses up to about 60 m.

Large-scale levee failures, similar to those of the Amazon and Rhone fans, have not been identified in the geological record, although the slump in the Waitemata Group (Fig. 14) is a possible analogy. On a smaller scale, 15 m thick slumps of thin-bedded turbidites, possibly of levee origin, occur in Cretaceous rocks of southern Chile (Winn and Dott, 1979).

CONCLUSIONS

Submarine fan studies are presently in a state of flux. The seismically derived information from modern fans concerning facies geometry and internal stratigraphy cannot yet be applied very easily in the geological record, where the scale of observation is commonly very much smaller. Conversely, features in the geological record cannot always be related to parts of modern fans. Information is gradually becoming available to link fan development with fluctuations of relative sea level, but there is an urgent need for precise dating within modern fans. Information from smaller sand-rich fans is needed to complement the data from large fans such as the Amazon, Mississippi and Rhone. Finally, tectonic setting clearly influences fan development in major ways; however, there are too few well-studied fans in each tectonic setting to allow any models to be formulated.

REFERENCES

Basic sources of information

Bouma, A.H., Normark, W.R. and Barnes, N.E. (eds.), 1985, Submarine fans and related turbidite systems: New York, Springer-Verlag, 351 p.
A well-organized compendium of information from many different ancient and modern situations. About one third of the volume is devoted to the results of the drilling that took place during DSDP Leg 96.

Pickering, K.T., Hiscott, R.N. and Hein, F.J., 1989, Deep marine environments; clastic sedimentation and tectonics: London, Unwin Hyman, 416 p.
This is the latest textbook on turbidites and submarine fans. It is organized into three parts, 1) on facies, processes, sequences and controls, 2) on deep-water basin elements, and 3) on plate tectonics and sedimentation.

Weimer, P. and Link, M.H., eds., 1991, Seismic facies and sedimentary processes of submarine fans and turbidite systems: New York, Springer Verlag, 447 p.
This volume appeared in January, 1992, too late for any ideas to be incorporated in this paper. The emphasis is on large-scale systems, and seismic facies in ancient and modern submarine fans. The book represents an important source of new information.

Wilgus, C.K., Hastings, B.S., Posamentier, H.W., Ross, C.A. and Kendall, C.G.St.C., eds., 1988, Sea level changes: an integrated approach: Society of Economic Paleontologists and Mineralogists, Special Publication 42, 407 p.
Collection of papers emphasizing conceptual basis of sequence stratigraphy plus numerous case studies of sea level change from the geological record.

Other references

Advocate, D.M. and Link, M.H., 1981, Summit mobil home park field trip stop, *in* Link, M.H., Squires, R.L. and Colburn, I.P., eds., Simi Hills Cretaceous turbidites, southern California: Society of Economic Paleontologists and Mineralogists, Pacific Section, Field Guide, p. 125-127.

Bouma, A.H., 1962, Sedimentology of some flysch deposits: Amsterdam, Elsevier, 168 p.
Many measured section of turbidites, and initial documentation of the "Bouma sequence".

Bouma, A.H. and Coleman, J.M., 1985, Mississippi Fan: Leg 96 program and principal results, *in* Bouma, A.H., Normark, W.R. and Barnes, N.E., eds., Submarine fans and related turbidite systems: New York, Springer-Verlag, p. 247-252.

Ciro, J., Kowsmann, R.O., Flood, R.D., Manley, P.L. and Pirmez, C., 1988, Evolucao Quaternaria pos-glacial do cone submarino do Amazonas: um modelo retrogradente: Anais do 35 Congreso Brasileiro de Geologia, v. 2, p. 451-465.

Clari, P. and Ghibaudo, G., 1979, Multiple slump scars in the Tortonian type area (Piedmont basin, northwestern Italy): Sedimentology, v. 26, p. 719-730.
Excellent documentation of large slump scars believed to have formed close to the slope break.

Cohen, Z., 1976, Early Cretaceous buried canyon: influence on accumulation of hydrocarbons in Helez oil field, Israel: American Association of Petroleum Geologists, Bulletin, v. 60, p. 108-114.

Crowell, J.C., 1957, Origin of pebbly mudstones: Geological Society of America, Bulletin, v. 68, p. 993-1009.

Damuth, J.E. and Embley, R.W., 1981, Mass-transport processes on Amazon cone, western equatorial Atlantic: American Association of Petroleum Geologists, Bulletin, v. 65, p. 629-643.

Damuth, J.E., Flood, R.D., Kowsmann, R.O., Belderson, R.H., and Gorini, M.A., 1988, Anatomy and growth pattern of Amazon deep-sea fan as revealed by long-range side-scan sonar (GLORIA) and high-resolution seismic studies: American Association of Petroleum Geologists, Bulletin, v. 72, p. 885-911.

Damuth, J.E., Kolla, V., Flood, R.D., Kowsmann, R.O., Monteiro, M.C., Gorini, M.A., Palma, J.J.C. and Belderson, R.H., 1983a, Distributary channel meandering and bifurcation patterns on the Amazon deep-sea fan as revealed by long-range side-scan sonar (GLORIA): Geology, v. 11, p. 94-98.

Damuth, J.E., Kowsmann, R.O., Flood, R.D., Belderson, R.H. and Gorini, M.A., 1983b, Age relationships of distributary channels on Amazon deep-sea fan: implications for fan growth pattern: Geology, v. 11, p. 470-473.

Dingus, W.F. and Galloway, W.E., 1990, Morphology, paleogeographic setting, and origin of the middle Wilcox Yoakum Canyon, Texas coastal plain: American Association of Petroleum Geologists, Bulletin, v. 74, p. 1055-1076.

Droz, L. and Bellaiche, G., 1985, Rhone deep-sea fan: morphostructure and growth pattern: American Association of Petroleum Geologists, Bulletin, v. 69, p. 460-479.

Elmore, R.D., Pilkey, O.H., Cleary, W.J. and Curran, H.A., 1979, Black shell turbidite, Hatteras Abyssal Plain, western Atlantic Ocean: Geological Society of America, Bulletin, v. 90, p. 1165-1176.

Enos, P., 1969, Anatomy of a flysch: Journal of Sedimentary Petrology, v. 39, p. 680-723.

Feeley, M.H., Buffler, R.T. and Bryant, W.R., 1985, Depositional units and growth pattern of the Mississippi Fan, *in* Bouma, A.H., Normark, W.R. and Barnes, N.E., eds., Submarine fans and related turbidite systems: New York, Springer-Verlag, p. 253-257.

Feeley, M.H., Moore, T.C., Jr., Loutit, T.S. and Bryant, W.R., 1990, Sequence stratigraphy of Mississippi Fan related to Oxygen isotope sea level index: American Association of Petroleum Geologists, Bulletin, v. 74, p. 407-424.

Fischer, P.J., 1979, The evolution of a late Paleocene submarine canyon and fan system: the Meganos Formation, southern Sacramento basin, California: Geological Society of America, Cordilleran Section, Field Trip Guidebook (San Jose, Cal., 1979), p. 1-10.

Goodwin, R.H. and Prior, D.B., 1989, Geometry and depositional sequences of the Mississippi Canyon, Gulf of Mexico: Journal of Sedimentary Petrology, v. 59, p. 318-329.

Gregory, M.R., 1969, Sedimentary features and penecontemporaneous slumping in the Waitemata Group, Whangaparaoa Peninsula, north Auckland, New Zealand: New Zealand Journal of Geology and Geophysics, v. 12, p. 248-282.
Excellent illustrations of some of the largest slumps ever described. Many of the slumps involve thin-bedded turbidites — could these be levee failures similar to those on fans such as the Rhone and Mississippi ?

Hein, F.J., 1982, Depositional mechanisms of deep-sea coarse clastic sediments, Cap Enragé Formation, Quebec: Canadian Journal of Earth Sciences, v. 19, p. 267-287.

Hesse, R., 1974, Long-distance continuity of turbidites: possible evidence for an early Cretaceous trench — abyssal plain in the East Alps: Geological Society of America, Bulletin, v. 85, p. 859-870.

Heezen, B.C., 1956, Corrientes de turbidez del Rio Magdalena: Societa Geografica de Colombia, Bolletin, v. 51/52, p. 135-143.

Heezen, B.C. Ericson, D.B. and Ewing, M, 1954, Further evidence for a turbidity current following the 1929 Grand Banks earthquake: Deep-Sea Research, v. 1, p. 193-202

Heezen, B.C., Menzies, R.J., Schneider, E.D., Ewing, W.M. and Granelli, N.C.L., 1964, Congo submarine canyon: American Association of Petroleum Geologists, Bulletin, v. 48, p. 1126-1149.
Excellent documentation of the relationship between river behaviour, turbidity current genesis and cable breaking.

Kolla, V. and Coumes, F., 1985, Indus Fan, Indian Ocean, *in* Bouma, A.H., Normark, W.R. and Barnes, N.E., eds., Submarine fans and related turbidite systems: New York, Springer-Verlag, p. 129-136.

Kuenen, P.H. and Migliorini, C.I., 1950, Turbidity currents as a cause of graded bedding: Journal of Geology, v. 58, p. 91-127.
This paper established the modern turbidite concept, and is one of the most important papers in sedimentology this century. Required reading, and not only for historical reasons.

Link, M.H., 1983, Sand rich turbidite facies of the Upper Cretaceous Chatsworth Formation, Simi Hills, California, *in* Link, M.H., Squires, R.L. and Colburn, I.P., eds., Simi Hills Cretaceous turbidites, southern California: Society of Economic Paleontologists and Mineralogists, Pacific Section, Guidebook, p. 63-70.

Lowe, D.R., 1975, Water escape structures in coarse-grained sediments: Sedimentology, v. 22, p. 157-204.
Extensive discussion of fluid escape, with the first detailed interpretation of dish structures and associated features.

Lowe, D.R., 1982, Sediment gravity flows; II. Depositional models with special reference to the deposits of high-density turbidity currents: Journal of Sedimentary Petrology, v. 52, p. 279-297.

Manley, P.L. and Flood, R.D., 1988, Cyclic sediment deposition within Amazon deep-sea fan: American Association of Petroleum Geologists, Bulletin, v. 72, p. 912-925.

Martinsen, O.J., 1989, Styles of soft-sediment deformation on a Namurian (Carboniferous) delta slope, Western Irish Namurian Basin, Ireland, *in* Whateley, M.K.G. and Pickering, K.T., eds., Deltas; sites and traps for fossil fuels: Oxford, Blackwell Scientific Publications, Geological Society Special Publication 41, p. 167-177.

McGovney, J.E. and Radovich, B.J., 1985, Seismic stratigraphy and facies of the Frigg fan complex, *in* Berg, O.R. and Woolverton, D.G., eds., Seismic stratigraphy II: American Association of Petroleum Geologists, Memoir 39, p. 139-154.

McHargue, T.R. and Webb, J.E., 1986, Internal geometry, seismic facies, and petroleum potential of canyons and inner fan channels of the Indus Submarine Fan: American Association of Petroleum Geologists, Bulletin, v. 70, p. 161-180.

Middleton, G.V. and Southard, J.B., 1984, Mechanics of sediment movement: Society of Economic Paleontologists and Mineralogists, Notes for Short Course 3, p. 8-1-8-34.
The most concise explanation of the mechanics of various types of sediment gravity flows.

Mutti, E., 1979, Turbidites et cones sous-marins profonds, *in* Homewood, P., ed., Sedimentation detritique (fluviatile, littorale et marine): Short course notes, Institut de Geologie de l'Universite de Fribourg, Switzerland, p. 353-419.

Mutti, E., 1985, Turbidite systems and their relations to depositional sequences, *in* Zuffa, G.G., ed., Provenance of arenites: Dordrecht, D. Riedel Publishing Company, p. 65-93.

Mutti, E. and Ricci Lucchi, F., 1972, Le torbiditi dell'Appennino settentrionale: introduzione all'analisi di facies: Memorie della Societa Geoloiga Italiana, v. 11, p. 161-199. English Translation by T.H. Nilsen, 1978, International Geology Review, v. 20, p. 125-166.
One of the most influential papers on turbidites ever written. Some ideas have changed, but this is still required reading. It established universal turbidite facies and facies associations.

Natland, M.L., 1933, The temperature- and depth-distribution of some Recent and fossil foraminifera in the Southern California Borderland: Scripps Institution of Oceanography, Technical Series, v. 3, p. 225-230.
Detailed comparison of Plio-Pleistocene foraminifera (600 samples at 10-foot intervals!) with modern ecological zones in the Pacific.

Normark, W.R., 1970, Growth patterns of deep-sea fans: American Association of Petroleum Geologists, Bulletin, v. 54, p. 2170-2195.

Normark, W.R., 1978, Fan valleys, channels and depositional lobes on modern submarine fans: characters for recognition of sandy turbidite environments: American Association of Petroleum Geologists, Bulletin, v. 62, p. 912-931.

Normark, W.R., Piper, D.J.P. and Hess, G.R., 1979, Distributary channels, sand lobes, and mesotopography of Navy submarine fan, California Borderland, with applications to ancient fan sediments: Sedimentology, v. 26, p. 749-774.

Normark, W.R., Piper, D.J.W. and Stow, D.A.V., 1983, Quaternary development of channels, levees and lobes on middle Laurentian Fan: American Association of Petroleum Geologists, Bulletin, v. 67, p. 1400-1409.

O'Connell, S., Stelting, C.E., Bouma, A.H., Coleman, J.M., Cremer, M., Droz, L., Meyer-Wright, A.A., Normark, W.R., Pickering, K.T. and Stow, D.A.V., 1985, Drilling results on the lower Mississippi Fan, *in* Bouma, A.H., Normark, W.R. and Barnes, N.E., eds., Submarine fans and related turbidite systems: New York, Springer Verlag, p. 291-298.

Picha, F., 1979, Ancient submarine canyons of Tethyan continental margins, Czechoslovakia: American Association of Petroleum Geologists, Bulletin, v. 63, p. 67-86.

Piper, D.J.W. and Normark, W.R., 1981, Re-examination of a Miocene deep-sea fan and fan-valley, southern California: Geological Society of America, Bulletin, v. 82, p. 1823-1830.

Piper, D.J.W., Stow, D.A.V. and Normark, W.R., 1984, The Laurentian Fan; Sohm Abyssal Plain: Geo-Marine Letters, v. 3, p. 141-146.

Piper, D.J.W., Shor, A.N. and Hughes Clark, J.E., 1988, The 1929 "Grand Banks" earthquake, slump, and turbidity current, *in* Clifton, H.E., ed., Sedimentological consequences of convulsive geological events: Geological Society of America, Special Paper 229, p. 77-92.

Pilkey, O.H., 1988, Basin plains; giant sedimentation events, *in* Clifton, H.E., ed., Sedimentologic consequences of convulsive geologic events: Geological Society of America, Special Paper 229, p. 93-99.

Posamentier, H.W. and Vail, P.R., 1988, Eustatic controls on clastic deposition II — sequence and systems tract models, *in* Wilgus, C.K., *et al.*, eds., Sea-level changes: an integrated approach: Society of Economic Paleontologists and Mineralogists, Special Publication, 42, p. 109-124.

Posamentier, H.W., Jervey, M.T. and Vail, P.R., 1988, Eustatic controls on clastic deposition I — conceptual framework, *in* Wilgus, C.K., *et al.*, eds., Sea-level changes: an integrated approach: Society of Economic Paleontologists and Mineralogists, Special Publication 42, p. 109-124.

Ricci Lucchi, F. and Valmori, E., 1980, Basin-wide turbidites in a Miocene, over-supplied deep-sea plain: a geometrical analysis: Sedimentology, v. 27, p. 241-270.

Stelting, C.E. and DSDP Leg 96 Shipboard Scientists, 1985, Migratory characteristics of a mid-fan meander belt, Mississippi Fan, *in* Bouma, A.H., Normark, W.R. and Barnes, N.E., eds., Submarine fans and related turbidite systems: New York, Springer-Verlag, p. 283-290.

Uchupi, E. and Austin, J.A., Jr., 1979, The stratigraphy and structure of the Laurentian Cone region: Canadian Journal of Earth Sciences, v. 16, p. 1726-1752.

Vail, P.R., 1987, Part 1; seismic stratigraphy interpretation procedure, *in* Bally, A.W., ed., Atlas of seismic stratigraphy: American Association of Petroleum Geologists, Studies in Geology no. 27, v. 1, p. 1-10.

Walker, R.G., 1965, The origin and significance of the internal sedimentary structures of turbidites: Proceedings of the Yorkshire Geological Society, v. 35, p. 1-32.
Comparison of turbidite structures with those made in flume experiments, following the publication of the Bouma sequence in 1962.

Walker, R.G., 1973, Mopping up the turbidite mess, *in* Ginsburg, R.N., ed., Evolving concepts in sedimentology: Baltimore, The Johns Hopkins Press, p. 1-37.
A philosophical history of the turbidite concept, based on the ideas of Thomas H. Kuhn. Read the paper to understand the title!

Walker, R.G., 1975a, Generalized facies models for resedimented conglomerates of turbidite association: Geological Society of America, Bulletin, v. 86, p. 737-748.
Defines descriptive parameters, and shows how four models were constructed using those parameters.

Walker, R.G., 1975b, Nested submarine channels at San Clemente, California: Geological Society of America, Bulletin, v. 86, p. 915-924.

Walker, R.G., 1978, Deep water sandstone facies and ancient submarine fans: models for exploration for stratigraphic traps: American Association of Petroleum Geologists, Bulletin, v. 62, p. *932-966.*
A submarine fan model of the channel — depositional lobe type, influential in its time, but now obsolete because it ignored external controls, especially sea level fluctuations.

Walker, R.G., 1985, Mudstones and thin-bedded turbidites associated with the Upper Cretaceous Wheeler Gorge conglomerates, California: a possible channel-levee complex: Journal of Sedimentary Petrology, v. 55, p. 279-290.
Introduces the idea of "CCC turbidites", and relates levee features to thick channelled conglomerates. This example is on the scale of a single channel-levee system in the Rhone Fan (see Droz and Bellaiche, 1985).

Weagant, F.E., 1972, Grimes gas field, Sacramento Valley, California, *in* King, R.E., ed., Stratigraphic oil and gas fields. American Association of Petroleum Geologists, Memoir 16, p. 428-439.

Weimer, P., 1989, Sequence stratigraphy of the Mississippi Fan (Plio-Pleistocene), Gulf of Mexico: Geo-Marine Letters, v. 9, p. 185-272.
Excellent documentation of the seismic facies of the seventeen Mississippi fan sequences; the paper is a goldmine of information.

Weimer, P., 1990, Sequence stratigraphy, facies geometries, and depositional history of the Mississippi Fan, Gulf of Mexico: American Association of Petroleum Geologists, Bulletin, v. 74, p. 425-453.

Winn, R.D., Jr. and Dott, R.H., Jr., 1979, Deep-water fan-channel conglomerates of Late Cretaceous age, southern Chile: Sedimentology, v. 26, p. 203-228.

14. Introduction to Carbonate and Evaporite Facies Models

Noel P. James, Department of Geological Sciences, Queen's University, Kingston, Ontario K7L 3N6

Alan C. Kendall, School of Environmental Sciences, University of East Anglia, Norwich NR4 7TJ England

THE SEDIMENTS ARE BORN, NOT MADE

This deceptively simple phrase encapsulates the main theme of carbonate and evaporite sedimentation. It also highlights the differences between such deposits and the terrigenous clastic facies described in preceding chapters. Terrigenous clastic sediments are made primarily by the disintegration of parent rocks and are transported to the depositional environment. Once there, patterns of texture and fabric are impressed upon them by the hydraulic regime. The signatures of such facies are in their sedimentary structures and grain-size variations (Table 1). Carbonate and evaporite sediments are "born" as precipitates or skeletons within the depositional environment. For carbonate sediments, this attribute has profound consequences, namely 1) sediment composition is fundamental in characterizing the depositional environment, 2) grain size variations need not signal changes in hydraulic regime, 3) large structures such as platforms are produced entirely by sediments formed in place, they are self-generating and self-sustaining, 4) the temporal and spatial style of accumulation depends upon the nature of the sediments themselves. Consequences for evaporites include: 1) mineralogy reflects the type of water being evaporated and the salinity of bottom brines, 2) many sediments are never transported but grow in place, at or below the sediment surface, and 3) most are shallow water (<10 m) or pelagic deposits.

As carbonate sediments and facies have become better understood over the last two decades (Bathurst, 1975; Wilson, 1975; Scholle *et al.*, 1983), attention has shifted to the dynamics of sediment accumulation. Compilations for evaporites have appeared more recently (Dean and Schreiber, 1978; Sonnenfeld, 1984; Schreiber, 1988; Warren, 1989; Melvin, 1991). The library of modern and ancient examples has grown to the point where true comparative sedimentology can now be practised, revealing previously unrecognized, universal themes in sedimentation. Nevertheless, as illustrated in the following chapters, consensus has yet to be reached on many fundamentals of sediment dynamics.

Dynamic stratigraphy demands that the input distilled from modern and ancient environments should be as fully understood as possible. Problems arise for some carbonates because the ecology of extinct rock-forming organisms may not be fully known. These difficulties are even more prevalent for evaporites because many have no Holocene analogue.

In the following chapters the facies are considered first and then placed in an allostratigraphic context. In many instances evaporites are a minor, but nevertheless important, component of other facies models, e.g., interdune evaporites in eolian facies, coastal sabkhas in carbonate or siliciclastic peritidal facies. However, when evaporites and evaporitic carbonates fill entire basins, or evaporites form laterally extensive shelf deposits, they warrant separate facies models (see Table 2 in Chapter 19). This introduction summarizes themes important to all carbonate and evaporite accumulations.

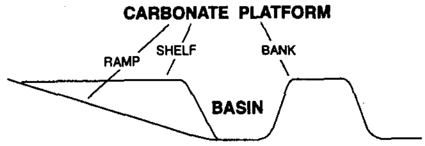

Figure 1 A sketch showing the different geometries of platforms and their terminology. No scale is intended.

SOME TERMINOLOGY

Words used to describe carbonate and evaporite accumulations vary greatly, as do their meanings (Ginsburg and James, 1975; Wilson, 1975; Read, 1985; Geldsetzer *et al.*, 1988). Although they can form across the environmental spectrum, the thickest carbonates accrete as platforms while the thickest evaporites form as basinal deposits. To maintain continuity, the following section defines the terms used in this book.

Platforms

A *carbonate platform* (Fig.1) is a large edifice formed by the accumulation of sediment in an area of subsidence. Most such structures have a flat top, possess steep sides and can be several kilometres thick and extend over many hundreds of square kilometres. A *carbonate shelf* is a platform tied to an adjacent continental land mass. This hinterland is a potential source of terrigenous clastic sediment, fresh water, terrigenous organic matter and nutrients. A craton many hundreds to thousands of kilometres across is called an *epeiric platform* when covered by shallow seawater. A *carbonate bank* is an isolated platform surrounded by deep ocean water and cut off from terrigenous clastic sediments. (Note that here "bank" is not synonymous with mound — a smaller, reef-like carbonate body that may lack definitive evidence of an organic framework, see Chapter 17). A *carbonate atoll* is a specific type of bank developed on a subsiding volcano. Similar banks, unrelated to volcanoes, are termed *faros*. Atolls and banks can be so dominated by reefs that their geological expressions are termed *reef complexes* or *carbonate buildups*.

The platform edge is critical. A *rimmed platform* (Fig. 2) has a segmented to continuous rampart of reefs and/or lime sand shoals along the margin that absorbs ocean waves. Modern warm water platforms are generally rimmed because corals are prolific and construct large reefs along the edges of shelves and banks. By absorbing waves and swells and dissipating storm energy, the rim generates a variety of lower energy environments. It also confines the movement of coarse-grained sediment to the lagoon/shallow platform and can potentially restrict water circulation, increasing the possibility of evaporites. Accumulation space is limited by sea level and carbonate facies are strongly differentiated.

An *unrimmed* or *open platform* (Fig. 2), is one in which there is no barrier. Unrimmed platforms occur today on the leeward side of large tropical banks and are the norm in all cool water settings. A *ramp* is an unrimmed shelf that slopes gently basinward at angles of less than 1 degree. Nearshore, wave-agitated facies grade into deeper water, low-energy deposits and there is no discernable break in slope. Because oceanic waves and swells can sweep directly onto and across the shallow seafloor of open shelves and ramps, 1) the energy level of most shallow water environments is high, 2) nearshore facies are complex, 3) sediment can easily be transported into deep water, 4) only the nearshore zone can keep pace with sea level rise, and 5) subtidal accumulation space will be controlled as much by the depth of wave abrasion as by sea level (Chapter 15). Since unrimmed platforms and ramps are affected by the same physical processes as terrigenous clastic shelves (Chapters 11, 12), they have similar facies. What sets them apart is the continual in place production of carbonate sediment and early cementation, which constantly alters the nature of the sea floor.

Lagoons and widespread shallow platforms may become restricted and hypersaline. Widespread shelf evaporites that pass basinward into open marine sediments are confined to rimmed platforms (Fig. 3). The absence of restrictive barriers on unrimmed platforms limits evaporites to marginal sabkha and associated salina deposits. In situations where the entire depositional basin is evaporitic, however, *evaporitic shelves* may occur without platform edge barriers. Theoretically, evaporite ramps could occur around evaporite basins; however, not one has been confidently identified. This is probably because rapid evaporite accumulation is restricted to shallow brines. Evaporites are either confined to marginal shelves built on the shallowest parts of older ramps, or they form on the deepest parts, when the adjacent basin desiccates.

Basins

Deep water environments are only significant repositories for carbonate sediment in post-Jurassic time, when pelagic calcareous microorganisms evolved. These planktonic foraminifera, green algae and tiny gastropods live in the upper parts of the water column and upon death sink to the seafloor as a pelagic rain (Fig. 2). Older basinal sediments are primarily terrigenous clastic or siliceous, with

Table 1 *Differences between terrigenous clastic, carbonate and evaporite sediments.*

Terrigenous Clastic	Carbonate	Evaporite
Climate is no constraint, sediments occur worldwide.	Most sediments occur in shallow, warm water environments.	Most sediments occur in shallow-water or mud flat environments.
Sediments are both terrestrial and marine.	Sediments are mostly marine.	Sediments occur only in restricted terrestrial and marine environments.
Grain-size reflects hydraulic energy of the environment.	Grain-size reflects the size of skeletons and precipitated grains.	Crystal size reflects nucleation and growth rate, or diagenetic alteration.
Mud indicates settling from suspension.	Mud commonly indicates prolific growth of organisms that produce tiny crystals.	Fine carbonates/sulphates indicate rapid precipitation.
Currents and waves form shallow-water sand bodies.	Many sand bodies form by localized physicochemical or biological production of carbonate.	Shallow-water sand bodies are rare.
Environmental changes are induced by widespread changes in hydraulic regimen.	Environmental change can be induced by localized buildup of carbonate, without change in hydraulic regimen.	Environmental change is induced by changes in basin dynamics.
Sediments remain unconsolidated in the depositional environment.	Sediments are commonly cemented on the seafloor.	Sediments are commonly cemented or form crystal crusts in the depositional environment.
Periodic exposure does not alter the sediments.	Periodic exposure results in intensive diagenesis.	Periodic exposure results in growth of intrasediment evaporites or wholesale dissolution.
Walther's law applies to most deposits.	Walther's Law applies to many, but not all, deposits.	Walther's law applies to few deposits.

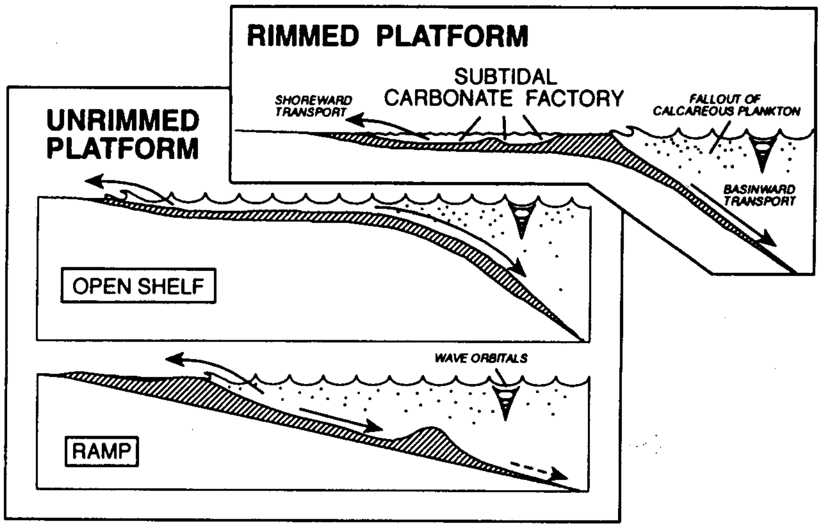

Figure 2 A sketch of rimmed and unrimmed platforms illustrating the position of the carbonate factory and the main directions of sediment transport. Note that open ocean waves and swells impinge on open shelves and ramps but are absorbed at the edge of the rimmed platform. Offshore banks are the same as these shelves and can have rimmed (generally windward) and unrimmed (generally leeward) margins.

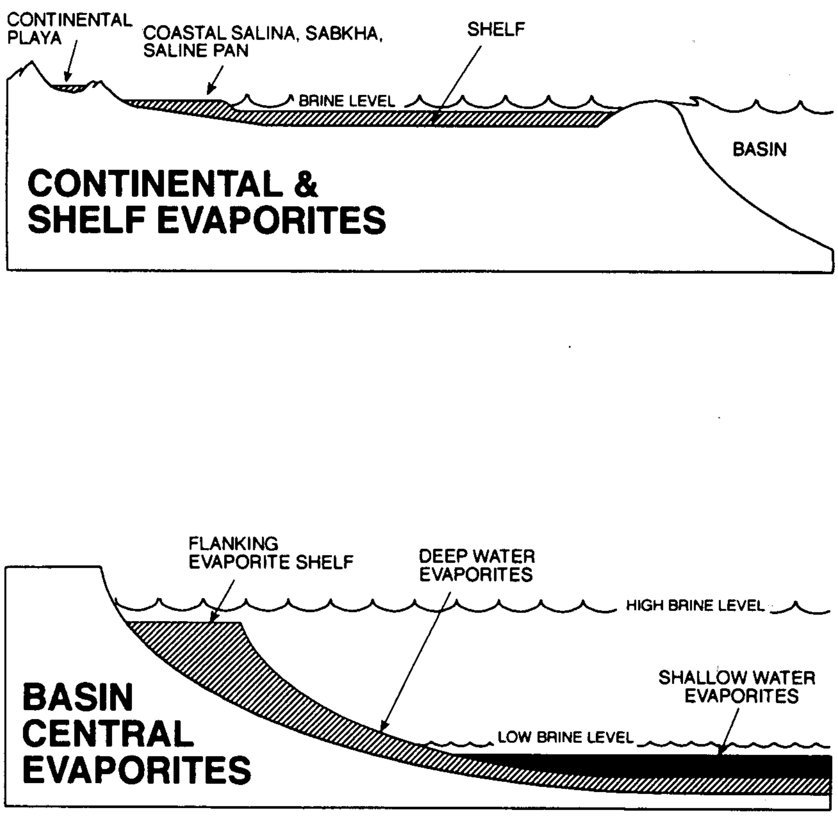

Figure 3 A sketch illustrating locations of the evaporite factory and resulting facies in continental, shelf and basin-central locations. Continental playa evaporites can be extremely large. Basin-central evaporites form as basin-margin shelves and deep water deposits when brine level is high and as shallow water deposits when brine level is low.

the only carbonate input coming from shallow platforms.

All large and thick evaporites occupy depositional basins that suffered partial or complete desiccation during isolation from the sea. Such *evaporite basins* can be flanked by *evaporitic shelves,* or alternatively, earlier carbonate shelves that become emergent during evaporitic episodes (Fig. 3). Evaporites cease to form during periods of flooding and the same basins become open- or restricted-marine environments.

THE SEDIMENT FACTORY

Carbonates

The *carbonate factory* (Fig. 2) is the shallow, illuminated seafloor. Particles of all grain sizes are born here, either crystallizing as skeletons or precipitating directly out of seawater. Sediments mostly remain in place forming widespread "subtidal" deposits (Chapter 15) or reefs and mounds (Chapter 17). Much of the abundant fine fraction is resuspended periodically and piles up as muddy peritidal flats against highs on the platform and along the shoreline (Chapter 16). Fine sediment is also swept seaward where, together with sediment gravity flows originating at the margin, it accumulates on the slope and on adjacent basin margin (Chapter 18). Regardless of facies, it is the factory that is at the core of carbonate deposition. All carbonate facies and carbonate stratigraphy depend on the "health" of this production unit.

Evaporites

The *evaporite factory* (Chapter 19) can operate in both terrigenous clastic and carbonate settings (Fig. 3). Evaporites similarly accumulate most rapidly in shallow water conditions. Export of sediment from this evaporite factory does occur, but it is substantially less than in carbonate settings because so much of the sediment is lithified initially, or quickly becomes cemented. Environments (see Table 2 in Chapter 19) range from continental lakes to coastal salinas and sabkhas to shelf-wide complexes. Evaporites can also develop in shallow- and deep-water basin centres.

The advantage of modelling evaporite systems is that deposition occurs by physico-chemical precipitation.

The original overall composition and mineralogy of an evaporite provide information about the type of water being evaporated, the brine temperature and salinity, and the degree of basin isolation. The disadvantages occur because, 1) most early models were chemical in nature and/or based upon few examples, 2) evaporites exposed in outcrop (uncommon) are much altered, and subsurface core is limited, 3) no areas of present-day evaporite deposition compare in size with many ancient basins (Fig. 4), 4) changes in depositional conditions are rapid, profound and commonly result in superimposed facies, making original environmental recognition difficult, 5) characteristically, new environments destroy and replace older ones, rather than moving laterally, so that associated facies are unreliable when interpreting poorly preserved deposits, and 6) evaporites are susceptible to wholesale, postdepositional change that can remove all primary features.

THE CONTROLS

For carbonate production and sediment accumulation to be at a maximum, the environment must be just right; not too deep, not too shallow; not too warm, nor too cold; not too fresh, but not too saline either; not too much terrigenous clastic sediment; not too many nutrients but neither too few (the *Goldilocks Window* of Goldhammer *et al.*, 1990). A similar depositional "window" controls evaporite accumulation. Water inflow must not be too much, nor too little: brine loss (reflux) must be allowed to occur, but must not be too great; evaporation rates must be high, but terrigenous clastic influx must be low. The principal regulators are climate, oceanography (including basin and/or shelf restriction) and tectonics, but for most carbonates, organism biology is the major factor.

Organism biology

Most carbonate sediments are produced biologically or by biochemical mediation. There are four sorts of carbonate particles: 1) *precipitates* – those grains formed by direct or biologically mediated precipitation of calcium carbonate, e.g., ooids and some lime mud; 2) *bioclasts* – the calcareous sheaths, shells, tests and spicules of the myriad of sessile, burrowing, drifting or swimming invertebrates, microbes and algae that live in shallow and deep water across the environmental spectrum; 3) *peloids* – grains of microcrystalline carbonate, generally agglutinated or cemented feces or diagenetically altered grains; and 4) *lithoclasts* – fragments of consolidated, hardened or lithified sediment. Precipitates around, and skeletons of, phototrophic organisms are particularly important because they rapidly produce enormous amounts of sediment. Such organisms are mostly photosynthetic microbes and algae, or invertebrates such as living stony corals, giant clams and big foraminifers, which have symbiotic phototrophs (light-dependent microorganisms) in their tissue. These symbionts, by taking over metabolic functions, allow otherwise small- or modest-sized invertebrates to precipitate large calcareous skeletons, but restrict such organisms to the photic zone. This bargain, large size for light dependence, restricts carbonate deposition to very specific settings.

We rely heavily upon observations from modern environments of deposition to interpret ancient sedimentary sequences and to construct facies models. This approach works, and is seen to work, because the composition of most sedimentary particles has remained the same through time; a quartz sand grain or an ooid is the same in the Pleistocene, Permian or Precambrian. Because organisms have changed with time, it is difficult, at first glance, to compare modern and specific ancient carbonate facies. This tends to intimidate those who are beginning the study of carbonates, but it should not. Carbonate-secreting organisms in the rock record, when viewed as sediment producers, do have living counterparts, although they may not even belong to the same phylum. Thus "carbonates are like Shakespeare; the plays remain the same, only the actors change". This is because, despite the numerous groups of organisms with hard parts, there are only two ways in which these hard parts are arranged either as whole, rigid skeletons (e.g., foraminifers, snails, corals) or as numerous individual segments held together in life

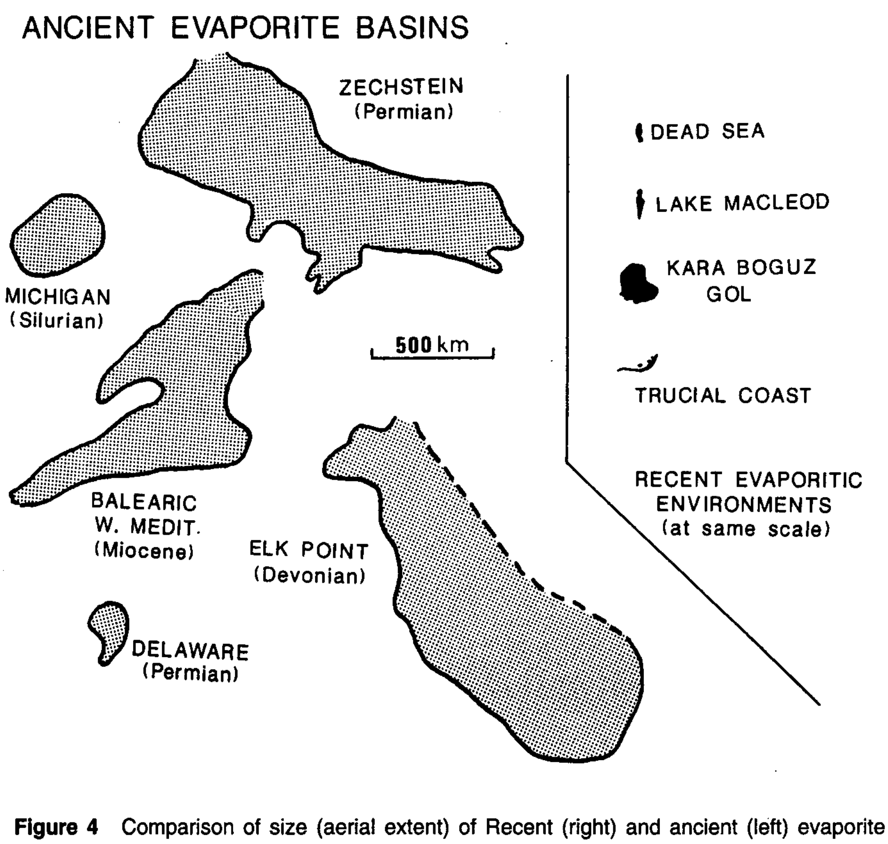

Figure 4 Comparison of size (aerial extent) of Recent (right) and ancient (left) evaporite settings.

by organic matter (e.g., trilobites, clams, crinoids). Table 2 lists the more important modern *carbonate* components and their fossil equivalents.

The sedimentology of organism remains should not be equated with their paleoecology. Evolution of the "modern" carbonate-producing community was gradual and took place in the Mesozoic. The shallow water Paleozoic brachiopod/echinoderm/tabulate and rugose coral/stromatoporoid/red algal assemblage was replaced by a green and red calcareous algae/scleractinian coral/mollusc/foraminiferal consortium. Many survivors from the Paleozoic era, such as the crinoids, stromatoporoids (sclerosponges), brachiopods and bryozoans, are still with us, but are abundant only in deep or cool, or less saline settings. Interestingly, these refugees (together with barnacles) produce most of the sediment on many modern cool water platforms.

But organisms are not just sediment producers. Grasses and microbes of various sorts are efficient sediment trappers, binders and stabilizers. Ichnofauna burrow through the sediment, moving and sorting particles, ingesting, processing and excreting sediment, forming grains (peloids) and diagenetically altering fine particles. A boring flora and fauna excavates into grains and hard substrates, and in the process breaks down the carbonate host and produces sediment. Large skeletons form elevations above the seafloor and create new environments. The carbonate platform is truly a living thing and, as the biosphere has evolved, its character has varied through geologic time.

Evaporitic environments are rarely completely lifeless, although hypersalinity does reduce organism diversity to low levels. Carbonate-secreting organisms are eliminated early in brine concentration so that almost all subsequent precipitation is inorganic. In the initial stages, however, microbes thrive within the brine and on the sediment bottom. Evaporitic sediments can be greatly modified by this addition of organic material, or by the binding and trapping activities of benthic microbial mats.

Climate

Evaporites are more sensitive to climate than any other sediment type. They provide unequivocal evidence of arid, but not necessarily warm, conditions (they occur in Antarctic playa lakes). Nevertheless, almost all ancient evaporites formed in warm climates because, when the atmosphere is undersaturated, more evaporation

Table 2 *The sedimentary aspect of modern warm and cool water carbonate components and their counterparts in the fossil record.*

Modern, Warm Water	Modern, Cool Water	Ancient Counterpart	Sedimentary Aspect
Corals	ABSENT	Corals, Stromatoporoids, Stromatolites, Coralline Sponges, Rudist Bivalves	Large components of reefs and biogenic mounds
Bivalves, Red Algae, Echinoderms	Bivalves, Red Algae, Brachiopods, Echinoderms, Barnacles	Red Algae, Brachiopods, Cephalopods, Trilobites	Remain whole or break apart into several pieces to form sand and gravel size particles
Gastropods, Benthic Foraminifera	Gastropods, Benthic Foraminifera	Gastropods Benthic Foraminifera	Whole skeletons that form sand and gravel size particles
Green (Codiacean) & Red Algae	Red Algae Bryozoans	Phylloid algae, Crinoids and other echinoderms, Bryozoans	Spontaneously disintegrate upon death to form many sand-sized particles
Ooids, peloids	ABSENT	Ooids, peloids	Concentrically laminated or micritic sand sized particles
Planktonic Foraminifera, Coccoliths, Pteropods	Planktonic Foraminifera, Coccoliths, Pteropods	Planktonic Foraminifera, Coccoliths (post-Jurassic), Styliolinids	Medium sand-sized and smaller particles in basinal deposits
Encrusting Foraminifera, Red Algae, Bryozoans	Encrusting Foraminifera, Red Algae, Bryozoans, Serpulid Worms	Red Algae, Renalcids, Encrusting Foraminifera, Bryozoans	Encrust on or inside hard substrates, build up thick deposits or fall off upon death to form sand grains
Dasyclad Green Algae	ABSENT	Dasyclad Green Algae	Spontaneously disintegrate upon death to form lime mud
Cyanobacteria and other calcimicrobes	Cyanobacteria and other calcimicrobes	Cyanobacteria and other calcimicrobes (especially pre-Ordovician)	Trap, bind and precipitate fine-grained sediments to form mats and stromatolites or thrombolites

occurs at higher temperatures.

Aridity is also prevalent in 1) *mountain-bounded basins at any latitude*, because the mountains act as rainfall-snowfall traps and barriers, resulting in basin-floor, rain-shadow deserts, 2) *continental areas in low to middle latitudes isolated from the ocean*, where temperatures are high and humidity low, creating high evaporation rates capable of generating brines that can even precipitate potash salts, and 3) *regions adjacent to cool, upwelling oceanic currents* which generate cool onshore winds with high humidity but low moisture content. These winds warm as they move inland, lowering their humidities and promoting evaporation.

The general climatic setting also partly controls the rate at which terrigenous clastic sediments are delivered to a shelf or basin by fluvial and eolian processes. This siliciclastic influx can partially or completely suppress the production of carbonate by 1) reducing water transparency, 2) clogging the feeding and/or respiratory apparatus of sessile benthic organisms and/or, 3) increasing nutrient and particulate organic content of the water. Reefs, in particular, can grow in nutrient-poor environments (Chapter 17). An increase in nitrates and phosphates can lead to displacement of coelenterates by filamentous algae and a dramatic increase in bioeroders (Hallock and Schlager, 1986). Climate also controls the amount and rate of evaporation or rainfall, and thus the composition of seawater, in shallow, partially restricted basins on or alongside continents. Furthermore, climate controls the "storminess" of the ocean and whether high energy is constant or episodic.

Oceanography

The ocean is inexorably linked to the atmosphere and climate, but there are inherent attributes which directly affect carbonate productivity.

Light penetration

Light penetration, which controls the phototrophs, varies with water depth, latitude (controls light refraction into the water) and water clarity. The last is markedly reduced where turbidity is high as a result of clastic runoff, particularly on west sides of tropical/subtropical oceans, or upwelling and high surface productivity above outer parts of platforms on eastern sides of oceans (Zeigler *et al.*, 1984). Carbonates have restricted distributions at these sites.

Water temperature

In open ocean situations there is a clear temperature stratification. Warm to cool surface waters extend down to −50 or −100 m, below which there is a decrease in temperature (thermocline). The deep ocean below about 1000 m is close to zero degrees. A similar stratification can be present in enclosed basins and shallow seas, but the temperature in many of them, especially if estuarine circulation is developed, is roughly the same from surface to seafloor.

A water temperature of about 20°C partitions carbonates in modern shallow seas into a warm water, low-latitude realm and a cool- to cold-water mid- to high-latitude realm. Carbonates of all types are produced on warm water platforms but such settings are dominated by direct precipitates and particles from phototrophic organisms. The photic zone is about 70 m deep in most places and it is in this zone that carbonate production is highest, being greatest in the upper 10-20 m. On modern *cool water platforms* the photic zone is of lesser importance because carbonates are generated almost entirely by nonphototrophic organisms; the only important phototrophs are coralline algae. The rates of sedimentation also seem to be much lower. Sediments which accumulate in deeper, cooler water parts of modern warm water platforms are much like those at higher latitudes. Whereas warm and cool water platforms have been differentiated in Cenozoic and Mesozoic sequences, their recognition in Paleozoic and Precambrian carbonates, although claimed, is less certain.

Water circulation

Unrimmed shelves and ramps have free circulation and open marine conditions are the norm. Fine-grained carbonates, suspended by storms and by organism activities, may be carried from where they form to quieter or deeper environments. Rimmed shelves commonly have poorer circulation and fine-grained sediment transport is curtailed. Carbonates are typically muddy, even in shallow environments subject to frequent high-energy storms. Furthermore, poor water circulation results in departures from oceanic water composition. Freshwater inflow into restricted shelves causes brackish conditions nearshore, or even bottom anoxia where persistent density stratification results. In arid climates, restricted shelves become hypersaline. For evaporites to form, however, the degree of restriction required is extreme (Lucia, 1972; Kendall, 1988), to the extent that large evaporite deposits are confined to basins that become isolated or nearly isolated from the open sea. Evaporative losses in such basins are not offset by inflow, and the water level drops below sea level; a process termed *evaporative drawdown*. Some interpretations of ancient, widespread and shallow cratonic seas (Shaw, 1964; Irwin, 1965) conclude that poor water circulation was the norm and resulted primarily from salinity variation, tidal and other currents being suppressed by friction.

Oxygenation

Because well-oxygenated waters are essential for the growth of skeletal invertebrates, any decrease in dissolved oxygen values reduces the diversity and then the abundance of such organisms in a predictable way. Partial to complete anoxia can be induced by 1) a stratification of the water column by pronounced temperature and/or salinity layering, reducing or arresting vertical mixing, or 2) a dramatic increase in nutrient supply to surface waters resulting from increased runoff or upwelling of deep ocean waters.

Salinity

Increasing salinity reduces biotic diversity (Chapter 15) (although this commonly is difficult to differentiate from the effects of fluctuating salinity) and above 40‰ most invertebrates disappear; calcareous algae, however, continue to be sediment producers for a time. Occasionally, tolerant skeleton-producing invertebrates thrive in salinities too high for calcareous mud-producing algae. These shells may accumulate in enormous numbers, as in Shark Bay (Western Australia). This serves as a reminder that not all hypersaline carbonates are muddy. The amount of carbonate generated by direct precipitation, however, increases with increasing salinity and the sediments grade insensibly into fine-grained evaporitic carbonates.

Tectonics

The tectonic setting controls the rate and style of subsidence and the nature of the foundation upon which a carbonate platform nucleates or on which evaporites accumulate. The effect of antecedent topography is most obvious during the early stages of rifting. Carbonate platforms nucleate on horsts and/or evaporites accumulate in grabens. On newly rifted, passive continental margins the rate of subsidence is predictable. Any changes in these rates occur slowly. Intracratonic basins have the same subsidence style and rate as mature passive margins. Thus, the space for sediment production and accumulation has been similar in these settings throughout geologic time. Platforms and ramps on the inboard side of foreland basins, toward the craton, have similar subsidence rates, but the style is more irregular and less predictable. Both subsidence and uplift occur as the basin responds to lithospheric flexure. Carbonate structures and evaporite accumulations in strike-slip basins and/or on thrust complexes are affected by unpredictable episodic and dramatic subsidence.

Paleotectonic setting also determines the nature of the adjacent hinterland and therefore, in part, the rate of terrigenous clastic sediment supply to the shelf or basin. Too much clastic sediment will "drown out" the carbonate or evaporite contribution. Finally, because platforms and basins are on moving tectonic plates, they may drift out of latitudes where carbonate/evaporite accumulations are favoured. Carbonate platforms may move out of a low-latitude, warm water belt and the sediments change to those dominated by cool water invertebrates, with lower accumulation rates. Alternatively, carbonate deposition may be replaced by terrigenous clastics as the platform moves into a more humid climatic belt. Similarly, evaporitic basins may be transported away from areas of negative water deficits so that evaporite accumulation ceases and either terrigenous clastics or carbonates take their place.

Carbonate platforms are most frequent along passive continental margins as 1) small banks atop horsts on newly rifted crust, 2) huge shelves along mature margins, 3) giant offshore banks, which continue to grow and coalesce as antecedent rift-blocks are buried, and 4) atolls around oceanic volcanoes. They are also familiar as 5) shelves around the margins of, and as banks within, shallow intracratonic basins. Although not as common on convergent margins, they do form irregular banks and shelves encircling fragmented and obducted tectonic slivers. Ramps are prevalent as the initial or foundation stages of rimmed platforms or as structures in their own right during geological periods when there were few large skeletal organisms to build reefs and form a rim. They occur most frequently in intracratonic basins or along the inner, craton side of foreland basins.

Apart from climatic control, large evaporite deposits only form in 1) hydrologically closed sedimentary basins in which outflow is less than inflow, 2) originally deep depressions, or areas which subside rapidly during evaporite accumulation, and 3) settings starved of terrigenous clastic sediment. Three types of basins are particularly susceptible to restriction and therefore potential sites of evaporite precipitation (Kinsman, 1974).

Intracratonic basins are long-lived, with active subsidence histories of tens of millions of years. Evaporite deposition tends to be episodic and superimposed so that evaporites are sandwiched between other sediment types. Although aerially extensive, the evaporites are typically thin (tens to hundreds of metres). If the evaporites are marine-derived, calcium sulphates are over-represented relative to halite. Some basins accumulate nonmarine evaporites. Evaporitic intervals are episodic and superimposed. Facies consist of shallow water and mud flat sequences (with both shelf and basin-central distributions) but episodes of basin starvation, together with subsidence, may generate depositional basins with several hundred metres of relief, in which "deep water" evaporites can accumulate.

Divergent plate margin basins occur within continental rift valleys, juvenile actively spreading oceans, and failed rifts (aulacogens). Evaporites can be thick, exceeding 5 km in many instances. They are generally composed of halite but also may contain $MgSO_4$ deficient potash salts. Such compositions suggest the influence of hydrothermal fluids, either as the source of the evaporites or substantially modifying the seawater source (Hardie, 1990). Where continued spreading has generated wide oceans, evaporite deposition essentially ceases and the older evaporites now occur as linear belts along the newly formed passive continental margins.

Remnant ocean basins at convergent plate boundaries, under appropriate conditions of restriction and climate, can change into enormous and deep evaporite basins. Desiccation of these basins, under conditions of intense evaporative loss, may create shallow water environments several kilometres below world ocean level. These are situations that have no parallel today.

AUTOSTRATIGRAPHY

Once carbonate and/or evaporite production begins in earnest the sediments accumulate by vertical and/or lateral accretion. *Vertical accretion* typifies carbonate and evaporite systems, in that sediments are produced in place and so, with time, inexorably build up toward sea level, (or the local brine level in a desiccated evaporite basin) even though they may never reach it. Shallowing-upward is inherent in the carbonate system and is common in evaporite settings. *Lateral accretion* of carbonates occurs because the factory is too shallow to retain the sediments or because they are piled up against a shoreline, forming a prograding sedimentary wedge. Whereas both lateral and vertical accretion will occur on a carbonate shelf, vertical accretion is probably more typical on carbonate banks (because there are few highs around which strandline facies can nucleate) and in large evaporite basins. Walther's Law is clearly applicable to lateral accretion but may not always apply during vertical accretion, because new environments may be created simply by shallowing or restricting water movement. If exposed, carbonate and evaporite platforms will be subject to diagenesis in the meteoric realm, the nature and extent of which depends upon both intrinsic (mineralogy, previous history, porosity) and extrinsic (climate, time) factors (James and Choquette, 1990).

Since carbonate and evaporite production and accumulation are predominantly shallow water phenomena and the controls are dynamic, the depositional systems are always in imminent danger of being shut down. For carbonates this occurs by intersecting, or being intersected by a critical interface that limits deposition. Such interfaces are 1) air/water (exposure and shutdown of all carbonate production), 2) base of photic zone (the demise of phototrophic organisms), 3) base of the zone of wave abrasion (above which bottom currents and wave action may lead to erosion and cementation), 4) O_2 minimum zone (extinction of all higher plants and animals), 5) thermocline (water is too cold for most carbonate-producing organisms), 6) pycnocline (the salinity is too great for most organisms). These interfaces cause the *bounding discontinuities* and are responsible for the conspicuous packaging of carbonate facies successions. Changes in the water balance within evaporitic settings are commonly fast, and result in equally abrupt vertical changes in evaporite mineralogy and brine depth (and consequent evaporite facies). This may also lead to cessation of evaporite deposition or its sudden appearance.

ALLOSTRATIGRAPHY

Space for accumulation must be created in order for deposition to continue, even if sediment is being produced at a rapid rate. For carbonate systems, this *accumulation* space is that space available for deposition between the seafloor and any critical interface. This is where the combined effects of the controls come into play in a dynamic way. The principal variables that determine the size of this space through time are the rates of 1) subsidence, 2) eustasy, 3) sedimentation (carbonate, evaporite and siliciclastic), and 4) for evaporitic systems, brine-level suppression below sea level. Excellent discussions of the interaction of these variables in carbonate systems are found in Kendall and Schlager (1981), Tucker and Wright (1990), Goldhammer *et al.* (1990) and Einsele *et al.* (1991), whereas evaporite systems are discussed in Kendall (1988).

The concepts of seismic and sequence stratigraphy were developed using the principles of terrigenous clastic sedimentation (Vail *et al.*, 1977; Van Wagoner *et al.*, 1988). Carbonates and evaporites have only recently been interpreted using these techniques (Sarg, 1988; Tucker, 1991). There is currently no consensus as to the response of sedimentation to eustasy largely because the same principles of sedimentation do not generally apply to both terrigenous clastics and carbonates/evaporites. Again, it is the same problem — there is no in situ factory for terrigenous clastics. Eustatic changes affect terrigenous clastic systems by controlling accumulation space and hence shifting the locus of sedimentation from one site to another. Eustatic changes in carbonate and evaporite systems determine the health or very existence of the sediment factory.

Such differences affect the dynamics of sedimentation, and thus allostratigraphy. To illustrate this point we generalize and contrast sedimentation on a terrigenous clastic shelf and basin with that on a rimmed carbonate shelf and basin, during a long-term (third-order) fluctuation in relative sea level with superimposed short-term (fourth- and fifth-order) perturbations (Fig. 5). A cautionary note — these are end members and if similar comparisons are made between terrigenous clastic shelves and carbonate ramps or open shelves, the differences are less pronounced. Evaporites are not restricted to either setting but have been placed mostly in the carbonate example because they are commonest there.

Lowstand systems tract

Terrigenous clastics. Sediments bypass the exposed shelf and are deposited in deep water on the slope and basin margin. Sand-rich submarine fans, fed from fluvial systems which cross the shelf, form at the base of slope during early stages of sea level fall. Later phases are characterized by initial filling of incised valleys on the shelf and the formation of mud-prone lowstand wedges on the slope and on top of earlier submarine fans.

Carbonates. Exactly the opposite occurs. The carbonate factory is shut down, or confined to a small fringing shelf on the slope. The adjacent slope and basin are thus starved of carbonate sediment, except for planktonic carbonate, and then only in Jurassic and younger settings. A contrasting view (Jacquin *et al.*, 1991) suggests that the narrow shelf is a source of much sediment and deep water sedimentation is active. Offshore banks or shelves bordering a carbonate hinterland are subject to subaerial diagenesis, the intensity of which depends upon climate, relief (extent of sea level fall), time of exposure and original mineralogy, resulting in a karst subaerial unconformity bounding surface. When shelves border a landmass of terrigenous clastic sediments, although subaerial diagenesis is common, they are also likely to be veneered by prograding fluvial deposits that can spill over the shelf edge, creating a terrigenous clastic lowstand fan or wedge. This results in alternating carbonate and terrigenous clastic sediments on the shelf and in the basin (Chapter 3).

Evaporites. Basin-central evaporites, often of great thickness, are characteristic when basins become isolated or greatly restricted by lowered sea level. The extent of water-level drop is greatly magnified by evaporative drawdown. Brines in basins that experience only partial drawdown rarely reach halite saturation and are characterized by marginal gypsum wedges and basinal, deep water laminated gypsum/evaporite carbonates (Tucker, 1991). Basins subject to nearly complete desiccation have shallow water mud flat evaporites on the basin floor. Such deposits are typically dominated by halite and can contain some of the more soluble potash salts. Because evaporite deposition occurs in near isolated environments, the elevation of the basin rim (relative to sea level), rather than the elevation of the depositional site, is of primary importance, While slight drops in sea level can allow basins to desiccate, slight rises may drown basins and quickly eliminate evaporite deposition altogether. Evaporite accumulation also causes onlap of the basin flanks, unrelated to sea level rise.

Transgressive systems tract

Terrigenous clastics. Incised valleys on the shelf are filled and estuarine sedimentation accompanies flooding. There is a rapid landward shift in facies belts, little widespread shelf deposition and the slope and basin are largely sediment starved, culminating in a maximum flooding surface.

Carbonates. In contrast, this period of long-term relative sea level rise allows the carbonate factory to operate at optimum capacity, slowed only by short periods of incipient drowning. Migration of an oxygen-minimum zone onto the platform can also cause periodic shutdown. Progressive addition of new accumulation space results in the infilling of previous topography, accumulation of thick, subtidal-dominated sediment packages and growth of reefs. Amalgamated subtidal units are common. Vertical sediment accretion or facies backstepping is the typical mode of sedimentation. Reefs, which have the greatest potential of all carbonates to track sea level rise (because of their relatively high growth rates), can build exceptionally high (stratigraphically thick) reliefs. The amount of off-platform sediment transport depends upon the effectiveness of the rim and the rates of carbonate sediment production. Prograding carbonate and/or evaporite tidal flats do not generally reach the shelf edge and can be stranded during short-term sea level changes. A maximum flooding surface can cap the transgressive systems tract. The condensed section develops when parts of the platform fall so far below the base of the photic zone that carbonate production is reduced dramatically or stops entirely.

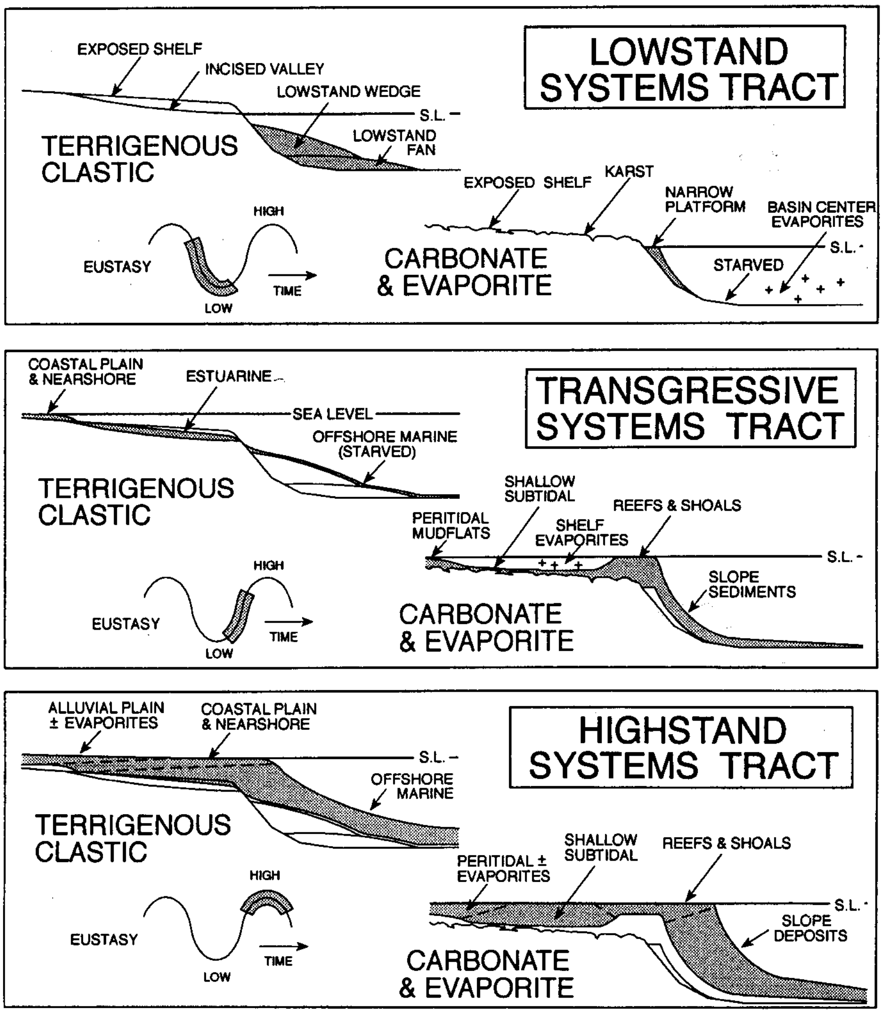

Figure 5 Diagrams illustrating the general sedimentary response of terrigenous clastic versus carbonate-evaporite shelves to long-term (third-order) changes in sea level. Shaded sequences formed during the indicated positions of sea level.

Evaporites. If the rim is continuous and well developed it can be a barrier to water circulation. Short-term fourth- or fifth-order sea level falls partially to completely restrict movement of marine waters onto the shelf, increasing the potential for shelf evaporites. Subtidal evaporites can develop only on the platform during these short-term, sea level falls, and will generally be confined to onshelf or onbank basins.

Highstand systems tract

Terrigenous clastics. Early phases encompass eustatic rise and stillstand while later phases record eustatic stillstand and the beginnings of sea level fall. There is general widespread shelf deposition. Aggradation typifies early stages and is usually succeeded by pronounced progradation. Depending upon the rate of sediment supply, the top of this systems tract can contain extensive fluvial and alluvial facies. Slope and basin sedimentation increase dramatically during late stages.

Carbonates. Carbonate and terrigenous clastic settings are most alike during this situation. The rate of addition of new accumulation space is low and under many circumstances periods of deposition alternate with roughly equal periods of exposure. The carbonate factory shrinks and becomes localized. During early stages antecedent depositional topography on the shelf is filled in. Reefs reach sea level and begin to expand laterally. Prograding tidal flat caps may periodically reach the shelf edge. Relatively short episodes of subaerial exposure result in moderate diagenetic change to carbonates.

During late stages, because the platform is essentially at mean sea level, the factory operates only intermittently, when flooded due to short-term changes in sea level. The main factory is at the shelf margin, producing a "shelf margin systems tract" (Sarg, 1988). Since accumulation space on the platform top is small, peritidal deposition is common. Few reefs develop and biostromes or sand shoals are the norm. The platform exports much sediment, especially from the margin facies, resulting in coarse-grained sediment-gravity flows and thick prograding or forestepping wedges of slope sediment. Sediments on the platform top are intensively altered by long periods of meteoric diagenesis.

Evaporites. Prograding alluvial and strandline terrigenous clastic facies can form isolated saline lakes on alluvial plains and salinas behind beach ridges. The reduced accumulation space and propensity for poor circulation on the carbonate platform top is ideal for thin shelf and peritidal evaporite accumulation. Diachronous units of sabkha and salina evaporites may be widespread. Under exceptional conditions of a rimmed platform, short-term falls in sea level may result in large hypersaline lagoons or shelves within which subtidal evaporites form. If the climate is arid and rimmed shelves are markedly restricted, widespread thin subtidal evaporites develop surmounted by thick peritidal evaporites.

CYCLICITY

The vertical, cyclic repetition of carbonate and/or evaporite facies is a hallmark of carbonate platforms and evaporite basins (Wilson, 1975; Kendall and Schlager, 1981; Algeo and Wilkinson, 1988). Carbonate cycles tend to record deposition in progressively shallower environments *(shallowing-upward)*; evaporites may display vertical changes in mineralogy indicating increasing salinity *(brining-upward)* or, less commonly, decreasing salinity *(freshening-upward)*. Cycles are m-scale to 100-m scale and their universality means that the mechanisms are either inherent in the system (autostratigraphic) or the platform is responding to some outside control (allostratigraphic) that has been present since Precambrian time, or both. The drive to produce a shallowing-upward, brining-upward or freshening-upward sediment package by either lateral or vertical accretion is inherent in the systems; what is much more difficult to determine is why and how numerous packages are stacked in a variety of different ways (Chapters 15, 16, 18, 19).

Thin evaporite units probably form in time intervals too short to have been markedly influenced by sea level changes. On the other hand, thicker, >0.1 km, evaporites are invariably compound units, commonly markedly cyclic. The delicate balance of influx, reflux and brine residence time that controls evaporite deposition is particularly sensitive to changes in sea level in marine-fed basins and evaporite shelves. It is therefore not surprising that sea level changes have been seen as controls of evaporite basin cyclicity. Climate, however, also controls the water balance in evaporite environments. Climate changes alone, or in combination with sea level changes, are also possible causes of evaporite cyclicity. Continental evaporites, particularly those forming in basins above sea level, will obviously respond only to climate (and tectonic) changes.

SUMMARY

Carbonate and evaporite facies, while controlled to a large degree by eustasy, are also defined and determined by the nature of the in situ sediment factory. They are therefore fundamentally different from terrigenous clastic sediments. This theme pervades the following chapters on carbonate facies models. Evaporite facies are treated in a single chapter. This is because they are differentiated on the basis of sedimentary features, and so independent of geographic setting and associated facies, carbonate or terrigenous clastic. Identification of environmental facies depends more on the stratigraphic relationship of evaporites to other facies and their distributions relative to depositional basins.

ACKNOWLEDGEMENTS

This introduction is much improved by the helpful and constructive comments of C.A. Cowan, R.G. Walker, P.-A. Bourque, M. Coniglio and G.M. Harwood.

REFERENCES

Basic sources of information

Bathurst, R.G.C., 1975, Carbonate sediments and their diagenesis: Amsterdam, Elsevier, 658 p.
Contains good summaries of carbonate components and their modern environments of deposition.

Crevello, P.D., Wilson, J.L., Sarg, J.F. and Read, J.F., eds., 1989, Controls on carbonate platform and basin development: Society of Economic Paleontologists and Mineralogists, Special Publication 44, 405 p.
Numerous articles on the response of different carbonates of various ages to intrinsic and extrinsic regulatory parameters — a good casebook.

Franseen, E.K., Watney, W.L., Kendall, C.G.St.C. and Ross, W., eds., 1991, Sedimentary modelling: computer simulations and methods for improved parameter definition: Kansas Geological Survey, Bulletin 233, 524 p.
Numerous studies modelling different carbonate depositional systems.

Kendall, A.C., 1988, Aspects of evaporite basin stratigraphy, *in* Schreiber, B.C., ed. Evaporites and hydrocarbons: New York, Columbia University Press, p. 11-65.
Contains sections dealing with basinal models, the inapplicability of Walther's law, and relations of evaporites to sea level changes.

Melvin, J.L., ed., 1991, Evaporites, petroleum and mineral resources: Amsterdam, Elsevier, 556 p.
Includes several excellent and exhaustive papers on non-marine, sabkha and shallow-water evaporites, some with excellent bibliographies.

Read, J.F., 1985, Carbonate platform facies models: American Association of Petroleum Geologists, Bulletin, v. 69, p. 1-21.
A succinct and important summary of the different types of platforms and ramps, with many examples — the best recent synthesis.

Schlager, W., 1981, The paradox of drowned reefs and carbonate platforms: Geological Society of America, Bulletin, v. 92, p. 197-211.
One of the first papers to critically look at the controls of platform development, an important place to start.

Scholle, P.A., Bebout, D.G. and Moore, C.H., eds., 1983, Carbonate depositional environments: American Association of Petroleum Geologists, Memoir 33, 708 p.
A beautiful synthesis of all carbonate (and some evaporitic) depositional environments, illustrated with colour photographs and diagrams — a critical source book for any student.

Schreiber, B.C., ed., 1988, Evaporites and hydrocarbons: New York, Columbia University Press, 475 p.
Compilation of papers covering evaporite stratigraphy and most aspects of marine-derived evaporites.

Warren, J.K., 1989, Evaporite sedimentology: Englewood Cliffs, Prentice Hall, 285 p.
Probably the best place to start; important because it discusses models for the origin of large-scale shelf and basinal evaporites.

Wilgus, C.K., Hastings, B.S., Posamentier, H.W., Ross, C.A. and Kendall, C.G.St.C., eds., 1988, Sea level changes: an integrated approach: Society of Economic Paleontologists and Mineralogists, Special Publication 42, 407 p.
Collection of papers emphasizing conceptual basis of sequence stratigraphy plus numerous case studies of sea level change from the geological record.

Wilson, J.L., 1975, Carbonate facies in geologic history: Berlin, Springer-Verlag, 471 p.
The single most important source of information on carbonate deposits of all ages, including thought provoking syntheses.

Other references

Algeo, T.J. and Wilkinson, B.H., 1988, Periodicity of mesoscale Phanerozoic sedimentary cycles and the role of Milankovitch orbital modulation: Journal of Geology, v. 96, p. 313-322.

Dean, W.E. and Schreiber, B.C., eds., 1978, Notes for a short course on marine evaporites: Society of Economic Paleontologists and Mineralogists, Short Course No. 4, 395 p.

Einsele, G., Ricken, W. and Seilacher, A. eds., 1991, Cycles and events in stratigraphy; Berlin, Springer-Verlag, 955 p.

Geldsetzer, H.H.J., James, N.P. and Tebbutt, G., eds., 1988, Reefs; Canada and adjacent areas: Canadian Society of Petroleum Geologists, Memoir 13, 775 p.

Ginsburg, R.N. and James, N.P., 1975, Holocene carbonate sediments of continental shelves, *in* Burke, C.A. and Drake, C.L., eds., The geology of continental margins: New York, Springer-Verlag, p. 137-155.

Goldhammer, R.K., Dunn, P.A. and Hardie, L.A., 1990, Depositional cycles, composite sea-level changes, cycle stacking patterns, and the hierarchy of stratigraphic forcing: examples from alpine Triassic platform carbonates: Geological Society of America, Bulletin, v. 102, p. 535-562.

Hallock, P. and Schlager, W., 1986, Nutrient excess and the demise of coral reefs and carbonate platforms: Palaios, v. 1, p. 389-398.

Hardie, L.A., 1986, Stratigraphic models for carbonate tidal-flat deposition, *in* Hardie, L.A. and Shinn, E.A., eds., Carbonate depositional environments, Part 3: Tidal flats: Colorado School of Mines Quarterly, v. 81, p. 59-73.

Hardie, L.A., 1990, The roles of rifting and hydrothermal $CaCl_2$ brines in the origin of potash evaporites, an hypothesis: American Journal of Science, v. 290, p. 43-106.

Irwin, M.L., 1965, General theory of epeiric clear water sedimentation: American Association of Petroleum Geologists, Bulletin, v. 49, p. 445-459.

Jacquin, T., Vail, P.R., Arnaud-Vanneau, A., Arnaud, H. and Ravenne, C., 1991, Systems tracts and depositional systems in a carbonate setting: a study of continuous outcrops from platform to basin on the scale of seismic lines: Marine and Petroleum Geology, v. 8, p. 122-139.

James, N.P. and Mountjoy, E.W., 1983, Shelf-slope break in fossil carbonate platforms, *in* Stanley, D.J. and Moore, G.T., eds., The shelf-slope break; critical interface in continental margins: Society of Economic Paleontologists and Mineralogists, Special Publication 33, p. 189-206.

James, N.P. and Choquette, P.W., 1990, Limestones — the meteoric diagenetic environment, *in* McIlreath, I.A. and Morrow, D.W., eds., Diagenesis: Geoscience Canada Reprint Series 4, p. 35-74.

Kendall, C.G.St.C. and Schlager, W., 1981, Carbonates and relative changes in sea level: Marine Geology, v. 44, p. 181-212.

Kinsman, D.J.J., 1974, Evaporite deposits on continental margins: 4th Symposium on Salt, Cleveland, Ohio, Northern Ohio Geological Society, v. 1, p. 255-259.

Lucia, F.J., 1972, Recognition of evaporite - carbonate shoreline sedimentation, *in* Rigby, J.K. and Hamblin, W.K., eds., Recognition of ancient sedimentary environments: Society of Economic Paleontologists and Mineralogists, Special Publication 16, p. 160-191.

Nelson, C.S., ed., 1988, Cool water carbonate sediments: Sedimentary Geology, v. 60, 367 p.

Postamentier, H.W., Jervey, M.T. and Vail, P.R., 1988, Eustatic controls on clastic deposition — conceptual framework, *in* Wilgus, C.K., *et al.*, eds., Sea level changes; an integrated approach: Society of Economic Paleontologists and Mineralogists, Special Publication 42, p. 109-124.

Read, J.F., 1985, Carbonate platform facies models; American Association of Petroleum Geologists, v.69, p.1-21.

Reading, H.G., ed., 1986, Sedimentary environments and facies: Oxford, Blackwell Scientific Publications, 615 p.

Sarg, J.F., 1988, Carbonate sequence stratigraphy, *in* Wilgus, C.K., *et al.*, eds., Sea level changes; an integrated approach: Society of Economic Paleontologists and Mineralogists, Special Publication 42, p. 155-182.

Shaw, A.B., 1964, Time in stratigraphy: McGraw-Hill, New York, 365 p.

Sonnenfeld, P., 1984, Brines and evaporites: Orlando, Academic Press, 613 p.

Tucker, M.E., 1991, Sequence stratigraphy of carbonate-evaporite basins: models and application to the Upper Permian (Zechstein) of northeast England and adjoining North Sea: Journal of Geological Society of London, v. 148, p. 1019-1036.

Tucker, M.E. and Wright, V.P., 1990, Carbonate sedimentology: Oxford, Blackwell Scientific Publications, 482 p.

Vail, P.R. and Todd, R.G., 1981, North Sea Jurassic unconformities, chronostratigraphy and sea-level changes from seismic stratigraphy: Petroleum geology of the Continental Shelf of Northwest Europe, Proceedings, p. 216-235.

Vail, P.R., Mitchum, R.M. Jr., Todd, R.G., Widmier, J.M., Thompson, S., III, Sangree, J.B., Bubb, J.N. and Hatlelid, W.G., 1977, Seismic stratigraphy and global changes in sea level, *in* Clayton, C.E., ed., Seismic stratigraphy — application to hydrocarbons: American Association of Petroleum Geologists, Memoir 26, p. 49-212.

Van Wagoner, J.C., Postamentier, H.W., Mitchum, R.M., Vail, P.R., Sarg, J.F., Loutit, T.S., and Hardenbol, J., 1988, An overview of the fundamentals of sequence stratigraphy and key definitions, *in* Wilgus, C.K., *et al.*, eds., Sea level changes; an integrated approach, Society of Economic Paleontologists and Mineralogists, Special Publication 42, p. 39-46.

Zeigler, A.M., Hulver, M.L., Lottes, A.L. and Schmachtenberg, W.F., 1984, Uniformitarism and palaeoclimates: inferences from the distribution of carbonate rocks, *in* Brenchley, P., ed., Fossils and climate: New York, John Wiley, p. 3-25.

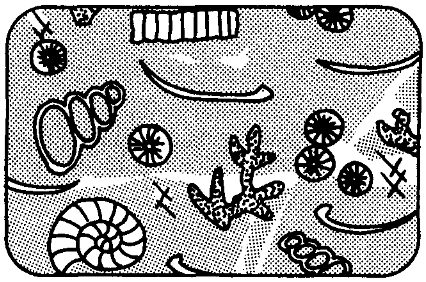

15. Shallow Platform Carbonates

Brian Jones, Department of Geology, University of Alberta,
Edmonton, Alberta T6G 2E3

André Desrochers, Ottawa-Carleton Geoscience Centre,
Department of Geology, University of Ottawa, Ottawa, Ontario K1N 6N5

INTRODUCTION

The shallow illuminated seafloor is the place where carbonate is fixed most rapidly by plants and animals and where carbonate particles precipitate most easily. While material may be exported from this factory to form tidal flats or slope deposits, much also stays in place, to be preserved as what are euphemistically called subtidal limestones. The focus of this chapter is the origin, composition, facies and stratigraphy of these platform sediments.

The dynamics of this environment are outlined in Figure 1. The starting point (upper left) is the carbonate factory where the nature of the sediment is dictated by evolution, organism biology, climate, salinity, water depth, and clastic sediment influx. Once formed, the fate of the carbonate sediments is dictated by wind waves, tides, storms, and large-scale oceanic currents. The balance between sediment production and sediment transportation determines the growth potential of the platform.

Carbonate platforms are dynamic depositional systems because fluctuations in sea level and variations in the rate and style of subsidence cause ever-changing environmental condi-

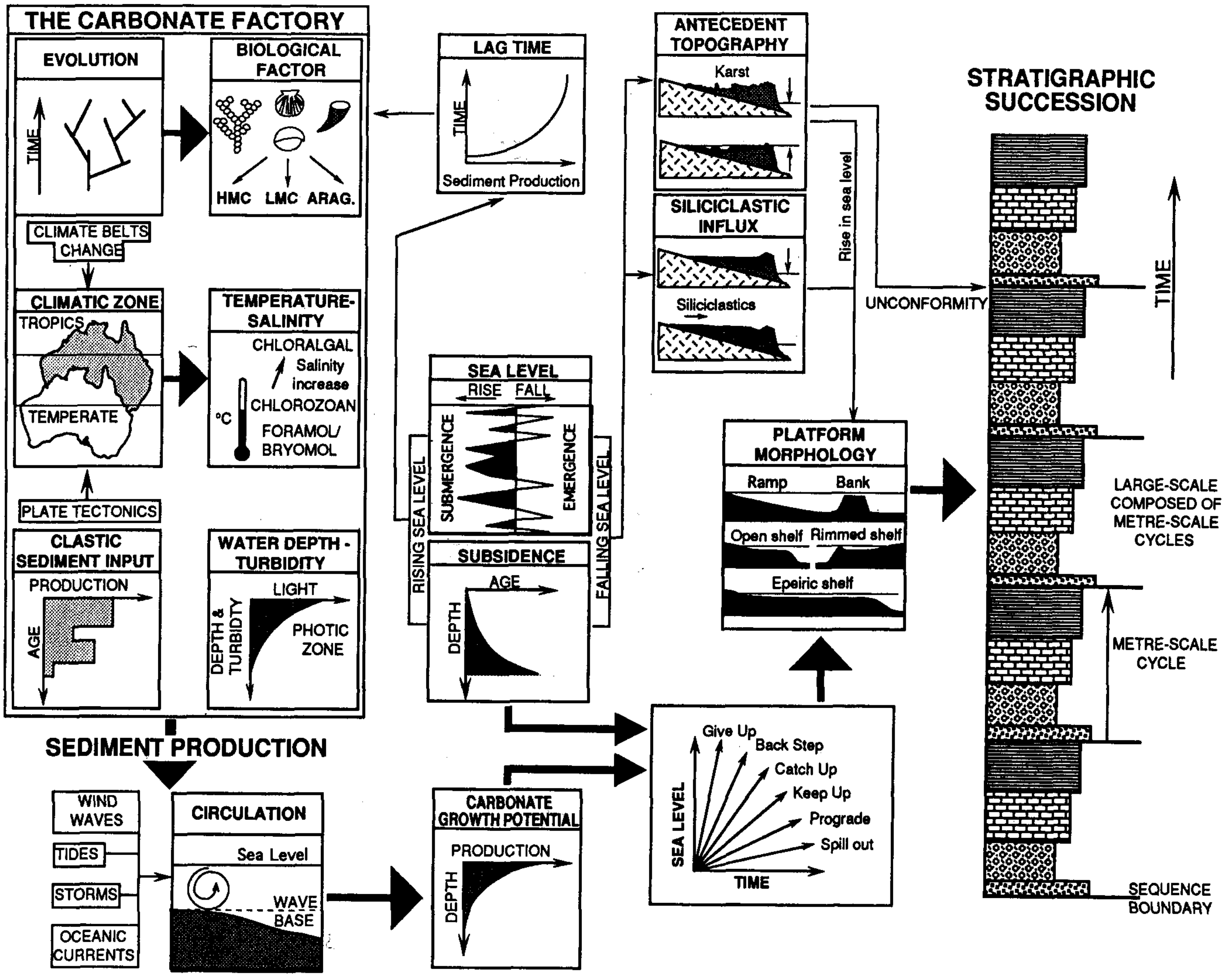

Figure 1 Diagram summarizing the main factors that control the formation of carbonate successions on platforms.

tions (centre). A drop in sea level may lead to siliciclastic sediment influx or karsting of previously deposited carbonates. Karst topography can control platform morphology during subsequent flooding. The vertical accumulation of platform sediments (right) is governed by the interplay between carbonate growth potential, the rate of change in relative sea level, and platform morphology.

The first section of this chapter outlines factors that control sediment production and distribution in the carbonate factory. The second presents platform facies models and uses modern and ancient examples to illustrate variations that can be expected in each type. The third part examines the factors that determine carbonate accumulation on platforms through time. The fourth illustrates the response of platforms to the dynamic changes that occur through time.

THE CARBONATE FACTORY

Location

The main environmental factors which determine the health of the carbonate factory are outlined in Chapter 14. A carbonate factory can form in any part of the world where shallow water, marine conditions exist. A fully functional factory will only be established, however, in areas isolated from extensive siliciclastic influx. The broad continental shelf stretching from North Carolina southward to the Florida Keys, for example, is the site of both siliciclastic and carbonate sedimentation (Fig. 2). Siliciclastic sedimentation occurs in the north because numerous rivers shed detrital sediment onto the shelf. Carbonate sedimentation occurs south of Miami mainly because siliciclastic sediments are absent. The Belize, West Florida (Fig. 2), and Queensland shelves are variants of this general scheme because they have siliciclastics on the inner shelf and carbonates on the outer shelf.

The areal dimensions of a carbonate factory are governed by the size of the platform and extent of siliciclastic sedimentation. Because benthic phototropic organisms are the source of most carbonate sediment in warm water factories, the vertical dimension is determined by the depth of the photic zone, usually 80 to 100 m. Information regarding cool water carbonate factories is sparse because they have not received as much study as their warm water counterparts. The cool water factory seems to be effective to depths of 350 m (or more) because most sediment is derived from skeletons of nonphototrophic organisms. Depths below the photic zone on and around warm water platforms are characterized by cool water and pelagic carbonate sedimentation.

Of particular importance to the construction of subtidal platform facies models and their interpretation in the rock record are sediment composition, the relationships between sediment and environment and the distribution of fossilized benthic organisms.

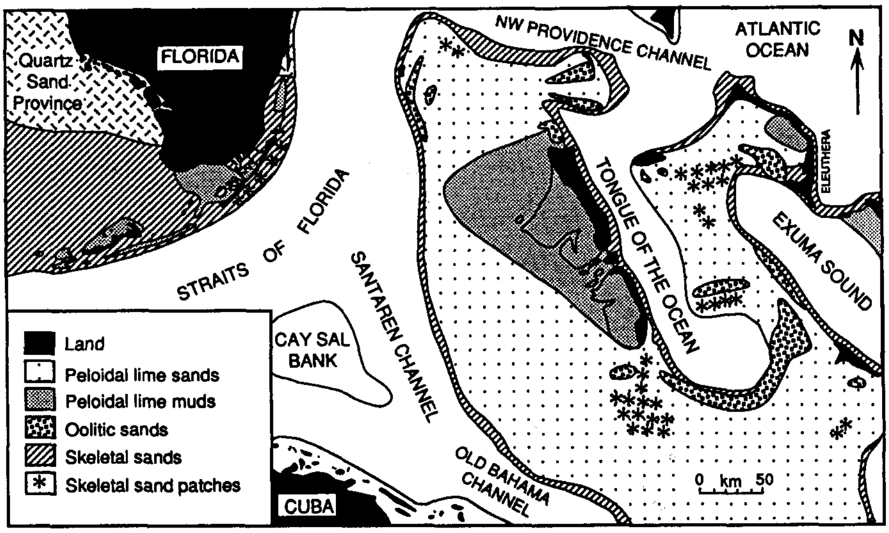

Figure 2 Map showing regional facies distribution on the Bahama Bank and the coasts of Florida. Modified from Wanless and Dravis (1989).

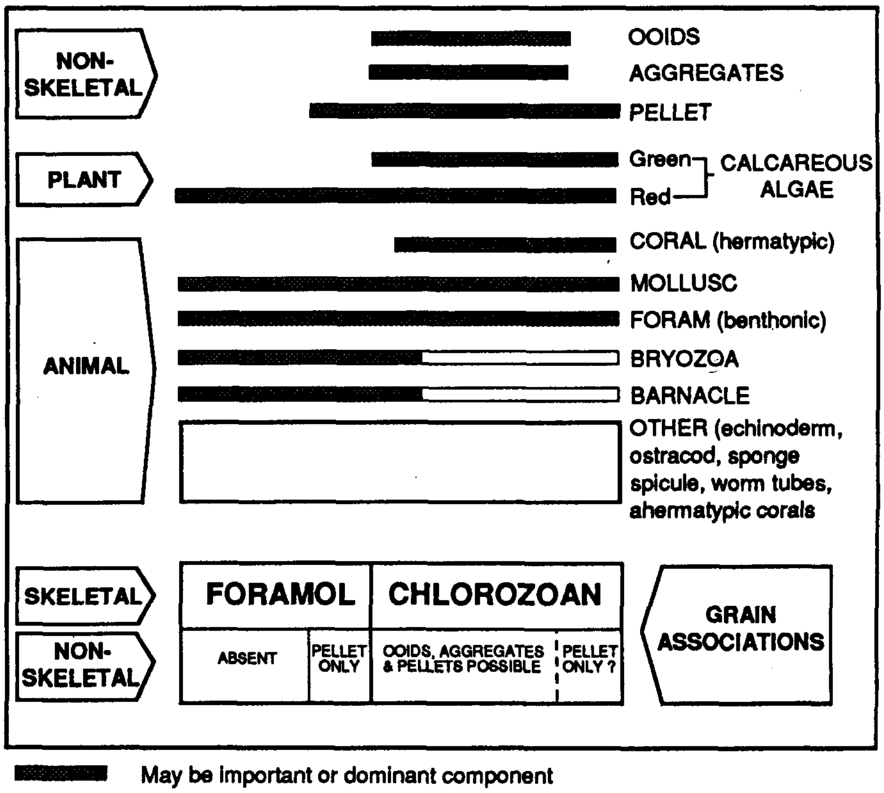

Figure 3 Comparison of foramol and chlorozoan carbonate assemblages. Modified from Lees and Buller (1972).

Sediment composition

On a global scale, modern carbonate sediments are largely controlled by temperature and salinity (Chapter 14) and can be divided into a *foramol* and a *chlorozoan* assemblage (Fig. 3). The foramol assemblage, composed of benthic foraminifera, molluscs, barnacles, bryozoa, and calcareous red algae characterizes cool water settings. Recent studies of modern and ancient cool water shelf carbonates have highlighted the importance of bryozoa and the term *bryomol* has been applied to these distinctive sediments (Nelson *et al.*, 1988). Conversely, the chlorozoan assemblage, dominated by hermatypic corals and calcareous green algae in addition to the foramol components, occurs in warm water areas where water temperature is above 18°C. Foramol and chlorozoan assemblages develop in places where salinities range between 32 and 40‰. Elevated salinities in tropical regions cause the demise of corals but not calcareous green algae. Thus, a *chloralgal* association usually occurs at salinities of >40‰. Ooids and aggregates are restricted to the chlorozoan assemblage. Pellets are more common in the chlorozoan assemblage than in the foramol association.

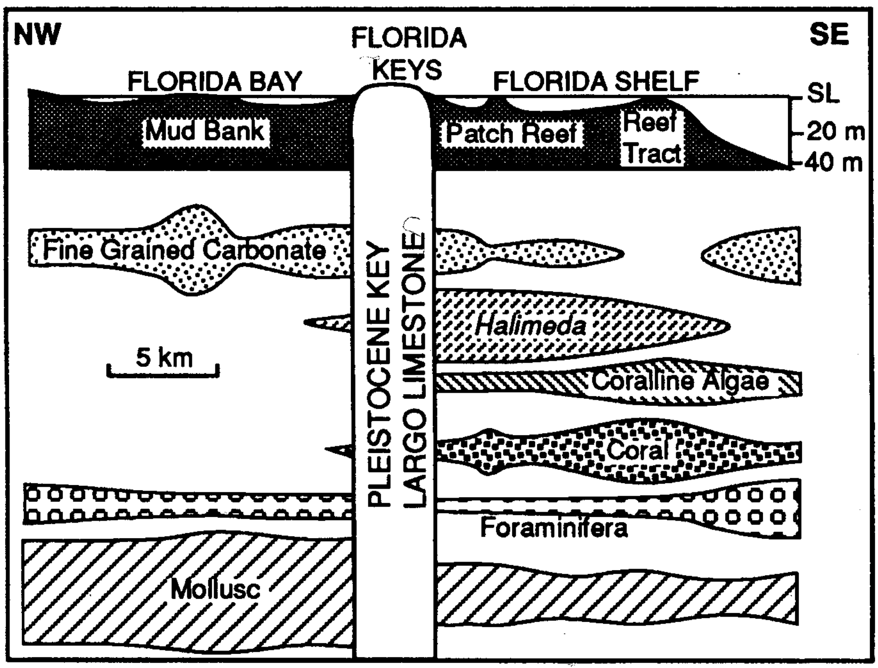

Figure 4 Distribution and origin of bioclasts across Florida Bay and Florida Shelf. Note that the sediment is derived from a diverse array of organisms. Modified from Ginsburg (1956).

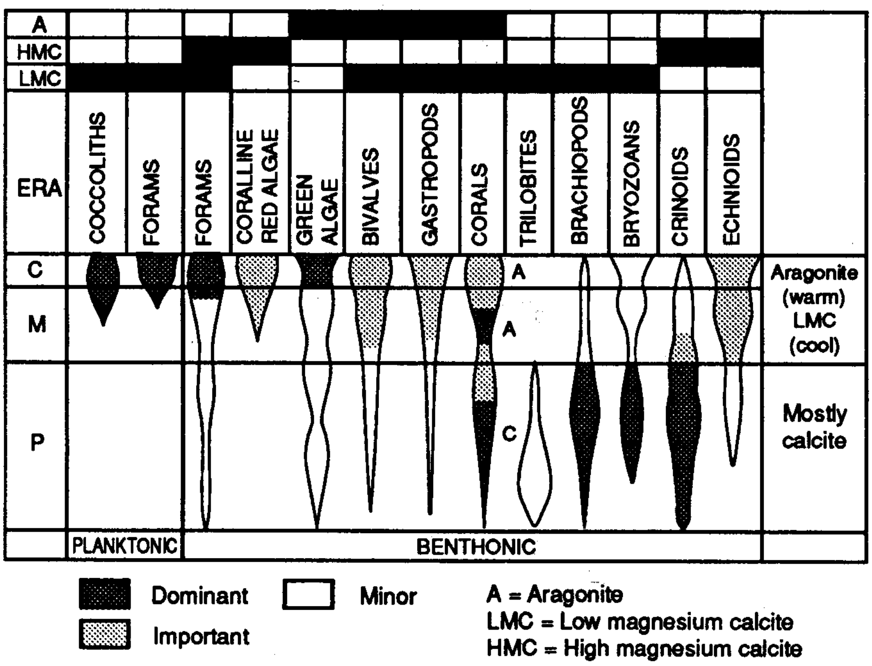

Figure 5 Distribution of main groups of animals and plants through the Paleozoic (P), Mesozoic (M), and Cenozoic (C). The fact that the different groups of animals and plants have skeletons formed of different mineralogies means that there are substantial differences between the Paleozoic and Mesozoic/Cenozoic sediments and cool versus warm water sediments (compare with Figure 3). Adapted from Wilkinson (1982).

Analysis of carbonate sediment from any platform, such as the Florida Shelf (Fig. 4), shows that it is largely skeletal material derived from plants and/or animals that secrete skeletal material with a specific composition (Scholle, 1978). Such precipitation is governed by the metabolic processes of the organisms and so, even under similar environmental conditions, different organisms will precipitate low magnesium calcite (LMC), high magnesium calcite (HMC), or aragonite. The chlorozoan and chloralgal assemblages (Fig. 3) are mostly aragonite and HMC. The foramol and bryomol assemblages are composed of HMC and LMC. Evolution becomes an important consideration because different groups of organisms, each with its characteristic mineralogy, were important at different times in geological history (Fig. 5). These mineralogies are variably preserved in the fossil record; aragonite fossils are commonly dissolved whereas HMC and LMC components are usually preserved.

Lithofacies

Although initial sediment composition is determined to a large degree by skeletal architecture, resultant lithofacies are also determined by the overall energy spectrum and the effectiveness of sediment binding. In general terms, except for platform margin facies, lithofacies on rimmed platforms are muddy while those on open, unrimmed platforms are grainy.

Mudstone

Calcareous mud in warm water settings comes from the breakdown of green calcareous algae (e.g., *Penicillus, Halimeda;* Fig. 6), inorganic precipitation from seawater, and/or from the disintegration of large skeletal particles into their smallest crystallographic unit. These muds accumulate in quiet water areas that are not affected by tidal and/or strong oceanic currents. Such habitats are found in deep water shelf areas below wave base or in the lee of islands and shoals. Conversely, calcareous mud can accumulate in moderate- to high-energy areas if it is bound into place by cyanobacterial mats, sea grasses like *Thalassia*, or trees such as mangroves. Recognizing low-energy as opposed to moderate- or high-energy mudstone facies is difficult because they are lithologically similar. They are best differentiated on the basis of faunal composition/diversity and sedimentary structures.

Aragonitic muds are rare or absent in cool water settings because the organisms that produce the aragonite are scarce. Mud in these settings is formed from the bioerosional breakdown of benthic skeletons or the accumulation of pelagic ooze.

Wackestone and packstone

Wackestones and packstones are transitional between low-energy mudstones and high-energy grainstones in warm water settings. They are not common in cool water settings because of the overall lack of mud. Such sediments generally accumulate on warm water platforms where current activity has been insufficient to remove the mud. As such they tend to be located away from the edges of platforms or on deeper parts of ramps where there is some protection. In areas of moderate to high energy they are organically bound.

Many wackestones and packstones are formed of pellets that reflect the activity of burrowing (e.g., ghost shrimps) and grazing (e.g., sea cucumbers) animals. If cemented early, such fecal pellets are preserved and become the dominant constituent of resultant wackestones or packstones.

Bafflestone and bindstone

Plants can induce deposition through baffling and binding. They also provide ideal substrates for calcareous epibiontic organisms. Although plants typically root in muds and sands, coarser material may be incorporated if it is transported into the area by storms. Such facies are easy to recognize in modern warm and cool water settings, because the plants are obvious (Fig. 7). Their recognition in ancient succes-

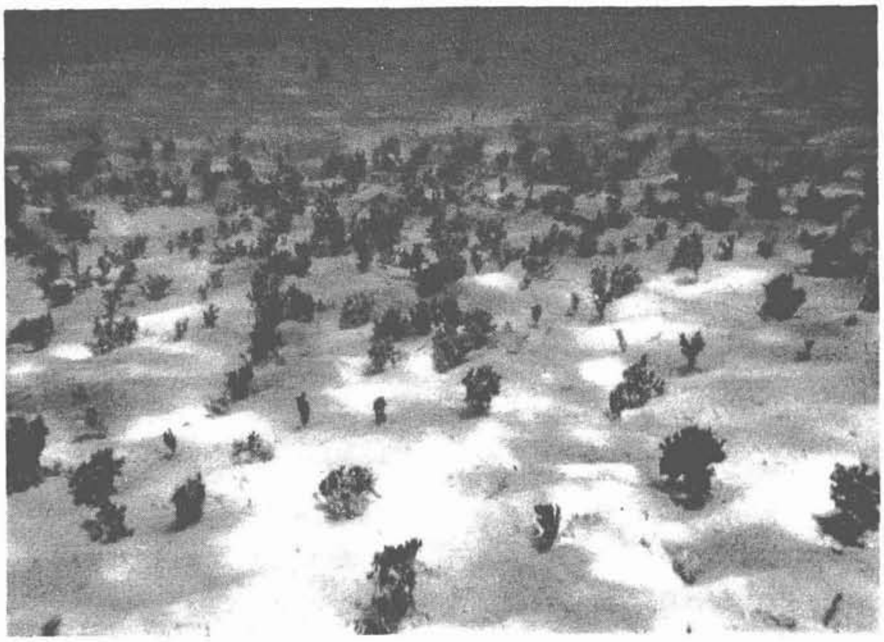

Figure 6 General view of lagoonal seafloor covered with skeletal sand and mud with numerous green calcareous algae *(Halimeda)*, each about 10 cm high. Water is about 3 m deep. Frank Sound, Grand Cayman Island, West Indies.

Figure 7 General view of *Thalassia* grass which is stabilizing sand and mud in the inner part of a shallow lagoon in water about 3 m deep. The mound is about 50 cm across and was formed from sediment expelled by the burrowing shrimp *Callianassa*. The dark-coloured sediment is material that has been brought up from sediments below the surface where conditions are reducing.

sions is difficult because the organic tissue of plants is lost following their rapid decay. Examples of fossilized *Thalassia* grass and/or mangrove roots are the exception rather than the rule. Poor sorting of sediment, or the presence of identifiable mound-like structures may provide some clues. Knowledge of the associated fauna/flora, however, may be the best evidence because some taxa are known to be specific to seagrass meadows or mangroves. Gastropods and foraminifera are particularly useful because certain forms live only on grass blades or submerged tree roots (Jones and Hunter, 1990).

Bindstones produced through the trapping action of algal mats may be easier to recognize because they are generally laminated. Conversely, burrowing organisms (e.g., shrimp, crabs; Fig. 8) may remove all trace of such laminations as they homogenize the sediment.

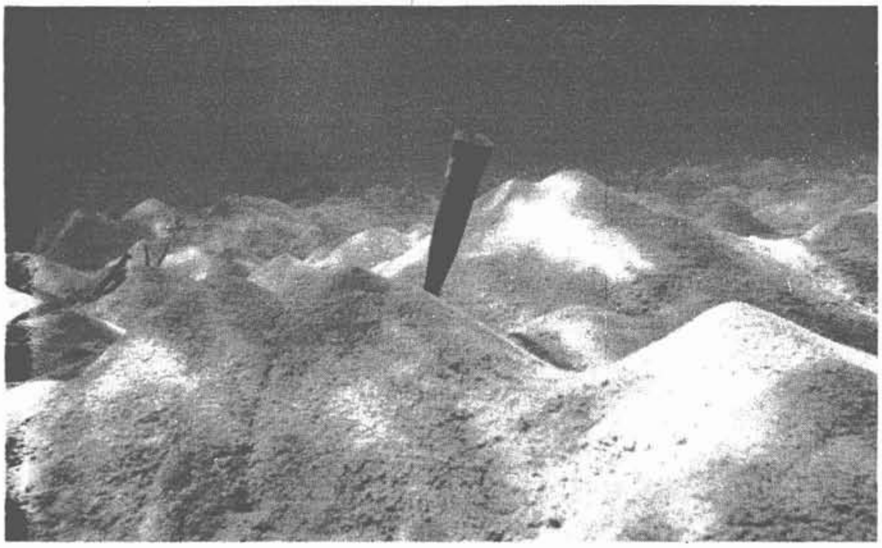

Figure 8 General view of shelf sands in 5 m of water that have been extensively bioturbated by burrowing shrimp *(Callianassa)*. Such burrowing activity will homogenize the sediment and completely destroy other original sedimentary structures. Hammer handle is 20 cm long.

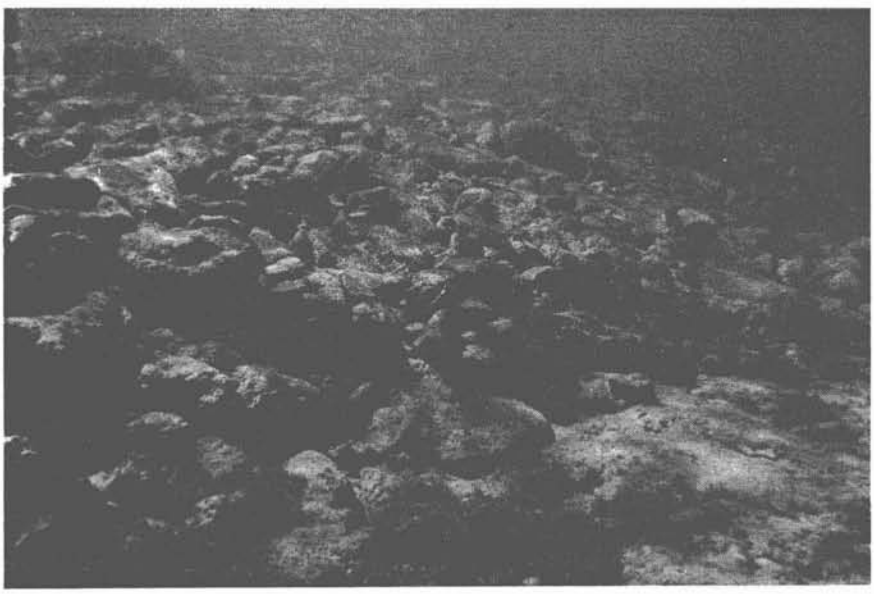

Figure 9 Boulders from a rimming reef prograding over lagoonal sands. Most clasts are coral heads that are transported during storms. Large clasts in the foreground are 50 cm in diameter. East Sound, Grand Cayman Island.

Grainstone and rudstone

Grainstones in cool water settings are well-washed skeletal sands derived from bryozoa, molluscs, brachiopods, and foraminifera. Further information on the depositional setting of such grainstones can be deduced from the bioclasts. Skeletal morphology has been used to define environmentally sensitive subfacies in the widespread bryozoa-rich facies that characterize cool water platforms (Nelson *et al.*, 1988; James and Bone, 1991).

Warm water grainstones, formed of bioclasts, ooids, and/or peloids, usually occur in high-energy areas, such as shoals and beaches. In some cases high-energy conditions are constant (e.g., tides and/or oceanic waves and currents). In other instances the environments are only periodically subjected to storm-induced high-energy conditions which remove the mud but leave coarser-grained sediment behind. Haloes of gravels and boulder-rich sediments (rudstones) are common around patch reefs or behind barrier reefs (Figs. 9, 10). Such sediment may be generated catastrophically during storms or through the everyday breakdown of the reefs by bioerosion.

Storm deposits

Storms can quickly and radically alter sediment distribution on any part of the platform that is above storm wave base. Although their effect on shallow water carbonates is the most obvious it must be remembered that the base of storm-generated waves may reach tremendous depths. Nelson *et al.* (1982) noted that storm waves produced current velocities of up to 11 cm/sec at depths down to 100 m on the Three Kings Plateau, northern New Zealand.

Storm waves and currents cause extensive remobilization of sediments and basinward transport of sands and muds. This leaves beds of grainstone-packstone with distinctive sedimentary structures that will be interbedded with the fairweather, bioturbated wackestone-mudstone (Figs. 11, 12). Hummocky cross-stratified grainstone and graded grainstone-packstone are two types of tempestite that commonly form between fairweather and storm wave base. Tempestite beds can, however, range from interbedded grainstone-mudstone to amalgamated grainstone depending upon water depth, frequency and intensity of storms, and proximity to the source area or shoreline (Aigner, 1985; Sami and Desrochers, 1992). Other storm-generated features in tempestites include scoured bases, swaly cross stratification, grading, gutter casts, interference ripple caps, shell coquinas and condensation horizons (see Kreisa, 1981).

Storm deposits can be recognized by evaluating geomorphologic, stratigraphic, and biostratinomic evidence. Geomorphic evidence includes the formation of offbank spillover lobes and onbank sand lobes (Aigner, 1985) which appear to develop after the passage of hurricanes over shallow water areas (Ball, 1967; Hine, 1977). Stratigraphic evidence includes sharp-based skeletal layers that commonly overlie erosional surfaces and fining-upward sequences (Aigner, 1985). Biostratinomic evidence includes excellent preservation of articulated shells despite movement from their original life position. This occurs because the shells are rapidly buried by storm-transported sediment and there is little opportunity for postmortem breakdown by biological and physical processes. Storms will commonly transport or move large masses of skeletal material from their place of growth. Thus, coral heads can be transported for considerable distances before being deposited elsewhere on the platform. This process may be accelerated if the coral basal attachment had previously been weakened by bioerosion.

Distribution of biota

Animals and plants are sensitive to their surrounding environment. The biota will change in concert with variations in light level, oxygen content, water temperature, sedimentation rate, water depth, substrate condition, water turbidity, and food availability across a carbonate platform (Heckel, 1972; Pickerill and Brenchley, 1991). This dependence of the biota on the environment is important because it provides valuable information about the carbonate factory that cannot be obtained from lithofacies alone.

At the broadest scale, information pertaining to the different benthic communities and their distribution provide vital clues regarding depositional conditions. On modern rimmed platforms *Thalassia* banks grow on the inner shelf whereas patch reefs and mobile sands occur on the outer shelf. Such faunal zonations across shelves have, for example, also been broadly outlined for the Permian of the Southern Alps (Flügel, 1981a) and the Triassic of Northern Calcareous Alps (Flügel, 1981b).

More detailed community analysis can help elucidate paleogeography. Boucot (1975), for example, developed

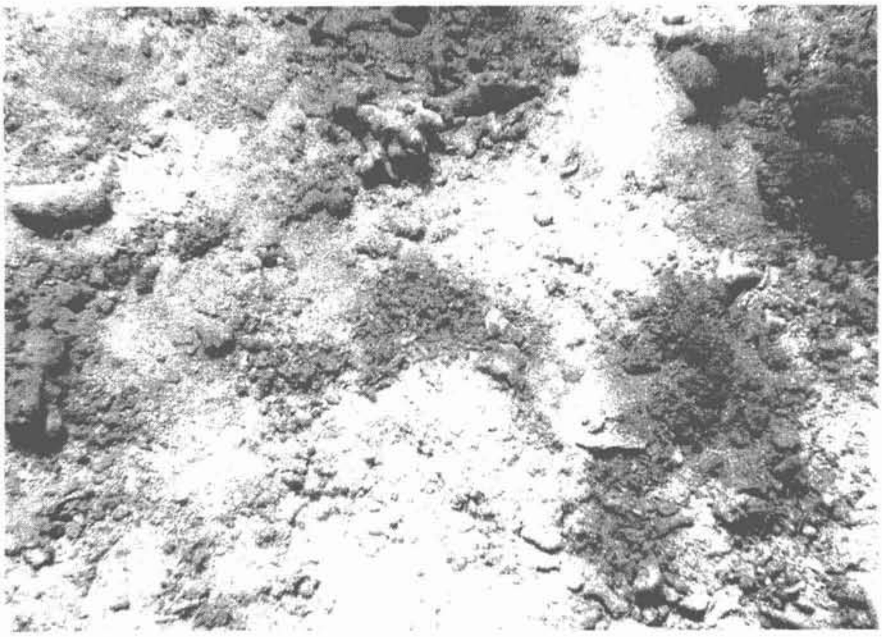

Figure 10 Coarse sands and gravels on outer part of shelf. Clast at upper right is 10 cm long. Water is about 1.5 m deep.

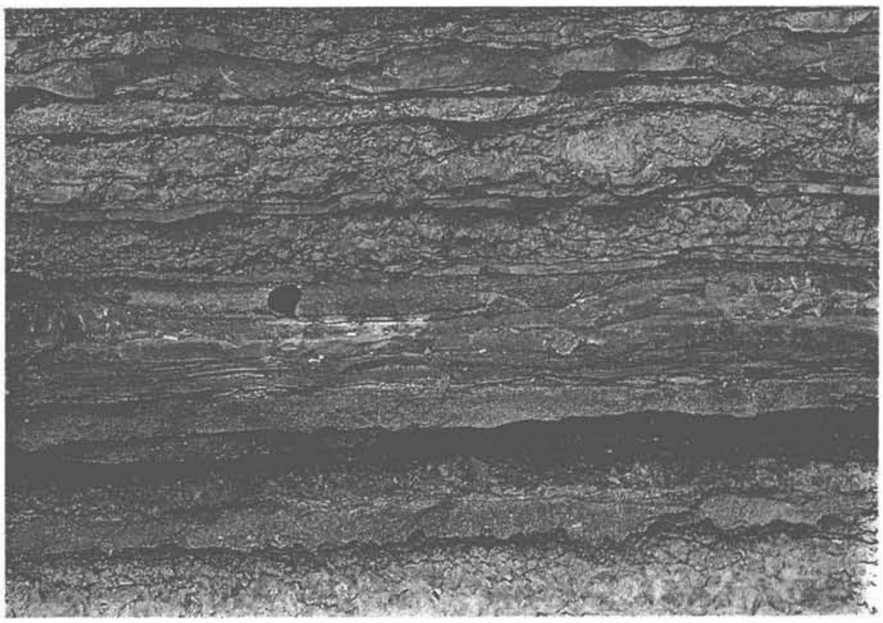

Figure 11 Interbedding of thin, sharp-based tempestite units and thicker, normally bedded lime mudstones. Lens cap (55 mm in size) is located on packstone-filled depression between two hummocks of a HCS tempestite unit with a gradational, intraclastic base. Bescie Formation (Lower Silurian), Anticosti Island, Quebec.

Figure 12 A graded tempestite unit with gradual transition from intraclastic coarse-grained grainstone up into laminated fine-grained grainstone overlain by nodular bedded mudstones. Note sharp scoured base. Pencil is 15 cm long. Bescie Formation (Lower Silurian), Anticosti Island, Quebec.

the concept of benthic assemblages for Paleozoic successions. Such assemblages, based largely on brachiopods, include different communities that occur repeatedly in different parts of a region but always in the same position relative to the shoreline.

Biota can also be used to decipher specific environmental factors. The diversity and abundance of the biota is an indication of the overall health of the carbonate factory (Fig. 13). Departure from normal open ocean conditions leads to a drop in faunal diversity because various elements of the biota cannot tolerate the stress induced by the change in salinity. The loss of diversity, however, is commonly compensated for by an increase in the number of individuals of the species that survive. Similarly, the biota can provide information about the consis-

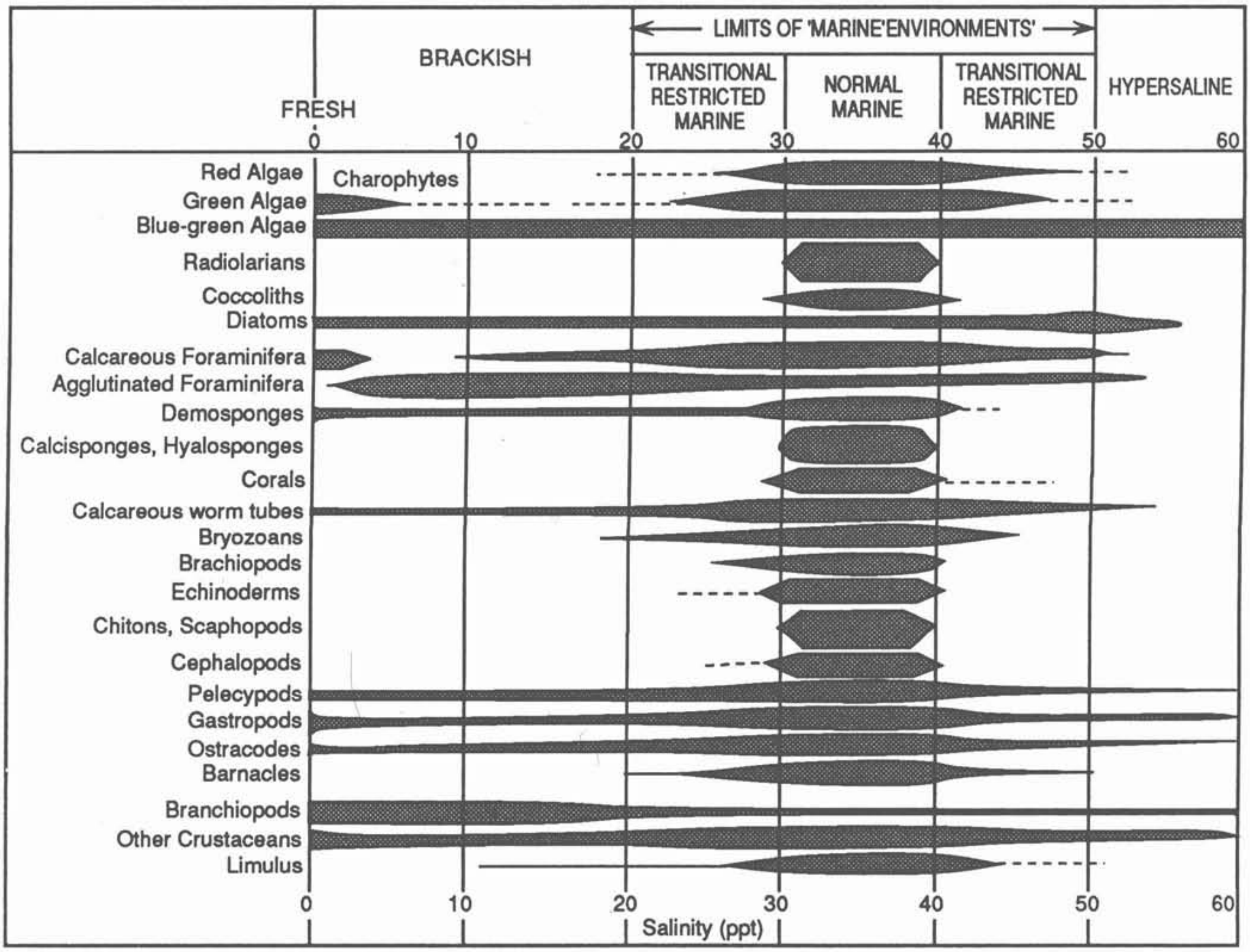

Figure 13 Effect of salinity on modern plants and animals. This diagram clearly shows how a decrease or increase in salinity will severely limit the diversity of the fauna and flora. Modified from Heckel (1972).

tency of the substrate; for example, it is the biota that usually leads to the recognition of hardgrounds and firmgrounds (Fig. 14).

PLATFORM FACIES MODELS

Platform morphology determines subtidal facies distribution. In most cases, however, the poor exposure of ancient successions or the lack of seismic profiles precludes an assessment of original platform morphology. Thus, the challenge is often to use the facies architecture to interpret platform type. This challenge is accentuated by the difficulty that can be encountered in translating the interpreted environmental parameters into a precise depositional setting! Geography is crucial because it is the spatial relationship between lithofacies and/or biofacies that usually provides the vital information. In the following section general facies attributes are outlined first and then amplified by specific modern and ancient examples.

Unrimmed shelves

Unrimmed shelves are swept by onshore waves because there is no barrier along their seaward margin. Such shelves range from ramps where slopes are relatively uniform (a few metres/km or <1°) and merge gradually into a relatively shallow basin (Ahr, 1973; Read, 1983, 1985) to open shelves (distally steepened ramp of Read, 1985) where there is an increase in gradient in the outer, deep shelf area (Ginsburg and James, 1974) before it merges with the deeper, oceanic basin. The nature of the shelf edge may vary along strike. The West Florida Shelf, for example, has a ramp profile without a major break in slope (~1-2°) in its northern portion; a distinct shelf edge with concave-up, outer slope profile (up to 12°) in its central part; and a steeper but similar profile (~5°) in its southern portion.

Modern, unrimmed shelves (Fig. 15) are characterized by 1) a seafloor, 10 to 300 km wide, gently sloping offshore from a continental area, 2) facies belts of variable width that closely parallel bathymetric contours, 3) gradual transition of facies belts from inner, shallow shelf to outer, deep shelf to basin, 4) high-energy, carbonate sands in the wave- and/or tide-agitated, inner shelf (above fairweather wave base), 5) skeletal muddy sands to muds in quiet, deeper outer shelf (below fairweather wave base) that are only periodically affected by storms, 6) no continuous reef trends, and 7) localized patch reefs and sand shoals.

Holocene, warm water

Modern, warm water, unrimmed platforms are the sites of low or moderate energy processes controlled by waves, local tides and/or oceanic currents. High-energy conditions may be induced by hurricanes. Modern examples include the ramp off the Trucial Coast (Fig. 16) and the open shelves of West Florida and Campeche (Fig. 17). Much of the sediment on these shelves is not in equilibrium with present-day shelf hydrodynamic processes. Sands on the West Florida Shelf, for example, formed in water about 5 m deep during the early Holocene, are now stranded near the shelf edge in water 80 to 100 m deep.

The Persian (Arabian) Gulf, a typical foreland basin, is a shallow, asymmetric sea with its deep axis (<100 m) near the steeper Iranian coast (Fig. 16). The north side receives terrigenous sediment from the mountainous Iranian coast. Almost pure carbonate sediment accumulates on the Arabian side because there is little siliciclastic material being brought into the area. Sediments off the Trucial Coast accumulate on a ramp (<35 cm/km). A transect perpendicular to strike crosses 1) a back ramp with microbial intertidal flats that pass landward into broad evaporitic sabkhas and skeletal-pelletal sands to pelleted lime muds in protected coastal lagoons, 2) a shallow ramp with high-energy skeletal/oolitic sand shoals, beach-barrier systems and coral reefs, 3) a deep ramp that is transitional from aggre-

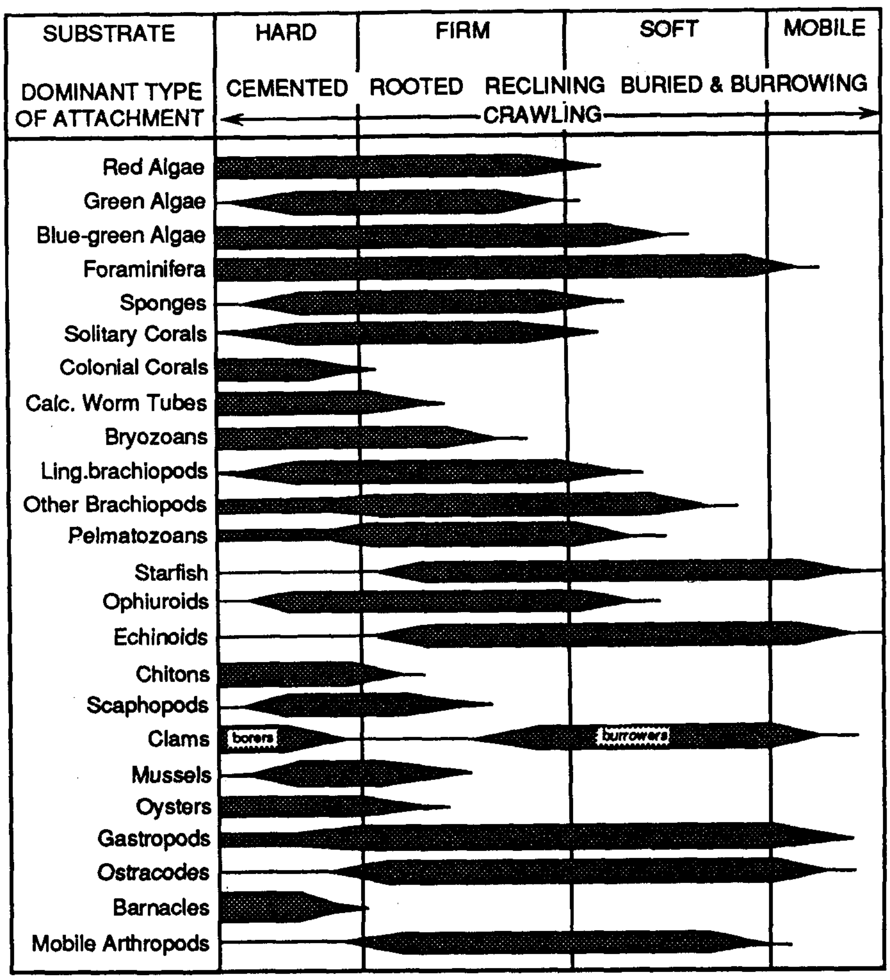

Figure 14 Substrate preferences for modern animals and plants. Modified from Heckel (1972).

gate/skeletal sands dominated by molluscs and foraminifera to skeletal muddy sands (mud-supported) dominated by mollusc debris, and 4) a gradual transition into bivalve-rich marls (>20% terrigenous material) of the deeper axial zone that contain coccoliths. Sediment distribution is controlled by NW winds (shamals) that generate waves several metres high that move sediment to depths of 30 m. Local tidal currents are less important. The biota is influenced by water circulation, especially in the restricted lagoons where stagnation leads to elevated salinities (>70‰). Although the biota in open gulf waters (salinities ~40-50‰) resemble the typical chlorozoan assemblage, the coral fauna is less diverse and codiacean algae are absent.

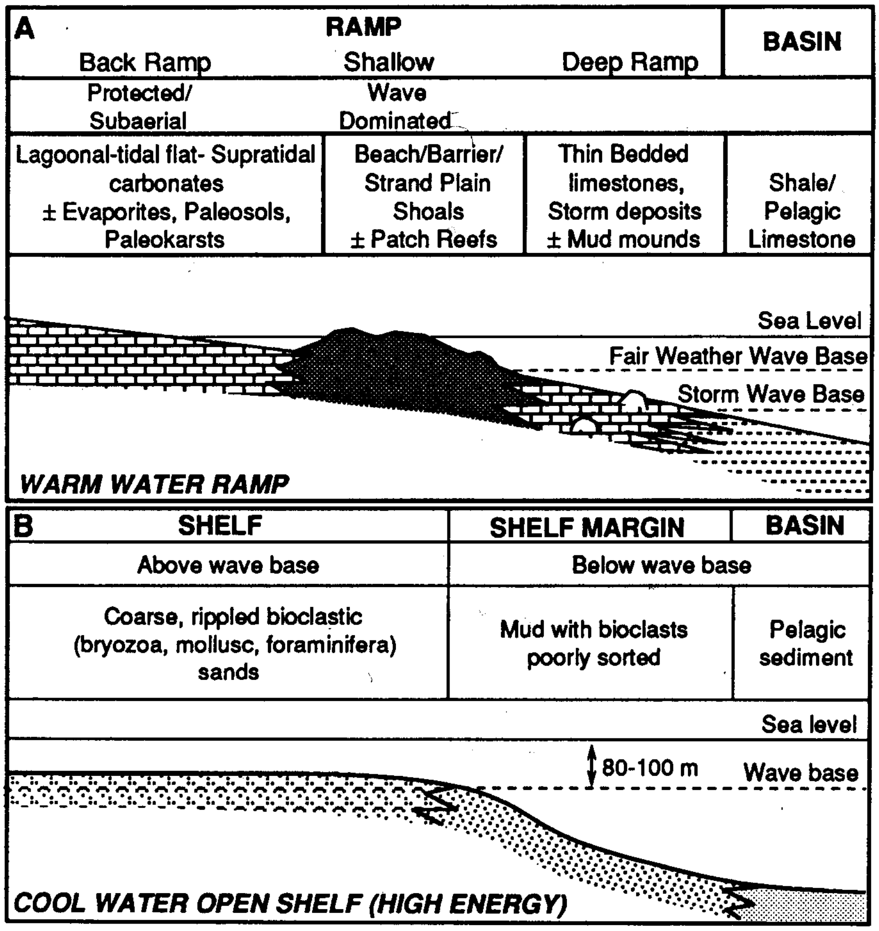

Figure 15 Facies models for unrimmed shelves (A) warm water ramps, and (B) cool water open unrimmed shelf (high energy).

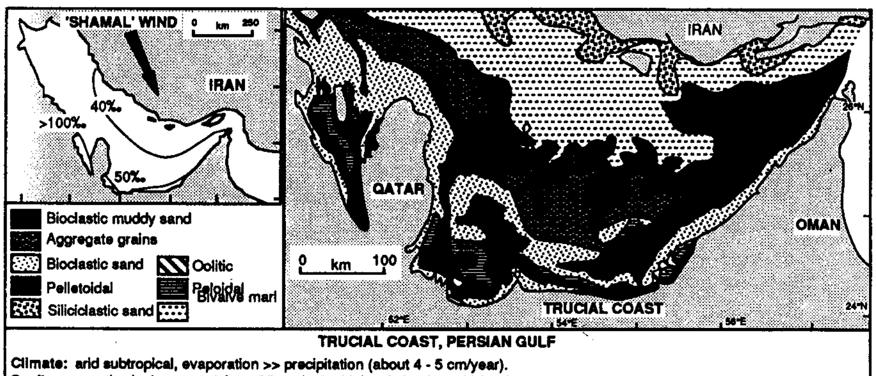

Figure 16 Distribution of facies on the ramp off the Trucial Coast in the Persian Gulf with summary of conditions that control sediment formation. Modified from Purser (1973, 1983).

The West Florida and Campeche shelves, on opposite sides of the Gulf of Mexico (Fig. 17), have contrasting styles of sedimentation. The Gulf of Mexico is a partially enclosed, microtidal, low-energy pericontinental sea that is essentially wind dominated. Although SE to NE waves associated with the Trade Wind Belt prevail, most energy comes from waves crossing the deep waters of the open gulf. Shelf sedimentation is controlled by waves and, to a lesser extent, by tides. Hurricanes, however, radically modify sedimentation.

Facies on the West Florida Shelf (Fig. 17) which parallel the shoreline include 1) inner shelf quartz/molluscan sands, 2) outer shelf coralline algal sands, 3) shelf edge oolitic, peloidal, and lithoclast sands (mainly relict), and 4) slope planktonic foraminiferal oozes with up to 30 per cent clay minerals. Landward of the shelf edge, small carbonate buildups are covered by branching and massive corals, bryozoans, and *Halimeda*. The facies architecture on the Campeche Shelf differs from that on the West Florida Shelf (Fig. 17) because there are no siliciclastic sands on the inner shelf, and isolated organic buildups occur at the shelf edge on top of antecedent highs.

Ancient, warm water

The Jurassic Smackover Formation in the southern United States accumulated on a ramp characterized by ooid grainstones, packstones, and sandstones in the nearshore belt (Moore, 1984). Further offshore, peloidal/bioclastic wackestones and foraminiferal mudstones were deposited in a deeper, lower energy setting. The deepest water areas were covered by organic-rich, laminated mudstones. Other examples of ancient ramps include those in the Upper Cambrian to Middle Ordovician carbonates of the Appalachians in Virginia (Read, 1980; Markello and Read, 1981) and possibly the Lower Carboniferous of South Wales (Tucker and Wright, 1990).

Holocene, cool water

Modern, unrimmed platforms in cool water settings include the relatively low-energy ramp of the Gulf of Gabès in the Mediterranean (Fig. 18) and the high-energy, swell-dominated Rottnest Shelf off western Australia (Fig. 19).

The Gulf of Gabès and its northern, shallower extension which extend for 200 km along the east coast of Tunisia, have a gently seaward-dipping seafloor with the 50 m depth contour situated up to 80 km offshore (Fig. 18). The main depositional belts, parallel to shoreline and bathymetric contours, are 1) a wave-agitated inner shelf above wave base at 20 to 30 m, 2) a quiet, low-energy outer shelf in water 30 to 80 m deep, and 3) a deeper shelf in water more than 100 m deep. The wave-agitated, inner shelf is rimmed landward by a low-relief rocky coast with local sabkhas and salinas. Except for a narrow nearshore band of quartzose sands, the inner shelf sediments are bioclastic sands distributed in a complex mosaic of sedimentary facies, especially in areas of sea grass meadows. The sediment is locally muddy because of baffling and stabilization by these sea grasses. Coarser and better sorted bioclastic sands occur where the sea grass is absent or in areas exposed to waves. Shelf sediments are coralline algae, foraminifera, molluscan and bryozoan debris, and locally, abundant *Halimeda* plates. The mixture of these bioclasts suggests that this area is transitional between foramol- and chlorozoan-type sediments.

The wave-dominated Rottnest Shelf lies on a passive continental margin that flanks a continental area of low relief and sluggish drainage (Fig. 19). Bryozoans and calcareous red algae dominate along with molluscs, foraminifera, echinoderms, pteropods, ostracods, and brachiopods. The inner shelf, up to 100 m deep, is veneered by wave-rippled cross-stratified sand. The outer shelf, 100-170 m deep, is covered by bioturbated bryozoan sand to sandy mud and the upper continental slope (>170 m) is blanketed by muddy planktonic carbonate.

Ancient, cool water

Examples of ancient carbonate successions that formed on temperate, unrimmed platforms are rare, probably because of the problems associated with identifying ancient temperate water carbonates. One example of this type of succession is mid-Cenozoic carbonates of the Eucla Platform in southern Australia (James and Bone,

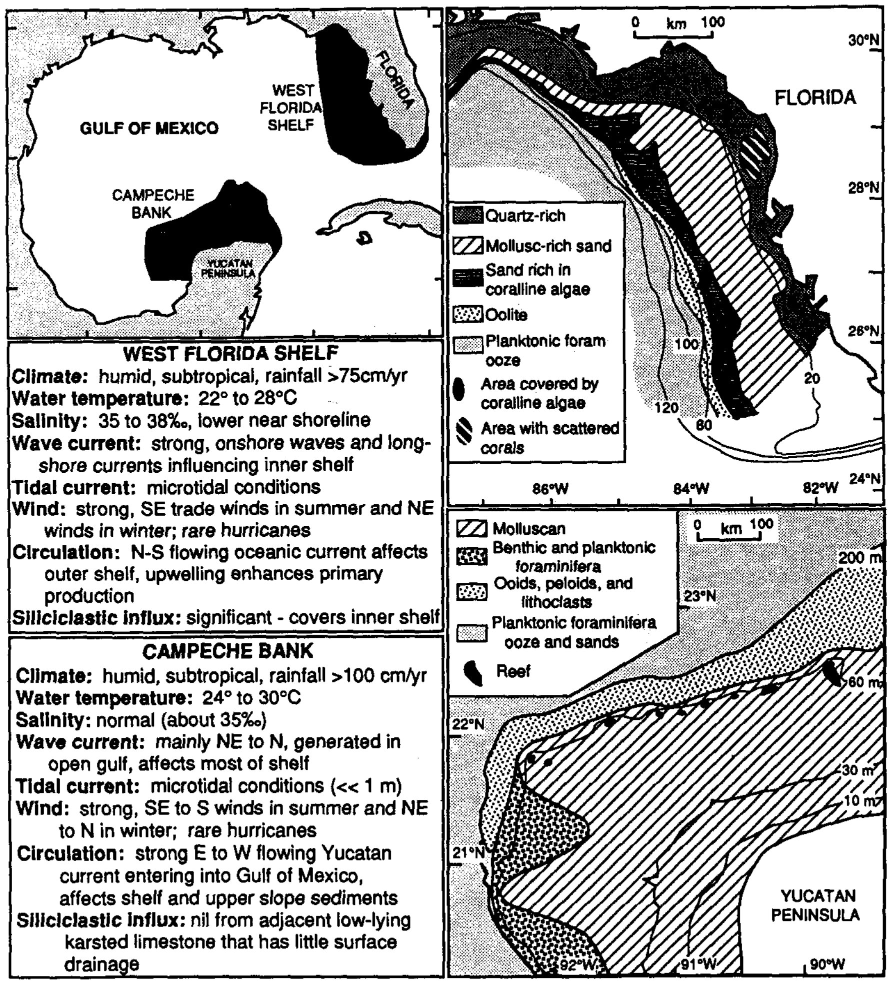

Figure 17 Comparison of facies distribution on the unrimmed West Florida Shelf (upper right) and the Campeche Bank (lower right) and summary of conditions that control sediment formation.

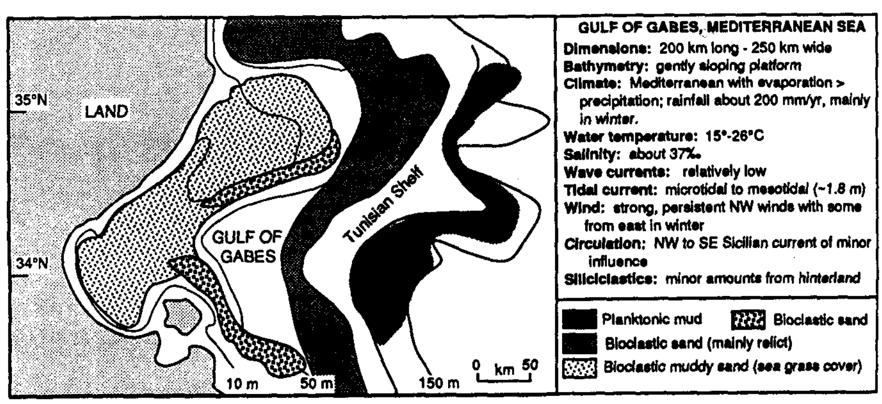

Figure 18 Facies distribution in the Gulf of Gabès, Tunisia and summary of conditions that control sediment formation. The open shelf is mantled by sediments that are a mixture of cool and warm water components. Modified from Purser (1983).

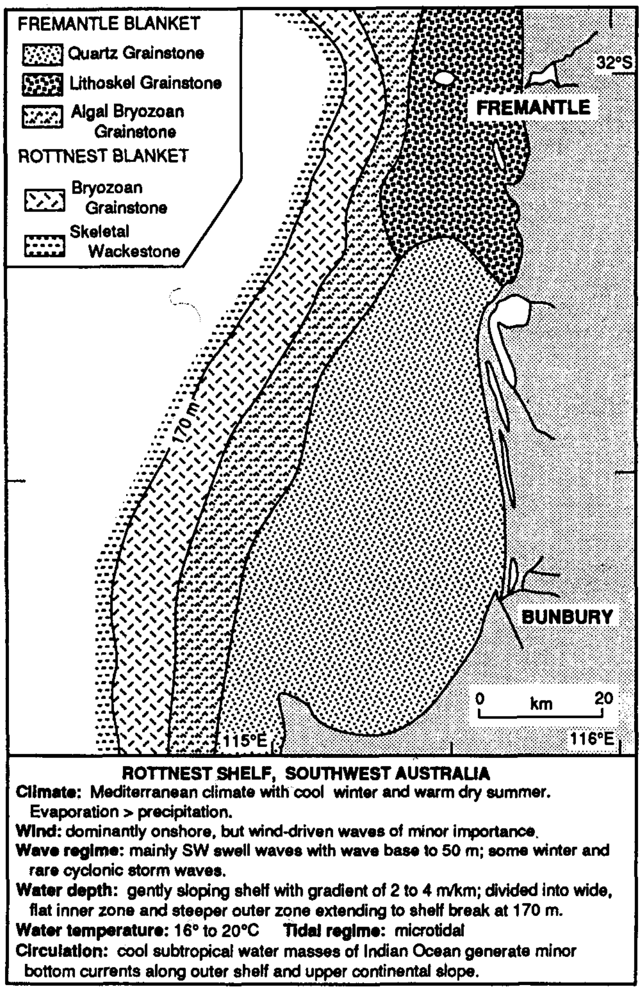

Figure 19 Facies distribution on the Rottnest Shelf, Western Australia and summary of conditions that control sediment formation. Modified from Collins (1988).

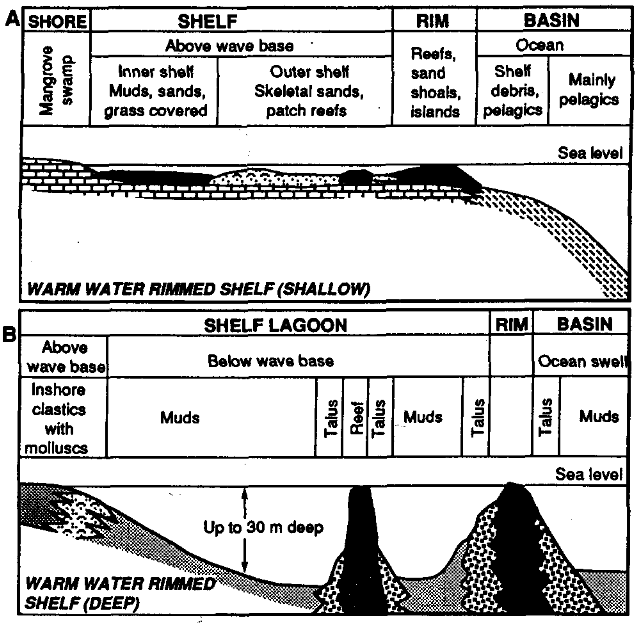

Figure 20 Facies models for warm water (A) and cool water (B) rimmed shelves. The latter is modified from Sellwood (1986).

1991). The limestones are largely skeletal grainstones with bioclasts derived from bryozoa, bivalves, brachiopods, and some corals. Facies include a lower cross-bedded and an overlying thin-bedded facies that probably represent subaqueous dunes and interdunes that originated in water more than 70 m deep. This example is interpretable because the rocks can be compared directly to the modern cool water carbonate sediments offshore. Interpretations of older carbonates are more equivocal because it has proven difficult to decouple the effects of evolution and environment. Nevertheless, Brookfield (1988) suggested that Trenton limestones in the Middle Ordovician of southern Ontario were probably deposited in such a setting. The brachiopod-bryozoa-crinoid-dominated faunas in these limestones are strikingly similar to the benthic biota on modern temperate shelves in the Southern Ocean.

Rimmed shelves

Rimmed shelves differ from open shelves because reefs, sand shoals and/or islands located along their seaward margin effectively reduce connection between the open ocean and shelf. The type and distribution of facies is related to shelf depth (Fig. 20). Shallow water shelves have grass-covered sands and muds on their inner parts and skeletal sands and patch reefs on their outer parts. Deep water shelves, with lagoons up to 30 m deep, are generally floored by muds. Steep-sided reefs, surrounded by haloes of reef talus, can form on the outer shelf whereas molluscan sands can develop in shallower, nearshore areas .

Holocene

The Florida (Fig. 21), Belize (Fig. 22), and Queensland shelves are modern examples. The Florida Shelf is covered by carbonate sediments whereas the Belize and Queensland shelves are mantled by siliciclastic and carbonate sediments. A comparison between the Florida and Belize shelves illustrates the effect of water depth on facies distribution.

The Florida Shelf, with water less than 20 m deep, is covered by biogenic sediment (Fig. 21) with most of the mud being derived from the breakdown of calcareous algae such as *Halimeda* and *Penicillus*. Patches of corals along the shelf edge are separated by areas of loose sediment. The outer shelf, subjected to high-energy conditions generated by onshore waves, is either bare Pleistocene limestone or rippled sand. Patch reefs and sessile organisms occur throughout. The inner shelf is covered by fine-grained sediment that is inhabited by *Thalassia*, algae (e.g., *Halimeda*, *Penicillus*), molluscs, coralline algae, echinoids, and small corals. Burrowing worms, molluscs, and crustaceans homogenize the sediment. Carbonate banks (e.g., Tavernier and Rodriguez banks) occur inboard over depressions in the underlying Pleistocene limestone basement.

The Belize Shelf facies (Fig. 22) comprises 1) an inshore siliciclastic belt, 2) a central trough-shaped lagoon ranging from 6 m deep in the north to 60 m deep in the south, 3) pinnacle reefs and atolls (faroes) in the shelf lagoon, and 4) a barrier reef that restricts circulation across the shelf. Nearshore siliciclastic facies of quartzose sands are derived from onshore Pleistocene deposits. Sedimentation in the shelf lagoon is controlled by water depth and salinity. Fine-grained sediments, accumulating in deeper parts

FLORIDA SHELF

Climate: rainfall of 90cm/yr on south part of shelf to 165 cm/yr around Miami. Subtropical, temperature of 19 to 30°C but with rare periods in winter when cold fronts move south.
Size: 5 to 10 km wide, 300 km long, south and southwest of Miami.
Wind: southeast trades during summer, wind from northeast in winter.
Ocean current: onshore waves generated by winds; strong on shelf edge, weak on inner part of shelf. Wave base less than 3 m.
Tidal range: 0.7 m. **Water temperature:** 18 to 30°C. **Salinity:** 35 to 38‰
Shelf margin: margin in 8 to 18 m deep water; upper slope of 8 to 18°.
Hurricanes: waves and currents generated by these storms cause considerably damage and move large amounts of sediment.

Figure 21 Facies distribution on a segment of the Florida Shelf near Key Largo and summary of conditions that control sediment formation. Modified from Enos (1977).

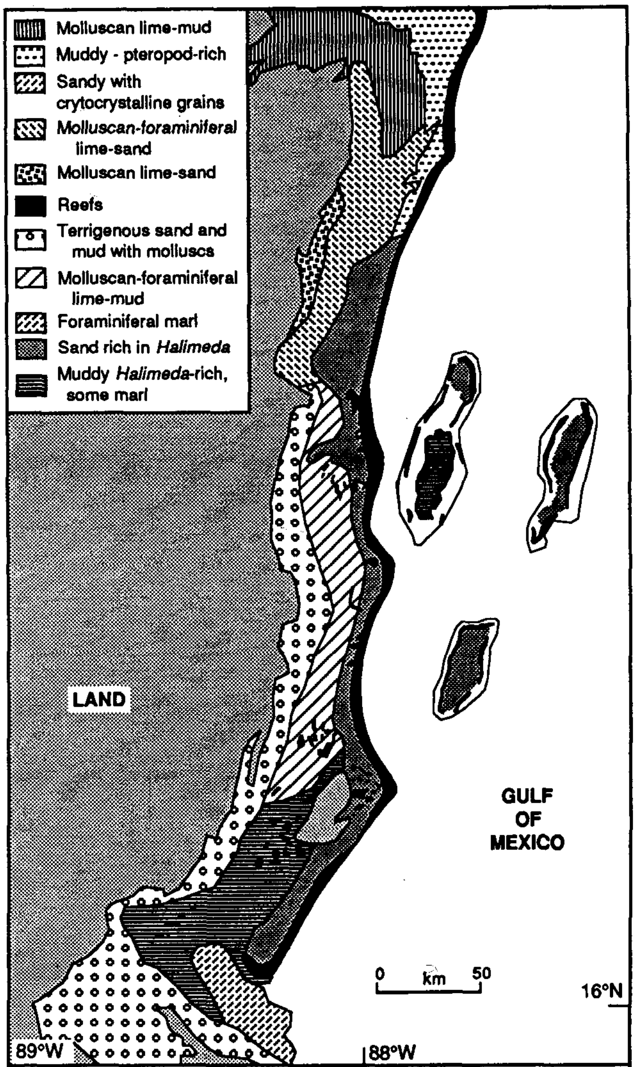

BELIZE SHELF

Climate: Subtropical, temperatures of 24 to 27°C; rainfall average of 25 cm/yr in north, 70 cm/yr in south. Cold air from north in October to January. Average of 1 hurricane every 6 years.
Wind: predominantly from east
Ocean current: Predominantly from east due to Caribbean current.
Water depth: Up to 50 m on shelf, shallowest in north (<10 m)
Shelf Margin: rimmed by 3 to 10 km wide barrier (<3 m water depth), with coral reefs and islands along entire length. Steep on oceanward side.
Salinity: Generally 35.7‰ to 36.1‰, well mixed to depths of 30 -50 m. Decreases to north and south due to influxes of freshwater. Slightly higher in north lagoon due to lower rainfall.

Figure 22 Facies distribution on the Belize Shelf and summary of conditions that control sediment formation. Modified from Purdy (1974), Ginsburg and James (1974).

of the lagoon where energy levels are lowest, display two main trends. First, in an west-east direction, the carbonate content changes from 30 per cent nearshore to 90 per cent near the barrier reef. Second, in a north-south direction, reflecting increasing water depth, there is a gradual change in dominant bioclasts from molluscs and foraminifera in the north, to green algal *(Halimeda)* plates in the centre, to foraminifera *(Gypsina)* tests in the south. Coarse sediment shed from the pinnacle reefs and atolls accumulates as leeward blankets. The barrier reef rim has rubble on the crest and an apron of sand on its landward side.

Ancient

The Dachstein Limestone (Late Triassic) in the northern calcareous Alps, contains numerous examples of rimmed shelves. Such shelves, with rims of reefs or oolitic grainstone shoals (Schäfer and Senowbari-Daryan, 1981), encompass a complex set of facies that parallel the shoreline. Other examples of rimmed platforms occur in the Devonian of the Canning Basin, Australia (Playford, 1980); the Upper Cambrian through Devonian strata of Nevada (Tucker and Wright, 1990); and the Devonian of western Canada.

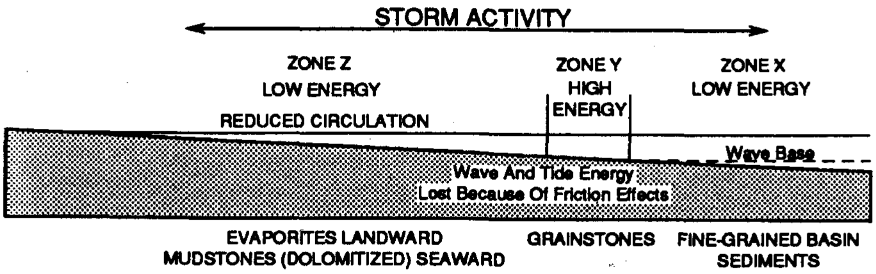

Figure 23 Facies model for an epeiric shelf (from Irwin, 1965).

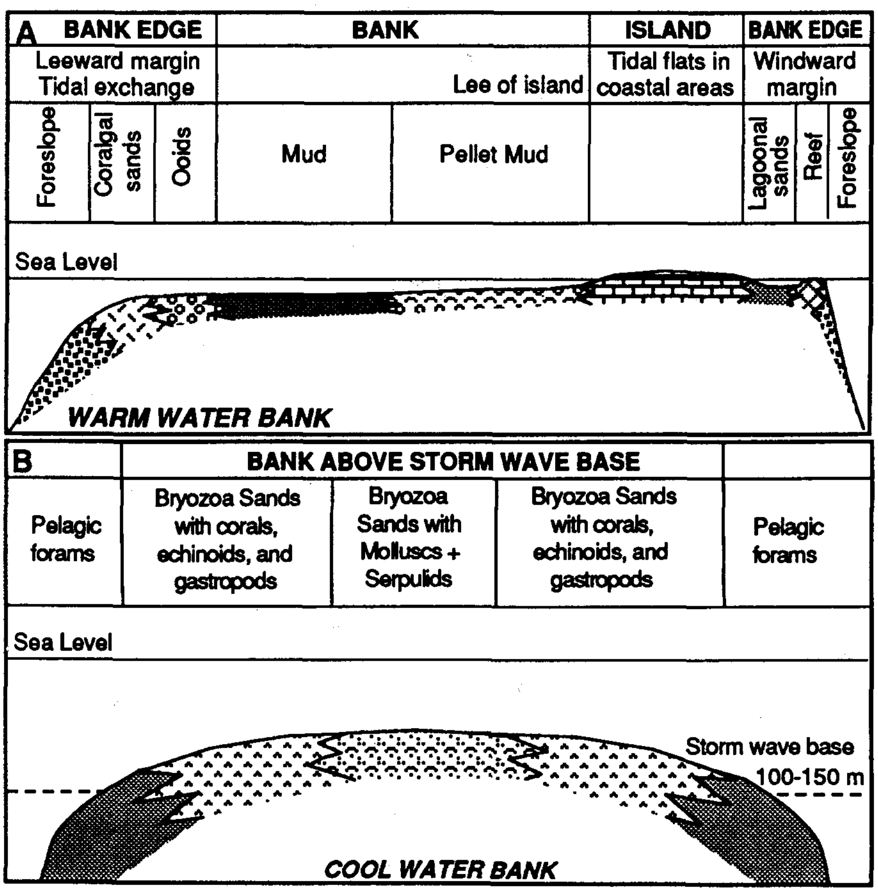

Figure 24 Facies models for carbonates on warm water (A) and cool water (B) banks.

Epeiric shelves

The lack of modern epeiric seas means that ancient examples must be used to model the depositional characteristics of these vast shallow water (<10 m) systems. The rocks present a dilemma because it is difficult to explain how such sediments could all be formed in 'normal' seawater. Why are evaporites generally lacking from such shelves?

Irwin (1965) suggested that epeiric shelves were quiet, shallow water areas not influenced by tidal activity. He divided them into, 1) zone X for the open ocean below wave base, 2) zone Y for a narrow high-energy zone that was under the influence of tidal exchange, and 3) zone Z for the platform beyond the effects of tidal exchange (Fig. 23). This model assumed that tidal currents were not maintained across the platform because of the dampening effect of shallow water. Thus, epeiric shelves were viewed as enormous areas of restricted circulation, affected only by wind-induced waves. Storm activity strongly influenced sediment and biota distributions. Storms caused piling of water in a downwind direction and when the storm had finished, water surged back across the platform, creating currents capable of transporting and sorting skeletal material.

Ginsburg (cited in Pray, 1981) proposed three models that might permit the requisite seawater bathing of epeiric shelves, 1) prograding coastal complexes, an autocyclic model with shoreline-fringing banks prograding across the open shelf, 2) banks and seaways formed because the shelf is dissected by channels that allow water circulation, and 3) wind flushing, a model that is essentially the same as that suggested by Irwin (1965). Pratt and James (1985) suggested that epeiric shelf deposition was controlled by tidal activity and storms. They argued that tides were not dampened and thus viewed an epeiric shelf as a shallow, tidally swept sea characterized by scattered islands and banks of varying sizes. Although shallow subtidal sediments dominate the sequence, each island and bank gave rise to its own intertidal and supratidal complexes (Chapter 16).

Examples of successions formed in epeiric seas are known from the late Precambrian to Ordovician of China, the Cambro-Ordovician of North America, the Triassic to Jurassic of Europe, and the Tertiary of the Middle East (Tucker and Wright, 1990).

Banks

Modern warm water banks tend to be covered by water less than 20 m deep whereas cool water banks are submerged to depths of 200-300 m (Fig. 24).

Holocene, warm water

Modern banks in a warm water setting are characterized by their large areas of shallow water (e.g., Bahama Bank – 96,000 km^2), isolation due to surrounding deep oceanic water, steep faulted margins (>40°), water circulation controlled by tides and waves, and storms that significantly influence sediment transportation. In the simplest sense, warm water banks have coarse sediments around their periphery where tidal activity and/or wind-driven waves produce high-energy conditions. The shallow (< 6 m but locally up to 20 m), quiet water central parts are characterized by muds and pellet muds (Fig. 24). This pattern can be substantially modified by islands that block the effect of cross bank winds or by storms that periodically sweep across the bank. Comparison of the facies of the Great Bahama (Fig. 25) and Caicos (Fig. 26) banks illustrates the variation that can occur in response to different water circulation patterns.

The correlation of lithofacies and biofacies on the Great Bahama Bank (Table 1) shows that the sediment is largely biogenic. Coralgal and oolite lithofacies line bank margins whereas the oolitic-grapestone and lime mud-pellet mud lithofacies occur on the bank interiors. Reefs grow on the eastern margin where wave action keeps water moving, oxygenation high, turbidity low, and salinity and water temperature normal. Andros Island, on the windward, eastern margin prevents the east-west movement of water across the bank. Thus, most cross bank currents are weak and can only move mud. This protected area, characterized by pellet muds and mud, is dis-

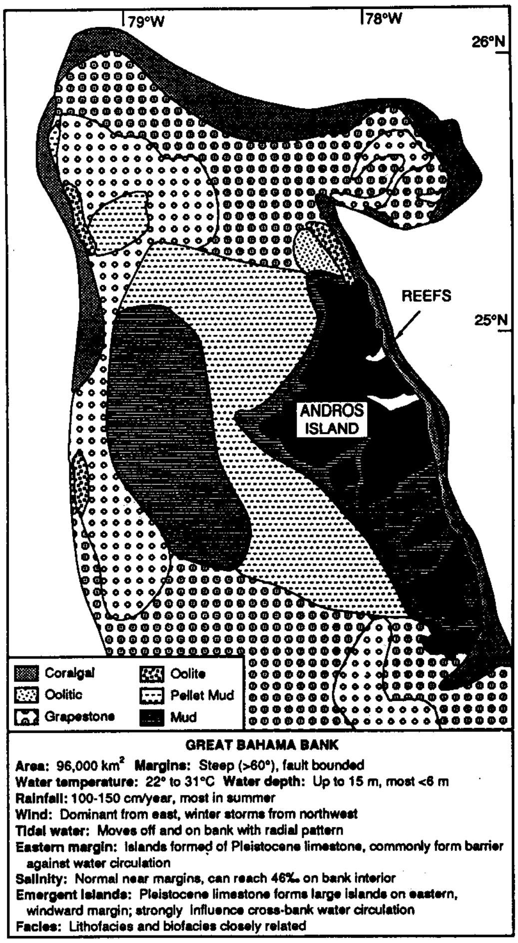

Figure 25 Facies distribution on the Great Bahama Bank and summary of conditions that control sediment formation. Modified from Purdy (1963a, 1963b).

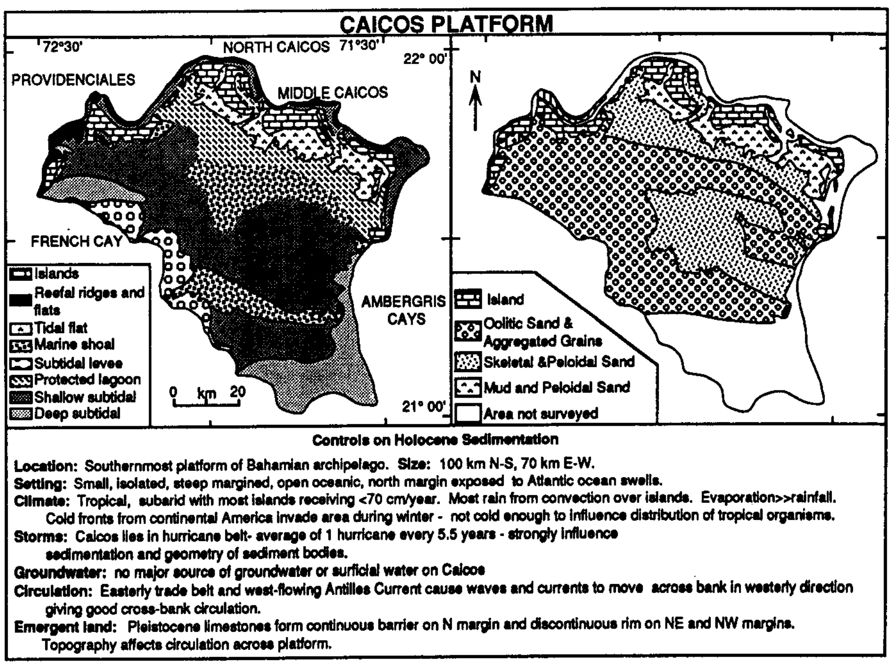

Figure 26 Facies distribution on the Caicos Platform and summary of conditions that control sediment formation. Modified and greatly simplified from Wanless and Dravis (1989).

turbed only during storms or by the winter winds which blow from the northwest. During the summer, stagnation of water on the centre of the bank coupled with high evaporation causes elevated salinities and a modified benthic biota.

The Caicos Bank has islands only on its northern margins (Fig. 26). Reefs are present in front of these islands where swells from the open Atlantic impinge on the bank. There is good circulation over the rest of the bank because of westward-flowing currents and waves generated through the combination of easterly trade winds and the westerly flowing Antilles Current. There are no areas of stagnation and so the lithofacies, which are not linked to the biofacies, are different from those on the Great Bahama Bank. Extensive mud accumulation is localized to tidal flats on the southern, leeward sides of the islands. The rest of the bank is covered by skeletal, aggregate grain and ooid sand.

Table 1 *Lithofacies, habitats, and communities of the Great Bahama Bank. Habitat refers to environment in which a particular group of organisms live, community refers to group of organisms which live together. After Bathurst (1975).*

Lithofacies	Habitat	Community
Coralgal	Reef	*Acropora palmata*
	Rock pavement	plexaurid (sea whip)
	Rocky shore	littorine
	Rocky ledges and prominences	*Millepora*
	Unstable sand	*Strombus samba*
Oolitic and grapestone	Stable sand	*Strombus costatus*
Oolite	Mobile oolite	*Tivela abaconis*
Mud and pellet sand	Mud and muddy sand	*Didumnum candidum* and *Cerithidea costata*

Ancient, warm water

Ancient examples of warm water banks occur in the Devonian of western Canada. The Golden Spike Reef in the Leduc Formation, for example, was a platform rimmed by stromatoporoid reefs (Walls, 1983). The platform interior was covered by interbedded skeletal, sand flat grainstones and packstones and peritidal planar stromatolites. Some spectacular examples of ancient banks occur in the Triassic strata of northern Italy (Fig. 27) where it is possible to drive around exhumed platforms.

Holocene, cool water

Banks in cool water settings are generally covered by biogenic gravels and sands derived from bryozoa, molluscs,

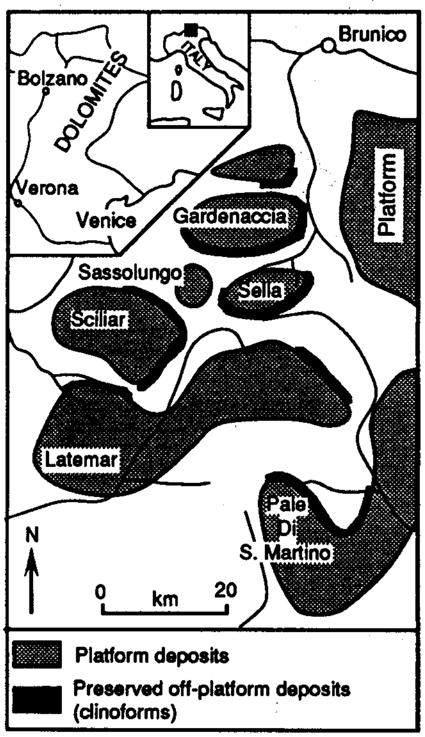

Figure 27 Bank and platform distribution in the Triassic successions of the Dolomites in northern Italy. Modified from Bosellini and Rossi (1974).

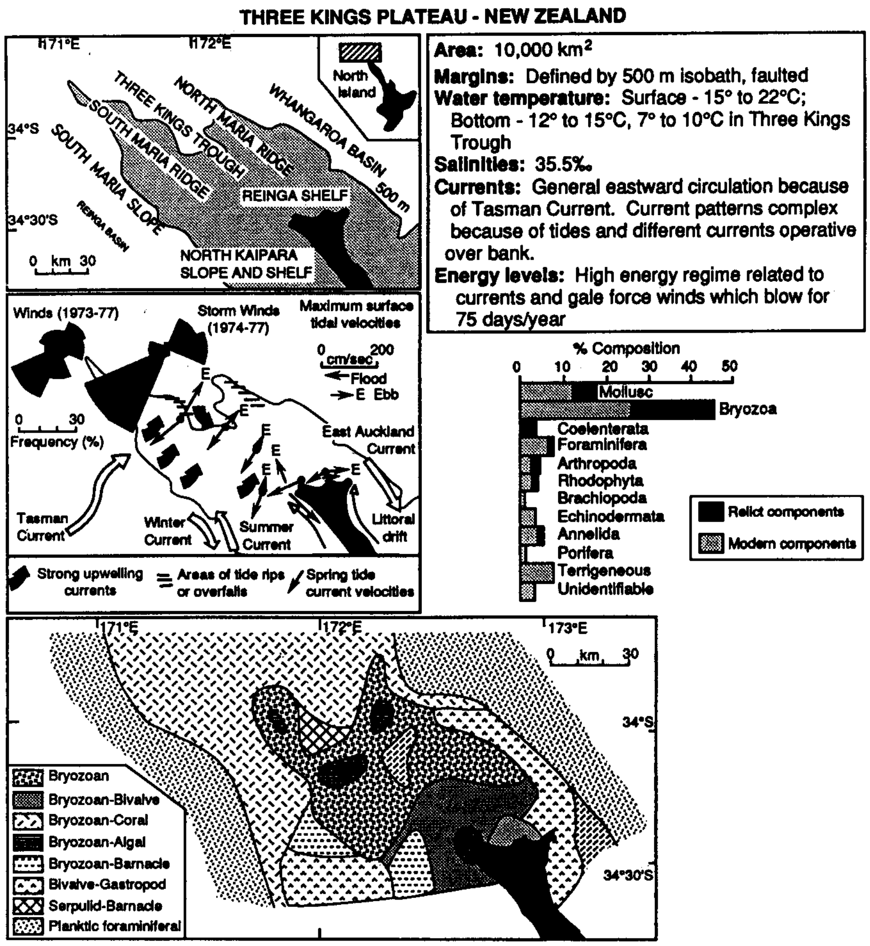

Figure 28 Summary of conditions, facies distribution, and sediment composition on Three Kings Plateau, northern New Zealand. Modified from Nelson *et al.* (1982).

echinoids, corals and gastropods (Fig. 28). Zonation of lithofacies across the bank is only evident in the skeletal composition of the sediments.

Modern examples include the Three Kings Plateau and Rockall Bank (Wilson, 1979, Scoffin *et al.*, 1980). Three Kings Plateau, New Zealand (Fig. 28), which lies in a zone of active nutrient upwelling, is swept by vigorous wind and storm waves and tidal currents. The seafloor is covered by bryozoa/bivalve/ahermatypic coral sands and gravels that lack mud to depths of 1500 to 3000 m. Facies belts are depth related. Biotic communities include 1) bivalve (bryozoan) facies (<150 m) on particulate substrates, 2) bryozoan (coralline algae-barnacle) facies (85 to 250 m), 3) ahermatypic coral (bryozoan-serpulid) facies (200 to 1000 m) on coarse and rocky substrates, and 4) planktonic foraminifera (>1000 m) in the peripheral basin sediments. Active skeletal production is limited to inshore regions, areas of rough seafloor topography, and ridge and bank crests. Most sediment seems to have been produced during low sea level stand(s) associated with the last glaciation.

Drowned carbonate platforms

Drowning of a platform occurs when the rate of sea level rise outpaces the rate of vertical sediment accumulation due to fault-induced subsidence, rapid glacio-eustatic sea level rises, or shutting down of carbonate production (Schlager, 1981). Such drowning is marked by a transition from shallow- to deep-water facies, a change from benthic to pelagic organisms, cementation forming hardgrounds, production of Fe- and Mn-oxides, and phosphate formation.

Modern examples of drowned platforms are common in the Pacific and Indian Oceans. Cay Sal Bank (Fig. 2) and the Blake Plateau are examples of drowned platforms in the Atlantic/Caribbean. On the latter, now in 2000 to 4000 m of water, pelagic sediments and Fe and Mn precipitates are being deposited on shallow water Cretaceous carbonates. Ancient examples of drowned carbonate seamounts occur in the Jurassic successions of the Apennines in Italy (Bice and Stewart, 1990) where pelagic limestones overlie shallow water platform carbonates.

CONTROLS ON DEVELOPMENT OF CARBONATE PACKAGES

The stratigraphy of subtidal platform carbonates is the sum of a number of different controls (Chapter 14). The most important universal, extrinsic controls are tectonic subsidence (Schlager, 1981; Cleotingh *et al.*, 1985), eustatic changes in sea level (Chapter 2), plate movement (Davies *et al.*, 1989) and clastic sediment input (Doyle and Roberts, 1988; Budd and Harris, 1990; Lomando and Harris, 1991). Specific to this setting, however, are the intrinsic controls of antecedent topography, biotic evolution, carbonate growth potential and lag time.

Antecedent topography – blueprint for sedimentation

In modern settings, antecedent topographic features are commonly the blueprint for sedimentation. Thus, many islands, shoals and barrier and patch reefs are located on highs in the antecedent topography where phototropic organisms were closer to sea level and thus in a better position for photosynthesis. Such highs are also the site of increased agitation and thus suitable for ooid shoal formation. Conversely, antecedent topographic lows become sheltered, quiet water areas where muds preferentially accumulate. The Belize Shelf (Purdy, 1974) and the Trucial Coast (Purser, 1973) are excellent examples of platforms that have a Holocene facies architecture related to antecedent topography.

Antecedent karst topography is controlled by climatic conditions and, to a

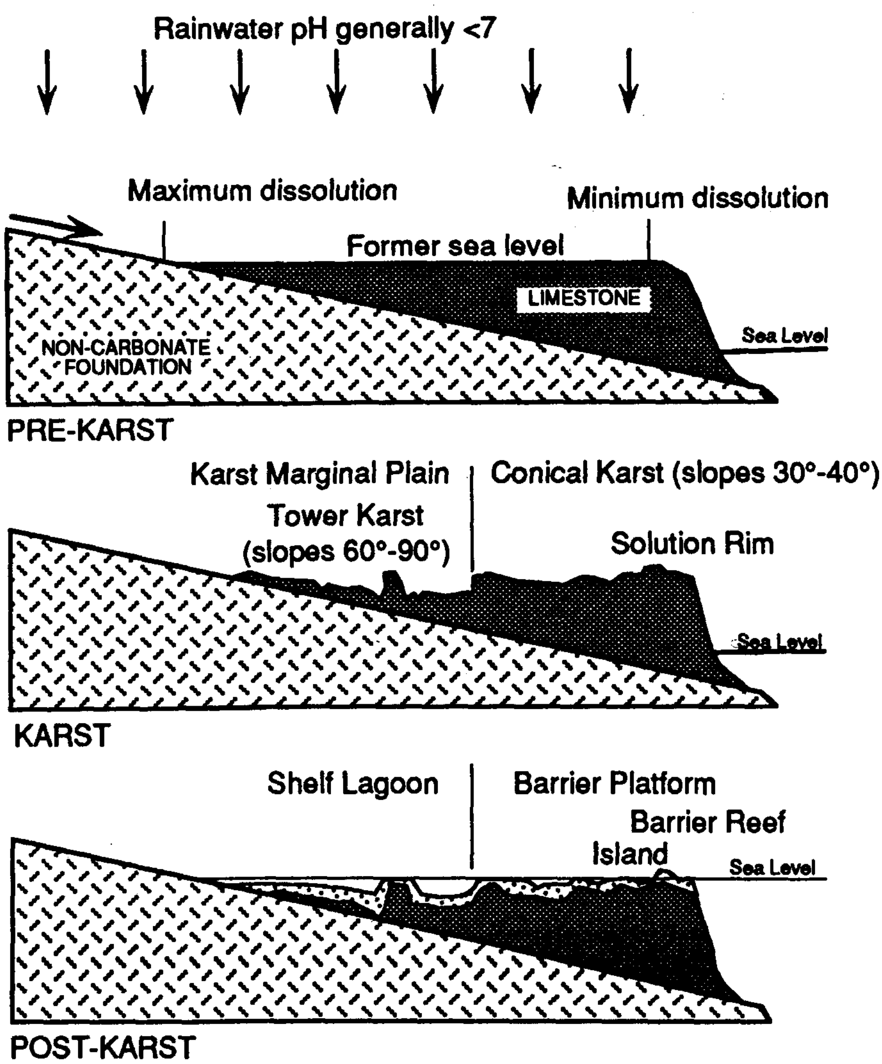

Figure 29 Diagrammatic illustration of evolution of karst terrains and influence that this can have on the location of reefs and facies during later transgressions. From Purdy (1974).

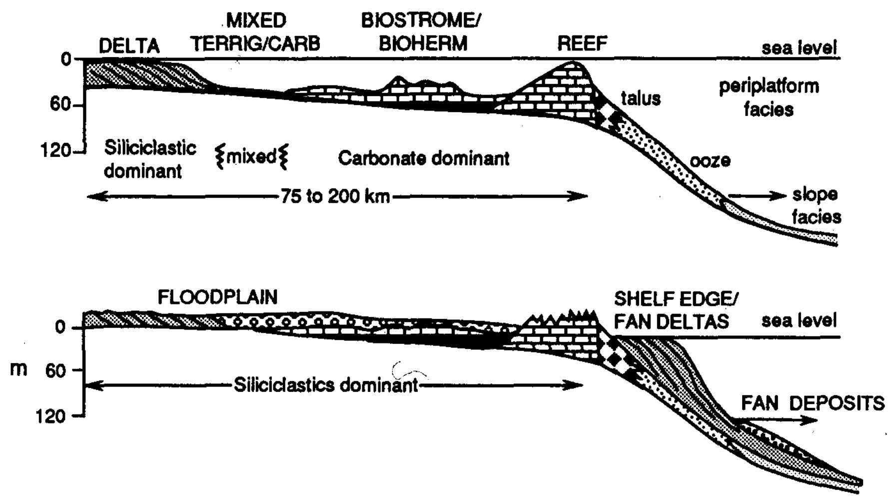

Figure 30 Diagrammatic illustration showing progradation of coastal siliciclastic deposits over platform carbonates on the Northeast Australian Platform during lowstand periods. Modified from Davies *et al.* (1989).

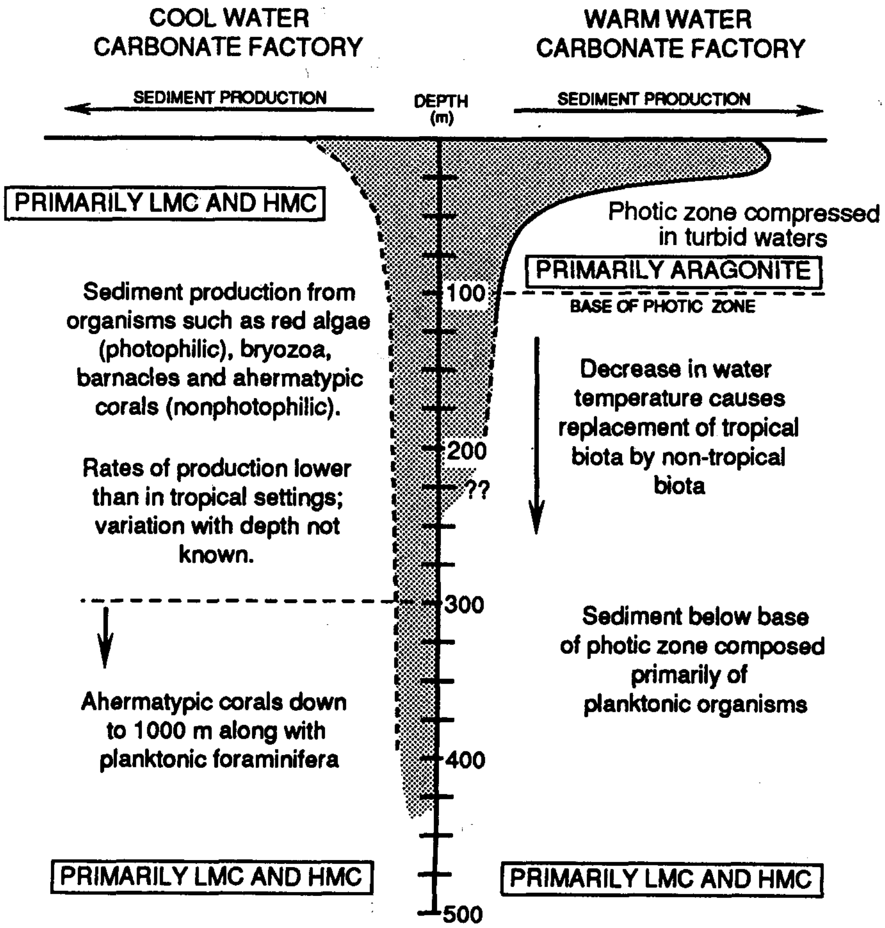

Figure 31 Comparison of carbonate sediment production in cool water and warm water areas. The speculative nature of sediment production rates of the cool water carbonates (dashed line) reflects the lack of detailed information from these areas.

lesser extent, the composition of the exposed carbonates. Warm water carbonates exposed to a wet, tropical climate are quickly lithified and a rugged karst terrain commonly results (Fig. 29). Cool water carbonates exposed to temperate climates do not react so radically and a much more subdued karst topography results. Exposure, however, does not guarantee karst development. Pleistocene lowstands on the Northeast Australia Platform, for example, led to the seaward progradation of coastal siliciclastic sediments. As a result, only the topographically higher carbonates of the barrier reef rim were karsted (Fig. 30). Pre-existing features such as old reefs and shoals, terraces formed by shoreline erosion, or siliciclastic river deposits can also influence later depositional patterns.

Biological evolution

Evolution is important because carbonate production is tied to biota. Most Paleozoic bioclasts, for example, were calcite whereas the majority of Mesozoic and Cenozoic skeletal particles were aragonite (Fig. 5). Nevertheless, modern and ancient facies patterns are comparable because subtidal carbonate sediments have been produced in a similar range of environments throughout the geological record.

Evaluating the role(s) of nonskeletal organisms such as grasses and microbes through time is difficult because of their poor preservation potential. The role of soft-bodied animals in burrowing and bioturbation of sediment through time can be evaluated through the ichnofossils that occur in many carbonate successions. Droser and Bottjer (1989), for example, suggested that there was a major increase in depth and extent of bioturbation in the Early Paleozoic.

Carbonate growth potential

The average growth potential of modern reefs and carbonate platforms is about 100 cm/k.y., a rate that exceeds the rates of relative sea level rise caused by long-term subsidence or eustatic sea level changes (Schlager, 1981). It seems unlikely that these extrinsic processes could outpace the growth of healthy carbonate platforms except in situations where sea level change is accelerated due to rapid fault-controlled subsidence or quick rises associated with glacial melting.

Insights into the growth potential of carbonate platforms can be obtained by calculating the amount of sediment generated by modern carbonate-secreting organisms, examining carbonate productivity changes with depth and position on shelf, and considering long-term accumulation rates on ancient carbonate platforms. Estimating the rates of vertical carbonate accumulation is complicated because sediments may have been deposited through lateral progradation rather than vertical accretion (Hardie *et al.*, 1991). It must also be remembered that the thickness of sediment produced during a given period is controlled by the accumulation space, not the rate of sediment production.

Estimates of sediment production can be calculated by considering the amounts of sediment produced through the breakdown of skeletal organisms in the carbonate factory. Neumann and Land (1975) estimated that calcareous algae in the Gulf of Abaco, northern Bahamas, produced up to 168 x 10^{10} kg of sediment over the last 5500 years. Even though this estimate was based on selected algae (i.e., a small proportion of total production), it still represents an overproduction of 190 per cent compared to the amount of sediment on the platform. Such calculations suggest that most sediment produced in the factory is transported onshore or into the nearby ocean basin.

The rate of carbonate production is depth dependent (Fig. 31). In warm water settings, production is highest and relatively constant to depths of about 15 m because this zone is usually inhabited by numerous carbonate-secreting phototrophic organisms. Sediment production in cool water settings is generally lower than that in warm water settings and does not show such variation with depth.

Carbonate productivity also varies across a platform. Sediment production in back reef and lagoonal areas of the Florida Keys translates into vertical accretion rates of 40 and 20 cm/k.y., respectively (Bosence, 1989). These values are comparable to estimates of Holocene sedimentation rates (muddy lagoon – 10-20 cm/k.y.; shallow subtidal – 40-60 cm/k.y.; deeper ramp/shelf – 10-20 cm/k.y.) averaged over several thousand years (Read *et al.*, 1990). These values are, however, lower than the average carbonate growth potential based on highly productive Holocene margin reef and sand shoal environments. Cool water carbonates accumulate at much slower rates (James and Bone, 1991).

Estimates of long-term accumulation rates of ancient carbonate deposits are about two orders of magnitude less than those in modern warm water settings (Fig. 32). Cool water Cenozoic platform limestones, however, accumulated at rates similar to those of some ancient platforms. Some differences between modern and ancient sedimentation rates are due to the fact that ancient successions include numerous breaks related to hardground development, sea level fluctuations, or subaerial exposure. Sediments in metre-scale Phanerozoic cycles, typical of many ancient carbonate platforms, may have accumulated in 3-30 per cent of the time represented by the sequence; the rest of the time being represented by such breaks in sedimentation (Wilkinson *et al.*, 1991).

Carbonate platforms throughout geological time appear to have been the sites of rapid carbonate production and high growth potential. Nevertheless, the actual rates have varied through time with the highest rates being coincident with periods when reef-building organisms were abundant (Bosscher and Schlager, pers. comm.). The Early Carboniferous, for example, was a time when carbonate ramps were the dominant settings for carbonate accumulation, possibly because of the absence of large skeletal framebuilders and water temperatures and productivity profiles that were different from other times (Wright and Faulkner, 1990).

Lag time

The initial stage of a transgression is not well understood, mainly because there is little direct evidence in terms

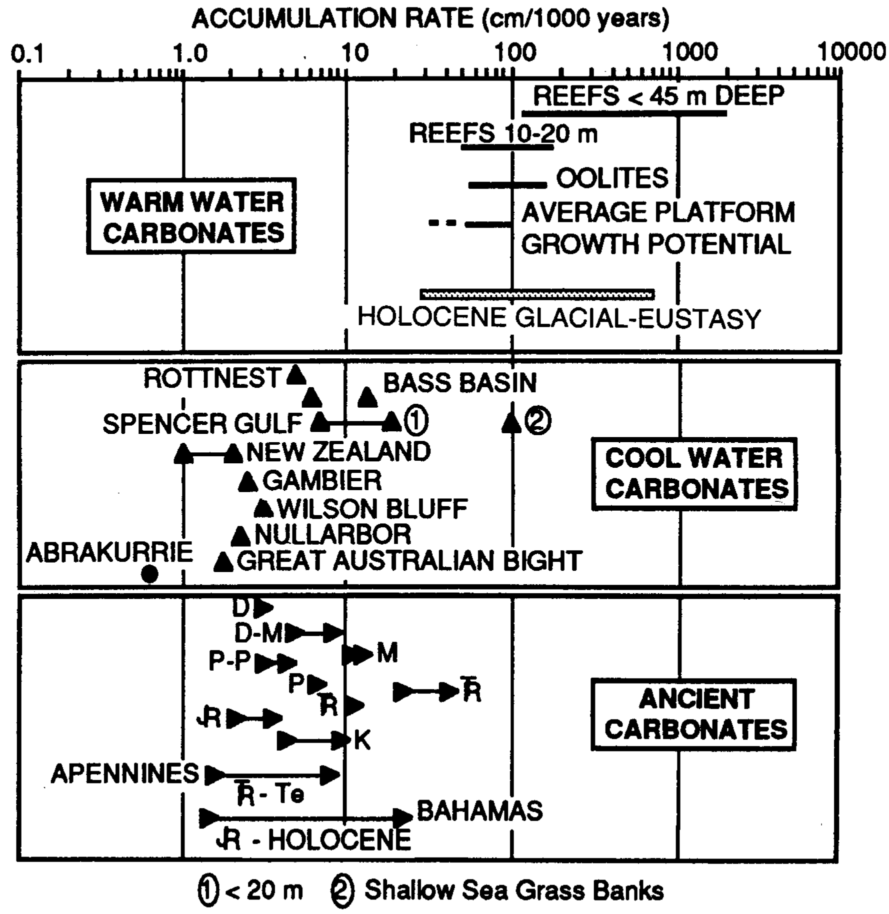

Figure 32 Comparison of estimated accumulation rates for warm water carbonates, cool water carbonates, and ancient carbonates. Modified from James and Bone (1991).

of sediment. It has been suggested that a minimum depth of water, the lag depth, is needed before circulation becomes effective enough to allow sediment production, accumulation, and dispersal (Ginsburg, 1971; Hardie and Shinn, 1986). Estimates of 1 to 2 m for the lag depth are based on some Holocene shallowing-upward cycles in Florida Bay (Enos, 1977) and the Bahamas (Harris, 1979) that have a basal 0.5 m thick layer of mangrove peat overlain by carbonates. The upward change from peat to carbonates records the evolution from initial platform flooding to the establishment of an active carbonate factory.

In some settings, the lag time is that interval when sediments deposited during the preceding period of subaerial exposure (e.g., terra rossa, freshwater carbonate sediments) are removed and/or modified by erosion. In addition, boring organisms (e.g., sponges, worms, bivalves) may colonize the new seafloor (Chapter 4). Thus, marine borings can be superimposed on the unconformity that marks the sequence boundary (Desrochers and James, 1988; Jones and Hunter, 1989).

PLATFORM RESPONSE TO EUSTASY

Developing a single model that incorporates all the variables that control vertical sediment accretion is complicated because of the numerous factors involved. Consequently, modelling is generally based on the two or three variables deemed the most important. Even if sediment is produced rapidly, it can only build up on the platform if there is sufficient accumulation space. Thus, relative changes in sea level are the major control over the style of sedimentation because this ultimately controls the space available on the platform (Chapter 14). There are three end member states associated with specific parts of a long-term third-order change in relative sea level (Fig. 33).

Exposure

If sea level falls below the edge of the platform, the carbonate factory is shut down and production ceases and the sediments are subject to meteoric diagenesis (Figs. 33, 34).

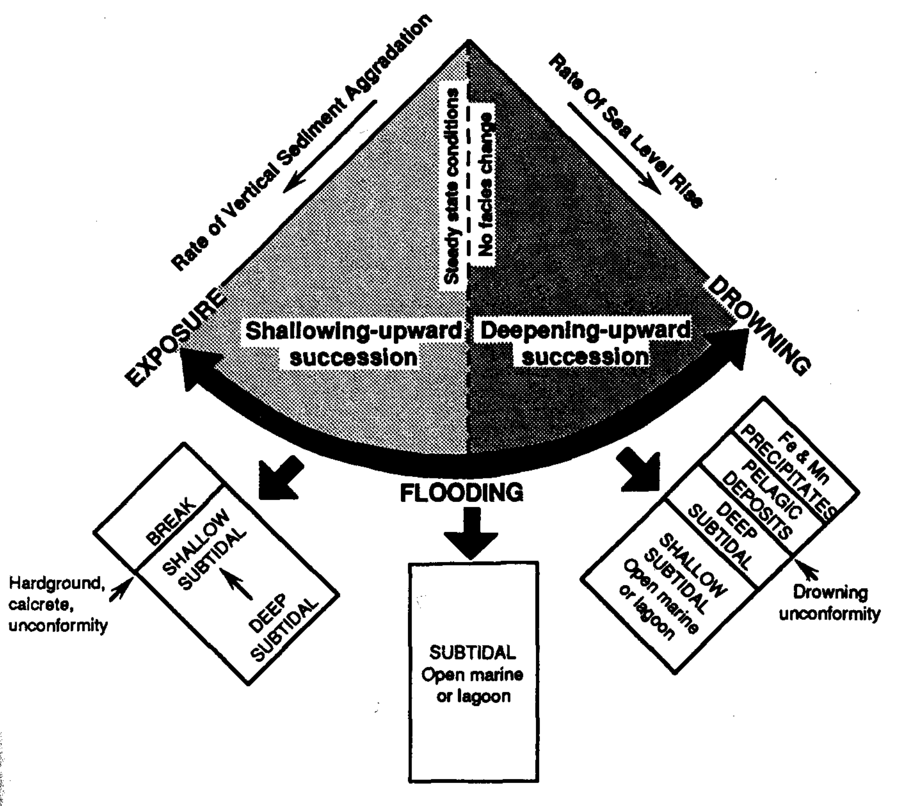

Figure 33 Schematic diagrams illustrating the type of succession that forms as the rate of sea level rise and the amount of carbonate sediment production varies.

Drowning

During transgression, a rapid rise in relative sea level may drown the platform (Figs. 33, 34). This generally occurs because the carbonate factory is submerged below the photic zone and cannot produce sufficient sediment to keep pace with the rise in sea level. Hardgrounds, which may develop in such situations, form submarine unconformity bounding surfaces or drowning unconformities (Schlager, 1989). An unconformity of similar appearance can also form if the carbonate factory is shut down through nutrient poisoning or choking by siliciclastic sediments during a sea level highstand (Schlager, 1989).

Unless platform drowning is tectonically induced and subsidence is into such deep water that little sediment is produced, the seafloor may eventually rise and reenter the photic zone, due to slow and steady sediment accumulation or a drop in sea level. Rapid sedimentation can then resume. Reefs on these incipiently drowned platforms, which generally have a higher vertical accretion rate than the subtidal platform seafloor, may keep up with sea level and thereby create a rimmed platform with a deep lagoon (Kendall and Schlager, 1981). Cool water platforms are usually viewed as incipiently drowned because accumulation rates are slow and/or off platform sediment transport is active.

Flooding

In a steady state situation, water depth over the platform is just right for maximum sediment production and accumulation space is maintained by a combination of platform subsidence and sea level rise (Figs. 33, 34). The rates of Holocene carbonate deposition on warm water platforms are greater than long-term rates of relative sea level changes on passive margins and intracratonic basins (Schlager, 1981). The rates of accumulation on cool water platforms, however, are less or even nil when the depositional surface lies above wave base and hardgrounds form as water is rapidly pumped through the sediment by wave action.

Variations on a theme

The rate of sea level change is important because different rates of flooding will trigger different responses from the carbonate factory (Kendall and Schlager, 1981; Scaturo *et al.*, 1989), as it does in reefs (Chapter 17).

Backstep (transgression)

Backstepping denotes the movement and reestablishment of a shelf margin toward the shelf interior. A rapid, relative sea level rise causes growth on the preexisting shelf to cease or slow down and the reef margin establishes itself in a more landward position thereby reducing platform width (Fig. 34).

Catch-up (transgression — early highstand)

In this situation, an initially rapid increase in the rate of relative sea level rise is followed by a decrease. The depositional surface remains in water depths conducive to high sediment production rate, and as the rate of relative sea level rise slows, carbonate sedimentation promotes vertical accumulation, thereby allowing the seafloor to *catch up* with sea level. Although vertical sediment accretion dominates, progradation will began as soon as the rate of creation of new accumulation space decreases with time. This leads to the deposition of thick, subtidal-dominated sequences characterized by an overall shallowing-upward trend that may be capped by prograding tidal flats.

Keep-up (transgression)

Keep-up occurs when the rate of sediment accumulation 'keeps-up' with the rate of relative sea level rise (Fig. 34) and accumulation space is continually being created. In this situation there is virtually no change in depositional conditions and facies are maintained throughout the period of rising sea level (steady state situation). Vertical sediment accretion dominates and thick, subtidal-dominated successions can form. Prograding tidal flats or sand shoal bodies are generally absent.

Progradation, fillup, and spillout (highstand)

This is the period when sediment production starts to exceed the rate of relative sea level rise and a fundamental change in the overall balance of the system occurs (Fig. 34). Under such conditions excess sediment becomes available for movement off the platform. Basinward transportation promotes platform margin progradation (Chapter 18) thereby expanding the width of the platform and potentially, the size of the carbonate factory. Conversely, shoreward transportation of sediment will promote tidal flat progradation over the platform (Chapter 16) thereby reducing platform width and decreasing the size of the carbonate factory.

SUBTIDAL PLATFORM CARBONATE STRATIGRAPHY

Thick successions of shallow water carbonate deposits commonly include repetitive metre-scale subtidal cycles. These differ from the classic peritidal cycles (Chapter 16) because they formed through sedimentation in shelf settings beyond the reach of prograding tidal flats or shoreline sandbodies.

Metre-scale cycles

Metre-scale subtidal cycles include successions with no depositional or erosional breaks (depositional cycles), and successions with diagenetic caps (diagenetic cycles).

Depositional cycles

Such cycles are typified by an upward increase in grain size, bed thickness, and cross bedding and other high-energy structures and thus differ from fining- and thinning-upward peritidal cycles. Furthermore, they are not capped by intertidal facies or subaerial exposure features. These shallowing-upward cycles appear to be the dominant cycle type on unrimmed shelves, especially ramps, throughout the geological record (Lohmann, 1976; Markello and Read, 1982; Aigner, 1985; Calvet and Tucker, 1988; Osleger, 1991). Upper Cambrian carbonates of Utah, for example, contain shallow to deep subtidal cycles formed of burrowed wackestone with open marine faunas that grade up into oncolitic-skeletal packstone that is capped by clean oolitic grainstone (Osleger, 1991). These cycles form a continuum across the carbonate ramp and are genetically linked to one another by shared lithofacies.

Diagenetic cycles

These cycles have a cap characterized by subaerial or submarine diagenetic features. The subtidal facies, formed in shallow to deep subtidal environments, include a single lithofacies, alternations of two lithofacies, or most commonly, vertically repeated lithofacies.

Cycles with subaerial diagenetic caps are common on banks. The Middle Triassic Latemar Limestone (Fig. 35) of the Dolomites region, northern Italy, contains about 600 cycles. Each cycle is composed of a basal, shallow subtidal packstone-grainstone unit overlain by a thin dolomitized cap with vadose cements, pisoids and other evidence of calichification (Goldhammer *et al.*, 1987). Exposure must have been linked to frequent drops in sea level because

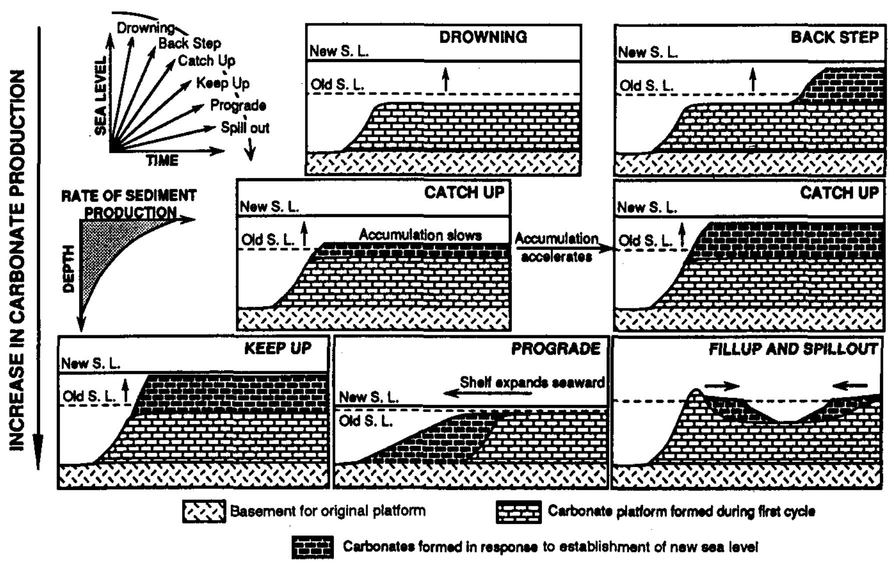

Figure 34 Diagrams illustrating growth of carbonate platforms once the rate of sediment production exceeds the rate of sea level rise.

the absence of peritidal deposits precludes exposure through tidal flat progradation.

Cycles capped by submarine diagenetic features occur on deep open shelves. The Oligo-Miocene Abrakurrie Limestone of southern Australia, for example, is a cool water, deep shelf (>50 m) deposit which contains numerous cycles with well-cemented hardground caps. Comparison with modern, swell-dominated shelves suggest that this type of cycle resulted from sedimentation when the shelf was below the depth of wave abrasion and cementation took place when the shelf was above wave base and subject to active water pumping (Fig. 36).

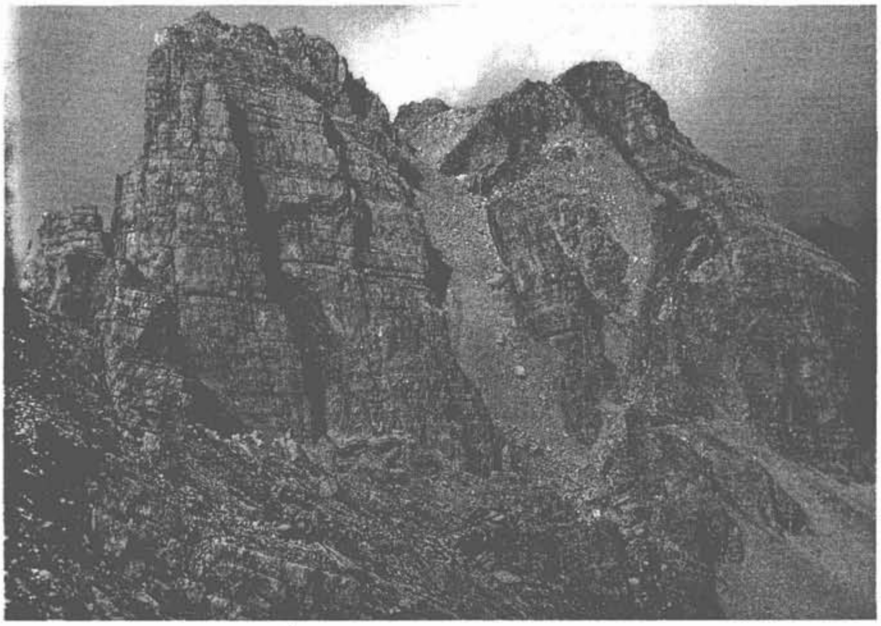

Figure 35 General view of the Triassic Latemar Limestone in northern Italy. This ca. 100 m-thick carbonate succession, formed of stacked metre-thick cycles, accumulated in the interior of a bank. Photograph courtesy Noel James.

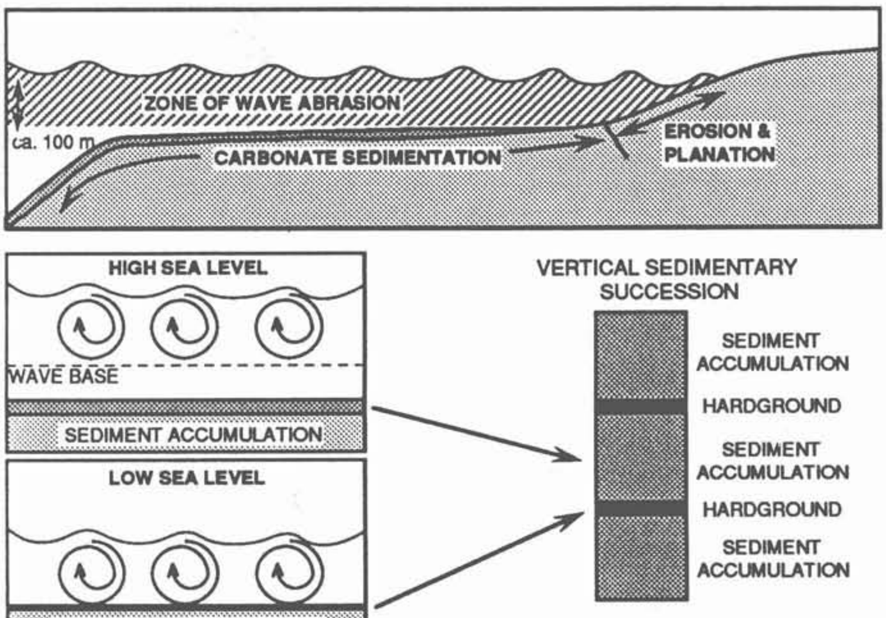

Figure 36 Diagram summarizing effect of high sea level and low sea level on the carbonate successions forming on temperate water shelves such as the Great Australian Bight Shelf. Note the effect that sea level has on the formation of hardgrounds. Modified from James and Bone (1991).

Autocyclic versus allocyclic controls

Mechanisms proposed for the generation of repeated metre-scale subtidal cycles include autocyclic processes (vertical accretion, variations in sediment production and redistribution), allocyclic processes (episodic subsidence, short-term eustasy) or a combination of both. The nature of these cycles may also be influenced by energy regimes which are dictated by platform geometry and local climate.

Autocyclic processes

Vertical accretion of sediments on a platform will occur in situations where carbonate growth potential exceeds the rate of relative change in sea level. This simple relationship can be radically altered by storm and wave reworking and sediment redistribution that together may limit vertical sediment accretion and keep the seafloor below the zone of optimal carbonate productivity. The critical element of this autocyclic process is the depth of the storm wave base.

Allocyclic processes

Allocyclic processes for forming metre-scale subtidal carbonate cycles involve episodic subsidence or short-term sea level fluctuation. Sea level change caused by episodic subsidence is unlikely unless the lithosphere or local fault blocks can oscillate with similar short frequencies. It is also hard to imagine that repeated tectonic pulses over a long period of time could produce repetitive metre-scale cycles, especially in relatively stable tectonic settings such as passive margins.

The simplest driving mechanism for the repetition of metre-scale subtidal cycles would seem to be short-term eustatic sea level fluctuations (Goldhammer *et al.*, 1987; James and Bone, 1991; Osleger, 1991). This mechanism is in part supported by actualistic models such as glacio-eustasy that are driven by orbital perturbations (i.e., Milankovitch cycles). There is good evidence that Middle Triassic Latemar megacycles, formed of five thinning-upward cycles, were controlled primarily by composite eustatic sea level changes in the Milankovitch band (Goldhammer *et al.*, 1987).

Thick successions of depositional subtidal cycles on stable cratonic interiors and passive margins appear to be the product of short-term eustatic sea level fluctuations that act in concert with intrinsic factors such as storm and wave reworking (Osleger, 1991). This process of wave reworking is a subsidiary but critical mechanism in the generation of subtidal cycles because it controls the upward limit of sediment accumulation. Fluctuations of the seafloor below and above this critical depth of wave reworking associated with short-term changes of eustatic sea level and/or storm activity may explain subtidal cycles with submarine diagenetic caps that form on deep shelves (Abrakurrie type, James and Bone, 1991).

Relationship of cycles to platform geometry

Subtidal cycles seem to be more common on open shelves than on rimmed platforms where peritidal cycles appear to dominate. This relationship is probably due to differences in the energy regimes. Unrimmed platforms are influenced by high-energy conditions because oceanic waves and swells, which wash directly on and across the shallow shelf, cause constant submarine erosion and offshore transport of sediment. This inhibits aggradation above the depth of wave abrasion and limits progradation of tidal flat or shoreline sandbodies across the platform. In contrast, reef-rimmed platforms are characterized by low-energy conditions because oceanic waves and swells are absorbed and storm activity is dissipated along the protective reef. Fine-grained sediments, which accumulate in restricted shallow lagoons, can be fed onto prograding tidal flats and widespread peritidal facies develop. Thus, peritidal cycles are common on rimmed platforms unless they are inhibited by other factors.

Large-scale sequences

Less is understood about 10-1,000 m-thick carbonate successions that contain repetitive small-scale subtidal cycles. In the Alpine Triassic, for example the long-term systematic vertical changes in the stacking pattern of the high-frequency cycles (fourth- and fifth-order) seem to have been dictated by a low-frequency (third-order) rise and fall of sea level against a background of overall slow tectonic subsidence (Goldhammer *et al.*, 1990). In particular, the increase in the rate of addition of new accumulation space on the rising limb of a third-order sea level change resulted in thick cycles and condensed megacycles due to missing beats of submergence. These long-term systematic changes occur irrespective of the allocyclic or autocyclic origin of the high-frequency cycles. Composite eustacy seems to impose a hierarchy of stratigraphic forcing that provides a link between metre-scale cyclostratigraphy and large-scale sequence stratigraphy.

CONCLUSIONS

Subtidal portions of carbonate platforms are complex depositional environments that are critical to the health of the entire carbonate depositional system. Complexity arises because the biota on these platforms, which are the source of most of the sediment, respond to *all* changes in the variables that control conditions on the platform. Once formed, the sediments then come under the control of water movement generated by tidal exchange, ocean currents, wind currents, and storms. The effect of such currents on facies distribution and sequence generation has been largely underestimated. Knowledge of carbonate platforms is disproportionally slanted towards those in warm water settings. More information is required from cool water settings before further advances can be made with respect to the full spectrum of carbonate platforms.

Our understanding of the mechanisms that govern the vertical development of facies on carbonate platforms is largely based on a comparative approach with modern facies analogs and knowledge of the dynamics of subtidal carbonate environments. There is need for a rigorous process-based approach to the interpretation of large-scale sequences built by stacked small-scale cycles. Allocyclic eustatic controls play a fundamental role in determining sequence development on platforms, a fact that it is implicit to many of the approaches used in computer modelling. In future, however, subsidiary autocyclic processes such as wave base reworking and redistribution will also have to be factored into the computer models.

ACKNOWLEDGEMENTS

We are grateful to Noel James who helped us to improve the quality of this paper by critically reading and extensively revising numerous earlier versions. Funding for preparation of the manuscript, and research on carbonate facies came from the Natural Sciences and Engineering Research Council of Canada.

REFERENCES

Basic sources of information

Aigner, T., 1985, Storm depositional systems: Lecture Notes in Earth Sciences 3: Berlin, Springer-Verlag, 174 p.

A readable, process-oriented summary of modern and ancient storm deposits, concentrating on ramp carbonates.

Flügel, E., 1982, Microfacies analysis of limestones: Berlin, Springer-Verlag, 633 p.

An exhaustive well-illustrated text focused on the composition of platform facies. An excellent source of detailed information.

Goldhammer, R.K., Dunn, P.A. and Hardie, L.A., 1990, Depositional cycles, composite sealevel changes, cycle stacking patterns and the hierarchy of stratigraphic forcing: examples from Alpine Triassic platform carbonates: Geological Society of America, Bulletin, v. 102, p. 535-562.

An interesting paper that discusses the role of composite eustasy in generating kilometre-thick sequences formed of stacked metre-thick cycles. Uses computer modelling to compliment stratigraphic analysis of Alpine Triassic platform carbonates.

Nelson, C.S., 1988, Non-tropical shelf carbonates-modern and ancient: Sedimentary Geology, v. 60, 367 p.

A collection of 33 papers that provides an excellent introduction to the realm of cool water carbonates with reference to modern and ancient examples.

Schlager, W., 1981, The paradox of drowned reefs and carbonate platforms: Geological Society of America, Bulletin, v. 92, p. 197-211.

A pioneering paper that contains lucid explanations of some of the basic controls of sediment accretion on platforms.

Tucker, M.E. and Wright, V.P., 1990, Carbonate sedimentology: Oxford, Blackwell Scientific Publications, 482 p.
An informative review of shallow, warm water carbonates using modern and ancient examples from all ovcr the world. A good compliment to Nelson's (1988) book on cool water carbonates.

Wilgus, C.K., Hastings, B.S., Posamentier, H.W., Ross, C.A. and Kendall, C.G.St.C., eds., 1988, Sea level changes: an integrated approach: Society of Economic Paleontologists and Mineralogists, Special Publication 42, 407 p.
Collection of papers emphasizing conceptual basis of sequence stratigraphy plus numerous case studies of sea level change from the geological record.

Other references

Ahr, W.M., 1973, The carbonate ramp: an alternative to the shelf model: Transactions of the Gulf Coast Association of Geological Societies, v. 23, p. 221-225.

Ball, M.M., 1967, Carbonate sand bodies of Florida and the Bahamas: Journal of Sedimentary Petrology, v. 37, p. 556-591.

Bathurst, R.G.C., 1975, Carbonate sediments and their diagenesis: Amsterdam, Elsevier, 658 p.

Bice, D.M. and Stewart, K.G., 1990, The formation and drowning of isolated carbonate seamounts: tectonic and ecological controls in the northern Apennines, *in* Tucker, M.E., Wilson, J.L., Crevello, P.D., Sarg, J.R. and Read, J.F., eds., Carbonate platforms, facies, sequences and evolution: International Association of Sedimentologists, Special Publication 9, p. 145-168.

Bosellini, A. and Rossi, D., 1974, Triassic carbonate buildups of the Dolomites, northern Italy: Society of Economic Paleontologists and Mineralogists, Special Publication 18, p. 209-233.

Bosence, D.W.J., 1989, Biogenic carbonate production in Florida Bay: Bulletin of Marine Sciences, v. 44, p. 419-433.

Boucot, A.J., 1975, Evolution and extinction rate controls: Developments in palaeontology and stratigraphy: Amsterdam, Elsevier, 427 p.

Brookfield, M.E., 1988, A mid-Ordovician temperate carbonate shelf — the Black River and Trenton Limestone groups of southern Ontario, Canada: Sedimentary Geology, v. 60, p. 137-153.

Budd, D.A. and Harris, P.M., 1990, Carbonate-siliciclastic mixtures: Society of Economic Paleontologists and Mineralogists, Reprint Series 14, 272 p.

Burrollet, P., 1979, La mer pélagienne: Géologie Méditéranéenne, v. 6, 1345 p.

Calvet, F. and Tucker, M.E., 1988, Outer ramp cycles in the Upper Muschelkalk of the Catalan Basin, northern Spain: Sedimentary Geology, v. 57, p. 185-198.

Cloeting, S., McQueen, H. and Lambeck, K., 1985, On a tectonic mechanism for regional sea level variations: Earth and Planetary Sciences Letters, v. 75, p. 157-166.

Collins, L.B., 1988, Sediments and history of the Rottnest Shelf, southwest Australia: a swell-dominated, non-tropical carbonate margin: Sedimentary Geology, v. 60, p. 15-50.

Davies, P.J., Symonds, D., Feary, D.A. and Pigram, C.J., 1989, The evolution of the carbonate platforms of northeast Australia, *in* Crevello, P.D., Wilson, J.L., Sarg, J.F. and Read, J.F., eds., Controls on carbonate platform and basin development: Society of Economic Paleontologists and Mineralogists, Special Publication 44, p. 233-258.

Desrochers, A. and James, N.P., 1988, Early Paleozoic surface and subsurface paleokarst: Middle Ordovician carbonates, Mingan Islands, Quebec, *in* James, N.P. and Choquette, P.W., eds., Paleokarst: New York, Springer-Verlag, p. 183-210.

Doyle, L.J. and Roberts, H.H., 1988, Carbonate-clastic transitions: Developments in Sedimentology 42, Amsterdam, Elsevier, 304 p.

Droser, M.L. and Bottjer, D.J., 1989, Ordovician increase in extent and depth of bioturbation: implications for understanding early Paleozoic ecospace utilization: Geology, v. 17, p. 850-852.

Enos, P., 1977, Holocene sediment accumulation of the South Florida shelf margin, *in* Enos, P. and Perkins, R.D., eds., Quaternary sedimentation in South Florida: Geological Society of America, Memoir 147, p. 1-130.

Flügel, E., 1981a, Lower Permian *Tubiphytes/Archaeolithoporella* buildups in the southern Alps (Austria and Italy), *in* Toomey, D.F., ed., European fossil reef models: Society of Economic Paleontologists and Mineralogists, Special Publication 30, p. 143-160.

Flügel, E., 1981b, Paleoecology and facies of Upper Triassic reefs in Northern Calcareous Alps, *in* Toomey, D.F., ed., European fossil reef models: Society of Economic Paleontologists and Mineralogists, Special Publication 30, p. 260-291.

Galli, G., 1991, Mangrove-generated structures and depositional model of the Pleistocene Fort Thompson Formation (Florida Plateau): Facies, v. 25, p. 297-314.

Ginsburg, R.N., 1956, Environmental relationships of grain size and constituent particles in some south Florida carbonate sediments: American Association of Petroleum Geologists, Bulletin, v. 40, p. 2384-2427.

Ginsburg, R.N. and James, N.P., 1974, Holocene carbonate sediments of continental margins, *in* Burke, C.A. and Drake, C.L., eds., The geology of continental margins: New York, Springer-Verlag, p. 137-155.

Goldhammer, R.K., Dunn, P.A. and Hardie, L.A., 1987, High-frequency glacio-eustatic sea level oscillations with Milankovitch characteristics recorded in Middle Triassic cycle platform carbonates, northern Italy: American Journal of Science, v. 287, p. 853-892.

Hallam, A., 1984, Pre-Quaternary sea-level changes: Annual Review of Earth and Planetary Science, v. 12, p. 205-243.

Haq, B.U., Hardenbol, J. and Vail, P.R., 1987, Chronology of fluctuating sea levels since the Triassic: Science, v. 235, p. 1156-1167.

Hardie, L.A., Dunn, P.A. and Goldhammer, R.K., 1991, Field and modelling studies of Cambrian carbonate cycles, Virginia Appalachians — Discussion: Journal of Sedimentary Petrology, v. 61, p. 636-646.

Hardie, L.A., and Shinn, E.A., 1986, Carbonate depositional environments: modern and ancient. Part 3: Tidal Flats: Colorado School of Mines, Quarterly, v. 81, 74 p.

Harris, P.M., 1979, Facies anatomy and diagenesis of a Bahamian ooid shoal: Sediments 7, Comparative Sedimentology Laboratory, University of Miami, 163 p.

Heckel, P.H., 1972, Recognition of ancient shallow marine environments, *in* Rigby, J.K. and Hamblin, W.K., eds., Recognition of ancient sedimentary environments: Society of Economic Paleontologists and Mineralogists, Special Publication 16, p. 226-286.

Hine, A.C., 1977, Lily Bank, Bahamas: history of an active oolite sand shoal: Journal of Sedimentary Petrology, v. 42, p. 1554-1581.

Howell, P.D. and van der Pluijm, B.A., 1990, Early history of the Michigan Basin: subsidence and Appalachian tectonics: Geology, v. 18, p. 1195-1198.

Irwin, M.L., 1965, General theory of epeiric clear water sedimentation: American Association of Petroleum Geologists, Bulletin, v. 49, p. 445-459.

James, N.P. and Bone, Y., 1991, Origin of a deep cool water Oligo-Miocene limestone, Eucla Platform, Australia: Sedimentology, v. 38, p. 323-341.

James, N.P. and von der Boch, C.C., 1991, Carbonate shelf edge of southern Australia: a prograding open platform margin: Geology, v. 19, p. 1005-1008.

Jones, B. and Hunter, I.G., 1989, The Oligocene-Miocene Bluff Formation on Grand Cayman: Caribbean Journal of Science, v. 25, p. 71-85.

Jones, B. and Hunter, I.G., 1990, Pleistocene paleogeography and sea levels on the Cayman Islands, British West Indies: Coral Reefs, v. 9, p. 81-91.

Kendall, C.G.St.C. and Schlager, W., 1981, Carbonates and relative changes in sea-level: Marine Geology, v. 44, p. 181-212.

Koerschner, W.F. and Read, J.F., 1989, Field and modelling studies of Cambrian carbonate cycles, Virginia Appalachians: Journal of Sedimentary Petrology, v. 59, p. 654-687.

Kreisa, R.D., 1981, Storm-generated sedimentary structures in sub-tidal marine facies with examples from the Middle and Upper Ordovician of southwestern Virginia: Journal of Sedimentary Petrology, v. 51, p. 823-848.

Lees, A., 1975, Possible influences of salinity and temperature on modern shelf carbonate sedimentation: Marine Geology, v. 19, p. 159-198.

Lees, A. and Buller, A.T., 1972, Modern temperate water and warm water shelf carbonates contrasted: Marine Geology, v. 13, p. 1767-1773.

Lohmann, K.C., 1976, Lower Dresbachian (Upper Cambrian) platform to deep-shelf transition in eastern Nevada and western Utah: an evaluation through lithologic cycle correlation: Brigham Young University, Geological Studies, v. 23, p. 860-878.

Lomando, A.J. and Harris, P.M., 1991, Mixed carbonate-siliciclastic sequences: Society of Economic Paleontologists and Mineralogists, Core Workshop 15, 569 p.

Markello, J.R. and Read, J.F., 1981, Carbonate ramp to deeper shale shelf transitions of an upper Cambrian intrashelf basin, Nolichucky Formation, southwest Virginia Appalachians: Sedimentology, v. 28, p. 573-597.

Markello, J.R. and Read, J.F., 1982, Upper Cambrian intrashelf basin, Nolichucky Formation, southwestern Virginia Appalachians: American Association of Petroleum Geologists, Bulletin, v. 66, p. 860-878.

Moore, C.H., 1984, The Upper Smackover of the Gulf Rim: depositional systems, diagenesis, porosity, evolution and hydrocarbon production, *in* Ventress, W.P.S., Bebout, D.G., Perkins, B.F. and Moore, C.H., eds., The Jurassic of the Gulf Rim: Society of Economic Paleontologists and Mineralogists, Gulf Coast Section, p. 283-308.

Nelson, C.S., 1988, An introductory perspective on non-tropical shelf carbonates: Sedimentary Geology, v. 60, p. 3-12.

Nelson, C.S., Hancock, G.E. and Kamp, P.J.J., 1982, Shelf to basin, temperate skeletal sediments, Three Kings Plateau, New Zealand: Journal of Sedimentary Petrology, v. 52, p. 717-732.

Nelson, C.S., Keane, S.L. and Head, P.S., 1988a, Non-tropical carbonate deposits on the modern New Zealand Shelf: Sedimentary Geology, v. 60, p. 71-94.

Nelson, C.S., Hyden, F.M., Keane, S.L., Leask, W.L. and Gordon, D.P., 1988b, Application of bryozoan zoarial growth-form studies in facies analysis of non-tropical carbonate deposits in New Zealand: Sedimentary Geology, v. 60, p. 301-322.

Neumann, A.C. and Land, L.S., 1975, Lime mud deposition and calcareous algae in the Bight of Abaco, Bahamas: a budget: Journal of Sedimentary Petrology, v. 45, p. 763-786.

Osleger, D., 1991, Subtidal carbonate cycles: implications for allocyclic versus autocyclic controls: Geology, v. 19, p. 917-920.

Pickerill, R.K. and Brenchley, P.J., 1991, Paleoscene 12. Benthic macrofossils as paleoenvironmental indicators in marine siliciclastic facies: Geoscience Canada, v. 18, p. 119-138.

Playford, P.E., 1980, Devonian 'Great Barrier Reef' of Canning Basin, Western Australia: American Association of Petroleum Geologists, Bulletin, v. 64, p. 814-840.

Pratt, B.R. and James, N.P., 1985, The St. George Group (Lower Ordovician) of western Newfoundland: tidal flat island model for carbonate sedimentation in shallow epeiric seas: Sedimentology, v. 33, p. 313-343.

Pray, L.C., 1981, Shelf processes: carbonates, *in* Dott, R.H. and Byers, C.W., eds., Society of Economic Paleontologists and Mineralogists, Research conference on modern shelf and ancient cratonic sedimentation — the orthoquartzite-carbonate suite revisited: Journal of Sedimentary Petrology, v. 51, 343-344.

Purdy, E.G., 1963a, Recent calcium carbonate facies of the Great Bahama Bank. I. Petrography and reaction groups: Journal of Geology, v. 71, p. 334-355.

Purdy, E.G., 1963b, Recent carbonate facies of the Great Bahama Bank. II. Sedimentary facies: Journal of Geology, v. 71, p. 472-497.

Purdy, E.G., 1974, Karst-determined facies patterns in British Honduras: Holocene carbonate sedimentation model: American Association of Petroleum Geologists, Bulletin, v. 58, p. 825-855.

Purser, B.H., 1973, The Persian Gulf: Berlin, Springer-Verlag, 471 p.

Purser, B.H., 1983, Sedimentation et diagenese de carbonate neriteques recents: Paris, Editions Technip, v. 2, 389 p.

Read, J.F., 1980, Carbonate ramp-to-basin transitions and foreland basin evolution, Middle Ordovician, Virginia Appalachians: American Association of Petroleum Geologists, Bulletin, v. 64, p. 1575-1612.

Read, J.F., 1985, Carbonate platform facies models: American Association of Petroleum Geologists, Bulletin, v. 66, p. 860-878.

Read, J.F., Osleger, D.A. and Elrick, M., 1990, Computer modelling of cyclic carbonate sequences: Geological Society of America , Short Course Notes 1990 Annual Meeting, Dallas, 35 p.

Sami, T. and Desrochers, A., 1992, Episodic sedimentation on an Early Silurian storm-dominated carbonate ramp, Becscie and Merrimark formations, Anticosti Island, Canada: Sedimentology, (in press).

Scaturo, D.M., Strobel, J.S., Kendall, C.G.St.C., Wendte, J.C., Biswas, G., Bezdek, J. and Cannon, R., 1989, Judy Creek: a case study for a two-dimensional sediment deposition simulation, *in* Crevello, P.D., Wilson, J.L., Sarg, J.F. and Read, J.F., eds., Controls on carbonate platform and basin development: Society of Economic Paleontologists and Mineralogists, Special Publication 44, p. 63-76.

Schäfer, P. and Senowbari-Daryan, B., 1981, Facies development and paleoecological zonation of four Upper Triassic patch-reefs, Northern Calcareous Alps near Salzburg, Austria, *in* Toomey, D.F., ed., European fossil reef models: Society of Economic Paleontologists and Mineralogists, Special Publication 30, p. 241-259.

Schlager, W., 1989, Drowning unconformities on carbonate platforms, *in* Wilgus, C.K., *et al.*, eds., Sea level changes — an integrated approach: Society of Economic Paleontologists and Mineralogists, Special Publication 42, p. 15-25.

Scholle, P.A., 1978, A color illustrated guide to carbonate rock constituents, textures, cements and porosities: American Association of Petroleum Geologists, Memoir 27, 241 p.

Scoffin, T.P., Alexandersson, E.T., Bowes, G.E., Clokie, J.J., Farrow, G.E. and Milliman, J.D., 1980, Recent, temperate sub-photic, carbonate sedimentation: Rockall Bank, northeast Atlantic: Journal of Sedimentary Petrology, v. 50, p. 331-356.

Sellwood, B.W., 1986, Shallow-marine carbonate environments, *in* Reading, H.G., ed., Sedimentary environments and facies: Oxford, Blackwell Scientific Publications, p. 283-342.

Shinn, E.A., 1963, Spur and groove formation in the Florida Reef Tract: Journal of Sedimentary Petrology, v. 33, p. 291-303.

Teichert, C., 1959, Cold- and deep-water coral banks: American Association of Petroleum Geologists, Bulletin, v. 42, p. 1064-1082.

Turmel, R. and Swanson, R., 1964, Rodriguez Bank, in Guidebook for Field Trip No. 1, Geological Society of America Convention 1964: New York, Geological Society of America, p. 26-33.

Walls, R.A., 1983, Golden Spike Reef Complexes, Alberta, *in* Scholle, P.A., Bebout, D.G. and Moore, C.H., eds., American Association of Petroleum Geologists, Memoir 33, p. 445-453.

Wanless, H.R. and Dravis, J.J., 1989, Carbonate environments and sequences of Caicos Platform, Field Trip Guidebook T374: 28th International Geological Congress, Washington, American Geophysical Union, 75 p.

Wilkinson, B.H., 1982, Cyclic cratonic carbonates and phanerozoic calcite seas: Journal of Geological Education, v. 30, p. 189-203.

Wilkinson, B.H., Opdyke, B.M. and Algeo, T.J., 1991, Time partitioning in cratonic carbonate rocks: Geology, v. 19, p. 1093-1096.

Wilson, J.B., 1979, Biogenic carbonate sediments on the Scottish continental shelf and on the Rockall Bank: Marine Geology, v. 33, p. 85-93.

Wright, V.P. and Faulkner, T.J., 1990, Sediment dynamics of Early Carboniferous ramps: a proposal: Geological Journal, v. 25, p. 139-144.

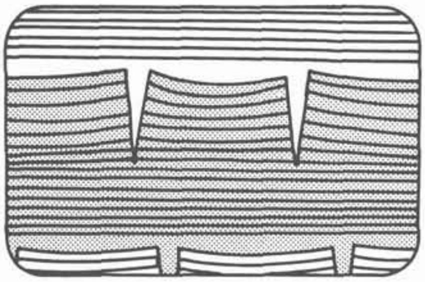

16. Peritidal Carbonates

Brian R. Pratt, Department of Geological Sciences, University of Saskatchewan, Saskatoon, Saskatchewan S7N 0W0

Noel P. James and Clinton A. Cowan, Department of Geological Sciences, Queen's University, Kingston, Ontario K7L 3N6

INTRODUCTION

Limestones and dolostones composed of calcareous sediment deposited in very shallow seawater and on muddy tidal flats are probably the most conspicuous carbonate facies in the rock record (Fig. 1). The term *peritidal* (from the Greek *peri*, meaning around or near, and tidal, relating to tides) was coined in passing by Folk (1973) and has proven a useful general name for the spectrum of nearshore and shoreline depositional environments and facies.

What distinguishes these rocks is their wide variety of features that can be compared directly with modern analogues, making them both easy to recognize in the field and important paleobathymetric indicators. The facies are generally arranged vertically in a *shallowing-upward sequence* (James, 1984), now referred to as a *shallowing-upward succession*, in which marine sediments are overlain successively by muddy carbonates deposited in paleoenvironments subject to varying periods of exposure. This vertical stacking of peritidal and related facies is a valuable record of the dynamics of carbonate platform development, on both large and small scales. It hints at extrinsic factors such as relative sea level change and climate, and records the effect on periodically exposed sediment of biotic evolution through geologic time. Peritidal carbonates are also economically important because they host Pb and Zn deposits and frequently form hydrocarbon reservoirs.

In this chapter, we first summarize the tidal flat environment from a Recent standpoint. We then discuss how the record of carbonate tidal flats may have changed through time in response to biological evolution and provide ancient examples of commonly encountered peritidal facies, with evidence for their interpretation. Finally, we outline how peritidal facies are preserved in the stratigraphic record, describe current hypotheses used to explain stratigraphic repetition and suggest how these facies can best be used in sequence stratigraphic analysis.

Figure 1 Panorama of Cambrian shallow water limestones and dolostones, Dezaiko Range, east-central British Columbia. Distinctive "stripy" bedding of lower unit, to the right of the small ice field, is from peritidal facies of the Snake Indian Formation. The unit in the middle of the photograph is the Eldon Formation, consisting of locally dolomitized subtidal limestones, and the left side comprises peritidal limestones of the Lynx Group.

THE PERITIDAL ENVIRONMENT

The understanding of tidal flat carbonate rocks underwent a dramatic boost with the largely petroleum company-funded research on Holocene tidal flats during the 1950s and 1960s. This produced comprehensive studies on shallow water sedimentation of south Florida (Ginsburg, 1956; Gebelein, 1977; Enos and Perkins, 1979), Andros Island of the northern Bahamas (Hardie, 1977), Belize (Wantland and Pusey, 1975), the Arabian (Persian) Gulf (Purser, 1973), and Shark Bay, Western Australia (Logan *et al.*, 1970, 1974). Observations from these areas were quickly applied to ancient examples (e.g., Beales, 1958; Roehl, 1967; Matter, 1967; Laporte, 1967; Ginsburg, 1975; Schwarz, 1975), which ushered in the modern era of carbonate sedimentological thinking. These Holocene examples, together with more recently studied flats in the Caicos Islands (Wanless *et al.*, 1988) and southern Australia (Burne and Colwell, 1982; Belperio *et al.*, 1988) are fundamental reference points for the interpretation of carbonate rocks and illustrate the wide variety of potentially preservable peritidal environments. The carbonate tidal flat is an easily accessible area and students are encouraged to explore for themselves a modern example.

Three bathymetric zones are recognized in the nearshore setting: subtidal, intertidal and supratidal (Fig. 2).

The subtidal zone is permanently submerged and ranges from low-energy, lagoonal environments to higher energy shoals. Semimonthly neap tides may briefly expose the shallowest portions. The intertidal, or littoral, zone lies between normal low- and high-tide levels and is therefore submerged on a diurnal or semidiurnal basis. It is generally dissected by subtidal creeks and dotted with brackish or saline ponds. The supratidal zone is above normal high tide, and is flooded only during storms and semimonthly spring tides. It may become evaporitic in semiarid and arid climates, and for these supratidal flats the Arabic word *sabkha* has been adopted by sedimentologists (Chapter 19).

The three-fold environmental subdivision is only an approximation, however, since tidal flats are often geographically complex, and tidal range can be modified by winds. While the environments are due to the variable submergence and emergence brought about by lunar tides, little sediment is transported onto the flats by the daily rise and fall in sea level. It is storms, which stir up the adjacent offshore sediments and drive sediment-laden waters up the tidal creeks and onto the flats, that result in sediment deposition. Even so, it is still the depositional environments, which are generated by daily lunar tides, that contain the distinctive sedimentary features that allow us to pinpoint facies so precisely. One approach to the analysis of environmental subdivision is to assign a specific, quantitative "exposure index" to lithologic features based on Holocene examples (see Hardie, 1977), but few ancient deposits have been described in this way (Smosna and Warshauer, 1981).

Marine coastlines can be separated into microtidal (<2 m), mesotidal (2-4 m) and macrotidal (>4 m) settings. Tidal range depends on basin shape and water depth. Strong tidal currents are generated when water is forced through relatively narrow straits or mouths of bays or over shallow shoals. Modern peritidal carbonate environments are exclusively microtidal. There is as yet no satisfactory way of judging ancient tidal range, but the scarcity of sedimentary structures formed by strong tidal currents suggests that most ancient carbonate peritidal settings were also microtidal.

Where do they form?

Carbonate sediment, generated mostly in the subtidal zone (the *carbonate factory*), can be subsequently transported and molded into tidal flats by physical processes. In this sense, tidal flats are repositories of allochthonous sediment, and accrete as wedges along shorelines (e.g., Qatar, Shark Bay, Spencer Gulf), in the lee of rocky islands (e.g., northern Bahamas, Caicos, Belize), spits (e.g., Florida) and reefs and shoals (e.g., Trucial Coast), and as discrete islands and banks in shallow seas (Fig. 3). This last setting is inferred from ancient examples because modern shelves are comparatively narrow and not directly analogous to the broad epeiric seas that were common in the past.

For muddy tidal flats to form they must be protected from open ocean swells and such protection can be provided by a platform rim or in the case of a ramp or unrimmed platform, by nearshore carbonate sand shoals (Fig. 4). Muddy tidal flats do not, therefore, generally occur in the facies spectrum of high-energy, unrimmed platforms, except behind nearshore shoals or islands.

Holocene carbonate tidal flat environments

Shallow subtidal and lower intertidal

The shallow seafloor oceanward of modern tidal flats is generally a bio-

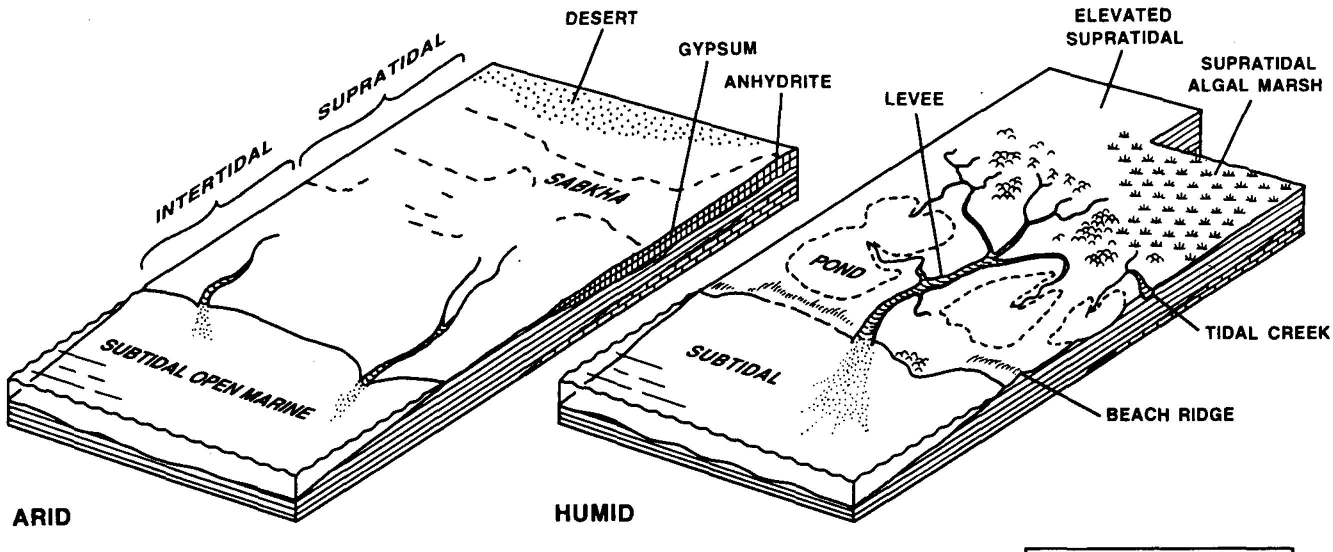

CARBONATE TIDAL FLATS

Figure 2 Block diagram showing the main morphological elements of a carbonate tidal flat. Left: a hypersaline tidal flat with few channels bordering a desert and developing evaporite deposits (based on modern Persian [Arabian] Gulf). Right: normal-marine tidal flat with many creeks, or channels, and ponds in a humid to sub-humid setting (based on modern Bahamas).

turbated and pelleted lime mud variably rich in shelly material from benthic oganisms, and commonly supports a cover of sediment-stabilizing sea grasses (Chapter 15). Protective low-relief banks of cross-stratified oolitic or bioclastic sand are present in some higher-energy nearshore areas where wave agitation is frequent.

In tranquil settings of normal salinity, the lowermost intertidal zone tends also to be a thoroughly bioturbated mixture of lime mud, pellets and bioclasts. This sediment is usually covered during low tide with an ephemeral microbial ("algal") slick that is the source of food for grazing organisms such as gastropods and worms. Crabs, shrimps, worms and fish are responsible for the bioturbation in the underlying sediment. Many low-energy flats are fronted by beaches of bioclastic sand winnowed from creeks and ponds or the adjacent seafloor during storms. Beach sands can be partially lithified by synsedimentary cement composed of aragonite fibres or bladed and micritic high-Mg calcite, forming gently seaward-dipping layers of beachrock. Beachrock tends to be crumbly and easily eroded, and supports a hard-substrate biota of encrusting and boring invertebrates, plants and microbes.

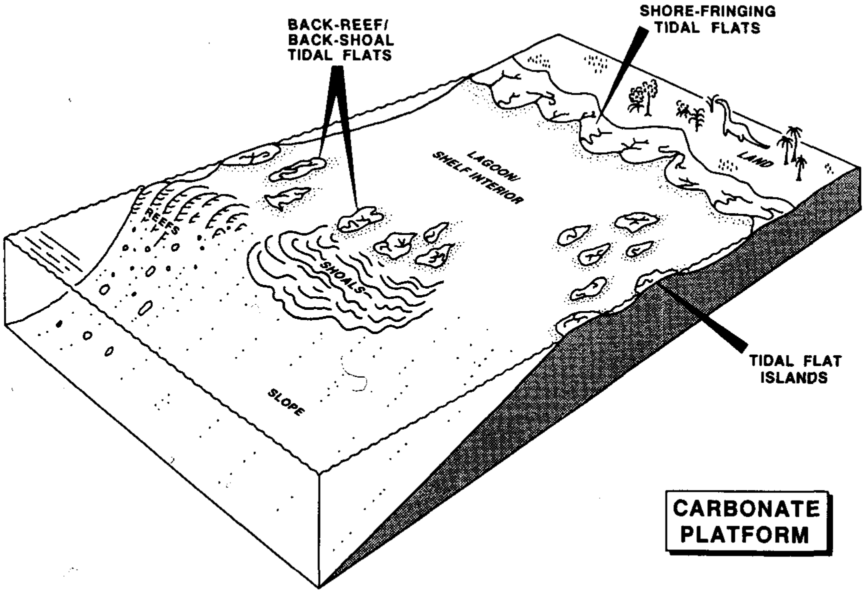

Figure 3 Block diagram of a carbonate platform, with basinward to left and landward to right, showing possible locations of tidal flats: in the lee of reefs and carbonate sand shoals, as islands, and as shoreline deposits.

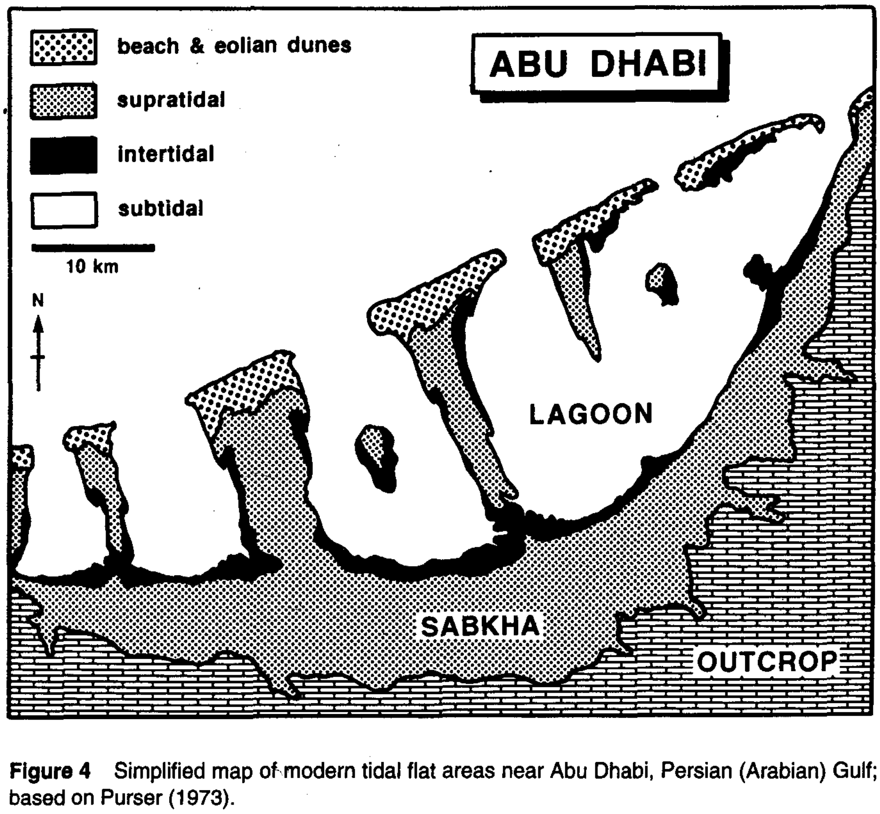

Figure 4 Simplified map of modern tidal flat areas near Abu Dhabi, Persian (Arabian) Gulf; based on Purser (1973).

Intertidal flats

Higher in the intertidal zone, microbial mat cover is more permanent, and forms thick, leathery carpets that can be locally shrunken, torn and folded over (Fig. 5). These exhibit various surface features such as pustules, blisters, wrinkles, crenulations or small, domical stromatolites. These mats are composed of a variety of filamentous and coccoid cyanobacteria ("blue-green algae") and bacteria, and are responsible for the millimetre-scale lamination exhibited by most of the sediment beneath them. The taxonomic makeup and surface appearance of such mats varies with degree of subaerial exposure and can be reflected in the microscopic nature of the underlying lamination. This type of lamination was called "algal" or "cryptalgal" before geologists became familiar with the detailed biological nature of the mats; "microbial" seems now to be the preferred adjective.

Ponds and creeks

Ponds containing brackish or hypersaline water are a common feature of the intertidal zone (Fig. 6), especially in more humid climates. These contain a restricted biota of microbial mats, foraminifera, gastropods, small bivalves, shrimps, ostracodes, and nematode and polychaete worms that is adapted to fluctuating salinity. This assemblage, living in a stressed environment, is typically one of high numbers of individuals but low species diversity, different from the immediate offshore biota. Copses of mangroves are usually present, except in the most arid areas. Also characteristic of the intertidal zone are permanently submerged tidal creeks or channels that are the conduits for tidal flooding and draining (Fig. 6). Such tidal creeks (least common in arid settings) are up to several metres deep and tens of metres wide, and contain a basal lag of semilithified intraclasts eroded from the surrounding flats and flanking levees, and bars of bioclastic sand winnowed from the ponds. Supratidal levees protrude above high-tide level and are microbially laminated. Creeks migrate laterally, as they do in siliciclastic tidal flats, and leave behind a vertical succession of cross-stratified, intraclastic and bioclastic sand overlain in turn by bioturbated bioclastic and peloidal lime mud and microbially laminated sediment. The amount of lateral migration of creeks and the proportion of the internal facies mosaic of intertidal flats that is generated by such migration are not well understood, but studies of modern flats suggest that it may be considerable (Hardie, 1977).

Supratidal flats

Most of the sediment surface in the upper intertidal and supratidal zones is covered by microbial mats that are typically shrunken into desiccation polygons and commonly dislodged into chips or intraclasts. The laminated sediment beneath these mats is generally fine grained with occasional coarser intercalations that reflect deposition by exceptional storms and, in some regions, by winds blowing off the neighbouring land surface. Beds and nodules of anhydrite precipitate in these sediments in arid settings (Chapter 19). In many areas, the supratidal zone is the locus of widespread synsedimentary cementation by microcrystalline aragonite, high-Mg calcite, or dolomite. This forms lithified pavements a few centimetres thick that are usually broken into intraclasts by forces exerted during crystal growth, groundwater pore pressure, or the roots of halophytic (salt-tolerant) plants such as grasses and mangroves. Evaporating sea spray can be responsible in some arid areas for fans and isopachous layers of fibrous aragonite that encrust stable substrates such as beachrock and shells, forming objects termed coniatolites.

Landward parts of the supratidal zone grade into eolian deposits, soils or freshwater marshes and lakes, or onlap bedrock surfaces, depending on the region's geography and climate. Marshes and lakes, which exist in the more humid areas and have fluctuating water chemistry, are characterized by microbial mats and stromatolites; these are partially lithified by high-Mg calcite cement and calcification of organic substrates, and are interbedded with thin-bedded, locally bioturbated lime mud and bioclastic and peloidal carbonate sand deposited during storms. Much of the microbially laminated sediment shows fenestral fabric, i.e., the presence of millimetre-

Figure 5 Upper intertidal microbial mat mainly composed of filamentous cyanobacteria *(Microcoleus)* that has shrunken into desiccation polygons. Boca Jewfish, Bonaire; trowel is about 25 cm long.

Figure 6 Oblique aerial photograph of the tidal flats on the northeast coast of Andros Island, Bahamas, looking north. Offshore subtidal is to the left. The white areas along the channel edges are supratidal levees. The dark patches are intertidal microbial flats between the levees and around the periphery of the mainly subtidal ponds. The field of view is about 3 km across.

to centimetre-sized subhorizontal, sheet-like pores formed as voids bridged by microbial mats or as molds of degraded mats. Decimetre-scale tepee structures (Fig. 7), consisting of disrupted and overthrust crusts of lithified, tufa-like fenestral sediment giving an inverted V-shaped cross section, form in areas of groundwater discharge (Kendall and Warren, 1987). These also contain complex generations of internal sediment and aragonite and high-Mg calcite cements.

Geological evolution of peritidal facies

Biological and environmental developments through geologic time have exerted an important influence on the nature of carbonate tidal flats. This is manifest in several ways, via 1) the increase in diversity of carbonate-secreting organisms and consequent change in sediment type, 2) the evolution of bioturbating and herbivorous invertebrates, and 3) the evolution of angiosperms.

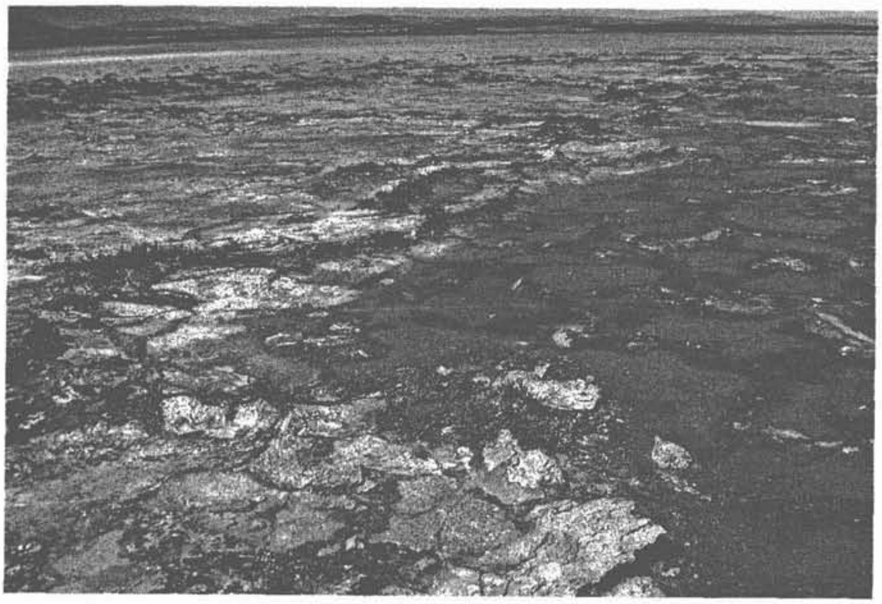

Figure 7 The supratidal flat at Fisherman Bay, Spencer Gulf, southern Australia. The polygonal crusts are lithified and have been thrust into teepees by episodic groundwater resurgence. Crusts in the foreground are roughly 30 cm across.

Figure 8 Outcrop of lenticular and wavy beds of wave-rippled peloidal grainstone (light coloured) in argillaceous dolostone (dark coloured), probably deposited in the lower intertidal zone. Petit Jardin Formation (Upper Cambrian), Port-au-Port Peninsula, western Newfoundland; lens cap is 6 cm across.

The subtidal carbonate factory was in its infancy during Precambrian time, when $CaCO_3$ was extracted from seawater by inorganic and microbial processes only. Peritidal strata during this phase in Earth's history are composed of ooids, intraclasts, stromatolites, supratidal tufas, and variable amounts of lime mud. Some subtidal units are entirely siliciclastic, and large-scale cyclicity of alternating calcareous and noncalcareous facies (e.g., Grotzinger, 1986; Bertrand-Sarfati and Moussine-Pouchkine, 1988) may have involved basin-wide, or greater, changes in carbonate saturation of seawater. The dramatic increase in skeleton-secreting and sediment-ingesting invertebrates beginning in Cambrian time meant that the carbonate factory changed in character and increased its output manyfold. New types of sedimentary particles appeared, in the form of abundant shells, fecal pellets, and carbonate mud from the breakdown of fragile skeletons and other biologically influenced precipitates. This no doubt changed the nature of tidal flats by causing increased mobility of the substrate, making it less and less likely to be cemented quickly or encrusted by stromatolite-forming microbial mats except in hypersaline areas (Pratt, 1982). It has been commonly held (Garrett, 1970) that grazing invertebrates such as gastropods caused intertidal stromatolites to become scarce after the Proterozoic, but the above sedimentary reasons rather than ecologic pressure seem likely to have been responsible for this decline.

Proterozoic tidal flat carbonates are distinctive too because, in comparison with other Precambrian carbonate facies and younger sediments, they were the preferred sites of diagenetic silica precipitation and formation of chert nodules (Maliva *et al.*, 1989). These cherts are important because they host the bulk of the Precambrian fossil record (Knoll *et al.*, 1991).

Bioturbation became a sediment-modifying process in Late Proterozoic time. Diversification of microbes, especially those involved in the breakdown of organic material, must have occurred in tandem with invertebrate diversification and the resulting appearance of new organic substances. The organic content and therefore the geotechnical properties of tidal flat sediments surely changed in the early Paleozoic. The effect of bioturbation seems to have increased dramatically after the late Paleozoic or earliest Mesozoic (Thayer, 1983; Bottjer and Ausich, 1986; Pratt, 1991). This was heralded by the evolution of a more diverse fauna including animals, such as certain shrimps and crabs, capable of burrowing as deeply as 1 m. Consequently, tidal bedding that would have been preserved in the Precambrian and early Paleozoic was commonly destroyed by infaunal activity, except in the upper intertidal and supratidal zones. Furthermore, intertidal to supratidal sedimentary and organosedimentary structures that escaped destruction were often subsequently bioturbated when buried by subtidal or lower intertidal sediments with an active deeply burrowing infauna.

Evolution of angiosperms since Cretaceous time has meant that the disruption of tidal flat sediments by halophytic plants has become a characteristic of Cenozoic deposits. In addition, shallow subtidal sea bottoms are especially well stabilized by the rhizomes (roots) of angiosperm sea grasses *(Thalassia, Posidonia, Cymodocea)*. Such grasses also support a prolific encrusting biota that supplies fine-grained carbonate sediment to the factory. These carpets of sea grasses, however, are disrupted only by intense storms, causing "blowouts" (Wanless, 1981), and we suggest that pre-Cenozoic subtidal sediments, especially silt- and sand-sized particles, might have been more readily moved onto tidal flats than they are now, because they were not bound by these grasses. This is analogous to the suggestion that the post-Devonian presence of widespread terrestrial plant cover, with its stabilizing, soil-forming and weathering attributes, affected the subaerial sedimentary system of the Earth. It may partly explain why some early Paleozoic intertidal carbonates look so much like siliciclastic counterparts from settings that lack significant seagrass communities.

Ancient peritidal carbonate facies

Environmental interpretation of peritidal limestones and dolostones is easily achieved in the broad sense, especially when they contain features unequivocally of subaerial origin. However, some facies cannot be assigned confidently to a bathymetric position, and for these Walther's Law must be invoked. Furthermore, tidal processes involve such a variety of energy regimes, sediment sizes and climates that there may be a limit as to

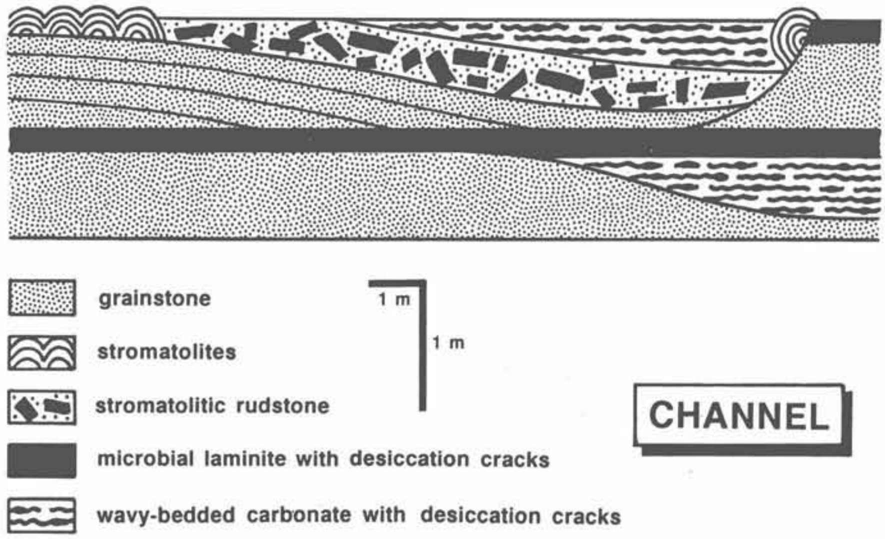

Figure 9 Simplified outcrop sketch of hypothetical channel or creek deposits cut into tidal flat facies, based on examples from the Waterfowl Formation (Upper Cambrian, Rocky Mountains, Alberta; Waters *et al.*, 1989) and Elbrook-Conococheague Formations (Middle and Upper Cambrian, Virginia; Koerschner and Read, 1989).

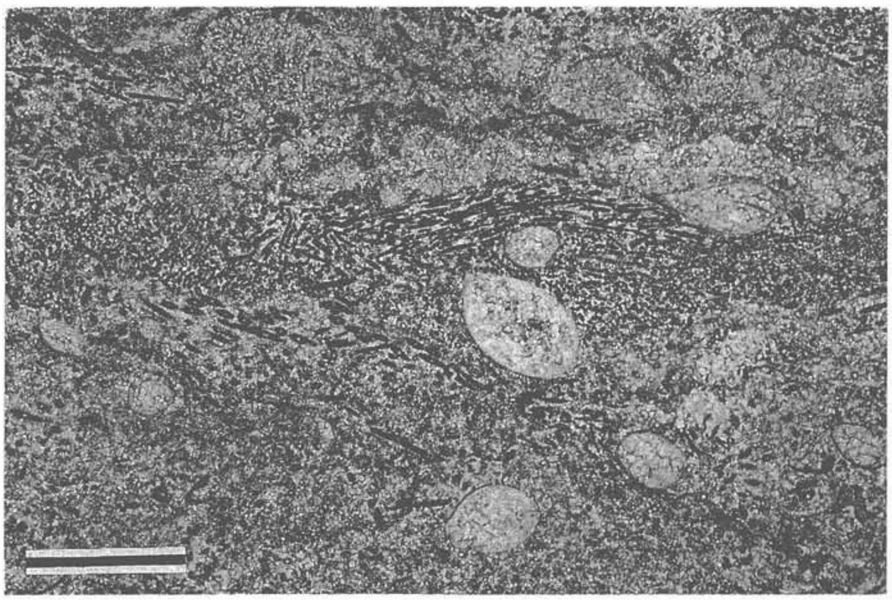

Figure 10 Thin section photomicrograph of limestone composed of loosely packed micrite, micrite peloids, articulated ostracode valves, and calcimicrobe *(Girvanella)* filaments with organic-rich walls. This sediment is interpreted to have been deposited in a tidal flat pond because of the low-diversity biota and the calcification of filamentous cyanobacterial thalli. Table Point Formation (Middle Ordovician), Port-au-Port Peninsula, western Newfoundland; scale bar is 1 mm.

how precise an interpretation one can make. The present level of detail is generally at the scale of units decametres to metres in thickness; few studies have gone down to the scale of individual beds and laminae.

Shallow subtidal and lowermost intertidal facies

Precambrian subtidal rocks are the most difficult to recognize, because the carbonate was produced by inorganic or microbially mediated precipitation, and there were no distinctive skeleton-secreting organisms. Such subtidal facies tend to be variably siliciclastic, or frequently dolomitized lime mudstone with local oolitic, peloidal or intraclastic beds. Nearshore limestones of Phanerozoic age are fossiliferous, commonly bioturbated to some degree, and may exhibit patch reefs and oolites. Units of thinly interbedded bioturbated lime mudstone and wackestone and ripple or dune cross-laminated grainstone that are overlain by rocks exhibiting clearly supratidal facies are typical. Subtidal and lower intertidal carbonates of Mesozoic and Cenozoic age are commonly thick bedded and totally bioturbated, reflecting the post-Paleozoic increase in the diversity and effect of the bioturbating fauna.

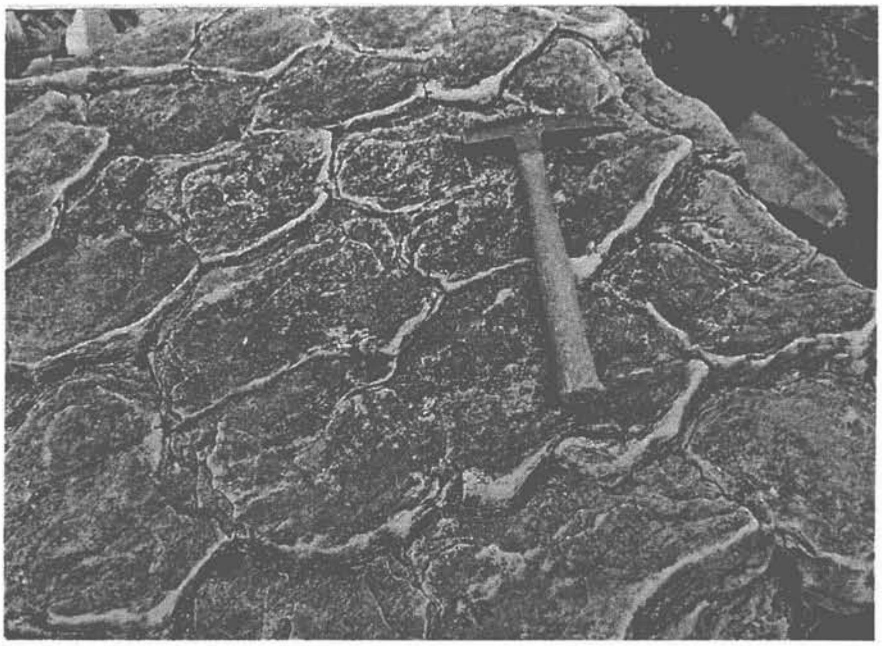

Figure 11 A bedding plane of desiccation-cracked polygons in which the edges of each polygon are curled up, probably because the original microbial mats shrivelled upon exposure. East Arm Formation, Upper Cambrian, Bonne Bay, western Newfoundland; hammer is 30 cm long.

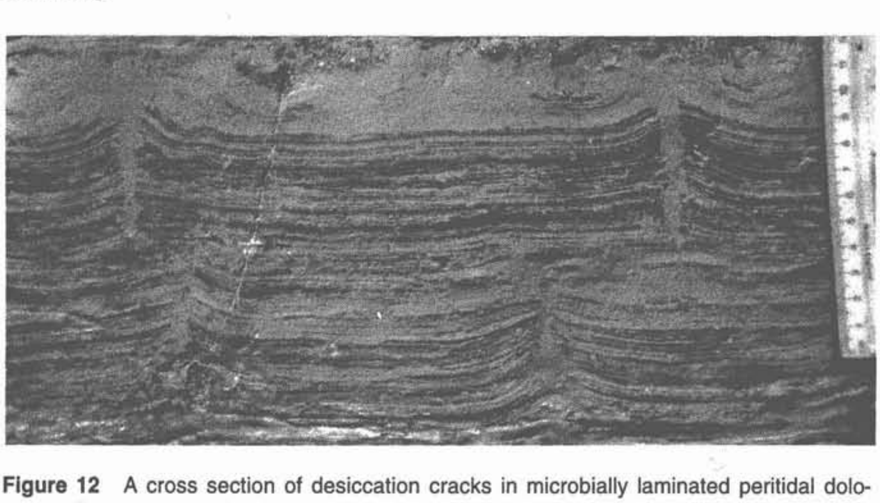

Figure 12 A cross section of desiccation cracks in microbially laminated peritidal dolostones; Providence Island Dolomite, Middle Ordovician, Lake Champlain, New York State.

Intertidal flat facies

Wavy-, lenticular- and flaser-bedded peloidal lime mudstone or grainstone (calcisiltite) and dolomitized argillaceous lime mudstone (sometimes interbedded with small hemispheroidal stromatolites), arising from the alternation between slack water and sediment transport by both unidirectional currents and waves under lower flow regime, are particularly distinctive of Precambrian and lower Paleozoic sequences (Fig. 8). This facies is directly comparable to the tidal bedding in siliciclastic peritidal deposits, including those forming in many modern settings (see Reineck and Singh, 1980). The carbonate strata, however, commonly contain intraclastic horizons which are absent in siliciclastic counterparts. Phanerozoic intertidal facies frequently have bioclastic layers. Well-sorted coquinas were likely washed in from the subtidal zone by storms, whereas poorly sorted shelly deposits containing a low-diversity assemblage of gastropods or bivalves probably represent the in situ intertidal fauna. Laminae that appear laterally continuous, undulating and uniform in thickness, are typically intercalated in this facies, and record periods of stabilization or binding of the substrate by a microbial mat. This tidal bedding can be burrowed in Phanerozoic sequences, and in the lower Paleozoic the trace fossil fauna is dominated by a low-diversity assemblage of horizontal burrows and U-shaped forms like *Arenicolites* and *Diplocraterion.* As with subtidal deposits, post-Paleozoic intertidal sediments are likely to be thoroughly churned: bioturbated, poorly fossiliferous lime mudstone units may be interpreted as intertidal if other criteria, such as vertically juxtaposed beds with desiccation cracks, are evident.

Tidal creek facies

Rocks specifically interpreted as having accumulated in tidal creeks or channels piercing intertidal flats are relatively uncommon. The reasons for this are mainly 1) the rarity of laterally extensive exposures that intersect the possible margins of channels once they stop migrating laterally, 2) the difficulty in distinguishing creek fills from regressive packages with a basal, higher-energy component that resulted from tidal flat progradation, 3) the similarity between bedforms and lateral-accretion bedding from bar migration in channels and inclined and tabular cross stratification from migrating offshore carbonate sand shoals, and 4) the difficulty in separating creeks in tidal flats from channels between adjacent offshore islands or shoals. The presence of flat-pebble and blocky intraclasts derived from the surrounding flats and levees, respectively, along with bipolar (herringbone) cross stratification typically exhibiting reactivation surfaces and *tidal bundles* (couplets of sandy and muddy laminae), seem to be diagnostic of creek or channel deposits (e.g., Pratt and James, 1986). Grainstone beds with erosional bases and containing stromatolite or thrombolite mounds in some Proterozoic and Cambrian sequences are reasonably interpreted as channel deposits, (Koerschner and Read, 1989; Wright *et al.*, 1990). Waters *et al.* (1989) and Cloyd *et al.* (1990) have mapped Cambrian channels at least 10 m wide and 1 m deep with erosional bases, filled with lateral-accretion beds of individually graded, locally bipolar cross-laminated grainstone containing desiccation-cracked lime mud drapes and reactivation surfaces (Fig. 9). Care must be taken in late Proterozoic and early Paleozoic carbonates, however, to differentiate subaerial (desiccation) cracks and other cracks of submarine origin (Knoll and Swett, 1990; Cowan and James, 1992).

Beach facies

Beaches, which also have not been reported frequently from ancient tidal flat sequences, are characterized by seaward-dipping, low-angle laminae and thin beds of grainstone, often with hardgrounds exhibiting bored surfaces. This facies passes laterally to subtidal deposits in the seaward direction and tidal-bedded strata in the landward direction (e.g., Inden and Moore, 1983; Waters *et al.*, 1989). Steeper shorelines, such as Tertiary and Quaternary examples from the Mediterranean and Red seas, are often onlapped by gravelly beds of well-rounded pebbles and large shells.

Pond facies

Recognition of schizohaline pond deposits on humid intertidal flats may be impossible in most rock sequences unless the ponds were particularly long-lived. In one example (Pratt, 1979), burrowed wackestone containing ostracodes and horizontal meshes of *Girvanella* filaments with organic-rich walls (Fig. 10) are intercalated within burrowed and microbially laminated lime mudstone and tidal-bedded dolostone and lime mudstone. The restricted biota of this deposit, the well-preserved microbial remains, and its lenticular geometry within a peritidal sequence argue against a normal-marine subtidal environment.

Supratidal facies

Microbially laminated limestone or dolostone, usually with desiccation cracks and coarser rippled layers, is a common peritidal rock type (Figs. 11, 12); such rocks, however, may be

Figure 13 Polished slab of clotted and peloidal lime mudstone showing microbial lamination and fenestral fabric of laminoid, millimetre- to centimetre-sized, cement-filled pores. This distinctive fabric probably formed in the upper intertidal or lower supratidal zone. Eldon Formation (Middle Cambrian), Exshaw, Alberta; scale bar is 1 cm.

Figure 14 Thin section photomicrograph of peloidal and clotted micrite containing bioclasts (mainly ostracodes and gastropods) and exhibiting fenestral fabric. Upper parts of the laminoid fenestral pores have pendant fringes of fibrous calcite cement (grey coloured) suggesting that this sediment was deposited in the upper intertidal zone and that the fibrous calcite precipitated as marine or mixed waters percolated through the pores during low tides. Table Point Formation (Middle Ordovician), western Newfoundland; scale bar is 1 mm.

upper intertidal or supratidal in origin. In older Phanerozoic sequences, a supratidal setting might be inferred if bioturbation is rare or absent, or there is evidence for prolonged subaerial exposure such as evaporites, karst horizons or paleosols. Intercalated within many microbially laminated rocks are intraclastic horizons, which are analogous to pavements of microbial mat chips or fragments of cemented crusts in modern supratidal environments. Fenestral lime mudstone and peloidal grainstone (Fig. 13) are common (Shinn, 1983b) and, by analogy with tidal flats of Florida and the Bahamas, were probably deposited in moist supratidal "algal marshes" or around ponds. This facies sometimes exhibits features, such as pendant fibrous cement (Fig. 14), brecciated crusts and tepees, pisolites and pores with geopetal sediment floors, suggestive of flushing by downward-percolating seawater and rainwater and upward-flushing by groundwaters in a subaerial environment. Precambrian supratidal deposits often contain digitate stromatolites, millimetres to centimetres in diameter, which have been interpreted as supratidal, tufa-like aragonite precipitates (e.g., Grotzinger, 1986). Post-depositional leaching of evaporites causes collapse brecciation in supratidal facies.

THE PERITIDAL SHALLOWING-UPWARD SUCCESSION

Ancient peritidal carbonate lithofacies are characteristically organized stratigraphically into metre- to decametre-thick, shallowing-upward successions (Fig. 15) each with a basal subtidal unit, intermediate intertidal facies, and an upper supratidal unit with or without a terrestrial horizon on the top (James, 1984; Wright, 1984; Tucker and Wright, 1990). Contacts between the members are gradational or sharp and may show evidence of local synsedimentary scour. Walther's Law tells us that, if there are no major depositional breaks, we can reconstruct the ancient environmental mosaic by dealing out each facies like a deck of cards. There are departures from this ideal pattern, however, and it is not unusual to find the supratidal member overlain by intertidal facies, or components missing because of nondeposition or erosion.

Characteristics

The lithologic nature of the subtidal → intertidal → supratidal succession is variable, reflecting the broad spectrum of intertidal and supratidal depositional environments, the dictates of biotic evolution and past changes in ocean chemistry. Such peritidal shallowing-upward successions can be subdivided into two types, low energy (Figs. 16, 17) and high energy (beach; Fig. 18) , and both may show the effects of climate, such as thin beds of evaporites, especially anhydrite (Chapter 19).

In the simplest case, and referring only to the Phanerozoic, low-energy shallowing-upward successions have a burrow-mottled, variably argillaceous lime mudstone to wackestone or packstone lowest member, often with a basal bioclastic and intraclastic grainstone or rudstone as a transgressive lag on top of the pre-existing succession (Fig. 16). Patch reefs may be present in the subtidal member. The intertidal member exhibits thin-, lenticular- and wavy-bedded, variably bioturbated lime mudstone and bioclastic, peloidal and sometimes oolitic grainstone, locally with small domical stromatolites. This grades upward to an upper intertidal and supratidal member that is usually a microbially laminated, locally desiccation-cracked, slightly argillaceous lime mudstone frequently exhibiting fenestral fabric, with thin interbeds of intraclastic horizons and laminae of peloidal or bioclastic grainstone. If the sediments were laid down in an arid climate, nodular to wavy beds of anhydrite may displace and replace sediment of the intertidal and supratidal members (Fig.16). Higher-energy cycles (Fig. 18) also have a bioturbated subtidal bioclastic basal member, but the intertidal component is made up of bioclastic and/or locally oolitic grainstones representing beach deposits. These may exhibit inclined- and cross-stratification and hardgrounds. The upper intertidal and supratidal units are generally desiccation-cracked microbial laminites.

Both kinds of shallowing-upward successions can have a capping horizon of marsh sediments, paleosol or calcrete. Successions may be separated from overlying units by a karst surface caused by subaerial weathering, or an erosion surface formed during the environmental shift responsible for the next succession. Supratidal sediments may show the diagenetic effects of groundwater dis-

Figure 15 A shallow pit excavated on the Holocene sabkha; Abu Dhabi, United Arab Emirates. The roughly 1 m of section is composed of light-hued subtidal sediment at the base, overlain in turn by conspicuous black intertidal microbial mats with desiccation cracks and light-coloured supratidal sediment and capped by eolian quartz-rich sands. Photo courtesy P. Scholle.

charge, such as tepees, cements and leaching of evaporites.

A warning! Tidal creek or channel fills can look suspiciously like shallowing-upward successions produced by tidal flat progradation (Fig. 18). Predictably, they should be composed of a basal intraclastic, peloidal and bioclastic grainstone lag or bar facies, overlain by thin-bedded and bioturbated lime mudstone and wackestone, and capped by microbially laminated lime mudstone, recording waning energy conditions as the creek is abandoned (e.g., Waters *et al.*, 1989; Cloyd *et al.*, 1990). Unless a channel margin or lateral-accretion bedding is exposed, or blocky intraclasts from margin collapse are present, these deposits could easily be misunderstood.

Geometry

To interpret how any particular peritidal shallowing-upward succession may have developed there must be firm local and regional lateral control on the distribution of units; bed or event correlation must be demonstrable. Besides walking or tracing out individual beds, the lithologic features that may be widely correlatable in peritidal successions are subaerial exposure horizons (karst surfaces, collapse breccias and paleosols), evaporite beds and siliciclastic horizons resulting from sea level fall. We recognize two geometries. *Laterally continuous* metre-scale successions are widespread, possibly platform-wide, and correlatable. *Laterally discontinuous* metre-scale successions are local in extent and noncorrelatable and supratidal facies can be traced laterally into intertidal and/or subtidal facies over kilometre-scale distances.

Origin

An aspect of carbonate sedimentology that has become a maxim over the last decade, for Phanerozoic rocks at least, is that healthy carbonate platforms, i.e., those not stressed by environmental conditions like cold water, hypersalinity, turbidity or nutrient poisoning that hinder organism growth, can produce enough carbonate sediment to aggrade, and commonly a surplus, causing progradation, while relative sea level rises (Schlager, 1981). Shallow water sediments thus overlie deeper water facies. Each shallowing-upward peritidal succession records the vertical and lateral accretion of a single tidal flat to a level just exceeding high-tide mark; if there was no subsidence or sea level change, the thickness of the intertidal-supratidal component might approximate the tidal range, but if there was any relative sea level change, the thickness is no indication of this at all.

There are currently three models used to explain how a shallowing-upward succession forms 1) as a prograding wedge, 2) as a simultaneously

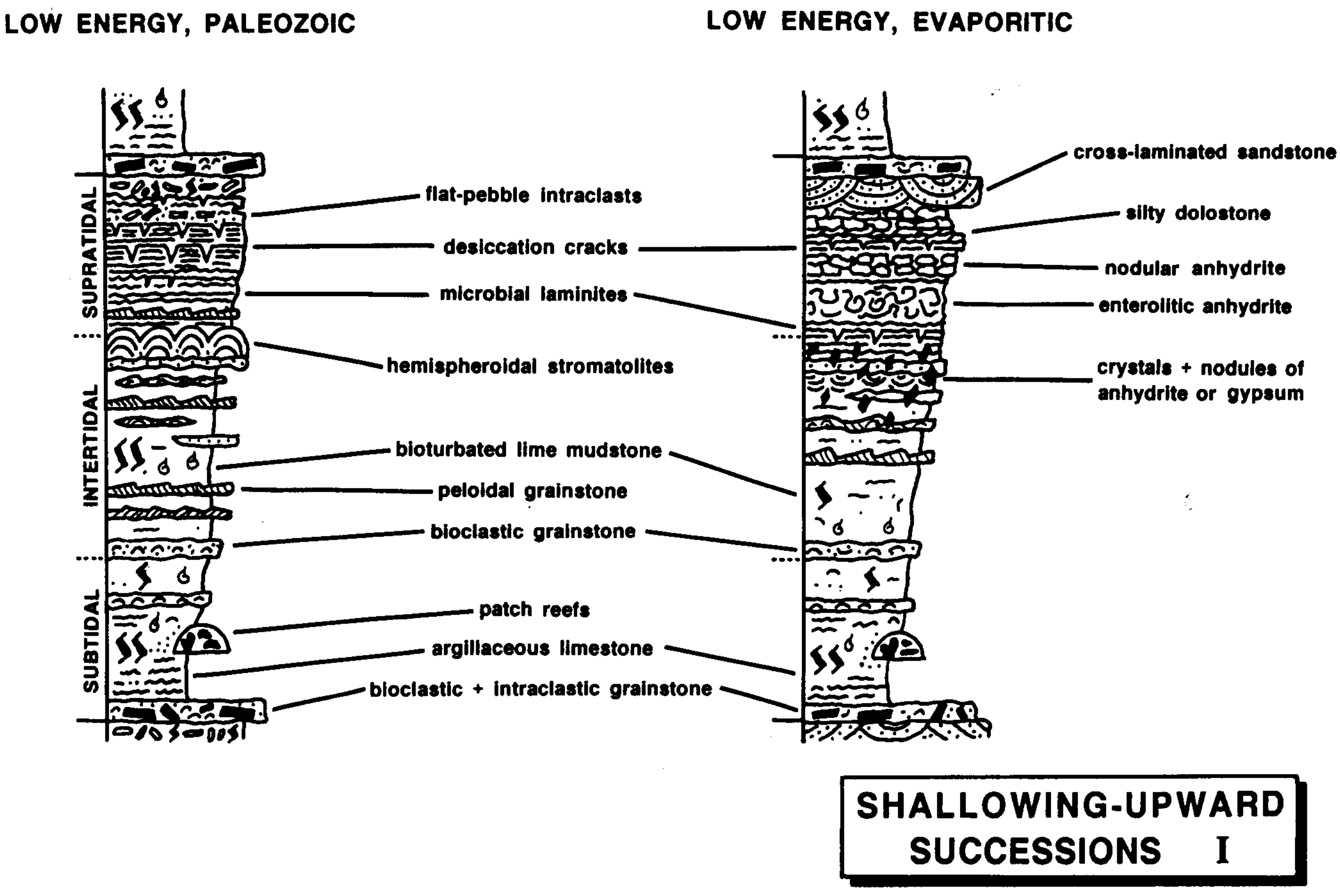

Figure 16 Hypothetical vertical profiles of individual low-energy, metre-scale, peritidal shallowing-upward successions. Left: from the lower Paleozoic; upper Paleozoic examples might exhibit calcretes at the top. Right: an evaporitic example (Chapter 19). No scale is implied, but each succession is typically 1-10 m thick.

aggrading sheet or, 3) as a mosaic of tidal flat islands (Fig. 19).

The prograding wedge

Holocene shallow-marine and peritidal environments are dynamic in that they shift geographically over geologically short periods of time in response to both local and regional changes in climate, prevailing wind direction, current pattern, and sediment supply. A single coastline, for example, may possess tidal flats that are accumulating and prograding, and tidal flats that are dormant or are eroding (e.g., Shinn *et al.*, 1969; Strasser and Davaud, 1986). Regardless, to generate a single, laterally extensive wedge that has peritidal, shallowing-upward attributes throughout, the tidal flat must prograde laterally from a nucleus. Such accretion can develop seaward from land, outward from islands, or shelfward from platform margin buildups and/or shoals. It must be stressed that deposition on the tidal flat is a physical process. Sediment generated on the platform is swept onto the flats by storms producing the gradually prograding tidal flat wedge. As such, the size and dynamics of the peritidal wedge are primarily a function of the health and nature of the source area (the subtidal carbonate factory) and the way in which sediment is redistributed on the platform (i.e., how much is transported to the flats, how much stays in place, how much is transported offshore into deep water).

The Holocene record of sea level change is one of rapid rise between 11 ka and 6 ka, followed by decelerated rise from 6 ka to the present. There are, unfortunately, few tidal flats that have been cored in enough detail to provide a good three-dimensional stratigraphic picture of deposition during this period. As a result of this small data base it is difficult to make generalizations. Nevertheless, at present there appear to be two styles of progradation (Fig. 20), *simple offlap* and *staggered offlap* (Hardie and Shinn, 1986). Simple offlap is typified by the gradually prograding wedge along the southern coast of the Persian (Arabian) Gulf. Staggered offlap is characterized by the northern Bahamas tidal flats. In the latter case the tidal flat does not seem to have prograded but instead aggraded behind a protecting beach ridge. The vertical succession is mainly burrowed sediment, reflecting deposition in a variety of pond, channel and intertidal flat environments, capped by laminated upper intertidal to supratidal sediments. It is thought that tidal flat sedimentation began only when the offshore carbonate sand bar emerged to become a barrier. Once the flat aggraded to sea level, progradation took place by a series of jumps followed by back filling (Hardie, 1986). Such successions in the rock record should

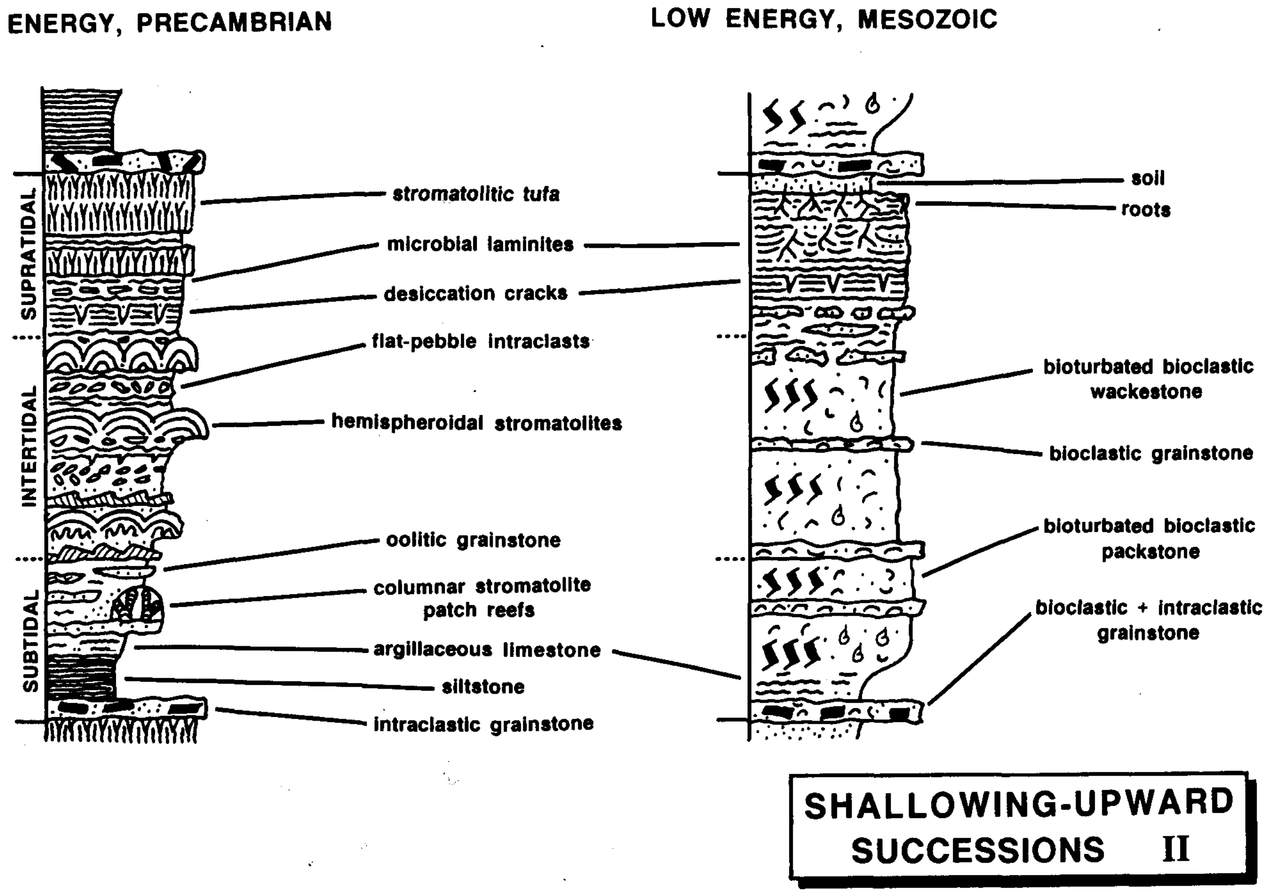

Figure 17 Hypothetical vertical profiles of individual low-energy, metre-scale, peritidal shallowing-upward successions from the Precambrian (left) and Mesozoic (right). A comparison of these with the Paleozoic example in Figure 16 shows some of the lithologic changes exerted by biotic evolution through geologic time.

contain remnants of these barriers. The Abu Dhabi sabkha is reported to have buried barriers (Warren and Kendall, 1985) and may have also developed, in part, through staggered offlap.

For a wedge of tidal flat sediment to prograde from the strandline across an entire platform, accumulation of sediment must occur under relatively stable hydrographic conditions (i.e., sea level and climate) for the length of time represented by progradation. A rapid rise in sea level would flood the broad supratidal flat and halt progradation, whereas any fall in sea level would strand the tidal flat before transplatform progradation was complete.

This style of accumulation has been proposed to explain the extensive Cambro-Ordovician peritidal strata of the southern Appalachians (Hardie, 1986). Metre-scale peritidal shallowing-upward successions of this epeiric platform have been correlated (but not traced) for distances greater than 100 km parallel and perpendicular to depositional strike. Progradation at this scale, however, would produce vast areas of abandoned supratidal flats behind the prograding shoreline, far distant from the subtidal source of sediment and exposed to protracted subaerial diagenetic effects. Since constant and uniform subsidence would inundate this supratidal surface, progradation must have taken place while relative sea level was stationary or gradually falling. If progradation was simple offlap, then successions will be laterally continuous. If progradation was staggered offlap, successions will be discontinuous and separated by lenticular beach deposits.

Simultaneously aggrading sheet

In this situation, continuous in situ carbonate sediment production results in aggradation of the seafloor steadily to sea level. The entire platform becomes intertidal and then supratidal, and can be completely exposed before flooding and deposition of the next overlying succession (Fig. 19). There are no Holocene analogues for this process; it is derived entirely from interpretation of the rock record, and therefore is poorly constrained. Platform-wide peritidal exposure under these circumstances cannot be *intertidal* per se, because it is unlikely that tides could operate across such a vast horizontal distance all at once. Instead, alternating flooding and exposure would have to be induced through the movement of the sea surface by periodic storm surges or persistent winds. Such a style of *occasional* exposure and submergence may be difficult to distinguish in the rock record from true *intertidal* conditions. This hypothesis demands that at least some sediment be produced on the flats when the whole platform is in the intertidal-supratidal environment. Such accretion could predictably produce platform-wide, laterally continuous, metre-thick shallowing-upward successions, such

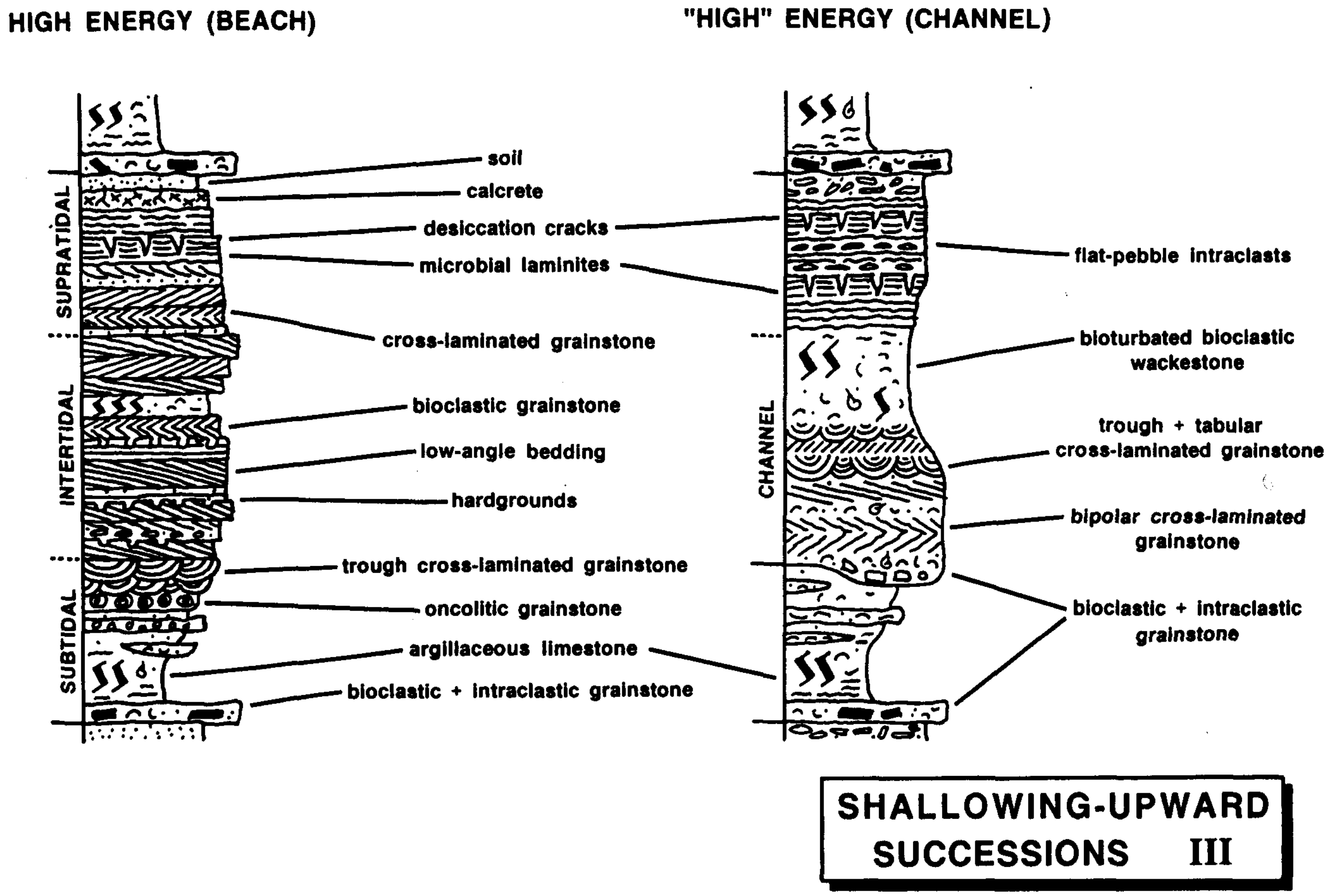

Figure 18 Hypothetical vertical profiles of individual high-energy, metre-scale, peritidal shallowing-upward successions, from a setting characterized by beach development (left) and a tidal flat penetrated by channels or creeks (right).

as those inferred from Cambrian strata by Koerschner and Read (1989).

Tidal flat islands

An alternative model has been postulated to explain shallowing-upward peritidal successions that are demonstrably laterally discontinuous (Pratt and James, 1986). In this *tidal flat island* model deposition is envisioned as taking place on a platform dotted by a mosaic of exposed low-relief islands and intertidal banks separated by subtidal source areas (Fig. 19), with the whole complex shifting laterally and vertically through time in response to a range of local and regional hydrographic conditions. Such islands are developed today in Florida Bay and illustrate two modes of Holocene accumulation, 1) physically deposited mud banks capped by prograding intertidal and supratidal sediments, and 2) entirely supratidal deposition of a coastal mud flat, later dissected by erosion (Enos and Perkins, 1979; Wanless and Tagett, 1989). These islands, however, have not migrated much during the relatively short period of Holocene flooding. If viable, this tidal flat island model severely limits the architectural predictability of ancient platforms, as the constituent facies, particularly the supratidal caps, are of inherently limited regional extent.

Asymmetry

Why is a metre-scale, peritidal shallowing-upward succession asymmetric? The characteristic asymmetry of a typical shallowing-upward succession, i.e., subtidal (A), intertidal (B) and supratidal (C) stacked in ABC → ABC *hemicycles* (Figs. 16, 17, 18), as opposed to full CBABC cycles, is generally attributed to problems with the source area during platform inundation. If the flooding which begins a succession were gradual, then the seafloor during initial submergence is thought to have been too wave swept and/or too shallow or restricted to produce much carbonate sediment. Thus there is a "lag time" or "lag depth" (Hardie, 1986) before the seafloor becomes deep enough to actively produce sediment that is subsequently moved onto the tidal flats. In some successions this time interval is represented by a coarse-grained "transgressive" facies at the base, whereas in others there is no obvious record of this hiatus in deposition. Alternatively, if flooding was rapid, then supratidal facies (C) would be rapidly drowned and intertidal facies (B) would not have time to accumulate.

PERITIDAL CYCLOSTRATIGRAPHY

The stratigraphic record of ancient peritidal carbonates tends to be one of persistent repetition of the basic metre-scale, shallowing-upward succession, imparting a characteristic *cyclic* or, more appropriately, *rhythmic* appearance to the strata. While Holocene tidal flats sometimes provide an analogue for the generation of one

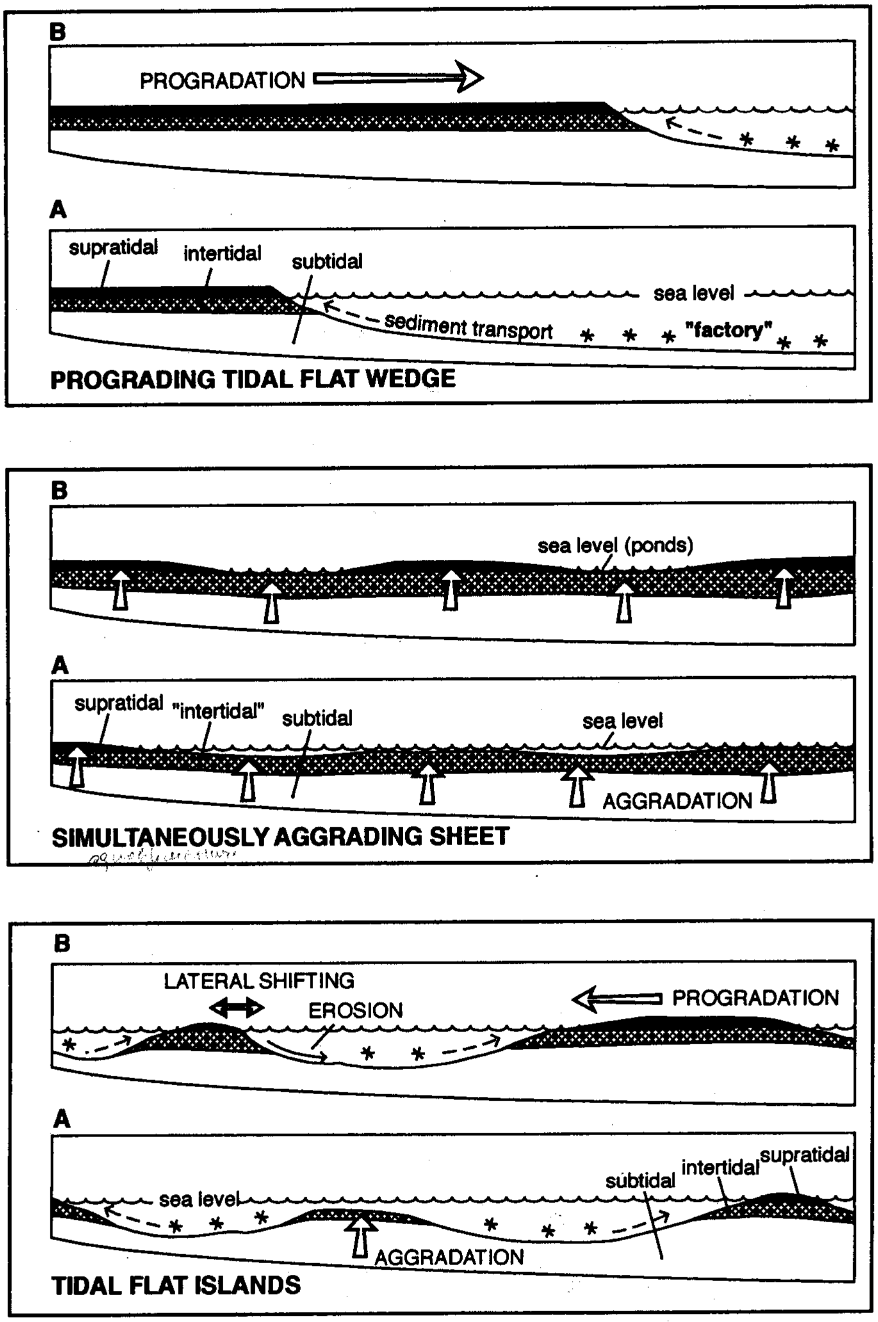

Figure 19 Diagrams illustrating various ways in which a metre-scale, peritidal, shallowing-upward succession can form. A prograding wedge is generated by sediment transported onto the tidal flat from the offshore carbonate factory. A simultaneously aggrading sheet accretes vertically to sea level and the whole platform becomes sequentially intertidal and then supratidal. Tidal flat islands nucleate and accrete by aggradation and progradation and shift in response to hydrographic forces.

shallowing-upward succession, the cause of stratigraphic repetition must be derived from the rock record. The Pleistocene history of climate and sea level change, although the most detailed and best understood of past epochs, has left a stratigraphic record of limited usefulness because sea level fluctuations were so large that they did not result in stacked metre-scale shallowing-upward successions. Consequently, there is currently much discussion as to what causes the rhythmic stacking into thick stratigraphic packages of ancient shallowing-upward successions. Debate has centred around the question of whether the new space made available for each successive shallowing-upward succession is the result of 1) recurring sea level changes (perhaps eustatic) at the same scale and temporal rhythm as the lithologic packaging; or 2) a high-frequency packaging mechanism *intrinsic* to processes of carbonate sedimentation which are superimposed on a low-frequency or irregular sea level rise. These are the *allocyclic* and *autocyclic* mechanisms, respectively, (see also Wilkinson, 1982). The two stacking mechanisms are not necessarily mutually exclusive, and it is uncertain at the moment whether or not evidence for either mechanism can be isolated in the rock record (Hardie *et al.*, 1991; Read *et al.*, 1991).

There is good evidence that a typical shallowing-upward succession was deposited within a time span of 10-100 k.y. (Algeo and Wilkinson, 1988). This is a scale of resolution beyond that provided by biostratigraphic methods. Much of the time represented by stacked shallowing-upward successions, however, is accounted for by hiatuses. Thus the time of deposition for a given tidal flat succession may be only a small fraction of the total apparent stratigraphic time; Wilkinson *et al.* (1991) have suggested as little as 3-30 per cent for some successions.

Autocyclicity

The driving force behind autocyclicity is the dynamics of sedimentation on the platform. Assuming optimum conditions, production rates for shallow-marine carbonate detritus could potentially provide enough sediment over a period of 10-100 k.y. to account for tidal flat aggradation to sea level or progradation of many tens to perhaps hundreds of kilometres under essentially static sea level conditions on a gradient which experienced typical passive-margin rates of subsidence (see also Hardie and Shinn, 1986).

Progradation is inherently limited by the sediment budget of the carbonate platform. For example, in a model first proposed by Ginsburg (1971; see Bosellini and Hardie, 1973; Mossop, 1979), a tidal flat wedge is envisioned as prograding across a gently inclined, gradually subsiding platform under static or slowly changing sea level (Fig. 19). As progradation covers the platform, the subtidal source area for tidal flat sediments becomes increasingly smaller (and deeper). Eventually the source area is too small or too deep to provide sediment for the tidal flat, so sedimentation stops. If relative sea level continues to rise, however, soon the whole platform will once again be subtidal and, after a lag period, the carbonate factory will be robust enough for sediment production, and the cycle will begin again.

The meagre areal coverage of present-day tidal flats makes it difficult to envision a platform literally choking itself off through hundreds of kilometres worth of tidal flat progradation under steady-state sea level and subsidence conditions. Furthermore, it should be emphasized that interpretations of platform-wide progradation in ancient examples are usually based on correlation of strata assumed to be diachronous, not on continuous stratigraphic exposure.

Under conditions of platform-wide *aggradation* it is thought that, once flooded, a shallow platform could generate enough sediment in situ that the whole seafloor would inexorably build to sea level (Fig. 19). Fundamental to this hypothesis is the ability of the "intertidal" and "supratidal" environments to produce sediment. The next cycle would accrete once relative sea level rise had submerged the platform in water deep enough for subtidal sedimentation to begin again. Critics of this hypothesis argue that, in order for the sediment surface to intersect the air/water interface on a platform-wide scale, there must be a sea level fall (albeit minor — a metre or less?), because it is unlikely that the seafloor would everywhere build right up to sea level of its own accord. This model is based on examples where shallowing-upward successions are correlated on a regional scale and assumed to be synchronous deposits.

Tidal flat islands are in part aggradational and in part progradational and their location is thought to shift through time in response to changing hydrographic conditions (Fig. 19). During intervals of prolonged static sea level, or slow sea level rise, they would, like the

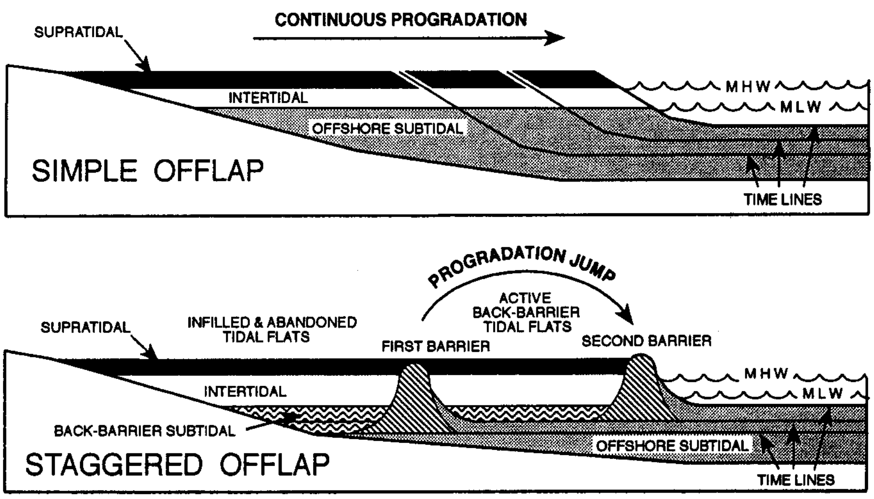

Figure 20 A diagram depicting two styles of tidal flat progradation envisioned from Holocene tidal flats. Simple offlap takes place by continuous progradation. Staggered offlap takes place by formation of an offshore bar which creates a leeward, protected setting in which tidal flat aggradation occurs. Once the flat builds to sea level it becomes dormant until another bar forms seaward and the process of backfilling begins again. Adapted from Hardie (1986).

prograding wedge, gradually choke off local source areas, eventually becoming dormant. For sedimentation to begin again after a period of local stasis and probably protracted exposure of supratidal flats, there must be creation of new accumulation space. Under conditions of more rapid long-term sea level rise, and continually renewed accumulation space, the islands would form a series of laterally discontinuous peritidal units.

These autocyclic models express a basic premise that pervades current thinking about peritidal carbonates. Persistent and ubiquitous stratigraphic repetition of the basic shallowing-upward succession seems to indicate that these systems are, *at least in part,* intrinsically self-governing.

Allocyclicity

The extrinsic factors of subsidence and eustacy, which cause relative sea level change, have long been assumed to exert strong control on *large-scale* peritidal stratal patterns. High-frequency, low-amplitude sea level changes, the fourth- and fifth-order fluctuations of sequence stratigraphy (Chapter 2), are commonly invoked to drive the packaging of metre-scale, shallowing-upward peritidal successions (Grotzinger, 1986; Koerschner and Read, 1989; Read *et al.*, 1991). In this situation, a metre-scale rise in relative sea level provides a *window of opportunity*, in the sense of both time and accumulation space, for the generation of a single shallowing-upward succession (Fig. 21). Deposition occurs while sea level is rising and at its apex, and is arrested by sea level fall.

Formation of the shallowing-upward succession in this window is envisioned in different ways by different workers. All three styles of accretion presented above are viable within this scheme (prograding wedge, Grotzinger, 1986; aggradation, Koerschner and Read, 1989; and tidal flat islands, Strasser, 1988). Extrinsically controlled metre-scale successions of many kinds, including peritidal, have also been called *punctuated aggradational cycles* (PACs; Goodwin *et al.*, 1986) or more recently *metre-scale allocycles* (Anderson and Goodwin, 1990). Such cycles are metre-scale units, bounded by surfaces of abrupt change to deeper or disjunct facies and comprising a suite of contemporaneous facies, all of which shallow upward. The peritidal portions of such cycles are thought to be aggradational, but there is no reason why they could not be progradational (either wedges or islands).

The most commonly postulated external controls to drive, or at least reset, the system at the end of each shallowing-upward succession are rhythmic eustatic change or jerky subsidence. While spasmodic subsidence with the required short frequency has been documented from seismically active areas and for passive margins where listric faulting is common (e.g., Cisne, 1986; Hardie *et al.*, 1991), the importance of subsidence rate changes as a control on stratigraphic rhythmicity in peritidal shallowing-upward successions is unclear. Sudden base level drops have not been observed in modern passive margin platforms, and ancient epeiric settings, where much of the peritidal record is found, seem unlikely to have experienced metre-scale, high-frequency spasms of subsidence. Because there is currently no known frequency to such tectonism, it is difficult to use, and as yet impossible to model this mechanism as a universal control of stratigraphic rhythmicity. Nevertheless, the mechanism should not be dismissed as a potential control, especially in tectonically active regimes (e.g., Fischer, 1964; Knight *et al.*, 1991).

In the early to mid-1970s studies of DSDP sediment cores and relict coral reef terraces demonstrated that the Pleistocene record of eustatic change is one of superimposed orders of sea level variation (orders, in the sense of both magnitude and frequency; Chapter 2). Deep sea sediments were analyzed for oxygen isotopes (as proxy to glacial ice volume) and revealed a long-term (100 k.y.), 100 m-scale, asymmetric sea level oscillation. Pleistocene fossil reef data suggested that a shorter term (20 k.y.) sea level oscillation was superimposed on the longer term fluctuation. These various orders of eustatic change have been correlated to those predicted for icehouse glaciation driven by celestial mechanics, i.e., the Milankovitch rhythm (e.g., Fischer, 1986). It has been postulated that the stratigraphic rhythmicity apparent in ancient peritidal carbonates reflects a similar *composite eustasy* (Goldhammer *et al.*, 1987), both icehouse and greenhouse, of celestial origin. If astronomically forced composite eustasy is indeed the primary driver in the packaging of shallowing-upward successions, then presumably modulation of various orders of superimposed eustatic cycles could have provided potentially limitless rhythms to the stratigraphic record (Bova and Read, 1987; Koerschner and Read, 1989; Read *et al.*, 1991).

The common challenge to allocyclicity is that extrinsic controls on peritidal sedimentation are neither demonstrable in, nor theoretically re-

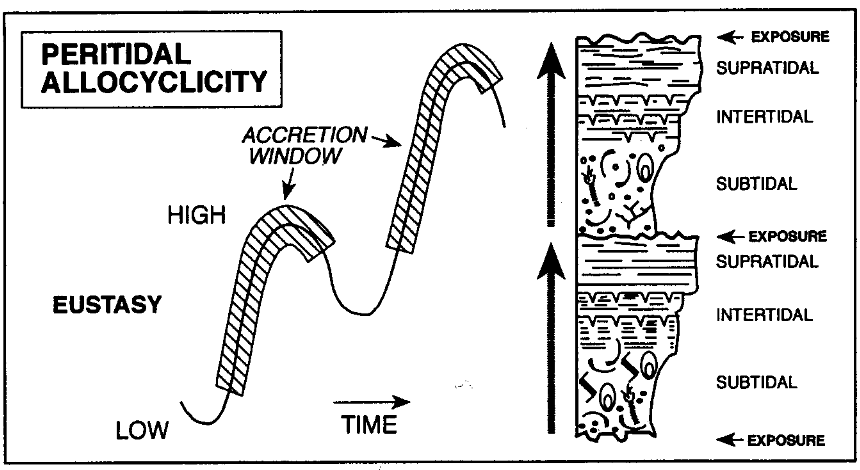

Figure 21 A diagram illustrating the relationship between fluctuating sea level and stacked metre-scale, peritidal, shallowing-upward successions. Sea level rise provides a window of opportunity for the succession to accrete as a prograding wedge, as a simultaneously aggrading sheet or as tidal flat islands. Sea level fall terminates accretion and results in subaerial exposure.

quired to generate metre-scale shallowing-upward successions. It is hard, however, to imagine sea level remaining static for a long period of time, and therefore difficult, if not impossible, to dismiss some extrinsic control on succession development. Allocyclic, platform-wide event stratigraphy should not be underestimated, but its deterministic role in peritidal cyclostratigraphy is still uncertain.

The search for controls and rhythms

Significant effort has recently been devoted to unravelling the meaning of possible stratigraphic rhythms in stacked shallowing-upward successions by numerical analysis. Because peritidal carbonates are so sensitive to changes in climate and sea level, it was widely suspected (hoped?) that this rhythmicity might retain a causative signal of ancient climate and sea level fluctuations. If allocyclic eustatic control on stratal packaging is assumed, then reconstruction of the strata-generating sea level curve can be used as a tool to correlate and explain temporally correlative strata (Read and Goldhammer, 1988).

At the current level of understanding and data base, it is not possible to isolate unequivocal evidence in the rock record for either allocyclic or autocyclic control on most peritidal stratal patterns. Reasonable-looking, synthetic, one-dimensional stratigraphic sections can, however, be generated by varying the critical input parameters of cycle amplitude, duration and asymmetry, bathymetry for each facies, lag time (depth), type of sediment, sedimentation rate, regional and local subsidence, isostatic compensation, wave damping, tidal range, and platform slope and dimension (Grotzinger, 1986; Read *et al.*, 1986; Goldhammer *et al.*, 1987; Spencer and Demicco, 1989). These sections can then be compared to actual examples and eventually a match may be achieved. When similar modelling techniques are used to simulate two-dimensional (multisection) architecture it is often found that the time needed for a peritidal wedge to prograde across the platform is longer than that predicted by Milankovitch rhythms, and the wedges become *stranded.*

Techniques, such as relative time series analysis and *Fischer plotting,* which made a good case for allocyclic forcing of some examples of platform carbonate rhythmicity, i.e., stratigraphic patterns attributable to rhythmic Milankovitch composite eustasy (Goldhammer *et al.*, 1987, 1990), cannot be used for the analysis of metre-scale *peritidal* shallowing-upward successions. Relative time series analysis to reveal the rhythms of sedimentation are invalid for progradational wedges, either local or platform-wide in extent, because such deposits are by nature diachronous, and thicknesses of resultant shallowing-upward successions vary with position on the regional gradient and/or platform topography. Fischer (1964) presented a graphic means of plotting time versus cumulative thickness for laterally continuous, stacked, peritidal shallowing-upward successions. Fischer plots have often been used in recent studies of cyclic strata because they are designed to reveal changes in accumulation space which deviate from that space generated solely by subsidence; these deviations are postulated to result from changes in sea level. However, interpretations of Fischer plots are essentially model driven. For them to be viable two assumptions must be satisfied: 1) each peritidal succession must have been deposited in the same amount of time as every other succession in the chain, and 2) there must be few, if any, missing tidal flat successions. The use of Fischer plots is therefore dubious for any peritidal successions which formed as prograding wedge-shaped tidal flats. It is likely that variations in both the tempo and magnitude of changes in accumulation space, however they are caused, account for stacks of shallowing-upward successions which vary in thickness. Whereas demonstration of allo- or autocyclic control of stratal patterns in stacked shallowing-upward successions appears out of reach at this time, more sophisticated models, particularly those which integrate peritidal rhythms with coeval subtidal and perhaps offplatform stratal patterns, hold promise.

PERITIDAL SEQUENCE STRATIGRAPHY

The concepts of sequence stratigraphy were developed in terrigenous clastic successions and carbonates have only recently been analyzed in this fashion (Chapter 14). *Systematic* packaging of the basic metre-scale shallowing-upward succession is less common and seems less straightforward, or less well developed in carbonates compared to siliciclastics. This difference likely reflects the fundamental differences between carbonate and siliciclastic sediments generally. We have, therefore, avoided the term *parasequence* in this treatment of carbonate tidal flat deposits.

Peritidal deposits are not indicative of any particular systems tract because the controls on tidal flat development, such as climate, platform circulation, wind patterns and tidal range, vary with each platform's unique history and configuration. Nevertheless, tidal flat deposits are potentially useful in delineating sequences and their component systems tracts in two ways, 1) geographic position of the tidal flat on the platform may track long-term changes in sea level, and 2) changes in large-scale accumulation space, and thus sequences, can be recognized through analysis of stacking patterns (packaging) of shallowing-upward successions.

Tracking sea level

Tidal flats can be the first facies overlying a sequence boundary, deposited as the rate of relative sea level fall decreases and the sea slowly floods back across the platform. As third-order sea level fluctuates in response to long-term, large-amplitude driving forces, the location of the strandline on the platform will change. If conditions are favourable for their development, land-fringing tidal flat deposits will mark the position of coastal onlap through the third-order eustatic cycle (i.e., the "onlap-offlap" geometry of Hardie, 1986; Fig. 22). Sarg (1988) documented the utility of tidal flats at the outcrop scale in a sequence stratigraphic context for the Permian of New Mexico, where a sequence boundary and shelf-margin wedge systems tract were recognized in part by the downdip, basinward position of onlapping tidal flat deposits.

Stacking

The stratigraphic patterns of *laterally continuous,* metre-scale, shallowing-upward successions generated by prograding tidal flat wedges, can be envisaged in the framework of long-term changes in relative sea level. Third-order sea level changes are thought to "modulate" the higher-frequency, fourth- and fifth-order sea level cycles represented by the tidal flat successions. This has two consequences.

Long-term, third-order fluctuations in sea level should carry the window of opportunity in which each individual metre-scale succession is formed back and forth across the platform. Depending upon the balance between different rates of subsidence, eustasy and sedimentation, the window will be geographically repositioned during each consecutive fourth or fifth-order change in relative sea level to result in backstepping, offlapping or stacking of peritidal shallowing-upward successions. Figure 22 illustrates, in a conceptual way, how this might work on an inclined shelf. If the rate of change of long-term relative sea level is *low,* the geographic position of successive windows should remain roughly the same. Thus, peritidal successions in lowstand (position 1) and early highstand (position 3) systems tracts will probably be stacked in one place and will be relatively thin because the rate of addition of new accumulation space is low. If the rate of change is *high,* the window should be forced backward and forward across the shelf. This will likely result in either relatively thick, backstepped tidal flat successions (position 2 – transgressive systems tract) or relatively thin successions which offlap in a shingled fashion (position 4 – late highstand or early lowstand systems tracts). It must be stressed that the distance of progradation in each case will be specific to each peritidal package on each shelf.

Long-term sea level rise should accentuate short-term rises and suppress short-term falls; long-term falls in sea level will have the opposite effect. The relative proportions of subtidal, intertidal and supratidal facies in successive shallowing-upward successions may change systematically in response to this long-term modulation of short-term changes in accumulation space. This relationship is as yet hypothetical, and interpretations of such controls in ancient strata are necessarily model driven.

SUMMARY

Peritidal limestones and dolostones exhibit a large number of easily recognized sedimentary and biosedimentary structures. While some of these are individually equivocal bathymetric indicators (stromatolites or wave-rippled beds, for example, can form in subtidal areas), in most cases the features can be used collectively to make a firm environmental conclusion. A boon to interpreting ancient peritidal facies is the wealth of knowledge gained from modern settings. Very often a one-to-one lithologic comparison can be made, leading to a refined understanding of paleoenvironments and paleoclimates in individual cases. A *hierarchy of models* has been formulated that deals with successive levels of interpretation of peritidal carbonate strata.

These kinds of rocks fall into two main depositional systems, low-energy tidal flats and higher-energy beaches. The facies associations are fairly distinctive for each setting: this is the first tier of models to guide basic interpretations.

The vertical record of peritidal facies commonly shows a trend from subtidal limestone through intertidal sediments to supratidal deposits, at a metre scale, as tidal flats aggrade to sea level and prograde laterally. Peritidal models are therefore shown as shallowing-upward successions as a reminder of these dynamic processes.

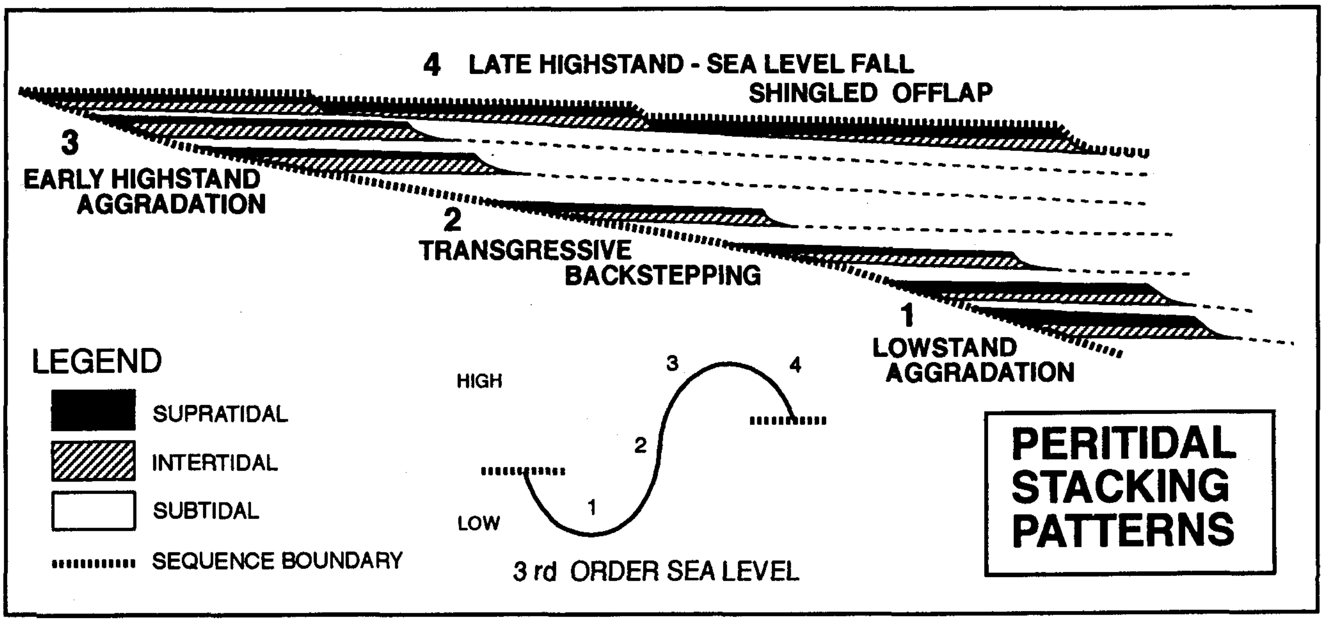

Figure 22 A diagram illustrating the hypothetical stratigraphy of metre-scale, peritidal, successions between two sequence boundaries. Each succession formed by progradation which took place in the window of opportunity produced by short-term fourth- and fifth-order fluctuations in relative sea level during a long-term, third-order rise and fall of sea level. Slow, third-order, sea level-controlled movement of the strandline will dictate where tidal flats develop on the shelf. The balance between sea level changes, sedimentation, and subsidence will dictate how successive tidal flats will stack, backstep or offlap.

These models, as predictors, point to departures from the norm and other irregularities that might have important implications regarding intrinsic or extrinsic controls on deposition. They also provide a framework within which the diagenesis of the sediment can be tracked.

Peritidal carbonates occur repetitively in stratigraphic sequences, often in a seemingly regular, or cyclic, fashion. There is much debate about whether these metre-scale, shallowing-upward successions are platform-wide responses to allogenic forces such as spasmodic subsidence or episodic eustasy, or whether they represent localized tidal flat shorelines and islands shaped by autogenic, i.e., hydrographic, controls. Sedimentologists have their work cut out for them by these models; we are now charged with the job of deciding, if possible, which one best explains our own successions, or if a new approach is necessary. It is an exciting field of research, one that weds careful and precise field observations with increasingly sophisticated numerical modelling.

ACKNOWLEDGEMENTS

This article is an outgrowth of several research projects funded by the Natural Sciences and Engineering Research Council of Canada. An early draft of the text was critically read by E.C. Turner.

REFERENCES

Basic sources of information

Bathurst, R.G.C., 1975, Carbonate sediments and their diagenesis: Amsterdam, Elsevier, 658 p.
Still a good summary of several modern examples.

Ginsburg, R.N., ed., 1975, Tidal deposits: a casebook of Recent examples and fossil counterparts: New York, Springer-Verlag, 428 p.
Many examples of both siliciclastic and carbonate tidal deposits.

Goldhammer, R.K., Dunn, P.A. and Hardie, L.A., 1990, Depositional cycles, composite sea-level changes, cycle stacking patterns, and the hierarchy of stratigraphic forcing: Examples from Alpine Triassic platform carbonates: Geological Society of America, Bulletin, v. 102, p. 535-562.
Manipulation of sedimentological data for computer models to show eustatic effects on a shallow platform.

Hardie, L.A., ed., 1977, Sedimentation on the modern carbonate tidal flats of northwest Andros Island, Bahamas: Johns Hopkins University, Studies in Geology 22, 202 p.
Carbonate tidal flat sediments and biology in a humid setting.

Hardie, L.A. and Shinn, E.A., 1986, Carbonate depositional environments, modern and ancient. Part 3: tidal flats: Colorado School of Mines, Quarterly, v. 81, 74 p.
The place to start, a thorough discussion of peritidal carbonate sediments, facies and depositional models.

Koerschner, W.F. and Read, J.F., 1989, Field and modelling studies of Cambrian carbonate cycles, Virginia Appalachians: Journal of Sedimentary Petrology, v. 59, p. 654-687
Lower Paleozoic peritidal facies and manipulation for computer models trying to show controls by eustasy.

Logan, B.W., Hoffman, P. and Gebelein, C.D., 1974, Evolution and diagenesis of Quaternary carbonate sequences, Shark Bay, Western Australia: American Association of Petroleum Geologists, Memoir 22, 358 p.
Carbonate tidal flat sediments, including stromatolites, in a hypersaline setting.

Pratt, B.R. and James, N.P., 1986, The St George Group (Lower Ordovician) of western Newfoundland: tidal flat island model for carbonate sedimentation in shallow epeiric seas: Sedimentology, v. 33, p. 313-343.
Lower Paleozoic facies and outline of autocyclic island model.

Purser, B.H., ed., 1973, The Persian Gulf: Holocene carbonate sedimentation and diagenesis in a shallow epicontinental sea: Heidelberg, Springer-Verlag, 47 p.
Description of carbonate peritidal sediments in an arid setting.

Shinn, E.A., 1983a, Tidal flats, *in* Scholle, P.A., Bebout, D.G. and Moore, C.H., eds., Carbonate depositional environments: American Association of Petroleum Geologists, Memoir 33, p. 171-210.
Read in conjunction with this article; a colour-illustrated, review of carbonate tidal flat sediments and facies.

Tucker, M.E. and Wright, V.P., 1990, Carbonate sedimentology: Oxford, Blackwell, 482 p.
Succinct review of peritidal carbonate sediments, facies and models.

Wilgus, C.K., Hastings, B.S., Posamentier, H.W., Ross, C.A. and Kendall, C.G.St.C., eds., 1988, Sea level changes: an integrated approach: Society of Economic Paleontologists and Mineralogists, Special Publication 42, 407 p.
Collection of papers emphasizing conceptual basis of sequence stratigraphy plus nimerous case studies of sea level change from the geological record.

Other references

Algeo, T.J. and Wilkinson, B.W., 1988, Periodicity of mesoscale Phanerozoic sedimentary cycles and the role of Milankovitch orbital modulation: Journal of Geology, v. 96, p. 313-322.

Anderson, E.J. and Goodwin, P.W., 1990, The significance of metre-scale allocycles in the quest for a fundamental stratigraphic unit: Journal of the Geological Society of London, v. 147, p. 507-518.

Beales, F.W., 1958, Ancient sediments of Bahaman type: American Association of Petroleum Geologists, Bulletin, v. 42, p. 1845-1880.

Belperio, A.P., Gostin, V.A., Cann, J.H. and Murray-Wallace, C.V., 1988, Sediment-organism zonation and the evolution of Holocene tidal sequences in southern Australia, *in* de Boer, P.L., van Gelder, A. and Nio, S. D., eds., Tide-influenced sedimentary environments and facies: Dordrecht, Reidel Publishing Company, p.475-497.

Bertrand-Sarfati, J. and Moussine-Pouchkine, A., 1988, Is cratonic sedimentation consistent with available models? An example from the Upper Proterozoic of the West African craton: Sedimentary Geology, v. 58, p. 255-276.

Bosellini, A. and Hardie, L.A., 1973, Depositional theme of a marginal marine evaporite: Sedimentology, v. 20, p. 5-27.

Bottjer, D.J. and Ausich, W.I., 1986, Phanerozoic development of tiering in soft substrata suspension-feeding communities: Paleobiology, v. 12, p. 400-420.

Bova, J.A. and Read, J.F., 1987, Incipiently drowned facies within a cyclic peritidal ramp sequence, Early Ordovician Chepultepec interval, Virginia Appalachians: Geological Society of America, Bulletin, v. 98, p. 714-727.

Burne, R.V. and Colwell, J.B., 1982, Temperate carbonate sediments of northern Spencer Gulf, South Australia: a high salinity 'foramol' province: Sedimentology, v. 29, p. 223-238.

Cisne, J.L., 1986, Earthquakes recorded stratigraphically on carbonate platforms: Nature, v. 323, p. 320-322.

Cloyd, K.C., Demicco, R.V. and Spencer, R.J., 1990, Tidal channel, levee, and crevasse-splay deposits from a Cambrian tidal channel system: a new mechanism to produce shallowing-upward sequences: Journal of Sedimentary Petrology, v. 60, p. 73-83.

Cowan, C.A. and James, N.P., 1993, Diastasis cracks: mechanically generated synaeresis-like cracks in an Upper Cambrian shallow water oolitic carbonates: Sedimentology, in press.

Demicco, R.V., 1985, Platform and off-platform carbonates of the Upper Cambrian of western Maryland: Sedimentology, v. 32, p. 1-22.

Enos, P. and Perkins, R.D., 1979, Evolution of Florida Bay from island stratigraphy: Geological Society of America, Bulletin, v. 90, p. 59-83.

Fischer, A.G., 1964, The Lofer cyclothems of the Alpine Triassic, *in* Merriam, D.F., ed., Symposium on cyclic sedimentation: State Geological Survey of Kansas, Bulletin 169, p. 107-149.

Fischer, A.G., 1986, Climatic rhythms recorded *in* strata: Annual Review of Earth and Planetary Science, v. 14, p. 351-376.

Folk, R.L., 1973, Evidence for peritidal deposition of Devonian Coballos Novaculite, Marathon Basin, Texas: American Association of Petroleum Geologists, Bulletin, v. 57, p. 702-725.

Garrett, P., 1970, Phanerozoic stromatolites: non-competitive ecological restriction by grazing and burrowing animals: Science, v. 169, p. 171-173.

Gebelein, C.D., 1977, Dynamics of Recent carbonate sedimentation and ecology: Cape Sable, Florida: Leiden, E.J. Brill, 120 p.

Ginsburg, R.N., 1956, Environmental relationships of grain size, Florida carbonate sediments: American Association of Petroleum Geologists, Bulletin, v. 40, p. 2384-2427.

Ginsburg, R.N., 1971, Landward movement of carbonate mud: new model for regressive cycles in carbonates (abst.): American Association of Petroleum Geologists, Bulletin, v. 55, p. 340.

Goldhammer, R.K., Dunn, P.A. and Hardie, L.A., 1987, High frequency glacio-eustatic sea level oscillation with Milankovitch characteristics recorded in Middle Triassic platform carbonates in northern Italy: American Journal of Science, v. 287, p. 853-892.

Goodwin, P.W., Anderson, E.J., Goodman, W.M. and Saraka, L.J., 1986, Punctuated aggradational cycles: implications for stratigraphic analysis: Paleoceanography, v. 1, p. 417-429.

Grotzinger, J.P., 1986, Cyclicity and paleoenvironmental dynamics, Rocknest platform, northwest Canada: Geological Society of America, Bulletin, v. 97, p. 1208-1231.

Hardie, L.A., 1986, Stratigraphic models for carbonate tidal-flat deposition, *in* Hardie, L.A. and Shinn, E.A., eds., Carbonate depositional environments; Part 3: Tidal flats: Colorado School of Mines, Quarterly, v. 81, p. 59-74.

Hardie, L.A., Dunn, P.A. and Goldhammer, R.K., 1991, Field and modelling studies of Cambrian carbonate cycles, Virginia Appalachians – Discussion: Journal of Sedimentary Petrology, v. 61, p. 636-646.

Inden, R.F. and Moore, C.H., 1983, Beach environment, *in* Scholle, P.A., Bebout, D.G. and Moore, C.H., eds., Carbonate depositional environments: American Association of Petroleum Geologists, Memoir 33, p. 209-265.

James, N.P., 1984, Shallowing-upward sequences in carbonates, *in* Walker, R.G., ed., Facies models: Geological Association of Canada, Geoscience Canada Reprint Series 1, p. 213-228.

Kendall, G.C.St.C. and Warren, J.K., 1987, A review of the origin and setting of tepee structures and their associated fabrics: Sedimentology, v. 34, p. 1007-1027.

Knight, I., James, N.P. and Lane, T., 1991, The Ordovician St. George unconformity, northern Appalachians: The effects of convergent lithospheric dynamics at the St. Lawrence Promontory on the Sauk-Tippecanoe Sequence boundary: Geological Society of America, Bulletin, v. 103, p. 1200-1225.

Knoll, H.A. and Swett, K., 1990, Carbonate deposition during the Late Proterozoic era: an example from Spitzbergen: American Journal of Science, v. 290A, p. 104-132.

Knoll, A.H., Swett, K. and Mark, J., 1991, Paleobiology of a Neoproterozoic tidal flat/lagoon complex: the Draken Conglomerate Formation, Spitzbergen: Journal of Paleontology, v. 65, p. 531-570.

Laporte, L.F., 1967, Carbonate deposition near mean sea-level and resultant facies mosaic: Manlius Formation of New York State: American Association of Petroleum Geologists, Bulletin, v. 51, p. 73-101.

Logan, B.W., Davies, G.R., Read, J.F. and Cebulski, D.E., 1970, Carbonate sedimentation and environments, Shark Bay, Western Australia: American Association of Petroleum Geologists, Memoir 13, 223 p.

Maliva, R.G., Knoll, A.H. and Siever, R., 1989, Secular change in chert distribution: a reflection of evolving biological participation in the silica cycle: Palaios, v. 4, p. 519-532.

Matter, A., 1967, Tidal flat deposits in the Ordovician of Maryland: Journal of Sedimentary Petrology, v. 37, p. 601-609.

Mossop, G.D., 1979, The evaporites of the Ordovician Baumann Fiord Formation, Ellesmere Island, Arctic Canada: Geological Survey of Canada, Bulletin 298, 52 p.

Pratt, B.R., 1979, The St. George Group (Lower Ordovician), western Newfoundland: sedimentology, diagenesis, and cryptalgal structures: Unpublished M.Sc. thesis, Memorial University of Newfoundland, 254 p.

Pratt, B.R., 1982, Stromatolite decline – a reconsideration: Geology, v. 10, p. 812-815.

Pratt, B.R., 1991, Asteroid impact on brachiopods?: Lethaia, v. 24, p. 457-459.

Radke, B.M., 1980, Epeiric carbonate sedimentation, Ninmaroo Formation (Upper Cambrian-Lower Ordovician), Georgina Basin: BMR Journal of Australian Geology & Geophysics, v. 5, p. 183-200.

Read, J.F. and Goldhammer, R.K., 1988, Use of Fischer plots to define third-order sea-level curves in Ordovician peritidal cyclic carbonates, Appalachians: Geology, v. 16, p. 895-899.

Read, J.F., Grotzinger, J.P., Bova, J.A. and Koerschner, W.F., 1986, Models for generation of carbonate cycles: Geology, v. 14, p. 107-110.

Read, J.F., Koerschner, W.F., III, Osleger, D.A., Bollinger, G.A. and Coruh, C., 1991, Field and modelling studies of Cambrian carbonate cycles, Virginia Appalachians – Reply: Journal of Sedimentary Petrology, v. 61, p. 647-652.

Reineck, H.-E. and Singh, I.B., 1980, Depositional sedimentary environments: Berlin, Springer-Verlag, 549 p.

Roehl, P.O., 1967, Stony Mountain (Ordovician) and Interlake (Silurian), facies analogs of recent low-energy marine and subaerial carbonates, Bahamas: American Association of Petroleum Geologists, Bulletin, v. 51, p. 1979-2032.

Sarg, J.F., 1988, Carbonate sequence stratigraphy, *in* Wilgus, C.K., *et al.*, eds., Sea-level changes: an integrated approach: Society of Economic Paleontologists and Mineralogists, Special Publication 42, p. 155-182.

Schlager, W., 1981, The paradox of drowned reefs and carbonate platforms: Geological Society of America, Bulletin, v. 92, p. 197-211.

Schwarz, H.-U., 1975, Sedimentary structures and facies analysis of shallow marine carbonates: Berlin, Springer-Verlag, Contributions to Sedimentology 3, 100 p.

Shinn, E.A., 1983, Birdseyes, fenestrae, shrinkage pores and loferites: a reevaluation: Journal of Sedimentary Petrology, v. 53, p. 619-628.

Shinn, E.A., Lloyd, R.M. and Ginsburg, R. N., 1969, Anatomy of a modern carbonate tidal flat, Andros Island, Bahamas: Journal of Sedimentary Petrology, v. 39, p. 1201-1228.

Smosna, R. and Warshauer, S.M., 1981, Rank exposure index on a Silurian carbonate tidal flat: Sedimentology, v. 28, p. 723-731.

Spencer, R.J. and Demicco, R.V., 1989, Computer models of carbonate platform cycles driven by subsidence and eustacy: Geology, v. 17, p. 165-168.

Strasser, A., 1988, Shallowing-upward sequences in Purbeckian peritidal carbonates (lowermost Cretaceous, Swill and French Jura Mountains): Sedimentology, v. 35, p. 369-383.

Strasser, A. and Davaud, E., 1986, Formation of Holocene limestone sequences by progradation, cementation, and erosion: two examples from the Bahamas: Journal of Sedimentary Petrology, v. 56, p. 422-428.

Thayer, C.W., 1983, Sediment-mediated biological disturbance and the evolution of marine benthos, *in* Tevesz, M.J.S. and McCall, P.L., eds., Biotic interactions in Recent and fossil benthic communities: New York, Plenum, p. 479-625.

Walker, K.R., Read, J.F. and Hardie, L.A., 1989, Cambro-Ordovician carbonate banks and siliciclastic basins of the United States Appalachians: Field Trip Guidebook T161, 28th International Geological Congress, American Geophysical Union, Washington, D.C., 88 p.

Wanless, H.R., 1981, Fining-upwards sedimentary sequences generated in seagrass beds: Journal of Sedimentary Petrology, v. 51, p. 445-454.

Wanless, H.R., Tyrrell, K.M., Tedesco, L.P. and Dravis, J.J., 1988, Tidal-flat sedimentation from Hurricane Kate, Caicos platform, British West Indies: Journal of Sedimentary Petrology, v. 58, p. 724-738.

Wanless, H.R. and Tagett, M.G., 1989, Origin, growth and evolution of carbonate mudbanks in Florida Bay: Bulletin of Marine Science, v. 44, p. 454-489.

Wantland, K.F. and Pusey, W.C., 1975, Belize Shelf – Carbonate sediments, clastic sediments, and ecology: American Association of Petroleum Geologists, Studies in Geology 2, 599 p.

Warren, J.K. and Kendall, C.G.St.C., 1985, Comparison of sequences formed in marine sabkha (subaerial) and salina (subaqueous) settings – modern and ancient: American Association of Petroleum Geologists, Bulletin, v. 69, p. 1013-1023.

Waters, B.B., Spencer, R.J. and Demicco, R.V., 1989, Three-dimensional architecture of shallowing-upward carbonate cycles: Middle and Upper Cambrian Waterfowl Formation, Canmore, Alberta: Bulletin of Canadian Petroleum Geology, v. 37, p. 198-209.

Wilkinson, B.R., 1982, Cyclic cratonic carbonates and Phanerozoic calcite seas: Journal of Geological Education, v. 30, p.189-203.

Wilkinson, B.H., Opdyke, B.N. and Algeo, T.J., 1991, Time partitioning in cratonic carbonate rocks: Geology, v. 19, p. 1093-1096.

Wong, P.K. and Oldershaw, A.E., 1980, Causes of cyclicity in reef interior sediments, Kaybob Reef, Alberta: Bulletin of Canadian Petroleum Geology, v. 28, p. 411-425.

Wright, V.P., 1984, Peritidal carbonate facies models: A review: Geological Journal, v. 19, p. 309-325.

Wright, V.P., Ries, A.C. and Munn, G., 1990, Intraplatformal basin-fill deposits from the Infracambrian Huqf Group, east Central Oman, *in* Roberston, A.H.F., Searle, M.P. and Ries, A.C., eds., The geology and tectonics of the Oman region: Geological Society of London, Special Publication No. 49, p. 601-616.

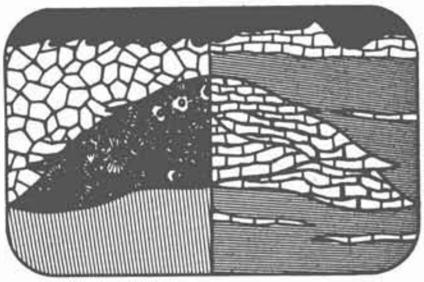

17. Reefs and Mounds

Noel P. James, Department of Geological Sciences, Queen's University, Kingston, Ontario K7L 3N6

Pierre-André Bourque, Département de Géologie, Université Laval, Québec, Québec G1K 7P4

INTRODUCTION

Ancient reefs and mounds were *biologically constructed reliefs* which grew on the seafloor and are now bodies of massive carbonate surrounded by bedded strata (Fig. 1). It is a challenge to formulate facies models for such features because they were primarily biological, and so their growth was governed as much by interactions within the evolving biosphere as by universal physical laws.

This article is an integration of themes or threads which run through geological time and characterize reefs and mounds of all ages. Because there are some structures in the geological record which have no living counterparts, the approach has been to use the modern to formulate principles, the modern and the rock record to outline structure and the rock record to discuss stratigraphy.

REEFS AND MOUNDS

When we think of reefs, visions of clear tropical water, luxuriant coral growth and brightly coloured fish generally spring to mind (Fig. 2). Such reefs are built by large corals and abundant algae and stand as impressive structures above the surrounding seafloor. Our vision quickly becomes blurred, however, in quiet, murky or deep water where these structures have varied relief, are constructed by different organisms and are as much piles of sediment as hard rock. Such reliefs, which do not readily fit our idea of reefs, are variably called banks, shoals, knolls or mounds. Because many "reefs" in the geological record were like these structures and because there were neither corals nor coral-like metazoans in many geological periods, there has for decades been an ongoing debate as to what constitutes an ancient "reef" (see Dunham (1970), Heckel (1974), Longman (1981), James (1983) and Geldsetzer *et al.* (1989)). In this review, *reefs* are those structures which were, like modern reefs, constructed by large, usually clonal elements (on average >5 cm in size), and capable of thriving in energetic environments; *mounds* are those structures which were built by smaller, commonly delicate and/or solitary elements in tranquil settings. Viewed in the context of geological time, there are probably many more mounds than reefs.

The different types of ancient reefs and mounds are most usefully conceptualized on a quaternary diagram (Fig. 3). The main framework elements of reefs are scleractinian corals and tabulate "corals", coralline sponges (including stromatoporoids) and encrusting calcareous algae or microbes (in the form of stromatolites/thrombolites). There are three types of mounds: *microbial mounds* and *skeletal mounds* were organically controlled, and are collectively called *biogenic mounds*; *mud mounds* were formed by inorganic accumulation of mud with variable amounts of fossils. The division between biogenic mounds and *mud mounds* depends on the nature of the accumulation/construction controls, not on the percentage of fossils. For instance, less than 10 per cent fenestrate bryozoans may have controlled the construction of a skeletal mound by baffling and trapping lime mud. The fossils in skeletal mounds are smaller versions of the reef builders together with calcareous algae, bryozoa, spiculate sponges, richtofenid brachiopods orudist bivalves. Microbial mounds are made of stromatolites/thrombolites, calcimicrobes (Renalcids, *Tubiphytes* etc.) and mud. Organisms which form mounds are gradational into, and can be important elements of, reefs or vice versa. Microbes and corals are common examples.

Figure 1 An exhumed reef, approximately 600 m in length and 300 m in height, in the Proterozoic Little Dal Group, Mackenzie Mountains, Northwest Territories, Canada. The castellated core of microbial limestone is surrounded by coarse flanking beds of reef talus. Photograph G. Narbonne.

Many reefs and mounds are fractal. The smallest elements, stromatolites, individual corals or clusters of delicate skeletons, repeat, forming ever larger structures. Corals and other calcareous benthos, for example, form heads, which in turn cluster to form coral knobs; clusters of coral knobs form reefs; clusters of reefs form reef complexes. This is particularly evident in mounds, where small clusters of organisms construct metre-size lenses (variously called calyptra in the Cambrian, saccoliths in the Permian), which are stacked on top of one another to form impressive geological structures or mound complexes.

Two terms, bioherms and biostromes, are commonly used to designate biogenically constructed geological structures. A *bioherm* is a lens-shaped reef or mound; a *biostrome* is a tabular rock body, usually a single bed of similar composition. Another commonly used generic epithet with no compositional, size or shape connotation is *carbonate buildup.*

The preceding terms carry no implication of scale. While the shape of reefs in plan varies from subcircular "patch reefs" to linear "barrier reefs", mounds are generally subcircular to elongate. During geological periods when large calcareous skeletal and microbial structures were common, reefs grew as fringing reefs inboard, as patch reefs across platforms, and as semicontinuous to continuous barrier reefs along platform margins. Coeval mounds developed in quiet water settings across the platform, on ramps or on the slope. During geological periods when there were no large reef builders, mounds were the only buildups and grew leeward of sand shoals, on deep water ramps and on slopes.

THE ORGANISM/SEDIMENT MOSAIC

Reefs and mounds generally comprise three facies (Fig. 4), 1) *Core facies* — massive, unbedded carbonate with or without skeletons, 2) *Flank or fore reef facies* — bedded carbonate sand and conglomerate of in place and/or core-derived material, dipping and thinning away from the core, and 3) *Interreef or open platform facies* — subtidal limestone or terrigenous clastic sediment, unrelated to reef growth. The focus of this review is the core facies.

Sedimentary processes

Modern reefs and mounds

Any living reef or mound is a delicate balance between 1) upward growth of in place calcareous elements (metazoan and microbial), 2) continuing destruction by a host of raspers, borers and grazers, 3) prolific sediment production by rapidly growing, short-lived, attached calcareous benthos, and 4) concurrent inorganic or organically induced cementation (Fig. 4). The large skeletal metazoans (e.g., corals) generally remain in place after death, except when so weakened by bioeroders that they are toppled by storms. Their irregular shape and growth habit result in roofed-over cavities that can be inhabited by smaller, attached calcareous benthos. En-

Figure 2 Large, shallow water, branching corals *(Acropora palmata)* about 1 m in height, growing just in the lee of the reef crest, offshore Grand Cayman Island, British West Indies.

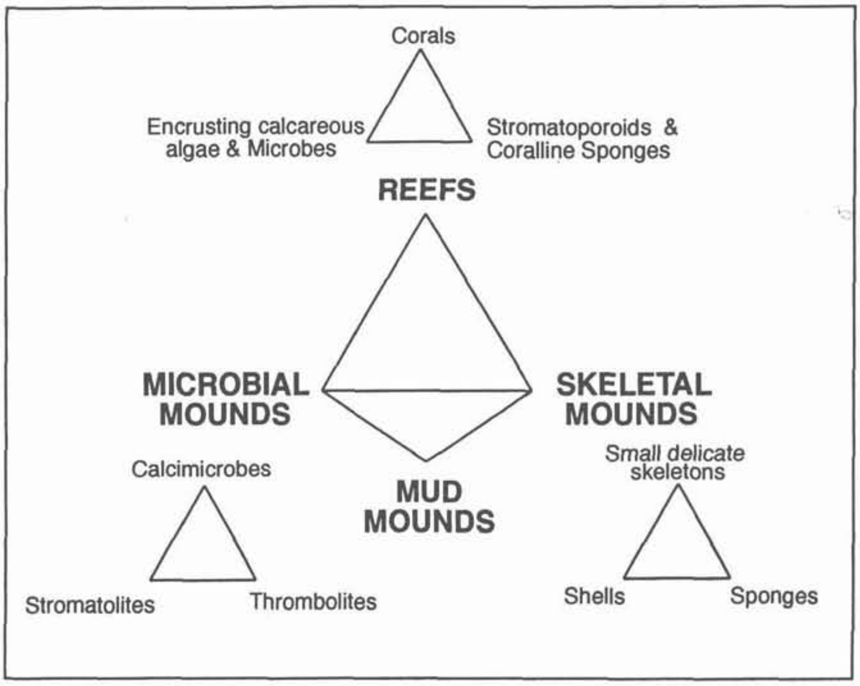

Figure 3 A conceptual classification of reefs and mounds.

crusting organisms growing over dead surfaces aid in stabilization. Branching reef-builders can also be preserved in place, but are just as commonly fragmented by storms into sticks and rods which form skeletal conglomerates.

Mounds are a variable mixture of skeletons and muddy sediment. Skeletons, if present, usually remain in place after death but not necessarily in growth orientation. Core sediment can be bioturbated.

Most sediment is produced by the postmortem disintegration of segmented (e.g., calcareous green algae) or nonsegmented (e.g., bivalves, brachiopods, foraminifers) organisms. These taxa grow on the reef/mound surface or in the many nooks and crannies between skeletons. Additional sediment is generated by bioeroders: boring organisms (worms,sponges bivalves) produce lime mud; rasping organisms, generally herbivores (echinoids, fish), graze the surface creating copious quantities of carbonate sand and silt. The sediment accumulates around the buildups as an apron, lodges between skeletons as a matrix and filters into growth cavities as geopetal internal sediment.

Rigidity of many reefs is accomplished by organisms encrusting or growing on top of one another. Mound cohesion is achieved through the binding action of grasses and algae. Many reefs and mounds are also preferential sites for synsedimentary cement precipitation (Schroeder and Purser, 1986), and are hard limestone just below the growing surface.

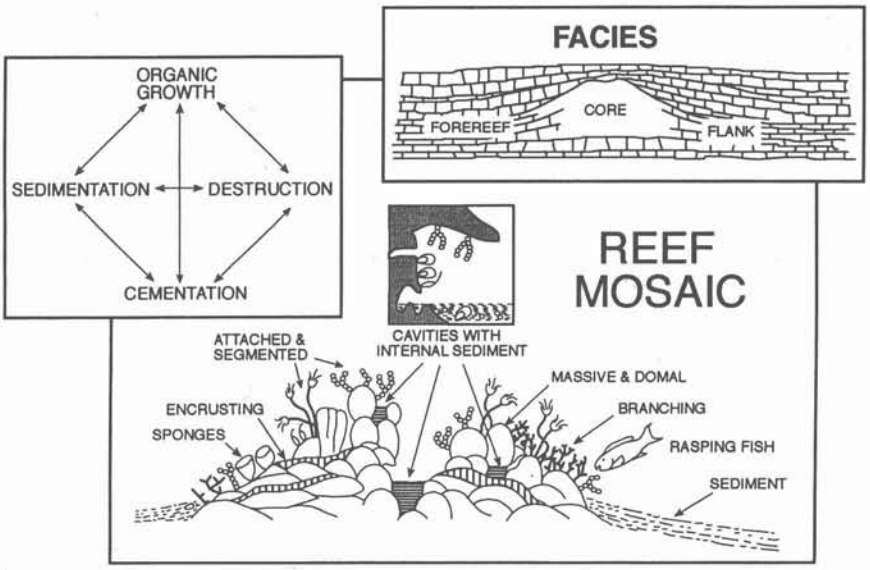

Figure 4 A diagrammatic cross section of the different facies which comprise a reef or mound (upper right) and the organism-sediment mosaic which typifies a growing reef, whose composition is the sum of the four different processes illustrated in the inset.

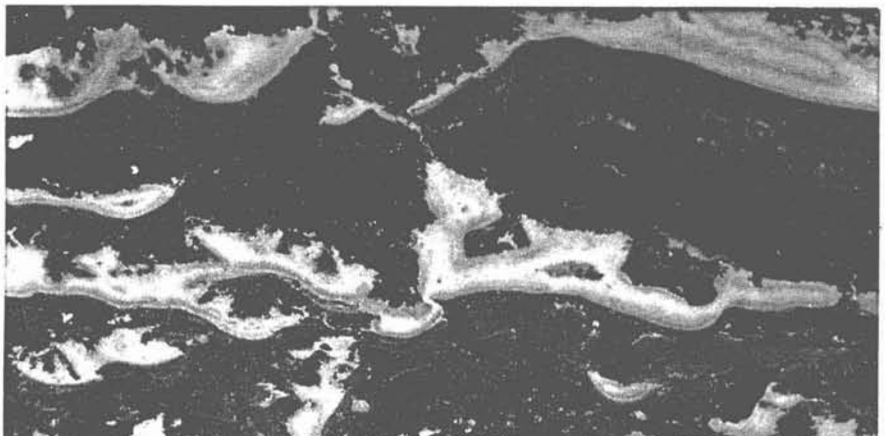

Figure 5 Stromatactis, composed of cavities with digitate roofs and flat sediment floors which are centripetally filled by white, isopachous crusts of cement. Dark limestone is lime mudstone to wackestone. Basal unit (Facies A) of Devonian "récifs rouges", Croisette Quarry, Vodelée, Belgian Ardennes. Scale bar is 5 cm.

Ancient reefs and mounds

Results of these processes can be seen in many Phanerozoic reefs and mounds, and especially in Mesozoic and Cenozoic structures, which are decidedly "modern" in composition. Paleozoic buildups do not appear to have been affected very much by boring organisms but were typically sites of intense synsedimentary cement precipitation; some reefs contain so much cement that they have been called "cementation reefs". Precambrian buildups (Fig. 1), with their limited biological components, were mainly constructive and contained few cavities but seem to have been particularly susceptible to erosion by waves and currents.

Our ability to distinguish between biogenic mounds and mud mounds depends on our facility to recognize the organic components, to interpret the ecological role played by the organisms or to determine the origin of the fine-grained carbonate.

Primary cavities in many carbonate mounds are enigmatic. They seem to have formed mainly during early diagenesis below the seafloor by collapse of material, either through 1) dewatering of lime mud, or compaction, 2) slumping and downslope creep of cohesive but unlithified sediment, or 3) decay of partially lithified organic tissue (especially sponges). Because collapse occurred in relatively homogeneous mud, the collapsed material left a digitate roof and accumulated as geopetal sediment on the cavity floor. Frondose or platy skeletons may have acted as umbrellas, protecting underlying sediments during collapse. Cavities are isolated or organized into a network in which the flatness of the floors was enhanced by water circulation.

Some cavities were subsequently centripetally cemented and such cement can form up to 40 per cent by volume of a given mound. These spar bodies (Fig. 5) were originally mistaken for fossils and given the name *Stromatactis* and have since been the subject of much controversy (Bathurst, 1982). Almost all workers have commented on the similarity of these carbonate mounds, regardless of their age. Some have concluded a common origin and by implication a common origin for the mound facies containing stromatactis or stromatactis-like structures (Bathurst, 1982; Pratt, 1982), whereas others have made a case for multiple origins (Bourque and Gignac, 1983; Lees, 1988). Such spar bodies are mainly, but not exclusively, a Paleozoic phenomenon, suggesting some sort of organic control.

The growth window

Although modern coral reefs and mounds are only part of the Phanerozoic spectrum, because they are alive today we can examine the factors which control their growth (Choat *et al.*, 1988 and other Coral Reef Symposia volumes are an excellent source for this evolving data base).

Modern coral reefs and mounds

The modern growth window (Fig. 6) is determined by the combination of factors which control growth of the major organism, in this case corals. Hermatypic (reef-building) corals grow in waters between 18° and 36°C, but are best adapted to form reefs in waters between 25° and 29°C. Periodic exposure is not necessarily lethal (Fig. 7) and some intertidal corals are out of water for many hours daily. The salinity window ranges from 22‰ to 40‰, but most corals grow best in waters between 25‰ and 35‰.

Hermatypic, reef-building corals are cnidarians which contain light-dependent, photosynthetic symbiotic microorganisms (zooxanthellae). Such symbionts enable hermatypic corals to produce calcium carbonate several times faster than ahermatypic (non reef-building), azooxanthallate corals. Light decreases exponentially with depth and the lower limits of hermatypic coral and calcareous green algal growth are 80-100 m. Vertical growth rates below 15 m decrease in a non-linear, possibly exponential fashion. While most corals are heterotrophs and micropredators, some, including the major reef corals *Acropora, Pocillopora* and *Porites,* are autotrophs and can meet their energy requirements entirely by photosynthesis. Coral growth form is in part an adaptation to varying light conditions. Other important animal-plant symbionts are alcyonarians (soft corals), tridacnid bivalves (giant clams), cyanobacteria-associated sponges and ascidians.

Coral reefs flourish in nutrient-impoverished oceanic regions largely because they retain and recycle nutrients very efficiently, using inorganic nutrients from the water and waste products (ammonia, organic phos-

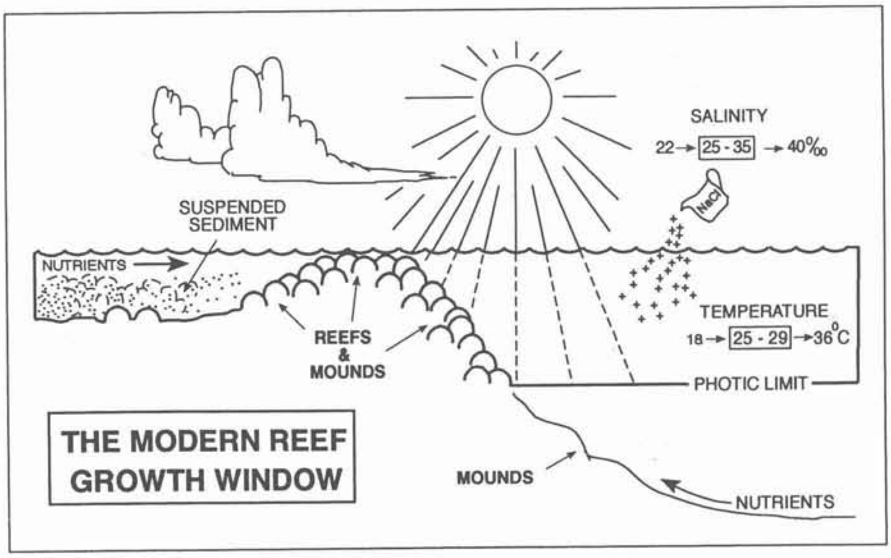

Figure 6 A sketch depicting the environmental window in which modern coral-algal reefs grow best. Numbers for temperature and salinity define the growth limits of corals, boxes enclose optimum values.

Figure 7 Shallow reef corals exposed during low tide on the northern Great Barrier Reef, Australia. The large colonies average 1 m in width.

phates) from the animal host. Even though the waters are low in nutrients, adequate amounts are supplied in energetic environments by high water flux across the reef. Increased nutrient levels, from upwelling on the outer platform and runoff on the inner platform, lead to dramatic changes in reef structure (Hallock and Schlager, 1986). At intermediate levels the animal-plant symbionts are replaced by more heterotrophic forms and "fouling organisms" such as filamentous algae, fleshy algae and small suspension-feeding animals (barnacles and bivalves). Reefs still grow in such regions only because herbivores graze back the algae. Thus the paradox, that increased nutrient supply, by enabling other organisms to thrive, leads to modified or arrested reef growth.

While coarse sediment in high-energy settings may cause abrasion, it is fine-grained suspended sediment that is most inimical to coral growth because it decreases light penetration and covers or clogs the polyps. It is difficult to decouple the effect of fine terrigenous sediment and nutrients on coral reef growth because they usually occur together. Fine sediment alone does not arrest coral reef growth but limits it to sediment-tolerant corals (Cortez and Risk, 1985; Johnson and Risk, 1987; Acker and Stearn, 1990), which either grow rapidly to rise above the substrate or are able to remove sediment from their polyps. Modern reefs in such environments are distinguished by comparatively low diversity, exceptionally large corals and relatively little coral cover.

Ancient reefs and mounds

Although we cannot be certain about the physiological tolerances of all fossil reef-builders, some generalities are possible. Scleractinian corals, the modern reef-building corals, evolved in the Triassic and were probably zooxanthallate and reef-building by Late Triassic, certainly by Middle Jurassic, time. Tabulate corals are a diverse group of several organisms and it is not clear whether they contained similar symbionts (Coates and Jackson, 1987; Cowan, 1988). Rudist bivalves, mound builders of Cretaceous seas, are related to modern, zooxanthallate tridacnid bivalves and their ability to form large skeletons is thought by many to be the result of symbiosis (Kaufmann and Johnson, 1988). Fossil sponges, both spiculate and soft bodied, and coralline sponges (hard skeletoned such as stromatoporoids, archaeocyathans) are poorly understood (Wood, 1990), but modern sponges on outer shelf reefs commonly contain cyanobacterial symbionts. Regardless, for those organisms that did contain phototrophic symbionts, light and nutrients would have been important limiting factors.

Many reefs and mounds built by archaeocyathans, spiculate sponges, stromatoporoids, tabulate corals, calcareous algae, and rudists are surrounded and buried by fine terrigenous clastic sediment, implying that these organisms had some method of removing fine detritus. Mounds are limited to regions of lower wave energy and, if constructed by phototrophic organisms, probably grew within a similar window. If they were nonphototrophic, the mounds could have grown in any environment and any water depth. The critical interfaces governing deep water mound facies are 1) the oxygen-minimum surface that marks the lower limit of bioconstruction, 2) storm wave base, below which delicate organisms will baffle and stabilize mud, 3) the photic/subphotic interface above which photosynthetic organisms will proliferate, and 4) the base of active reef growth above which large skeletal reef-building organisms, when present, will replace the mound communities. In general, the most significant is the photic/subphotic interface.

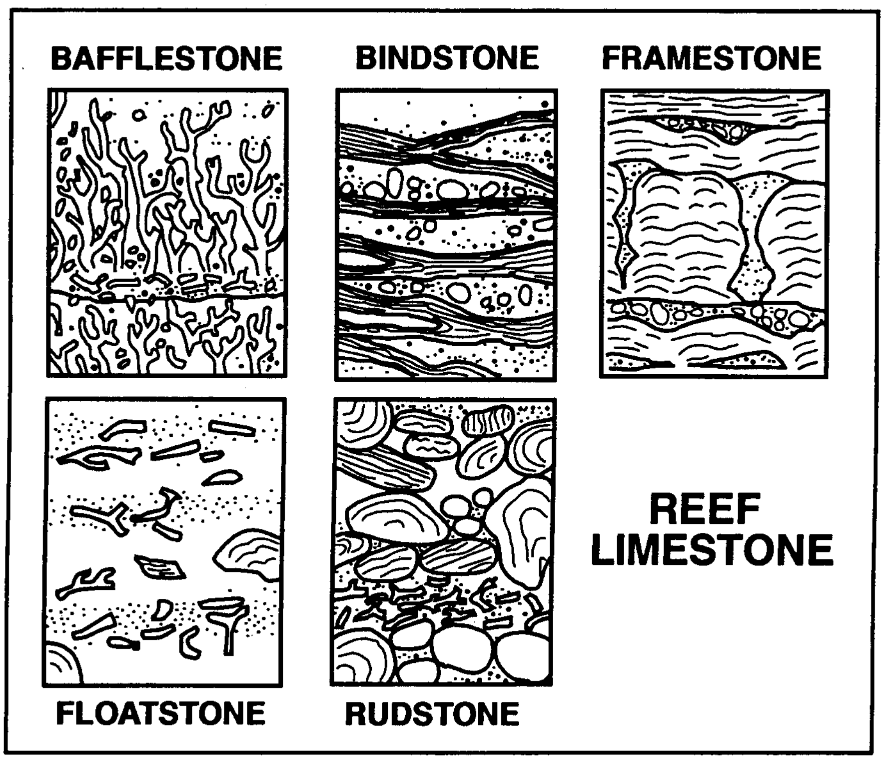

Figure 8 An interpretive sketch of the different types of reef and mound limestone recognized by Embry and Klovan (1971). Autochthonous limestones (top) are found in the core facies while allochthonous limestones (bottom) typify the flank or fore reef facies.

REEF AND MOUND LIMESTONE

Ancient reefs and mounds are usefully interpreted on the basis of several criteria, 1) the relative abundance and the relationship between organic components and sediment, i.e., the type of limestone, 2) the diversity of the larger fossils, and 3) the growth form of these organisms.

Rock classification

Many classifications have been proposed for reef carbonates, but the most descriptive and widely used is a modification of Dunham's (1962) textural classification of lime sand- and mud-rocks proposed by Embry and

Klovan (1971; Fig. 8) which is partly descriptive and partly interpretive. As the library of fossil reefs and mounds has increased in the last 20 years the separation between allochthonous flanking sediment and autochthonous core limestone has become blurred. This is especially true for mud-rich lithologies in mounds, which are well classified as floatstones, or even wackestones (see discussion of skeletal mounds) with no connotation of physical deposition. Alternatively, coarse skeletal particles such as phylloid algal plates accumulate with the texture of rudstone, which is inappropriate for essentially in place accumulations; Davies and Nassichuk (1990) suggest the term *platestone* for such lithologies. Other modifications have been suggested by Cuffey (1985). There is no real term for reef limestone composed of calcified microbes, and we suggest using the general term *boundstone* (Dunham, 1962).

Fossil diversity
Relative abundance of different fossils is potentially one of the most useful observations when interpreting reefs and mounds. It must always be kept in mind, however, that only the calcareous part of the community, and moreover only part of that, is preserved. Organism diversity is, together with competitive interaction, a product of all those factors which affect growth (see reef window). Recent observations indicate that interruption by extrinsic factors such as hurricanes, outbreaks of predators (e.g., crown-of-thorns starfish, gastropods), die off of important grazers (e.g., echinoids) or major water temperature and salinity perturbations (e.g., El Nino) rearrange coral community structure. Undisturbed buildups have relatively low diversity because competitive dominants have eliminated inferior species. Structures subject to frequent or intense disturbance have higher species richness because competitive domination is repeatedly interrupted, giving inferior species a chance to persist. Reefs and mounds prone to the highest rates of disturbance are less diverse because only small numbers of resistant or rapidly colonizing species persist. Thus, patchiness and evidence of extensive fragmentation and debris formation should be expected in the most diverse fossil buildups. Low diversity is also a characteristic of new communities (those that have moved into a new environment) and those subject to severe and continuing physical/chemical stress.

Growth form and environment
The relationship between organism shape and environment is one of the oldest and most controversial topics in biology and paleontology. Limitations of applying these concepts directly to fossil reefs and mounds have been emphasized by Stearn (1982) who stresses that no general patterns are applicable to all reefs, and that variations in shape are the result of interactions between environmental factors and the genetically dictated growth pattern of the organism. Nevertheless, the relationship between organism and

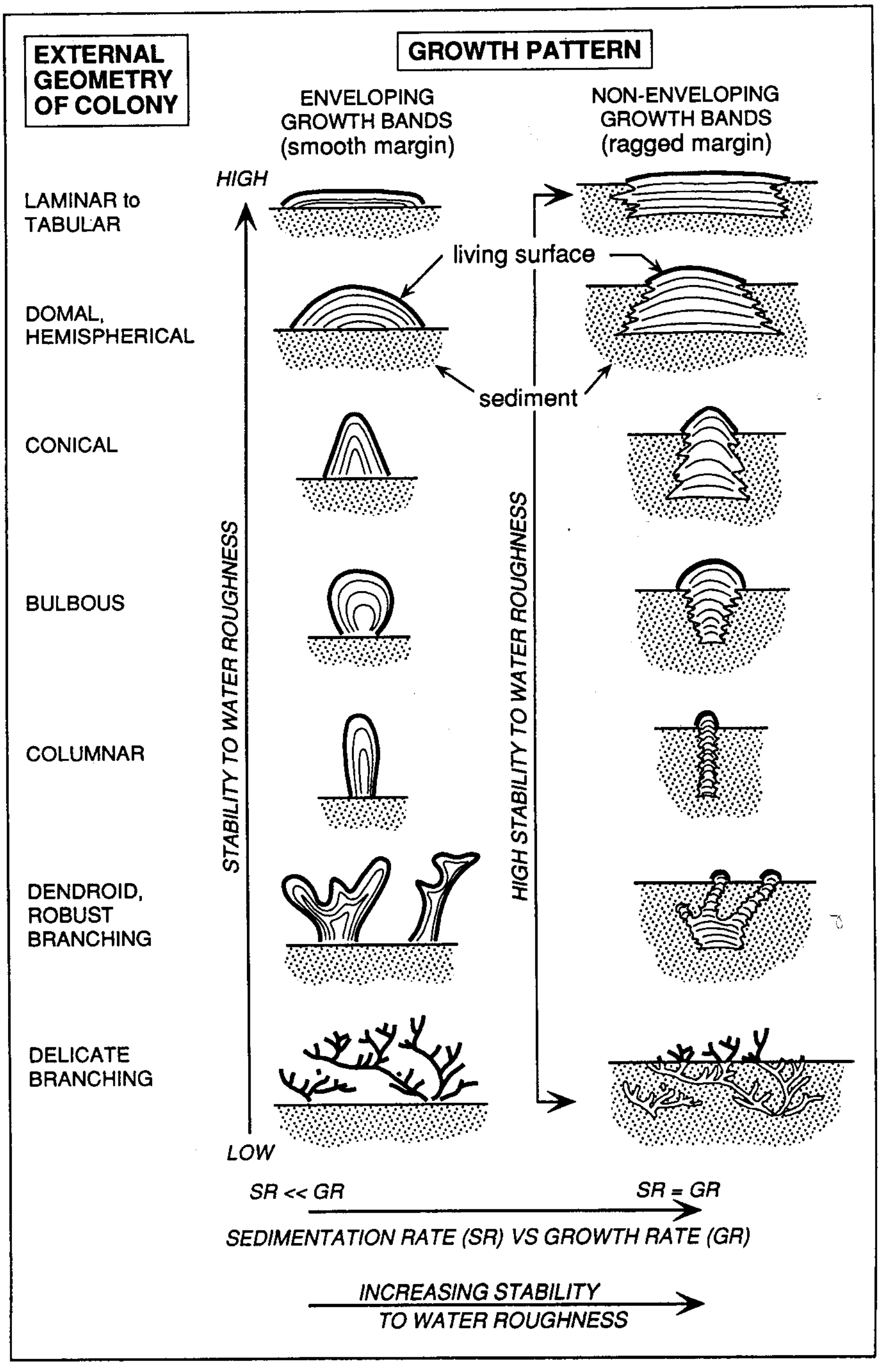

Figure 9 Control of water roughness and sedimentation rate on resulting external and internal geometry of fossil metazoan colonies.

surrounding sediment in the rock record, does allow us to make some useful generalizations.

Rate of sedimentation and water roughness in particular exert an important influence on the growth pattern of an individual colony. Relationship between external shape and internal growth banding geometry of a fossil colony can be used to infer the relative rates of sedimentation and water roughness (Fig. 9). The two growth forms, *enveloping* (Fig. 10) and *nonenveloping* (Fig. 11) result from the position of the living surface at the time of growth. That position is expressed in corals by successive growth bands, whereas among the stromatoporoids, it is latilaminae. Enveloping forms indicate decreasing stability to water roughness with an increasing height to width ratio. Those skeletons whose base is cemented to a hard substrate (scleractinian corals) are more stable in rough water than those which sit on or in the sediment (stromatoporoids). Progressive burial of the skeleton (Fig. 9, right column) increases its stability. Although margin raggedness of a skeleton may come about in various ways (e.g., encrustation by other organisms), partial burial that forces the living surface to move up is a common cause. The ragged nature of a skeletal margin is therefore a measure of the capacity of an organism to keep pace with sedimentation and hence, an indication of the rate of sedimentation. The implication is that skeletons with smooth margins that did not cement to one another and grew above the sediment surface were sensitive to variations in water roughness and thus confined to low-energy environments; those with ragged margins were partially buried and so could grow in any environment and stand rough water conditions. This is reflected by the zonation of stromatoporoid reefs (Fig. 12).

FACIES

The attribute which separates reefs from mounds is the organisms which constructed them. Reefs were built by clonal skeletons or organo-sedimentary elements (e.g., stromatolites) which could grow in many directions, attain large sizes and most important, encrust other elements and/or sediments. Mounds were generally constructed by relatively delicate and/or solitary organisms with restricted body shapes. Reefs had the *potential* to grow and thrive in high-energy, shallow environments, whereas mounds did not (the "wave resistant" attribute of Lowenstam, 1950). Thus, reefs could construct reliefs at platform margins which affected circulation and sedimentation across the top of the whole platform, whatever its size. Mounds were passive players in platform development although their large size may have generated separate sedimentary environments. They were, however, common foundations for platform margin reefs.

Since reefs grew in shallow, high-energy settings, they show distinct lateral as well as vertical facies zonations, a response to variations in water depth and energy. Many mounds grew in quiet water and commonly have only a vertically zoned core facies surrounded by a flanking sediment facies.

REEFS

Attributes

These structures were built by organo-sedimentary stromatolites and thrombolites and/or skeletal metazoans, particularly tabulate corals, scleractinian corals and stromatoporoids. Binding was accomplished mainly by calcareous red algae in the Phanerozoic and stromatolites in the Precambrian. Their facies distribution is generally the same as that of modern coral reefs with the caveat that it is not clear whether all stromatoporoid and tabulate coral reefs built structures up into the surf zone. Modern reef facies characteristics are directly applicable to Mesozoic and

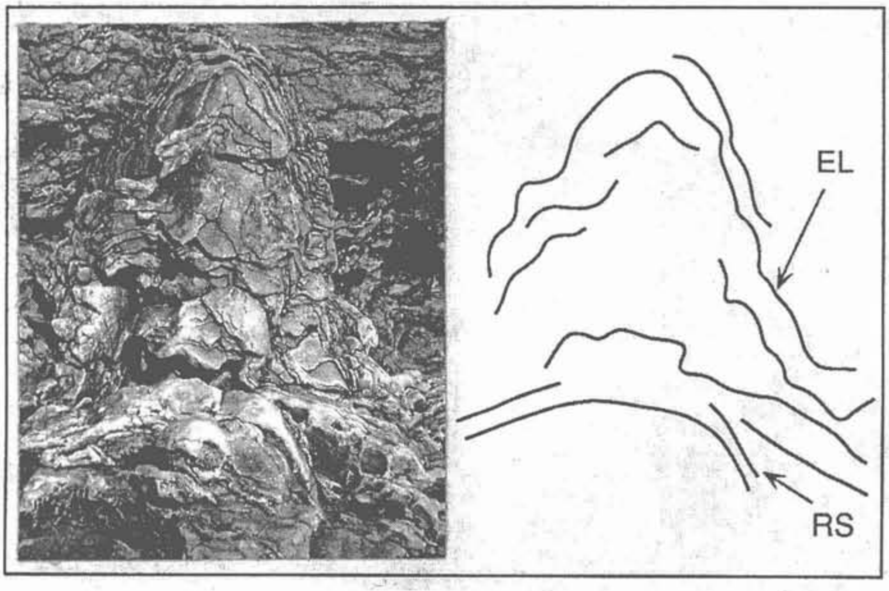

Figure 10 Outcrop photograph and sketch of a stromatoporoid skeleton with enveloping latilaminae (EL) indicating a low rate of sedimentation. Stability to water roughness would be low, unless the skeleton rooted into the sediment (RS) during early stages of growth. Skeleton is 80 cm in height. Upper Silurian Gotland, Sweden.

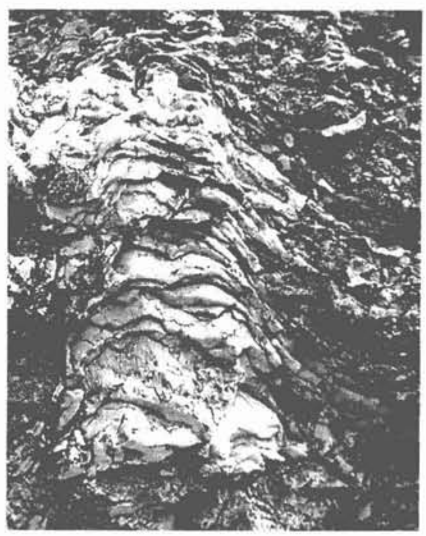

Figure 11 Stromatoporoid skeleton (nonenveloping) with ragged margin (right) indicating a relatively high rate of sedimentation and high stability to water roughness. Skeleton is 60 cm in height. Upper Silurian, Gotland, Sweden.

Cenozoic coral-algal reefs, and, with the above caveat, useful for the interpretation of Paleozoic and Proterozoic structures as well.

Scleractinian coral reefs

Depth zonation

Modern reefs exhibit depth zonation (Fig. 12) because of decreasing wave energy, light intensity and to a lesser extent temperature, with increasing bathymetry (e.g., Graus and Macintyre, 1989). The *Reef Front Facies* lies between about 10 m (the base of surface wave action) and 100 m. This is an environment of diverse reef-builders varying in shape from hemispherical to branching to columnar to dendroid to sheet-like. Accessory organisms and various niche dwellers such as bivalves, gastropods, coralline algae, segmented calcareous algae and sponges are common. Below about 30 m wave intensity is low, light is attenuated and most reef corals are prone and plate-shaped (Fig. 13), forming framestones to floatstones. Pockets, streams and chutes of skeletal, especially calcareous algal, sand occur between areas of dense coral growth. The *Fore Reef Facies* is generally gravel and sand composed of whole or fragmented skeletal debris, blocks of reef limestone and skeletons of reef builders. Such deposits grade basinward into muds exhibiting many of the attributes described in the chapter on carbonate slopes (Chapter 18). This zonation is particularly sensitive to perturbations of the growth window, particularly a decrease in light, which leads to a shallowing of all zones.

Energy zonation

Growing as they do in the trade-wind belts, modern shallow water reefs exhibit a strong windward-leeward zonation (Fig. 12). This is true whether they form the margins of large platforms or are isolated structures inboard.

Zonation is best developed in windward locations (Fig. 14). The *Reef Crest Facies*, which extends to a depth of 15 m at most, receives most of the wind and wave energy. Composition depends upon the degree of wind strength and swell height and periodicity of cyclonic storms. Only organisms that can encrust, generally sheet-like forms, are able to survive where wind and swell are constant and intense. If wave and swell intensity are more episodic or only moderate to strong, encrusting forms still dominate but can be bladed or have short, stubby branches. Where wave energy is moderate, robust branching corals proliferate. The large numbers of branching corals on modern reefs are due to their rapid evolution in the late Cenozoic. Hemispherical to massive forms characterize this zone in older scleractinian reefs. The *Reef Flat Facies* varies from a pavement of cemented, large skeletal clasts with scattered rubble and coralline algal nodules in areas of intense waves and swell, to shoals of well-washed lime sand in areas of moderate wave energy. Most material comes from the reef crest and is swept onto the pavement during cyclonic storms. Vagaries of wave refraction may pile the sands into cays and islands which in turn protect small, quiet water environments adjacent to the reef crest. The protected *Back Reef Facies* is where much of the mud formed on the reef comes out of suspension. This, coupled with the prolific growth of sand- and mud-producing bottom

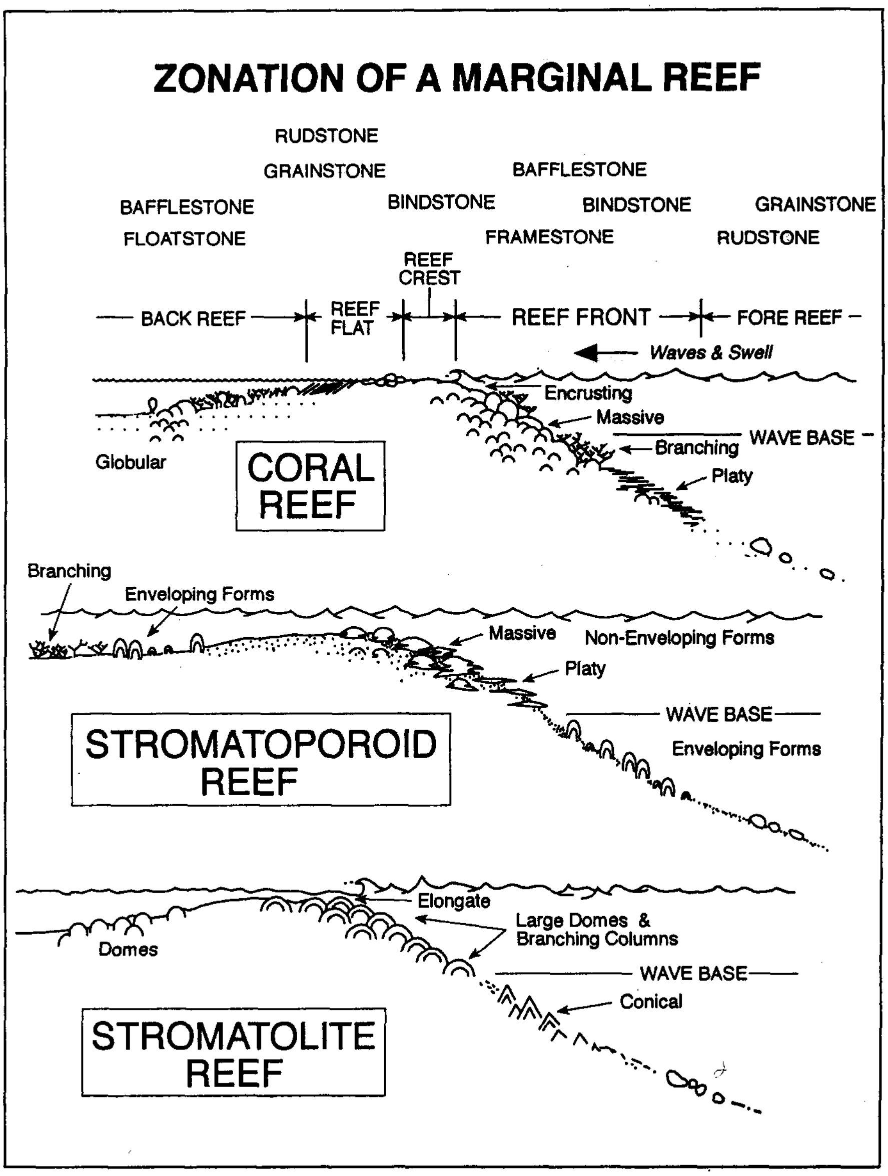

Figure 12 Cross sections through hypothetical, zoned marginal coral (mainly Cenozoic), stromatoporoid (mainly Siluro-Devonian) and stromatolite (mainly early Proterozoic) reefs. Rock types and growth forms are illustrated for each facies.

fauna, such as calcareous green algae, results in mud-rich lithologies. Corals here are stubby and dendroid, and/or large, globular forms which extend above the substrate to withstand episodic agitation and quiet muddy periods.

Reefs on the leeward side of banks can be strikingly different, either because of reduced wave activity or because of "bad water". The bad water is formed on the platform by fine-grained sediment production, oxygen depletion, heating or evaporation. It is usually driven off the bank downwind, across the leeward margin, inhibiting reef growth to a depth of several tens of metres. Such shallow leeward margins can, therefore, be bare rock floors covered by soft fleshy algae or hard coralline algae with active reef growth taking place only in deeper water, below this interface.

Nutrient/sediment zonation

There is commonly a cross-shelf zonation in reef composition that partly reflects the outboard decrease in fine sediment and nutrients. *Inner shelf reefs* are characterized by 1) quickly growing corals with a high tolerance for fine sediment but unable to withstand turbulent waters, 2) large and abundant heterotrophic sponges, 3) low epifaunal diversity, 4) few soft corals, and 5) abundant soft algae and few calcareous algae. *Outer shelf reefs* (in areas of little upwelling) are distinguished by 1) slow-growing autotrophic corals which cannot withstand suspended sediment but are adapted to high-energy seas, 2) reduced numbers of sponges, most of which contain photosynthetic symbionts, 3) common tridacnid bivalves in the Pacific, 4) high epifaunal diversity, and 5) prolific calcareous algae.

Stromatoporoid reefs

Stromatoporoids are thought to be related to a class of fossil sponges which resembles modern sclerosponges (dense, hard calcareous porifera). Since modern sclerosponges are not shallow reef builders we must rely on ancient reef case histories (e.g., Geldsetzer *et al.*, 1988) to construct a general energy zonation (Kobluk, 1975; Bourque *et al.*, 1986; Fig. 12). Although there were encrusting stromatoporoids, most, unlike corals, sat on or were anchored in the sediment. High-energy zones like the reef crest, were inhabited by large, nonenveloping, ragged-margin forms (often referred to as massive forms) which were solidly rooted in the sediment. Plate-like stromatoporoids, bound together by algae, microbes and/or cement, are also known to have occurred in rough water environments. The totally enveloping smooth forms occupied quiet water zones, either below wave base or in sheltered areas of the back reef (domal, bulbous, dendroid forms) and the lagoon (delicate stick-like amphiporoids). These skeletons were commonly reworked during cyclonic storms and redeposited as rubble units associated with peritidal facies.

Since stromatoporoids did not typically have an encrusting habit, it is doubtful that they were successful builders in the surf zone. Sand- and gravel-rich facies containing reworked ragged skeletons of stromatoporoids, up to several tens of centimetres high (an indication of scouring and digging during storms; Kershaw, 1979) are probably an expression of the inability of stromatoporoids to withstand surf conditions.

Stromatolite reefs

There are comparatively few studies of stromatolite reefs (see Geldsetzer *et al.*, 1988 for some excellent recent reports). Stromatolites were constructed

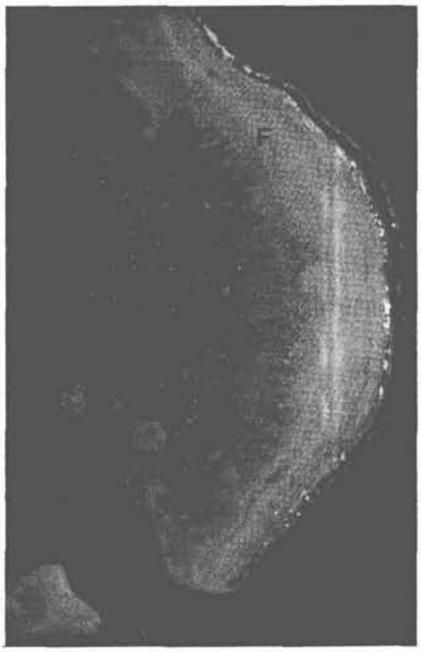

Figure 14 Aerial view of a zoned "ribbon reef" which is part of the discontinuous rim along the eastern margin of the northern Great Barrier Reef, Australia. Wind and wave approach are from the Coral Sea (east = right). The reef crest is a narrow wave-swept band at the extreme right. The reef flat (F) is a cemented rubble and coral pavement about 1 km wide and exposed at low tide. The back reef (B) deepens gradually into the lagoon (west = left) and is an area of abundant coral growth and isolated patch reefs.

Figure 13 Large overlapping platy corals (*Montastrea* sp. and *Agaricia* sp.) at 45 m water depth on the reef front, Discovery Bay, Jamaica. Plates are 0.2 to 1.0 m in width.

by microbes which trapped and bound sediment and, perhaps more important, induced precipitation of calcium carbonate. Shallow water Proterozoic buildups were formed by stromatolitic domes, linked domes, columnar stromatolites and their elongate equivalents in high-energy settings (Fig. 12). Surrounding sediments are generally intraclastic. Isolated deep subtidal and slope reefs (?below fairweather wave base) were built primarily by conical (conoform) stromatolites. Late Archean and early Proterozoic (2.7-1.5 Ga) buildups can contain spectacular synsedimentary cements. The microbial communities were probably less susceptible to environmental factors (salinity changes, nutrient supply) and pressures of community succession than later metazoan reefs (Grotzinger, 1989).

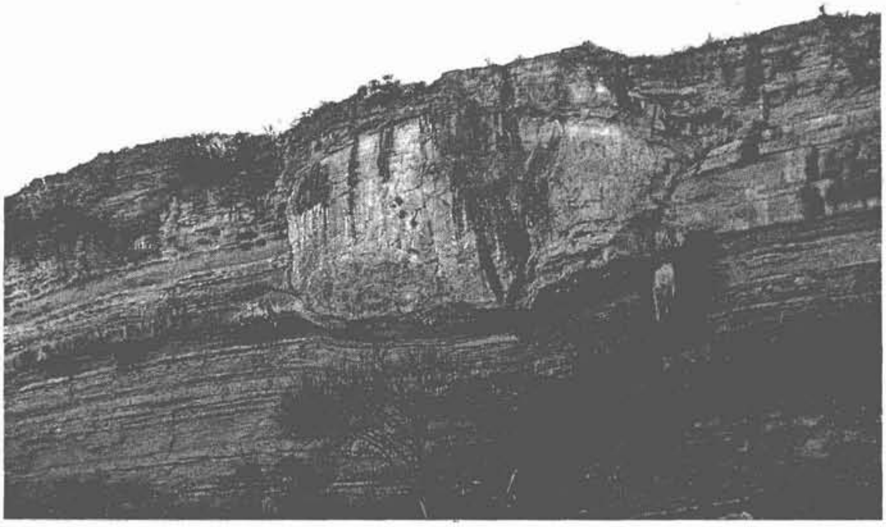

Figure 15 An Upper Cambrian microbial mound (centre), about 12 m in thickness, exposed in cliffs of siltstone, shale and limestone along the Llano River, central Texas, U.S.A.

MOUNDS

Carbonate mounds (Fig. 15) are known mostly from the rock record. Single component mounds existed in the past, but recent studies have shown that many are not homogeneous but composite, containing a mosaic of facies. Two good mid-Paleozoic examples are the famous Waulsortian mounds and récifs rouges (Figs. 16, 17, 18) in which each end member, skeletal and microbial facies is represented. The true Waulsortian mounds (Lees, 1988) were early Carboniferous deep water buildups composed of stacked facies representing a depth zonation (Lees and Miller, 1985). The late Devonian (Frasnian) "récifs rouges" are also deep water carbonate mounds and show a depth-dependent vertical succession of facies (Boulvain, 1990). With the exception of some calcimicrobial mounds, which appear to have been able, like modern calcareous algae, to grow in high-energy environments, most mounds seem to occur in preferred locations, 1) arranged just downslope on gently dipping platform margins, 2) in deep basins, and 3) spread widely in tranquil reef lagoons or wide shelf areas.

The shape of carbonate mounds varies from flat lenses to conical piles with slopes of up to 40°, suggesting that they had significant relief above the seafloor. Critical to recognition of original depositional relief are the relationships between mound facies and

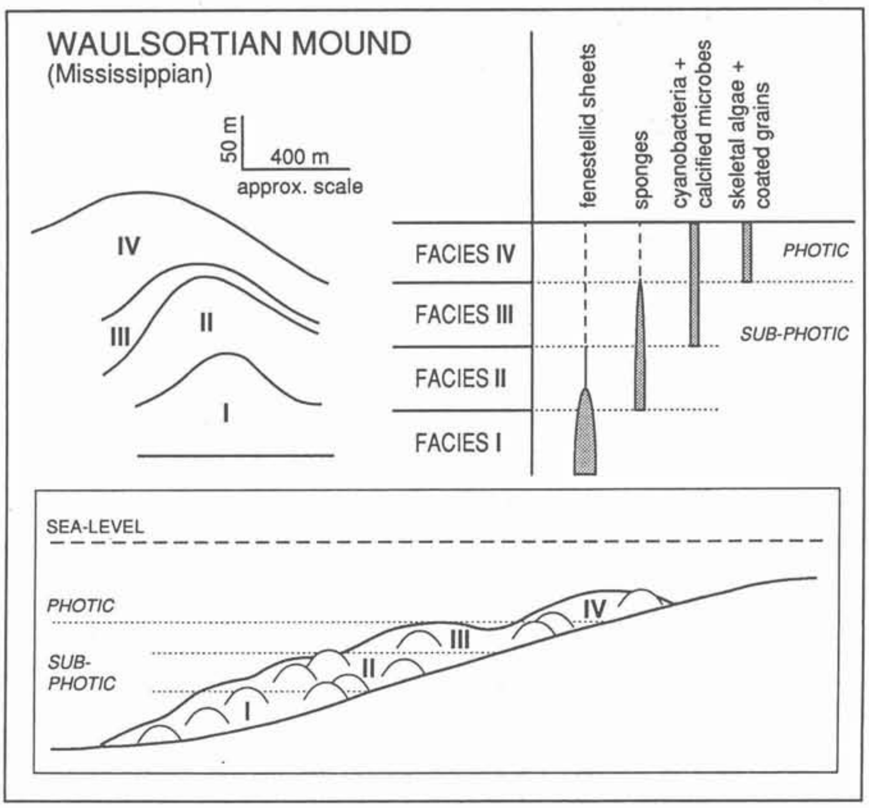

Figure 16 Facies distribution and depth zonation of Waulsortian biogenic mounds. (Top) complete facies succession in a Belgian Waulsortian mound (type area); growth surfaces approximately parallel facies limits. (Top, right) Ecological assemblages and depth zonation. Facies I=fenestrate bryozoan mound; Facies II=sponge mound; Facies III=sponge/cyanophyte (thrombolites+calcimicrobes); Facies IV=skeletal algae/mud and spar mound. (inset) Distribution of facies on a carbonate ramp. After Lees and Miller (1985).

surrounding regional beds. Some may be "stratigraphic reefs", sensu Dunham (1970), with little original relief while growing.

Skeletal mounds are generally bafflestones, bindstones, floatstones and wackestones with lime mud, although muddy sand occurs. The massive to well-bedded carbonates that flank on-shelf mounds are extensive accumulations of skeletal debris and chunks of wholly to completely lithified lime mudstone. These flank beds can be volumetrically greater than the core itself and almost bury it.

Microbial mounds
Attributes

These rocks are formed by the action of microbes, namely cyanobacteria, true algae, diatoms and other autotrophs which can either calcify directly, induce calcification or trap and bind sediment (Riding, 1991). The rocks have been collectively called "microbialites" (Burne and Moore, 1987). While most such microbes are/were phototrophic and so restricted to shallow water, some are/were chemautotrophs and so not depth limited. The most familiar elements are stromatolites and/or thrombolites (Fig. 19) of various types (Kennard and James, 1986). Less familiar are the small calcified microfossils collectively called "calcimicrobes" (Fig. 20) of uncertain affinity (James and Gravestock, 1989) which include such forms as *Renalcis, Epiphyton, Girvanella* and *Tubiphytes.* Most contentious, however, is the origin of carbonate mudstone (or microspar) in these structures which varies from clotted ("structure grumeleuse") to mottled to homogeneous. Because bacteria can induce carbonate precipitation, which is commonly clotted, much of this mudstone may be microbial. Alternatively much of the mud may be a direct inorganic precipitate or breakdown of calcimicrobial micrite. The organo-sedimentary product of microbes, being sensitive to diagenesis, is frequently difficult to recognize.

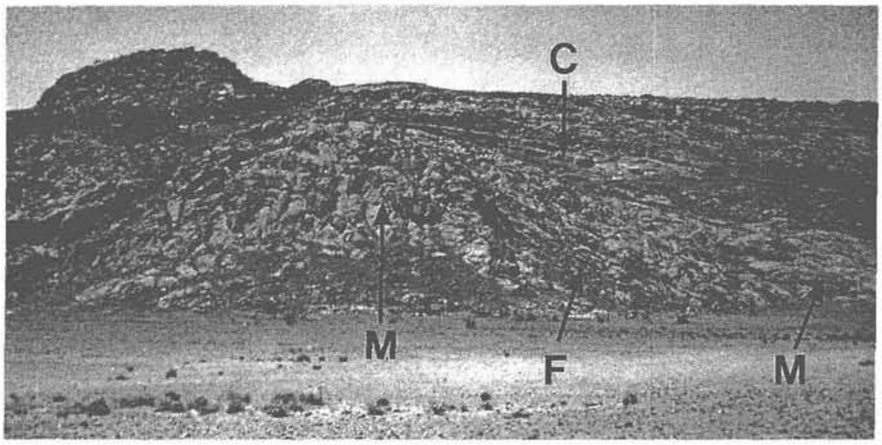

Figure 17 Field photograph of Waulsortian mounds (M) with flanking (F) and capping (C) beds. The central mound is approximately 40 m in height. Lower Carboniferous of the Béchar Basin, Djebel Kébir, Algerian Sahara.

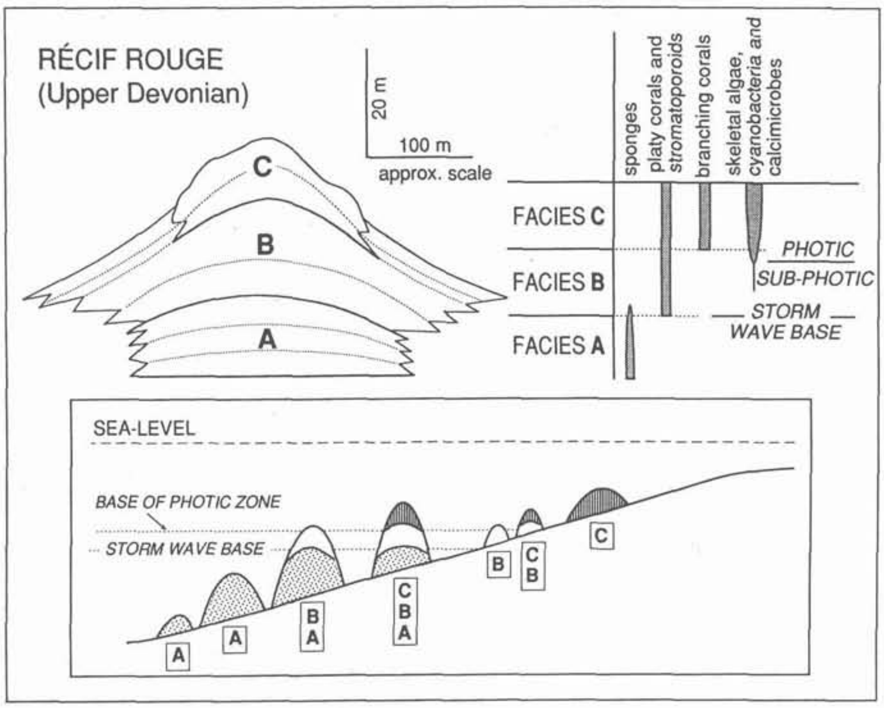

Figure 18 Facies mosaic and vertical succession of an Upper Devonian "récifs rouges" of Belgium. (Top, left) complete facies succession; dotted lines are growth surfaces. (Top, right) ecological assemblages and depth zonation. (Inset) Conceptual model of distribution of various types of monogenic and composite mounds on a slope with stacking order of facies for each mound. Facies A = red, stromatactis, sponge-rich mound; Facies B = pink coral/stromatoporoid/mud mound; Facies C = grey coral/thrombolite/calcimicrobe mound.

Modern analogues

Uncertainty about the origin of microbial mounds comes from the fact that, because modern marine environments are dominated by metazoans and grasses, microbial buildups, like stromatoporoid reefs, are restricted to stressed environments such as high-energy tidal sand shoals (Dill *et al.*, 1986; Fig. 21), marginal marine ponds, saline and freshwater lakes and saline embayments (Burne and Moore, 1987; Kobluk and Crawford, 1990). Yet, there is the suggestion that they are present in coral reefs, especially as cement/microbe consortia (Pratt, 1982; Riding *et al.*, 1991).

Skeletal mounds
Attributes

The skeletal builders acted as mud bafflers, trappers, binders and stabilizers. Three broad groups are distinguished: 1) the small delicate skeletons such as bryozoa (particularly fenestrate forms), delicate branching or solitary corals and stromatoporoids, skeletal algae (dasyclads, codiaceans and corallines), phylloids and related forms, archaeocyathans and hard coralline sponges (Fig. 22), 2) the shelly organisms such as rudist bivalves and rhytophenid brachiopods, and 3) the spiculate sponges. Microbial encrustation and binding may be present in all structures.

Spiculate sponges are a peculiar group in this regard. They are sessile organisms composed of a spicular skeleton (amorphous silica or calcium carbonate) enclosed in an organic matter-rich body. Construction potential of such organisms is high, but their fossilization potential is weak because the sponge body can easily be destroyed by oxidation of organic matter and dissolution of the spicular skeleton. Mounds with fossil sponges are known and in some instances they have been preserved by bacterial activity (calcification during biodegradation or encrustation; Flügel and Steiger, 1981). But there are other mounds, commonly referred to as mud mounds (see below), where the fine-grained carbonate is extremely rich in sponge spicules, but where well-preserved sponge bodies are few. In this

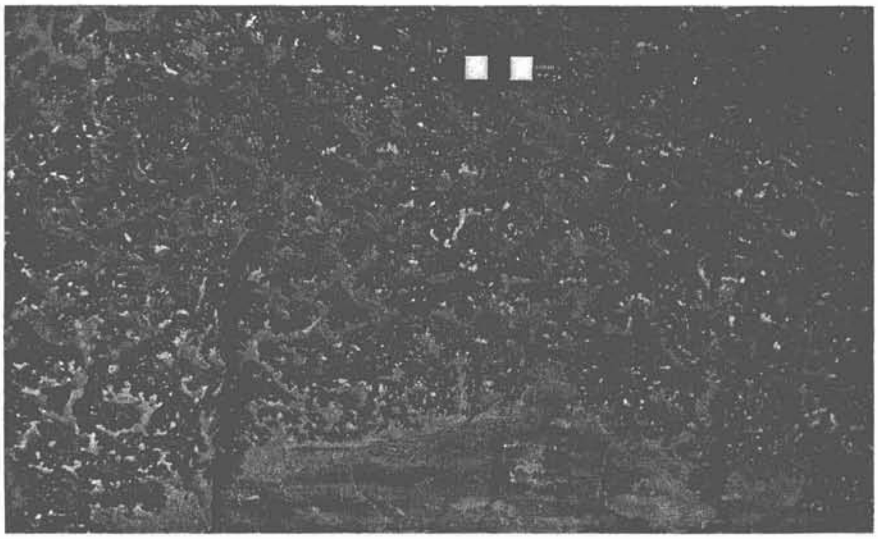

Figure 19 Core of a thrombolite illustrating the clotted microbial fabric in Upper Cambrian Limestone, Amadeus Basin, central Australia. Scale divisions in centimetres.

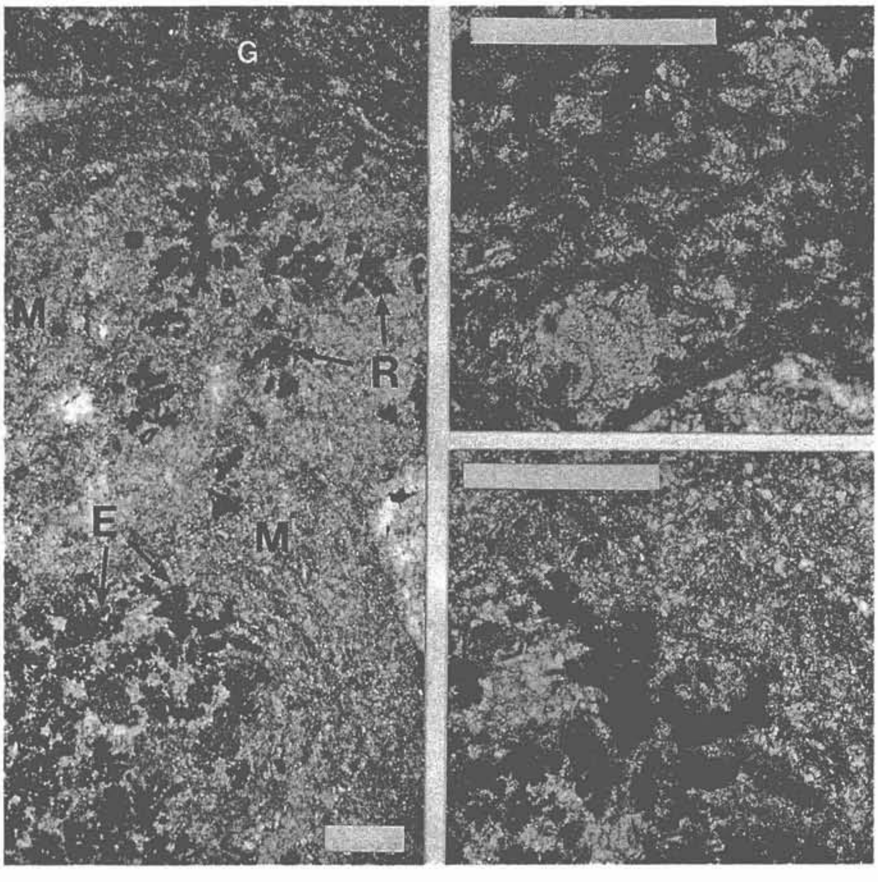

Figure 20 Calcimicrobe boundstone. (Left) *Girvanella* (G), *Epiphyton* (E), *Renalcis* (R), ?microbial spar and microspar (M) boundstone; scale bar is 1 mm. (Upper right) detail of *Girvanella*; scale bar is 0.5 mm. (Lower right) detail of *Epiphyton* 'encrusted' by ?microbial spar and microspar; scale bar is 1.0 mm. Large clast of Lower Cambrian limestone in St. Roch Formation conglomerate, L'Islet Warf, Québec, Canada.

Figure 21 Underwater photograph, at a depth of about 8 m, of stromatolites growing in subaqueous ooid sand dunes, Lee Stocking Island, Bahamas. Photograph R. Dill. Diver for scale.

last case, it is probable that sponges were responsible for mound growth, but our ability to recognize them is limited (Bourque and Gignac, 1983).

Modern analogues

Potential general modern analogues are found across the environmental spectrum. Shoals of algae and corals (Boscence *et al.*, 1985; McNeill, 1988; Fig. 23) and banks of mud bound by grass and burrowed by decapods (Wanless and Tagett, 1989) occur on the inner, protected parts of platforms or ramps which contain coral reefs. Tracts of calcareous algal *(Halimeda)* banks occur below a depth of 20 m in areas of upwelling and nutrient excess (papers in Roberts and Macintyre, 1988) where coral reefs have been excluded. Mounds constructed by non reef-building (ahermatypic) corals (Mullins *et al.*, 1981; Stanley and Cairns, 1988; Bernecker and Weidlich, 1990) and crusts (lithoherms) (Messing *et al.*, 1990) grow in waters hundreds of metres deep. Skeletal mounds rich in bivalves and vestimentiferan tubeworms (Fig. 24) also grow in deep water around seeps of petroleum, methane, hypersaline brines and vents of hydrothermal waters (Callender *et al.*, 1990). Tiny sponge-rich buildups grow in arctic waters (Van Wagoner *et al.*, 1990; Eliuk, 1991).

Mud mounds

Attributes

Mud mounds are reliefs of lime mud that supported a variable benthic flora and/or fauna. Two problems bedevil our understanding of mud mound genesis: the source of particulate mud and its stabilization mechanisms. Lime mud can come from an external source and be hydrodynamically concentrated (as soft pellets) to form mounds or it can be produced in situ by organisms (degradation of delicate skeletons, microbial production). When mud mounds are surrounded and buried by carbonate sediments both sources are possible, but when surrounded by siliciclastic facies (Fig. 25) the mound must have been the mud factory.

Modern analogues

One of the most frustrating aspects of studying carbonate mud mounds is the absence of modern analogues. Except for microbes, which are thought to be able to produce particulate lime mud (Camoin and Maurin, 1988; an hypothesis for which there is no modern example), there are no known mud producers on the scale of modern delicate green algae. Structures that come closest to mud mounds are seagrass-stabilized shallow water mud banks, supporting a variable volume of benthic flora and fauna or the deep water current-formed lithoherms in the Straits of Florida. No fossil analog to modern seagrass has been shown to have stabilized ancient mud mounds although early seafloor cementation is a conspicuous attribute of many ancient mud mounds.

AUTOSTRATIGRAPHY AND ECOLOGICAL SUCCESSION

The composition, diversity and organization of reef- and mound-building assemblages commonly change as the structures grow. This is due both to intrinsic biological interactions which lead to ecological succession or *autostratigraphy* and to external environmental controls which result in *allostratigraphy*. As both are/were operative in all reefs and mounds, usually simultaneously, they are difficult to separate in the geological record.

Ecological succession is manifest in reefs and mounds as an increase in species diversity, biomass, structural

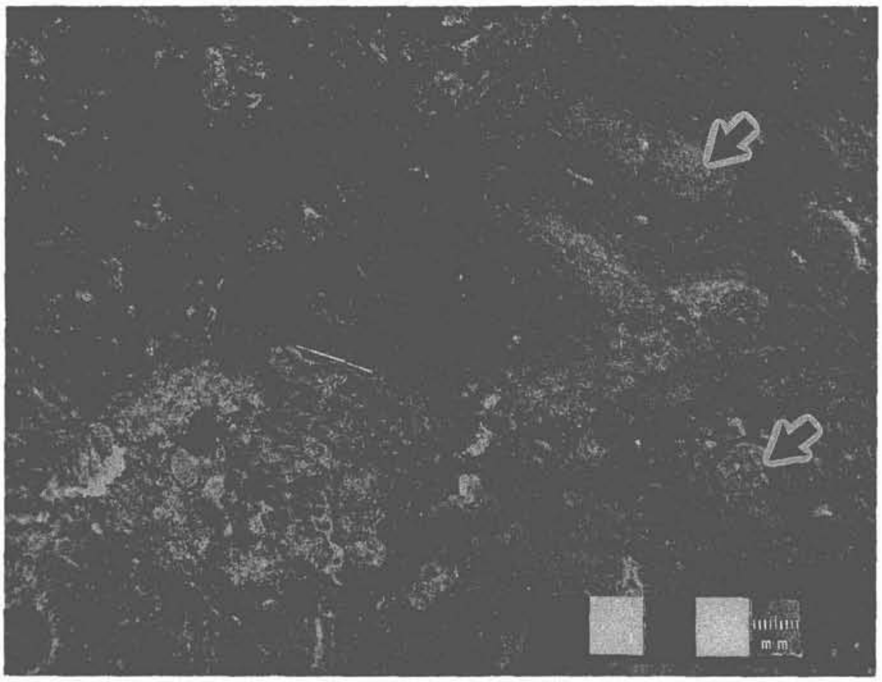

Figure 22 Outcrop photograph of calcareous sponges (arrows) and encrusting calcareous algae (irregular dark lines) in one of the skeletal mounds along the margin of the Permian "Reef" Complex, New Mexico, U.S.A. Scale divisions in centimetres.

Figure 23 Polished slab of a plastic-impregnated core through a Holocene skeletal mound, Rodriquez Key, Florida, U.S.A. The large skeletons are branching coral (*Porites* sp.) and the numerous smaller fossils are cross sections through platy green calcareous algae (*Halimeda* sp.)

complexity and stability through time. The stages of succession have been called *stabilization*, colonization, diversification and domination (Fig. 26; Walker and Alberstadt, 1975; James 1983). 1) The *Stabilization Stage* is a shoal or accumulation of skeletal lime sand composed of pelmatozoans, bivalves, brachiopods, or calcareous algae. Surfaces can be colonized by algae, plants (sea grasses) and/or animals that send down roots or holdfasts to bind and secure the substrate. 2) The *Colonization Stage* is characterized by few species, sometimes massive or lamellar forms, but more commonly monospecific clusters or clumps of branching fossils. The branching shapes created many small subenvironments or niches which were populated by other attached and encrusting organisms. 3) In the *Diversification Stage* the number of major reef-building taxa is usually more than doubled, and the greatest variety in growth habit is encountered. With this increase in form and diversity of framework and binding taxa comes increased nestling space, i.e., surfaces, cavities, nooks and crannies, leading to an increase in diversity of debris-producing organisms (Fig. 27). The structure is frequently high enough above the seafloor to affect water circulation and thus change sedimentation patterns. At this point not only are surrounding sedimentary environments altered but, in the right location, the reef itself can, because its margins now reach from shallow to deep water, develop an energy zonation. 4) The most common lithology in the *Domination Stage* is a limestone formed by a few taxa with one growth habit, generally encrusting to laminated. Most buildups show the effects of rough water at this stage, in the form of beds of rudstone.

In more general terms the first two stages are really pioneer or developmental phases whereas the last two are climax or mature phases (Fig. 26; see Copper, 1988, for an excellent discussion). Such *pioneer communities* are composed of generalists which are small, solitary, generally erect, hardy and fast growing, have high recruitment and reproduction rates, and are of wide geographic distribution. They can readily adapt to new substrates and tolerate abundant suspended matter. Assemblages are of generally low diversity and dominated by one or two elements, poorly zoned and characterized by clumps of fossils with spaces between. A *climax community* is composed of clonal, long-lived, commonly endemic specialists who occupy narrow environmental niches, are slow growing and of large to gigantic size and have a wide variety of shapes. The community is one of high biomass which completely covers the seafloor and in which nutrients are conserved and efficiently recycled, but it is vulnerable to catastrophe.

Considered against this background, most mounds fit the concept of a pioneer community or stages 1 and 2, while most reefs fit the concept of a pioneer community or mound unit succeeded by a climax community or stages 3 and 4. The basal mound unit is an elevated, firm to hard substrate upon which the reef or climax community could grow. This topographic high can, however, be antecedent, i.e., a pre-existing seafloor high of whatever composition (pre-existing dead reef, karst hill, terrigenous sand shoal), in which case the climax or reef commu-

Figure 24 Lower Cretaceous (Albian) chemosynthetic mound composed of abundant bivalves and serpulid worm tubes surrounded by deep water, outer shelf to slope, fine-grained, terrigenous clastic sediments. Helicopter for scale.

Figure 25 An Upper Carboniferous (Middle Pennsylvanian) Waulsortian-like mound in the Blue Mountains, northwestern Ellesmere Island, Arctic Canada. The 300 m-thick structure occurs in dark, slope to basin calcareous shales. Photograph B. Beauchamp.

nity nucleated directly on the seafloor. Such a situation is common in modern seas where living reefs are located on highs formed by underlying Pleistocene reefs, modified by prolonged karstification.

Thus, in the geological record, ecological succession generates three types of structures (Fig. 28), 1) mounds, 2) mounds gradationally overlain by reefs, and 3) reefs nucleated directly on pre-existing hard, commonly elevated, surfaces. These styles depend upon the local environment and geological period. During periods when a wide spectrum of organisms were present all three can be expected. Mounds during these times will be pioneer communities which were prevented from developing into climax communities ("arrested successions" of Copper, 1988) by their location in unsuitable environments, generally on the inner platform or in deep water. In geological periods when benthic communities lacked organisms capable of producing large elements, buildups rarely passed the pioneer stage, and mounds were the norm.

The autostratigraphy of an individual buildup may comprise two to four stages, or if disrupted, illustrate stacked stages. While periodic disturbances were necessary for diversity, major catastrophes which destroyed the community are manifest as breaks (hardgrounds, subaerial exposure surfaces). These catastrophes reset the clock and, depending on the local environment, the overlying buildup may be a mound (pioneer) or reef (climax). The size and frequency of units within a buildup are allostratigraphic, a function of external controls.

AUTOSTRATIGRAPHY - ECOLOGICAL SUCCESSION

STRUCTURE	STAGE		LIMESTONE	DIVERSITY	SHAPE
REEF	Climax	Domination	Bindstone Framestone	Low	Laminate Encrusting
		Diversification	Framestone Bindstone	High	Domal Massive Lamellar Branching Encrusting
MOUND	Pioneer	Colonization	Bafflestone Floatstone	Low	Branching Lamellar
		Stabilization	Grainstone Rudstone	Low	Skeletal Debris

Figure 26 A sketch of the four divisions of the core facies that can be generated by ecological succession of the reef builders. (Right) the most common types of limestone, relative species diversity and shape of the reef builders found in each part. (Left) The stages of growth. Mounds typically exhibit the first two stages while reefs can exhibit all four stages.

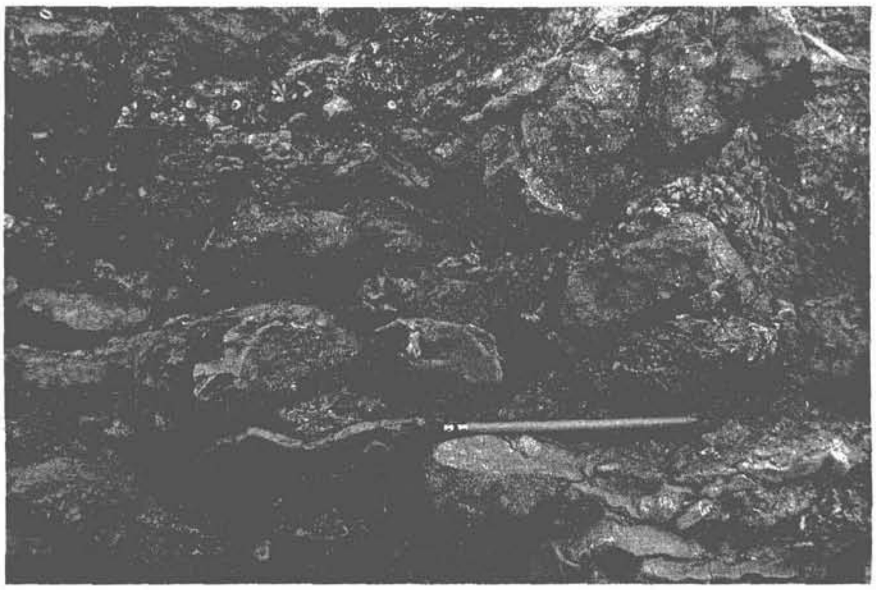

Figure 27 A reef core framestone (diversification stage) of massive stromatoporoids and domal and branching tabulate corals in the Lower Devonian on Ellesmere Island, Canada.

ALLOSTRATIGRAPHY AND SEQUENCE STRATIGRAPHY

Holocene history of living reefs

The allostratigraphy of reefs and mounds is a function of 1) varying conditions in the growth window, 2) ecological succession, 3) antecedent topography, and 4) the rates of sea level rise and organism growth. Reef growth during the Holocene rise in sea level, as revealed by extensive drilling during the last 15 years (Macintyre and Glynn, 1976; Davies and Hopley, 1983; Davies and Montaggioni, 1985; Davies *et al.*, 1985; Macintyre, 1988), illustrates several themes. Even though rates may be different in the ancient, the stratigraphic record is still a measure of the interplay between them, from which first-order interpretations can be made.

Start-up

Reef start-up can take place 1) during sea level rise following exposure, 2) during sea level fall when the seafloor comes into the growth window, 3) when the seafloor is raised by mound development into the growth window, 4) when factors inimical to reef growth are turned off. The nature of the initial community depends on where in the growth window accretion begins (e.g., inboard/outboard, shallow water/deep water) and the nature of the substrate (e.g., flat soft-sediment seafloor, elevated hard substrate). Reef growth during the Holocene transgression generally began on Pleistocene limestone or other hard substrates. There seems to be no pattern to initial reef growth; some reefs started as shallow or intermediate depth communities immediately, other reefs experienced lag times of up to 2,000 years and did not begin to grow until the water was more than 20 m deep. In general, however, mid-to inner-shelf reefs show delayed start-up whereas shelf margin reefs illustrate immediate growth. Accretion rates of inner shelf reefs increased dramatically once the barrier reef reached sea level.

Growth strategies

The Holocene sea level curve is one of early rapid rise, late slowing and final stability. Reef accretion during this period illustrates one of several strategies (Neumann and Macintyre, 1985; Fig. 29). *Keep-up Reefs* maintained their crests at or near sea level, tracking sea level rise. *Catch-up Reefs* began as shallow reefs which became deeper as rise rate exceeded accretion rate, only to grow upward and catch up with sea level. Alternatively, they started on a deep substrate and then grew up to sea level. Once reefs of either type reached sea level they maintained a near-surface crest or developed a capping facies of subtidal pavements to storm-ridge deposits. At this point growth was limited to the seaward margin and reefs prograded laterally over their own reef front and fore reef sediments. *Give-up Reefs* initially grew as did the others but then succumbed to changing environmental conditions and died. All studies note that the responses of reef growth to sea level rise varied greatly, even within the same reef. In Papeete, for example, keep-up reefs typify the windward margin, catch-up reefs characterize the leeward margin and give-up is the fate of muddy patch reef margins (Montaggioni, 1988). Growth strategies were independent of reef fabric, form and setting.

Drowning

Reefs can turn off and die for a variety of reasons. The most obvious reason, that sea level rise was too rapid for the reefs to keep up, is not the answer. This is because Holocene reefs can have extraordinarily high growth rates which potentially exceed any rise in sea level except that related to tectonics. Schlager (1981) has argued, mainly on the basis of abundant evidence of progradation in the rock record, that ancient reefs were also capable of similar rapid growth rates. Changes in the growth window are more likely to be the cause of reefs giving up. "Drowning" is defined by Schlager (1990) as "submergence of the platform top below the photic zone" by a rise in sea level or shallowing of the photic limit. Alternatively many reefs which grew along the steep edges of platforms during the early Holocene seem to have been killed by some combination of increased turbidity, nutrient excess or hot saline waters which swept off the shelves when sea level flooded the wide shallow platforms (the "bad water" syndrome). Even today most windward Bahamian reefs grow opposite islands which protect them from these bank waters, otherwise they are "shot in the back" by the very waters they helped generate by restricting circulation on the platform (Neumann and Macintyre, 1985).

Ancient reefs

Keep-up reefs in the rock record should illustrate homogeneous vertical sequences of roughly similar facies. Alternating framework and detrital reef

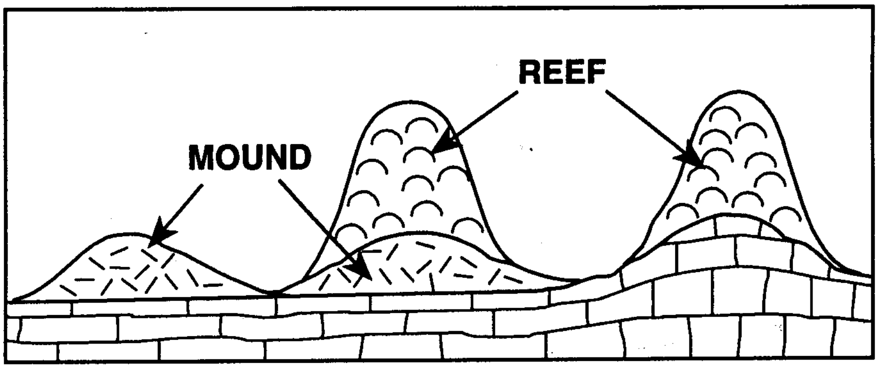

Figure 28 A sketch illustrating the stratigraphic relationship between reefs and mounds. Mounds can be separate structures or be gradational upward into reefs while reefs can cap mounds or grow directly on the flat or elevated seafloor.

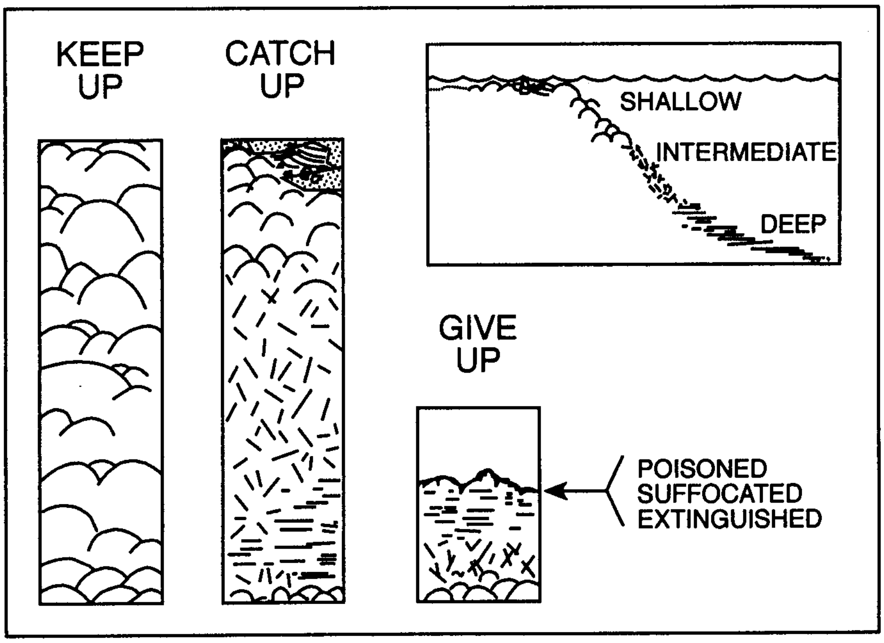

Figure 29 Growth strategies illustrated by reefs during a period of rising sea level; after Neumann and Macintyre (1985). (Inset) The shallow, intermediate and deep zones of reef growth. Keep-up reefs track sea level and have uniform facies throughout (in this case, all shallow water facies). Catch-up reefs can have an initial shallow water facies, then lag behind sea level rise for a short period only to grow upwards through progressively shallower waters to reach sea level; such reefs display shallowing-upward facies trends. Give-up reefs start to grow but are killed off by excessive nutrients (poisoned), abundant fine sediment (suffocated) or rapid subsidence below the photic zone (extinguished). The top of a give-up reef can be a hardground or it can grade upward into a deep water mound.

flat facies will be typical of reefs that tracked sea level but did not exceed it. Massive framework facies will characterize reefs that grew in intermediate water depths, never accreting fast enough to build into the surf zone.

Catch-up reefs should illustrate either a deepening and then shallowing-upward succession or just shallowing-upward. The shallowing-upward parts often resemble sequences produced by ecological succession. *Give-up*

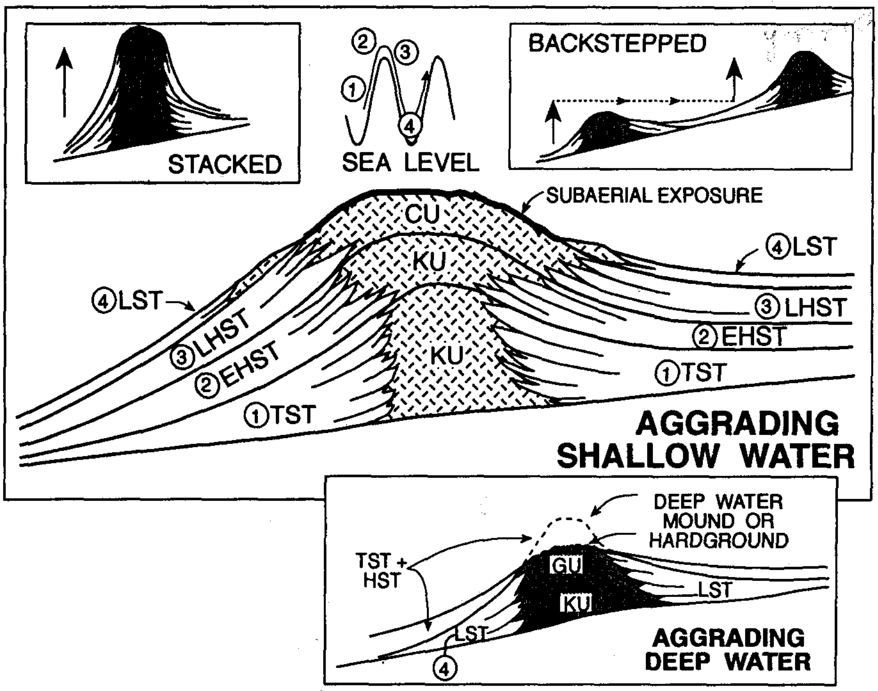

Figure 30 A sketch illustrating aggrading reef growth during a rise and fall in sea level when fluctuations were large and of short period and/or the reef builders could barely match rates of sea level rise. In relatively shallow water aggradation is mainly during TST, EHST and LHST phases; in deep water aggradation is only during LST and the top of the reef is drowned or replaced by a deep water mound during sea level rise. Such reefs may be stacked to form large complexes or if sea level is very rapid may backstep upslope (insets).

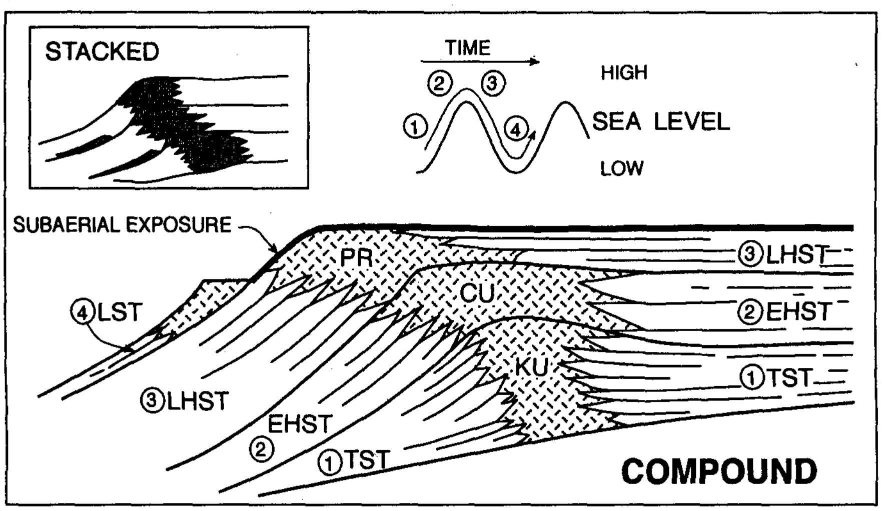

Figure 31 A sketch illustrating compound reef growth patterns during a rise and fall in sea level when the scale and period of sea level fluctuations were intermediate and/or reef builders could match the fastest rates of sea level rise. The motif is one of aggradation followed by progradation. TST are mostly keep-up; EHST are catch-up and LHST are prograding. Inset shows stacking of reefs as the result of growth during several major fluctuations in sea level.

reefs can display a variety of successions (Fig. 29) depending on whether they were smothered by sediment (terrigenous or carbonate), poisoned by nutrient excess or extinguished by failing light. Poisoned or extinguished reefs are overlain by hardgrounds, different communities or mounds.

The geometry of ancient reef bodies is controlled by the nature of relative sea level fluctuations and the ability of reef-building organisms to track these sea level changes (e.g., Polmar, 1991). Variations in the shape and composition between reefs at any given time will also reflect the shape of the sea level curve, especially the amplitude and period of the sign curve. The responses are of course hierarchical and can be superimposed, resulting in a myriad of slightly different geometries. Most, however, are variations of the three illustrated in Figures 30, 31 and 32. In each case the response of the reef is expressed as a transgressive systems tract (TST), an early highstand systems tract (EHST), a late highstand systems tract (LHST) and a lowstand systems tract (LST).

Aggrading reefs

Aggrading reefs (Fig. 30), which can be perpetually submerged, are characterized by upward growth and develop when the amplitude of sea level fluctuation is large and the period short, and/or when the reef builders can barely match the rate of sea level rise. Two variations are possible, shallow water reefs and deep water reefs.

1. *Shallow water reefs.* TST reefs are narrow but thick, with near vertical margins and little perireefal sediment. They grew in a keep-up, but lag mode and the reef community was an intermediate depth one. EHST reefs are still keep-up to catch-up in the form of shallower water assemblages. LHST reefs are catch-up and may exhibit local exposure and minor progradation. LST reefs are prograding providing there is sufficient perireefal sediment for a foundation.
2. *Deep water reefs.* These buildups developed on deeply submerged platforms or in basins and accreted only when sea level fell far enough to bring the seafloor into the growth window. TST reefs are give-up in style, being extinguished as the water became too deep. The EHST and LHST are sedi-

ments, hardgrounds or mounds on top of the reefs. LST is characterized by start-up and catch-up reefs, which may have reached sea level, but usually did not, during the bottom of sea level fall, only to give-up again as sea level rose.

Successive periods of reef growth can result in stacked structures with relative relief above surrounding sediments dependent upon rates of inter-reef sedimentation during lowstands. Alternatively, if long-term sea level rise is rapid then reefs may not be stacked but will have nucleated progressively upslope, generating a "backstepping" motif.

Compound reefs

These buildups (Fig. 31), which have a prominent aggradational and progradational motif, formed when the amplitude and period of sea level fluctuations were intermediate or the reef builders had no trouble matching the fastest rates of sea level rise. TST reefs, with plenty of accumulation space were continuously in a catch-up or more commonly keep-up mode, and this part of the reef is usually the narrowest and thickest. EHST reefs caught up to sea level and formed wide reef flat facies with growth focused on the oceanward side. LHST reefs had little accumulation space, exhibit extensive progradation and have wide reef flat facies. LST reefs were narrow fringing structures downslope and built on variably cemented fore reef sediments which may have been subject to slumping.

Prograding reefs

These reefs (Fig. 32), which grew in shallow water, were often perpetually exposed and expanded laterally. They formed when sea level changes were relatively small and of long duration and/or the reef builders could have easily exceeded the rates of sea level change. The prograding style was established soon after nucleation because accumulation space was minimal. TST reefs are typically zoned structures but the style of EHST and LHST reefs depended upon reef-basin relief. If relief was large then progradation would continue and wide reef flats could have developed. If relief was minimal then reef geometry would be lost and the seafloor would come to resemble a biostrome. LST development would be represented by a slight downshift in facies.

Ancient mounds

Whatever their location, on shelves or in deeper water, common features of biogenic mounds are their well-defined vertical zonation and near absence of lateral zonation. In on-shelf or upper slope mounds, which are dominantly skeletal mounds, vertical zonation is energy dependent. These mounds are exemplified by the late Paleozoic platy algal mounds (Fig. 33). A complete vertical sequence goes through three successive stages, 1) a basal accumulation of bioclastic muddy sediments without baffling or binding (mud mound stage), 2) a core of lime-mud-rich platy algal bafflestone (skeletal mound stage) built in relatively low energy level, below wave base, and 3) a crestal bindstone of encrusting skeletal organisms (foraminifera, *Tubiphytes*; skeletal mound stage to reef stage) when the biogenic pile reached higher energy level (active wave base). If the mound crest was maintained in rough water, a sand shoal would cap the mound. Similar types of zonations are found in on-

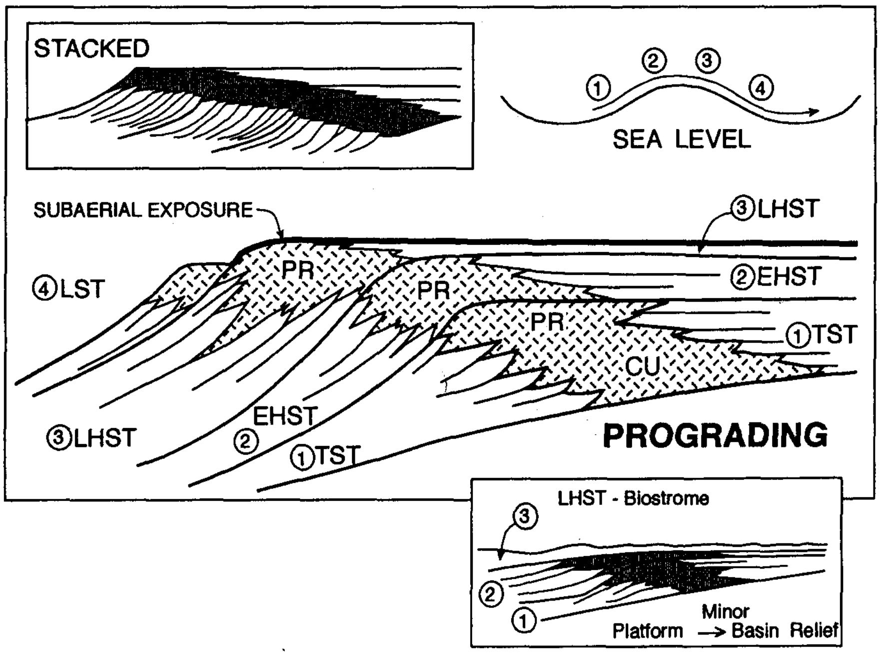

Figure 32 A sketch illustrating prograding reef growth during a rise and fall in sea level when changes in sea level were small and of long duration and/or the reef builders could easily exceed the rates of sea level change. If platform-basin relief was large progradation prevails during LHST and LST but if small then biostromes or sand shoals can develop. Inset shows the result of repeated progradation.

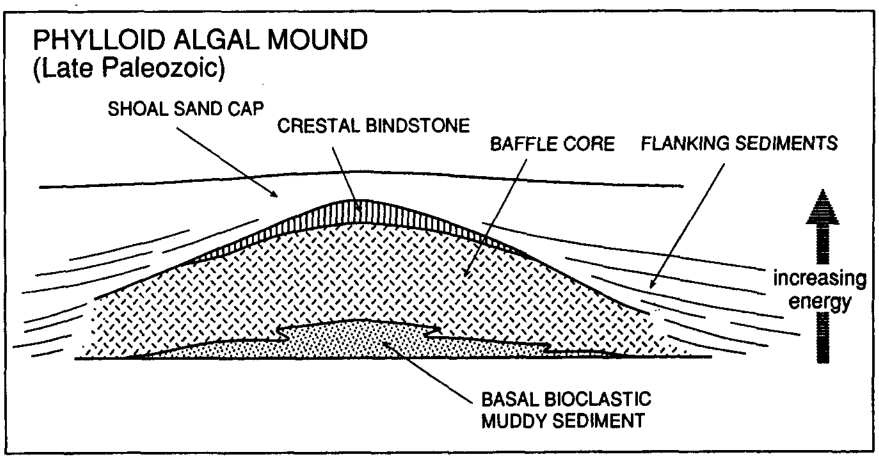

Figure 33 Idealized on-shelf skeletal mound showing energy-dependent vertical zonation. Modified from Wilson (1975).

shelf rudist mounds (Wilson, 1975).

Most deep water mounds are similar to aggrading reefs in their development and response to sea level change. They are composed of facies that developed below, near, or slightly above storm wave base. Unlike reefs, where sea level changes may have caused sharp boundaries and discontinuities between facies, sea level changes in mounds will be detectible only by changes in the normal facies succession of a given mound type, a feature not detectible in seismic profiles. For instance (Fig. 34), assuming that A-B-C is a complete shallowing-upward facies sequence of a mound, any break or reversal in the sequence will indicate sea level change. The succession ABCBA indicates slow transgression, ABCA rapid transgression; AC rapid sea level fall.

Figure 34 illustrates, starting from a depth-zonation model of deep water biogenic mounds (that of Fig. 18), how mounds responded to sea level changes and the vertical successions that resulted in various systems tracts. Reef growth strategies (Fig. 29) also apply to mounds. In TST situations mounds were in a keep-up or catch-up mode. Under conditions of slow sea level rise the upper surface of the mounds kept pace with sea level rise and there was no facies change. If sea level rise was relatively rapid most mounds were in a catch-up situation and there was a reversal of the vertical sequence. The deeper mounds became give-up, but start-up mounds developed on shallower parts of the slope. In an EHST situation the mounds were in a keep-up mode and developed normal depth-controlled sequences. Shallower mounds may have acted as foundations for reefs. LHST mounds showed the complete depth-zoned vertical sequence and ultimately were capped by prograding marginal reefs or isolated aggrading reefs.

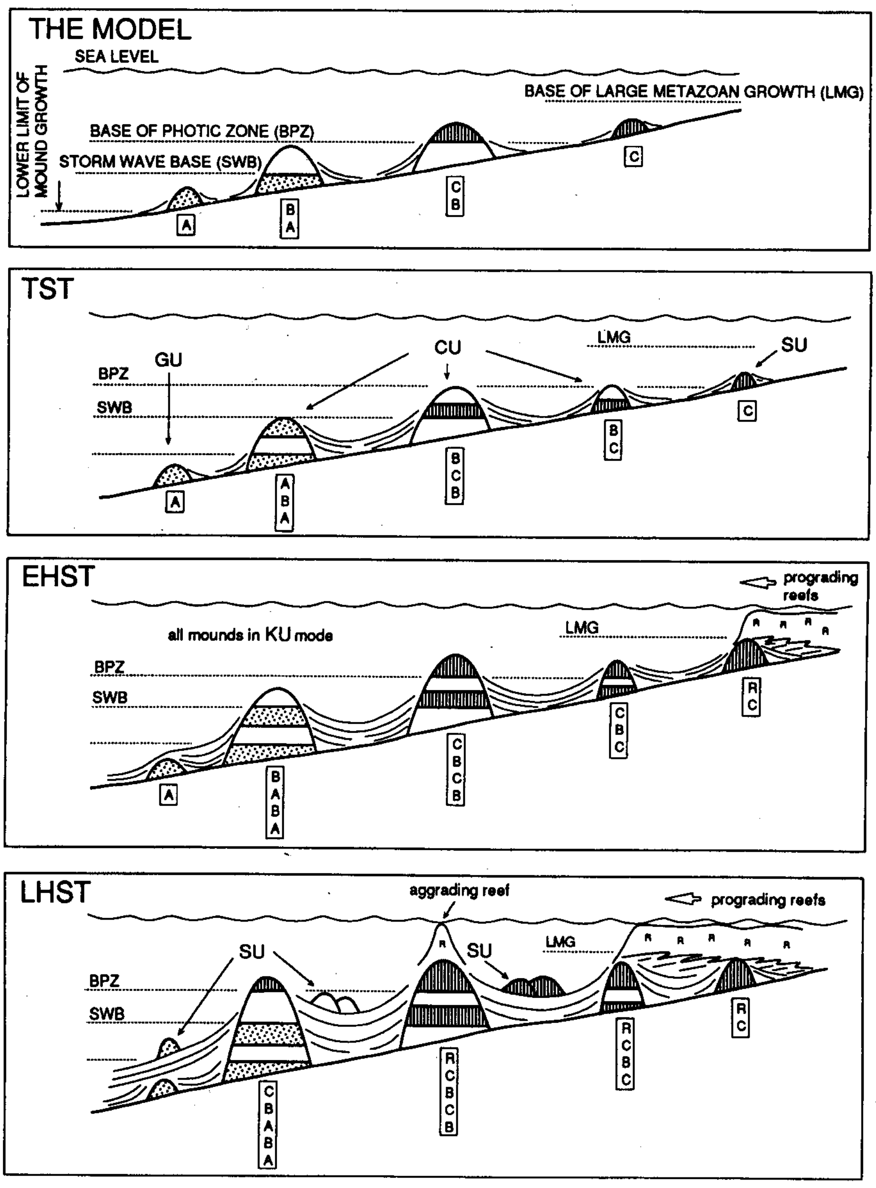

Figure 34 Sketch illustrating response of depth-zoned biogenic mounds to sea level changes and the resulting vertical succession in various systems tracts. CU = catch-up, GU = give-up, SU = shallow-up, R = reef; letters A, B, C correspond to facies in Figure 18.

GEOLOGICAL HISTORY OF REEFS AND MOUNDS (Fig. 35; Table 1)

Introduction

The history of Phanerozoic reefs and mounds has recently been reviewed by James and Macintyre (1985), Sheehan (1985), Fagerstrom (1987), Copper, (1988) and Talent (1988). Descriptions of Precambrian buildups can be found in Geldsetzer *et al.* (1988) and Grotzinger (1989).

1. Archean (Beginnings)

The oldest recognizable buildups are late Archean (2.5-2.7 Ga) stromatolitic mounds occurring as atoll-like buildups around subsiding volcanoes or linear belts on early cratonic crust. If there are earlier structures they have been rendered largely unrecognizable by metamorphism.

2. Proterozoic (First extensive reefs and mounds)

The formation of cratons flooded by shallow seas during earliest Proterozoic time coincided with the appearance of diverse buildups. Reefs and mounds were constructed by stromatolites that grew across the environmental spectrum. Extensive barrier reefs, fringing reefs and pinnacle reefs developed on carbonate platforms and patch reefs and mounds grew in terrigenous clastic-dominated settings. Latest Proterozoic reefs are poorly documented but some spectacular buildups (Fig. 1) (Aitken, 1988) illustrate construction by a transitional community of stromatolites and calcimicrobes (?calcareous algae). They have a distinctly Phanerozoic architecture with cavities, internal sediments and fibrous cements.

3. Early Cambrian – Early Ordovician (Age of uncertainty)

The very earliest (Tommotian) Cambrian buildups are skeletal mounds built by calcimicrobes and archaeocyathans, together with an ever-increasing fauna of other skeletal invertebrates. Archaeocyathans, however, disappeared at the end of early Cambrian time. Late Cambrian buildups are once again simple stromatolitic/thrombolitic or calcimicrobial mounds (Kennard and James, 1986), much like older late Proterozoic buildups. In early Ordovician these mounds were gradually populated by an evolving biota of sponges, calcareous algae and primitive corals.

4. Middle Ordovician – Devonian (Spectacular stromatoporoid reefs)

This period is the acme of Paleozoic reef development, coinciding with the appearance of bryozoans, rugose and tabulate corals and stromatoporoids. While Ordovician structures were built by a variety of organisms, Silurian and Devonian buildups were constructed primarily by stromatoporoids forming the full spectrum of reefs and mounds. The stromatoporoids inhabited most shallow subtidal environments while tabulate and colonial rugose corals were more common in turbid and deeper water settings. Calcimicrobes were particularly prominent in Devonian buildups.

Toward the end of Devonian time there was an extinction of shallow-marine animals on a huge scale. Most stromatoporoids, rugose corals, tabulate corals and brachiopods disappeared resulting in the demise of this successful ecosystem.

5. Mississippian – Middle Triassic (Many mounds)

This period in earth history is characterized by few large skeletal metazoa, and all buildups are mounds, generally on slopes and ramps and on the inner parts of platforms. Mississippian structures are commonly skeletal to mud mounds with variable proportions of fenestellid bryozoa, sponges or codiacean and dasycladacean algae and locally spectacular pelmatozoan-rich flanking beds. Most Pennsylvanian and early Permian mounds are rich in the phylloid algae *Archaeolithophyllum, Eugoniophyllum* and *Ivanovia* and/or the enigmatic platy organism *Paleoaplysina.* These organisms are augmented and then replaced by tubular foraminifera, stromatolites, the ?calcimicrobe *Tubiphytes,* and a wide variety of calcareous inozoan and sphinctozoan sponges in middle and late Permian buildups. Remarkably, this fauna seems to have passed through the Permian extinction relatively unscathed, and even though there are no earliest Triassic reefs, Middle Triassic buildups are virtually identical to those of the late Permian (Stanley, 1988). This Permian hold-over fauna was largely extinguished by an extinction event at the end of Middle Triassic time.

6. Late Triassic – Early Jurassic (First modern reefs)

This is when reefs become "modernized" due largely to the evolution of scleractinian corals, new forms of coralline and codiacean algae and a wide variety of endolithic organisms. Late Triassic reefs and mounds were built primarily by scleractinian corals, calcisponges, and calcareous algae. They formed buildups across the environmental spectrum, including dis-

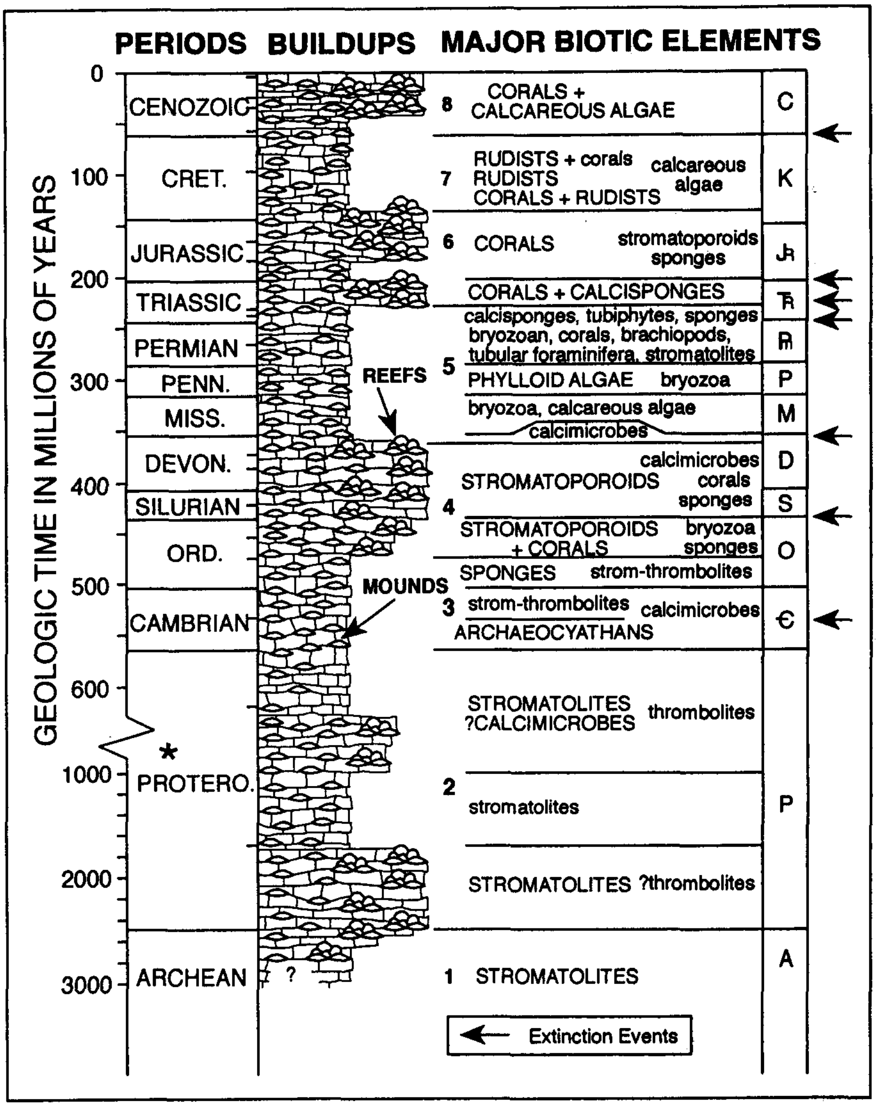

Figure 35 An idealized stratigraphic column representing geological time and illustrating periods when there were only mounds and those times when there were both mounds and reefs. Numbers indicate different associations of reef- and mound-building biota; * = scale change.

placed low-latitude terranes. This community was terminated by the end-Triassic mass extinction event and although corals again became dominant reef-builders, calcisponges never regained their previous importance.

Earliest Jurassic time was a protracted period without significant reef growth. Although a wide spectrum of structures similar to living reefs and mounds characterizes late Jurassic time, the two commonest types are 1) shelf-margin ramp and barrier reefs dominated by corals and/or stromatoporoids and a wide spectrum of accessory taxa, and 2) deep water slope and basin sponge-algal mounds below normal wave base and near lower limits of the photic zone. The reefs grew as patches on wide platforms, as belts of patch reefs near shelf margins and as caps on pre-existing deep water mounds.

7. Cretaceous
(Rudist bivalve mounds)
The Jurassic reef-building community persisted into early Cretaceous time, but was gradually augmented and locally replaced by rudist bivalves. Early Cretaceous buildups at the seaward shelf edge consisted of deeper coral-algal communities (?below wave base) and shallower caprinid-radiolitid rudist communities. Interior shelf basins were bordered by caprinid-dominated buildups. Middle Cretaceous buildups were dominated by rudists forming mounds of low-diversity, loosely constructed, essentially unbound bafflestone with coherence due to interlocking and cocementation. The structures were rarely large, mostly in the form of mounds stacked upon one another and separated by layers of bioclastic sediment, much of which was produced by frequent destruction of unbound frameworks by storms. Late Cretaceous shelf margin buildups, particularly post-Cenomanian, consisted of rudist-coral communities in which radiolitids and hippuritids were more abundant than nodular to hemispherical and planar corals.

Table 1 *Studies of reefs and mounds in specific geological periods, mainly since 1980 (see Fig. 35).*

Period	Reference
Living	Acevedo *et al.* (1989); Acker & Stearn (1990); Bosence *et al.*, (1985); Callender *et al.* (1990); Cortez & Risk (1985); Eliuk (1991); Ginsburg & Schroeder (1973); Gaus & Macintyre (1989); James & Ginsburg (1979); Johnson & Risk (1987); Messing *et al.* (1990); Mullins *et al.* (1981); Van Wagoner *et al.* (1990).
Holocene	Chappell & Polach (1976); Choi & Ginsburg (1982); Davies & Montaggioni (1985); Davies & Hopley (1985); Davies *et al.* (1985); Longman (1981); Macintyre (1988); McNeill (1988); Montaggioni (1988); Neumann & Macintyre (1985); Tudhope (1989); Wanless & Tagett (1989).
8. Cenozoic	Bernecker & Weidlich (1990); Crame (1980); Dabrio *et al.* (1981); Esteban (1979); Geister (1980); Pedley (1979); Polmar (1991); Riding *et al.* (1991).
7. Cretaceous	Camion *et al.* (1988); Kaufman & Johnson (1988); Scott (1988); Scott (1990); Scott *et al.* (1990).
6. Triassic-Jurassic	Crevello & Harris (1984); Flügel & Steiger (1981); Frost (1981); Palmer & Fursich (1981); Schafer (1984); Stanton & Flügel (1989).
5. Mississippian-Triassic	Bolton *et al.* (1982); Bridges & Chapman (1988); Brown & Dodd (1990); Cranston (1990); Davies & Nasichuk (1990); Davies *et al.* (1988); Flügel & Reinhardt (1989); Hileman & Mazzulo (1977); Lees & Miller (1985); Lees *et al.* (1985); Reid & Ginsburg (1986); Tedesco & Wanless (1989).
4. Ordovician-Devonian	Bourque & Gignac (1983); Bourque *et al.* (1986); Burchette (1981); Copper & Brunton (1991); Moore (1988); Playford (1980); Shaver & Sundermann (1989); West (1988).
3. Cambro-Ordovician	Barnaby & Read (1990); James (1981); James & Gravestock (1990); Pratt & James (1982); Rees *et al.* (1989); Rowland & Gangloff (1988); Toomey & Nitecki (1979); Webby (1984).
2. Proterozoic	Aitken (1988); Grotzinger (1989).
1. Archean	Grotzinger (1989).

8. Cenozoic
(Return of modern reefs)
The terminal Cretaceous event led to the extinction of rudists and most Cenozoic reefs were, like living reefs, constructed by scleractinian corals and calcareous algae. Paleocene reefs are not common but a major Eocene radiation of new hermatypic coral genera resulted in extensive reef development. The acme of Cenozoic reef growth appears to have been the Oligocene with subsequent plate rearrangement and climatic deterioration destroying some habitats (Mediterranean) and isolating others (Caribbean, Indo-Pacific).

Finally, a paradox — living reefs are atypical of the Cenozoic! During early Pleistocene time quickly growing, branched corals such as the *Acroporidae, Poritidae and Seriatoporidae* evolved rapidly, dominating most shallow water environments. Thus, the Cenozoic shallow water reef corals with shapes much like those of stromatoporoids and stromatolites, were replaced by these newly evolved, highly branching forms.

ACKNOWLEDGEMENTS
This manuscript draws heavily on our research supported by the Natural Sciences and Engineering Research Council of Canada.

REFERENCES

Basic sources of information

Choat, J.H., *et al.*, 1988, Proceedings of the Sixth International Coral Reef Symposium: Townsville, Australia, 3 volumes.
These proceedings and those of preceding symposia held every four years are an invaluable source of information on the biology and geology of coral reefs.

Fagerstrom, J.A., 1987, The evolution of reef communities: New York, J. Wiley & Sons, 600 p.
A sound introduction to the wide diversity of Phanerozoic reef communities.

Geldsetzer, H.H.J., James, N.P. and Tebbutt, G.E., 1988, Reefs, Canada and Adjacent Areas: Canadian Society of Petroleum Geologists, Memoir 13, 775 p.
A gold mine of information! A total of 115 short case studies of Precambrian, Paleozoic and early Mesozoic reefs organized chronologically.

Harris, P.M., 1983, ed., Carbonate buildups: a core workshop: Society of Economic Paleontologists and Mineralogists, Core Workshop No. 4, 593 p.
A total of 21 short, succinct, well-illustrated papers on reefs of all ages, with emphasis on depositional facies and diagenesis.

Heckel, P.H., 1974, Carbonate buildups in the geologic record: a review, *in* Laporte, L.F., ed., Reefs in time and space: Society of Economic Paleontologists and Mineralogists, Special Publication 18, p. 90-155.
A detailed account of reefs or buildups, their classification and zonation with geological time and general models of reef formation.

Hopley, D., 1982, The geomorphology of the Great Barrier Reef: Quaternary Development of Coral Reefs: New York, J. Wiley & Sons, 453 p.
Although concentrating on the Great Barrier Reef, this book contains a great deal of information on modern reefs in general.

James, N.P., 1983, Reef environment, *in* Scholle, P.A., Bebout, D.G. and Moore, C.H., eds., Carbonate depositional environments: American Association of Petroleum Geologists, Memoir 33, p. 345-440.
An overview of the sedimentology of modern and ancient reefs with numerous colour illustrations and photographs; read in conjunction with this paper.

James, N.P. and Macintyre, I.G., 1985, Carbonate depositional environments, Part 1: Reefs: Colorado School of Mines Quarterly, v. 80, no. 3, 70 p.
Articles on the zonation, depositional facies and diagenesis of modern and ancient reefs.

Laporte, L.F., ed., 1974, Reefs in time and space: Society of Economic Paleontologists and Mineralogists, Special Publication 18, 256 p.
Seven papers dealing with various aspects of modern and fossil reefs.

Roberts, H.H. and Macintyre, I.G., eds., 1988, *Halimeda*: Coral Reefs, v. 6, p. 121-271.
A special issue with numerous papers on modern mounds composed primarily of the calcareous alga Halimeda *and its role as a sediment producer.*

Schroeder, J.H. and Purser, B.H., 1986, eds., Reef diagenesis: Berlin, Springer-Verlag, 455 p.
A series of 19 case studies of Phanerozoic reefs emphasizing diagenesis but with many excellent accounts of facies.

Stanley, G.D., Jr. and Fagerstrom, J.A., eds., 1988, Ancient reef ecosystems issue: Palaios, v. 3, p. 110-250.
An issue with 12 papers devoted to the paleoecology of reefs and mounds; including several excellent summary contributions.

Toomey, D.F., ed., 1981, European fossil reef models: Society of Economic Paleontologists and Mineralogists, Special Publication 30, 546 p.
A total of 17 papers with emphasis on latest Paleozoic, Mesozoic and Cenozoic structures.

Wilson, J.L., 1975, Carbonate facies in geologic history, Heidelberg, Springer-Verlag, 471 p.
Still the best overall reference to fossil reefs with succinct descriptions and numerous references.

Other References

The pertinent literature is so large and interdisciplinary that only selected papers, mostly published since 1980, are listed here. Citations to earlier papers can be found in James, 1983, 1984 and James and Macintyre, 1985. See Table 1 for selected references organized by geological period.

Acevedo, R., Morelock, J. and Olivieri, R.A., 1989, Modification of coral reef zonation by terrigenous sediment stress: Palaios, v. 4, p. 63-85.

Acker, K.L. and Stearn, C.W., 1990, Carbonate-siliciclastic facies transition and reef growth on the northeast coast of Barbados, West Indies: Journal of Sedimentary Petrology, v. 60, p. 18-25.

Aitken, J.D., 1988, Giant "algal reefs", Middle/Upper Proterozoic, Little Dal Group (>1200 Ma), Mackenzie Mountains, N.W.T., Canada, *in* Geldsetzer, H.H.J., James, N.P. and Tebbutt, G.E., eds., Reefs, Canada and adjacent areas: Canadian Society of Petroleum Geologists, Memoir 13, p. 13-23.

Barnaby, R. and Read, J.F., 1990, Carbonate ramp to rimmed shelf evolution: Lower to Middle Cambrian continental margin, Virginia Appalachians: Geological Society of America, Bulletin, v. 102, p. 391-404.

Bathurst, R.G.C., 1982, Genesis of stromatactic cavities between submarine crusts of paleozoic carbonate mud buildups: Journal of the Geological Society of London, v. 139, p. 165-181.

Bernecker, M. and Weidlich, O., 1990, The Danian (Paleocene) coral limestone of Fakse, Denmark: A model for ancient aphotic, azooxanthallate coral mounds: Facies, v. 22, p. 103-138.

Bolton, K., Lane, H.R. and LeMone, D.V., 1982, Symposium on the paleoenvironmental setting and distribution of the Waulsortian facies: El Paso Geological Society and University of Texas at El Paso, 202 p.

Bosence, D.W.J., Rowlands, R.J. and Quine, M.L., 1985, Sedimentology and budget of a Recent carbonate mound, Florida Keys: Sedimentology, v. 32, p. 317-343.

Boss, S.K. and Liddell, W. D., 1987, Patterns of sediment composition of Jamaican fringing reef facies: Sedimentology, v. 34, p. 77-88.

Boulvain, F., 1990, Sédimentologie et diagenese des monticules micritiques frasniens "F2j" de belgique: D.Sc. thesis, Université Libre de Bruxelles, Belgium, 535 p. (unpublished).

Bourque, P.-A. and Gignac, H., 1983, Sponge-constructed stromatactic mud mounds, Silurian of Gaspé, Québec: Journal of Sedimentary Petrology, v. 53, p. 521-532.

Bourque, P.-A., Amyot, G., Desrochers, A., Gignac, H., Gosselin, C., Lachambre, G. and Laliberté, J.-Y., 1986, Silurian and Lower Devonian reef and carbonate complexes of the Gaspé Basin, Québec – a summary: Bulletin of Canadian Petroleum Geology, v. 34, p. 452-489.

Bridges, P.H. and Chapman, A.J., 1988, The anatomy of a deep water mud-mound complex to the southwest of the Dinantian platform in Derbyshire, UK: Sedimentology, v. 35, p. 139-162.

Brown, M.A. and Dodd, J.R., 1990, Carbonate mud bodies in Middle Mississippian strata of southern Indiana and northern Kentucky: end members of a Middle Mississippian mud-mound spectrum: Palaios, v. 5, p. 236-243.

Burchette, T.P., 1981, European Devonian reefs: a review of current concepts and models, *in* Toomey, D.F., ed., European fossil reef models: Society of Economic Paleontologists and Mineralogists, Special Publication 30, p. 85-142.

Burne, R.V. and Moore, L.S., 1987, Microbialites: organosedimentary deposits of benthic microbial communities: Palaios, v. 2, p. 241-254.

Callender, W.R., Staff, G.M., Powell, E. and Macdonald, I.R., 1990, Gulf of Mexico hydrocarbon seep communities V. biofacies and shell orientation of autochthonous shell beds below storm wave base: Palaios, v. 5, p. 2-14.

Camoin, G. and Maurin, A.-F., 1988, Roles of micro-organisms (bacteria, cyanobacteria) in the formation of mud mounds. Examples from the Turonian strata of Jebels Bireno and Mrhila (Tunisia): Comptes Rendu Academie Sciences, Paris, *Serie II*, p. 401-407.

Camoin, G., Bernet-Rolande, M.-C. and Philip, J., 1988, Rudist-coral frameworks associated with submarine volcanism in the Maastrichtian of the Pachino area: Sedimentology, v. 35, p. 123-138.

Chappell, J. and Polach, H.A., 1976, Holocene sea-level change and coral-reef growth at Huon Peninsula, Papua, New Guinea: Geological Society of America, Bulletin, v. 87, p. 235-239.

Choi, D.R. and Ginsburg, R.N., 1982, Siliciclastic foundations of Quaternary reefs in the southernmost Belize Lagoon, British Honduras: Geological Society of America, Bulletin, v. 93, p. 116-126.

Coates, A.G. and Jackson, J.B.C., 1987, Clonal growth, algal symbiosis, and reef formation by corals: Paleobiology, v. 13, p. 363-378.

Copper, P., 1988, Ecological succession in Phanerozoic reef communities: is it real?: Palaios, v. 3, p. 136-151.

Copper, P. and Brunton, F., 1991, A global review of Silurian reefs, *in* Bassett, M.G., Lane, P.D. and Edwards, D., eds., The Murchison Symposium: London, Palaeontological Association, Special Papers in Palaeontology 44, p. 225-260.

Cortes, J.N. and Risk, M.J., 1985, A reef under siltation stress: Chuita, Costa Rica: Bulletin of Marine Science, v. 36, p. 339-356.

Cowen, R., 1988, The role of algal symbiosis in reefs through time: Palaios, v. 3, p. 228-232.

Crame, J.A., 1980, Succession and diversity in the Pleistocene coral reefs of the Kenya coast: Palaeontology, v. 23, p. 1-37.

Cranston, C.C., 1990, Late Mississippian Girvanella-bryozoan mud mounds in southern West Virginia: Palaios, v. 5, p. 460-471.

Crevello, P.D. and Harris, P.M., 1984, Depositional models for Jurassic reefal buildups, *in* Ventress, W.P.S., Bebout, D.G., Perkins, B.F. and Moore, C.H., eds., Jurassic of the Gulf Rim: Gulf Coast Section, Society of Economic Paleontologists and Mineralogists, p. 57-102.

Cuffey, R.J., 1985, Expanded reef-rock textural classification and the geologic history of bryozoan reefs: Geology, v. 13, p. 307-310.

Cummings, E.R., 1932, Reefs or bioherms?: Geological Society of America, Bulletin, v. 43, p. 331-352.

Dabrio, C.J., Esteban, M. and Martin, J.M., 1981, The coral reef model of Nijar, Messinian (uppermost Miocene) Almeria Province, southwest Spain: Journal of Sedimentary Petrology, v. 51, p. 521-541.

Darwin, C., 1842, Structure and distribution of coral reefs: Berkeley, University of California Press, from 1851 edition, 214 p.

Davies, G.R. and Nassichuk, W.W., 1990, Submarine cements and fabrics in Carboniferous to Lower Permian, reefal, shelf margin and slope carbonates, northwestern Ellesmere Island, Canadian Arctic archipelago: Geological Survey of Canada, Bulletin 399, 77 p.

Davies, G.R., Richards, B.C., Beauchamp, B. and Nassichuk, W.W., 1988, Carboniferous and Permian reefs in Canada and adjacent areas, *in* Geldsetzer, H.H.J., James, N.P. and Tebbutt, G.E., eds., Reefs, Canada and adjacent areas: Canadian Society of Petroleum Geologists, Memoir 13, p. 565-574.

Davies, P.J. and Hopley, D., 1983, Growth facies and growth rates of Holocene reefs in the Great Barrier Reef: BMR Journal of Australian Geology and Geophysics, v. 8, p. 237-252.

Davies, P.J. and Montaggioni, L.F., 1985, Reef growth and sea level change: the environmental signature: Proceedings of the Fifth International Coral Reef Symposium, Tahiti, v. 3, p. 477-511.

Davies, P.J., Marshall, J.F. and Hopley, D., 1985, Relationships between reef growth and sea level in the Great Barrier Reef: Proceedings of the Fifth International Coral Reef Congress, Tahiti, v. 3, p. 95-103.

Dill, R.F., Shinn, E.A., Jones, A.T., Kelly, K. and Steinen, R.P., 1986, Giant subtidal stromatolites forming in normal salinity waters: Nature, v. 324, p. 55-58.

Dunham, R.J., 1962, Classification of carbonate rocks according to depositional texture, *in* Ham, W.E., ed., Classification of carbonate rocks: American Association of Petroleum Geologists, Memoir 1, p. 108-122.

Dunham, R.J., 1970, Stratigraphic reefs versus ecologic reefs: American Association of Petroleum Geologists, Bulletin, v. 54, p. 1931-1932.

Eliuk, L., 1991, Siliceous sponge communities, biological zonation, and Recent sea level change on the Arctic margin, ice island results; discussion: Canadian Journal of Earth Sciences, v. 28, p. 459-462.

Embry, A.F. and Klovan, J.E., 1971, A Late Devonian reef tract on north-eastern Banks Island, N.W.T.: Bulletin of Canadian Petroleum Geology, v. 19, p. 730-781.

Esteban, M., 1979, Significance of the Upper Miocene coral reefs of the western Mediterranean: Palaeogeography, Palaeoclimatology, Palaeoecology, v. 29, p. 169-189.

Flügel, E. and Steiger, T., 1981, An Upper Jurassic sponge-algal buildup from the northern Frankenalb, West Germany: Society of Economic Paleontologists and Mineralogists, Special Publication 30, p. 371-397.

Flügel, E. and Stanley, G.D., Jr., 1984, Reorganization, development and evolution of post-Permian reefs and reef organisms: Paleontographica Americana, v. 54, p. 177-186.

Flügel, E. and Reinhardt, J., 1989, Uppermost Permian reefs in Skyros (Greece) and Sichuan (China): implications for the late Permian extinction event: Palaios, v. 4, p. 502-518.

Frost, S.H., 1981, Oligocene coral biofacies in the Vicentin, northeast Italy, *in* Toomey, D.F., ed., European reef models: Society of Economic Paleontologists and Mineralogists, Special Publication 30, p. 483-451.

Geister, J., 1980, Calm water reefs and rough water reefs of the Caribbean Pleistocene: Acta Paleontologica Polonica, v. 25, p. 541-556.

Ginsburg, R.N. and Schroeder, J.H., 1973, Growth and submarine fossilization of algal cup reefs, Bermuda: Sedimentology, v. 20, p. 575-614.

Graus, R.R. and Macintyre, I.G., 1989, The zonation patterns of Caribbean coral reefs as controlled by wave and light energy input, bathymetric setting and reef morphology: computer simulation experiments: Coral Reefs, v. 8, p. 9-18.

Graus, R.R., Macintyre, I.G., and Herghenroder, B.E., 1984, Computer simulation of the reef zonation at Discovery Bay, Jamaica: Hurricane disruption and long-term physical oceanographic controls: Coral Reefs, v. 3, p. 59-68.

Grotzinger, J.P., 1989, Facies and evolution of Precambrian carbonate depositional systems: emergence of the modern platform architype, *in* Crevello, P.D., Wilson, J.L., Sarg, J.F. and Read, J.F., eds., Controls on carbonate platform development: Society of Economic Paleontologists and Mineralogists, Special Publication 44, p. 79-106.

Hallock, P. and Schlager, W., 1986, Nutrient excess and the demise of coral reefs and carbonate platforms: Palaios, v. 1, p. 389-398.

Hileman, M.E. and Mazzulo, S.J., 1977, Upper Guadalupian Facies, Permian Reef Complex, Guadalupe Mountains, New Mexico and Texas: Permian Basin Section, Society of Economic Paleontologists and Mineralogists, Publication 77-16, 508 p.

James, N.P., 1981, Megablocks of calcified algae in the Cow Head Breccia, western Newfoundland: vestiges of a lower Paleozoic continental margin: Geological Society of America, Bulletin, v. 92, p. 799-811.

James, N.P. and Ginsburg, R.N., 1979, The seaward margin of Belize barrier and atoll reefs: International Association of Sedimentologists, Special Publication 3, 191 p.

James, N.P. and Gravestock, D., 1990, Lower Cambrian shelf and shelf margin buildups, Flinders Ranges, South Australia: Sedimentology, v. 37, p. 455-480.

Johnson, D.P. and Risk, M.J., 1987, Fringing reef growth on a terrigenous mud foundation, Fantome Island, central Great Barrier Reef, Australia: Sedimentology, v. 34, p. 275-288.

Kauffman, E.G. and Johnson, C.C., 1988, The morphological and ecological evolution of Middle and Upper Cretaceous reef-building rudistids: Palaios, v. 3, p. 194-216.

Kennard, J.M. and James, N.P., 1986, Thrombolites and stromatolites: two distinct types of microbial structures: Palaios, v. 1, p. 492-503.

Kershaw, S., 1979, Functional and environmental significance of skeletal morphology in stromatoporoids: Ph.D. thesis, Cardiff, University of Wales (unpublished).

Kobluk, D., 1975, Stromatoporoid paleoecology of the southeast margin of the Miette carbonate complex, Jasper Park, Alberta: Bulletin of Canadian Petroleum Geology, v. 23, p. 224-277.

Kobluk, D.R and Crawford, D.R., 1990, A modern hypersaline organic mud and gypsum-dominated basin and associated microbialites: Palaios, v. 5, p. 134-149.

Lees, A., 1988, Waulsortian "reefs": history of a concept: Mémoire Institut Géologique Université de Louvain, v. 34, p. 34-45.

Lees, A. and Miller, J., 1985, Facies variation in Waulsortian buildups, Part 2; Mid-Dinatian buildups from Europe and North America: Geological Journal, v. 20, p. 159-180.

Lees, A., Hallet, V. and Hibo, D., 1985, Facies variation in Waulsortian buildups, Part 1; a model from Belgium: Geological Journal, v. 20, p. 133-158.

Longman, M.W., 1981, A process approach to recognizing facies of reef complexes, *in* Toomey, D.F., ed., European fossil reef models: Society of Economic Paleontologists and Mineralogists, Special Publication 30, p. 9-40.

Lowenstam, H.A., 1950, Niagaran reefs of the Great Lakes area: Journal of Geology, v. 58, p. 430-487.

Macintyre, I.G., 1988, Modern coral reefs of western Atlantic: new geological perspective: American Association of Petroleum Geologists, Bulletin, v. 72, p.1360-1369.

Macintyre, I.G. and Glynn, P.W., 1976, Evolution of modern Caribbean fringing reef, Galeta Point, Panama: American Association of Petroleum Geologists, Bulletin, v. 60, p. 1054-1072.

McNeill, D.F., 1988, Initiation and development of tidal-inlet reef mounds, South Florida: Proceedings of the Sixth International Coral Reef Symposium, Australia, v. 3, p. 513-518.

Mesolella, K.J., Sealy, H.A. and Matthews, R.K., 1970, Facies geometries within Pleistocene reefs of Barbados, West Indies: American Association of Petroleum Geologists, Bulletin, v. 54, p. 1899-1917.

Messing, C.G., Neumann, A.C. and Lang, J.C., 1990, Biozonation of deep-water lithoherms and associated hardgrounds in the northeastern Straits of Florida: Palaios, v. 5, p. 15-34.

Montaggioni, L.F., 1988, Holocene reef growth history in mid-plate high volcanic islands: Proceedings of the Sixth International Coral Reef Symposium, Australia, v. 3, p. 455-460.

Moore, P.F., 1988, Devonian reefs in Canada and adjacent areas, *in* Geldsetzer, H.H.J., James, N.P. and Tebbutt, G.E., eds., Reefs, Canada and adjacent areas: Canadian Society of Petroleum Geologists, Memoir 13, p. 367-390.

Mullins, H.T., Newton, C.R., Heath, K. and Van Buren, H.M., 1981, Modern deep-water coral mounds north of Little Bahama Bank: criteria for recognition of deep-water coral bioherms in the rock record: Journal of Sedimentary Petrology, v. 51, p. 999-1015.

Neumann, A.C. and Macintyre, I.G., 1985, Reef response to sea level rise: keep-up, catch-up or give-up: Proceedings of the Fifth International Coral Reef Congress, Tahiti, v. 3, p. 105-110.

Palmer, T.J. and Fursich, F.T., 1981, Ecology of sponge reefs from the Upper Bathonian (Middle Jurassic) of Normandy: Palaeontology, v. 24, p. 1-25.

Pedley, H.M., 1979, Miocene bioherms and associated structures in the Upper Coralline Limestone of the Maltese Islands; their lithification and paleoenvironment: Sedimentology, v. 26, p. 577-593.

Playford, P.E., 1980, Devonian "Great Barrier Reef" of the Canning Basin, Western Australia: American Association of Petroleum Geologists, Bulletin, v. 64, p. 814-840.

Polmar, L., 1991, Reef geometries, erosion surfaces and high-frequency sea level changes, upper Miocene Reef complex, Mallorca, Spain: Sedimentology, v. 38, p. 243-270.

Pratt, B.R., 1982, Stromatolitic framework for carbonate mudmounds: Journal of Sedimentary Petrology, v. 52, p. 1203-1227.

Pratt, B.R. and James, N.P., 1982, Cryptalgal-metazoan bioherms of Early Ordovician age in the St. George Group, western Newfoundland: Sedimentology, v. 29, p. 543-569.

Rees, M.N., Pratt, B.R. and Rowell, A.J., 1989, Early Cambrian reefs, reef complexes, and associated lithofacies of the Shakleton Limestone, Transantarctic Mountains: Sedimentology, v. 36, p. 341-361.

Reid, P. and Ginsburg, R.N., 1986, The role of framework in Upper Triassic patch reefs in the Yukon (Canada): Palaios, v. 1, p. 590-600.

Riding, R., 1991, ed., Calcareous algae and stromatolites: Heidelberg, Springer-Verlag, 571 p.

Riding, R., Martin, J.M. and Braga, J.C., 1991, Coral-stromatolite reef framework, Upper Miocene, Almeria, Spain: Sedimentology, v. 38, p. 799-819.

Rowland, S.M. and Gangloff, R.A., 1988, Structure and paleoecology of Lower Cambrian reefs: Palaios, v. 3, p. 111-135.

Schafer, P., 1984, Development of ecologic reefs during the latest Triassic (Rhaetian) of the Northern Limestone Alps: Paleontographica Americana, v. 54, p. 210-218.

Schlager, W., 1981, The paradox of drowned reefs and carbonate platforms: Geological Society of America, Bulletin, v. 92, p. 197-211.

Schlager, W., 1990, Depositional bias and environmental change — important factors in sequence stratigraphy: Sedimentary Geology, v. 69, p. 109-130.

Scott, R.W., 1988, Evolution of late Jurassic and early Cretaceous reef biotas: Palaios, v. 3, p. 184-193.

Scott, R.W., Fernandez-Mendiola, P.A., Gili, E. and Simo, A., 1990, Persistence of coral-rudist reefs into the late Cretaceous: Palaios, v. 5, p. 98-111.

Searle, D.E. and Flood, P.G., 1988, Halimeda bioherms of the Swain Reefs, Southern Great Barrier reef: Proceedings of the Sixth International Coral Reef Symposium, Australia, v. 3, p. 139-144.

Shaver, R.H. and Sunderman, J.A., 1989, Silurian seascapes: water depth, clinothems, reef geometry, and other motifs — a critical review of the Silurian reef model: Geological Society of America, *Bulletin*, v. 101, p. 939-951.

Sheehan, P.M., 1985, Reefs are not so different — They follow the evolutionary pattern of level bottom communities: Geology, v. 13, p. 46-49.

Stanley, G.D., Jr, 1982, Triassic carbonate development and reef building in western North America: Geologische Rundschau, v. 71, p. 1057-1075.

Stanley, G.D., Jr., 1988, The history of Early Mesozoic reef communities: a three-step process: Palaios, v. 3, p. 170-183.

Stanley, G.D., Jr. and Cairns, S.D., 1988, Constructional azooxanthallate coral communities: an overview and implications for the fossil record: Palaios, v. 3, p. 233-242.

Stanton, R.J. and Flügel, E., 1989, Problems with reef models: the Late Triassic Steinplatte "reef" (Northern Alps, Salzburg/Tyrol, Austria): Facies, v. 20, p. 1-138.

Stearn, C.W., 1982, The shapes of Paleozoic and modern reef-builders: a critical review: Paleobiology, v. 8, p. 228-241.

Stoddart, D.R., 1969, Ecology and morphology of recent coral reefs: Biological Reviews, v. 44, p. 433-498.

Talent, J.A., 1988, Organic reef-building episodes of extinction and symbiosis? Senckenbergiana lethaea, v. 69, p. 315-368.

Tedesco, L.P. and Wanless, H.R., 1989, Role of burrow excavation and infilling in creating the preserved depositional fabric of Pennsylvanian phylloid mounds of southeastern Kansas, *in* Watney, W.L., French, J.A. and Franseen, E.K., eds., Guidebook for sequence stratigraphic interpretations and modelling cyclothems: Kansas Geological Society, p. 179-191.

Toomey, D.F. and Nitecki, M.H., 1979, Organic buildups in the Lower Ordovician (Canadian) of Texas and Oklahoma: Fieldiana, New Series, v. 2, 181 p.

Tudhope, A.W., 1989, Shallowing-upwards sedimentation in a coral reef lagoon, Great Barrier Reef of Australia: Journal of Sedimentary Petrology, v. 59, p. 1036-1051.

Van Wagoner, N.A., Mudie, P.J., Cole, F.E., and Daborn, G., 1990, Siliceous sponge communities, biological zonation, and Recent sea level change on the Arctic margin: Ice Island results: Canadian Journal of Earth Sciences, v. 26, p. 2341-2364.

Wahlman, G.P., 1988, Subsurface Wolfcampian (Lower Permian) shelf-margin reefs in the Permian Basin of west Texas and southeastern New Mexico, in Permian Rocks of the Midcontinent: Midcontinent Society of Economic Paleontologists and Mineralogists, Special Publication 1, p. 177-204.

Walker, K.R. and Alberstadt, L.P., 1975, Ecological succession as an aspect of structure in fossil communities: Paleobiology, v. 1, p. 238-257.

Wanless, H.R. and Tagett, R.P., 1989, Origin and dynamic evolution of carbonate mudbanks in Florida Bay: Bulletin of Marine Science, v. 44, p. 454-489.

Webby, B.D., 1984, Ordovician reefs and climate: a review, *in* Bruton, D.L., ed., Aspects of the Ordovician System: Paleontological Contributions from the University of Oslo, 8, p. 87-98.

West, R.R., 1988, Temporal changes in Carboniferous reef mound communities: Palaios, v. 3, p. 151-169.

Wood, R., 1990, Reef-building sponges: American Scientist, v. 78, p. 224-235.

Woodley, J.D., *et al.*, 1981, Hurricane Allen's impact on Jamaican coral reefs: Science, v. 214, p. 749-755.

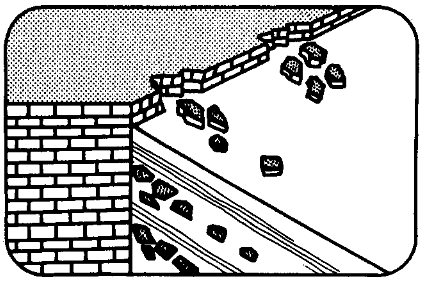

18. Carbonate Slopes

Mario Coniglio, Department of Earth Sciences, University of Waterloo, Waterloo, Ontario N2L 3G1

George R. Dix, Department of Earth Sciences, Carleton University, Ottawa, Ontario K1S 5B6

INTRODUCTION

Carbonate slopes encompass a suite of environments which pass seaward from shallow water, sunlit platform margins to the dark, deep, ocean basins. Accordingly, they are variably affected by changing seawater chemistry, temperature, pressure and biota with depth. Slopes also bear witness to extreme scales of sedimentary processes, from episodic and catastrophic margin collapse to quiet and persistent rain of fine-grained sediment. These environments are fundamental links in the carbonate facies spectrum. Their deposits are often the only record of the history of carbonate platforms that are now hidden, eroded, tectonized, dolomitized or metamorphosed. They contain a more complete sedimentary record of sea level change than adjacent, periodically exposed platforms as exemplified by the detailed record of Quaternary climatic variation. Finally, carbonate slopes are host to base metal and hydrocarbon deposits and have acted as conduits through which metalliferous and petroleum-rich fluids have migrated to platform host rocks (Cook, 1983; Eberli, 1988; Dix and Mullins, 1992).

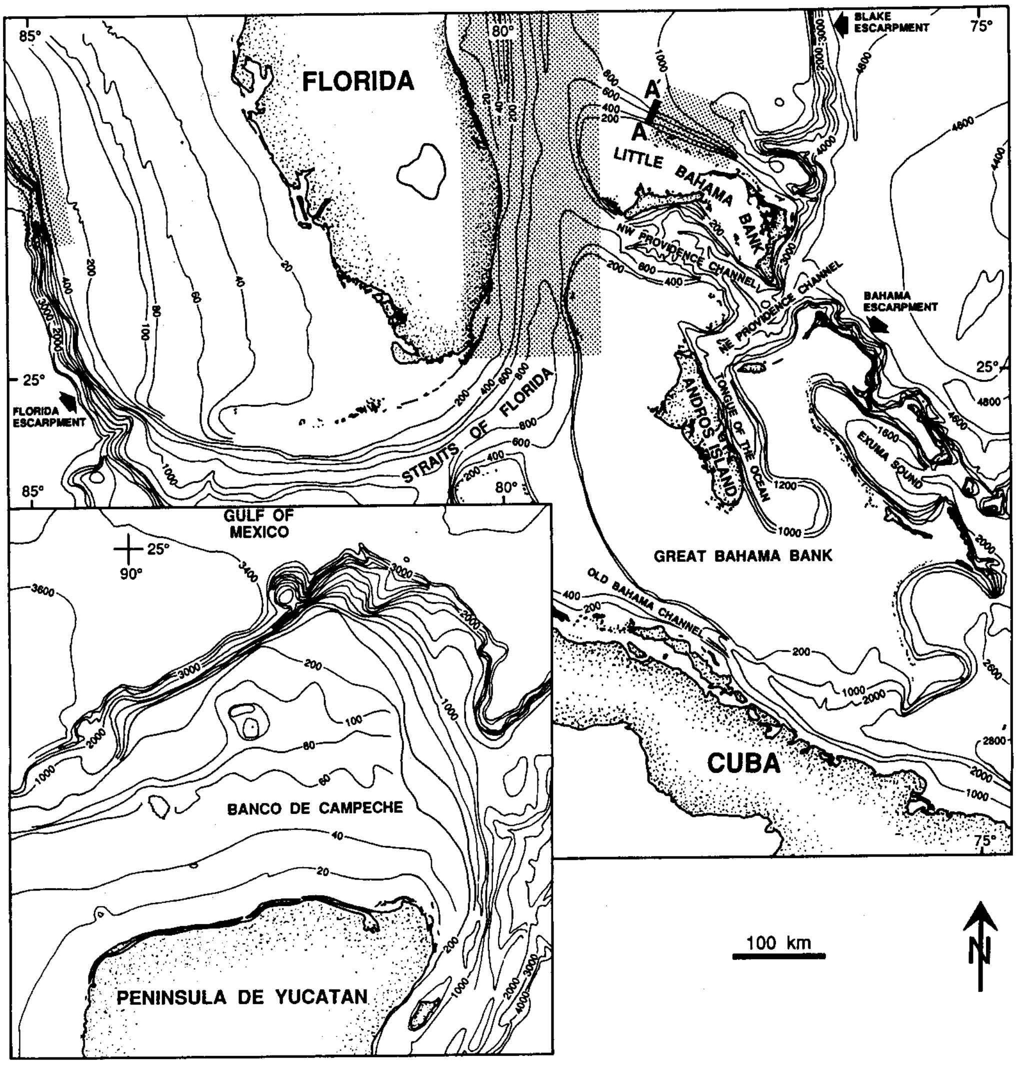

Figure 1 Bathymetry of Bahamas-Florida region and Banco de Campeche area. Stippled areas are shown in detail in Figures 5 (north of Little Bahama Bank), 11a (Straits of Florida), and 16a (west of Florida), respectively. Line A-A' is shown in Figure 13. Contours are in metres. Modified from Perry (1984).

Study of modern carbonate slopes has lagged behind research on shallow water and pelagic carbonates. Prior to 1985, the structure, stratigraphy and shallow subsurface lithology of this realm came from short (<12 m) piston cores, dredge hauls, bottom-sediment grab samples, seismic-reflection profiles, side-scan sonar, and underwater photographs supplemented by a few direct observations from submersibles. Carbonate slopes and platforms were initially excluded from the Deep Sea Drilling Project. Since 1985, however, the Ocean Drilling Program has provided a wealth of new seismic, pore water, and core data from across-slope transects of carbonate and mixed siliciclastic-carbonate slopes. Two areas with extensive drilling now include the northern Bahamas (Leg 101; Austin, Schlager *et al.*, 1986, 1988) and the Great Barrier Reef, Australia (ODP Leg 133 Scientific Party, 1991; Davies, McKenzie *et al.*, in press).

The best studied carbonate slopes in today's oceans are those in the northern Bahamas-Florida region (Fig. 1), augmented by more local studies in Belize, Jamaica, Grand Cayman, and several atolls in the Pacific and Indian oceans. These slopes provide good actualistic models with which to interpret ancient carbonate slopes. Unfortunately, they are all essentially pure carbonate depositional systems, in contrast to many ancient slope deposits which include a large percentage of terrigenous clastic rocks. Whether this disparity is important awaits research associated with recent deep-ocean drilling off northeast Australia along the largest modern pericontinental mixed carbonate-siliciclastic platform margin (Davies, McKenzie *et al.*, in press). Actualistic modelling is further hampered because 1) Cenozoic and Mesozoic carbonates are unlike older sediments in terms of platform or pelagic sediment mineralogy (Wilkinson, 1979), 2) although a few ancient submarine carbonate fans have been documented, no modern equivalents have been described, and 3) until recently, slopes along modern carbonate ramps were poorly documented.

In this chapter we examine the products and processes that characterize carbonate slopes and discuss a variety of facies models. A fundamental precept throughout is that the geometry and preserved sedimentary record of carbonate slope deposits are inextricably linked to the evolution of the adjacent shallow water platform or ramp. Actualistic input into the models is drawn mainly from the Bahama-Florida region. Data from ancient slope successions are used to temper and refine the actualistic bias, and bring to light aspects of slope sedimentation that now can only be viewed dimly through a curtain of burial diagenetic effects, tectonic deformation or paleoceanographic conditions that are not replicated in today's oceans.

SLOPE TYPE AND MORPHOLOGY

The shape, orientation, size and facies of a carbonate slope are linked to a variety of intrinsic and extrinsic factors (Fig. 2), their interplay leading to important differences when compared to siliciclastic slopes (Table 1).

Slope types

Differences in slope gradient are influenced by sediment budget (gain versus loss) and/or locus of deposition. *Depositional* or accretionary slopes demonstrate net accumulation (Figs. 3,4). The locus of sedimentation can be 1) along the upper slope, with sediment thickness decreasing seaward, or 2) distal from the platform edge, in which case the bulk of sediments *bypass* the upper slope. Individual slopes may have bypass (including erosional) and depositional segments. For example, the northern slope off Little Bahama Bank has a steep upper portion eroded by vigorous turbidity currents and a gentle lower segment, where products of mass wasting come to rest, explaining, at least in part, the typical concave profiles of some carbonate slopes. The upper part of the southwest Florida slope, in contrast, is the site of abun-

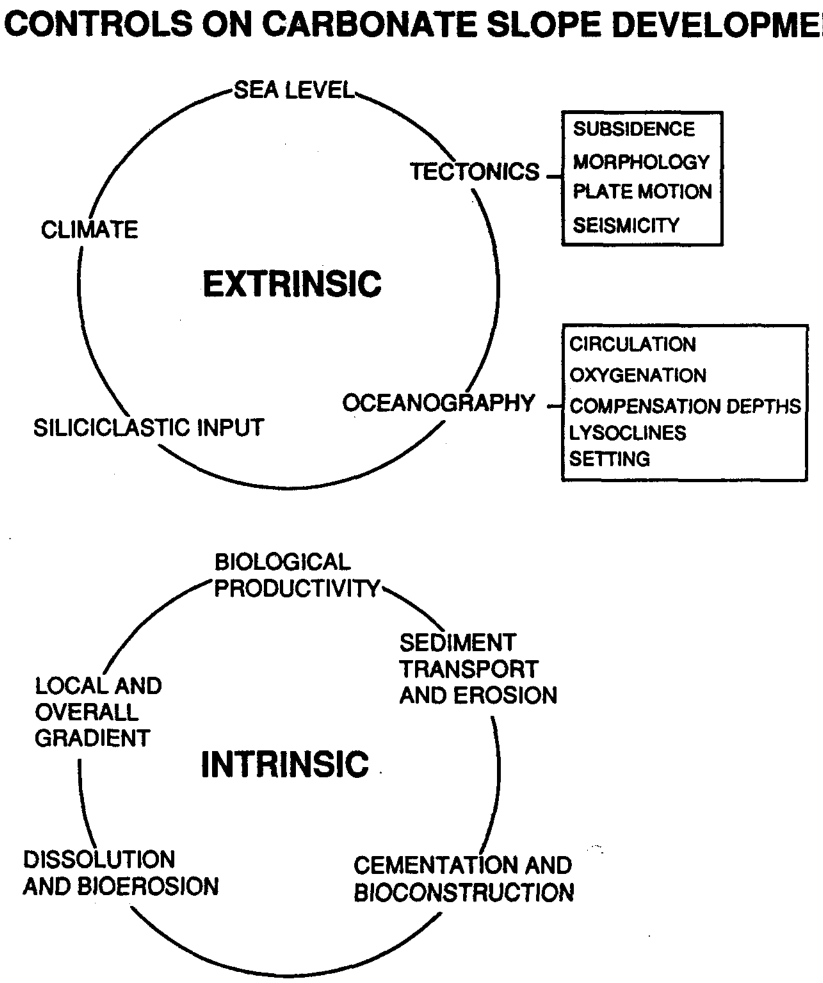

Figure 2 Extrinsic and intrinsic controls on carbonate slope development.

dant sedimentation and intermittent gravity flow transport but the lower slope is the site of erosional gullies and sediment bypassing.

Erosional slopes illustrate net sediment loss. On seismic profiles, they are characterized by truncated reflectors and relatively steep gradients (Fig. 3). Such slopes adjacent to actively producing, shallow water platforms are also bypass in nature, with sediment accumulating at the base where it can be reworked by bottom currents or dissolved. Slide masses and large fallen blocks that accumulate within cones of talus at the base of erosional and bypass slopes may act as local dams preventing finer grained sediment from

Table 1 *Comparison of carbonate and siliciclastic slopes.*

	Carbonate Slopes	**Siliciclastic Slopes**
Nature of sediment	platform, pelagic, hemipelagic	pelagic and hemipelagic
	turbidity currents occur during shallow flooding of adjacent platform	turbidity currents occur during lowstands
Response to platform emergence	shutdown carbonate factory, pelagics dominate periplatform ooze	slope erosion and offlap, more sand to slope
Response to platform submergence	drowned margin facies contribute to slope	stranded sand bodies, fine-grained sediments prevail
Sediment dispersal pattern	point source rare; more common line source from numerous shallow gullies in upper slope	large submarine canyons form point source with resultant formation of submarine fans
Constructions	base of slope aprons (erosional or bypass slopes), slope aprons (depositional slopes) next to rimmed or open platforms; rare submarine fans	submarine fans common
Success of actualistic facies models	difficult to apply to Triassic and older slopes and slopes with significant terrigenous component	application is relatively straightforward
Slope angles	relatively high (avg. 5-15°), increases with height	relatively low (avg. 3-6°), does not increase with height
Slope profiles	concave	slightly convex or straight
Response to to upper slope erosion	reefs can repair damaged margin	lack repair mechanism
Potential for oversteepening	high — as slopes become steeper they become more easily cemented in marine environment (positive feedback)	low — lack of lithificiation results in slumping that effectively prevents oversteepening
Submarine cementation	common, allows oversteepening with resultant catastrophic collapse	uncommon
Pressure solution	tends to remove primary sedimentary structures on beds tops and bottoms such as sole marks and diagnostic ichnofossils	not significantly affected
	penetrative clast contact fabrics in conglomerates may result from pressure solution	less likely to show pressure solution interpenetration depending on clast lithology
Affect of calcite and aragonite compensation depths	dissolution can occur on lower slopes, lowering seafloor and increasing topographic gradient and potential for failure	dissolution does not occur
Diagenetic beds	beds can be created by diagenetic unmixing of carbonate	diagenetic beds do not occur except locally in carbonate-rich parts of some successions
Nodular beds	common (primary and diagenetic)	common primary (isolated ripples, load casts, etc.) rare diagenetic nodules (concretations) in carbonate-rich parts of some successions

moving downslope.

Escarpments along some erosional slopes or bypass margins attest to removal of significant volumes of material. The shelf edge along the Mesozoic carbonate platform of eastern North America, for example, was cut back in places up to 30 km (Jansa, 1981). Erosional slopes such as the Blake, Bahama and west Florida escarpments may have retreated landward as much as 5 to 15 km (Fig. 1; Mullins *et al.*, 1986). These steep slopes are due to faulting, erosion by contour currents, carbonate dissolution by corrosive bottom waters and acidic brine seeps, and mechanical weakening caused by organisms which bore into, dissolve, or disaggregate the rockface (Paull *et al.*, 1990; Twichell *et al.*, 1990). Escarpments can also develop from sliding and gravity current erosion initiated by sediment overload.

Erosional slopes have the lowest preservation potential and their existence must be inferred from abundant slope-derived material that is preserved in more distal facies. The more complete record afforded by depositional slopes provides practically all of the information obtained on ancient carbonate slope successions and much of what is known from modern carbonate slopes.

Slope morphology

Modern carbonate slopes are generally steeper than their terrigenous counterparts (Table 1). Modern carbonate slopes tend toward concavity with the angle of the upper slope increasing with slope height. The slope north of Little Bahama Bank, for example, is steepest near the top (≈4° in 200-900 m water depth) and more gentle below (1-2°; Fig. 5a). Carbonate slopes adjacent to open platforms with relatively deep margins ("distally-steepened ramp" *sensu* Read, 1985) resemble siliciclastic slopes in profile (e.g., west Florida, Banco de Campeche; Fig. 1).

Steepening of a carbonate slope, particularly the upper slope, can result from 1) organic binding and framework building by reef-forming organisms, 2) submarine cementation, and 3) shallow subsurface lithification. Early lithification may act to delay large-scale failure. Other factors that can control slope gradient include 1) inheritance of predepositional paleoplatform margin morph-

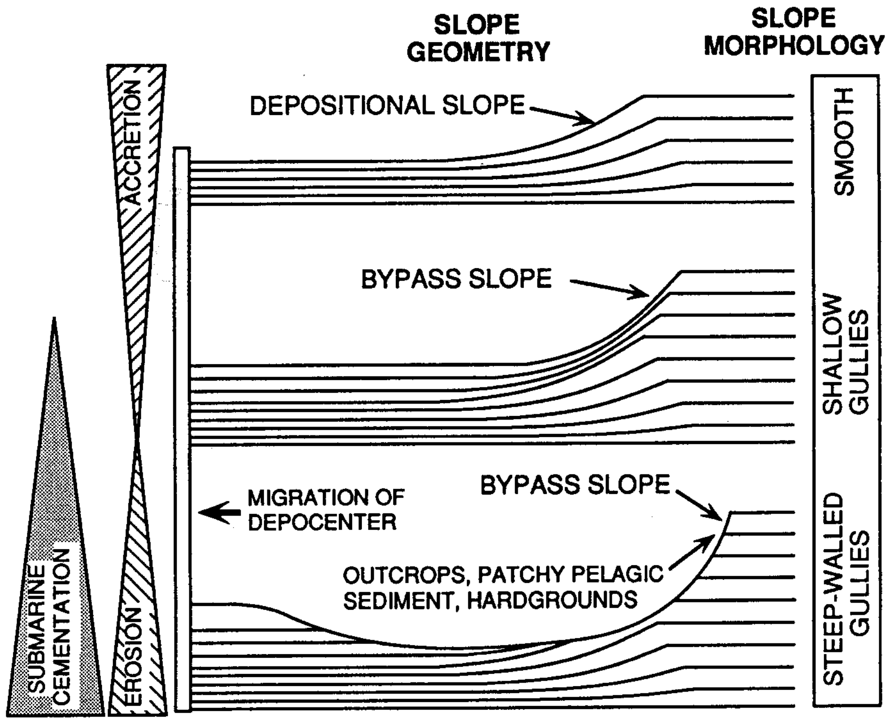

Figure 3 Relationship between slope geometry, morphology, sediment budget, and propensity for seafloor lithification based on Bahamas and ancient platforms. Modified from Schlager and Camber (1986).

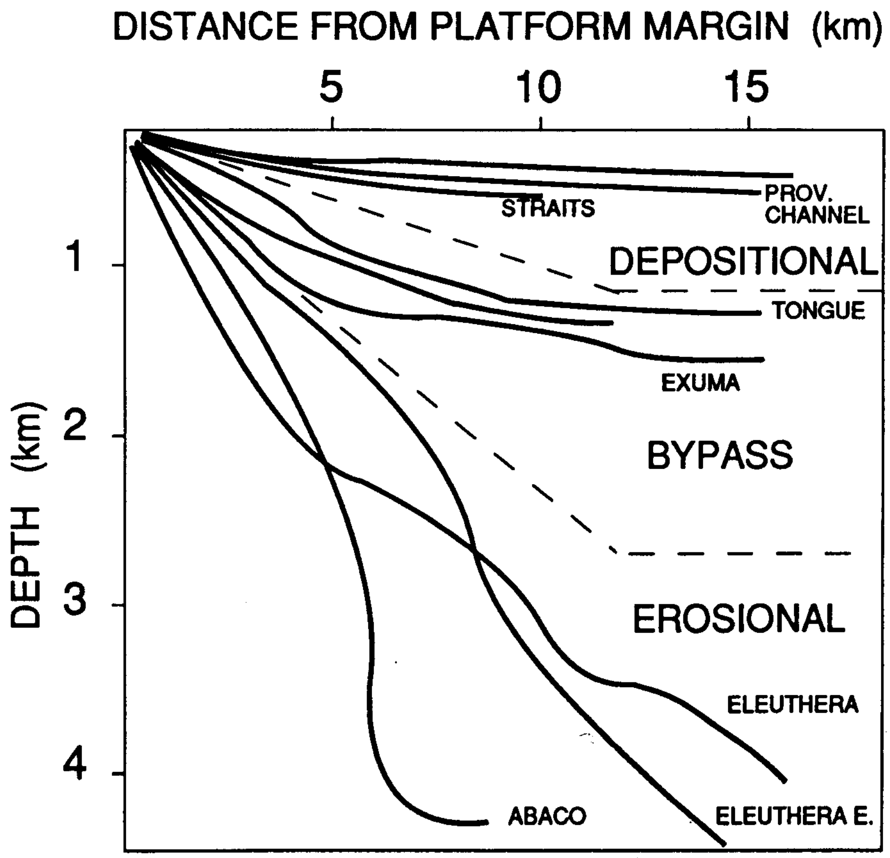

Figure 4 Bathymetric profiles of various Bahamian platform slopes and relation to depositional regime. Modified from Schlager and Ginsburg (1981).

ology, especially along collapsed margins or rimmed platforms, 2) shallow water reefs attempting to migrate upslope during sea level rise, thus forming areas of slightly elevated bathymetry on slopes, and 3) sediment fabric. Kenter (1990) noted that gradients are steeper (30-40°) for sediments with cohesionless, grain-supported fabrics (with or without mud), than those of paleoslopes dominated by mud-supported, cohesive fabrics (<15°). Pure muds have slope angles of less than 5°.

One important characteristic of many modern carbonate slopes is the presence of numerous parallel incised gullies, oriented perpendicular to the margin (Fig. 5a,b). Such gullies form by erosion associated with downslope gravity flows. Once incised, a gully will perpetuate itself by acting as a conduit for further flows. The presence of a gullied slope has three important implications, 1) numerous parallel gullies form a *line source* of sediment supply from the platform and upper slope to the lower slope (Schlager and Chermack, 1979), 2) facies belts will be parallel to the platform margin, and 3) specific facies will be restricted to certain portions of a developing slope.

SEDIMENT TYPES

Slope sediments have several origins: pelagic, platform, hemipelagic, and in situ or autochthonous carbonate. Relative proportions vary spatially and temporally according to 1) proximity to continental hinterland, 2) proximity and productivity of the shallow water "carbonate factory", 3) latitudinal changes of tectonic plates which may promote or impede carbonate production (e.g., Davies *et al.*, 1989), 4) biologic evolution, especially affecting the source role of pelagic biota and reef-building organisms, 5) locus of deposition of platform-derived sediment, 6) oceanographic setting. Intermixed platform-derived and pelagic carbonate muds have been named *periplatform ooze* analogous to their pelagic counterpart (Schlager and James, 1978), and commonly consist of a mixture of aragonite and various Mg-calcites. We use the more general term *periplatform* carbonate to refer to sediment which contains similar mixed sources, regardless of grain size.

The sedimentary input, preserved at the seafloor, is also governed by the ambient saturation state of overlying seawater relative to the carbonate minerals, aragonite, calcite and Mg-calcite. For each mineral, chemical oceanographic gradients are expressed by a *lysocline,* or depth at which dissolution rates increase markedly, and a *compensation depth*, or depth at which rate of supply equals rate of dissolution. These critical depths vary globally according to temperature as controlled by latitude and water depth; changing pCO_2 associated with depth and different water masses; influx of individual carbonate mineralogies; influx of terrigenous sediments; and deep ocean circulation patterns (see Scholle *et al.*, 1983b). A decrease in temperature and rise in pCO_2 causes the lysocline and compensation depths to shallow. Intersection of these oceanographic chemical gradients with the sediment-water interface results in downslope changes in the diagenetic alteration potential proportional to the mixture of aragonite and Mg-calcite in periplatform carbonate. Despite a reasonable understanding of the chemical dynamics of seawater (Morse and Mackenzie, 1990), a more difficult problem to solve is exactly how much dissolution and removal of metastable minerals has occurred prior to burial.

Pelagic sediment

The term *pelagic* means "of the open sea", and excludes shallow platforms, reefs and other reef-associated settings (Jenkyns, 1986). Pelagic sediments in the modern ocean are restricted to deep basins, and are mixed with platform-derived sediment along platform margins (Scholle *et al.*, 1983b). Pelagic particles are typically less than a few micrometres to a few tens of micrometres in size and consist predominantly of the calcareous and siliceous skeletal remains of zooplankton and phytoplankton. Accumulating on the seafloor, they form *pelagic ooze*. Noncarbonate grains include diatoms, radiolarians, volcanic detritus, cosmogenic detritus (tektites), and authigenic mineral precipitates. Pelagic sediments are siliceous or dominated by red clays below the calcite compensation depth (Atlantic ≈ 5500 m; Pacific ≈ 4500 m).

Modern pelagic carbonates contain

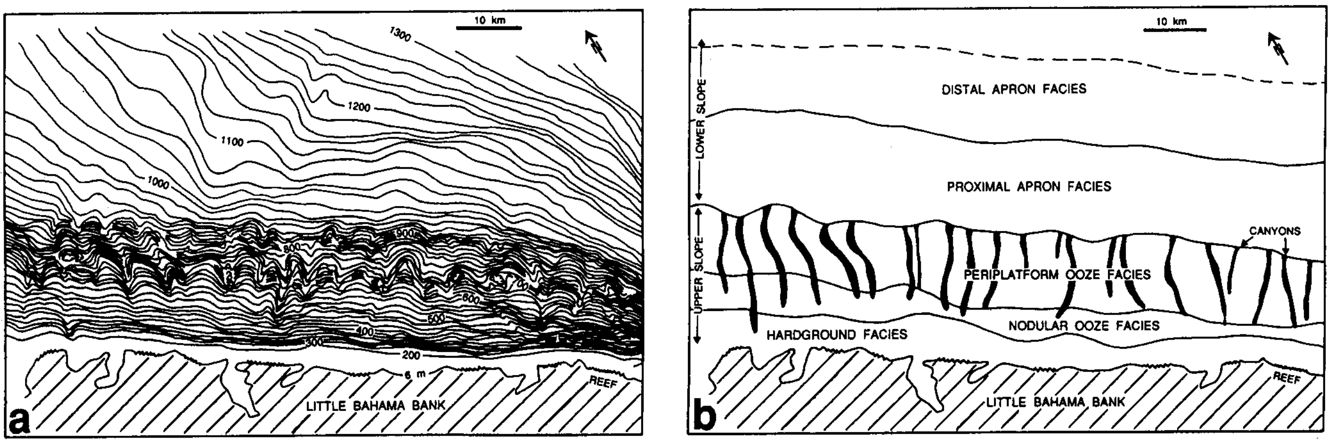

Figure 5 Slope north of Little Bahama Bank. Location is shown in Figure 1. Modified from Mullins *et al.* (1984). a) Bathymetric map with contours in metres showing steep upper slope (200-900 m) dissected by numerous gullies and gentle lower slope (900+ m). Closed contours in upper slope are submarine slide scars. b) Open ocean, near surface, sedimentary facies showing transition from upper slope hardgrounds through nodular ooze and gullies to lower slope gravity flow facies.

two end members, 1) *nannofossil ooze*, dominantly composed of the broken (<20 μm) and whole (<100 μm) coccolithophorids (planktonic algae), and 2) *foraminiferal ooze*, predominantly composed of planktonic foraminifers typically ranging from 1-2 mm in size. Both of these components are calcite. Aragonitic planktonic gastropods, or pteropods, reach a few millimetres in length and locally contribute significantly to the calcareous pelagic fraction. Sedimentation of planktonic microfossils is assisted by their ingestion by predatory organisms in the surface waters and subsequent transfer to the ocean floor within fecal pellets. *Pelagic calcareous sediment has been volumetrically important only since Jurassic time, coincident with the appearance of planktonic foraminifers and coccolithophorids.* Thus, Pre-Jurassic pelagic facies are typically radiolarian-rich, siliceous ooze or shale. Nautiloids, tentaculitids, and styliolinids, although common, were volumetrically minor sediment contributors.

Platform carbonate

Typically off-platform transport of shallow water allochems contributes varying proportions of mud-size algal and inorganically precipitated aragonite needles, blades of Mg-calcite and aragonite, mud- to sand-sized skeletal and nonskeletal debris, lithoclasts, and bioeroded particles (e.g., sponge chips). Locally, coarser periplatform sediments contain gravels and boulder-sized lithoclasts derived from shallow water facies or carbonate bedrock. Due to the absence of calcareous pelagic sediment in pre-Jurassic time, older slope carbonates are mostly platform-derived sediment. Diagenetic alteration, however, all but eliminates a clear understanding of the origin of this very fine-grained sediment.

Modern platform-derived carbonate is hybrid in its mineralogy. Relative proportions of aragonite, calcite and Mg-calcite vary according to the productivity of the carbonate factory as controlled by sea level, biotic composition of the shallow water facies, and distance from the shallow platform margin. Seaward transport of platform-derived sediment may be on the order of hundreds of kilometres if carried by oceanic currents. North of Little Bahama Bank, half of the sedimentary constituents in surface sediment 50 km from the bank margin are bank derived, and bank-derived material can be detected at distances 120 km from the platform (Heath and Mullins, 1984).

Hemipelagic terrigenous clastics

The term *hemipelagic* is used here to refer to fine-grained terrigenous material that enters the marine system at the coast, either by coastal erosion or fluvial transport (Pickering *et al.*, 1989). These terrigenous, usually clay-sized particles, are transported by water or wind across the shelf and deposited on the slope to form terrigenous "background" sediment. In modern carbonate slopes, the clay-sized particles are thoroughly mixed with carbonate sediment.

Hemipelagic terrigenous clastics can travel great distances along the slope margin prior to deposition, carried by deep water currents. One of the best ancient examples in Canada is the Upper Devonian Ireton Formation (Western Canadian Sedimentary Basin), which consists of a mixed siliciclastic-carbonate facies that forms a basin fill enveloping facies around Leduc Formation platform carbonates (Stoakes, 1980). Modern hemipelagic clays form muddy sediment drifts within the southern Straits of Florida between Cuba and Florida (Brunner, 1986). Hemipelagic clays can also form discrete clay-rich beds sandwiched between periplatform carbonate, as found in Pleistocene strata north of Little Bahama Bank (Austin, Schlager *et al.*, 1986). Off northeast Australia, hemipelagic sediment forms a volumetrically important constituent along the slope immediately seaward of the Great Barrier Reef, transported seaward across the exposed epicontinental platform during sea level lowstands as well as carried along strike of the slope via currents (Davies, McKenzie *et al.*, in press).

Autochthonous carbonate

Included in this category are fecal pellets derived from epifauna and infauna, seafloor Mg-calcite cement, peloidal Mg-calcite cement precipitated within foraminifer tests, and skeletal debris associated with biota indigenous to the slope environment. Siliceous sponge spicules form a locally important supply of noncarbonate sediment. Deep water mounds, a common facies in some slope settings, are described in Chapter 17.

DEPOSITIONAL PROCESSES AND PRODUCTS

Sediment is transported to and accumulates within the slope setting by suspension settling, gravity (resedimented) flow, rock fall, and submarine creeping and sliding. Also important are bottom currents which can winnow and rework these deposits, or prevent accumulation entirely, resulting in periods of no net accumulation during which submarine dissolution or lithification is active.

Suspension settling facies

Whereas pelagic sediment accumulates from a continuous rain of individual particles or fecal pellets falling through the water column, fine-grained platform-derived particles are transported off the shallow water platform by oceanic processes (tidal flux, storms, and oceanic currents), forming concentrated to dilute sediment-seawater mixtures (Fig. 6). These plumes can dissipate, in which case material

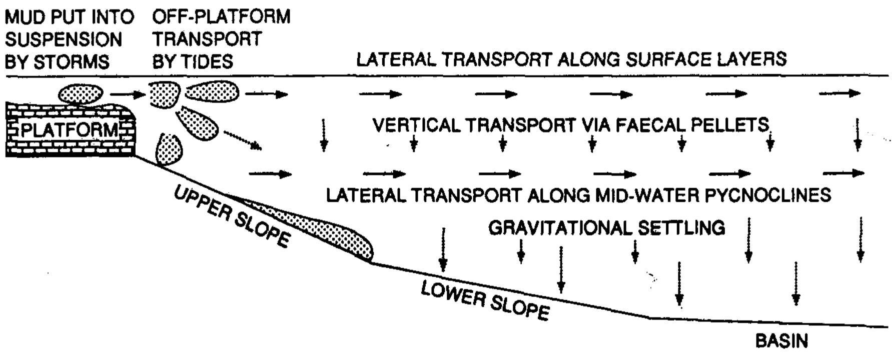

Figure 6 Schematic diagram illustrating modes of vertical and lateral transport of platform-derived fine-grained carbonate. Modified from Heath and Mullins (1984).

rains down to the seafloor, or moves downslope as unconfined and confined dilute turbidity currents (lutite flows). Such flows can also move along mid-water density interfaces from which sediment rains down on the basin floor. These plumes also form along the slope during mass wasting.

Recognition of suspension deposition in ancient slopes can be difficult, especially where diagenetic overprinting obliterates textural evidence. Yet, a common facies association in many ancient slope sequences is interbedded, finely crystalline, dark grey to black, lime mudstone and shale, forming evenly and continuously rhythmic sequences (Figs. 7a; 8a,b). In places where the carbonate is finely laminated, suspension deposition may have occurred within an oxygen minimum zone which limited bioturbation. Oxygenated slopes are commonly intensively bioturbated, obliterating primary sedimentary laminations and possibly encouraging the formation of nodular bedding.

Sediment gravity flow facies
Deposition from these relatively high-energy events is essentially instantaneous with reduced flow competency. Several types of gravity flow mechanisms may operate during the downslope journey.

Turbidites
These gravity flows, which can originate on the platform margin and rework sediment anywhere along the slope, can be unconfined or laterally confined and extend for many kilometres onto the lower slope and out onto the adjacent basin floor. Distinguishing distal parts of fine-grained turbidites from suspension sediments, whether platform-derived or pelagic in origin, can be difficult. Turbidite thickness varies from a few centimetres to several metres. In ancient carbonate slope successions, turbidites are commonly interbedded with shale (Figs. 7b, 9). Such deposits, however, must be carefully distinguished from sediments deposited by contour currents (see below). Application of the Bouma turbidite divisions is quite successful in understanding flow regimes in most calciturbidites. Pressure solution initiated during burial diagenesis greatly decreases the preservation potential of bedding surface structures, especially in carbonate-shale sequences, resulting in common abrupt carbonate-to-shale transitions.

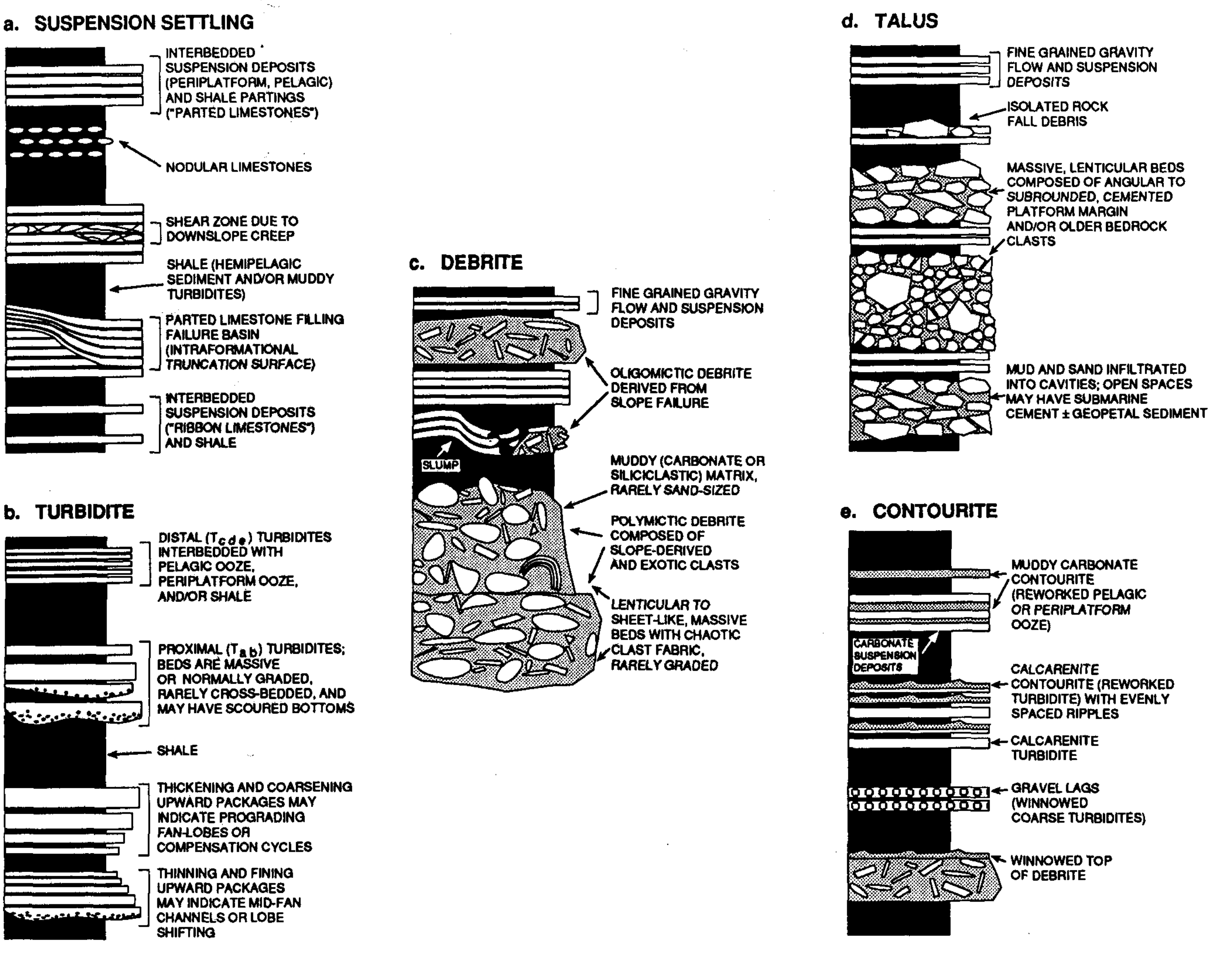

Figure 7 Generalized hypothetical sequences for various slope facies. Scale is variable, ranging from 5 cm thick beds for fine-grained suspension deposits to debrites and talus beds up to several tens of metres in thickness.

Grain flow deposits

An inverse grading in thin (<5 cm) beds created by dispersive pressure induced by grain to grain interaction is predicted for depositional units deposited by grain flow. The importance of this process in modern or ancient carbonate slope deposits is uncertain because so few have been described (Mullins, 1983).

Debrites and conglomeratic deposits

Massive, thick slope limestone conglomerates have been called debrites, debris sheets or avalanches, olistostromes, and mass breccia flows (Pickering *et al.*, 1989). True debris flows have a mud and water matrix characterized by a combined strength and buoyancy that allows the flow to carry clasts that are denser than the bulk density of the flow itself (Middleton and Hampton, 1976). Many so-called "debrites" (the deposits of debris flows) have a granular matrix that is noncohesive; more likely transport mechanisms in these cases are turbulence and grain interactions. Modern examples indicate that debris flows can travel large distances, up to

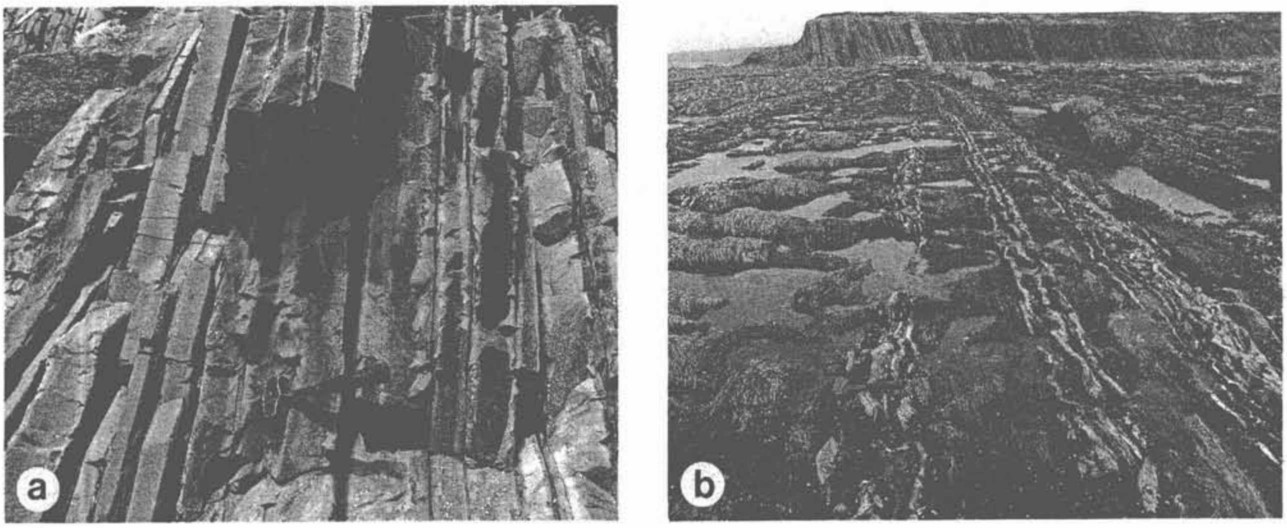

Figure 8 Field photographs illustrating examples of fine-grained, deep water, carbonate-shale facies, Cambro-Ordovician Cow Head Group, western Newfoundland. From Coniglio and James (1990), published with permission of Blackwell Scientific Publications. Stratigraphic top is toward left. Hammer for scale. a) Continuously bedded, parted lime mudstones separated by thin shale partings. b) Continuously bedded, ribbon limestones extending for hundreds of metres without change in thickness or fabric. These finely laminated to massive beds are interbedded with turbiditic and hemipelagic shale.

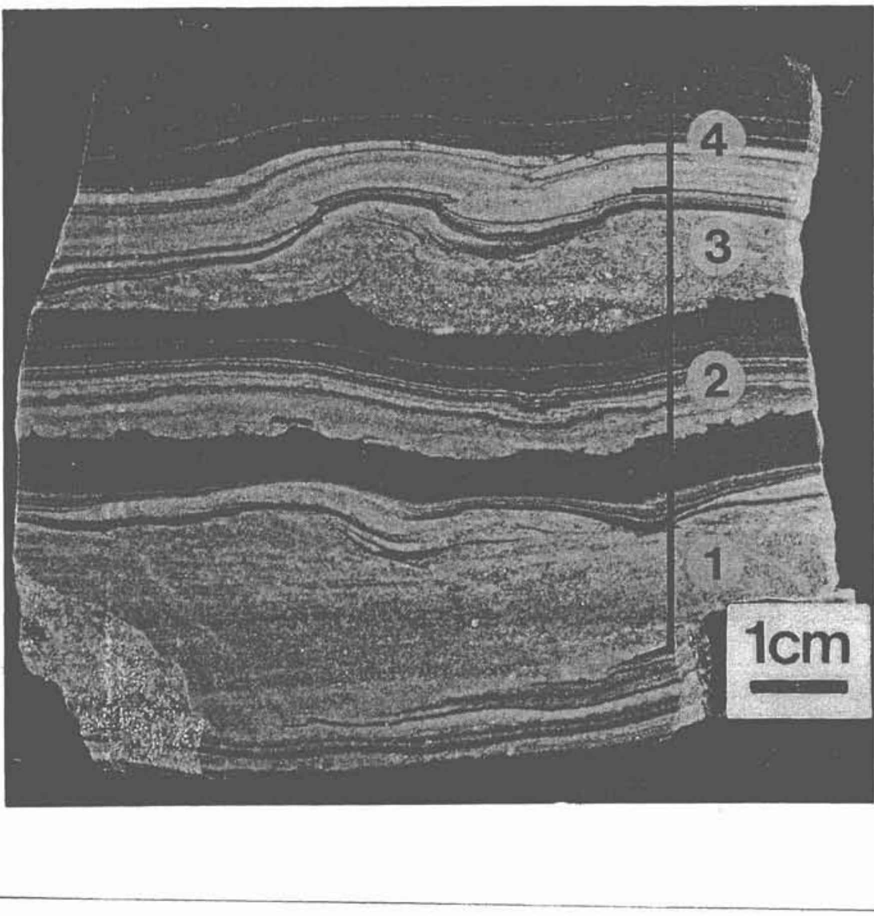

Figure 9 Slab of completely dolomitized carbonate turbidites interbedded with shale. Layer 1 illustrates basal scour and upward gradation into fading ripples which pass laterally into muddy (shale) troughs; this is overlain by shale. Layer 2 shows a massive loaded basal division overlain by a division of graded laminations and then shale. Layer 3 has a distorted massive basal division of dolomitized calcarenite which grades rapidly upward to dolomitized calcisiltite with fading ripples. Layer 4 shows parallel-laminated dolomitized calcisiltite followed by graded laminations and then shale. Cow Head Group, western Newfoundland. From Coniglio and James (1990), published with permision of Blackwell Scientific Publications.

100 km away from their source.

Debrites range from a few decimetres to several tens of metres in thickness. Thicker beds may be the result of amalgamation of two or more flows but such amalgamated beds are usually difficult to recognize. Most debrites and similar deposits are sheet-like in three dimensions. Lenticular beds are common locally, and their margins may be abrupt, steep and lobate, or form feather edges due to gradual pinch out. The base of a debrite can be erosional and sharply defined, but conformable contacts are common and may occur even where underlying beds are finer grained. Injection structures resulting from loading are typically preserved in thicker flows. Sole marks are rare. Upper contacts are abrupt or pass upward into parallel and rippled turbidites that probably resulted from the same flow event (e.g., Krause and Oldershaw, 1979). Tops may be planar or hummocky, the latter formed by large projecting boulders.

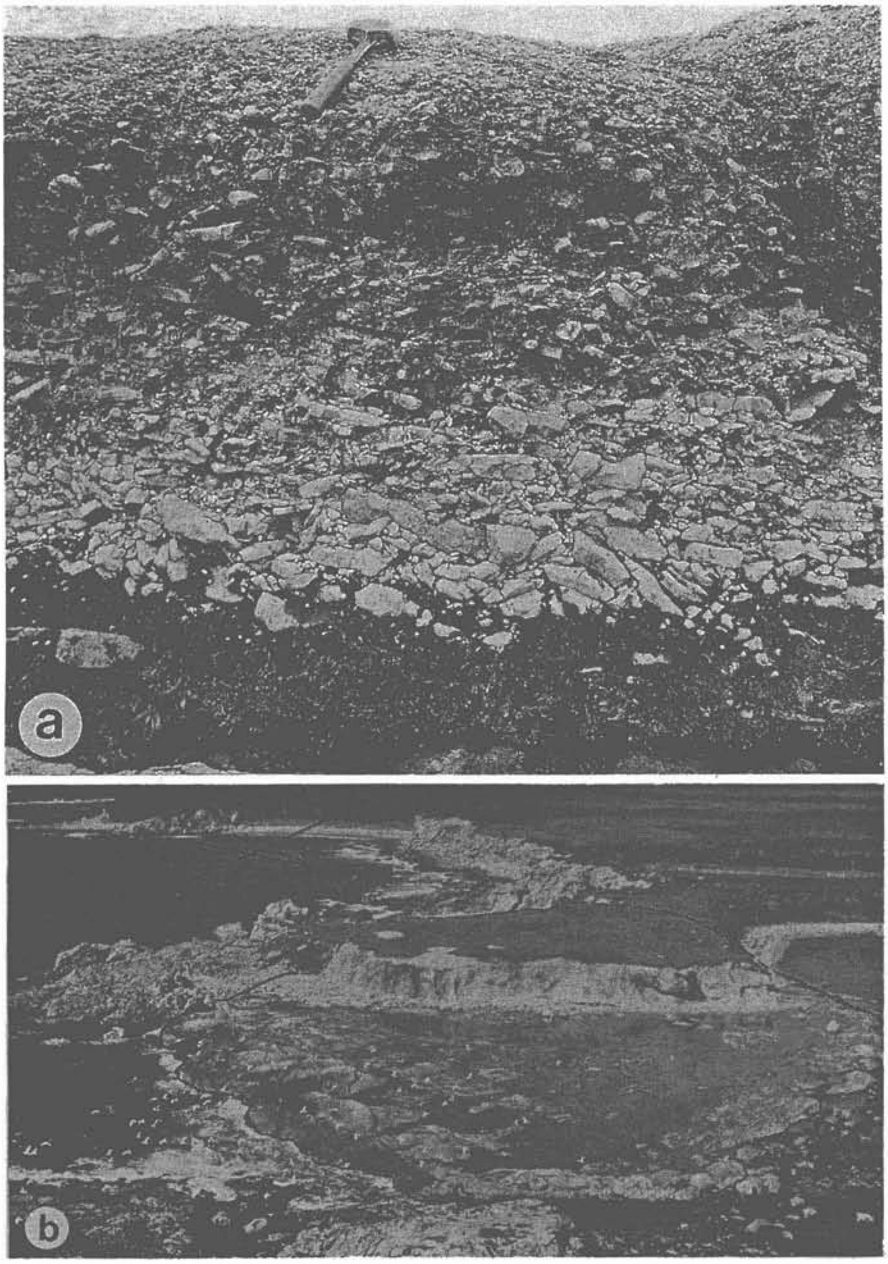

Figure 10 Conglomeratic beds of the Cow Head Group, western Newfoundland. a) Conglomerate with calcarenite matrix demonstrates exceptionally well-preserved normal grading of clasts. Packing fabric varies from clast-supported to condensed by pressure solution. Tabular aspect decreases with decreasing clast size. Hammer for scale. b) Oblique aerial photograph illustrating "magabreccia" bed exposed along the intertidal platform in Gros Morne National Park. The small cliff at the centre of the photograph is 8 m high and is developed in the "alpha boulder", a 50+ m clast composed of a biohermal facies (now forms grass-covered hill above cliff) and an off-reef calcarenite (now forms low-tide platform in foreground). This coarse bed is interpreted to have accumulated at the toe-of-slope and may be a debris flow or talus deposit. Photograph courtesy N. Hames.

These deposits are typically poorly sorted, lack stratification, and are described as having a random or chaotic clast arrangement (Fig. 7c). There are, however, examples of normal (Fig. 10a) and reverse grading, clast alignment near the base, sides or top of the deposits, local clast imbrication, and swirled domains in which clasts display a gradual change in flat clast orientation. Clast packing is also variable with both framework- and matrix-supported deposits being common. Modification of depositional fabric via pressure solution (based on stylolite occurrences) is common and results in an interpenetrating or condensed clast fabric. Clasts are rounded to angular, and sizes vary from gravel- to house-sized boulders with maximum clast size and bed thickness commonly being correlated (Fig. 10b). Recent work off the Nicaraguan Rise in the Caribbean Sea has shown 100 m-blocks of platform margin/slope facies incorporated into enormous mass flow megabreccias that extend for 16 km downslope, 28 km along slope and reach 100 m in thickness (Hine *et al.*, 1991).

Matrix varies from any combination of fine-grained carbonate (including silt- and sand-sized particles) to terrigenous mud. Because debris flows move across pre-existing slope sediment, the matrix can contain reworked slope sediment. The positive relief of debris flows allows their surfaces to be winnowed by strong bottom currents, producing interparticle spaces that can subsequently become filled with submarine cement and/or younger infiltrated sediment.

Proximity to the paleomargin is commonly indicated by the most abundant and thickest conglomerates, with the largest sizes and variety of clasts. Polymictic conglomerates result from the mixing of platform-derived exotic clasts (which may be variable themselves) with slope-derived clasts and matrix. Oligomictic conglomerates are almost always the result of erosion and redeposition of slope limestone in the form of tabular clasts (limestone chips) and interparticle matrix. The slope origin of limestone chips is difficult to prove, but can be inferred by microfacies similar to in situ slope limestones. Rafts of coherently bedded, slope-derived limestone several tens of metres in size are identical to in situ slope limestones. During progressive downslope transport, these rafts become fragmented to yield matrix and tabular clasts. Soft-sediment folding, faulting, fracture cleavage formation and brecciation characterize such rafts and lucidly illustrate the high degree of limestone lithification relative to the plastically deformed, argillaceous interbeds.

Talus facies

Talus forms downslope-widening conical accumulations along the top of the slope, below steep upper forereef escarpments (e.g., James and Ginsburg, 1979; Colacicchi and Baldanza, 1986), and along the base of canyon walls and fault scarps (Cook and Mullins, 1983). Individual blocks can also be left stranded on the slopes and, depending on their size, form local bathymetric highs. Talus blocks probably fall freely or tumble into place. Merging of adjacent talus cones forms a distinctive but narrow facies belt. Few ancient examples of talus have been described probably because of their restricted proximal location (Fig. 10b). Blocks are similar to those occurring in debrites and it is likely that many failed talus accumulations eventually evolve into debris flows. The interparticle matrix comprises mud and sand filtered into interparticle cavities (Fig. 7d). Talus sediments are the most likely facies to contain geopetal sediments which provide information as to slope gradient and orientation.

Contourite facies

Contourites, or sedimentary deposits which accumulate from currents flowing parallel to the slope, occur in modern carbonate slope environments. Semiconical carbonate sand drifts are present at depths of about 800 m within the Straits of Florida, approach 600 m in thickness, are up to 60 km in width and 100 km in length, and extend outward from the northwest corners of two major platforms (Fig. 11a). These contourites are typi-

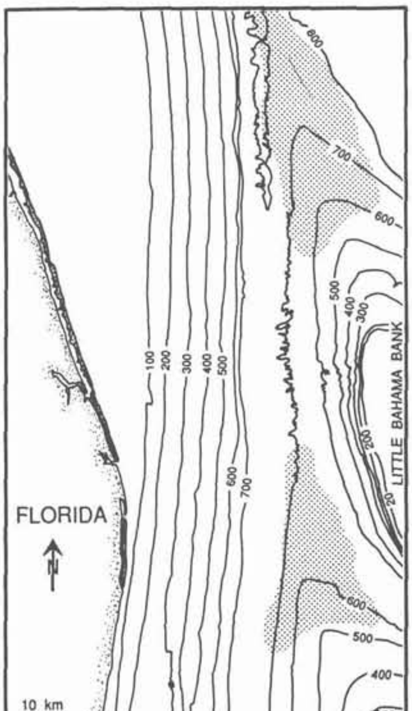

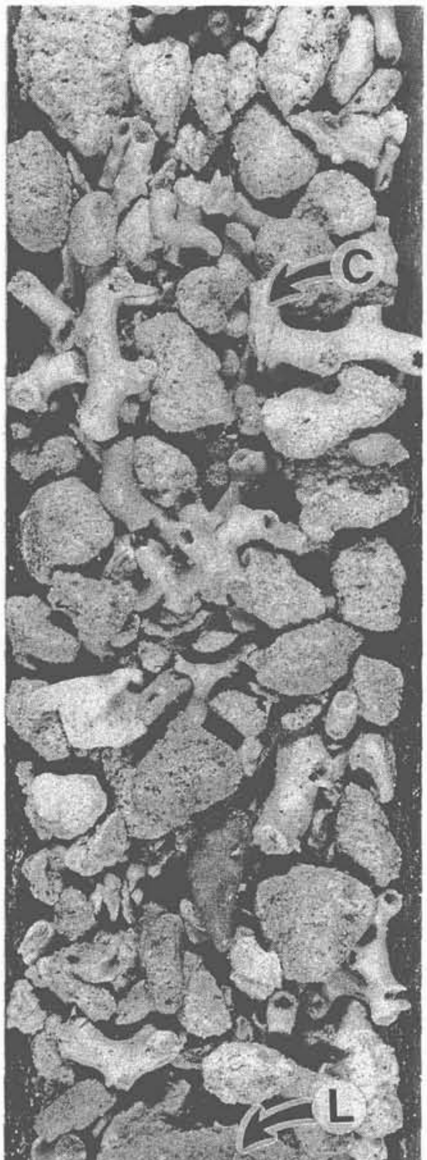

Figure 11 Current washed carbonate sands in northern Straits of Florida. a) Bathymetric map showing approximate outlines of hemiconical sediment drifts (stippled) extending from the northwest margin of platforms. Contours in metres. Location of map is shown in Figure 1. Modified from Mullins *et al.* (1980a). b) Coarse gravels and sands in core from ODP Site 626, rich in lithoclasts (L) and deep water corals (C). Core is 6 cm wide. See Fig. 11a for location. From Austin, Schlager (1986); photograph courtesy Ocean Drilling Program.

Figure 12 Slide mass in Cow Head Group, western Newfoundland, consisting of variably deformed lime mudstones and showing basal scour into underlying shales. Stratigraphic top is to left. Hammer for scale. From Coniglio (1986), published with permission of the *Canadian Journal of Earth Sciences*.

cally periplatform sands and local gravels (Fig. 11b), in the form of lags characterized by a high degree of sorting, evenly spaced ripples, lack of mud matrix, and sharp lower and upper contacts (Fig. 7e). Hardgrounds are present locally. Such deposits form as a result of thorough washing by the strong Florida Current. Sediment drifts between Florida and Cuba contain a high percentage of mud because bottom currents are weaker (Brunner, 1986).

Interpretation of contourites in ancient deep water carbonates remains weakly supported (e.g., Bein and Weiler, 1976; Cook, 1983). In the case of sandy contourites, a diagenetic origin for the lack of mud matrix (i.e., alteration of mud to pseudospar) must first be ruled out. In addition, sharp upper and lower contacts can be caused by pressure solution. Contourites may be partially reworked turbidites or hemipelagites and, as such, may have the characteristics of all three. The least equivocal criterion for the interpretation of a contourite origin is that flow direction must be parallel to the slope. This can be demonstrated if it is possible to determine slope orientation from unambiguous turbidite paleocurrents.

Submarine slides and related evidence of slope failure

Intraformational truncation surfaces, shear zones, and detached slide masses are all products of slope failure and form in any of the preceding facies. The first two provide evidence for an ancient slope; the third, like gravity flows, can be preserved either downslope or within an adjacent basin. Causes of slope failure are varied and interrelated. Sediment overloading and seismic activity are the two most obvious. Excessive pore pressures can also be important in stimulating failure on a gentle slope. Eberli (1988) hypothesized that changing grain size within turbidites establishes a vertical gradient in consolidation and physical properties, such that even on a gentle (1°) slope, numerous stacked calciturbidites create a propensity for intraformational failure.

Although *slump* is a general term used to denote soft-sediment deformation, it is too ambiguous to correctly describe the style or mechanism of failure. Instead, following Nardin *et al.* (1979), a *slide* is the movement of a rigid, internally undeformed mass along a discrete shear surface. The surface can be curved, producing a *rotational slump*, or planar, producing a *translational glide*. Such distinction is seldom possible in ancient sequences. Sliding gives rise to a slide mass (Fig. 12). The detachment surface is called an *intraformational truncation surface*. Although the initial slide mass may begin its journey downslope as a cohesive, coherently bedded entity, progressive internal deformation can lead to formation of a debris flow. Evidence for slide masses or incipient slides can be seen on seismic profiles from modern settings (Fig. 13), and includes hummocky surfaces created by creep lobes, initial dissection of strata or large "pull-aparts", and compressional folds. Slide masses with little deformation may not be distinguishable in a stratigraphic sequence, particularly if lateral exposure is limited and the slide mass is compositionally identical to surrounding sediment. On a smaller scale, *sedimentary boudins* have previously been considered to represent stretching and necking of a bed due to downslope creep or turbidity current drag on the seafloor (e.g., McCrossan, 1958; Hubert *et al.*, 1977). These features, however, are almost certainly early diagenetic concretions whose orientations are unrelated to paleoslope configuration (Coniglio, 1985).

Truncation surfaces recognized on modern slopes as trough and concave depressions are referred to as *slide scars*. On modern and ancient slopes, these localized intraslope failure basins are identified by the abrupt termination of older truncated strata and the anomalous thickening of infilling younger units (Fig. 13). The giant truncation surface along the distal edge of the west Florida shelf, now buried by younger sediment, extends for at least 120 km along the Florida Escarpment and is up to 30 km across. As much as 350 m of stratigraphic section was removed, and presumably transported over the Florida Escarpment into the abyss of the Gulf of Mexico (Mullins *et al.*, 1986). Because of the scale/discontinuous outcrop problem, recognizable truncation surfaces in ancient sequences are usually much smaller, and illustrate from less than 1 m to more than 100 m of bedding truncation (Fig. 14).

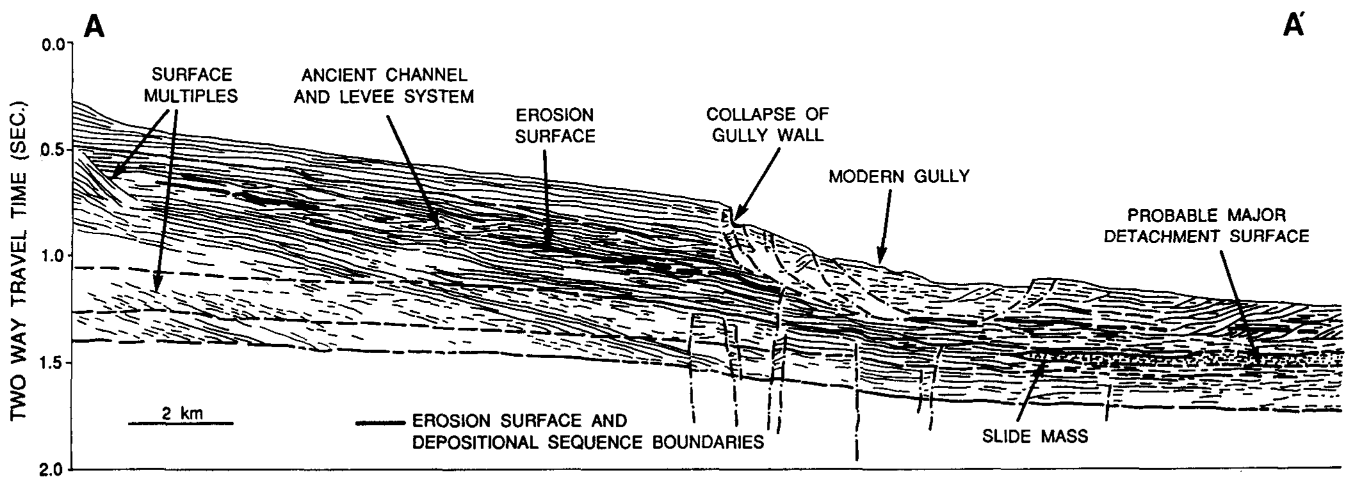

Figure 13 Interpreted seismic line from north of Little Bahama Bank (Line A-A' in Fig. 1) displays evidence for downslope creep, truncated surfaces and glide planes. Modified from Harwood and Towers (1988).

Downslope *creep* is caused by bedding parallel translation along a well-defined surface or diffuse *shear zone* lacking a basal shear plane (e.g., Cook and Mullins, 1983) and is probably a long-term process characteristic of slope environments within an unlithified sediment pile. Shear zones also occur below intraformational truncation surfaces and in the basal parts or margins of slide masses. Numerous small-scale bedding disruptions can occur in shear zones, including intrafolial drag folding, faulting, fragmentation and rotation of beds, and homogenization or reorientation of laminations. Creep or subsurface shear zones can also be localized along intervals containing water-rich turbidites (Eberli, 1988).

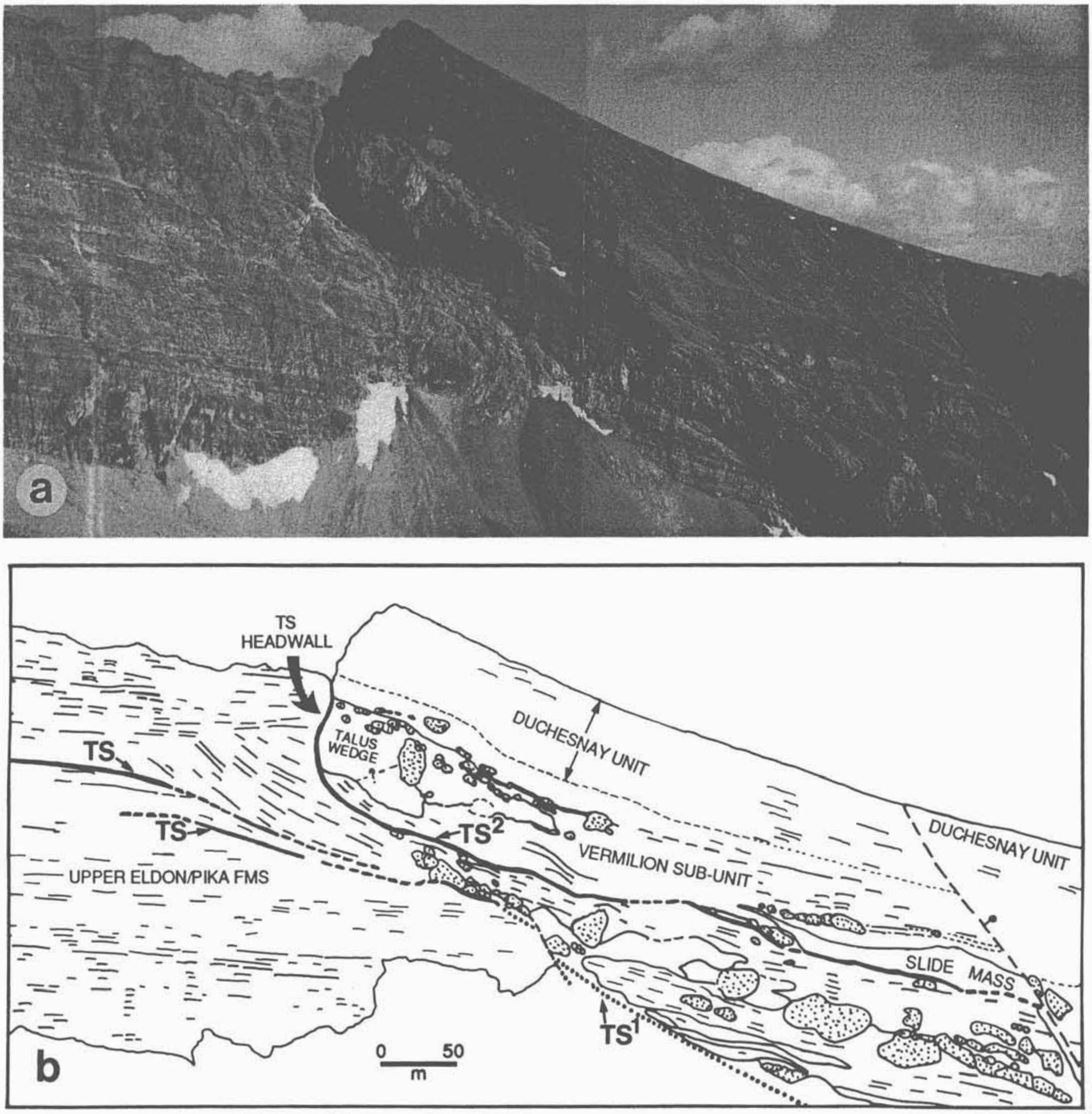

Figure 14 a) Cross-strike exposure of the upper Eldon and Pika formations on the southeast wall of Verdant cirque, Middle Cambrian, Canadian Rocky Mountains, Alberta. b) Line drawing of photography in (a). Bedded, peritidal platformal strata were truncated by two surfaces (TS) that converge to form a single, sub-Vermilion truncation surface (TS^1) to the right. This surface is onlapped by argillaceous sediments of the Vermilion sub-unit, which contain prominent megaconglomerates (large boulders are stippled) and calcarenite bodies. Subsequent progradation of the platform occurred, shown by the prominent foresets above this surface. The margin failed once again producing the intra-Vermilion truncation surface (TS^2) that clearly shows a nearly vertical headwall. Minor failures along this margin subsequently deposited the talus wedge that abuts the escarpment. Photograph and interpretation by D. Stewart.

Sedimentation rates

Sedimentation rates are extremely variable even along different portions of the same slope. In the northern Bahamas and western Florida, rates are commonly 1-3 cm/1000 years but range from zero (where no net accumulation occurs) to as high as 60 cm/1000 years (e.g., Tongue of the Ocean) where mass wasting predominates. Brooks and Holmes (1990) report an extremely high rate of 2.5 m/1000 years from the upper slope in southwestern Florida during a sea level highstand with abundant shallow water production of carbonate. Lateral variation is also expected. When pelagic sedimentation is dominant in slope environments, low rates, on the order of a few centimetres/1000 years will be characteristic. These rates may be higher than pelagic settings, however, because of productivity pulses associated with upwelling and platform margin currents (e.g., Gardulski *et al.*, 1986).

FACIES ASSOCIATIONS

Introduction

Facies variations observed in the highly segmented, modern Bahamian slopes demand unique combinations of oceanographic and geomorphologic conditions and are therefore too restricted to be adopted as general carbonate slope facies models. The position of slopes relative to prevailing oceanographic-atmospheric dynamics also determines whether coarser-grained sediment is transported *on-platform* (windward) or *off-platform* (leeward). Rapid facies variation along and between slopes further compounds the difficulty of capturing the essence of slope deposition. Modern carbonate slopes do, however, exhibit unambiguous depth/distance facies relationships (laterally and in the shallow subsurface).

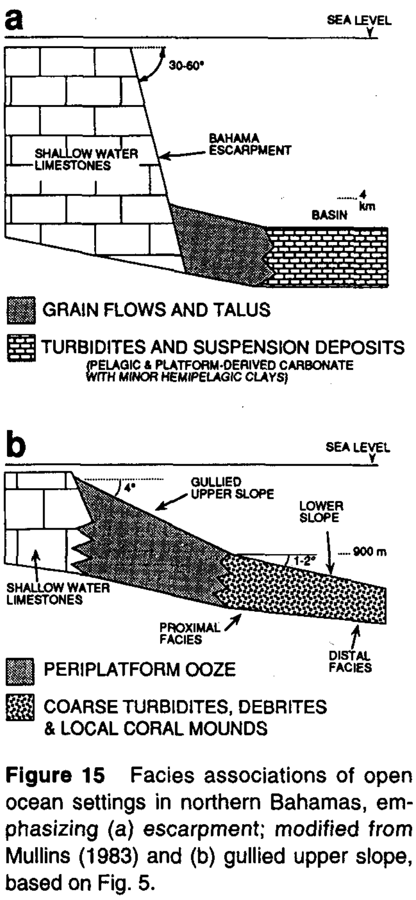

Figure 15 Facies associations of open ocean settings in northern Bahamas, emphasizing (a) escarpment; *modified from* Mullins (1983) and (b) gullied upper slope, based on Fig. 5.

Modern platform slopes

In an open ocean setting, i.e., where a platform margin faces the broad fetch of an ocean and is therefore influenced by surface and subsurface currents (e.g., north of Little Bahama Bank; Fig. 1), two different facies associations occur (Mullins and Neumann, 1979). The first, with predominantly platform-derived sands and slope lithoclasts, forms talus and gravity flow accumulations along a steep (erosional) escarpment (Fig. 15a). Facies belts are narrow, form parallel to the platform margin, and grade abruptly seaward into basinal turbidites and suspension-deposited muds. In the second, the steep upper slope is formed by peri-platform ooze with intermittently active slope gullies containing coarse resedimented debris (Figs. 5b, 15b). There is a downslope reduction in the degree of submarine cementation due to decreasing influence of current activity. The lower slope contains an apron of coarse gravity flow deposits and local coral mounds. Seaward facies transition illustrates a gradation from mud- to grain-supported fabrics of debris flows across the lower slope.

The relatively deep margin off west Florida, which is also in an open ocean setting, illustrates a threefold division of facies parallel to the strike of the margin — hardgrounds, sand and bioturbated pelagic ooze (Fig. 16). The reworked, washed sand facies and hardgrounds of the outer shelf and shelf margin are due to the Loop Current, a current within the Gulf of Mexico which flows southward parallel to the margin. In contrast to the open ocean Bahamian settings, gravity flow deposits are absent along the west Florida slope, although large-scale gravity-controlled mass wasting has been important (Mitchum, 1978; Doyle and Holmes, 1985; Mullins *et al.*, 1986). Because pelagic sedimentation dominates depositional facies along the outer slope the mineralogic composition of sediments is predominantly calcite, whereas along the Bahamas margins a hybrid mineralogy (aragonite, Mg-calcite) is common at similar water depths and distances from the shallow water platform. A comparison between the northwestern Bahamas rimmed platform slope and the western Florida slope is found in Table 2.

Slopes within the *open seaways* between carbonate platforms (e.g., Florida Straits and Northwest Providence Channel; Fig. 1) are susceptible to considerable influence by bottom currents, related to oceanic circulation and slope-derived turbidity currents, and illustrate a considerable variety of facies associations. Of particular note are sediment drifts, coral banks, lithoherms (Fig. 17a), chaotic debris flows and slides (Fig. 17b), and what might be referred to as a "diagenetic slope" (Fig. 17c). The latter reflects the decreasing influence of submarine cementation with depth coincident with decreasing current activity across the slope. This is well developed along the northern windward slope of Grand Bahama Bank, a gentle (1-2°) ramp-like incline, with the following transition in facies: hardgrounds, <375 m depth; nodular oozes, 375-500 m; and unlithified periplatform oozes at greater depths. There are few coarse-grained platform-derived sediments along this margin.

Closed seaway settings, are characterized by Tongue of the Ocean and Exuma Sound, Bahamas (Fig. 1; Mullins and Neumann, 1979). In Tongue of the Ocean, facies associations are similar to those in open ocean settings, but the facies belts are narrower, marginal slopes steeper and, because of the surrounding shallow water platforms, sediment influx is multi-directional (Mullins, 1983). Three concentric facies belts are parallel to the bank margin (Schlager and Chermak, 1979), 1) a gullied bypass slope facies, consisting of periplatform ooze with coarse debris in gully axes, 2) a basin margin facies of proximal turbidites forming small coalescing "fans", and 3) a basin facies of interbedded periplatform ooze and thinly bedded fine-grained turbidites (Fig. 18). Due to the narrow width of this seaway, platform-derived sediment effectively dilutes pure pelagic sediments such that there is no discrete pelagic facies.

There is no concentric facies pattern in Exuma Sound. Instead, a single Quaternary debris sheet covers much of the basin floor. Yet, gullied slopes are present and turbidites become finer toward the basin centre. Episodic and spatially discrete occurrences of debrites should be expected within closed seaways enclosed by normal sequences of interbedded ooze and turbidites (Mullins, 1983), as found in ancient slope sequences (e.g., Cook *et al.*, 1972).

Subsurface facies associations

Modern slopes

A comparison of short (<12 m) cores from north of Little Bahama Bank and west Florida demonstrates considerable variation in facies associations, both laterally and vertically, related to the different geological settings and slope evolution (Fig. 19). Deep sea drilling along the northern margin of Little Bahama Bank, however, documents spatial and temporal facies variations to subsurface depths of 300 m (middle to late Miocene age; Austin, Schlager *et al.*, 1986). Even though the margin has been prograding since the early Miocene, and has produced a seaward-thinning periplatform wedge overlying pelagic carbonates, it is clear that the same environments did not simply undergo seaward translation with bank-margin progradation (Harwood and Towers, 1988).

Ancient slopes

Vertical successions in ancient carbonate slopes typically contain disorganized, unpredictable arrays of coarse- and fine-grained facies, such as debrites, the hallmark of carbonate slope deposition, which punctuate sequences of fine-grained suspension deposits. Naturally, local slope morphology and sediment budget significantly influence the type of sediment that accumulates. Thus certain slopes, or parts of slopes may be turbidite-dominated or characterized by beds of periplatform ooze punctuated by debrites. Systematic thickening-upward sequences indicative of prograding depositional lobes or other attributes of submarine fan deposition (discussed below) are not common.

Early diagenesis and cyclic sedimentation

Early diagenetic processes are important in both modern and ancient carbonate slope deposits. Bored and mineralized hardgrounds, nodular chalks and limestones, and shallow-burial concretionary layers all attest to early lithification with fragmented beds commonly occurring as clasts within debrites. In modern systems, the presence of fine-grained and abundant aragonite establishes a strong diagenetic gradient facilitating early lithification. In addition, the alteration of Mg-calcites appears to contribute sufficient Mg, along with seawater diffusion, to establish shallow-burial dolomitic carbonates along some slopes (Dix and Mullins, 1992).

Aragonite cycles in modern slopes

Aragonite cycles, or alternating aragonite-rich and aragonite-poor layers, are common to both Bahama and Florida slopes, as well as other modern periplatform settings. Gardulski *et al.* (1986) describe Bahamian cycles as being *platform-driven* with aragonite percentages directly related to productivity in shallow water platform environments. In contrast, the greater depth of the margin along the open west Florida shelf effectively limits the seaward extent of the shallow water carbonate factory, and hence slope deposition is dominated by pelagic settling. Gardulski *et al.* (1986) considered the west Florida cycles as *pelagic-driven*, linked to planktonic-oceanographic dynamics.

Cycles in the Bahamas are asymmetric fluctuations of high-Sr aragonite (derived from the adjacent platforms), and correlate well with oxygen isotope stratigraphy indicating an association with climatically driven interglacial and glacial sea level changes (Fig. 20a). Elevated aragonite content coincides

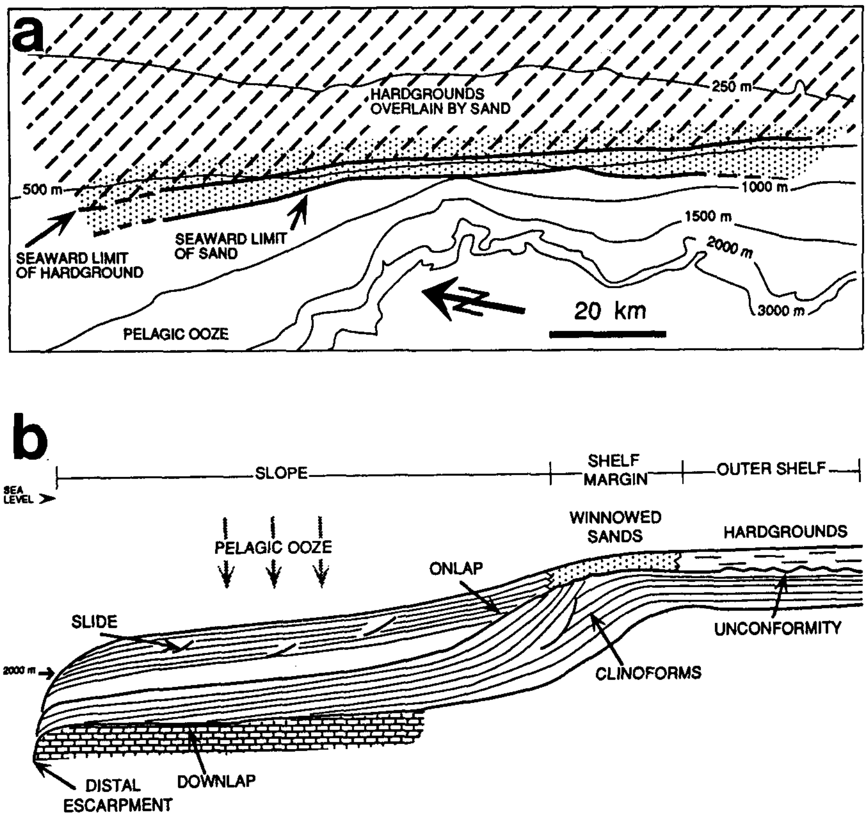

Figure 16 Slope adjacent to deep open shelf margin off western Florida. a) Bathymetry and surficial facies. Contours in metres. Location is shown in Figure 1. Modified from Mullins *et al.* (1988b). b) Schematic cross-section illustrating geometry and major facies. Note lenticular geometry of youngest slope sequence thins landward due to onlap and thins abruptly seaward along the distally-steepened slope. Figure not drawn to scale. Modified from Mullins *et al.* (1988b).

with maximum platform productivity and *highstand shedding* (Droxler and Schlager, 1985). There is considerable debate as to the reasons for lowered aragonite percentages. Droxler *et al.* (1983, 1988) maintain that, in addition to decreased aragonite production due to platform exposure, aragonite was also lost through seafloor dissolution. The timing of the Bahama minima coincides well with carbonate minima in the Pacific, Indian, and North Atlantic oceans, some of which can be shown to be due to carbonate dissolution. Boardman *et al.* (1986) suggest that the variation in percentages marks a purely autocyclic control resulting from alternate flooding and exposure of the shallow water carbonate factory.

West Florida cycles (Fig. 20b) are out of phase with the Bahamian cycles, and are not asymmetric. Maximum aragonite percentages are not always associated with climate extremes, and aragonite is a low-Sr variety characteristic of planktonic pteropods rather than platform-derived sediment. Elevated percentages of aragonite, Mg-calcite, dolomite, and insoluble residue coincide with glacial periods as determined by oxygen isotope stratigraphy. These cycles are considered to be a product of increased planktonic productivity and dilution by hemipelagic clays. There is no evidence of dissolution to account for the depleted aragonite intervals.

A third, slightly different cyclic relationship occurs off the northern Bahamas (Dix and Mullins, 1988). The Plio-Pleistocene cycles of carbonate content and high-Sr aragonite are negatively covariant; i.e., intervals of high aragonite correspond to decreased total carbonate content, due to increased terrigenous clastic content. Such increased deposition of clay would occur if bottom current strengths decreased between platforms with rising sea level during the glacial-to-interglacial transition (Brunner, 1986).

Limestone-shale/marl cycles in ancient slopes

Of all the various fine-grained facies found in ancient carbonates slopes, none is more visually striking than the thick, monotonously interbedded limestone-shale (or marl) sequences which can extend for hundreds of metres along strike with little or no change in bed thickness (Fig. 8). Recent studies suggest that this limestone-shale association is largely the product of shallow-burial diagenesis (e.g., Hallam, 1986; Ricken, 1986; Coniglio and James, 1990). Most thin-bedded lime mudstones were deposited from dilute turbidity currents or from suspension settling. Lithification of the limestone seems to have taken place by early dissolution of carbonate from the

Table 2 *Comparison of Bahamian (rimmed platform) and west Florida (open platform) slopes. Based on Mullins* et al. *(1988b).*

	NW Bahamas	West Florida
Morphology	gullies are important in upper bypass slope	smooth and gentle; lacks gullies; no upper bypass slope
	slope becomes more gentle in a seaward direction	slope becomes more steep in a seaward direction
Influence of line source on sediment dispersal	strongly controlled	shelf margin position of Loop Current eliminates potential control by line source
Turbidites and debris flows	major contributor to lower slope and basin margin facies	relatively minor contributor to slope
Slides	important	important
Pelagic sedimentation	most abundant along upper bypass slopes and in regions not diluted by sediment gravity flows, winnowing by bottom currents, or carbonate compensation depths	dominant depositional process
Cyclicity	aragonite cycles are platform-driven with peak aragonite abundances during warm interglacial intervals	aragonite cycles controlled by higher pteropod productivity during glacial intervals
Sediment composition	bank-derived Mg-calcite and aragonite are important	calcite from planktonic foraminifera and coccoliths is most important
Diagenetic potential	early submarine cementation encourages formation of slope-derived clasts during slope failure	no oblivoius source for slope-derived clasts; fine-grained nature of sediment reduces permeability of sediment discouraging submarine cementation
Distribution of slope facies	variety encouraged by segmentation of banks and basins	3 main facies belts with Loop Current as major control
Seismic facies	numerous seismic facies	simple configuration

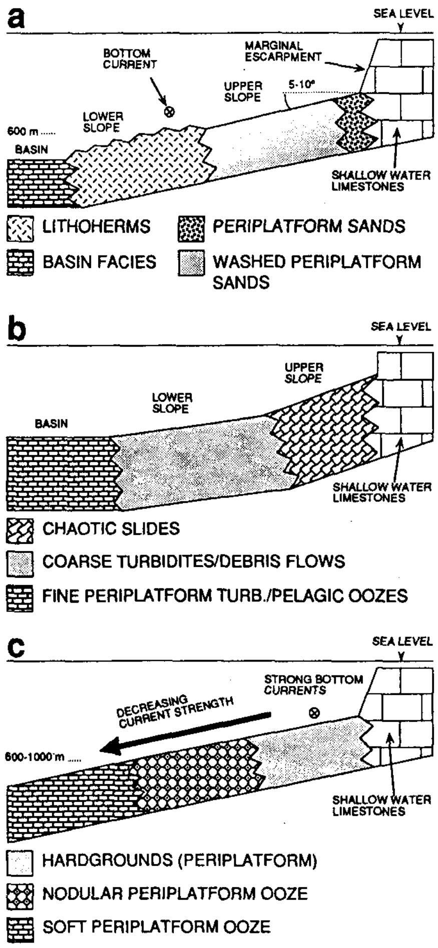

argillaceous interlayers and reprecipitation in the carbonate layers. This precipitation also cemented local grainy turbidites and formed nodules to layers of diagenetic lime mudstone. Later pressure solution during burial usually enhances all limestone-shale or limestone-marl contacts.

Such limestone-shale cycles are characteristic of many Paleozoic slope carbonates and, although partially diagenetic, the initial depositional signal of carbonate sediment alternating with argillaceous sediment may be a response to the same controls that produce aragonite cycles on modern slopes.

FACIES MODELS

Earlier attempts to model carbonate slope facies have highlighted three common elements, 1) the considerable spatial and temporal facies variation, 2) the propensity for carbonate sediments to accumulate along the slope from a line source or a multitude of feeder channels, and 3) the difference between siliciclastic and carbonate slope sedimentation in response to sea level fluctuations. McIlreath and James (1979; 1984) established two basic models — bypass and depositional (Fig. 21) — based on relief between platform and basin and

Figure 17 Facies associations of open seaways of the northern Bahamas. a) Example of periplatform sands and lithoherms influenced by the bottom-sweeping Florida Current. Modified from Mullins and Neumann (1979). b) Chaotic slide facies changing downslope into gravity flows and pelagic ooze. Modified from Mullins (1983). c) Diagenetic slope reflecting decreasing current strength passing from hardground through nodular ooze to ooze with increasing water depth. Note that the upper slope north of Little Bahama Bank (Fig. 5b) clearly displays these current-controlled facies. Modified from Mullins *et al.* (1980b).

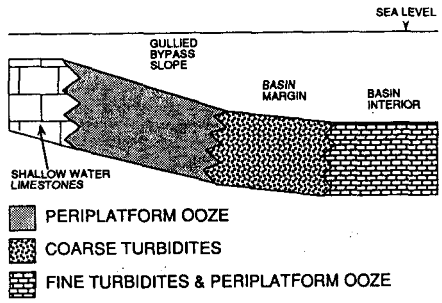

Figure 18 Facies associations of closed seaways of the Bahamas. Based on Schlager and Chermak (1979).

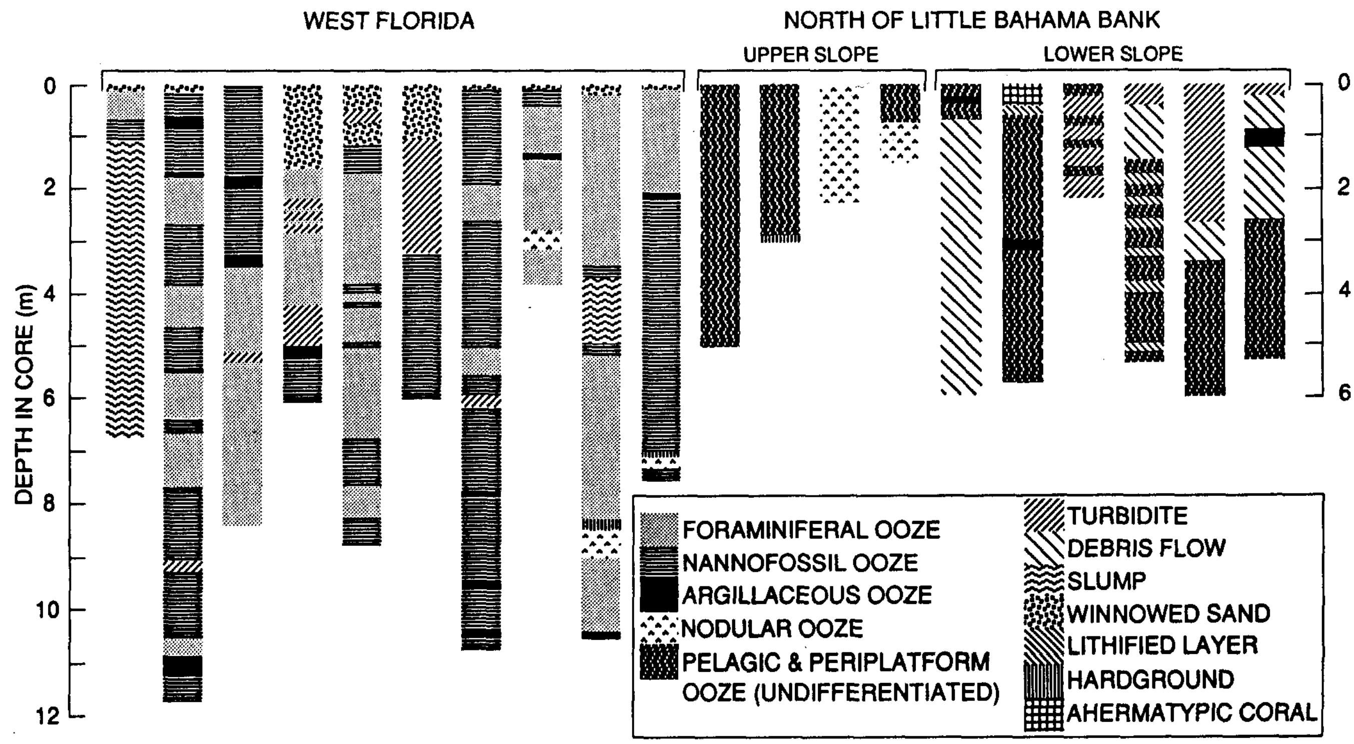

Figure 19 Shallow subsurface slope facies from west Florida and north of Little Bahama Bank. Diagram is based on parts of figures in Mullins *et al.* (1984) and Mullins *et al.* (1988a).

the nature of the platform margin facies. Cook *et al.* (1972) took an alternate approach by considering the wedge of sediment underlying slopes as forming an apron adjacent to the shallow water platform, and distinguishing two end members by the position of the apron top relative to the shallow water margin. Facies and facies associations were not a prime criterion for distinguishing slope types. Only one facies, however, was set aside: the debris sheet model was used to explain extensive megabreccias resulting from collapse of a platform margin. Using the apron-platform geometry, Mullins and Cook (1986) recently proposed a facies classification using nomenclature similar to that used for terrigenous sedimentary gravity flow facies (Mutti and Ricci Lucchi, 1978). This approach emphasizes similarities and differences between siliciclastic fans and carbonate aprons.

Carbonate slope facies models based primarily upon geometry of the slope deposits and the adjacent platform margin appear to offer the most malleable models, in which the numerous possible facies and facies associations play an important complimentary, but secondary role.

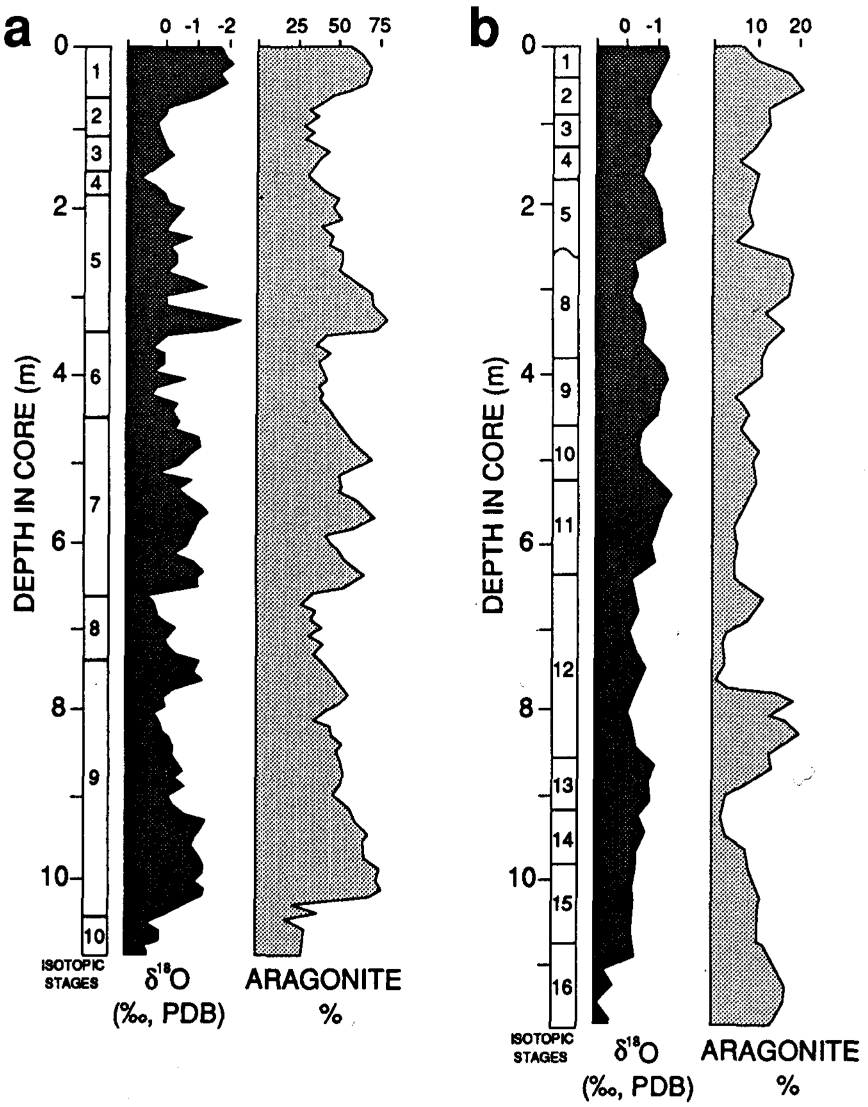

Figure 20 Aragonite abundance and oxygen isotope composition cycles if the shallow subsurface. Aragonite cycles from the Bahamas (a) appear asymmetric whereas those from west Florida (b) show less asymmetry. See text for details. Diagram is based on parts of figures in Droxler *et al.* (1983) and Gardulski *et al.* (1986).

Carbonate aprons

Aprons are wedge-shaped to lenticular bodies that generally thicken towards the platform margin. Facies belts closely parallel the platform margin. Three types of apron-platform geometries are recognized, 1) rimmed platform slope aprons, 2) rimmed platform base-of-slope aprons, and 3) open platform slope aprons.

Rimmed platform slope apron

Carbonate slope aprons extend without break from the basin along gentle (<4°) gradients up to a shallow water platform margin (Fig. 22a). This is similar to what has been regarded as the depositional slope model (McIlreath and James, 1979; 1984). A line source of platform-derived sediment originates from numerous channels dissecting shoals, reefs and islands along the platform margin. Downslope sediment transport along such carbonate aprons is predominantly via unchannelized sheet flows. Because gravity deposits may be initiated anywhere along the slope, correlation of these deposits will be fraught with problems except for megabreccias resulting from sea level change or seismically induced failure of platform margins (e.g., James and Stevens, 1986). Turbidites and debris sheets are common but do not develop systematic vertical sequences; instead, they are characterized by randomly distributed broad sheets of carbonate gravity flow facies interbedded with suspension deposits. General coarsening- or fining-upward trends can, however, result from progradation or retrogradation of the adjacent platform margin (Fig. 23). Slope aprons are not described from modern oceans because modern platforms typically possess steep forereef escarpments, and in places upper slope escarpments, which are a function of glacially induced Quaternary sea level fluctuations. Ancient examples include the Devonian of Alberta, the Siluro-Devonian of Nevada, and the Permian of west Texas (Cook, 1983).

Rimmed platform base-of-slope apron

A base-of-slope apron forms downslope from the platform-slope break along relatively steep (>4°) margins (Fig. 22b). Sediment is supplied from a line source which typically takes the form of a series of closely spaced gullies transporting shallow water and slope-derived sediment through some portion of the upper to middle (bypass) slope. Sediment emerging from a gullied slope would initially follow a dispersal path outlining a series of small, interleaved fan-shaped deposits while broadly defining platform margin-parallel facies belts. As with carbonate slope aprons, systematic vertical sequences are not expected. Prominent facies to be expected at the top of a base-of-slope apron would be coarse debrites and talus, especially if a steep escarpment is present. Good examples of modern base-of-slope aprons occur along several margins in the northern Bahamas (Mullins and Cook, 1986), off Belize (James and Ginsburg, 1979) and Jamaica (Land, 1979). There are several well-described ancient examples as well, including the Middle Cambrian of the Canadian Rocky Mountains (McIlreath, 1977), the Cambro-Ordovician of western Newfoundland (James and Stevens, 1986), and the Cretaceous of Mexico (Enos, 1977).

Open (unrimmed) platform apron

Because the platform margin is below depths at which the carbonate factory operates, sediments forming aprons adjacent to such shelves are likely to be dominantly pelagic in origin (Fig. 22c). Mass-wasting deposits include pelagic turbidites and debrites, the latter of which can contain clasts derived from the platform margin or fragmented beds of early lithified pelagite. The generally finer grained nature of the deeper platform margin sediment implies that submarine cementation (and therefore production of clasts) may not be as important as along shallower rimmed platform margins. Pre-Mesozoic aprons adjacent to open platform margins will be highly argillaceous.

Both modern and ancient examples of carbonate aprons adjacent to open platform margins (distally steepened ramps) are rare, although in the latter case, this more likely reflects the difficulty in differentiating between rimmed shallow water platforms and open platforms in the rock record. Modern slopes adjacent to open shelves include west Florida and Banco de Campeche, Mexico. An ancient example is the early Proterozoic of Northwest Territories (Grotzinger, 1986).

Carbonate submarine fans

Carbonate submarine fans appear to be rare in the rock record, but several have been described from the Paleozoic (Cook, 1983; Cook and Mullins, 1983), Mesozoic (Ruiz-Ortiz, 1983; Wright and Wilson, 1984; Watts and Garrison, 1986; Cooper, 1989), and Tertiary (Gökten, 1986). No modern-day examples have been documented.

Ancient carbonate fans are interpreted to have been built from a point source, similar to their siliciclastic "channel-feeding-lobe" (Chapter 13) counterparts, developing at the base of a slope fed from a major submarine channel (Fig. 22d). Facies associations and types are also similar (Fig. 24). In carbonate systems, inner fan facies

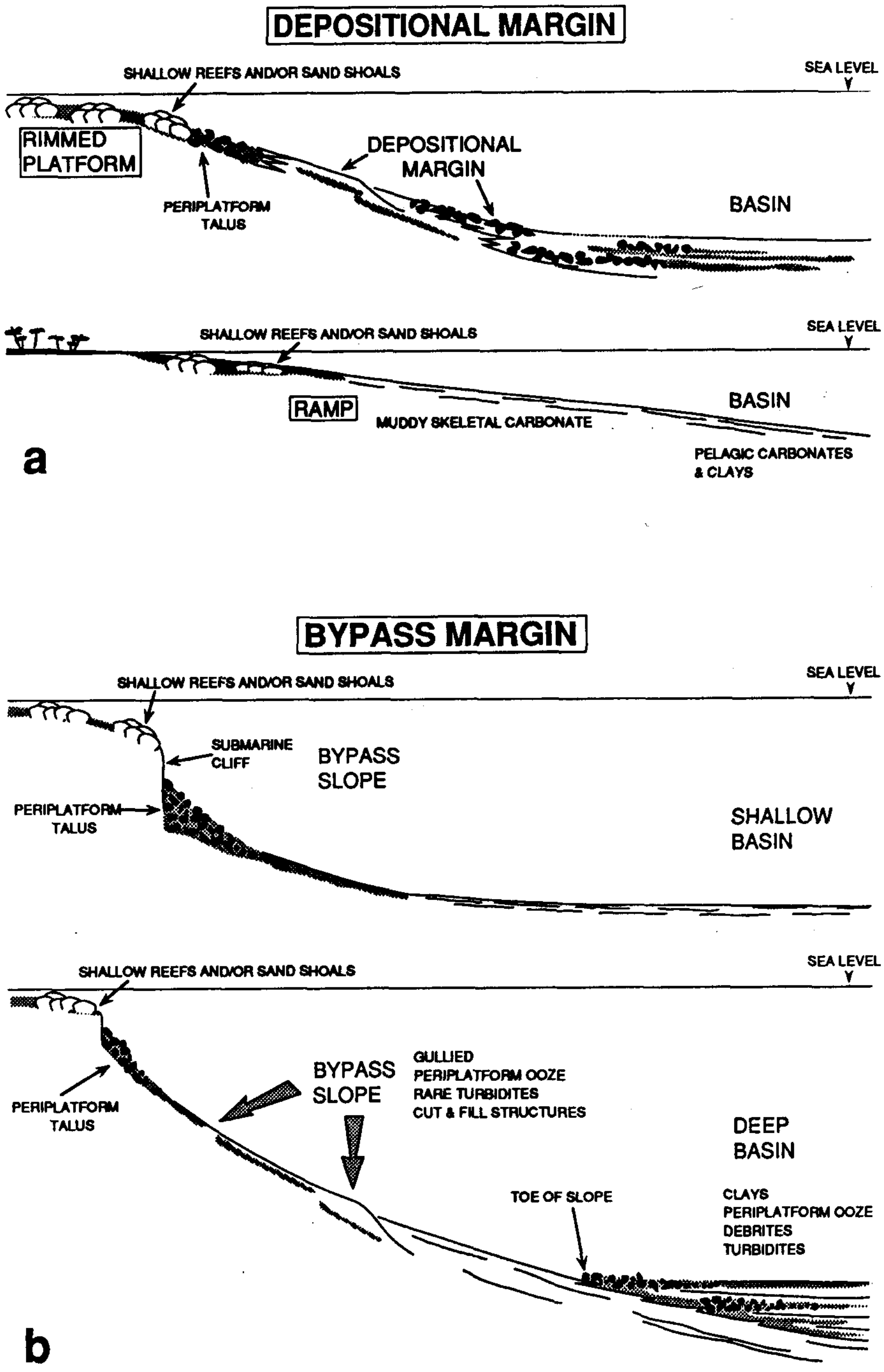

Figure 21 Facies models for depositional and bypass margins. Modified from James and Mountjoy (1983).

include debris flow conglomerates and coarse proximal turbidites deposited in feeder channels and associated with submarine slides. Mid-fan deposits comprise thinning- and fining-upward strata deposited as braided distributary channels. Thickening- and coarsening-upward turbidite sheets are inferred to represent outer fan-lobe sheets. Thin-bedded laterally continuous turbidites may represent fan fringe, basin plain, or interchannel facies (Mullins and Cook, 1986). Sediment disperses in a radial fashion, yet if numerous fans develop along a slope also fed by a line source, the distinctive fan geometry and facies succession may be blurred.

In the previous older submarine fan models (Walker, 1979), suprafan lobes are a major structural component. However, reappraisal of siliciclastic facies associations based on multichannel seismic facies analysis (Chapter 13) illustrates that channel-feeding-lobe fan systems do not characterize a general fan model. In light of this, future investigations of carbonate submarine fan systems need to be cognizant of channel-levee complexes, stacked thick sandy turbidites, synsedimentary deformed sediment, and debrites. Carbonate submarine fan systems may prove to be more common in the rock record than is generally recognized.

SEA LEVEL CHANGES AND SEQUENCE STRATIGRAPHY

The sequence anatomy of carbonate slopes, comprising allostratigraphic units and the lithologic succession are difficult to predict because shifting sea level causes so many changes in the ambient physical, biological and chemical conditions of deposition. Furthermore, the relative importance of these parameters on sedimentation often changes as base level shifts. Sequence anatomy can be influenced, however, without any change in sea level, for example, through seafloor dissolution due to rise of chemical oceanographic boundaries, erosion or sedimentation related to variations in bottom-sweeping currents, or changes in the tectonics of the hinterland as it affects terrigenous sediment input into coastal areas (Schlager, 1991).

Despite this complexity, the management of a slope above the common carbonate mineral lysoclines and compensation depths when the adjacent platform is flooded should be directly controlled by production and off-platform transport of shallow water carbonate sediment (Wilson, 1975; Kendall and Schlager, 1981; James and Mountjoy, 1983). The greatest rates of slope aggradation and progradation from off-platform transport of mud and coarser detritus appear to be associated with platform flooding, establishing conditions for highstand shedding when sedimentation rate matches or exceeds the rate of relative sea level rise, or when the shallow water carbonate factory's production rate is maximized.

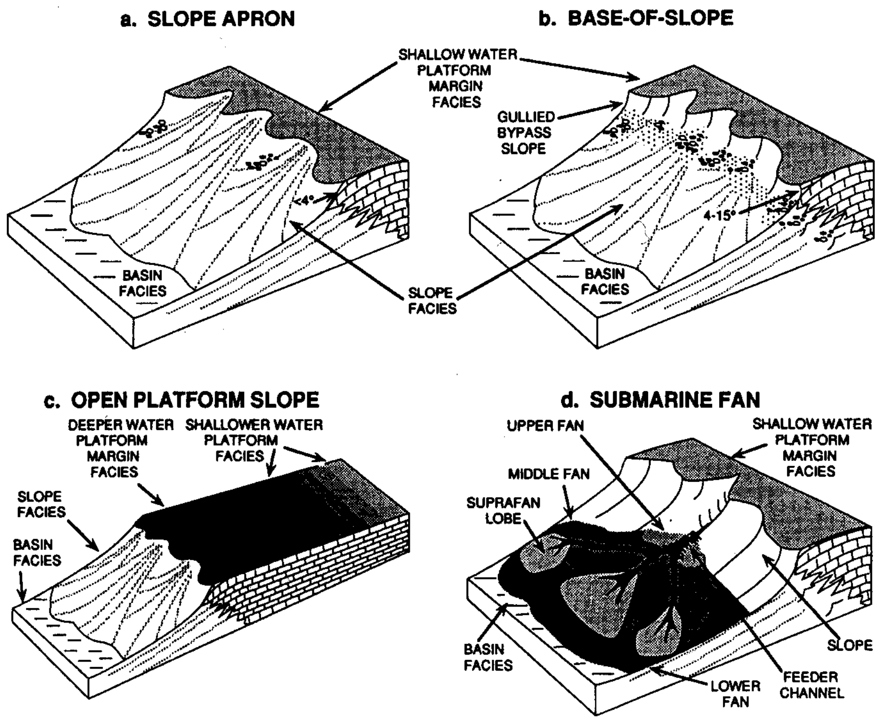

Figure 22 Block diagram facies models for a) carbonate slope apron, b) carbonate base-of-slope apron, c) carbonate deep open platform slope, and d) carbonate submarine fan (a and b are modified from Mullins and Cook, 1986).

Exposure

A drop in sea level to below the shallow, rimmed paleoplatform margin creates the potential for a new platform to grow on the upper part of the old slope, although constant erosion can prevent any significant platform development on top of steep slopes. This new platform will have a relatively small area for shallow water sediment production. Consequently, calcitic pelagic sediment in Mesozoic and Cenozoic sequences may predominate due to reduction in the input of platform-derived aragonite and Mg-calcite whereas Paleozoic slopes become sediment starved, resulting in an increase in the relative amount of shale, the default sediment.

During lowered sea level, the exposed and lithified platform margin will be weakened by physical and chemical processes, potentially leading to collapse and accumulation of sediment gravity flow, slide and talus deposits. Whether sufficient sediments in carbonate systems accumulate to generate recognizable *lowstand systems tracts* analogous to siliciclastic lowstand fans (Sarg, 1988) is debatable. Along a pericontinental shelf margin siliciclastics can prograde across the shelf and down the new slope, thereby establishing a terrigenous clastic lowstand systems tract. From sequence stratigraphic studies of relatively pure carbonate systems, however, the lowstand systems tract appears to be either thin or absent (Fig. 25; Eberli and Ginsburg, 1989; Pomar, 1991; Yose, 1991). In contrast, Masetti *et al.* (1991) have suggested that the greatest rate of slope progradation in Triassic platforms of northern Italy occurred during sea level lowstands. The problem of highstand versus lowstand slope deposition remains a key area for research.

Because of greater water depths at the margin, the sedimentary regime on open platform slope aprons remains unaffected by small sea level fluctuations that would otherwise intermittently expose and flood a shallow, rimmed platform margin. Large-scale sea level drops, however, particularly if the platform margin is in relatively shallow water, may impart a clear shallow water, platform-derived carbonate contribution to the apron.

Flooding

With a gradual rise in sea level, such that the rate exceeds sediment production, the lowstand margin and platform facies backstep, onlapping the previously exposed platform and forming a *transgressive systems tract* (TST; Fig. 25). Superimposed on this overall rise and landward onlap may be short intervals of rapid rise followed by stillstands during which carbonate platforms can catch-up. If of prolonged duration, aggradational sequences can develop. Submarine cementation tends to be common in the lime mud-rich lithofacies that characterize the platform margin because of the longer time available for pore-fluid migration and cement precipitation (Sarg, 1988). Any mass wasting from such margins will produce slope aprons characterized by abundant mud-rich intraclasts.

As the rate of relative sea level rise approaches sediment production rates, the *maximum flooding surface* (MFS) is attained with decreasing onlap (Fig. 25). Condensed sequences or hardgrounds may form on the platform during this peak in onlap. When sediment production rates exceed sea level rise, or during a stillstand, the *highstand systems tract* (HST) prograding sigmoid/oblique clinoforms develop and downlap onto the older transgressive systems tract (Fig. 25). Submarine cementation tends to be minor and gravity flows derived from such systems will reflect the uncemented, grain-rich and mud-poor lithofacies that characterize the platform margin.

Highstand shedding should promote greater mass wasting where slopes become overloaded, or margins become oversteepened. The most vigorous off-platform transport may occur, however, during early flooding of the platform margin, decreasing during subsequent increased water depth if much of the platform surface is placed below wave base (e.g., Brooks and Holmes, 1989). Rapid outbuilding of the margin forming a highstand systems tract may lead to alternating development of accretionary and bypass margins. In fact, evolution from an accretionary to bypass margin may repeat itself many times if oversteepening of the bypass margin gives way to collapse and lower gradients (Schlager and Ginsburg, 1981).

Drowning

Sediment production on the platform can be temporarily or permanently shut down during transgression, creating a starved slope. Such drowning conjures up images of the platform lying in the murky depths due to a rapid rise in relative sea level related either to eustasy or tectonics (Schlager, 1981). Certainly, rates of shallow water sediment production and off-platform transport appear to decrease with increasing water depth over the platform. But,

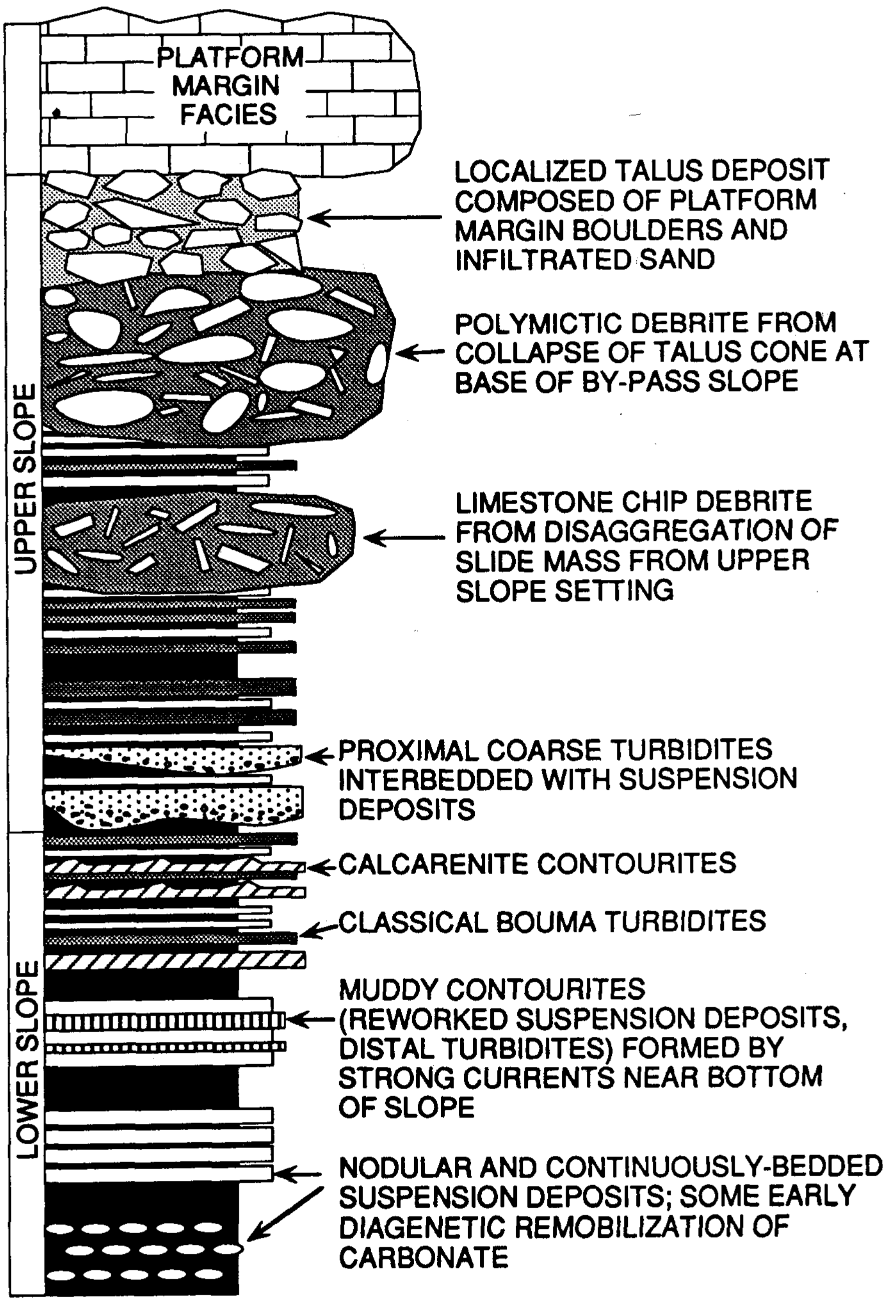

Figure 23 Generalized hypothetical sequence of slope facies resulting from progradation of the adjacent shallow water platform.

progradational stacking of slope sequences can still be generated adjacent to platforms which sit at depths below those commonly considered for the carbonate factory (0-20 m; Glaser and Droxler, 1991).

Since water *quality*, in addition to water depth, may play an important role in controlling platform growth potential, locally retarded shallow water carbonate production and/or high rates of off-platform transport may lead to diminished accumulation rates along some margins and to incipient drowning (Dominguez *et al.*, 1988). Excessive nutrients (Hallock and Schlager, 1986), derived from either upwelling or across-platform transport of lagoon waters, can inhibit carbonate production. Thus, drowning can occur during formation of a transgressive systems tract in very shallow water. Tectonic plate motion and a platform's latitudinal change through successive water masses, with changing temperature, salinity and/or water clarity characteristics, can form a long-term control on carbonate productivity and resulting platform aggradation (Davies *et al.*, 1989). No sea level change is required for these nutrient or tectonic influences.

Drowning in deep or shallow water should lead to a starved or condensed sequence characterized by low rates of mostly pelagic deposition (in post-Paleozoic strata) with possible development of phosphatic hardgrounds. Subsequent sequence boundaries within overlying pelagic strata will be parallel or subparallel or mounded to the contact with underlying slope carbonates, although bottom currents may keep some areas devoid of pelagic sediment. Hemipelagic terrigenous muds or siliceous ooze may be the prevalent sediment type on the drowned platform and slope in pre-Mesozoic systems.

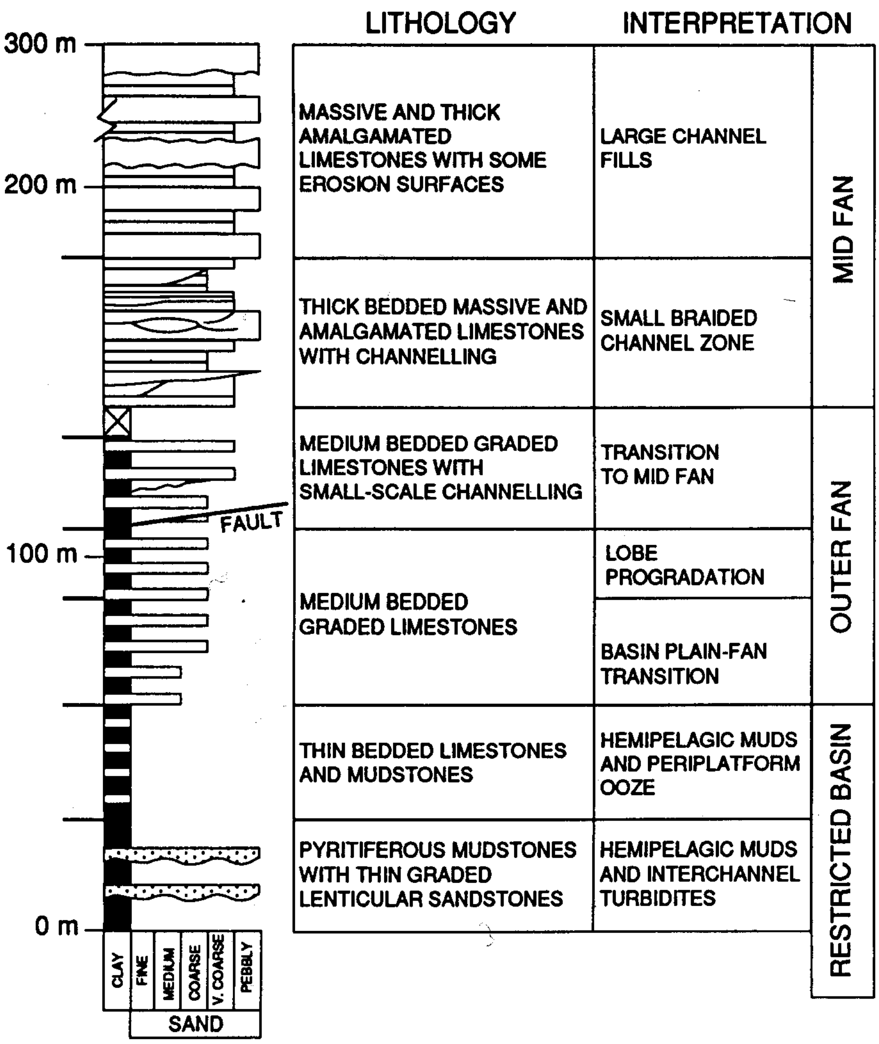

Figure 24 Summary log of major lithofacies in Jurassic carbonate submarine fan sequence at Peniche, Portugal. Modified from Wright and Wilson (1984).

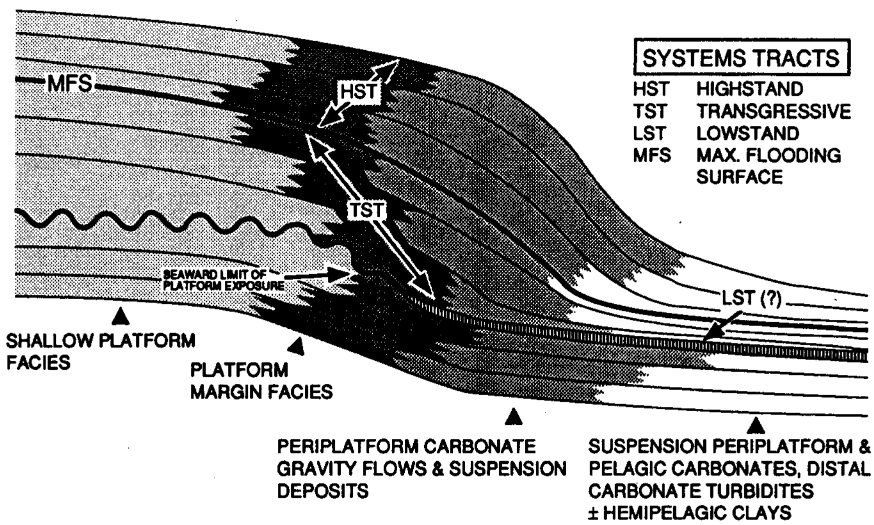

Figure 25 Geometry of carbonate sequences with generalized facies associations. Platform exposure leads to a thin, condensed lowstand systems tract (LST?) or hiatal surface. Rising sea level creates a backstepping transgressive systems tract (TST) which progressively onlaps the previously exposed platform. Condensed, thin sequences may occur along the slope. With greater sediment production than sea level rise, a highstand systems tract (HST) progrades out over the maximum flooding surface (MFS), creating a sequence of downlapping strata. Modified from Sarg (1988).

SUMMARY

In the first edition of *Facies Models*, McIlreath and James (1979) underscored the need for future refinement of their models to include more study of modern carbonate slopes in the Bahama region and beyond. Over the last decade, considerable research has resulted in a greater understanding of many previously unstudied, relatively pure carbonate slopes in the northern Bahamas-Florida region, together with parts of the Caribbean, as well as the Pacific and Indian Oceans. Across-slope drill transects begun by the Ocean Drilling Program in 1985 ushered in a new era of research. The choice of the northern Bahamas for the inaugural Leg 101 was in partial recognition of the need for better understanding of the facies architecture of modern carbonate slopes. Recent ODP transects off northeast Australia provide a new vantage point from which to investigate the dynamics of basin-to-platform transitions in mixed siliciclastic-carbonate depositional systems. Future research investigating open shelves within different oceanographic systems will also, no doubt, provide further understanding of slope sedimentation and development along this alternate type of carbonate margin.

The variety of facies, slope morphologies, internal stratigraphy, and sedimentary processes characterizing even a single slope illustrate that carbonate slopes continually adjust toward a dynamic equilibrium with a host of interrelated climatic, oceanographic, sedimentological, tectonic, and sea level eustatic factors. Past attempts to model slopes provided snapshots of numerous facies associations which characterize the variability of this depositional system and the various geometric configurations of carbonate slopes. Recognizing the dynamic interrelationship between numerous parameters affecting slope facies, our approach has been to underscore their inherent spatial and temporal variability. This knowledge allows us to better understand observed facies associations and temper predictions of lateral and vertical facies development in both modern and ancient carbonate slopes.

ACKNOWLEDGEMENTS

The preparation of this manuscript was made possible by an NSERC operating grant to MC. Much of that part of the manuscript written by GRD was prepared while at the Department of Geological Sciences, University of British Columbia. Noel James provided photographs as well as encouragement and stimulation throughout. We thank D. Stewart and the Ocean Drilling Program for providing photographs. M. Kunert assisted with drafting of several diagrams.

REFERENCES

Basic sources of information

Cook, H.E., Hine, A.C. and Mullins, H.T., eds., 1983, Platform margin and deep water carbonates: Society of Economic Paleontologists and Mineralogists, Short Course 12, 573 p.
These voluminous notes include separate chapters on modern carbonate platform margins (Hine, 1983), modern Bahamian slopes and basins (Mullins, 1983), and ancient carbonate margins, slopes, and basins (Cook, 1983).

Einsele, G., Ricken, W. and Seilacher, A., eds., 1991, Cycles and events in stratigraphy: Berlin, Springer-Verlag, 955 p.
Numerous articles on deep water carbonates, limestone-shale rhythms and the relationships between sea level fluctuation and slope deposition.

Flügel, E., 1982, Microfacies analysis of limestones: New York, Springer-Verlag, 633 p.
Good summary of facies and microfacies in allochthonous carbonate deposits in deep marine environments.

McIlreath, I.A. and James, N.P., 1984, Carbonate slopes, *in* Walker, R.G., ed., Facies models: Geoscience Canada Reprint Series 1, p. 245-257.
An updated version of the first comprehensive synthesis of modern and ancient carbonate slopes.

Mullins, H.T. and Cook, H.E., 1986, Carbonate apron models: alternatives to the submarine fan model for paleoenvironmental analysis and hydrocarbon exploration: Sedimentary Geology, v. 48, p. 37-79.
An examination of the similarities and differences between carbonate aprons and submarine fans. The authors adopt a facies classification similar to that used by Mutti and Ricci Lucchi (1978) for deep water siliciclastic sediments.

Scholle, P.A., Bebout, D.G. and Moore, C.H., eds., 1983a, Carbonate depositional environments: American Association of Petroleum Geologists, Memoir 33, 691 p.
A superbly illustrated source including chapters dealing with the fore-reef (Enos and Moore, 1983), basin margin (Cook and Mullins, 1983) and pelagic carbonates (Scholle et al., *1983b).*

Tucker, M.E. and Wright, V.P., 1990, Carbonate sedimentology: Oxford, Blackwell Scientific Publications, 482 p.
Concise, up-to-date synthesis of facies models for deep water, resedimented carbonates. Several informative studies on ancient sequences are nicely summarized.

In addition to the above, there are several SEPM publications containing numerous individual papers dealing with general concepts and with specific ancient and modern carbonate slopes.

Cook, H.E. and Enos, P., eds., 1977, Deep-water carbonate environments: Society of Economic Paleontologists and Mineralogists, Special Publication 25, 336 p.

Crevello, P.D. and Harris, P.M., eds., 1985, Deep-water carbonates: Buildups, turbidites, debris flows and chalks – a core workshop: Society of Economic Paleontologists and Mineralogists, Core Workshop 6, 527 p.

Crevello, P.D., Wilson, J.L., Sarg, J.F. and Read, J.F., eds., 1989, Controls on carbonate platform and basin development: Society of Economic Paleontologists and Mineralogists, Special Publication 44, 407 p.

Doyle, L.J. and Pilkey, O.H., eds., 1979, Geology of continental slopes: Society of Economic Paleontologists and Mineralogists, Special Publication 27, 374 p.

Harris, P. and Grover, G.A., 1989, Subsurface and outcrop examination of the Capitan Shelf margin, northern Delaware Basin: Society of Economic Paleontologists and Mineralogists, Core Workshop 13, 481 p.

Other references

Austin, J.A., Jr., Schlager, W., Palmer, A.A. 1986, Proceedings, Initial Reports, ODP, Leg 101, College Station, Texas, 569 p.

Austin, J.A., Jr., Schlager, W., Palmer, A.A. 1988, Proceedings, ODP, Scientific Results, Leg 101, College Station, Texas, 501 p.

Bein, A. and Weiler, Y., 1976, The Cretaceous Talme Yafe Formation: a contour current shaped sedimentary prism of calcareous detritus at the continental margin of the Arabian Craton: Sedimentology, v. 23, p. 511-532.

Boardman, M.R., Baker, P.A., Dulin, L.A., Kenter, R.J., Hunter, G.E. and Keifer, K.B., 1986, Banktop responses to Quaternary fluctuations in sea level recorded in periplatform sediments: Geology, v.14, p. 28-31.

Brooks, G.R. and Holmes, C.W., 1989, Recent carbonate slope sediments and sedimentary processes bordering a non-rimmed platform: Southwest Florida continental margin, *in* Crevello, P.D., Wilson, J.L., Sarg, J.F. and Read, J.F., eds., Controls on carbonate platform and basin development: Society of Economic Paleontologists and Mineralogists, Special Publication 44, p. 259-272.

Brooks, G.R. and Holmes, C.W., 1990, Modern configuration of the southwest Florida carbonate slope: Development by shelf margin progradation: Marine Geology, v. 94, p. 301-315.

Brunner, C.A., 1986, Deposition of a muddy sediment drift in the southern Straits of Florida during the Late Quaternary: Marine Geology, v. 69, p. 235-249.

Colacicchi, R. and Baldanza, A., 1986, Carbonate turbidites in a Mesozoic pelagic basin: Scaglia Formation, Apennines – comparison with siliciclastic depositional models:Sedimentary Geology, v. 48, p. 81-105.

Coniglio, M., 1985, Origin and diagenesis of fine-grained sediments, Cow Head Group (Cambro-Ordovician), western Newfoundland: Unpublished Ph.D. thesis, Memorial University, St. John's, Newfoundland, 684 p.

Coniglio, M., 1986, Synsedimentary submarine slope failure and tectonic deformation in deep-water carbonates, Cow Head Group, western Newfoundland: Canadian Journal of Earth Sciences, v. 23, p. 476-490.

Coniglio, M. and James, N.P., 1990, Origin of fine-grained carbonate and siliciclastic sediments in an early Palaeozoic slope sequence, Cow Head Group, western Newfoundland: Sedimentology, v. 37, p. 215-230.

Cook, H.E., 1979, Ancient continental slope sequences and their value in understanding modern slope development, *in* Doyle, L.J. and Pilkey, O.H., eds., Geology of continental slopes: Society of Economic Paleontologists and Mineralogists, Special Publication 27, p. 287-305.

Cook, H.E., 1983, Ancient carbonate platform margins, slopes and basins, *in* Cook, H.E., Hine, A.C. and Mullins, H.T., eds., Platform margin and deep water carbonates: Society of Economic Paleontologists and Mineralogists, Short Course 12, p. 5-1 – 5-189.

Cook, H.E., McDaniel, P.N., Mountjoy, E.W. and Pray, L.C., 1972, Alloch-thonous carbonate debris flows at Devonian bank ("reef") margins, Alberta, Canada: Bulletin of Canadian Petroleum Geology, v. 20, p. 439-497.

Cook, H.E. and Mullins, H.T., 1983, Basin margin environment, *in* Scholle, P.A., Bebout, D.G. and Moore, C.H., eds., Carbonate depositional environments: American Association of Petroleum Geologists, Memoir 33, p. 540-617.

Cook, H.E. and Taylor, M.E., 1991, Carbonate-slope failures as indicators of sea level lowerings: American Association of Petroleum Geologists, Bulletin, v. 75, p. 556 (abstract).

Cooper, D.J.W., 1989, A longitudinal carbonate fan from the Jurassic of the Oman Mountains: the Guweyza Limestone Formation of the Hamrat ad Duru: Sedimentary Geology, v. 61, p. 253-275.

Davies, P.J., Symonds, P.A., Feary, D.A and Pigram, C.J., 1989, The evolution of the carbonate platforms of northeast Australia, *in* Crevello, P.D., Wilson, J.L., Sarg, J.F. and Read, J.F., eds., Controls on carbonate platform and basin development: Society of Economic Paleontologists and Mineralogists, Special Publication 44, 233-258.

Davies, P.J., McKenzie, J., *et al.*, in press, Proceedings, Initial Reports, ODP, Leg 133, College Station, Texas.

Dix, G.R. and Mullins, H.T., 1988, A regional perspective of shallow-burial diagenesis of deep-water periplatform carbonates from the northern Bahamas: *in* Austin, J.A., Jr., Schlager W., *et al.*, Proceedings, ODP, Scientific Results, Leg 101, College Station, Texas, p. 279-304.

Dix, G.R. and Mullins, H.T., 1992, Shallow burial diagenesis of deep-water carbonates, Northern Bahamas: Geological Society of America, Bulletin, v. 104 , p. 305-315 .

Dominguez, L.L., Mullins, H.T. and Hine, A.C., 1988, Cat Island platform, Bahamas: An incipiently drowned Holocene carbonate shelf: Sedimentology, v. 35, p. 805-819.

Doyle, L.J. and Holmes, C.W., 1985, Shallow structure, stratigraphy, and carbonate sedimentary processes of west Florida upper continental slope: American Association of Petroleum Geologists, Bulletin, v. 69, p. 1133-1144.

Droxler, A.W., Bruce, C.H., Sager, W.W. and Watkins, D.H., 1988, Pliocene-Pleistocene variation in aragonite content and planktonic oxygen-isotope record in Bahamian periplatform ooze, hole 633A, *in* Austin, J.A., Jr., Schlager, W., *et al.*, Proceedings, ODP, Scientific Results, Leg 101, College Station, Texas, p. 221 -244.

Droxler, A.W. and Schlager, W., 1985, Glacial versus interglacial sedimentation rates and turbidite frequency in the Bahamas: Geology, v. 13, p.799-802.

Droxler, A.W., Schlager, W. and Whallon, C.C., 1983, Quaternary aragonite cycles and oxygen-isotope record in Bahamian carbonate ooze: Geology, v. 11, p. 235-239.

Eberli, G.P., 1988, Physical properties of carbonate turbidite sequences surrounding the Bahamas — implications for slope stability and fluid movements, *in* Austin, J.A., Jr., Schlager, W., *et al.*, Proceedings, ODP, Scientific Results, Leg 101, College Station, Texas, p. 305-314.

Eberli, G.P. and Ginsburg, R.N., 1989, Cenozoic progradation of northwest Great Bahama Bank, a record of lateral platform growth and sea-level fluctuations, *in* Crevello, P.D., Wilson, J.L., Sarg, J.F. and Read, J.F., eds., Controls on carbonate platform and basin development: Society of Economic Paleontologists and Mineralogists, Special Publication 44, p. 339-351.

Einsele, G., 1982, Limestone-marl cycles (periodites): diagnosis, significance, causes — a review, *in* Einsele, G. and Seilacher, A., eds., Cyclic and event stratification: Berlin, Springer-Verlag, p. 8-53.

Enos, P., 1977, Tamabra Limestone of the Poza Rico Trend, Mexico, *in* Cook, H.E. and Enos, P., eds., Deep-water carbonate environments: Society of Economic Paleontologists and Mineralogists, Special Publication 25, p. 273-314.

Enos, P. and Moore, C.H., 1983, Fore-reef slope environment, *in* Scholle, P.A., Bebout, D.G. and Moore, C.H., eds., Carbonate depositional environments: American Association of Petroleum Geologists, Memoir 33, p. 508-537.

Gardulski, A.F., Mullins, H.T. and Oldfield, B., 1986, Carbonate mineral cycles in ramp slope sediment: eastern Gulf of Mexico: Paleoceanography, v. 1, p. 555-565.

Glaser, K.S. and Droxler, A.W., 1991, High production and highstand shedding from deeply submerged carbonate banks, northern Nicaragua Rise: Journal of Sedimentary Petrology, v. 61, p. 128-142.

Gökten, Y.E., 1986, Paleocene carbonate turbidites of the Sarkisla Region, Turkey — their significance in an orogenic basin: Sedimentary Geology, v. 49, p. 143-165.

Grotzinger, J.P., 1986, Evolution of early Proterozoic passive-margin carbonate platform, Rocknest Formation, Wopmay Orogen, N.W.T., Canada: Journal of Sedimentary Petrology, v. 56, p. 831-847.

Hallam, A., 1986, Origin of minor limestone-shale cycles: climatically induced or diagenetic: Geology, v. 14, p. 609-612.

Hallock, P. and Schlager, W., 1986, Nutrient excess and the demise of coral reefs and carbonate platforms: Palaios, v. 1, p. 389-398.

Harris, P.T., Davies, P.J. and Marshall, J.F., 1990, Late Quaternary sedimentation on the Great Barrier Reef continental shelf and slope east of Townsville, Australia: Marine Geology, v. 94, p. 55-78.

Harwood, G.M. and Towers, P.A., 1988, Seismic sedimentologic interpretation of a carbonate slope, north margin of Little Bahama Bank, *in* Austin, J.A., Jr., Schlager, W., *et al.*, Proceedings, ODP, Scientific Results, Leg 101, College Station, Texas, p. 263-278.

Heath, K.C. and Mullins, H.T., 1984, Open-ocean, off-bank transport of fine-grained carbonate sediment in the northern Bahamas, *in* Stow, D.A.V. and Piper, D.J.W., eds., Fine-grained sediments: deep water processes and facies: London, Blackwell Scientific Publications, p. 199-208.

Hine, A.C., Locker, S.D., Hallock, P. and Mullins, H.T., 1991, Strongly contrasting modes of slope failure and erosion along the carbonate margins of three open seaways; Northwest Nicaraguan Rise: American Association of Petroleum Geologists, Bulletin, v. 75, p. 595-596 (abstract).

Hiscott, R.N. and James, N.P., 1985, Carbonate debris flows, Cow Head Group, western Newfoundland: Journal of Sedimentary Petrology, v. 55, p. 735-745.

Hubert, J.F., Suchecki, R.K. and Callahan, R.K.M., 1977, The Cow Head Breccia: sedimentology of the Cambro-Ordovician continental margin, Newfoundland, *in* Cook, H.E. and Enos, P., eds., Deep-water carbonate environments: Society of Economic Paleontologists and Mineralogists, Special Publication 25, p. 125-154.

James, N.P. and Ginsburg, R.N., 1979, The seaward margin of Belize barrier and atoll reefs: International Association of Sedimentologists, Special Publication 3, 191 p.

James, N.P. and Mountjoy, E.W., 1983, Shelf-slope break in fossil carbonate platforms — an overview, *in* Stanley, D.J. and Moore, G.T., eds., The shelf-break critical interface on continental margins: Society of Economic Paleontologists and Mineralogists, Special Publication 33, p. 189-206.

James, N.P. and Stevens, R.K., 1986, Stratigraphy and correlation of the Cambro-Ordovician Cow Head Group, western Newfoundland: Geological Survey of Canada, Bulletin 366, 143 p.

Jansa, L.F., 1981, Mesozoic carbonate platforms and banks of the eastern North American margin: Marine Geology, v. 44, p. 97-117.

Jenkyns, H.C., 1986, Pelagic environments, *in* Reading, H.G., ed., Sedimentary environments and facies: London, Blackwell Scientific Publications, p. 343-397.

Kendall, C.G.St.C. and Schlager, W., 1981, Carbonates and relative changes in sea level: Marine Geology, v. 44, p. 181-212.

Kenter, J.A.M., 1990, Carbonate platform flanks: slope angle and sediment fabric: Sedimentology, v. 37, p. 777-794.

Krause, F.F. and Oldershaw, A.E., 1979, Submarine carbonate breccia beds — a depositional model for two-layer, sediment gravity flows from the Sekwi Formation, (Lower Cambrian), Mackenzie Mountains, Northwest Territories, Canada: Canadian Journal of Earth Sciences, v. 16, p. 189-199.

Land L.S., 1979, The fate of reef-derived sediment on the north Jamaican island slope: Marine Geology, v. 29, p. 55-71.

Land L.S. and Moore, C.H., Jr., 1976, Deep forereef and upper island slopes, north Jamaica, *in* Frost, S.H., Weiss, M.P. and Saunders, J.B., eds., Reefs and related carbonates — ecology and sedimentology: American Association of Petroleum Geologists, Studies in Geology 4, p. 53-67.

Ludvigsen, R., 1989, The Burgess Shale: not in the shadow of the Cathedral Escarpment: Geoscience Canada, v. 16, p. 51-59.

Masetti, D., Neri, C. and Bosellini, A., 1991, Deep-water asymmetric cycles and progradation of carbonate platforms governed by high-frequency eustatic oscillations (Triassic of the Dolomites, Italy): Geology, v. 19, p. 336-339.

McCrossan, R.G., 1958, Sedimentary boudinage structure in the Devonian Ireton Formation of Alberta: Journal of Sedimentary Petrology, v. 28, p. 316-320.

McIlreath, I.A., 1977, Accumulation of a Middle Cambrian, deep-water limestone debris apron adjacent to a vertical submarine carbonate escarpment, southern Rocky Mountains, Canada, *in* Cook, H.E. and Enos, P., eds., Deep-water carbonate environments: Society of Economic Paleontologists and Mineralogists, Special Publication 25, p. 113-124.

McIlreath, I.A. and James, N.P., 1979, Carbonate slopes, *in* Walker, R.G., ed., Facies Models: Geological Association of Canada, Geoscience Canada Reprint Series 1, p. 133-149.

Middleton, G.V. and Hampton, M.A., 1976, Subaqueous sediment transport and deposition by sediment gravity flows, *in* Stanley, D.J. and Swift, D.J.P., eds., Marine sediment transport and environmental management: New York, John Wiley and Sons, p. 197-217.

Mitchum, R.M., 1978, Seismic stratigraphic investigation of west Florida slope, Gulf of Mexico: American Association of Petroleum Geologists, Studies in Geology 7, p. 193-223.

Morse, J.W. and Mackenzie, F.T., 1990, Geochemistry of sedimentary carbonates: Developments in Sedimentology 48, Amsterdam, Elsevier, 707 p.

Mullins, H.T., 1983, Modern carbonate slopes and basins of the Bahamas, *in* Cook, H.E., Hine, A.C. and Mullins, H.T., eds., Platform margin and deep water carbonates: Society of Economic Paleontologists and Mineralogists, Short Course 12, p. 4-1 – 4-138.

Mullins, H.T., Gardulski, A.F., Hinchey, E.J. and Hine, A.C., 1988b, The modern carbonate ramp slope of central west Florida: Journal of Sedimentary Petrology, v. 58, p. 273-290.

Mullins, H.T., Gardulski, A.F. and Hine, A.C., 1986, Catastrophic collapse of the west Florida carbonate platform margin: Geology, v. 14, p. 167-170.

Mullins, H.T., Gardulski, A.F., Hine, A.C., Mellillo, A.J., Wise, S.W., Jr. and Applegate, J., 1988a, Three-dimensional sedimentary framework of the carbonate ramp slopes of central west Florida: A sequential seismic stratigraphic perspective: Geological Society of America, Bulletin, v. 100, p. 514-533.

Mullins, H.T., Heath, K.C., Van Buren, H.M. and Newton, C.R., 1984, Anatomy of a modern open-ocean carbonate slope: northern Bahama Bank: Sedimentology, v. 31, p.141-168.

Mullins, H.T. and Neumann, A.C., 1979, Deep carbonate bank margin structure and sedimentation in the northern Bahamas, *in* Doyle, L.J. and Pilkey, O.H., eds., Geology of continental slopes: Society of Economic Paleontologists and Mineralogists, Special Publication 27, p. 165-192.

Mullins, H.T., Neumann, A., Wilber, R.J. and Boardman, M.R., 1980b, Nodular carbonate sediment on Bahamian slopes: Possible precursors to nodular limestones: Journal of Sedimentary Petrology, v. 50, p. 117-131.

Mullins, H.T., Neumann, A., Wilber, R.J., Hine, A.C. and Chinburg, S.J., 1980a, Carbonate sediment drifts in northern Straits of Florida: American Association of Petroleum Geologists, Bulletin, v. 64, p. 1701-1717.

Mutti, E. and Ricci Lucchi, F., 1978, Turbidites of the northern Apennines: Introduction to facies analysis: International Geology Review, v. 20, p. 125-166.

Nardin, T.R., Hein, F.J., Gorsline, D.S. and Edwards, B.D., 1979, A review of mass movement processes, sediment and acoustic characteristics, and contrasts in slope and base-of-slope systems versus canyon-fan-basin floor systems, *in* Doyle, L.J. and Pilkey, O.H., eds., Geology of continental slopes: Society of Economic Paleontologists and Mineralogists, Special Publication 27, p. 61-73.

ODP Leg 133 Scientific Party, 1991, A chronicle of carbonate platform development: Geotimes, April 1991, p. 22-26.

Paull, C.K., Freeman-Lynde, R., Bralower, T.J., Gardemal, J.M., Neumann, A.C., D'Argenio, B. and Marsella, E., 1990, Geology of the strata exposed on the Florida Escarpment: Marine Geology, v. 91, p. 177-194.

Perry, R.K., compiler, 1984, Bathymetry of the Gulf of Mexico and the Caribbean Sea: American Association of Petroleum Geologists, Scale 1:3, 289, 263.

Pickering, K.T., Hiscott, R.N. and Hein, F.J., 1989, Deep marine environments: London, Unwin Hyman, 416 p.

Pomar, L., 1991, Reef geometries, erosion surfaces and high-frequency sea level changes, upper Miocene reef complex, Mallorca, Spain: Sedimentology, v. 38, p. 243-270.

Read, J.F., 1985, Carbonate platform facies models: American Association of Petroleum Geologists, Bulletin, v. 69, p. 1-21.

Ricken, W., 1986, Diagenetic bedding, a model for marl-limestone alternations: New York, Springer-Verlag, 210 p.

Rudolph, K.W. and Lehmann, P.J., 1989, *Platform evolution and sequence* stratigraphy of the Naturna platform, South China Sea, *in* Crevello, P.D., Wilson, J.L., Sarg, J.F. and Read, J.F., eds., Controls on carbonate platform and basin development: Society of Economic Paleontologists and Mineralogists, Special Publication 44, p. 353-361.

Ruiz-Ortiz, P.A., 1983, A carbonate submarine fan in a fault controlled basin of the Upper Jurassic, Betic Cordillera, southern Spain: Sedimentology, v. 30, p. 33-48.

Sarg, J.F., 1988, Carbonate sequence stratigraphy, *in* Wilgus, C.K, *et al.*, eds., Sea level changes: an integrated approach: Society of Economic Paleontologists and Mineralogists, Special Publication 42, p. 155-181.

Schlager, W., 1981, The paradox of drowned reefs and carbonate platforms: Geological Society of America, Bulletin, v. 92, p. 197-211.

Schlager, W., 1991, Depositional bias and environmental change — important factors in sequence stratigraphy: Sedimentary Geology, v. 70, p. 109-130.

Schlager, W. and James, N.P., 1978, Low-*magnesian calcite limestones forming* at the deep-sea floor, Tongue of the Ocean, Bahamas: Sedimentology, v. 25, p. 675-702.

Schlager, W. and Chermak, A., 1979, Sediment facies of platform-basin transition, Tongue of the Ocean, Bahamas, *in* Doyle, L.J. and Pilkey, O.H., eds., Geology of continental slopes: Society of Economic Paleontologists and Mineralogists, Special Publication 27, p. 193-208.

Schlager, W. and Ginsburg, R.N., 1981, Bahama carbonate platforms — The deep and the past: Marine Geology, v. 44, p. 1-24.

Schlager, W. and Camber, O., 1986, Submarine slope angles, drowning unconformities, and self-erosion of limestone escarpments: Geology, v. 14, p. 762-765.

Scholle, P.A., Arthur, M.A. and Ekdale, A.A., 1983b, Pelagic environment, *in* Scholle, P.A., Bebout, D.G. and Moore, C.H., eds., Carbonate depositional environments: American Association of Petroleum Geologists, Memoir 33, p. 620-691.

Stoakes, F.A., 1980, Nature and control of shale basin fill and its effect on reef growth and termination: Upper Devonian Duvernay and Ireton formations of Alberta, Canada: Bulletin of Canadian Petroleum Geology, v. 28, p. 345-410.

Stow, D.A.V. and Shanmugam, G., 1980, Sequence of *structures in fine-grained* turbidites: comparison of recent deep-sea and ancient flysch sediments: Sedimentary Geology, v. 25, p. 23-42.

Twichell, D.C., Parson, L.M and Paull, C.K., was 1990, Variations in the styles of erosion along the Florida escarpment, eastern Gulf of Mexico: Marine and Petroleum Geology, v. 7, p. 253-266.

Walker, R.G., 1979, Turbidites and associated coarse clastic deposits, *in* Walker, R.G., ed., Facies Models: Geological Association of Canada, Geoscience Canada Reprint Series 1, p. 171-188.

Watts, K.F. and Garrison, R.E., 1986, Sumeini Group, Oman-evolution of a Mesozoic carbonate slope on a south Tethyan continental margin: Sedimentary Geology, v. 48, p. 107-168.

Watts, K.F. and Blome, C.D., 1990, Evolution of the Arabian carbonate platform margin slope and its response to orogenic closing of a Cretaceous ocean basin, Oman, *in* Tucker, M.E., Wilson, J.L., Crevello, P.D., Sarg, J.R. and Read, J.F., eds., Carbonate Platforms — facies sequences and evolution: International Association of Sedimentologists, Special Publication 9, p. 291-323.

Wilkinson, B.H., 1979, Biomineralization, paleoceanography, and the evolution of *calcareous marine organisms*: Geology, v. 7, p. 524-527.

Wilson, J.L., 1975, Carbonate facies in geologic history: New York, Springer-Verlag, 471 p.

Wright, V.P. and Wilson, R.C.L., 1984, A carbonate submarine-fan sequence from the Jurassic of Portugal: Journal of Sedimentary Petrology, v. 54, p. 394-412.

Yose, L.A., 1991, Part 2: Sequence stratigraphy of mixed carbonate/volcaniclastic slope deposits flanking the Sciliar (Schlern)-Catinaccio Buildup, Dolomites, Italy, *in* Bradner, R., Flügel, E., Koch, R. and Yose, L.A., The northern margin of the Schlern/Sciliar-Rosengarten/Catinaccio Platform, Guide-book Excursion A: Dolomieu Conference on Carbonate Platforms and Dolomitization, p. 17-39.

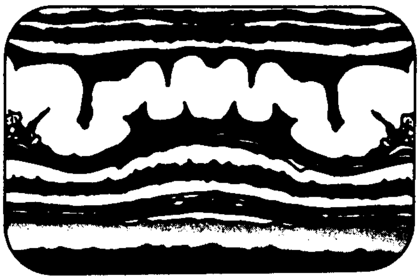

19. Evaporites

Alan C. Kendall, School of Environmental Sciences, University of East Anglia, Norwich NR3 7TJ England

INTRODUCTION

Evaporites are chemical sediments precipitated from brines. They may form anywhere there is a substantial deficit in the water budget due to evaporation. The feedstock for most large evaporite deposits is believed to have been seawater, but groundwaters are the sources for many evaporites in continental settings. Carbonates are commonly interlaminated with the more soluble materials and should also be considered, when they are precipitated by similar processes, as evaporites.

A diverse group of minerals occur in evaporites, but most are rare to minor components. The more important minerals are shown in Table 1. The diversity of marine-derived evaporite minerals is more limited. Dissolved constituents in modern seawater are dominated by sodium and chloride, and only 12 components have concentrations greater than 1 ppm. The proportions of major ions in seawater are constant and apparently have been since late Precambrian times. This constancy implies that seawater evaporation followed similar pathways in the past.

Evaporites are formed in a wide range of depositional settings, from soils to lacustrine environments on continents, and from the supratidal to the deep subaqueous realm in the marine setting. Evaporite minerals may crystallize in these environments at the brine/air interface or, less commonly, within the brine itself, on the floor of a brine pool, in brine-soaked sediments as displacive or incorporative crystals, or as efflorescent crusts in the capillary fringe of subaerially exposed settings. The crusts have low preservation potential. Consequently, evaporite deposits can be described as being 1) subaqueous accumulations of surface-nucleated *crystals*, or *crystal cumulates*, 2) subaqueous bottom precipitates, or *crusts*, 3) diagenetically emplaced *intrasediment precipitates*, which may replace, displace or incorporate nonevaporite or previously formed evaporite host sediments, or 4) *clastic accumulations* of evaporite particles. After deposition, evaporites are subject to many early diagenetic processes that 1) alter the original mineralogy and sediment fabric to varying degrees (including complete obliteration of original characteristics), or 2) lead to complete removal by dissolution. Thus many evaporites are not strictly primary precipitates: they are diagenetic minerals emplaced within other sediments, or are diagenetic replacements of true primary precipitates.

In this chapter the overall controls on evaporite precipitation are discussed; a new classification of evaporite facies emphasizing sedimentary features rather than geographic settings is introduced; and facies models for continental, basin marginal and basin

Table 1 *Common evaporate minerals. From Hardie (1984).*

anhydrite	$CaSO_4$	leonhardtite	$MgSO_4 \cdot 4H_2O$
aphthitalite (glaserite)	$K_2SO_4 \cdot (Na,K)SO_4$	leonite	$MgSO_4 \cdot K_2SO_4 \cdot 4H_2O$
antarcticite	$CaCl_2 \cdot 6H_2O$	loewite	$2MgSO_4 \cdot 2Na_2SO_4 \cdot 5H_2O$
aragonite	$CaCO_3$	magnesium calcite	$(Mg_xCa_{1-x})CO_3$
bassanite	$CaSO_4 \cdot {}^1/_2H_2O$	mirabilite	$Na_2SO_4 \cdot 10H_2O$
bischofite	$MgCl_2 \cdot 6H_2O$	nahcolite	$NaHCO_3$
bloedite (astrakhanite)	$Na_2SO_4 \cdot MgSO_4 \cdot 4H_2O$	natron	$Na_2CO_2 \cdot 10H_2O$
burkeite	$Na_2CO_3 \cdot 2Na_2CO_4$	pentahydrite	$MgSO_4 \cdot 5H_2O$
calcite	$CaCO_3$	pirssonite	$CaCO_3 \cdot Na_2CO_2 \cdot 2H_2O$
carnallite	$MgCl_2 \cdot KCl \cdot 6H_2O$	polyhalite	$2CaSO_4 \cdot MgSO_4 \cdot K_2SO_4 \cdot 2H_2O$
dolomite	$CaCO_3 \cdot MgCO_3$	rinneite	$FeCl_2 \cdot NaCl \cdot 3KCl$
epsomite	$MgSO_4 \cdot 7H_2O$	sanderite	$MgSO_4 \cdot 2H_2O$
gaylussite	$CaCO_3 \cdot Na_2CO_2 \cdot 5H_2O$	schoenite (picromerite)	$MgSO_4 \cdot K_2SO_4 \cdot 6H_2O$
glauberite	$CaSO_4 \cdot Na_2SO_4$	shortite	$2CaCO_2 \cdot Na_2CO_3$
gypsum	$CaSO_4 \cdot 2H_2O$	sylvite	KCl
halite	$NaCl$	syngenite	$CaSO_4 \cdot K_2SO_4 \cdot H_2O$
hanksite	$9Na_2SO_4 \cdot 2Na_2CO_3 \cdot KCl$	tachyhydrite	$CaCl_2 \cdot 2MgCl_2 \cdot 12H_2O$
hexahydrite	$MgSO_4 \cdot 6H_2O$	thenardite	Na_2SO_4
kainite	$MgSO_4 \cdot KCl \cdot 1{}^1/_4H2O$	thermonatrite	$Na_2CO_3 \cdot H_2O$
kieserite	$MgSO_4 \cdot H_2O$	trona	$NaHCO_3 \cdot Na_2CO_3 \cdot 2H_2O$
langbeinite	$2MgSO_4 \cdot K_2SO_4$	van'thoffite	$MgSO_4 \cdot 3Na_2SO_4$

central evaporites are presented.

CONTROLS ON EVAPORITE PRECIPITATION

Conditions necessary for the formation and preservation of substantial evaporite deposits are stringent, thus the major controls of evaporite deposition need to be included in any treatment of dynamic facies models. The type of evaporite produced is a product of the degree of brine concentration, the brine composition, and the hydrology and climate of the depositional site.

Brine concentration

The order in which evaporite minerals precipitate is controlled by their relative solubilities, the least soluble minerals precipitating first. Calcium carbonate begins to precipitate from seawater concentrated 1.8 times; gypsum begins precipitating at 3.8 times seawater concentration, and halite only when the brine reaches a concentration 10.6 times that of seawater (McCaffrey *et al.*, 1987). Magnesium sulphate first appears at brine concentrations of about 70 times seawater, whereas a 90 times concentration is needed to precipitate potassium-bearing phases. The composition of an ancient marine-derived evaporite deposit is therefore, in part, a measure of the brine concentration reached at the depositional site. This is partially controlled by climatic factors.

If brine and air are at the same temperature, water can only be evaporated when its vapour pressure exceeds the partial pressure of water in the atmosphere (= its relative humidity; Kinsman, 1976a). The vapour pressure of a brine varies with the chemical activity of water in that brine, itself a function of the brine's ionic strength or salinity. The mineralogy of evaporites is therefore strongly controlled by climatic variables. Low humidities are required to evaporate brines to the concentrations needed to precipitate minerals of high solubility, e.g., if the relative humidity of air over an evaporite basin exceeds 76%, brines cannot be concentrated by evaporation to halite saturation. Over oceans, mean relative humidities are near 100%, whereas at low-latitude coasts, humidities fall to 70-80%. Humidities low enough to allow primary potassium and magnesium salts to precipitate (below 67%) are confined to regions distant from oceans. These salts will not occur in marginal marine evaporitic environments. Today, the only significant region of potash salt precipitation is in the Qaidam Basin of western China, a region 1500 km from the nearest ocean, in an orographic desert.

Brine composition

Compositions of continental waters are more variable than seawater, so that a greater diversity of evaporite minerals form when they are evaporated. As each mineral phase is precipitated during evaporation, it removes components from solution, so modifying the remaining brine composition. Evaporation pathways of brines are largely determined by the initial Ca:[HCO_3 + CO_3] *ratio*, and the Ca:SO_4 ratio (Eugster and Hardie, 1978). The first ratio determines whether the remaining brine will become alkaline and depleted in calcium, or will become neutral and depleted in carbonate species. The *second ratio*, at the stage of gypsum saturation, determines whether a brine will become depleted in calcium or sulphate. Waters with Ca < CO_3 + HCO_3, upon evaporation precipitate alkaline carbonates, whereas those with Ca > CO_3 + HCO_3 may evolve into brines that precipitate sodium sulphates.

Mineralogical, geochemical and

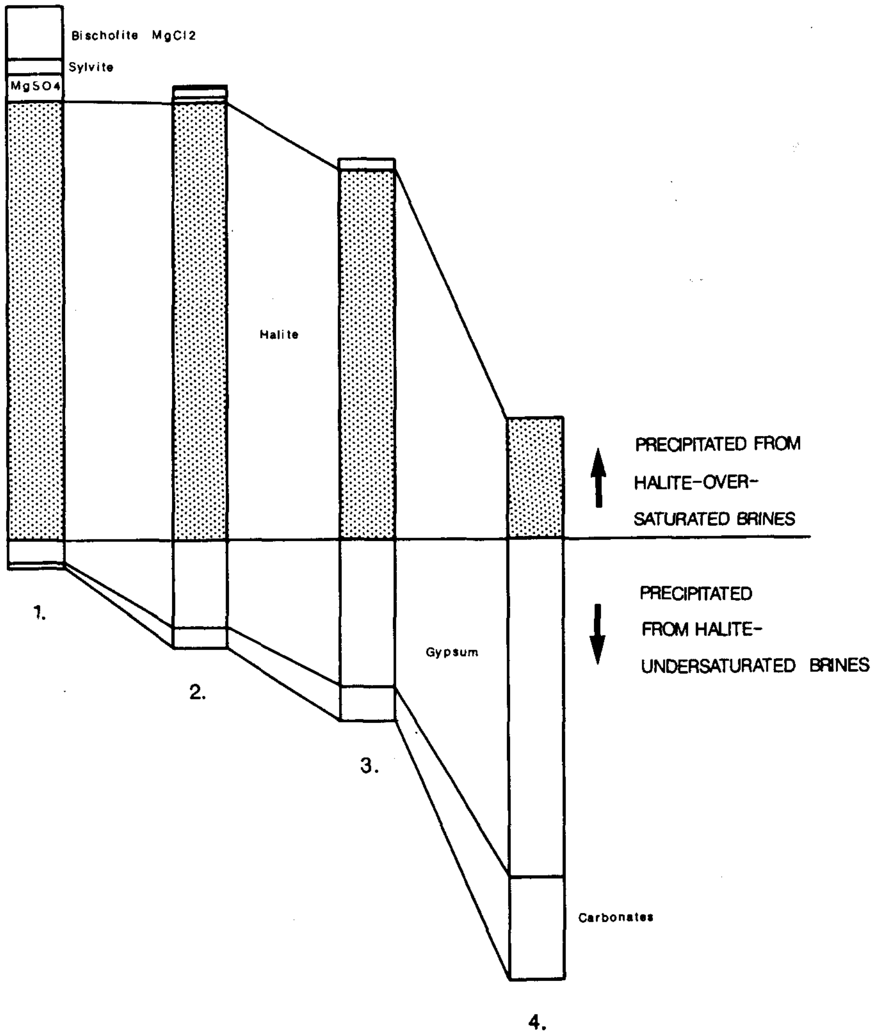

Figure 1 Comparison of evaporite compositions expected from seawater evaporation (1), compared with average compositions of (2) Zechstein evaporites, (3) "average" evaporites (dominantly from cratonic basins; rift/juvenile oceanic evaporites would be more halite dominated), and (4) anhydrite-dominated sequences. Data modified from Borchert and Muir (1964).

sedimentological criteria for discriminating between marine and nonmarine evaporites have been proposed by Hardie (1984) and Smoot and Lowenstein (1991). Most controversial are Hardie's (1990) suggestions that the commonest potash salts were precipitated from hydrothermal brines or from evaporated seawater modified by mixing with these brines. Salts composed of halite-sylvite-carnallite ± tachyhydrite ± bischofite (the magnesium sulphate-poor evaporites) cannot be derived from seawater evaporation. Many of these evaporites occur in rift and transtensional strike-slip basins, locations where there are upwelling hydrothermal $CaCl_2$ brines, rich in Na^+, K^+, and Ca^+ but poor in Mg^+ and SO_4^{2-}. These brines, driven upward thermally, may enter closed or partially closed basins, there to mix with surface waters. Evaporation of these mixed waters will precipitate magnesium sulphate-poor evaporites.

Magnesium sulphate-poor evaporites also occur in cratonic sag basins where rising deep-seated hydrothermal brines are not expected. However, the hydraulic head, produced during the desiccation of deep evaporite basins, may cause underlying groundwaters to migrate upward and enter the basin (Kendall, 1989). In this way pre-existing $CaCl_2$ brines or newly formed $CaCl_2$ waters, generated during dolomitization of limestones, enter the basin and modify surface waters in the same manner as Hardie proposed.

Basin hydrology

All models of evaporite deposition involve a consideration of basin hydrology. Evaporite depositional systems are dynamic and open, and must be considered in terms of inter-related water and salt budgets (Logan, 1987).

Inflow of water and salts

Large volumes of seawater are required to form evaporite deposits. A single batch of seawater, even in a deep basin, cannot produce any significant deposit.

Basin restriction

Although large volumes of water are required, the depositional site must not be too open or brines will constantly be diluted; evaporation is unable to prevent dilution from unrestricted surface-water inflow. Evaporite basins must therefore be restricted or isolated from the sea. The ratio between the surface area of the basin and the cross sectional area of any inlet must be at least $>10^6$:1 for gypsum to form, and for halite, the inlet must be at least eight orders of magnitude smaller than the basin area (Lucia, 1972).

All marine-derived evaporite sequences are deficient in the more soluble phases (Fig. 1). Thus the brine components forming the missing more-soluble phases must have been exported from the basin. The size of any inlet to a halite-precipitating basin, however, is so small that there must, in reality, be complete surface disconnection of the basin from the open ocean (Lucia, 1972). In such isolated basins there is no opportunity for *surface* reflux of remaining brines back to the sea.

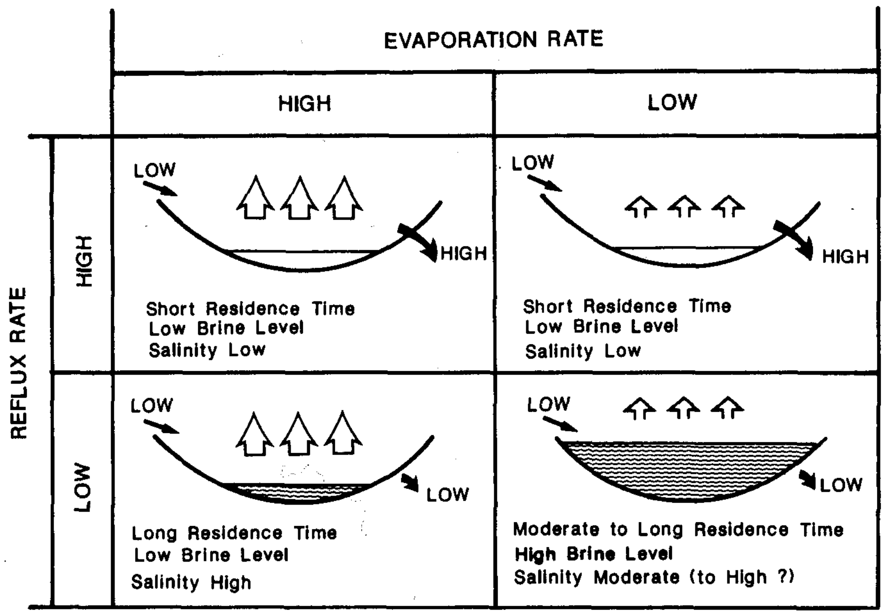

Figure 2 Models of isolated evaporite basins. Evaporative drawdown occurs in response to low influx rates (relative to evaporative losses). Deep water evaporites only form in basins with low rates of reflux and evaporation; all others experience significant desiccation. However, with low rates of evaporation, long time periods are necessary to concentrate the entire brine volume in the basin to the point where evaporites accumulate.

Inflow rates into isolated basins

Disconnected but marine-fed basins must gain their water by seepage through permeable barriers, and may receive a significant proportion of their water from continental sources. But seepage through barriers is unable to offset evaporative losses in the basin. The loss of brine volume, and a consequent lowering of the basin brine level is termed *evaporative drawdown* (Maiklem, 1971). When evaporation losses exceed inflow, nothing can prevent basins from desiccating. Preservation of a perennial brine in basins (required for "deep-water" evaporites) necessitates 1) episodic seawater input into the basin over the barrier, 2) a reduction in the evaporation rate, or 3) additional seepage inflow from the basin periphery or from the basin floor.

Brine reflux in isolated basins

Loss of the more soluble components in isolated basins must be by reflux through the basin floor. It is unreasonable, however, to expect that significant brine reflux can occur over the main part of an evaporite basin floor. If it were permeable enough to allow wholesale brine export, then this same permeability should also allow upward seepage of groundwater. Brines in the basin thus would be constantly diluted by this upward seepage, and brines of any significant concentration could not be generated. As fast as they form, they would sink away through the permeable basin floor, or be diluted by inflow. Thus a major prerequisite for evaporite deposition in basins is the presence of a basal aquitard, one capable of confining brines within basins (Logan, 1987). Such a basal seal in large basins is unlikely to be everywhere complete. Porous parts are potential sites for brine reflux or for upward seepage of groundwaters into the basin.

Inflow-outflow ratios in basins

Surface brines can only occur where losses from a basin (evaporation + brine reflux) are more or less balanced by inflow through the barrier (+ basin-floor seepage inflow, rainfall and additions of continental surface waters). If inflow exceeds water losses, the basin fills and becomes more dilute: if losses exceed inflow, the basin desiccates. The balance between losses and inputs also determines the salinity of basin brines (Fig. 2). Brine salinity is partially a function of the residence time of water in the basin (Logan, 1987). With low reflux rates, residence times are long, and evaporation may be able to concentrate brines to high concentrations. When air humidities are high, however, brines cannot be concentrated beyond a certain point. When residence times are short (high reflux rate), brines spend insufficient time in the basin to be concentrated to high salinities, before being exported from the basin. Regardless of the aridity of the climate, only evaporite minerals of relatively low solubility (carbonates, gypsum) are precipitated.

Neither influx nor reflux rates will be stable during a basin's history. Sea level changes increase or decrease the hydraulic head between ocean and the basin brine level, so increasing or decreasing the amount of seepage inflow. Sediment aggradation causes brine levels to rise, reducing hydraulic head and rates of seepage influx. Sediment aggradation is also associated with lateral overstep of basin flanks, expanding the area for possible brine reflux. Sites of influx and/or reflux may also become choked by precipitates or sediment, progressively reducing or stopping flow.

Variations in the inflow-reflux ratio cause changes in the volume of surface brine retained within a basin and the evaporite mineral being precipitated. Such changes may, however, occur without any change in climate.

EVAPORITE FACIES

Today, the relatively small area of continental crust with shallow seas limits evaporite deposition to continental lake basins and arid shorelines. This

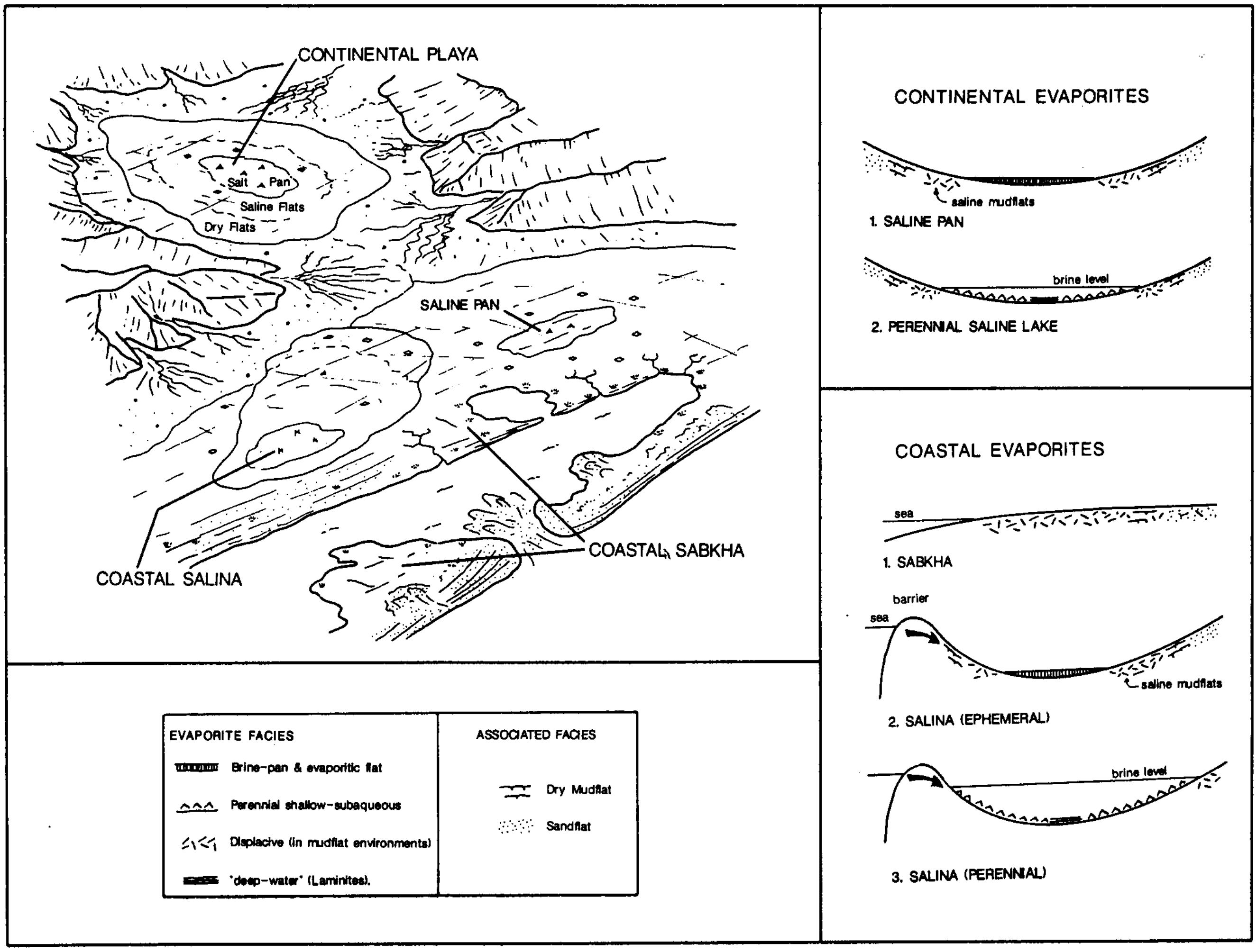

Figure 3 Modern evaporite depositional environments; diagram courtesy of C.R. Handford. Evaporites form in non-marine interior basins with playa lakes, salt pans and mud flats (continental sabkhas), coastal supratidal mud flats (marine sabkhas) and marine-fed, coastal lagoons and salt pans (salinas).

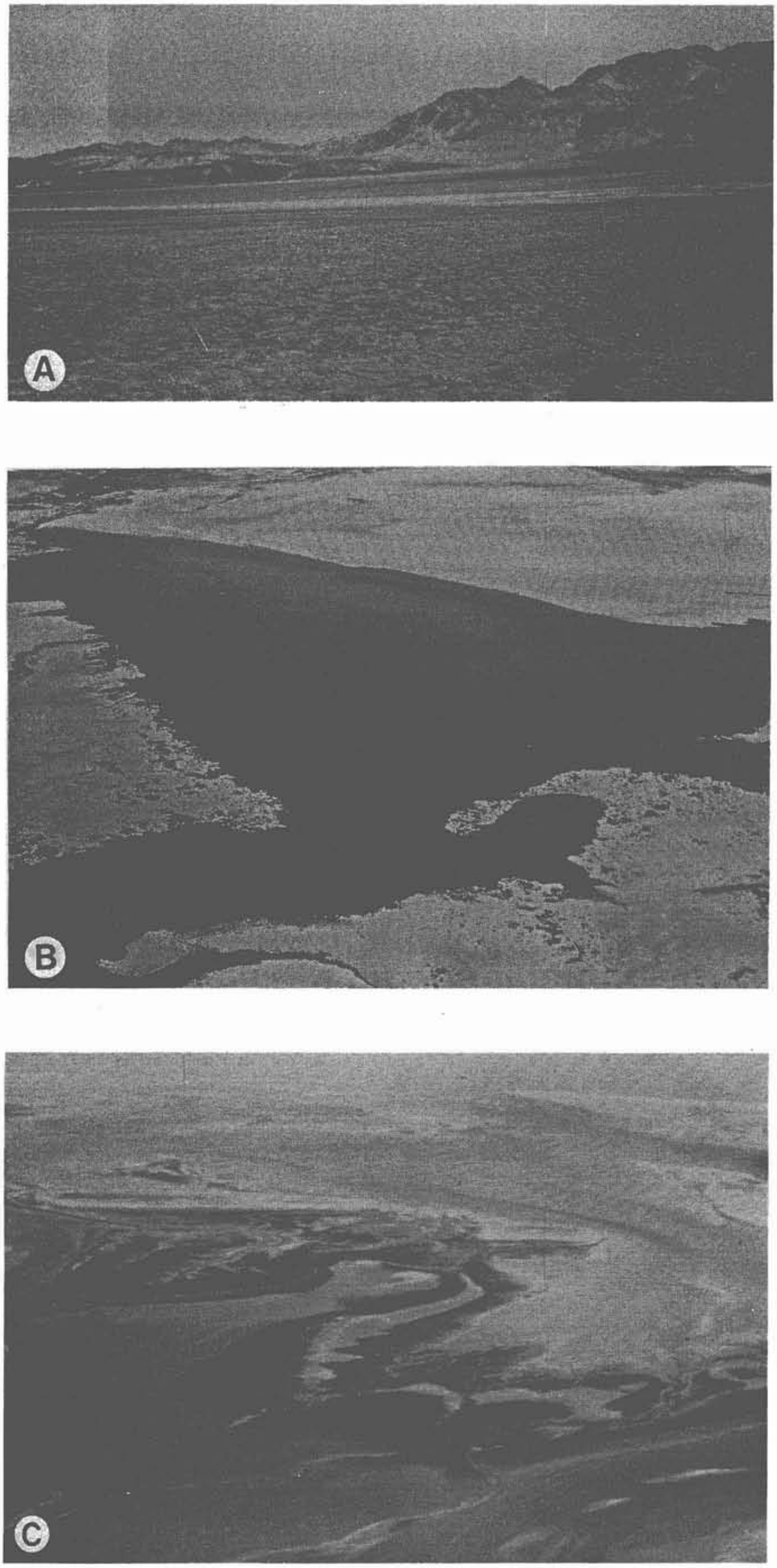

has not been the case in the past.

Evaporite sequences are generated in a variety of modern geographic settings (Fig. 3, 4). They grade into each other, are affected by similar depositional processes, and can produce similar facies. Identification of the geographic setting of ancient evaporites thus may depend more upon associated facies than upon internal characteristics.

The absence of Recent deep basinal and widespread shallow-marine evaporitic settings (Fig. 5) means that ancient evaporites of this type are identified by comparing their facies with those of ephemeral and permanent playa lakes and with small marine-fed salinas. In the absence of Recent analogs, models explaining the distribution and extent of these ancient facies (particularly those that cover hundreds of thousands of square kilometres, exceed several kilometres in thickness, or which directly overlie oceanic basement) must be determined by deductive reasoning coupled with information about the physicochemical behaviour of brine systems. One of the most important environmental parameters to be determined for these ancient evaporites is the depth of brine during their deposition.

Brine depth

Schreiber *et al.* (1976) recognized three main environmental settings for subaqueous evaporites (Fig. 6).

Figure 4 A) An interior basin: view of Death Valley, California with alluvial fans flanking mountains in background; salt pan in middle-distance (about 4 km wide), and saline mud flat (with efflorescent crusts) in foreground. B) A salina: aerial view of part of Lake MacLeod basin with perennial lake (about 2 km wide) fed by seepage through barrier (part of seepage face in foreground) and evaporite flats in background. C) A coastal sabkha: oblique view of NW Abu Dhabi sabkha. Supratidal sabkha in foreground; intertidal algal belt is the dark zone (1-2 km wide); seaward of this is the lagoon (20 km across), barrier islands and open Persian Gulf in far distance. Photo courtesy R.K. Park.

Identification was based on sedimentary structures. Criteria used include 1) structures indicating wave and current activity, identifying high-energy intertidal and shallow subtidal environments, 2) algal structures (in the absence of wave- and current-induced structures), believed to indicate a deeper environment, but one still within the photic zone, and 3) widespread, evenly laminated sediments, lacking evidence of current and algal activity (but associated with gravity-displaced sediments) characterizing the deepest, subphotic environment. There are problems with the use of these criteria.

Stromatolites may grow in protected, shallow water settings and the absence of current structures from algal-bearing sediments is not necessarily a criterion of greater depth. It may also be impossible to discriminate between planar stromatolites and organic films, formed by a passive

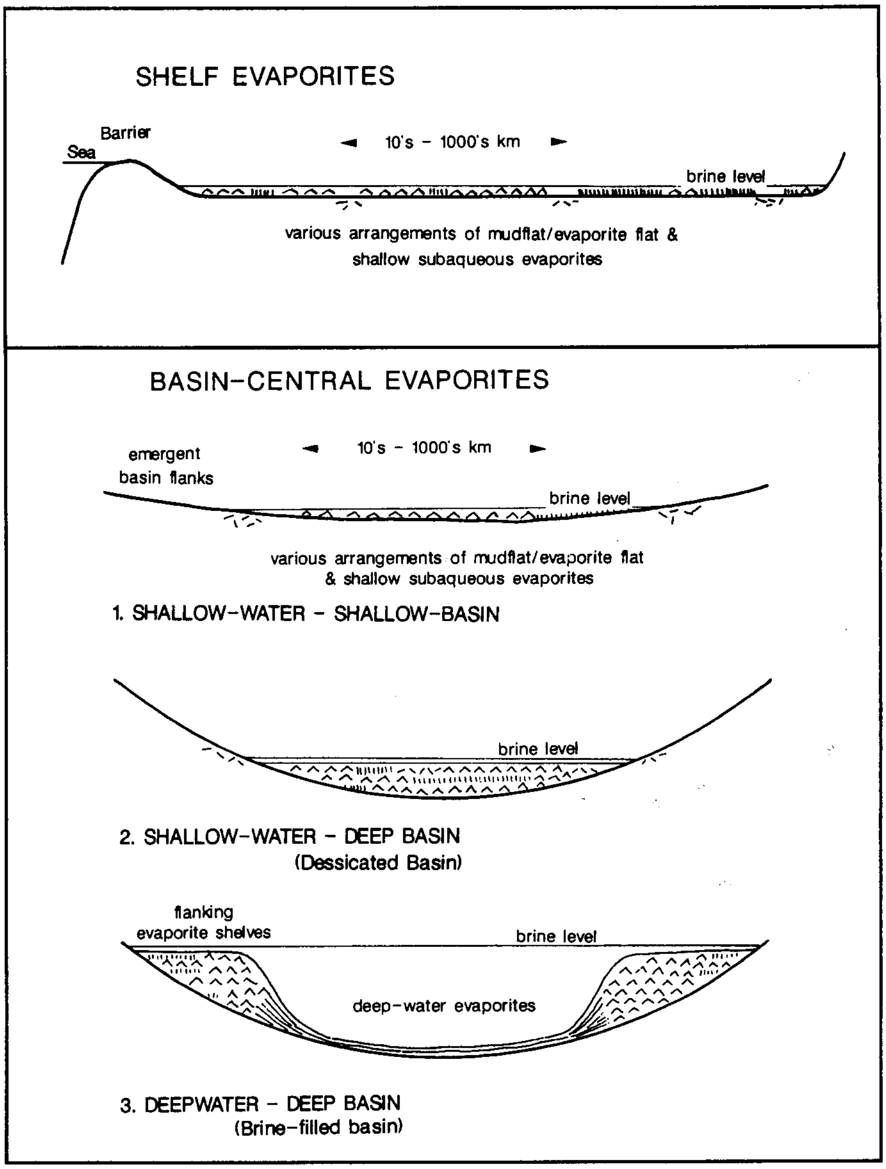

Figure 5 Evaporite depositional environments, in addition to continental and coastal settings, represented in the rock record. For key see Fig. 3.

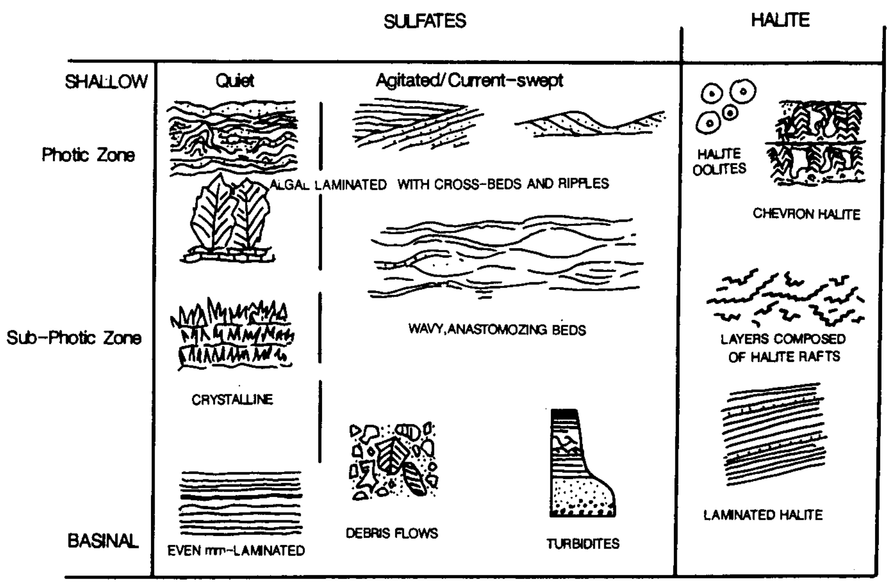

Figure 6 Main physical environments of subaqueous evaporite deposition and the chief sulphate and halite facies present in each. Modified from Schreiber *et al.* (1973).

accumulation of organic detritus, which have no depth significance.

Widely correlatable lamination is not unique to deep water environments. Similar lamination occurs in evaporites deposited in subaerial, but ephemerally flooded, environments (see Figure 18 later in this chapter)

Dissolution surfaces and bottom-grown crusts may also be used to assess depositional depth in evaporites. An abundance of dissolution surfaces implies each water influx into the depositional site dissolved part of the previously precipitated evaporite. Thus each flooding event diluted the entire brine column (Adams, 1969; Warren, 1982). This can only happen when brine volumes are small, implying shallow brine depths. Despite the shallow water origin (5-10 m) of some evaporites lacking dissolution surfaces, the presence or absence of these surfaces reflects a feature of fundamental importance. Environments affected by dissolution events are composed of repeatedly dissolved and reprecipitated salts, whereas those of deeper environments are not subjected to such recycling.

Continued growth of evaporite crystals on the sediment surface requires that they be in contact with supersaturated brines. Evaporative concentration leading to supersaturation, however, only occurs at the air-brine interface. In deep bodies of stratified brine, descent of supersaturated brines will be prevented by the density stratification, and bottom-grown crusts should not form.

Even when brine stratification is absent, as it is for brief periods in the present-day Dead Sea (Steinhorn, 1985; Anati *et al.*, 1987), there is no drive to transport supersaturated brines to the deep basin floor. They do not differ substantially in density and should mix with the main part of the brine long before reaching the bottom.

Advection of supersaturated brines probably affects brines down to a salinocline or thermocline (20-40 m). Where the basin floor lies at shallower depths it should be affected by advecting brines, and bottom crusts could potentially grow. Unless supersaturation can be achieved by means other than surface evaporation, evaporite crusts should record precipitation in brines only a few tens of metres deep.

Three main groups of evaporite facies are here recognized (Table 2), 1) *mud flat* facies in which evaporites accumulate within pre-existing sediments in episodically flooded, subaerial environments, 2) *shallow water* facies, typically characterized by evaporites containing dissolution surfaces/bottom-grown crusts, and 3) *deep water* facies characterized by the presence of laminations and gravity-displaced sediments, and lacking indications of shallow water environments. Deep water evaporites may, however, be deposited in only a few tens of metres of brine, whereas many shallow water evaporites are deposited on evaporitic flats that only become flooded during storm surges or particularly high tides. Since here all depositional events are subaqueous, the interpreted environment is so identified, even though the depositional site may be subaerially exposed for most of the time.

Table 2 *Evaporite facies.*

1. **MUD FLAT EVAPORITES** formed by displacive evaporite growth in pre-existing sediments.
   - A) *DRY MUD FLAT FACIES*: evaporites non-accumulative, former presence revealed by modifications to primary depositional and desiccation structures.
   - B) *SALINE MUD FLAT FACIES*: evaporites persistent* as crystals/nodules; few sedimentary structures survive in host sediments.

2. **SHALLOW WATER EVAPORITES** formed by precipitation and/or sedimentation from shallow surface brines (usually <5 m deep) which are permanent or ephemeral features of the environment.
   - A) *EVAPORITE FLAT FACIES*: laminated clastic evaporites precipitated and deposited from unconfined ephemeral brine- and flood-sheets+. Dissolution features usually absent or subdued because of cyanobacterial coatings and frequency of flooding. Transitional into —
   - B) *BRINE PAN (EPHEMERAL SALINE LAKE) FACIES*: evaporites precipitated/deposited from ephemeral but confined bodies of brine. Laminated detrital evaporites and/or alternations of evaporite crusts and saline mud flat detrital layers (with displacive evaporite crystals). Well-developed dissolution surfaces and patterned ground phenomena. Cyanobacterial mats in less saline settings. Transitional into —
   - C) *SHALLOW PERENNIAL LAKE FACIES*: evaporites deposited/precipitated from permanent shallow brines. Evaporite crusts with flood-introduced detrital layers; dissolution surfaces in shallower parts; buried crystal terminations in deeper. Cyanobacterial mats in less saline shallower settings. Transitional into 3A

3. **DEEP WATER EVAPORITES** precipitated or emplaced in brines generally deeper than 20-40 m (but deep-water-appearing evaporites may occur in brines only a few metres deep). Characteristically they lack dissolution surfaces and bottom crusts.
   - A) *BASIN FLOOR FACIES*: sediments with fine, even, and widely distributed laminations.
   - B) *BASIN MARGIN FACIES*: basin floor laminated/shallow water crusts, with resedimented evaporites — turbidites, slumps and mass flow deposits.

* Evaporites may later be removed by undersaturated groundwaters, making distinction from dry mud flat facies difficult.

+ Growth of displacive evaporites within evaporite flat sediments superimposes saline mud flat characteristics.

MUD FLAT EVAPORITES

These evaporites grow in occasionally flooded, but essentially subaerially exposed, saline mud flats around playa lakes and salina ponds, and in supratidal flats or coastal sabkhas. Here there is an imbalance between evaporative outflow and seepage inflow such that brine tables lie within the sediment. Flooding events, produced by storms, spring tides or wind set-up, punctuate the history of these areas and are the chief depositional agents. The brine table usually occurs less than a metre below the surface so that all sediments reside within phreatic or capillary zones.

Sedimentary processes

Saline mud flats are equilibrium deflation-sedimentation surfaces with a topography controlled by the brine table and its gradients. Wind removes particulate material that has dried out on the flats, but this can be inhibited by cyanobacterial mats or efflorescent crusts. Disruption of upper sediments by efflorescent crust growth creates materials sensitive to wind action and formation of clay dunes. Gypsum crystals, precipitated in uppermost sediments, may concentrate as lag deposits or be swept together as gypsum dunes.

The shallow water table allows evaporation to occur with concomitant concentration of pore fluids. Thus saline mud flats are sites of brine formation regardless of the salinities of the inflowing groundwaters. The brine type and the mineralogy of the evaporites that precipitate from them are, however, highly dependent upon the chemical composition of the ground- and floodwaters. Continuing evaporation generates a pronounced groundwater concentration gradient away from input sites (commonly toward the basin centre in playas, and away from the sea in coastal sabkhas). Progressively more saline minerals can be precipitated and preserved in these directions.

Little, if any, evaporite precipitation occurs from surface brines; instead evaporites grow within soft, brine-soaked sediments to form intrasediment evaporites (Fig. 7A), or at the surface, by evaporation of groundwater, as ephemeral efflorescent crusts (Fig. 7B). Precipitation results from brine evaporation from the capillary fringe, or by reactions between the brine and the host sediment (including previously formed evaporites). Host sediments are typically siliciclastic or carbonate muds, but may be sands or earlier precipitated evaporites.

Sediment is transported onto mud flat surfaces episodically: by spring tide or storm-backup sheet floods in coastal sabkhas, or by storm-fed sheets in playas downslope (or downwind in playas). These sediment additions are only preserved where the brine table rises a corresponding amount. Otherwise the extra sediment dries out and is deflated. Where flood-introduced sediments persist, the episodic nature of depositional events imparts a lamination. This is continuously disrupted and destroyed between flooding events by the growth and dissolution of ephemeral evaporite crystals and crusts, and by episodes of surficial drying that cause extensive and multiple mud-cracking.

Efflorescent crusts of saline minerals accumulate on mud flats during groundwater discharge and evaporation (Figs. 7B, 8), or by the evaporation to dryness of ponded floodwaters. Because evaporation is both rapid and complete, crusts include metastable and highly soluble salts. Rain and floodwaters dissolve the more soluble constituents to form concentrated but chemically "simple" brines. Ultimately such brines may reach basin-central ponds or brine pans.

Thicker saline crusts are similar to those of salt pans but are surficial and ephemeral features. Growth of evaporite crystals causes volume increase and the formation of salt blisters (Fig. 8A), salt-thrust polygons (Fig. 8B,C); or, when affected by rain, highly irregular dissolution surfaces with considerable relief (Fig. 9).

Even salts that survive dissolution by floodwaters and become buried are ephemeral when underlying groundwaters are undersaturated. Upward movement of undersaturated brine, caused by evaporative losses near the

Figure 7 Recent mud flat evaporites. A) Displacive lenticular gypsum crystals forming "gypsum mush" layer, Abu Dhabi sabkha. Photo courtesy B.C. Schreiber. B) Ephemeral halite crust with "pop-corn"-like growths (10 cm across): Howz-e-Soltan salt lake, Iran. Although halite forms the most conspicuous surface evaporite, gypsum is the only phase accumulating within the sediment. Photo courtesy F. Fayazi.

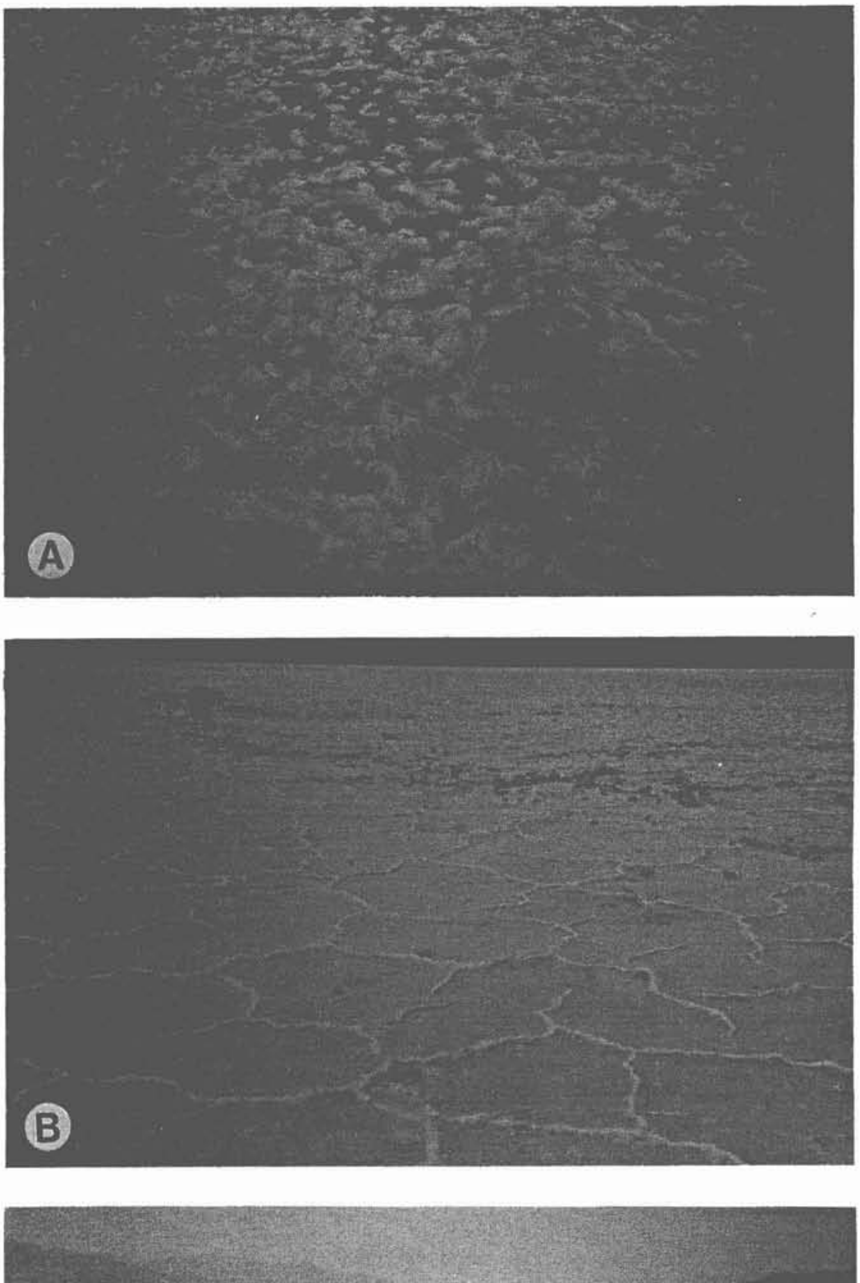

Figure 8 Surface features of salt pan, Death Valley, California. A) "Puffy-ground" (small salt blisters) on dry mud flat marginal to salt pan (photograph 3 m across in foreground). B) Thin salt crust with polygonal fracture system and growth of efflorescent salt in fractures. C) Salt-crust polygons with upthrust edges (photograph 4 m across) in foreground.

surface, dissolves the buried remnants of the salt crust and reprecipitates it at the new surface. Further away from the input sites, however, groundwaters become increasingly more saline and calcium sulphate, or even halite, may become stable within the sediment. Minerals in surface crusts thus do not usually reflect the character of evaporite minerals preserved in underlying sediments. Many fine-grained, dolomitic redbed sequences probably represent deposits of these evaporitic, but essentially non-evaporite-preserving, environments.

Sedimentary facies of host sediments

Two types of mud flat are distinguished in playas (Hardie *et al.*, 1978; Smoot and Lowenstein, 1991) and the same concepts can be adopted for salinas (Handford, 1991) and for marine-marginal sabkhas. Saline mud flats lie closer to saline lakes, salt pans, salina ponds or the sea, whereas dry mud flats occur in more distal locations and may pass laterally into coarser sand flats.

Dry mud flats

Depositional and desiccation structures (Figs. 10, 11) are generally preserved. Mud and sandy laminae form during and after flooding but these become partially disrupted by mud cracks, sheet cracks and the growth and subsequent dissolution of saline minerals. Dry mud flats are covered with efflorescent saline crusts between flooding events. When saline crusts begin to dissolve in floodwaters, introduced coarser sediment is trapped in depressions on the dissolving crust. Upon burial and complete dissolution of saline crusts, these coarser sediments are preserved as irregular coarser-grained patches (*sand-patch fabric*, Fig. 11C).

Slowly aggrading dry mud flats are composed of more massive sediments (Castens-Seidell, reported in Hardie, 1986; Smoot and Lowenstein, 1991). Here, most of the sediment deposited during flooding events subsequently blows away in the wind, only material deposited in mud cracks survives. Upon drying out, the surface becomes covered by new mud cracks which are able to trap new sediment during subsequent floods. Repeated mud cracking and sediment filling, together with growth and dissolution of halite crystals, generates massive mudstones.

Saline mud flats

These mud flats are composed of sediments in which lamination and desiccation structures have been destroyed by the growth of abundant intrasediment evaporite crystals. Floods cause partial dissolution of previously precipitated evaporites and sediment collapses into the cavities formed. Repeated episodes of these processes produces a chaotic mix of evaporite crystals within an unlaminated mud matrix (Figs. 12, 13A).

Mud flat evaporite facies

Intrasediment evaporite crystals grow by incorporating sediment (trapped as inclusions within the growing crystals), or displacively, by pushing aside the sediment, or by both processes (Fig. 13A). The amount of evaporite emplaced within sediments varies enormously (Fig. 12).

Saturation of groundwaters with respect to calcium and magnesium carbonates occurs quickly. This causes precipitation of 1) calcite cement or caliche layers in coarse-grained sediments, such as alluvial fan sands and gravels surrounding playas, 2) micron-sized high-Mg calcite and protodolomite soft muds, or 3) travertines and pisolitic caliche when precipitation occurs at peripheral springs. In arid coastal settings, seawater also quickly becomes carbonate saturated in the intertidal zone, causing formation of cemented crusts.

Intrasediment gypsum crystals most commonly exhibit a discoidal hemipyramidal habit (flattened normal to the c-axis, Fig. 7A) and may be complexly twinned to form rosettes (desert roses). Gypsum grows displacively within

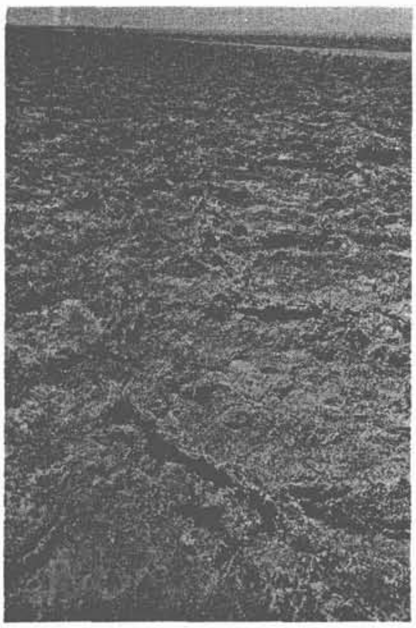

Figure 9 Markedly upthrust polygons, partially dissolved to form highly irregular, 0.5 m relief. Devil's Golf Course, Death Valley, U.S.A.

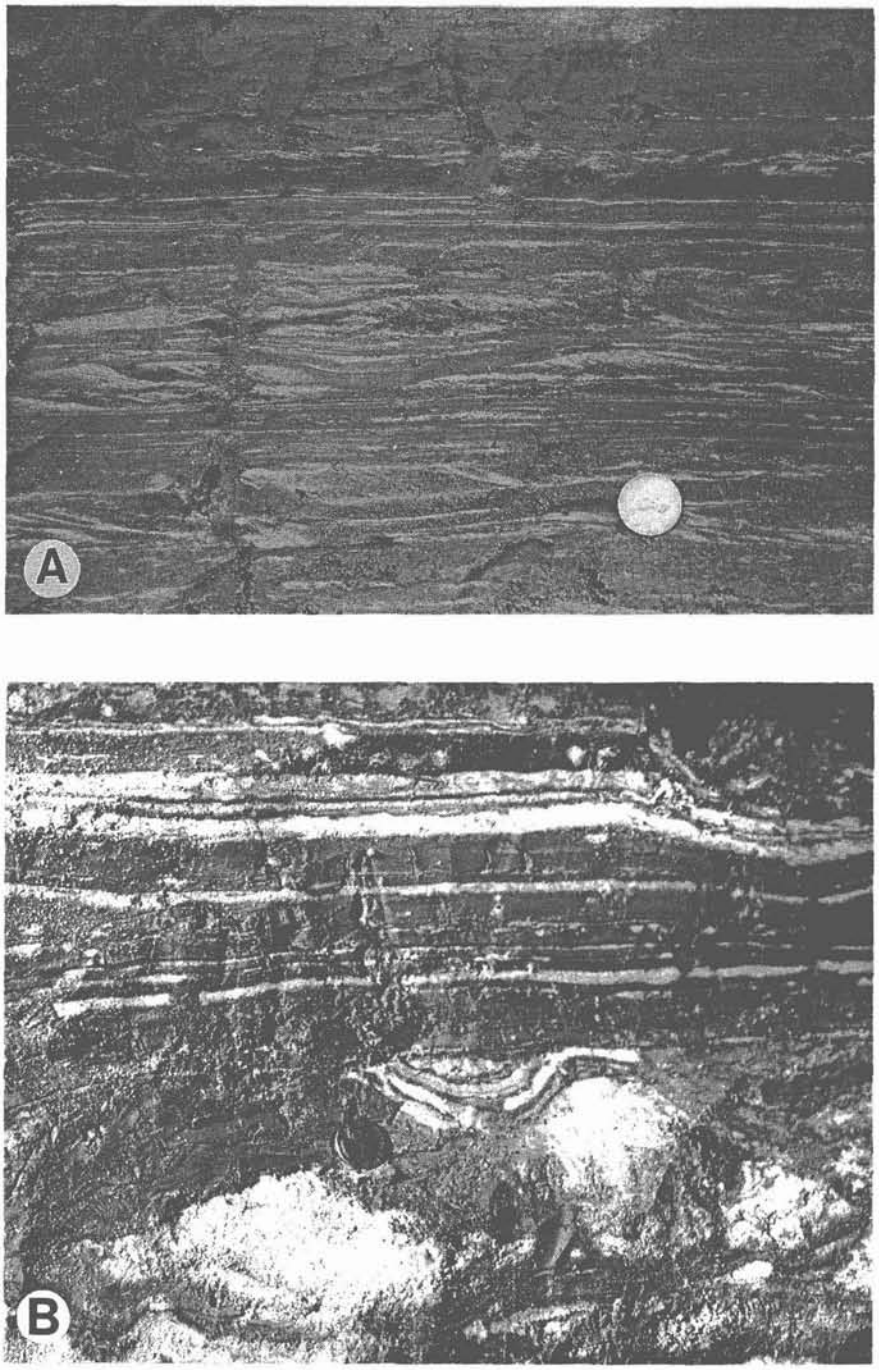

Figure 10 Recent mud flat sediments. A) Flaser-bedded clastic playa sediment with clay drapes (5 cm coin for scale). B) Contorted gypsum and red mud; note truncated gypsum layers marking former playa surface (5 cm coin for scale), Bristol Dry Lake (California); photo courtesy C.R. Handford.

cyanobacterial mats or fine-grained sediments (sometimes forming crystal mushes), or grows poikitically within sandy sediments, where it occurs as large, lenticular crystals. Gypsum precipitation causes calcium depletion in groundwaters, and the increased Mg/Ca ratio of brines may promote dolomitization of pre-existing aragonite and precipitation of magnesite. Dolomitization of aragonite also releases strontium that precipitates as celestite.

Anhydrite has a more restricted distribution in mud flats and is confined to the capillary zone. It may replace earlier gypsum (Butler *et al.*, 1982), or be newly formed. Nucleation of anhydrite requires a seasonal high temperature above 35°C, and is only preserved where mean annual temperatures exceed 20°C (Kinsman, 1976a). It forms discrete nodules and bands of coalesced nodules (Fig. 14), some of which may take the form of ptygmatic (enterolithic) layers. Nodules grow by host-sediment displacement, and replacement and dilution of the host sediment may occur to such an extent that this is relocated to internodule areas or reduced to mere partings between the anhydrite nodules. Much of this *mosaic anhydrite*, however, may have replaced gypsum, rather than being displacive. Pseudomorphs are uncommon because of flowage, adjustment during compaction, and continued growth of primary anhydrite. Composite anhydrite nodules are remnants of gypsum crystal clusters, and massive anhydrite forms from gypsum mush layers. Such soft anhydrite layers become deformed into enterolithic folds and microdiapirs with continued anhydrite growth (Fig. 15).

Displacive anhydrite growth is not the only mechanism for generating nodules. Primary gypsum nodules occur (West *et al.*, 1979), and gypsum and anhydrite regularly alter backward and forward, dependent upon temperature changes and flooding or rainfall events (Gunatilaka *et al.*, 1985). Much nodular and bedded nodular anhydrite in Recent and ancient evaporites has replaced gypsum-pan (salina) deposits, rather than being displacive or replacive after displacive gypsum (Hardie, 1986).

The addition of displacive gypsum and anhydrite in mud flat sediments raises the sediment surface. If the water table fails to rise a corresponding amount, the upper parts of the sediment dry out and blow away. Deflation exposes anhydrite and gypsum at the surface and truncates layering and other structures present within these sediments (Figs.10, 14B, 15).

Displacive halite in modern playa sediments has been described (Gornitz and Schreiber, 1981; Handford, 1982) but it is uncertain if precipitation occurred beneath shallow brines, or within mud flat capillary zones. Crystals commonly grow preferentially along cube corners and edges (especially when they are precipitated from highly supersaturated brines), forming cubes with hopper-like pyramidal hollows on each face. In extreme cases, skeletal/dendritic halite crystals are generated (Fig. 13b). Sediments with abundant displacive halite cubes (Fig. 12) are termed *haselgebirge* (Arthurton, 1973). Halite also occurs as salt crusts on coastal sabkha surfaces, as veneers around grains in the upper part of the capillary zone, and as solid cubes in sands. Halite is not an accumulative phase here, but dissolves diurnally in morning dew, is blown away, or dissolves in floodwaters.

SHALLOW WATER EVAPORITES

Deposition of most shallow water evaporites occurs in brines at or near saturation with respect to gypsum or halite, and in environments that may have been subject to strong wave and current action, causing sediment

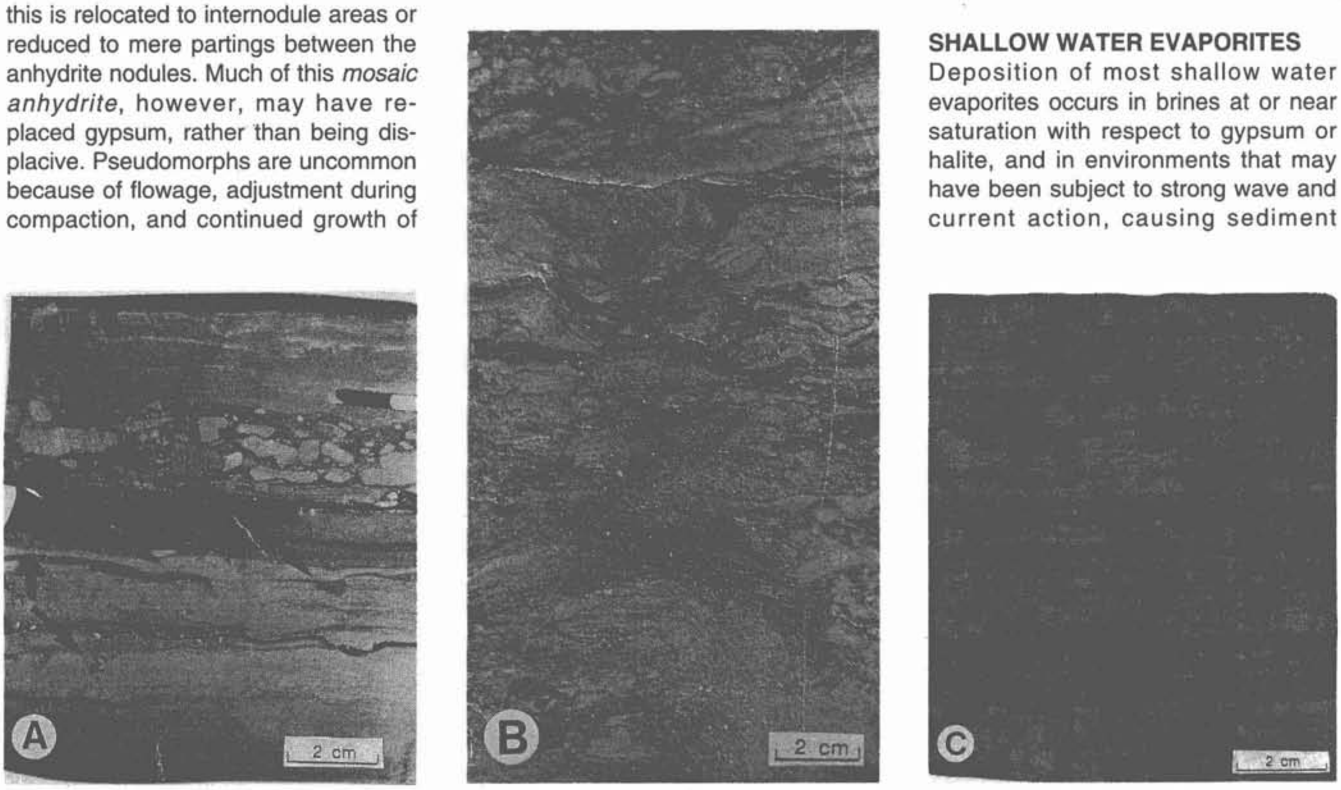

Figure 11 Ancient dry mud flat dolomites. A) Centimetre-bedded silty dolomites with erosive bases and sediment-filled moulds after displacive halite hopper crystals (arrowed). B) Silty dolomite, originally laminated but now highly disrupted by superimposed generations of desiccation cracks and (?) repeated growth and dissolution of evaporites. Both from Paradox Formation (Pennsylvanian), Utah. C) Herald Formation (Ordovician of Saskatchewan) dolomites with irregular patches of coarser sediment (sand patch fabric), believed to have accumulated on top of former saline crusts, filling depressions created during floodwater dissolution.

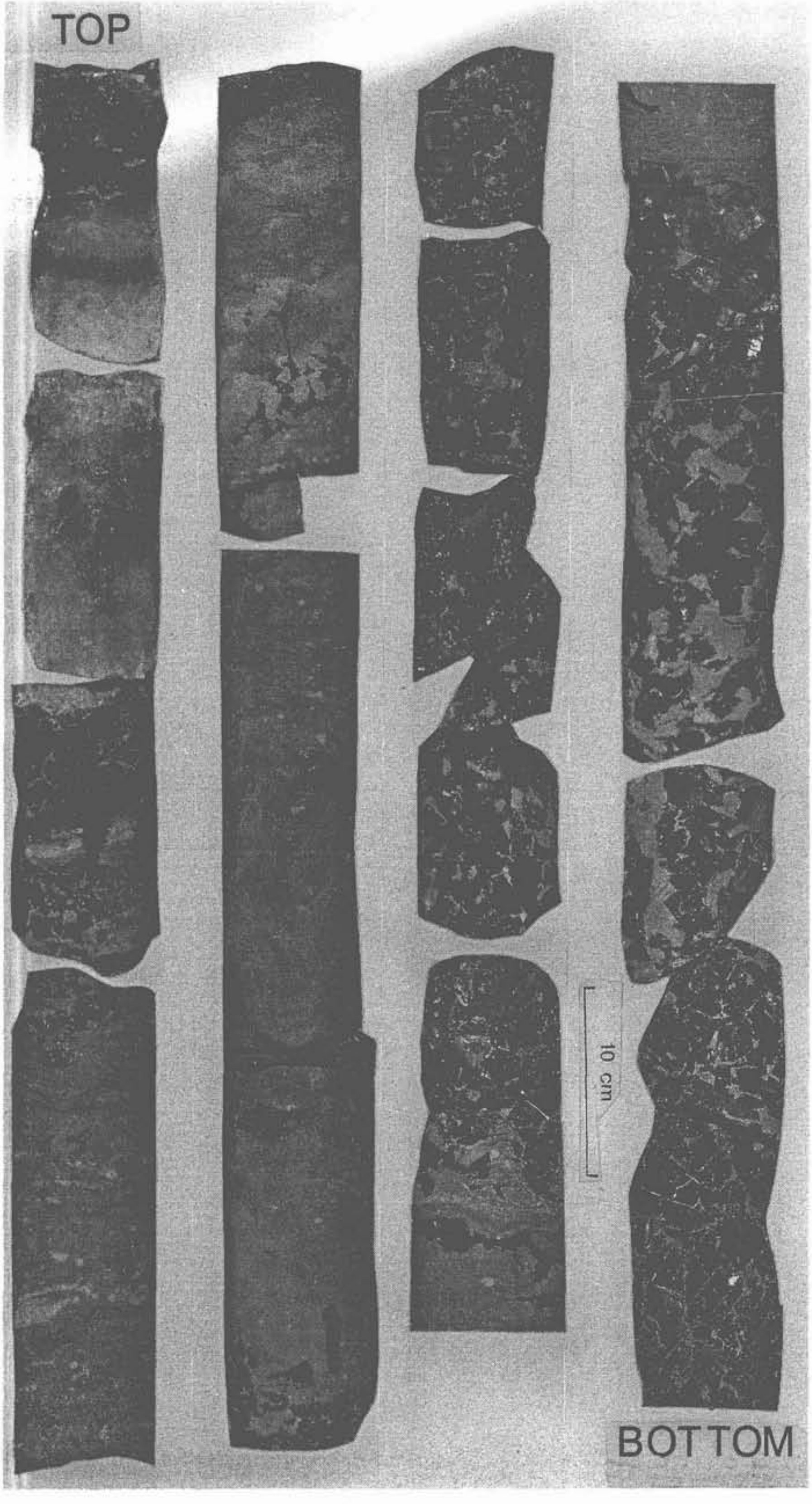

Figure 12 Upward passage from red silty and anhydritic mudstone with abundant displacive halite (haselgebirge) to similar sediments with lesser amounts of halite crystals (with hopper morphology) and bedded halite with thin anhydrite and clay laminae. Sequence marks a change from a saline mud flat to a salt pan deposit. Lotsberg Salt (M. Devonian), N. Alberta.

scour, transport and redeposition. Most facies probably form in brines less than 5 m deep. Cyanobacterial activity is important in more protected environments and many sediments are subject to periodic drying.

Most of our original understanding of these evaporites came from interpretations of ancient examples (Hardie and Eugster, 1971; Schreiber *et al.*, 1973; Vai and Ricci Lucchi, 1977; Garrison *et al.*, 1978). More recently studies of artificial salt ponds (Busson, 1982; Orti Cabo and Busson, 1984) and of Recent salinas (Arakel, 1980; Kushnir, 1981; Perthuisot, 1981; Warren, 1982; Logan, 1987) have confirmed older interpretations and suggested others.

Shallow water evaporites occur in shallow perennial and ephemeral playa lakes and in marine-fed salina ponds, these being typically surrounded by mud- or evaporite-flats. Ephemeral saline lakes are also termed salt pans. They grade insensibly into mud flat-like environments where evaporites accumulate as detrital sediments or by surface precipitation. These *evaporite flats* are occupied for brief episodes by unconfined brine sheets, usually only a few centimetres deep.

Three present-day shallow water evaporite environments can be recognized: perennial saline lakes, salt pans, and evaporite flats. Evaporites with shallow water features also occur in ancient deposits where they form laterally extensive deposits unlike those of Recent examples. Some of these may form by lateral accretion in depositional environments similar to those of the present, whereas others may require explanations that are drastic departures from present-day settings (see sections *Basin-marginal (shelf) evaporites* and *Basin-central evaporites).*

Sedimentary processes

Perennial saline lakes persist for tens to thousands of years without drying up. They require substantial perennial inflow — a large river, an inlet or a highly permeable barrier. During wet periods/seasons they may greatly expand, flooding surrounding flats.

Evaporation at the lake surface generates concentrated surface brines in which saline minerals nucleate and grow. Brines and crystals sink but, unless the entire brine column is saturated, the crystals dissolve before reaching the lake bottom. This dissolution progressively increases brine concentrations until crystals no longer dissolve and they begin to accumulate on the lake floor.

The minerals precipitating from surface waters are determined by the chemical composition of the inflow, the evaporation/inflow ratio, and the previous history of the lake. If evaporation just slightly exceeds inflow, only minerals of low solubility (carbonates) will be precipitated. For more soluble minerals to be precipitated, the evaporation/inflow ratio must be higher, and bottom brines must be dense enough to support the surface brine for sufficient time to allow it to become supersaturated with respect to the saline mineral. When bottom brines are not dense enough, surface brines sink before supersaturation is reached.

Lakes experiencing a progressive reduction in their inflow exhibit a progressive change from precipitating low to high solubility salts. But lakes affected by short term decreases in inflow may display no change in precipitation because the change in the evaporation/inflow ratio is not matched by a sufficient change in the density of the entire lake brine.

Dissolution of the uppermost evaporite deposits in shallow perennial lakes occurs during freshening events (storms, wet seasons) when mixing of the entire brine column is complete. Wind turbulence causes mixing, and during strong persistent winds there may be wind setup where brines are driven or kept upslope. Migration of lake margins for tens of kilometres is controlled by changes in wind conditions, and brine sheets may be disconnected from a lake to move over neighbouring mud- or evaporite-flats.

Wave action is limited by restricted depth and/or fetch. Maximum expenditure of wave energy occurs at lake margins where evaporite crystals may be continuously moved and abraded *as they grow*. This forms rippled sands and gravels composed of rounded crystal clasts.

Crystal growth at brine surfaces produces small, thin and platy or needle-like crystals or brine-displacing, hollow hopper-shaped crystals. Crystals may coalesce into floating rafts. Crystals and rafts float on the brine surface, *held up by surface tension*, until they grow large enough to sink, or are spilled by waves. They can be transported downwind to accumulate at shorelines, but most accumulate on lake floors forming loosely packed layers of *cumulate* crystals.

Carbonates may also be chemically or biochemically precipitated in surface waters to produce sediments similar to those of freshwater lakes (Dean and Fouch 1983; Eugster and Kelts 1983; Allen and Collinson, 1986). They form carbonate units between evaporites during episodes of lake dilution, or form seasonal partings between evaporite laminae.

Crystal crusts precipitate on lake bottoms from well-mixed supersaturated brines. They overgrow cumulate crystals or older crusts, or nucleate on stable substrates (e.g., cyanobacterial mats; Fig. 16). Crusts deposited at greater depths are protected from dissolution during flood events by a density stratification developed between the inflow and the bottom brine, and become draped by detrital or chemical laminae. Those in shallower parts are partially dissolved during freshening events and may be difficult to distinguish from saline pan deposits (see below).

Shallow lakes with bottom brines at or below gypsum saturation support luxuriant cyanobacterial mats (Fig. 16). Gypsum and carbonates precipitate in and upon the mats.

Salt pans are occupied by ephemeral bodies of brine that form when inflow temporarily exceeds outflow. A return to normal evaporative conditions causes such lakes to shrink and disappear. Repeated floods generate sequences

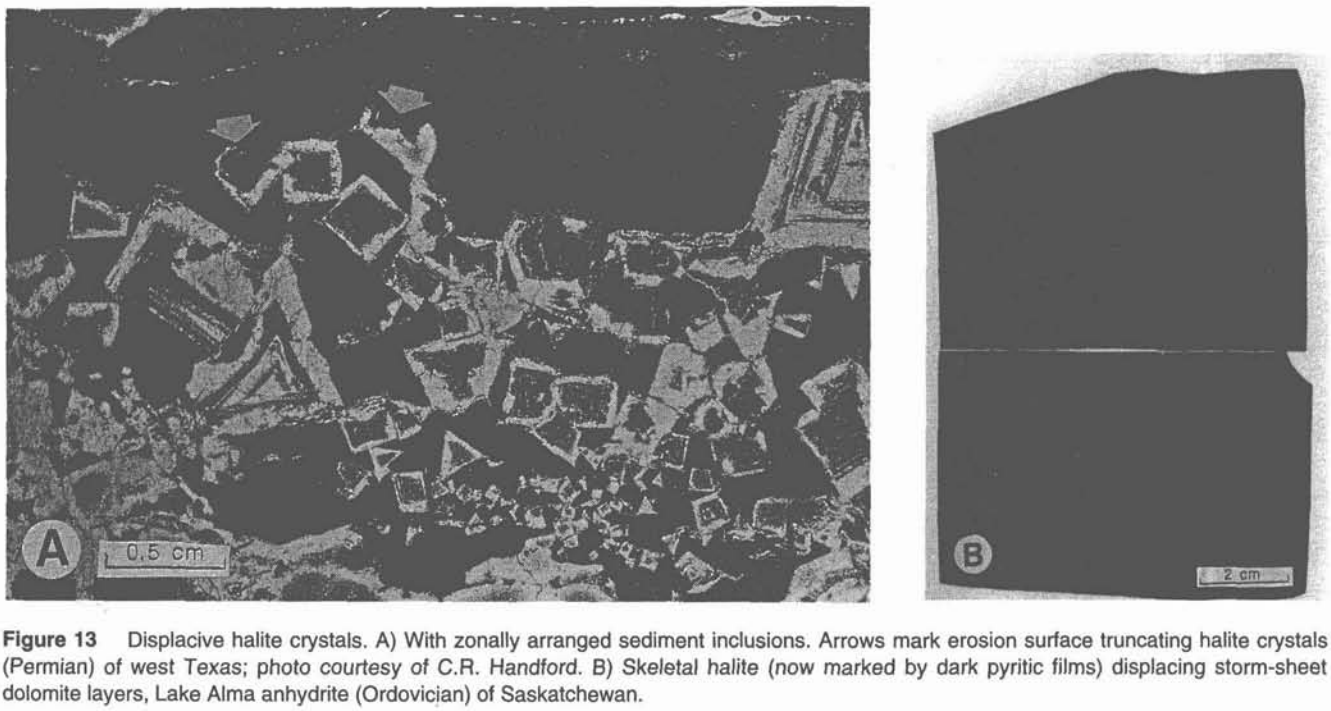

Figure 13 Displacive halite crystals. A) With zonally arranged sediment inclusions. Arrows mark erosion surface truncating halite crystals (Permian) of west Texas; photo courtesy of C.R. Handford. B) Skeletal halite (now marked by dark pyritic films) displacing storm-sheet dolomite layers, Lake Alma anhydrite (Ordovician) of Saskatchewan.

composed of thin salt crusts (of halite, trona, gypsum or mirabilite/thenardite) separated by crystal-rich mud partings and dissolution surfaces (Fig. 17).

During floods, shallow brackish lakes form, and fine-grained sediments, introduced by floodwaters, are deposited as thin layers. Floodwaters also dissolve 1) efflorescent saline crusts on surrounding flats, and 2) previously precipitated salt crusts of the salt pan. After floods, lake waters concentrate by evaporation. At first they precipitate cumulate crystals, but eventually crystals grow on the lake floor as crusts. If several minerals are precipitated they exhibit a "bull's-eye" distribution pattern, with the most soluble minerals confined to the centre of the lake and precipitated just prior to complete lake desiccation. Newly exposed salt crusts have high porosities with crystal interstices occupied by saturated brine. Salt surfaces are kept moist by evaporative draw and by precipitation of dew on hydrophilic salt surfaces during cold nights. The evaporation rate falls to values as low as 1/170th of the rate from standing bodies of the same brine, so the brine level rarely drops more than a few metres beneath the surface. Nevertheless brines continue to concentrate by evaporation, with development of overgrowth cements on salt crystals, precipitation of more soluble minerals in pore spaces, and growth of displacive crystals within mud layers. Continued crystal growth causes crust expansion and formation of polygonal fractures with overthrust edges (Fig. 8C). Preferred brine evaporation in fractures (Fig. 8B) causes localized precipitation of efflorescent crusts. This widens cracks and continues the upturn of polygon margins to form relief up to 50 cm on the pan surface that traps eolian dust.

Because each flood introduces new salts (from surrounding flats and the hinterland), less salt in the pan is dissolved than was precipitated during preceding lake concentration stages. Each salt layer is largely composed of material that has been repeatedly dissolved and reprecipitated.

Gypsum pans differ from more saline salt pans. During floods gypsum is more commonly reworked than dissolved, and accumulates as crystal lags and intraclasts at the base of mud layers. Also after mud layers are de-

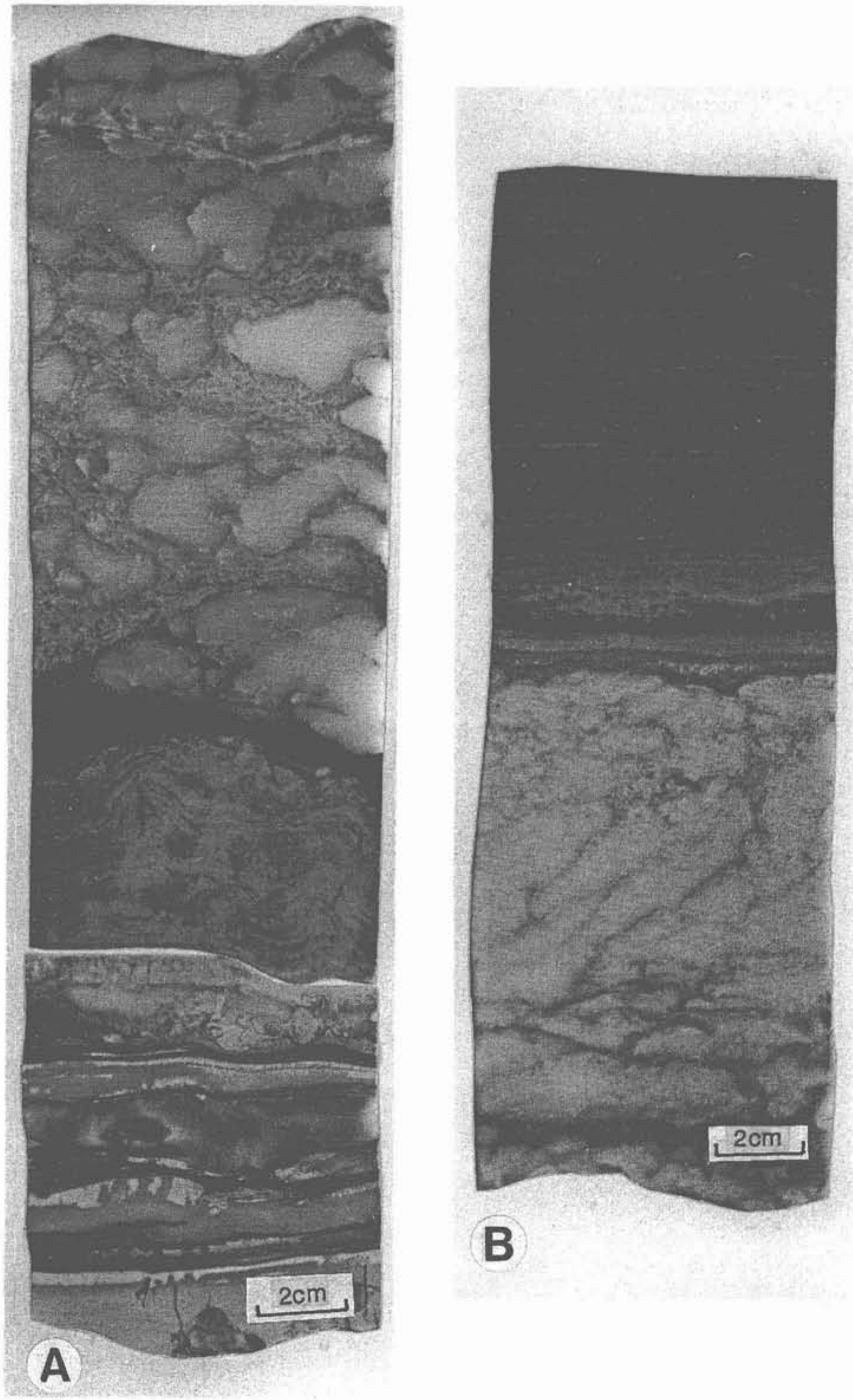

Figure 14 Sabkha cycles in Frobisher Evaporite (Mississippian of Saskatchewan). A) Laminated microdolomites (probably hypersaline lagoon) overlain by cyanobacterial mat containing anhydrite pseudomorphs of vertically oriented lenticular gypsum crystals, and nodular mosaic anhydrite. B) Upper part of sabkha cycle shown in (A) with inclined rows of nodular mosaic anhydrite (after subaqueous gypsum), truncated by erosion surface and overlain by laminated micrites of succeeding lagoonal member. Nature of anhydrite suggests deposition partly occurred in a salina on the sabkha surface.

posited, they are colonized by cyanobacterial mats. Their contorted surfaces are the template for later gypsum precipitation as surface crusts and as cements that grow beneath the blistered surfaces. Surfaces are exaggerated by continued gypsum crystal growth that buckles, domes and fractures the layers even more.

Evaporite flats are only occupied ephemerally by brine sheets. These are only a few centimetres thick but may cover areas of several hundred square kilometres. They form as outflows from saline lakes, either seasonally, when lowered evaporation rates allow lakes to expand, or episodically, when wind stresses detach brine sheets. Evaporite flats are also affected by flood sheets: ephemeral events caused by lower salinity inflows. Floods cause dissolution of earlier evaporites. This material reprecipitates as the floodwaters evaporate, with the formation of laterally persistent thin beds or laminae (Fig. 18), some traceable over the entire extent of the flooding, perhaps hundreds or thousands of square kilometres.

Evaporite flats occur in essentially the same geographic settings as mud flats but probably form in environments with greater frequency of flooding and an abundant supply of detrital evaporite.

Cyanobacterial mats are important during deposition of thin layered to laminated gypsum on evaporite flats. Brine sheets, upon evaporation, precipitate crusts composed of tiny acicular crystals. These are reworked by later brine or flood sheets to form detrital laminae, the main features of which may be controlled by cyanobacterial mats. Mats collect and bind evaporite sediment and, as the flood subsides, the coarser load is deposited as a traction layer or as a settle-out to form a normally graded lamina. The cyanobacteria grow through this, reestablish themselves on the surface, and protect the underlying sediment from erosion during the next flood.

Shallow water evaporite facies

An abundance of shallow water clastic textures and structures, coupled with the presence of desiccation features, crystal crusts, and cyanobacterial mats makes identification of well-preserved shallow water evaporites relatively straightforward. Difficulties arise when depositional features are lost or obscured by later diagenesis, or when these sediments are modified by diagenetic overprinting, as when the depositional environment desiccates and becomes subject to mud flat processes.

Laminated sulphates

Shallow water laminites consist of current-deposited carbonate micrite and clastic silt- and sand-sized gypsum crystals/cleavage fragments in reverse- and normally graded laminae. Crystals originally grew as bottom crusts that were later broken and reworked, or were precipitated brine-surface crystals that sank. All particles eventually become overgrown by cement, and laminae are converted into interlocking gypsum crystal mosaics.

Cross bedding, ripple-drift bedding (Fig. 19), basal scoured surfaces and rip-up clasts testify to environments with periodic high-energy events such as floods and storms. Reverse-graded laminae probably form when an upward segregation of coarser particles occurs in highly concentrated, flowing sand sheets. These occur in extremely shallow waters during storm surges, characteristic of evaporite flats. Shallow water deposition is also demonstrated by the presence of micritic, organic-rich stromatolites; by bird or dinosaur footprints; or by fossil brine shrimp or their fecal pellets.

Gypsum laminites altered to anhydrite rarely provide sufficient evidence for precise environmental reconstruction.

Gypsum crusts

This facies occurs as crusts and superimposed beds of vertically standing, elongate and commonly swallow-tail twinned crystals (Fig. 20), less than a centimetre to over five metres in height. Crystals are commonly eu-

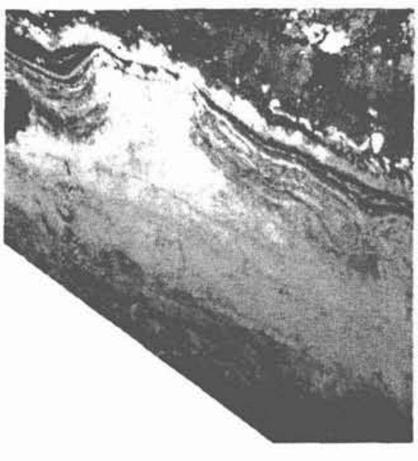

Figure 15 Surface trench about 50 cm deep in Abu Dhabi sabkha with diapiric layers of anhydrite (after gypsum); upper sediment layer truncating anhydrite is a storm-washover and eolian carbonate-clastic unit. Photo courtesy R.K. Park.

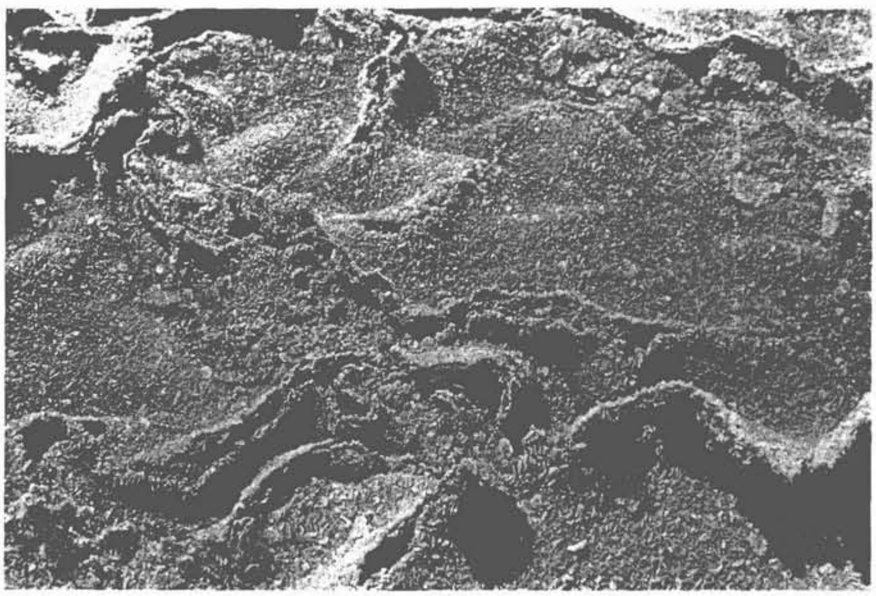

Figure 16 Rubbery, wrinkled cyanobacterial mat encrusted with gypsum crystals, 1-2 mm long; Hyeres salt lagoons, S. France. Photo courtesy G.M. Harwood.

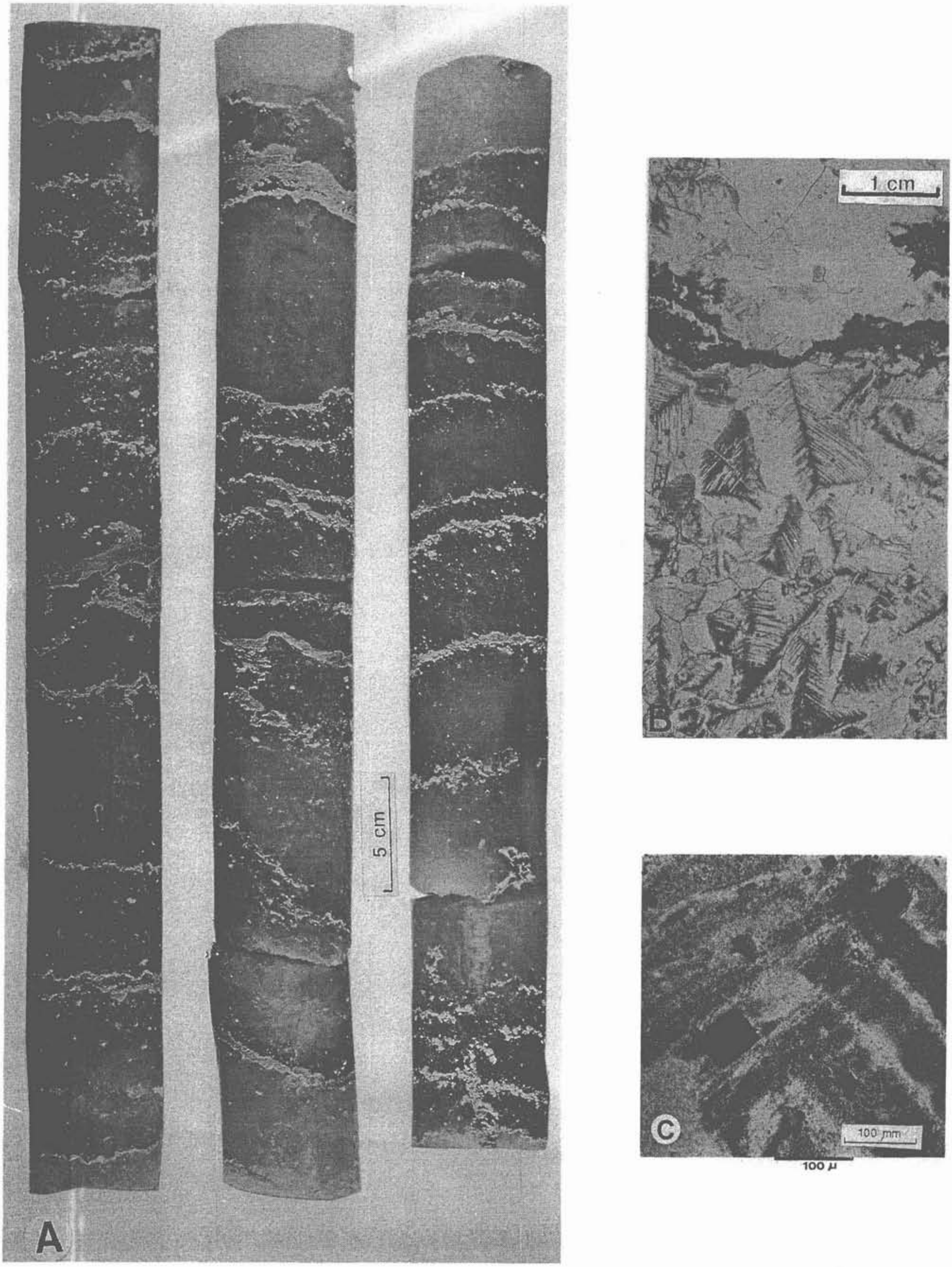

Figure 17 Brine-pan halite. A) Crusts of chevron halite with laminae of anhydrite, lower Prairie Evaporite, Saskatchewan. B) Thin section through chevron halite layer containing cloudy, inclusion-rich, and clear, void-filling crystals. The former are truncated by an anhydrite lamina. Thin section loaned by N.C. Wardlaw. C) Detail of single chevron halite crystal with alternations of brine-filled inclusion-rich, and clear halite growth layers. Photo courtesy C.R. Handford.

hedral, and define a vertical palisade fabric or radiating upward-conical clusters. Crystals are separated by micritic carbonate or fine-grained gypsum; or secondary overgrowth produces an interlocking crystal mosaic. Other crystals exhibit bizarre growth and twinning patterns and suffer crystal-splitting to generate palmate clusters of subparallel subcrystals (Fig. 21; see Orti-Cabo and Shearman, 1977). Twinning occurs at a variety of angles, probably because of organic matter incorporation along curved crystal faces; the greater the impurity, the more obtuse the twinning angle. Sometimes only one twin arm grows.

The crystals contain faint lamination (Fig. 21), defined by carbonate and anhydrite inclusions, which pass through the crystalline beds, parallel to bedding. Inclusions may parallel crystal faces, recording successive growth stages, or may be more planar, defining dissolution surfaces. Many crystals have invaded cyanobacterial mats (Fig. 22B).

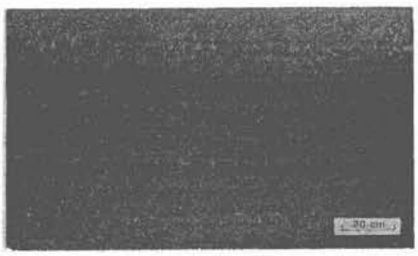

Figure 18 Thin-bedded to laminated clastic gypsum from evaporite flat; Lake MacLeod (Western Australia). Beds are laterally persistent across basin and record precipitation events after successive floods.

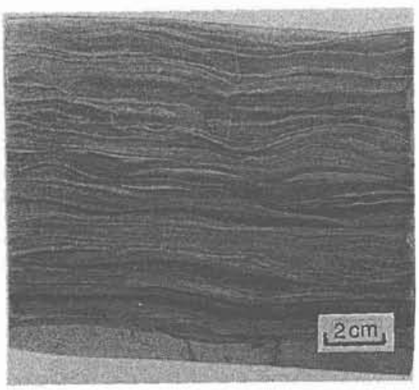

Figure 19 Laminated anhydrite with minor disseminated dolomite defining lamination, ripples, minor cross stratification and scoured surfaces. Poplar Beds (Mississippian) of Saskatchewan.

Larger gypsum crystals form in environments of constant and active brine flow: brine ponds that are drained during wet seasons only develop clastic gypsum layers or crusts composed of centimetre or smaller crystals. Internal lamination and included cyanobacterial mats indicate crystals

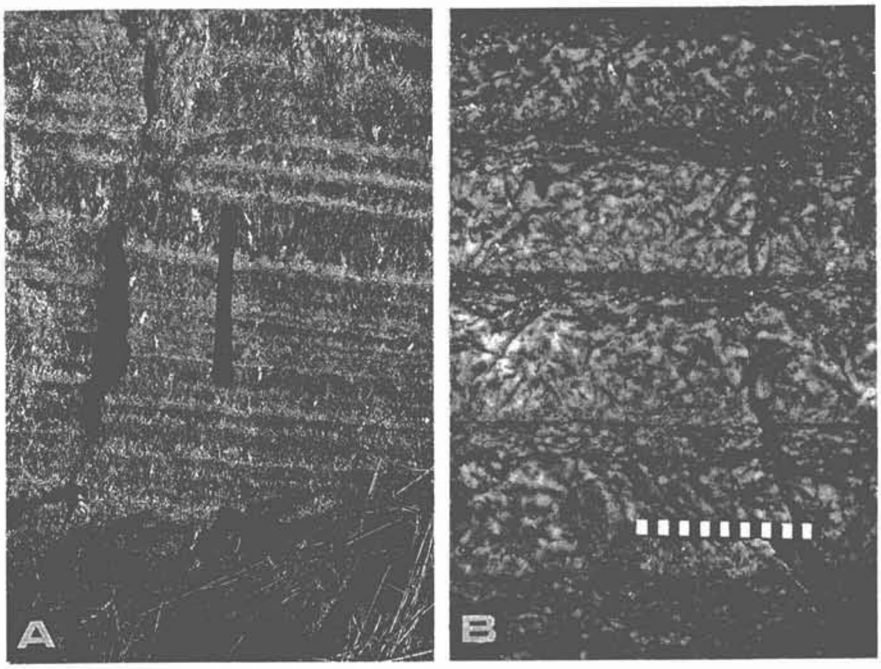

Figure 20 Coarsely crystalline gypsum facies. A) Palisades of gypsum crystals (scale bar 6 cm long), Miocene of Sicily. Photo courtesy B.C. Schreiber. B) Layered anhydrite with pseudomorphs after gypsum crystals, Otto Fiord Formation (Pennsylvanian), Ellesmere Island (scale bar divisions in cm). Photo courtesy N.C. Wardlaw.

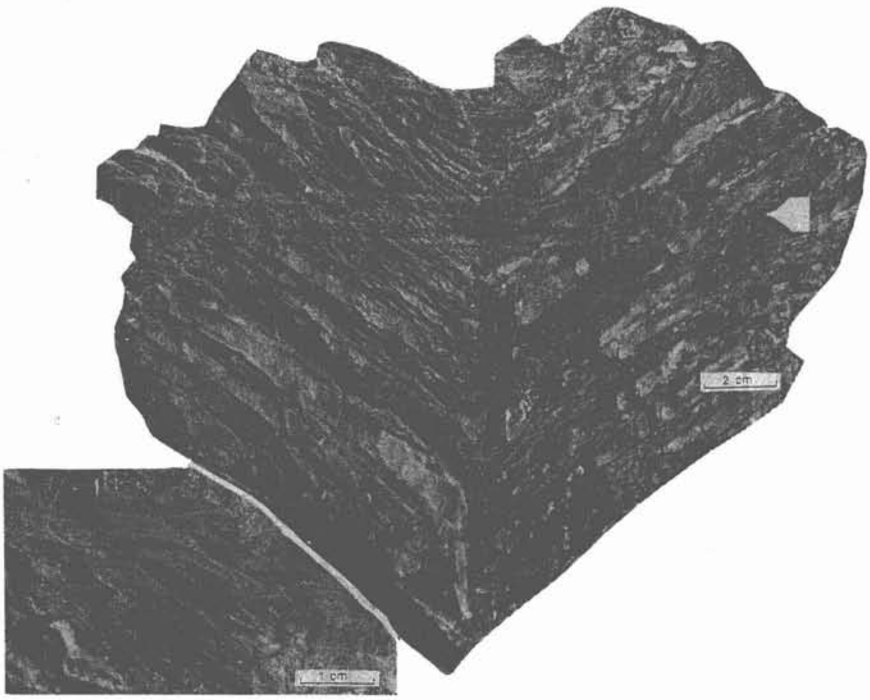

Figure 21 Swallow-tail twinned gypsum crystal (25 cm across) with dissolution surfaces at arrow. Inset is a cleavage plane surface of the same crystal with inclusion-defined growth layers. Photo courtesy B.C. Schreiber.

grew poikilitically, enclosing surficial veneers of sediment. Episodes of slight undersaturation create minor dissolution surfaces that truncate crystals. Renewed precipitation, however, occurs on the etched surfaces, burying them within the crystal (Fig. 21).

Beds composed of gypsum crystals may be difficult to identify when converted to anhydrite. During burial they are replaced by mosaic anhydrite (Rouchy, 1976; Loukes and Longman, 1982; Kendall and Harwood, 1989) which can closely resemble, and be confused with displacive nodular anhydrite. When the original gypsum crystals grew and poikilitically enclosed carbonate laminae associated with planar dissolution surfaces (Fig. 21) the nodular anhydrite retains such lamination and can easily be mistaken for a replacement of laminated gypsum. Gypsum crusts may also be replaced by halite, sylvite or polyhalite; the crystals being outlined by anhydrite. Such replacements only occur in the shallowest of brine ponds where there is a great temperature contrast between the brine layer and gypsum crystals beneath the pond floor.

Coarse clastic gypsum

Gypsum sands and pebbly sands, composed of worn gypsum cleavage fragments with variable amounts of carbonate and other materials, may locally be abundant, but rarely constitute major rock units. They do, however, indicate that gypsum can be transported and deposited in the same manner and environments as other clastic sediments, so long as the water body is gypsum saturated. These sands exhibit structures indicative of current or wave activity, or may be penecontemporaneously disturbed and contain load casts. Clastic gypsum occurs as shoestring sands or as sand sheets representing channel, beach, offshore shoal or spit deposits, or it may occur as beds between layers of laminar gypsum or gypsum crusts.

Halite crusts

There are detailed descriptions of halite crusts from the ancient (Wardlaw and Schwerdtner, 1966; Brodylo and Spencer, 1987), from Recent salt pans (Shearman, 1970; Lowenstein and Hardie, 1985) and from experimental studies (Arthurton, 1973). Various halite growth habits are observed but the most important are chevron halite (Fig. 17) and crusts composed of cornet-shaped crystals. Inclusions in crystals are concentrated into layers parallel to cube faces (Fig. 17C), so that, in crystals with corners uppermost, the zoning appears as chevrons with upwardly pointing apices.

Most upper surfaces of halite layers are either crystal growth faces (interruption in growth caused only by temporary and slight brine undersaturation: characteristic of perennial lakes), or truncation surfaces associated with cavities (recording more extreme episodes of brine undersaturation and halite dissolution; characteristic of saline pans). Each layer is composed of two types of halite: an inclusion-zoned halite, and a clear halite cement filling

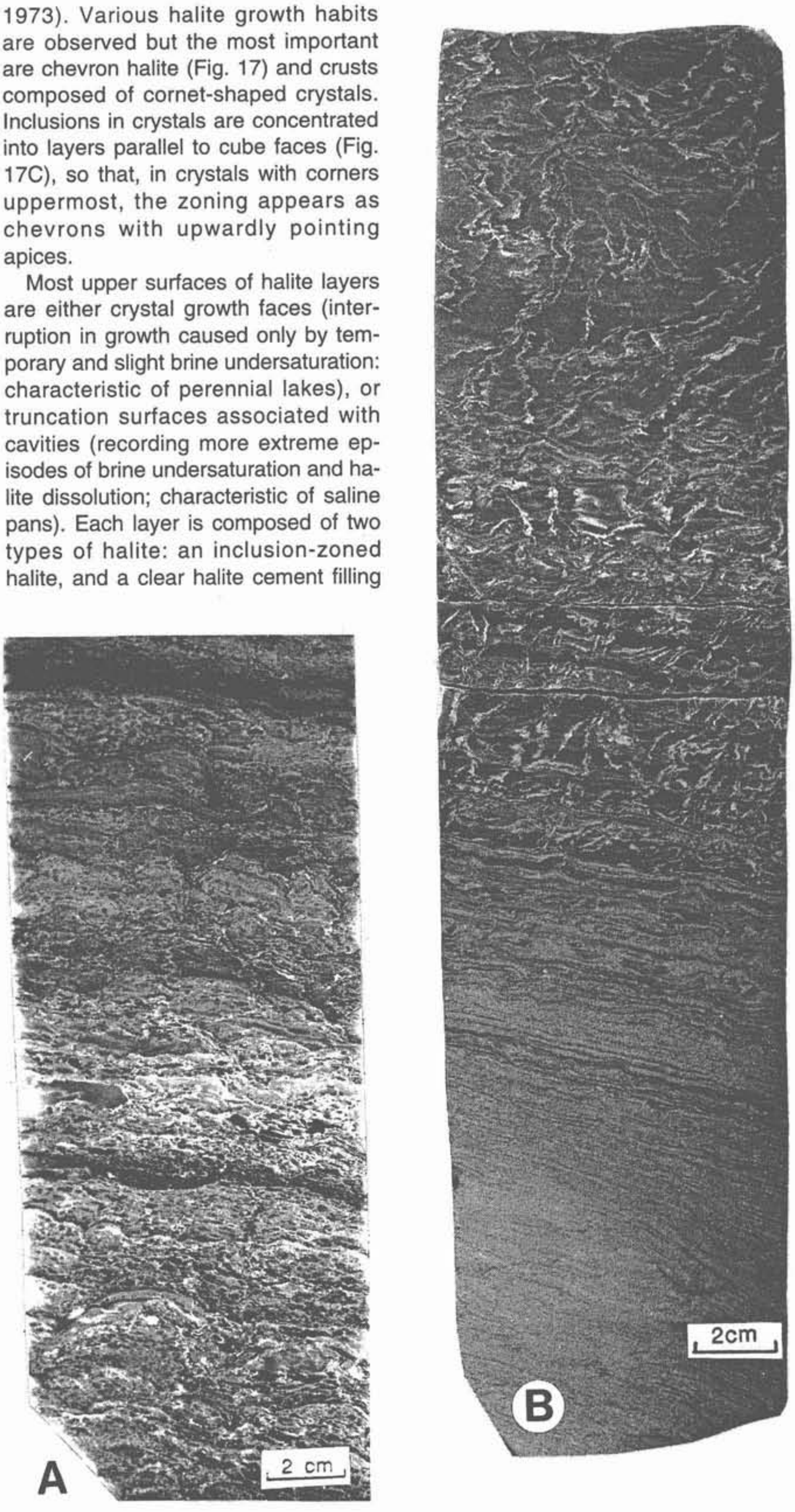

Figure 22 A) Anhydrite after displacive gypsum crystals that grew in mud-cracked stromatolitic carbonate. Each gypsum crystal is now a small, angular anhydrite "nodule", Souris River Formation (Upper Devonian), Saskatchewan. B) Anhydrite after gypsum crystals that grew within cyanobacterial mat, Souris River Formation, Saskatchewan.

porosity between zoned halite crystals or in dissolution cavities (Fig. 17B).

Inclusion-rich and -poor layers in chevron halite crystals (Fig. 17C) form from brines with different degrees of supersaturation. Thus they record rapid changes in brine concentration. This only occurs in small brine volumes, implying chevron halites are shallow water precipitates.

Detrital halite

Detrital halite is probably more important than published studies suggest; it is particularly susceptible to recrystallization. When preserved it is composed of fragmentary surface-grown hopper crystals and small cubes that may represent overgrown hoppers, crystals precipitated during brine mixing, or reworked material from bottom-growing crusts. Detrital halite commonly is ripple marked, exhibits cross bedding, and includes other detrital material. Karcz and Zak (1987) suggest that hydraulic behaviour of halite in brine is similar to that of the quartz/water system. Crystal growth continues after deposition and the detrital origin is easily obscured.

Detrital halite dominates higher energy environments, situations where crystals are subject to constant bottom movement, and crust development is prevented (Weiler *et al.*, 1974). Constant motion promotes halite precipitation onto grain surfaces with the formation of halite ooids.

Potash salts

Less is known about origins of potash-magnesia salts. The primary nature of sylvites in varved sylvinites is indicated by the intimate association with halite-preserving subaqueous textures (Lowenstein and Spencer, 1990). Sylvite layers were crystal cumulates that crystallized as a result of surface brine cooling. Wardlaw (1972) described crusts of bottom-grown carnallite, interbedded with layers of detrital halite. The presence of tachyhydrite in these evaporites, a mineral that cannot survive exposure to the atmosphere, indicates evaporite deposition was entirely subaqueous.

Most potash-magnesia salts, however, are diagenetic replacements of, or additions to, earlier halite or sulphate deposits. All textures and structures may be diagenetic, but less altered beds may still exhibit surprisingly well-preserved depositional features. Lowenstein (1988) describes primary textures in halite and anhydrite (originally gypsum) from potash ore beds of the Permian Salado Formation of West Texas-New Mexico. In the Salado and the Prairie Evaporite, sylvite and some carnallite are early diagenetic cements that fill intercrystalline porosity and solution cavities created in brine pan halite crusts (Fig. 23; Lowenstein and Spencer, 1990). These can be matched with Recent occurrences from brine pans. Here carnallite cements are precipitated as warm, potassium-rich surface brines descend below the saline pan surface during desiccation phases. Cooling of such brines causes them to become supersaturated with respect to carnallite.

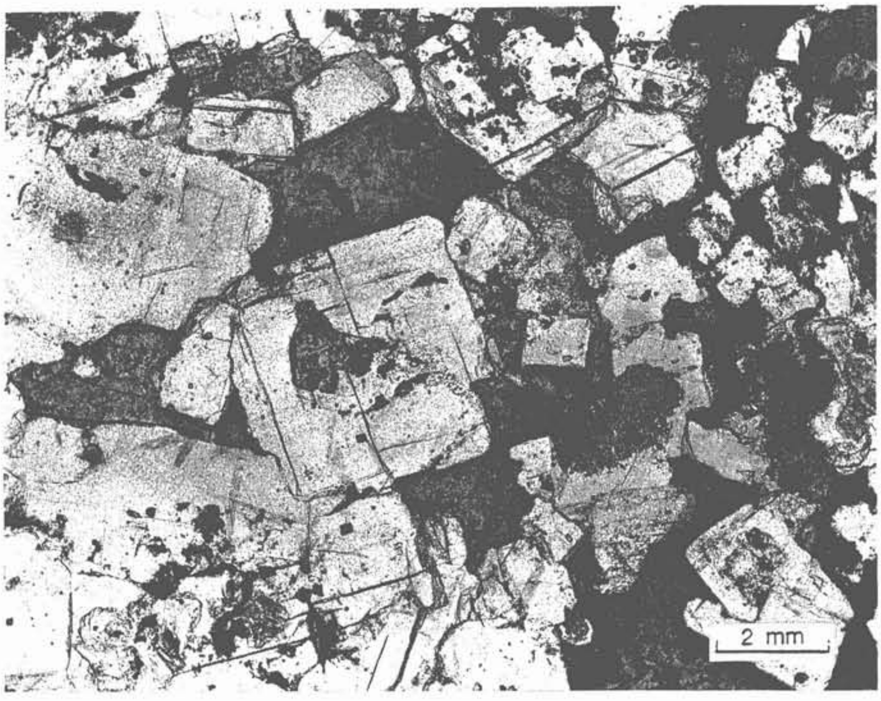

Figure 23 Thin section photograph of halite cubes surrounded by void-filling carnallite cement (dark grey) and mudstone (black); McNutt Potash zone, Salado Formation (Permian), New Mexico. Photo courtesy T.K. Lowenstein.

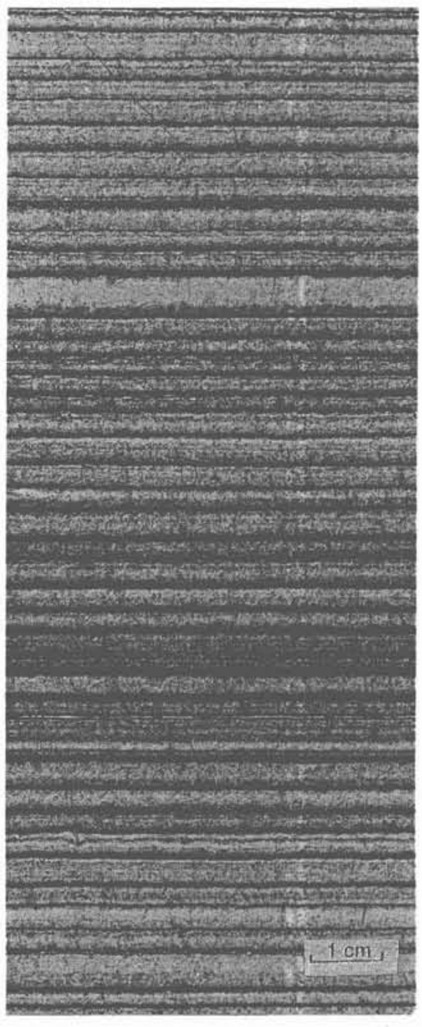

Figure 24 Thin section photograph of organic-rich calcite (dark) and anhydrite (light) laminae from the Permian Castile Formation. Photo courtesy W.E. Dean.

DEEP WATER EVAPORITES

Deep water evaporites are controversial. Almost every deposit identified as a deep water evaporite has also been, at some time, interpreted as having formed in a shallow water or supratidal setting. For some people, evaporite basins may have been deep enough to sink battleships in, but for others the floors of the same basins would have been barely moist.

Because there are no suitable modern analogs for deep water evaporites, identification of these facies is based entirely upon ancient examples. Nucleation and crystal growth occurs at the brine surface and crystals settle through the brine column as a pelagic rain to form cumulate deposits. Some gypsum and halite, however, grow on the bottom. Theoretically, evaporite crystals might also precipitate within stratified brines during diffusive mixing of the different layers (Raup, 1982).

The distinctive features of deep water evaporites reflect the relatively large size and volume of the brine body. Deep water evaporites are usually identified by their vertical and lateral continuity. Large bodies of brine do not fluctuate in composition in response to short-term changes because the large volume of brine acts as a buffer. Regular interlaminations of minerals of different solubility do occur, however, and record short-term variations in the salinity of surface brines. The majority of inferred deep water evaporites are laminar to thin bedded, and individual laminae are traceable for long distances: they may be basin wide. Stratigraphic units composed of laminar evaporitic carbonates, sulphates and halite may extend over thicknesses of tens to hundreds of metres, and are correlatable laterally over whole basins (tens to hundreds of kilometres). It is this vertical and lateral constancy that is one of the main arguments for the presence of a substantial body of brine.

Turbidites and mass flow deposits composed entirely, or in part, of resedimented evaporites may also be emplaced within deep water environments. Originally formed in shallower parts of a basin, their lateral transport implies the existence of relief in the basin and deposition within the deep water setting.

Sedimentary processes

Depositional processes in deep water evaporitic environments are believed to have been essentially similar to those in perennial salt lakes. Most perennial saline lakes more than a few metres deep are density or temperature stratified, with denser brine at the bottom (Neev and Emery, 1967;

Figure 26 Anhydrite pseudomorphs of bottom-grown gypsum crystal crusts with draped anhydrite-calcite laminae. Swallowtail twinning evident in former crystals at arrows. Greater part of gypsum now replaced by nodular anhydrite. Lower Anhydrite member of Castile Formation, west Texas.

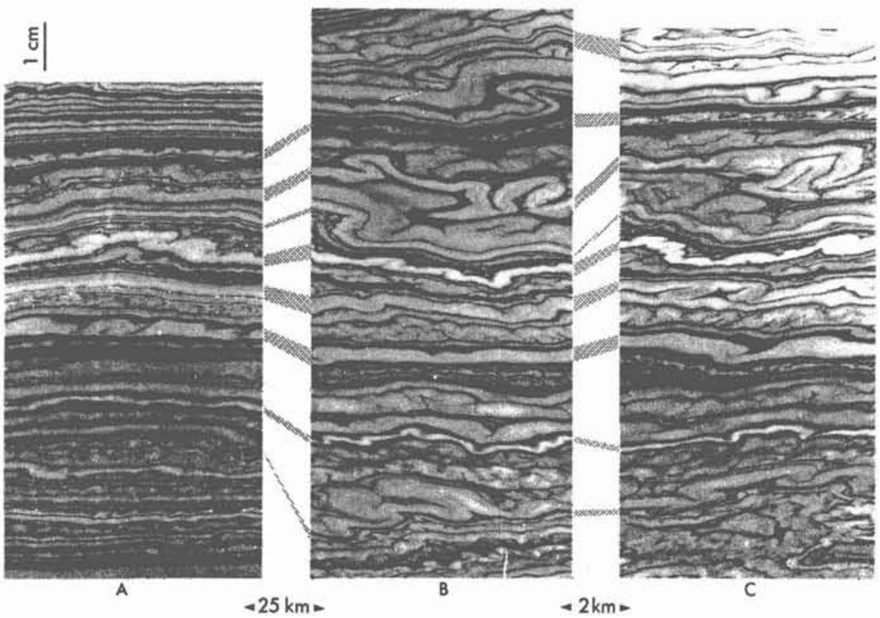

Figure 25 Correlation of carbonate, organic matter and anhydrite laminae, all enterolithically folded (slumped?): Ratner Member of Prairie Evaporite, N. Alberta. Photo courtesy G.R. Davies.

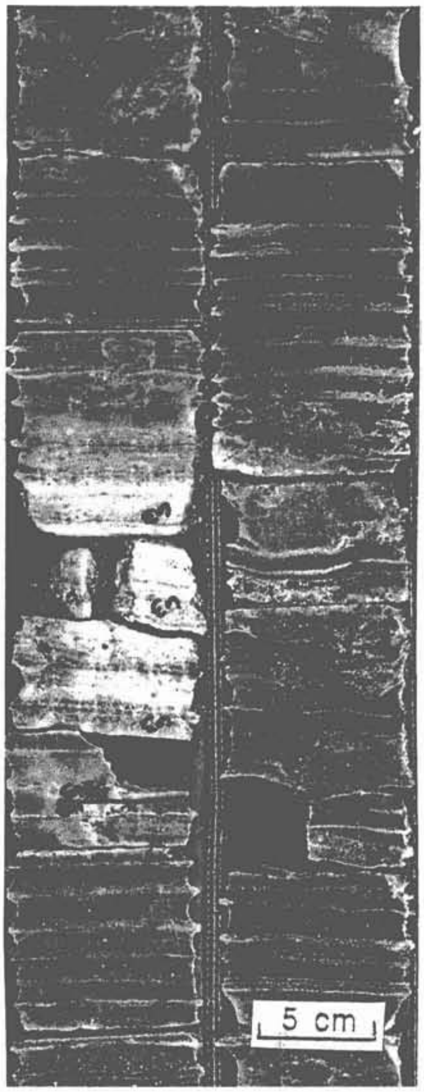

Figure 27 Laminated deep water anhydrite-halite, Paradox Formation, Utah.

Spencer, 1982). Ancient deep water evaporites are similarly considered to have been precipitated from stratified brine systems. This has important implications: 1) the denser bottom brine protects previously precipitated evaporites from dissolution during flooding/dilution events, 2) stratification prevents surface brines from reaching the lake bottom, so that growth of bottom crusts is prevented or curtailed, and 3) bottom brines become anoxic, allowing organic matter to be preserved and/or allowing bacterial reduction of sulphate to proceed.

Deep water evaporite facies

Laminar sulphates and carbonates

Laminar sulphate (originally gypsum), either alone or in couplets or triplets with carbonate and/or organic material, is the most common deep water evaporite facies (Figs. 24, 25). It passes vertically up or down into laminar carbonates that are probably also of evaporitic origin. Laminar sulphate may also pass vertically into laminar halite, or contain intervals of resedimented material. Laminae are thin, usually only 1-2 mm thick, and are typically bounded by smooth flat surfaces. Within short vertical sequences laminae tend to be of near uniform thickness, and individual laminae are traceable over long distances (tens to hundreds of kilometres).

Laminar deposits are commonly interpreted as being seasonal or annual increments — varves. It has never been conclusively shown that evaporite laminae are truly annual, but it is commonly stated that no other hypothesis explains all the features of these evaporites. Evaporitic carbonate laminae in Searles Lake and the Dead Sea may be seasonal, but are not annual; only one lamina is deposited every three or four years.

Laminar carbonates and sulphates record deposition in a brine body whose bottom was unaffected by wave and current action. Such stagnant, permanently stratified bodies of brine need not, however, be particularly deep. Well-developed brine stratification can dampen wave motion at shallow depths, leading to a false impression of depth in the bottom sediments. The Castile Formation has almost universally been recognized as a deep water deposit, deposition having occurred from brines hundreds of metres deep. Yet even here identification of former crusts of bottom-grown gypsum crystals (Fig. 26), suggests deposition may have occurred from brines only tens of metres deep (Kendall and Harwood, 1989).

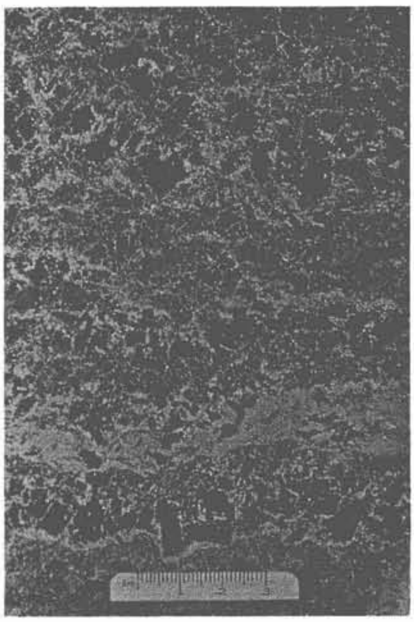

Figure 28 Bottom-growth halite from Paradox Formation, Utah. Cubic terminations of clear halite crystals are outlined by overlying laminae of anhydrite (white). The absence of dissolution at the top of halite crusts indicates deposition was from waters deep enough to allow crusts to escape the effects of brine-dilution events (responsible for the anhydrite precipitation).

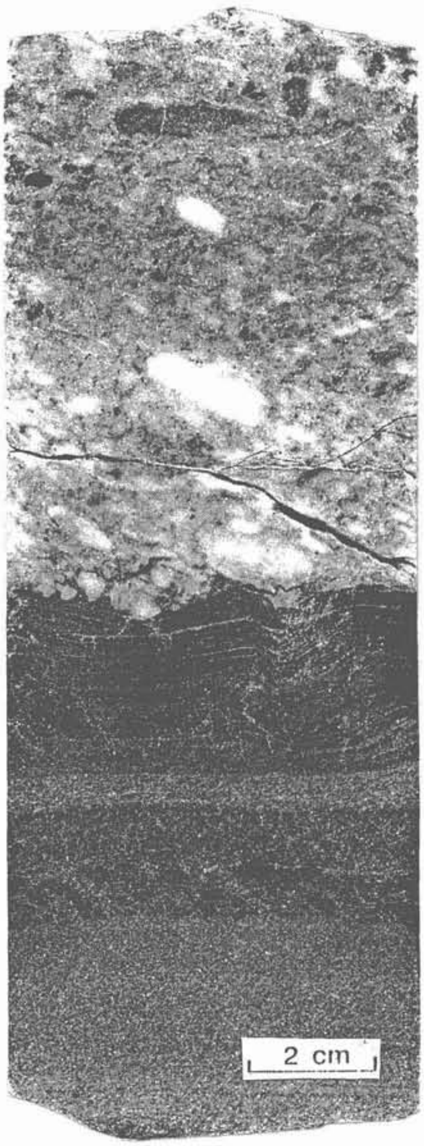

Figure 29 Graded clastic anhydrite bed with white and dark bituminous clasts overlying dark laminated anhydrite (with other layers having a finely clastic texture). Zechstein-1 anhydrite, West Germany. From Schlager and Bolz (1977); photograph supplied by Shell Oil Company.

Laminated and bedded halite

Deep water halite is difficult to recognize because most examples have suffered recrystallization. Even so, inferred deep water halite is invariably finely laminated (Fig. 27; also Czapowski, 1987) and contains anhydrite-carbonate laminae similar to those of deep water laminated sulphates. Even finer lamination within salt layers occurs, defined by variations in inclusion content. The fineness and perfection of this lamination indicates the original halite must have been fine grained and probably represents accumulations of cumulate crystals. Salt layers and laminae of this type have been traced for kilometres (Anderson *et al.*, 1972; Schreiber *et al.*, 1973).

Some presumed deeper water halites are composed of large bottom-nucleated crystals (Nurmi and Friedman, 1977; Beyth, 1980; Fig. 28). A deeper water setting is suggested by 1) the clear, inclusion-free character of the halite crystals, and 2) an absence of dissolution surfaces associated with anhydrite laminae. Instead, anhydrite buries and defines the crystal terminations of the bottom crusts. Bottom growth of halite in deeper water settings has yet to be satisfactorily explained. Possibly much of the facies was deposited in only a few tens of metres of brine, but this cannot be assumed and does not explain the deep water halite of the Dead Sea. Here halite growth may be due to density flows of very concentrated brines from brine pans in the shallow southern sub-basin, or may form by the mixing of these brines with less concentrated Dead Sea brines. Other halite may have precipitated from a subsurface brine that enters the Dead Sea along faults through older underlying salts.

Gravity-displaced evaporites

Clastic evaporite intervals within deep water laminated evaporites are slump, mass flow, density current or turbidity current deposits. Their presence is probably the best indication of a large body of brine being present during deposition. They also imply the existence of unstable slope conditions in the basin. Gypsum and anhydrite turbidites (Figs. 29, 30) are similar to their nonevaporite equivalents. Sometimes entire Bouma sequences are present, but most beds are composed only of graded units, or possess poorly developed parallel laminae in their uppermost parts (Schlager and Bolz, 1977). Mass flow deposits are represented by breccias composed of clasts of reworked sulphate (Fig. 31), either alone or with carbonate fragments. They are intimately associated with units affected by slumping.

Resedimented halite deposits are rarely identified. Their nature is only clearly established when they contain entrained nonevaporite clasts (Czapowski, 1987).

EVAPORITE FACIES MODELS

Facies models have been formulated for modern evaporitic settings: continental playa basins and marginal marine environments (coastal sabkhas + salinas). They have also been deduced for ancient deep water basins. However, the presence of the same depositional facies in different geographic settings, and the vast extent of many ancient evaporites (with no modern parallel), makes it difficult to use geography-based models directly for ancient evaporites. Distributions of presumed marine evaporites in depositional basins are believed to be equally important.

Facies models can be devised for continental, basin-marginal (shelf) and basin-central deposits. The need to establish a nonmarine origin before continental evaporites are positively identified is obvious, but this is not always easy. Many evaporites now considered marine could have been affected, to varying degrees, by nonmarine inflow.

The term *basin* requires definition. Tectonic and depositional basins must be distinguished. Evaporites are usually only preserved in structural basins but may have been formed in depositional basins or on wide platforms that had no central depression. Basin is used here only for depositional basins.

Krumbein and Sloss (1963) identified basin-central and basin-marginal evaporite distributions, and this aspect was discussed by Warren (1989). All present-day marine-fed evaporite environments (sabkhas and salinas) are basin-marginal; we have no modern representative of *marine* basin-central evaporites, although similar depositional patterns occur in larger salinas. (Almost all continental evaporites are basin central.) The important difference between these settings is that basin-central evaporites occupy the entire depositional basin, whereas shelf evaporites pass laterally into normal-marine strata elsewhere. An intervening preserved barrier facies (or a nonsequence marking the former presence of a barrier) occurs between evaporite and open-marine facies on shelves. For basin-central evaporites it is the entire exposed rim of the basin that forms the necessary restricting barrier. Thus basin-central evaporites should be represented on basin rims by nonsequences (Kendall 1988). In basin-margin (shelf) settings the solubility of evaporites increases away from the basin centre, whereas in basin-central evaporites, this increase

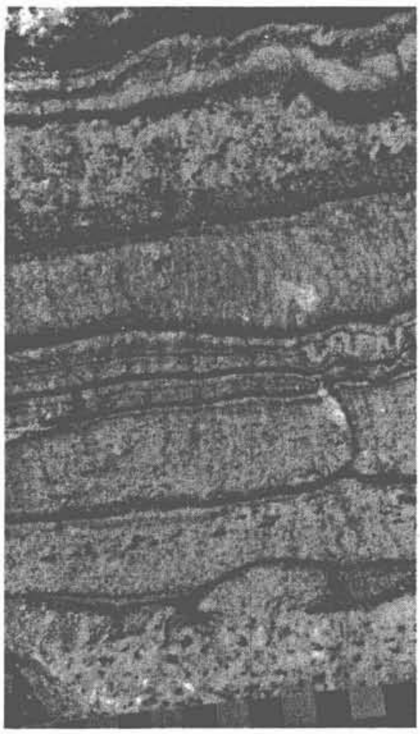

Figure 30 Amalgamated gypsum turbidites (now anhydrite), some of which display pronounced grading. Z1 Anhydrite (Permian Zechstein), S Harz (Germany); scale in cm. Photo courtesy G.M. Harwood.

Figure 31 Mass flow deposit from Z1 Anhydrite, composed of rounded blocks of anhydrite (probably reworked fragments of gypsum crusts from a shallow water platform) and associated with turbidites and mm-laminated anhydrites. Near Walkenried, S-Harz, Germany. Photo courtesy G. Harwood.

may occur toward the basin-centre or away from a confining barrier. Finally, basin-central evaporites are lowstand system tract deposits, filling the entire basin and forming when sea level drops below basin rims, whereas basin-marginal evaporites are components of transgressive and (especially) highstand system tracts. However, if the barrier occurs at the shelf edge, almost the entire shelf may be evaporitic and evaporite-accumulating. There are no modern equivalents of such wide evaporitic shelves.

CONTINENTAL EVAPORITES

The basic model

The basic facies model for continental evaporites is a closed basin with a shallow groundwater table and a more-or-less centrally located playa lake. Continental evaporites of any substantial volume are confined to the central parts of these basins, particularly in association with salt pans and playa lakes, and their surrounding saline mud flats. These areas are the lowest parts of the drainage basins, environments characterized by almost horizontal and largely vegetation-free surfaces of fine-grained sediments (Fig. 4A).

Where the groundwater table intersects the surface at the deepest parts of the basin, a saline lake or a salt pan forms and is concentrically surrounded by saline and dry mud flats (Fig. 32). The latter may grade into sand flats, with or without alluvial fans. These trap most coarse detritus and only the finest material reaches the basin centre. Apart from sheetwash flow during storms, water circulation is generally confined to the subsurface, although ephemeral or perennial streams may cross playas to feed ephemeral or perennial lakes.

Evaporites accumulate in playa basins where groundwaters discharge. Many playas, however, have water tables so deep that no discharge occurs, and these playas have smooth, hard and dry surfaces. They contain little evaporite and none accumulates.

An association with alluvial fan and ephemeral stream deposits, eolian sediments, redbeds and lacustrine carbonates all suggest nonmarine origins. Evaporites precipitated exclusively from continental groundwaters are not commonly recognized in the rock record. This rarity (particularly of pre-Tertiary examples) may reflect the ephemeral nature of many continental evaporite basins and of evaporites in the depositional environment. Many evaporites move upward at the same rate as sediment accretion, and so are nonaccumulative. Thus many evaporative environments leave no record in the form of evaporite deposits. Their former presence, however, can be deduced from the presence of crystal moulds and the modification of depositional structures.

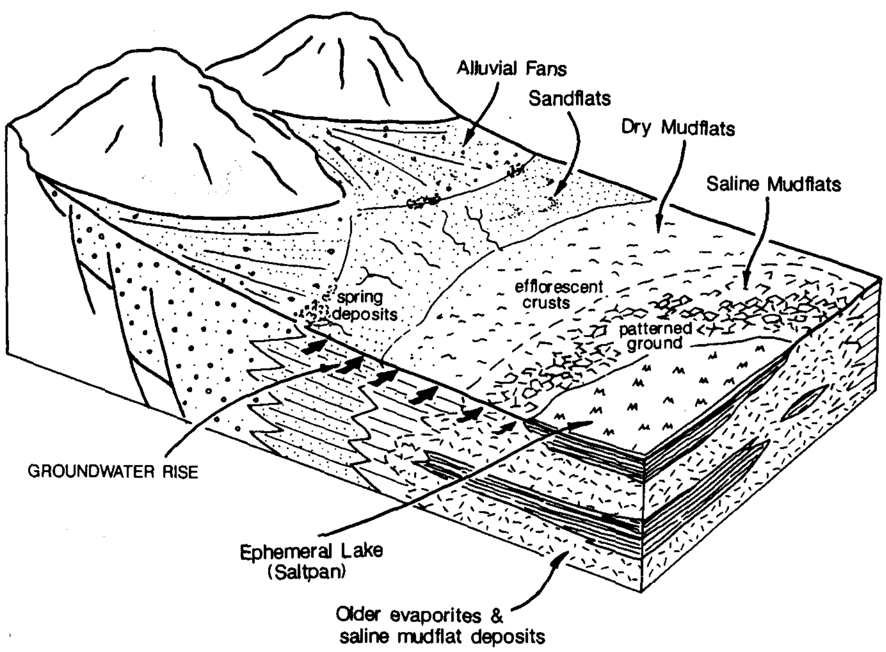

Figure 32 Schematic block diagram showing depositional framework for the continental evaporite (playa complex) model. Modified from Eugster and Hardie (1975).

Variations from the basic model

The climate and groundwater composition (discussed elsewhere), geological setting and the groundwater source are the main factors causing variations from the basic facies model. They also determine the type, amount and distribution of the evaporites in continental settings.

Geologic/Geographic setting

Five main settings are recognized (Smoot and Lowenstein, 1991), each characterized by different arrangements and associations of environments.

1. Rain-shadowed deep basins bounded by mountains (intermontane basins), like those of the desert and semi-desert basins of the western U.S.A., central British Columbia, the Andes, some East African rift valleys and the Tibetan Plateau, are characterized by an *alluvial fan – saline pan association*. Basins are fringed by alluvial fans and contain salt-encrusted ephemeral saline lakes ringed by mud flats and sand flats. Inflow into the pan is confined to groundwater influx and aperiodic storm runoff. An ancient example is the saline pan deposits of the Wilkins Peak Member (Eocene Green River Formation, Green River Basin, Wyoming).

2. Intermontane basins fed by perennial streams constitute an important variant. The stream produces a permanent lake. Examples of this *alluvial fan – perennial-stream – perennial saline lake* association are the shallow Great Salt Lake of Utah and Lake Urmia of Iran (both surrounded by mud flats), and the deeper and narrower Dead Sea of Israel, where alluvial fans enter the lake directly. Beds of cumulate nahcolite and halite in the Green River Formation of the Piceance Basin (Colorado) accumulated in a perennial saline lake, unlike the situation in neighbouring Wyoming.

3. Wide shallow basins are dominated by ephemeral stream floodplains and dune fields. Large areas

become aperiodically inundated by ponded floodwaters that slowly evaporate, precipitating a saline crust. Complete desiccation gives rise to a salt pan (with an area perhaps only 1/100th of that originally inundated) fringed by a saline mud flat or wide dry mud flats. The Lake Eyre Basin of Australia is the largest example of this *ephemeral-stream – dune field – saline pan* association. Ancient examples include part of the Lower Permian Rotliegendes of northern Europe, and Devonian halites associated with redbeds in the Lower Elk Point Group of western Canada.

4. Lake Chad (north-central Africa) is a shallow but freshwater lake surrounded by eolian dune fields with small interdune saline pans and saline mud flats. The lake is fed by perennial rivers. It is the only Recent example of a *perennial stream – perennial lake – dune field* association.

5. Saline pans, or perennial lakes directly fed by groundwater occur in old channel systems, hollows on glacial sediments, and in karst depressions. The preservation potential of these deposits is low.

Groundwater source

In the basic model groundwaters move radially from the hinterland, converging toward the basin centre (which also marks the hydrographic low point of the basin). Flow is assumed to be horizontal and shallow subsurface. This produces a concentric pattern of increasing groundwater salinity and a "bull's eye" pattern of salt deposition (more saline salts in the centre, Fig. 33). However, when the deepest part of the basin floor is not centrally located, or when groundwater enters the basin predominantly from one side, this ideal pattern is disturbed and becomes asymmetric.

There is a tendency for less mineral segregation to occur in river-fed than in groundwater-fed playa systems. Brine compositions in lakes fed by perennial streams are less affected by prior precipitation of less saline salts (in peripheral playa flats). River waters retain their carbonate and sulphate content, and low-solubility salts precipitate within the lake. In solely groundwater/floodwater-fed pans, less soluble constituents are retained on surrounding flats, and pan salts are dominated by more soluble salts, and can be monomineralic.

Extrinsic controls on continental evaporite facies

Except for basins that might be inundated or isolated, continental evaporites are unaffected by sea level changes.

The most important extrinsic control is climate. The history of present-day and many ancient playa lake complexes has been one of alternating wet and dry conditions, with corresponding transgressive, freshened, nonevaporite-precipitating lakes, and regressive (shrinking) saline lake or saline pan stages. Variations between arid and less arid conditions cause replacement of perennial lakes by salt pans or even dry mud flats, lake levels to rise and fall, lake margins to expand and contract, the amount of clastic sediment to vary, and water chemistry to change.

During prolonged episodes of aridity, groundwater tables may be lowered such that ephemeral lakes (saline pans) drain, convert to dry mud flats and perhaps are encroached upon by aeolian dunes. Lessened aridity, on the other hand, is marked by partial or complete dissolution of earlier-formed salts, by deposition of basal transgressive conglomerates and beach deposits over former playa flat deposits, and by deposition of nonsaline lacustrine sediments, amongst which oil shales may be conspicuous.

The effects of climate change are not straightforward in perennial lakes that occupy topographically subdivided depressions. Different sub-basins may develop opposite sedimentary sequences. Where lakes have asymmetric water supply and a lowered brine level (such as Great Salt Lake in Utah) the sub-basin still fed by a perennial river becomes less saline. This is because the inflow, although diminished, now dilutes a smaller volume of lake brine. In contrast, sub-basins now cut off from inflow, desiccate and become more saline. These opposite sequences are caused by the same environmental change, a lowered water level, produced by increased aridity.

Increased sediment supply, caused by tectonism and climatic changes, dilutes evaporite accumulation. Salt pan and perennial lake deposits (composed of salt crusts) are thereby replaced by clastic muds containing displacive evaporite crystals.

BASIN-MARGINAL (SHELF) EVAPORITES

Models for coastal sabkhas, marginal marine salinas and for ancient large evaporites are discussed.

Coastal sabkhas

These supratidal areas (Fig. 4C) are described in Chapter 16. They may merge insensibly landward with continental sabkhas (playas), and landward parts of coastal sabkhas are affected by continental groundwaters. Thus evaporites typical of nonmarine settings (e.g., trona) can be emplaced within marine-derived sediments.

Coastal sabkhas are products of both depositional and diagenetic processes, the most important being the emplacement of early diagenetic calcium sulphate, less commonly of halite. Indigenous sediments reflect the offshore sediment mosaic, but may contain substantial amounts of detrital sediment from the hinterland. Offshore sediments are washed over the sabkha surface during storms that episodically inundate seaward parts.

Groundwaters beneath sabkhas become more concentrated toward sabkha interiors, and all but the very seaward and landward margins may be halite saturated. Concentration occurs by evaporation from the capillary fringe and by dissolution of earlier-formed evaporites (particularly halite). Evaporative losses are replenished by downward seepage of storm-driven floodwaters and/or by gradual intrasediment flow, fluxing either from the seaward margin or from a continental reservoir that affects landward parts of the sabkha (Patterson and Kinsman, 1981). The water table inclines seaward but brine migration is slow. Movement is limited by the low permeability of the predominantly muddy sediments and by permeability barriers such as buried algal mats (Bush, 1973) and cemented layers (McKenzie *et al.*, 1980). These subdivide the sabkha sedimentary prism into hydrologic zones. Vertical movement of groundwaters only occurs where these barriers are broken.

Sabkhas that widen as a result of coastal progradation have a characteristic sedimentary sequence (Figs.

14, 34) consisting of subtidal sediments (commonly restricted lagoonal) at the base; intertidal sediments, including cyanobacterial mats and cemented crusts; and a capping supratidal deposit with abundant displacive gypsum (+ anhydrite). Displacive gypsum grows within intertidal and subtidal sediments once these are located beneath the sabkha environment.

Variations in sabkha sequences

1. *Diastrophic control.* Shallowing-upward sequences terminated by marine sabkhas can form from three different events, simple progradation, eustatic falls in sea level, or brine level drops caused by evaporative drawdown. The first two also affect nonevaporite sequences and Chapter 16 discusses the different hypotheses for shallowing-upward carbonate successions, of which evaporite-capped successions form only a variant. Two problems arise when successions are interpreted simply as progradational events; one also relates to nonevaporite successions, the other is intrinsic to the sabkha environment.

Present-day sabkhas are protected from the full impact of onshore storms by beach barriers or offshore islands. This protection allows the sabkha to prograde. Once the lagoon behind the barrier becomes filled with sediment, further progradation requires formation of another barrier, seaward of the first, behind which progradation can be renewed. Widespread cycles composed of fine-grained sediments and capped by sabkhas thus should not accrete laterally in a uniform manner, but do so in a series of jumps, as offshore bars develop into barriers. Wide sabkha sequences should contain remnants of these barriers. The entire sediment body should be an arid-zone equivalent of a chenier plain, an environment described by Picha (1978) from Kuwait, by West *et al.* (1979) from the Mediterranean coast of Egypt, and by Warren and Kendall (1985) from Abu Dhabi, but which still appears not to have been documented in the ancient.

Many ancient evaporites interpreted to have been generated in sabkha environments overlie open marine carbonates, rather than restricted lagoonal deposits. Here we must assume either that 1) barriers were absent and mud flats were protected from wave attack by the extensiveness and shallowness of the offshore environment, or 2) the sabkha interpretation of the evaporites is incorrect (see below).

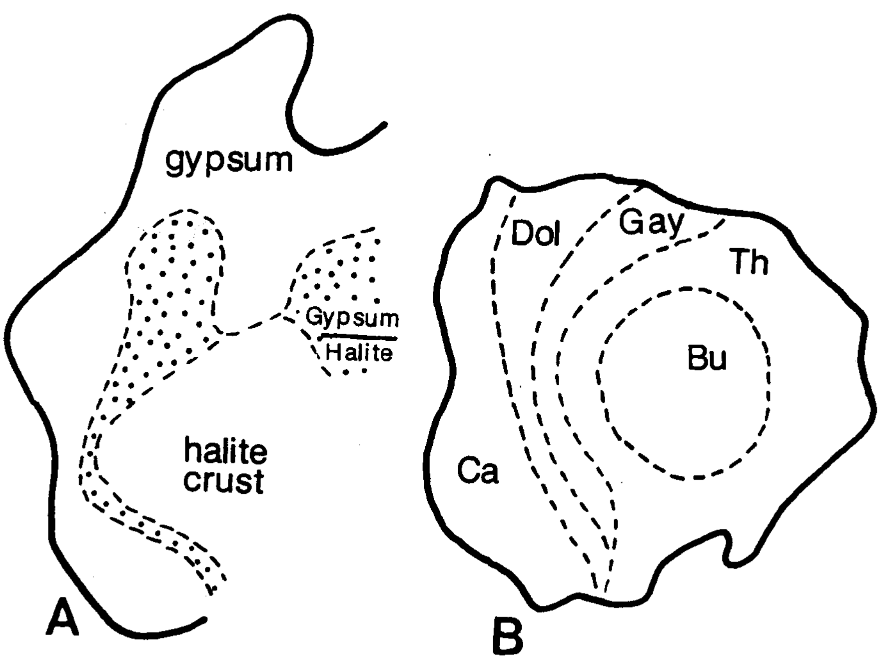

Figure 33 Saline mineral zonation in playas. A) Yotvata Sabkha (Israel), after Amiel and Freidman (1971). B) Deep Spring Lake, California, after Jones (1965), Ca = calcite/aragonite, Dol = dolomite, Gay = gaylussite, Th = thenardite, Bu = burkeite.

The second problem concerns the preservation potential of wide sabkhas. These need low-gradient, stable shelves, locations where active lateral flow of groundwaters is uncommon. Arid environments are subject to continual evaporation losses and, unless this water loss is replenished, the supratidal environment dries out and is subject to wind erosion. Wide sabkhas thus require a regional groundwater flow system that allows the water table to rise as the sabkha progrades. Without such a groundwater system, the upper evaporite-bearing sediments in the areas beyond seawater flood-recharge would be entirely removed by deflation. Warren and Kendall (1985) interpret dolomitized subtidal sequences, with erosive upper surfaces and nodular anhydrite after displacive gypsum, but lacking overlying supratidal units, as having formed in this way. A seaward-dipping gradient to the sabkha groundwater surface would also cause additional sediment (mainly eolian) to be deposited as the brine surface rises, but requires the presence of a large neighbouring landmass with sufficient relief to act as a recharge area for the groundwater system. For many widespread evaporite units, interpreted as sabkhas, this requirement has not be substantiated. Neither have the thick eolian supratidal sections of more landward parts of these sabkha complexes been identified. For these reasons the interpretation of many widespread evaporites as sabkha deposits is suspect.

Sediment emergence, with the formation of widespread exposure surfaces and the overprinting of formerly subaqueous sediments by mud flat processes, can occur by relative falls in water level independent of any sediment progradation. Falls may be due to global external events (e.g., glaciations) or to increased restriction and subsequent evaporative drawdown. No obvious criteria exist to distinguish cycles generated by sediment progradation from those that reflect episodes of evaporative drawdown.

2. *Nature of the host sediment.* This determines the permeability and hence the amount of drainage in the sabkha sediment, the further evolution of sabkha brines, and the subsequent compactional history of the evaporite de-

posit. Impermeable sediments inhibit brine reflux and, by curtailing downward seepage of floodwaters, extend the width of the area affected by flood recharge. Carbonates (particularly aragonite) in host sediments are of major importance. Their dolomitization releases calcium that reacts with sulphate in groundwaters to form additional gypsum and anhydrite. This increased sulphate precipitation and dolomitization reduces the sulphate and magnesium content of brines in sabkha interiors to low levels and causes magnesite (precipitated earlier) to dissolve. Reflux of brines capable of dolomitizing deeper-lying carbonates causes gypsum precipitation in these sediments. Extensive sulphate growth in subtidal carbonates between sabkha evaporites may obscure evidence of the cyclic nature of an evaporite deposit and create a single thick, composite unit. In noncarbonate sediments, dolomitization is absent, the sabkha brines retain 60-70 per cent of their sulphate, much less gypsum is precipitated, and brines remain magnesium-rich and so magnesite remains stable. The sulphate-rich brines formed in noncarbonate sabkha sediments react with earlier-formed gypsum to form polyhalite (Holser, 1966).

Differences in sediment coherency dictate subsequent compactional history. Lithified or coherent sediments preserve pseudomorphs after gypsum crystals or halite crystal moulds. Compressible sediments (particularly organic-rich varieties, e.g., cyanobacterial mats), on the other hand, allow gypsum and anhydrite nodules to grow, to coalesce and compact, perhaps even to form sluggy or even-layered anhydrites (Shearman and Fuller, 1969; Mossop, 1974).

3. *Nature of the offshore water body.* Commonly this is normal marine to slightly hypersaline and well below gypsum saturation. Thus subtidal and intertidal sediments beneath sabkha evaporites are bioturbated and skeletal-rich, with cyanobacterial mats (if present) confined to upper intertidal environments. Where sabkhas border more saline water bodies, sediments beneath sabkha evaporites are laminated (burrowing biota absent) and cyanobacterial mats may extend down well into subtidal environments (browsing biota absent). Where offshore waters precipitate and preserve gypsum, the sabkha sequence forms the uppermost unit of a subaqueous unit. Subaqueous evaporites are transported onto the sabkha by storms, there to form clastic beds of gypsum, anhydrite or even halite debris. Such sabkha sequences would be largely composed of such beds and might be difficult to distinguish from shallow subaqueous evaporites.

Marginal marine salinas

Relatively small marginal marine salinas occur above sea level in depressions on sabkhas, between coastal dunes, or in ephemeral stream deltas or fan deltas. Those lying below sea level (Fig. 4B) are of greater importance in terms of size, persistence and the thickness of evaporite that can be deposited and preserved. They occur in tectonic depressions and behind coastal barriers. Marine inflow may be via minor inlets through the barrier, surface flow across a supratidal flat, or by passage through the barrier, discharging into the salina as springs, brine sheets or as seepages. Salinas are covered by water for brief or long periods (ephemeral and perennial salinas), but in both cases evaporite deposition is primarily by precipitation from a surface brine, rather than by precipitation within a sediment. Salinas associated with wide, high-relief barriers differ markedly from sabkhas in that they are unaffected by tide/storm surges. They therefore lack transported marine sediment (unless this is wind-introduced).

Salinas can be large and comparable with small- to medium-sized ancient evaporite basins, e.g., the Ranns of Kutch (India), 30,000 km^2 (Glennie and Evans, 1976), Lake MacLeod (Western Australia), 2,000 km^2 (Logan, 1987).

Salinas and continental playa lake

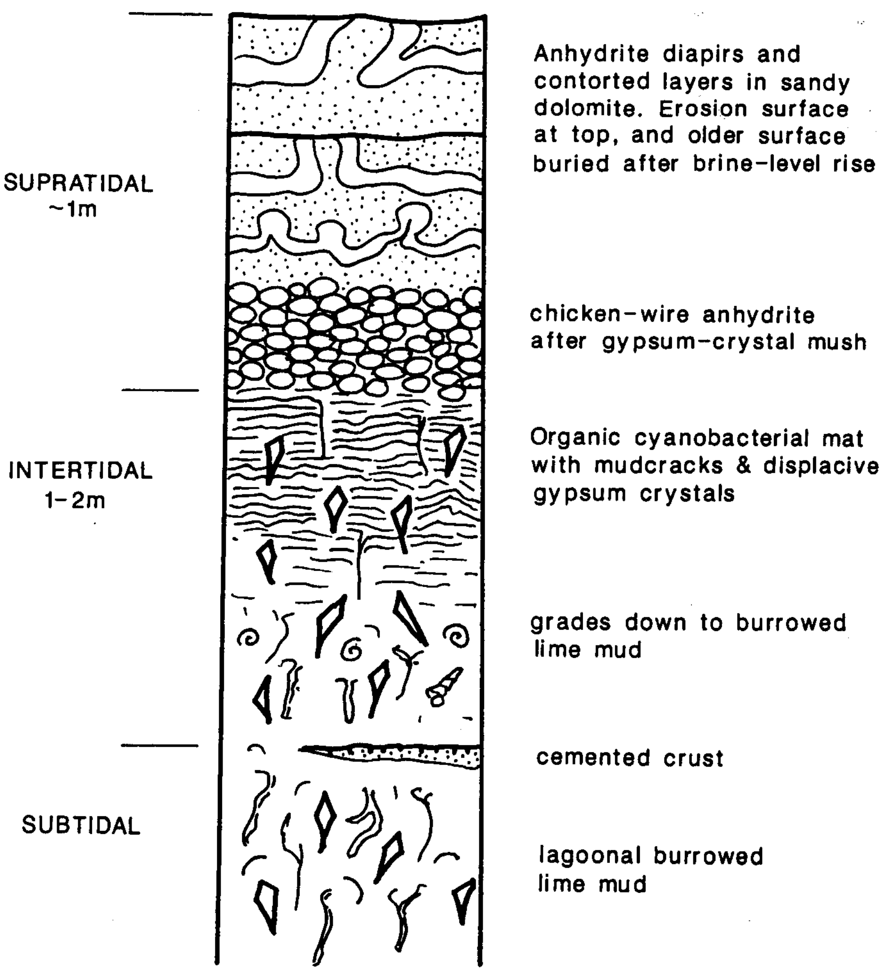

Figure 34 Simplified vertical section through sabkha sequence at Abu Dhabi.

complexes are similar. Both contain subaqueous and subaerial subenvironments in which evaporites accumulate. These may be arranged in similar fashions and depositional processes and products are comparable. They commonly consist of an ephemeral or perennial saline lake located in the lowest parts of a depression, surrounded by saline mud flats that pass outward into peripheral dry mud flats.

Variations in salina sequences

The variation in mineralogy and facies within salina evaporites is controlled by factors similar to those controlling continental playa evaporites. Climate controls the maximum salinity to which brines can be concentrated, but inflow-reflux ratios more commonly determine the concentrations actually reached. These ratios are determined by the presence or absence of surface inflow, the nature (width and permeability) of the barrier, the hydraulic head between sea level and brine level in the salina (these all determine inflow rates), size of the salina (controls losses by evaporation), and the effectiveness of basal aquitard (controls brine seepage losses). These are discussed in the section *Basin-central evaporites.*

Ancient widespread shelf evaporites

Many evaporites are composed of shallow water and/or mud flat facies, but must have accumulated on a scale and in settings different from those occurring today. The main problem with interpreting these evaporites is to determine whether they were 1) generated during progradation of marginal-marine evaporitic environments comparable with those of the present day (in which case they are diachronous), or 2) they formed simultaneously in evaporitic settings significantly larger than any today. This is a major unresolved problem for many large evaporites: often the problem simply has not been addressed. Detailed stratigraphic study of some evaporites suggests the second explanation can be correct. These evaporites must have formed in vast expanses of evaporitic lagoons and mud flats, reaching tens to hundreds of thousands of square kilometres in extent, over which brine depths were only a few metres deep (or even shallower). Episodically they became emergent. Tidal influences were minimal; deposition was affected more by storms that created laminated clastic gypsum sands. Storms reworked subaqueous sediments from shallow evaporitic lagoons and transported the resultant carbonate and clastic evaporite sands onto neighbouring flooded evaporitic flats. Cyanobacterial mats were ubiquitous in evaporitic flat and shallow subaqueous environments where brines had salinities below halite saturation.

Stratiform evaporite units, 5 to 50 m thick, of mixed subaerial and shallow water evaporites were generated in these settings. The lateral persistence of thin beds over large areas with only minor changes in thickness, mineralogy or facies indicates they formed on broad, flat shelf areas, areas which could be affected by rapid transgressions. Other widespread evaporites are more variable laterally, accumulated in a mosaic of smaller environments, and may have been diachronous. Both types of evaporite commonly form the upper parts of shallowing-upward cycles with underlying open-marine or restricted-marine carbonates. These, in areas of continued subsidence, may be vertically stacked to form thick sedimentary packages (Chapter 16). Landward they may interfinger with continental siliciclastics.

Internal characters of shelf evaporites suggest they were deposited on mud- and evaporitic-flats, or subaqueously in shallow lagoons. Mud- and evaporite-flat sediments form shoaling-upward cycles but, according to Warren (1989) are not easily correlated across a platform because of limited continuity of individual facies. They are deposited as a facies mosaic of saline and dry mud flats that separate local brine pans. Here brine pans, saline and dry mud flat environments

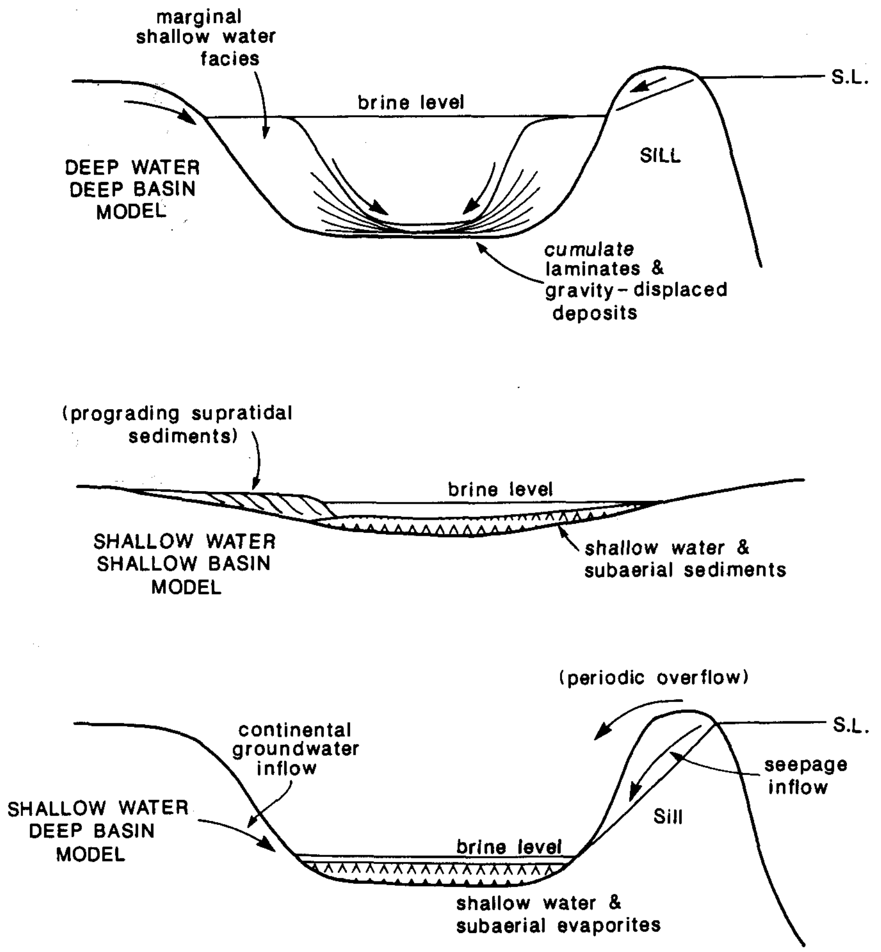

Figure 35 Depositional models for basin-central evaporites.

may be comparable in size and facies to modern coastal marine equivalents, however, the lateral extent of the evaporite itself may have no modern counterpart. Host sediments may be fine-grained clastics and carbonates, or composed of detrital gypsum.

Much evaporite, previously interpreted as widespread sabkha deposits, could have been deposited in salinas. Relicts of subaqueously formed gypsum are abundant in many "classic" sabkha anhydrites — the Upper San Andres Formation (Warren and Kendall, 1985) of the Texas Panhandle, the Miocene of Iran (Purser, 1979), and the Permian Bellerophon Formation of northern Italy (Hardie, 1986), the Jurassic Arab evaporites and overlying Hith Anhydrite of the Arabian Gulf (Mitchell *et al.*, 1988), large parts of the lower Buckner anhydrites of the U.S.A Gulf Coast (Mann, 1988), and Mississippian basin-marginal anhydrites of the Williston Basin (Fig. 14; Lindsay and Roth, 1982).

Widespread areas of shallow subaqueous evaporite precipitation also have no modern counterpart, although the facies developed can be matched in perennial coastal salina and continental playa lakes. These evaporites are also commonly cyclic and composed of shallowing-upward units 2-50 m thick, underlain by transgressive open-marine sediments, and terminated by thin sabkha sequences. Units can be traced over distances of tens to hundreds of kilometres, e.g., San Andres Formation of west Texas (Elliott and Warren, 1989), Yates Formation anhydrites of west Texas (Crawford and Dunham, 1982), and the Ferry Lake Anhydrite of east Texas (Loucks and Longman, 1982).

In the absence of a recent analog, it is difficult to account for evaporites deposited in continuous shallow brine bodies. Comparison with the large salina of Lake MacLeod (Western Australia), however, suggests that those apparently composed of subaqueous laminated gypsum may have been deposited on evaporite flats. Other evaporites, however, such as bottom-grown gypsum or cumulate halite, must have been deposited subaqueously. Those composed of large gypsum crystals indicate deposition in relatively stable bodies of brine, this facies being confined to deeper

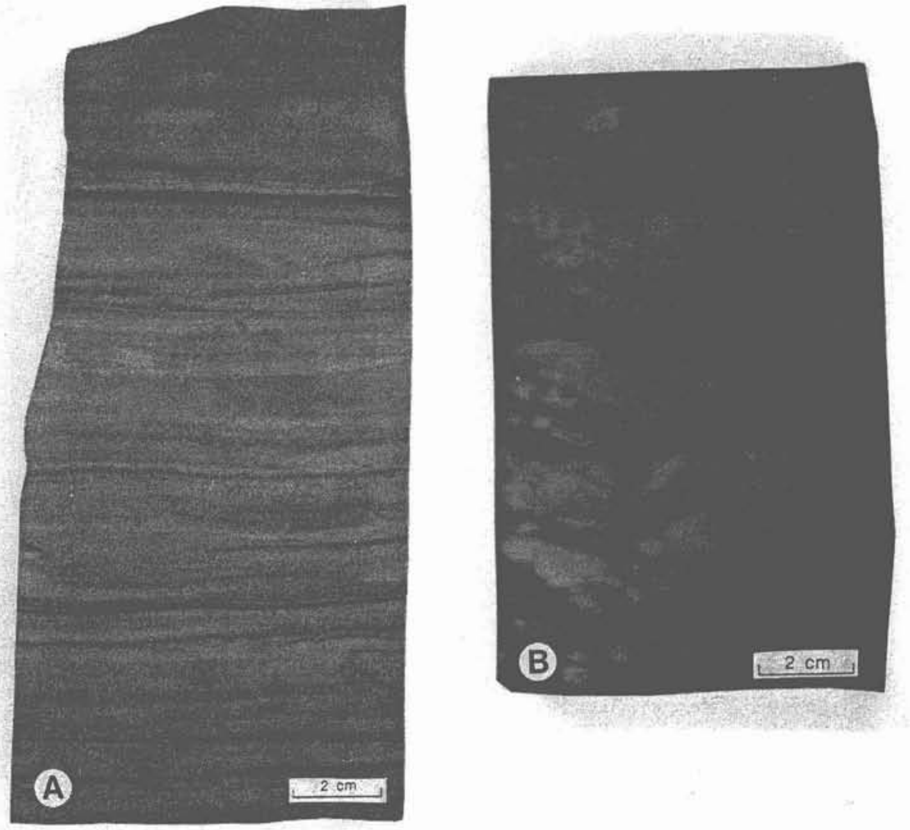

Figure 36 Upper Red River (Herald Fm.) evaporite cycle, Saskatchewan. A) Inferred dry mud flat deposits with cm-bedding (storm-flood deposits ?), desiccation cracking. B) Nodular mosaic anhydrite after bottom-grown gypsum crystal.

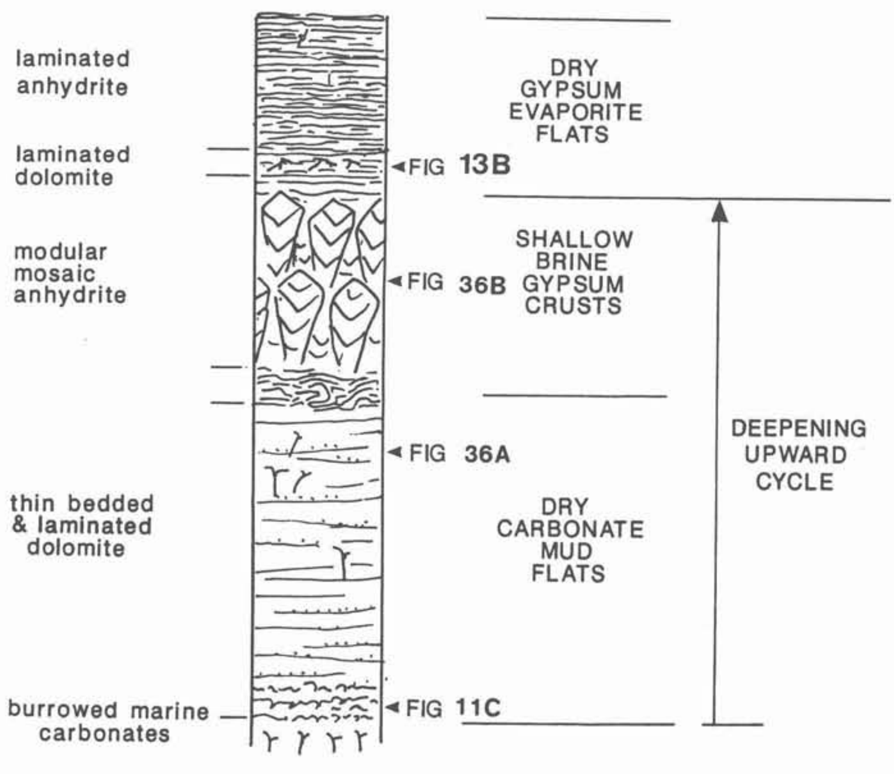

Figure 37 Schematic diagram of Upper Red River (Herald Formation) evaporite cycle, Saskatchewan, showing both "brining-up" and deepening-up character.

parts of Recent salina successions (Warren, 1982) or to salt ponds that are not drained nor subject to brine mixing (Orti-Cabo *et al.*, 1984).

Warren (1991) speculates that wide bodies of shallow brine precipitate gypsum under near-equilibrium conditions where evaporation kept brine surfaces below sea level, and brine depths limited to only a few tens of centimetres. An underlying aquitard (probably formed as underlying sediments became cemented by evaporites), high humidities in the overlying air mass, and frequent resupply from storms and seepage kept the environment from drying up. It is difficult, however, to imagine how brines in such areas could be replenished without interrupting the normal depositional conditions. These dilution events should be recorded within the evaporites. We lack a viable depositional model for these evaporites.

BASIN-CENTRAL EVAPORITES

There are no modern equivalents of marine basin-central evaporites (although evaporites form a minor component of Dead Sea sediments). These basin-wide stratigraphic units may be thin (<5 m) or thick (hundreds to thousands of metres) and consist of shallow-water/subaerial evaporites, with or without evaporites of deep water aspect. Deep brine-filled basins may contain marginal slope and deeper basin-central facies.

Evaporites deposited in low-relief basins are similar to shelf evaporites, except for their basin-central distribution. They are exclusively composed of shallow water or mud flat facies. In basins that had high relief, shallow-water/subaerial facies may have formed on basin-marginal shelves, been the terminal phases of the basin fill (after depositional relief was eliminated), or accumulated on the floors of largely desiccated basins during periods of evaporative drawdown. Evaporites of deep water aspect are confined to the basin-centre. Near basin edges they may pass laterally into thicker shallow water facies, perhaps with an intermediate facies belt of slope deposits, characterized by reworked evaporites, mass flow deposits, slumps and turbidites (see Fig. 38 in this chapter).

Thick basin-central evaporites are composite stratigraphic units, intercalated with marine or restricted-marine carbonates. Carbonates represent less saline evaporitic intervals or episodes when the entire evaporite basin was flooded by normal marine waters (transgressive or highstand system tract deposits).

Three main types of evaporite depositional basin can be distinguished (Fig. 35). In most basins, however, these basin types represent stages that they pass through and most have compound fills. This is not surprising since the brine level in a basin is most unlikely to have been constant. Evaporite deposition usually implies surface disconnection with the ocean, thus brine levels rapidly change or fluctuate in response to even slight changes in the rates of inflow, outflow and evaporation. These rates are controlled by climate and the degree of basin restriction. Basin restriction, in turn, is controlled in part by changes in tectonism or sea level.

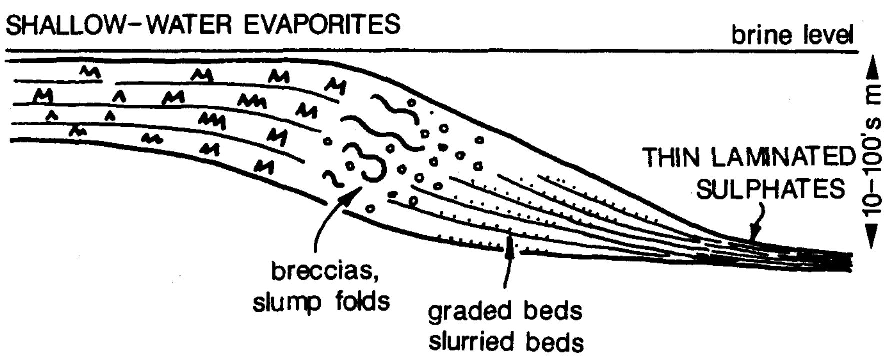

Figure 38 Schematic diagram of deep water and slope evaporitic environments. After Schlager and Bolz (1977).

Shallow water, shallow basin model

This model accounts for relatively thin (<10 m thick) evaporites with basin-central distributions. This last feature alone should be sufficient to prevent these evaporites being compared with present-day coastal sabkhas, but a similarity in evaporite facies has commonly resulted in this misinterpretation. They are developed within cratonic basins which did not subside rapidly and were never excessively deep.

Evaporites of this type are composed of shallow-subaqueous and mud flat facies and commonly form the upper parts of carbonate cycles exhibiting signs of upward-increasing restriction. They have usually been interpreted as shallowing-upward cycles but are better identified as "brining-upward" cycles (Longman *et al.*, 1983), particularly when the evidence for shoaling is equivocal. In evaporite-terminated cycles of the Ordovician upper Red River (Herald) Formation of the Williston Basin (Kendall, 1976, 1988) and the Middle Devonian Lucas Formation of the Michigan Basin (Park, 1987) thin-bedded laminated evaporitic dolomites containing desiccation cracks, cyanobacterial mats and evidence of deposition by storms (Figs. 11C, 36A) pass upward into nodular anhydrite, the majority of which forms pseudomorphs after subaqueous gypsum crusts composed of large, vertically aligned crystals (Fig. 36B). In these cycles the uppermost, more saline parts were deposited in more stable, subaqueous environments than the less saline carbonates that underlie them (Fig. 37) and which resemble dry mud flat deposits. The brining-up cycles thus are also deepening-upward cycles.

Deep water, deep basin model

Evaporite basins that were deep depressions at least partially filled with brine are dominated by evaporites of deep water aspect. On basin floors, these are mm-laminated evaporites (sulphates or halite), whereas on marginal slopes, reworked platform evaporites may occur. The presence of a high-relief basin is usually shown by 1) the presence beneath evaporites of deep water clastic or carbonate sediments (commonly of a starved basin aspect), 2) the occurrence of depositional slope facies in both the older and evaporite sediments, or 3) the presence of high pre-evaporite carbonate buildups. When initial basin slopes are gentle, the basin periphery becomes the depositional site of thick shallow water gypsum evaporites that build upward and outward into the basin, and a ramp or platform is constructed (Schlager and Bolz, 1977). In large part, the difference in sedimentation rate between basin centre and flanks is a result of the greater degree to which brines can be evaporated in shallower waters. Because deposition is slower in basin centres, steep depositional slopes may develop at the platform edge. Upper parts of slopes are sites of slumping and mass flow, whereas lower parts contain graded beds emplaced by turbidity currents (Fig. 38).

The same basin-filling pattern as occurs during calcium sulphate deposition is present when some deeper water halites (and even some potash salts) are precipitated (Colter and Reed, 1980). Stratigraphic units in the Permian Zechstein evaporites of the North Sea thicken from the basin to a marginal depositional shelf. This evidence suggests the salts were deep water deposits. Deep water potash salts constitute a major problem. In order for a basin to fill with brine concentrated enough to precipitate potash salts, each batch of seawater would first have to precipitate the greater part of its sodium chloride as halite. The amount of halite precipitated would equal in volume the entire depositional basin, so that no deep basin would be left in which to precipitate the potash salts (Schmalz, 1969).

Depositional models for deep water evaporite basins were reviewed by Logan (1987). *Stratopycnal basins* have subhorizontal density layering and, when they have surface inflow, are the classic evaporite basins of King (1947), Scruton (1953) and Hite (1970). This model is unsound hydrodynamically (Kendall, 1988). Strong winds (needed to promote evaporation) mix waters down to depths of several tens of metres, so that upper parts of the brine develop a vertical density structure (i.e., an *isopycnal basin*) similar to that of Hamelin Pool (Shark Bay, Australia). Here salinities reach 72‰. For gypsum to be precipitated in Hamelin Pool, inflow must be reduced to 10% of its already restricted rate (Logan, 1987). This would confine influx to channels through a permanently emergent sill, and brine levels in the basin would fall below sea level. Seepage inflow through the barrier would occur, but not surface reflux. Thus, the basin would be a variant of a *seepage inflow basin*: one modified by some surface inflow. Halite precipitation at Hamelin Pool would require complete surface disconnection.

Isolated or highly restricted basins experience drawdown and thus differ only in degree from *shallow water, deep basins*. The main problem (discussed earlier) is to explain how any surface brine can be retained in desiccating basins.

Hydrodynamic considerations suggest deep water evaporites were precipitated from brines that were laterally uniform (Kendall, 1988), although they were probably density stratified. This means that at any given time, evaporites of the same mineral facies are deposited throughout the basin. Vertical changes in mineral facies in the Castile Formation occurred almost simultane-

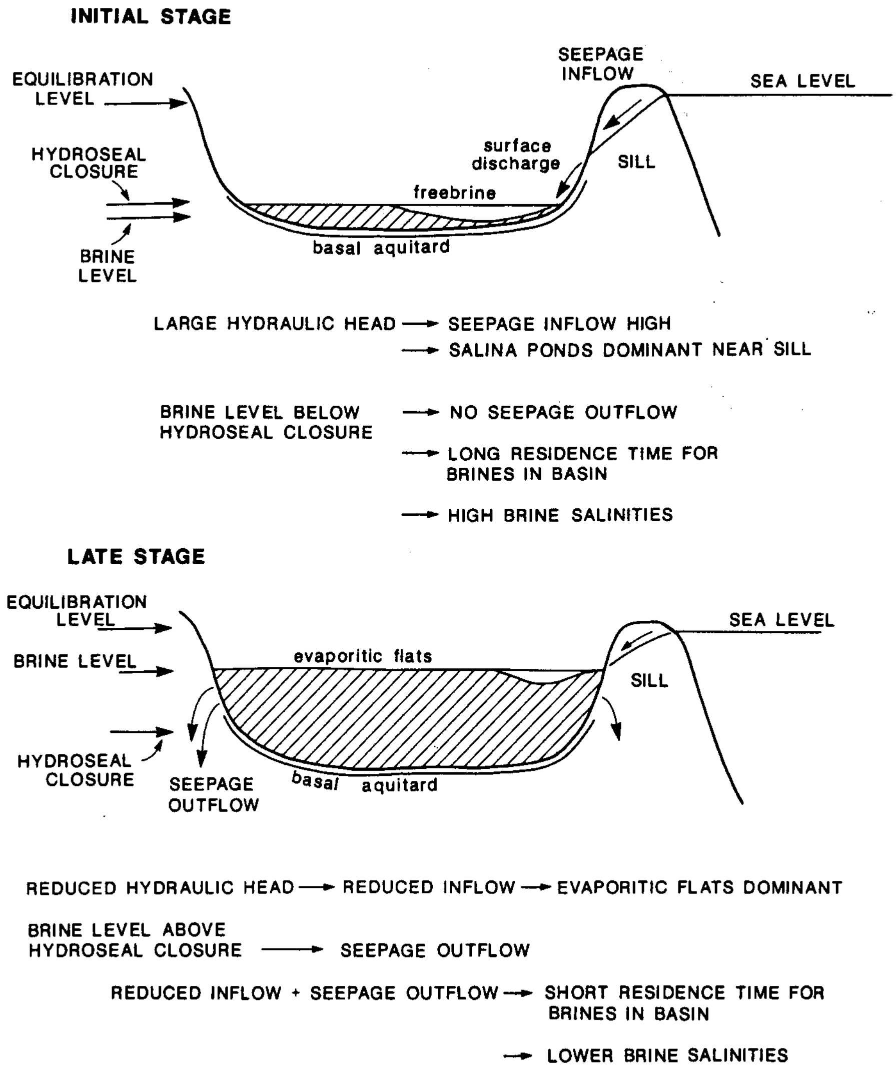

Figure 39 Diagrams illustrating two stages in the development of seepage basins, Initial stage above, with large hydraulic head (between equilibration- and brine-levels) and brine levels located below hydroseal closure (low reflux), and late stage below, with reduced hydraulic head and brine levels above hydroseal closure (seepage outflow of basin brines). The consequences of these variations are shown with respect to brine residence times and brine salinities. Diagrams based upon work of Logan (1987). In the late stage it is assumed that no diagenetic seal is formed that curtails brine reflux (see Fig. 40).

ously over the entire basin (Anderson *et al.*, 1972), confirming this inference.

Shallow water, deep basin model
Most thick basin-central evaporites seem to have been deposited in deep basins subject to significant evaporative drawdown. They were therefore isolated or extremely restricted basins and obtained much of their inflow by seepage. Like those of the previous model, these evaporites are underlain by deep water marine sediments. Unlike them, they are composed of shallow water and/or mud flat facies. The facies developed depends upon the depth of brine retained in the basin, and the inflow/reflux ratio (Logan, 1987; Kendall, 1988).

Evaporite accumulation in evacuated deep basins is only possible where there is a basal aquitard, either a pre-existing impermeable layer on the basin floor, or one created by evaporite cementation during initial, and leaky, stages of brine concentration. The aquitard lines at least part of the basin floor enclosing a topographically closed volume. Within this hydrosealed part of the basin, long-term storage of brine occurs.

Two different situations can be contrasted (Fig. 39). When brine surfaces lie within the hydrosealed part of the basin, and the seepage discharge rate is greater than evaporation, water flows into the basin. Evaporites and brines are confined to parts of the basin underlain by the hydroseal. Reflux occurs 1) at slow rates through the seal, or 2) during short episodes when floods raise the brine level above the hydroseal. Consequently, brine residence times in the basin are long, and evaporation is able, with appropriate climatic conditions, to concentrate brines. Highly saline salts can accumulate. In contrast, when brine levels lie above the hydroseal, the basin is more open. Brines are lost by seepage outflow in marginal areas where the basal aquitard is absent. This loss reduces residence times of basin brines and they are exported before they can be concentrated. Only salts with low solubility are precipitated.

There is no simple relationship, in isolated basins, between the type of evaporite deposited and sea level change. Brine salinities are controlled by brine residence times in the basin. These are determined primarily by the absolute and relative rates of water flow into, and brine reflux out of, the basin. One of the most direct methods of changing the inflow is to change sea level. When sea level rises (but not high enough to cause drowning of the basin rim: this would terminate evaporite deposition) the hydraulic head between the sea and the depressed brine level in the basin is increased. This results in greater volumes of water seepage through the permeable barrier. If reflux rates are unchanged, this enhanced influx increases brine residence times and promotes higher brine salinities. In disconnected basins therefore, sea level rises are marked by deposition of evaporites of increased solubility. Lowered sea levels cause reduction in influx rates, decreased brine residence times, and deposition of evaporites of lower solubility. These effects are opposite to those expected in basins having free connection with the ocean (compare Hite, 1970). Kendall (1988) suggested the upward sequence from anhydrites to carbonates in the Middle Devonian of northern Alberta (Muskeg and Sulfur Point formations), usually interpreted as reflecting a sea level rise, may in fact be interpreted as a product of a sea level fall which terminated with the deposition of the overlying nonmarine Watt Mountain unit.

Inflow/reflux rates may also change as a result of evaporite aggradation (Fig. 39). Initially, evaporite deposition is confined to the bottom and central parts of a basin where reflux is severely limited by an underlying aquitard. Residence times of brines are long, brines are concentrated to high salinities, and highly saline evaporites precipitated. With continued evaporite accretion the depositional area expands onto basin flanks where the aquitard is absent. Increasing amounts of brine reflux occur, progressively reducing residence times of brines. As brine salinities drop, the more soluble phases cease being precipitated (some may even begin to dissolve) and an upward sequence of decreasing mineral solubility is generated (Fig. 40). Kendall (1988) used this model, based upon the work of Logan (1987) at Lake MacLeod, to explain cyclicity in the Pennsylvanian Paradox evaporites of Utah and Colorado.

Most evaporite sequences, even those associated with onlap of basin flanks, have upward increases in mineral solubility. Here, lateral expansion of depositional areas was not coupled with decreases in brine residence times, and this implies the presence of efficient seals on basin flanks. Commonly, however, these flanks are composed of only slightly older carbonates that undoubtedly were still perme-

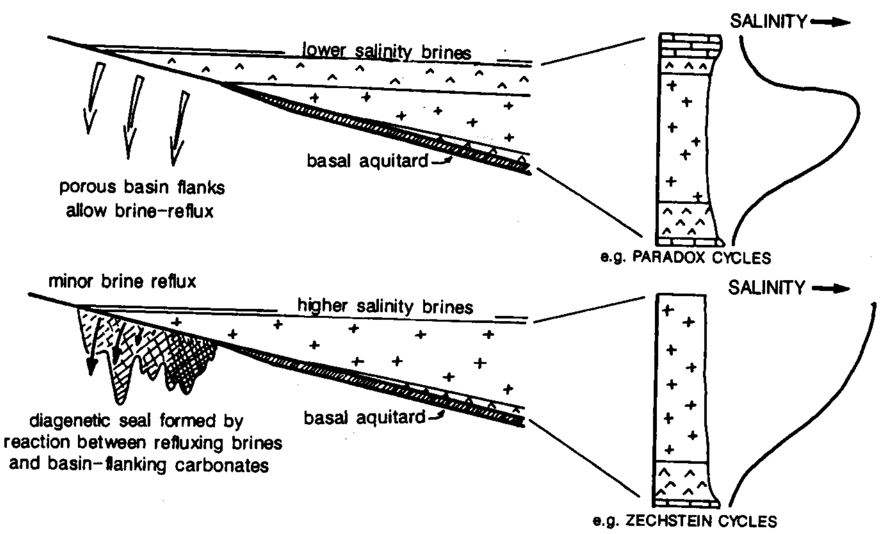

Figure 40 Diagrams showing inferred depositional sequences in basins without a hydroseal at basin-flank locations (top), and basins that develop a diagenetic hydroseal as a result of reaction of refluxing brines with flanking carbonate sediments or rocks (bottom). G.M. Harwood is jointly responsible for the concept of diagenetic sealing of evaporite basins.

able during the evaporite depositional episode. This suggests evaporite basins can be self-sealing: porosity in rocks and sediments of basin flanks, upon contact with concentrated brines, is occluded by evaporite cement or is eliminated by evaporite replacement (Fig. 40). In particular, dolomitization of flanking carbonates (almost universally associated with evaporite basins) is accompanied by precipitation of calcium sulphates as replacive nodules or cements that eliminate porosity.

Evaporite sequences that do exhibit upward decreases in mineral solubility possibly are confined to basins in which basin flanks are clastics (less susceptible to evaporite replacement and porosity loss), or in which conduits for refluxing brines were repeatedly opened by tectonism. Both explanations apply, for instance, to the formation of the Paradox Basin evaporites.

Finally, changes in aridity cause variations in evaporite mineralogy and facies within isolated and desiccated basins. These changes may be seasonal (as in Lake MacLeod; Logan 1987) or long term. The presence of free brine in a basin indicates inflow exceeds losses from reflux and evaporation. When evaporation losses exceed inflow, surface brines disappear. Increases in aridity thus promote development of evaporite flat environments where, if brine residence times are long (low reflux rates), evaporites of high solubility accumulate in the sediment. Decreases in aridity allow perennial or seasonal surface brines to be present, but may prevent accumulation of more soluble mineral phases.

SUMMARY

Evaporite facies are better defined by internal sedimentary/early diagenetic characters than by inferred geographic environments. Three main evaporite facies are recognized, mud flat, shallow-, and deep-water evaporites. Three main assemblages of evaporite facies are identified: 1) continental evaporites, that accumulate in basins largely unaffected by sea level changes, 2) basin-marginal evaporites, largely of marine origin and deposited as part of transgressive and highstand system tracts, and 3) basin-central evaporites, believed to be largely of marine origin but which could have been influenced by continental groundwaters. Basin-central evaporites only form when the entire depositional basin becomes restricted or isolated and thus are lowstand system tract deposits. Evaporative drawdown in such basins may, however, greatly amplify the effects of sea level falls.

ACKNOWLEDGEMENTS

I thank Noel James and Gill Harwood for carefully reviewing earlier versions, and for suggesting (imposing!) necessary changes for improvement (and increased brevity). Many people have been generous in supplying illustrations and have been credited in the main part of the paper. To those whose ideas I have used without credit, I apologize but offer the excuse that it is now impossible to acknowledge everyone within reviews of this type. Mr. P. Judge and Ms. S.M. Davies were responsible for the excellent drafting and photography, respectively.

REFERENCES

Basic sources of information

Anderson, R.Y., Dean, W.E., Kirkland, D.W. and Snider, M.I., 1972, Permian Castile varved evaporite sequence, west Texas and New Mexico: Geological Society of America, Bulletin, v. 83, p. 59-86.
Classic work on deep water evaporites, but see Kendall and Harwood (1989).

Arthurton, R.S., 1973, Experimentally produced halite compared with Triassic layered halite-rock from Cheshire, England: Sedimentology, v. 20, p. 145-160.
Beautifully illustrated, well worth reading.

Butler, G.P., Harris, P.M. and Kendall, C.G.St.C., 1982, Recent evaporites from the Abu Dhabi coastal flats, *in* Handford, C.R., Loucks, R.G. and Davies, G.R., eds., Depositional and diagenetic spectra of evaporites: Society of Economic Paleontologists and Mineralogists, Core Workshop 3, p. 33-64.
Well illustrated account of the "classic sabkha".

Eugster, H.P. and Kelts, K., 1983, Lacustrine chemical sediments, *in* Goudie, A.S. and Pye, K., eds., Chemical sediments and geomorphology: precipitates and residua in the near-surface environment: London, Academic Press, p. 321-36.
Detailed treatment of saline lake mineralogy and brine chemistry.

Hardie, L.A., 1984, Evaporites: marine or non-marine?: American Journal of Science, v. 284, p. 193-240.
Extensive treatment of criteria to be used in distinguishing marine and nonmarine evaporites. Dispels previous views that nonmarine evaporites are insignificant and that they always differ mineralogically and geochemically from marine evaporites

Hardie, L.A., 1990, The roles of rifting and hydrothermal $CaCl_2$ brines in the origin of potash evaporites: an hypothesis: American Journal of Science, v. 290, p. 43-106.
Continues discussion of the nonmainre origin of many ancient evaporites, here suggesting most potash salts are associated with hydrothermal waters.

Hardie, L.A. and Eugster, H.P., 1971, The depositional environment of marine evaporites: a case for shallow, clastic accumulation: Sedimentology, v. 16, p. 187-220.
Still highly recommended and beautifully illustrated.

Hardie, L.A., Lowenstein, T.K. and Spencer, R.J., 1985, The problem of distinguishing between primary and secondary features in evaporites, *in* Schreiber, B.C. and Harner, H.L., eds., Sixth Symposium on Salt, Alexandria, VA, Salt Institute, v. 1, p. 11-40.
Difficult to obtain, but an important paper dealing with a matter of vital importance to facies modelling, sorting diagenetic from depositional factors.

Hovorka, S., 1987, Depositional environments of marine-dominated bedded halite, Permian San Andres Formation, Texas: Sedimentology, v. 34, p. 1029-1054.
Critical discussion of depositional setting of halites.

Kendall, A.C. 1988, Aspects of evaporite basin stratigraphy, *in* Schreiber, B.C., ed., Evaporites and hydrocarbons: New York, Columbia University Press, p. 11-65.
Discusses relationship of evaporites to sea level change, and evaporite models.

Logan, B.W., 1987, The MacLeod Evaporite Basin, Western Australia: American Association of Petroleum Geologists, Memoir 44, 140 p.
Superbly illustrated account of major Recent evaporite basin, with sections concerned with evaporite models: emphasizes dynamic nature of evaporite basins. A "must read".

Lowenstein, T.K., 1988, Origin of depositional cycles in a Permian "saline giant": the Salado (McNutt zone) evaporites of New Mexico and Texas: Geological Society of America, Bulletin, v. 100, p. 592-608.
Excellent use of modern environmental data in the interpretation of an ancient deposit.

Melvin, J.L., ed., 1991, Evaporites, petroleum and mineral resources: Amsterdam, Elsevier, 556 p.
A compilation of papers dealing with all aspects of evaporites, well recommended.

Purser, B.H., 1985, Coastal evaporite systems, *in* Friedman, G.M. and Krumbein, W.E., eds., Hypersaline ecosystems: The Gavish sabkha: New York, Springer-Verlag, p. 72-102.
Extensive review of coastal sabkhas.

Richter-Bernburg, G., 1985, Zechstein-Anhydrite — Facies und Genese: Geologisches Jahrbuch, Reihe A, v. 85, 82 p.
Reviews a lifetime's work on these deep water evaporites.

Schreiber, B.C., ed., 1988, Evaporites and hydrocarbons: New York, Columbia University Press, 475 p.
Compilation of papers dealing with all aspects of evaporites, well recommended.

Warren, J.K., 1989, Evaporite sedimentology: Englewood Cliffs, Prentice Hall, 285 p.
Probably the best place to start; uneven treatment of some aspects.

Warren, J.K. and Kendall, C.G.St.C., 1985, Comparison of sequences formed in marine sabkha (subaerial) and salina (subaqueous) settings — modern and ancient: American Association of Petroleum Geologists, Bulletin, v. 69, p. 1013-1023.
Useful summary.

Other references

Adams, S.S., 1969, Bromine in the Salado Formation, Carlsbad Potash District, New Mexico: New Mexico State Bureau of Mines and Mineral Resources, Bulletin, v. 93, 122 p.

Allen, P.A. and Collinson, J.D., 1986, Lakes, *in* Reading, H.G., ed., Sedimentary environments and facies: Oxford, Blackwells, p. 63-94.

Amiel, A.J. and Friedman, G.M., 1971, Continental sabkha in Arava Valley between Dead Sea and Red Sea: significance for origin of evaporites: American Association of Petroleum Geologists, Bulletin, v. 55, p. 581-592.

Anati, D.A., Stiller, M., Shasha, S. and Gat, J.R., 1987, Changes in the thermohaline structure of the Dead Sea: 1979-1984: Earth and Planetary Science Letters, v. 84, p. 109-121.

Arakel, A.V., 1980, Genesis and diagenesis of Holocene evaporitic sediments in Hutt and Leeman lagoons, Western Australia: Journal of Sedimentary Petrology, v. 50, p. 1305-1326.

Beyth, M., 1980, Recent evolution and present stage of Dead Sea brines, *in* Nissenbaum, A., ed., Hypersaline brines and evaporitic environments: Amsterdam, Elsevier, p. 155-166.

Borchert, H. and Muir, R.O., 1964, Salt deposits: the origin, metamorphism and deformation of evaporites: Princeton, Van Nostrand-Reinhold, 338 p.

Brodylo, L.A. and Spencer, R.J., 1987, Depositional environments of the Middle Devonian Telegraph Salts, Alberta, Canada: Bulletin of Canadian Petroleum Geology, v. 35, p. 186-196.

Bush, P., 1973, Some aspects of the diagenetic history of the sabkha in Abu Dhabi, Persian Gulf, *in* Purser, B.H., ed., The Persian Gulf, New York, Springer-Verlag, p. 395-407.

Busson, G., ed., 1982, Geologie Mediterraneene (Nature et genese des facies confines): Annales de l'universite de Provence, v. 9(4), p. 303-591.

Colter, V.S. and Reed, G.E., 1980, Zechstein 2 Forden Evaporites of the Atwick No. 1 borehole, surrounding areas of N.E. England and the adjacent southern North Sea, *in* Füchtbauer, H. and Peryt, T., eds., The Zechstein Basin with emphasis on carbonate sequences: Contributions to Sedimentology 9, p. 115-129.

Crawford, G.A. and Dunham, J.B., 1982, Evaporite sedimentation in the Permian Yates Formation, Central Basin Platform, Andrews County, West Texas, *in* Handford, C.R., Loucks R.G. and Davies, G.R., eds., Depositional and diagenetic spectra of evaporites, Society of Economic Paleontologists and Mineralogists, Core Workshop 3, p. 238-275.

Czapowski, G., 1987, Sedimentary facies in the oldest rock salt (Na1) of the Leba Elevation (northern Poland), *in* Peryt, T.M., ed., The Zechstein facies in Europe: Lecture Notes in Earth Sciences, v. 10, Berlin, Springer-Verlag, p. 207-224.

Dean, W.E. and Fouch, T.D., 1983, Lacustrine environment, *in* Scholle, P.A., Bebout, D.G. and Moore C.H., eds., Carbonate depositional environments: American Association of Petroleum Geologists, Memoir 33, p. 97-130.

Elliott, L.A. and Warren, J.K., 1989, Stratigraphy and depositional environment of the Lower San Andres Formation in the subsurface and equivalent outcrops: Chavez, Lincoln and Roosevelt Counties, New Mexico: American Association of Petroleum Geologists, Bulletin, v. 73, p. 1307-1325.

Eugster, H.P. and Hardie, L.A., 1978, Saline Lakes, *in* Lerman, A., ed., Chemistry, geology and physics of lakes: New York, Springer-Verlag, p. 237-293.

Garber, R.A., Levy, Y. and Friedman, G.M., 1987, The sedimentology of the Dead Sea; Carbonates and Evaporites, v. 2, p. 43-57.

Garrison, R., Schreiber, B.C., Bernoulli, D., Fabricius, F.H., Kidd, R.B. and Meliere, F., 1978, Sedimentary petrology and structures of Messinian evaporitic sediments in the Mediterranean Sea. Leg 42A, Deep Sea Drilling Project, *in* Hsü, K.J. and Montaderi, L., *et al.*, Initial Reports of the Deep Sea Drilling Project, v. 42, p. 571-611.

Glennie, K.W. and Evans, G., 1976, A reconnaissance of the Recent sediments of the Ranns of Kutch, India: Sedimentology, v. 23, p. 625-647.

Gornitz, V.M. and Schreiber, B.C., 1981, Displacive halite hoppers from the Dead Sea: some implications for ancient evaporite deposits: Journal of Sedimentary Petrology, v. 51, p. 787-794.

Gunatilaka, A., Al-Temeemi, A., Saleh A. and Nassar, N., 1985, A new occurrence of bassanite in recent evaporitic environments, Kuwait, Arabian Gulf: Journal University of Kuwait (Science), v. 12, p. 157-166.

Handford, C.R., 1982, Sedimentology and evaporate genesis in a Holocene continental-sabkha playa basin, Bristol Dry Lake, California: Sedimentology, v. 29, p. 239-253.

Handford, C.R., 1991, Marginal marine halite: sabkhas and salinas, *in* Melvin, J.L., ed., Evaporites, petroleum and mineral resources: Amsterdam, Elsevier, p. 1-66.

Hardie, L.A., 1986, Ancient carbonate tidal-flat deposits: Colorado School of Mines Quarterly, v. 81, p. 37-57.

Hardie, L.A., Smoot, J.P. and Eugster, H.P., 1978, Saline lakes and their deposits: a sedimentological approach, *in* Matter A. and Tucker, M.E., eds., Modern and Ancient Lake Sediments: International Association of Sedimentologists, Special Publication 2, p. 7-41.

Harvie, C.E., Weare, J.H., Hardie, L.A. and Eugster, H.P., 1980, Evaporation of seawater: calculated mineral sequences: Science, v. 208, p. 498-500.

Hite, R.J., 1970, Shelf carbonate sedimentation controlled by salinity in the Paradox Basin, Colorado and Utah, *in* Rau J.L. and Delwig L.F., eds., Third Symposium on Salt: Cleveland, Northern Ohio Geological Society, v. 1, p. 48-66.

Hite, R.J., 1986, The sulphate problem in marine evaporites, *in* Schreiber, B.C., ed., Proceedings of the 6th International Symposium on Salt, Toronto: The Salt Institute, Alexandria, Virginia, v. 1, p. 217-230.

Holser, W.T., 1966, Diagenetic polyhalite in Recent salt from Baja California: American Mineralogist, v. 51, p. 99-109.

Hovorka, S.D., 1989, Depth evolution of the Delaware Basin — Castile/Salado transition: Society of Economic Paleontologists and Mineralogists, Core Workshop 13, p. 441-449.

Jones, B.F., 1965, The hydrology and mineralogy of Deep Springs Lake, Inyo County, California: U.S. Geological Survey, Professional Paper 502-A, 56 p.

Karcz, I. and Zak, I., 1987, Bed forms in salt deposits of the Dead Sea brines: Journal of Sedimentary Petrology, v. 57, p. 723-735.

Kendall, A.C., 1976, The Ordovician carbonate succession (Bighorn Group) of southeastern Saskatchewan: Saskatchewan Department of Mineral Resources, Report 180, 185 p.

Kendall, A.C., 1989, Brine mixing in the Middle Devonian of western Canada and its possible significance to regional dolomitization: Sedimentary Geology, v. 64, p. 271-285.

Kendall, A.C. and Harwood, G.M., 1989, Shallow-water gypsum in the Castile Formation — significance and implications, *in* Harris, P.M. and Grover, G.A., eds., Subsurface and outcrop examination of the Capitan Shelf Margin, Northern Delaware Basin: Society of Economic Paleontologists and Mineralogists, Core Workshop No. 13, p. 441-450.

King, R.H., 1947, Sedimentation in Permian Castile Sea: American Association of Petroleum Geologists, Bulletin, v. 26, p. 535-763.

Kinsman, D.J.J., 1975a, Rift Valley basins and sedimentary history of trailing continental margins, *in* Fisher, A. and Judson, S., eds., Petroleum and global tectonics: Princeton, Princeton University Press, p. 83-126.

Kinsman, D.J.J., 1975b, Salt floors to geosynclines: Nature, v. 255, p. 375-378.

Kinsman, D.J.J., 1976a, Evaporites: relative humidity control on primary mineral facies: Journal of Sedimentary Petrology, v. 46, p. 273-279.

Kinsman, D.J.J., 1976b, Sabkha facies nodular anhydrite and paleotemperature determination (abstr.): American Association of Petroleum Geologists, Bulletin, v. 60, p. 688.

Krumbein, W.C. and Sloss, L.L., 1963, Stratigraphy and sedimentation: San Francisco, Freeman, 660 p.
Chapter 13 discusses basin-marginal and basin-central evaporites.

Kushnir, J., 1981, Formation and early diagenesis of varved evaporitic sediments in a coastal hypersaline pool: Journal of Sedimentary Petrology, v. 51, p. 1193-1203.

Lindsay, R.F. and Roth, M.S., 1982, Carbonate and evaporite facies, dolomitization and reservoir distribution of the Mission Canyon Formation, Little Knife Field, North Dakota, *in* Christopher, J.E. and Kaldi, J., eds., Proceedings of 4th International Williston Basin Symposium, Regina, p. 153-179.

Longman, M.W., Fertal, T.G. and Glennie, J.S., 1983, Origin and geometry of Red River dolomite reservoirs, western Williston Basin: American Association Petroleum Geologists, Bulletin, v. 67, p. 744-771.

Loucks, R.G. and Longman, M.W., 1982, Lower Cretaceous Ferry Lake Anhydrite, Fairway Field, east Texas: Society of Economic Paleontologists and Mineralogists, Core Workshop 3, p. 130-173.

Lowenstein, T.K. and Hardie, L.A., 1985, Criteria for the recognition of salt pan evaporites: Sedimentology, v. 32, p. 627-644.

Lowenstein, T.K. and Spencer, R.J., 1990, Syndepositional origin of potash evaporites: petrographic and fluid inclusion evidence: American Journal of Science, v. 290, p. 1-42.

Lucia, F.J., 1972, Recognition of evaporite-carbonate shoreline sedimentation, *in* Rigby, J.K. and Hamblin, W.R., eds., Recognition of ancient sedimentary environments: Society of Economic Paleontologists and Mineralogists, Special Publication 16, p. 160-191.

Maiklem, W.R., 1971, Evaporative drawdown — a mechanism for water-level lowering and diagenesis in the Elk Point Basin: Bulletin Canadian Petroleum Geology, v. 19, p. 487-501.

Mann, S.D., 1988, Subaqueous evaporites of the Buckner Member, Haynesville Formation, northeastern Mobile County, Alabama: Transactions, Gulf Coast of Association of Geological Societies, v. 38, p. 187-196.

McCaffrey, M.A., Lazar, B. and Holland, H.D., 1987, The evaporation path of seawater and the coprecipitation of Br^- and K^+ with halite: Journal of Sedimentary Petrology, v. 57, p. 928-937.

McKenzie, J.A., Hsu, K.J. and Schneider, J.F., 1980, Movement of subsurface waters under the sabkha, Abu Dhabi, UEA, and its relation to evaporative dolomite genesis: Society of Economic Paleontologists and Mineralogists, Special Publication 28, p. 11-30.

Mitchell, J.C., Lehman, P.J., Cantrell, D.L., Al-Jallal, I.A. and Al-Thagafy, M.A.R., 1988, Lithofacies, diagenesis, and depositional sequence: Arab-D Member, Ghawar Field, Saudi Arabia: Society of Economic Paleontologists and Mineralogists, Core Workshop 12, p. 459-514.

Mossop, G.D., 1974, The evaporites of the Baumann Fiord Formation, Ellesmere Island, Arctic Canada: Geological Survey Canada, Bulletin 298, 52 p.

Murray, R.C., 1969, Hydrology of south Bonaire, Netherlands Antilles — a rock selective dolomitization model: Journal of Sedimentary Petrology, v. 15, p. 987-1035.

Neev, D. and Emery, K.O., 1967, The Dead Sea, depositional processes and environments of evaporites: Israel Geological Survey, Bulletin 41, 147 p.

Nurmi, R.D. and Friedman, G.M., 1977, Sedimentology and depositional environments of basin-central evaporites, Lower Salina Group (Upper Silurian), Michigan Basin, *in* Fisher, J.H., ed., Reefs and evaporites — concepts and depositional models: American Association of Petroleum Geologists, Studies in Geology 5, p. 23-52.

Orti-Cabo, F. and Shearman, D.J., 1977, Estruturas y fabricas deposicionales en las evaporitas del mioceno superior (Messiniense) de San Miguel de Salinas (Alicante, Espana): Instituto de Investigaciones Geologicas, Diputacion Provincial Universidad de Barcelona, v. 32, p. 5-54.
Description and interpretation of gypsum crystal habits.

Orti-Cabo, F. and Busson, G., eds., 1984, Introduction to the sedimentology of the coastal salinas of Santa Pola (Alicante, Spain): Revista d'Investigacions Geologiques, v. 38/39, p. 1-235.

Orti-Cabo, F., Pueyo, J.J., Geisler-Cussy, D. and Dulau, N., 1984, Evaporitic sedimentation in the coastal salinas of Santa Pola (Alicante, Spain): Revista d'Investigacions Geologiques, v. 38/39, p. 925-220.

Park, S.G., 1987, Deposition, diagenesis, and porosity development of the Middle Devonian Lucas Formation in the West Branch oil field, Ogemaw County, Michigan: unpubl. M.Sc. thesis, Kalamazoo, Western Michigan University.

Parrish, J.T., Ziegler, A.M. and Scotese, C.R., 1982, Rainfall patterns and the distribution of coals and evaporites in the Mesozoic and Cenozoic: Palaeogeography, Palaeoclimatology, Palaeoecology, v. 40, p. 67-101.

Patterson, R.J. and Kinsman, D.J.J., 1981, Hydrologic framework of a sabkha along the Arabian Gulf: American Association of Petroleum Geologists, Bulletin, v. 65, p. 1457-1475.

Perthuisot, J.P., 1981, Sebkha et Melah near Zarzis, a Recent paralic salt basin (Tunisia), *in* Evaporite deposits: Houston, Gulf Publishing Co., Editions Technip, p. 11-17 and 92-95.

Picha, F., 1978, Depositional and diagenetic history of Pleistocene and Holocene oolitic sediments and sabkhas in Kuwait, Persian Gulf: Sedimentology, v. 25, p. 427-449.

Purser, B., 1979, Les paleosabkhas du Miocene inferieur dans le sud-est de l'Iran: Bulletin Centre de Recherche Exploration-Production Elf-Aquitaine, v. 4, p. 235-244.

Raup, O.B., 1982, Gypsum precipitation by mixing seawater brines: American Association of Petroleum Geologists, Bulletin, v. 66, p. 363-367.

Rouchy, J.M., 1976, Sur la genese de deux principaux types de gypse (finement lite et en chevrons) du Miocene terminal de Sicile et d'Espagne meridionale: Revue de Geographie Physique et de Geologie Dynamique (2), v. 18, p. 347-364.

Schlager, W. and Bolz, H., 1977, Clastic accumulation of sulphate evaporites in deep water: Journal of Sedimentary Petrology, v. 47, p. 600-609.

Schmalz, R.F., 1969, Deep-water evaporite deposition: a genetic model: American Association of Petroleum Geologists Bulletin, v. 53, p. 798-823.

Schreiber, B.C., Friedman, G.M., Decima, A. and Schreiber, E., 1973, Depositional environments of the Upper Miocene (Messinian) evaporite deposits of the Sicilian Basin: Sedimentology, v. 23, p. 729-760.

Scruton, P.C., 1953, Deposition of evaporites: American Association of Petroleum Geologists, Bulletin, v. 37, p. 2498-2512.

Shearman, D.J., 1970, Recent halite rock, Baja California, Mexico: Institute of Mining and Metallurgy, Transactions, v. 79B, p. 155-162.

Shearman, D.J. and Fuller, J.G., 1969, Anhydrite diagenesis, calcitization, and organic laminites, Winnipegosis Formation, Middle Devonian, Saskatchewan: Bulletin of Canadian Petroleum Geology, v. 17, p. 469-525.

Smoot, J.P. and Lowenstein, T.K., 1991, Depositional environments of non-marine evaporites, *in* Melvin, J.L., ed., Evaporites, petroleum and mineral resources: Amsterdam, Elsevier, p. 189-347.

Sonnenfeld, P., 1984, Brines and evaporites: Orlando, Academic Press, 613 p.

Spencer, R.J., 1982, The geochemical evolution of Great Salt Lake, Utah: unpubl. Ph.D. thesis, Baltimore, Johns Hopkins University, 309 p.

Steinhorn, I., 1985, The disappearance of the long term meromictic stratification of the Dead Sea: Limnology and Oceanography, v. 30, p. 451-472.

Taylor, J.C.M., 1980, Origin of the Werraanhydrit in the U.K. Southern North Sea — a reappraisal, *in* Füchtbauer, H. and Peryt, T., eds., The Zechstein Basin with emphasis on carbonate sequences: Contributions to Sedim- entology 9, p. 91-113.

Vai, G.B. and Ricci Lucchi, F., 1978, Algal crusts, autochthonous and clastic gypsum in a cannibalistic evaporite basin: a case history from the Messinian of Northern Apennines: Sedimentology, v. 24, p. 211-244.

Wardlaw, N.C., 1972, Syn-sedimentary folds and associated structures in Cretaceous salt deposits of Sergipe, Brazil: Journal of Sedimentary Petrology, v. 42, p. 572-577.

Wardlaw, N.C. and Schwerdtner, W.M., 1966, Halite-anhydrite seasonal layers in Middle Devonian Prairie Evaporite Formation, Saskatchewan, Canada: Geological Society of America, Bulletin, v. 77, p. 331-342.

Warren, J.K., 1982, The hydrological setting, occurrence and significance of gypsum in late Quaternary salt lakes in South Australia: Sedimentology, v. 29, p. 609-637.

Warren, J.K., 1991, Sulphate dominated sea-marginal and platform evaporitic settings: sabkhas and salinas, mudflats and salterns, *in* Melvin, J.L., ed., Evaporites, petroleum and mineral resources: Amsterdam, Elsevier, p. 69-187.

Weiler, Y., Sass, E. and Zak, I., 1974, Halite oolites and ripples in the Dead Sea, Israel: Sedimentology, v. 21, p. 623-632.

West, I.M., Ali, Y.A. and Hilmy, M.E., 1979, Primary gypsum nodules in a modern sabkha on the Mediterranean coast of Egypt: Geology, v. 7, p. 354-358.